

Giorgio Lollino  
Daniele Giordan  
Cristian Marunteanu  
Basiles Christaras  
Iwasaki Yoshinori  
Claudio Margottini  
*Editors*



# Engineering Geology for Society and Territory – Volume 8

Preservation of Cultural Heritage



 Springer

---

Engineering Geology for Society  
and Territory – Volume 8

---

Giorgio Lollino • Daniele Giordan  
Cristian Marunteanu • Basiles Christaras  
Iwasaki Yoshinori • Claudio Margottini  
Editors

# Engineering Geology for Society and Territory – Volume 8

Preservation of Cultural Heritage

 Springer

*Editors*

Giorgio Lollino  
Daniele Giordan  
Institute for Geo-hydrological Protection  
National Research Council (CNR)  
Turin  
Italy

Cristian Marunteanu  
Faculty of Geology and Geophysics  
University of Bucharest  
Bucharest  
Romania

Basiles Christaras  
Department of Geology  
Aristotle University of Thessaloniki  
Thessaloniki  
Greece

Iwasaki Yoshinori  
Geo Research Institute  
Osaka  
Japan

Claudio Margottini  
ISPRA-Institute for Environmental  
Protection and Research  
Geological Survey of Italy  
Rome  
Italy

ISBN 978-3-319-09407-6      ISBN 978-3-319-09408-3 (eBook)  
DOI 10.1007/978-3-319-09408-3  
Springer Cham Heidelberg New York Dordrecht London

Library of Congress Control Number: 2014946956

© Springer International Publishing Switzerland 2015

This work is subject to copyright. All rights are reserved by the Publisher, whether the whole or part of the material is concerned, specifically the rights of translation, reprinting, reuse of illustrations, recitation, broadcasting, reproduction on microfilms or in any other physical way, and transmission or information storage and retrieval, electronic adaptation, computer software, or by similar or dissimilar methodology now known or hereafter developed. Exempted from this legal reservation are brief excerpts in connection with reviews or scholarly analysis or material supplied specifically for the purpose of being entered and executed on a computer system, for exclusive use by the purchaser of the work. Duplication of this publication or parts thereof is permitted only under the provisions of the Copyright Law of the Publisher's location, in its current version, and permission for use must always be obtained from Springer. Permissions for use may be obtained through RightsLink at the Copyright Clearance Center. Violations are liable to prosecution under the respective Copyright Law.

The use of general descriptive names, registered names, trademarks, service marks, etc. in this publication does not imply, even in the absence of a specific statement, that such names are exempt from the relevant protective laws and regulations and therefore free for general use.

While the advice and information in this book are believed to be true and accurate at the date of publication, neither the authors nor the editors nor the publisher can accept any legal responsibility for any errors or omissions that may be made. The publisher makes no warranty, express or implied, with respect to the material contained herein.

*Cover Illustration:* fotolia/#61631350/Temple of Juno © lapas77

Printed on acid-free paper

Springer is part of Springer Science+Business Media (www.springer.com)

---

## Foreword

It is our pleasure to present this volume as part of the book series of the Proceedings of the XII International IAEG Congress, Torino 2014.

For the 50th Anniversary, the Congress collected contributions relevant to all themes where the IAEG members have been involved, both in the research field and in professional activities.

Each volume is related to a specific topic, including:

1. Climate Change and Engineering Geology;
2. Landslide Processes;
3. River Basins, Reservoir Sedimentation and Water Resources;
4. Marine and Coastal Processes;
5. Urban Geology, Sustainable Planning and Landscape Exploitation;
6. Applied Geology for Major Engineering Projects;
7. Education, Professional Ethics and Public Recognition of Engineering Geology;
8. Preservation of Cultural Heritage

The book series aims at constituting a milestone for our association, and a bridge for the development and challenges of Engineering Geology towards the future.

This ambition stimulated numerous conveners, who committed themselves to collect a large number of contributions from all parts of the world, and to select the best papers through two review stages. To highlight the work done by the conveners, the table of contents of the volumes maintains the structure of the sessions of the Congress.

The lectures delivered by prominent scientists, as well as the contributions of authors, have explored several questions: ranging from scientific to economic aspects, from professional applications to ethical issues, which all have a possible impact on society and territory.

This volume testifies the evolution of engineering geology during the last 50 years, and summarizes the recent results. We hope that you will be able to find stimulating contributions which will support your research or professional activities.



A handwritten signature in blue ink that reads "Giorgio Lollino".

Giorgio Lollino



A handwritten signature in blue ink that reads "Carlos Delgado".

Carlos Delgado

---

## Preface

This volume examines the unique role of engineering geology in cultural heritage (CH) conservation from rapid and slow environmental dynamics, also including climate change impact and disaster risk reduction. It introduces various approaches to protect heritage from irreplaceable loss and considers ways to draw upon heritage as an asset in building the resilience of communities and nations to disasters.

Cultural heritage represents the legacy of the human kind on the planet Earth. It is evidence of millennia of adaptation of humans to the environment. Cultural heritage can be intangible (e.g. traditional knowledge, customs, ritual practices or beliefs) and tangible, the latter including various categories of places, from cultural landscapes and sacred sites to archaeological complexes, individual architectural or artistic monuments and historic urban centres.

The sites and remains are not always in equilibrium with the environment. They are continuously impacted and weathered by several internal and external factors, both natural and human-induced, with rapid and/or slow onset. These include major sudden natural hazards, such as earthquakes or extreme meteorological events, but also slow, cumulative processes such as the erosion of rocks, compounded by the effect of climate change, without disregarding the role of humans, especially in conflict situations.

In recent decades, many sites of significant cultural heritage value have suffered damage, occasionally irreversible, from natural and human-induced processes, resulting in the destruction of countless historical properties, museums and archives that hold the history of humanity within their walls. Cultural landscapes and natural heritage are being destroyed, and with them valued ecosystem services. These risks may be extensive, spanning entire countries or regions, or they may be more localised, such as those posed by fires, floods or landslides where they regularly affect particular heritage sites.

Often, disasters also affect traditional knowledge, practices, skills and crafts that ensure the cultural continuity of cultural heritage, as well as the means for its maintenance and conservation.

Typical examples of hazards affecting cultural heritages are the Bam earthquake in Iran (2003), the destruction of Bamiyan Buddhas from Taliban in Afghanistan (2001), the slow weathering of stones in Petra monuments (Jordan), the structural damage, also due to settlements, to Angkor Temples (Cambodia), the collapse of buildings in Pompei (Italy) and many other cases worldwide.

Against this background, engineering geology and Earth Science in general may play an essential role in the conservation and management of cultural properties. The relevance and potential of these areas of study was not fully appreciated in the past. At present, however, their contribution is increasingly acknowledged as the need for an interdisciplinary approach, which would bring together art history, science, management and socio-economic concerns, has become more and more apparent.

As a matter of fact, the protection of Cultural Heritages from geotechnical and geological hazards is a border area between Science for Conservation of Cultural Heritages and Earth Science. Conservators have to develop the proper restoration project, taking into consideration and having understood geological processes acting on the site and monument; in the mean

time, engineering geology has to implement a mitigation plan and monitoring system that are fulfilling the request of low impact and perfect integration of solutions into the archaeological context. Typical example of connection points between these two major categories is the usage of solution that can damage the CH or the cultural landscape, even if reducing the natural processes acting on the site; similarly, the use of materials that, during time, can lose original properties, generating salts, oxides, etc., that may affect the integrity and conservation of CH. In this context also the proposed monitoring systems need to fulfil the requirement of low environmental impact and minimum interference with the archaeological remains.

The above reflections, without obviously being exhaustive of the problem list, clearly underline the impact that the Earth Sciences have had in the construction, development and maintenance of the cultural properties; it is self evident that the same disciplines have to assume, today and in the future, a fundamental role in all the policies that are necessary for the protection and conservation of the heritage.

This passage has never been very clear in the past, since the archaeology and the conservation aspects had a strong centrality and autonomy. This point of view is now less evident, with more attention to the integration of different sciences. Indeed it is possible to affirm that the protection of the cultural heritage represents an interdisciplinary process (and not multi-disciplinary) to the border-line among art history, science, policies for management and exploitation.

In conclusion, it is possible to say that engineering geology ([www.iaeg.info](http://www.iaeg.info)) highly contributes to the conservation of Monuments and Sites, being the science devoted to the investigation, study and solution of the engineering and environmental problems, which may arise as the result of the interaction between geology and the works and activities of man as well as to the prediction of and the development of measures for prevention or remediation of geological hazards.

Thus, Engineering Geology embraces:

- the definition of the geomorphology, structure, stratigraphy, lithology and groundwater conditions of geological formations;
- the characterisation of the mineralogical, physic-geomechanical, chemical and hydraulic properties of all earth materials involved in construction, resource recovery and environmental change;
- the assessment of the mechanical and hydrological behaviour of soil and rock masses;
- the prediction of changes to the above properties with time;
- the determination of the parameters to be considered in the stability analysis of engineering works and of earth masses;
- the improvement and maintenance of the environmental condition and of the properties of the terrain.

From the above it is quite evident as engineering geology (in the widest sense of the term) is a major science for the protection and conservation of cultural heritages from environmental degradation and disruption; then, engineering geology is now more relevant in the current international standards on culture heritage protection and development, which are the result of several decades of ethical reflection, experience, research and consensus building in a rapidly changing world situation.

---

# Contents

<b>1</b>	<b>Engineering Geology in Shaping and Preserving the Historic Urban Landscapes and Cultural Heritage: Achievements in UNESCO World Heritage Sites</b> . . . . .	<b>1</b>
	Claudio Margottini	
<b>Part I Conservation of Heritage of Earthen Structure, Earth Mound, Dam, Rock Monument, and Rock Cavern</b>		
<b>2</b>	<b>Microtremor Measurements at Mogao Grottoes, Dunhuang, China for Preliminary Dynamic Characterization for Performance During Earthquake</b> . . . . .	<b>31</b>
	Yoshinori Iwasaki, Koichi Nakagawa, Yuzo Ishikawa, Chikaosa Tanimoto, Keigo Koizumi, Kazuo Oike, Lanming Wang, Xudong Wang, and Qinglin Guo	
<b>3</b>	<b>CEN TC 346 Conservation of Cultural Heritage-Update of the Activity After a Height Year Period</b> . . . . .	<b>37</b>
	Vasco Fassina	
<b>4</b>	<b>A Study on the Present States of Different Rocks of Ancient Monuments in Sri Lanka</b> . . . . .	<b>43</b>
	Upali Silva de. Jayawardena	
<b>5</b>	<b>Analysis of the Stability of a Rock Cavern: The Fontanelle Cemetery</b> . . . .	<b>47</b>
	Anna Scotto di Santolo, Lorenza Evangelista, and Aldo Evangelista	
<b>6</b>	<b>Measurement of the Joint Displacement Along Masonry Wall Using Digital Photogrammetry for the Structural Stability of the Borobudur Temple, Indonesia</b> . . . . .	<b>53</b>
	Tomofumi Koyama, Ichita Shimoda, and Yoshinori Iwasaki	
<b>7</b>	<b>Earth Pyramids: Precarious Structures Surviving Recurrent Perturbations</b> . . . . .	<b>59</b>
	Giovanni B. Crosta, Riccardo Castellanza, Roberto de Franco, Alberto Villa, Gabriele Frigerio, and Grazia Caielli	
<b>8</b>	<b>Evaluation of the Stability of Underground Cavities in Calcarenite Interacting with Buildings Using Numerical Analysis</b> . . . . .	<b>65</b>
	Matteo Oryem Ciantia, Riccardo Castellanza, Claudio di Prisco, Piernicola Lollino, Jose Antonio Fernandez Merodo, and Gabriele Frigerio	

<b>9</b>	<b>Estimation of Hydraulic Environment Behind the Mogao Grottoes Based on Geophysical Explorations and Laboratory Experiment. . . . .</b>	<b>71</b>
	Koizumi Keigo, Oda Kazuhiro, Ito Misae, Piao Chunze, Tanimoto Chikaosa, Iwasaki Yoshinori, Yoshimura Mitsugu, Wang Xudong, Guo Qinglin, and Yang Shanlong	
<b>10</b>	<b>Application of Photogrammetry to the Survey of the Yokosuka Arsenal Dry Dock No. 1, Japan. . . . .</b>	<b>75</b>
	Yukiyasu Fujii, Kunio Watanabe, Takaharu Shogaki, and Katsuhiro Kikuchi	
<b>Part II Engineering Geology and Preservation of Cultural Heritage</b>		
<b>11</b>	<b>Engineering Protection of the Territory, Monitoring and Safeguarding of the Immovable Cultural Heritage of the Historical Centre of Kiev . . . .</b>	<b>83</b>
	Yuriy Maslov	
<b>12</b>	<b>The Acropolis Hill of Athens: Engineering Geological Investigations and Protective Measures for the Preservation of the Site and the Monuments . . . . .</b>	<b>89</b>
	George Koukis, Lambros Pyrgiotis, and Athanasia Kouki	
<b>13</b>	<b>Preservation of Saint George’s Church at Cairo, Egypt . . . . .</b>	<b>95</b>
	Andreas Antoniou, Efthymis Lekkas, and Nikitas Chiotinis	
<b>14</b>	<b>Preservation of Sanukite, the Highly Sophisticated Music Instrument Made of Andesite . . . . .</b>	<b>99</b>
	Shuichi Hasegawa, Seiko Tsuruta, and Munekazu Maeda	
<b>15</b>	<b>Resistance of Buried Archeological Site to One-dimensional Mechanical Loading . . . . .</b>	<b>103</b>
	Dominique Ngan-Tillard, Wim Verwaal, Arno Mulder, Hans Huisman, and Axel Muller	
<b>16</b>	<b>Trostburg Castle in South Tyrol—Engineering Geological Investigations on the Castle Hill. . . . .</b>	<b>107</b>
	Lempe Bernhard, Mehnert Lucia, Scherzer Kathrin, Festl Judith, and Thuro Kurosch	
<b>17</b>	<b>The Geology of the Hill of Summersberg Castle in Gufidaun (South Tyrol, Italy) and Its Geotechnical Challenges in Mitigation Works . . . . .</b>	<b>113</b>
	Ellecosta Peter, Lempe Bernhard, and Thuro Kurosch	
<b>18</b>	<b>Engineering Geological Conditions and Instability of Mycenaean Tombs in Cephallonia, Greece. . . . .</b>	<b>117</b>
	Charalambos Saroglou and Andreas Sotiriou	
<b>19</b>	<b>Slope Geometry Design, Deformations and Failures of Ancient Quarries in Zhejiang Province, China . . . . .</b>	<b>123</b>
	Lihui Li, Xiaolong Deng, and Zhifa Yang	

<b>20</b>	<b>Underground Tunneling to Match Social Development and Preservation of Historical and Cultural Heritage: Bangalore Metro Line UG-1</b> . . . . .	129
	Giuseppe M. Gaspari, Namita Gopeenatha, and Prathap Muniyappa	
<b>21</b>	<b>Three Dimensional Pore Geometry and Fluid Flow of Kimachi Sandstone Under Different Stress Condition: Suggestion to Conservation of Tuffaceous World Cultural Heritage</b> . . . . .	135
	Manabu Takahashi, Naoki Takada, Minoru Sato, and Weiren Lin	
<b>22</b>	<b>Application of Non Destructive Ultrasonic Techniques for the Analysis of the Conservation Status of Building Materials in Monumental Structures</b> . . . . .	139
	Basile Christaras, Francesco Cuccuru, Silvana Fais, and Helen Papanikolaou	
<b>Part III Engineering Geology Problem of Preservation and Restoration of the Cultural Heritage</b>		
<b>23</b>	<b>Mechanisms of Rock Cracking on Huashan Rock Paintings</b> . . . . .	147
	Fang Yun, Qiao Liang, Yan Shaojun, Peng Pengcheng, and Zhu Qiuping	
<b>24</b>	<b>Stability Analysis of Wine Cellars Cut into Volcanic Tuffs in Northern Hungary</b> . . . . .	153
	Mariann Mocsár-Vámos, Péter Görög, Márta Borostyáni, Balázs Vásárhelyi, and Ákos Török	
<b>25</b>	<b>The Historical Stone Architecture in the Ossola Valley and Ticino: Appropriate Recovery Approaches and Solutions</b> . . . . .	159
	Zerbinatti Marco, Bianco Isabella, and Piumatti Paolo	
<b>26</b>	<b>Engineering Geology Problems and Seismic Vulnerability of Ancient Structures in Central Asia</b> . . . . .	165
	N.G. Mavlyanova	
<b>27</b>	<b>Limestone Weathering and Deterioration in the Tebessa Roman Wall N E Algeria</b> . . . . .	169
	A. Boumezbeur, H. Hmaidia, and B. Belhocine	
<b>Part IV Engineering Geology Problems and Preservation of Chinese Caves and Earthen Architecture Site</b>		
<b>28</b>	<b>Earthquake Environments at Mogao Grottoes, Dunhuang, China</b> . . . . .	177
	Yoshinori Iwasaki, Chikaosa Tanimoto, Yuzo Ishikawa, Keigo Koizumi, Koichi Nakagawa, Kazuo Oike, Xudong Wang, Qinglin Guo, and Lanming Wang	
<b>29</b>	<b>The Engineering Geological Problems and Conservation of Cliff Face of Dunhuang Mogao Grottoes, China.</b> . . . . .	183
	Xudong Wang, Qinglin Guo, Shanlong Yang, Qiangqiang Pei, and Yuquan Fan	

<b>30</b>	<b>Control of Rockfall and Mudflow at a Hillside Buddhist Temple Site in Northwest China</b> . . . . .	189
	Huyuan Zhang, Bo Yang, Yi Chen, and Jinfang Wang	
<b>31</b>	<b>Field Tests on Anchoring Mechanism of the Bamboo-Steel Cable Composite Anchor with Single Reinforcement</b> . . . . .	193
	Jingke Zhang, Wenwu Chen, Faguo He, and Lei Tian	
<b>32</b>	<b>The Disease Characteristics and Conservation Technique of the Bezeklik Grottoes at Turpan in Xinjiang</b> . . . . .	199
	Wenwu Chen, Jingke Zhang, Faguo He, Guanping Sun, and Lei Tian	
 <b>Part V Geoheritage, Geosites, Geoparks: Contributions of the Engineering Geology in the Management of Natural and Cultural Landscape</b>		
<b>33</b>	<b>The Stone Bridges on the Po River at Turin (NW Italy): A Scientific Dissemination Approach for the Development of Urban Geological Heritage.</b> . . . . .	207
	Giulia Poretti, Alessandro Borghi, Anna d'atri, Giovanna Antonella Dino, Simona Ferrando, Chiara Groppo, Luca Martire, Edoardo Accattino, Sergio Enrico Favero Longo, Rosanna Piervittori, and Franco Rolfo	
<b>34</b>	<b>Directions in Geoheritage Studies: Suggestions from the Italian Geomorphological Community.</b> . . . . .	213
	Irene Bollati, Paola Coratza, Marco Giardino, Lamberto Laureti, Giovanni Leonelli, Mario Panizza, Valeria Panizza, Manuela Pelfini, Sandra Piacente, Alessia Pica, Filippo Russo, and Andrea Zerboni	
<b>35</b>	<b>Endangered Geoheritage in Bangladesh: A Case Study of Eocene Sylhet Limestone and Adjoining Areas, Jaflong, Sylhet.</b> . . . . .	219
	Ismail Hossain and Mowsumi Nahar	
<b>36</b>	<b>Estimation of Recreation Attractiveness and Geomorphic Risks for Recreational Purposes: Case of Nalychevo Nature Park (Kamchatka, Russia).</b> . . . . .	223
	Iuliia Blinova and Andrey Bredikhin	
<b>37</b>	<b>Recovery of Ancient Groundwater Supply Systems and Old Abandoned Mines: Coupling Engineering Geosciences and Geoheritage Management</b> . . . . .	227
	Maria Eugénia Lopes, Maria José Afonso, José Teixeira, João P. Meixedo, J. Filinto Trigo, Maria João Dias Costa, Luís C. Gama Pereira, and Helder I. Chaminé	
<b>38</b>	<b>Influence of Geological Structures and Weathering in Formation and Destruction of Cone-Shaped Rocky Houses of the Kandovan Village, Iran</b> . . . . .	231
	Ebrahim Asghari Kaljahi, Farideh Amini Birami, and Masoud Hajjalilue	

<b>39</b>	<b>The Ivrea Morainic Amphitheatre as a Well Preserved Record of the Quaternary Climate Variability (PROGEO-Piemonte Project, NW Italy) . . . . .</b>	235
	Franco Gianotti, Maria Gabriella Forno, Roberto Ajassa, Fernando Cámara, Emanuele Costa, Simona Ferrando, Marco Giardino, Stefania Lucchesi, Luigi Motta, Michele Motta, Luigi Perotti, and Piergiorgio Rossetti	
<b>40</b>	<b>The Monviso Ophiolite Geopark, a Symbol of the Alpine Chain and Geological Heritage in Piemonte, Italy. . . . .</b>	239
	Franco Rolfo, Gianni Balestro, Alessandro Borghi, Daniele Castelli, Simona Ferrando, Chiara Groppo, Pietro Mosca, and Piergiorgio Rossetti	
<b>41</b>	<b>The Morainic Amphitheatre Environment: A Geosite to Rediscover the Geological and Cultural Heritage in the Examples of the Ivrea and Rivoli- Avigliana Morainic Amphitheatres (NW Italy) . . .</b>	245
	Stefania Lucchesi, Franco Gianotti, and Marco Giardino	
<b>42</b>	<b>LiDAR-Helped Recognition and Promotion of High-Alpine Geomorphosites . . . . .</b>	249
	Ludovic Ravanel, Philip Deline, and Xavier Bodin	
<b>43</b>	<b>Assessment of Ancient Stone Quarry Landscapes as Heritage Sites . . . . .</b>	253
	Heldal Tom and Meyer Gurli	
<b>44</b>	<b>Multimedia and Virtual Reality for Imaging the Climate and Environment Changes Through Earth History: Examples from the Piemonte (NW Italy) Geoheritage (PROGEO-Piemonte Project). . . . .</b>	257
	E. Giordano, A. Magagna, L. Ghiraldi, C. Bertok, F. Lozar, A. d'Atri, F. Dela Pierre, M. Giardino, M. Natalicchio, L. Martire, P. Clari, and D. Violanti	
<b>45</b>	<b>Relationships Between Geoheritage, and Environmental Dynamics in the Tanaro Valley (NW Italy): Geological Mapping and Geotourist Activities for a Proper Management of Natural and Cultural Landscapes. . . . .</b>	261
	E. Giordano, M. Natalicchio, L. Ghiraldi, M. Giardino, F. Lozar, and F. Dela Pierre	
<b>46</b>	<b>An Application for Geosciences Communication by Smartphones and Tablets. . . . .</b>	265
	Emmanuel Reynard, Christian Kaiser, Simon Martin, and Géraldine Regolini	
<b>47</b>	<b>Methodologies and Activities to Promote Geotourism. The Case Study of the Cannobina Valley (NW Italy) . . . . .</b>	269
	Luca Ghiraldi, Marco Bacenetti, Luigi Perotti, Marco Giardino, and Paolo Millemaci	
<b>48</b>	<b>Geomorphological Hazard in Hypogeum Karst Touristic Landscape: An Example from Frassassi Cave (Central Italy) . . . . .</b>	273
	P. Farabollini, D. Aringoli, M. Materazzi, and G. Pambianchi	

<b>Part VI Monitoring and Modelling Applications for the Diagnosis of the Actual Conditions, Preservation and Management of Cultural Heritage</b>	
<b>49 Instrumental Geophysical Diagnose: Help to Historical Monuments Reconstruction Works</b> . . . . .	281
Mihai Mafteiu, Cristian Marunteanu, Victor Niculescu, and Sanda Bugiu	
<b>50 Rockfalls Monitoring Along Eastern Coastal Cliffs of the Favignana Island (Egadi, Sicily): Preliminary Remarks</b> . . . . .	287
Luca Falconi, Alessandro Peloso, Claudio Puglisi, Augusto Screpanti, Angelo Tati, and Vladimiro Verrubbi	
<b>51 Landslide Hazard Assessment, Monitoring and Conservation of Vardzia Monastery Complex</b> . . . . .	293
Claudio Margottini, Jordie Corominas, Giovanni Battista Crosta, Paolo Frattini, Giovanni Gigli, Ioshinori Iwasaky, Giorgio Lollino, Paul Marinos, Claudio Scavia, Alberico Sonnessa, Daniele Spizzichino, and Daniele Giordan	
<b>52 Implementation of advanced monitoring System Network in the Siq of Petra (Jordan)</b> . . . . .	299
Giuseppe Delmonaco, Gabriele Leoni, Claudio Margottini, and Daniele Spizzichino	
<b>53 Effects of Moisture Content on the Strength and Wear Resistance of Chalk</b> . . . . .	305
John Cripps, Nurul Liyana B. Awang Rosli, Barnabas Harris, and Roger Lewis	
<b>54 Characterization of Adobes in the Central Plateau of Angola</b> . . . . .	311
Pedro Elsa, Duarte Isabel, Varum Humberto, and Pinho António	
<b>55 Remote Sensing Techniques in a Multidisciplinary Approach for the Preservation of Cultural Heritage Sites from Natural Hazard: The Case of Valmarecchia Rock Slabs (RN, Italy)</b> . . . . .	317
Margherita Cecilia Spreafico, Francesca Franci, Gabriele Bitelli, Valentina Alena Girelli, Alberto Landuzzi, Claudio Corrado Lucente, Emanuele Mandanici, Maria Alessandra Tini, and Lisa Borgatti	
<b>56 Dynamic Response of the Giotto's Bell-Tower, Firenze, Italy</b> . . . . .	323
Maurizio Ripepe, Massimo Coli, Giorgio Lacanna, Emanuele Marchetti, Maria Teresa Cristofaro, Mario De Stefano, Valentina Mariani, Marco Tanganelli, and Paolo Bianchini	
<b>57 Damage to the Bangudae Petroglyph in South Korea and a Scheme for Its Conservation</b> . . . . .	329
Su-Gon Lee, Steve Hencher, Ji-Won Kim, Sung-Bu Cho, Ho-Dam Lee, Sun-Hyun Park, Gun-Su Kim, and Young-Suk Lee	

<b>58</b>	<b>Consolidation and Restoration of the Moletta's Tower (Circus Maximus: Roma): Site Investigation and Monitoring</b> . . . . .	335
	Roberto Brancaleoni, Federico Celletti, Fabio Garbin, Giuliano Padula, Luigi Serio, and Daniele Spizzichino	
<b>59</b>	<b>Multi-scale Detection of Changing Cultural Landscapes in Nasca (Peru) Through ENVISAT ASAR and TerraSAR-X</b> . . . . .	339
	Deodato Tapete, Francesca Cigna, Rosa Lasaponara, and Nicola Masini	
<b>60</b>	<b>Structural Assessment of Case Study Historical and Modern Buildings in the Florentine Area Based on a PSI-Driven Seismic and Hydrogeological Risk Analysis</b> . . . . .	345
	Fabio Pratesi, Deodato Tapete, Gloria Terenzi, Chiara Del Ventisette, and Sandro Moretti	
<b>61</b>	<b>Documentation, Digital Survey and Protection for a Multidisciplinary Knowledge of Some Urban Historic Landscape in Italy</b> . . . . .	351
	Alessandro De Masi	
<b>62</b>	<b>Analysis of Rockfall Individual Risk at the Feifeng Underground Caves (Zhejiang Province, China) by Using 2D and 3D Runout Models</b> . . .	357
	X.L. Wang, L.Q. Zhang, P. Frattini, S. Lari, G.B. Crosta, and F. Agliardi	
<b>63</b>	<b>Rock Mass Instabilities in Tatlarin Underground City (Cappadocia-Turkey)</b> . . . . .	361
	İsmail Dinçer, Ahmet Orhan, Paolo Frattini, and Giovanni B. Crosta	
<b>Part VII Preservation of Cultural Heritage from Natural Hazards</b>		
<b>64</b>	<b>Preservation of Saint John Chapel in Dukla from Landslide Natural Hazard</b> . . . . .	369
	Zbigniew Bednarczyk	
<b>65</b>	<b>Behavior of Buildings in Reinforced Concrete During an Earthquake: Case Study</b> . . . . .	375
	Samir Bouhedja, Boualem El Kechebour, and Ahmed Boukhaled	
<b>66</b>	<b>Stabilization of the Landslide in the Brda River Scarp at the Abutment of the Historical Bridge of the Narrow-Gauge Railway (Koronowo, Poland)</b> . . . . .	381
	Marek Kulczykowski, Lesław Zabuski, Teresa Mrozek, Izabela Laskowicz, and Waldemar Świdziński	
<b>67</b>	<b>Importance of Mortars Characterization in the Structural Behavior of the Monumental and Civil Buildings: Case Histories in L'Aquila (Italy)</b> . . . . .	387
	Elena Pecchioni, Raimondo Quaresima, Fabio Fratini, and Emma Cantisani	
<b>68</b>	<b>Natural Hazard Affecting the Katskhi Pillar Monastery (Georgia)</b> . . . . .	393
	Claudio Margottini, Daniele Spizzichino, Alberico Sonnessa, and Luca Maria Puzzilli	

<b>69</b>	<b>Ambient Noise Recordings in the Circo Massimo and <i>Vallis Murciae</i> Areas: Main Results Compared with the Dynamic Response of the XII Cen. A.D. Torre Della Moletta</b> . . . . .	399
	Emiliano Di Luzio, Francesco Fazio, Sebastiano Imposa, and Giuseppe Rannisi	
<b>70</b>	<b>Susceptibility Assessment of Subaerial (and/or) Subaqueous Debris-Flows in Archaeological Sites, Using a Cellular Model</b> . . . . .	405
	Valeria Lupiano, Maria Vittoria Avolio, Marco Anzidei, Gino Mirocle Crisci, and Salvatore Di Gregorio	
<b>71</b>	<b>The Latomiae of Syracuse: A Geotechnical Mapping Through Rock Reflectivity</b> . . . . .	409
	Mastelloni Maria Amalia, Ercoli Laura, Nocilla Alessandra, Nocilla Nicola, Sciortino Rosanna, and Zimbardo Margherita	
<b>72</b>	<b>Sacred Historical Heritage Affected by Landslides in the Polish Flysch Carpathians</b> . . . . .	415
	Izabela Laskowicz and Teresa Mrozek	
<b>73</b>	<b>Preservation of Cultural Heritage of Sant’Agata de’ Goti (Italy) from Natural Hazards</b> . . . . .	421
	Anna Scotto di Santolo, Filomena de Silva, Domenico Calcaterra, and Francesco Silvestri	
<b>74</b>	<b>A Study for Preserving the Freisa Terroir (Central Piedmont—Northwestern Italy) from Soil Erosion</b> . . . . .	427
	Roberto Ajassa, Caterina Caviglia, Enrico Destefanis, Giuseppe Mandrone, and Luciano Masciocco	
<b>75</b>	<b>Rockfall at the Arvanitia Pathway, Nafplio, Greece: Protection of the Site with Respect to Its Unique Natural Beauty and Archaeological Interest</b> . . . . .	431
	Garyfalia Konstantopoulou, Natalia Spanou, and Vaia Kontogianni	
<b>76</b>	<b>Andalusian Cultural Heritage and Natural Hazards Prevention</b> . . . . .	437
	Jesús Garrido and M <sup>a</sup> Lourdes Gutiérrez	
<b>Part VIII The Role of Historical Archives in the Assessment, Management and Valorization of Cultural Landscapes</b>		
<b>77</b>	<b>Using Documentary Data to Reconstruct Social Responses and Local-Based Adaptation Strategies to Landslide and Flood Hazards in N Czechia</b> . . . . .	443
	Pavel Raška, Vilém Záborský, and Jakub Dubiřar	
<b>78</b>	<b>Historical Archives Data for the Reconstruction of Geomorphological Modifications in the Urban Area of Turin (NW-Italy)</b> . . . . .	447
	Stefania Lucchesi and Marco Giardino	

<b>79</b>	<b>Reconstructions, Transfers and Forced Abandonments Brought About by Earthquakes and Landslides in the Historical Centres of Southern Italy: The Role of Primary Sources</b> . . . . .	453
	Fabrizio Terenzio Gizzi, Maria Rosaria Potenza, Maria Sileo, and Cinzia Zotta	
<b>80</b>	<b>Relevance of Database for the Management of Historical Information on Climatic and Geomorphological Processes Interacting with High Mountain Landscapes</b> . . . . .	459
	Guido Nigrelli and Marta Chiarle	
<b>81</b>	<b>Dynamic Geomorphology and Historical Iconography. Contributions to the Knowledge of Environmental Changes and Slope Instabilities in the Apennines and the Alps</b> . . . . .	463
	Giardino Marco, Mortara Giovanni, Borgatti Lisa, Nesci Olivia, Guerra Cristiano, and Lucente Corrado Claudio	
<b>Part IX Weathering and Preservation of Building Stones and Other Materials</b>		
<b>82</b>	<b>Stone Masonry Material of a Medieval Monastic Glass Production Centre, Pomáz (Hungary)</b> . . . . .	471
	Á. Török, B. Szabó, and J. Laszlovszky	
<b>83</b>	<b>Statistical Models for Predicting the Mechanical Properties of Travertine Building Stones After Freeze-Thaw Cycles</b> . . . . .	477
	Amin Jamshidi, Mohammad Reza Nikudel, Mashalah Khomehchiyan, and Ahmad Zalooli	
<b>84</b>	<b>Geological Problems of the Cave Monastery Complex of Vardzia (Georgia)</b> . . . . .	483
	Bezhan Tutberidze and Tamara Tsutsunava	
<b>85</b>	<b>Conserving Scotland's Built Heritage: A Petrographic Investigation on the Effects of Deicing Salts on Scottish Sandstones</b> . . . . .	487
	Callum Graham, Martin Lee, Vernon Phoenix, and Maureen Young	
<b>86</b>	<b>Gypsum Decay Simulation: Risco de las Cuevas Case Study, Madrid, Spain</b> . . . . .	491
	David Martín Freire-Lista, Vladimir Greif, Mónica Álvarez de Buergo, and Rafael Fort	
<b>87</b>	<b>Deterioration of Stone and Mineral Materials from the Roman Imperial "Villa of the Antonines" at Ancient Lanuvium</b> . . . . .	495
	Gregory A. Pope, Deborah Chatr Aryamontri, Laying Wu, and Timothy Renner	
<b>88</b>	<b>Stone Masonry Arch Bridges: In situ Testing and Stability Analyses by Using Numerical Methods; Examples from Hungary</b> . . . . .	503
	Bögöly Gyula, Görög Péter, and Török Ákos	

<b>89</b>	<b>Quantitative Analysis of Salt Crystallization–Dissolution Processes on Rock-Cut Monuments in Petra/Jordan</b> . . . . .	507
	Kurt Heinrichs and Rafiq Azzam	
<b>90</b>	<b>Staining Tests for Granitic Stone Conservation</b> . . . . .	511
	Maria Heloisa Barros de Oliveira Frascá, Fabiano Cabañas Navarro, and Eduardo Brandau Quitete	
<b>91</b>	<b>The Effect of Biodeterioration by Bird Droppings on the Degradation of Stone Built</b> . . . . .	515
	Harith E. Ali, Suhail A. Khattab, and Muzahim Al-Mukhtar	
<b>92</b>	<b>Changes in Petrophysical Properties of the Stone Surface due to Past Conservation Treatments in Archaeological Sites of Merida (Spain)</b> . . . . .	521
	Natalia Perez-Ema, Monica Alvarez de Buergo, Rosa Bustamante, and Miguel Gomez-Heras	
<b>93</b>	<b>Synthesis and Characterization of a Calcium Oxalate-Silica Nanocomposite for Stone Conservation</b> . . . . .	525
	Noni Maravelaki, Anastasia Verganelaki, Vassilis Kilikoglou, and Ioannis Karatasios	
<b>94</b>	<b>Freeze-Thaw and UV Resistance in Building Stone Coated with Two Permanent Anti-graffiti Treatments</b> . . . . .	531
	Paula María Carmona-Quiroga, María Teresa Blanco-Varela, and Sagrario Martínez-Ramírez	
<b>95</b>	<b>Monitoring of Cultural Heritage Decay in Rome: Analysis of Soiling and Erosion Phenomena</b> . . . . .	535
	Raffaella Gaddi, Mariacarmela Cusano, Patrizia Bonanni, Carlo Cacace, and Annamaria Giovagnoli	
<b>96</b>	<b>Fluorescent Microscopy of Stained Thin Sections: A Direct Tool for the Evaluation of Pore Space Characteristics in Porous Rocks</b> . . . . .	539
	Richard Přikryl	
<b>97</b>	<b>Influence of Fântânița Lake (Chalk Lake) Water on the Degradation of Basarabi–Murfatlar Churches</b> . . . . .	543
	Rodica-Mariana Ion, Radu-Claudiu Fierascu, Irina Fierascu, Raluca-Madalina Senin, Mihaela-Lucia Ion, Mirela Leahu, and Daniela Turcanu-Carutiu	
<b>98</b>	<b>Condition Survey on XIV–XVIII Century Funerary Monuments in the Cloisters of St. Anthony Basilica in Padua</b> . . . . .	547
	Vasco Fassina, Simone Benchiarin, and Gianmario Molin	
<b>99</b>	<b>Micro-Fabric, Pore-Size Distribution and Water Absorption of Consolidated Porous Limestone</b> . . . . .	553
	Zita Pápay and Ákos Török	
<b>100</b>	<b>The Bentheim Sandstone: Geology, Petrophysics, Varieties and Its Use as Dimension Stone</b> . . . . .	557
	C. Wim Dubelaar and Timo G. Nijland	

---

<b>101 Comparative Analysis of the Mechanical Properties of Water Saturated and Air Dry Volcanic Tuffs . . . . .</b>	<b>565</b>
B. Vásárhelyi and Á. Török	
<b>102 Influence of Salt and Moisture on Weathering of Historic Stonework in a Continental-Humid, Urban Region . . . . .</b>	<b>569</b>
I. Egartner, H. Schnepfleitner, and O. Sass	
<b>103 Monitoring of the Thermal-Moisture Regime at St. Jacob's Church in Levoča UNESCO Site, Eastern Slovakia. . . . .</b>	<b>577</b>
Jan Vlcko, Vladimír Greif, Eudovít Kubičár, Danica Fidriková, and Kralovičová Lenka	
<b>Author Index . . . . .</b>	<b>581</b>



The Istituto di Ricerca per la Protezione Idrogeologica (IRPI), of the Italian Consiglio Nazionale delle Ricerche (CNR), designs and executes research, technical and development activities in the vast and variegated field of natural hazards, vulnerability assessment and geo-



risk mitigation. We study all geo-hydrological hazards, including floods, landslides, erosion processes, subsidence, droughts, and hazards in coastal and mountain areas. We investigate the availability and quality of water, the exploitation of geo-resources, and the disposal of wastes. We research the expected impact of climatic and environmental changes on geo-hazards and geo-resources, and we contribute to the design of sustainable adaptation strategies. Our outreach activities contribute to educate and inform on geo-hazards and their consequences in Italy.

We conduct our research and technical activities at various geographical and temporal scales, and in different physiographic and climatic regions, in Italy, in Europe, and in the World. Our scientific objective is the production of new knowledge about potentially dangerous natural phenomena, and their interactions with the natural and the human environment. We develop products, services, technologies and tools for the advanced, timely and accurate detection and monitoring of geo-hazards, for the assessment of geo-risks, and for the design and the implementation of sustainable strategies for risk reduction and adaptation. We are 100 dedicated scientists, technicians and administrative staff operating in five centres located in Perugia (headquarter), Bari, Cosenza, Padova and Torino. Our network of labs and expertizes is a recognized Centre of Competence on geo-hydrological hazards and risks for the Italian Civil Protection Department, an Office of the Prime Minister.



---

# Engineering Geology in Shaping and Preserving the Historic Urban Landscapes and Cultural Heritage: Achievements in UNESCO World Heritage Sites

1

Claudio Margottini

---

## Abstract

Cultural heritage represents the legacy of human being to the planet earth. It is the evidence of 1,000 years of past generation evolution, to adapt our living condition to environment. Cultural heritage can be intangible (e.g. tradition, custom) and tangible, the latter including various physical objects, from historic landscapes and human transformed landscapes to sacred sites, archaeological sites, monumental sculpture, monumental painting, architecture and town planning. The above sites and remains are clearly not in equilibrium with environment. They are continuously impacted and weathered by several internal and external factors, both natural and human, with rapid and slow onset. Natural hazards are a clear example of such factors as well as long term weathering decay of rocks, until the effect of climate change, without disregarding the role of men, especially in war areas. In this context, an essential role on conservation and management of cultural properties has been identified by engineering geology and earth science in general. This approach was not very evident in the past, and now more attention to the integration of different sciences is demanded. Indeed, it is possible to affirm that the protection of the cultural heritage represents an interdisciplinary process (and not multi-disciplinary) at the border-line among art, history, science, policies for management and exploitation. In recent decades, many significant sites of cultural heritage have suffered damage, occasionally irreversible, from natural processes. This paper is presenting some case studies developed by United Nations Educational, Scientific and Cultural Organization (UNESCO) to protect and maintain important cultural heritage sites and historic urban landscapes, mainly in Country of the world recently involved in military conflicts or requiring international assistance and cooperation due to the dimension of the disaster or the relevance of threatened monument.

---

## Keywords

Engineering geology • Cultural heritage • Historic urban landscape • Diagnosis • Conservation

---

## 1.1 Introduction: The Beginning of Human Era

During almost the whole of human history, since at least 3 million years ago, mankind has lived by carrying out the two basic activities of hunting (or fishing) and gathering edible items of any kind (from fruit to insects). We are unusual among animals in combining the two functions, and we have been greatly helped in both by the development of language. But basically, as hunter-gatherers, we have lived by doing what comes naturally.

---

C. Margottini (✉)  
ISPRA—Geological Survey of Italy, Via Vitaliano Brancati 60,  
00144 Rome, Italy  
e-mail: claudio.margottini@gmail.com

A radical change came roughly 10,000 years ago, after the last glacial age, when people first learned how to cultivate crops and to domesticate animals, what can certainly be considered the most significant development in human history. This process takes place during the Stone Age, for tools are still made of flint rather than metal, but it is a dividing line, which separates the old Stone Age (Paleolithic) from the new Stone Age (Neolithic). It has been rightly called the Neolithic Revolution.

Part of the reason for this development are linked to the end of the most recent cold phase of the last ice age ( $22 \pm$  Kyears, cal. B.P.) This created new temperate regions, in which humans could live comfortably, especially after the de-glaciation which ended in the Holocene climatic optimum ( $8.5 \pm$  Kyears, cal. B.P) (Margottini and Vai 2004).

It is not hard to imagine, in these circumstances, a strong human impulse to abandon the hunt of wild animals and to settle, instead, in regions where edible plants were growing in sufficient quantity to be worth cultivating and protecting (by weeding around them, for example). Some human groups adapt to a new way of life, although the adaptation was quite slow.

If the impulse was to settle, there was also a strong incentive to ensure that animals remained nearby as a supply of food. This would support attempts to herd them, to pen them in enclosures, or to entice them near the settlement by laying out fodder.

Beginning with the Age of Agriculture, however, humans began to prosper, and population began to grow intensely (one of the basic realities of ecology is that when any organism has excess food and available habitat, its numbers increase). Farming produced a lot more food than had ever been available in the past, and population grew in response. More people then needed more food, so production was increased, allowing population to grow even further.

From an anthropological perspective, the convergence of agriculture, a settled existence, and population growth brings a number of significant changes that we identify with the emergence of human civilization.

One of the first changes concerned the process of planning, designing and construction of structures for human settlements. Architectural works, in the material form of buildings, are often perceived as cultural symbols and as work of art. Historical civilizations are often identified with their surviving architectural achievements.

Nevertheless, architectural works are not related to construction only. They represent the synthesis of a complex system that, in the different historical ages, is guided by the genius of human beings, but it depends from availability and types of construction materials (natural geological resources), it is magnified by the available social and economic conditions also in term of morphological conditions (e.g. defensive settlements on top of cliff), it is also influenced by local meteorological conditions (Margottini and Spizzichino 2014).

Before the heavy environmental impact of human growing at world wide level, concentrating population in a limited number of megalopolis, and also introducing construction techniques that are similar all over the planet (Gregotti 2001), most of urban centers were representing the synthesis of the fore-mentioned four elements and, as a consequence, quite often they constitute unique and spectacular urban landscapes, since they harmonize local architecture based on local natural resources in a given historical climate and socio-economic conditions. These ancient towns and villages are part of the concept of Historic Urban Landscape (HUL) promoted by UNESCO (Bandarin and Van Oers 2012).

The following Fig. 1.1 is reporting the conceptual framework for the Historic Urban Landscape as previously described.

In all of the above elements but mainly in availability of natural resources and defensive morphological constrains, earth sciences are playing a fundamental role. Their integration, even if with different weight and importance, demonstrate how geology and geomorphology are the real conditioning sciences in the urban town evolution, before the industrial era, deeply shaping human settlements. Such geologically dependency ended in the twentieth century when steel and reinforced concrete (the liquid stone, according to the definition provided by the famous Italian Architect Pier Luigi Nervi) became a universal building material, together with the new science of construction based on mathematical modeling.

An attempt to classify the geodiversity of historic urban landscapes was recently proposed by Margottini and Spizzichino (2014), showing the relationship between

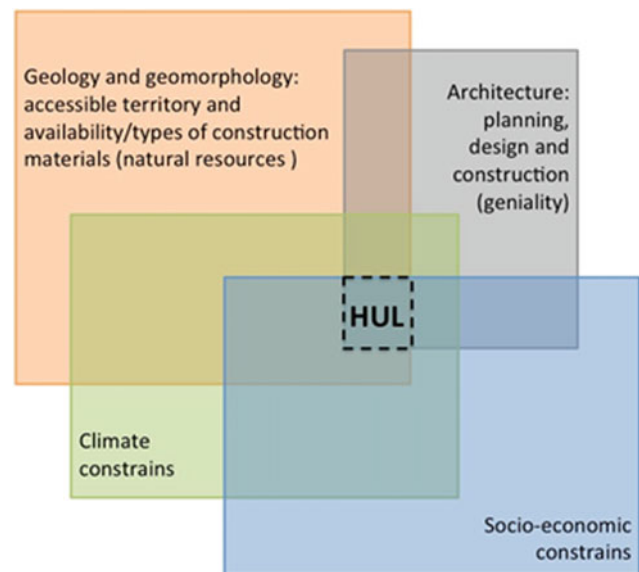


**Fig. 1.1** Conceptual framework for Historic Urban Landscape (HUL) (Margottini and Spizzichino 2014, modified)

**Table 1.1** An attempt to classify the geo-diversity of Historic Urban Landscape (Margottini and Spizzichino 2014)

Clay based urban landscapes		Soft rock-based urban landscapes		Hard rock-based urban landscapes		Complex environment	
Sun-dried bricks buildings	Burnt bricks buildings	Buildings realized with soft rock	Historic settlements directly built up into soft rock	Squared blocks	Rounded natural blocks	Mixed materials	Continuous evolution in time
				Big size	Small size	Small size	

building materials and human settlements (Table 1.1). For major details refer to Margottini and Spizzichino (2014)

In the mean time, ancient towns and villages are experiencing the ageing, which often means the growing of the settlement but also the weathering and degradations of parent materials, as well as the impact of environmental dynamics and hazards on architecture. The latter often associated with the changing of socio-economic conditions, and then of the investments for maintenance.

More in detail, any of the above described genetic factors of HUL, is evolving during the time, requiring mitigation strategies and adaptation policies to new conditions. Natural resources, used in the construction of buildings and monuments, can weather when exposed to exogenic factors; defensive settlements, built up in step morphology, can experience mass movements, in severe climate conditions. Buildings and high rise monuments, on unconsolidated soils, show settlements which may re-occur, after centuries, for a modification of the underground water table. Variability of climate can produce flooding in plain villages originally planned in dry period. The modification of socio-economic conditions can generate a different urban landscape, e.g. for lack on maintenance or for increasing of living conditions, such as with the advent of motor vehicles. The changing of

urban planning perspective, from one dominating Empire to another.

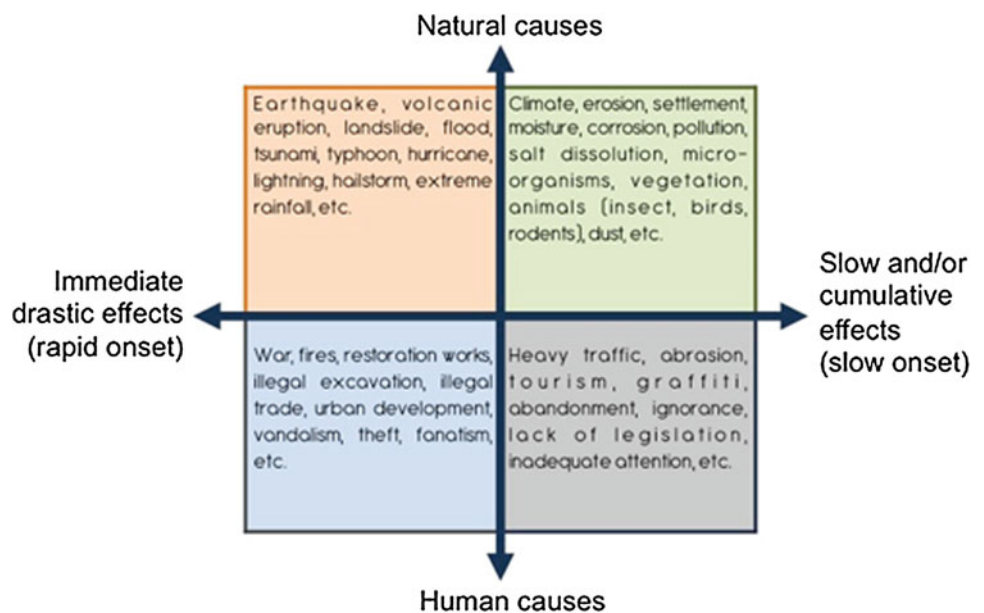
To better understand the threats to Historic Urban Landscape and Cultural Heritage in general, see the following Fig. 1.2 (ICCROM 2006). All the individual threats, with natural and/or human cause, represent the effects of ageing and external hazards that limited the preservation of monuments and sites. In other words, they identify the evolution history of HUL along the time.

As a matter of fact, the modern protection of Historic Urban Landscapes, need to investigate both original genetic factors and their time evolution, in terms of damage phenomena and adopted maintenance/restoration policies.

Clearly, the threats affecting the conservation and preservation of HUL and cultural heritage are also components of the four constitutive elements originating the settlements, but occurring after the construction of them, during their evolution in time (Fig. 1.3).

As a matter of fact, the protection of Historic Urban Landscapes (HUL) and Cultural Heritages (CH) from ageing and external hazards, as above defined, is, in many cases, a border area between Science for Conservation of Cultural Heritages and Engineering Geology. Such assumption is clearly relevant for those threats having a well-defined

**Fig. 1.2** Threats facing Historic Urban Landscape and Cultural Heritage in general (ICCROM 2006, modified)



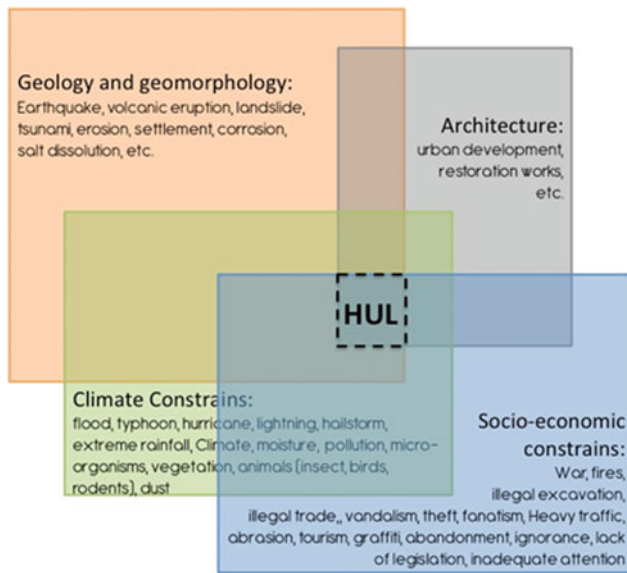


**Fig. 1.3** The threats affecting the conservation of HUL and cultural heritage during time and their relationship to the four constitutive elements originating the settlements

geological and geomorphological origin, but also in others. An ideal method should consider that any conservation policies and management of HUL has to be anticipated by a proper diagnosis of current conditions, based on its evolution, highlighting major critical preservation threats, after having investigated the cultural and scientific origin of settlement.

The science of engineering geology is then playing a major role in the identification of internal causes for material or site deterioration and of external processes acting on the settlement, also considering any appropriate monitoring system. Finally, solutions and mitigations need to fulfill the request of low impact and perfect integration into the archaeological contest.

In the following paragraphs some case studies highlighting the relationship among geology, architecture, climate and socio-economic factors in the development of the Historic Urban Landscape are discussed, together with the experience in conservation. The examples are mainly related to UNESCO World Heritage Sites and have been divided according to the proposed classification of the geo-diversity of Historic Urban Landscape, in Table 1.1 (Margottini and Spizzichino 2014).

## 1.2 Clay Based Urban Landscapes (Sun-Dried Bricks Buildings): The Red Fortress of Shar-e-Zohak (Afghanistan)

### 1.2.1 The Origin

The Shahr-e-Zohak fortress represents the easternmost archaeological remains of the famous UNESCO property of Bamiyan Cultural Landscape. It rises on the top of a hill at the

confluence of the Kalu and the Bamiyan rivers, about 15 km east of the city of Bamiyan and 115 km west-northwest of Kabul. The site is thought to have been founded during the Buddhist period, in the 6th–7th century A.D., but the present fortification remains are dated to the Islamic period and are those that tried in vain to oppose to the advance of the Mongol army, that invaded the region in 1221 A.D. Due to its strategic position, providing excellent measures of natural defence, Shahr-e-Zohak was once the principal fortress protecting the entrance to the city of Bamiyan during the reigns of the Shansabani Kings in the 12th–13th centuries A.D. (Minorsky 1943; Dupree 1977), though archaeological evidence testify the existence of a fort on this site since the times of the White Huns (6th century A.D.). The citadel itself, containing the royal quarters, is placed on the topmost part of the hill, on its southern side, separated from the plateau by a E-W oriented valley and it's protected by three more orders of walls. These defensive walls lay along the southern flank of the small valley and are punctuated by a number of watchtowers used as surveillance posts.

The buildings of Shahr-e-Zohak are made of mud bricks placed on top of stony foundations and covered with mud plaster (Fig. 1.4). Bricks are made of sun-dried red clay resulting from the weathering of the local terrain (Zohak Formation, see next paragraph), consisting of conglomerate and marl. Stones used for the foundations substantially consist of pebble- to cobble-sized rounded clasts of fluvial origin, probably deriving from the local riverbeds.

### 1.2.2 The Evolution During the Time

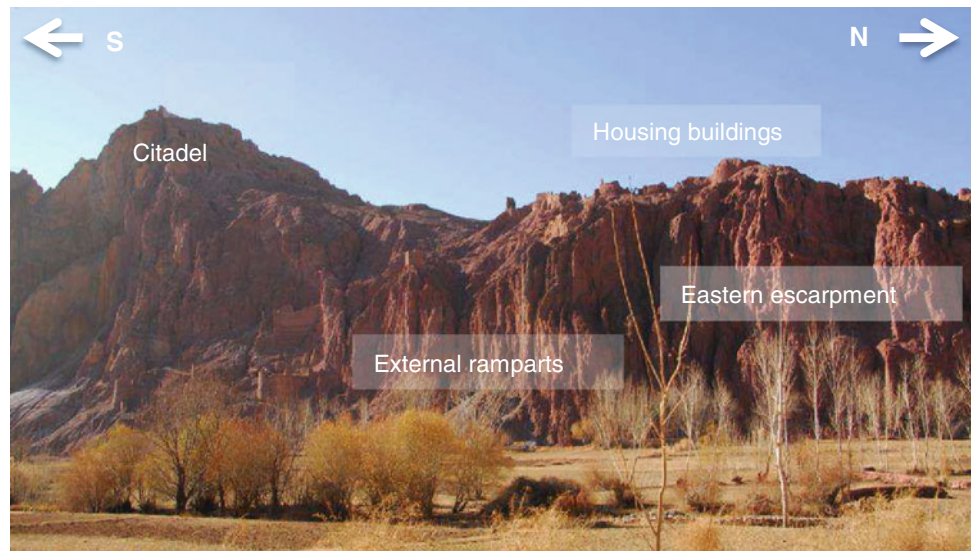
After the Mongol invasion and the subsequent destruction and abandonment, the citadel was never rebuilt and only the extremely dry climate of the region preserved the mud walls from a total ruin.

Nevertheless, a major damage is now recorded to the archaeological site, due to the internal weathering of mud brick and to geomorphological processes acting on the cliff. Both these phenomena are acting from very long time as consequence of rainfall and snowmelt. Rainfall is relatively low in the region, with average value of 133 m, from available data (Cock 2012). More complex is to estimate the impact of snowmelt but, likely, very severe for the low water release and infiltration into soil and architectural structure.

### 1.2.3 Diagnosis of Current Conditions

The Bamiyan valley is hosted in a wider Tertiary intermountain basin bounded to the south by the Koh-e-Baba Mountains and by the Khwaja-Ghar and Koh-e-San Chaspan Ranges to the north (Lang 1972). The basin has been filled with an about

**Fig. 1.4** General view of Shar-e-Zohak red fortress



1,500 m thick succession of continental deposits. In the area, dominant is the Zohak Formation (Eocene), a more than 1,000 m thick succession of alternating red conglomerate and marl, deposited by huge en-masse flows.

The area is affected by many erosional processes, such as gullies, solifluction, erosional basin, earth flow and rock fall. Such phenomena cause large debris accumulation and alluvial fan at the toe of the escarpment. The geomorphological map of Fig. 1.5 is reporting such processes.

Gully erosion is also producing important water runoff concentration, especially on the external steep sides of the hill; on top of citadel, sometimes gully erosion is directly affecting the monuments and ramparts. As an example, the wall and related cisterns, located in the upper citadel are clearly siphoned from the water coming from the erosional sheets located behind them, at higher elevation, in a more clayey strata (Fig. 1.6).

Mud bricks from the historic architecture are also exposed to rainfall and snow; especially with the latter, during snowmelt, they are affected by weathering due to softening of clay constituting the binding material.

#### 1.2.4 Conservation Strategies and Management

The conservation plan for the Citadel of Shar-e-Zohak require a mitigation plan for soil erosion and water run off. The two process are spatially differentiated since in the upper part, where the material is richer in clay component, there are more soil and sheet erosion; in the lowest-top part of the settlement there are mainly gully erosion while, in the and steep side of the cliff, the gully erosion is extremely amplified and requiring a special attention. According to the

above differentiation there are three main zones on the hill, each one needing a specific strategy of water control and erosion mitigation. Following, from the lowest part of the hill till the top, are the proposed mitigation works, which follow the concept of eco-friendly intervention and low environmental impact.

*Steep side of the hill* the energy of water is very high and the gullies are often vertical, especially in Eastern escarpment. Reduction of water is the main measure, to achieve with a new open water channel along the main access path and diverting the flows on top of citadel from the very eroded Eastern flank to the Western one. Construction of some stone check dams, where the velocity of water if very high and erosion very relevant. Original inhabitants already implemented stone check dams and this technique is quite easy to manage from local workers and perfectly integrated in the archaeological context.

*Lowest-top part of the citadel* in this area there is the need to diversify the water runoff and limiting speed velocity. According to specific design, a series of check dams has been proposed. They are made of stone and wood where the discharge is higher and only wood where the amount of water and channel section is limited. A channel diverting from free water Eastern flank to Western was already discussed.

*Upper part of citadel* this area is more clayey and sheet erosion and earth flow are prevailing. It is expected to limit the erosion with a series of wooden buried fence and shrub planting, likely in agreement with local people and realizing a special shrub nursery. Wooden check dams are also expected in the small channels.

The following Fig. 1.7 is reporting the synthesis of planned eco-friendly intervention.

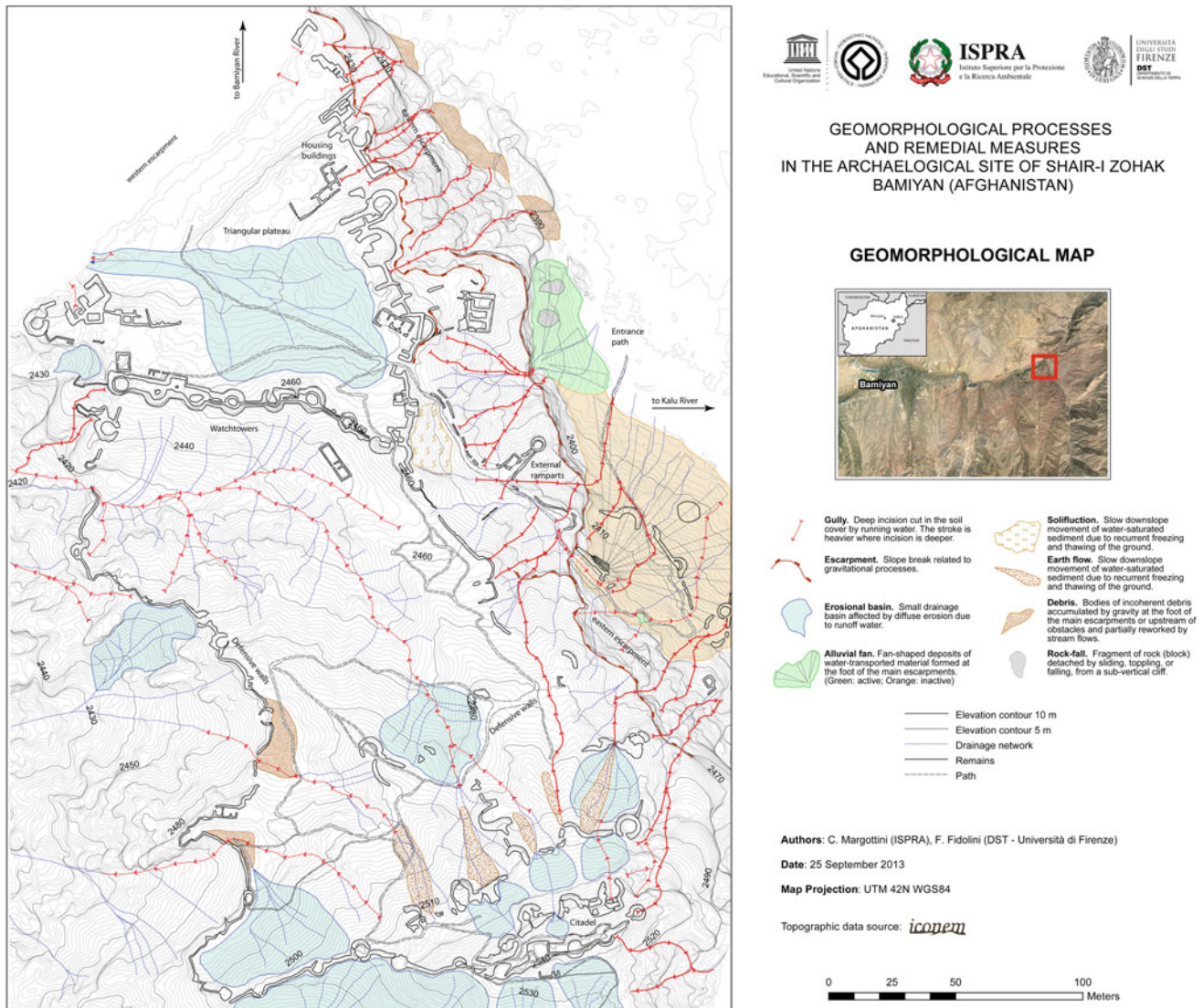


**Fig. 1.5** Geomorphological map of the Zohak site (Margottini et al. 2014)

### 1.3 Clay Based Urban Landscapes (Burnt Bricks Buildings): The Minaret of Jam (Afghanistan)

#### 1.3.1 The Origin

The Minaret of Jam is a UNESCO World Heritage Site in the Shahrak district of Ghur province, western Afghanistan. It stands by the Hari river, in a narrow rocky valley flanked by mountains that rise up to 2,400 m. The monument is 65 m high and is built entirely of fired bricks. It is famous for its intricate brick, stucco and glazed tile decoration, which consists of alternating bands of geometric patterns and Kufic and Nashki calligraphy of verses from the Qur'an. It is not clear from where the bricks were obtained but, not far

from Jam, in the area of heart, along the Hari Rud river there are still many furnaces producing good quality materials. The minaret was probably built between 1163 and 1203, and it is the only remains of an important town of the Gurid period. The town was likely destroyed by Genghis Kan and the remains buried by following floodings (Bruno and Margottini 2011).

The following Fig. 1.8 is giving a general view of the Hari Rud and Jam Rud valley.

#### 1.3.2 The Evolution During the Time

The minaret, that is 65 m high, is presently leaning 3.4°, producing a top displacement of 3.35 m.

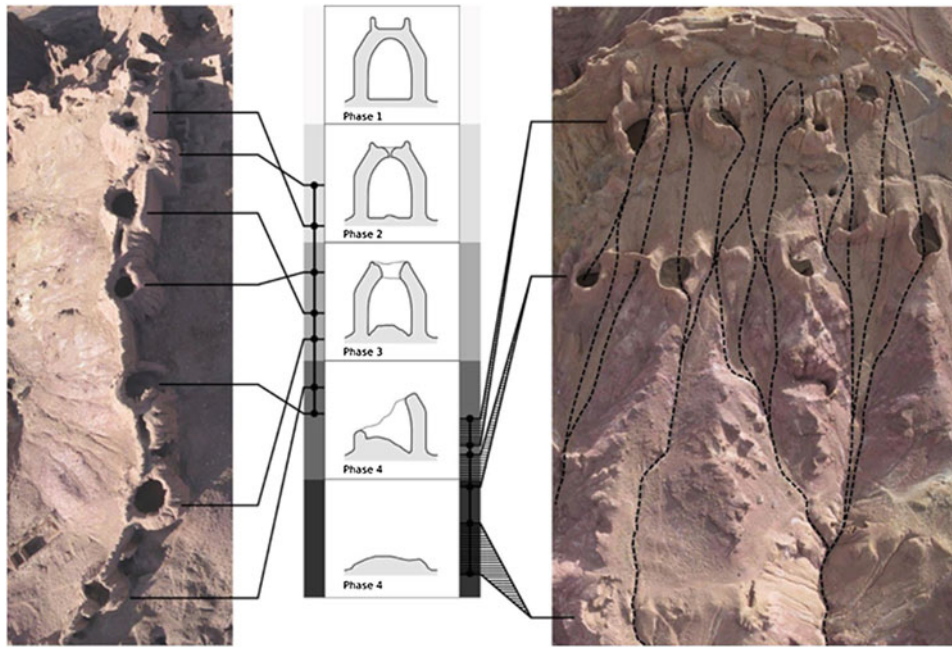


**Fig. 1.6** Different recognized phases in the dismantling of wall and cisterns in the upper citadel (Courtesy of ICONEM, France)

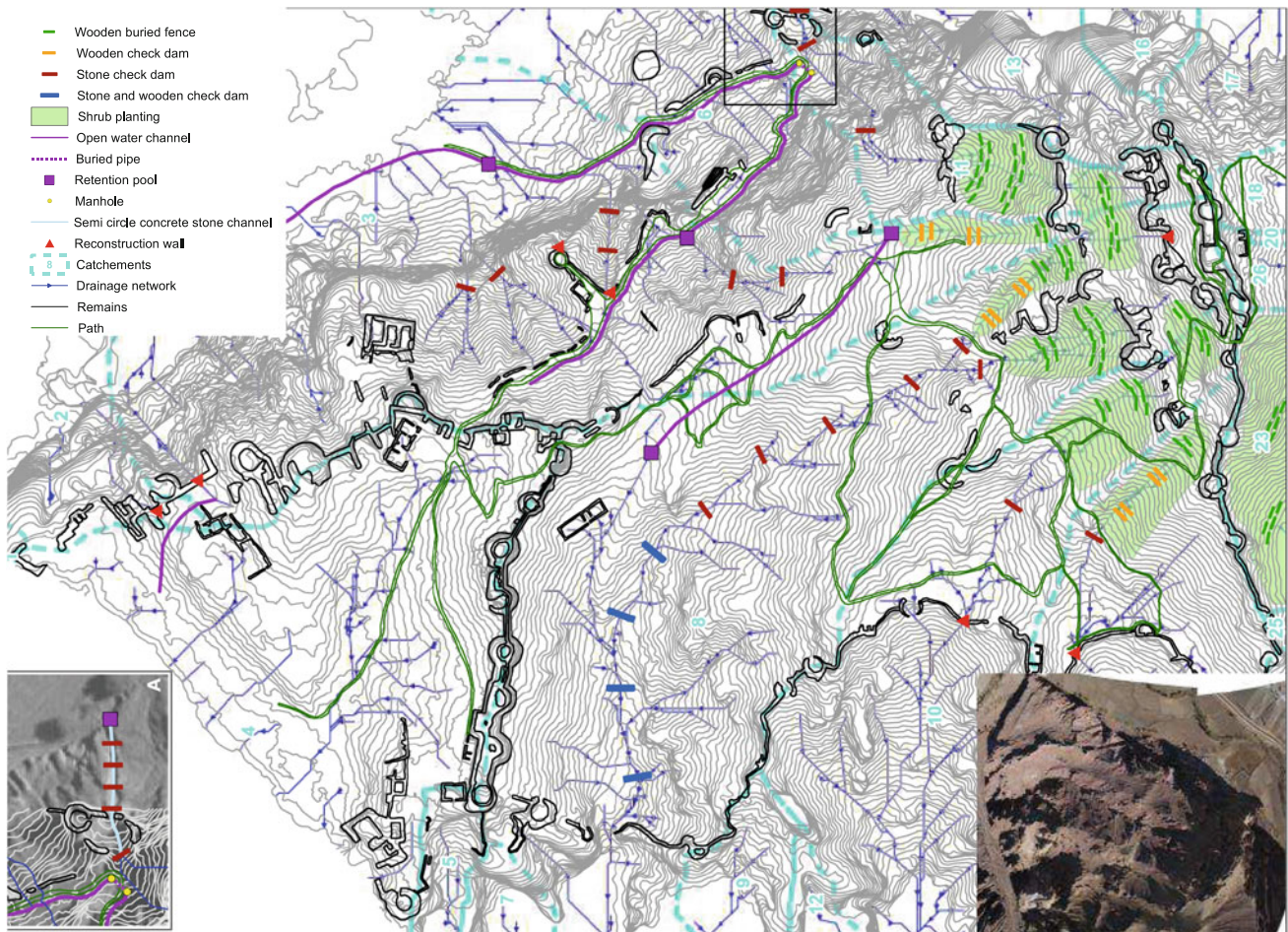


**Fig. 1.7** Eco-friendly intervention for soil erosion and water control in Shar-e-Zohak (Margottini et al. 2014)



**Fig. 1.8** The Hari Rud and Jam Rud valley with the remain of the minaret of Jam and the floodplain where the city were built, now covered by 3–4 m of alluvial deposits. Some of the settlements were also in the cliff

The minaret was clearly affected by a severe flooding, since the level entrance is about 2.80 m below present day topographic surface, originated by the accumulation of alluvial deposit. Also the minaret, in its recent history, was most likely affected by embankment erosion and under-excavation of the Hari Rud river (Fig. 1.9). Water table rising during flood periods and embankment erosion probably also produced a reduction of bearing capacity in limited period of time. Finally, seismic activity probably also contributed to the present endanger situation.

### 1.3.3 Diagnosis of Current Conditions

The minaret of Jam is located in a narrow valley, at the confluence of two rivers: the Hari Rud with the Jam Rud. The local geology (Bruno and Margottini 2011) is strongly affected by mountain environment, with a bedrock covered by coarse alluvial and slope talus deposits. In detail, the bedrock is composed by massive granite/granodiorite, covered by few orders of alluvial deposit; the flanks of the valley are covered by debris cone/talus slope materials. The



**Fig. 1.9** The embankment in 1963, 1986 and 1999, showing the river Hari Rud quite close to the minaret

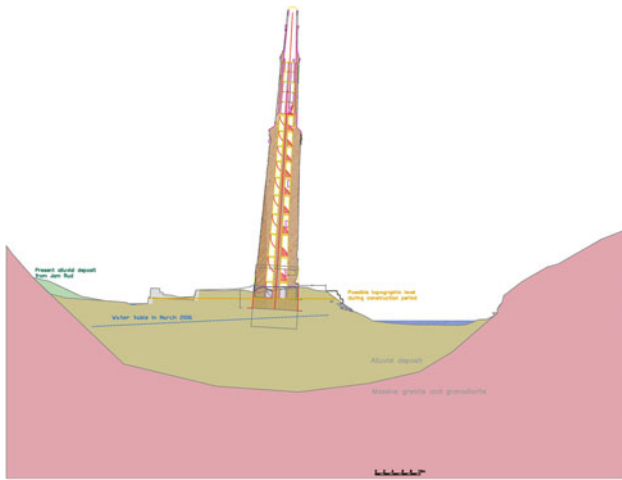


**Fig. 1.10** Geological section through the valley

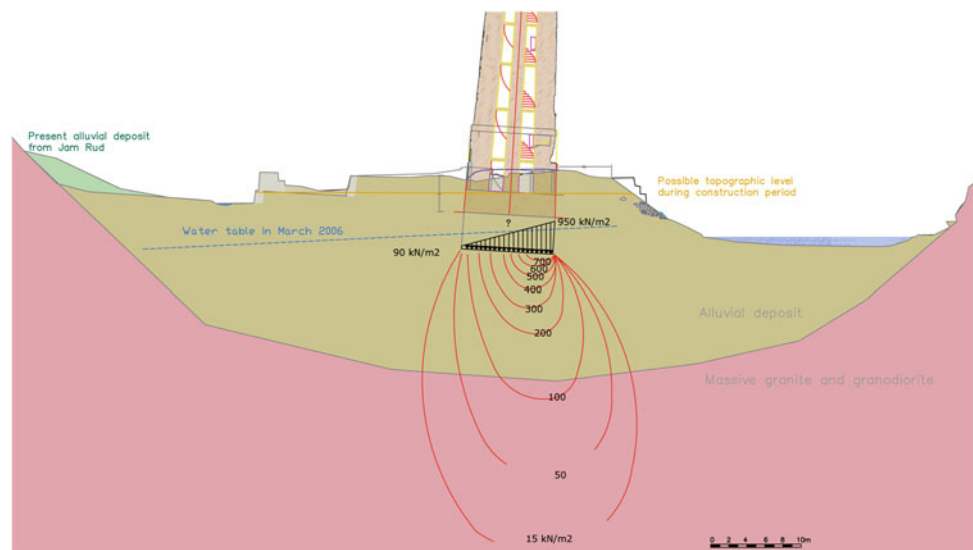
joint interpretation of vertical electrical sounding and the seismic refraction data gives a good correlation on the depth of the bedrock that seem to be at about 20–25 m in correspondence of the Minaret (Fig. 1.10).

Geophysical investigations also revealed the presence of possible archaeological remains of the ancient town of Jam, covered under a few meters of alluvial deposits.

The minaret is presently leaning  $3.4^\circ$ , producing a top displacement of 3.35 m. The total axial load of the structure is 32,630 kN; the foundation is now changing its original gravity load distribution, from an average load of 415–90 kN/m<sup>2</sup> in tensile border and 950 kN/m<sup>2</sup> in the compressive one, Menon et al. (2004). The foundation it is not very clear, in depth, extent and composition.

Due to the inclination, the center of gravity of the tower is presently just at the border of foundation (Fig. 1.11). The total gravity load was originally far away from the ultimate

**Fig. 1.11** Distribution of structure overload in the soil, after the inclination



bearing capacity of the soil, for the geological information available. Moreover, in particular conditions such as flooding period and/or erosion of the embankment, the allowable conditions are quite close to the ultimate ones. Also, the high leaning of the structure is concentrating the gravity load to the border of the minaret, thus very much reducing the factor of safety of net bearing capacity from the ultimate.

As consequence of the above it is possible to say that the minaret is in endangered situation with potential risk of collapse in case of severe flooding and embankment erosion or even in case of earthquake activity.

### 1.3.4 Conservation Strategies and Management

In order to develop a long term conservation plan for such a unique and endangered Cultural Heritage of Afghanistan and with the coordination of UNESCO, a proper seismic, geological, geomorphological, geotechnical and geophysical investigation were performed in 2003–2005 (Bruno and Margottini 2011), revealing important features about soil stratigraphy and foundation typology. Also some initial restoration works were performed in the period 2005–2009, to reduce the structural degradation on the minaret. Also, it is worthwhile to mention the important flooding of April 2007, destroying the 20 years river protection gabions, leaving the water very close to the minaret foundations and then requiring an emergency intervention. Such intervention was planned and executed in this remote area of Afghanistan, after having investigated the main hydrologic and hydraulic features of the area (Beta Studio 2007). It is sufficiently reasonable to say that the leaning of the minaret is related to the reduction of bearing capacity due to embankment erosion during heavy flooding. The work was conducted with local expertise and workers, without being able to visit the



**Fig. 1.12** The emergency restoration work of Jam embankment after the destruction caused by a flooding in 2007

site for security reasons. The following Fig. 1.12 is reporting the final result of emergency intervention.

## 1.4 Historic Urban Landscapes Made up of Soft Rock (Buildings Realized with Soft Rock): Orvieto (Italy)

### 1.4.1 The Origin

Orvieto is a major historic town in Central Italy, endowed with an inestimable artistic heritage dating back to the Etruscan period. The ancient town was built on the top of an elliptical slab (1,500 m 700 m) composed by a soft pyroclastic rock (tuff), delimited by vertical cliffs up to 60 m high, which is formed by the “Orvieto and Bagnoregio Tuff”, a soft rock formation erupted by a centre of the Bolsena volcanic district about 330,000 years BP and overlying overconsolidated

marine clay (Cencetti et al. 2005). The site of this settlement (etruscan period 8–9th centuries B.C.) has in fact been identified with the Etruscan center of *Velzna* (Volsinii in Latin), a city which began to flourish in the beginning of the 6th century B.C. This economic prosperity was based mainly upon the production of ceramics and on bronze work. From a political point of view, *Velzna* was in the forefront of the struggle against Roman expansionism, as a result of which in 254 B.C., having been occupied by the enemy armies, it was razed to the ground. After the destruction the town was periodically inhabited by some “Barbarians” troops, in the way to Rome. Only in the 11th century Orvieto became a Comune or City-State and in 1860 was annexed to the Italian Kingdom, which later became the Italian Republic.

The peculiar geology of the cliff the town is built on that allowed the inhabitants to excavate the caves that cross and overlap one another under the urban fabric, over the course of Orvieto’s 3,000 years of history. These can be read in close connection with the history above ground, because of the indispensable and complementary services that the underground city assured to the city on the surface. The history of Orvieto dates since approximately 3,000 years, during which different events have happened, peoples and dominations have followed, the city grew spreading and stratifying, changing the allocation of sites and modifying the morphology of the landscape. The present Urban Landscape is the final results of all these events, showing how the history of the town in strictly connected and linked to its geological setting (Fig. 1.13).

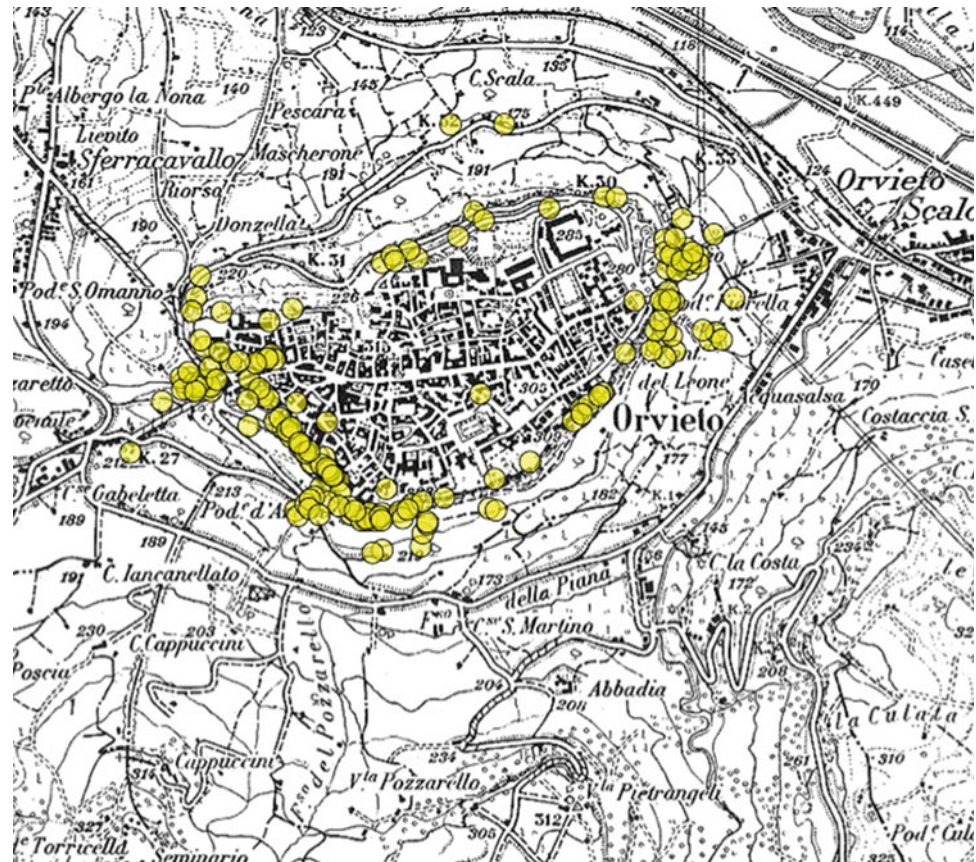
### 1.4.2 The Evolution During the Time

The Orvieto’s ancient hilly rests on a tuffaceous slab that overlies an overconsolidated clayey stratum, where numerous landslides systematically occur. The clay stratum has been affected, since prehistoric times, by failures and more



**Fig. 1.13** The settlements of Orvieto, composed by a soft pyroclastic rock overlying low plasticity and over-consolidated marine clay

**Fig. 1.14** Historical landslides in Orvieto in the period 1139–1986 A.D.



or less slow movements that have left scarps and terraces still having a sharp relief and large extension.

A widespread historical investigation was developed for the settlement, collecting as much as possible of available information in local and central libraries and archives. The result is a data set of 197 individual rock fall and mass movements for Orvieto since 1139 A.D. (Fig. 1.14), which clearly overlap with the main geomorphological features of the areas, developed with traditional field survey investigation (Martini and Margottini 1999).

The Orvieto case differs only marginally from other towns of the same region (Bardano, Rocca Ripesena, Rocca Sberna, Civita di Bagnoregio) which developed in similar morphological conditions and, as a consequence, currently show similar instability phenomena. Orvieto was included in the list of towns to be consolidated entirely with State funds by Royal Decree no. 1067 of 4 March 1937. Since that date and up to the present, a number of works have been carried out for the consolidation and stabilization of the Rock, which have made it possible to protect and preserve it. In particular, the worsening of the instability processes led to the passing of a national law (230/78 and subsequent amendments) for urgent consolidation works on the Rock to protect its historic-artistic heritage.

### 1.4.3 Diagnosis of Current Conditions

The general picture of the instability of the Hill and Rock of Orvieto (Cencetti et al. 2005) is closely connected with the lithological characteristics of the two morphological entities (clay hill and soft pyroclastic rock). Along the slopes of the hill, which are made up of basal clays covered by an extensive layers of detritus, landslide movements result from rotational and translational slides, which can involve the rock type. A typical example of this kind is the Porta Cassia landslide, which was first reported in 1904 and covers an area of about 2.5 ha, with a sliding surface depth varying from 3–4 m up to 10–11 m. The main cause of these landslides is to be found in the saturation processes of the detritus layers or of the most superficial parts of the basal clays. This saturation is connected with the presence of the water table described earlier.

Along the perimeter of the tuffaceous plate, however, the rock failure mechanisms are many and can be traced to: the lowering of blocks along the upper edge, falls or toppling of blocks in the middle-upper part, and the basal fracturing of prisms of various sizes (Cencetti et al. 2005).

The rock failure mechanisms of the Rock are closely connected with the fracturing of the tuffaceous mass, very

evident along all of its perimeter, which is the result of the cooling stages of the high-temperature pyroclastic flow.

The instability processes are due to the different deformability of the plate compared to the underlying clays, to the high state of stress at the foot of the tuffaceous wall, and to the alteration of the mechanical characteristics of the rock types due mostly to atmospheric agents.

Added to these causes are anthropic activities, linked to the millenary presence of man, who exploited the tuff of the Rock for use as a building material. Also significant are the concessions issued by the local authorities for the extracting of pozzolana from inside the Rock, resulting in the excavating of the caves which characterize subterranean Orvieto today.

#### 1.4.4 Conservation Strategies and Management

Only in 1977, following two major landslides, which affected Orvieto's tuff rock (1972 and 1977), the Italian Government, Regione Umbria and local Municipality decided to assume a new cultural position of great responsibility, not only to stop the landslides, but also to plan and implement permanent and long-lasting interventions. In 1977, a geological and technical study was carried out on the entire Orvieto cliff. The study made it clear that the problem of rehabilitating and consolidating the cliff and the inhabited town centre was a multi-disciplinary and global one, and that it went beyond the financial possibilities of a local budget. Thus, following in-depth discussions among the various political groups, Law 25 May 1978 No. 230 was adopted calling for "Urgent actions for the consolidation of the cliff

of Orvieto and hill of Todi to safeguard the landscape and historical, archaeological and artistic heritage of the two towns".

Developed activities, with some examples in Fig. 1.15, included the following (Cencetti et al. 2005):

- the water network, including the conduction network and the reservoir, were completely rebuilt.
- the gullies originating into the rock tuff were entirely diked, reshaped, and partially covered, in order to reduce or eliminate the erosion processes taking place, such as the deepening of the bed and the collecting of unstable material at the sides of the valleys;
- the slopes of the hill were reforested, improvements were made to control the flow of water, and all springs were tapped;
- the edge of the Rock was also reshaped, with the building of walls, impermeabilization works, and the planting of greenery;
- works were also carried out to stabilize the landslides along the slopes of the hill, including the building of support structures, trenches, drainage wells and the morphological rearrangement of the slopes;
- the tuffaceous wall was consolidated following a plan with active anchorages at the foot of the Rock (so as to obtain a partial recompression of the tuff) and passive anchorages located on the upper part of the wall;
- the existent city walls standing on the Rock and built in various historical periods were consolidated and restored for preservation, which involved removing plant growth, cementing and cramping loose stones, replacing deteriorated stones, raising the walls, and building underpinings and buttresses;

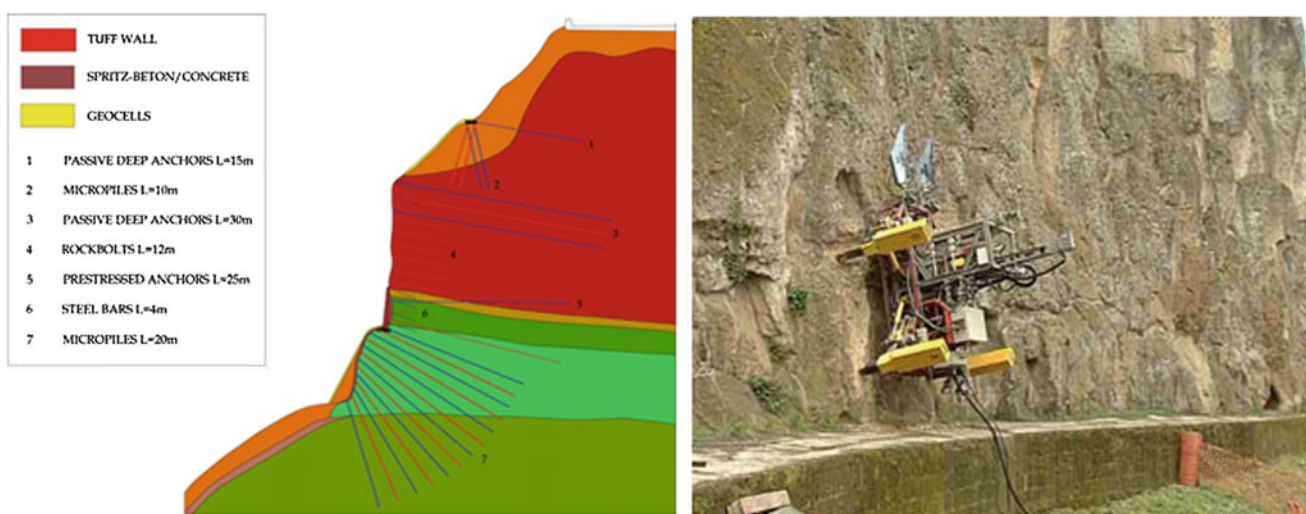


**Fig. 1.15** Typology of consolidation works on the cliff (Soccolato et al. 2013) and automatic robot drilling machine, for anchoring in vertical cliff of Orvieto (Courtesy Endro Martini)

- the numerous artificial caves in the tuffaceous rock were also consolidated, to prevent the roofs from collapsing and the surface from caving in; depending on the historical and archeological importance of the cave, the choice was made whether to simply fill them with mortars of lightened pozzolana mixtures, or to consolidate them with support works, the reinforcing of the walls and cementing, cramping and bracing. Some of these caves are now open to the public and are one of the most interesting tourist attractions.

In this context, the Observatory for the Permanent Monitoring and Maintenance of the Orvieto Hill was set up by the Regional Government of Umbria. The Observatory is the Regional instrument for the control and management along the time of the territory and of the remediation works.

## 1.5 Historic Urban Landscapes Made up of Soft Rock (Historic Settlements Directly Built up into Soft Rock): Bamiyan (Afghanistan)

### 1.5.1 The Origin

In the great valley of Bamiyan, 200 km northwest of Kabul, central Afghanistan, two huge standing Buddha statues were carved out of in situ sedimentary, at an altitude of 2,500 m. The Emperor Kanishka probably ordered the sculpturing of the smaller Buddha around the 4th century A.D., while initiation of the great Buddha seems to date from the 5th century A.D. Some descendants of Greek artists who went to Afghanistan with Alexander the Great started the sculpturing, which lasted until the 6th century A.D.

Together with the Statues, the rupestrial settlement of Bamiyan was growing, with more than 800 individual caves and temple (Figs. 1.16, 1.17). It was one of the major religious centre on the Southern branch of the silk road.

The outcropping rocks in the area are mainly conglomerate, with some strata of siltstone that largely slake when wet. The lower part of the cliff is predominantly siltstone, with two main set of discontinuities spaced every 20–40 cm. The central part of the cliff is mainly conglomerate, well cemented and with a limited number of vertical discontinuities mainly paralleling the profile of the slope.

Caves and Statues were carved inside these materials, taking also benefit from the some large de-tensioning cracks, almost vertical and parallel to the slope. Back wall of the Statues is exactly one of these large cracks.

In the valley, due to the presence of alluvial clay, adobe houses made of sundried brick and straw were also realized.

### 1.5.2 The Evolution During the Time

The cliff is affected by many geomorphological processes which include (Margottini 2014): water infiltration, gully erosion, progressive opening of discontinuities in the outer parts of the cliff, weathering and slaking of siltstone levels, toppling of large external portions as well isolated blocks along the cliff face, occurrence of mud flows probably when the siltstone is saturated, sliding of a large portion of the slope, accumulation of debris at the toe (Fig. 1.18).

### 1.5.3 Diagnosis of Current Conditions

Under the worldwide astonishment, the two statues were demolished on March 2001 by the Taliban, using mortars, dynamite, anti-aircraft weapons and rockets. The Buddhists as well as the world community, UN and UNESCO failed to convince the Taliban to avoid the destruction of this cultural heritage. Nevertheless, since 2002 UNESCO is coordinating a large international effort for the protection of the World

**Fig. 1.16** The cultural landscape of the Bamiyan valley, with the empty Western Giant Buddha niche, cavities on the cliff and adobe in the floodplain



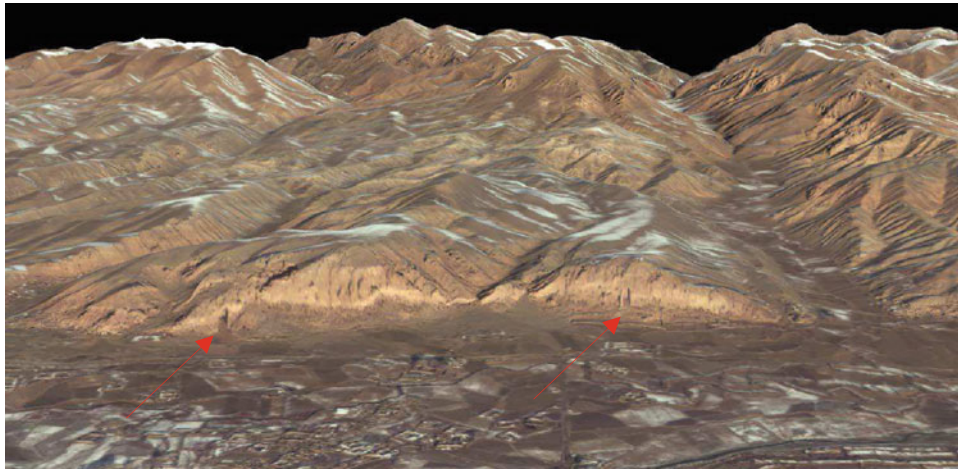


**Fig. 1.17** The 3D Bamiyan terrain model textured with colour IKONOS ortho-image and the Western (*left*) and Eastern (*right*) niches, from Gruen et al. (2004)

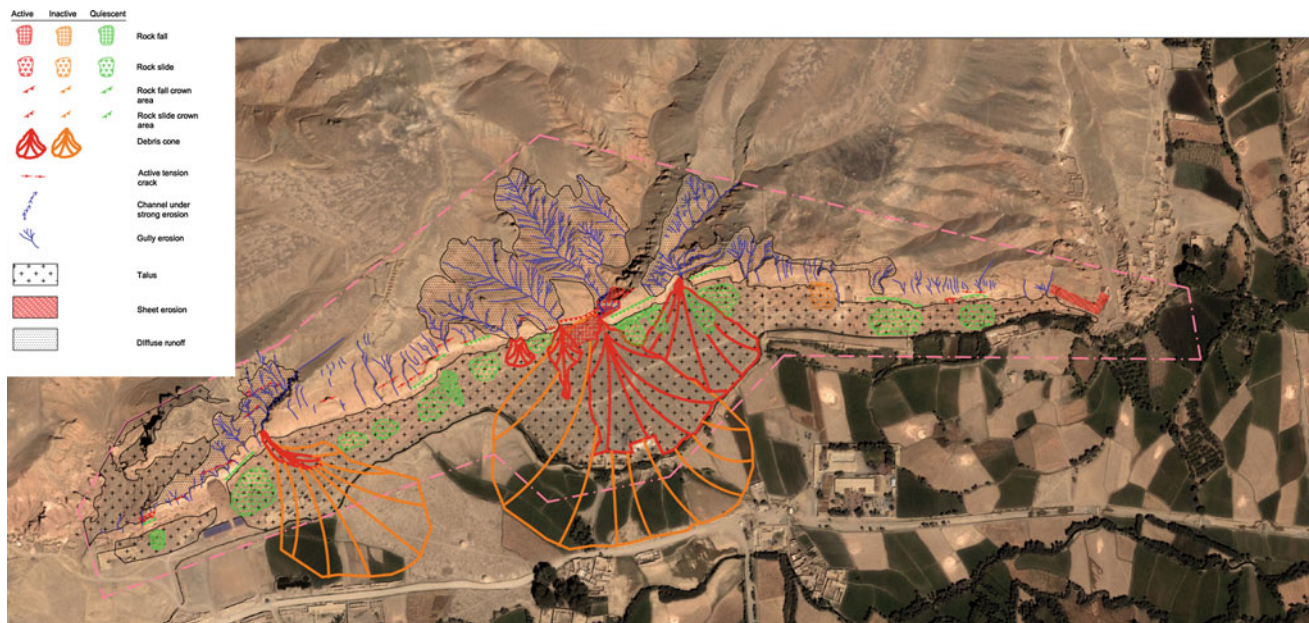


**Fig. 1.18** Geomorphological map of the Bamiyan cliff (Margottini 2014)

Heritage Site of Bamiyan and the future development of the area.

The explosion of March 2001 (Fig. 1.19), as well as demolishing the statues, reduced the stability of the slope, mainly in the outer parts of the niches.

#### 1.5.4 Conservation Strategies and Management

In order to develop an emergency consolidation of both niches after the Taliban destruction, the following survey and activities were performed on the site (Margottini 2014):

- the inventory of geological and geomorphological feature and existing mass movements;
- the identification of predisposing factors to slope instability (climatology, petrology, mineralogy, sedimentology, seismology, geophysical properties of rocks, mechanical behaviour of both rock masses (in situ and laboratory) and discontinuities, discontinuities distribution);
- the investigation of potential triggering mechanisms of landslides;
- the kinematic analysis to identify potential failure mechanisms for cliff and niches;
- the numerical stability analysis of cliff and niches, to identify the relationship between shear strength along the potential failure surface and conditions required to trigger the collapse;
- experiences in previous restoration/consolidation works;



**Fig. 1.19** Explosion and destruction of the Western and Eastern Giant Buddha Statues

- a manual crack gauge monitoring system was also installed in the niches, showing no movement in the period September 2003–present. An other manual crack gauge network was also installed along many relevant fractures along the entire cliff;
- Automatic crack gauge monitoring system operating at the time of stabilisation works (November–December 2003 and April–May 2004).

Finally, the field data, kinematic analysis, mathematical modelling, caves and crack distribution and detail inspection of the effect of the explosion allow the preparation of project for the emergency consolidation of both niches.

The stabilisation activities for the outer part of Eastern Buddha niche started in October 2003 till the beginning of December 2003 in the. A second operational phase was implemented in the period April–June 2004 and the final one in the period September–November 2006.

The practical activities included four different steps (Margottini 2014):

- *the installation of a monitoring system*, to evaluate in real time any possible deformation of the cliff. Sensor were designed to monitor the entire working area, connected with an alarm system, to make workers in safe conditions;
- *the realisation of temporary protection* includes steel ropes, and two iron beams suitable to avoid lateral deformation, inside the niche from an unstable cliff and blocks. Among the temporary work, a wire net was installed on the back side of both niches to allow archaeologists to work on the ground floor in safe conditions, just after the consolidation of the niche's wall;
- *the final stabilisation* of the East niche. In these area anchors, nails and grouting were executed (Fig. 1.20), in order to reduce the risk of rock fall and collapse; particular care was addressed to the problem of grouting

material since the very high slaking capability of silt-stone. The anchors placed in 2003 were pre-grouted to avoid any oxidation and then percolation inside the niche. From 2004 it was decide to use only stainless steel materials, even if not pre-grouted.

- *minimization of intervention* (anchor/nail head finishing) complete the execution of work. Anchor and nail heads were designed to be placed slightly inside the rock and then covered by a mortar allowing a total camouflage of the work. A number of tests on the better mixture, between cement, local clay/silt and water, to be used for covering the anchor/bolt heads, were also designed and developed in 2003, in cooperation with ICOMOS experts. The results highlight the better chromatic, stability and robustness of the mixture.

Some minor consolidation and impermeabilisation works were also implemented in the Western Buddha niche in 2006.

Finally, after the stabilisation of the external part of the Eastern Buddha niche, in 2009–2012 the inner back wall (shear zone of explosion) was stabilised by means of small anchors and limited grouting also aimed at fixing the still existing original part of the Statue plaster, jointly executed by Engineering Geologists and Conservators (Fig. 1.21).

## 1.6 Hard Rock-Based Urban Landscapes (Squared Blocks, Big Size): Machu Picchu (Peru)

### 1.6.1 The Origin

The famous archaeological site of Machu Picchu is situated in southeastern Peru, approximately 100 km to the northwest of Cusco. The citadel of Machu Picchu was built on a steep

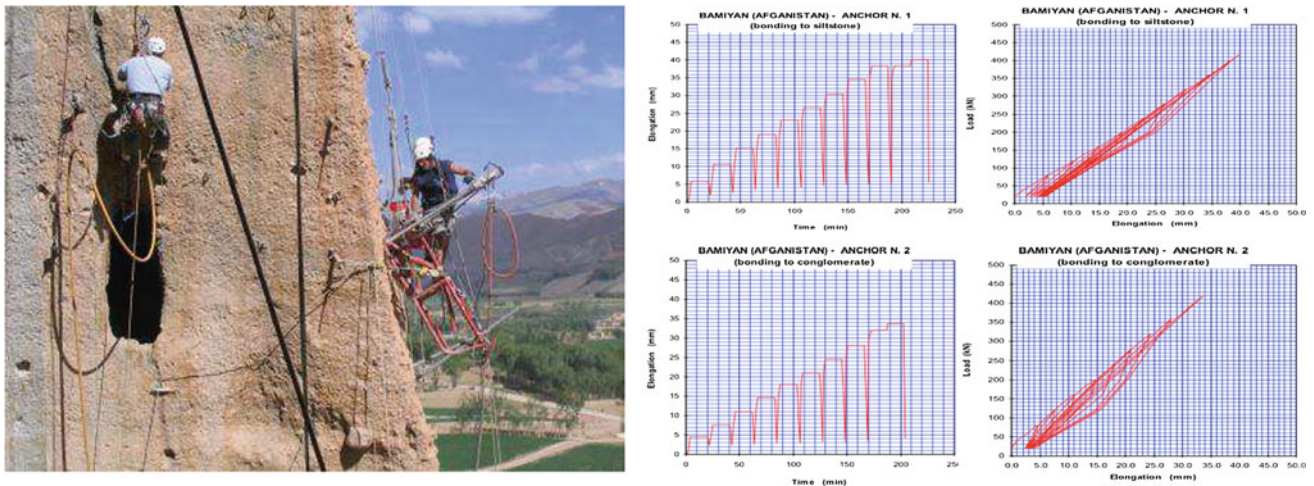
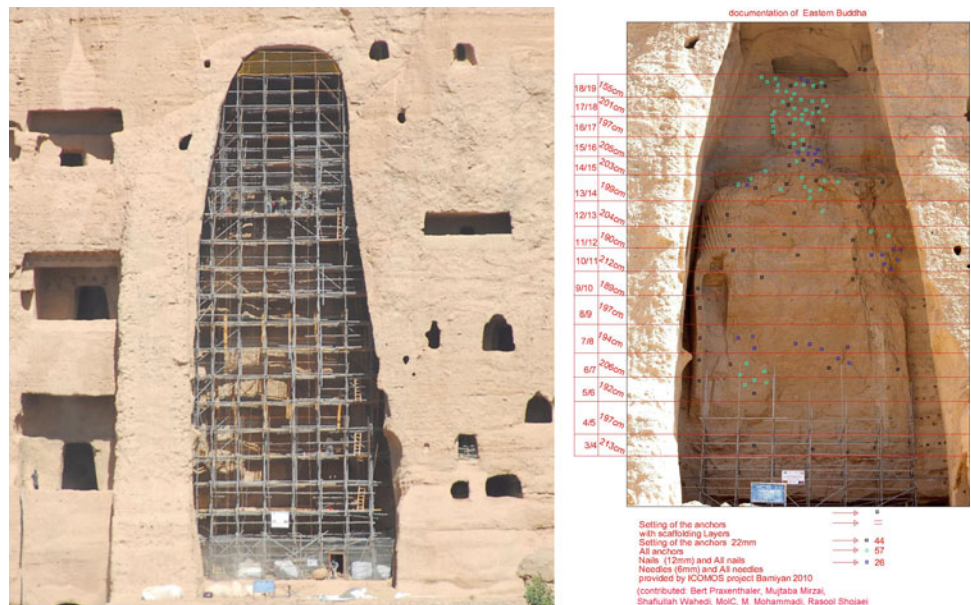


**Fig. 1.20** Anchoring the Eastern Buddha niche (*left*) and anchor suitability tests for siltstone and conglomerate, in 1 m length anchor (*right*). The load (kN) and respective time (min) and elongation (mm)

are reported showing, till 40 t, the uphold of elastic domain and still the missing of any permanent deformation for the tested anchors

**Fig. 1.21** The scaffolding for the stabilisation of back wall shear zone and the position and typology of installed anchors (diam. 22, 12, 6 mm)



ridge, about 500 m above the incised meanders of the Urubamba River (Fig. 1.22).

UNESCO declared Machu Picchu a World Heritage site in 1983. This site was discovered for modern archaeology by Hiram Bingham in 1911, and since then, it has been under continuous scientific study.

Recent study (Margottini et al. 2008) have shown and proved that the final choice of the site for the realization of the magnificent and mysterious city (symbol of the heyday of the Inca empire), is very likely the result between the geomorphologic process affecting the area and human

evolution of the site, taking into consideration the constraints caused by the original landscape to human settlement, in connection with the availability of rock material for building constructions (Fig. 1.23). In other words, the possibility that the site was originally chosen because of the availability of weathered granitic material (easily managed for building construction) is actual one of the main accepted hypothesis. The mentioned material could also be the consequence of palaeo-landslide(s) affecting the area. One of the main inputs to such interpretation came from the recent discovery of a wide potential landslide on which the citadel was probably



**Fig. 1.22** Machu Picchu and the surroundings



**Fig. 1.23** Possible borrowing quarry/paleo landslide deposit of archaeological site of Machu Picchu (*left*) and methodologies for squared hard rock block production (*right*)

built. Depending on the particular topographical and morphological situation, the area was presumably used as a borrowing cave for building construction or as a foundation basement of entire neighborhoods of the city (Fig. 1.24).

### 1.6.2 The Evolution During the Time

Machu Picchu served a permanent population of about 300 with a peak of 1,000 when the Inca emperor was in

residence. When Bingham stumbled upon the ruins of the beautiful Andean Inca community, it had endured nearly intact for over four centuries without suffering from foundation failures or landslide damage (Wright et al. 1997; Bingham 1930). The potential ravages of time, steep mountain slopes, and excessive rainfall were overcome by the exceptional ability of the Inca engineers to construct good building foundations and install effective drainage systems. These two Inca achievements delivered Machu Picchu to the 20th century scientists in a condition nearly as



**Fig. 1.24** Location of the quarry (locally “cantera”) for the production of stones to be used in Machu Picchu construction

it had existed when it was abandoned in the 16th century. It was occupied between 1450 and 1540 A.D., with some people remaining until 1572 A.D. (Rowe 1990).

Since that period, many mass movements occurred all around the site, damaging the andenas and many important buildings (Fig. 1.25). Likely also earthquake contributed to such deterioration.

A historical research on available documentation, both scientific and religious, allow the identification of some events that have affected or potentially hit the site (e.g. earthquake), in the period 1591–1999. In detail, 55 earthquakes within 200 km from the site, 13 mass movements and

12 floodings on the Urubamba river have been identified, giving a picture of the threats affecting the area and the site (Fig. 1.26).

### 1.6.3 Diagnosis of Current Conditions

The geological and geomorphological investigations conducted in the area of Machu Picchu highlight the presence on many slope instabilities (Fig. 1.27), mainly with low depth. Several slope instability phenomena have been identified and classified according to mechanism, material involved

**Fig. 1.25** Machu Picchu at the time of discovery from Hiram Bingham in 1911 (Bingham 1930)



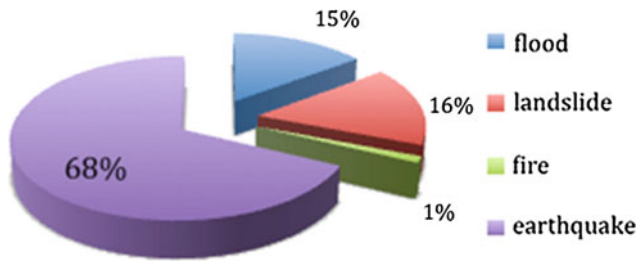


**Fig. 1.26** Extreme events affecting the Machu Picchu region, in the period 1581–1999 (Martini and Paolini 2006)

and state of activity. They are mainly related to rock falls, debris flows, rock slides and debris slides. Origin of phenomena is kinematically controlled by structural asset and relationship with slope face (rock falls, rock slide and debris slides); the so accumulated materials is the source for debris flow.

In the area of the Carretera (access road to Machu Picchu) a precise mapping of debris deposits and past debris flows was carried out, leading to a zonation of processes.

The situation of the slope with the citadel is more complex due to the strong structural control of the master joints on the slope evolution. In this, planar rock slides are mainly affecting the NE flank while rock falls are predominant on SE cliff.

### 1.6.4 Conservation Strategies and Management

A low environmental impact monitoring system has been established on the area having the purpose to minimize equipments usage and, in the mean time, to collect reliable data on surface deformations. The monitoring network comprise a GPS, multitemporal laser scanner survey, Ground based Radar interferometry (GB-SAR) and Satellite Interferometric Synthetic Aperture Radar (InSAR).

The preliminary results are confirming the field evidences of slope deformation but, in the mean time, they require a longer period of observations since the sliding processes are relatively slow (Fig. 1.28).

**Fig. 1.27** Geomorphological map of Machu Picchu area (Canuti et al. 2009)

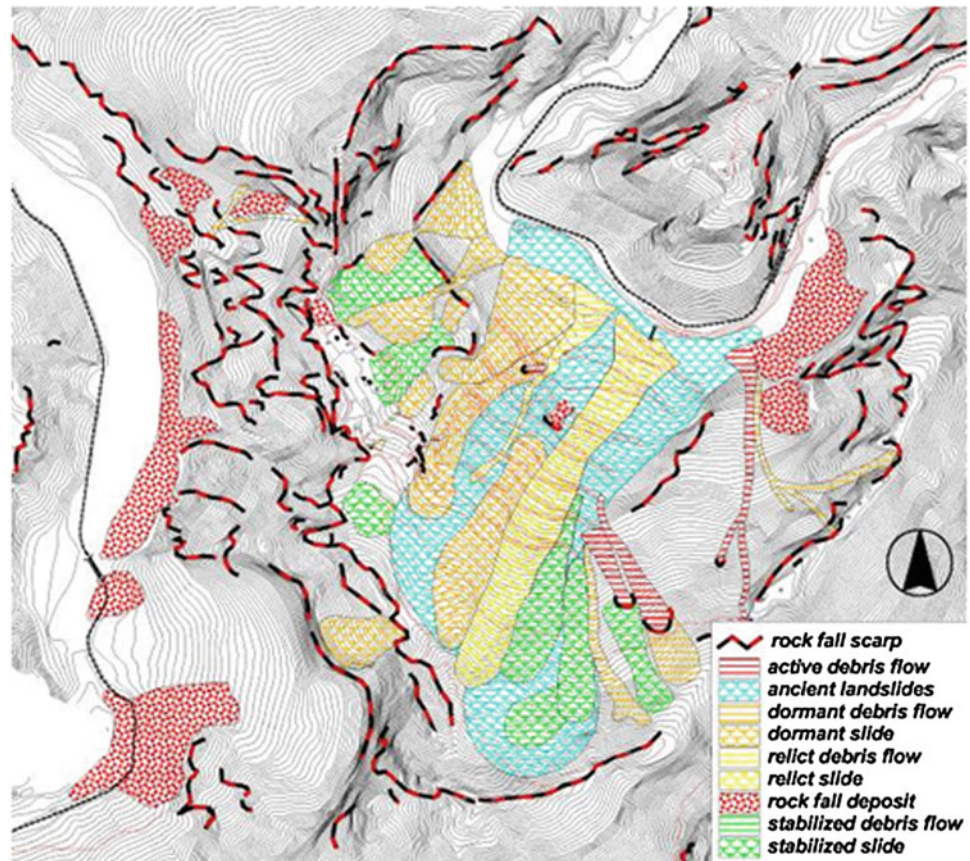
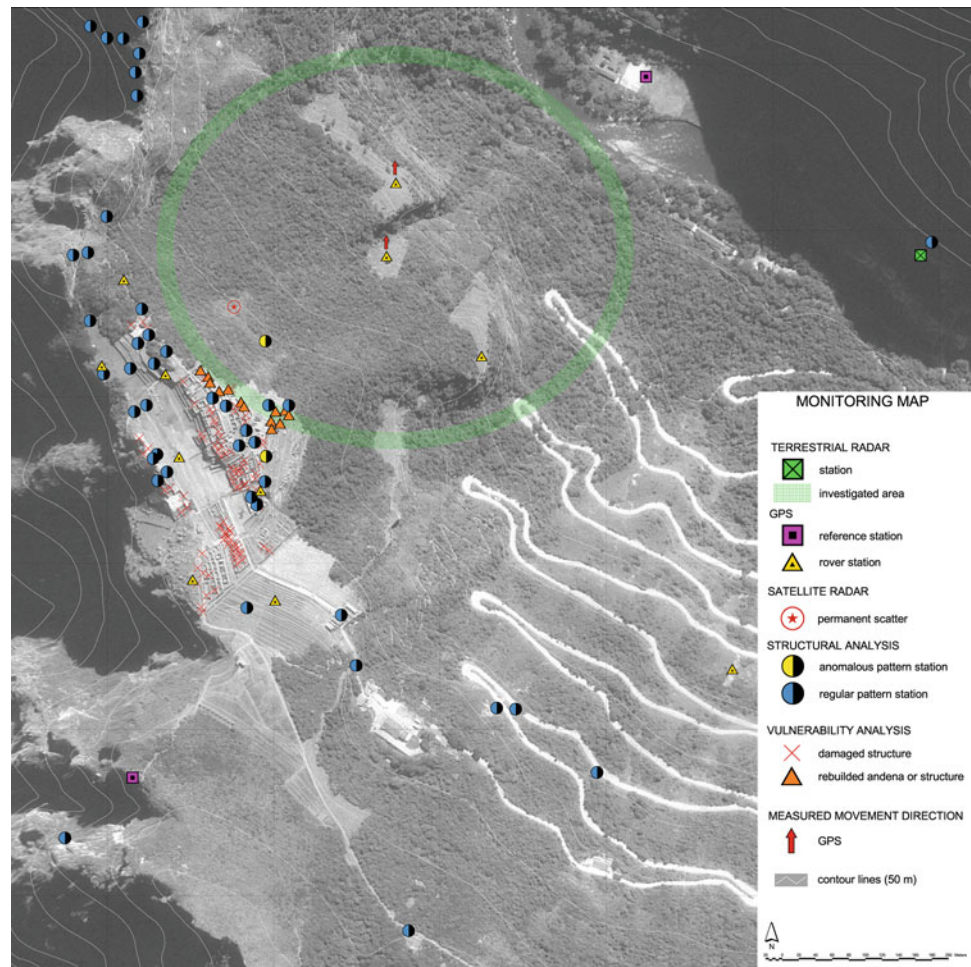


**Fig. 1.28** Integrated map of surface deformation evidences and present monitoring data



## 1.7 Hard Rock-Based Urban Landscapes (Squared Blocks, Small Size): Orongo-Easter Island (Chile)

### 1.7.1 The Origin

The ceremonial village's of Orongo is constituted by 53 stone masonry houses realized thanks to the wide availability of highly fractured basalt rock. More in detail the houses were constructed by means of local stones pleased one over the other, with the shape of a cavity. Rocks are already available and fractured from cooling of volcanic lava available in the surrounded area and do not need to be re-shaped.

The village has been built in about Huri-Moai period (about XVI–XVIII c) (Mulrooney et al. 2009), in the Eastern Island (Orongo village) due to the availability of squared hard rock block in small size, as a consequence of likely rapid cooling of lava flow (Fig. 1.29).

Until the mid-nineteenth century 'Orongo' was the centre of the birdman cult, which hosted an annual race to bring the first manutara (sooty tern) egg from the islet of Motu Nui to

Orongo. The site has numerous petroglyph, mainly of tangata manu (birdmen). Worthwhile is the ceremonial centre of Mata Ngarau. This site is extremely important for Rapa Nui culture due to its unique petroglyphs and dominant view of the surrounding landscape, ocean and motus. Mata Ngarau is located inside the village of Orongo, in one of the most spectacular sites within Rapa Nui National Park, on a narrow plateau between Rano Kau crater and a 250 m cliff to the waters of the Pacific Ocean. The site is composed by individual rock blocks, hanging over 200 m of high slope cliff (Fig. 1.30).

The first half of the ceremonial village's 53 stone masonry houses was investigated and restored in 1974 by American archaeologist William Mulloy. In 1976 Mulloy assisted by Chilean archaeologists Claudio Cristino and Patricia Vargas completed the restoration of the whole complex which was subsequently investigated by Cristino in 1985 and 1995. Orongo enjoys a dramatic location on the crater lip of Rano Kau at the point where a 250 m sea cliff converges with the inner wall of the crater of Rano Kau. Orongo now has world heritage status as part of the Rapa Nui National Park.

**Fig. 1.29** The stone masonry houses of Orongo village



**Fig. 1.30** The ceremonial centre of Mata Ngarau



### 1.7.2 The Evolution During the Time

The flank of Rano Kau caldera is continuously affected by rock mass movements, as consequence of the important discontinuity pattern affecting the lava and steep slope. Energy of the sea waves in the lower part and chemical alteration in the whole surface are also playing an important role. The flank of Rano Kau caldera was been inventoried (starting from May 2003) in the slope flank located below the archaeological site. From a geomorphological point of view, the landslide can be classified as a rock-slide, initially triggered as a rotational slide in the upper crown area. The following Fig. 1.31 is reporting some evidence of recent and historical mass movement along the cliff below the historical urban landscape of Orongo. Remarkable is the landslide of Nov. 2007 which occurred in a very hazardous slope of the caldera. The rock slide, in highly weathered volcanic material, might affect, in future evolution, the conservation of the lake inside the caldera, located at topographic level higher than the sea. The crown area is localised at approx. 100 m a.s.l. The mobilised material, according to a preliminary morphometric analysis, is about 5,000 m<sup>3</sup>.

### 1.7.3 Diagnosis of Current Conditions

Geological, geomorphological, structural analysis, kinematic analysis, rock laboratory investigations and slope stability calculation with FEM have been executed.

Landslide risk assessment and surveys, has highlighted a condition of instability, concerning both the scale of slope of the outer edge of the crater below the village of Orongo, both as regards the area immediately below the ceremonial centre of Mata Ngarau. This instability process is actually in evolution as evidenced by the photos from 2003 until today. Kinematic analysis, seismic passive environmental noise and slope stability analysis has been carried out in order to define failure mechanism, unstable potential blocks and safety factors along the SW cliff. In dry condition the factor of safety value has been calculated equal to 1.05, close the potential unstable condition for the slope. The minimum value for the Safety Factor drops below unity (the simulation has been performed in static condition) under the fully saturated slope condition.

Below the ceremonial centre of Mata Ngarau a specific passive analysis, by means of portable seismometer

**Fig. 1.31** Detected rock slide on the external edge of Ranu Kau volcanic caldera, below the historical urban landscape of Orongo

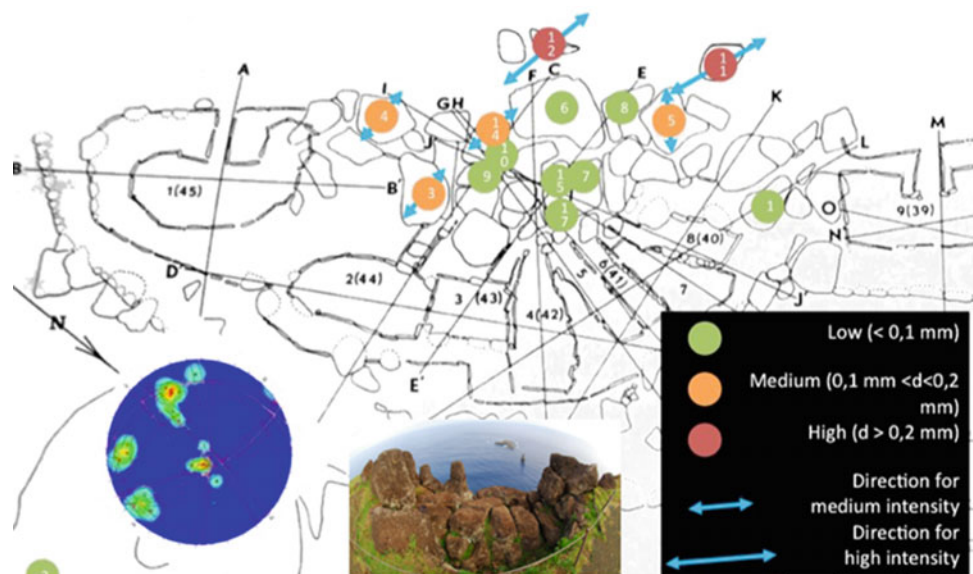


(velocimeter), has been conducted on the individual block constituting the monument (Fig. 1.32). The use of portable seismometer allowed the measurement of environmental noise characteristics for many as possible blocks, compared with bedrock measurements developed outside the site (Margottini 2013). The results show a clear correlation of most unstable blocks with largest intensity of ground motion and versus of it. The analysis was carried out by means of comparing response spectra, horizontal to vertical spectral ratio and intensity/direction of horizontal motion.

In detail:

- major displacement ( $>0.2$  mm) is detected in the blocks prominent to the cliff, looking at the sea (top in the figures), characterised by red colour;
- minor displacement ( $<0.1$  mm, green) is noticed in blocks located in the inner part of the ceremonial altar, suggesting a satisfactory degree of connection among individual blocks;
- horizontal components are almost showing the same direction, for medium and high detected values of motion;

**Fig. 1.32** Plan of Mata Ngaroa ceremonial altar in Rapa Nui (Easter Island, Chile) and intensity/direction of horizontal components of environmental noise. The single measurement have been ranked in three categories of intensity (low, medium and high)



Such techniques demonstrates a remarkable degree of maturity and the possibility to be applied in rock fall prediction. In fact, most critical blocks of the ceremonial altar are those hanging to the 250 m cliff, for which a serious treat could be logically posed. Also the missing of scatter among single data suggest an internal consistency of the experiment.

#### 1.7.4 Conservation Strategies and Management

A preliminary proposal of stabilization, aimed at finding eco-friendly solutions, was developed by Margottini and Spizzichino (2012). The following remedial measures has been foreseen:

Waterproofing of ground surface avoiding infiltration and pore pressure excess:

- Surface water collection and channelling;
- Draining trench for sub-surface water flowing;
- Protection of material potentially prone to slide;
- Metallic net with green re-forestation;
- Strengthening the rock with grouting.

Slope consolidation:

- Scaling of unstable block
- Deep anchor with steel cable on top;
- Stabilisation of unstable individual block.

The philosophy of the entire project is based on the combination of two different approaches, the first aimed at reducing the destabilizing forces (water infiltration elimination and reduction in the unstable soil, avoiding pore

pressure excess), the second aimed to the increase of those resistant (increase resistance at the rock scale mass with, net, grouting, bolts, etc.).

### 1.8 Hard Rock-Based Urban Landscapes (Rounded Natural Blocks)

Compared with the squared rock blocks, the rounded ones have more difficulties in placing on site and need important mortar support. The strength characteristics of the structure, in fact, is definitely poorer, especially under dynamic stress. This type of material has a great spread along all the historic towns and small communities grown along the rivers alluvial deposition areas. In these places, such material could be recovered and used in an effortless and very economical way. It does not require special processing (sizing) and can be put in place both dry (e.g. perimeter walls, simple masonry) and with various types of mortar. Wonderful example is the Aztec historic site of Tiuanacho (Mexico, II c. A.D.), where many volcanic boulder, likely transported by many erosional phenomena, have been used for the construction of the large pyramids (Fig. 1.33). Binding mortar have been also studied by many authors.

Along the time, key hazards suffered by prehispanic populations and buildings in the region included tectonic movements, volcanic events, and agricultural risks such as early or late frosts, as well as drought, torrential rainfall events, hailstorms, floods, and erosion. Needless to say, these factors are often interrelated (de Tapia 2012).

**Fig. 1.33** Some details from Teotihuacan monumental complex (Mexico City) and the rounded volcanic rocks, small size, used as main source for construction



Other villages built up with this type of construction material are typical of almost all the ‘high valley’ of the River Tevere in the Umbria region (Central Italy). The historic villages of Ficulle and Parrano in Central Italy are a classic example of HUL due to type and availability of such material. Result of such kind of construction technique is the evident vulnerability to earthquakes, even with a low vibratory ground motion and the very rapid ageing of structure, requiring frequent intervention to replace the mortar between the blocks (Margottini and Spizzichino 2014).

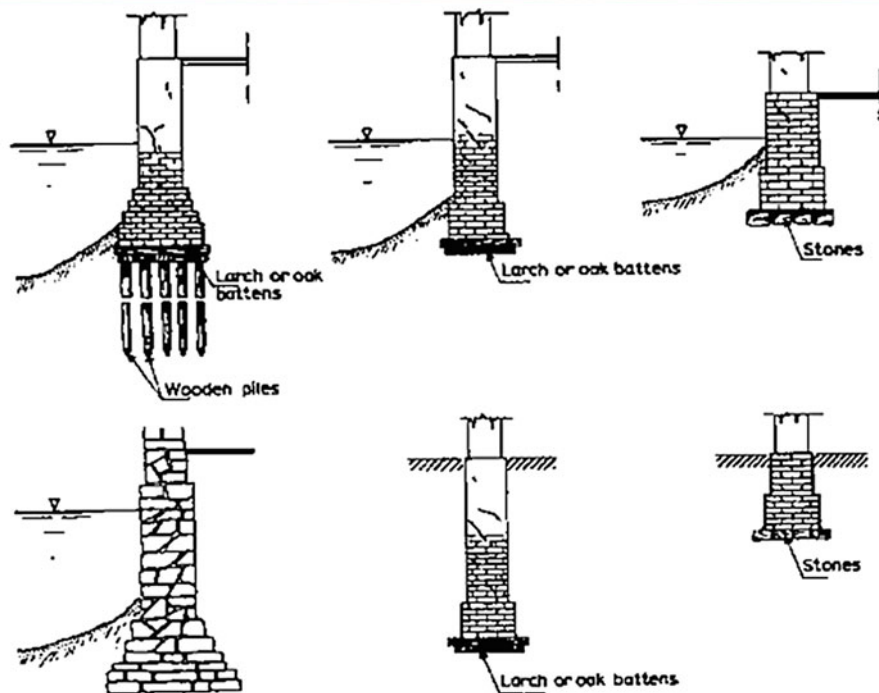
## 1.9 Complex Environment: Venice (Italy)

### 1.9.1 The Origin

The city of Venice is made up of 117 islands that are linked together by water canals, numerous small bridges, as well as three large bridges of the Grand Canal.

Venice has a rich and diverse architectural style, the most famous of which is the Gothic style. The style originated in 14th-century Venice, where the confluence of Byzantine style from Constantinople met Arab influence from Moorish Spain. These buildings of grandeur are still very well preserved. Key to its construction is an ancient method of using raised foundations, which effectively elevate ground zero to a height where buildings can be safeguarded from tidal waters (Fig. 1.34). This involves the hammering of thousands of pilings—large wooden stakes commonly made from alder—through the water and into the underlying sand and clay. Each piling is positioned very closely to its neighboring stake, one after the other, ultimately forming a raised wooden platform. Once a certain number of pilings has been driven into the earth, the tops are evened off and a substrate (or foundation layer) of wood and marble laid over the top. A stone foundation is then placed on top of the horizontal timbers. The foundations rest on the piles, and buildings of brick or stone sit above these footings.

**Fig. 1.34** Example of Venetian buildings and foundations. Wooden piles were mainly used for external buildings walls while, internal wall foundations were mainly executed enlarging the masonry (Colombo and Colleselli 1997)



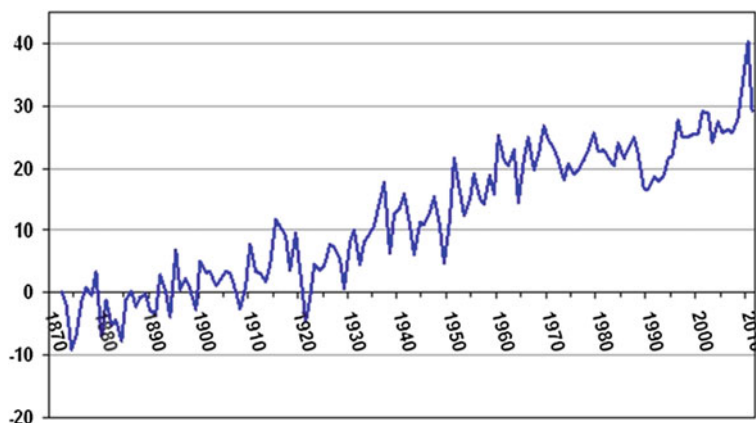


**Fig. 1.35** Sea level rising in the Venice lagoon in the period 1872–2011 (Campostrini 2012); about half reflects actual sea level rise in the upper Adriatic; the remainder is attributed to land subsidence induced

by natural processes and anthropogenic groundwater extraction in the 1960s (Gatto and Carbognin 1981)

### 1.9.2 The Evolution During the Time

The town of Venice is affected by different environmental problems that are all related to: fluctuations in Sea Level, which is related to tides and atmospheric conditions (Fig. 1.35); relative Sea Level Rise which is related to land subsidence and climate change.

Subsidence is related to both geological subsidence and anthropogenic groundwater extraction, the latter inducing consolidation of soil and then further settlement. The natural subsidence is thought to be composed of a long-term component ( $10^6$  yr) due to the retreat of the Adriatic plate subducting beneath the Apennines (Carminati et al. 2003) and a short-term component ( $10^3$ – $10^4$  yr) controlled by climatic changes through glaciation cycles (Pirazzoli 1996; Carminati and Di Donato 1999).

Present day subsidence has been recently studied using the PSInSAR™ method by Bock et al. (2012), which estimated a total value of about 1.5 mm/yr in the town of Venice, in the period April 2003 and October 2007 (Fig. 1.36). Thus, values are quite different in other surrounding areas and also changing rate over the time.

They both affect the building stability in terms of modification of bearing capacity and degradation of foundation materials. Also, relevant to the overall building stability are the modification and variation of load along time.

### 1.9.3 Diagnosis of Current Conditions

Steady sea level rise and land subsidence, as above described, have resulted in increased flooding conditions in the lagoon. Relative sea level changes have resulted in increased frequency and severity of flooding (called “acqua alta”—literally high water), which had reached about two events per year greater than 1.2 m after the 1960s (Camuffo and Sturaro 2004). The last decade has seen an increase in exceptionally high events in the Venice Lagoon (Figs. 1.37, 1.38) (<http://www.comune.venezia.it>).

### 1.9.4 Conservation Strategies and Management

The “acqua alta” (flooding) phenomena in Venice is posing a serious threat to conservation and management. Even if the phenomena have always occurred in the millenary history of Venice, the present situation is leading to a not sustainable development of the City.

Thus, also the fortunes of Venice have always been connected with the sea. In the past (since the XIV century), the Venice’s strategy included two main different targets:

- Defence of the city from flooding
- Grant access to the port.

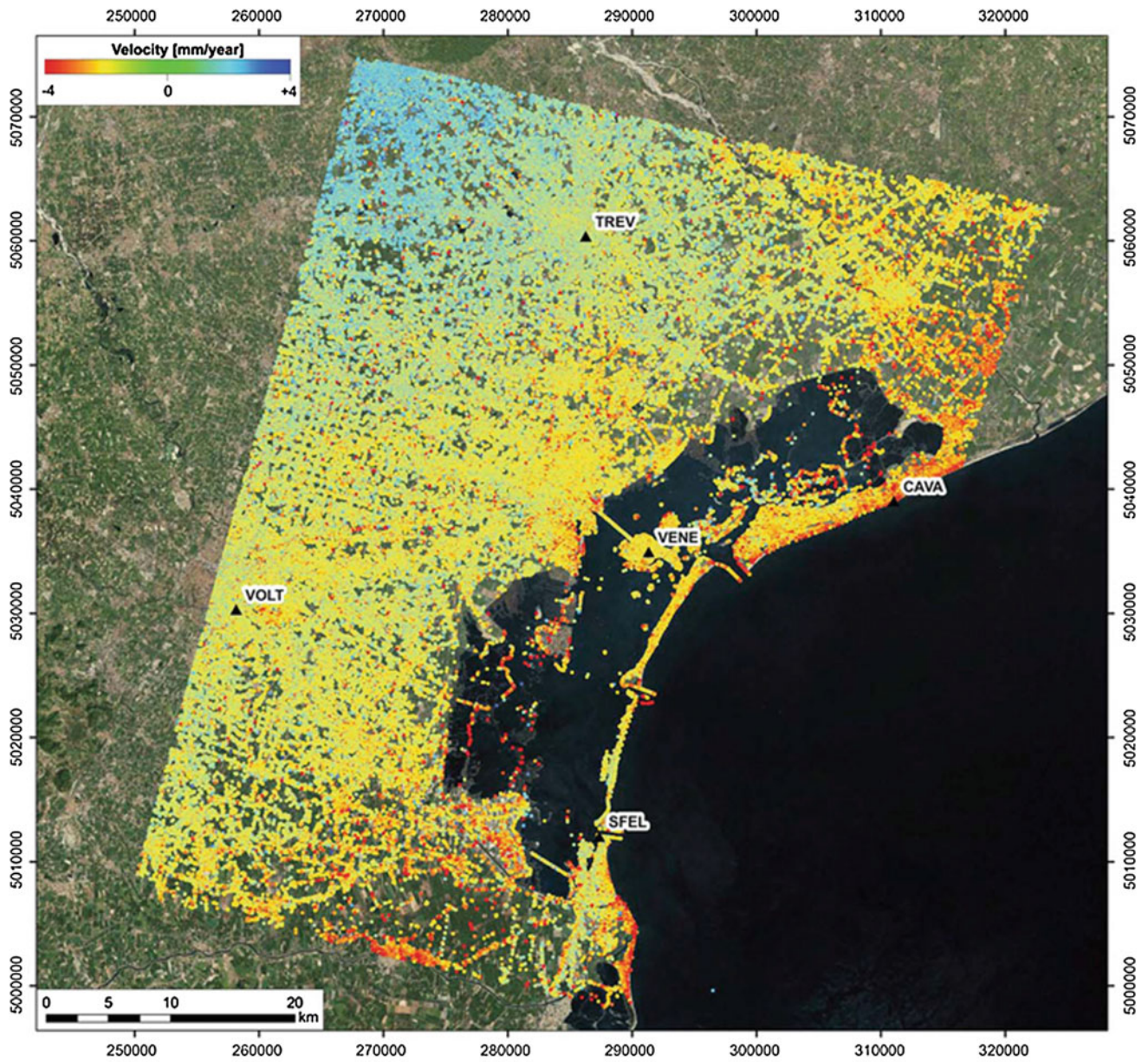


**Fig. 1.36** Annual average rate of line of sight surface displacement in mm/yr estimated for all the PS identified in the area (Bock et al. 2012)

**Fig. 1.37** Number of floodings (“acqua alta”) per decade in Venice, in the last century (Campostrini 2012)

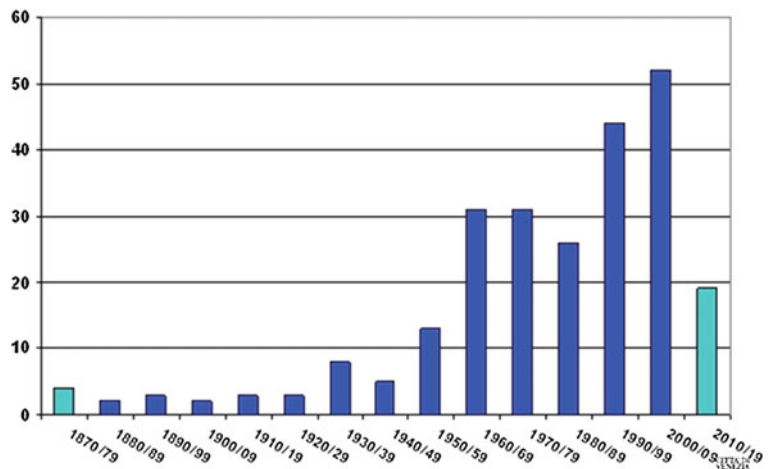




**Fig. 1.38** The “acqua alta” phenomena of 4th Nov 1966 (192 cm) (Campostrini 2012)

Both the above issues are now essential for the conservation of the town. For this reason, the Italian Government, lunched in 1987 the Mose system.

The system (<http://www.mosevenezia.eu/>) is being constructed to safeguard Venice and the entire lagoon area (550 km<sup>2</sup>) from high waters. It consists of barriers made up of mobile gates able to temporarily separate the lagoon from the sea and protect Venice from both exceptional destructive events and more frequent high tides, even if the sea level rises significantly (Fig. 1.39).

The barriers are being constructed at the lagoon inlets of Lido, Malamocco and Chioggia, the three openings in the barrier island through which tides propagate from the Adriatic sea into the lagoon.

In normal tidal conditions, the gates in the barriers rest in housing structures in the seabed in the inlets, completely invisible and without modifying exchanges between sea and

lagoon. They are raised only when necessary to block the incoming tide and avoid flooding of the lagoon and built-up areas. Four barriers made up of a total of 78 independent gates are being constructed (<http://www.mosevenezia.eu/>).

The design started in 1987, the construction on 2003 and the completion is expected on 2016 (<http://www.mosevenezia.eu/>).

## 1.10 Conclusions

The present paper is showing the “constrains” that geology is posing to the urban planning and constructions of Historic Urban Landscapes and Cultural Heritage in general. The same geological factors are very often at the origin for the decay of chemical/physical/mechanical properties of the rock (ageing); jointly with external environmental conditions and natural hazards they constitute the threats that are affecting the short, medium and long term conservation of monuments and sites.

As a matter of fact, the protection of Historic Urban Landscapes (HUL) and Cultural Heritages (CH) from ageing and external hazards is, in many cases, a border area between Science for Conservation of Cultural Heritages and Engineering Geology. Such assumption is clearly relevant for those threats having a well-defined geological and geomorphological origin, but also in others. An ideal method should consider that any conservation policies and management of HUL has to be anticipated by a proper diagnosis of current conditions, based on its evolution, highlighting major critical preservation threats, after having investigated the cultural and scientific origin of settlement.

In conclusion, the science of engineering geology can play a major role in the identification of internal causes for material or site deterioration and external processes acting on the settlement, also considering any appropriate monitoring system.

Last but not least, any solution and mitigation need to fulfill the request of low impact and perfect integration into the archaeological contest.

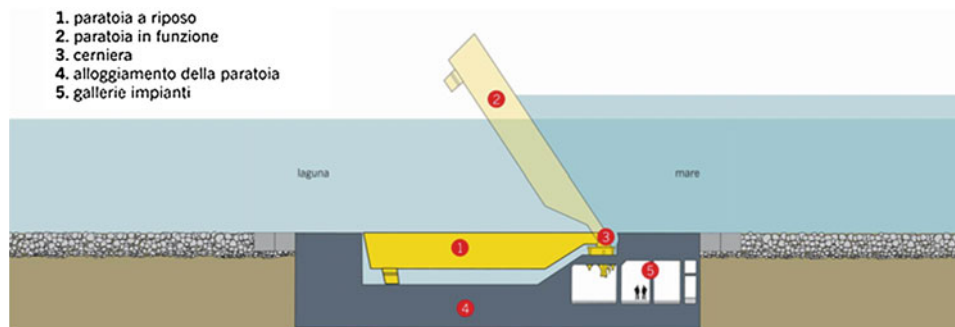


**Fig. 1.39** The “Mose” system (1 on rest; 2 in activity) (<http://www.mosevenezia.eu/>)

## References

- Bandarin F, Van Oers R (eds) (2012) *The historic urban landscape*. Wiley, London
- Beta Studio (2007) *Safeguarding of the Minaret of Jam in Afghanistan*. UNESCO Internal Report
- Bingham H (1930) *Machu Picchu, a citadel of the Incas*. Hacker Art Books, New York. ISBN 978-0-87817-252-8. OCLC 6579761
- Bock Y, Wdowinski S, Ferretti A, Novali F, Fumagalli A (2012) Recent subsidence of the Venice Lagoon from continuous GPS and interferometric synthetic aperture radar. *Geochemistry, Geophysics, Geosystems*, G3. Research letter, vol 13, no 3, 28 Mar 2012, Q03023. doi:[10.1029/2011GC003976](https://doi.org/10.1029/2011GC003976)
- Bruno A, Margottini C (2011) The Jam minareth in Afghanistan: emergency works and long term stabilisation. In: Iwasaki Y (ed) *Proceedings of the special session on geo-engineering for conservation of cultural heritage and historical sites*. 14th Asian regional conference, ISSMGE May 26, 2011, Hong Kong, 26 May, 2011
- Campostrini P (2012) Climate risk management at the local level and protection of Venice's cultural heritage. In: *Proceeding of the conference: building cities resilience to disasters in Europe: protecting cultural heritage and adapting to climate change*. Venice, 19–20 Mar 2012. Accessed 15 Mar 2014
- Camuffo D, Sturaro G (2004) Use of proxy-documentary and instrumental data to assess the risk factors leading to sea flooding in Venice. *Glob Planet Change* 40:93–103. doi:[10.1016/S0921-8181\(03\)00100-0](https://doi.org/10.1016/S0921-8181(03)00100-0)
- Canuti P, Margottini C, Casagli N, Delmonaco G, Falconi L, Fanti R, Ferretti A, Lollino G, Puglisi C, Spizzichino D, Tarchi D (2009) *Monitoring, geomorphological evolution and slope stability of Inca citadel of Machu Picchu: results from Italian INTERFRASI project*. In: (a cura di): Sassa K, Canuti P, Landslides: disaster risk reduction. Springer, Berlin, ISBN: 978-3-540-69966-8
- Carminati E, Di Donato G (1999) Separating natural and anthropogenic vertical movements in fast subsiding areas: the Po plain (N. Italy) case. *Geophys Res Lett* 26:2291–2294. doi:[10.1029/1999GL900518](https://doi.org/10.1029/1999GL900518)
- Carminati E, Doglioni C, Scrocca D (2003) Apennines subduction-related subsidence of Venice (Italy). *Geophys Res Lett* 30(13):1717. doi:[10.1029/2003GL017001](https://doi.org/10.1029/2003GL017001)
- Cencetti C, Conversini P, Tacconi P (2005) The Rock of Orvieto (Umbria, Central Italy). *Giornale di Geologia Applicata* 1 (2005):103–112. doi:[10.1474/GGA.2005-01.0-10.0010](https://doi.org/10.1474/GGA.2005-01.0-10.0010)
- Cock DE (2012) Bamiyan Province climatology and temperature extremes in Afghanistan. *Defense technology area (DTA) Report* 343, NR 1601, ISSN 1175-6594
- Colombo P, Colleselli F (1997) Preservation problems in historical and artistic monuments of Venice. In: *Proceedings of international symposium on geotechnical engineering for the preservation of monuments and historic sites*. Naples, 3–4 Oct, 1996, Balkema, Rotterdam
- de Tapia EMC (2012) Silent hazards, invisible risks: prehispanic erosion in the Teotihuacan Valley, Central Mexico. In: Cooper Jago, Sheets Payson (eds) *Surviving sudden environmental change answers from archaeology*. University Press of Colorado, Boulder
- Dupree NH (1977) *An historical guide to Afghanistan*. Afghan Air Authority, Afghan Tourist Organization, Kabul, 492 pp
- Gatto P, Carbognin L (1981) The Lagoon of Venice: natural environmental trend and man-induced modification. *Hydrol Sci Bull* 26(4/12):379–391
- Gregotti V (2001) *Architettura e postmetropoli*. Passaggi Einaudi, Torino
- Gruen A, Remondino F, Zhang L (2004) The bamiyan valley: landscape modeling for cultural heritage visualization and documentation. In: Gruen A, Murai S, Fuse T, Remondino F (eds) *ISPRS, processing and visualization using high-resolution images*, vol XXXVI-5/W1, WG V/6 18–20 Nov 2004, Pitsanulok
- ICCROM (2006) *Introducing young people to the protection of heritage sites and historic cities. A practical guide for school teachers in the Arab Region*, 2nd edn.
- Lang J (1972) Bassins intramontagneux néogènes de l'Afghanistan Central. *Rev Geogr Phys Geol Dynam* 14, 4(2):415–427
- Margottini C (2013) On the protection of cultural heritage from landslides. In: Margottini C, Canuti P, Sassa K (eds) *Landslide science and practice: risk assessment and mitigation*. Springer, Heidelberg. ISBN: 978-3-642-31318-9
- Margottini C (ed) (2014) *After the destruction of Giant Buddha Statues in Bamiyan (Afghanistan) in 2001. A UNESCO's emergency activity for the recovering and rehabilitation of cliff and niches*. Springer, Berlin. ISBN: 978-3-642-30050-9, doi:[10.1007/978-3-642-30051-6](https://doi.org/10.1007/978-3-642-30051-6)
- Margottini C, Fidolini F, Iadanza C, Trigila A, Barthélemy P, Ruther H, Ubelmann Y, Wessels S (2014) *Geomorphological processes and remedial measures in the archaeological site of Shair-e-Zohak*. UNESCO Internal Report
- Margottini C, Spizzichino D (2012) *Proposal of slope stability works at Orongo ceremony village*. Italian Institute for Environmental Protection and Research, Internal Report
- Margottini C, Spizzichino D (2014) *How Geology Shapes Human Settlements*. In: Bandarin F, Van Oers R (eds) *Reconnecting the city*. Wiley, London
- Margottini C, Panizza M, Spizzichino D (2008) The huge landslide on which the Machu Picchu citadel was founded. In: 33rd IGC congress in Oslo, 6–14 Aug 2008
- Margottini C, Vai GB (eds) (2004) *Litho- Palaeoenvironmental map of Italy during the last two climatic extremes*. Litografia Artistica Cartografica s.r.l, Bologna
- Martini E, Margottini C (eds) (1999) *Le frane storiche di Todi ed Orvieto*. CD ROM Regione Umbria
- Martini G, Paolini S (2006) *Regional environmental setting of the Inca park*. Minister of Education, University and Research—ENEA, INTERFRASI project, Final Internal Report
- Menon A, Lai CG, Macchi G (2004) Seismic hazard assessment of the historical site of jam in Afghanistan and stability analysis of the minaret. *J Earthq Eng* 8(1):251–294
- Minorsky V (1943) Some Early Documents in Persian (II). *J Roy Asiatic Soc Great Brit Irel* 1:86–99
- Mulrooney M, Ladefoged T, Stevenson C, Hao S (2009) The myth of A.D. 1680: new evidence from Hanga Ho'onu, Rapa Nui (Easter Island). *Rapa Nui J* 23(2):94–105
- Pirazzoli PA (1996) *Sea level changes, the last 20,000 years*. Wiley, Chichester, 211 pp
- Rowe JH (1990) Machu Picchu a la luz de documentos de siglo XVI. *Historica* 14(1):139–154
- Socodato F, Tortoioli L, Martini E, Mazzi AM (2013) The orvieto observatory. In: Margottini C, Canuti P, Sassa K (eds) *Landslide science and practice: risk assessment and mitigation*. Springer, Heidelberg, ISBN: 978-3-642-31318-9
- Wright KR, Kelly JM, Valencia ZA (1997) Machu Picchu: ancient hydraulic engineering. *J Hydr Eng ASCE* 123(10):838–843

---

**Part I**

**Conservation of Heritage of Earthen Structure,  
Earth Mound, Dam, Rock Monument,  
and Rock Cavern**

# Microtremor Measurements at Mogao Grottoes, Dunhuang, China for Preliminary Dynamic Characterization for Performance During Earthquake

Yoshinori Iwasaki, Koichi Nakagawa, Yuzo Ishikawa, Chikaosa Tanimoto, Keigo Koizumi, Kazuo Oike, Lanming Wang, Xudong Wang, and Qinglin Guo

## Abstract

Mogao Grottoes, Dunhuang, China, is a world heritage of UNESCO created in steep cliff with 50–60 m in height. Micro-tremor measurements and seismic refraction surveys have been carried out as a preliminary study to obtain dynamic characteristics. The site surface geology consists of young sediment of conglomerate in Pleistocene period above granite rock. A velocity sensor with a natural period of 0.5 s was used to monitor the micro-tremors at several points on the top terrace of the cliff and the lower plain in front of the cliff. Two survey lines of some 40 m for refraction survey were performed along which P and S waves were monitored. The velocities obtained from the both refraction lines are in the range of 500–700 m/s. and 1.6–4.0 km/s. for S and P waves respectively. The monitored micro-tremors were in less than a few m kins and the intensities of the motions were changed with time. Particle motions at the most observed sites shows the perpendicular direction to the cliff of EW is the predominant direction irrespective the intensity of the motions. Predominant period of spectral ratio of SW to UD direction shows about 2 s at the top terrace of the cliff and 1 s at the lower plain in front of the cliff. The thickness of the top surface layer of conglomerates is estimated about 125–180 m below the lower plain and 250 m or more. Another characteristic period was found at a period of 0.3–0.4 s. that might be caused by cliff-edge vibration.

## Keywords

Mogao grottoes • Protection heritage • Micro-tremor

## 2.1 Introduction

The geology of Mogao Grottoes is young conglomerate of Pleistocene in geological period was rather easy to excavate horizontal caves in ancient time. The area belongs to dry

desert zone of annual rain of about 30 mm/year. The strength of the conglomerate is rather high because of high tension of negative water pressures under very dry weather condition. However, strong wind that brings sand grains against the cliff wall and has resulted in failures and structural damages.

Y. Iwasaki (✉)

Geo Research Institute, 4-3-2 Itachi-bori, Nishi-ku,  
Osaka 550-0012, Japan  
e-mail: yoshi-iw@geor.or.jp

K. Nakagawa

Osaka City University, Osaka, Japan

Y. Ishikawa

Shizuoka University, Shizuoka, Japan

C. Tanimoto

International Institute for Advanced Studies, Tokyo, Japan

K. Koizumi

Osaka University, Suita, Japan

K. Oike

Kyoto University of Art and Design, Kyoto, Japan

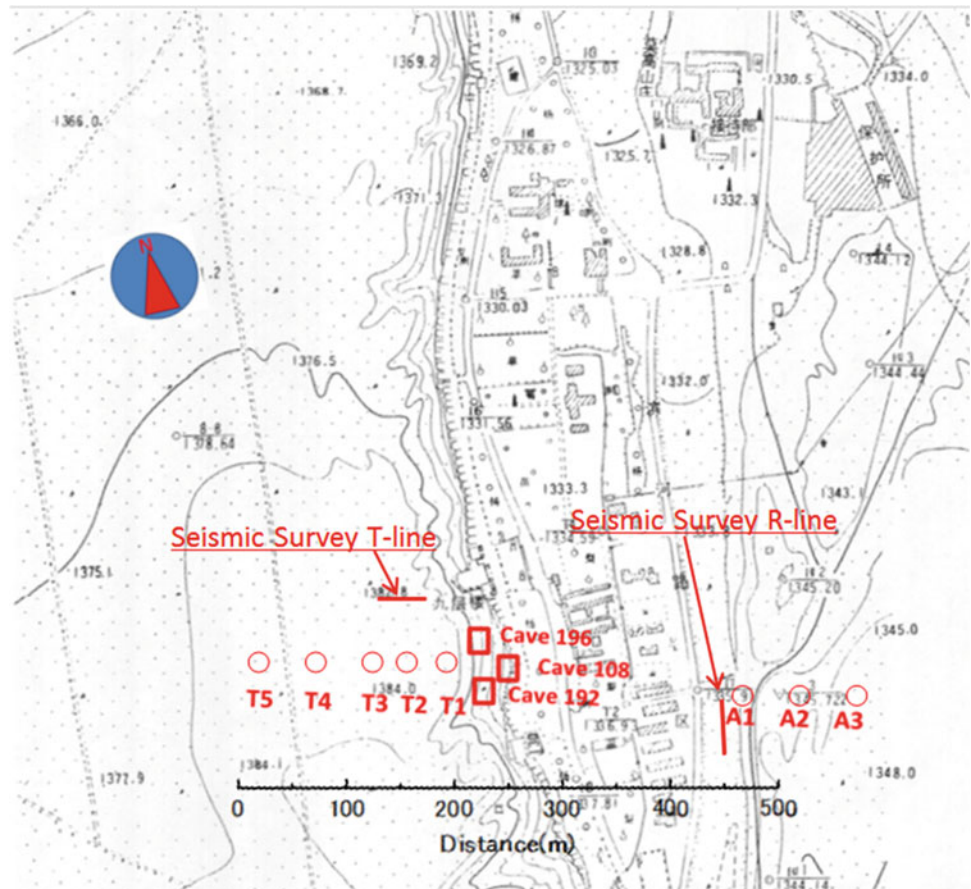
L. Wang

Dunhuang Academy, Dunhuang, China

X. Wang · Q. Guo

Lanzhou Institute of Seismology, Lanzhou, China

**Fig.2.1** Micro tremor measurement points at Mogao Grottoes



Systematic fractures parallel to the cliff wall were identified another geological feature that weakens the stability of the caves in the cliff. The dynamic characteristics of cliff at Mogao Grottoes under earthquakes depend upon cliff shape as well as dynamic properties of the ground. Micro-tremors and seismic refraction survey were performed to estimate the dynamic characteristics at the Mogao Grottoes, Dunhuang, China.

## 2.2 Microtremor Measurement

Mogao Grottoes is a group of horizontal caves that were excavated from vertical cliff as shown in Photo-1. The cliff is around 40–50 m in height and the geology of the cliff consists from gravel layers deposited in Pleistocene geological period. In front of the cliff face, caves had been excavated in four different levels.

Two vertical joint systems have been identified that run parallel and perpendicular to the cliff face.

Micro-tremor measurement was carried out at several points as shown in Fig. 2.1 at the top terrace ground and lower plane as well as at the floor of caves along the cliff.

One of the typical ground motions is expected at the edge of the cliff, T1 site. The recorded motions for 16 min. are shown in Fig. 2.2. The amplitude of the tremor was in the level of less than *mkine* (=10–3 cm/s) with the largest amplitude in the east-west direction.

The particle motions are shown for four time sections from 22 to 37 min. In horizontal plan, the predominant direction of motion is found in about east-west that is the perpendicular to the cliff face.

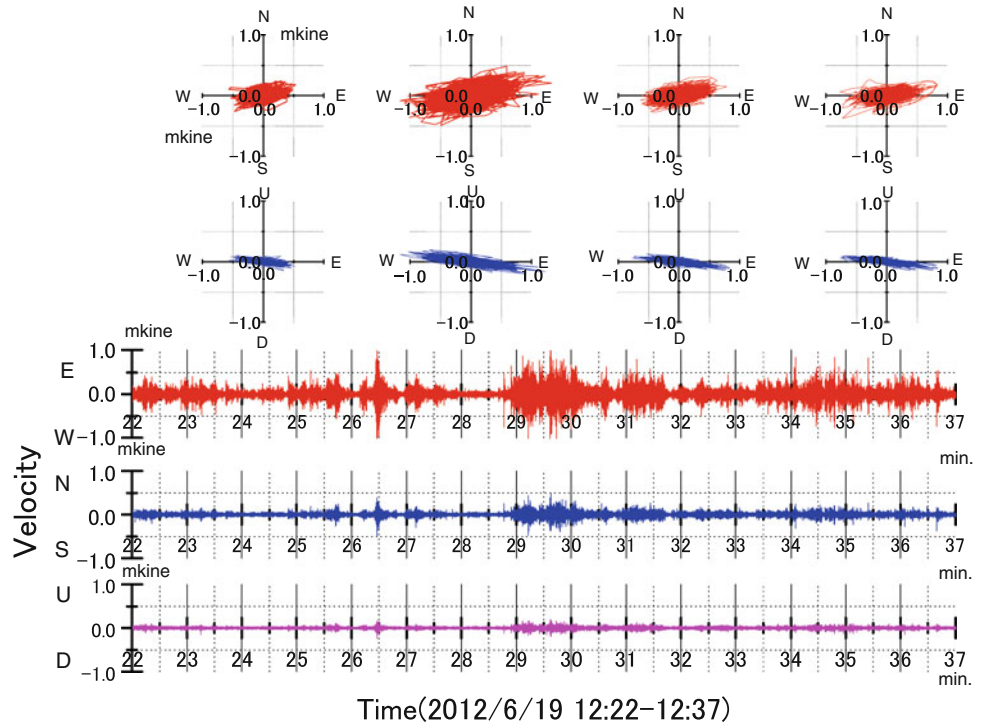
Micro tremors at five points on the terrace (T5, T4, T3, T2, and T1) and three points on the lower ground (A1, A2, and A3) were monitored independently at different time by one seismometer.

Figure 2.3 shows loci of particle motion for each site for a horizontal plane of EW-NS as well as a vertical plane of EW-UD directions.

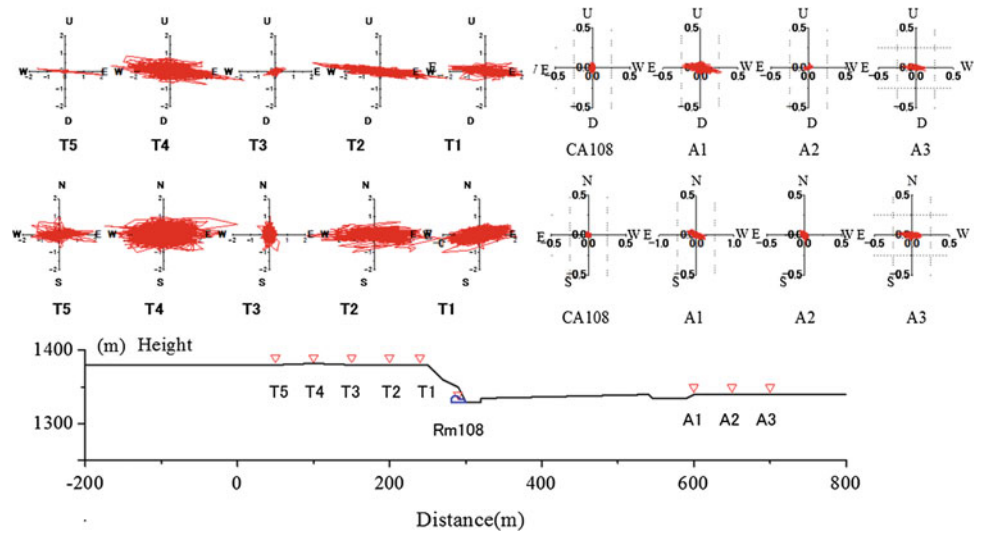
Except two points of T3 on the terrace and A2 on the lower ground, the rest of the most sites show the west-east direction is the most predominant direction, which coincides with the perpendicular direction to the present cliff.

A special site of the floor level in Cave 108, which locates at the bottom of the cliff, does not show any predominant direction of motions.

**Fig.2.2** Micro tremor recorded at T1



**Fig.2.3** Predominant direction of particle motion along from the west to east



Nakamura (2000) indicates the possible physical interpretation on the ratio of spectra of horizontal and vertical components related with the thickness of surface layer.

Figure 2.4 shows changes of the spectral ratios of the horizontal EW components to the vertical UD along the monitored line. In lower ground, 1 s period is noticed as the most predominant component except A2. This 1 s is also found at the Cave 108.

The predominant period at sites on the terrace shows 2–3 s as well as 1 s for the most sites except at T3 site.

### 2.3 Velocity Measurement of Deposited Layers

Small scaled refraction surveys were carried out at two experimental lines of T-line and R-line as shown in Fig. 2.1. An example of S-wave at T-line is shown in Fig. 2.5. P wave is about 1.6 km/s with some exception as high as 3–4 km/s. Most of the arrival waves caused by shear source were in a range of 500–700 m/s with low velocity of about 200 m/s.

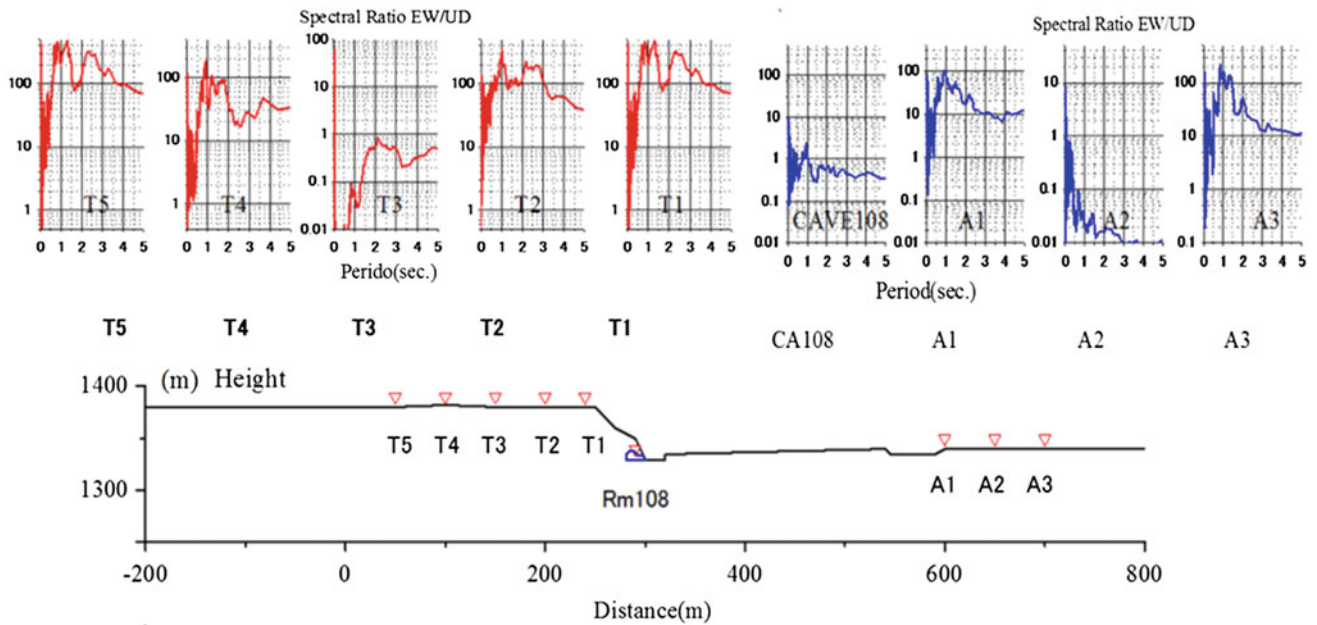


Fig. 2.4 Characteristics of predominant period of spectral ratio

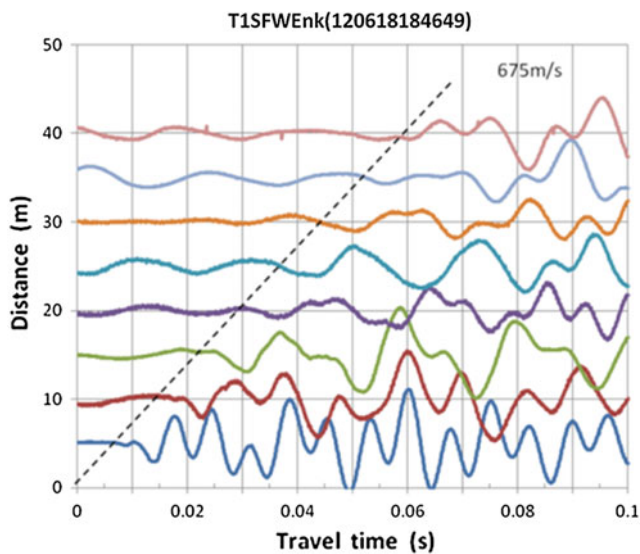


Fig. 2.5 Example of arrival waves by shear wave source

The preliminary obtained velocities of 1.6 km/s. for P-waves and 0.5–0.7 km/s. for S-wave, respectively are considered as reasonable value for the very densely hardened conglomerates under dry climates.

## 2.4 Surface Structure Inferred by Microtremors

The basic characteristic obtained by micro tremor measurement was strong tendency of predominant direction in the east-west direction. This is very much reasonable since the

direction coincides with the cliff that runs south to north. The predominant mode of the micro tremor is considered as controlled by the existence of the cliff.

The thickness of the sedimentary deposit under river bed side may correspond to 1 s of the predominant period of the spectral ratio, which may be estimated as one quarter of the wave length of the upcoming shear wave in the deposit. If we assume the shear wave velocity in the surface deposit as  $V_s = 500\text{--}700$  m/s, the thickness of the surface layer that is one quarter of the wave length becomes about 125–180 m.

At the same time, the predominant period of the spectral ratio on the terrace ground is about 2–2.5 s. If the same values are applied, the thickness is expected 250 m. The heights of lowland and terrace are about 1,330 and 1,370 m respectively. If the above estimated depths are applied, the height of the base rock is around 1,205–1,150 m under the low land and 1,120 m terrace.

## 2.5 Conclusions

Based upon in-situ study, some basic characteristics have been obtained as the basic information to consider the seismic protection for the Mogao Grottoes.

Several conclusions are summarized as follows,

- (1) Micro tremor measurements resulted in predominant direction of motions in east-west direction, which is perpendicular against the cliff.
- (2) Predominant period of the spectral ratio is about 1 s and 2–3 s in the lower ground and top of the cliff respectively.

- (3) Short period was predominant in caves and should be studied further.
- (4) Preliminary study of the seismic survey in the field provided velocity of P-wave and S-wave in the surface deposit as  $V_p = 1.6$  km/s, 3–4 km/s and  $V_s = 0.5$ –0.7 km/s.
- (5) Based on the predominant period, the thickness of the surface layer is estimated as 120–180 m for lowland and 250 m for terrace area.

**Acknowledgments** The authors express their sincere thanks to great supports for field work by members of Dunhuang Academy and the live

discussion with members of Lanzhou Institute of Seismology, China. This work was supported by MEXT/JSPS Grant-in-aid for Scientific Research (A) (22254003).

---

## Reference

Nakamura Y (2000) Clear Identification of fundamental idea of Nakamura's technique and its application, Paper 2656, 12 WCEE, Auckland, New Zealand. (<http://www.iitk.ac.in/nicee/wcee/article/2656.pdf>)

---

# CEN TC 346 Conservation of Cultural Heritage- Update of the Activity After a Height Year Period

3

Vasco Fassina

---

## Abstract

A specific European standardisation activity in the field of conservation of cultural heritage is essential to acquire a common unified scientific approach to the problems relevant to the preservation and conservation of the cultural property. A scientific approach is essential for the conservation of cultural heritage as a preliminary basis that will ensure effective planning of ordinary and extraordinary maintenance works, as well to assure their efficacy and durability. The scope of CEN TC 346 is to establish standards in the field of the processes, practices, methodologies and documentation of conservation of tangible cultural heritage to support its preservation, protection and maintenance and to enhance its significance. This includes standardization on the characterization of deterioration processes and environmental conditions for cultural heritage and the products and technologies used for the planning and execution of conservation, restoration, repair and maintenance. Up to now seventeen EN standards were published according to a matrix-based method in which three main topics have been developed. In 2014 seven more standards will be published.

---

## Keywords

CEN TC 346 • Conservation cultural heritage • Standardization

---

### 3.1 Scope of CEN TC 346

The main objective of CEN/TC 346 is drafting European standards which will help conservation professionals in their conservation and restoration work. It will also ensure that European experts can exchange information on test and analysis methods for the conservation of cultural heritage. This standardization activity will harmonize and unify methodologies in the European area.

The initial scope of CEN/TC 346, as approved in 2002, was the standardization in the field of definitions and terminology, methods of testing and analysis, to support the

characterization of materials and deterioration processes of movable and immovable heritage, and the products and technologies used for the planning and execution of their conservation, restoration, repair and maintenance (Many authors 1994; Many authors 2001; Many authors 2002).

Standardization in the field of conservation of cultural property will:

- improve methodology, protocols, guidelines to allow implementations of better practices or define equipment for preservation and conservation;
- improve the efficiency and pertinence of the diagnosis with a subsequent better management of funding for the conservation/restoration works and therefore increasing the number of conservation projects and spin-off economic benefits/opportunities for new investment, and consequent job creation;

---

V. Fassina (✉)  
CEN/TC346-Conservation of Cultural Heritage, Fine Arts of  
Veneto, Venice, Italy  
e-mail: vasco.fassina@gmail.com



**Fig. 3.1** a, b. Temperance statue, Carrara marble. In 1900 (*left*) the state of conservation was rather good, in 1976 (*right*) some missing parts are visible due to marble dechoesion after heavy atmospheric pollution exposure

- give precise and appropriate indication on the kind of diagnosis studies to be performed, promoting in this way conservation works on an increasing number of artifacts;
- increase longevity and reduce maintenance costs of conservation works, therefore reducing costs in the on a long-term range because conservation operations will be needed less frequently over time spaced out;
- facilitate professional mobility and international trade and increase the employment opportunities especially for young conservators, restorers, technicians etc...
- facilitate the exchanges between interested parties in Europe, respecting cultural identities, through the use of a common vocabulary.

### 3.2 Objectives of CEN TC 346 as Revised in the New Business Plan Approved in Venice in 2012

In 2012 a new Business Plan was prepared and it was decided to change the title from Cultural Property into Cultural Heritage and to prepare standards on a need-based approach. It was also specified the scope as following:

standards will be established in the fields of the processes, practices, methodologies and documentation of conservation of tangible cultural heritage to support its preservation, protection, and maintenance and to enhance its significance. This includes standardization on the characterization of deterioration processes and environmental conditions used for the planning and execution of its conservation, restoration, repair and maintenance (Many authors 2012).

In accordance with the objective of the revised BP the previous working structure composed by five WGs was changed into eleven WGs to cover the objectives in the period 2012–2015 described in the new BP.

### 3.3 Benefits Expected from the Work of CEN TC 346

To explain better the advantage of a good standardisation in the field of Cultural Heritage we report an example of a Venetian monument which was restored in 1976 as it was strongly decayed. The Porta della Carta, built in XIV century as the entrance door of Ducal Palace, was preserved in a rather good state for four centuries and the only damage observed were ascribed to the natural weathering agents. Comparison between two pictures taken at the beginning of XIX century and after seventy years respectively (Fig. 3.1a, b), shows a sharp increase in the marble decay, ascribed to the contemporary pollution increase occurring in the Venetian district as a result of the industrialization of Porto Marghera, the industrial area, created at the beginning of 1930s (Fassina 1994; Fassina et al. 2002).

In 1976 the conservation work of the whole Porta della Carta started, thanks to a funding of the Venice in Peril fund, and it was completed in a three year period. In 2001 in the framework of the National Research Council Project finalized to the Safeguard of Italian Cultural Heritage in cooperation with the Venice Superintendence for Monuments Care a check of the durability of restoration materials used in 1976 restoration work and of the condition was carried out. The results obtained allow us to conclude that the decay processes, which has caused missing of pieces of marbles and disintegration of carved surfaces (as it is possible to observe from the comparison of Fig. 3.1a and 1b), since the industrialization until 1976, seems to be arrested or slowed down (Fassina et al. 2002; Favaro et al. 2005).

We believe that a good standardization process is a useful tool to increase the durability of conservation works therefore reducing costs on a long-term range because conservation operations will be spaced out.

Up to now seventeen EN standards were published according to a matrix-based method in which the following three main topics have been developed:

- general guideline, terminology and characterization of materials constituting cultural property;
- evaluation of methods and products for conservation works of inorganic porous materials;
- indoor/outdoor climate-Specifications and measurement

### 3.4 Relevant Standards for the Conservation of Inorganic Porous Materials

Some relevant standards for the conservation of stone materials have been developed and will be described and discussed one after the other.

EN 16096:2012- Condition survey and report of built cultural heritage. *This standard gives guidelines for a condition survey of built cultural heritage.* It states how the condition of the built cultural heritage should be registered, examined, documented and reported on. It encompasses evaluation of the condition of a building or other structure mainly by visual observation, together—when necessary—with simple measurements. The relevant data and documentation on the built cultural heritage should be collected and included in the report. This standard can be applied to all built cultural heritage such as buildings, ruins, bridges and other standing structures. Archaeological sites and cultural landscapes are not dealt with in this standard.

This standard does not specify how to carry out a diagnosis of the built cultural heritage. For listed/protected immovable heritage specific national rules for expert documentation and works may apply.

As feed-back since its publication it has been considered in many European countries as a useful guidance for the preliminary assessment of the condition of built heritage.

EN 16085:2012- Methodology for sampling from materials of cultural property-general rules. *This standard provides a methodology and criteria for sampling cultural property materials for their scientific investigation. It covers, for example, how to characterize the material(s), assess the condition, determine the deterioration causes and/or mechanism(s) and decide on and/or evaluate the conservation treatment(s).* Apart from sampling, this document also provides requirements for documentation, and handling of sample(s). This standard does not deal with the decision making process for taking a sample nor how the sample is to be used. Sampling requires people with manual skill and knowledge of the cultural property. This is a general standard for sampling of materials constituting cultural property in order to characterize them during all stages of conservation. The sampling procedure depends on the type and condition of the material to be sampled, the specific case under study and the type of investigation chosen. Sampling is invasive and invariably causes damage, however small. It should only be undertaken if there is strong justification for it and in the closest consultation with those having responsibility for the object and those who will be studying the samples. The consultation should consider whether the same information could be obtained by non-invasive methods.

Regarding issues dealing with the evaluation of methods and products for conservation works of inorganic porous materials an important general draft for the evaluation of water repellent treatments was developed by considering standardized measurements of appropriate parameters (single test methods) to assess the performance of the product.

prEN 16581: 2014 “Surface protection for porous inorganic materials-laboratory test methods for the evaluation of the performance of water repellent products” is a *standard specifying the methodology for laboratory evaluation of the performance of water repellent products.* It is based on the measurement of several parameters which assess the performance of the product using standard test methods before and after ageing. The main goal of a water repellent is to reduce the penetration of liquid water and soluble substances into porous materials by changing its surface properties through capillary action. A water repellent product when applied to the surface of a material decreases its surface tension and prevents wetting of the surface. Many deterioration mechanisms result from the presence of water and therefore the reduction of water absorption may positively influence the preservation of porous inorganic materials.

A water repellent should fulfil the following requirements:

- (a) to reduce the absorption of liquid water in the material,
- (b) to minimize change of water vapour permeability,
- (c) to minimize change in colour and gloss of the substrate,
- (d) to produce no harmful by-products after the application,
- (e) to have a good chemical stability.

Water repellent products should be applied on the surface of heritage objects only after they have been tested on representative samples of porous inorganic materials in the laboratory.

In order to evaluate the durability and in service performance of a water repellent product applied on the substrate, ageing tests representing the environment in which the porous inorganic material is located must be carried out.

The following six standards applied to porous inorganic materials either untreated or subjected to any treatment or ageing have been already published.

- (i) EN 15801:2010. Determination of water absorption by capillarity. *This standard specifies a method for determining the water absorption by capillarity.* The water absorption experiment provides information about the material’s transport properties for liquid water. The draft is based on the process of water capillary rise to calculate the water absorption coefficient (AC) and to determine the amount of water absorbed (Qi) at different times. Capillarity measurements are carried out on untreated specimens and repeated after treatments and/

or ageing of treated material on the same specimen and measuring the amount of absorbed water at the same time intervals.

- (ii) EN 15803:2010. Determination of water vapour permeability ( $\delta p$ ). *This standard specifies a method for determining the water vapour permeability (WVP)*. It measures the amount of water vapour passing through the specimen over time in static conditions. A flux of water vapour through the specimen occurs when the partial pressure of water vapour differs between the two opposite surfaces of the specimen.
- (iii) EN 15802:2010. Determination of static contact angle. *This standard specifies a method for the measurement of the static contact angle of a water drop deposited on the tested surface*. The draft is used to assess the degree of water-repellency of a surface. Determination of static contact angle is carried out on untreated specimens and repeated after treatments and/or ageing of treated material on the same specimens. The contact angle  $\theta$  of a liquid on a surface is used to estimate the wetting properties of the material by calculating its solid-liquid-vapour surface tension.
- (iv) EN 15886:2010. Colour measurement of surfaces. *This standard describes a test method to measure the surface colour of porous inorganic materials, and their possible chromatic changes*. No reference to the appearance of glossy surfaces is described. The measurement of the surface colour of a specimen is performed on untreated specimens and repeated after treatments and/or ageing of treated material on the same specimens. When the number of readings has been determined, the measuring points for the after-treatment colour measurement shall be localized by reference coordinates in order to ensure precise repetition of the measurement. A grid delimiting the measurement field may be useful for this purpose, depending on specimen size.
- (v) EN 16302:2013. Measurement of water absorption by pipe method. *This standard specifies a method to measure the amount and rate at which water is absorbed through the test surface that is in contact with water*. Measurements are carried out on untreated specimens and the measurements repeated after treatment and/or ageing of treated material on the same specimens. The test is performed by measuring the volume of water absorbed through a defined surface under low pressure and within a specified time. This test can be performed in situ or in the laboratory and can be used to measure vertical and horizontal water transport. Penetration of driving rain into wall surfaces results in horizontal transport. Under actual conditions, the rate of rain penetration depends on prevailing wind

conditions as well as on the composition and condition of the exposed surfaces.

- (vi) EN 16322:2013. Determination of drying properties. *This standard specifies a method for the determination of the drying behaviour of porous inorganic materials*. The drying properties of materials can be calculated from a curve that indicates the weight loss of the mass of water inside the sample, as a function of time, during a drying experiment. Usually the drying of specimens saturated with water consists of two phases. The first drying phase is characterized by transport of liquid water to the surface followed by evaporation. The surface remains wet allowing evaporation at a constant rate, as water moves to the surface fast enough to compensate for the losses due to evaporation. The evaporation at the surface is determined to a large extent by the test boundary conditions. These are temperature, relative humidity and the flow velocity of the ambient air. The slope of the drying curve during the first drying phase therefore reflects these conditions.

The second drying phase starts when the amount of water brought to the surface becomes too small to keep the surface wetted and the rate of evaporation decreases. Transport of liquid water to the surface is no longer possible and only the less efficient vapour diffusion mechanism remains available.

Some materials, e.g. adobe or sandstones containing clay, do not dry in this typical two-phase drying curve. For example, in the case of material treated with water repellent, the first drying phase does not exist.

---

## References

- Many authors (1994) Community action plan in the field of cultural heritage, Council decision O.J. 94/C 235/01 Bruxelles
- Many authors (2001) STOA (Scientific and technological Options Assessment), Technological requirements for solutions in the conservation and protection of historic monuments and archaeological remains, developed for the European Parliament, Directorate-General for European Panel on the Application of Science to Cultural Heritage, Bruxelles, October 2001
- Many authors (2002) BT N 6732, Conservation of cultural property—New CEN/TC, Bruxelles, 19 December 2002
- Many authors (2012) CEN TC 346-N0358, Business Plan—Final draft revised during the ninth plenary meeting in Venice, (29th–30th March, 2012), and approved with Resolution N 117/2012
- Fassina V (1994) The influence of atmospheric pollution and past treatments on stone weathering mechanisms of Venetian monuments. *Eur Cultur Herit Newslett Res* 8(2):23–35
- Fassina V, Favaro M, Naccari A (2002) Principal decay patterns on venetian monuments, in natural stone, weathering phenomena, conservation strategies and case Studies. In: Siegesmund S, Volbrecht A, Weiss T (eds) *The geological society*, London, Special Publications, 205, 2002, pp 381–391
- Favaro M, Menichelli C, Bassotto L, Fassina V (2002) Preliminary results on the behaviour of restoration materials used in the past on

monuments in relation to their durability and to decay processes case study: Porta della Carta in Venice. In: Guarino A (ed) 3rd International congress on science and technology for the safeguard of cultural heritage in the Mediterranean Basin Alcalá de Henares, July 9–14, 2001, 2002, pp 204–209

Favaro M, Simon S, Menichelli C, Fassina V, Vigato P (2005) The four virtues of the Porta della Carta, ducal palace, Venice—assessment of preservation state and re-evaluation of the 1979 restoration. *Stud Conserv* 50(2005):109–127

Upali Silva de. Jayawardena

---

## Abstract

Buddhism was introduced to Sri Lanka in 4th century BC. Since then various Buddha statues, monuments and temples have been built by various rulers in different parts of the country. The author carried out a research on the rock materials used for the construction of ancient Buddha statues remaining in archaeological sites. The observations indicate that the rock types namely migmatite, biotite gneiss, hornblende biotite gneiss, microcline bearing biotite gneiss and marble have been used for sculpturing. Statues made from highly fractured rocks like quartzite and pegmatite, very strong rocks like charnockite, pink granite and dolerite, and sedimentary limestone are not presently seen in any site. Most of the marble statues are broken in to several pieces due to the effects of both physical and chemical weathering processes. Statutes made from other rocks are still remaining without any major damage. A few statues have been made from the bedrock at the site itself. The other statues or the rock materials or both have been moved from different locations to the present sites. These statues are located on flat terrains, isolated small hillocks, some isolated large exposed rocks and erosional remnants like inselbergs surrounded by flat lands.

---

## Keywords

Buddha statues • Archaeology • Rock types • Climate • Weathering

---

## 4.1 Introduction

Sri Lanka has a recorded history of over 2500 years. Ancient chronicles have mentioned that the irrigation systems in Sri Lanka were operating since 6th and 5th centuries BC. The most significant event in the country's history was the arrival of Arahath Mahinda who brought Buddhism to the Island when "Devanampiyatissa" was the king in 307BC. Since then Buddhism influenced the life of people through the centuries under the ruling of different kings (Siriweera 2001).

---

U.S. de. Jayawardena (✉)  
Department of Civil Engineering, University of Peradeniya,  
Peradeniya, Sri Lanka  
e-mail: udesja@pdn.ac.lk

There are a large number of protected ancient archaeological monuments in Sri Lanka. Statues of Lord Buddha, monumental structures and temples were built by ancient kings to honor the Buddha. Some of them are made of rocks and others are mainly of bricks and wood. Most of the Buddha statues made of hard rocks are still remaining. Though finding an exact period is difficult, according to legends and chronicles the huge partially finished Buddha statue carved out of bedrock at Dowa Temple, Ella, could be the oldest statue in Sri Lanka. It is believed that this 36 feet height statue has been built during the reign of King Valagamba (104–77 BC) in the 1st century BC. There are no historical records on the previous Buddha statues in Sri Lanka. The statues made of rocks after the 1st century BC have subjected to the effects of various climatic conditions in a longer period (Siriweera 2001).

### 4.1.1 Sri Lanka in Brief

Sri Lanka is an Island in the Indian Ocean. Physiographically Sri Lanka consists of a central mountainous mass or central highland surrounded by a low, flat plain on all sides and extending to the sea (Vitanage 1970). Sri Lanka is considered to have a humid tropical climate. On the basis of rainfall, the dryness and topography, Sri Lanka can be divided into three climatic zones namely the Dry Zone (rainfall less than 2,000 mm), the Intermediate Zone (rainfall between 2,000 and 3,000 mm) and the Wet Zone (rainfall above 3,000 m) (Walker 1962), (Fig. 4.1).

Geologically nine tenth of Sri Lanka is made up of high grade metamorphic rocks of Precambrian age i.e., older than 570 million years, belonging to one of the ancient and stable parts of the earth's crust, called the South Indian Shield. The remaining rocks are sedimentary rocks of predominantly of Miocene age in the north-west (and one place of south east) with some Jurassic sediments preserved in small faulted basins. There are recent sedimentary formations, identified as Pleistocene deposits in a few locations. Intruding the metamorphic rocks of Sri Lanka are some granites, dolerites, pegmatites, quartz veins and a carbonatite (Cooray 1967). Charnockite, quartzite, marble, granulite, migmatite, gneisses (garnet sillimanite graphite gneiss, hornblende biotite gneiss, biotite gneiss, calc gneiss, cordierite gneiss, wollastonite-scapolite gneiss, granitic gneiss etc.) and amphibolites are the common Precambrian metamorphic rocks found in

Sri Lanka. The widely distributed rocks within the country are charnockite, hornblende biotite gneiss, biotite gneiss, migmatite, quartzite, marble and granitic gneiss. Most of these metamorphic rocks are very hard and strong. Therefore it may take a longer time for weathering. Weathering is not uniform in any place in the country and the thickness changes drastically from place to place.

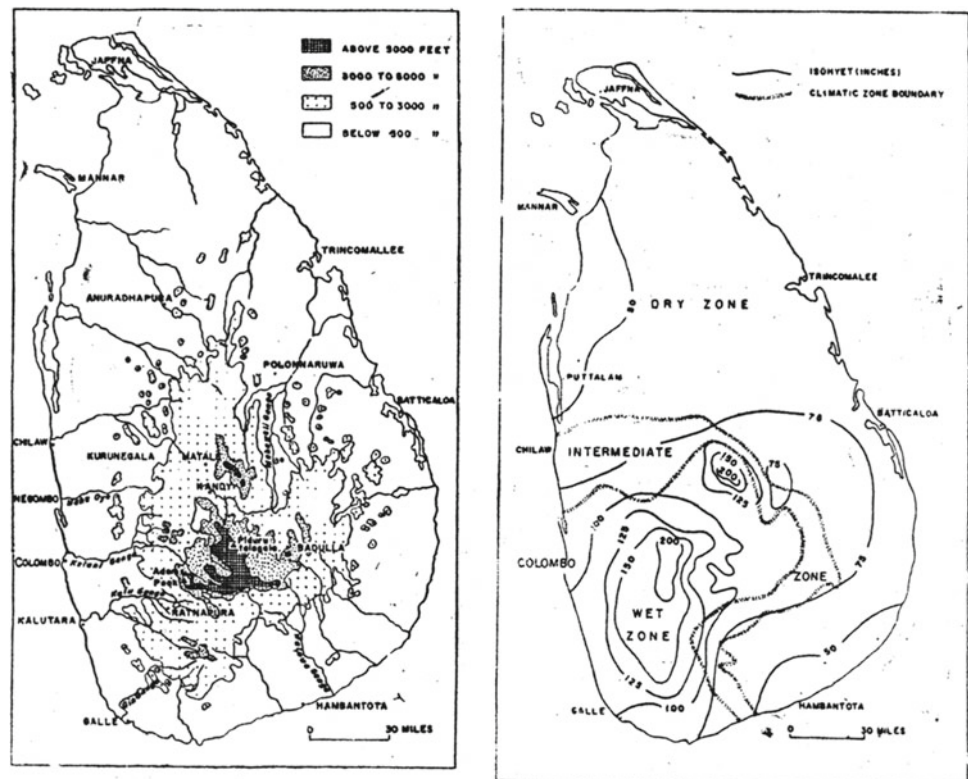
### 4.1.2 Objective

Although there are various types of monuments made of rocks, the author carried out a research on the natural rock materials used for the constructions of ancient statues of Load Buddha which can be presently seen in archaeological sites. The objective of this paper is to describe the type of original rock materials, their present conditions, effect of dry and wet climatic condition and methods to be applied for protection.

## 4.2 Method of Study

Statues made from the natural rocks in archaeological sites were carefully observed. The rock types, effect of physical and chemical weathering conditions, fractures and filling materials, effects of rain and groundwater and the geomorphology of the surrounding area were studied to describe the

**Fig. 4.1** Climatic zones and relief map of Sri Lanka (Herath 1973)



present condition of them. The general geology of the surrounding areas where the statues are located at present was also studied to identify the sources of rock materials (Fig. 4.2).

### 4.3 Observations and Discussions

The oldest Buddha statue (1st century BC) at Dowa Temple (Bandarawela-Badulla road) has been made by carving the vertical surface of charnockitic hornblende biotite gneiss rock. This temple is situated in a part of the central highland, at a height of about 1,200 m from MSL. This is the only statue that can be seen now in the Wet Zone mountain areas (Fig. 4.2). Other than this there are no evidences for ancient Buddha statues built by rocks in central highlands or mountain areas in Sri Lanka. The surface is faded or slightly discolored due to irregular weather conditions but it has not subjected to serious chemical weathering. This is an

incomplete statue. Except this, all other Buddha statues made of rocks are situated in low flat plains or isolated small hill-ocks, some isolated large exposed rocks and erosional remnants like inselbergs surrounded by flat lands. And also these locations are situated in the Dry Zone where the annual rainfall is low and the day temperature is high. The other large single standing statues made of rocks are situated at Aukana, Sasseruwa, Buduruwagala, and Maligawila (Fig. 4.2). A large recumbent Buddha statue and seated Buddha statues are situated at Tantirimale. There are five statues at Buduruwagala but only one standing statue shows the features of Lord Buddha. It is the tallest (15 m) Buddha statue in the country. There are four Buddha statues, two in seated postures, one standing posture and one recumbent posture at Galviharayya, Polonnaruwa.

The rock type of 12 m high single statue at Aukana is granitic gneiss/quartzo-feldspathic gneiss. It has been carved from the solid part of inselberg situated at a little higher elevation than the surrounding area. The surface of the statue is fully faded and discolored. Some micro cracks due to the effect of physical weathering can be seen at the surface. Statues at Tantirimale have been made by carving an in-situ elongated outcrop of same rock type, granitic gneiss/quartzo-feldspathic gneiss mixed with microcline feldspar. These are also faded and discolored with more micro cracks on the surface. Standing statues at Buduruwagala and Sasseruwa have been made by carving the exposed bedrock of migmatitic charnockitic biotite gneiss. Some parts of these statues are broken. This may be due to physical weathering or separation of pieces when those were sculptured.

Statues at Galvihareya, Polonnaruwa have been carved out of in-situ elongated bedrock of garnetiferous migmatitic hornblende biotite gneiss. This exposed rock is now fully discolored and developed or expanded cracks can be seen on the surface of the statues. In addition, some places of the cracks are chemically weathered and very thin highly weathered materials can be seen in the cracked parts of the statue.

All these previously mentioned Buddha statues have been made by carving the in-situ bedrock and the back sides of the statues are directly connected to the bedrock. The Maligawila Buddha statue in standing posture has been made by carving a single crystalline limestone (marble) block and the other parts of the bedrock or boulder cannot be seen. This 14 m high single statue had been in free standing position for a longer time. However by the time it had been found in 1951 it was already broken into several pieces. In 1980 the statue was reconstructed with latest techniques and raised again. Most of the parts of the surface of the statue are chemically weathered and open spaces like gravel size cavities can be seen.

Statues made from marble rock can be seen at Anuradhapura, Seruwila, Triyaya, Medirigiriya, Polonnaruwa, Sampur, Kalametiya, Kuchchiveli, Kantale, Pulkunawa,

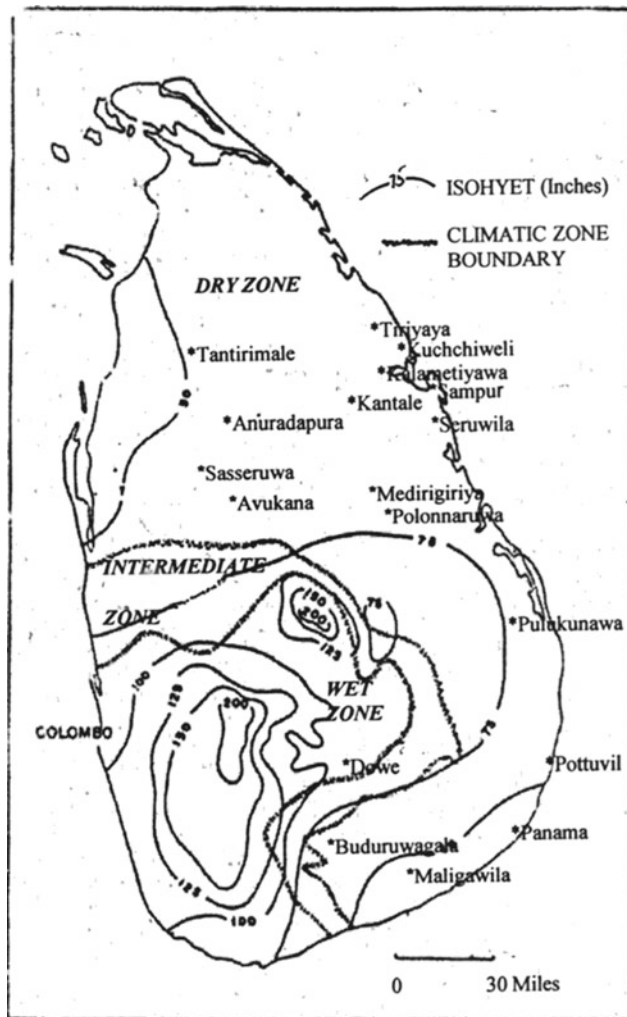


Fig. 4.2 Locations of the study area

Potuvil, and Potuvil-Panama road. The outer surfaces of all of these marble statues are chemically weathered and tiny cavities on the rough surfaces can be seen. The broken parts of these faded and discolored statues have been plastered by cement mortar in recent years. Reconstructed Anuradhapura Samadi Statue and Seruwila statue (seated posture) are now under shelters to protect from weathering. Madirigiriya and Polonnaruwa seated posture statues and other standing statues (more than 2 m height) at Tiriyaya, Medirigiriya, Sampur and Potuvil, are kept in open spaces. Some of these statues have already been broken and not reconstructed. The statue at Kalametiya, in Trincomalee is completely broken and some parts are eroded. Statues found at Kuchichiveli and Kantale have been moved to the Trincomalee museum. A few rocky monuments which are located in the coastal zone (Potuvil and Potuvil-Panama road) may have been affected by wind-blown silt and sand in addition to the weathering effects from the atmosphere. Those effects could be minimized by covering with roofs and glass shelters from the sides and maintaining the sites frequently. Crystalline limestone (marble) or dolomitic marble is the type of solid rock of all these statues. But the bedrock of the places where these statues are located is not either marble or dolomitic marble. The bedrocks are migmatitic biotite gneiss, hornblende biotite gneiss or microcline biotite gneiss. Therefore all these marble statues or the boulders of marbles or both have been moved from different places where they have been sculptured or collected.

Remains of Buddha statues made of microcline bearing biotite gneiss rock at Rataveli Vihara, on Potuvil-Panama road and Pulukunawa are already broken. Statue found at Toluwila, Anuradhapura has been made of microcline biotite gneiss. Faded and discoloured statue is now kept in the museum. These are also carved out of single rock boulders but the bedrock locations may not be very far away. All of these statues have been carved out before the 7th century AD.

Statues made from highly fractured rocks like quartzite and pegmatite and sedimentary limestone (weakest rock) are not seen or remaining in any site now. The most important thing is the absence of statues made of charnockite (metamorphic) and pink granite (igneous) which are very strong rocks in Sri Lanka (Jayawardena 2001). No statues have been made from dolerite (igneous) which is another strong

rock which occurs as narrow thin veins. Sculpturing and carving out of these strong rocks may be a time consuming activity and need very careful attention to avoid over-breaking. The compressive strength of the rock types of these statues are less than charnockite and pink granite.

The effect from sunlight, rain and flood, and the growing of roots of trees are the major impacts to these archaeological sites. Those effects from sunlight and rain should be minimized by applying suitable engineering methods. However there are no major effects from growing roots and flood.

---

#### 4.4 Conclusion

The observation indicates that the rock types namely migmatite, biotite gneiss, hornblende biotite gneiss, microcline bearing biotite gneiss and marble (crystalline limestone or dolomitic) have been used to sculpturing in ancient times. All marble rocks have been subjected to physical and chemical weathering and erosion than the other rock types. Except one, all other Buddha statues are located in low elevation terrains in Dry Zone of Sri Lanka. The effects of the climate and the surrounding areas could be minimized by covering with roofs and glass shelters on the sides and maintaining the sites frequently.

---

#### References

- Cooray PG (1967) An introduction to the geology of Ceylon, Department of National Museums, Government Press, Colombo, p 340
- Herath JW (1973) Industrial clays of Sri Lanka. Geological Survey Department publication, Sri Lanka p113
- de Jayawardena US (2001) A study on the engineering properties of Sri Lankan rocks. *J Ins Eng, SL*, pp 07–22
- Siriweera I (2001) Rajarata civilization and kingdoms of South-West. Dayawansa Jayakody & Company, Sri Lanka p447
- Vitanage PW (1970) A study of the geomorphology and morphotectonics of Ceylon. In: Proceedings of the second seminar on geological prospecting methods and techniques, United Nations, New York, USA, pp 391–405
- Walker RC (1962) The hydrometeorology of Ceylon, Part 1. Government Press, Ceylon, Canada Colombo Plan Project

Anna Scotto di Santolo, Lorenza Evangelista, and Aldo Evangelista

## Abstract

The paper reports the study conducted to evaluate the stability condition of one the most suggestive rock cavity located in the city of Naples (Italy), the *Fontanelle* (little fountains) Cemetery. It is a chamber and pillar cavity, with a rectangular and elongated plan, consisting of three naves. The cavern was excavated in the Neapolitan Yellow Tuff, a soft rocks widespread used as construction material in the city and its origin goes back to the 16th century while its expansion to the 17th century, when the city was quickly battered by popular uprising, famines, earthquakes, eruptions of the Vesuvius and epidemics. The cavity was addresses to different uses; destined to become an ossuary in the 18th century, progressively turned into a Christian worship place, suffering many events during 400 years of life, until it finds, in the modern age, its stability as a place of worship. The paper reports the numerical analyses by means of a 3D finite difference code, carried out to evaluate the stability condition of the cavity and the hill on which was excavated, taking into account the various stages of life. The results obtained show that there are some stability problem for the roof of the cavity; further investigations on the shape of the pillars, partially hidden by the fill, and on the mechanical properties of the tuff are needed for a more satisfactory evaluation.

## Keywords

Tuff • Numerical analysis • Cavern • Stability conditions • 3D FLAC

## 5.1 Introduction

The city of Naples lies on a morphologic and a geologic complex context, dominated mainly from the presence of pyroclastic soil, originated from the superimposition of various volcanic activities, produced from the Caldera of the Campi Flegrei and from the Somma-Vesuvio (Fig. 5.1).

The main base formation is the Neapolitan Yellow Tuff (NYT), that sometimes is emerging or is founded at various depths from the ground level. Above the tuff is present the pyroclastic sequence, constituted mainly by cohesionless silty sand (pozzolana) sometimes with gravels (pomici).

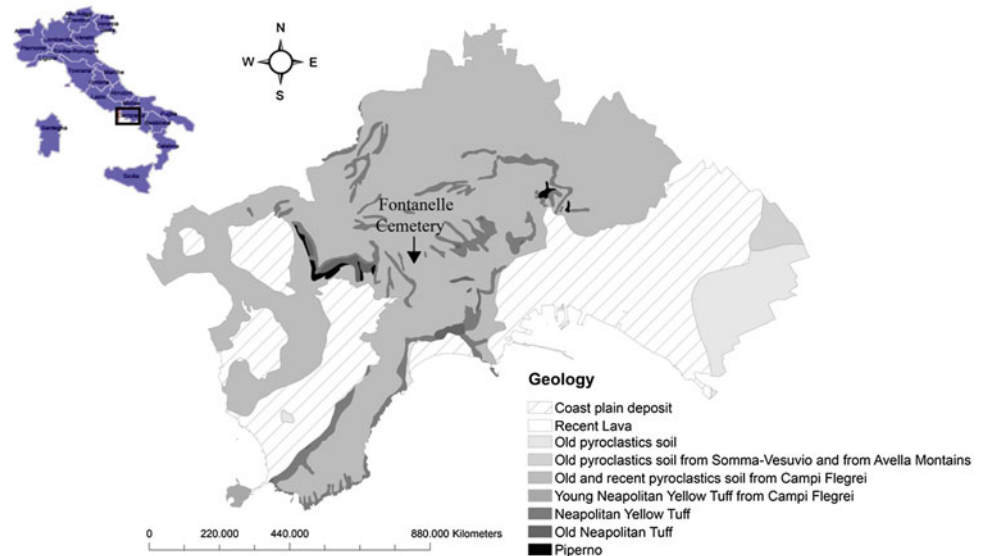
Given its good mechanical properties, the tuff has been excavated through the centuries for religious purpose, water supply or for connected different area of the city. Nowadays about 700 cavities are registered all over the city, but a considerable number of them are located mainly in the western area; that chosen, afterwards, for the pagan—and later Christian—cemeteries. In this area, in fact, the backbone of the hills is the NYT, covered by pyroclastic soils (pozzolana and pumices) was easily eroded by rain water; going on through the centuries the erosion exposed the underlying tuff on the sides of the valleys, creating the optimal conditions for quarrying it as a construction material. Just outside the ancient Greek—Roman necropolis, the

---

A. Scotto di Santolo (✉)  
Università telematica Pegaso, Centro Direzionale, Piazza Cenni, 2,  
80143 Naples, Italy  
e-mail: anna.scottodisantolo@unipegaso.it

L. Evangelista · A. Evangelista  
DICEA Università degli Studi di Napoli Federico II, Via Claudio  
21, 80125 Naples, Italy

**Fig. 5.1** Location of the *Fontanelle Cemetery* and geology map of Napoli, Italy



*Fontanelle Cemetery* is located; a cavity that has no particular architectural features, nor its size (width and height) comparing with the other quarries, but due its complex story, it is particularly suggestive becoming part of the cultural heritage of the city. The origin of the quarry may be traced back to the XVI century, and its expansion to the XVII century.

Even if the cavity has been interested by several inspections, a systematic and exhaustive campaign of geological, geotechnical and structural investigations has never been performed. Due to the complexity of the problem, a number of uncertainties remain concerning the hidden geometry of the cave, the properties of the debris material and about the mechanical characterization of the rock mass due to the presence of persistent joint system in this weak rock.

## 5.2 The *Fontanelle Cemetery*

Even if one of the major uncertainties is connected the unknown details of the excavation technique, the *Fontanelle Cemetery*, recall the most widespread practice used in Central and Southern Italy for the extraction of the tuff. It is a “chamber and pillars” cavity, regular in plan, with a rectangular shape elongated in a north–south direction. The caver has a width equal to 40 m and a length of 105 m, with a total area of more than 3,000 m<sup>2</sup>. The roof is supported by nine isolated pillars (P1–P9) and four further vertical elements or septum (SE1–SE4) protruding from the walls (Fig. 5.2a) that generate three naves. The main one is called “navata degli Appestati” (nave of the plague stricken persons) while the second one is the “navata dei Preti” (nave of the priests). The caver has two direct access and on the right entering, there is a third secondary aisle with an inclination

of 45° respect to the other ones and a smaller span, called “navata dei Pezzentelli”(nave of the small beggars). The height of the “navata dei Preti” is 7 m, while the “navata degli Appestati” is 10 m high. The naves sections have a trapezoidal shape with a flat roof and walls inclined of 10°–15° to the vertical; the pillars, consequently, have a structural section decreasing with depth (Fig. 5.2b).

The cover above the roof (tuff plus pyroclastic soils) ranges between 8 and 10 m. In the entrance and in the central chamber the height of the roof rises up to 12.0 m, while the cover is 30 m thick.

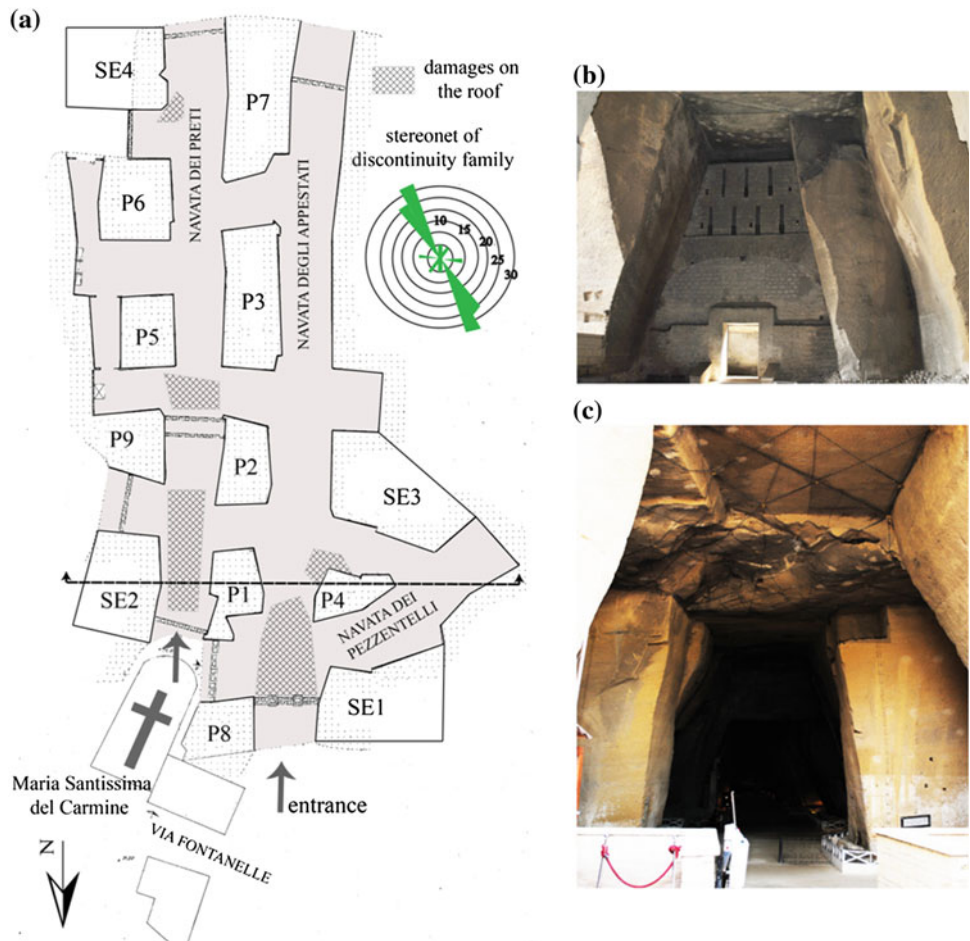
The material below the present floor level (72 m a.s.l.) is composed by an inter-bedding of anthropic fill and cineritic levels of different grain size and alluvial origin. The floor of the ancient quarry lies at an average depth of 9.0 m from the actual walking level. It is therefore believed that the pillars, for a substantial stretch, are buried in the filling material.

An intense fracturation is present in the central part of the roof at the entrance (e.g. Fig. 5.2b), with a prevailing northwest-southeast orientation. A second discontinuity system is detected where there are variations of height of the cavity oriented in the east–west direction. A few vertical discontinuities have been found in the *navata dei Pezzentelli*, at the intersection between the roof and the pillar. The statistical analysis of the discontinuities detected is reported in Fig. 5.2.

## 5.3 Consideration on the Stability Condition of the Cavern

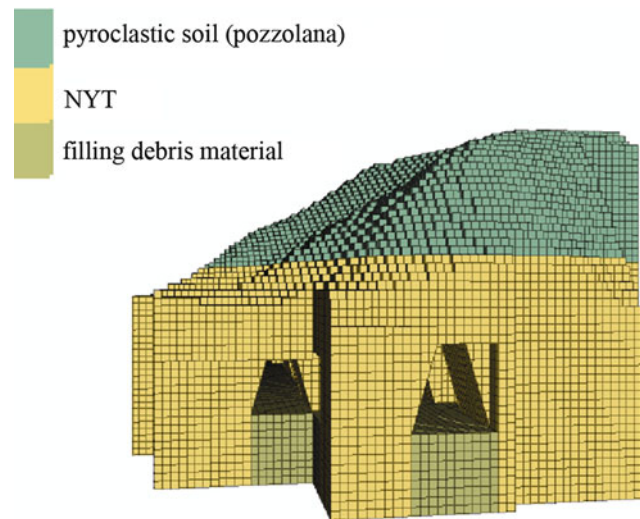
The geometry analyzed was lightly simplified respect to the reality. The Fig. 5.3 reports the structured mesh and the geotechnical model utilized. The elements are square bricks

**Fig. 5.2** Plan of the *Fontanelle* Cemetery and pictures of the entrances **a** plan view; **b** and **c** pictures of the entrance



of 100 cm and u-wedge (of the same dimensions) for the splayed portals for a total of about 300,000 elements. The boundary conditions are fixed displacements at vertical walls in direction normal to the surface and fixed in all direction at

the bottom. This approximation is almost negligible in our case since the low value of Poisson coefficient assumed.



The stratigraphy is made off, starting from the top the hill: pyroclastic loose soil named “pozzolana” and pyroclastic soft rocks, NYT. As mentioned before the floor of the cavity was filled by debris materials during time (Aversa and Evangelista 1998). Moreover the materials have not yet been deeply investigated, especially for the debris that represent a very particular materials, so that the physical and mechanical properties adopted in the calculation are the main value reported in the literature for Neapolitan ones (e.g. Evangelista et al. 2000; Picarelli et al. 2006). At the first time the properties of the intact rock tuff have been assumed for the model. The materials were modelled like elastic–plastic, using a Mohr–Coulomb failure criterion. The physical and mechanical parameters adopted are shown in Table 5.1.

**Fig. 5.3** 3D FLAC model

**Table 5.1** Mechanical properties of materials

Material	$\gamma$ (kN/m <sup>3</sup> )	$\phi$ (°)	c (kPa)	B (kPa)	G (kPa)	$\sigma_t$ (kPa)
Pozzolana	15.0	33	15	1.8e4	7.5e3	4.9
NYT	14.0	29	800	5.0e5	4.2e5	98.0
Debris	13.0	25	7	1.2e4	3.6e3	1.0

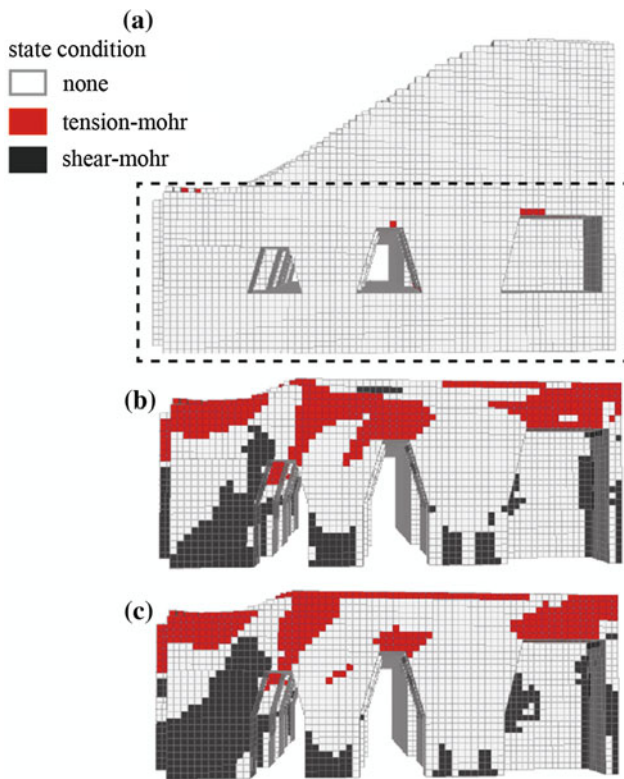
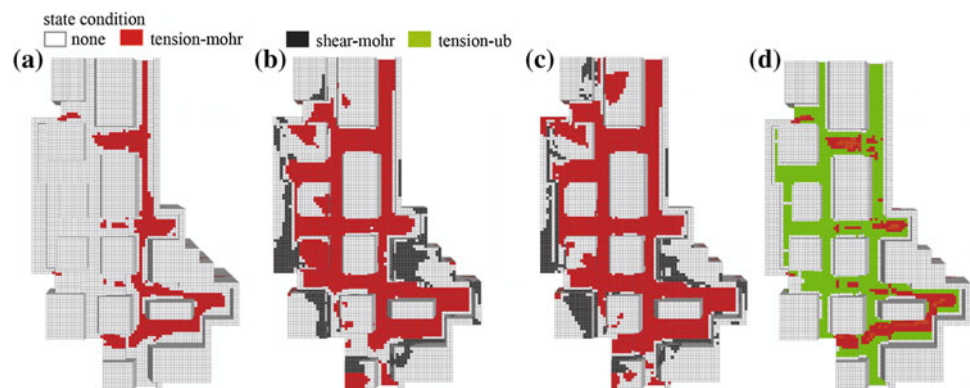


**Fig. 5.4** Plastic point: initial condition (a) and strength reduction methods for the NYT:  $c$  and  $\sigma_t$  (b) all parameters (c)

The strength reduction methods implemented into the code was utilised to investigate the properties of the rock mass and the possible evolution of failure mechanisms. With this procedure the safety factor (FOS) is obtained as the ratio between the rock cohesion and the value of cohesion in correspondence of which it highlights the failure condition as the friction was kept constant. This FOS also coincides with the safety factor in terms of compressive strength. The results of these analyses are reported in Figs. 5.4b and 5.5b. The same approach was utilized for all mechanical properties in order to obtain the possible mechanical parameters for

**Fig. 5.5** Plastic zone: initial condition (a);  $c$  and  $\sigma_t$  reduction (b); FOS conditions (c) and for ubiquitous joint model



an equivalent rock mass. These results were reported in Figs. 5.4c and 5.5c. Figures 5.4 and 5.5 report the distribution of the plastic zones calculated.

The tension plastic zones are concentrated on the roof. At initial condition the portions of the cavity mainly affected by tension failure are the “navata degli appestati” and the “navata dei pezzentelli” (Fig. 5.5a). The vertical stresses at the base of the pillars are lower than compressive strength of the intact rock at initial condition, but during strength reduction method shear failure may occur. These results were compared with that obtained for a ubiquitous joint model reported in di Santolo and Evangelista (2013) (Fig. 5.5d). The plastic points, relative to the initial conditions, are similar to those of Mohr–Coulomb model regarding the failure mechanisms with a wide plasticization in the roof. These results are, also, in agreement with the in situ observations that show the presence of cracks that affects mainly the roof.

## 5.4 Conclusion

A numerical study is presented to evaluate the stress state conditions of the cavity, conducted by the commercial code FLAC 3D Version 5 (Itasca 2012). Through these numerical analyses, it was tried to reproduce the present stress state of the structural components; it was analyzed the sequence of the excavations and the subsequent filling up of the cavity. Two different strength reduction methods was adopted to back-analyzed the mechanical properties of the rock mass, due to presence of a systematic system of joint and due to the lack of their mechanical characterization. The results furthermore show that the critical failure mechanism involved mainly the roof (local collapse) and some pillars in agreement with the observed failure occurred in the past. In order to obtain more reliable quantitative evaluation of the stability condition of this suggestive site a further stage of investigations is necessary.

## References

- Aversa S, Evangelista A (1998) The mechanical behaviour of pyroclastic rock: yield strength and destructureation effects. *Rock Mech Rock Eng* 31(1):25–42
- Scotto di Santolo A, Evangelista A, Evangelista L (2013) The Fontanelle Cemetery: between legend and reality. In: *Proceedings of 2nd international symposium on geotechnical engineering for preservation of monuments and historic sites*, Naples, 30–31 May
- Evangelista A, Feola A, Flora A, Lirer S, Maiorano RMS (2000) Numerical analysis of roof failure mechanism in soft rocks. In: *GeoEng2000*, Melbourne
- Itasca (2012) *FLAC 3D (Fast Lagrangian Analysis of Continua) Version 5.0*. Itasca Consulting Group, Inc FLAC, Minneapolis
- Picarelli L, Evangelista A, Rolandi G, Paone A, Nicotera MV, Olivares L, Scotto di Santolo A, Lampitiello S, Rolandi M (2006) Mechanical properties of pyroclastic soils in Campania Region. In: *Proceedings of international workshop on characterization and engineering properties of natural soils*. Taylor & Francis, London, pp 2331–2383

# Measurement of the Joint Displacement Along Masonry Wall Using Digital Photogrammetry for the Structural Stability of the Borobudur Temple, Indonesia

Tomofumi Koyama, Ichita Shimoda, and Yoshinori Iwasaki

## Abstract

For the preservation and restoration of masonry structures, it is significantly important to evaluate their stability properly and measurement of cracks/joints along masonry walls will be useful to investigate the deformation of masonry structures. In this study, the newly developed crack/joint deformation measurement system using digital photogrammetry was applied to investigate the structural stability of the Borobudur Temple, Indonesia. In the newly developed crack/joint measurement system, a pair of reflective targets is employed at the measurement points around the cracks/joints as gauges and the digital camera image of the targets is obtained by taking photos using digital camera. Employing image processing and photogrammetry, the two dimensional displacement in local coordinates of the cracks/joints can be calculated from digital images of targets. For the site investigation and measurements in the Borobudur Temple, five different joints along the masonry wall (with high possibility for displacement) were selected and monitored. After 8 months of the monitoring, the normal displacement of about 0.6 mm was observed at two of five selected joints and groundwater will play important roles for joint displacement.

## Keywords

Crack/joint measurement • Masonry structures • Borobudur temple • Image processing • Digital photogrammetry

## 6.1 Introduction

Borobudur is believed to be constructed during the late 8th to mid-9th century by the Sailendra dynasty at the middle of Kedu plain of Central Java. This temple was constructed by approximately 55,000 m<sup>2</sup> andesite stone blocks, a dark

volcanic rock, above artificial fill on a natural small hill. Length of the foot of this square temple platform is 120 m on a side. The temple consists of six lower square shape stages, three upper round stages and a bell shape stupa on the top. Top most of the stupa was decorated by a finial. The total height of the temple including this finial is estimated as 42 m (however, the conjectural image of this finial is still under discussion and waiting reconstruction) (see Fig. 6.1). A total of 1,460 Buddhist scriptures and 1,212 decorative relief panels were engraved on the wall of the square six stages, and 432 seated Buddha images were installed in each niche. Furthermore, 72 seated Buddha images were covered in the see-through lattice shaped stupas on the upper round stages surrounds the central main stupa.

Below the andesite structure, a manmade well compacted foundation composed of a mixture of andesite fragments in loamy soil was confirmed in 0.5–8.5 m layers of thickness.

T. Koyama (✉)

Faculty of Safety Science, Kansai University, Osaka, Japan  
e-mail: koyama@geotech.kuciv.kyoto-u.ac.jp

I. Shimoda

Department of World Heritage Studies, Tsukuba University,  
Tsukuba, Japan

Y. Iwasaki

Geo-Reserch Institute, Osaka, Japan

**Fig. 6.1** The Borobudur Temple (after <http://en.wikipedia.org/wiki/Borobudur>)



Three natural hill layers were confirmed under these man-made layers. Uppermost layer of the natural hill is the high permeability loam with andesite chip layer of 2.0–13.5 m in thickness (Horizon A). Second layer is the weathered tuff layer of 0.5–3.5 m in thickness (Horizon B), and third layer is the tuff rock layer (Horizon C).

Bearing capacity is the important index for evaluating the structural stability. The low bearing capacity of the manmade foundation caused uneven settlement throughout Borobudur, and a tendency of the displacement is that the uneven settlement is more predominant than outward sliding. Although there was rain water evacuation through the stepped drainage system of each pyramid stages, displacement of the foundation provoked joint openings and infiltration of the rain water into the platform. Flowing water carried away the foundation soil to the outside of platform, and caused further platform displacement. Against these structural problems, previous restoration work by UNESCO and Indonesian government implemented several countermeasures. A new reinforcement concrete structure was installed between the stone platform and manmade foundation layer in order to support the entire load of platform and upper stone structure. Since 1983, just after the restoration project of UNESCO, several monitoring initiatives were started by the Borobudur Heritage Conservation Office (BHCO) to investigate the stability of masonry structure.

In this study, the newly developed crack/joint deformation measurement system using digital photogrammetry was applied to investigate the structural stability of the Borobudur Temple, Indonesia.

## 6.2 Crack/Joint Measurement Using Photogrammetry: Theory and Methodology

In the newly developed crack/joint deformation monitoring system using photogrammetry, image processing is applied to identify centroids of circles of reflective targets taken on the images (Kanazawa et al. 2012). The reflective targets

were designed with glass beads arranged in circles to induce a strong diffuse reflection of incident light (see Fig. 6.2). There are four circles on each reflective target and the distance of one pair of circles on both sides of the crack is measured. The circles on the target also act as marks for the perspective projection and the change of the distance is interpreted as displacement.

The digital imageries are categorized into two (white and black) areas through binarization based on the threshold of intensity value. The 2-D coordinates of the centroids of the circles is obtained by calculating the center of gravity of white areas for each circle (Trinder 1989). Assuming the  $x$ - and  $y$ -coordinates are  $x = 1-n$  and  $y = 1-m$  in the image coordinate system, the  $x$ - and  $y$ -coordinates ( $x$ ,  $y$ ) of the gauge imageries are calculated by using the following equations.

$$x = x_0 + a_x \frac{\sum_{i=1}^n \sum_{j=1}^m (q(i,j) \times x_{ij})}{\sum_{i=1}^n \sum_{j=1}^m q(i,j)} \quad (6.1a)$$

$$y = y_0 + a_y \frac{\sum_{i=1}^n \sum_{j=1}^m (q(i,j) \times y_{ij})}{\sum_{i=1}^n \sum_{j=1}^m q(i,j)} \quad (6.1b)$$

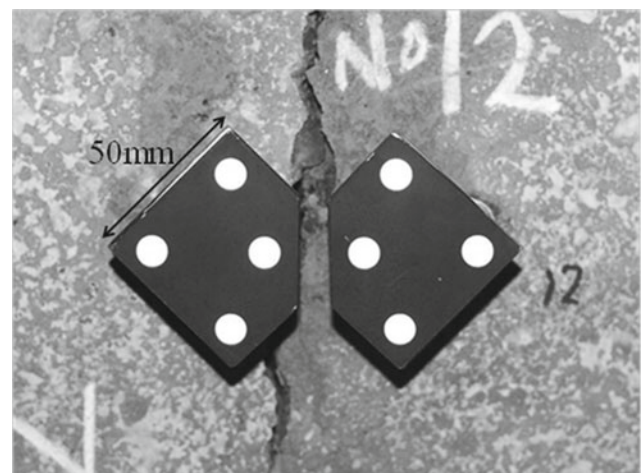


**Fig. 6.2** Reflection target used in digital photogrammetry

where,  $x_0$  and  $y_0$  are the origin of the image coordinate system,  $ax$  and  $ay$  are the pixel size,  $q(i, j)$  is the intensity value of the pixel  $(i, j)$ .

The image seen from the front view of the targets is calculated using the perspective projection (Penna 1991). The perspective projection is based on the collinearity condition, which means that a measurement point, the camera and the measurement point's imagery appearing on the image taken can be connected by a straight line (Ohnishi et al. 2006). The concept of collinearity condition is shown in Fig. 6.3. The Eqs. (6.2a, 6.2b) shows the relation between the  $x$ - $y$  coordinates in the original image coordinate system and the  $x'$ - $y'$  coordinates in the image coordinate system defined in the front view of the targets (see Fig. 6.4). There are eight unknowns in total, namely  $b_i$  ( $i = 1-8$ ). Because Eqs. (6.2a, 6.2b) is established for one known point, at least four known points are required to solve the equation.

$$x' = \frac{b_1x + b_2y + b_3}{b_7x + b_8y + 1} \quad (6.2a)$$

$$y' = \frac{b_4x + b_5y + b_6}{b_7x + b_8y + 1} \quad (6.2b)$$

The  $x$ - $y$  coordinates for the centers of four circles are substituted for  $(x', y')$  in Eqs. (6.2a, 6.2b) and unknown  $b_i$  is obtained by the least-squares method in practice. Finally, the distance between the pair of circles on both sides of the crack is calculated and the change of the distance can be evaluated as the change of crack width and/or crack length.

The procedure of the crack/joint measurement is summarized as follows; (1) the reflective targets are attached around the cracks/joints as gauges, (2) a digital image of the targets is taken from an arbitrary camera position and angle,

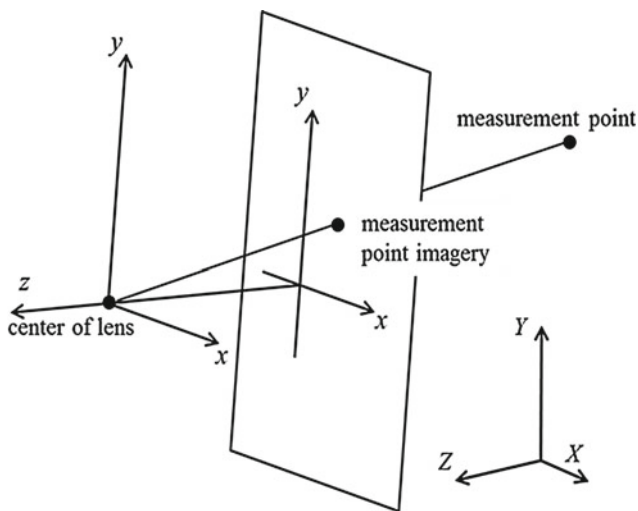


Fig. 6.3 Measurement point means a circle of the reflective targets

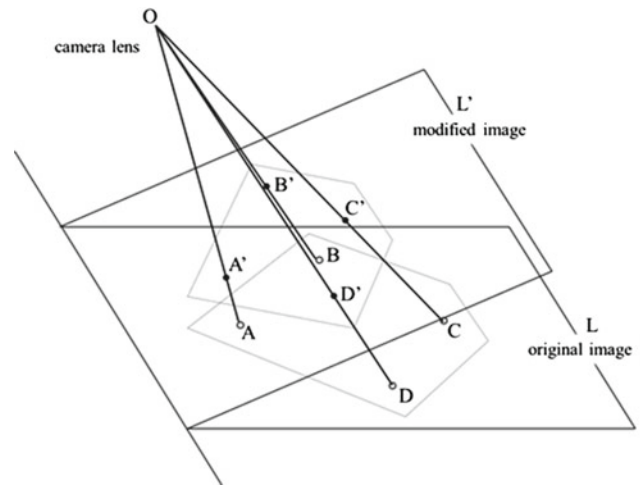


Fig. 6.4 The image  $L'$  from the front view of target is calculated by this perspective projection

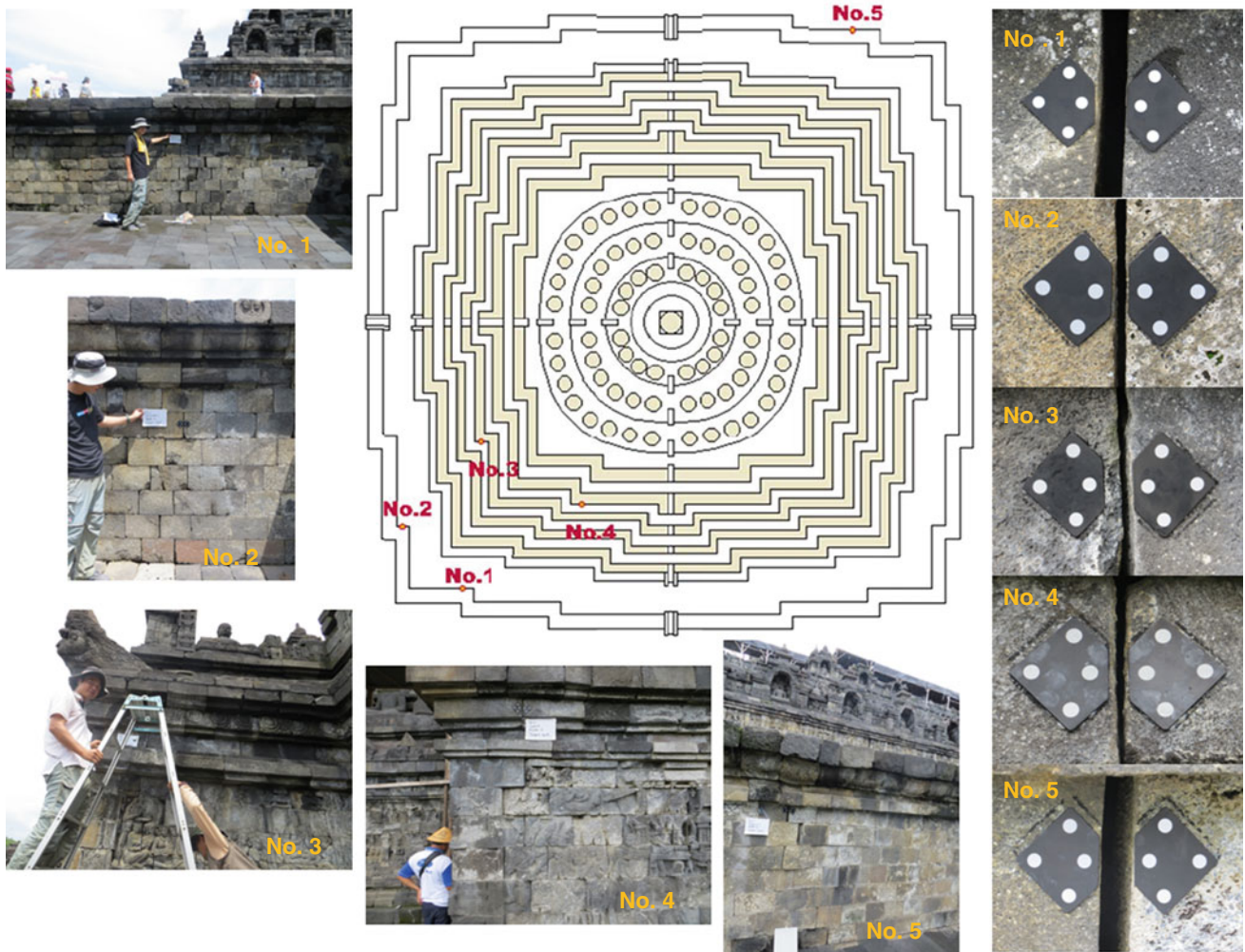
(3) the digital image taken at an arbitrary camera angle is converted to the image facing the target by the perspective projection, (4) the 2-D coordinate values of the centroids of the circles on the image are measured by using the image processing, and (5) the change of the distances between the circles of the targets on the both sides of the crack indicates the displacements in the tensile and shear directions.

The displacement measurement in both normal and shear directions can be measured in the accuracy and precision of about 20  $\mu\text{m}$  when the image is taken 1.0 m away from the cracks/joints (Kanazawa et al. 2012).

### 6.3 Joint Measurement at the Borobudur Temple, Indonesia

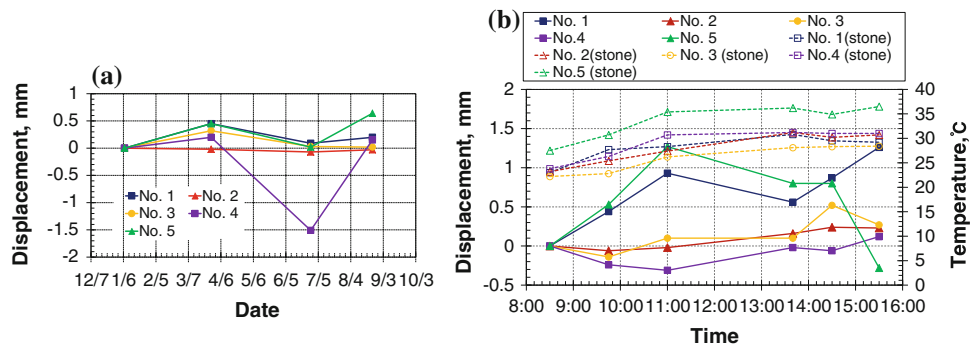
For the site investigation and measurements in the Borobudur Temple, five different joints along the masonry wall were selected at the southwest and northeast corner of the gallery, where relatively large opening was observed (see Fig. 6.5). The joints displacement was measured three times (on 28 March, 28 June and 24 August, 2013). The BHCO is also measuring the joint opening of the lowest platform by the vernier caliper currently and this monitoring is the complementary research. Additionally, the hourly change was also measured once (on 24 August, 2013) to investigate the effect of temperature (measured at the stone surface) on the joint displacement.

Figure 6.6a and b show the monthly and hourly joint displacement for each target, respectively. From Fig. 6.6a, relatively larger joint displacement of more than 0.5 mm was observed at the joint No. 1 and 5. The hourly change of joint displacement is more drastic (see Fig. 6.6b) especially for



**Fig. 6.5** The location of five different joints along the masonry wall in the Borobudur Temple, Indonesia

**Fig. 6.6** The joint displacement for five selected joints (No. 1–5), **a** monthly change (for 8 month) and **b** hourly change with temperature change



joints No. 1 and 5. However, the maximum temperature difference is about 10 °C and the effect of temperature on the joint displacement will be small considering the coefficient of linear expansion of stone. Therefore, some other factors (such as groundwater) may affect the joint displacement and should be further investigated.

### 6.4 Concluding Remarks

In this study, the newly developed crack/joint deformation measurement system using digital photogrammetry was introduced to investigate the structural stability of the Borobudur Temple, Indonesia. Since this system does not

require experts' knowledge/skill for the measurement and electricity like commonly used crack gauge (just attaching the reflective target and taking photos), the measurement can be carried out easily by anybody and the measurement cost is significantly decreased. To increase the accuracy of the measurement, the number of taking photos should be increased (although displacement can be calculated using one photo) and taking photos with different rotation angle of camera is necessary to reduce the effect of lens distortion.

**Acknowledgment** First of all, we would like to express our grateful appreciation to the many experts in the Borobudur Heritage Conservation Office; Mr. Iscandar Muria Siregar, Mr. Nahar Cahyandaru, Mr. Basuki Rachamad, Mr. Brahmantara, Mr. Rony Muhammad, Ms. Ari Swastikawati, Ms. Dian Ekarini, Mr. Panggah Ardiyansyah, Mr. Yudi Suhartono. In addition, we would like to thank to Dr. Hans Leisen, Dr. Esther von Plehwe Leisen, and Dr. Eberhard Wendler who are the project member of the Germany project for conservation of Borobudur. We also would like to express our thanks to Prof. Nishiyama, Okayama University and Dr. Yano, Kyoto University for useful comments and

discussions as well as technical support for photogrammetry. Finally our deepest appreciation to Mr. Nagaoka Masanori and many UNESCO members who gave us the research occasion and coordinate the project in Borobudur.

---

## References

- Kanazawa A, Nishiyama S, Yano T, Kikuchi T (2012) Measurement of the crack displacement using digital photogrammetry for evaluation of the soundness of tunnels. In: Proceedings of GEOMATE 2012, KL Malaysia, paper ID:250, Nov 14–16
- Ohnishi Y, Nishiyama S, Yano T, Matsuyama H, Amano K (2006) A study of the application of digital photogrammetry to slope monitoring systems. *Int J Rock Mech Min Sci* 43:756–766
- Penna MA (1991) Determining camera parameters from the perspective projection of a quadrilateral. *Pattern Recogn* 24(6):533–541
- Trinder JC (1989) Precision of digital target location. *Photogram Eng Remote Sens* 55:883–886

---

# Earth Pyramids: Precarious Structures Surviving Recurrent Perturbations

7

Giovanni B. Crosta, Riccardo Castellanza, Roberto de Franco,  
Alberto Villa, Gabriele Frigerio, and Grazia Caielli

---

## Abstract

Earth pyramids are tall tapered spires, slender or stocky, made of rock or soil material. This type of features have been marginally studied. Even if they are often included in parks and geosites. We start from this lack of studies to analyse the geometrical and physical-mechanical characteristics considering some case studies in northern Italy. Because of their geometrical characteristics these elements are intrinsically weak and can be used as indicators of past external perturbations. We performed laboratory characterization and numerical modelling to analyse the involved actions, the stability and the reaction to dynamic perturbations.

---

## Keywords

Earth pyramids • Hoodos • Characterization • Stability • Modeling • Vibrations

---

## 7.1 Introduction

Earth pyramids, also known as hoodos and fairy chimneys are characteristic tall (from a few meters up to some tens of meters) tapered spires, slender or stocky, made of rock or soil material. In this research we concentrate on these natural earth structures and especially on their appearance typical of the alpine mountainous areas. These elements are formed by a sort of block-in-matrix materials, where the matrix ranges in size from silt to gravel and the large particles reach the size of large blocks up to some meters in diameter. The

matrix is generally incoherent with a slight cohesion associated to a small percentage of clay particles, weak cementation and overconsolidation. In alpine environments they are associated to diamictos, poorly sorted unlithified glacial deposits (moraines, glacial till, lodgment till), transported and deposited by glacial action or mixed action by fluvial and glacial action. These spire-like features are often characterized by a termination which coincides with a large rock block capable to protect the underlying weak column. Earth pyramids are present at various sites and often have been included in parks and geosites (geological, geomorphological or geomorpho sites) because of their exceptional beauty. Notwithstanding this importance in geosites their exceptional features have been marginally studied (Gortani 1906; Kleblsberg 1927; Muller 1932; Schaffer 1932; Scheidegger 1958; Perna 1958) whereas some more attention has been devoted to the formation of rocky hoodos.

Because of their geometry and characteristics, earth pyramids are intrinsically sensitive to external perturbations. In particular they can be subject to direct runoff erosion along the basal topography or the pyramid stem, or to seismic shaking and other meteoric actions. As a consequence their stability can provide some useful information about the recurrence time of perturbations as well as about their magnitude.

---

G.B. Crosta (✉) · R. Castellanza · A. Villa · G. Frigerio  
Department of Earth and Environmental Science, Università di  
Milano Bicocca, Piazza della Scienza 4, 20126 Milan, Italy  
e-mail: giovannibattista.crosta@unimib.it

R. Castellanza  
e-mail: riccardo.castellanza@unimib.it

R. de Franco · G. Caielli  
Institute for the Dynamics of Environmental Processes, National  
Research Council of Italy (IPDA-CNR), Via Mario Bianco, 9,  
20131 Milan, Italy  
e-mail: roberto.defranco@idpa.cnr.it



**Fig. 7.1** Location and aspect of the earth pyramids in Zone (BS)

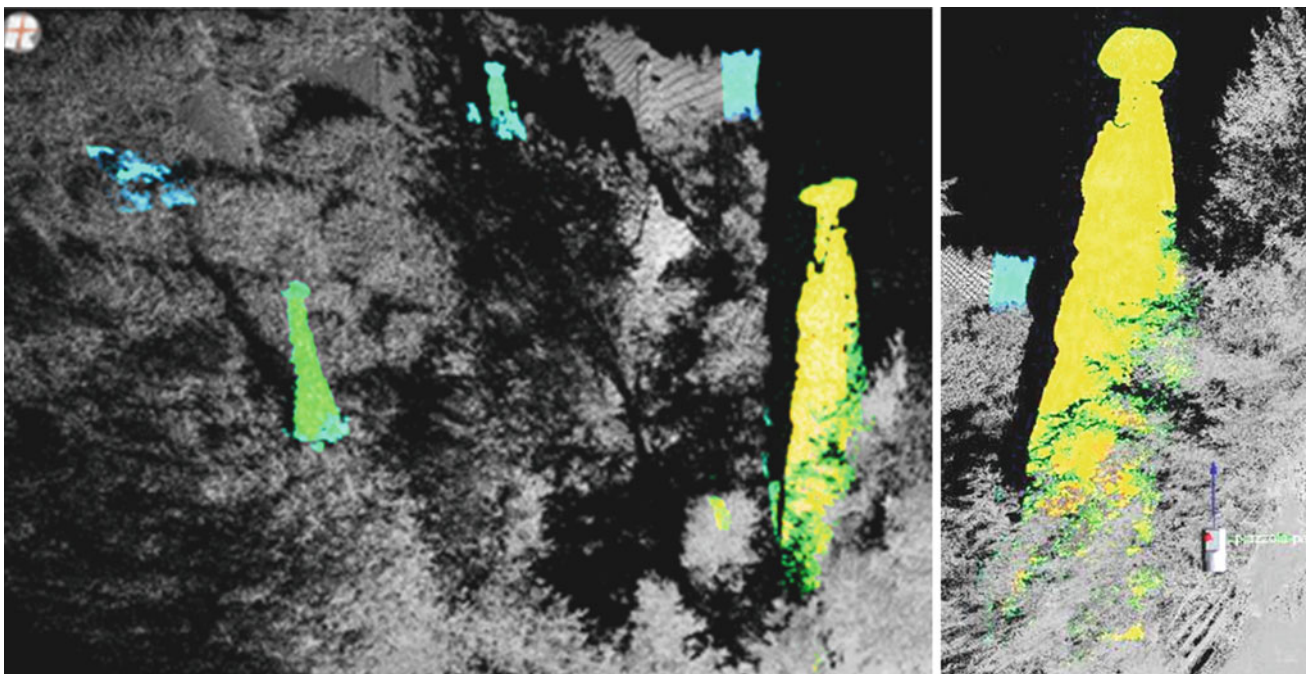


**Fig. 7.2** Example of TLS 3D model for site 1 (Zone), on the *right* the pyramid n°1: height 26.75 m, maximum diameter 9.5 m and minimum diameter 1.85 m

To improve the knowledge about these features we performed a series of topographic surveyings and sampling campaigns at different sites to characterize the morphology and the physical-mechanical properties of the forming

materials. In situ geometrical description and ambient noise measurements have been completed at different sites evaluating the changes in seismic spectra along several profiles.

**Fig. 7.3** Grain size distribution for the three sites

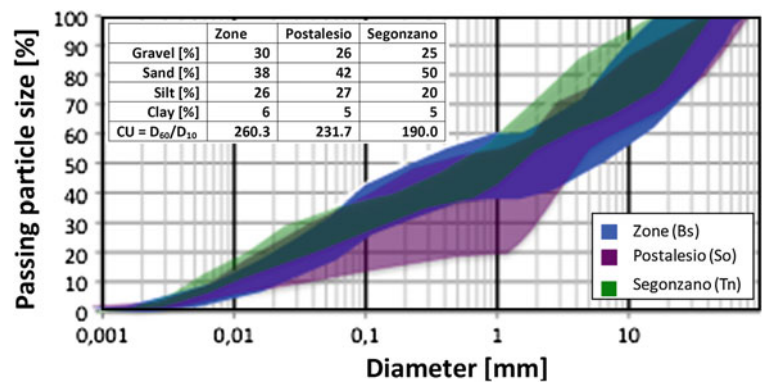
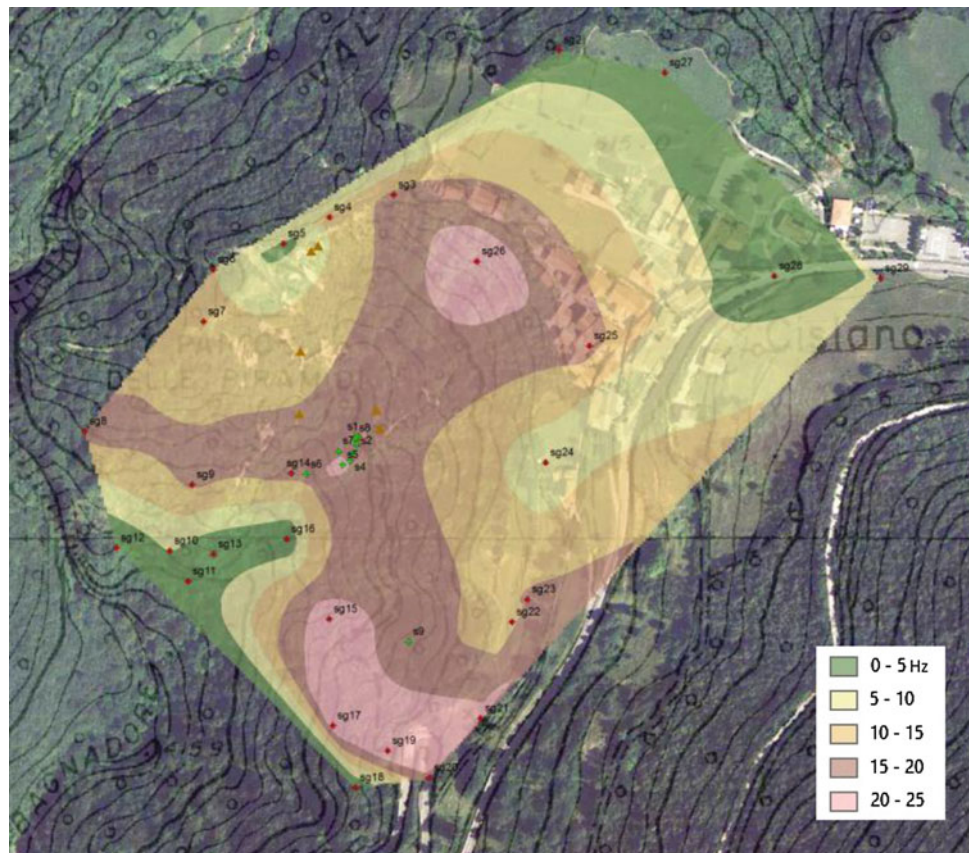


**Fig. 7.4** Ground natural frequency maps for site 1 (Zone (BS))



## 7.2 In Situ Surveyings

Three sites, in the Central Italian Alps (Zone (Fig. 7.1), Segonzano, Postalesio) have been considered in the present work. By performing a series of detailed TLS surveys it has been possible to detect with enough accuracy the 3D shape both of the earth pyramids and the surrounding topographic surface (see Fig. 7.2).

For each site a sampling campaign has been performed in order to characterize the granulometric size distribution of the block-in-matrix materials and direct shear test on the matrix forming the earth pyramids. As shown in Fig. 7.3 the matrix is made of a well graded soil with relevant fractions of gravel, sand, silt and clay typical of diamictites.

Geophysical in situ investigations included a detailed noise measurements performed by using a digital mobile seismic station (Lennartz M24) equipped with triaxial velocimeter (Lennartz 5 s). The data acquired with SESAME (Haghshenas et al. 2008) procedure were analyzed in the

**Fig. 7.5** Ratio H/V of spectral amplitudes along alignment 2 (site 1) (inset for alignment position; *dot line* are the station point positions)

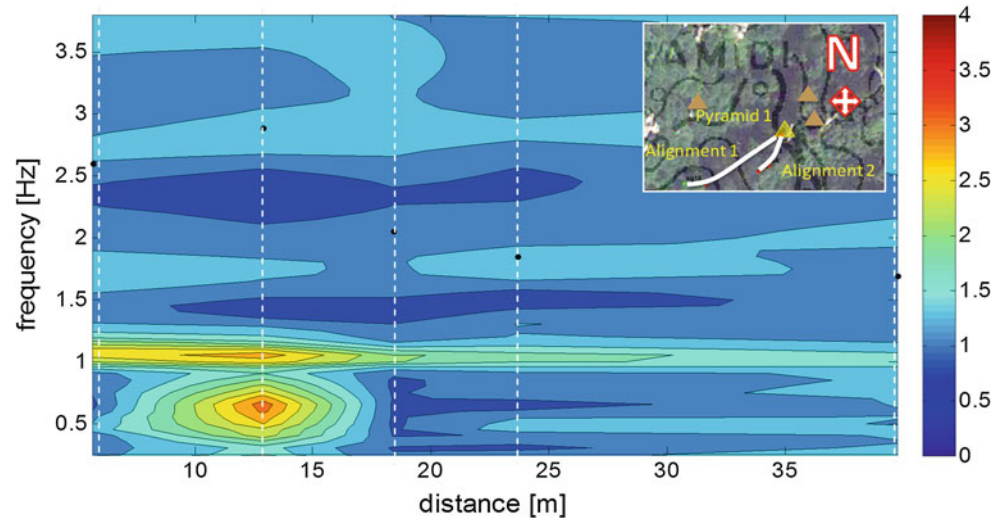
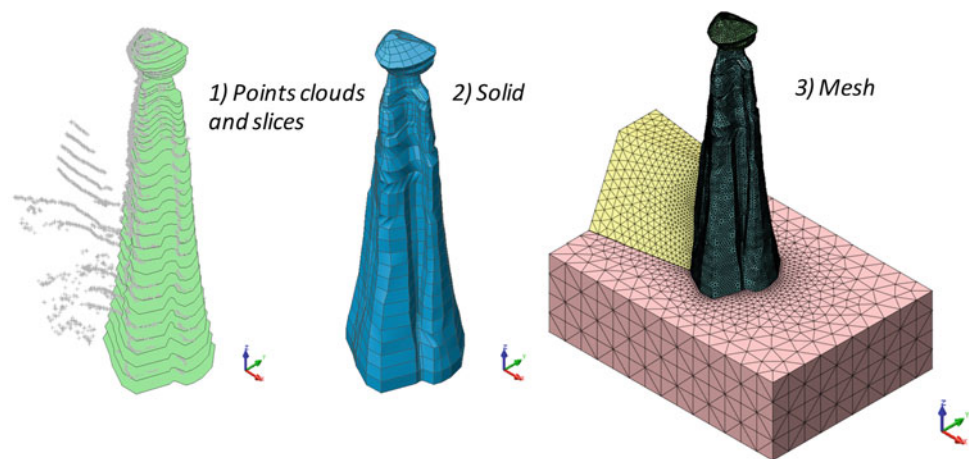


**Fig. 7.6** Example of 3D mesh for earth pyramids 1 at Zone



frequency domain in order to obtain the natural frequency of the subsoil deposit on which the earth pyramids are resting on and the depth of the soil-bedrock interface using the Nakamura methods (1989). Figure 7.4 is a map of the natural frequency for the site 1 (Zone).

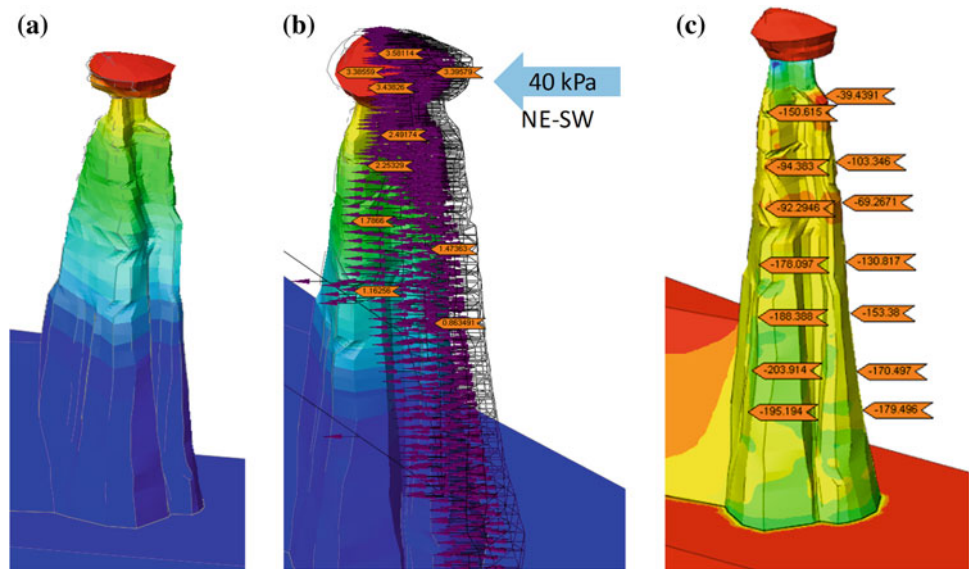
In order to evaluate the natural frequency of the pyramids and to verify the real source of the micro-tremors we performed a series of micro-tremors measurements along two alignments (shown in Fig. 7.5) with acquisition points at different distances from the pyramid base. The results are shown as contour plot of H/V spectral ratio as a function of distance from the pyramid base in the low frequency range (0.5–4 Hz) (see Fig. 7.5). A marked peak at 1.2 Hz is observed and a clear attenuation is recorded beyond the distance of 30 m from the pyramids base. This frequency is assumed to be the dominant vibration frequency of pyramid 1.

### 7.3 Numerical Modelling

Both analytical and numerical analyses have been performed on the earth pyramids model. An example of 3D numerical analyses performed for pyramid 1 at Zone is shown. In Fig. 7.6 the adopted 3D mesh derived from the TLS geometrical model presented in Fig. 7.2.

Performing an analysis of the Eigen-values the stiffness of the block-in-matrix material has been back-calculated obtaining a mode 1 natural frequency equal to 1.2 Hz. A Young modulus  $E$  equal to 0.6 GPa and a Poisson ratio  $\nu$  equal to 0.25. In Fig. 7.7a for the displacements the mode 1 at 1.2 Hz are shown. Once the stiffness parameters of the block-in-matrix materials have been estimated a static analyses with a pressure load equivalent to a wind action close to the maximum recorded in the area was performed. As a results an horizontal displacement of 3.6 mm at the top

**Fig. 7.7** Example of eigenvalue analyses and time history analyses



of the pyramid have been evaluated (Fig. 7.7b). In Fig. 7.7c the vertical stresses are depicted, with a maximum value of about 800 kPa estimated at the contact between the top block and the column. This examples show a possible deterministic approach for evaluating the behavior of earth pyramids when subjected to environmental loads (wind or earthquakes actions).

## 7.4 Conclusion

Vibration of these column like features have been examined. We suggest the possible use of earth pyramids to evaluate the level of maximum ground acceleration typical of the sites that could have occurred during the lifetime of such structures. In fact, such delicate features can be found in alpine areas characterized by weak to moderate seismicity. Analytical solutions as well as 3D finite element numerical simulations have been performed to analyze their stability and the required characteristics to resist typical local perturbations. A series of numerical analyses have been

performed to evaluate the stresses generated taking into account environmental loads.

## References

- Gortani M (1906) Le piramidi di erosione ed i terreni glaciali di Fielis in Carnia. *Mondo Sotterraneo*, a. II, n. 5–6, pp 75–81, tav. 1, 1 cartina, Udine
- Haghshenas E, Bard PY, Theodulidis N (2008) SESAME WP04 team empirical evaluation of microtremor H/V spectral ratio. *Bull Earth Eng* 6(1):75–108
- Klebelsberg RV (1927) Beitrage zur Geologie der Sudtiroler Dolomiten. I. Ruckzugstande der Eiszeitgletscher in den Dolomitentalern. *Zeits. Der Dt. Geol. Ges.*, Bd. 79, n. 3, pp 280–337
- Muller W (1932) Die Entstehung der Erdpyramiden. Dolomiten, 18 Juli 1932, Bolzano
- Schaffer FX (1932) Uber die Erdpyramiden am Ritten bei Bozen. *Verhandlungen d. Geol. Bundesanstalt*, n. 11–12, pp 163–165, Vienna
- Scheidegger (1958) A physical theory of the formation of hoodoos. *Pure appl Geophys* 41(1):101–106
- Perna G (1958) Le piramidi di terra di Segonzano e del Renon. *Natura Alpina*, a. IX, n.1, pp 3–7, fig 4, tav.1, Trento
- Nakamura Y (1989) A method for dynamic characteristics estimation of subsurface using microtremor on the ground surface. *Q Rep RTRI* 30(1):25–33

---

# Evaluation of the Stability of Underground Cavities in Calcarene Interacting with Buildings Using Numerical Analysis

8

Matteo Oryem Ciantia, Riccardo Castellanza, Claudio di Prisco, Piernicola Lollino, Jose Antonio Fernandez Merodo, and Gabriele Frigerio

---

## Abstract

Soft and highly porous rocks such as calcarenites are very common in all Mediterranean region. Due to their porous calcareous structure these rocks are prone to water induced weathering mechanisms. Natural onshore and inland underground cavities are evidence of such phenomena. The collapse of cliffs and underground cavities is usually the long-term result of a complex hydro-chemo mechanical process taking place at the micro-scale. Experimental results mainly give evidence of: (a) a marked and instantaneous reduction in strength and stiffness for these porous rocks when macro-pores are filled with water, (b) a slow successive reduction in strength and stiffness occurring in the long-term due to dissolution processes; (c) a more pronounced weakening of the rock material as a consequence of wetting and drying cycles. In the present work a methodological path to cope with deterministic assessment of the stability of natural and anthropic caves will be presented. The following steps will be adopted: (i) experimental study: execution of an experimental campaign to identify the physics of the processes taking place at both the micro-scale and the macro-scale; (ii) theoretical study: extend the concept of strain hardening-non mechanical softening to the time evolution of  $c$ - $f$  reduction; (iii) numerical study: present the 3D numerical results of a real case-study showing the capability of the proposed methodology to cope with risk assessment in complex geomechanical situations concerning weathering, as for underground cavities.

---

## Keywords

Weathering • Soft-rocks • Numerical modelling • Risk assessment

---

M.O. Ciantia (✉)

Universitat Politècnica de Catalunya-BarcelonaTech, C. Jordi Girona, 31, Barcelona, Spain  
e-mail: matteo.ciantia@upc.edu

R. Castellanza

Università degli studi Milano Bicocca, Piazza della scienza 4, Milan, Italy  
e-mail: riccardo.castellanza@unimib.it

C. di Prisco · G. Frigerio

Politecnico di Milano, Piazza Leonardo da Vinci 32, Milan, Italy  
e-mail: claudio.diprisco@polimi.it

---

P. Lollino

CNR-IRPI, Via Amendola 122/I, Bari, Italy  
e-mail: p.lollino@ba.irpi.cnr.it

J.A.F. Merodo

Geological Hazards Group, Instituto Geológico y Minero de España, c/Ríos Rosas, 23, 28003 Madrid, Spain  
e-mail: jose.fernandez@igme.es

## 8.1 Introduction

Formations of calcarenite are common in many regions of Mediterranean coast. These are affected by weathering processes induced by a chemo-mechanical degradation of the rock mass in contact with water. In the southern part of Italy the number of karstic and manmade caves, excavated within the underground environment, are remarkably high, thus producing significant risk conditions for the population and the local economy. A large number of failures of both natural underground caves and anthropic cavities (Parise and Lollino 2011; Vattano et al. 2012) have been registered in the recent decades. The sinkhole that developed in the urban center of Gallipoli in 2007 (Fig. 8.1a) is an exceptional example that motivates the authors in their research activity.

The factors that govern the changes of rock masses around caves prior to failure are of multiple natures. For karstic caves, the changes mainly depend on the hydro-chemo-mechanical processes inside the rock mass and therefore generally develop in the long term. For man-made caves (Fig. 8.1b), instead, failures frequently occur just few years after the end of the extraction works as a consequence of: (i) the low strength of the rock, (ii) variations of either geometrical or loading conditions around the cave, (iii) creep phenomena, (iv) degradation, with time of the rock properties due to weathering processes (Ciantia et al. 2012, 2013). To cope with weathering processes affecting the calcarenites of either natural or anthropic structures, the authors have undertaken the following research activities: (i) an experimental study for defining at both micro and macro scales the weathering processes; (ii) a theoretical study for developing a constitutive model suitable for reproducing the previously

identified degradation processes; (iii) a numerical study for making available a numerical tool for analyzing boundary value problems. In the present work a synthesis of both experimental and theoretical studies is reported.

## 8.2 Modelling Weathering: A Hydro-Chemo-Mechanical Process

Calcarenites are sedimentary soft rocks formed by the cementation of calcareous grains originally unbonded. The grains, with an organogeous origin, are calcareous shells. At the death of the animals the shells are accumulated at the bottom of the same marine environment in which they were formed. By means of an exhaustive set of 2 and 3D micro-investigations the microstructure (Ciantia et al. 2014a) two different types of bonds between grains were recognized: (i) the diagenetic bonds (DG in Fig. 8.2), identified as the bonds formed during diagenesis and composed by  $\text{CaCO}_3$ ; (ii) the second type of bonds, named depositional bonds (DP in Fig. 8.2), is composed by less densely packed material formed by small calcite micrograins held together by microscopic calcite crystals.

This explains the lighter color of these bonds when observed with an optical microscope. Often, a bond is the result of the superimposition of these two types of microstructures, as the surface of diagenetic bonds is usually covered by a layer of loosely packed microcrystals. It was observed (Ciantia et al. 2014a) that this double bonding nature explains the macroscopic behavior of the material when inundated with water. In particular the short term debonding (STD) is the result of the inundation process:

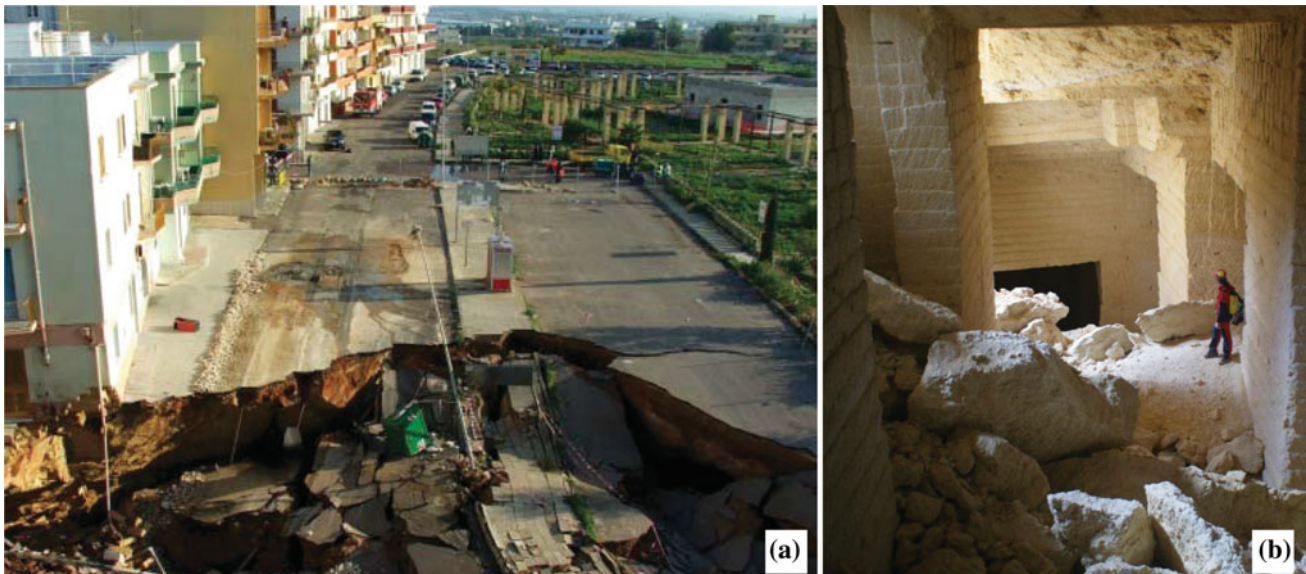


**Fig. 8.1** a Sinkhole in Gallipoli due to the collapse of an anthropic cave (Polimeno 2007), b partial collapse underground cavities in Canosa di Puglia

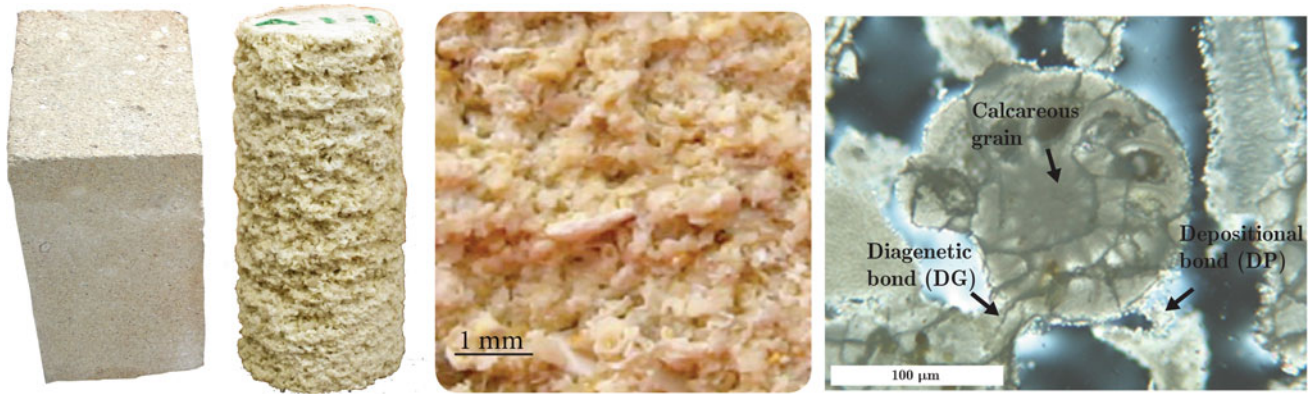


**Fig. 8.2** From left to right: block of calcarenite, cylindrical sample, surface photograph and typical thin-sections obtained where diagenetic bond (DG) and depositional bond (DP) are clearly visible

water penetrates through the porous structure, damages the depositional bonds causing an instantaneous drop in strength and stiffness. On the other hand the long term debonding (LTD) is the result of the chemical dissolution of diagenetic bonds taking place when calcarenite is flooded by water for a long period of time. The driving variable of this two hydro microscale weathering mechanisms were found to be the normalized suspended mass,  $\zeta_{sus}$ , and dissolved mass,  $\zeta_{dis}$ , respectively (see Ciantia et al. 2014b). In this work the concept of non-mechanical softening driven by the two latter mentioned scalar quantities ( $\zeta_{sus}$  and  $\zeta_{dis}$ ) introduced by Ciantia et al. (2013) using a multiscale approach, is extended to the practical methodology of the  $c$ - $\phi$  reduction numerical technique (Griffiths and Lane 1999; Aliguer et al. 2013). This allows us to obtain a physical time evolution of the safety factor. In fact it was found that the evolution of the yield locus due to the weathering mechanism could be described by the two scalars  $\zeta_{sus}$  and  $\zeta_{dis}$  (Fig. 8.3a). Since the latter two are function of saturation degree,  $S_r$ , ionic concentration of chemical species in the bulk fluid and dissolution kinetic constants, a direct relationship between strength and time can be obtained if the hydraulic problem is solved. As explained by Ciantia and Hueckel (2013) the worst scenario is the one described by a rapid saturation and consequent fresh water recycle. Under these conditions the suspended mass turns to depend only on the saturation time and the dissolution kinetics only. Henceforth, using specific weathering experimental test results that describe the strength evolution with  $S_r$ , for the STD and time for the LTD (Fig. 8.3b), it is possible to build the  $c$ - $\phi$  reduction coefficient—time abacus for calcarenite (Fig. 8.3c). Consequently the classical  $c$ - $\phi$  reduction numerical analysis combined with the just presented abacus enables to build a safety factor ( $F_s$ )-time graph.

### 8.3 3D Numerical Analysis for the Risk Assessment of a Cavity

In order to describe the methodology presented in the previous section a representative case study of a man-made cave excavated in a calcarenite deposit in the urban area of Canosa di Puglia (Southern Italy) is here presented. The complex 3D geometry concerning the interaction of cave excavated about two centuries ago within a calcarenite deposit belonging to the “Calcarenite di Gravina” formation and a 4 storey building (Fig. 8.4).

The questions at hand are (i) what is the current safety factor of such a complex ground-structure interaction problem and (ii) how does it evolve if the rock-mass undergoes the STD and LTD weathering mechanism? The commercial code MIDAS GTS was used to perform the 3D numerical analyses. Laboratory experimental tests on the intact and artificially weathered material extracted in site were performed in order to calibrate the elastic-perfectly plastic Mohr-Coulomb constitutive model was adopted for the FEM simulations. In this way, as explained in the previous section, using the abacus in Fig. 8.3c to each reduced  $c$ - $\phi$  run a predicted time to that corresponding level of damage is obtained (Fig. 8.5).

### 8.4 Conclusions

In this paper a methodological approach for hazard assessment of underground caves affected by rock weathering has been described. The hydro-chemo-mechanical mechanisms occurring at the micro scale level were identified by means of

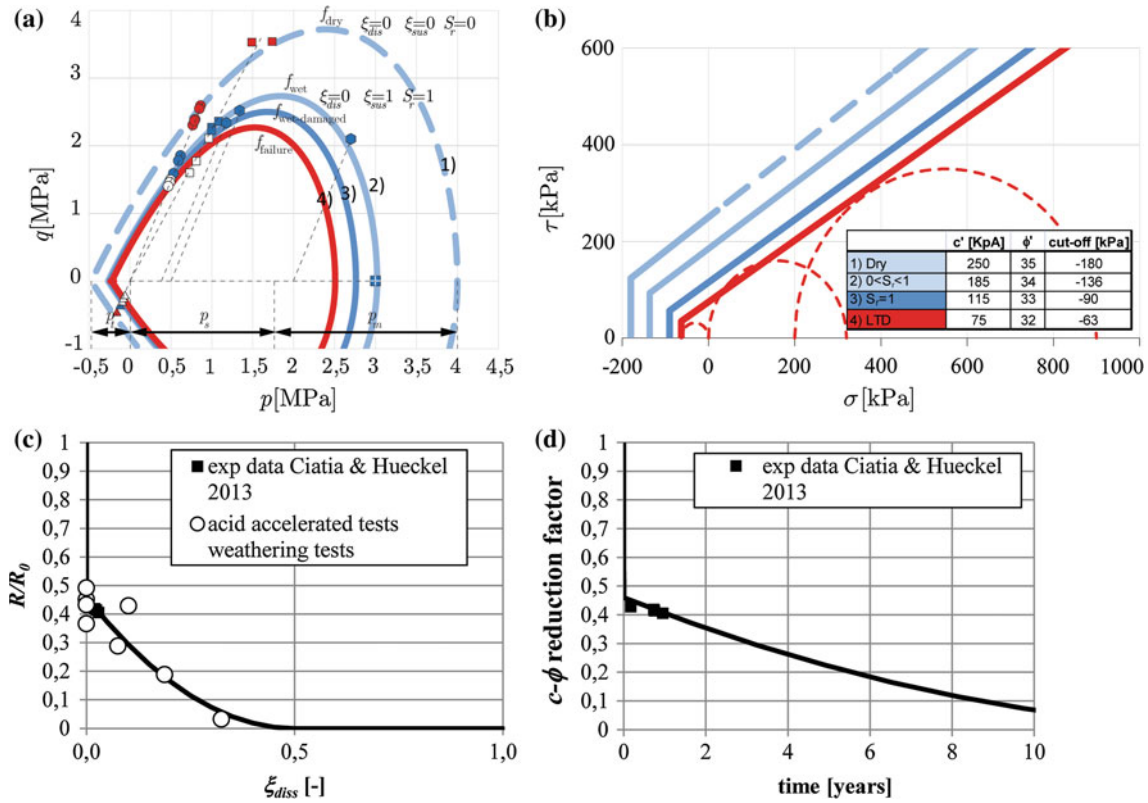


**Fig. 8.3** a Yield locus evolution with  $\xi_{sus}$  and  $\xi_{dis}$  for a closed surface strain hardening plasticity model, b extension of yield shrinkage due to weathering effect to  $c-\phi$  reduction, c evolution of strength with  $S_r$  and  $\xi_{dis}$  and d corresponding  $c-\phi$  reduction factor in function of time

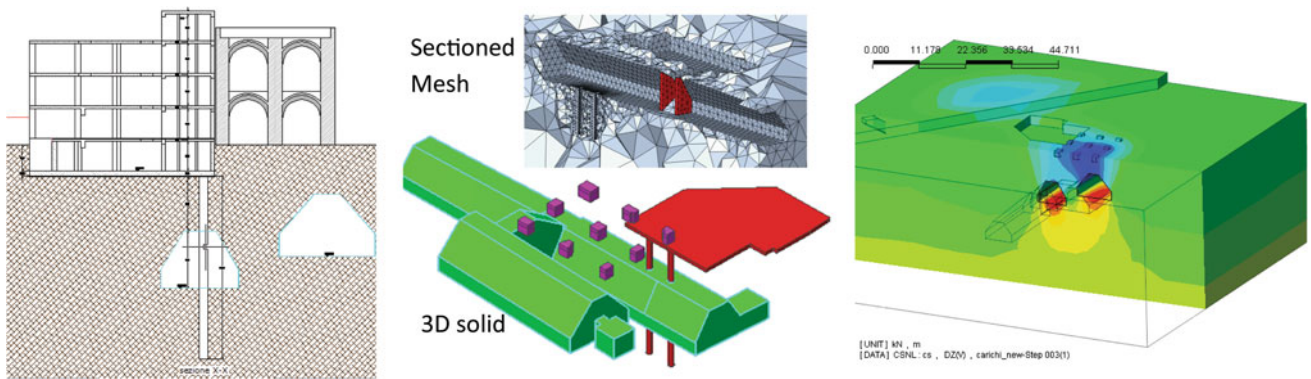


**Fig. 8.4** From left to right: Cross section of the model, 3D numerical reconstruction of the cavity and vertical displacement field of one of the simulations

specific experimental tests. In the worst weathering scenario, degree of saturation and dissolution kinetics constants were found to be the driving variables of the non-mechanical component of weathering. The concept of extended hardening laws used in advanced constitutive models was extended

to the classical  $c-\phi$  reduction methodology. The final result is a  $c-\phi$  reduction—time abacus that allows in a very practical manner to predict the weathering induced time evolution of the safety factor of very complex ground-structure interaction problems.

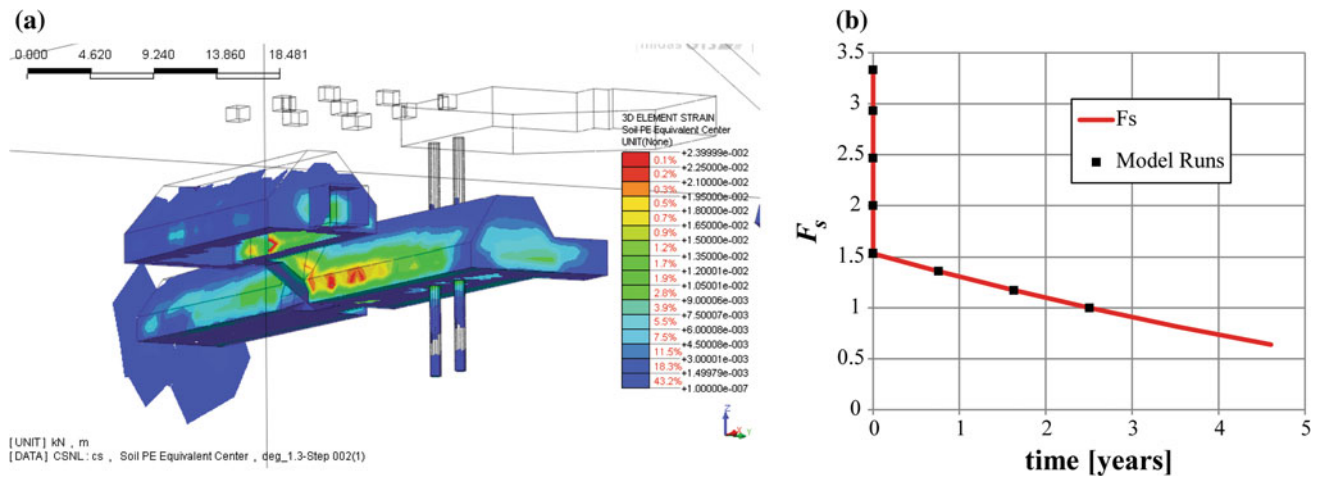


**Fig. 8.5** a Equivalent plastic strain contour fill and b predicted safety factor time evolution

## References

- Aliguer I, Carol I, Alonso EE (2013) Numerical analysis and safety evaluation of a large arch dam founded on fractured rock, using zero-thickness interface elements and a  $c$ - $\phi$  reduction method. *COMPLAS XI*:1233–1243
- Ciantia MO, Castellanza R, di Prisco C, Hueckel T (2012) Experimental methodology for chemo-mechanical weathering of calcarenites. In: Laloui L, Ferrari A (eds) *Multiphysical testing of soils and shales*. Springer, Berlin, pp 331–336
- Ciantia MO, Hueckel T (2013) Weathering of submerged stressed calcarenites: chemo-mechanical coupling mechanisms. *Géotechnique* 63(9):768–785
- Ciantia MO, Castellanza R, di Prisco C (2013) Chemo-mechanical weathering of calcarenites: experiments and theory. In: *Coupled phenomena in environmental geotechnics* (ads Manassero et al). Taylor & Francis, London, pp 541–548
- Ciantia MO, Castellanza R, Hueckel T, Crosta G (2014a) Mineral suspension and dissolution: their role in weakening of inundated soft carbonatic rocks. *Eng Geol* (submitted)
- Ciantia MO, Castellanza R, di Prisco C (2014b) Experimental study on the water-induced weakening of calcarenites. *Rock Mech Rock Eng*. doi: [10.1007/s00603-014-0603-z](https://doi.org/10.1007/s00603-014-0603-z)
- Griffiths DV, Lane PA (1999) Slope stability analysis by finite elements. *Géotechnique* 49(3):378–403
- Parise M, Lollino P (2011) A preliminary analysis of failure mechanisms in karst and man-made underground caves in Southern Italy. *Geomorphology* 134:132–143
- Polimeno A (2007) Il crollo di via Firenze in Gallipoli. *l'intervento dei vigili del fuoco*, *Geologi e Territorio*, 4-2006/1-2007, 13–19 (in Italian)
- Vattano M, Audra P, Bigot JY, De Waele J, Madonia G, Nobécourt JC (2012) Acqua Fitusa Cave: an example of inactive water-table sulphuric acid cave in Central Sicily. In *Rend. Online Soc Geol It* 21:637–639

# Estimation of Hydraulic Environment Behind the Mogao Grottoes Based on Geophysical Explorations and Laboratory Experiment

Koizumi Keigo, Oda Kazuhiro, Ito Misae, Piao Chunze, Tanimoto Chikaosa, Iwasaki Yoshinori, Yoshimura Mitsugu, Wang Xudong, Guo Qinglin, and Yang Shanlong

## Abstract

There is moisture movement under the ground as a factor contributing to salt damage at the arid regions. Some parts of wall paintings of the Dunhuang Mogao Grottoes, which is a World Heritage site, have been seriously damaged by the crystallization of salts. This damage is likely to have been caused by short-term factors such as rainwater and flooding, and a long-term factor, namely, groundwater movement. In order to preserve the grottoes, it is important to know the relationship between underground moisture and salts. The purpose of this study is to understand the moisture content and salinity in conglomerate layers behind the Mogao Grottoes by the geophysical explorations and laboratory experiment. The resistivity characteristics of the field sample focused on water saturation with salinity were determined by laboratory tests. By obtaining the distribution of water saturation from the electric resistivity method in the study site, the moisture content in the ground was estimated. To confirm the reliability of the estimation, RI-density log was implemented. These results indicate there is relationship between the hydric environment and salinity concentration in each depth behind the Mogao Grottoes.

## Keywords

Stone heritage • Electrical resistivity • Moisture environment • Salinization

K. Keigo (✉) · O. Kazuhiro · I. Misae  
Osaka University, 2-1 Yamadaoka, Suita, 565-0871 Japan  
e-mail: koizumi@civil.eng.osaka-u.ac.jp

P. Chunze  
Hytec Geotechnical Consultant, 2-11-9 Miyahara, Yodogawa-ku,  
Osaka, 532-0003 Japan

T. Chikaosa  
Earth Watch Corp, 1-10-206 Toyotsu, Suita, 564-0051 Japan

I. Yoshinori  
Geo Research Institute, 4-3-2 Itachibori, Nishi-ku, Osaka,  
550-0012 Japan

Y. Mitsugu  
Soil and Rock Engineering, 2-21-1 Shonaisakaemachi, Toyonaka,  
561-0834 Japan

W. Xudong · G. Qinglin · Y. Shanlong  
Dunhuang Academy, Dunhuang city, China

## 9.1 Introduction

The Dunhuang Mogao grottoes are located 25 km southeast of Dunhuang City. The grottoes were excavated over about 1,000 years, from 366 A.D., and extend about 40 m in height and 2 km in north–south length. Presently, 492 caves, 2,400 painted sculptures and 45,000 m<sup>2</sup> of mural are preserved; additionally, the grottoes were registered as a World Heritage site in 1987.

The Mogao grottoes were cut into the western cross section of a cliff that resulted from the erosion of the old fan deposits by the Daquan River. The grottoes were basically formed by the reasonable consolidated conglomerate layer which can be excavated by human-beings (Kuchitsu and Duan 1992).

The present cliff is divided into five layers: Q<sub>2</sub>A–D and Q<sub>3</sub>. The upper layer (Q<sub>3</sub>) consists of unconsolidated conglomerate and forms the upper portion of the grottoes. The lower layer (Q<sub>2</sub>) is formed by conglomerate consisting of old

fan deposits. Most of the caves are within the Q<sub>2</sub>C and Q<sub>2</sub>D layers, although a few are within the Q<sub>2</sub>B layer.

Recrystallization of soluble salts can be observed owing to the particular desert conditions surrounding the Mogao grottoes, and likely occurs as a result of evaporation of water that became loaded with salt when the surrounding rock reacted with fluids such as rainwater. Such processes cause salt damage in the caves, resulting in the deterioration or collapse of murals as a result of recrystallization of the soluble salts. Salt damage is observed mostly on the ceiling of a cave in the upper layer and is confirmed at the bottom of side wall of a cave in the lower layer. The movement of water (rainwater and floodwater in the upper and lower layers, respectively) may dissolve salt within the ground. Salt damage has occurred in more than 70 caves in the grottoes and is an issue that must be addressed in order to preserve the grottoes.

To prevent salt damage to the walls of the caves, it is necessary to elucidate the movement of water and soluble salts in the ground around the Mogao grottoes. Moisture behavior in the area can be classed as short term (e.g., rain, flood) or long term (e.g., groundwater). In order to elucidate the mechanisms of the salt damage, this study is intended to estimate moisture conditions, especially salinity, in the ground behind the Mogao grottoes. First, electrical resistivity distribution within the cliff of the grottoes is measured in the field by electrical survey. However, because there are abundant soluble salts in the ground, it is difficult to estimate moisture conditions based on the resistivity distribution without considering soluble salts. Therefore, the characteristics of the electrical resistivity distribution are examined by laboratory experiments focusing on relationship between the degree of water saturation and the salt content by using filed samples. Finally, the moisture conditions of the ground are estimated by converting the resistivity distribution into distribution of water saturation using the results of the laboratory experiments.

## 9.2 Electrical Resistivity Distribution

Electrical resistivity was measured at the top of the cliff of the Mogao grottoes. A borehole was located at a point 150 m west of the Nine-story Pagoda that is the landmark feature of the grottoes. The borehole reached a depth of 120 m. The two-pole method was carried out. Figure 9.1 shows the measurement results, and Fig. 9.2 illustrates a cross-sectional view showing Line100gake and LineV100. It is clear that the electrical resistivity is higher for shallow ground than for deep ground. In particular, a lower resistivity zone of about 45  $\Omega$  m exists at 40–80 m depth; additionally, the higher resistivity zone in the vicinity of 100 m depth appears to be a localized phenomenon. A lower resistivity zone can be seen over the

caves in Line100gake. Accurate measurement of resistivity was impossible in the section between LineV100 and Line100gake because the steel wires for the environmental stations were buried in the ground. The results of this measurement indicated that a lower resistivity zone, which may affect the caves, is present at the back of the Mogao grottoes.

## 9.3 Characteristics of Electrical Resistivity of Local Samples

In this study, moisture conditions in the ground behind the Mogao grottoes are estimated from electrical resistivity distribution measured by field survey. In general, electrical resistivity changes under the influence of various elements; therefore, it is important to interpret the resistivity distribution by laboratory tests. In this section, we discuss the relationship between electrical resistivity and water saturation using field samples.

### 9.3.1 Methods

Experiments were conducted in the laboratory to elucidate the relationships between electrical resistivity and water saturation of field samples under changing salt concentration. The samples are conglomerates which were collected near the Mogao grottoes. First, salts contained in the samples were leached by filtering with distilled water. Then, salts were impregnated by injecting aqueous solution that dissolved the certain quantitative saturated salt into the samples leached salts. While gradually drying samples, resistivity and weight measurements of the samples were repeated several times. The experiment was conducted based on four patterns: Case-A calculated the average value of all samples; twice amount of Case-A in Case-B; Case-C gives the

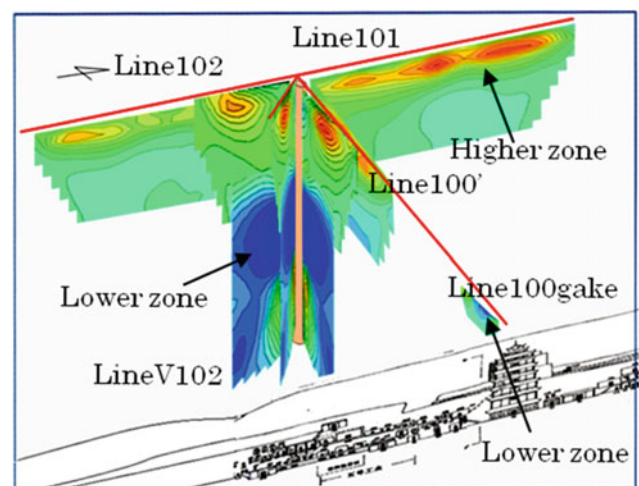
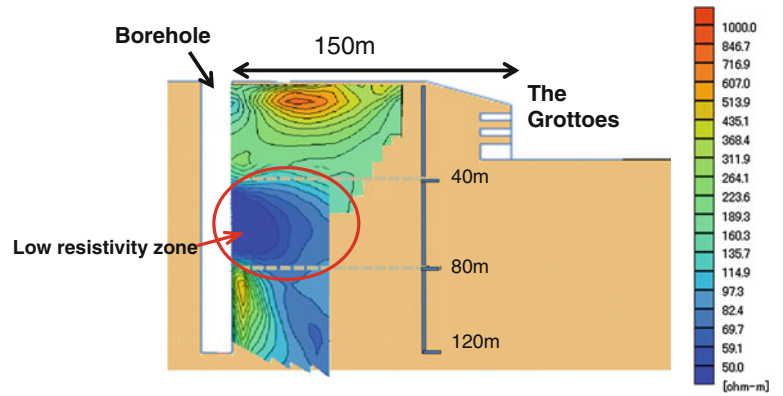


Fig. 9.1 Results of measurements

Fig. 9.2 Cross-sectional view



maximum value of all samples; and Case-D provides the upper limit, i.e., the maximum amount of salt that was detected in aqueous solution in pore water.

9.3.2 Results and Discussion

The measurement results are shown in Fig. 9.3; the black-framed inset of Fig. 9.3 is shown in Fig. 9.4. Electrical resistivity increased gradually with increasing degree of saturation, increasing rapidly when the degree of saturation became less than 10 %. The resistivity changes were small in the range of high water saturation; however, with increases in salt impregnation, the lower resistivity is indicated. For resistivity of 45 Ω m (i.e., the lowest resistivity obtained in field measurements), Case-B exhibited saturation of 100 %, Case-C a saturation of 85 %, and Case-D a saturation of 55 %. The lowest resistivity zone, in the ground behind the Mogao grottoes, exhibited resistivity of 45 Ω m; therefore, the possibility that the degree of saturation is at least 55 % (i.e., conversion ratio of NaCl is  $16.7 \times 10^{-3}$ ) was confirmed.

9.4 Moisture Conditions Behind the Grottoes

This section estimates moisture conditions in the area behind the Mogao grottoes based on the results of Sect. 9.3. The resistivity distribution in the field survey was converted into two types of water saturation distributions using the results of laboratory experiments.

Figure 9.5 illustrates the distribution of water saturation. Figure 9.5a shows the distribution of water saturation reflecting the ground environment of Case-B, while Fig. 9.5b shows the distribution of water saturation reflecting the ground environment of Case-D; it is clear that the degree of water saturation is higher in Case-B than in Case-D. These figures cover the same range of resistivity distribution, and the difference in the amount of soluble salts is reflected in the distribution of water saturation. Moreover, for 50–100 m depth, the degree of saturation is 100 % for Case-B and 55 % for Case-D. Near the top of the caves, the degree of saturation is 60.1 % for Case-B and 46.6 % for Case-D.

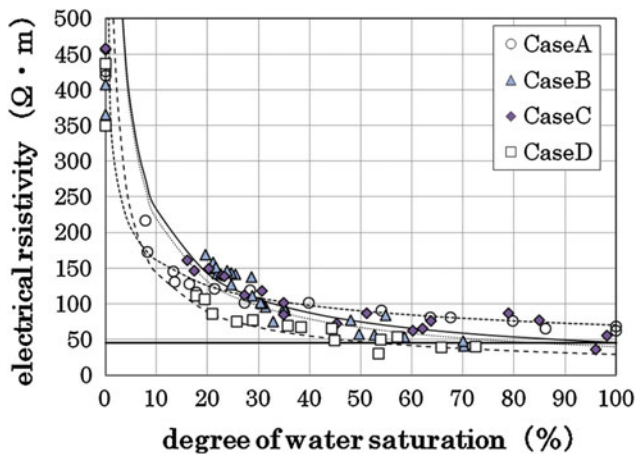


Fig. 9.3 Measurement results

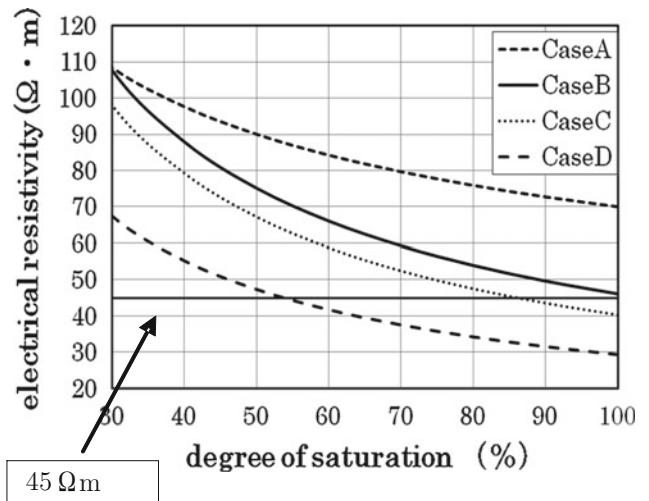
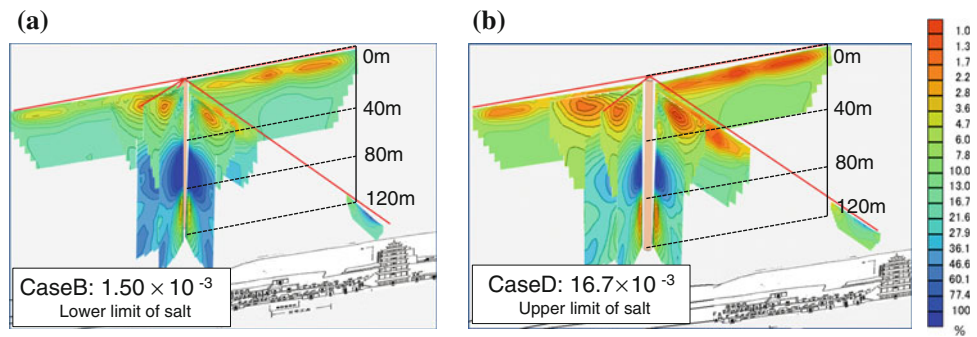


Fig. 9.4 Inset lower resistivity zone

**Fig. 9.5** Distribution of water saturation. **a** *Case-B* lower limit of salt. **b** *Case-D* upper limit of salt



## 9.5 Estimation of Moisture Environment of the Ground Behind the Grottoes by RI-Density Log

RI-density log is carried out to evaluate the results obtained by the electrical resistivity in the borehole and the results of the lab experiments. Figure 6 shows the result of saturation. The evaluation was not intended in the casing part from G.L.0 to 30 m. The degree of saturation which is the depth from 40 to 80 m corresponds with the low resistivity zone obtained by the electrical resistivity method. The peaks of saturation in the section indicate from 55 to 60 %. The result corresponds with the result when salinity becomes maximum.

## 9.6 Conclusions

The resistivity distribution behind the Mogao grottoes was measured by the field surveys, and lower resistivity zones were confirmed at 40–80 m depth and on the top of the caves. In subsequent laboratory experiments, the resistivity characteristics of the field samples with respect to changing water and salt concentrations were identified, and the resistivity distribution derived from the field survey was converted into a distribution of water saturation using the results of laboratory experiments. The results indicated that deep ground is subject to relatively high water saturation

compared to shallow ground. The degree of saturation was more than 55 % when electrical resistivity was  $45 \Omega \text{ m}$ , which was the lowest resistivity measured in the field; therefore, the low resistivity in the surrounding ground is likely to indicate at least 55 % water saturation. The results obtained by the electrical resistivity method correspond with the result of RI density log. In conclusion, water saturation is relatively high at 40–80 m depth, indicating that moisture behind the Mogao grottoes would be exerting an influence on the caves. Our next research should be clarified how to control the moisture movement to the caves through the on-site monitoring.

## References

- Adachi K (2001) Study of water distribution by resistivity measurement Dunhuang Mogao Grottoes. In: 56th annual meeting of J.S.C.E, pp 642–643
- Kitano Y (1994) The chemical composition of land waters in the Dunhuang area and of evaporites in various desert areas of China. *Sci Conserv* 33:1–26
- Kuchitsu N, Duan X (1992) Geological environment of the Dunhuang Mogao-Grottoes, Gansu Province China. *Sci Conserv* 31:79–80
- Miyazaki T, Nishimura T (2011) *Soil physical experimentation*, vol 103. University of Tokyo Press, Tokyo, pp 95–96
- Tanimoto Y (2007) The state of water and salts in the Dunhuang Mogao Grottoes. In: 36th Symposium on Rock Mechanics, pp 141–146

Yukiyasu Fujii, Kunio Watanabe, Takaharu Shogaki, and Katsuhiro Kikuchi

---

## Abstract

Digital documentation by photogrammetry was applied to the Yokosuka Arsenal dry dock No. 1, which is established in 1871. Vertical and horizontal sections near the gate can be generalized from digital surface model of the dock. Leakage of seepage seawater from the joints of building stones can be identified on both sides of the walls near the gate of the dock. However, the vertical section on the southern wall had been deformed compared to the one on the northern wall. This deformation might be caused from deformation of backfill materials or underground geological sediments. Geological sediments inside the northern wall is Pleistocene, however it is Holocene inside the southern wall, depend on the geomorphological map before construction of the dock. In addition, the southern wall of the dock was collapsed and repaired in 1879. Therefore, it is estimated that geo-technical underground condition of the northern side is better than the southern side of the dock near the gate.

---

## Keywords

Deformation • Pleistocene sediment • Backfill material • Building stone • Seepage water

---

## 10.1 Introduction

There are six dry docks in the United States Naval Base, Yokosuka city, Japan (Fig. 10.1). Three of them, from No. 1 to No. 3, have been constructed with building stones. The oldest one is dry dock No. 1 which had been constructed from 1867 to 1871 under the supervision of French engineers, Verny and Florent. It is one of the most important

constructions in Japan, because it's the oldest dry dock with building stones. In addition, its construction methods and techniques have been applied to the following construction of Japanese dry docks.

During the excavation of mount Hakusen for the construction of the dry dock No. 1, an animal bone had been discovered. A German geologist, Professor Heinrich Edmund Naumann, studied and identified it as a species of elephants. And he named it "Naumann elephant", which is one of the exterminated elephants. Therefore, the underground is composed of Pleistocene mud sediments. It was suffered from 1923 Great Kanto earthquake. However, there was no serious damage by the earthquake in the dock.

The dry dock No. 1 is still in use today. However, the surfaces of building stones have been weathered by seawater and winds. In addition, water leakage from the joints of the building stones can be identified in some areas near the gate. It is needed to survey the stability of the dock to prepare for the future great earthquake. Therefore, digital documentation by photogrammetry was conducted to the dock near the gate.

---

Y. Fujii (✉)

Fukada Geological Institute, Tokyo, Japan  
e-mail: fujii@fgi.or.jp

K. Watanabe

Geosphere Research Institute, Saitama University, Saitama, Japan

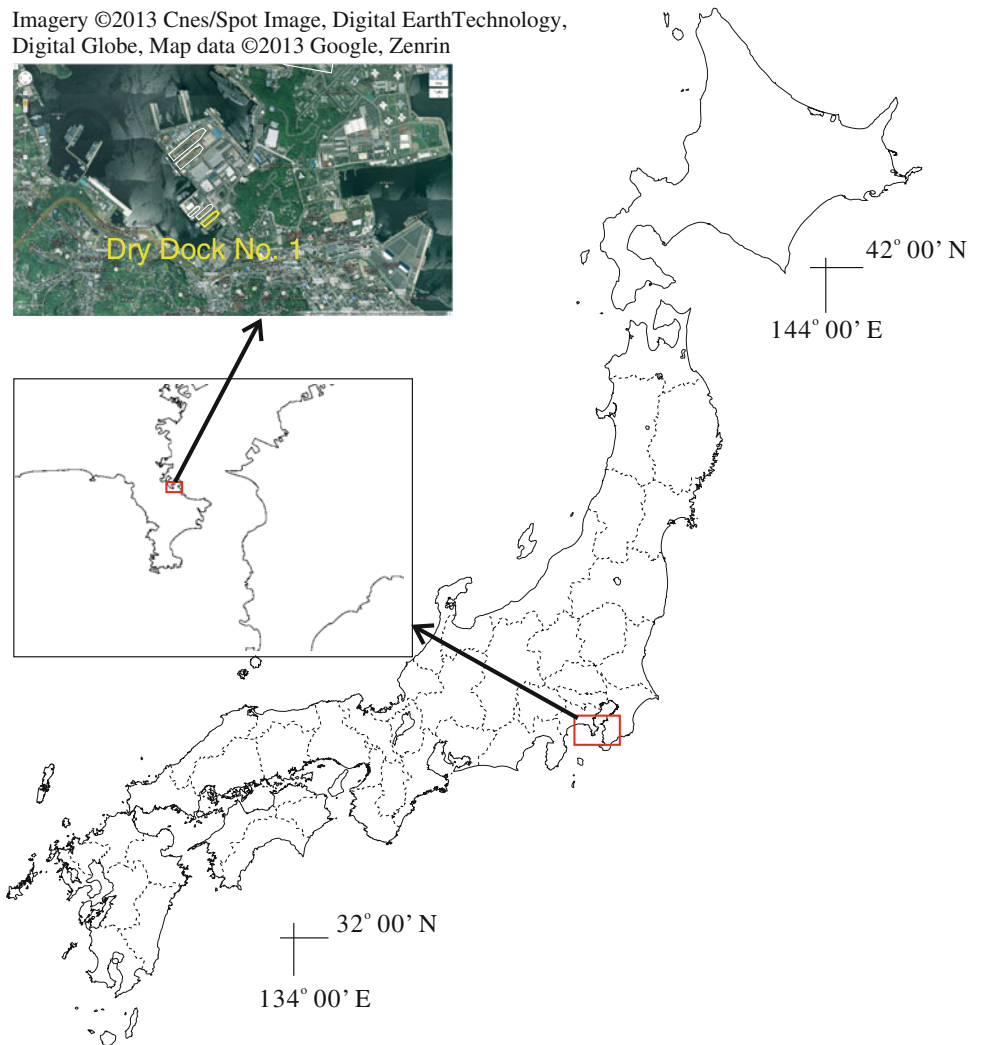
T. Shogaki

National Defense Academy of Japan, Yokosuka, Japan

K. Kikuchi

Yokosuka City Museum, Yokosuka, Japan

**Fig. 10.1** Location map of the Yokosuka Arsenal dry dock No. 1, in United States Naval Base, Yokosuka city, Japan



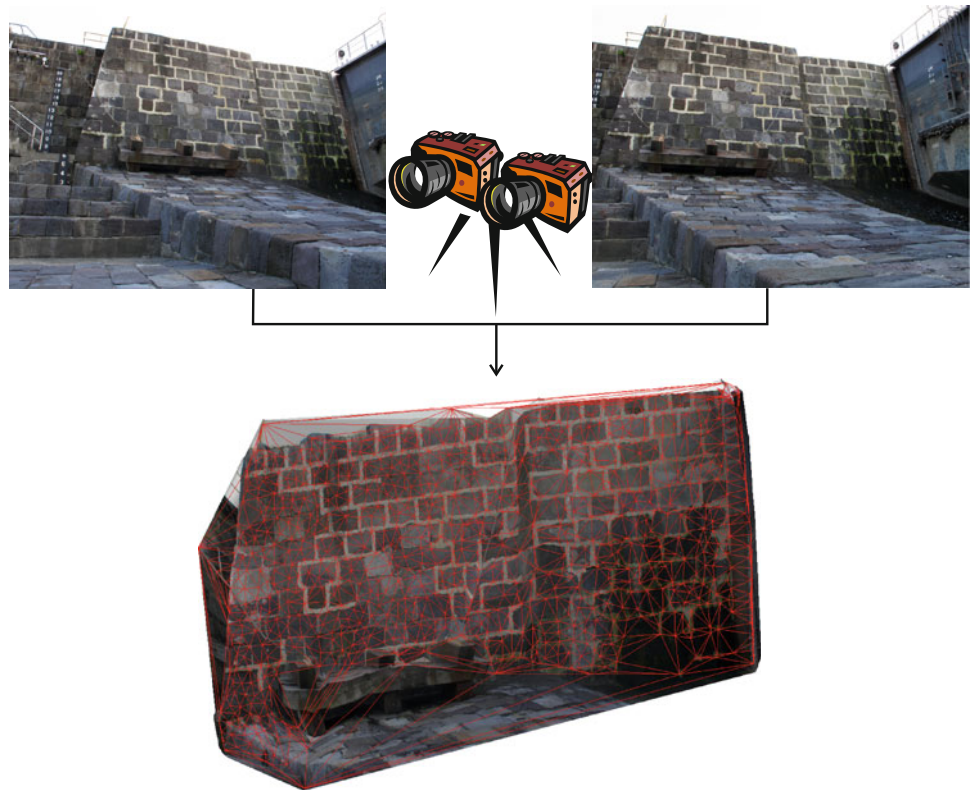
## 10.2 Photogrammetry

Photogrammetry is a science measuring objects on photographs (Linder 2003). Obviously, a single photograph has only two-dimensional information, as it is a two-dimensional plane. If two photographs of the same object are taken from different directions and positions, a stereoscopic picture is formed and three-dimensional (3-D) information of the object can be gain. The photographs are called as a pair of stereo-photographs. Historically, photogrammetry has been used to construct topographic maps from stereo-photographic pairs of aerial photographs. This technique can also be applied to close-range mapping with a hand-held camera (Atkinson 2003).

Three-dimensional mapping of the dry dock No. 1 near the gate was carried out by means of close-range digital photogrammetry. Nineteen pairs of stereo-photographs were taken from different positions. Using the pairs of stereo-photographs, three-dimensional morphology of the dock can

be constructed (Fig. 10.2). Data for camera positions and directions when taking the photographs are used to get the three-dimensional information. However, it is very difficult to get accurate positions and directions at the same time when taking the photographs. Before taking the photographs, many control points were put on the walls of the docks. Coordinates of the control points essential to the photogrammetric evaluation were determined by the use of a geodetic Total Station (TS). The camera positions and directions can be inversely calculated from the control points by means of a least squares adjustment. 3-D digital photogrammetric software was employed to calculate the camera positions and to get 3-D information on the surface of the dock. The results of photogrammetric survey will be shown as a perspective view of three-dimensional surface model of the dock (Fig. 10.3). The model is composed of triangle irregular network with texture mapping (photo image). The dock has about 140 m long, 30 m width and 9 m depth. The model covers about 30 meters long from the gate. Blue plane shows Tokyo Peil (T.P.: average sea-level of Tokyo Bay),

**Fig. 10.2** A pair of stereo-photographs was taken in the dock with hand-held stereo-camera (*upper*). And a digital surface model (*lower*), which is constructed with triangle irregular network (*red line*), was generated by photogrammetric software



and red lines show two vertical cross sections and two horizontal cross sections on the wall.

### 10.3 Results

After making three-dimensional surface model of the dry dock No. 1, some vertical and horizontal cross sections can be created in the software. The vertical section on the

northern wall near the gate, which is right side from a view point of inside of the dock, is almost straight. However, the vertical section on the southern wall is curved a little (Fig. 10.4). Therefore, the southern wall near the gate is a little deformed and expanded into the inside of the dock.

About horizontal cross sections, their formations are complicated compare to vertical ones. About the closest part to the gate, the cross-sections are curved with round shape. Such formations can be recognized on both north and south

**Fig. 10.3** Perspective view of three-dimensional surface model of the dry dock No. 1, near the gate. This model was combined with 19 different digital surface models (Fig. 10.2 lower shows one model). *Blue surface* shows seawater surface about T. P. = 0 m. *Red lines* show vertical and horizontal cross sections on the wall inside the dock. *Straight lines* are on the northern wall, and *break lines* on the southern wall. The width of the dock (the length of gate) is about 25 m

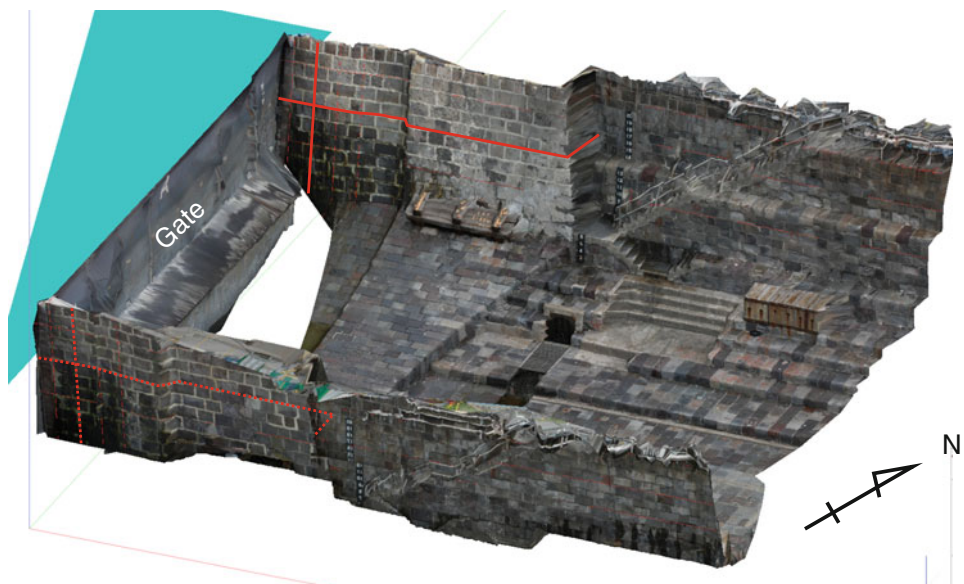
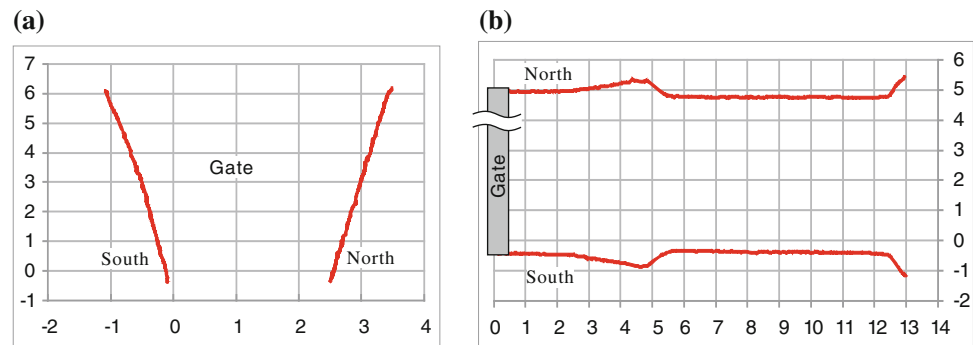


**Fig. 10.4** Vertical (a) and horizontal (b) cross sections generated from Fig. 2.2. Figures have a scale marked in meters. Notice that horizontal scales are exaggerated about two times for vertical sections (a)



walls of the dock near the gate. Therefore, this is not deformed one and it may be original designed formation.

## 10.4 Discussion

Only the southern wall near the gate is deformed and expanded a little into the inside of the dry dock No. 1. This deformation might be caused by the different condition of geology around the dock. Dry dock No. 1 was constructed after the excavation of Mount Hakusen which was composed of Pleistocene mud sediments. Old geomorphological map,

before the construction of the dock, shows that the axis of the dock was almost parallel to the ridge of Mount Hakusen. In addition, the northern wall near the gate was located in the middle of Mount Hakusen, and the southern side was located near the surface of Mount Hakusen (ARSENAL D'IOKOSKA 1869). Therefore, geological sediment inside the northern wall is Pleistocene. However it might be Holocene inside the southern wall. In addition, the northern wall of the dry dock No. 1 was collapsed in January, 1879 (Fig. 10.5). The wall was repaired next month (JACAR 1879). Therefore, it is estimated that geo-technical underground condition of the northern side is better than the southern side of the dock near the gate.

Seawater leakage can be identified on both sides near the gate in the dry dock No. 1. Seawater is leaked from the joints of building stones. Therefore seawater might be come through the backfill materials as seepage water. The amount of the leakage seawater in the other dry docks constructed with stones, for example No. 2 and 3, is not so much compare to the dry dock No. 1. This difference might be caused by the different design of the docks near the gate. The walls of both sides near the gate in the dry dock No. 1 are gradually curved from the gate to about 5 m locations (Fig. 10.4). This formation cannot be recognized in the other dry docks in Yokosuka Naval Base. This design formation is estimated to be ease to concentrate strain around the gate in the dock. This might be another important problem for the stability of the dock.

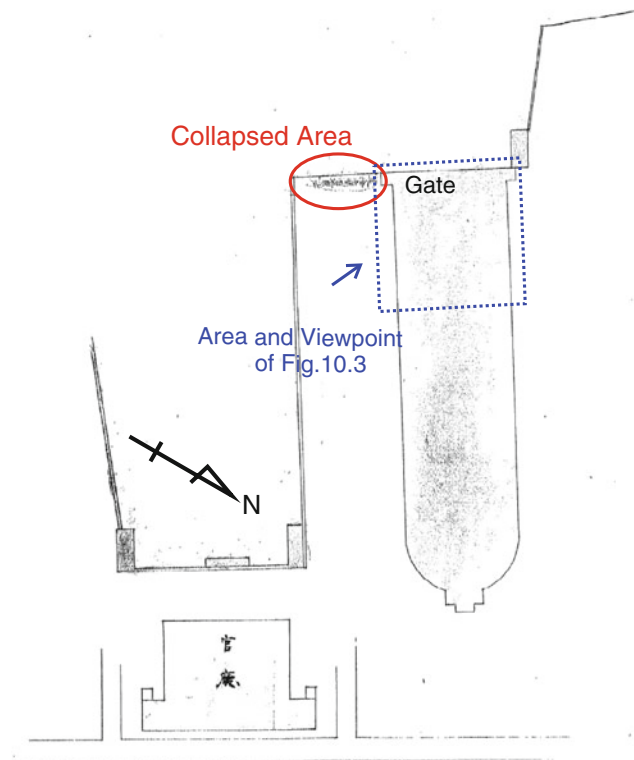


**Fig. 10.5** Collapsed area of the southern wall in the dry dock No.1. Modified form JACAR (1879)

## 10.5 Summary

The dry dock No. 1 in the United States Naval Base, Yokosuka city Japan, was documented by photogrammetry. Some water leakage from the joints of building stones can be identified in some area near the gate. In addition, a little deformation can be recognized on the southern wall near the gate. Future research, for example measurement of water

leakage, more study from the viewpoint of design formations and borehole survey near the gate, will be needed for the study of stability of the dry dock No. 1.

**Acknowledgment** This research is one of the productions by the academic committee on the technical evaluation of historical structures constructed during and after the Edo era, The Japanese Geo-Technical Society Kanto branch. We acknowledge support from the U.S. Naval Base Yokosuka for this research.

## References

- Atkinson KB (2003) Close range photogrammetry and machine VISION. Whittles Pub, London, p 384
- Linder W (2003) Digital photogrammetry theory and applications. Springer, Berlin, p 189
- ARSENAL D'IOKOSKA (1869) Plan general indiquant la situation des travaux en avril (construction map written in French)
- JACAR (Japan Center for Asian Historical Records) (1879) Ref. C09112825300

---

**Part II**

**Engineering Geology and Preservation  
of Cultural Heritage**

---

# Engineering Protection of the Territory, Monitoring and Safeguarding of the Immovable Cultural Heritage of the Historical Centre of Kiev

11

Yuriy Maslov

---

## Abstract

The substantial part of the historical centre of Kiev with the architectural heritage located in the zones of a geological risk, i.e. zones of the development of the dangerous natural and technogenic processes. The town-building activity without taking into account the geological risk can considerably decrease the effectiveness of the efforts for the heritage conservation. The problem is that to the risk decrease and to increase the heritage stability and the steady existence of the objects with a common infrastructure. At the basis of the concept is stated a forestall strategy, a monitoring of the surrounding and the heritage objects with use of the contemporary technologies. There are represented the special features of the program—purposive approach to the solution of the problem of the preservation and conservation of the architectural heritage at the urbanized territory under the conditions of the increasing ecological and technogenic risk of the geological environment. The distinctive special feature of this approach is a consideration of the significant role of the upper lithosphere for the stability of the bases of the architectural heritage and the ground-based technosphere of the city.

---

## Keywords

Safeguarding • Heritage • Geological risk • Lithosphere

---

### 11.1 The Main Problem

The substantial part of the of the historical centre of Kiev with the immovable heritage is located in the zones of a geo-ecological risk, i.e. zones of the development of the dangerous natural and tecnogenic processes in the environment. The town-building activity without taking into account this risk can considerably decrease the effectiveness of the efforts for the heritage safeguarding.

The main problem is to reduce the geo-ecological risk, to increase the stability of the territory and a long-term sustainability of cultural and natural heritage, including the urban infrastructure (Maslov 2012). At the basis of the concept use of a strategy to risk forestall, including monitoring of the surrounding environment and the objects of heritage (Starostenco et al. 2011). The special feature of this approach—take in account the significant role of the upper lithosphere for the stability of the bases of the immovable heritage and the ground-based techno-sphere of the city.

---

Y. Maslov (✉)

Ukrainian Scientific and Designed Corporation “Ukrrestavratsia”  
of Construction Academy of Ukraine (Kiev), 6, Boryspilska  
Street, Kiev 02099, Ukraine  
e-mail: ymaslov@ukr.net

---

### 11.2 The Features of the Territory

The historical centre of Kiev is located on the right-bank of the Dnieper. This part of the city from the immemorial time formed the unique urban landscape and till now has the



**Fig. 11.1** Panorama of the right bank of the Dnieper

important role of the city forming. Natural dominants of the right banks are decorated with the whole chain of the architectural ensembles, historical parks and gardens.

The most significant objects of the immovable cultural heritage which create the historical silhouette of the city are concentrated on this territory.

There are the Saint Sophia Cathedral and Kiev Pechersk Lavra from the World Heritage List among them. They are under patronage of Convention Concerning the Protection of the World Cultural and Natural Heritage of UNESCO including their buffer zones. In connection with the special importance of objects in this territory and the manifestation here of the dangerous geological processes, this part of Kiev requires special attention and protection (Fig. 11.1).

### 11.2.1 Reasons of Emergence of the Problem

The sources of problem lie in the natural features of the territory and in the results of anthropogenic activity in the territory. There are significantly different the engineering geological conditions of the left-bank and the right-bank territory of Kiev. The simple engineering and geological conditions are inherent to the left low coast of the Dnieper. There are no manifestations of the dangerous geological processes here.

The most adverse natural features of the right bank territory of Kiev are the following: geo-morphological contrasts of a relief; territory arrangement on a joint of structures of the crystal base; location of territory at the junction of the structures of the crystalline basement and existence of tectonic breaks; presence of gaps in the sedimentary cover; presence of rocks in the geological structure with low strength and deformation properties (loess, sandy, loam, sand, clay) the loess; presence of zones of geodynamic activity and intense neo-tectonic movements that create the conditions for erosion of soil masses and enhancing of gravitational processes.

Among the main environmental risk factors in the area—a manifestation of endogenous (seismicity, modern tectonic movements of the earth's crust) and exogenous (erosion, landslides, suffusion, subsidence, flooding, water logging, subsidence of the surface) processes which, when anthropogenic impacts acquire destructive character (Fig. 11.2).

Dangerous factors of anthropogenic impact on this area are the following: the mechanical effect of the techno-sphere ground; violation of the balance components groundwater conditions change flow of surface and ground water—filling erosive network (gullies, ditches, channels of small rivers and streams); forming arrays of bulk sediments with low filtration properties; barrage effect as a result of small rivers and streams); forming arrays of bulk sediments with low filtration properties; barrage effect as a result of device structures on the way flow; condensation under the new buildings, backwater groundwater underground structures, topography changes, and other elements of the natural topography changes, and other elements of the natural landscape in the process of urban development; presence undermined area of land on the slopes of the valley of the Dnieper.

Point loads on the earth surface from high-rise buildings of weight, as a kind of mechanical influence, especially within the intersection of the zones tectonic breaks and areas of geodynamic stresses can trigger seismicity induced by overloading the power of the crystalline basement. Intensification of urban development has led to the formation of negative physical fields in the subsurface, including vibration, thermal and electrical. Thus, all of these processes are major reasons of the emergence and exacerbation of the problem.

## 11.3 The Choice of Approaches to Solving the Problem

The problem can be solved by the implementation of two fundamentally different options: the first option—the response to the devastating effects of adverse processes, the second option—their prediction and anticipation. The first option is intended solely for the repair activities of a local nature, which relate to the elimination of the consequences of negative phenomena in certain areas and sites of architectural heritage. The need for measures to eliminate the consequences of the development of dangerous situations are often caused by a lack of information about the natural and man-made processes and their manifestations, as well as of the existence of a number of new facilities that were created without regard to their impact on the environment.



**Fig. 11.2** Historical centre of Kiev. Scale 1: 50,000. 1 Buffer zone of the St. Sophia Cathedral, 2 Buffer zone of the Kiev-Pechersk Lavra, 3 Buffer zone of the St. Andrew Church, 4 Buffer zone of the St. Cyril Church

The main drawback of this embodiment is that this requires an excessive expenditure of money and effort. The second option is aimed at implementing the strategy of pre-emption through the development of the advanced monitoring systems and neutralize threats.

In this connection the second embodiment has been chosen for the problem solution.

## 11.4 Solution of the Problem: The Strategy of Pre-emption and Neutralize Threats

### 11.4.1 The Essential Features of the Strategy

Preservation of immovable cultural heritage depends on compliance with the ecological balance in the upper layers of the lithosphere. Therefore, the strategy includes preservation of historical and cultural target area, which includes monuments, which are regarded as integral parts of natural-technical systems, urban infrastructure and urban values, expanding the boundaries of the target zone to a depth of lithosphere and physically combining them. The main place in this triad takes cultural heritage that defines intended subordinate role of other components. The strategy should cover an area outside of each local object of the heritage, that

enables to track the development of the negative processes in the subsurface, the distribution of which takes place in the adjacent parts of the territory, as well as emerging in the environment at large distances from the local objects, organize all the activities with the application of technical, organizational and investment funds to determine the most efficient ways to reduce natural and man-made influences.

### 11.4.2 Priority Actions

Among the priorities the implementation of the chosen strategy are the following: implementation of instrumental observations deformations of the earth surface in a complex interaction of exogenous, endogenous and man-made processes; study of rhythm exogenous geological processes, particularly erosion-gravity, to assess the potential of the territory of the geodynamic and geological risk; identification of spatio-temporal parameters of differentiation and changes of endogenous tectonic crustal movements and assess their impact on the dynamics of the exogenous processes; detection and systematization dangerous for the stability of the geological environment changes in the operation of engineering systems and communications in specific geotechnical conditions; mapping of risk zones—

manifestations dangerous exogenous, endogenous, natural and man-made processes which regulate and developing, engineering and monitoring activities to reduce it; the use of geographic information system for monitoring and forecasting the development of hazardous natural and man-made processes in the subsurface.

### 11.4.3 Preventive Measures

Basis of preventive measures should be the development of monitoring territorial, local and object levels.

Monitoring system at the territorial level subsystem must include: precise geodetic observations of the horizontal and vertical deformations of the earth's surface in the territory; hydro-geological monitoring site for tracking groundwater regime, moisture regime zones aeration, flow drainage adit; seismological monitoring for tracking origin earthquake zones in terms of man-made influences, zoning study areas and create measures to reduce seismic risk; use of aerial photographs and satellite imagery to track and trace trends in the development of dangerous anomalies in the geological environment.

Geodetic control points of the observation network for changes in the position of deep frames must be located within the fault-block structures, as well as of places of dangerous natural and anthropogenic processes affecting the stability of the geological environment.

Seismological monitoring network should be established taking into account the location of discontinuous zones of violations to assess their potential activity.

Monitoring at the local level as a single system, which should include: comprehensive surveillance engineering geological processes, the efficiency of engineering protection, state structures and territories during periods of restoration, repair, rehabilitation and operation of the facility; analysis of the results of observations, calculations and modeling, recommendations for the strengthening of engineering protection, strengthening structures and facilities, etc.; design additional measures to ensure the reliability and efficiency of facilities engineering protection, prevention of socio-environmental impacts; implementation of the necessary additional measures with the active geological supervision.

Monitoring at the local level also provides, inter alia: field engineering and geophysical observations in order to detect anomalies in the surface layers of the geological environment; control of the stress-strain state of soil masses, landslide areas and failures, revealing their structural and tectonic features; spatial control of deformations over ground and underground parts of the objects of architectural heritage in view of the static and dynamic effects, dynamics

of stress-strain state of inhomogeneous grounds of ancient structures and additional loads on structures due to accumulative fatigue processes in building materials and construction, as well as in an inhomogeneous structure of the actual geological cut in the base of the building, reducing the stability margin as a result of non-uniform sediment banks and buildings and structures; technical inspection of equipment engineering, geotechnical engineering networks and facilities in local areas.

The results of monitoring at the local level should be the basis for project planning and implementation of measures for the protection of local areas of engineering territory, engineering protection and preservation of cultural heritage.

### 11.4.4 Protective Measures

Based on the significant features of the area the most preferential directions for engineering protection measures on the territory and the objects of immovable heritage are: increasing load-bearing capacity of the foundations of buildings and strengthening the bases of buildings including active strengthening foundation soils, strengthening of the construction systems with help of dimensional frames; development of restraint devices and supporting anti-landslide structures, including retaining walls, for wall-drainage in the presence of groundwater, anchorages, bowls, cover nets; development of device contour drains to catch leaks from water-host on earth and underground structures to sites of architectural heritage and their protection zones; development of device horizontal, vertical, combined drains, reservoir drainage, water-down wells of various types in combination with or instead of their drains; regulation of the flow of surface water and ground water protection slopes of infiltration and erosion; device coatings, plugging cracks, holes, pits, the elimination of potholes, craters, gullies and drainage outside the landslide-prone areas.

---

## 11.5 Conclusion

Based on the most significant features of the area and the principles outlined above as the urgent engineering protection measures are: unloading the top parts of landslide slopes, the establishment of surface drainage systems on landslide slopes, organization of the cobbled surfaces around the monuments and landscaping of the slopes; strengthening of the local artificial slopes located around the monuments with help of the integumentary grids with the anchors and planting with bushes; development of the restraint devices and supporting anti-landslide structures, including retaining walls with drainage; modernization of water-bearing

engineering networks with the device of automatic leaks control; decommissioning of the deep adit-drainage systems on the slopes of the Dnieper, which lost its value due to changes in the hydro-geological regime; artificially increasing the load carrying capacity of the monuments' bases using geo-jet technology; reinforcement and grouting of cracks in structural elements of the monuments.

## References

- Maslov YA (2012) Ecological and technogenic risks during the building in the historical areas of Kiev. *Zhishchnoe stroitel'stvo* 10-P:32–36. (ISSN: 0044-4472)
- Starostenco VI et al (2011) Problems of preservation of architectural heritage of Kiev historical centre under conditions of growing ecological and technogenic risk. *Geophys J Inst Geophys*

# The Acropolis Hill of Athens: Engineering Geological Investigations and Protective Measures for the Preservation of the Site and the Monuments

George Koukis, Lambros Pyrgiotis, and Athanasia Kouki

## Abstract

A detailed engineering geology study was conducted in the Acropolis hill aiming to the examination of the geological, tectonic, hydrogeological, geomechanical conditions and the seismicity in relation to the slope stability problems. The hill is covered by limestones of a thickness up to 35 m, underlain at the base of the steep slopes by the schist-sandstone-marl phase in a continuous sedimentation without unconformities. On the basis of the examined lithologic, tectonic and microtectonic conditions and those of natural processes of rock weakening, it is clear that on the upper surface (where the monuments are found) not any anxiety would be justified. On the slopes certain places were indicated as attaining unfavourable stability conditions, without suggesting an immediate danger for the monuments. Some of these measures, such as anchoring of the loosened rock masses and filling of the cracks with mortar, have been applied in parts of the NE and E-SE mainly slopes.

## Keywords

Acropolis hill • Engineering geology • Geotechnical measures

## 12.1 Introduction

In 1975 was established an interdisciplinary organization, the Committee for the Preservation of Acropolis Monuments, with main task to save the monuments on the Sacred Rock. The rock was seen by the Committee as a monument in itself,

so it adopted the hard-and fast-rule that in no case whatsoever should the rock formation be changed in any way.

The work carried out, consisted of a methodic investigation of those agents and mechanisms which could directly or indirectly influence the safety conditions of the Acropolis hill (Andronopoulos and Koukis 1976, 1988; Koukis 1982).

Firstly, the lithological and tectonic structure of the hill constituting formations was examined. A detailed mapping of the area, at a scale of 1:500 has been effected with a study of the tectonics and compilation of the relevant maps. Also, the hydrogeological and seismicity maps were compiled, while an appreciation of certain physical-mechanical features and the erosional-weathering processes was made.

---

G. Koukis  
Department of Geology, University of Patras, Patras, Greece  
e-mail: g.koukis@upatras.gr

L. Pyrgiotis (✉)  
Institute of Geology and Mineral Exploration, National Center of Sustainable Development, Athens, Greece  
e-mail: lpyrg@igme.gr

A. Kouki  
EYDE-PATHE, Ministry of Infrastructure, Transport and Networks, Athens, Greece  
e-mail: kouki.nassia@gmail.com

## 12.2 Geology and Tectonics

The Acropolis hill is covered by thick-bedded and massive limestones of Upper Cretaceous age, resting on the formations of the so-called Athens schists, consisting at the base of

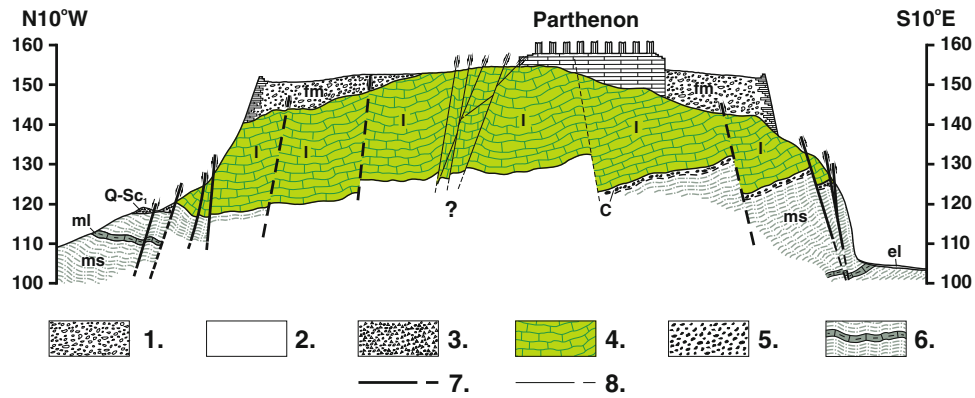


**Fig. 12.1** Geological section of the Acropolis hill. 1. Artificial earthfill (fm), 2. Eluvial mantle (el), 3. Talus (Q-Sc), 4. Limestones (I), 5. Conglomerates (C), 6. Schist-sandstone-marl series (ms-ml), 7. Fault

observed and its probable extension, 8. Main fractures on the Acropolis plateau

the slopes of the schist-sandstones-marl series. At the southern and western slopes a horizon of conglomerates appears, having a thickness up to 10 m. These develop upwards, through an evolutionary transition, to the limestones of a thickness 30–35 m, implying an autochthonous stratigraphic series of a continuous sedimentation without unconformities (Fig. 12.1).

The limestones appear with an intense and multifarious rupturing and are strongly karstified with the presence of cavities and caves. This explains the strong erosional action

by the water of an extend and thick limestone formation, residues of which consist the remaining hills in the town of Athens, including Acropolis.

The above sedimentary rocks are folded together in a syncline structure with a fold axis fluctuating around the direction E-W. The differential mechanical behaviour of the schists-sandstones and the limestones (plasticity and inflexibility respectively) explain the observed asymmetric and disharmonic folds, through the exertion of tectonic stresses during the folding (Fig. 12.2).

**Fig. 12.2** South slope of the hill. Contact of limestones and the underlain series



As it has been revealed from the microtectonic analysis in certain positions of the slopes, unfavourable conditions occur (mainly on the northern and eastern slopes), due to the orientation of main plane of weakness in conjunction with the presence of major faults, karstic caves and open intersected fissures of considerable width and length.

The more recent loose deposits are usually of a limited thickness and cover, at places, the geologic basement on the slopes. The artificial earthfill on the upper surface of the Acropolis reaches (at the south side) the thickness of 14 m (Fig. 12.1).

### 12.3 Seismicity, Hydrogeological and Engineering Geological Conditions

According to existing seismic data of the wider area, the Acropolis hill is included in a zone of low seismic activity and the seismic risk deemed to be considerably low (criteria: the Corinthian style columns located at the south side of the Acropolis and those of Olympian Zeus are still standing).

The hydrogeological regime is characterized by the creation of a poor hanging aquifer in the contact of the permeable limestones with the underlying impervious formations, which is regularly discharged through three small springs.

As far as the geomechanical characteristics of the rocks participating in the structure of the hill, from a partial sampling and laboratory testing, aiming to the determination of indicative values for the various lithological horizons, quite satisfactory strengths were found.

Especially, the unconfined compression strength for limestones ranges between 40–45 MPa, for schistose sandstone-marls 33 and 11 MPa (cores vertical and parallel to bedding respectively), while the strength of moderately weathered sandstones 12 MPa and slightly weathered and fine material 38 MPa (it is obvious the influence of texture, degree of weathering and the orientation of bedding planes). In the conglomerate the values are ranging from 23–25 MPa. The estimated values of the modulus of elasticity for the limestones range between 1,000 and 27,500 MPa (being relatively low), in the schistose sandstone-marls 15,000 MPa, the conglomerates 62,500 MPa and in sandstones 25,000 up to 62,500 MPa while the Poisson's ratio is 0.29 for limestones 0.15–0.22 for sandstones and 0.21 for sandstone-marls.

Concerning the rupture, the limestone rock in the greater part of the western and southern slopes is cohesive and compact, while on the northern and eastern slopes, the conditions are more unfavourable and the initially high mechanical properties are, thus, considerably, reduced and correspond to the residual strength of the fractured rocks.

### 12.4 Protective Measures

Out of the present study, for the improvement of the stability conditions of the rock and the preservation of the monuments a series of protective measures were proposed.

The necessity of studying the problem of intervention in the rock by selecting the most suitable methodology was stressed, for reasons mainly connected with the historical importance of the Acropolis and the efficiency of the measures.

According to the existing testimonies the first measures for the stability of the hill have been taken in 1930s (Balanos 1938) with the construction of high masonry walls intended to serve both as gravity walls and as supports for the load of overhanging rocks, filling of cracks with stones and mortar based on lime, joining the loose rock with iron rods and underpinning with rendered rubble. Also, in 1950s analogous additional works were taking place but based on the non reinforced concrete. These measures have proved insufficient and not satisfactory, having as a result the cracks in the walls, the washing out of the cement, so exhibiting stability problems while the detachment and falling down of rock blocks is continuing. Also these operations have changed the view of the rock formation and obstructed further observation of progressive deterioration.

The most systematic effort for the consolidation of the rock aiming to cope with 22 unstable zones begun in 1977, based on the results of the above study and the executed hereafter more detailed rock mechanic analyses (Hackl and Arvanitakis 1979). The consolidation work had two phases, first temporary buttressing and then the final treatment. The access to the cliff was succeeded with the construction of a stepped adjustable scaffolding while all of areas for consolidation were drawn up at a scale of 1:20. Particularly these measures covered only some parts of the rock-hill, mainly on the northern and eastern sides, follow the next procedure (Monokrousos 1984; Committee for the Preservation of the Acropolis Monuments 1985; Arvanitakis and Monokrousos 1988):

#### *1st Phase*

- Containing the parts of the rock in danger of falling by means of wire netting.
- Cleaning away of the earth, roots and any material causing the rock to disintegrate.
- Cleaning out the cracks and filling them with mortar based on highly durable cement.
- Channeling off the rainwater through terracotta drainage pipes installed in the crevices not yet sealed off. The crevices were then covered with white cement mortar adjusted to the colour of the rock.

**Fig. 12.3** Eastern slope. Limestone rock after filling of the cracks and joints with cement and with the plates of anchoring



#### 2nd Phase

- Securing of the loosened rock masses with the installation of anchors (Fig. 12.3). As the most proper kind of anchoring was judged, out of the studies made, that of combining anchoring at specific points and along the entire length using rods of ribbed steel that adheres two and a half times better than smooth steel. An electrically operated rotating drill is used to open up the holes for the anchors, which can bore to a depth of 35 m.
- The anchoring was done under tension, so that strengthening will be effected right from the beginning. Anchoring rod with a cone at the tip is inserted down the hole; the cone is unscrewed from above, it opens out and gets a firm grip on the rock where it is sound (anchoring at a specific point). The anchor plate is screwed on at the surface and the anchor rod is placed under tension.
- The ends of the rods are fitted with sockets, so that they may be linked and reach the desired depth. The space between the rod and the rock wall is filled with cement mortar, which secures anchoring along the entire length and helps protect the anchor from corrosion.
- The anchor head and rod are made of an alloy of stainless steel with chrome, nickel, molybdenium and titanium in proportions of 18/10/2/0.5. The resistance to oxydation of such alloys when they are under pressure, has been

tested and found that they do not oxydize in cases of minor cracks.

The as above consolidation work lasted for ten nearly years (1977–1988) covered in the NE and E-SE slopes, an area of 11,400 m<sup>2</sup> out of a total rock surface to be stabilized of 24,000 m<sup>2</sup>. The average anchor length was 12.3 m, each anchor corresponding to a slope surface of 92 m<sup>2</sup>.

#### References

- Andronopoulos B, Koukis G (1976) Engineering Geology study in the Acropolis area- Athens. Engineering Geology Investigations, No. 1, Institute of Geological and Mining Research (I.G.M.R.), Athens (In Greek with extensive English conclusions and legends of the coloured maps and sections)
- Andronopoulos B, Koukis G (1988) Engineering Geology problems in the Acropolis of Athens. In: Marinos P, Koukis G (eds) Proceedings of international symposium “The Engineering Geology of Ancient Works, Monument and Historical Sites”, IAEG, Balkema, Rotterdam, vol 3, pp 1819–1831
- Arvanitakis M, Monocrousos D (1988) Consolidation work on the sacred rock of the Acropolis. Athens. In: Marinos P, Koukis G (eds) Proceedings of international symposium “The Enginnering Geology of Ancient Works, Monument and Historical Sites”, IAEG, Balkema, Rotterdam, vol 3, pp 1833–1837
- Balanos N (1938) Les monuments de l’ Acropole. Relevement et Conservation, vol 1 text vol 2 plates, Paris

- Hackl E, Arvanitakis M (1979) Der Akropolishugel von Athen. Rock Mech. Suppl. 8:317–322
- Koukis G (1982) Slope stability problems of the Acropolis hill of Athens, Greece. Proceedings of IV international congress, IAEG, vol III, New Delphi
- Ministry of Culture–Committee for the Preservation of the Acropolis Monuments (1985) The Acropolis of Athens–Conservation, Restoration and Research 1975–1983. Published by the Committee for the Preservation of the Acropolis Monuments, Ministry of Culture, Athens
- Monokrousos D (1984) Basic principles concerning the study and application of protection measures in the rock of the Acropolis of Athens. Technical report, Ministry of Culture and Science, Athens (In Greek)

Andreas Antoniou, Efthymis Lekkas, and Nikitas Chiotinis

---

## Abstract

Saint George's church is characterized as one of the most important monuments of Greek Orthodoxy heritage at Egypt. The church is a unique and massive building complex combining the elements of a number of different structural systems constructed at different periods of time. More specific, there were three major periods of construction that influence present behavior: Roman period, 1909 construction and 1941 reconstruction. Although the subsurface conditions are not very favorable (man-made materials with significant thickness), this paper presents the ability of the building to resist the potential impacts caused by dewatering operation taking into account the prevailing geological and geotechnical conditions, since cracks and local failures were observed mainly during the fluctuations of Nile River and during the dewatering process. Finally, the estimated settlements from previous reports were reconsidered and monitoring methods recommended.

---

## Keywords

Saint george • Egypt • Dewatering • Settlement • Monitoring

---

## 13.1 Introduction

The Saint George Church at Mar Girgis area, Cairo, Egypt (Fig. 13.1), is a unique and massive masonry building complex combining the elements of a number of different

structural systems constructed at different periods of time. Portions of the existing structures, particularly those lying within the cylindrical portion of the church, are believed to have been erected during Roman times, but the foundation elements that were encountered suggest even earlier Pharonic workmanship at the lower levels. The first written references to Mar Girgis monastery occur in the 14th and 15th centuries; however, the Greek Orthodox community had presence in Old Cairo from 5th century. The three major periods of construction that influence present behavior are as follows: Roman period, 1909 construction and 1941 reconstruction (extensive demolition, construction of new exterior wall and restoration of many interior surfaces).

---

A. Antoniou  
Division of Geotechnics, School of Civil Engineering, National Technical University of Athens, 9 Heroon Polytechniou St, 157 80 Athens, Greece  
e-mail: andreasan19@yahoo.com

E. Lekkas (✉)  
Department of Dynamic Tectonic Applied Geology, Faculty of Geology and Geoenvironment, National and Kapodistrian University of Athens, University Campus, 157 01 Athens, Greece  
e-mail: elekkas@geol.uoa.gr

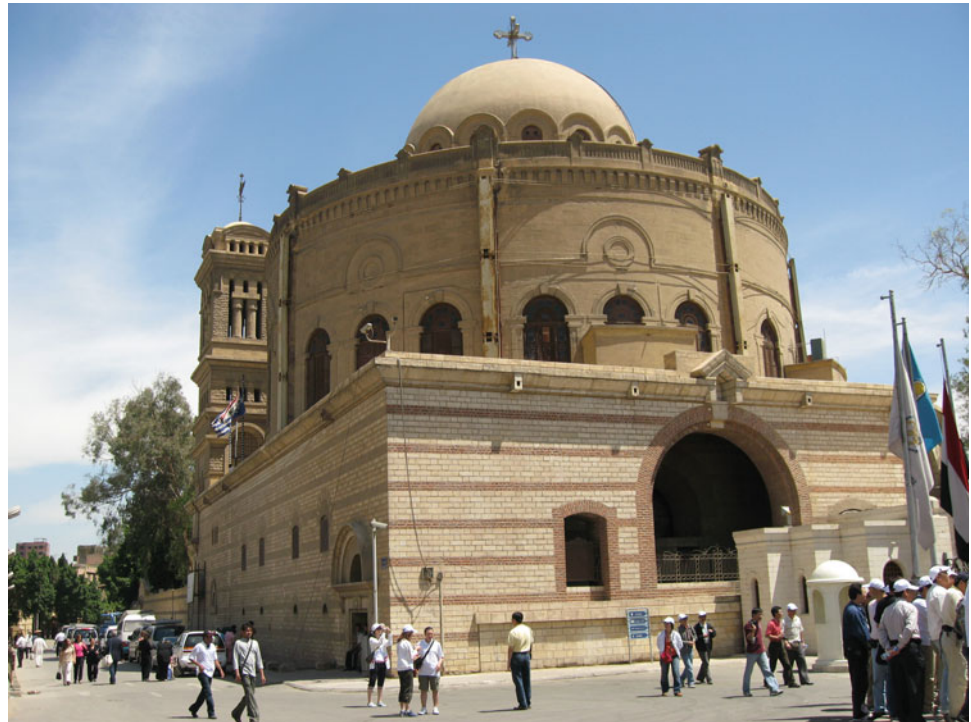
N. Chiotinis  
Department of Interior Architecture, Decoration and Design, Technological Educational Institute of Athens, Agiou Spyridonos, 122 10 Athens, Greece

---

## 13.2 History and Pathology of the Monument

The circular Roman tower is one of the most fundamental elements of the church. It was constructed in masonry and measures 28.6 m in diameter and was built

**Fig. 13.1** View of the Saint George Church at Mar Girgis area, Cairo, Egypt



immediately adjacent to the Nile River. The foundation is believed to have been constructed on native dense alluvial sands, silts and clayey soils, during the low water periods of river flow. The tower carries loads due to the massive thickness of the walls as well as to the addition of cross walls.

The central elevated dome and its associated walls, built above the present level of the upper terrace, are supported by series of arches that span to a circular colonnade. The flat portion of the roof is carried on a vaulted arch system, while the vault loads are transferred to the inner colonnade and the main exterior rotunda walls. The entire building rests upon a concrete slab located at terrace which in turn transfers all loads to the Roman structure below.

During the third period of construction, structural modifications have been performed using a hard cement mortar. According to CDM report (2002) the masonry church structure is judged to be at moderate risk to continued damage from any external movements caused by excessive construction vibrations, excessive differential settlements from ground water lowering or seismic events. From their point of view some areas of major concern are:

- The cupola window arches which are cracked through the entire thickness of the masonry arches.
- The ceiling of the hollow clay block vaulted roof is cracked around the peak of the vaults.
- The bases of six central columns have unsupported areas underneath them.

- The interior central core colonnade of masonry arches supporting the main sanctuary floor are slightly cracked due to stress concentrations.
- The eight cracked marble columns in the central well area that are supporting the intermediate period masonry above give the appearance of instability.

The internal ancient Roman stairway is suffering from deterioration and degradation.

### 13.3 Geotechnical Conditions

Three separate subsurface investigations in different time have been performed in the area of Saint George's church. Based on boreholes' findings and results from in situ and laboratory tests, the following geotechnical units encountered (CDM 2002).

#### *Fill layer*

This layer ranges in depth from 4.0 to 14.5 m below ground surface, while the average depth of fill is about 11.5 m below ground surface. The depth of fill is deeper north of Saint George's church and slopes gradually up towards the south. The fill is comprised of red bricks, asphalt, timbers, gravel, sand, and fines.

#### *Stratum 2*

This layer was encountered in all boreholes at Saint George's church. All boreholes were ended in Stratum 2, while its thick was over 13 m in places, and its depth was

significantly deeper than other areas in the city of Old Cairo. This layer was comprised of very loose to dense, yellowish to brown and grey, silty—clayey sand with gravel, limestone fragments and clay in some places. According to Unified Soil Classification System (USCS) this layer characterized as silty sand with no cohesion. In CDM's report stratum 2 divided in two sub-stratums: 2a which is presented as cohesive and 2b which is presented as non-cohesive.

#### *Limestone layer*

This layer was not encountered in any of boreholes in Saint George's church area and estimated to be significant deeper in this area than other parts of Old Cairo.

Some of the physical properties of the aforementioned geotechnical units are presented to Table 13.1 as results from laboratory tests.

Groundwater table encountered at each borehole during drilling, its depth fluctuated from 6 to 7.50 m below ground surface. Water readings measured in boreholes should not necessarily be considered to represent stabilized groundwater levels, while water levels are expected to fluctuate seasonal.

### 13.4 Groundwater Lowering

The existing high groundwater level in the Old Cairo area has flooded lower floor levels of some ancient structures. The Contract 102 (Johnson and Malhotra 2000) groundwater control system has been constructed to lower the water table below that floor levels. The groundwater control system consists of groundwater lowering elements and discharge elements, which namely are: (a) perforated shafts, (b) filter walls adjacent and connected to the perforated shafts, (c) horizontal perforated drainage systems below building floor, which will discharge to collection shafts or to the closest perforated shafts, (d) discharge pipes installed using micro-tunneling technique, and (e) shafts collecting the water from the horizontal drains.

The entire groundwater control system operates by gravity flow, thus pumping is not required to discharge the water into the main sewer. CDM refers that the groundwater will typically be lowered within fill layer, which is a non-homogenous material with a wide range of grain sizes. The CCJM (Johnson and Malhotra 2000) design calculations of the groundwater control system were based on using a range

**Table 13.1** Mean values of physical parameters of geotechnical units

Soil type	LL	PL	W %	Fines %	$\gamma_d$ , kN/m <sup>3</sup>
Fill	44	15	40	36	17.56
Stratum 2a	41	17	34	75	18.20
Stratum 2b	–	–	23	23	19.72

of permeability. The highest permeability assumed was  $1.5 \times 10^{-4}$  m/s and the lowest permeability was  $4 \times 10^{-5}$  m/s. CDM design calculations were based using permeability equal to  $4 \times 10^{-5}$  m/s.

In order to calculate the radius of influence for various drawdowns as well as coefficient of permeability the following equation was used:

$$R_0 \sim C * h * k^{0.5} \quad (13.1)$$

where  $R_0$  is the radius of influence, C is a factor equal to 3,000 for radial flow to pumped wells (simulation of perforated shafts) and between 1,500 and 2,000 for line inflow to trenches or to a line of wellpoints (simulation of filter walls), h is the drawdown in meters and k is the permeability (m/s). Table 13.2 presents the radius of influence for various drawdowns and permeability values.

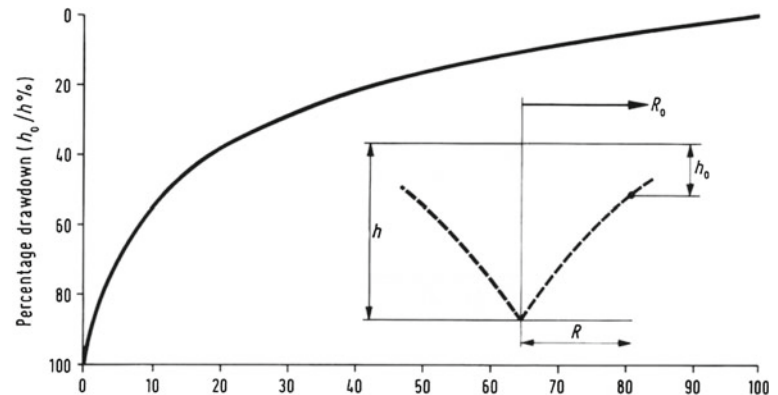
### 13.5 Estimation and Monitoring of Settlements

For Saint George church and according to Contract 102 (Johnson and Malhotra 2000) it was decided a maximum drawdown of 2.5 m below the present average level. According to CDM's report (2002) the Old Cairo area has historically flooded periodically before the construction of the Aswan High dam on the Nile River. These floods caused loading and unloading of the soils for at least decades up to hundreds of years as the vertical effective stresses in the soil changed with the rising and falling waters. Finally CDM concluded that the maximum settlements varied from 0.7 to 0.9 cm for the most realistic cases. It has to be considered that parts of the church are founded on shallow depth,

**Table 13.2** Radius of influence for given drawdown and coefficients of permeability

Drawdown (m)	Permeability k (m/s)	Type of drawdown	$R_0$ (m)
2	$4 \times 10^{-5}$	Perforated shafts	38
2	$4 \times 10^{-5}$	Filter walls	19
2	$1.5 \times 10^{-4}$	Perforated shafts	73.5
2	$1.5 \times 10^{-4}$	Filter walls	36.7
3	$4 \times 10^{-5}$	Perforated shafts	57
3	$4 \times 10^{-5}$	Filter walls	28.5
3	$1.5 \times 10^{-4}$	Perforated shafts	110
3	$1.5 \times 10^{-4}$	Filter walls	55
5	$4 \times 10^{-5}$	Perforated shafts	97
5	$4 \times 10^{-5}$	Filter walls	47.5
5	$1.5 \times 10^{-4}$	Perforated shafts	184
5	$1.5 \times 10^{-4}$	Filter walls	92

**Fig. 13.2** Relation of drawdown to distance from centre of cone of depression (CIRIA 1986)



although the inner part of the church is built on remnants of a Roman tower. This tower has a deep foundation in significantly deeper soils than the foundations of the outer structures. The foundation of the tower is not expected to experience settlements, while for the very conservative case, differential settlements of less than 10 mm may occur, between the deeply founded interior and the shallower founded exterior structures of the church.

Based on various theories for the estimation of settlements and calculate Young's modulus equal to 9 MPa for fill materials, while in a conservative approach the preconsolidation of fill material was not taken into account, the authors calculated settlements up to 9 mm at the areas of filter wall and perforated shaft. In certain distances from shaft and wall, various diagrams (Fig. 13.2, Ciria 1986), which relate the drawdown to distance from center of cone of depression, can be used.

Finally, after the termination of the groundwater lowering, differential settlements were observed between parts of the Roman Tower and the structures around the perimeter terrace. Those settlements were less than one centimeter and confirm not only CDM's calculations but also the above-mentioned calculations.

Before the beginning of the renovation of the church, another monitoring program with additional Elevation Reference Points (ERPs) at the inner columns and walls of the outer circle of the Roman Tower and the 1941s additional structures should be performed. Readings should be taken

weekly for a period not less than six months. In case of no additional movements the works of renovation will commence.

### 13.6 Conclusions

Saint George church is located at Mar Girgis area in the old city of Cairo, Egypt, and combines the elements of a number of different structural systems constructed at different periods of time. Since the existing high groundwater level has flooded the lower floor levels it was decided as part of a greater dewatering project to lower the water table. Therefore this paper presents the geotechnical evaluation of the encountered subsurface layers, as well as estimates the expected settlements, which are in good agreement with the measured.

### References

- Camp Dresser and McKee International (CDM) (2002) Old Cairo Ground Water Lowering, Greek Orthodox church of Saint George evaluation. Final report, United States Agency for International Development
- Johnson CC, Malhotra PC (CCJM) (2000) Contract 102, Old Cairo Area Project. Works at Mar Girgis church. (In CDM's final report)
- Somerville SH (1986) Control of groundwater for temporary works. Report 113, (CIRIA), (ed) London

# Preservation of Sanukite, the Highly Sophisticated Music Instrument Made of Andesite

Shuichi Hasegawa, Seiko Tsuruta, and Munekazu Maeda

## Abstract

Sanukite is a special volcanic rock that had erupted about 13 Ma in northern Shikoku of southwest Japan. Petrologically it belongs to aphyric andsite. Sanukite is much harder and finer-grained than the ordinary volcanic rocks. Although its density is  $2.60 \text{ g/cm}^3$ , its P-wave velocity is about 6 km/s. This high P-wave velocity is unique characteristics of sanukite. Dr. Hitoshi Maeda made the first stone xylophone (“sekkin” petrophone) in 1981. He has continued the analyses into the specific vibrational properties and wave forms of sanukite and he created many musical instruments of stone known by the name “Sanukitephone.” We believe that sanukite and Sanukitephones will be the future World Heritage. Sanukite is globally important rock and its resource is limited. As sanukite is the symbolic rock of Sanuki District (Kagawa Prefecture), we must hurry to establish preservation system as one of the member of the Global Geopark Network.

## Keywords

Sanukite • Andesite • Music instrument • Preservation

## 14.1 Introduction-What Is Sanukite?

Sanukitoids, which characterize the Setouchi volcanic belt, SW Japan, include unusually high-Mg andesites (Tatsumi 1983: Fig. 14.1). They were generated by slab melting and subsequent melt-mantle interactions under unusual tectonic settings such as where warm lithosphere subducted into hot upper mantle (Tatsumi 1983). Setouchi magmatism took place within the short period of 12–15 Ma. Tatsumi (2006) suggests that the magmatism was caused by subduction of very young lithosphere of the Philippine Sea plate.

S. Hasegawa (✉) · S. Tsuruta  
Faculty of Engineering, Kagawa University, Hayashicho,  
Takamatsu, 2217-20, Japan  
e-mail: hasegawa@eng.kagawa-u.ac.jp

M. Maeda  
Kagawa Prefecture Resources Institute, Ejiricho, Sakaide,  
1571-1, Japan

Sanukite is a special volcanic rock that had erupted about 13 Ma in northern Shikoku of Setouchi volcanic belt, SW Japan (Fig. 14.2). It was named by Weinschenk in 1891 after Sanuki District, the old name of Kagawa Prefecture in northeast Shikoku. Petrologically it belongs to aphyric andsite. Under the microscope sanukite can be seen to be minutely grained and is composed mainly of glass, orthopyroxene, magnetic iron ore, and plagioclase (Fig. 14.3). It is characterized by the existence of sporadic magnesian olivine and orthopyroxene in its phenocrysts. These phenocrysts are particularly valuable in the genetic models for the andsite.

## 14.2 Physical Property of Sanukite

Sanukite is much harder and finer-grained than the ordinary igneous rocks. Although its density is  $2.60 \text{ g/cm}^3$ , its P-wave velocity is about 6 km/s (Fig. 14.4). This high P-wave

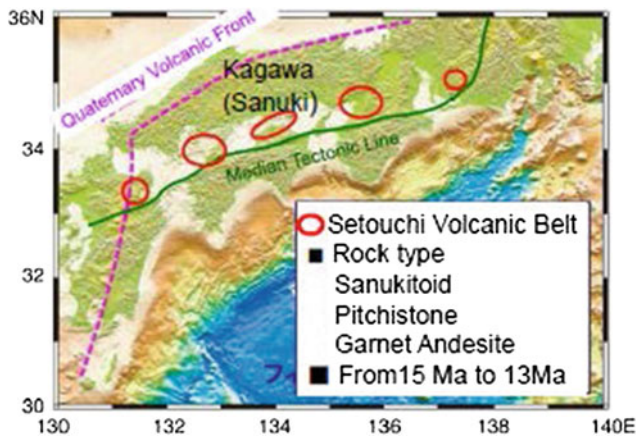


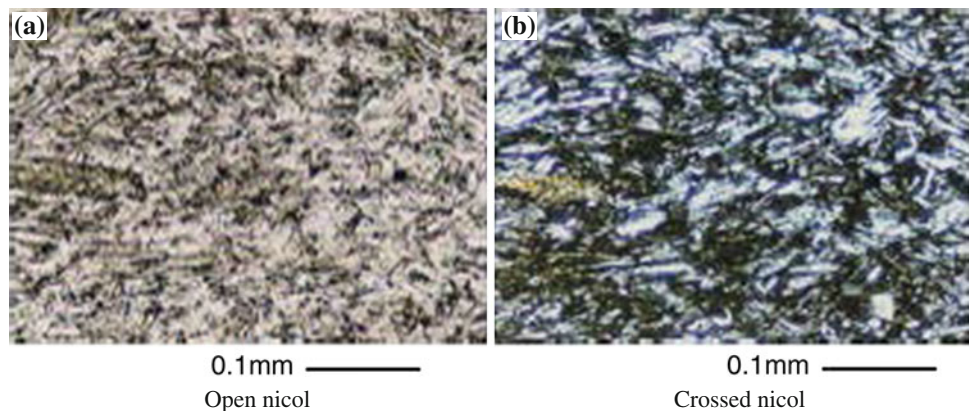
**Fig. 14.1** Locality of Kagawa and sanukite (Modified after Tatsumi (2006))



**Fig. 14.2** Weathered surface of sanukite (Modified after Tatsumi (2006))

velocity is unique characteristics of sanukite. Fresh sanukite is black in color. Hydrated white weathering crusts have been formed at the rate of  $4.1 \mu\text{m/ky}$  (Kuchitsu and Iijima 1990).

**Fig. 14.3** Texture of sanukite under the microscope. **a** Open nicol, **b** Crossed nicol



### 14.3 Use of Sanukite as Stone Implements

More than ten thousand years ago, paleolithic people noticed this stone, with its fine-grained, sharp cleft edges, and used it to make innumerable stone tools for their daily needs. Kayanam in Kagawa Prefecture has been identified as main source site of sanukite stone implements by X-ray fluorescence analysis (Higashimura and Warashina 1975; Warashina and Higashimura 1975).

### 14.4 Sanukite as Miracle Percussion Instruments

The sanukite that has beautiful and clear tone when striking is locally known as “clanging stones” and “tinkling stones” (Fig. 14.5).

Dr. Hitoshi Maeda has devised and produced various kinds of percussion instruments made of sanukites. Tuned percussion instrument made of sanukites were first made produced in 1981 as “sek-kin”, instrument with two and a half octaves and similar to the glockenspiel (Kishi et al. 2001). He has continued the analyses into the specific vibration properties and wave forms of sanukite and he has created many musical instruments of stone known by the name “Sanukitephone.” The instruments are divided into four major types: (1) “Sekkin” (Xylophone shapes, or “stone xylophones), (2) “Sou” (Sets of hanging bells, or “stone bell sets.”), (3) “Rou” (“Field stone” shapes, with simple cuts), (4) “Kei” (“Gong shapes.”), and others. He has also applied piezo-sensing technology to amplification of weak inaudible vibrations.

Some of sanukite percussion instruments were presented to Buddhist temples in Japan, the National Center Hall in Taiwan, the University of Munich, Washington State University, and others. Many well-known percussionists, such as Stomu Yamashita and Lionel Hampton have admired

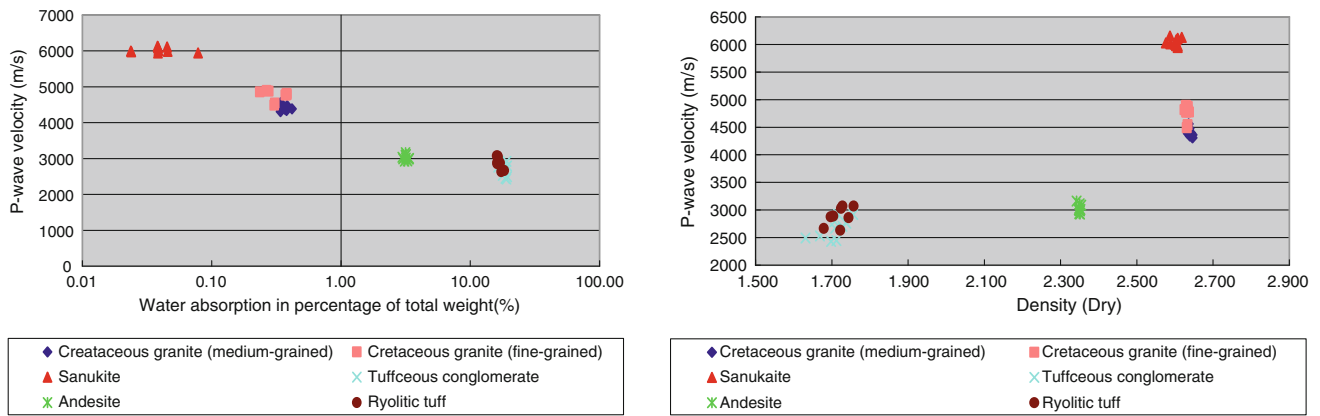
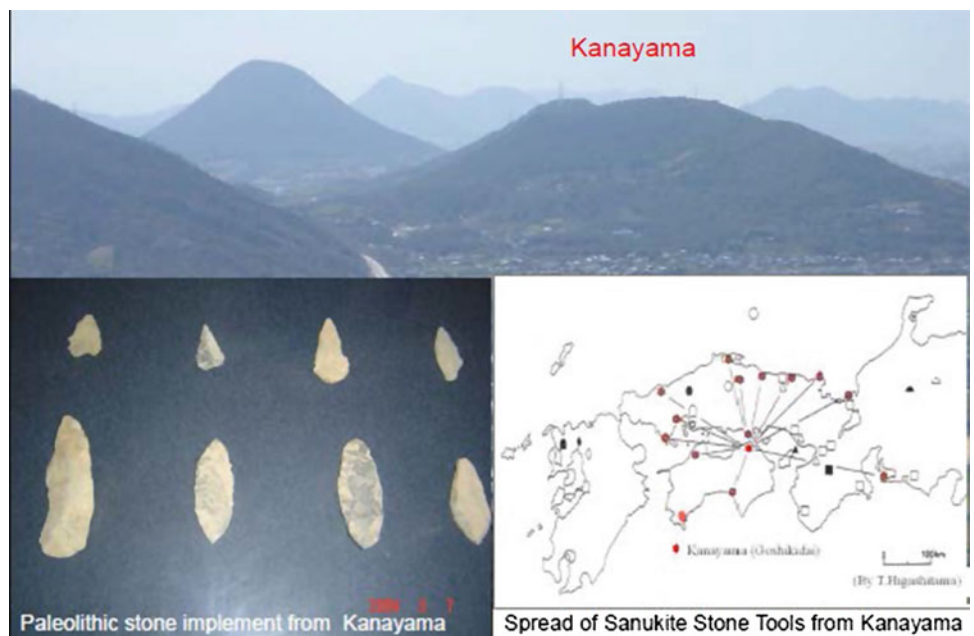


Fig. 14.4 Physical property of sanukite and other rocks in Kagawa Prefecture

Fig. 14.5 Spread of sanukite stone implements from Kanayama during the Palaeolithic and Postglacial (Jomon, Yayoi) ages. (modified after Higashimura and Warashina)



(modified after Higashimura & Warashina)

these instruments and have used them in their concerts (Fig. 14.6).

The sounds made by Sanukitephone remind listeners of ancient memory from the Earth and the Universe. As only few vibration analyses have done (e.g. Kishi et al. 2001), mechanism of beautiful sound is still mystery. We believe that sanukite and Sanukitephones will be the future World Heritage. Sanukitephone is still in progress with the aids of famous musicians.

### 14.5 Preservation of Sanukite and Succession of Sanukite Percussion Instruments

As Mt. Kayamana which yields sanukite is private poverty, we now plan a scheme for preservation by the concept of geopark.

Kagawa (Sanuki) will be served as a unique geopark, featuring with a combination of the following unique three strong characteristics:

- (1) Unique Seouchi volcanism which produced sanukitoid and sanukite,
- (2) Unique monadnocs, comprised of mesas and volcanic necks resulting from of the Setouchi volcanic activities. Mt. Kanayama is one of their manadocs.
- (3) Unique stone cultures since Paleolithic Age.

Stone culture has arisen in Kagawa and make using use of the many diverse property properties of volcanic rocks. The Setouchi volcanic activity produced not only very hard sanukite, but it also produced soft, tuffaceous rocks and medium-hard andesite, which has have been used for stone Budda images, and stone lanterns. Sanukite is a symbol of stone culture in Sanuki District (Kagawa Prefecture).

**Fig. 14.6** Sanukite music instruments produced by Dr. Hotshi Maeda. **a** Kin, **b** Sou, **c** Rou, **d** Kei



Kagawa University is taking the lead in this project's scientific research and has prepared documents of for 30 geosites in Sanuki. Last year we made a presentation to Governor Hamada at the prefectural government. The Kagawa Association of Corporate Executives has formed a team to prepare for the registration of the area of as an official Japanese Geopark.

## 14.6 Concluding Remarks

We believe that sanukite and Sanukitephone will be the future World Heritage. Sanukite is globally important rock and its resource is limited. As sanukite is the symbolic rock of Sanuki District (Kagawa Prefecture), we must hurry to establish preservation system.

## References

- Higashimura T, Warashina T (1975) Sourcing of sanukite stone implements by X-ray fluorescence analysis, *Jour. Archaeol Sci* 2:169–178
- Kishi K, Maeda H, Sugai M (2001) A new percussion instrument “hokyo” made of Sanukite. *Acoust Sci Technol* 22:209–218
- Kuchitu N, Iijima A (1990) The weathering rate of sanukite (in Japanese), *Abst of 97th Annual Meeting of Geological Society of Japan*, p 286
- Tatsumi Y (1983) High-magnesian andesites in the setouchi volcanic belt, southwest japan and their possible relation to the evolutionary history of the shikoku inter-arc basin, *Geodynamics of the Western Pacific-Indonesian*
- Tatsumi Y (2006) High-mg andesites in the setouchi volcanic belt, southwestern japan: analogy to archean magmatism and continental crust formation? *Annu Rev Earth Planet Sci* 34:467–499
- Warashina T, Higashimura T (1975) Sourcing of sanukite implements by X-ray fluorescence analysis II, *Jour. Archaeol Sci* 5:283–291

Dominique Ngan-Tillard, Wim Verwaal, Arno Mulder, Hans Huisman, and Axel Muller

---

## Abstract

Our article focuses on wetland archeological sites that are subjected to one dimensional compression by the placement of a soil body for the construction of a line infrastructure or a landfill. We study the resistance to mechanical loading of ecofacts that are often investigated in archeological prospection works: charred and non charred plant remains and shells. We conducted one dimensional compression tests on assemblies of ecofacts, sand samples seeded manually with ecofacts and natural soils rich in ecofacts and used X-ray micro-tomography to evaluate the integrity of the ecofacts as function of loading. We assumed that fragmentation of ecofacts results in a loss of archeological value if particles become too small to be recovered. The ecofacts tested so far are unlikely to get crushed when included in an archeological soil above which a sand embankment of 1 to 10 m height is constructed. Some might however be deformed, flattened and re-aligned.

---

## Keywords

Ecofacts • One dimensional compression • Damage • X-ray micro-computed tomography

---

D. Ngan-Tillard (✉) · W. Verwaal · A. Mulder  
Faculty of Civil Engineering and Geosciences,  
Delft University of Technology, PO Box 50482600 GA,  
Delft, The Netherlands  
e-mail: d.j.m.ngan-tillard@tudelft.nl

H. Huisman  
Cultural Heritage Agency of the Netherlands,  
PO Box 16003800 BP, Amersfoort, The Netherlands

H. Huisman  
Dutch Cultural Heritage Agency,  
The Netherlands Leiden University,  
Amersfoort, The Netherlands

H. Huisman  
Faculty of Archeology, Leiden University, PO Box 95152300 RA,  
Leiden, The Netherlands

A. Muller  
ADC Archeologie, PO Box 15133800 BM, Amersfoort,  
The Netherlands

---

## 15.1 Introduction

Archaeological remains are increasingly considered to be valuable; as a link to the past, as a part of cultural heritage and as a source for scientific research. Development plans must now be preceded by research to establish whether archaeological remains would be damaged by these plans. If damage is likely, there are two basic options: either the plans are adapted to enable preservation in situ, or the archaeological remains are excavated in a rescue-excavation prior to construction. The decision is, in many cases, hampered because the effects of developments on archaeological sites are unknown. Then, archaeologists take the “better safe than sorry” approach, sites are excavated. Within the framework of a Dutch programme on the in situ preservation of buried archeological sites in the Province of Flevoland, we proposed to develop a protocol to enable sound judgments when assessing the mechanical impact of line infrastructure on archaeological sites. The protocol will avoid non necessary archaeological excavations.

Our article focuses on wetland archeological sites that are subjected to 1D compression by the placement of a sand body for the construction of a line infrastructure. The largest threats to archeological sites buried underneath a sand embankment are thought to be (Huisman et al. 2011): (i) the destruction of specific types of vulnerable artefacts or ecofacts embedded in heterogeneous and deformable soils, (ii) the loss of the relationship between remains and soil features, (iii) the deformation of soil features and layers, hampering their interpretation, and, (iv) the loss of stratigraphic information that would make it possible to separate remains from different periods. We illustrate below the methodology that we have adopted to predict the “fate” of various ecofacts (carbonized and non carbonized organics) and shells packed in a layer or found as inclusions in soft soils and aeolian sands. Such remains are among the most friable materials that are commonly studied during archeological research. Little is known about their mechanical resistance. Our approach is inspired from experimental studies on crushable (carbonate) sands in which particle damage is assessed as function of vertical stress, before, at and, after yield stress during mechanical loading for packings more or less dense made of grains of given sizes and shape. It presents the originality of relying on micro-CT scanning (Tarplee et al. 2011) to track particle damage. Fragmentation is assumed to result in a loss of archeological value if particles become too small to be recovered.

## 15.2 Laboratory Testing

### 15.2.1 X-Ray Microtomography

X-ray micro-computed tomography uses the principle of attenuation of X-ray by matter. X-ray attenuation is mainly function of the thickness and density of the matter as well as the energy of the X-ray beam and the atomic number of the matter. The dependency between attenuation and density renders possible the visualisation of structures within objects made of materials of various densities. Resolution is function of object size, in our case, 35–70 and 5–10  $\mu\text{m}$  for 70 and 10 mm diameter samples, respectively. X-ray microtomography presents several advantages over traditional techniques such as sieving or micro-morphological analysis of thin sections: remains can be observed in 3D, in their context as well as in vivo during testing. Nevertheless, training is needed to be able to identify ecofacts. Atlases of micro-CT scans of seeds, fruits, or bones do not yet exist!

### 15.2.2 Mechanical Testing of Reconstituted Samples

First, we explored the mechanical resistance of the charred ecofacts: wood fragments, hazelnut shells and cereal grains (Ngan-Tillard et al. under submission). We conducted individual crushing tests on ecofacts of millimetric size. We determined their strength, compressibility and mode of failure, and categorized them. The ecofacts showed a variety of behaviours ranging from very brittle, very stiff to very ductile, very compressible, with sudden splitting to progressive degradation before peak force. The weakest particles failed at less than 5 N. Then, we prepared assemblies of friable ecofacts and compressed them one-dimensionally. At several stages of the mechanical compression, we examined the sample integrity by micro-CT scanning. Figure 15.1 illustrates the degree of details of our images and micro-structural changes as function of loading for charred hazelnut shells.

Deformation modes varying from brittle tensile failure with limited particle rearrangement to grain crushing and indentation by neighbours, with large permanent intra- and inter-grain deformation have been found to reflect the particle behaviour during individual crushing tests and their coordination number in the oedometer ring. Microscopic damage by splitting or crushing was limited at the macroscopic yield stress. It occurred at stresses less than 80 kPa for the weakest assemblies made of loosely packed wood charcoals and carbonized seeds and in all cases at stresses below 320 kPa. Note that one can assume a unit weight of 18  $\text{kN/m}^3$  to translate stress to height of sand column above ground level. After loading—to any stress—and partial or full unloading, we noticed significant permanent deformation. In comparison to the in situ conditions, where the particles are surrounded by soft soils, larger stress concentrations from the lower number of particle contacts can be expected in our tests. As a result a conservative estimate, i.e. worst case, for particle damage as function of vertical stress level is obtained.

Second, as ecofacts are embedded in soil in most common situations at archeological sites, we tested soil samples with archeological inclusions. The tests on fine aeolian sand seeded with charred inclusions showed the beneficial effect that particle confinement by sand has on the preservation of charred particles during one-dimensional loading. The charcoal pieces were found to be unaffected by loading. They were supported all around by sand rather than having a few contact points with neighbouring particles. While subjected to stresses above 1,500 kPa, they were not placed

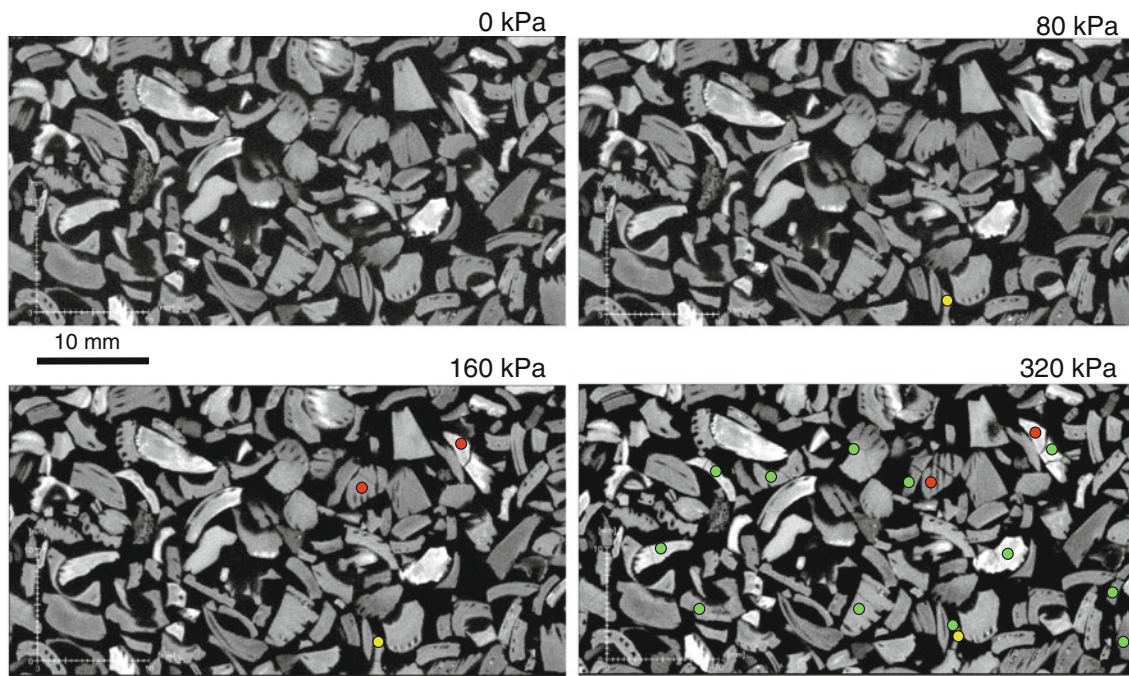


**Fig. 15.1** Zoom on hazelnut shell fragments at the horizontal mid-section of the oedometer sample, at initial state and after 80, 160 and 320 kPa loading. Arrows point at cracks and ellipses highlight crushed

zones. Limited damage occurs after 80 (yellow dots) and 160 kPa (red dots) loadings. Damage is significant at 320 kPa (green dots)

under tensile/flexural loading. Stress arching also developed during testing in sand surrounding the soft charred particles which protected them from high stress concentration and eliminated the risk of local crushing.

On the opposite, stiff particles embedded in a softer material (hazelnuts shell fragments in clay for example) attract stresses. The stress concentration factor is however less than when particles are not supported by a (soft) matrix. Our trials to reconstitute clayey mixtures with weak and light inclusions have failed so far. We noticed bubbles and flat voids around the inclusions on the scans of our mixtures.

### 15.2.3 Mechanical Testing of Natural Soils Containing Ecofacts

Third, we mimicked in the laboratory the in situ loading situation by oedometric testing on real soils that have not yet loaded by construction work. We also stimulated the effect of higher embankments by conducting some tests at stresses up to 4 times higher than those applied in situ. We tested two types of soils: a reed peat containing plant remains such as wood branches, rootlets, seeds and fruits and a detritus clayey peat rich in shells, mainly ostracoda (shrimp mussels). We completed our mechanical testing by a X-ray microtomography and a botanical analysis of the oedometric specimens after testing. In some cases, sub-specimens were

scanned for a better evaluation of the integrity of delicate ecofacts. We compared our observations to those made on intact specimens kept as reference.

We noticed that a number of (non carbonized) seeds and fruits included in the very compressible peat could resist to stresses up to 200 kPa without being crushed (Fig. 15.2, left) while several branches and rootlets were flattened making the identification of their specie possibly more difficult. We observed that ostracoda embedded in a clayey organic matrix were not damaged, even after loading up to 490 kPa. On the other hand, those forming a shelly lamination within the sample were severely crushed (Fig. 15.2, right).

## 15.3 Validation

We validated the outcome of our laboratory research by observations made on the same type of reed peat and detritus peat sampled after the in situ placing of a soil body corresponding to a loading of about 50 and 100 kPa, respectively. On one hand, the cores of both soils were, as expected stiffer, stronger and less permeable than those recovered before the placing of the soil body. This can be seen as beneficial for the ecofacts that they contain as transport processes and possible deterioration processes are slower. It is only during recovery and release of vertical stress that tensile cracks were formed in the compressed cores. On the other hand,

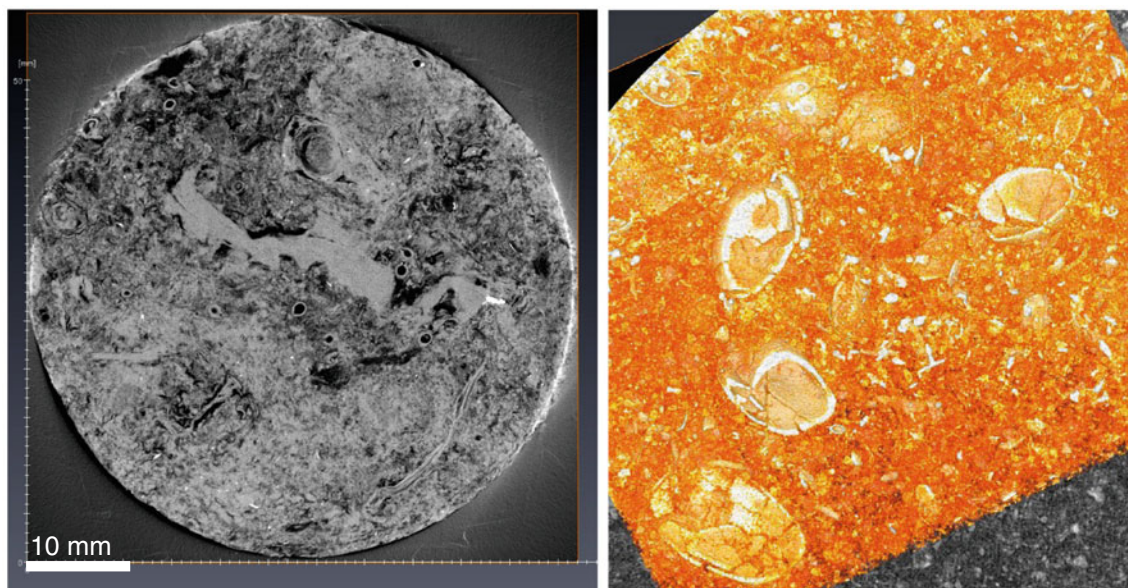


**Fig. 15.2** *left* scan of a 60 mm sample of peat compressed up to 200 kPa, partially desaturated. After compression, many millimetric fruits and seeds showing no sign of crushing are visible. *Right* sub-scan

of a 60 mm oedometer sample of detritus clayey peat compressed up to 490 kPa. Compression caused crushed of millimetric ostracoda shells

traditional techniques used to study botanical content and soil micro-structure (microscopic observation after loosening the soil sample or thin section of soils after water replacement by acetone and resin impregnation) become prohibitively time-consuming due to the material compacity. Micro-CT scanning offers an alternative to traditional methods. It allows a rapid investigation of the samples, whatever their degree of compression is. Scanning organic samples after partial de-saturation enhances plant remains on scans.

Our X-ray micro-scans of samples compressed in situ confirmed the observations made on samples compressed in the laboratory. Several species of seeds and fruits and ostracoda presenting no sign of degradation could be spotted.

foundation piles still has to be examined in details. Oedometer tests conducted up to high stresses (490 kPa) have already shown that particle crushing occur in specific conditions. The loss of archeological context by relative displacement of the archeological remains with respect to their matrix is being investigated by testing natural archeological clayey samples containing charred inclusions. Our most detailed micro-CT observations have been made at a resolution of 5  $\mu\text{m}$ . They will be completed by a micromorphological analysis of thin sections made in intact and deformed samples taken at (archeological) sites partially loaded by a sand body. This will allow us to check the integrity of organic tissues at the cell scale.

## 15.4 Conclusion

To conclude, loose assemblies of friable charred ecofacts are likely be damaged by the construction of medium height embankments (3–5 m). However, such assemblies are unlikely to be found at an archeological site. In most cases, ecofacts are embedded in a soil matrix and the matrix has a beneficial effect on the preservation of the ecofacts. The ecofacts tested so far are unlikely to get crushed when included in an archeological soil above which an embankment of 1–10 m height is constructed. They might however be deformed, flattened and re-aligned. Their resistance to higher loads generated, for example, underneath the tip of

## References

- Huisman DJ, Bouwmeester J, de Lange G, van der Linden Th, Mauro G, Ngan-Tillard DJM, Groenendijk M, de Ridder T, van Rooijen C, Roorda I, Schmutzhart D, Stoevelaar R (2011) De invloed van bouwwerkzaamheden op archeologische vindplaatsen, Rijksdienst voor het Cultureel Erfgoed, [www.cultureelerfgoed.nl/bouwen-en-archeologie](http://www.cultureelerfgoed.nl/bouwen-en-archeologie)
- Ngan-Tillard DJM, Dijkstra J, Verwaal W, Mulder A, Huisman DJ, Müller A (under submission) Under pressure: a laboratory investigation into the effects of mechanical loading on charred organic matter in archaeological sites
- Tarplee MFV, van der Meer JJM, Davis GR (2011) The 3D microscopic ‘signature’ of strain within glacial sediments revealed using X-ray computed microtomography. *Q Sci Rev* 30:3501–3532

Lempe Bernhard, Mehnert Lucia, Scherzer Kathrin, Festl Judith, and Thuro Kurosch

---

## Abstract

Constructed in the 13th century, Trostburg Castle is situated on an impressive castle hill above the village Waidbruck (Ital. Ponte Gardena) in South Tyrol (Italy), about 17 km northeast of Bozen (Ital. Bolzano). The walls of Trostburg Castle are crossed by many cracks. There are various possible causes for these damages. On the one hand, there are geogenic causes, such as the curved surface of the castle hill (whaleback), composed of the volcanic Trostburg formation, and the low rock mass strength due to the adverse orientation of some joint sets. On the other hand there are anthropogenic influences. The castle was extended several times leading to a potential overload of the foundation walls. During the Second World War, Trostburg Castle was damaged, half-ruined and exposed to weathering for a long time. Probably a combination of various geogenic and anthropogenic causes led to the castle's recent damages. The geological conditions of the castle hill were investigated with a special focus on the petrography and the tectonic joints. The result of the work was a large-scale (1:2,500) geological map as well as detailed outcrop descriptions, focusing on petrographic and structural analyses, e.g. by thin sections and pole plot diagrams. A thin section microscopy analysis of different tuff and ignimbrite layers of the alternating Trostburg formation demonstrated that there is no sign of fluvial relocation of the grains after falling out from an eruption cloud. Therefore the tuffs of the Trostburg formation can be described as actual ash fall. As another result of this study besides the potential overload of the foundation, the steeply dipping joints parallel to the slope are one of the most important causes for many cracks in the walls of Trostburg Castle, making it necessary to monitor the joints as well as the cracks at least periodically.

---

## Keywords

Trostburg castle • Trostburg formation • Slope instabilities • Compressive strength • Structural damages

---

## 16.1 Introduction

Medieval castles are typical for the South Tyrolean scenery like the pale mountains of the Dolomites or the wide orchards in the valleys. Over the centuries many castles have

turned to picturesque ruins by fire, war or missing maintenance after losing their capacity of defense and habitation. Because funds for maintenance are enormous the preserved castles are still threatened of decay, which is caused by weathering as well as unfavorable or instable subsoil.

Strategic, political, economic and often prestigious considerations affected the laying of the foundation stone, construction and modification of the castles more than geological and geotechnical issues. These are the reasons why many castles are built at places, which are obviously unfavorable subsoil. Typical places are mountain spurs,

---

L. Bernhard (✉) · M. Lucia · S. Kathrin · F. Judith · T. Kurosch  
Technische Universität München, Arcisstraße 21, 80333 Munich,  
Germany  
e-mail: lempe@tum.de

ridges and brows with slopes as steep as possible providing best natural protection.

One good example is Trostburg Castle (Ital. Castel Forte) (Fig. 16.1), which was mostly constructed during the Middle Ages and remodeled during Renaissance. It has preserved its well-fortified appearance but the walls of Trostburg Castle are crossed by many cracks and there are various possible causes for these damages. On the one hand, there are geogenic causes, such as the curved surface of the castle hill (whaleback), composed of the volcanic Trostburg formation, and the low rock mass strength due to the adverse orientation of some joint sets. On the other hand there are anthropogenic influences.

To investigate the geological and geotechnical conditions of the castle hill two Master's theses (Mehnert 2011; Scherzer 2011) were assigned in cooperation with Dr. Volkmar Mair (Office for Geology and Building Material Testing of the Autonomous Province of Bolzano—South Tyrol, Kardaun (Ital. Cardano), Italy) and are the background for this paper.

## 16.2 Geographical and Historical Review

Trostburg Castle (Fig. 16.1) is situated on an impressive castle hill (627 m s.l.m.) at the eastern slope of the Valley of the Eisack river (Ital. Isarco) around 150 m above the village Waidbruck (Ital. Ponte Gardena) in South Tyrol (Italy), about 17 km northeast of Bozen (Ital. Bolzano). Waidbruck is located at the confluence of the Gröden creek (Ital. Rio Gardena) into the Eisack river.

Hohenbühel (2008) described the building history of the castle: In the 13th century (Romanic) Trostburg Castle was constructed as a small castle with a central, strongly fortified main tower (donjon = Bergfried) surrounded by small residential buildings and a bailey at the eastern side. In the first half of the 14th century parts of the western castle wall broke off and the round tower (“Römerturm”) was built on a knoll in the Southeast; in the 15th and 16th century (Gothic and Renaissance) the castle was widely extended and the walls and buildings were heightened, because the area of the castle hill was narrow. For example the donjon was raised from a height of around 13.5–22 m. During this time round bastions and the outer bailey in the South were constructed. In the 17th century modifications were made and the outer bailey was completed with a rectangular tower, called “Pfaffenturm”, the curtain walls in the “Hirschgraben” and a new gun turret (“Kaserne”). Three of the modifications at the main castle were the breakup of the western walls for larger windows and the heightening of the donjon about 2 m as well as of the medieval palas to get a new great hall. The curtain wall with parapet on the south side of the medieval castle was heightened and enlarged to a residential building in 1724 (Baroque). Since 1850 the decay of the buildings of the outer bailey started. Instabilities and the danger of break offs forced the partly deconstruction of the second and third floor to reduce the strain on the foundation walls of the southern and western wing of the main castle in 1864. Bombardment with anti-aircraft guns by German troops caused serious harms mainly at the roofs in 1943 and the successive neglect

**Fig. 16.1** Trostburg Castle, situated on volcanic rocks of the Trostburg formation (view from the southwest). On the *left* the medieval castle with the rectangular donjon; in the *middle* the outer bailey with a rectangular tower (“Pfaffenturm”) and a gun turret, on the *right* the round tower (“Römerturm”)



let degenerate Trostburg Castle into a half-ruin after the war. Further damages at the roofs were caused by storm loss in 1957. A large restoration between 1967 and 1977 saved the castle and it is now open for tourists and cultural events. But the walls of Trostburg Castle are still crossed by many cracks, which could be alarming.

### 16.3 Geological Settings

The hill of Trostburg Castle (*locus typicus*) is composed of the volcanic Trostburg formation, which is the lower part of the Athesian volcanic group “AVG”. The underlain beds are the Southalpine basement rocks, the Brixen quartzphyllites, with a metamorphic age of about 300–360 Ma (Variscan

orogeny), which are overlain by the Waidbruck conglomerate, that was only intermittently deposited. (Brandner et al. 2007; Gruber et al. 2007).

To the east, about 200 m above the castle, the Trostburg formation is overlain by rocks of the Bolzano quartzporphyry of the Lieg formation (acidic volcanic rock series of the AVG). (Brandner et al. 2007; Gruber et al. 2007).

The Trostburg formation (Fig. 16.2) consists of basic to intermediate volcanic rock series, such as tuffs, lavas and blocky ignimbrites/agglomerates that were deposited in the Permian (300–255 Ma). A thin section microscopy analysis of different tuff and ignimbrite layers of the alternating Trostburg formation demonstrated that there is a typical fluidal texture (Fig. 16.3) in the ignimbrites. Many grains of the tuffs are angular and partially razor-sharp edges of

**Fig. 16.2** Typical rocks of the Trostburg formation: well bedded, consolidated ash fall near the outer bailey and rarely bedded agglomerates near the round tower



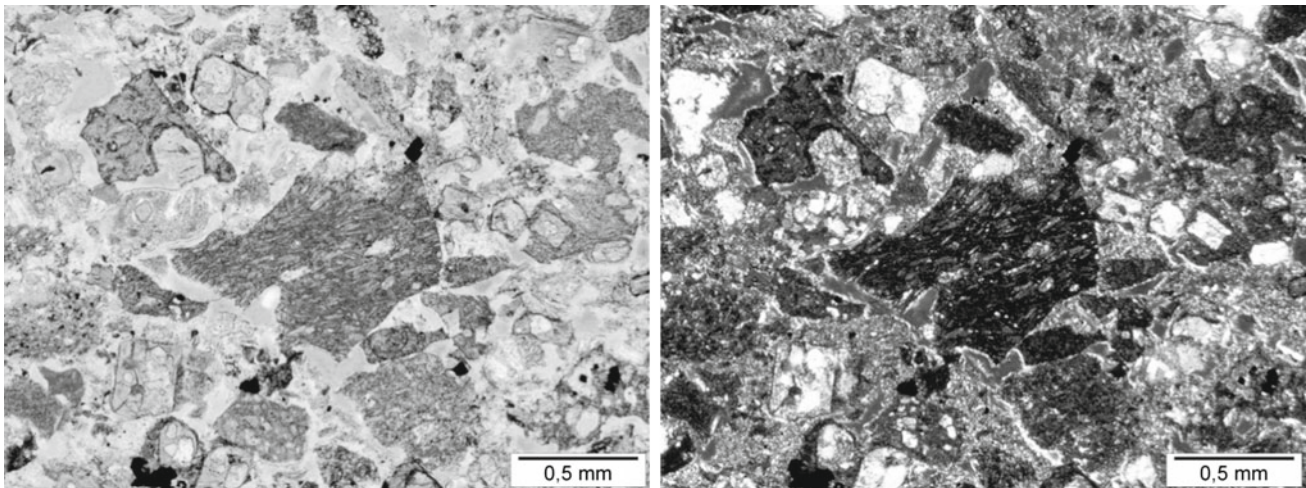


**Fig. 16.3** Photomicrographs of tuff; plane-polarized light (*left*) and crossed-polarized light (*right*). A rock fragment with razor-sharp edges

in a glassy matrix with flow-banding is visible in the middle (*photos* Dr. G. Grundmann 2011)

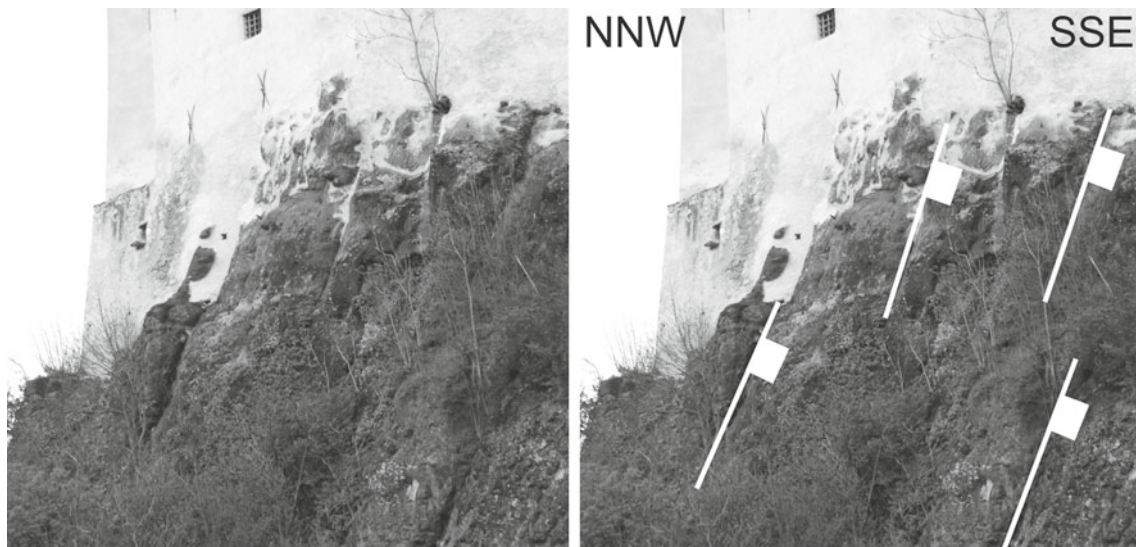


**Fig. 16.4** The foundation of Trostburg Castle on ignimbrites of the Trostburg formation. Besides the potential overload of the foundation Not the strength of the rocks, but the kinematic freedom offered by the

orientation of the discontinuities is responsible for the instabilities. On the *right* the orientation of the discontinuities are marked with “Müller-Fähnchen”

components can be found (Fig. 16.3). This implies that there is no sign of fluvial relocation of the grains after falling out from an eruption cloud. Therefore the tuffs of the Trostburg formation can be described as actual ash fall.

## 16.4 Stability Analysis

The structural analysis of more than 1,100 joints showed that there is no correlation between the joints in the Brixen quartzphyllites and the joints of the Trostburg formation.

The joint sets in the Brixen quartzphyllites show a wide diversity of strike and dip values, whereas the joints in the Trostburg formation can only be divided into four steeply dipping main sets, of which the NW/SE striking set is the most relevant one. The bedding dips slightly with only a few degrees towards the NW.

The uniaxial compressive strength of samples from the hill of Trostburg Castle is commonly between 25 and 50 MPa. But 25 MPa are enough for bearing the building loads. This suggests that the instabilities of the castle rock do not come from too low strengths of the castle hill.

## 16.5 Conclusion and Outlook

As a result of this study besides the potential overload of the foundation not the strength of the rocks, but the steeply dipping joints parallel to the slope are one of the most important causes for many cracks in the walls of Trostburg Castle (Fig. 16.4), making it necessary to monitor the joints as well as the cracks at least periodically.

**Acknowledgements** Our thanks go to Dr. Volkmar Mair (Office for Geology and Building Material Testing of the Autonomous Province of Bolzano—South Tyrol, Kardaun (Ital. Cardano), Italy) for his cooperation and assistance on site.

## References

- Brandner R, Gruber A, Keim L (2007) Geologie der westlichen Dolomiten: von der Geburt der Neotethys im Perm zu Karbonatplattformen, Becken und Vulkaniten der Trias. *Geo Alp* 4:95–121
- Gruber A, Gruber J, Keim L (Red.) (2007) Geologische Karte der Westlichen Dolomiten im Maßstab 1:25,000 West-Blatt. Kardaun (Amt für Geologie und Baustoffprüfung)
- Hohenbühel AV (2008) Trostburg—Zum Nutzen, zur Freude und zur Ehre. Verlag Schnell & Steiner, Regensburg, p 64
- Mehnert L (2011) Ingenieurgeologische Detailkartierung des Burgfelsens der Trostburg in Südtirol/Italien. Unpublished Master's thesis, Chair of engineering geology, Technische Universität München, Munich, p 99
- Scherzer K (2011) Ingenieurgeologische Detailkartierung des Burgfelsens der Trostburg in Südtirol/Italien. Unpublished Master's thesis, Chair of engineering geology, Technische Universität München, Munich, p 123

---

# The Geology of the Hill of Summersberg Castle in Gufidaun (South Tyrol, Italy) and Its Geotechnical Challenges in Mitigation Works

# 17

Ellecosta Peter, Lempe Bernhard, and Thuro Kuroschi

---

## Abstract

In 1957 and 1987, parts of the castle hill of Summersberg castle collapsed and pulled sections of the castle down onto the valley bottom and endangered an important access road. Due to this fact, the government of the Autonomous Province of Bolzano decided to ensure the castle hill. As the detailed geological structure of the castle rock and the reasons for its instability are unknown, an engineering geological mapping was investigated. Results suggest, that the castle hill has a shell-like structure: the core consists of a slightly foliated metagabbro. The foliation, folding and alteration increases towards the edge of the hill. The uniaxial compressive strength of samples from the inner region is commonly slightly higher than 100 MPa, while the outer part decreases to approximately 50 MPa. Field mapping indicates, that the fracture network is dominated by the effects of persistent faults spaced at 5–10 m. Most of the faults and associated fractures are very steep and run parallel to the slope. Therefore, we suggest a strong negative control on the natural slope stability. A structure model shows, that the castle hill could be divided into three parts with a different fracture system and with different failure mechanisms. Our findings suggest that not the strength of the rocks, but the kinematic freedom offered by the orientation of the discontinuities is responsible for the main instabilities. On this basis, a mitigation concept for the slope was drafted. It is comprised of steel networks, braced anchors, anchor beams and shotcrete

---

## Keywords

Castle summersberg • Gufidaun • Landslides • Rock consolidations • Compressive strength

---

## 17.1 Introduction

Medieval castles are for many people a romantic dream. However, many castles have since its construction problems with their stability. One recent example is Summersberg Castle (Ital. Castel Summersberg) (Fig. 17.1) in Gufidaun

(Ital. Gudon) (South Tyrol, Ital. Alto Adige), situated on a hill of metagabbro 70 m above the Villnöß-valley (Ital. Val di Funes). In the past, parts of the castle hill collapsed and pulled sections of the castle down onto the valley bottom (events are documented from 1957 and 1987 (Hepperger, n.d.), but other older ones are assumed) and endangered an important access road. Due to this fact, the government of the Autonomous Province of Bolzano decided to ensure the castle hill. This task was taken over by the office for the “Wildbach-und Lawinerverbauung Nord” (office for the construction of torrent and avalanche barrier north, Ital. Ufficio Sistemazione bacini montani nord). The mitigation works started 2009 and were completed in 2011.

---

E. Peter (✉) · L. Bernhard · T. Kuroschi  
Chair of Engineering Geology, Faculty of Civil, Geo and  
Environmental Engineering, Technische Universität, Munich,  
Germany  
e-mail: p.ellecosta@tum.de



**Fig. 17.1** Eastern Flank of the hill of Summersberg Castle with a clearly visible fault and associated fractures dipping to south. The

spatial position corresponds approximately to the spatial position of the Villnöß-line (Photo 26/04/2012)

Parallel to the mitigation works, the geological structure and some important rock properties of the castle hill were investigated as part of a bachelor's thesis. The whole castle hill was included in a detailed engineering geological mapping with emphasis on the fracture system and the compressive strength of the relevant rocks.

## 17.2 Geological Setting

The village Gufidaun, which belongs to the municipality Klausen (Ital. Chiusa), is located on a to northwest rising terrace-like hill on the east side of the Eisack-valley (Ital. Valle Isarco) south of the Villnöß-valley at about 720 m s.l.m. The terrace is bounded in the north by a steep and till to 120 m deep canyon of the Villnöß-river. Straight above the canyon on the northern edge of the terrace stands Summersberg Castle (first mentioned 1211, Weingartner 1998, p. 375).

The work area is located in the major tectonic unit of the Southalpine. Rocks of the southalpine basement, the Brixen-unit (Brixen quartz phyllite), form Gufidaun's underground. The Villnöß-valley itself runs along an EW-striking permian fault zone (Brandner et al. 2007) (Fig. 17.1), which was reactivated in the Alpine orogeny (Gruber et al. 2006) and is called the Villnöß-line (Cornelius-Furlani 1924, 121ff; Mutschlechner 1933, p. 94).

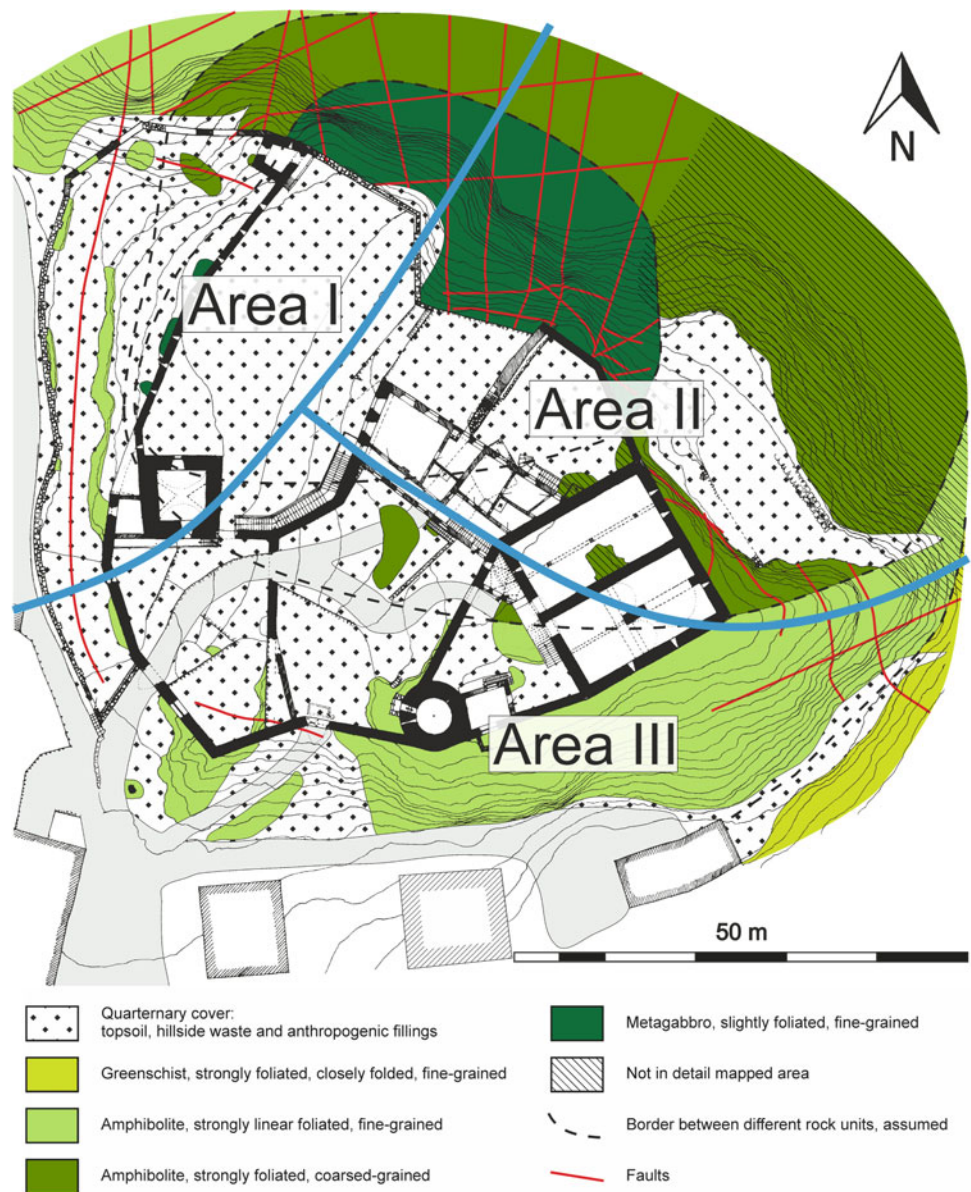
The castle hill is part of an amphibolite-metagabbro complex which is a basic intrusive body. The parent rock was an intrusion of gabbro into the early sediments of the Brixen-unit prior to the Variscan orogeny. About the intrusion age are so far no more detailed information available (Rofner et al. 2010, p. 39). During the Variscan orogeny, 360 to 310 Ma

(Rofner et al. 2010, p. 42) ago, the intrusion got a metamorphic overprint. Higher temperature and pressure (488–588 °C and 3–5 kbar (Rofner et al. 2010, p. 52)) transformed the gabbro to an amphibolite. As the rocks of the amphibolite-metagabbro complex are harder and tougher than the surrounding phyllites, they were etched out as whalebacks by the glaciers in the ice ages during the Pleistocene.

But already Cornelius and Cornelius-Furlani (1922, p. 110) and Cornelius-Furlani (1924, p. 126) realized that the amphibolite-metagabbro complex is not homogenous. It consists of several individual cores in which the primary magmatic fabric was preserved. These cores are separated by shear zones to which foliation gets stronger. This structure was formed during the Variscan metamorphism: By the deformation during metamorphism, the intrusion was broken into several pieces, separated by shear zones. In the area of the shear zones, the gabbro was converted to an amphibolite and even greenschist by the influence of deformation and fluids.

The castle hill itself is one of these cores where four rock types can be distinguished (Fig. 17.2). As you can see in Fig. 17.2, the core consists of a fine-grained and only slight foliated Metagabbro with a light alteration. To the edge of the castle hill, foliation and alteration increases so that in the south even a greenschist is found. The uniaxial compressive strength of samples from the two inner rock bodies is commonly slightly higher than 100 MPa, while the outer part of the greenschist decreases to approximately 50 MPa. The decrease is primarily due to the stronger foliation and alteration. But 50 MPa are still big enough to bear the building loads. This suggests that the instabilities of the castle rock do not come from too low strengths of the castle hill (Ellecosta et al. 2013).

**Fig. 17.2** Geological map of the castle hill. Clearly visible is the shell-like structure of the castle rock and its many faults in the northern part. Area I-III represents different parts with their own fracture system (based on Kulturkommission Bozen 1942)



### 17.3 Stability Analysis and Mitigation Concept

In an engineering geological mapping it turned out that the border area of the castle hill, especially the northern hillside to the valley, is loosened up profound. The reason is an amount of faults and associated fractures (Figs. 17.2 and 17.3), which occur on average every 5–50 cm. In addition, most of the faults and the associated fractures are very steep and run parallel to the slope. Therefore, we suggest a strong negative control on the natural slope stability (Fig. 17.3).

Due all-in all 649 structure measurements it was possible to create a structure model of the castle hill. As you can see in Fig. 17.2, the castle hill can be divided into three parts with a different fracture system and own failure mechanism

- Area I is located in the northwest of the castle hill. It has an orthogonal fracture system with a plenty of very steep inclined fractures. The generally flat dipping foliation doesn't exist here, respectively isn't effective as a joint set. When comparing Figs. 17.2 and 17.3 it is remarkable that many fractures run parallel or perpendicular to the slope. This is the reason why this area is dominated by rockfalls.
- Area II is located in the northeast of the castle hill. The fracture system here is generally not as steep as in Area I and has less directions. But in this area, the foliation is effective so that an additional flat dipping joint set exists, which dips in right to the valley. This also can cause slidings beside rock falls.
- Area III is located in the southern section of the castle hill. There are only 3 joint sets, which are very steep and

**Fig. 17.3** Rock area below the north tower; clearly visible are the numerous, parallel to the slope and up to 10 cm wide opened fractures that break down the rocks (photo 13/04/2010)



mostly N–S-orientated. This means that the fractures run diagonal to the slope. The foliation is again effective so that the flat to NW dipping joint set exists again. Since the most fractures run diagonal to the slope and the foliation dips to the hillside, no clear slope failure mechanism can be detected and no failure is to be expected.

These results show that there is no significant difference between the different rock bodies. The findings indicate that the kinematic freedom offered by the orientation of the discontinuities is responsible for the instabilities (Fig. 17.3).

To protect the castle from further damage and to prevent collapses of the rocks, the castle hill was ensured. In a first step, the northslope was cleared up from vegetation and loose jointed rock bodies. In the second step, the area to be protected was covered with a steel mesh, fixed with rock nails and anchor systems (6–12 m long, pretensioned injection anchors with an anchor density with 1 anchor to 1.5 m<sup>2</sup>) placed over the entire area. In a third step, the anchors were braced together with steel cables and the entire surface sealed with shotcrete. The uppermost regions of the rock on which the castle directly rests was additionally secured with anchor beams.

## 17.4 Conclusion and Outlook

Our findings suggest that not the strength of the rocks, but the kinematic freedom offered by the orientation of the discontinuities is responsible for the instabilities. Thanks to the complex mitigation works, the endangered areas of the castle and the castle hill could be secured, so that no further loss of buildings is to be expected. In addition, there is no more danger of rock falls/slidings from the area directly below the castle, which could threaten the road in the valley floor. Our work and the presented results allow a better understanding of the geological structure of the castle hill and his rock mechanical behavior.

**Acknowledgements** At this point, my thanks goes to the office for the “Wildbach-und Lawinerverbauung Nord”, especially representative Dr. Paul v. Hepperger and the office for “Geologie und Baustoffprüfung”, especially representative Dr. Volkmar Mair for their cooperation and assistance on site. Another thanks goes to the owner of Summersberg Castle, the family Zingerle for the great cooperation and the inhabitants of the “Unterburg” for the permission to access the private garden and to take samples from there.

## References

- Brandner R, Gruber A, Keim L (2007) Geologie der westlichen Dolomiten: von der Geburt der Neotethys im Perm zu Karbonatplattformen, Becken und Vulkaniten der Trias. *Geo. Alp*, 4:95–121, Innsbruck
- Cornelius HP, Cornelius-Furlani M (1922) Über gangförmige Eruptivbreccien aus dem Villnößtal (Südtirol)—*Centralblatt für Mineralogie, Geologie und Paläontologie*, 4:110–114, Stuttgart
- Cornelius-Furlani M (1924) Zur Kenntnis der Villnösser Linie. *Verh. Geol. B.-A.*, 7: 125–131, Vienna (Geologische Bundesanstalt)
- Ellecosta P, Lempe B, Thuro K (2013) The geology of the castle rock of Castle Summersberg in Gufidaun/South Tyrol and its geotechnical challenges in securing works. In: 19. Tagung Ingenieurgeologie. 13–15 March 2013 in Munich
- Gruber A, Brandner R, Keim L (2006) Permische Grabenbildung und ihre Vererbung in alpidischer Extensions- und Kompressionstektonik am Nordwestrand der südtiroler Dolomiten. *Pangeo-conference Innsbruck*, 1 p., Abstract, Innsbruck
- Hepperger P. v. (n.d.): Technischer Bericht zur Sanierung von Schloß Summersberg in Gufidaun. Unpublished report, Autonome Provinz Südtirol, Bolzano, p. 2
- Kulturkommission Bozen (1942) Burg Summersberg Gufidaun, Lageplan und Längsschnitt, Maßstab 1:200. Bolzano (family archive Zingerle)
- Mutschlechner G (1933) Geologie der Peitlerkofelgruppe. *Jb. Geol. B.-A.*, 83: 75–112, Vienna (Geologische Bundesanstalt)
- Rofner V, Tropper P, Mair V (2010) Petrologie, Geochemie und Geologie des Amphibolit/Metagabbro Komplexes von Gufidaun (Südtirol, Italien). *Geo.Alp*, 7: 39–53, Innsbruck
- Weingartner J (1998) Die Kunstdenkmäler Südtirols, Band 1, Eisacktal, Pustertal, Ladinien, p 776. Bozen/Bolzano (Athesia) and Innsbruck/Vienna (Tyrolia)

---

# Engineering Geological Conditions and Instability of Mycenaean Tombs in Cephallonia, Greece

18

Charalambos Saroglou and Andreas Sotiriou

---

## Abstract

The paper presents the engineering geological behaviour of a calcarenite on the stability of Mycenaean tombs in the archaeological site of Mazarakata in Cephallonia Island. The geological setting of the site is characterized by the presence of faults, which delineate the fracture pattern. This along with the range of hardness of the sedimentary rock controls primarily the stability of the tombs. The geological conditions are described and the engineering geological behaviour of the calcarenite is investigated. It was assessed that the progressive weathering and deterioration of the calcarenite would lead to further instability and potential collapse of the tombs.

---

## Keywords

Calcarenite • Faults • Archaeology • Instability

---

## 18.1 Introduction

The underground tombs are carved on the natural calcarenitic rock and are dated at the Mycenaean period, while they have been used in the period between 1390/70–1060/40 B.C. The tombs in Mazarakata area, Cephallonia have been found and investigated in 1813 by Colonel de Bosset, Commissioner of the Island. The stability of the investigated tombs presented herein is primarily controlled by the geological conditions prevailing on site. The impact of geological and geotechnical problems on the stability of Macedonian tombs and Vergina Royal tombs and the stabilization techniques have been reported by Christaras et al. (1997) and Arvanitakis et al. (1988) respectively. Similar cases of geological controls on

the Christian catacombs at Melos Island have been investigated by Arvanitakis and Miligos (1988).

---

## 18.2 Geological Setting

### 18.2.1 Site Geology and Tectonics

The prevailing geological formation in the area is calcitic sandstones with well-developed bedding and varying degree of diagenesis. The diagenesis is characteristic since it determines the strength and durability of the formation against erosion. Based on geological mapping, two horizons of the sandstone (characterized as calcitic sandstone) were distinguished, horizon A and horizon B (Fig. 18.1). Horizon A is a moderately to highly cemented calcarenite, having a Schmidt hammer hardness value between 20 and 30. This horizon has a thickness of 1.0–2.5 m and is capped by a highly cemented horizon (A1) with hardness values up to 40. Horizon A is underlain by horizon B, which is slightly cemented and has hardness between 10 and 20. The tombs are excavated mostly in horizon B and it is characteristic that their roof is more stable when formed in the overlying horizon. In the area of the site, two faults are encountered,

---

C. Saroglou (✉)  
Department of Civil and Environmental Engineering, Imperial  
College, London, SW7 2AZ, UK  
e-mail: c.saroglou@imperial.ac.uk

A. Sotiriou  
LE Office of Prehistorical and Classical Antiquities, Ministry  
of Culture, Athens, Greece

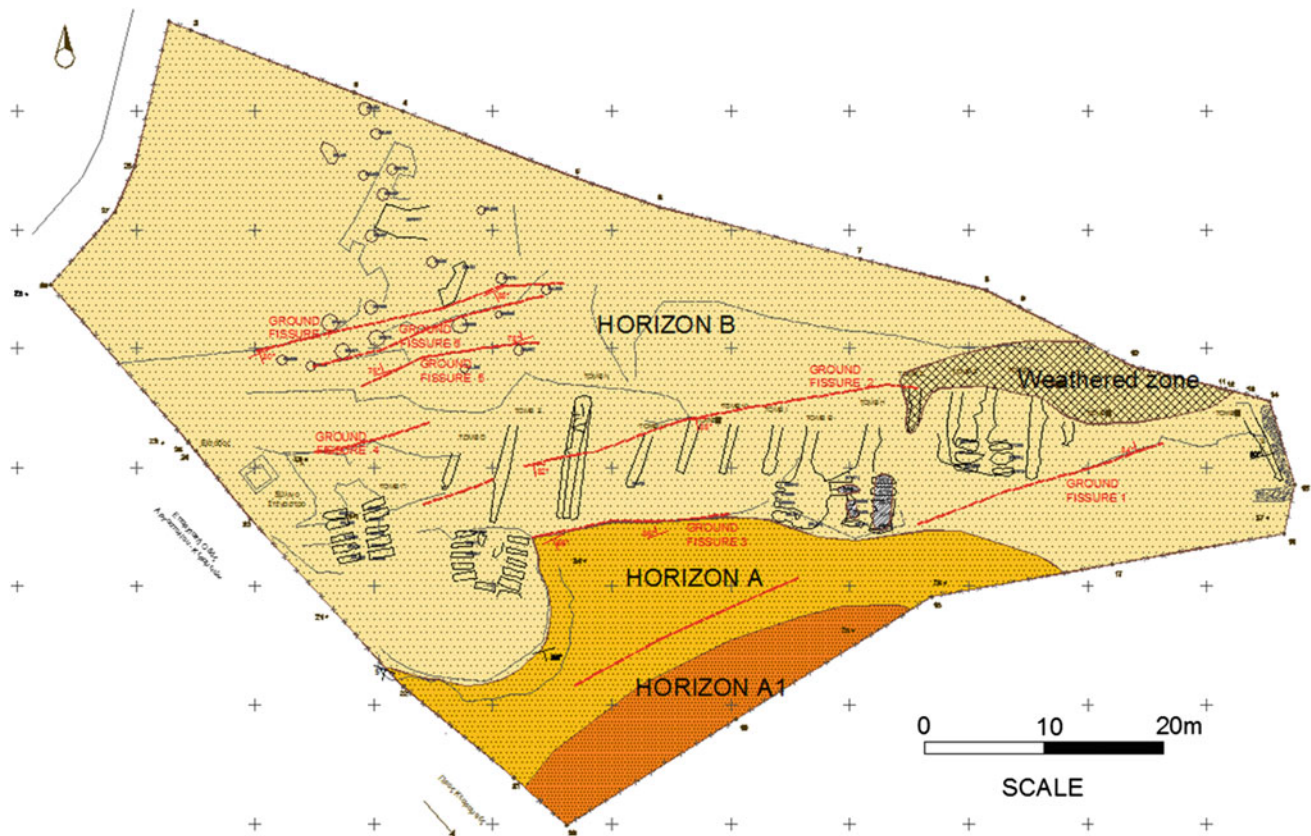


**Fig. 18.1** Geological map of archaeological site (ground fractures denoted with red)

one with an E–W and one with a NW–SE trend. A number of ground fissures exist and are aligned parallel with the faults, having an E–W trend (Fig. 18.2).

The island of Kephallonia is located in one of the most seismic zones of Greece. The strongest earthquakes recorded in the twentieth century were on 12 August 1953 ( $M_s$ : 7.2) and 17 January 1983 ( $M_s$ : 7.0) (Comninakis and Papazachos 1986) and it is estimated that the likely maximum annual magnitude is 5.17 R.

In order to decide on the most appropriate treatment methods for improving the behaviour of the calcarenites, petrographical analysis and tests for the determination of physical and mechanical properties were performed.

The fracture pattern of the formation and the varying strength of calcarenite horizons control primarily the stability of the walls and roof of the tombs.

### 18.2.2 Mineralogical Composition

The mineralogical composition of the calcarenite is rich in calcite and quartz. The main texture of the rock is micritic and microsparitic. The calcite crystals are found altered while fossils are commonly encountered filled with microcrystalline calcite (Fig. 18.3).

### 18.2.3 Mechanical Properties of Calcarenites

The physical and mechanical properties of the slightly to moderately cemented calcarenite (horizon A) where determined according to ISRM testing procedures (ISRM 2007). The properties are presented in Table 18.1. Additionally, jar slake tests were performed, in order to assess the degree of slaking, which resulted in moderate slaking degree according to the classification proposed by Santi and Shakoor (1997).

Kolaiti and Koumantakis (1991) determined the porosity of calcarenite of the study area equal to 17.6 % and the unconfined compressive strength equal to 25 MPa. The difference in strength is attributed due to the fact that the degree of cementation can differ significantly and thus the compressive strength of the calcarenite.

### 18.3 Instabilities of Tombs

The unstable conditions in both surface tombs, which were formed due to the collapse of the roof in the past, as well as underground tombs, are due to the intense loosening and deterioration of the calcarenite due to the action of surface processes (Fig. 18.4). The instabilities in the underground

**Fig. 18.2** Rosette diagram of encountered ground fractures on the surface and tombs

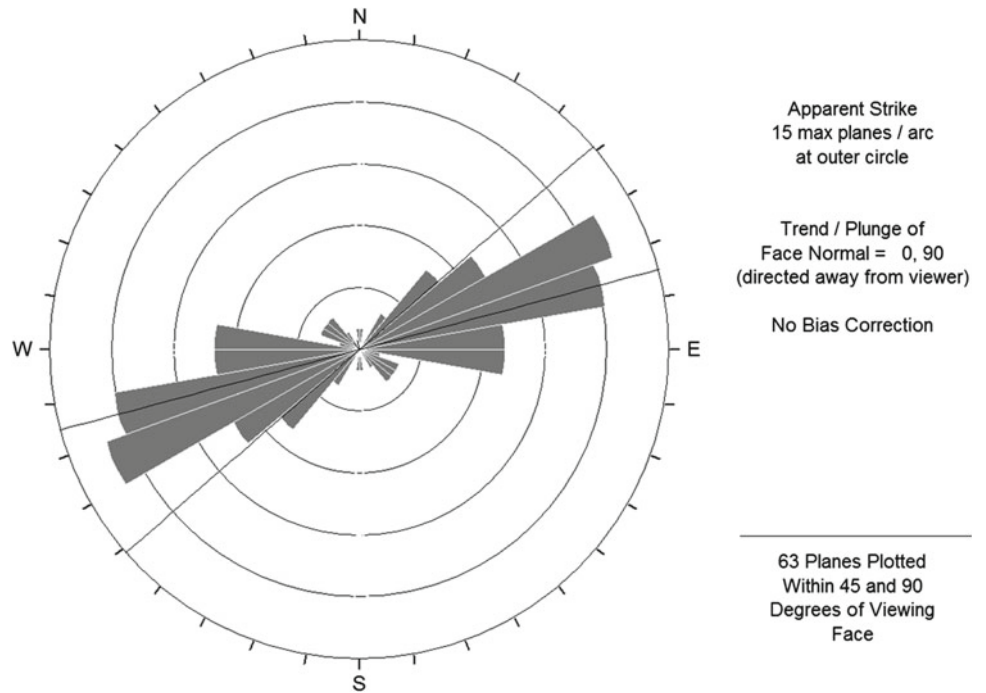


**Fig. 18.3** Scanning electron microscope (SEM) image of biomicritic, fossiliferous texture of calcarenite

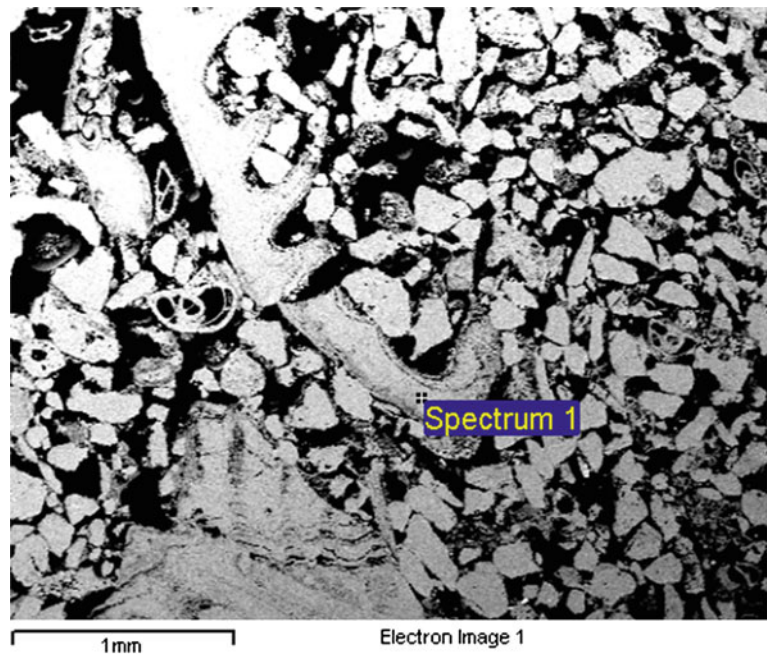


**Table 18.1** Physical and mechanical properties of calcarenite formation

Properties	Porosity (%)	Dry density (kN/m <sup>3</sup> )	Id <sub>2</sub> (%)	UCS (MPa)	E (MPa)
Calcarenite horizon A	19	22.8	64.6	1.5	590

tombs are primarily in the form of potential unstable calcarenite blocks formed at the sidewalls and roofs due to the presence of open joints, especially when they are wide or very wide.

The water infiltration and seepage in the tombs due to the presence of fissures and the high porosity of the calcarenite creates adverse conditions for the stability of the walls. Additionally, the immediate surface of the calcarenite is



**Fig. 18.4** Entrance of tombs showing the presence of fractures and deterioration of the walls by erosion processes

totally deteriorated and weathered up to a depth of about 10 cm, due to the organic action from insects and the presence of lichens.

The walls of surface tombs are often undermined to the different degree of weathering and varying strength of the calcarenite horizons and in some cases small overhanging blocks exist. The stability of the pit walls of the open surface tombs is marginal due to their small thickness and soft nature of the calcarenite.

---

#### 18.4 Stabilization and Improvement Measures

The stabilization and improvement measures of the tombs were distinguished according to whether their type of action is control of water or support of unstable weathered calcarenite.

The control of water infiltration was proposed through: (a) filling of open fractures with grout, (b) sealing of ground fissures on the surface in order to minimise the infiltration of water, (c) waterproofing of the area upslope of the tombs with a geomembrane and construction of surface runoff trenches. Additionally, the open surface tombs in the weathered weak calcarenite should be backfilled since the stability of their walls cannot be improved. Potentially unstable blocks in the surface and underground tombs can be

supported or anchored when applicable. The improvement of durability and strength of the calcarenite through application of different resin solutions on rock samples was evaluated. Based on slake durability tests, the slake durability index increases by 30 % approximately, while the water absorption reduces substantially. Luque et al. (2008) and Cultrone et al. (2012) have used adhesive and watertight solutions for the improvement of the behavior of calcitic biomicritic sandstones and concluded that these solutions can be very effective since they reduce the water absorption up to 100 %.

---

#### 18.5 Conclusion

The geological conditions that control the stability of the tombs are the friable and weak nature of the calcarenite, its high porosity and presence of extensive fractures, which allow water infiltration and its progressive weathering due to exposure to rain and wind as well as organic action. The improvement of the stability conditions of the tombs was rather difficult due to the very low strength and weathered condition of the hosting formation. The improvement of the stability was based on the control of water infiltration and supporting potentially unstable blocks. Finally, the improvement of durability of calcarenite with application of solutions was assessed and proved significant.

## References

- Arvanitakis M, Miligos C (1988). The early Christian catacombs at Melos island, Greece-study on the consolidation of the entrance. Proceedings of engineering geology of ancient works, monuments and historical sites, Balkema, p 319–325
- Arvanitakis M, Mira P, Asteriou A, Kotsopoulou E (1988) Stabilisation and protection of the sides of the trenches and pits of the Vergina Royal Tombs, Greece. Proceedings of engineering geology of ancient works, monuments and historical sites, Balkema, p 249–252
- Comninakis PE, Papazachos BC (1986) A catalogue of earthquakes in Greece and the surrounding area for the period 1901–1985. Aristotle University of Thessaloniki, p 167
- Charitaras B, Mariolakos I, Foundoulis J, Athanasias S, Dimitriou A (1997) Geotechnical input for the protection of some Macedonian Tombs in Northern Greece. In: IVth international symposium on the conservation of monuments in the Mediterranean Basin, Rhodes, pp 125–132
- Cultrone G, Luque A, Sebastián E (2012) Petrophysical and durability tests on sedimentary stones to evaluate their quality as building materials. *Q J Eng Geol Hydrogeol* 45:415–422
- ISRM (2007) The complete ISRM suggested methods for rock characterization, testing and monitoring: 1974–2006. In: Ulusay R, JA Hudson (eds) Suggested methods prepared by the commission on testing methods, Turkey, p 628
- Kolaiti E, Koumantakis J (1991) Engineering geological study of St. George Castle of Cephalonia (Ionian Islands, Greece). *Bull Eng Geol Env Springer* 43:61–67
- Luque A, Cultrone G, Sebastián E, Cazalla O (2008) Effectiveness of stone treatments in enhancing the durability of bioclastic calcarenite in (Granada, Spain). *Materiales de Construcción*. 58(292):115–128
- Santi PM, Shakoor A (1997) Characterization of weak and weathered rock masses. *Bull Assoc Eng Geol* 9:139–159

---

# Slope Geometry Design, Deformations and Failures of Ancient Quarries in Zhejiang Province, China

# 19

Lihui Li, Xiaolong Deng, and Zhifa Yang

---

## Abstract

There are many ancient quarry slope sites in Zhejiang Province, China. The typical quarries are Shanghuashan in Ningbo, Donghu, Houshan and Keyan in Shaoxing, Dafo Temple in Xinchang and so on. These slopes were excavated by the ancients 700 years even more than 2,000 years ago. Nowadays, these sites are all opened to the public for tourism. According to the field engineering geological investigations, the maximum height of the slopes is 60 m. Unique slope geometry design was made by the ancients to get larger production of stone and obtain safety of the workers: arc countertendency slope, arc slope in horizontal plane, supporting thin wall in the orthogonal direction to slope, triangular blocks supporting the top of the slope in a countertendency, horizontal bench along slope below fault etc. These geometries designed by the ancients can be reference for the modern quarry. Nowadays, deformations and failures occurred in some of the slopes: wedge failure, pressure shear or tensile crack, slide along the bedding plane or fault. Thoroughly engineering geology studies should be carried out as soon as possible to ensure the safety of the tourists and protect the ancient sites of quarry.

---

## Keywords

Ancient quarry slope • Slope geometry design • Deformation and failure

---

## 19.1 Introduction

There are many ancient quarry slope sites in Zhejiang Province, China. The typical quarries are Shanghuashan in Ningbo, Donghu, Houshan and Keyan in Shaoxing, Dafo Temple in Xinchang and so on. These slopes were excavated by the ancients 700 years even more than 2,000 years ago.

Nowadays, these sites are all opened to the public for tourism.

Donghu is located in Ruokui Mountain, 6 km east away to Shaoxing City. From Han Dynasty, the people began to excavate the stone. Till Sui Dynasty, the excavation had prevailed. After the excavation, the ponds and cliffs are the main scene of the quarry. Keyan is located at the foot of Keshan in Keqiao County, 12 km west to Shaoxing City. The excavation of it began in Han Dynasty, 1,800 years ago. Houshan is located in the Gaobu County, 12 km east to Shaoxing. The quarrying began at 2,000 years ago. The large chessboard stone and cloud stone is the most special scenery of the quarry (Fig. 19.1).

---

L. Li (✉) · X. Deng · Z. Yang

Key Laboratory of Shale Gas and Geoengineering, Institute of Geology and Geophysics, Chinese Academy of Sciences, Beijing, China

e-mail: lhli2942@mail.igcas.ac.cn



**Fig. 19.1** The chessboard stone (*left*) and the cloud stone (*right*) in Houshan quarry

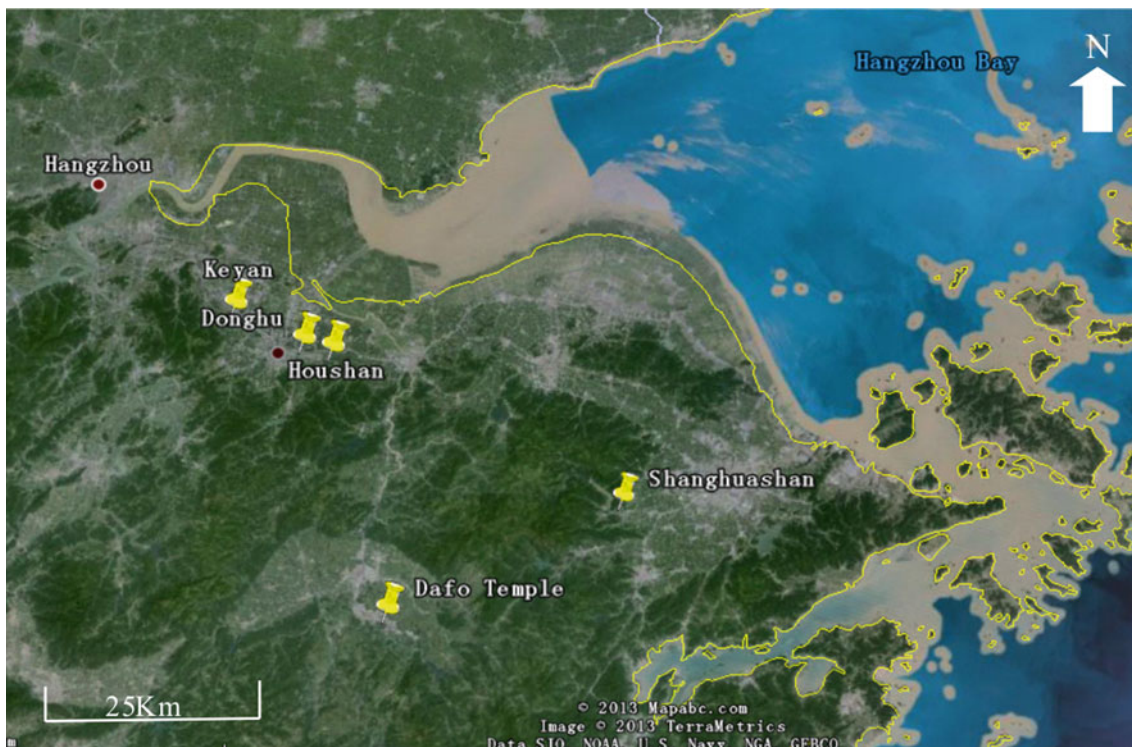
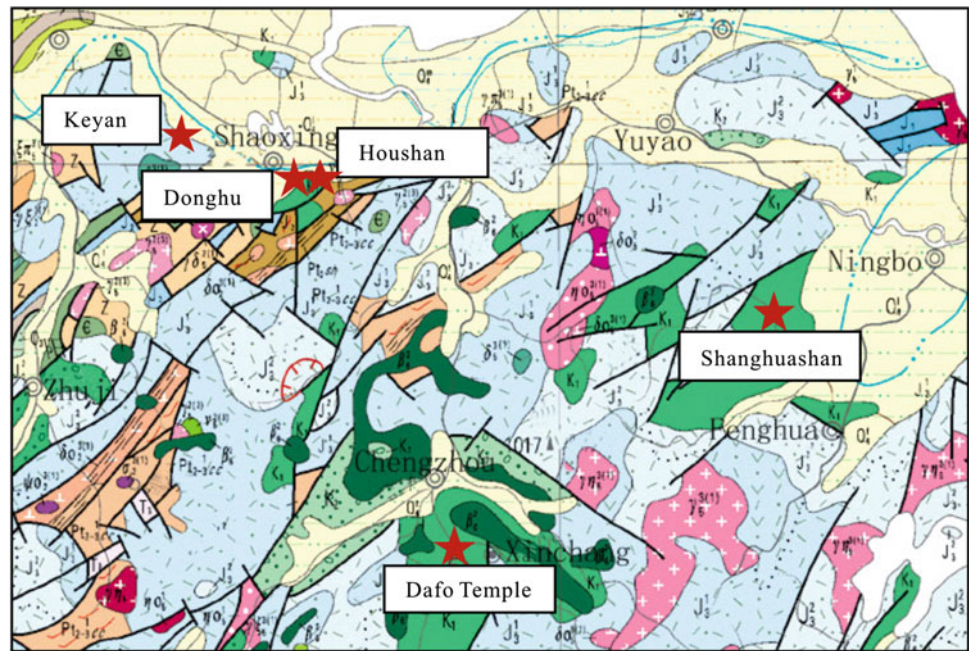


**Fig. 19.2** Location and topography of ancient quarries in Zhejiang Province, East China (drawn on topographical base of Google Map 2013)

Shanghuashan quarry is located in the Yinjiang Town, 25 km away from Ningbo City. According to the history record, the quarrying in Shanghuashan began in the Yuan Dynasty (1297), more than 700 years till now. Dafo

Temple is located in Xinchang County. The quarrying in Dafo Temple also began at 2,000 years ago. The location and topography of the ancient quarries was shown in Fig. 19.2.

**Fig. 19.3** The geological map of the ancient quarries



## 19.2 Geological Backgrounds

The outcrops of the four quarries of Keyan, Donghu, Houshan and Dofu Temple are the Chaochuan Formation ( $K_1C^1$ ) of Lower Cretaceous (BGMZP 1989). The outcrop of Shanghuashan is the Fangyan Formation ( $K_1f$ ). The stratum of Chaochuan Formation of Lower Cretaceous ( $K_1C^1$ ) is tuff breccia interbedded with sandstone and conglomerate. The stratum of  $K_1f$  is mainly medium to thick-bedded mauve siltstone interbedded with coarse gravel contained sandstone. The thickness of intact rock mass is about 0.4–4 m. Figure 19.3 gives the geological map of the other 5 quarries. The physical and mechanical parameters of the rocks are shown in Table 19.1.

The type of ground water in these areas belongs to fractured pore water. The water bearing formation is composed of gravel stone, siltstone intercalated with volcanoclastic rock of Lower Cretaceous. As the main recharge approach, the atmospheric precipitation penetrates directly into the rock mass along the fractured fissure. The underground water level varies apparently with the climatic variation especially in the rainstorm season, in which the underground water level rises up rapidly.

## 19.3 Special Slope Geometry

According to the field engineering geological investigations, the maximum height of the slopes is 60 m; the dip of each slope is almost vertical or antidip slope. Special slope geometry design was made by the ancients: arc countertendency slope, arc slope in horizontal plane, supporting thin wall in the orthogonal direction to slope, triangular blocks supporting the top of the slope in a countertendency, horizontal bench along slope below fault etc. Figure 19.4 shows the special slope geometry of the quarry slopes.

In Longyou caverns, there are also some special features in the structures of the caverns, such as the inclined ceilings, inclined sidewalls, the arc connection for in situ rock between pillar and ceiling, the iron-shaped horizontal cross-section of rock pillars and the L-shaped pillar base etc. Rock mechanical analyses were carried out numerically to compare the special structures and the common ones. The compared numerical results include tensile stresses, shear stresses, roof settlement, and wall bulge. The numerical results indicate that the special structures adopted benefit for the stability of the caverns (Li et al. 2006, 2007, 2011; Yang et al. 2011; Zhu et al. 2008).

**Table 19.1** Rock physical and mechanical parameters

Lithology	Natural density (g/cm <sup>3</sup> )	Elastic modulus (GPa)	Poisson's ratio	Cohesion (MPa)	Tensile strength (MPa)	Compressive strength (MPa)
Sandstone	2.470	32.85	0.152	56.60	15.043	142.48
Tuff (mean)	2.19	12.64	0.29	11.12	2.93	36.64

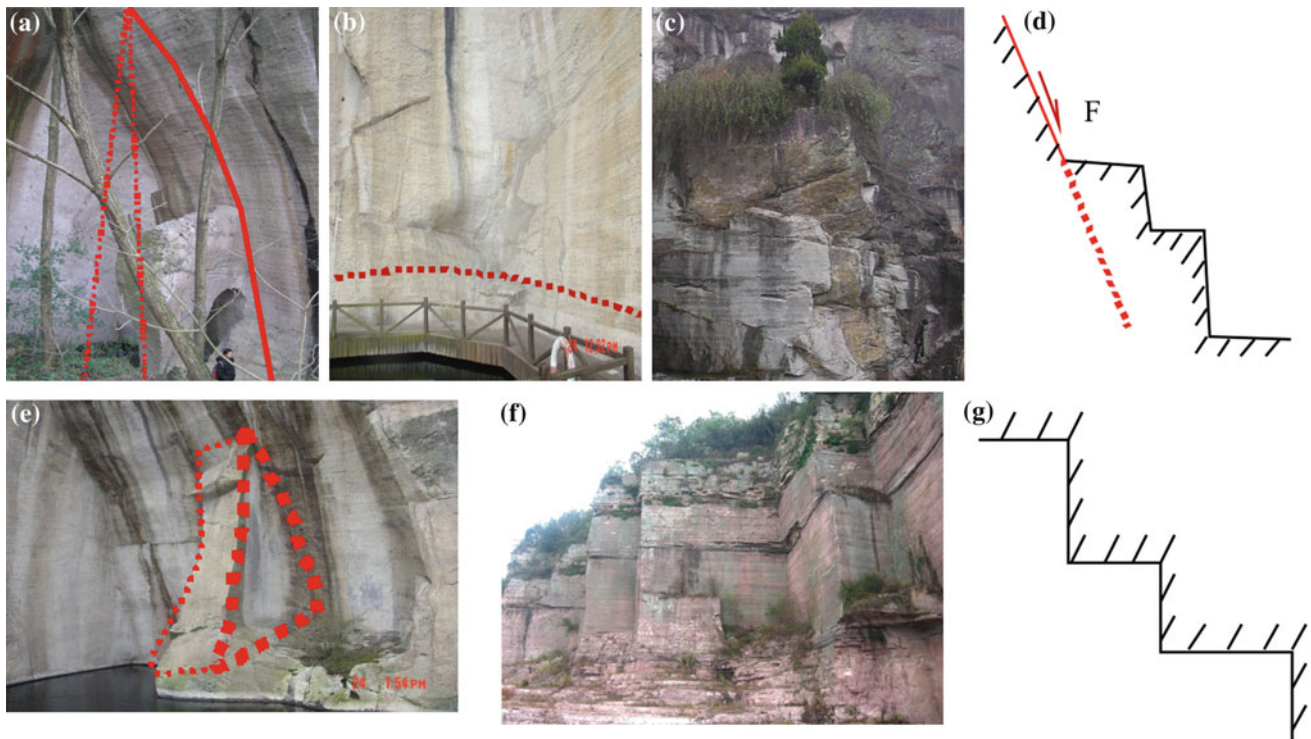


**Fig. 19.4** The geometry of the slopes adopted by the ancients **a** arc countertercenty slope, **b** arc slope in *horizontal plane*, **c** and

**d** horizontal bench along slope below fault, **e** triangular blocks supporting the slope, **f** zigzag slope and its *horizontal plane* (**g**)

Therefore, the special slope geometry of these quarry slopes maybe also the measures adopted by the ancients to get larger production of stone and obtain safety of the workers. More studies should be done to verify it. These geometries designed by the ancients can be referenced for the modern quarry.

## 19.4 Deformations and Failures of the Quarries

Nowadays, deformations and failure occurred in some of the slopes: wedge failure, pressure shear or tensile crack, slide along the bedding plane or fault. Figures 19.5 and 19.6 give the tendency of the rock fall and block sliding or toppling along structural plane and fault. The deformations or failures are mainly induced by the unreasonable exploiting for tourism. Moreover, the weathering of the rock mass is another reason for the failures. Figure 19.7 shows the cracks and flake weathering of the Yungu in Keyan. The Yungu is an in situ rock pillar left after quarrying. The reason why it was left is a secret, which made it be the most famous scenery in Keyan. However, there are many cracks occurred due to the long-term loading and the weathering. Therefore, thoroughly engineering geology studies should be carried out as soon as possible to ensure the safety of the tourists and protect the ancient sites of quarry.



**Fig. 19.5** The risk of rock fall in Donghu



**Fig. 19.6** The sliding of block along fault in Keyan

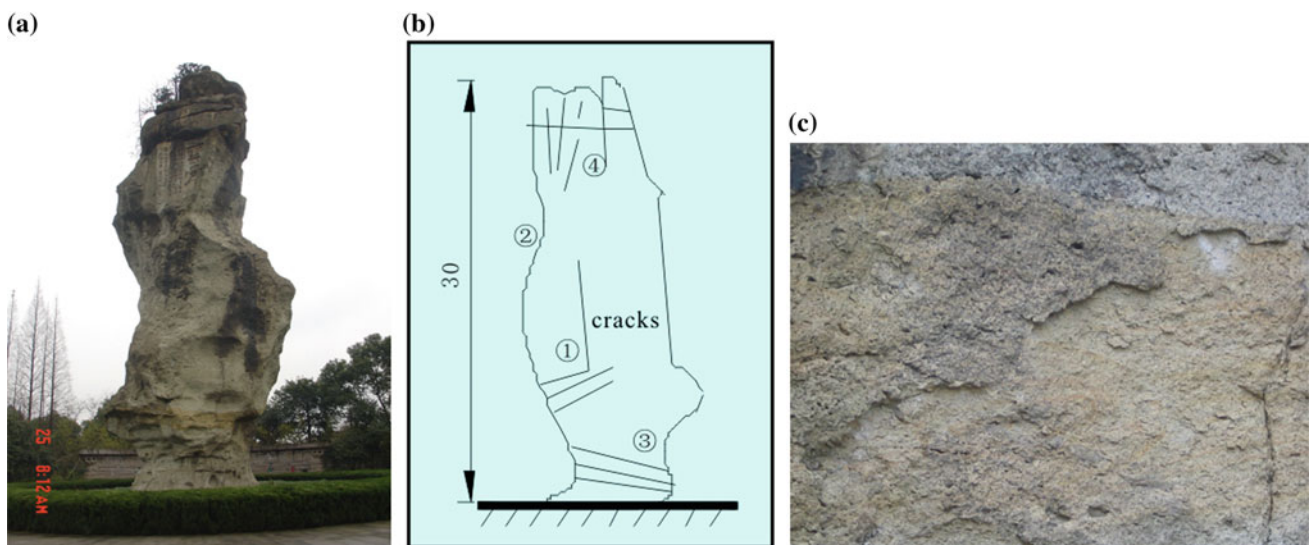


**Fig. 19.7** The cracks in the rock of Yungu in Keyan **a** the front side of the Yungu, **b** the cracks developed in the Yungu, **c** the flake weathering

## 19.5 Conclusion

- (1) The ancient quarry slopes in Zhejiang Province, China have a high value to study from the point view of engineering geomechanics.
- (2) The special geometries of the slopes are deserved to study thoroughly and maybe can be referenced by the modern quarry.
- (3) Many deformations and failures occurred in the quarry slopes due to the unreasonable exploiting for tourism. Thoroughly engineering geology studies should be carried out as soon as possible to ensure the safety of the tourists and protect the ancient sites of quarry.

**Acknowledgments** This work has been supported by the National Natural Science Foundation of China (No. 41172269 and No. 41372322).

---

## References

- BGMRZP (Bureau of Geology and Mineral Resources of Zhejiang Province) (1989) Regional geology records of Zhejiang Province. Geology Press, Beijing
- Li LH, Yang ZF, Liu JL, Lu M, Xu JH, Zheng J (2006) Research on the design of inclined walls in the ancient non-arched caverns: case study of the Longyou Caverns and the no. 3 grotto in Beixiangtang temple grottoes. In: Proceedings of the international symposium on protection of Longyou Grottoes in China
- Li L, Yang ZF, Yue ZQ (2007) The influence of cavern's structures on the long-term stability of Longyou large underground caverns. *J Eng Geol* 18(suppl):45–53
- Li LH, Yang ZF, Yue ZQ (2011) Special shapes and their effects on stability of Longyou Caverns, China. In: The 14th Asian regional conference on soil mechanics and geotechnical engineering, Hong-Kong, China
- Yang ZF, Yue ZQ, Li LH (2011) Design, construction and mechanical behavior of relics of complete large Longyou rock caverns carved in argillaceous siltstone ground. *J Rock Mech Geotech Eng* 3 (2):131–152
- Zhu JW, Bo S, Liu EC et al (2008) Mechanics idea of Longyou Grottoes structure. *Rock Soil Mech* 29(9):2427–2432

---

# Underground Tunneling to Match Social Development and Preservation of Historical and Cultural Heritage: Bangalore Metro Line UG-1

20

Giuseppe M. Gaspari, Namita Gopeenatha, and Prathap Muniyappa

---

## Abstract

The fast economical growth and the great development of Bangalore, Capital of Karnataka State in India, transformed the city in one of the biggest metropolises in India: the population almost doubled in the last 20 years, but without the contemporary and proper increase in public services and utilities. A special opportunity is nowadays given to the inhabitants: a profound change in public transports network has been developing, particularly with recent design and construction of metro line UG-1. The central portion of the line runs under the ancient historic centre of Bangalore, characterized by old buildings and a labyrinth of streets along which huge market activities take place. In order to manage such neuralgic and sensitive areas, special technologies were adopted to reduce the tunneling impact. The biggest issue was to match the civil works with preservation of the ancient heritage buildings of the area: the target is being achieved through an integrated design procedure, capable of taking into account results coming from site monitoring and the most recent developments of research in the field of building risk assessment.

---

## Keywords

Induced settlements • Risk analysis • Numerical modeling • Urban areas • Social development

---

## 20.1 Use of Underground Space: The Adoption of TBMs to Attenuate Settlements on the Surface and Reduce Traffic

The recent experience of the design of UG-1 metro line in Bangalore is referred to be a remarkable example of the main challenges related to urban tunneling in densely urbanized areas. The use of the underground space was deeply analyzed in order to maximize the possibility of using the narrow areas available to execute every intervention to

consolidate the ground and guarantee the stability of the existing building and the safe excavation of stations, tunnels and cut and cover structures. However, the limited availability of surface space imposed to take the advantage of supporting solutions such as propping directly on the buildings instead of intervening with grouting or injections.

EPB—Tunnel Boring Machines was chosen as the best solution in order to reduce settlements on the surface and the required working areas, thus decreasing the impact on the already chaotic traffic of the city. Every system widely known in literature for ground improvement was studied to be adapted to specific real conditions, characterized by a variable water table level and inconstant geology, with alternate strata of silty sand and sandy silt, detected on a bedrock that was found at different depth in different stretches of the alignment. Furthermore, presence of boulders was foreseen, thus requiring a specific geotechnical design for tunnels, stations, shafts and access ramps to avoid

---

G.M. Gaspari (✉)  
Geodata Engineering SpA, New Delhi, India  
e-mail: giuseppegaspari@hotmail.com

N. Gopeenatha · P. Muniyappa  
Geodata India Pvt. Ltd., New Delhi, India

unexpected collapses of the temporary structures at the construction phase.

### 20.1.1 The Study of Tunneling Impact on Historical Buildings

The study of deformations induced by the excavation of tunnels was very important in order to evaluate the expected damages, particularly on the most ancient buildings. At the stage of preliminary evaluation, the building risk assessment is based on empirical relations. These ones are widely confirmed by the direct experience of several projects and have been extensively validated in literature since many years. They allow an evaluation of the dimension and the shape of the subsidence basin due to excavation. However, in order to be as more consistent as possible with the geology and with the geotechnical characteristics of the ground, an integration of such a methodology with numerical analyses was often applied.

The limit values for deformations are given by Burland (1977) and Boscardin and Cording (1989), that defines different risk category based on the cracks present in the structure or expected to appear after tunneling. For structures with continuous foundation the limit values for deformation are given by Burland (1977) that defines different risk category based on the cracks present in the structure. For structures with isolated foundations the classification is given by Rankine (1988) that fixes limit values for settlement and angular deformation (Fig. 20.1).

### 20.1.2 The Adopted Solutions for the Ancient Heritage Buildings

In the number of buildings studied in the historical center of Bangalore, some of them were analyzed with particular

effort, considering both their cultural value and their social importance, such as the Victorian Age Vani Villas Hospital and the six centuries old Kote Venkateshwara Swamy Temple, in order to organize in the best way evacuation and protective measures on the buildings. The first is one of the leading and more important health-care and medical centers of the city.

The Temple is one of the most important religious hearths of the whole State of Karnataka, as the yearly increasing number of pilgrims and offers confirm. It stands just in front of one of the most famous masterpiece of the Region, the outstanding Tipu Palace, ultimate house of the last Maraja who tried to oppose to the British expansion in the early eighteenth Century (see Fig. 20.2).

In consideration of the analyses' results, that were showing quite a remarkable effect of the excavations on some of the above described buildings, specific drawings and reports were produced to list the countermeasures to be adopted for the specific structure both with the aim of a proper monitoring plan and with the purpose to guarantee the safety of inhabitants/users of the building facilities. The achieved target was that of preserving the archeological beauties and, in case, giving the shortest possible time for building reinstatement, reducing to the minimum the disturbance to people's life and to tourists ease of access.

## 20.2 Case History of an Archeological Heritage Preservation

The necessity to reduce or eliminate the hazard on such an ancient structure as the Temple described in Sect. 20.1.2, together with the requirement of guaranteeing the continuity of religious celebrations, imposed to apply innovative techniques for reducing damages due to geotechnical causes. A step by step sequence of actions was given to local Authorities to be applied on the studied buildings in order to

**Fig. 20.1** Vertical Settlements to evaluate induced deformations on the building

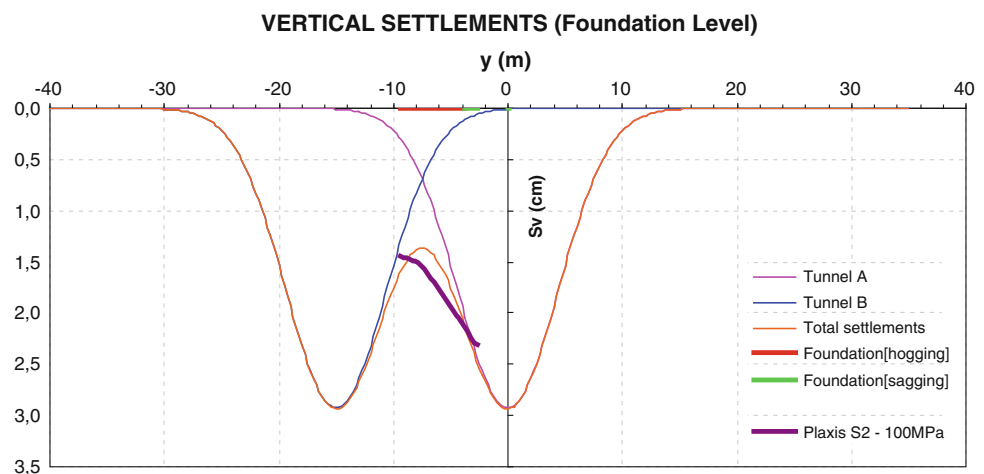




**Fig. 20.2** Typical examples of the historical heritage in Bangalore, just close by the tunnels: Kote Venkataramana Temple (*left*) and Tipu’s Palace of 1537 (*right*)

guarantee the maximum safety both for people and structures and in coherence with contents of the structural studies and of the Pre Condition Building Survey executed by the Contractor. With the purpose of limiting its tilt and counteracting the induced settlements during tunneling by giving a monolithic behavior to it, the ancient column in front of the East temple entrance was protected with an appropriate combination of propping and casings, with tendons to anchor the central body to the tower in front of it and to pins to be inserted in the foot-path.

Subsequent site visits clearly showed a better structural behaviour than expected from the lateral wall facing the tunnel alignment and from the internal tower, thus not requiring any propping but an evacuation plan during the time in which TBMs excavated close to such structures. In front of the wall, rigid barricades imposed the pedestrian to walk on opposite side of the road, while, inside the temple court, light barricades exactly demarcated accessible areas at every time, depending on the TBMs advancement and on the monitored parameters.

**Fig. 20.3** Monitoring instruments codes at Kote Venkataramana Temple

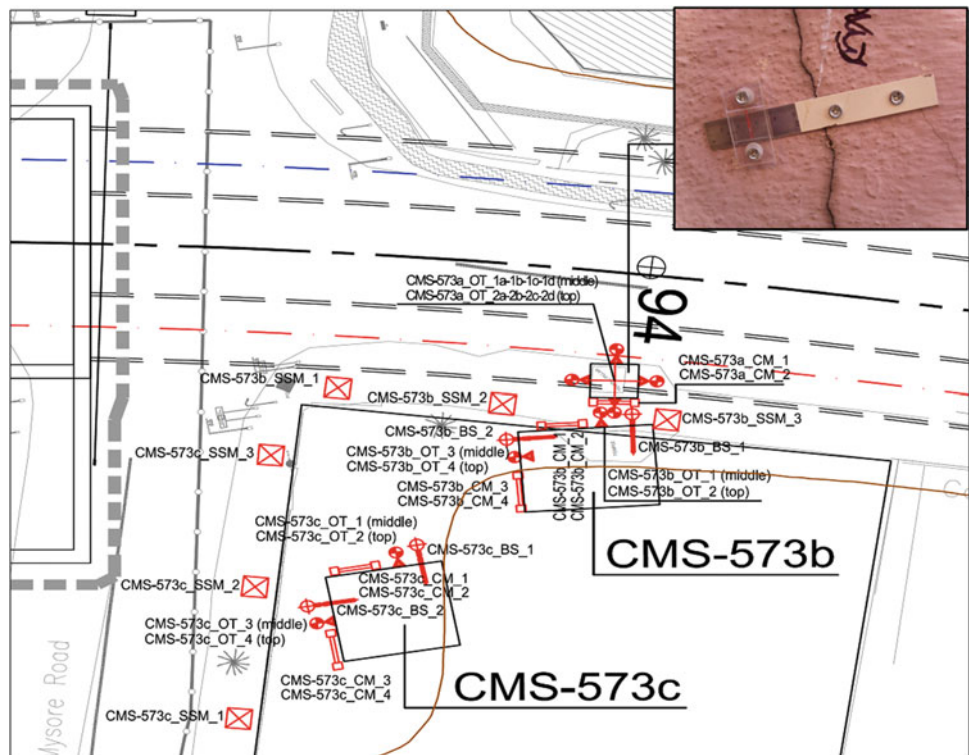




Fig. 20.4 Protective means for the monuments at Kote Venkataramana Temple

### 20.2.1 The Monitoring System Applied to the Temples Area

The most advanced and non-invasive monitoring techniques were adopted to define present condition and expected dynamics of the monument during tunneling.

Trigger values were set for all typologies of instrument in order to create a system of alert and alarm involving the Employer, the Engineer and the Designer in a multidisciplinary work. The actual trend assessment was the first target for sustainable mitigation strategies development.

Considering the importance of the building and its risk category, monitoring was required to both guarantee a continuous and proper check on the stability of the individual elements and to assure the safety of people.

Furthermore, a continuous check before, during and after the TBM excavation below the tunnels was recommended in order to verify the trigger, design and allowable levels provided in order to guarantee proper countermeasures and immediate action as per monitoring report on the instruments installed.

Instruments had minimum impact both on the structure and on the aesthetic of the heritage building such as the

example of the crack meter in Fig. 20.3. Furthermore, optical targets and base settlement markers were fixed on the building external walls without performing them and consequently without causing damage.

### 20.2.2 The Precautionary Measures and the Planned Countermeasures

Installation of monitoring system both on the structures and on the roads and footpath was followed by a precise plan of evacuation of certain areas of the temple complex according with TBMs advancement and by setting up a propping system on the column and on the main entrances of the area. Collecting and storage of the required material for propping of other portions of the buildings as per plan view shown in Fig. 20.4 was also required, in case assigned figures overpassed limits.

As soon as TBM face reached an assigned chainage, the main entrance to temple area was closed to everyone out of the temple religious authorities (who could access after a daily permission by the Engineer if safety condition were verified).

As the TBMs advanced, subsequent gates were opened and used for emergency exit at any time. Main entrance was propped in such a way to guarantee doors opening and religious ceremony to take place in the period between the transit of the two TBMs, but all propping remained in place until the second TBM passed through. Horizontal forces, tilting risk and differential vertical settlements were taken by horizontal propping dimensioned for this specific purpose.

Propping of the upper portion and of the cut-outs and windows of the tower was not required as they could cause

even more damages to the statues if executed by not specialized workers and in any case the flow of stresses in the structure was expected not to be affected by any impact from their presence, considering the very limited ratio between their area and the total mass of the masonry tower.

With the adequate propping provided, the aim of reducing the impact of induced cracks by the ground settlement, with no tilting of the structure, was achieved. However, by monitoring daily both the settlements at foundations and the angular distortion, an emergency plan was ready in order to avoid any damage.

---

## 20.3 Conclusions

Since 2010, a decisive alternative in public mass transport systems of Bangalore was planned as a network of metro lines was chosen to be the answer to growing demand for urban mobility. One of the most important concerns of the Designer of UG-1 line was to reduce the impact of the new civil works on the ancient heritage buildings of the old city center: the target was achieved through an appropriate set of monitoring instrumentation and countermeasures specifically developed.

---

## Reference

Gaspari GM et al (2012) Urban requalification opportunity and social responsibility of underground structures. The case of Bangalore Metro line UG-1—ITA-AITES World Tunnel Congress 2012 in Bangkok

# Three Dimensional Pore Geometry and Fluid Flow of Kimachi Sandstone Under Different Stress Condition: Suggestion to Conservation of Tuffaceous World Cultural Heritage

Manabu Takahashi, Naoki Takada, Minoru Sato, and Weiren Lin

## Abstract

During the confined triaxial compression test, we measured permeability of Kimachi sandstone by Transient Pulse test for three mutually perpendicular directions under effective confining pressure. In general, the permeability of Kimachi sandstones decreased slightly with increasing the effective confining pressure. Permeability anisotropy was also observed in the normal and two parallel directions to the bedding planes. We introduced the three-dimensional medial axis (3DMA) method to quantify the flow-relevant geometric properties of the voids structure in Kimachi sandstone. Using these data, we evaluated the number of connecting path between two faces, tortuosity and the shortest path distribution within an arbitrary region of Kimachi sandstone specimen. Geometrical information on the number of connecting path in an arbitrary volume CT data shows reasonable correlation between permeability anisotropy and mutually perpendicular directions normal and parallel to bedding planes. It is confirmed that pressurization effect on permeability caused by the decrease of the connecting path and the shortest path between arbitrary faces, and then caused a complex condition of on fluid pressure and fluid velocity.

## Keywords

Permeability anisotropy •  $\mu$ -focus • X-Ray CT • Medial axis distribution • Tortuosity • Number of connecting path • Numerical simulation • LBM

## 21.1 Introduction

Most of tuffaceous rock are widely used for building materials and monumental sculptures in antique culture, because of this kind tuff is relatively soft and easy to cut, and easy to take it. Tuffs are volcanic rocks, from the view point of

geological aspect, they are a typical rock consisting of consolidated volcanic ash ejected from vents during a volcanic eruption. Tuffs exist in a great assortment of colours, composition, grain size, sorting and textures which depends on each production areas and geological history. Fluid flow of water and related phenomenon is clearly recognized as one of the most important factors contributing to the weathering and deterioration of building rocks. The mechanical and hydraulic properties of tuffaceous rocks are a major and common concern in preservation of world cultural heritage and engineering fields. The permeability and specific storage of tuffaceous rocks and sedimentary are very important parameters for problems related to the buried evaluation of conservation of tuffaceous world cultural heritage. In this study, we provide some knowledge for understand the relation between geometrical information of voids space in tuff, which is taken from Shimane prefecture in Japan, and permeability and specific storage obtained by

M. Takahashi (✉) · N. Takada  
National Institute of Advanced Industrial Science and Technology,  
1-1-1 Hi-gashi, 305-8567 Tsukuba, Japan  
e-mail: takahashi-gonsuke@aist.go.jp

M. Sato  
Tsukuba University, Tsukuba, Japan

W. Lin  
Japan Agency for Marine-Earth Science and Technology,  
Yokosuka, Japan

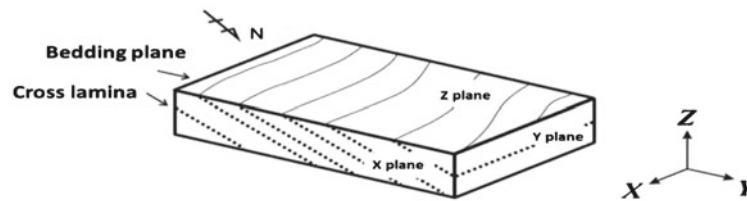


**Fig. 21.1** Schematic view of Bedding plane and Cross Lamina

permeating test of Transient Pulse test under various effective confining pressure.

## 21.2 Specimen

### 21.2.1 Geology of Kimachi Sandstone

Kimachi sandstone is one layer of the Miocene Omori Formation which is distributed around the south shore of Shinji Lake, southwest Japan. The Kimachi sandstone has a clear bedding plane and not clear cross lamina in cm size specimen, which is mainly caused by grain orientation and void space in microscopic scale, as shown in Fig. 21.1. It is a medium-grained tuffaceous sandstone (Kano et al. 1991). Average grain size is 0.5–1.0 mm and it consists of clastics derived from andesite lavas. It is composed of 80 % clasts and 20 % matrix. The Z axes of the specimens are vertical to the horizontal plane and their horizontal directions (X and Y direction) are arbitrary.

### 21.2.2 Properties of Testing Samples

The rock samples used are Kimachi sandstone, which were taken from Shimane prefecture in Japan. As shown in Table 22.1, Kimachi sandstone is tuffaceous and is characterized by large void ratio. Figure 21.2 shows pore size distribution of Kimachi sandstone by Mercury Intrusion Porosimetry. Twin peaks were observed in the almost range of 0.03–0.05  $\mu$  diameter and 0.4–0.6  $\mu$  diameter, and total porosity is about 21 %.

## 21.3 Permeability and Specific Storage of Kimachi Sandstone

Triaxial compression tests were carried out using the triaxial testing apparatus which is composed of the load frame, the axial actuator, the triaxial cell, the confining pressure

**Table 21.1** Properties of rock samples

Mass	(g/cm <sup>3</sup> )	2.23
Porosity	(%)	25.8
Speed of P-waves	(km/sec)	2.90
Speed of S-waves	(km/sec)	1.61
Dynamic Poisson's ratio		0.276
Dynamic Young's Modulus (MPa)	(MPa)	18,125

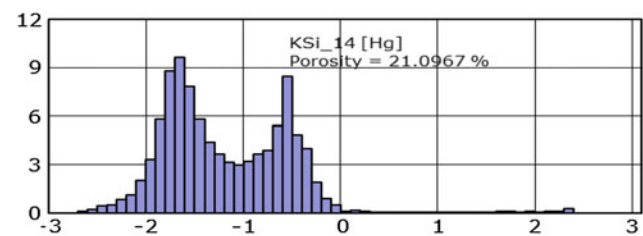


**Fig. 22.2** Pore size distribution of Kimachi sandstone by MIP

intensifiers, the pore pressure intensifiers, the digital controller, and the PC workstation. The stress control system is composed of digital servo control. This system allows us the high-precision control over stress management. Permeability and specific storage of Kimachi sandstone under effective confining pressure to 25 MPa were evaluated by rigorous analysis in Transient Pulse test. Triaxial compression tests were conducted in conformity to ISRM standards. The results of the tests were organized by putting compressive stresses and compressions to be positive values. Figure 21.3 show permeability evolution for three directions (a), and specific storage values for X, Y and Z directions (b). Permeability for Z direction showed the highest value and all three directions showed almost same effect on effective confining pressure. But, specific storage for Z direction showed the least value and those of X and Y direction showed almost similar value and same confining pressure dependency.

**Fig. 22.3** Effective confining pressure effect on permeability for three directions (a), specific storage of Kimachi sandstone with changing effective confining pressure (b)

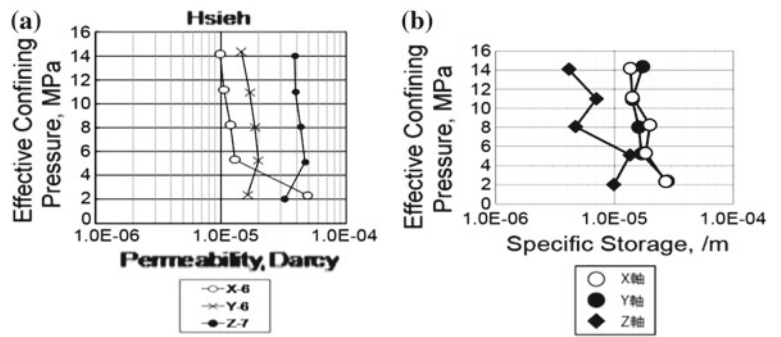


**Fig. 22.4** CT volume data under air and pressurization to 25 MPa

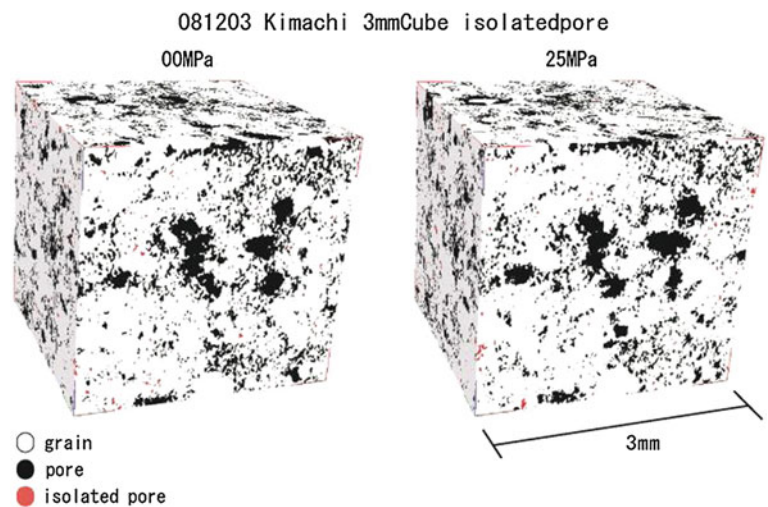


**Fig. 22.5** Geometrical information of Berea sandstone under air condition

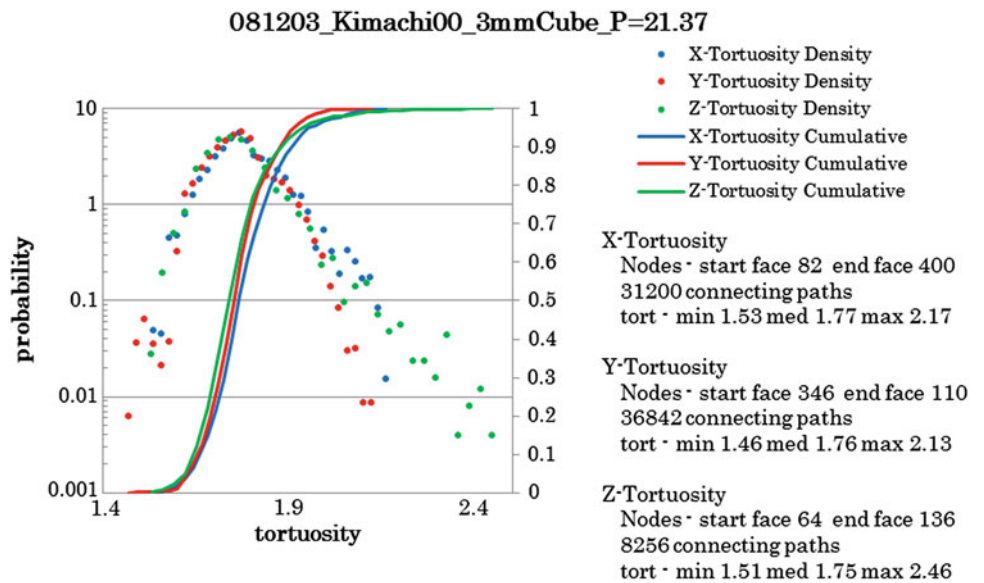
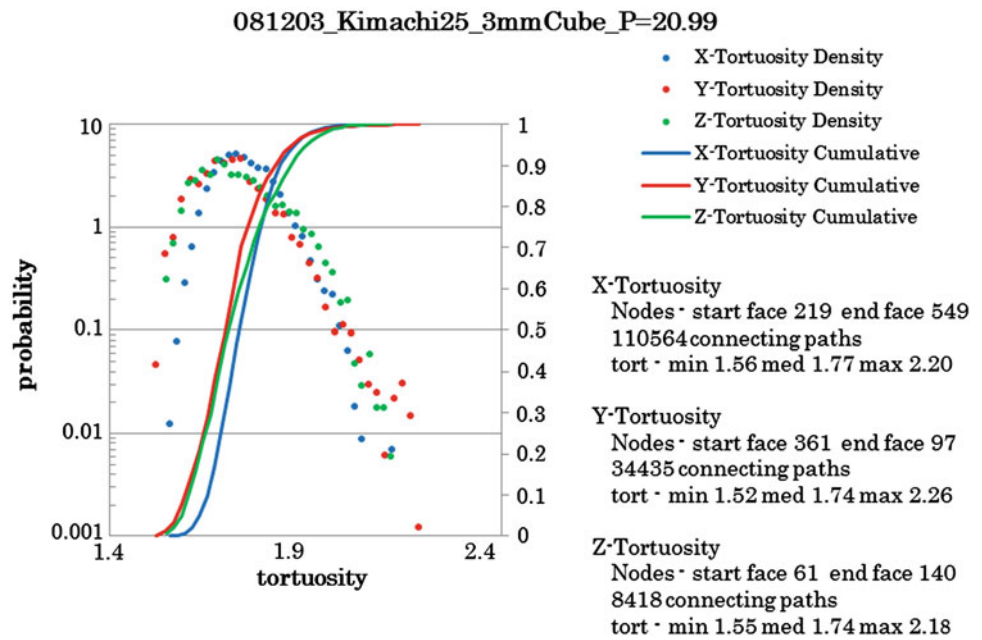


**Fig. 22.6** Geometrical information of Berea sandstone under pressurization to 25 MPa



## 21.4 Quantification of the Flow-Relevant Geometrical Information with $n$ Focus X-Ray CT

Figure 21.4 shows original CT volume data of 3mm voxel size under air and pressurization to 25 MPa. In this Fig., black region indicates void space, and red color indicates isolated pore space which is neglected in Medial Axis analysis (Lindquist and Venkatarangan 1999). From both CT images, we can recognize the differences of each size void space. Figures 21.5 and 21.6 show geometrical information of Berea sandstone under air and pressurization to 25 MPa. Maximum pressurization to 25 MPa is correspond to the stress condition at almost 1,000 m depth underground. Total bulk porosity decreased a little with under pressurization, those porosity data were obtained by Mercury Intrusion Porosimetry under air condition, and by subtraction volume compaction by pressurization from porosity in air condition. Number of connecting path for z direction showed the least value under air condition, but almost same value under pressurization. On the other hand, number of connecting path for x direction increased under pressurization. This geometrical information change due to pressurization are not sufficient for good explanation of permeability anisotropy. Permeability measurement method is considered as bulk estimation of rock physics, one of void connectivity. Geometrical information can't correlate well permeability phenomenon.

## 21.5 Conclusion

Permeability measurement of Kimachi sandstone was carried out to obtain the permeability and specific storage under effective confining pressure. The Kimachi sandstone has a not clear bedding plane and cross lamina in cm size specimen, which is mainly caused by grain orientation and pore distribution in microscopic scale. Permeability for vertical direction show larger value than those for horizontal two directions. Specific storage for three directions decreased with increasing effective confining pressure, and showed dominant reduction around the maximum strength. Using the data related to the connecting path and tortuosity of the Kimachi sandstone obtained by X ray CT, anisotropic phenomenon for different three perpendicular directions on permeability and specific storage are discussed with geometrical information, but both phenomenon can't correlate well.

## References

- Kano K, Takeuchi K, Matsuura H (1991) Geology of the Imaichi district. Geological Survey of Japan, Tsukuba
- Lindquist WB, Venkatarangan A (1999) Investigating 3D geometry of porous media from high resolution images. *Phys Chem Earth Part A* 25(7):593–599

# Application of Non Destructive Ultrasonic Techniques for the Analysis of the Conservation Status of Building Materials in Monumental Structures

Basile Christaras, Francesco Cuccuru, Silvana Fais, and Helen Papanikolaou

## Abstract

Some examples of application of ultrasonic methods were chosen in different test areas located in Southern Sardinia (Italy) and Northern Greece coastal areas: (1) Cagliari town (Southern Sardinia—Italy), masonry structure and architectural element of an ancient monument. (2) Dion archaeological site (N. Greece). The study on the above mentioned monument was focused on the application of ultrasonic techniques in the low frequency range (24–54 kHz), with the aim to verify the conservation status of their building materials by means of the study of the longitudinal ultrasonic pulses propagation. Compressional velocity has been related to the physical, textural and mineralogical-petrographic features of the investigated materials, to correlate their intrinsic properties with the elastic ones. On the base of the laboratory ultrasonic measures, in situ investigations have been performed to identify the areas affected by degradation, quantify the intensity of weathering and monitoring his evolution. In addition, the methodological approach used in this study has proved to be useful also to reconstruct the texture of walls under the plaster or in the outcropping masonry structures, where the degradation makes it difficult the macroscopic identification of building materials.

## Keywords

Ultrasonic velocity • Historical buildings • Monument protection • Weathering description

## 22.1 Introduction

The need to recover the historical buildings for a reuse allowed a significant expansion of non-destructive diagnostic investigations. With non-destructive tests it is now possible to get all the qualitative and quantitative parameters

useful to formulate a plan of recovery and preservation of a monumental structure.

Nowadays, the non-destructive ultrasonic method represents one of the most reliable diagnostic methods used in the building materials of monumental structures. The high relationship between propagation velocity of the ultrasonic pulses in stone materials and its physical, textural and mineralogical features is the strength of this method. The integrated analysis of ultrasonic method with the physical and mineralogical-petrographic data of building materials, allows obtaining important information about the conservation status of the monumental structures. The changes in time of the elastic properties, observed by means of ultrasonic measures, identify the evolution of degradation in building materials and provide useful information about the effectiveness of restoration works. In fact, alterations in the materials, normally, cause a decrease in the longitudinal

B. Christaras (✉) · H. Papanikolaou  
Laboratory of Engineering Geology and Hydrogeology, School of Geology, Aristotle University of Thessaloniki AUTH, Thessaloniki, Greece  
e-mail: christar@geo.auth.gr

F. Cuccuru · S. Fais  
Dipartimento Di Ingegneria Civile, Ambientale E Architettura DICAAR, Università Degli Studi Di Cagliari, Cagliari, Italy  
e-mail: sfais@unica.it

pulse velocity values and therefore the longitudinal velocity values can be considered representative of the elasto-mechanical behaviour of the stone materials.

## 22.2 The Case Study of Cagliari (Italy)

### 22.2.1 Materials and Methods

#### 22.2.1.1 Materials

The stones used in the building of the monumental structures of Cagliari (Italy), come from a prevalently carbonate succession, cropping only in the town hills, known as “Calcari of Cagliari Auct”. This sedimentary complex, attributed to Tortonian-Messinian, is formed by three different limestones which from top to bottom are called: *Pietra Forte*, *Tramezzario* and *Pietra Cantone*.

*Pietra Forte* is a bioclastic shelf limestone very compact, tenacious, very hard, poorly porous, even if in some cases can be intensely fractured and interested by many carsic cavities.

*Tramezzario* is a white, well lithified, bioclastic limestone without stratification. It can be characterized by an intense fracturation associated with the alteration and the disaggregation of the rock, making it very porous and making to assume it the characteristics of a loose rock.

*Pietra Cantone* is a bioclastic, limestone without stratification, frequently bioturbated. Generally it is a very soft stone, characterized by an elevated porosity and by an elevated percentage of matrix that make this rock very hygroscopic. The low cementation of the granules causes disaggregation in the rock, especially in conditions of strong humidity.

Samples of these limestones have been analyzed for determining their mineralogical and textural characteristics using respectively X-ray diffraction and thin sections observed to petrographic microscope.

The different textural characteristics of the three lithotypes regulate the intensity of the degrade process. In the cases of the *Pietra Cantone* and *Tramezzario*, that are characterized by

a high porosity (>20 %), the processes of erosion, alveolization, disaggregation and detachment (Fig. 22.1a, b) are frequent. In the matrix supported limestones (*Pietra Cantone*) a large quantities of water can be accumulated. This fact causes the degradation of the stone. In the *Pietra Cantone* is frequent the alveolization, that causes the formation, on the stone surface, of cavities (alveoles) which may be interconnected and may have variable shapes and sizes. *Pietra Forte*, that is a shelf limestone, is more resistant than the *Pietra Cantone* and *Tramezzario*. However, if the *Pietra Forte* is fractured, the materials near the discontinuities are subject to the oxidation and to the detachment (Fig. 22.1c).

#### 22.2.1.2 Laboratory and in situ Ultrasonic Measurements

One of the most effective tools in restoration and rehabilitation of monumental structures is the ultrasonic inspection which includes the assessment of damaged or altered zones, cracks, defects and elasto-mechanical characterization of stone materials (Galan et al. 1991; Christaras 1997; Casula et al. 2009; Fais and Casula 2010).

The ultrasonic techniques are effective both for laboratory and site conditions and they have increasingly been used to determine the dynamic properties of rocks and then their mechanical behaviour. In fact the ultrasonic velocity of a rock is closely related to the rock properties. Therefore, the velocities of longitudinal wave ( $V_p$ ) have been calculated for the different type of limestones under study (Table 22.1). The ultrasonic measurements have been performed, in laboratory condition, on prismatic unaltered specimens ( $12 \times 12 \times 24$  cm) prepared for the application of the ultrasonic techniques according to C.N.R.—I C R—Normal—22/86 (1986). The mentioned ultrasonic measurements were performed using the Portable Ultrasonic Non-Destructive Digital Indicating Tester (PUNDIT) by C.N.S. Electronics LTD.

On the basis of the results of the laboratory tests, in situ ultrasonic measurements on significant monumental structures in order to check zones of weakness, to assess the



**Fig. 22.1** Different types of degrade: **a** Alveolization of the *Pietra Cantone*, **b** Detachment of material from a wall of *Tramezzario*, **c** Detachment of material from an architectural element of *Pietra Forte*

**Table 22.1** Ultrasonic Velocities measured in laboratory

Lithotype	$V_p$ (m/s)
Pietra Cantone	3,000
Tramezzario	4,500
Pietra Forte	6,000

alterability of the investigated stones and evaluate the restoration effectiveness have been also carried out. In fact, as it is known, alterations in the material lower the ultrasonic velocity value, which can be considered representative of its elastic status. Longitudinal pulse ultrasonic velocities were measured in situ using the above mentioned portable ND indicating tester (PUNDIT) with 54 kHz transducers. As cases study, some architectural elements of the church of S. Chiara on the historical downtown of Cagliari, were tested. S. Chiara church is an important monument built in the seventeenth century in the historic district of Stampace. It was one of the most popular religious sites of the city in the past centuries. Nowadays, closed to worship, the church has become an important point of performance of cultural events such as visual art exhibitions, concerts and theatrical works.

## 22.3 Application

### 22.3.1 The Case of the Church of S. Chiara

In this paper the results obtained on an outside structural element (external pillar) of the church of S. Chiara are presented. Tests have been performed both by indirect (surface).

Ultrasonic measurements by indirect transmission have been carried out on the surfaces of the pillar to know the conditions of the building materials on its superficial parts. The measurements of the travel time of the ultrasonic signal from transmitter to receiver were carried out along parallel

profiles in a vertical direction and particular care was given to take measurements at the same level in all the profiles. Starting from the measured travel time of the ultrasonic signal and considering as space the distance between transmitter and receiver, the apparent propagation velocity at each observation point along the profiles was computed. The values of the longitudinal ultrasonic velocity were contoured to represent the distribution of the velocity on the investigated surfaces with the aim of detecting damages and degradation zones by studying the velocity variations. In fact, ultrasonic signal characteristics change as the wave propagates through the carbonate materials with varying properties such as porosity, pore types, mineralogical and petrographical composition also as a result of degradation. In Figs. 22.2a, b and 22.3a, b are reported both the acquisition schemes and the ultrasonic longitudinal velocity maps of the accessible faces of the pillar respectively named A, B, C and D. The low velocity areas (yellow zones) in the map represent mainly degradation of the limestones and weakness zones, as can be also deduced both comparing the in situ velocity measurements with the laboratory results and considering the information from the petrographical study.

## 22.4 The Case of Dion Archaeological Site (Greece)

### 22.4.1 Historical Data

Dion in Pieria of Macedonia was one of the most important religious centers of the ancient Greeks from the 5th century BC. Built at the eastern foothill of Mount Olympus, it was on the road leading from Thessaly to Macedonia. In antiquity it was just 1.5 km from the coast of the Thermaikos Gulf. Vaphyras, a navigable river passing to the east of the ancient city, provided a link to the sea, through the extensive marshlands and shallow lagoons of its estuary.

**Fig. 22.2** Acquisition scheme and ultrasonic longitudinal velocity maps of faces A and B

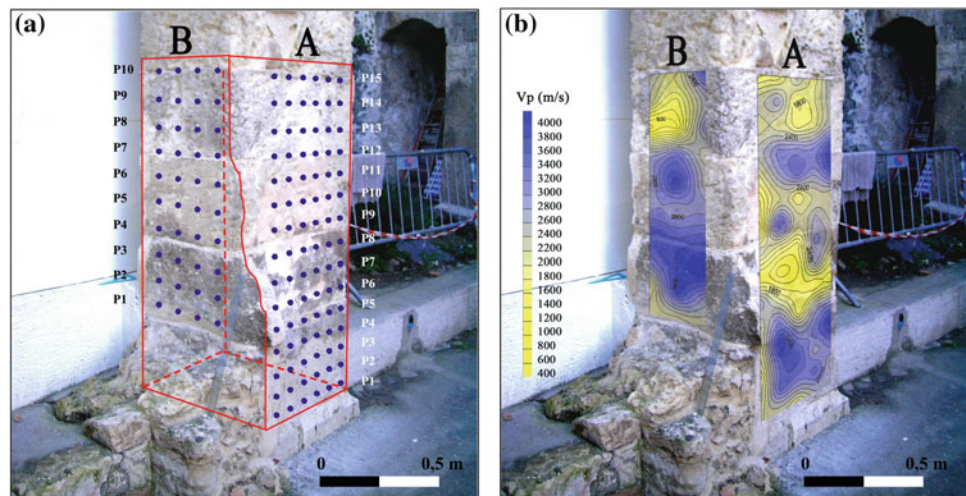
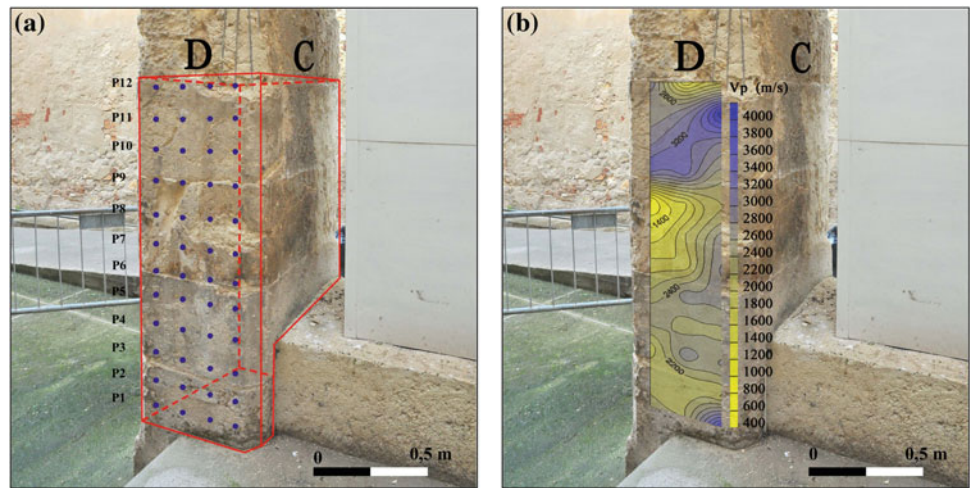


**Fig. 22.3** Acquisition schemes and ultrasonic longitudinal velocity maps of faces C and D



**22.4.2 Representative Application of Ultrasonic Technique**

The application was performed on conglomeratic blocks along the main street of the archaeological site. According to the mineralogical study, these conglomerates consist mainly

of limestone. Dolomite is also secondary found, together with trace of quartz and micas.

Ultrasonic velocity was used for mapping the weathering degree of the conglomeratic blocks (Fig. 22.4). For this purpose, a small portable UK140 I ultrasonic tester was used in the present investigation, additionally to a “Pundit Lab

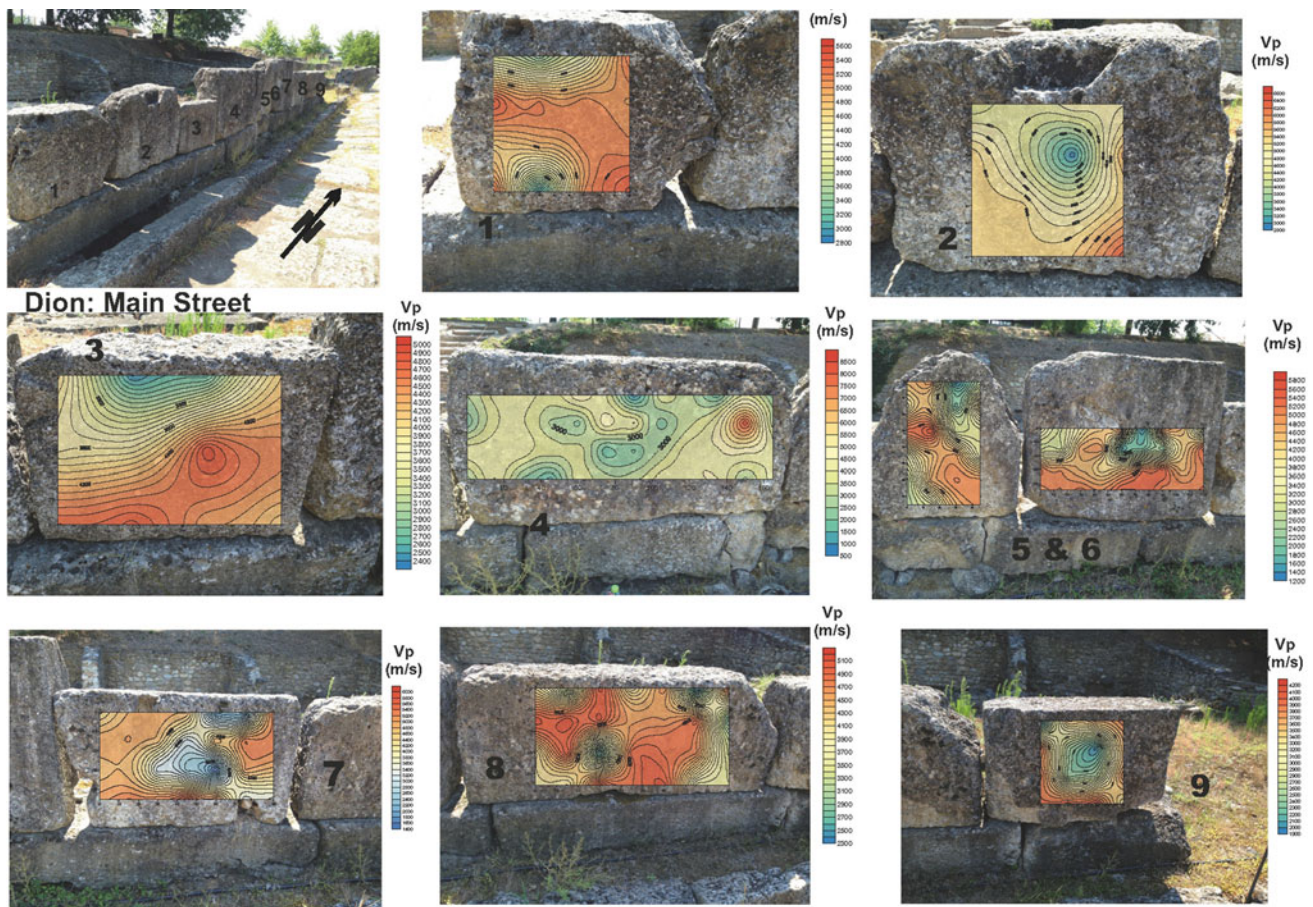


**Fig. 22.4** Ultrasonic velocity mapping related to the surface weathering of stones, along the main street of Dion archaeological site

ultrasonic tester” which was, also, used in our investigation. Measurements were applied, indirectly, on the same surface of the stones, which are located along the, S–N direction, street (Fig. 22.4). The measurements taken by indirect method (transducers placed on the same surface) are lower (about the 2/3) than those taken by direct method (transducers placed at the opposite sites of a stone), for the same stone, because the first measurements refer to the surface quality instead of the second which refer to the inner quality of the stone (Christaras 1998).

---

## 22.5 Conclusion

In this study, representative surfaces of calcareous pillars of Sta Chiara (Cagliari) and thin calcareous-conglomeratic plates of the main street of Dion archaeological site were mapped regarding to their surface weathering, using indirect ultrasonic technique.

The result of this weathering mapping can give information for the consolidation of these stones against weathering.

## References

- Casula G, Fais S, Ligas P (2009) Experimental application of 3-D Laser Scanning and acoustic techniques in assessing the quality of stones used in monumental structures. *Int J Microstruct Mater Prop* 4:45–56
- Christaras B (1997) Estimation of damage at the surface of stones using non-destructive techniques. In: Proceedings of the 5th international congress of structural studies, repairs and maintenance of historical buildings. San Sebastian, in *Advances in Architectural Series of Computational Mechanics Publications*, Southampton, pp 121–128
- Christaras B (1998) Non-destructive methods used for the estimation of the damage (weathering and cracks) of the building and ornamental stones. *PACT 55 (Revue du Conseil de l' Europe)*, pp 213–219
- Fais S, Casula G (2010) Application of acoustic techniques in the evaluation of heterogeneous building materials. *NDT E Int* 43:62–69
- Galan E, Guerrero MA, Vasquez MA, Maert F, Zezza F (1991) Marble weathering: relation between ultrasonic data and macroscopic observations. The case of the columns of the court of the lions at the Alhambra in Granada, Spain. In: Proceedings of the 2nd international symposium “The conservation of monuments in the Mediterranean Basin”. Geneve, Switzerland, pp 193–207
- Normal 22/86 (1986) Misura della velocità di propagazione del suono. *Normativa Materiali lapidei*, CNR-ICR, Rome

---

Part III

**Engineering Geology Problem of Preservation  
and Restoration of the Cultural Heritage**

Fang Yun, Qiao Liang, Yan Shaojun, Peng Pengcheng, and Zhu Qiuping

## Abstract

The rock cracking, inducing rock flaking and toppling, on the limestone cliff with Rock Painting is a dangerous threaten for the relics conservation. A detailed field investigation and statistics have been carried out. The geometrical sizes, shapes, fillings have been recorded. There are four sets of fractures control the broken. Non-destructive tests have been accomplished in situ for evaluating the property of the rock of the painting cliff. The temperature sensors were installed on and inside the rock cliff for studying the heat field of the cliff and cracked rock influenced by sunlight. Shear and tension stresses induced by the temperature fluctuation are main damage agents for rock cracking. Surface flow is another important threatens to the relics conservation.

## Keywords

Rock cracking • Huashan Rock Painting • Thermal stress • Water seepage

## 23.1 Introduction

The Huashan rock painting, a famous prehistorical relics in south China, distributing on a limestone cliff of right bank of Ming River, Ningming County, Guangxi Zhuang Autonomous Region, is composed by 111 groups of mysterious cliff images (Xu et al. 2006). The paintings were drawn from ca. 1680 to 4200 BP, it is Warring States to the Eastern Han Dynasty period in north China. These pictures reflect life-time, prayer and witchcraft activities of ancestors of Zhuang

minority with unique value for historical, scientific and artistic researches.

For thousands years exposed in nature surroundings, the pictures and the rock with pictures are being eroded seriously. The break and falling of the rockmass are the vital geological questions for the relics protection (Fang et al. 2007). The control and boost factors for the deteriorations have been focused on in this researches, such as initial fractures formed by the tectonic stress, swell and shrink stress induced by sunlight burning and chemical erosion by acid air.

The cleavage mechanism of the painted rock have been figured out and valuable advices have been provided for following treatments in this study.

F. Yun · Q. Liang (✉) · Y. Shaojun  
China University of Geosciences, No. 388 Lumo Road, Wuhan  
430074, People's Republic of China  
e-mail: shaojuncug@qq.com

P. Pengcheng  
Guangxi Administration of Cultural Heritage, No. 38 Sixian Road,  
Nanning 530023, People's Republic of China

Z. Qiuping  
Administration of Cultural Relics in Ningming County, No. 81  
Xingyuan Street, Chongzuo 532500, People's Republic of China

## 23.2 Geological Background

The strata of the cliff are Upper Carboniferous limestone. The occurrence of the layers is  $165^{\circ}$ – $190^{\circ}$   $\angle$   $16^{\circ}$ – $20^{\circ}$  and the cliff is a consequent slope with low apparent angle on the profile perpendicular to the cliff striking. Therefore, the main

rock fall take place along the tectonic discontinuous planes but the bedding. The layer beddings are the good seepage channel for water flow and form the Karst deposition on the painted surface.

The cliff of Huashan Rock Paints is belonging to a wall of a regional strike-slip fault, extends more than 20 km, Huashan Fault (F1) and the joints on the painted cliff mainly controlled by this fault. The fault is formed by compresso-shear force and strike to NNW with vertical dip angle. The west part has been eroded by Ming River and the vertical cliff, 140 m high and 300 m wide, been left for painting. It is a normal geological phenomenon that there are sets of fractures and faults associate with a region fault (Zhu 2005). Fault F2, is a branch vertical fault to F1 behind the cliff. This fault, striking to NE 25°, is formed by tension stress and intersection angle with F1 is 45°. A granite-porphry vein has been found along the fault valley, which obviously shows the opening character for easily injected by magma. Besides F2, a set of opening fractures can be found on the cliff. Another two sets of joints, one is vertical to the F1 and another intersect to the main fault with 15° (S1 and S2 in Fig. 23.1), are the conjugated shear joints formed by same stress field with F1. Some joints parallel to the F1 have been influenced by the unload effect of the river cutting and the width of aperture is high. Therefore, four sets of fracture, two opening fractures parallel to F1 and F2, two shear fractures associated with F1, formed the basic geological background of crack system on the rock-painting cliff.

Shape of the lower part of the cliff, painted with images, is recession for the erosion of the river and this is helpful for keeping the relics away from influence of the rainfall directly.

### 23.3 Cracking Rock Investigation

A detail filed investigation have been carried out for Huashan Rock Painting since September, 2009. The type, opening, length, filler material, dip direction and dip angle, distribution area and volume, etc. have been recorded for

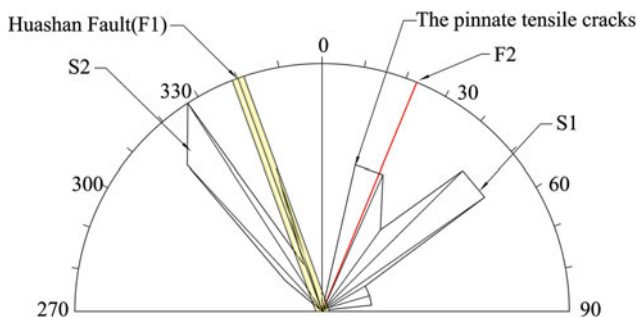


**Fig. 23.1** The rose diagram of the strikes of F1 and its associated cracks

every discontinuous rock mass. There are 418 cracked rock bodies and the total area is 25.7 m<sup>2</sup> according to the investigation results. The shapes of the cracked rocks are irregular, mostly lamellar and block (Fig. 23.2). The proportion of the lamellar rock is 77 %. The thickness of cracked rock bodies is mainly from 1 to 50 mm, and the average is 30.2 mm. The crack fillers are calcareous and argillaceous. 52 % are calcareous and only 3 % are pure argillaceous, 29 % are combined with calcite and clay and 16 % of the cracks are filled with nothing. The conclusion can be drawn that the cracks development controlled not only by water but also heat because of a lot of fractures filled with clay brought by wind or filled nothing. The weather thickness of limestone on the cliff is about 3 cm.

### 23.4 Field Temperature Monitor

The thermal stress is the main induction factor for the painting and rock weathering because the sun is shining directly on cliff, facing to west, at afternoon. A monitoring system has been installed to study the temperature of the broken and intact rock surface, the temperature fluctuation from the surface to 50 cm inside.

Two temperature probes have been installed on the surface of the cracked rock body and the intact rock mass (Fig. 23.3) separately, at the same time, a probe has been placed in the air to record the air temperature. The monitoring results from September 20 to October 10 have been shown in Fig. 23.4. The temperatures of the three sensors fluctuate synchronously, but the variations of amplitude are different. The peak temperature of the cracked rock body is higher than the intact rock mass, 58 °C for cracked rock but 54 °C for intact rock mass at a sunny afternoon of September 20 have been recorded. The records of two sensors are nearly the same temperature, up to 31 °C, at a rainy afternoon of September 30. The difference between broken rock to intact rock have been obtained by subtracting the two sensor records (Fig. 23.5). The curve shows that the temperature of cracked rock is lower than intact rock when there is no direct sunlight at night and morning but higher when the cliff is shined directly at afternoon. The reason is that the constant temperature mountain provides a good buffer for intact rock mass when the environment change but broken rock is fragile and variable. The thermal stress, between the broken rock and intact cliff, changes highly when the temperature fluctuate which is helpful for the rock crack growth.

Five sensors have been installed at the different depths, the surface, 5, 15, 30 and 50 cm, in a borehole to record the intact cliff influenced by the surroundings. The total records of a sunny day, September 20, have been show in Fig. 23.6. The temperature gradient from surface to 15 cm is high at 16:00 when the sun burning the cliff directly and shear stress

**Fig. 23.2** Lamellar cracked-rock (*left*) and block cracked-rock body (*right*)

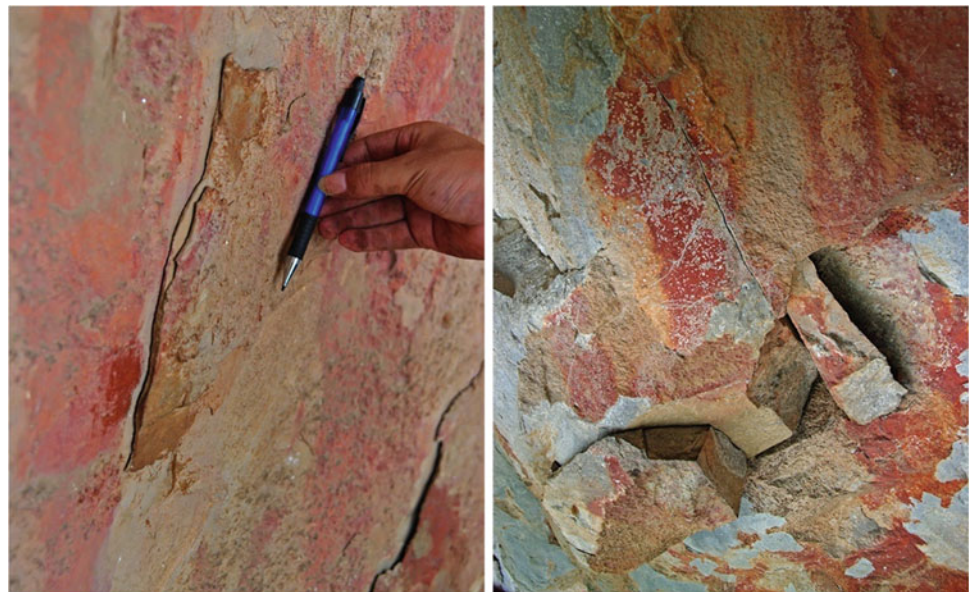


**Fig. 23.3** Temperature monitoring probes in site



**Fig. 23.4** Temperature curves of air, intact rock mass and cracked rock body from September 20 to October 10

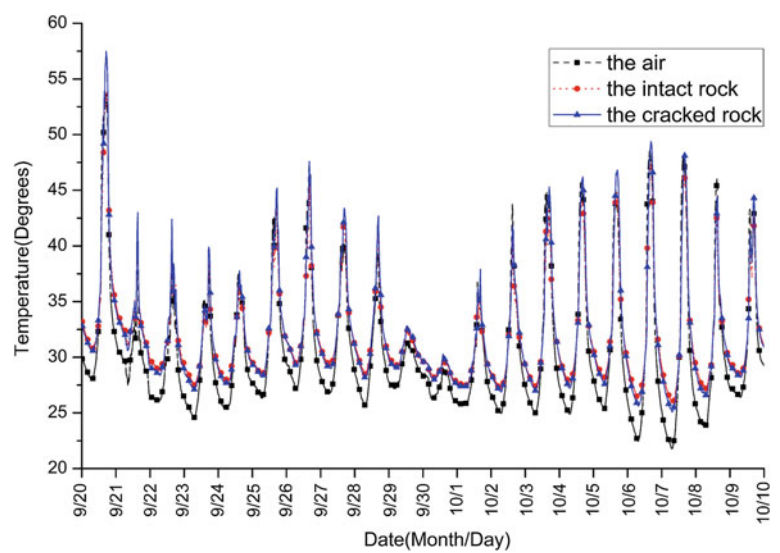


**Fig. 23.5** Temperature difference between cracked rock and intact rock from September 20 to 21

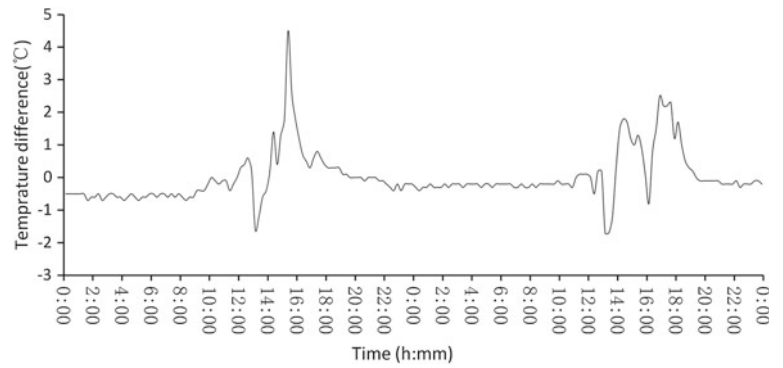
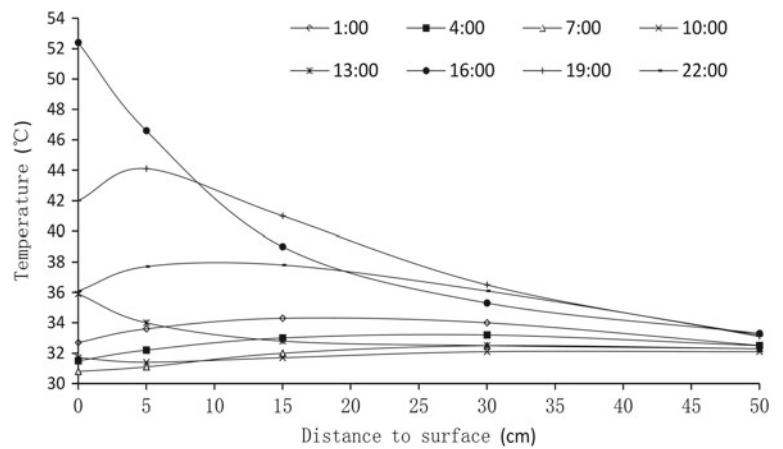


**Fig. 23.6** Temperature distribution curves of different time of borehole at September 20

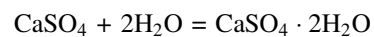
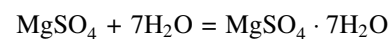
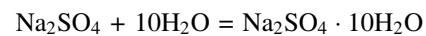


occurs when the surface swell by the heat transfer inside the cliff. Worse situation takes place after the sunset at 19:00, the cliff surface become cool quickly but the inside rock still keep high temperature, therefore the surface shrink but the inside swell and tension stress takes place. The shear and tension thermal forces on the cliff surface are boosting the weathering.

### 23.5 Surface Flow Influences

Surface flows on the cliff are another induction for cracking rocks. The flows mainly come from the fractures, beddings and karst channels and few from the rainfall directly. There are at least three negative effects of the surface flow, karst deposition, hydro pressure in fractures and salts accumulation. The karst depositions are containing, diluting and covering the painting. The hydro stresses are high when the cracks have been filled with water and tension stresses occur on the joints of the fractures. The acid gases,  $\text{CO}_2$ ,  $\text{SO}_2$ , etc mix with the rainfall and seepage into the fracture of mountain dissolve the limestone and dolomite. The solutes in the water transform into crystalline salts in cracks on the

cliff quickly for cliff exposing to the sun. Except calcite, gypsum, mirabilite, epsomite, etc. have been detected in the fillers of the fractures. These salts can absorb water at night and lose water at daytime for the temperature fluctuates every day.



The volume of hydrate crystals are higher than anhydrous crystals, therefore the cracks are expanded by the crystalline transform cycle.

Some other factors, plants, bacteria, induce negative effects for the relics protections too.

### 23.6 Conclusion

The investigation shows that the rock cracking and surface weathering are the main damage factors. There are four sets of fractures on painting cliff, two tensile and two shear

cracks and these are the main discontinuities for cracking rock. The sunlight is the main effect of weathering for the cliff face to west and irradiate by sun afternoon. A monitor system has been installed to study the temperature fluctuation of cracked rock and intact cliff. There are notable and complicated thermal stresses, accelerating the damage of relics, on the shallow part. Another important weathering agent is the surface flow, which bring hydro and crystalline pressures in the cracks.

## References

- Fang Y, Liu J, Wang J (2007) Stability studies of dangerous—rock slumping of Huashan rock art in Ningming County. *Sci Conserv Archaeol* 19(4):37–40 (in Chinese)
- Xu L, Fang Y, Wang J (2006) Research on the water permeation disease and environmental cure of Huashan Rock Art. *Saf Env Eng* 13(2):24–27 (in Chinese)
- Zhu Z (2005) *Tectonic geology*. China University of Geoscience Press, Wuhan (in Chinese)

Mariann Mocsár-Vámos, Péter Görög, Márta Borostyáni, Balázs Vásárhelyi, and Ákos Török

## Abstract

There are more than 570 underground wine cellars that were constructed from the 13th century in the city centre of a town (Miskolc) in NE Hungary. With the recent rapid urban development and the population growth many of the cellars are endangered and there is a risk of collapse and structural damage. The present paper focuses on the stability analyses of the slope with the cellars by using various data sets including field surveys, core drillings, laboratory analyses and slope stability modelling by Phase<sup>2</sup>, a finite element modelling software. The cellars are found in three levels within a vertical elevation of more than 80 m. The prevailing lithology is a Miocene andesite tuff with a thickness of 50–60 m. Besides andesite tuff 0.7–1 m-thick layers of sandstone, 0.2–0.5 m of clay and very thin 0.2–0.3 m of bentonite also occur. The sequence also contains a thin bed of rhyolite tuff. The andesite tuff is heterogeneous but it is considered as a typical bimrock with signs of redeposition. For understanding the geology 4 core drillings were made. Cylindrical tests specimens of cores were used for rock mechanical analyses. Laboratory tests included uniaxial compressive strength tests, indirect tensile strength tests and triaxial strength tests. The data set obtained from laboratory analyses and measured joints were used as input parameters for the 2D modelling by Phase<sup>2</sup> software.

## Keywords

Cellars • Volcanic tuffs • Stability analysis • Numerical methods

M. Mocsár-Vámos  
University of Debrecen, Debrecen, Hungary  
e-mail: mariannvamos@hotmail.com

P. Görög (✉) · M. Borostyáni · Á. Török  
Budapest University of Technology and Economics, Budapest,  
Hungary  
e-mail: gorog.peter@mail.bme.hu

M. Borostyáni  
e-mail: marta.borostyani@gmail.com

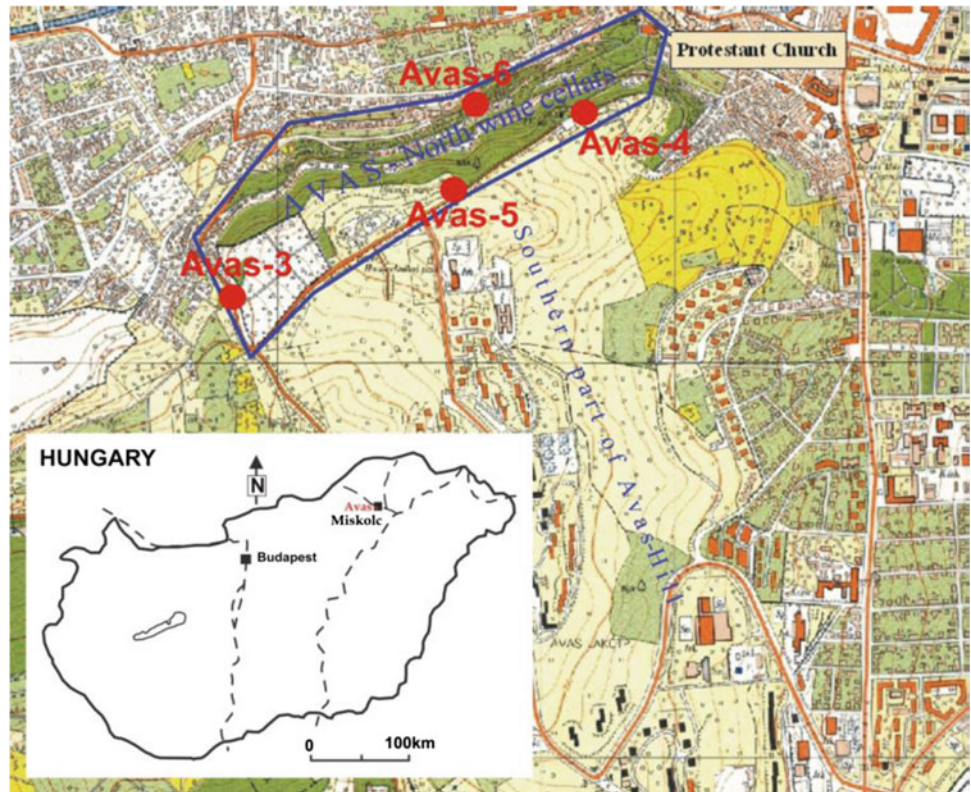
Á. Török  
e-mail: torokakos@mail.bme.hu

B. Vásárhelyi  
University of Pécs, Pécs, Hungary  
e-mail: vasarhelyib@gmail.com

## 24.1 Introduction

Large urban areas are composed of volcanosediments in Northern Hungary. The study area of the Avas Hill being the southern part of the Tardona-hill is located in the city of Miskolc with a maximum height of 211 m. The southern part of it is not very steep and built-in with ten-story residential buildings (Fig. 24.1). Steep slopes (25–65°) of the Northern part of the Avas Hill extending over 0.75 km<sup>2</sup> are densely built-in with cultural heritages, such as small houses and worship places as well as more than 570 cellars (Fig. 24.1). The less utilized road network, however, is in poor conditions. The extensive network of cellars and the heterogeneity of geological formations increase geological risks and induce landslides and surface instabilities on the steep slopes (Vámos et al. 2011).

**Fig. 24.1** Map of the Avas Hill with the location of the core drillings



The study area, the Avas hill is comprised of Sarmatian volcanosediments and located within the centre of the third largest town of Hungary, in Miskolc. The historical cellars of the hillside are almost 300 years old, many of them have good conditions, but there are numerous cellars which are forgotten or not maintained. These forgotten cellars have important impact on the stability of the northern part of the area. The aim of this study is to clarify the geological conditions and the related human impacts which led to the landslides (Vámos et al. 2012).

## 24.2 Geological Conditions

The site can be characterized by both double volcanic activity and periodically transgressive and regressive sedimentary systems. Due to the microclimatic conditions, the geological setting was beneficial for wine-production that led to the development of wine-cellars. The stability of the hillside depends on different geological strata that are weakened by cellars formed densely side by side as well as below and above each other, thus the site is prone to mass movements causing subsurface damages within the cellars.

The geological conditions of the northern steepest side of the Avas hill was described according to the lithological logs of the 4 new core drillings. The boreholes were cored to a

depth of 50–100 m (Kozák et al. 2013) (Fig. 24.1). The most important identified layers and lithologies are as follows:

- Silts: there are two different types of the silts. The first type is micaceous, with high fine sand content with slight similarities to the loess. The second type is a fine sandy aleurite (Fig. 24.2a).
- Clays: it is rather a weak claystone than soil, three different types of clays were identified. Close to the surface it is redeposited sandy and silty clay with low amount of swelling clay minerals and with some tuff debris. The second type of it is the most frequent layer at the study area with different depth, it consists of silty clay with limonite stains and at some part of it has fine graded sand content. The third type of it a bluish grey claystone, there are in it some conches and shells (Fig. 24.2b).
- Andesite tuffs: There are several redeposited andesite tuff layers with different thickness. The cellars were mainly cut into the thickest andesite tuff layer. It has several types differing in the grain size (Fig. 24.3c).
- Riolite tuff: It is strongly weathered tuff with lot of quartz mineral and small pumice grains. The riolitetuff layer is very thin.
- Sandstones: There are also three types of the sandstones. The first type of it is a polymikt sandstone with limonite, quartz and clay content. The size of the tuff grains in it is very coarse, and the structure of it is slightly laminated.

**Fig. 24.2** Samples of the different geological units after UCS test

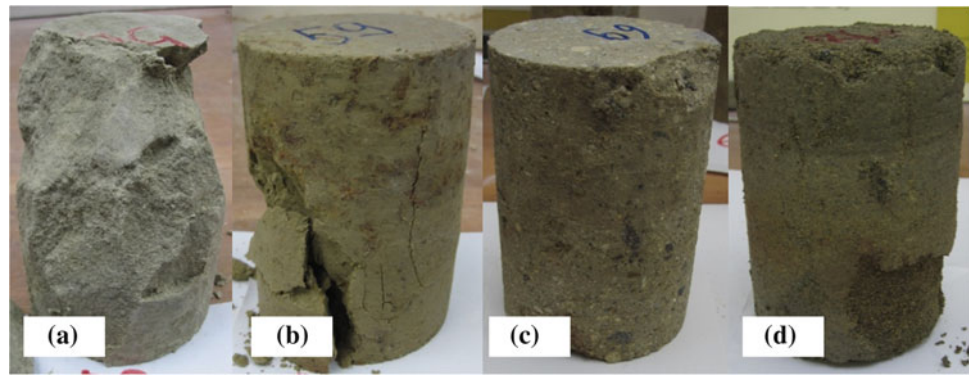
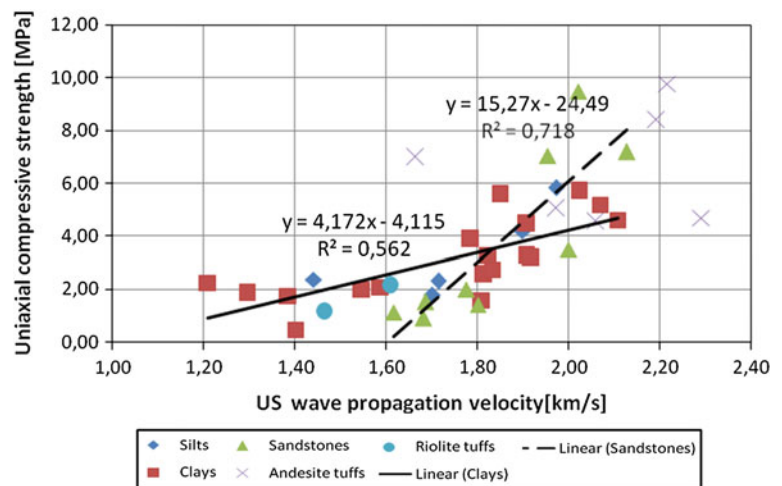


**Fig. 24.3** Relationship between the US wave velocity and the UCS values



The second type of it is clearly consists of fine sand originated from tuff with tuff binding and it is also slightly laminated with matrix framework. The third type is a volcanosedimentary sandstone with low binder content therefore it is porous, crumbling, laminated sandstone which basically consists of andesite-sand and sand-sized volcanic tuff grains (Fig. 24.2d).

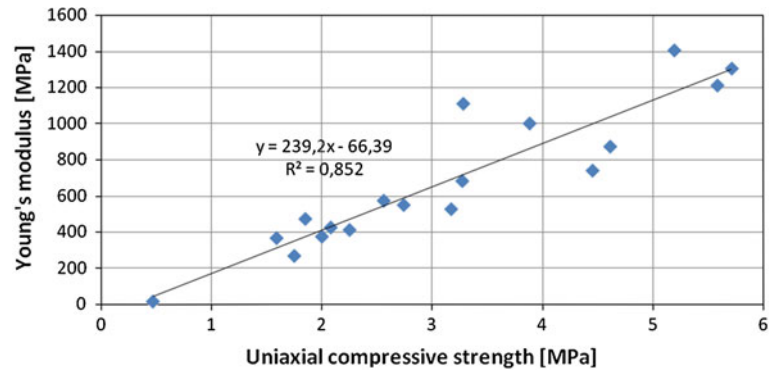
### 24.3 Petrophysical Properties of the Rock Materials

The cores were tested under laboratory conditions. The density, porosity, US wave propagation velocity of the specimen where measured according to the international standards before the destructive tests. The uniaxial compressive strength tests with displacement measurements and the triaxial tests were performed according the ISRM suggested methods (ISRM 1979, 1983). The first part of the investigations includes the test of 50 specimens. The results were evaluated using statistical methods.

The petrophysical parameters of the investigated 5 different rock types are plotted on diagrams. The largest numbers of tested specimens were clays, andesite tuffs and sandstones. The physical parameters of these to rocks were also evaluated statistically. Figure 24.3 shows the relationship between the US wave propagation velocity and the UCS of the specimen. Different relationships were found for the clays and for the sandstones. In case of the andesite tuffs no relationship was identified between this two physical parameters. It is most probably related to the different sizes of the andesite fragments within the tuff. The density of the andesite is much higher than the ground mass of the tuff, thus the US wave has higher velocity in the andesite than the tuff itself. The andesite tuff with larger andesite fragments has higher US wave velocity. The UCS value becomes smaller when the fragments are bigger, due to the fact that such grains fall out from the specimen during the strength test.

The range of UCS values is also shown in Fig. 24.3. It is in between 0.5 and 9.8 MPa, therefore all these rocks are considered as weak rocks. Figure 24.4 shows the relationship between the UCS and the Young's modulus of the clays.

**Fig. 24.4** Relation between the UCS and the Young's modulus values



There is a linear correlation between these two parameters with strong correlation coefficient (Fig. 24.4). The UCS values of the clays are in between 0.5 and 5.6 MPa, the Young's modulus values are in between 16 and 1,404 MPa.

## 24.4 Stability Analysis

The stability of the hillside was analyzed by Phase<sup>2</sup> software. The investigated geological cross section of the area was modeled according to the results of the core drillings. The hill slope consists of many thin layers, which are mainly clay layers (Fig. 24.5). The dip direction of the layers and the slope is the same, which is disadvantageous in point of the stability of the hill slope.

The input parameters of the different layers were determined according to the laboratory data, while the degree of jointing was described by using GSI system, and also taking into account the previous in situ measurements. According to the calculations the slope is considered stable with a factor of safety 2.0. The slip surface is located at greater depth within the strata above the layered, redeposited andesite tuff (Fig. 24.6).

In this section the influence of the cellars can be investigated only with reducing the parameters of the layers in which the cellars are cut. After 35 % reduction of strength parameters of this layers, the factor of safety remained almost the same, due to the fact that the slip surface is found at greater depth.

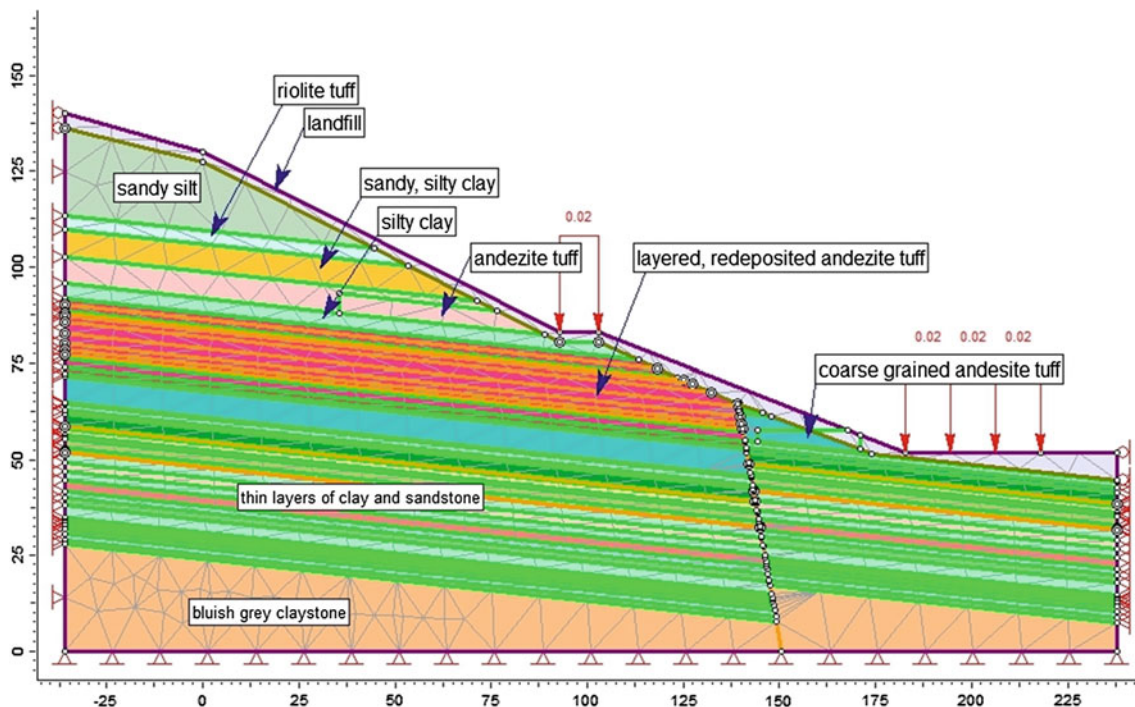
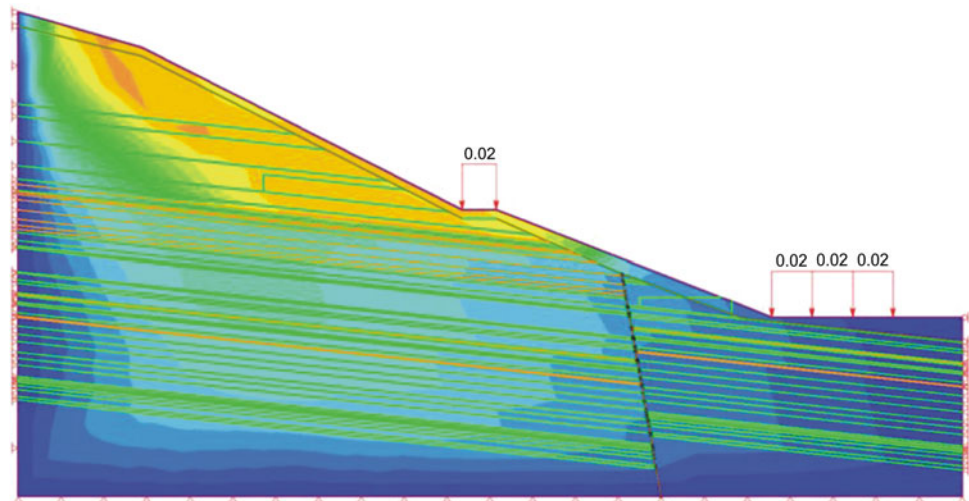


**Fig. 24.5** The strata of the hillside with the names of the most important layers

**Fig. 24.6** The location of the slip surface with factor of safety 2.0



## 24.5 Conclusions

The northern side of the Avas Hill has a very complex bedding and lithology according to the core drillings. There were 5 main rock types recognized in the cores, these rocks belong to the weak rocks, with a maximum uniaxial compressive strength of 10 MPa. The andesite tuff has the highest strength values, so it has the best quality rock in the area. The cellars without lining system were mainly cut in this rock.

According to the stability analyses the slope is globally stable, and the cellars have no impact on the global stability of the whole hillside. The landslides always occur after heavy rains, therefore the key parameter is the water-sensitivity of the investigated weak rocks. The thin clay layers with the same dip direction as the slope are dangerous when the water seeps on its surface reducing the shear strength of it.

The upper landfill layer continuously slides because of its weak strength parameters and the water infiltration. The impact of it can be seen at the area: cracked roads, moving gravity walls etc. The cellars can cause local failures on the surface when they are not maintained.

## References

- ISRM (1979) Suggestive methods for determining the uniaxial compressive strength and deformability of rock materials. *Int J Rock Mech Min Sci Geomech Abs* 16:135–140
- ISRM (1983) Suggested methods for determining the strength of rock materials in triaxial compression: revised version. *Int J Rock Mech Min Sci Geomech Abs* 20(6):285–290
- Kozák M, McIntosh RW, Plásztán J, Vincze L, Mocsár-Vámos M (2013) “Mapping and stability analysis, geophysics”- Results of a complex geological, geotechnical-engineering geomechanical pre-works on the Avas, Miskolc, Avas-North complex reconstructional program financed by the Municipality of Miskolc, Geokomplex Ltd. p 270 (in Hungarian)
- Vámos M, Léber T, Görög P, Kozák M, Török Á (2011) Slope stability analysis of volcanosediments undercut by cellars with FEM analyses. In: Anagnostopoulos A, Pachakis M, Tsatsanifos C (ed) *Proceedings of 147, the 15th European conference on soil mechanics and geotechnical engineering*, pp 1297–1334
- Vámos M, Kozák M, McIntosh RW, Léber T, Török Á (2012) Engineering geological investigations in the historical cellars of the Avas hill in Miskolc (North Hungary). *ACTA GGM Debrecina Geology, Geomorphology, Physical Geography Series* 6 (in press)

---

# The Historical Stone Architecture in the Ossola Valley and Ticino: Appropriate Recovery Approaches and Solutions

# 25

Zerbinatti Marco, Bianco Isabella, and Piumatti Paolo

---

## Abstract

Conservation and requalification of mountain vernacular architecture concerns a large area of the whole Alpine arch. Stone constructions are an important heritage both from the cultural, social and real-estate point of view. The paper proposes approaches to conservation and possible solutions developed by the international project Interreg-AlpStone. This study focuses on the traditional constructions located in the area between Italy (Ossola valley) and Switzerland (the canton of Ticino). In order to reuse these buildings it is necessary to ensure safety conditions according to current regulations. To do this and to promote local materials, the project firstly tested the mechanical behavior of the *serizzo Formazza* stone, largely used in traditional stone balconies. The obtained resistance values provided useful data for the future finding of safe architectural solutions. Secondly, the project studied how to improve the seismic behavior of the stone buildings without destroying their cultural value. The research project will soon produce a manual providing architectural guide-lines for appropriate stone buildings conservation.

---

## Keywords

Alpine architecture • Stone buildings • Cultural heritage • Preservation • Recovery

---

## 25.1 Introduction

The preservation of vernacular architectures located in the Alpine arch currently involves different kinds of subjects, such as local administrations, building owners and conservation experts. In fact, this architecture represents a remarkable heritage from different points of view. Firstly there is a cultural reason: mountain constructions reflect the wise adaptation of past generations to the mountain landscape, the climate condition and the available natural resources. Secondly, a social reason has recently emerged: while the 20th century mountains suffered a continuous

process of depopulation today a new realization about their potential is developing (Albert et al. 2011, Corrado 2010; Dematteis et al. 2013). This concept is directly connected with the real-estate reasons: once the value of the mountain and of the local know how is recognized, resettlement and eco-tourism become sources of a “green economy” (Bonomi 2011).

The international research project Interreg-AlpStone takes part in the challenge of giving new life to the Alpine territory. In particular the project involves the territory between Italy (Ossola Valley) and Switzerland (the canton of Ticino). This area has a rich heritage of stone constructions, which are the expression of a constructive know how that is intimately connected to the territory (Fig. 25.1). Unfortunately, during the decades following the Second World War, the migration from the peripheral Alpine areas led to the decay of its architectural heritage and to a widespread loss of the traditional knowledge.

---

Z. Marco (✉) · B. Isabella · P. Paolo  
Politecnico di Torino, Corso Duca degli Abruzzi 24, 10129 Turin,  
Italy  
e-mail: marco.zerbinatti@polito.it

**Fig. 25.1** Traditional stone buildings in Craveggia (Val Vigezzo, Italy)



In order to conciliate the protection of this cultural heritage with real-estate aspects, the Interreg-AlpStone project is finding technical solutions that give new life (as residences or tourism accommodations) to the local constructions by respecting the traditional architecture. Barns and stables have to be adapted to the current regulations (seismic adaptation, thermal insulation aspects, space management, ...). The aim is to establish some guide-lines for a respectful recovery of these buildings and, at the same time, to enhance locally available materials from the point of encouraging a local production chain.

The present paper shows the studies with regard to the mechanical behavior of the stone modillions and the seismic improvement of structures.

## 25.2 Methodology

Recovery techniques are often in conflict with the preservation of the architectural heritage. The primary aim of the project Interreg-AlpStone is to find technical solutions in order to guarantee both the safety conditions and the conservation of local stone buildings.

This section deals with the methods used to analyze the mechanical behavior of stone modillions and the improvement of seismic behavior.

### 25.2.1 Mechanical Behavior of Local Stone

The Interreg-AlpStone research project carried out a series of tests in order to define the mechanical behavior of the local *serizzo Formazza* lithotype.

This study was necessary in order to satisfy the Italian NTC (*Norme Tecniche di Costruzione*) regulations (related to the *Decreto Ministeriale* 14/01/2008), which oblige architects and engineers to verify the structural stability of

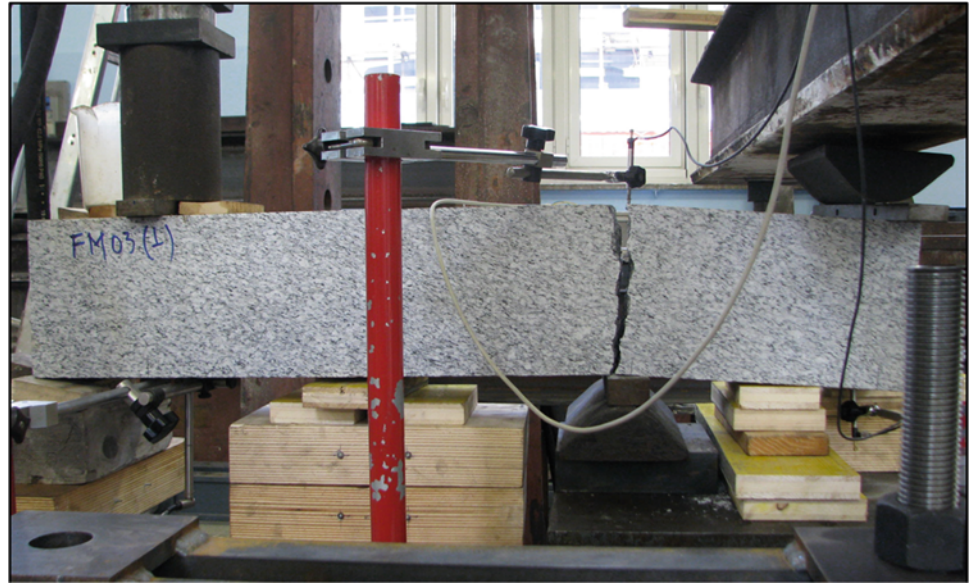
buildings and their components in case of earthquake. In the case of concrete modillions, experts can follow specific regulations for the tests, but there are not any regulation on stone modillions tests. The use of stone is therefore inevitably becoming very restricted in the field of recovery. However, the substitution of a stone balcony with a concrete one is rejected because of its incoherency with the traditional landscape. The study is therefore looking for a way to verify safety conditions to stone balconies too. A possible solution is to provide the stone modillions with steel elements which avoid material falling in cases of accidental breaks.

In order to properly plan a safe architectural solution, it was firstly necessary to evaluate the mechanical characteristics of stone elements currently in production. Samples of the local stone were tested in order to define the uniaxial compressive strength, the flexural strength test (Fig. 25.2), the static and dynamic elastic modulus (through ultrasonic test). Tests were carried out according to the UNI-EN regulations: the samples were dried and the direction of loading was set firstly parallel and secondly perpendicular to the bedding planes. The analysis of the results is still in progress. At the same time, sonic tests will be carried out in order to evaluate the mechanical characteristics of placed modillion. Technical solutions for the modillion issue will be consequently available in the near future.

### 25.2.2 Seismic Behavior Improvement

According to data supplied by the European research institute INGV (*Istituto Nazionale di Geofisica e Vulcanologia*), Piedmont territory has a quite frequent seismic activity, even if of low intensity. In particular, the analyzed area shows the lowest magnitude values of the region: the historical seismic map of Italy reveals that from 476 BC, Ossola valley and surrounding areas have not been object of earthquakes with magnitude  $M > 5$ . The stronger earthquakes felt in this area

**Fig. 25.2** Flexural strength test on a *Serizzo Antigorio* stone modillion



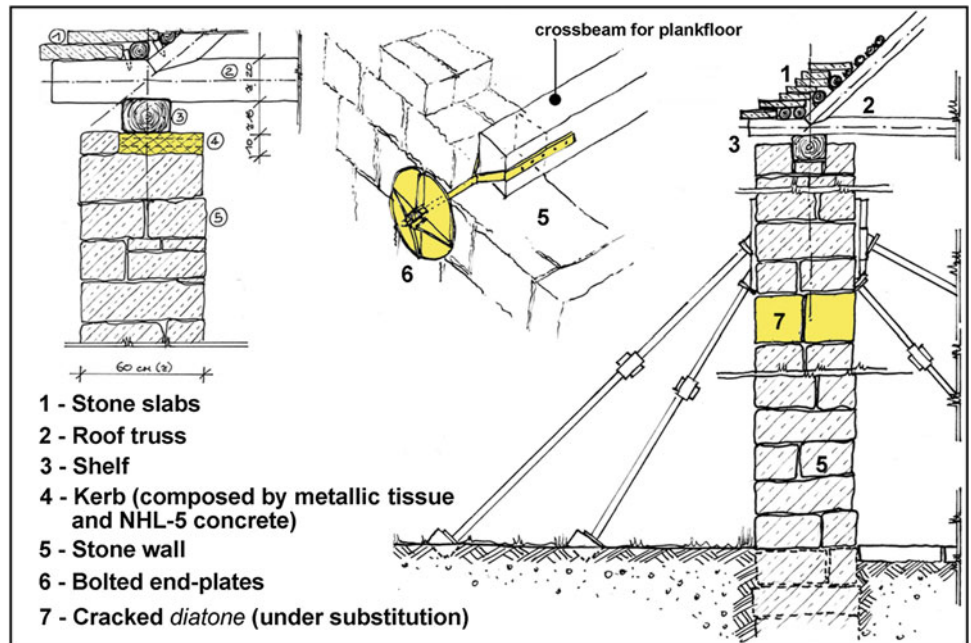
were in 1880, 1887 and 1891, when the macro seismic intensities joined the moderate value of 5-6 MCS. Currently, the Italian seismic classification is based on probabilistic analysis and the area of study presents a level of danger of 3A (in a scale from 1 to 4, where 1 is the higher value of danger). Consequently, regulations impose to take into account the seismic regulations while recovering the architectural heritage.

The goal is to find technical solutions providing a proper collaboration among structural components in order to activate a box behavior. Indirect techniques are available and more largely employed than the direct ones. Examples of direct restoration projects are the technique of *scuci e cuci*

for walls with cracks, the substitution of single stone elements, the pointing with mortar joints (except in case of dry stonework). The project has studied some possible indirect techniques, such as the following ones:

- Strengthening of stone walls at the top of the building, where the roof structure leans. It is possible to insert a tissue of brass steel fibers (which has got high values of resistance) in inorganic composites made up of natural hydrated lime (according to UNI EN 459-1 and 2) Fig. 25.3.
- Recovery of diatonic failures (a *diatone* is the stone element that connects the wall in the direction of the thickness). This technique allows steel strands with high

**Fig. 25.3** Sketches of technical solutions currently tested in yard



traction resistance to bond the masonry even in the cross direction. The research team currently evaluates the possibility of applying this system on sample buildings located in Veglio (Montecrestese, Ossola valley).

- Strengthening of stone constructions with the insertion of basalt fibers. They are stranded in way of bonding the dry-stone masonry, both in the height and in the cross-section directions. As part of the AlpStone project, this technique is currently tested for the seismic improvement of the dry-stone Lossetti tower located in Beura Cardezza (Italy). The tower, built during the Middle Age, is made up of big blocks of orthogneiss and presents evident structural failures (cracks, bowed wall). Moreover, the project is testing this technique on samples of real scale stone walls.
- The improvement of connections between horizontal and vertical elements in order to activate a box behavior. This can be achieved through the insertion of bracings with tie-beams and bolted end-plates Fig. 25.3.

Concerning the last point, the project developed three tests in situ in order to study the insertion of tie-beams and end-plates. Test were made on two dry-stone buildings, of which one with roof and the other one without roof. End-plates were submitted to traction effort. Results showed that the wall not stabilized by the roof resisted to the previewed 32,00 kN of effort without any change of position. Moreover, the wall with roof was submitted to higher traction efforts (over 67 kN). The steel bar reached the yield point and it after cracked, but the stone elements still didn't move.

### 25.3 Future Developments

The research project Interreg-AlpStone is still in progress and it is developing in parallel the different issues concerning the conservation of the traditional Alpine buildings and infrastructures. A branch of the project, as stated in Sect. 25.2.1, currently focuses on the finding of architectural solutions able to ensure safety conditions to stone balconies. To do this, sonic tests will be soon carried out on placed modillion. These tests will be developed through:

1. The use of ultrasound
2. The use of probes for the survey of acoustic emissions of strained stone elements. This kind of analysis will involve the colleagues G. Lacidogna and S. Invernizzi from Politecnico di Torino.

Another goal is the analysis of roofing system. Building roofs in the area between Italy and Switzerland are mainly built with *piode* (thick local stone slabs). The project studies the way to realize works of maintenance or renovation which

are respectful of the traditional architecture. Moreover, the project currently develops technical solutions for the thermal issues and the internal space management. The results of all these studies will be published in a manual providing a series of guide-lines for conservation professionals.

### 25.4 Conclusions

The recovery of vernacular buildings are issues that involve a growing number of subjects (local people, tourists, building owners, conservation experts, etc.). As a consequence, many research groups have studied different aspects of the topic. Nevertheless, almost no researchers have focused on the rich architectural heritage located in the territory between Italy and Switzerland. The international project Interreg-AlpStone currently studies the local stone constructions of this area with the aim of preserving their richness and stopping inappropriate recoveries.

The reuse of these stone buildings requires their adaptation to current regulations. Therefore, the project tested the mechanical behavior of the local stone in order to ensure the safety conditions of modillions such as the traditional balconies. Buildings further have to be recovered by taking into account the seismic regulations. The study has developed some possible solutions that satisfy the regulations while preserving the cultural value of the heritage. Many other aspects have to be considered for a respectful recovery, such as roofing systems, thermal insulation, space management, etc.

An aim of the project is to give a series of useful guide-lines for whoever has to recover an Alpine construction or analogous building. Nevertheless the proposed solutions are not rigid and have to be adapted case by case, according to the peculiarities of the construction and the locally available resources.

**Acknowledgments** All the authors are pleased to thank partners and people who contributed to the realization of this paper. We thank in particular: Elisa Genna (engineer) for the mechanical tests on stone samples she has carried on; Alessandro Grazzini (research fellow at ISEG Department, Politecnico di Torino) for the aid he has given in relation to the seismic improvements; Massimo Marian (geologist, CSL of VCO Province) for his good knowledge of stones he had shared.

### References

- Albatici R (2006) Local tradition and bioclimatic architecture in the Italian Alpine region. In: PLEA2006—The 23rd conference on passive and low energy architecture

- Albert F, Chiapparini C, Rossetti M, Antoniol E, Frisiero M, Carnevale G, Giani E (2011) Architettura alpina contemporanea a Vinigo, Workshop IUAV 2011
- Bonomi A (2011) La green economy può aiutarci a superare la crisi. Il Sole 24 ore (20 novembre 2011)
- Corrado F (2010) Fragile areas in the Alpine region: a reading between innovation and marginality. *J Alp Res/Revue de Géogr Alp* 98(3)
- Dematteis G, Corrado F, Onida M, Morandini M, Streifeneder T, Omizzolo A, Di Gioia A, Ferrario E, Zanini RC (2013) New perspectives of Alpine research. Mt Doss
- Modena C, Valluzzi MR, Da Porto F, Casarin F (2011) Structural aspects of the conservation of historic masonry constructions in seismic areas: remedial measures and emergency actions. *Int J Archit Herit Conserv Anal Restor* 5(4–5):539–558

N.G. Mavlyanova

---

## Abstract

The area of the Central Asian region was as a part of Great Silk Way and it is covering the territories of Kazakhstan, Kyrgyzstan, Tajikistan, Turkmenistan and Uzbekistan. This area is famous for some of the most beautiful and important examples of ancient Islamic architects. In present time most of buildings of monuments have deformations due to unfavorably impact of environment and seismic vulnerability is increasing. In the same time the territory of Central Asia is one of the most seismically active regions in the world. First available information about violent earthquakes of the past which occurred on the territory of Central Asia was found in works of famous scientists of the Orient. Macroseismic data on more than 500 strong earthquakes with magnitude  $M > 5$  are available from the historical manuscripts. Problem of decreasing of seismic vulnerability for historical monuments is considering in this paper.

---

## Keywords

Central Asia • Ancient structure • Earthquake • Deformation

---

## 26.1 Introduction

Preservation of historical monuments in the countries of the former USSR has the special features. Several times on last centuries a functional value of ancient structures was changing depending of change of a political system. These buildings of historical heritage were used as a school, factories, warehouses, shops, etc. Other reasons of deformations of ancient structures are unfavorably impact of environment and the restoration of these buildings when at 1970–1980 years of the 20th century restoration was conducted without research of influence of engineering geological conditions.

The important condition of engineering-geology research of ancient monuments for the aims of conservation and restoration is to find out the bearing capacity deficiency that means discrepancy between existing load and real capacity of soil foundation. The generally problems of construction damages are: salt efflorescence and damage to the walls. The foundations of monuments are ordinary brick masonry have been made of non burnt brick or dense clay. The salt efflorescence is result of ground waters rising have been connected with leakage of water from city sewerage systems and flowing waters from irrigation lands. The result of which are construction's distortions with further development of monument's deformations and destruction of whole construction.

The earthquakes on the territory of Central Asia are the most frequent and dangerous (can reach the magnitude 8). In XX century almost in each of five countries strong earthquake to magnitude more than 7 have occurred, led to human victims. The first available information about violent earthquakes of the past had been occurred on the territory of Central Asia was found in works of famous scientists of the Orient. Macroseismic data on more than 500 strong

---

N.G. Mavlyanova (✉)  
Sergeev Institute of Environmental Geoscience, Russian Academy  
of Sciences, Ulanskii per, 13, bld. 2, Moscow 101000, Russia  
e-mail: georisk2012@mail.ru

earthquakes with magnitude  $M > 5$  are available from historical manuscripts. Instrumental seismology in CA started in 1892 when 14 seismoscopes of the Russian Geographical Society had been installed in Tashkent. In May 1901 Repsold-Zelner instruments were installed and since July 13, 1901 regular stationary seismic observations has been started.

Some of the monuments have very long history (about 1,000 years). Many strong earthquakes with magnitude more than 7 ( $M > 7$ ) happened in this time: 1209—Khiva, 1822—Ferghana, 1902—Andijan, 1907—Karatage, 1946—Chatkal, 1976 and 1984—Gazly (near Bukhara city).

At present the process of deformation of monuments is increasing of their seismic vulnerability. Available data of macroseismic observations of ancient monuments of architecture show that even earthquakes with intensity in 3–4 points (by MSK-scale) can cause it's damage because of architectural monuments are strongly deformed. Therefore these monuments are sensitive on insignificant influences because the vulnerability of them is increasing.

## 26.2 Deformation of Ancient Structures

The most part of monuments of architecture in Central Asia is located in Uzbekistan. The famous historical cities including in World heritage list are: Bukhara, Samarkand, Khiva, Kokand, Shahrissayb. The Republic is world renowned for its monuments and cultural heritage assets given its history and position on the Great Silk Road. There are more than 7 thousand monuments (including 2,500 monuments of architecture, more than 2,700 monuments of archeology and etc.) are under of the governmental protection now in Uzbekistan. The architectural complex of monuments of Ichan-Kala in Khiva city and Tilla Kari madrasah on Registan square in Samarkand city are one of the largest ancient structures in Central Asia.

Unfortunately, damages to the monuments accumulated in the course of time are inevitable. The engineering-geological and geophysical investigations were conducted with the purpose to find the reasons of deformation of foundation of buildings of the monument of Ichan-Kala in Khiva city and Tilla Kari madrasah in Samarkand city and also for development of techniques for improving properties of soils.

### 26.2.1 Tilla Kari Madrasah in Samarkand

The madrasah of Tilla Kari (1646–1660) is located at the historical center of Samarkand on Registan square. By the first Ulugbek madrasah was constructed on this area in 1417–1420 then during of the time of government of Yalangshu Bahodir the second building is Sherdor madrasah

was constructed and last the Tilla Kari madrasah and mosque was built.

At definition of location it was necessary to find out a spatial combination of these structures and to create uniform architectural ensemble of the area of Registan. Tilla Kari madrasah was constructed in conditions worse in comparison with the earlier constructed monuments because of limitation of a choice of a place. All three monuments on Registan square had been founded on filled soils and deposits of ancient irrigation channels. The building of Tilla Kari madrasah has the traditional form of a square with the external sizes  $73 \times 76$  m in the plan, internal yard about  $45 \times 50$  m. On the western part of this building the Juma mosque with a dome of height about 32 m is located. The construction of a dome was completed in 1975 under the project of a architecture's Krukov K. By the conducted researches is established that the deformation of the building began in far last, it is probable from time of operation. These processes in the dome part which has begun in 1976 in connection with additional loading on the bases. The deformation from the weight of a completed dome above of the mosque is significant increasing. As a result of large non-uniform settlements of foundation the cracks on walls with wide of 8–10 sm, inclinations on a floor and columns of gallery inside of mosque under a dome part were formed (Khudaybergenov 1996).

The territory of Samarkand including the area of madrasah of Tillakori is covering basically by Quaternary proluvium loess soils deposits with thickness up to 80 m, with layers of sand and rubble. During the all historical period (about 2,500) as a result of activity of the man in territory of city were formed the filled soils. They were formed on a surface of loess soils as a result of transformation moving of accumulation. A level of underground waters of 15 m. Using geophysical methods is determined that the wetting of soils is non-uniform from 5 up to 36 %. The wetting of some zones is connected to outflow water from water and sewer networks, and also infiltration of atmospheric waters. The intensity of possible earthquakes is VIII (by MSK-scale). The soils of the basis are in a critical condition of stability and even at insignificant increase of their humidity the collapse process is increased (Fig. 26.1).

### 26.2.2 Deformations of Ancient Structures in Ichan-Kala in Khiva

Accordingly to archeology assessment in Khiva, this city was based in IV century on “The Great silk way” (Gulyamov 1957). In XIV century is known as one of large cities of Central Asia. In XVIII century the urban structures of Khiva suffered badly and on their place in XVIII–XIX century's new ones were constructed. The destroyed structures were

**Fig. 26.1** Tilla Kari madrasah (1646–1660). The *arrow* indicates to the dom was constructed in 1975



leveled on the areas and streets; therefore on the territory of the city the large layer of filled soils was formed. This part of Khiva, received the name of Ichan-Kala (internal fortress) became administrative, political and economic downtown of that time. The territory of Ichan-Kala has 26 ha. The rather small territory of Ichan-Kala contained two palaces, more than 60 madrasahs and little mosques, a cathedral mosque, covered market, caravans—sheds and baths, apartment houses of khan’s retainers, officials, clergy and whole-sale dealers. It was protected with defense city wall (Pugachenkova 1985). Since 1997 when Khiva was jubilated 2,500 anniversary of its history, UNESCO included Khiva into the list of cities of the world heritage.

Consequences of moistening of ground foundations of a monument results in non-uniform settlements of the bases, weathering of interbrick mortar as result of lixiviation of salts breaking stability of monuments. Evaporation causes salts have been formed on the outside of buildings from the water in the capillary zone. The key to this process in that external air temperature is different from the wall temperature and is higher, thus allowing evaporation at the surface. Field measurement of air, wet bulb and external wall temperatures support this argument. In addition the air temperature within buildings is normally lower than temperatures outside, thus creating a transverse gradient that encourages moisture movement to the outside walls. In moving to the outer wall of the building, salts will form mainly where moisture is greatest, that is to say, preferentially within the mortar. The formation of salts from solution by evaporation on the external walls of buildings in the capillary zone is one

major process that causes the break-up (weathering) of bricks, mortar, and stone (Legg and Myers 2000).

Also the natural factor influencing on the state of monuments is the condensation of moisture appearing in the zone of aeration. As it is known from a surface of a level of underground waters through capillary the moisture aspires upwards. This moisture in superficial parts of a ground under action of temperature evaporates and there is a process of drying. However in places, where the surface of ground is blocked by asphalt covering, stones, slabs there is no process of drying of ground, and there is a gradual accumulation of moisture in the zone of aeration. The occurrence of the condensed moisture is promoted by universal covering of the territory of the ensemble Ichan-Kala by asphalt, slabs, bricks and stones.

The next artificial factor regularly influencing on the state of the ground foundation of monuments is filling-up of artificial drainage systems. At the time of construction of the ensemble Ichan-Kala the artificial drainage systems were provided as ditch around defense wall and wells, reservoirs (“houses”). Still up to 1858 in the city there were no main communications, because the southern wall had a lake, and there was no gate at that time. In the period from 1858 to 1867 along the southern wall of Ichan-Kala the part of the reservoir was drained and the gate has appeared only to 1873. At that time the ditch and lake played roles as drainage network, and protective structures.

During the Soviet authority, especially since 1950 the general plans of Khiva of some times were developed. They provide allocation Ichan-Kala as reserved zone of

monuments. In this connection in 1970–1980 years all areas and streets were covered with asphalt, slabs, bricks, stones, which in turn negatively influenced on moisture changes. Also in 1980 the many wells were filled-up in the territory, the ditch and lake located in a southern part of Ichan-Kala were liquidated, and were covered with asphalt and concrete plates. In result the ditch and lake, which played a role of a drainage network were completely destroyed. Probably, it very strongly has affected to are increasing of moisture of ground in the basis of buildings and structures on an internal part of Ichan-Kala. Therefore, as one of the basic reasons of non-uniform deformation of architectural monuments are filling-up of wells in court yard of monuments and liquidation the ditch around of Ichan-Kala.

---

### 26.3 Conclusion

The estimation of seismic risk for monuments of architecture should be conducted for each construction separately since each historical construction is unique on soil conditions, on a

structure of the base, as a design, on the used materials of walls. The protection of these monuments and urban renewal in the areas around the monuments are essential to preserve the city's heritage for future generations and for international tourism.

---

### References

- Gulyamov Y (1957) The history of irrigation of Horezm from the ancient to present. FAN, Tashkent (in Russian)
- Khudaybergenov AM (1996) Analysis of engineering-geological causes of deformations of the madrasah Tillakori and recommendations for reinforcing the soil foundations. *Geol J Uzbekistan* 4 (1996):84–92
- Legg R, Myers R (2000) Salt damage to important Islamic Monuments at Bukhara and Khiva. In: Lane B, Usmanov B (ed) Proceedings of the regional workshop "Ground water and soil salinity related damage to the monuments and sites in Central Asia". Samarkand/Bukhara, Uzbekistan 2000, UNESCO, Tashkent, pp 61–91
- Pugachenkova G (1985) Central Asia: ancient monuments of IX–XIX centuries. Planeta, Moscow (in Russian)

A. Boumezbeur, H. Hmaidia, and B. Belhocine

---

## Abstract

Tebessa city is first build on what remained of an ancient Roman city called Thevest. It is surrounded by a famous wall of more than seven meters high and three meters thick. The stone used for building the wall comes from Turonian limestone from nearby quarries. It is a clear pinkish limestone containing small grains of calcite and bioclasts with micritic cement. On the wall, the stone material show varying signs of deterioration such as powdering, flaking, pitting, cracking and discoloration. On top of the observations made in the field, several other experimental techniques have been used to investigate the weathering intensity of the limestone in the laboratory. The first technique is the microscopic examination of thin sections made from weathered and sound limestones. Then density, specific gravity and ultrasonic velocity have been measured for a set of samples taken from both sound material from three quarries and weathered ones from different parts of the wall. Schmidt rebound test has also been undertaken to assess the resilience of both fresh and weathered materials. Geochemical analysis has also been carried out. The results show that the limestone of the wall is moderately to highly weathered with a loss of strength and resilience due mainly to the micropores and cracks which have been developed upon weathering. The salts (sulfates and chlorides) revealed by geochemical analysis explain the reason of flaking, spalling, pitting and discoloration observed on the stone. In order to take the appropriate preservation and restoration measures we have shown the mechanisms by which salts arrive inside the stone and crack it.

---

## Keywords

Salt weathering • Tébéssa • Limestone • Dimension stone

---

A. Boumezbeur (✉)

Laboratoire Environnement Sédimentaire et Ressources Minérales et hydriques de l'Algérie orientale, Département des Sciences de la Terre et de l'Univers, Faculté des sciences, Université de Tébéssa, Tébéssa, Algeria  
e-mail: Boumezbeura@yahoo.fr

H. Hmaidia · B. Belhocine

Département des Sciences de la Terre et de l'Univers, Faculté des sciences, Université de Tébéssa, Tébéssa, Algeria  
e-mail: hamaidiahacene@yahoo.fr

B. Belhocine

e-mail: Belhocine@yahoo.fr

---

## 27.1 Introduction

Tebessa is a city that has known the succession of several civilizations. It has been conquered by the Romans, Vandales, Byzantins and the Muslims. It was known by Thebes, Theves, Thevest and then Tebessa. The name Thevest was the name by which it was called at the arrival of the Muslims. Thevest city is build after the erection of the Hycatempyle in what is known today by Tebessa Al khalia. The Hycatempyle is constructed eight centuries before the Christ by the Phoenician.

Thevest or the actual Tebessa hosts several historical monuments, the most distinguished one being the Wall that surrounds the city. It forms a rectangle of 180 m × 160 m with 14 surveillance tours. It has three main gates: Caracalla, Solomon and Cirta (Fig. 27.1). It is three meters wide and seven to ten meters height. Other monuments such as the roman theater and the basilica are of a paramount importance.

An important part of the history of the city and its surroundings is getting erased. Unfortunately, when these traces are lost, it is forever. Vandalism on one hand, natural weathering processes on the other and the lack of maintenance are speeding the loss of the traces of the past human history and civilization in the area. We know that stones or rocks under the attack of the different environmental factor changes their mineralogical content as well as their textural integrity and consequently get decayed. This study comes to investigate the geology, mineralogy, the origin as well as the state of weathering and degradation of the stone of the Thevest Roman wall.

## 27.2 Geological Setting

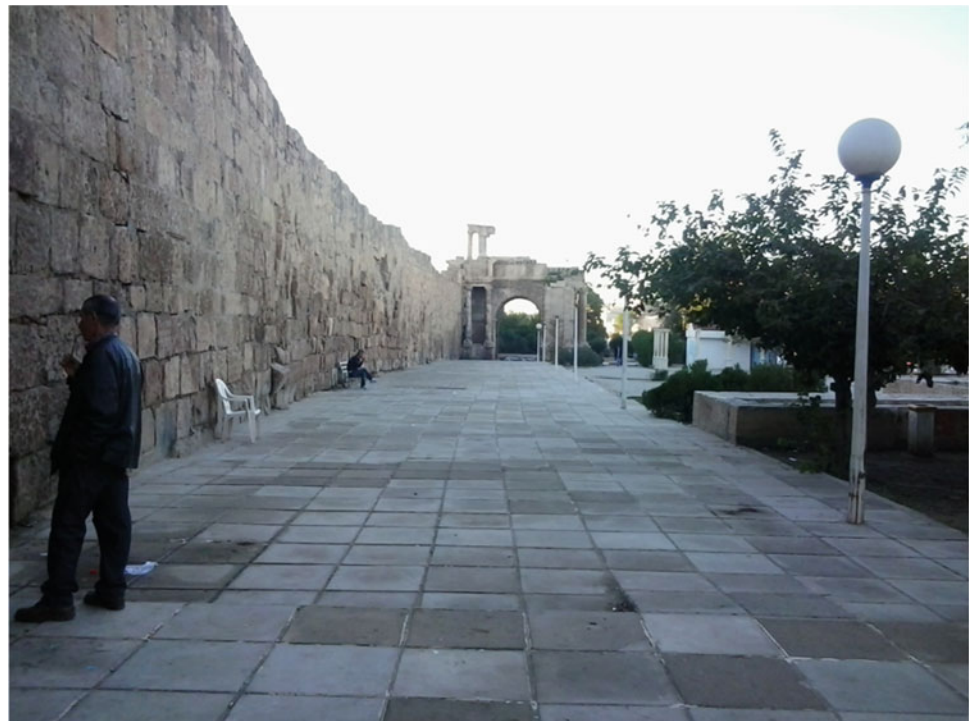
Tebessa area belongs to the autochthonous structure of the northern Aures mountain belt of the Saharan Atlas (Durozoy 1956; Villa 1969; Kowalski et al. 1997). It is a rift valley like structure bordered by high grounds and mountains of different altitudes. Geologically, the formations constituting the area are dominantly carbonates. The carbonate formations in

the area extend from the Albian up to the Eocene. Older formation which can be found is the Triassic outcrops, they occurs as elongated bodies of diapirs which consist of multicolored clay, dolomite gypsum and halite. They generally come to surface along deep tectonic accident at the borders of the depression (trough). Albian limestone outcrops in very limited area around Hamimet. It is a dark gray vacuolar dolomitized limestone. The vraconian is mainly composed of marl with few passages of limestone and argillite. On top of the vraconian comes the cenomanian which consist entirely of marl. The basin continues to receive sediments that alternate between marl and limestone. At the base of the upper Turonian, a well developed recifal facies was found in many part of the area where limestones are highly crystalline and highly fossiliferous. Turonian limestone outcrops in many areas in Tebessa. The Maestrichtian, which also outcrops over large areas, is constituted of a succession of fine beds of marl and limestone at its lower part and continues upward with mainly fine chalky limestone sediments. Eocene is mainly marl at its lower part and limestone with silex at its upper part.

## 27.3 Geological and Petrographical Characteristics of the Stone of the Wall

It is obvious that the stones used for the construction of the wall and the other monuments come from nearby quarries. Many references state that the building stone used for the wall comes from different places such as Djebel Ozmor,

**Fig. 27.1** The northern part of the wall and Karakalla Gate



Djebel Mizeb and from Tnoukla. The rapid examination of Tebessa geological map reveals an important deposit of hard and massive Turonian limestone at the vicinity of the city. The macroscopic and microscopic examination of the stone wall reveals the existence of more than one type of limestone. Travertine can be found scattered throughout the wall, it is a highly porous limestone. It shows the most advanced state of weathering of the stones of the wall. Its origin is not known yet (Fig. 27.2). Claire pinkish well crystalline and highly fossiliferous limestone building materials constitute an important part of the wall and mainly Caracalla Gate. This material is distinguished by its attractive appearance due to its color and its content of rudiste remains (genre Hippurites). This later material is comparable to the Turonian limestone of Al Gaaga localit . Beige Claire fine micritic limestone is also used in the construction of the wall. This later looks similar to the Turonian limestone of the outcrops surrounding the city such as Mizeb, Ozmor and Tebessa Al Khalia. Whitish chalky hard micritique limestone

has also been used in the construction of the wall. It probably comes from the Maestrichtian carbonates that are widespread in the area.

In thin section, turonian limestone are biomicritic to bi-osparitic, fine to coarse grained, with varying pore sizes and geometry. Section cut from material of the lower part of the wall are highly discolored and porous. Voids can be seen throughout the section. The purity of the limestone is tested by calcimetry using Bernard calcimeter. For the stones of the wall, the amount of insoluble residue which consists of clay and salts vary from 30 to 14 %. This figure is about 10 % for Ozmor and 25 % for Mizeb. Chemical analysis by XRF method shows that the stones of the wall contain along with the calcium carbonates which is the main component, other secondary constituents such as aluminum silicates and several types of salts (Table 27.1). Aluminum silicates are chiefly clay minerals. Among the salts present one can note magnesium and calcium sulfates, sodium chlorite, sodium sulfate, sodium carbonates, potassium chlorite...etc.

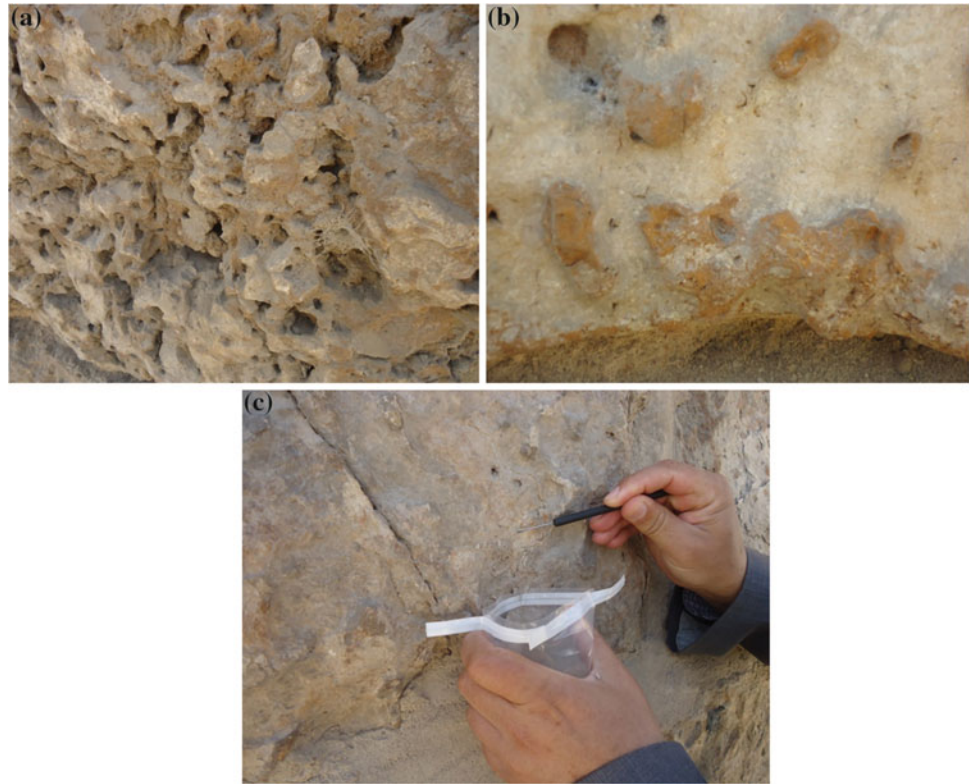


**Fig. 27.2** Travertinous highly porous limestone

**Table 27.1** Chemical analysis of the stone of the wall and Ozmor turonian limestone

	SiO <sub>2</sub>	Al <sub>2</sub> O <sub>3</sub>	Fe <sub>2</sub> O <sub>3</sub>	CaO	MgO	K <sub>2</sub> O	Na <sub>2</sub> O	SO <sub>3</sub>	Cl
Stone wall	3.42	2.052	1.01	91.72	0.76	0.04	0.16	0.096	0.004
Ozmor	3.54	2.26	1	91.33	1.23	0.06	0.14	0.27	0.05

**Fig. 27.3** Limestone showing an advanced state of weathering: **a** Alveolar weathering, **b** light colored crust tracing the surface, **c** loss of scales, efflorescence, subflorescence and cracking



## 27.4 State of Degradation of the Stone

From a quick look at the wall one can distinguish that the stones display a varying degree of stain. Completely discolored and covered by a thin black soft and silky film of probably oxidized sulfate material are found in the lower part of the wall. Stone displaying vacuoles of different dimensions are widespread. Efflorescent salt like material are also found on the stone surface. In some parts whitish powder like material are seen to cover the stone surface. Thin slivers parallel to the stone surface are easily detached (Fig. 27.3). Relief form of weathering, Fitzner and Heinrichs (2002) and Heinrichs and Fitzner (2002), where differential alteration displays nodes of iron ore like material can also be seen throughout the wall materials. The upper parts of the wall are slightly stained and less weathered.

Along with these observations, some test indices have been carried out in order to shed light on the effect of weathering on the physical properties of the stone. Specific gravity has been used to assess weathering grades by several authors (Irfan and Dearman 1978; Dobreiner and de Freitas 1986). For the same rock type, the weathered stone has a lower density than the fresh one as weathering is usually accompanied by loss of matter and replacement by lower density minerals.

Specific gravity values obtained for the wall stones vary from 1.01 to 2.22 while those of the presumed source rock vary between 2.3 and 2.7, Table (27.2). The values of the specific gravity for the other limestone rocks such Aptian, Maestrichtian and Eocene are all in the range of 2.15 and 2.6. It is clear that the specific gravity values of the stones of the wall are lower than those obtained for the rocks of Ozmor and Mizeb localities.

**Table 27.2** Specific gravity values of the studied materials

Samples	Wall stones	Ozmor	Mizeb
1	1.53	2.52	2.65
2	1.63	2.45	2.71
3	1.10	2.30	2.67
4	1.01	2.35	/
5	2.22	2.48	/

**Table 27.3** The porosity values of the studied materials

Samples	Wall stones (%)	Ozmor (%)	Mizeb (%)
1	2.80	2.13	2.00
2	3.00	3.08	2.10
3	3.80	2.80	1.90
4	2.90	4.90	/

**Table 27.4** Schmidt Hammer rebound number of the studied materials

Ech	Wall stones	Ozmor	Mizeb
1	25	30	38
2	27	32	42
3	30	34	36
4	32	31	44
5	22	36	32
6	14	32	30
7	16	29	39
8	34	31	28
9	12	26	50

The other test index used to assess weathering is the porosity (Irfan and Dearman 1978; Fookes et al. 1988). The porosity values of the stones of the wall are in the range of 1.8–3.8 %, those of Ozmor in the range of 1.13–9.8 % and Mizeb in the range of 1.9–2.3 % (Table 27.3). The porosity values do not seem to vary much between the stone of the wall and the limestone coming from Ozmor and Mizeb.

Schmidt Hammer which is used worldwide to estimate the compressive strength of the concrete is also used by the rock mechanic community as a tool to estimate the compressive strength of rocks (Deere and Miller 1966). It is a good and rapid tool for the assessment of weathered material. The rebound numbers obtained on different parts of the wall are in the range of 12–32. Samples of the rocks of Ozmar display a rebound of 26–36 and those of Mizeb 30–44 (Table 27.4). The lower values of the stones of the wall reflect that they have lost some of their hardness and strength upon weathering.

Another test index was also used for the diagnosis of weathering. It is the pulse ultrasonic velocity. This test is widely used to evaluate weathering of porous materials, the transit time is inversely proportional to the weathering state. Thus velocity values are greater for sound material than for weathered ones. As weathering goes by, voids, fissures, lesser density neofomed minerals become more and more abundant and hence the velocity through the material decreases. In our case, the lower velocity values obtained were for the stone wall about 3,000 m/s. Mizeb and Ozmor limestones display relatively higher values (Table 27.5).

**Table 27.5** Velocity values for the studied materials

Samples	Stones of the wall		Ozmor		Mizeb	
	Velocity dry (m/s)	Velocity humid (m/s)	Velocity dry (m/s)	Velocity humid (m/s)	Velocity dry (m/s)	Velocity humid (m/s)
1	4,226	3,000	3,642	4,611	5,531	5,090
2	4,883	3,408	4,500	4,435	6,891	6,000
3	5,184	4,775	5,250	6,060	5,313	6,164

## 27.5 Degradation Mechanism

The degradation of the stone of the wall is in fact caused by the interplay of several agents (Cardell et al. 2008). Salts, clays, relative humidity and wetting—drying are the main factors that lead to deterioration. Salt weathering is a well known phenomenon, the humidity carried soluble salt crystallize just under the surface when water becomes a vapor. These salt crystals exert a pressure and wedge small pieces of the surface. The repeated cycles of crystallization—hydration results in the formation of flakes parallel to the surface. The movement of the water in the porous material causes the appearance of a whitish crust on top of a weak powder like material; this phenomenon is known by powdering. The attack by aerosols containing salts in an appropriate relative humidity causes vacuolar weathering, well seen on the wall. It is much like the effect of sea spray on rocks. Clay minerals that are originally contained in the limestone, upon wetting—drying cycles, expand, shrink and exert pressure on the material forming what is known by scaling. The disrupting work of the clays is usually enhanced by the presence of salts. By being part of the absorbed layer of the clay it helps in absorbing more water and consequently more expansion.

## 27.6 Conclusion

The stones of the wall of the Roman wall of Thevest are brought from nearby quarries. They are mainly from the Turonian formation that surrounds the Antic City. The tones come more probably from tree localities Mizeb, Ozmor and Gaagaa. The stones display varying degree of weathering. The lower parts are the more affected. Weathering is displayed by discoloration, alveolar weathering, spalling, efflorescence, pitting and cracking. It is accompanied by an increase in porosity and water absorption and a decrease in the specific gravity, strength and ultrasonic velocity. The most important agent of weathering is salt crystallization and clay minerals expansion upon water and humidity migration throughout the stones.

## References

- Cardell C, Benavente D, Rodríguez-Gordillo J (2008) Weathering of limestone building material by mixed sulfate solutions. Characterization of stone microstructure, reaction products and decay forms. *Mater Charact* 59:1371–1385
- Deere DM, Miller RP (1966) Engineering classification and index properties for intact rock. Technical Report AFWL-TR-116, Air Force weapons Laboratory, Kirtland Air Force Base, New Mexico
- Dobreiner L, de Freitas ML (1986) Geotechnical properties of weak sandstones. *Geotechnique* 36:79–94. Durozoy et Lamber 1947: Compte rendu la tournée effectuée dans la région de Tébessa (plateau de Cheria) A.N.R.H de Tébessa, 40 p
- Fitzner B, Heinrichs K (2002) Damage diagnosis on stone monuments-weathering forms, damage categories and damage indices. In: Prikryl R, Viles HA (eds) Proceedings of the international conference, weathering and atmospheric pollution network (SWAP-NET 2011), Charles University, Prague, Czech Republic, 2002
- Fookes PG, Hawkins AB (1988) Limestone weathering: its significance and a proposed classification scheme. *Q J Eng Geol* 21:7–31
- Fookes PG, Gourley CS, Ohikere C (1988) Rock weathering in engineering time. *Q J Eng Geol* 21:33–57
- Heinrichs K, Fitzner B (2002) Deterioration in Petra, Jordan. In: Proceedings of the 9th international congress on the deterioration and conservation of stone, Venice, Italy 2002, pp 53–61
- Irfan TY, Dearman WR (1978) Engineering petrography of weathered granite. *Q J Eng Geol* 11:233–244
- Kowalski WM, Phrisat A, Hamimed M (1995) Analyse sédimentologique des sables du miocène des environs de Tébessa, Confins Algero-Tunisiens, annales scientifiques de l'Université de Franche-Comte, Besançon
- Vila JM (1996) Halocinèse distensive albienne à «glacier de sel» sous-marin et plissements tertiaires du secteur Ouenza-Ladjebel-Méridéf

---

**Part IV**

**Engineering Geology Problems and Preservation  
of Chinese Caves and Earthen Architecture Site**

Yoshinori Iwasaki, Chikaosa Tanimoto, Yuzo Ishikawa, Keigo Koizumi, Koichi Nakagawa, Kazuo Oike, Xudong Wang, Qinglin Guo, and Lanming Wang

---

## Abstract

This paper describes fundamental settings of the Mogao Grottoes, Dunhuang against earthquake damage. The potential damage caused by an earthquake might be generally estimated by Intensity scale. The intensity is related to human reaction and structural damages. Based upon the characteristics distribution pattern of the relation between magnitudes and epicentral distances or distances from faults, general effects to structures could be estimated as a preliminary base. Earthquake data from PCSeis (1606–2011) show little effects on the Mogao Grottoes. However, “*Sanwei Shan fault*,” which locates nearby the site, may cause a very big magnitude earthquake of  $M = 8$ . The active fault is extended to the very near to the Grottoes, the Sanwei Shan fault is identified as to produce the most dangerous earthquake to Mogao Grottoes in the future.

---

## Keywords

Mogao grottoes • Protection of cultural heritage • Earthquake risk • Active fault

---

Y. Iwasaki (✉)  
Geo Research Institute, 4-3-2 Itachi-bori, Nishi-ku, Osaka  
550-0012, Japan  
e-mail: yoshi-iw@geor.or.jp

C. Tanimoto  
International Institute for Advanced Studies, Kyoto, Japan

Y. Ishikawa  
Shizuoka University, Shizuoka, Japan

K. Koizumi  
Osaka City University, Osaka, Japan

K. Nakagawa  
Osaka University, Osaka, Japan

K. Oike  
Kyoto University of Art and Design, Kyoto, Japan

X. Wang · Q. Guo  
Dunhuang Academy, Dunhuang, China

L. Wang  
Lanzhou Institute of Seismology, Lanzhou, China

---

## 28.1 Introduction

Dunhuang is located at 1,900 km west of Beijing as shown in Fig. 28.1. The Mogao Grottoes (Fig. 28.2) in 25 km southeast of Dunhuang City is one of the world’s largest stone cave monument. During 1,000 years from 4th to 14th centuries, about 1,000 caves had been excavated at conglomerate cliff, and 492 caves are decorated with wall paintings and murals. They have been registered as the World Cultural Heritage since 1987.

---

## 28.2 Active Faults

In the past centuries, there are little documents that refer earthquake damage of the grottoes. At the same time, there is a mountain “*Sanwei Shan*” nearby the site, which is believed to have been built up by thrust movements of active “*Sanwei Shan Fault*.” Figure 28.2 shows the *Sanwei Shan Fault* that extends in the ENE direction with about 130 km in length. Active faults are discussed by Jiang (2009). There are other



**Fig. 28.1** Dunhuang in China

active faults that are located about 100 km south of the grottoes. These active faults are *Aerjin* and *Qilian* Active as shown in Fig. 28.2 as well.

Matsuda (1975) has proposed simple equation to estimate earthquake magnitude *M* that is caused by a fault movement of the length *L* as follows,

$$\text{Log}(L) = 0.6M - 2.9 \quad (28.1)$$

Based upon the above equation, magnitude of two earthquakes from Sanwei and Aerjing sub fault VI are estimated as *M* = 8.4 and *M* = 8.9 and shown in Fig. 28.3. Based upon the relative position of Mogao Grottoes and active faults, two types of earthquake risk should be considered. One is very big earthquake with strike slip movement with relatively long distance of about 100 km. Another

**Fig. 28.2** Active faults near the Mogao Grottoes

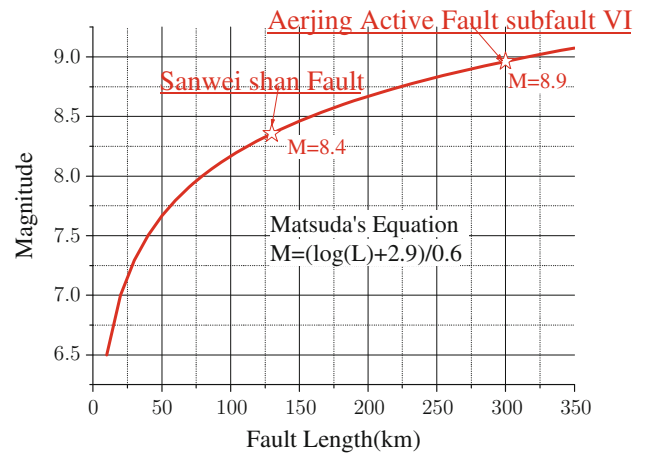
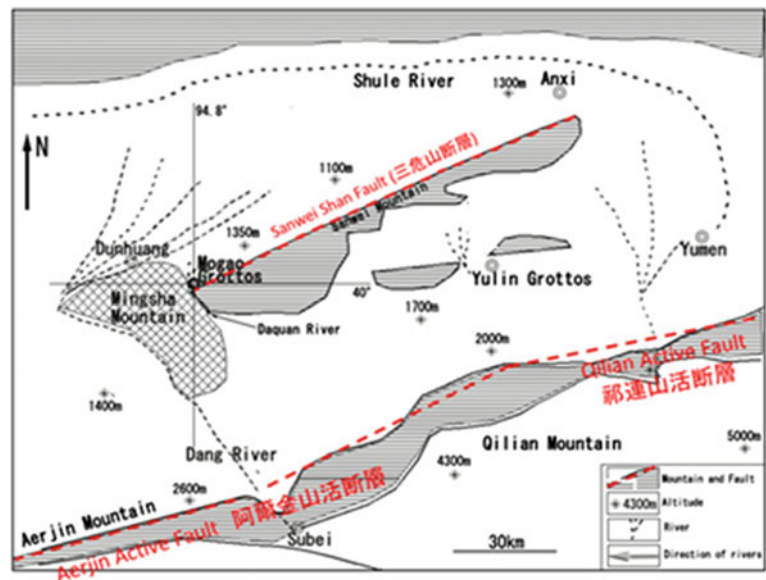


**Fig. 28.3** Estimated magnitude by Sanwei and Aerjing faults

type of earthquake is also very big earthquake with a very short distance.

The earthquake intensity depends on several factors of magnitude, distance of the site from the fault or epicenter, as well as depth of the earthquake.

Matsuzaki et al. (2006) studied intensity distributions by 554 earthquakes of magnitude from *M* = 5 to 8.2 from 1926 to 2005 in Japan and proposed the following relationship to estimate intensity at a site.

$$I_{JMA} = 1.36M_j - 4.03\text{log}(X + 0.00675 \cdot 100.5M_j) + 0.0155 \cdot h + 2.05 \quad (28.2)$$

where,

- M<sub>j</sub>*: magnitude,
- X*: distance from fault or epicentral distance (km),
- h*: depth(km).

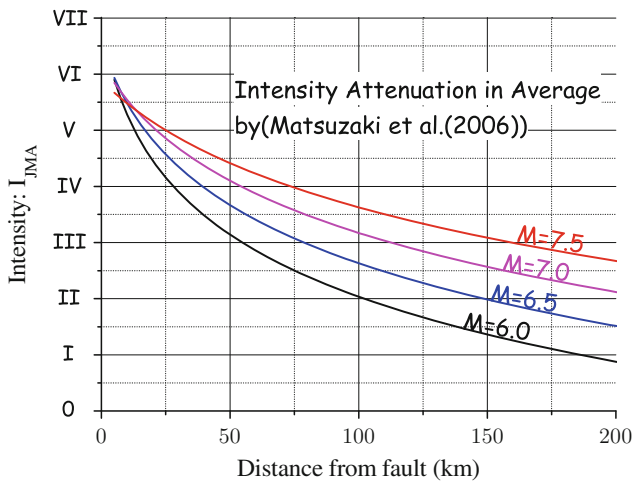


Fig. 28.4 Earthquake intensity by magnitude with epicentral distance



Fig. 28.5 Comparison between Japanese and Chinese intensity

Equation (28.2) was obtained for sites of various grounds in average. It was reported averaged deviation of the estimated intensity of  $-0.152$ ,  $+0.012$ ,  $+0.190$ , and  $0.416$  for rock, hard, medium, and soft ground respectively.

Fig. 28.6 Seismicity at Mogao Grottoes

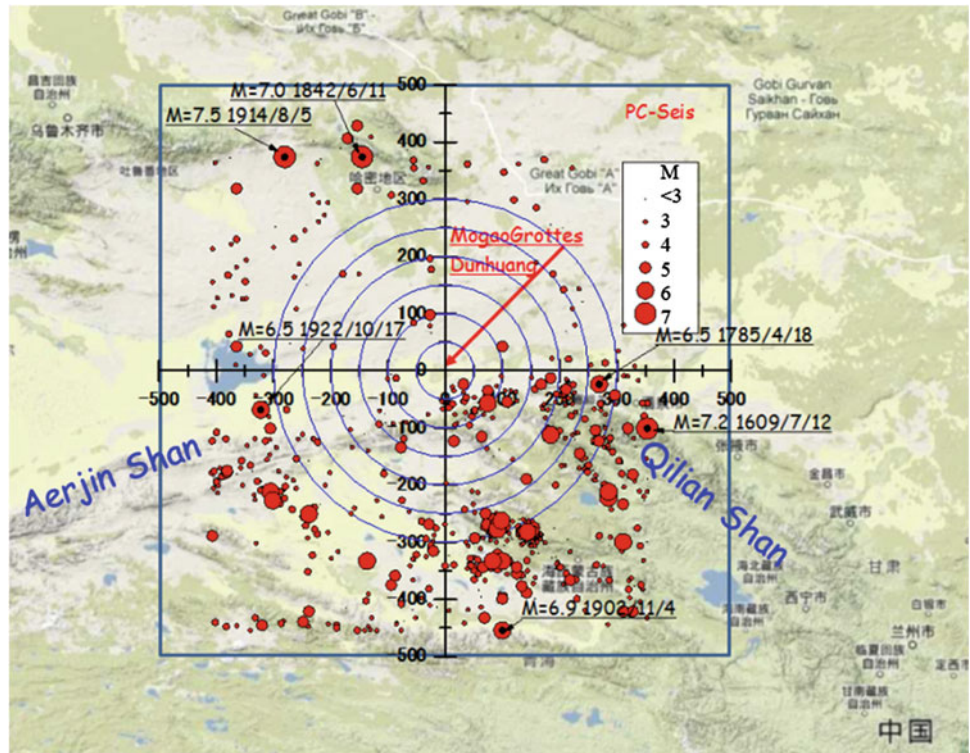


Figure 28.4 shows relationship between the observed intensity, magnitude, and distance from fault.

Figure 28.5 shows comparison of Japanese Earthquake Intensity and Chinese one.

### 28.3 Seismicity Near Dunhuang

Seismicity in the vicinity of Mogao grottoes has been collected from the earthquake catalogue that is provided by the PCSeis from 1606 to 2011.

These data are plotted in Fig. 28.6 with equi-radius of distance from the Mogao Grottoes, Dunhuang city. Seismicity Near Dunhuang. As shown in Fig. 28.6, most earthquakes took place south of Dunhuang, especially in east-south of Dunhuang along Qiliang Fault Belt. The effects of an earthquake to some site depend upon basically two factors of earthquake magnitude and distance from the epicenter or fault line.

Figure 28.7 shows the relationship of epicentral distance and magnitude in the past earthquakes from Mogao Grottoes. The earthquakes from active faults are also added in the Fig. 28.7 as possible earthquakes in the future.

General effects by the past earthquakes are shown to have given less than JMA intensity III(= Chinese Intensity VI) of little damages. The Sanwei Shan Fault is found as the only possible dangerous earthquake to give damaging intensity to Mogao Grottoes.

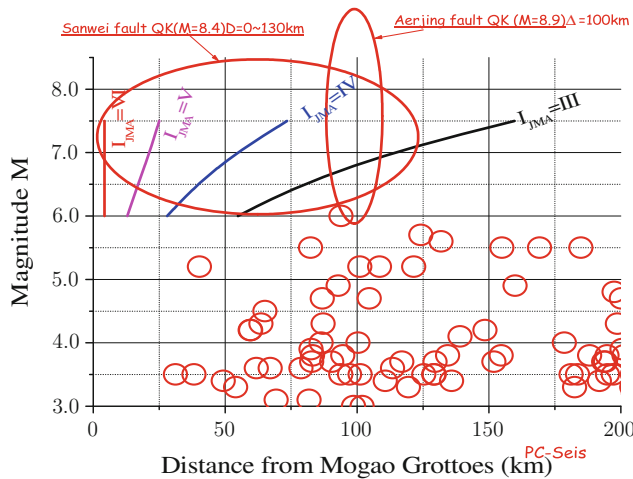


Fig. 28.7 Intensity attenuation with distance from fault

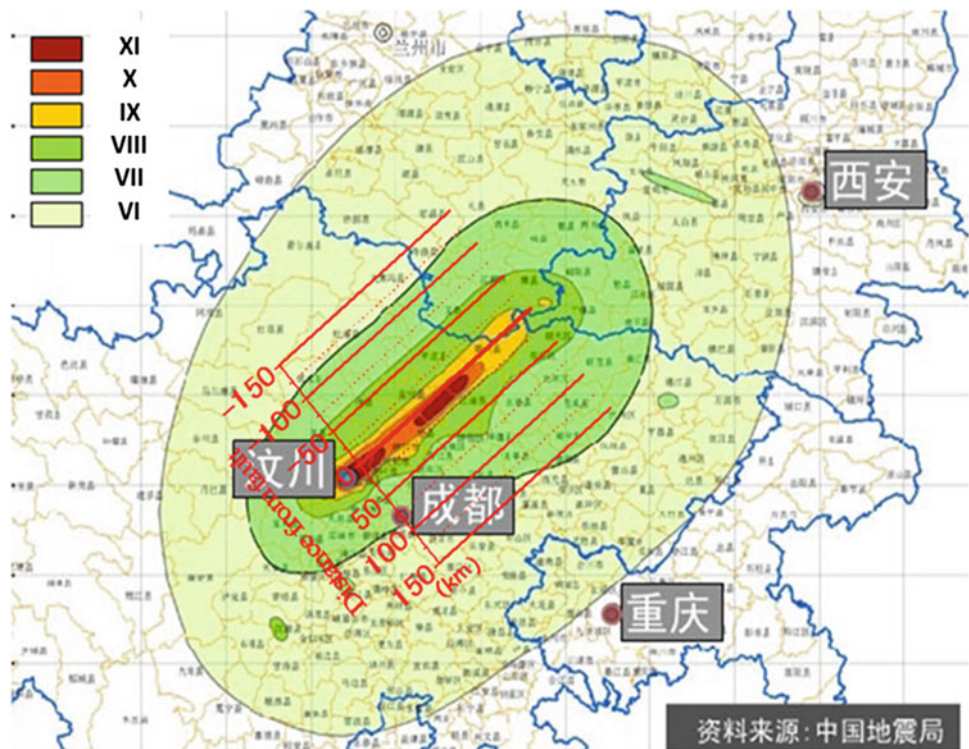
### 28.4 Intensity Map of Wenchuan Earthquake of M = 8, 2008/9/2

It is worthwhile to study intensity distribution caused by very big earthquake of magnitude 8. One of the good example may be Wenchuan Earthquake of M = 8, which occurred on September 2, 2008.

Figure 28.8 shows the earthquake intensity map provided by China Earthquake Administration.

The fault activated was believed within a long active fault of 300 km in length called as Longmenshan Thrust Zone.

Fig. 28.8 Intensity distribution for Wenchuan earthquake M = 8



The very near the fault zone of within a several km, the intensity was XI and X in Liudu, Chinese scale. When the distance becomes 100 km, the intensity decreases VII to VI that shall not cause severe damage to the structures.

Considering the above experience, Sanwei earthquake is anticipated to give much severe damages to Mogao Grottoes compared to Aejing Fault.

### 28.5 Conclusions

Based upon the seismic environmental study near the Mogao Grottoes, conclusions are obtained as follows,

1. Two active faults near the Mogao Grottoes are identified as Sanwei and Aejing active faults.
2. Estimated origins of earthquakes recorded in the past distribute in the Qiliang shan fault belt and far from the site and these earthquakes did not give any severe damages to Grottoes.
3. Aejing active may produce a big earthquake of M = 8.9, however the effects to the site are estimated not so severe because fault locates about 100 km from grottoes.
4. Sanwei fault, on the other hand, could give fatal damage to Mogao Grottoes because of the short distance from the fault as well as great magnitude by long fault length.
5. Further study needs to clarify the structure of Sanwei fault and dynamic geotechnical characterization of the site near the Mogao Grottoes to protect the world heritage.

## References

- Jiang W (2009) Discussion of estimation of strong ground motion and quantitative study of active fault structures, monthly report of science and technology from China 27, 2009年1月号(第27号)第27中国科学技术月报. [http://www.spc.jst.go.jp/hottopics/0901earthquake/r0901\\_jiang.html](http://www.spc.jst.go.jp/hottopics/0901earthquake/r0901_jiang.html) (in Japanese)
- Matsuda T (1975) Earthquake magnitude and its return period caused by active fault. *Jishin II* 28:269–283 (in Japanese)
- Matsuzaki K et al (2006) Attenuation relation of JMA seismic intensity applicable to near source region. *J Struct Const Eng AIJ*, No. 604, June 2006, 201–208 (in Japanese)

---

# The Engineering Geological Problems and Conservation of Cliff Face of Dunhuang Mogao Grottoes, China

29

Xudong Wang, Qinglin Guo, Shanlong Yang, Qiangqiang Pei, and Yuquan Fan

---

## Abstract

Located in northwest China, the Mogao Grottoes site at Dunhuang is one of first group of world cultural heritage sites in China. Due to the tectonic movement, long-time weathering unloading actions and construction of caves, there are cross-cutting structural cracks, vertical, horizontal, lengthwise tension cracks, and unloading cracks in the rock body of the Mogao Grottoes. The strong rainfall, sand and wind, and earthquake also threaten the permanent preservation of the Mogao Grottoes. Aiming at the main engineering geology problems at the Mogao Grottoes, various measures had been taken to ensure the stability of most cliff rock. The ongoing researches and construction of a monitoring and forewarning system at the Mogao grottoes can provide continual monitoring, allowing for the transition from rescue conservation to preventive conservation.

---

## Keywords

Mogao grottoes • Engineering geology • Cliff deterioration • Site conservation

---

## 29.1 Introduction

The Mogao Grottoes was constructed out of the eastern cliff of the Mingsha Mountain, and the site stretches 1,680 m from south to north. Because the Mogao Grottoes were dug in the conglomerate cliff cemented by the Quaternary calcium clay, and the caves mainly concentrate the Jiuquan group formed in Middle Pleistocene ( $Q_2$ ). Due to natural geological actions and human activities, the Mogao Grottoes bring a series of problems, such as the development of cracks in the cliff, weathering, collapse, disruption of the wall paintings, the floods, the wind and sand, and the earthquake.

---

X. Wang · Q. Guo · S. Yang · Q. Pei · Y. Fan  
National Research Center for Conservation of Ancient Wall  
Paintings, Dunhuang 736200, China

X. Wang · Q. Guo (✉) · S. Yang · Q. Pei · Y. Fan  
Dunhuang Academy, Dunhuang 736200, China  
e-mail: gqinglin@aliyun.com

---

## 29.2 Landform and Engineering Geological Features of the Cliff at the Mogao Grottoes

The Mogao Grottoes is situated on the upper part of the alluvial fan formed by the Daquan River, a contact zone between the uplift zone of the bedrock mountain area and the subsidence zone of Dunhuang Basin, with the sandy Mingsha Mountain to the southwest and the Sanwei Mountain to the southeast, which is composed of ancient metamorphic rock of Presinian Dunhuang rock group (Sun 1994).

The extant caves are located in the steep cliff near the west bank of the Daquan River, which basically stretches 1,680 m long from south to north. More than 90 % of the Mogao caves are concentrated in a 920-m long section of the Southern Area cliff, consisting of a lower steep cliff and an upper side slope, about 10–40 m high. The steep cliff ( $Q_2$ ) is 10–20 m high, which forms the wall rock of all the caves; the slide slope of Upper Pleistocene sandstone layer ( $Q_3$ ) at an incline of  $40^\circ$  forms the cover of the top caves. A broad

Gobi platform on the top of the caves, which is about 800–1,000 m away from the Mingsha Mountain, is the main passageway for the sand transportation. The Yumen group conglomerate of Lower Pleistocene series ( $Q_{1yal-pl}$ ), which covers the Tertiary argillaceous sandstone ( $N_2$ ) and is composed of grayish-brown conglomerate of siliceous or silicon-calcium cementation with clear stratification and hard texture, forms the material of the bottom caves. The Jiuquan group conglomerate of Middle Pleistocene series ( $Q_{2pl-al}$ ), composed of calcium or calcium-mud cementation mixed with fine sandstone lenticles, which is grey and has bedding structures, forms the wall rock of all the caves. The Gobi group conglomerate of the Upper Pleistocene series ( $Q_{3pl-al}$ ) is the layer of Gobi exposed on the top of the caves. It is composed of ash grey gravel layers mixed with lenticles of sand and dust layers, with bedding structures and loose structures. The part of Holocene series ( $Q_{4pl-al}$ ) is composed of loose sand-gravel layer, sandy loam, clay-like loam, aeolian sand and slope wash that are distributed in front of the caves (Wang et al. 2000) (Fig. 29.1).

### 29.3 Elements Influencing the Conservation of the Mogao Grottoes

Elements that influence the conservation of the Mogao Grottoes mainly include destruction of the cliff, strong rainfall, sand-carrying winds and earthquakes. They might

cause fatal destruction to the Mogao Grottoes. These elements are discussed in detail as follows:

#### 29.3.1 Destruction of the Rock Body

The main engineering geology problems for the cliff of the Mogao Grottoes are developmental cracks and severe surface weathering, which often result in collapse or sloping of the cliff. The developmental cracks in the cliff of the Mogao Grottoes can be divided into four main types (Fig. 29.2). First, there are the cracks vertical and parallel to the cliff. These cracks are not only long in length and large in number, but also have the greatest impact on the safety of the caves. The section between caves 96 and 15 shows the most severe vertical cracks. Second, we can find the transverse cracks vertical to the cliff. Usually these cracks are thin, short, rough and wavelike, with an opening of 1–5 mm at the bottom which extends 2–5 m upward along the cliff. They have a relative smaller impact on the safety of the caves. Third, we can find beveled tectonic cracks in the cliff. These cracks have flat and closed fissures without fillings, identical in attitude to the reversed faults produced by the neotectonic movement of the Sanwei Mountain in the south. The last one is horizontal cracks. They develop along the stratum of Jiuquan group and mainly appear in the south section of the cave zone, looking like interrupted horizontal lines on the cliff surface.

**Fig. 29.1** Geological map of the areas around the Mogao Grottoes (1 Lower Pleistocene series; 2 Mid Pleistocene series; 3 Upper Pleistocene series; 4 Holocene series; 5 Presinian system; 6 Fault; 7 Dike)

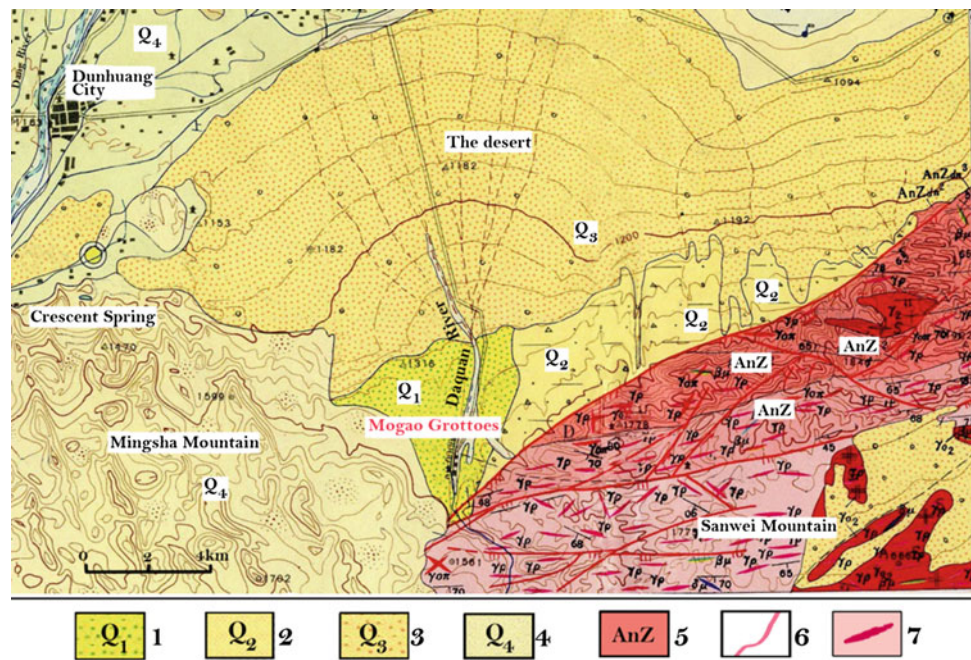
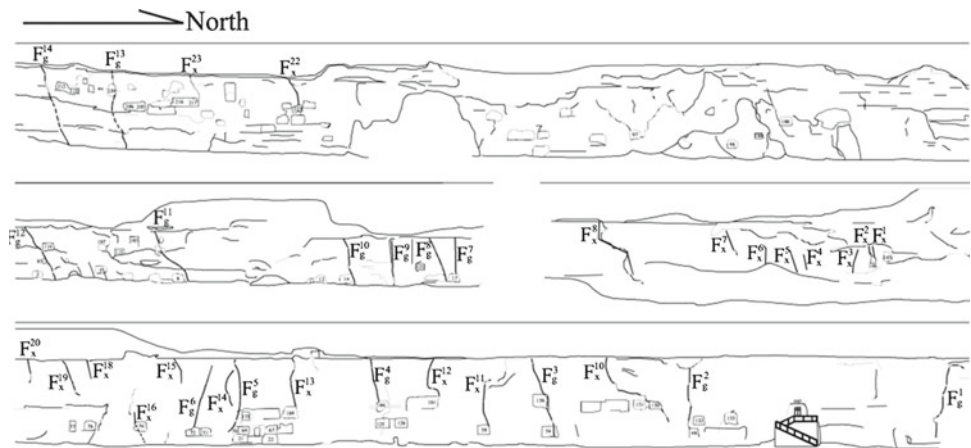


**Fig. 29.2** Representative fissure appeared on the cliff of the northern area



The main type of rock weathering at the Mogao Grottoes is physical weathering. As the environmental temperature and humidity vary with the climate, seasons, and day and night, obvious temperature stress will appear between the gravel and the binding materials in the conglomerate of the caves. Meanwhile, the clay minerals such as montmorillonite and chlorite will repeat the cycle of expanding after absorbing the water and shrinking after losing the water, resulting in damage to the cement structure of the gravels. The weathering degree and resultant deterioration vary with the topographical features or landforms at the Mogao Grottoes. As the weathering-resistant consolidation for the rock requires, Wang Xudong and Zhang Huyuan (Wang et al. 2009) have classified the weathering deterioration at the Mogao Grottoes into nine categories based on detailed field investigation. Each category is divided into strong, middle and weak levels according to their influences on visitors or on cultural relics in the cave zone.

### 29.3.2 Influence of Strong Rainfall Events, Wind and Sands and the Earthquakes on the Mogao Grottoes

Though the Mogao Grottoes lies in a very arid area, the rainfall events concentrated in summer often result in floods in the Daquan River, threatening the conservation of the caves.

The harm of sand and wind at the Mogao Grottoes mainly comes from the wind-sand flow formed by west and south winds, which cause a lot of sand to accumulate in the cave zone and erode the cliff as well as abrasively erode the wall paintings and statues in the caves (Wang et al. 2009).

The Mogao Grottoes is located a zone where seismic activities are frequent. There have been 15 recorded seismic activities since 417 AD, and the caves collapsed for many times in the history (Fu and Shi 2004).

## 29.4 Conservation Measures for the Mogao Grottoes Site

### 29.4.1 Consolidation of the Rock Body

Aiming at the main engineering geology problems at the Mogao Grottoes, various engineering measures such as support, retaining wall, fender and removal had been implemented to ensure the stability of most cliff rock in 1950s (Fig. 29.3). During recent 5 years, consolidation measures including cable anchoring, grouting cracks, consolidating thin-topped caves and consolidating the cliff surface against weathering have been taken to effectively strengthen the weathering-resistant and rain erosion-resistant properties of the cliff.

- With mechanical drilling pressure-type anchorage cables, the dangerous rocks between caves 201 and 204 were anchored into deeper stable rocks, not only remaining the original appearance, but also strengthening the stability of the rocks.
- The PS solutions are used to consolidate the strong and medium weathering gravels and outcrop sandstones for three times to improve their weathering-resistant, denudation-resistant properties and protect the deep rocks.
- Consolidating the tension cracks on the top of the cliff by filling grouting can prevent further weathering of the rocks along the cracks, strengthen the integrity of the rocks and prevent meteoric water from penetrating into the rocks and caves.
- Consolidation with the geotextiles and PS had protected the thin-topped caves against the rainfall effectively.
- The sloping cliff over the caves has a natural angle of repose, and surface debris is prone to fall down and threaten the safety of visitors. Therefore, the surface rocks on the slopes and the deterioration of previous consolidation structures should be treated comprehensively.



**Fig. 29.3** The Mogao Grottoes Cliff before consolidation in 1907 (*left*) and after consolidation in 2008 (*right*)

#### 29.4.2 Implementation of the Flood Control Project on the Daquan River at the Mogao Grottoes

A 2.4-km long flood bank was built on the left river bank, half on each side of the bridge leading to the cave zone. It was designed to resist against the once-in-three-centuries flood. On the right, a 1.2-km long flood bank was built on the upper reaches of the bridge, which was designed to resist against the once-in-a-century floods.

#### 29.4.3 Comprehensive Sand Control at the Mogao Grottoes

Prior to 1990s, the sand accumulated in front of the caves at the Mogao Grottoes was mainly cleared up manually. In 1989, a research was launched jointly by Dunhuang Academy, Institute of Environment and Engineering in Frigid and Arid Zone, Chinese Academy of Science, and the Getty Conservation Institute. As a result, experiments on chemical sand fixation were done on the top of the cliff; a sand-prevent system made of an A-shaped nylon net fence was built on top of the caves; and experiments on biological sand fixation were also done on the edge of the Mingsha Mountain by introducing the drip irrigation technology (Wang et al. 2005). Based on many years' research results, the sand-wind control project, as a part of the project on conservation and utilization of the Mogao Grottoes at Dunhuang began in 2008 and passed the acceptance check in 2012. It mainly includes high sand protecting barriers, sand protecting wheat grass grid, sand control by paving gravels, and sand-fixation tree belts.

#### 29.4.4 Construction of the Monitoring and Forewarning System

The monitoring and forewarning system can not only realize the information integration and sharing among the meteorology monitoring, micro environment monitoring, site monitoring, carrier monitoring, visitor-carrying capacity monitoring and safe guarding monitoring systems, improve the cooperation between different divisions, but also can confirm how to handle with different events encountered in the conservation, management and utilization of the site, make corresponding countermeasures, improve the management level.

### 29.5 Conclusion

- Consolidation measures including retaining walls, anchoring cables, and anti-weathering consolidation measures are combined to effectively protect the Mogao Grottoes and to prevent the damages of the wall paintings and statues due to the destruction of the cliff.
- Implementation of the flood-control project of the Daquan River at the Mogao Grottoes has got rid of the potential flood threats.
- Comprehensive sand-control measures taken on the top of the Mogao caves have prevented the Mogao Grottoes being damaged by sand and wind to a large extent.
- Construction of the monitoring and forewarning system at the Mogao Grottoes allows for the transition from passive conservation to preventive conservation, and attains leapfrog development in site conservation.

**Acknowledgment** This research was co-supported by funding from the China National Key Technology R&D Program (2013BAK01B01). The authors' special thanks go to Dr. ZHANG Huyuan, Lanzhou University, China for his useful comments that improved the manuscript substantially.

---

## References

- Fu C, Shi Y (2004) A study on the characteristic of the dynamic damage of the Mogao cave rock walls under the seismic load. *Northwest Seismol J* 3:266–273
- Sun R (1994) Review of the consolidation projects at the Mogao Grottoes. *Dunhuang Res* 2:14–29
- Wang W, Wang T, Zhang W et al (2005) The design of the comprehensive sand and wind control system at the Mogao Grottoes. *Arid Land Geogr* 28(5):614–620
- Wang X, Zhang M, Zhang H et al (2000) Engineering properties of the wall rocks at Dunhuang Mogao Grottoes. *Chin J Rock Mech Eng* 19(6):756–761
- Wang X, Zhang H et al (2009) Weathering features of the cliff of the Mogao Grottoes at Dunhuang and the conservation countermeasures. *Chin J Rock Mech Eng* 28(5):1055–1063

Huyuan Zhang, Bo Yang, Yi Chen, and Jinfang Wang

---

## Abstract

This paper takes the Shengjinkou Buddhist temple in the Northwest of China as an example to discuss the preservation countermeasures against geological hazards such as rockfall and mudflow. The Shengjinkou site is a famous Buddhist Temple along the ancient Silk Road constructed in 640–791 A.D., including grottos excavated in weak conglomerate rock and some earthen buildings made by mud-bricks. Engineering geological investigation indicated that the heritage site at a hillside is seriously threatened by rockfall and mudflow due to strong geological weathering and sudden rainfall. Therefore, engineering measures have to be taken to reduce the risk of geological hazards under the least intervention principle for heritage conservation. A safety netting system (SNS) mainly consisting of wire rope net was designed at the upside of the hill to prevent the rolling stones from striking grottos and visiting guests, and a diversion ditch was designed to conduct the sticky mudflow away from the earthen buildings. The preservation practice at Shengjinkou Grottos site proves that good cooperation between Engineering geologists and conservation scientists plays an important role in heritage conservation.

---

## Keywords

Geological hazards, heritage site • Rockfall • Mudflow • Shengjinkou grottos

---

## 30.1 Shengjinkou Buddhist Temple

The Shengjinkou Buddhist Temple is located in a mountain area, about 40 km east of Turpan City, Xinjiang Uygur Autonomous Region of China. According to the last archeological information, this temple was built from A.D. 640 to A.D. 791 through the Xizhou period of Tang to Gaochang Kingdoms, considered to be mainly served as the Royal monastery of Gaochang Kingdoms. Therefore, Shengjinkou

site is an important Buddhist art treasure in China and even in Central Asia along the Ancient Silk Road (Albert von Le Coq 1928) with special historical, artistic and cultural values.

Shengjinkou Buddhist Temple had been neglected for more than 1,000 years until 1920s when official organization and individuals undertaken a series of excavations in this area. Investigation indicates, at present, there are 8 caves and 8 earthen temples being remained at this site. The caves were excavated into weakly cemented conglomerate rock and distributed at a cliff 120 m long and 20 m high. All the caves are characterized by a horse-shoe section; both the vertical walls and arched roof were lined by mud-bricks. The earthen temples, distributed on the left river terrace about 1,700 m long and 14 m high above the Mutougou River, were constructed by mud-bricks, between them mud plaster was used as cementation.

---

H. Zhang (✉) · B. Yang · Y. Chen · J. Wang  
School of Civil Engineering and Mechanics, Lanzhou University,  
Lanzhou 730000, China  
e-mail: zhanghuyuan@lzu.edu.cn

This site was listed in the Great Relic's Conservation Program along the Silk Road by Chinese government in 2006 for its extremely abundant artifacts unearthed and profound Buddhist art. Followed began the engineering geological investigation and conservation design in 2008. From 2011 on, a stabilization project conducted to control mainly the geological hazards such as rock-fall and mud-flow etc. This paper reports the results of Engineering geological investigation and the engineering measurements, providing a case study of Engineering Geology to cultural heritage conservation.

### 30.2 Geological Settings of the Site

Shengjinkou site is located at the left terrace of Mutougou River that deeply cut into the Flaming Mountain, an intensively elevated geological belt with compact fold structures and faults, 1,600 km long in W–E direction and 5–15 km wide in N–S direction. Flaming Mountain is so named because it is abrupt up 300–500 m high from the sedimentary basins at two sides and characterized with red-colored stones just like burning flames. The bedrock at mountain area is classified as Jurassic, Cretaceous and Tertiary strata. The major rocks observed from the outcrop at the site are Cretaceous formation: thick-bedded mudstone interlaid by thin-bedded fine sandstone. It is the differential weathering between the mudstone and sandstone at the high mountain slope that results in serious geological threat to the site at hill side in forms of rock fall and mudflow.

Mutougou River is deeply cut into the Flaming Mountain. At the left bank of the river there exists a flat terrace (Fig. 30.1), composed of Quaternary sediments, that is, thick-bedded alluvial materials interlaid by residual. The alluvial sediments are classified mainly as weakly cemented conglomerate, serving as host rock of the caves, and as sand and gravels serving as the foundation of the temples.

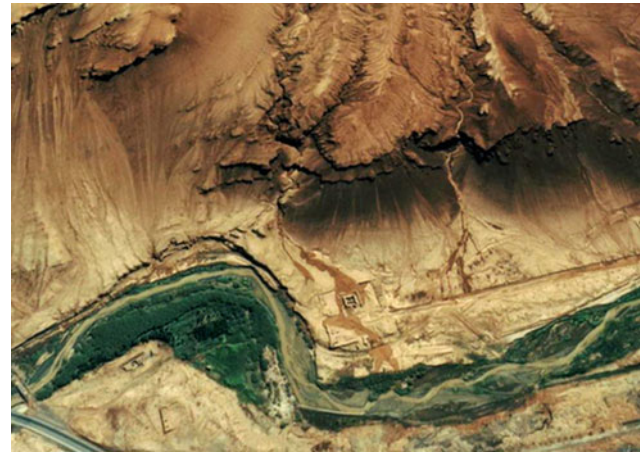


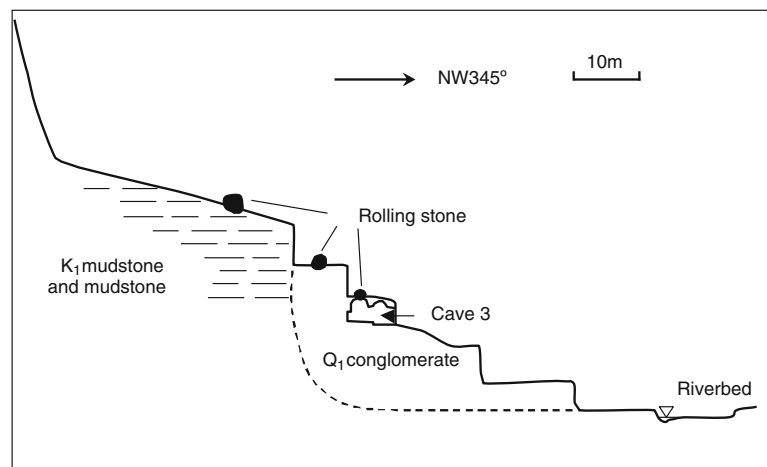
**Fig. 30.1** Shengjinkou Buddhist Temple attacked by mudflow after an rainfall on July 10, 2011

Meteorologically, Flaming Mountain area is also characterized by extremely dry and hot summer and violent windy spring all over China. The average annual rainfall is as less as 16.4 mm, but the evaporation as high as 2,837.8 mm. There are at least 32.7 days a year that the wind speeds is more than 17 m/s. The average temperature at summer is around 30 °C, and the max temperature is as high as 47.7 °C. All of these factors have established a framework for the fracture of sandstone and the severe physical weathering of mudstone, leading to the rockfall and mudflow hazards discussed in the followings.

### 30.3 Rockfall Hazard and Its Control

Field investigation shows that there are some big stones, as large as several tons, exist along the slope upward the caves. One big stone hit and even penetrated through the roof strata of Cave 3 just as shown in the typical section of the slope through Cave 3 (Fig. 30.2). Some other caves at top level

**Fig. 30.2** Cave 3 cross-section



were also damaged partially by rolling stones. It can be found that the rock-fall from the over slope possess a great threat to the safety of both caves and visiting guests at site area.

Investigation indicates that these big stones fall down from the high mountain area due to intensive differential weathering between Cretaceous mudstone and sandstone. The mudstone contains abundant clay minerals, which swell very easily when absorbed water after occasional rains. During dry season, weathered mudstone is eroded away continuously by aggressive strong wind, and recessed a portion of the outcrop, making the overlain sandstone layers into an over-hanged situation. Subjected to intensive deformation due to geological folding, the sandstone was originally fractured. Along with excessive recession of mudstone layers, sandstone blocks lose their sufficient support and get rid of the host sandstone layer, rolling down to the hill side area. Rock fall then takes place.

Detailed analysis reveals that the rolling stones possess great kinetic energy due to their giant volume and high falling height, just as the roof of Cave 3 have been damaged (Fig. 30.2). Obviously, rolling stones makes both the caves and the visitors into a dangerous situation. Eliminating the risky rocks at the source positions is very dangerous because the falling heavy rock bodies perhaps impact directly the caves at hillside. Also, stabilizing the risky rocks in situ seems not to be economic and feasible in technology because the source area is so high. Practically, a flexible guard fence, namely safety netting system (SNS), was designed at the hillside, upside of the caves, to passively stop the possible rolling stones that falling down from the high mountain area (Fig. 30.3). The net system consists mainly of steel posts anchored to the ground by wire cable, between the posts wire rope net is stretched. When a rolling stone hits the flexible net system, the kinetic energy can be absorbed by the deformation of the high-strength wire net and the steel brake rings connected to the anchoring cables. In fact, this kind of passive guard fence has been successfully used



**Fig. 30.3** SNS against rolling stones

worldwide to provide protection to railway (MOR 2004) and road etc., against rolling stone from high mountain slope.

### 30.4 Mudflow Hazard and Its Control

Mudflow is another geological hazard threatening the Shengjinkou site seriously, especially to the mud-brick temples (Fig. 30.4). Control of mudflow is a new task that firstly encountered in the conservation projects along the Silk Road in China (Li 2003). Field investigation indicates that mudflow had reached the biggest temple at least 7 times in history, where mud sediments accumulated as deep as 1.3 m. Fortunately, satellite photo in Fig. 30.1 recorded occasionally a mudflow event on July 10, 2011. Figure 30.1 shows clearly the mudflow path across the temple, coincided with that recorded by historical sediments.

It is found that strongly weathered Cretaceous mudstone provide abundant clay minerals along the slope surface as the source material for mudflow. Although the precipitation in the site area is as less as 16.4 mm on an annual average, the rainfall of a whole year is concentrated to limited times. As a result, at 2–3 year intervals, concentrated rainfall is big enough to produce runoff, making the weathered clay minerals in the small gullies from a dry condition into a saturated condition, and triggering a slow mudflow. In case of strong rainfall, the mudflow can spread long enough from the mountain gullies to the big temple as that occurred on July 10, 2011 (Fig. 30.1).

When reached the temple, flooded mudflow did not only bury partially the temple buildings, but also made the wall foundation saturated, resulted in differential deformation or even the whole falling down of the walls. A practical way to control the mudflow is to dig a diversion ditch, conducting the mudflow away from the temple. Figure 30.5 shows the diversion ditch under construction in May, 2013, which is an artificial channel with a single concrete embankment at downhill side.



**Fig. 30.4** Mudflow reached the mud-brick temple



**Fig. 30.5** Diversion ditch for mudflow control

The diversion ditch is designed as a wide, shallow channel, cut into the terrace sediments, with a concrete embankment constructed at the left side. Diversion ditch begins from a gully mouth where mudflow was spilled away from mountain slope, and ended to the main river bed with several steps at terrace edge. The major purpose of the diversion ditch is to introduce the intending mudflow directly to the main Mutougou River, so to prevent the temple to be flooded again by mudflow.

Frankly, there is a risk that the mudflow material tends to deposit again within the diversion ditch. Field investigation reveals that historical mudflow might be a sticky and dense liquid with very slow moving velocity. This can be proved by the fact that some mudflows stopped suddenly with a steep edge in a dried condition. From this meaning, the diversion ditch is exactly a sedimentation place rather than a drainage channel. Therefore, regular maintenance, such as cleanup of the sediments stopped within the ditch, is required in the future.

### 30.5 Summary and Conclusions

- (1) Major geological hazards at Shengjinkou Buddhist Temple include rockfall and mudflow, which are

attributed to the strong geological folding and differential weathering between Cretaceous mudstone and sandstone. Accompanying with the excessive weathering and recession of mudstone on outcrop, the overlain sandstone becomes over-hanged and finally falls down. Weathered mudstone contains abundant clay material which, in case of saturated by occasional rainfall, moves slowly as mudflow within small gullies on slope.

- (2) Big risky stones at mountain area are over-hanged at so high positions that it is difficult to be cleared off or stabilized in situ economically. Safety netting system is a practical selection to stop passively the rolling stones for protection of the caves and visiting guests.
- (3) A wide, shallow channel with a single concrete embankment was designed to divert the mudflow to main river bed directly. This diversion ditch can prevent the mud-brick temple being flooded afterward, but has a risk to stop or deposit the mud materials within the ditch. Regular cleanup of the diversion ditch becomes an additional maintenance.
- (4) Engineering Geology plays an important role in heritage conservation, which helps grasp the vital geological hazards encountered frequently in cultural site at mountain area, and select effective protection plans for heritage and visitor.

**Acknowledgements** The present work has been sponsored by National Key Project of Scientific and Technical Supporting Programs Funded by Ministry of Science & Technology of China (NO. 2013BAK01B01).

### References

- Albert von Le Coq (1928) Buried treasures of Chinese Turkestan. University Press, Oxford
- Ministry of Railways (MOR) of the People's Republic of China (2004) The flexible safety net for protection of slope along the line (TB/T3089-2004)
- Li Zuixiong (2003) Protection of ancient site in silk road. Science Press, Beijing

---

# Field Tests on Anchoring Mechanism of the Bamboo-Steel Cable Composite Anchor with Single Reinforcement

31

Jingke Zhang, Wenwu Chen, Faguo He, and Lei Tian

---

## Abstract

Under the influence of natural condition and human activities, the majority of earthen sites are suffering from the damage with different degrees, which are in urgent needs of rescuing and conservation. The previous conservation experiments and practices show that the conservation methods for the main body of earthen sites should adopt the traditional craft as far as possible to achieve the goal of “maximum compatibility, minimum intervention”. A type of the bamboo-cable composite bolt (a 7 @ 5 steel strands within the bamboo, with the length of 5 m) is chosen to carry out the field experiment of anchoring mechanism of composite bolts. The results indicate that: the main destruction way of composite anchor is that the composite material interface slips out of softening; the composite anchor axial stress distribution is exponential distribution with the pullout load increases; when pull-out load is smaller, interfacial shear stress shows the exponential function distribution, decreasing from the start to the end of the bolt, and the peak shear stress deviates to the end with the load increases; Steel strand axial stress is higher than the bamboo pipe axial stress; Composite bolt shows the material memory characteristics in the process of cycle pullout; The strain value of bamboo internal surface is higher than that of the outside surface in the same section; The limited pullout force is 238 KN in the bolt with the plats in end, whereas, it is 204 KN for the bolt without the anchor plates.

---

## Keywords

Bamboo-steel cable composite anchor • Single reinforcement • Anchorage performance • Interfacial mechanical transmission

---

## 31.1 Introduction

Since the 1980s, the earthen sites in arid and semi-arid areas have been carried out reinforcement tests and engineering practice, it is gradually realized that anchoring technology not only meets the needs of the mechanical stability control, also can better follow the idea and principle of cultural

heritage protection in China. The previous reinforcement tests and practice show that the reinforcement of the ontology should adopt the traditional craft as far as possible to achieve the goal of “maximum compatibility, minimum intervention” (Song-lin et al. 2001; Xun-guo 2009; Wu et al. 2010). Meanwhile, with the further study of scientific traditional craft, it is realized that the simple metal bolt and cement paste can not comply with the requirements of earthen sites protection. Therefore, it turns to the traditional bamboo—wood anchor and its secondary research. Under such circumstance, the bamboo-steel cable composite anchor based on the research of bamboo and steel attempts to be applied to the anchorage of the general volume of earthen sites, and finally achieved a comparatively successful

---

J. Zhang (✉) · W. Chen · F. He · L. Tian  
Key Laboratory of Mechanics on Environmental and Disaster in Western China, and School of Civil Engineering and Mechanics, Lanzhou University, Lanzhou 730000, China  
e-mail: zhangjink@lzu.edu.cn

engineering practice (Yan-jun et al. 2008; Sun et al. 2008; Ren et al. 2010; Hu-yuan et al. 2011). Due to its nonstandard, non-programmed, inhomogeneous and diameter—varied characteristics, composite anchor is completely different from other more mature reinforcing steel, steel strand and GFRP in other research area. Therefore, the study on anchoring mechanism of composite anchor is more difficult.

This article selects a type of the bamboo-steel cable composite anchor (within a 7 @ 5 specifications steel strand, 5 m long) as the object of study, carrying out the field anchorage test in the world's largest raw soil site—Jiaohe Ruins. The test installs strain gauges in different locations and surfaces of internal rod body for monitoring interface mechanics process under stress. Besides, the test adopts the method of cyclic loading and unloading for pullout.

### 31.2 Anchoring System of the Bamboo-Steel Cable Composite Anchor with Single Reinforcement

The bamboo-steel cable composite anchor rod with single reinforcement (Fig. 31.1) is composed of two pieces of bamboos, composite fillers, and 7  $\Phi$  5 mm steel strand (tensile strength 1,860 Mpa), steel strand is located in the middle of rod body, two pieces of bamboos with steel strapping butt into round, and are filled with composite fillers, the rod diameter is 90 mm. No scar, no fault and straight bamboo is often selected, and the inner and outer surfaces are coated with epoxy resin after cutting; composite filler is a mixture of fly ash, epoxy resin, asbestos, alcohol and curing agent; the end of steel strand is exposed to 200 mm. The outer surface of anchor is wrapped in a layer of glass cloth, and coated with epoxy resin adhesive. The

centering bracket is strapped with the 4 steel pipes. The HQM grip is used as anchorage, and anchor plate with the side length of 200 mm square steel, thickness is 16 mm. The anchor hole diameter is 150 mm, slope angle is 10–15°. The cement grout is mortar, cement type using 42.5 R, cement-sand ratio 1:1, water-cement ratio 0.4–0.6. The end of the anchor paints with bituminous to prevent corrosion.

### 31.3 Field Anchorage Tests Scheme

It is selected the lower part of the western cliff 5–4 sub-region of Jiaohe Ruins as anchorage test site. Facade of the cliff is nearly vertical, and surface is smooth without structural fissures, stratigraphic continuity and integrity are also good.

The LSS50H type bolt pull-out instrument produced by China Coal is used in the test, the center aperture of cylinder is 60 mm, cylinder stroke is 120 mm, the range of measurement is 0–500 KN. Strain acquisition is used by the DH3816 strain measurement system Ver3.0.1 version produced by Donghua Test, the range of measurement is  $-20,000$  to  $20,000 \mu\epsilon$ . Strain gauge is the BQ120-60AA (resistance value  $120.8 \pm 0.1 \Omega$ , sensitivity  $2.14 \pm 1\%$ ) produced by ZEMIC.

The length of bolt is 6000 mm, the starting end 0–1000 mm of bolt is selected as the reserved rod body in pull-out test, strain gauge is arranged in the inner surface of the steel stand rod, two pieces of bamboos and the outer surface of shaped anchor, arrangement position is in the same section, Specifically, a strain gauge is pasted in the 1000–4000 mm spacing 500 m and the 4000–6000 mm spacing 1000 mm respectively, a total of 36 strain monitoring points are used to monitor the axial strain (Fig. 31.2).

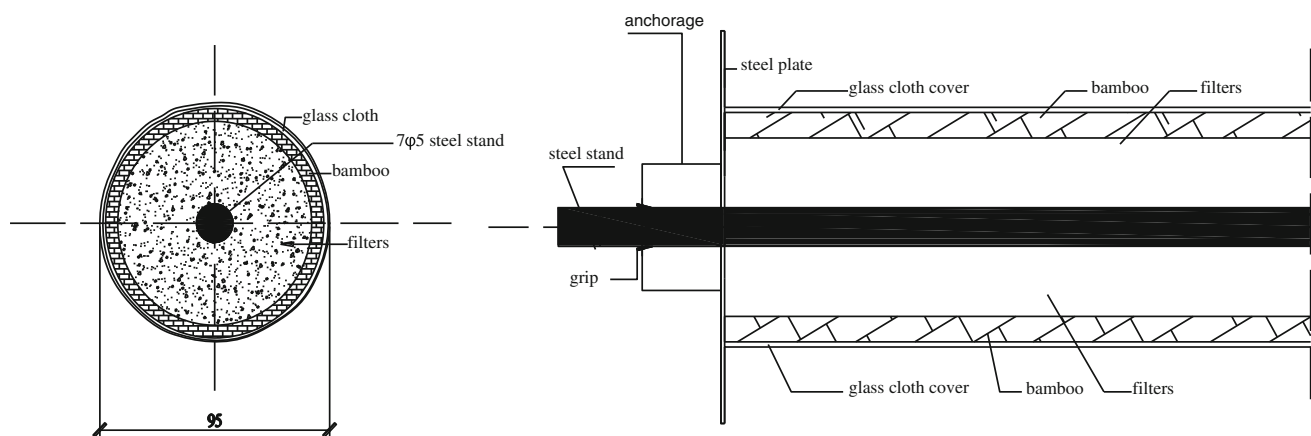
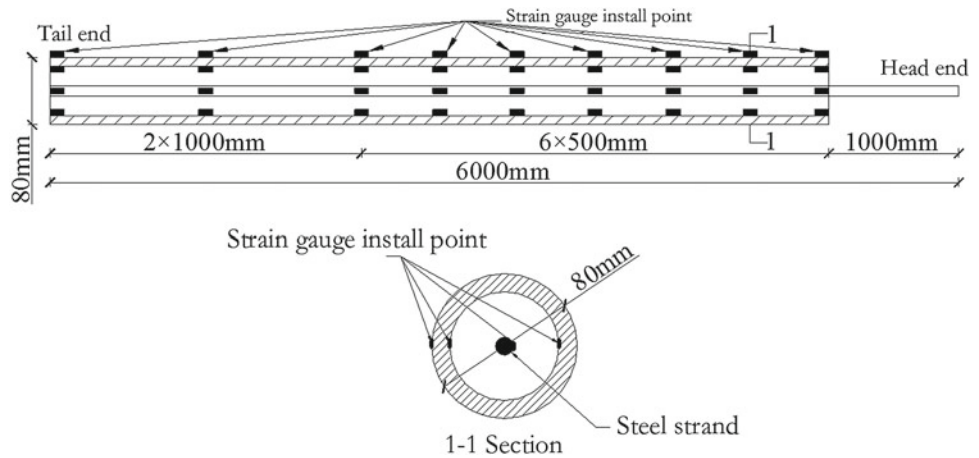


Fig. 31.1 Composite anchor structure with single steel stand

**Fig. 31.2** Strain monitoring arrangement of composite anchor with single steel stand



### 31.4 Results and Analysis

#### 31.4.1 Anchorage Performance

From the basic bolt test, it is verified that the ultimate bearing capacity of the test anchor with anchor plate at the end of the anchor has an additional loading cycle than the one without anchor plate (Figs. 31.3 and 31.4), the failure load of anchorage end with anchor plate is 238 KN, and the one without anchor plate is 204 KN.

#### 31.4.2 Interfacial Mechanical Characteristics of Transferring

##### 31.4.2.1 Interface Strain Variation Along the Anchor Axial with Time Steps

By analysis and statistics, it presents the distribution of the axial strain along the anchor shaft when load was applied to the strain of the steel strand, the inner and outer surface of the bamboo. From Figs. 31.5 and 31.6, it presents that the interface strain value changes obviously up and down along

with the load change. At the same time step, with the increasing load, the first step is to overcome the cohesive force(bond force), which will present that the strain capability in front is higher than that of the rear, and additionally, compressive stress will occur at 0 m. The phenomenon is due to the special structure of the composite anchor for the anchor clamp is installed on the steel strand and the anchor bearing plate are placed against the front side of the soil to prevent the outward deformation of the soil, resulting compressive stress to the anchor bamboo in the front of the anchor bolt. In addition, from Fig. 31.7, it presents that a parallel strain gauge is installed at the place of 1 m, and two-strain curves tend to parallel but no coincident. Because it is difficult to ensure that the pull-out instrument is completely perpendicular with the anchor in the field test, existing a partial pull phenomenon.

##### 31.4.2.2 The Interface Strain under Different Load Variation Along the Axial Bolt

As can be seen from Fig. 31.8, the steel strand at 1 and 2 m are all pulled under 34 KN load. The compressive stress occurs at 4 m. As the load increases to 102 KN, the

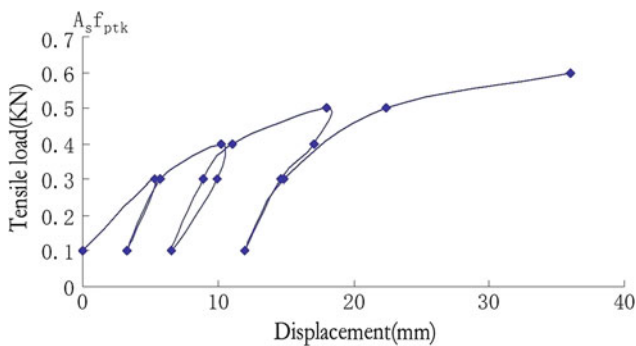


**Fig. 31.3** The basic test load-displacement curve of the bolt without anchor plate

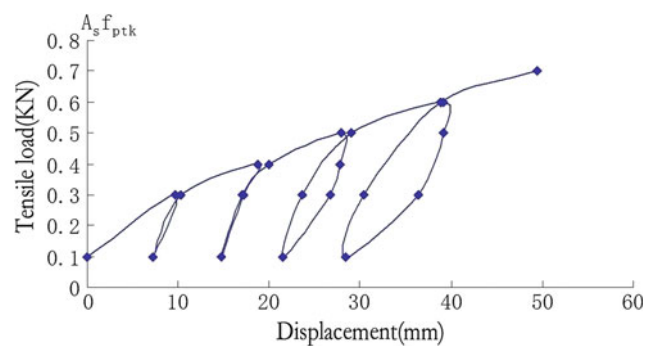


**Fig. 31.4** The basic test load-displacement curve of the bolt with anchor plate

**Fig. 31.5** Strain distribution of steel stand along the axial different position

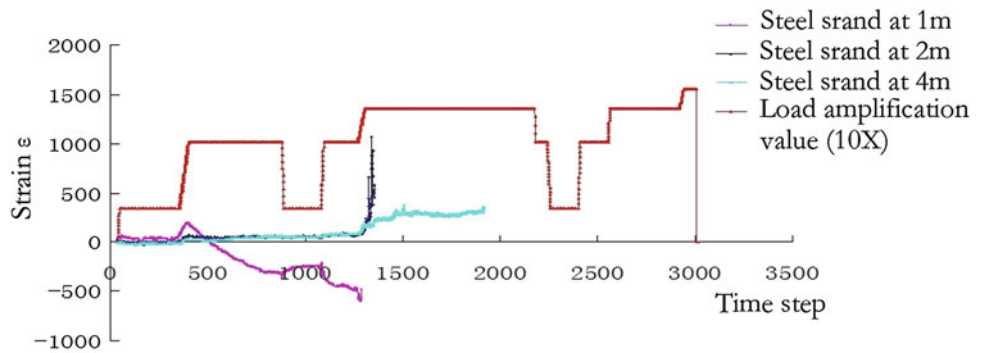


**Fig. 31.6** Strain distribution on the inner surface of bamboo along the axial different position

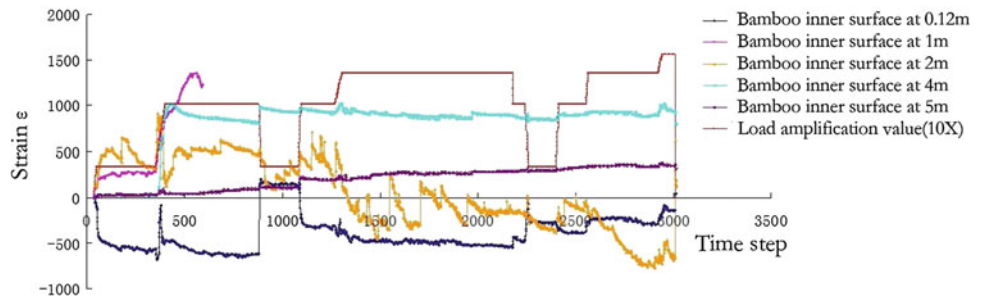


**Fig. 31.7** Strain distribution on the outer surface of bamboo along the axial different position

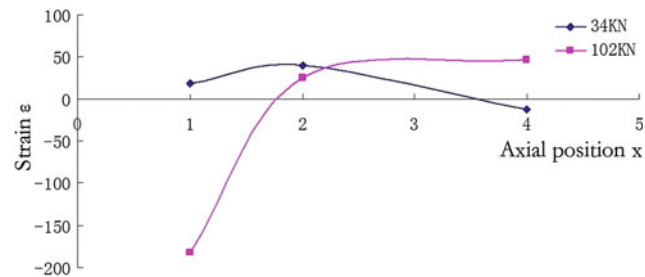
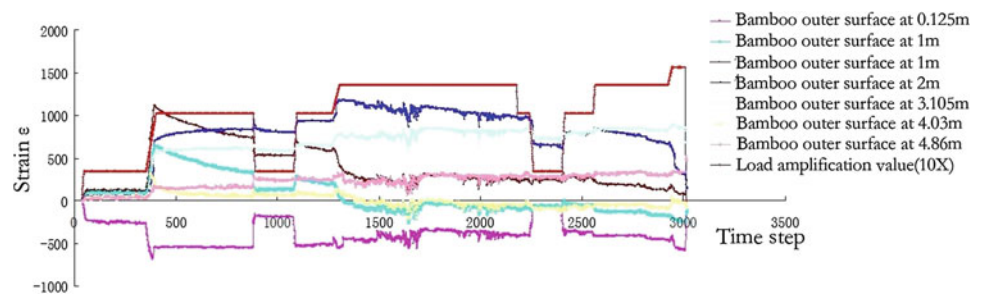


**Fig. 31.8** Strain distribution of steel strand along the axial under different loads

compressive stress occurs at the place of 1 m, and the tensile strain at 2 m is decreased, while subtle compressive strain occurs at 4 m.

The Figs. 31.9 and 31.10 present the strain distribution of the inner and outer of bamboo surface under different load

along with the axial direction. Just like the steel strand, compressive stress occurs at the anchor end is related to two factors. One is the shifting of anchor under tension. The other is that the front end soil confines outward deformation under the restriction of the anchor bearing plate, which prevents the front of bamboo’s collaborative deformations to appear the compressive stress. From the analysis of the curves trend, we can see that the bond stress along the anchor section is in asymmetrical distribution, that is, the bond stress reduces gradually from the front to the rear, and with the tensile force increasing, the peak of the bond stress transfers to the distance. In addition, as can be seen from the two Figures, under the load of 156 kN, the anchorage force can’t fully play out. The peak of the bond stress on the inner surface of bamboo transfers to the place near 4 m, however, due to lag effect of the surface, the peak of the bond stress just transfers to the place 3 m and the designed anchorage force should be greater than 156 kN.

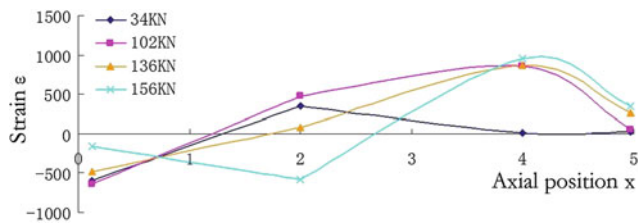


**Fig. 31.9** Strain distribution on the inner surface of bamboo along the axial under different loads

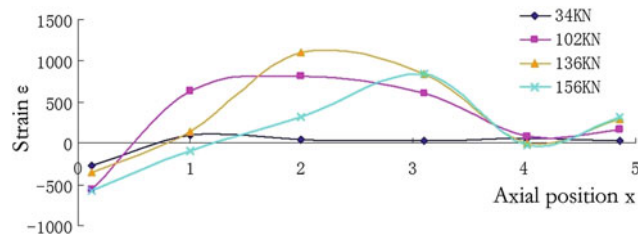


**Fig. 31.10** Strain distribution on the outer surface of bamboo along the axial under different loads

### 31.5 Conclusions

The results show that: the main destruction way of composite anchor is the composite material interface slipping out of softening; the composite anchor axial stress distribution is exponential distribution with the pullout load increases; when Load is smaller, interfacial shear stress shows the exponential function distribution, decreasing from the near-end to far-end, and the peak shear stress deviates to the far-end with the load increases; Steel strand axial stress is higher than the bamboo pipe axial stress; Composite anchor appears material memory characteristics in the process of cycle pullout; The strain value of bamboo internal surface is higher

than that of the outside surface in the same section; The limited pullout force is 238 KN in the end with the anchor plates and 204 KN without the anchor plates. The Test revealed that the interface mechanics distribution, interfacial mechanics process and the limited anchoring force of the bamboo-steel cable composite rock-bolt presented under the action of pull force are of great value to the improvement of the rod body as well as the completion, application and promotion of anchoring craft.

**Acknowledgements** This research was supported by the National Natural Science Foundation of China (Grant No. 51108218) and the national twelfth-five science and technology support program (Grant NO. 2013BAK01B01).

### References

- Hu-yuan Z, Xiao-dong W, Xu-dong W et al (2011) Bond-slip model for bamboo-steel cable composite anchor. *Rock Soil Mech* 32 (3):789–796
- Ren FF, Yang ZJ, Chen JF et al (2010) An analytical analysis of the full-range behaviour of grouted rockbolts based on a tri-linear bond-slip model. *Constr Build Mater* 24:361–370
- Song-lin Y, Guan R, Huan-chun Z (2001) Theoretical analysis and in situ experiment on load-transfer mechanism of bolt in cement. *Rock Soil Mech* 22(1):72–74
- Sun M-l, Li Z-x, Wang X-d et al (2008) Study on reinforcement of earthen sites by bamboo-steel composite anchor. *Chin J Rock Mech Eng* 27(supp.2):3381–3385
- Wu Z-m, Yang S-t, Zheng J-j et al (2010) Analytical solution for the pull-out response of FRP rods embedded in steel tubers filled with cement grout. *Mater Struct* 43:597–609
- Xun-guo Z (2009) Study on the reinforcement mechanism of fully grouted rock bolt considering the inter-action between bolt and wallrock Mass. *Metal Mine* 399:24–28
- Yan-jun Z, Hu-yuan Z, Qing-feng L et al (2008) Stress transfer model of bamboo-steel composite anchor. *Hydrogeology Eng Geol* 5:37–40

# The Disease Characteristics and Conservation Technique of the Bezeklik Grottoes at Turpan in Xinjiang

Wenwu Chen, Jingke Zhang, Faguo He, Guanping Sun, and Lei Tian

## Abstract

With the influence of the spread of Indian Buddhism, there are a large quantity of Grottoes with the variation in history, architectural art and functions distributing along the Silk Road in China. Bezeklik Grottoes at Turpan, Xinjiang is an important royal temple with significantly historical, scientific and artistic value along the Silk Road. The grottoes need urgent conservation because of the natural damage and human activities. Based on the field investigation and analysis, the types and characteristics of the main disease developing in the cliff and caves of Bezeklik Grottoes was clarified, furthermore, the genetic analysis of the disease was studied. The diseases of Bezeklik Grottoes are found out, which include carrier diseases, cave diseases and carrier a diseases associated with the cave. In accordance to the principle of diseases development, the appropriate conservation methods were proposed. The conservation engineering was finished with a satisfying effect. The similar grottoes in the same area can use the conservation experience of Bezeklik Grottoes as a successful reference.

## Keywords

Bezeklik grottoes • Cliff and caves • Diseases • Conservation methods

## 32.1 Introduction

Since the 1950s, China has being gathering experiences from the conservation projects of Dunhuang Mogao Grottoes, Yungang Grottoes, Longmen Grottoes, Maiji Mountain and Kizil Grottoes, however, a standard and formal level for conservation is still not formed. With the deep research on the conservation theory and practice, it is increasingly realized that the independent study on the personality of the grottoes plays a great deal of importance to the conservation

methods (Ramsay 1967; Lansheng et al. 1994; Junhui et al. 2003).

Bezeklik Grottoes is one of the grottoes with great historic, scientific and artistic values Xinjiang section of Silk Road in China. With more than 1,500 years history, it has already been proved to be of significant value on studying the history of Gaochang Uighur period. After the data collection, field investigation and mapping, field and indoor test, the disease characteristics of the Bezeklik Grottoes is revealed and the corresponding conservation methods are proposed.

W. Chen (✉) · J. Zhang · F. He · G. Sun · L. Tian  
Key Laboratory of Mechanics on Environmental and Disaster in Western China, and School of Civil Engineering and Mechanics, Lanzhou University, Lanzhou 730000, China  
e-mail: 754320957@qq.com

G. Sun  
e-mail: sungp@lzu.edu.cn

## 32.2 Overview of Bezeklik Grottoes

Bezeklik grottoes is a famous temple site in western china, and it is located in the west escarpment of Wood Groove and the mountainside of the main peak of Flaming mountains, with the distance of 40 km from the northeast of Turpan city.

Bezeklik Grotto owns the abundant caves and the richest frescoes among the existing grottoes in the Turpan region. Bezeklik Grottoes had gone through the history of Gaochang Period, Tang West-state period and Gaochang Uighur period. After the mid-15th century, the cave temple was scrapped and destroyed in pagan conflict and finally reduced to ruins unattended.

Turpan Basin is a typically continental, temperate and arid desert climate with the characteristic of the scarce rain and dry heat. The Flaming Mountains in the Grotto sites is north-west trend (about  $300^\circ$ ), and wood groove to  $20\text{--}30^\circ$  angle cut through the Flaming Mountains with the intersection to Shengjin ditch. The wind direction is generally from the southeast to the northwest. There is an U-shaped valley with a relative flat, 50–70 m width, 100–110 m height and about 13 % slope, whose sides are substantially straight, with the about 118 m height of debris on the left side of the Flaming mountain. The right bank is alluvial soil cliff (the bottom of soil cliff is the coffee and brown mudstone) and cave is dug in them (seen from Figs. 32.1 and 32.2).

The regional strata is alluvium and diluvium lower-middle Pleistocene ( $Q^{1-2al} + Pl$ ). It mainly distributes on the right bank of Wood Groove with micro stratification and the basic level. Its lower part is gray or pale yellow gravel Stone, and the roundness is sub-angular to sub-rounded with the thickness of 2 m, and it uncomfortably overlay on the Tertiary Shanshan Group ( $E^{sh}$ ) (seen from Fig. 32.2) with about 20 m yellow sandy silt in upper part. The Thousand Buddha Cave was excavated in the silt section.

Bezeklik Grottoes distributes above and below of the west cliff of Wood Groove. It can be divided into four zones (seen from Fig. 32.1). Firstly, caves from No. 1 to No. 7 are located in the northern end of the cliff. Secondly, caves from No. 8 to No. 39 are excavated in the middle of cliff with the fine space and appropriate location where there are the mainly existing caves so far. Thirdly, caves from No. 40 to No. 57, with the poor space and severe dilapidation, are



**Fig. 32.1** Distribution situation of the Bezeklik Grottoes



**Fig. 32.2** The typical stratigraphic section of cliff facade

separated from the second district. Fourthly, caves from No. 58 to No. 83, similar to former caves, are located below the cliff and built with adobe.

## 32.3 The Analysis of the Main Diseases

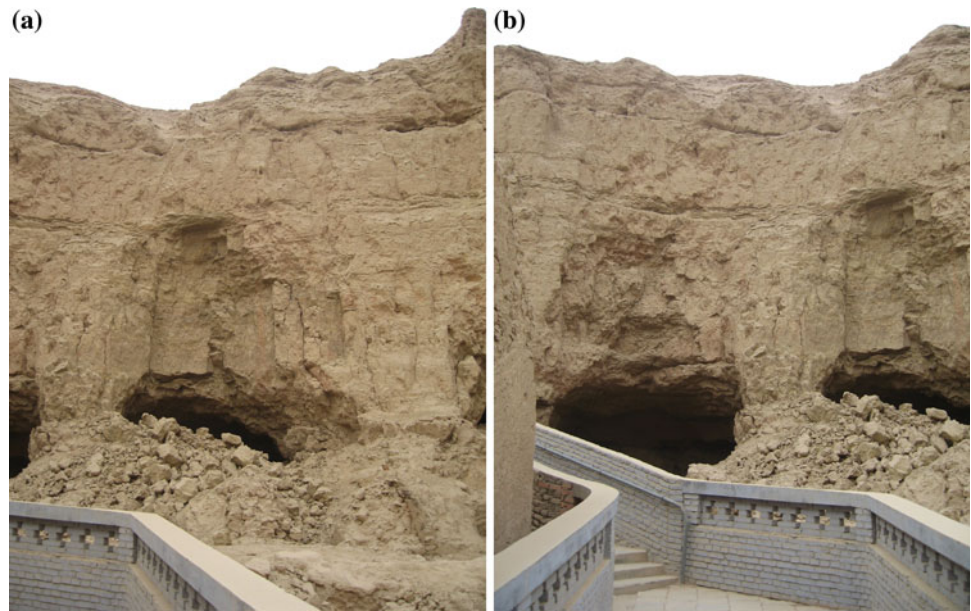
### 32.3.1 The Major Diseases of the Cliff Body

#### 32.3.1.1 The Main Diseases of the Cliff Body

##### (1) Collapse

1. The cliff body in Z1–Z3 caves distribution area  
This section of the cliff body is vertical with a  $60^\circ$  slope on the top. Z1, Z2, Z3 caves is near No. 11, No. 12, No. 13 caves and the visiting channel for tourists. Currently, the caves partly collapsed and led to the partial separation of top cliff body, the deformation and destruction of nearby cliff body, the accumulation of dilapidations in the lower part of the cliff body and the block of cave Z1. As the result of the collapse of the top, the slight suspend of the upper cliff body caused the collapse of the upper cliff body (seen from Fig. 32.3).
2. Cliff body in front of the Caves from No. 37 to No. 39  
The section of the cliff is located in the southernmost part of the current travel footway, and the upper footway flared and deformed due to the early adobe slump, thus which threatens the safety of visitors and the upper cave. Meanwhile, the collapse of adobe made the near slope suspend in the air, deformed and destructed. The unconformities

**Fig. 32.3** The lower part of cliff slump accumulation and cave collapse. **a** the collapse of the upper cliff. **b** the blocked Z2 cave



surface between the quaternary and Tertiary causes the poor slope integrity to easily collapse. Currently, the top of the slope has been suffering the heavy shock from visitors. By investigation, the causes of destruction are the dumping and scattering of the near adobe slope, which led to a further collapse of the upper footway (seen from Figs. 32.4 and 32.5).

(2) Gully

The gullies are mainly developing in the area of caves from No.1 to No.9. This section of cliff body suffers massive collapse, which led to the partial collapse near caves. As a result, the cliff is vertical with a separate block in northern side. There is a large crack parallel to the cliff face with the 1 m distance to the cliff edge. Its opening width is 15–20 cm which causes the inner and

external suspend of outer cliffs, and six large gullies develop on the top with the maximum cutting depth of 2 m. Caves from No. 1 to No. 8 were dug in this section. Therefore, the stability of the cliff body determines the survival of these 8 caves (seen from Figs. 32.6 and 32.7).

(3) Fissures

The fissure in No. 28 cave cliff body is the most typical one with a nearly vertical body in the Quaternary sandy strata. There are five fissures parallel to the cliff face developing inside the cliff body. With the characteristics of 3–5 cm fissure aperture, straight surface, no ups



**Fig. 32.4** The top of the dangerous cliff



**Fig. 32.5** Façade of the dangerous cliff



**Fig. 32.6** Façade of No. 1 dangerous cliff



**Fig. 32.7** Gully slump in the dangerous cliff

and downs, rough walls and the late topsoil filling in the middle, one of which cuts the No. 28 cave completely and forms the channel for rainwater infiltration (seen from Fig. 32.8). The fissures result from unloading of soil mass.

### 32.3.1.2 The Main Diseases of the Caves

The diseases of Bezeklik Grottoes are closely associated to the diseases of the cliff body. After investigations, the major diseases of caves are revealed: (1) cracks are developing among the soil mass and most of them penetrate to the cave and wall painting is destroyed (Fig. 32.9); (2) partial collapse and suspend of the cliff causes the disappear of cave (Fig. 32.10); (3) the fresco is being eroded by the rainwater infiltration due to the collapse of cave roof (Fig. 32.11); (4) Poor drainage of the roof causes rainwater infiltration to pollute the wall painting (Fig. 32.12).



**Fig. 32.8** Facade fissure of the dangerous cliff

### 32.3.2 The Analysis of the Causes of the Diseases

- (1) Flood erosion: Since Bezeklik grottoes is located in the canyon of Wood Goove with the Flaming Mountain, it is suffering the floods erosion for many years. After the bottom part of the cliff collapses, the upper part of the cliff will deform and generate the fissures because of the unloading. Moreover, it is another cause that the long-term water immersion will destroy the structure of soil mass.
- (2) Geological conditions  
In Turpan Basin, the temperature can reach 47 °C in summer and about -15 °C in winter. Meanwhile, frequent gale happens in the district. Both of climate factors will damage the structures of the soil-rock mass of the cliff. On the other side, the soil-rock mass is weak-weathered. As a result, the collapse will happen from the surface of the cliff and the caves will be strengthened.
- (3) Earthquake: the Wood Groove and the Flaming Mountains lie in the fissure of the seismic zone, therefore, the active earth's crust forms lots of large crevices inside the cliff body. These crevices cross the caves, causing the natural collapse of cliff body as a devastating power.
- (4) Winds and rainfall: The Flaming Mountains blocks the wind from the northern Tianshan Mountains. These valleys (including Wood Groove and Tuyu Ditch) were formed by flood erosion at history, which makes wind flowing by the sites. Furthermore, the crushing rock and backward protection facilities make the serious

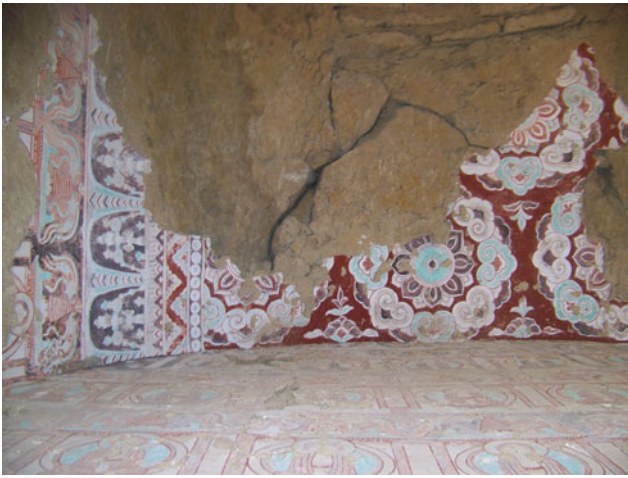


**Fig. 32.9** Tensile fissure at the top of No. 9 cave



**Fig. 32.11** The cave roof collapsed



**Fig. 32.10** The current status of No. 6 cave



**Fig. 32.12** The cave roof rainwater infiltration induced by poor drainage

erosion of the cliff. Besides, the concentration of rainfall creates a great deal of different-degree gullies among the cliff. Finally, the wall painting will be damaged by the rainfall infiltration.

- (5) Human activities: There is a road across the top of the cliff. Along the road, there are a lot of tourism service facilities. Consequently, a variety of vibration, domestic water infiltration and other human activities heavenly strengthened the stability of the cliff and the preservation of the wall painting.

## 32.4 Main Conservation Methods

The methods of cliff conservation include anchorage, fissure filling and grouting, masonry support, top gully remediation, and deformation monitoring. Among them, anchorage and masonry support is supposed to control the mechanical stability of the cliff. The methods of caves conservation include fissure grouting, anchorage, top masonry support and top waterproof remediation.

## 32.5 Conclusions

As a valuable site along the Silk Road, Bezeklik Grottoes has been suffering the collapse, gullies and fissures and other damages. Measures should be taken to conserve the grottoes which also are experiencing fissure, rainwater infiltration, collapse and other damages. Based on results of detailed investigation, the main causes for these damages are revealed. Mechanical stability control measures for cliff body are advised including anchoring, grouting, top-supporting and other measures. The whole process of conservation shall be strictly in accordance with the concept of “dynamic design, information construction”. Rescue conservation engineering

was finished with good effect. The success of the grottoes conservation can be set as an example for other grottoes with same diseases.

---

## References

- Junhui S, Langsheng W, Qinghai W et al (2003) Deformation and fracture features of unloaded rockmass. *Chin J Rock Mech Eng* 22 (12):2028–2031
- Lansheng W, Tianbing L, Qihua Z (1994) Epigenetic time dependent structure and human being project. Geology Publishing House, Beijing
- Ramsay JG (1967) Folding and fracturing of rocks. McGraw Hill, New York

---

Part V

**Geoheritage, Geosites, Geoparks: Contributions  
of the Engineering Geology in the Management  
of Natural and Cultural Landscape**

---

# The Stone Bridges on the Po River at Turin (NW Italy): A Scientific Dissemination Approach for the Development of Urban Geological Heritage

# 33

Giulia Poretti, Alessandro Borghi, Anna d'atri, Giovanna Antonella Dino, Simona Ferrando, Chiara Groppo, Luca Martire, Edoardo Accattino, Sergio Enrico Favero Longo, Rosanna Piervittori, and Franco Rolfo

---

## Abstract

This paper presents a minero-petrographic study of the rocks employed in the building of stone bridges over the Po River in the city of Turin (Piemonte Region—NW of Italy). In all the bridges, the dimension stones are present in different quantities and elements, either representing the only building material or associated with several artificial materials. The total number of bridges on the Po River is six, three of which are made of natural stones (Princess Isabella Bridge, King Umberto I Bridge and King Vittorio Emanuele I Bridge) and three are built with artificial materials with minor dimension stones (Balbis Bridge, Queen Margherita Bridge and Sassi Bridge). The lithologies of the six bridges have been identified in order to find out the corresponding geological units and the original quarry site. The stones mainly consist of rocks from the western Alps, with a prevalence of metamorphic rocks such as gneisses, as well as intrusive igneous rocks. Sedimentary rocks are minor represented.

---

## Keywords

Applied petrography • Geotourism • Geological heritage • Urban geology • Western Alps

---

G. Poretti · A. Borghi (✉) · A. d'atri · G.A. Dino · S. Ferrando · C. Groppo · L. Martire · F. Rolfo  
Dipartimento di Scienze della Terra, Università di Torino, Turin, Italy  
e-mail: alessandro.borghi@unito.it

G. Poretti  
e-mail: giulia.poretti@uniroma1.it

A. d'atri  
e-mail: anna.datri@unito.it

G.A. Dino  
e-mail: giovanna.dino@unito.it

S. Ferrando  
e-mail: simona.ferrando@unito.it

C. Groppo  
e-mail: Chiara.groppo@unito.it

---

L. Martire  
e-mail: luca.martire@unito.it

F. Rolfo  
e-mail: franco.rolfo@unito.it

E. Accattino · S.E.F. Longo · R. Piervittori  
Dipartimento di Scienze della vita e biologia dei sistemi,  
Università di Torino, Turin, Italy  
e-mail: edoardo.accattino@unito.it

S.E.F. Longo  
e-mail: sergio.favero@unito.it

R. Piervittori  
e-mail: rosanna.piervittori@unito.it

### 33.1 Introduction

The Po River rises from the Mount Monviso, runs for 652 km through the northern Italy (W–E direction) and flows in the Adriatic Sea. It is the longest Italian river and one of the most important because it has guaranteed, over the centuries, the development of the cities built on its banks. In particular the Po River has significantly influenced the development of urban and suburban design of Turin.

The purpose of the present work is to characterize the stone materials of the Turin's stone bridges from a petrographic and mineralogical point of view in order to achieve a new conceptual and operational discipline in the management of the geological heritage of the Piemonte Region (NW Italy). In this framework, the knowledge and enhancement of historic ornamental stones of Turin, ancient capital of the Kingdom of Savoy and current chief town of the Piemonte Region, may represent the starting point for a new geotouristic approach for the development of urban geological heritage (Fiora et al. 2002).

### 33.2 Bridges Description

The total number of bridges on the Po River is six, three of which are made of natural stones—King Vittorio Emanuele I Bridge (1803–1813), the Princess Isabella Bridge (1876–1880), the King Umberto I Bridge (1903–1907)—and three are made of artificial materials with minor dimension stones—Balbis Bridge (1926–1927), the Queen Margherita Bridge (1877–1882) and the Sassi Bridge (1926–1927) (Fig. 33.1).

The best evidence of the use of stone in the bridges of Turin is the King Vittorio Emanuele I Bridge, tangible sign of the Napoleonic power, that stands as a prototype for the new supplies of stone buildings in Piemonte. The exclusive use of the *Cumiana Stone* for its construction is documented at the State Archives of Turin. The slabs of the sidewalk, now completely replaced, is made up of blocks of *Balma Syenite* and *Canavese Diorite* for the roadway, whereas both the sidewalks are paved with *Cumiana Stone*.

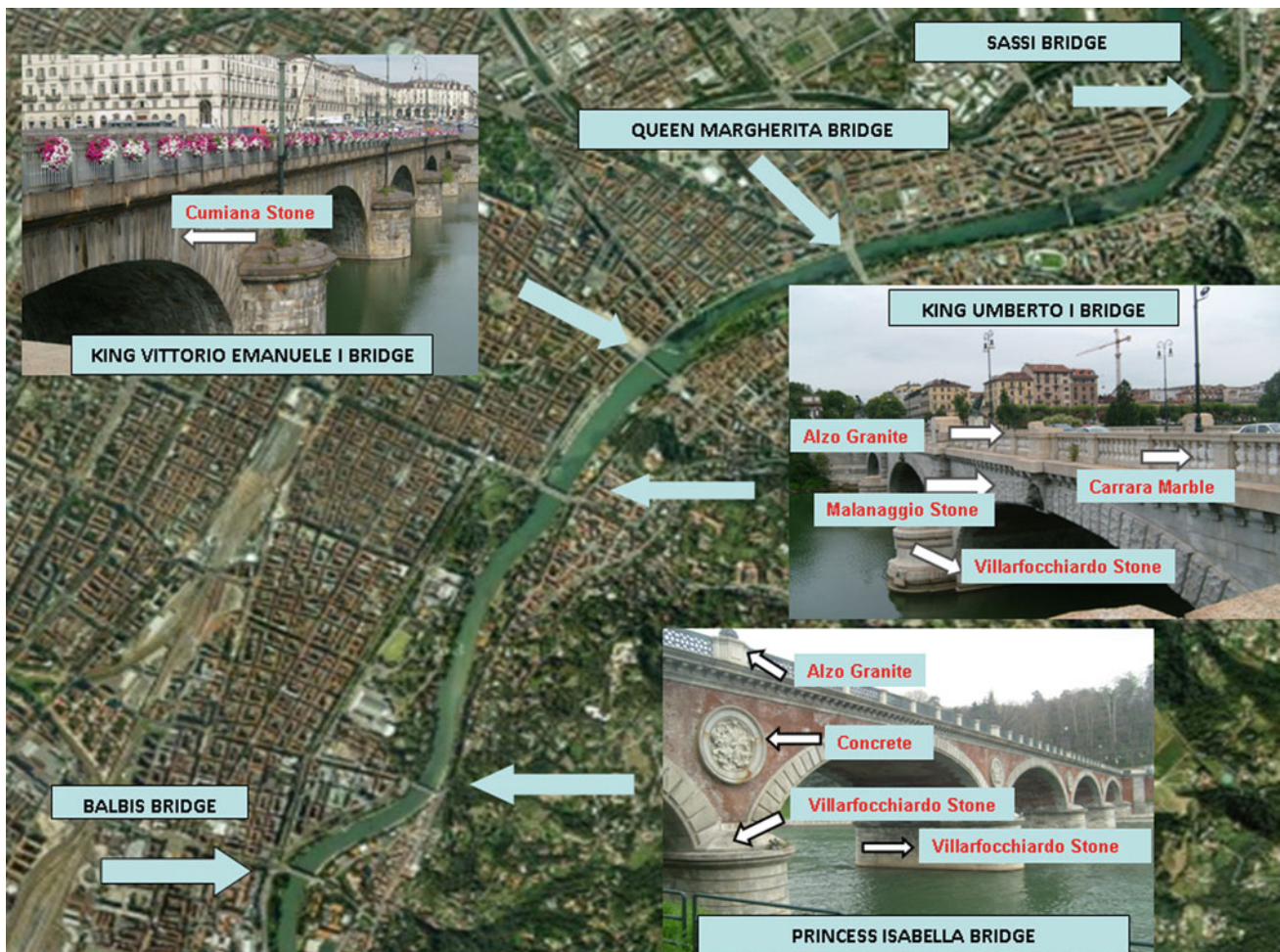


**Fig. 33.1** Satellite toponomastic map of Turin (from Google Earth®, 21/09/2013) with location of the Po River bridges

The construction of the Princess Isabella Bridge started in 1876 and was completed in 1880. This bridge shows five semielliptical arches of 24 m of light made of brick, built on high stacks made of the *Villarfocchiardo Stone*. For the realization of the pillars of the parapet, the *Alzo Granite* was used, which was also employed in the cornices of the rings. The flooring is made of slabs of *Luserna Stone* lined with blocks of *Villarfocchiardo Stone*. The rose windows of the eardrums, formerly made using the *Monte Fenera Sandstone*, are now completely replaced with a more durable material, being the sandstone not so suitable for withstanding the conditions of moisture and exposure to atmospheric agents.

The *Queen Margherita Bridge*, originally built employing brickwork and stone materials from the western Alps (Perino and Faraggiana 2002), in 1972 it was replaced with a new modern structure because of the poor state of conservation and the progressive increase in car traffic.

At the beginning of the twentieth century was built the new monumental King Umberto I Bridge (1903–1907). The structure of the bridge consists of three semielliptical arches built on pillars with semicircular rostrum and made of different Alpine stones, including the *Malanaggio Stone*, the *Villar Focchiardo Stone* and *Vaie Stone*. The decorations and the lining of the fronts, the cornice and frieze are made of *Alzo Granite*, while the pillars of the parapet are made of *white Carrara Marble*. The flooring of the sidewalk is made with slabs of *Malanaggio Stone* lined with blocks of *Alzo Granite*, whereas the roadway for car traffic and tramway was made using blocks of *Balma Syenite*.

Finally (1926–1927), Balbis and Sassi Bridges were made of reinforced concrete structure, with minor dimension stones. In particular, the window sill parapet of Balbis Bridge consists of *Aurisina Stone*, a gray limestone, while the floor of the Sassi Bridge sidewalk is made up of stone slabs consisting of *Cumiana Stone* and *Luserna Stone*.

### 33.3 Analytical Techniques

A minero-petrographic characterization of representative geological samples collected from historical quarries was performed in order to develop, for each ornamental rock used in the Turin bridges, a descriptive form containing all the information useful for their restoration and conservation. Rock samples were analysed using optical microscopy and scanning electron microscopy (Cambridge Stereoscan S360). An EDS (energy-dispersive X-ray spectrometer) equipped with a SDD (a silicon drift detector from Oxford Instruments) was used to determine the composition of the most discriminative minerals. Natural oxides and silicates were acquired as standards.

### 33.4 The Stone Materials

The stones used in the construction of the bridges were mostly exploited in the western Alps; they are mainly metamorphic rocks such as gneisses and intrusive igneous rocks. Sedimentary rocks are minor represented. This emphasizes the close connection between the architectonic and cultural history of Turin and its surrounding environment, strongly influenced by the presence of the Alpine Chain, which represents the source of the building materials employed in the bridges across the last two century.

The most widespread dimension stone is certainly the *Cumiana Stone*, an orthogneiss of Permian age employed in the King Vittorio Emanuele I Bridge. This gneiss belongs to the Dora-Maira Massif (Penninic Domain). It consists of millimetre porphyroclasts of K-feldspar surrounded by a foliated matrix of quartz, white mica, biotite, albite and epidote (Fig. 33.2a).

Another alpine gneiss employed in relevant quantities is the *Malanaggio Stone*, used for the covering of the King Umberto I Bridge. This amphibolic—biotitic orthogneiss of dioritic composition is exploited in the monometamorphic graphite-bearing complex of the Dora-Maira Massif outcropping along the Chisone Valley.

The *Villarfocchiardo Stone*, used in the piers of Princess Isabella Bridge, is exploited in the middle Susa valley. This is a leucocratic white to light greyish orthogneiss, characterized by the presence of tourmaline, which defines a mineralogical lineation (Fig. 33.2b).

The *Luserna Stone* is an orthogneiss quarried in the lower Pellice Valley. It is characterized by magmatic porphyroclasts of K-feldspar wrapped around by a pervasive foliation defined by the iso-orientation of phengite and, in minor amounts, biotite and chlorite. Quartz and albite, partially recrystallized during the Alpine metamorphic event, complete the mineral assemblage. Plates of *Luserna Stone* are present on the sidewalks of all the bridges, except for the King Vittorio Emanuele I Bridge.

The *Vaie Stone* was used only for coating the piers under the arches of the Umberto I Bridge. It is a very durable augen-gneiss quarried in the lower Susa Valley. It consists of K-feldspar porphyroclasts surrounded by a fine grained oriented matrix defined by alternating micaceous layers and albite—quartz domains.

Three magmatic rocks were used for the flooring and the balustrades of the stone bridges. The *Alzo White Granite* is an olleucocratic monzogranite of Permian age belonging to the Southalpine Domain, and outcropping on the western shore of the Orta Lake (Fig. 33.2c). It has been observed in the balustrades of the Princess Isabella and the King Umberto I bridges.

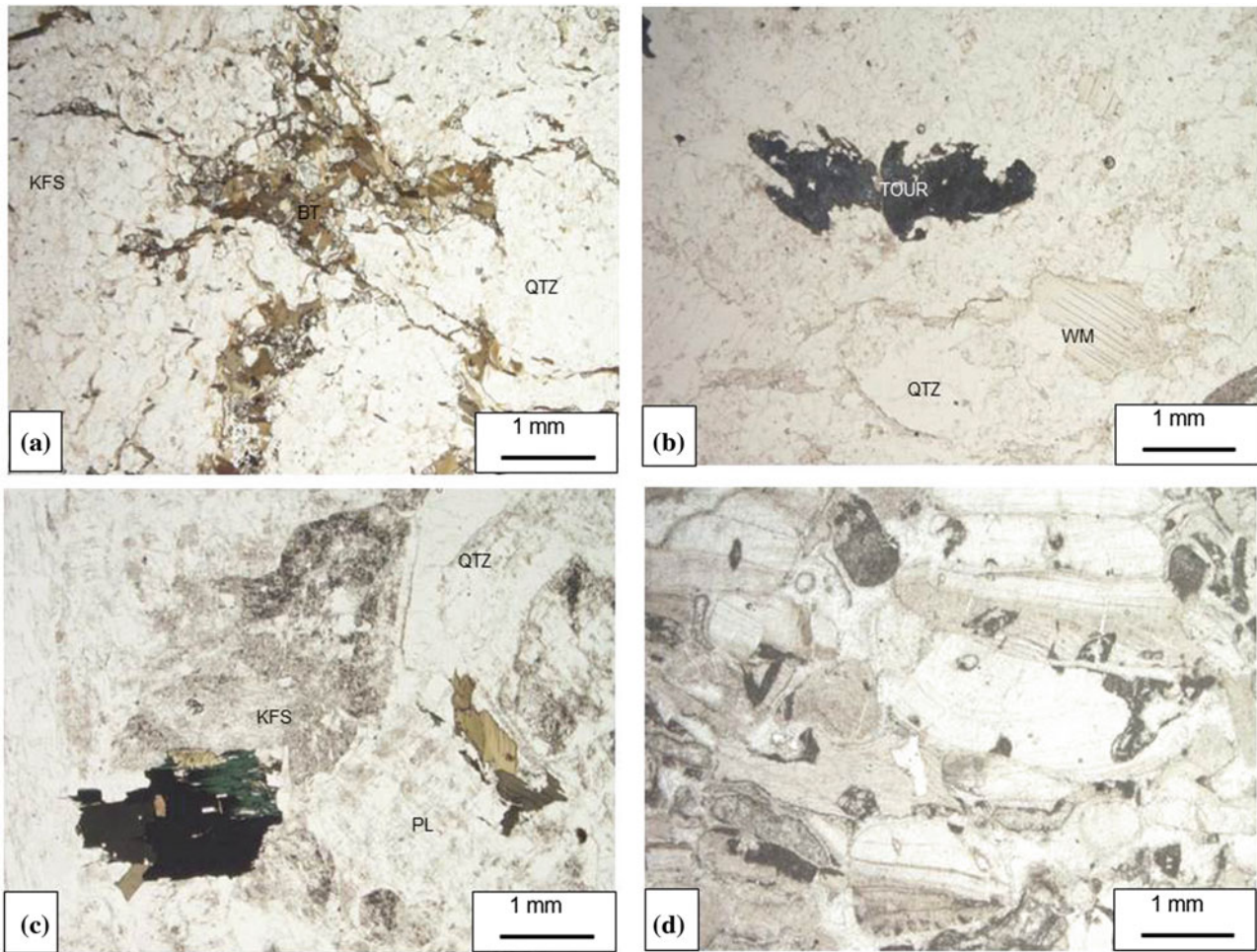


**Fig. 33.2** Representative optical microscope images (plane polarized light) of the main ornamental stones employed in the bridge buildings. **a** Cumiana Stone; **b** Villarfochiardo Stone; **c** Alzo Granite; **d** Aurisina. Mineral symbols according to Kretz (1983)

The *Balma Syenite* and *Canavese Diorite*, exploited from two small post-metamorphic intrusive bodies of Oligocene age, intruded in the metamorphic rocks of the Sesia-Lanzo Zone and outcropping along the Cervo Valley and Chiusella Valley, respectively. The *Balma Syenite* shows a typical grey-violet colour and a medium-grained size. Its mineralogical composition consists of K-feldspar, violet on the hand sample, minor amounts of plagioclase and very rare quartz. Amphibole and biotite occur among the femic minerals. The *Canavese Diorite* shows a granular texture and varies in colour from light gray to very dark depending on the grain size and on the percentage of femic minerals, represented by amphibole, biotite and rare pyroxene. They were used for the roadway of the King Vittorio Emanuele I and the King Umberto I bridges.

Some decorative elements of the bridges are made of sedimentary rocks. The sill of the balustrade of the Sassi Bridge is formed by blocks of *Aurisina stone*, a bioclastic limestone of Late Cretaceous age characterized by rudist bioclasts (Fig. 33.2d). It outcrops in the Friuli Platform

(Carso). The *Monte Fenera Sandstone*, a red Lower Jurassic sandstone from NE Piemonte, originally used for decorative purposes in the Isabella Princess Bridge, has been replaced by concrete because of degradation.

### 33.5 Discussion and Conclusions

To boost the fruition of the information about stone materials employed in Turin buildings and infrastructures, such as stone bridges, a widespread dissemination has to be enhanced.

Therefore, knowledge of stone resources, their mineral-petrographic features, their use and quarrying techniques from antiquity to the present, can provide a broad overview of the historical and cultural significance of these materials, stressing the importance of a relevant economic activity in the history and traditions of different cultures that followed over the centuries in the Mediterranean area.

The present study is part of a wider research project (PROGEO—Piemonte) which aims to create a comprehensive Knowledge Management Software Platform for the integrated, effective, and efficient management of such data to support understanding of cultural values, valuation, interpretation, ethics, and identity around all forms of cultural heritage (Giardino 2012). One of the steps of the dissemination process is the design and realization of a specific catalogue of natural stones used in the different areas of the Western Alps (e.g. significant stones employed in Turin bridges). This catalogue is aimed to recording: the full name of the stone (commercial and scientific), the location of the quarry site, the main applications in buildings and monuments, the macroscopic and microscopic description illustrated by extensive iconographic material. The main emphasis will be given to the stone types used for external installation as easily seen during touristic city tours.

The other step is to create a Knowledge Base of “linked open data” by integrating existing catalogue information with multimedia data, such as pictures of stones in different employment, degradation stages, etc.

In conclusion, the tour of Turin Stone Bridges will be part of a set of possible Geotouristic paths provided by “Museo Torino”, a virtual network of the main museums of the city, managed by the Municipality of Turin. It represents a cultural tourist route that will concur to the development of the heritage of the “stone-town”.

---

## References

- Fiora L, Alciati L, Borghi A, Callegari G, Derossi A (2002) Pietre piemontesi storiche e contemporanee. *L'informatore del marmista* 489:50–59
- Giardino M (2012) Progeo-Piemonte: a multidisciplinary research project for developing a proactive management of geological heritage in the Piemonte region. *Geologia dell'ambiente* 3:196–197
- Kretz R (1983) Symbols for rock-forming minerals. *Am Mineral* 68:277–279
- Perino AS, Faraggiana G (2002) *I ponti di Torino*. Ed. del Capricorno, Torino

Irene Bollati, Paola Coratza, Marco Giardino, Lamberto Laureti, Giovanni Leonelli, Mario Panizza, Valeria Panizza, Manuela Pelfini, Sandra Piacente, Alessia Pica, Filippo Russo, and Andrea Zerboni

---

## Abstract

In recent years, more and more attention has been focused on geological and geomorphological heritage. This has led to several investigations within the framework of conservation projects, both at administrative and scientific levels, involving national and international research groups whose purposes are the promotion of Earth Sciences knowledge and the conservation of geological heritage. This paper presents an overview of research and conservation projects in Italy, focusing mainly on geomorphological heritage. Members of the AIGeo Working Group on “Geomorphosites and cultural landscape” analysed the historical development of these research projects in order to identify possible innovation strategies to improve the awareness and knowledge of geodiversity and geoheritage of a wider public.

---

## Keywords

Italy • Geoheritage • Geomorphosites • Geotourism • Geodiversity

---

I. Bollati · G. Leonelli · M. Pelfini · A. Zerboni  
Dipartimento Di Scienze Della Terra “a. Desio”, Università Degli Studi Di Milano, Milan, Italy

P. Coratza · M. Panizza · S. Piacente  
Dipartimento Di Scienze Chimiche E Geologiche, Università Degli Studi Di Modena E Reggio Emilia, Modena, Italy

M. Giardino  
Dipartimento Di Scienze Della Terra, Università Degli Studi Di Torino, Turin, Italy

L. Laureti  
Dipartimento Di Scienze Della Terra E Dell’Ambiente, Università Degli Studi Di Pavia, Pavia, Italy

V. Panizza (✉)  
Dipartimento Di Storia, Scienze Dell’Uomo E Della Formazione, Università Degli Studi Di Sassari, Sassari, Italy  
e-mail: valeria@uniss.it

A. Pica  
Dipartimento Di Scienze Della Terra, Università Degli Studi Di Roma “La Sapienza”, Rome, Italy

F. Russo  
Dipartimento Di Scienze E Tecnologie, Università Degli Studi Del Sannio, Benevento, Italy

---

## 34.1 Historical Development

The attention of researchers has focused primarily on the inventory and assessment of sites of geological and particularly geomorphological interest—Geosites—in order to emphasise not only their scientific values but also their cultural and landscape contexts, as a support for particular biological and historic-architectonic assets. Researchers from various Italian Universities were involved in national and international projects. Within these projects, a common methodological approach for the survey, selection, cataloguing, assessment and appraisal of Geomorphological Sites was set up. This method was compared at an international level and tested in different areas.

The term “Geomorphosite”, introduced by Panizza 2001, synthesizes the interest for the heritage value of geomorphology and its relationships with human heritage. The complex and often close connection that can exist between Geoheritage, human history and cultural heritage, led to several scientific initiatives both at international and national level. Increasing interest in geomorphological heritage has inspired diverse projects, often in collaboration with the

local administrations. The recent inclusion of the Dolomites in the UNESCO World Heritage list is one of the main results of research on geomorphological heritage assessment and a new approach in geodiversity studies.

### 34.2 Research Lines and Methodological Issue

At an international level, many Italian researchers have been involved in studies carried out by the Working Group “Geomorphological sites” of the International Association of Geomorphologists (IAG). The Working Group was created during the 5th International Conference on Geomorphology held in Tokyo in 2001 with the aim to improve knowledge and scientific research on the definition, assessment, mapping, promotion and conservation of geomorphological heritage. During these 12 years of activities many improvements in the field of Geomorphosite research have been achieved (Reynard and Coratza 2013); nevertheless, several questions have not yet been solved and should be addressed in the future. In particular the WG decided to focus its future activities on the following new themes: (1) geomorphosites as key sites for environmental education; (2) the study of dynamic and sensitive geomorphosites; (3) the relationships between geoheritage and geodiversity.

The latter issue will be addressed in collaboration with the new WG “Geodiversity”.

In Italy numerous projects of research have been implemented and are under development:

- Improvements in field data collection and visual representation of landforms have led to new elements in geomorphological mapping (Carton et al. 2005; Coratza and Regolini-Bissig 2009). Applications of these new methodologies were improved by several research units. Among these, interesting proposals have been carried out by La Sapienza University of Rome, concerning geosite inventory in urban areas, also for urban geotourism proposals (Del Monte et al. 2013). Previous studies in the city of Rome have allowed geomorphosites, still recognizable in an intensely urbanized context, to be properly appraised. In order to disseminate scientific knowledge a geosite evaluation model has been developed. A further step concerns the implementation of a map containing essential scientific and cultural information (Fig. 34.1). The long tradition of geoheritage assessment carried out by Modena University researchers has dealt with the development of methodologies and tools for assessing the relationships between physical landscapes and quality of the environment (Panizza and Piacente 2003; Coratza and Giusti 2005; Piacente and Coratza 2005). This has led to the elaboration of applied methodologies dedicated

to facing problems concerning the transfer of scientific knowledge to end-users or local communities. Several geotourism initiatives have been carried out following agreements with local boards (Coratza et al. 2004; Castaldini et al. 2011).

- Geomorphological and geological heritage is analysed with a special focus on its relationships with cultural landscape and human history. With this aim, the Sannio University research unit focuses its studies on the relationships between the geological and geomorphological heritage of Irpinia and its historical and cultural landscape (Cartoian et al. 2011). Here geology and geomorphology interacted strongly with the social, economic and religious life of the local population. The willingness of the population to recover the landscapes of their memories has led to a profitable appraisal and clever promotion of the local geosites through the offer of naturalistic and cultural itineraries (Russo and Sisto 2012).
- Researches have been carried out on monitoring evolution rates of active geomorphosites in different morpho-climatic contexts (Reynard 2004), in order to evaluate risk scenarios in the context of tourism. The research group of Milan University has been working on active geomorphosites and variations of geomorphological processes: it is fundamental for forecasting evolutionary scenarios, especially regarding hazards and impacts on natural and cultural assets. The problem of dealing with active geomorphosites is twofold (Fig. 34.2): (a) changes in geomorphological processes may directly influence the value of sites of geomorphological interest; (b) active geomorphological processes may represent natural hazards and be a source of risk where tourist trails are present. Researches on active geomorphosites are in progress. Educational exemplarity and accessibility of active geomorphosites under investigation will allow the research results to be disseminated to the general public, with a further application for education regarding risk. For this reason, a methodology for mapping the hazards along tourist trails in relation to geotourism has been proposed for various sites of the Alps (Pelfini et al. 2009; Bollati et al. 2013).

Within the framework of assessing geomorphosites and their tourism potential, a new field of research is being carried out by the Sassari research unit, focusing on sites used for outdoor activities like free climbing or canyoning, or for active tourism in general. In particular, concerning climbing, a method of assessment was designed and tested on a number of important Italian climbing sites. As is often the case of leisure sports activities, the geomorphological resource is often the main motivation for destination choice. It is therefore advisable not to ignore the possible risks linked to the

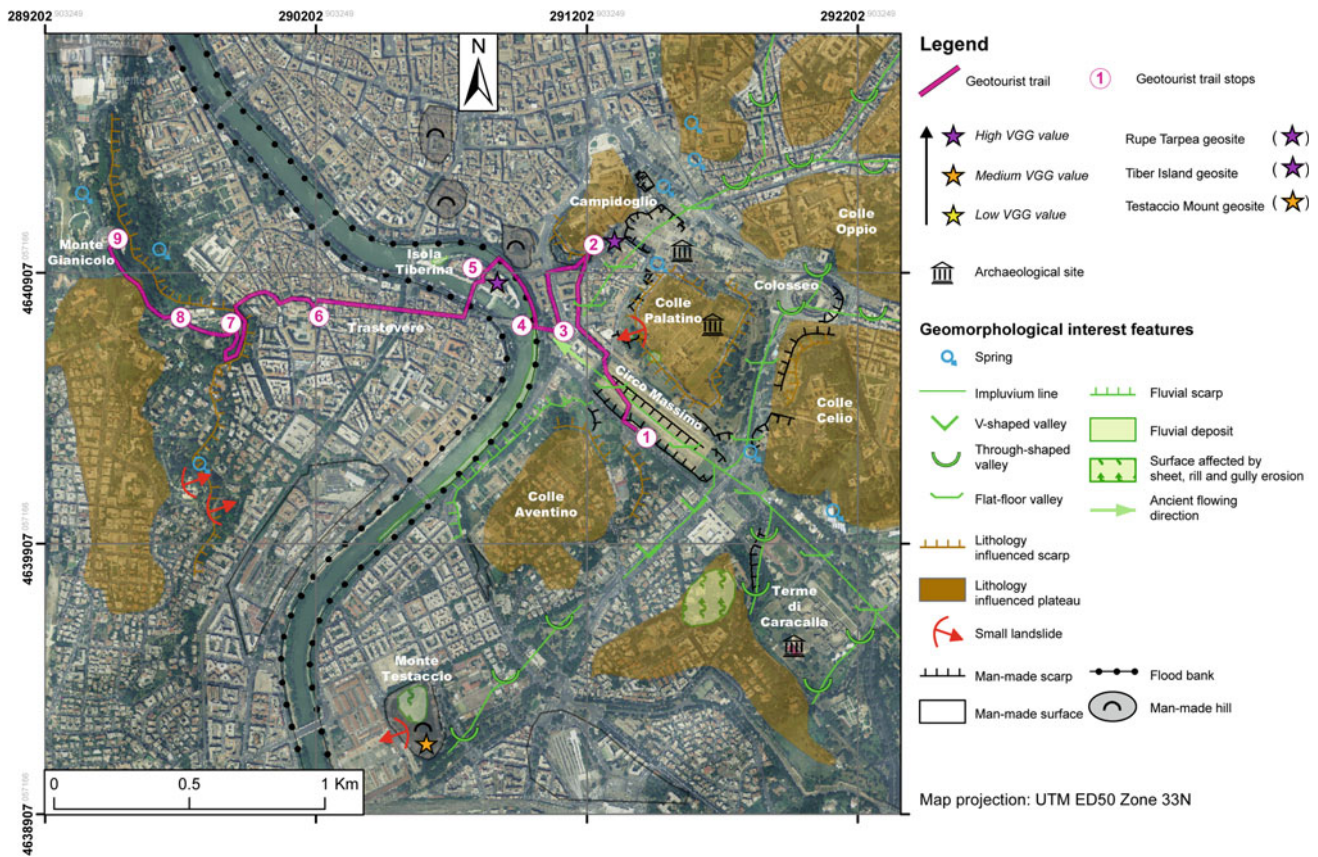
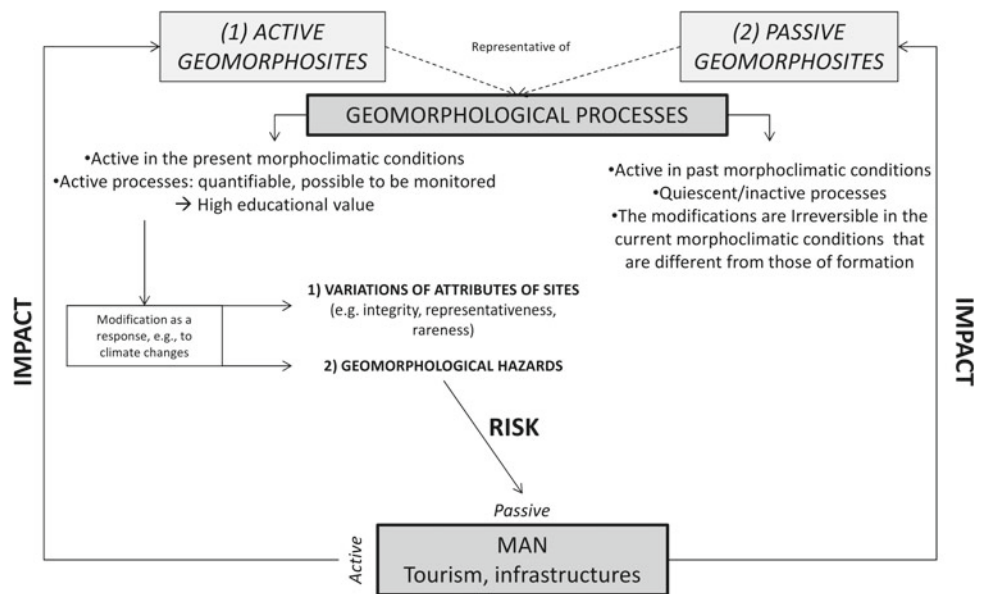


Fig. 34.1 Geotourism map of Rome city centre. Only the essential scientific information is shown on the map

Fig. 34.2 Typologies of geomorphosites according to their activity in present morphoclimatic conditions



dynamic nature of the environment in which these activities take place (Panizza and Manca 2006; Panizza and Mennella 2007).

- In order to provide a bridge between cultural heritage and potential geoheritage, a geoarchaeological approach is

suggested by the geoarchaeologists working unit from Milan University. From the methodological viewpoint, the geomorphologist/geoarchaeologist is asked to accomplish the geomorphological survey of an area where an archaeological/historical site is located (Panizza

and Piacente 2003). Integrated fruition of cultural and geomorphological heritage can be suggested by the creation of geo-archaeological pathways which may help users to understand the complexity of the geological landscape surrounding an archaeological/historical site and the ways in which humans and the environment have interacted in the past. A further step should be taken concerning the preservation of cultural heritage when considering active geomorphosites. In fact, in dynamic geomorphological contexts cultural heritage may suffer heavy threats and even complete destruction: various ongoing projects concerning the simultaneous enhancement of cultural and geomorphological heritage have been developed in diverse Italian and African regions (Biagetti et al. 2013). In the arid environment of North Africa, studies aim to combine the archaeological evidence with geomorphosites, in order to provide a way of increasing the tourist potential of the region, and to select areas that could be proposed for conversion into natural parks.

- Relationships between geomorphological heritage and parks are undergoing comprehensive development, including the proposal of interdisciplinary attractions such as geoarchaeological parks, mining and other georesources theme parks. The research unit of Pavia University, for instance, focused its studies on mining heritage. The persistence over time of mining villages and mining plants is a significant example of the influence of mining activities on land use and the natural landscape. As mining sites are abandoned, they deteriorate rapidly and are subject to recolonization by natural elements. Over the past two decades in some European countries, including Italy, the recovery of old mines has become more frequent, both in the Alps and in other regions (Laureti 2011). The results of investigations carried out on abandoned and deactivated mines in the provinces of Lecco, Bergamo and Brescia, led to the Lombardy Region issuing a law in 2009, which sets out the rules for the recovery and reuse of old mines.
- The social role of geological and geomorphological studies, according to a modern “geoethical vision” of the application of Science. The “Section on Geoethics and Geological Culture” was established in 2013 as a branch of the Italian Geological Society, thanks to experiences within the framework of the Italian Commission on Geoethics and to the contributions of individual researchers. It is also the Italian representative of the IAPG—International Association for Promoting Geoethics. The section provides a scientific and multidisciplinary platform aiming to promote debates on ethical problems applied to Geosciences, as well as studying and deliberating on the values of geological culture (Matteucci et al. 2012). By means of a systemic and functional approach, research can be developed towards a cultural type of geology capable of reconstructing the “historical map” of specific sites. In this way the “geological site” becomes the “place” above all others. Thus, one of the main goals of our disciplines is achieved: the implementation of “Social Geology” able to respond to the needs of the general public and increase the level of knowledge and responsibility at the same time (Panizza and Piacente 2003).
- With particular reference to Geomorphology, Panizza (2009) introduced the concept of Geomorphodiversity: “the critical and specific assessment of the geological features of a territory, by comparing them in a way both extrinsic and intrinsic and taking into account the level of their scientific quality, the scale of investigation and the purpose of the research”. A discussion about Geodiversity should start off from these grounds and remarks, also in order to avoid conceptual misunderstandings or drifting away towards fruitless schematizations.

### 34.3 New Directions

Although studies on geomorphological heritage share the same conceptual foundations and have common development stages, the various research groups followed several methodological approaches and lines of development. This diversity is in part due to the multiplicity of geographical contexts and application areas of research. In one sentence we can say this is part of the high geodiversity of Italy.

Many innovative themes can be outlined for the next developments in geoheritage assessment, geoconservation issues and geotourism activities including:

### References

- Biagetti S, Cancellieri E, Cremaschi M, Gauthier C, Gauthier Y, Zerboni A, Gallinaro G (2013) The Messak Project. Archaeology research for cultural heritage management in SW Libya. *J Afr Archaeol* 11:55–74
- Bollati I, Smiraglia C, Pelfini M (2013) Assessment and selection of geomorphosites and trails in the Miage Glacier Area (Western Italian Alps). *Environ Manage* 51:951–967 (Springer, New York)
- Cartoian E, Di Lisio A, Ferretta C, Magliulo P, Russo F, Sisto M, Valente A (2011) Esempi di aree di interesse geoturistico nel territorio Irpino-Sannita (Campania). In: Bentivenga M (ed) *Geologia dell’Ambiente, SIGEA Suppl. al n. 2/2011, Atti del Conv. Naz. Il patrimonio geologico: una risorsa da proteggere e valorizzare*, pp 388–400
- Carton A, Coratza P, Marchetti M (2005) Guidelines for geomorphological sites mapping: examples from Italy. *Géomorphol Relief Process Environ* 3:209–218
- Castaldini D, Conventi M, Coratza P, Dallai D, Liberatoscioli E, Sala L, Buldrini F (2011) *Carta Turistico-Ambientale della Riserva Naturale Regionale delle Salse di Nirano*. Fiorano Modenese, Tipolitografia Notizie, Modena

- Coratza P, Marchetti M, Panizza M (2004) Itinerari Geologici-Geomorfologici. N. 1 Passo Gardena-Crespeina-Colfosco; N. 2 Corvara-Vallon-Corvara; N. 3 La Villa-Gardenaccia-Val de Juel-La Villa. Fotoriva, Alleghe
- Coratza P, Giusti C (2005) Methodological proposal for the assessment of the scientific quality of geomorphosites. In: Piacente P, Coratza C (eds) Geomorphological sites and geodiversity. *Il Quaternario*, vol 18, issue 1, pp 305–311
- Coratza P, Regolini-Bissig G (2009) Methods for mapping geomorphosites. In: Reynard E, Coratza P, Regolini-Bissig G (eds) *geomorphosites*. München, Pfeil-Verlag, pp 89–103
- Del Monte M, Fredi P, Pica A, Vergari F (2013) A geotourist itinerary within Rome city center (Italy): a mixture of cultural and geomorphological heritage. *Geografia Fisica e Dinamica Quaternaria* 36(2):241–257
- Laureti L (2011) Le miniere abbandonate e dismesse della regione Lombardia. Loro recupero e valorizzazione. VII Conv. Naz. di Speleologia in cavità artificiali, Urbino 2010, Opera Ipogea, XIII(1–2):177–186
- Matteucci G, Gosso G, Peppoloni S, Piacente S, Wasowski J (2012) A hippocratic oath for geologists? *Ann Geophys* 55 (3):365–369
- Panizza M (2001) Geomorphosites: concepts, methods and examples of geomorphological survey. *Chin Sci Bull* 46:4–6
- Panizza M (2009) The geomorphodiversity of the dolomites (Italy): a key of geoheritage assessment. *Geoheritage* 1:33–42
- Panizza M, Piacente S (2003) *Geomorfologia culturale*. Pitagora Editrice, Bologna
- Panizza V, Manca P (2006) Morfologie di erosione fluviale e fruizione turistica. Un esempio nella Sardegna centro-orientale. *Rivista Geografica Italiana*, Firenze 113:527–547
- Panizza V, Mennella M (2007) Assessing geomorphosites used for rock climbing. the example of Monteleone Roccadoria (Sardinia, Italy). *Geogr Helvetica* 3:181–191
- Pelfini M, Brandolini P, Carton A, Piccazzo M (2009) Geotourist trails: a geomorphological risk-impact analysis. In: Reynard E, Coratza P, Regolini-Bissig G (eds) *Geomorphosites*. München, Pfeil-Verlag, pp 131–144
- Reynard E, Coratza P (2013) Scientific research on Geomorphosites. A review of the activities of the IAG working group on geomorphosites over the last twelve years. *Geografia Fisica e Dinamica Quaternaria* 36:159–168
- Reynard E (2004) Geotopes, Géo(morpho)sites et paysages géomorphologiques. In: Reynard E, Pralong JP (eds) *Paysage géomorphologiques*. Acts Séminaire 3<sup>e</sup> cycle, Univ. Lausanne, Instit. Géogr., Travaux et Recherches, vol 27, pp 124–36
- Russo F, Sisto M (2012) Valorisation culturelle et économique d'un territoire marginal à travers le tourisme: le cas de l'Irpinia (Campanie, Italie)". In: Giusti C (ed) *Géomorphosites 2009: imagerie, inventaire, mise en valeur et vulgarisation du patrimoine géomorphologique*. Actes Coll. Intern. Paris, 10–12 June 2009, pp 287–293

# Endangered Geoheritage in Bangladesh: A Case Study of Eocene Sylhet Limestone and Adjoining Areas, Jaflong, Sylhet

Ismail Hossain and Mowsumi Nahar

## Abstract

The Eocene Sylhet Limestone is highly endangered outcrops exposed only in the eastern bank of the Dauki River, Jaflong, Bangladesh. These outcrops and associated stratigraphic units have enormous geo-scientific and educational contents. So, the present study deals with the characterization, identification and evaluation of Jaflong Eocene Sylhet Limestone along with surrounding areas as a geoheritage. Characteristics of the calcitic-rich limestone indicate low energy shallow marine depositional condition. This limestone (48–50 Ma) also includes an abundant and diverse larger foraminifer assemblage and genera, a sparse diverse ostracode assemblage and a very rich, diversified dasycladalean algal assemblage. The foraminifer assemblage has zoogeographic affinities with Eocene Tethys and Indopacific assemblages. Overall evaluations provide score as Rank III of an open system of qualification of the geological heritage content as of its regional importance and the indicial, symbolic, documental and scenic types of abstract perception. Results and level of rank from different quantitative and qualitative assessment also provide excellent geoheritage category. However, the main entity, Eocene Sylhet Limestone of the area is in extremely vulnerable conditions, which recommend strong justification to grant protection at the level of geoheritage as well as geopark and it is so much important to make legal base for conservation.

## Keywords

Geoheritage • Sylhet limestone • Jaflong • Geopark • Geoconservation

## 35.1 Introduction

Jaflong is a spectacular scenic beauty and second largest tourist gathering (after Cox's bazar sea beach) in Bangladesh due to its picturesque exquisiteness with nearby tea gardens, waterfalls and also amazing cascade shape housing structure in Dauki city, southern fringe of Shillong Plateau, Meghalaya, India. The Eocene Sylhet Limestone succession exposed within the Dauki Fault zone in Bangladesh, just few

hundred meters from the Dauki city, Meghalaya. The limestone consists of a number of extensively faulted blocks of both crystalline and fossiliferous limestone, which is vastly Nummulitic-rich with abundant and diverse larger foraminifer assemblage and a sparse diversity of ostracode assemblage (Brouwers et al. 1992). The Sylhet Limestone stage was first named by Evans (1932) and later the term Sylhet Limestone was first used by Khan (1963) for limestone deposits in the area of Sylhet, Bangladesh. This oldest outcrop is now much endangered exposure having enormous geological significance for its larger foraminifer assemblage and the oldest Formation in this region. So, the scientific, intrinsic, economic, research, educational, functional and cultural or aesthetic values of Jaflong Eocene Sylhet Limestone and adjoining areas have the theoretical and practical

I. Hossain (✉) · M. Nahar  
Department of Geology and Mining, University of Rajshahi,  
Rajshahi, 6205 Bangladesh  
e-mail: ismail\_gm@ru.ac.bd

significance for student and researcher. Accordingly, it is an important opportunity to establish exposed Jaflong Eocene Sylhet Limestone and adjoining areas as a geological heritage and a geopark. The study area (Fig. 35.1a) is tectonically within the Sylhet trough, a sub-basin of the Bengal Basin in NE Bangladesh, developed in response to interaction of the emerging Shillong Plateau to the north and the prograding mobile Indo-Burman Fold Belt to the east. Stratigraphically, the sedimentary sequence of the area has been subdivided into Sylhet Limestone, Kopili Shale, Barail Sandstones and Dihing Formations consisting of a sequence from Eocene Sylhet Limestone to Recent Alluvium based on their lithological variations, sedimentary structures and depositional breaks of the sequence.

The aims of the study are to demonstrate visual significance of outcrops or areas, to evaluate the importance of the outcrops and the surrounding area, and call attention to make legal base for conservation of the exceptionally significant

geoscientific features. In this context, the present study involves the detailed investigations of Sylhet Limestone, including the petrogenetic processes of the rocks, types of microfossils and origin of faunas that took place during their origin in the Eocene and throughout their subsequent evolution until the Oligocene. Moreover, the geomorphological/ tectonic features of the areas are carefully evaluated for their aesthetic or scenic values. Diverse and rare geological objects of the area demand appeal to conserve those phases.

### 35.2 Characteristics of Sylhet Limestone

#### 35.2.1 Geochemistry

The standard chemical analyses of the samples and their chemical compositions were determined by Energy-Dispersive X-ray Fluorescence spectrometer at the Central

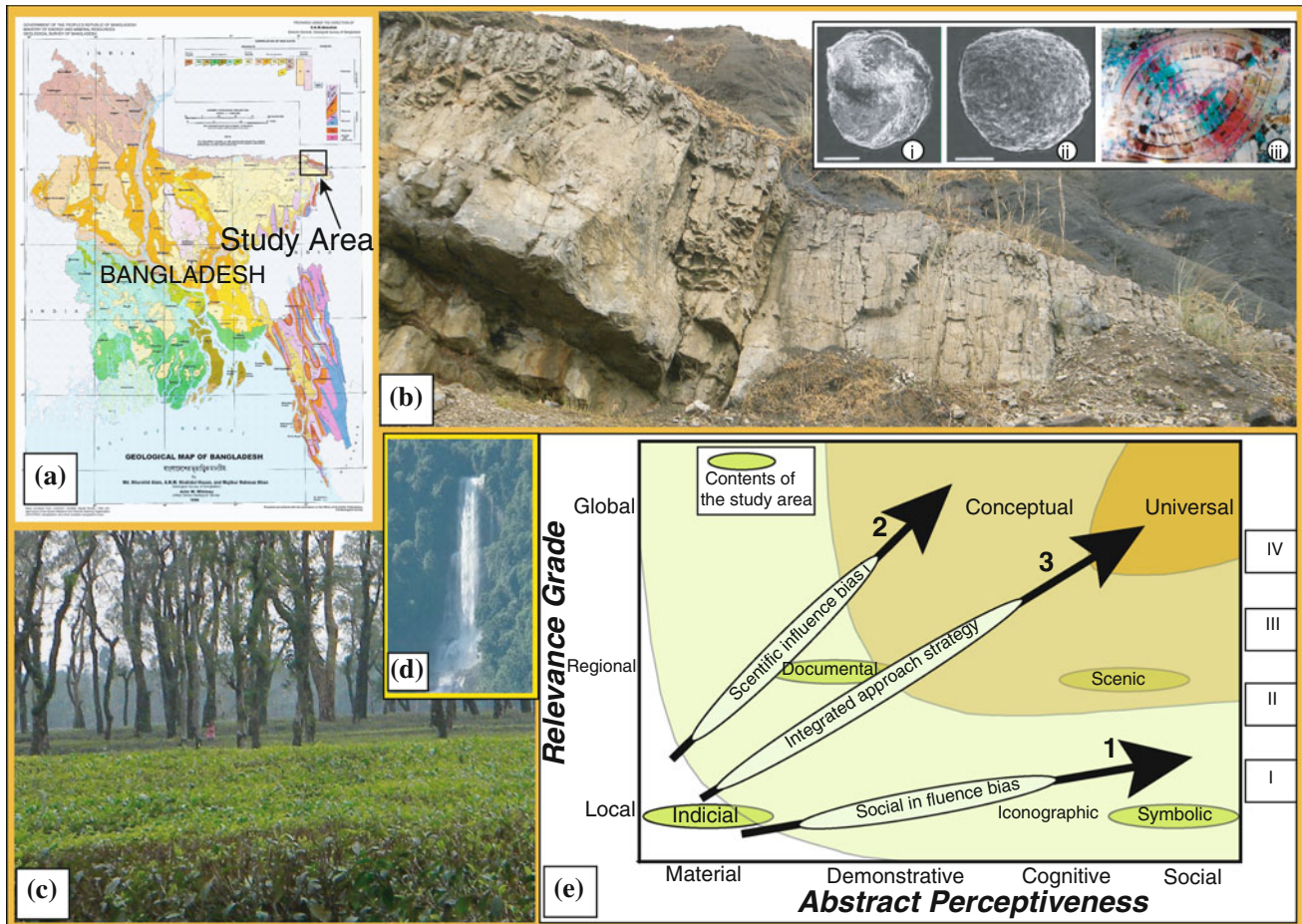


**Fig. 35.1** a Geological map of Bangladesh showing location of the study area. b Exposed endangered Eocene Sylhet Limestone (inset i. *Parafissurina sp.*, ii. *Cibicides sp.*, iii. *Nummulite* microphotograph), c Green carpet of tea garden, Jaflong, d A waterfall in the flank of the

Shillong Plateau, India, photograph taken from Tamabil area, Bangladesh, and e Applications of evaluation systems for the present geosite as a geological heritage indicate Rank III according to Reis and Henriques (2009)

laboratory, University of Rajshahi. Eocene Sylhet Limestone is dominantly calcite-rich carbonate rocks, which contains on average 64 wt% of CaO. The result of the major elemental analyses indicates that Ca concentration ranges between 32 and 61 wt% with mean value of 46.5 wt%. The silicon (Si) contents range between 1 and 6 wt% (av. 3.5 wt%), Fe between 0.3 and 6.6 wt% (av. 3.45 wt%), and Al between 0.5 and 2 wt% (av. 1.25 wt%).

### 35.2.2 Microfossils of Sylhet Limestone

The Eocene Sylhet Limestone (Fig. 35.1b) contains abundant microfossil faunas, dominantly *Nummulites* and diverse larger foraminifer assemblages including *Assilina*, *Discocyclina* and *Alveolina* with low diversity ostracode assemblage. Major benthic foraminifer taxa are *Nummulites pengaronensis*, *N. beaumonti*, *N. acutus*, *Discocyclina dispansa*, *D. undulate*, *D. sowerbi*, *Alveolina glubula*, *Assilina papillata*, *Anomalina sp.*, *Cibidoides perlucidus*, *Cibicides rakhienensis*, *Parafissurina sp.*, *Pellatispira glabra*, *P. inflata*, *P. irregularis*, *Peneroplis sp.*, *Quinqueloculina acuta* and *Q. sawaensis* (Brouwers et al. 1992). The Sylhet Limestone Formation in India also discover a very rich and diversified dasycladalean algal assemblage, include eleven species of the dasycladalean algae belonging to the three families *Dasycladaceae*, *Triploporaceae* and *Acetabulariaceae* (Humane et al. 2010). The highly Nummulitic Limestone was a consequence of an extensive marine transgression that ranged over most of the Bengal-Assam shelves. The algal assemblage suggests their luxuriant growth in the open lagoonal to shelf environment in the warm waters.

### 35.3 Area Characterization

Jaflong is situated in Tertiary hilly region around the lap of Hill Khasia, green flank of Shillong Plateau. Geomorphologically the area lies in the Meghalaya piedmont depression or Meghalaya foothills at international border between Bangladesh and India. The area presents rough and rugged topography including hillocks of different height and size, with numerous gullies, cliffs, number of stream channels and immediately lower regions have subsequent ox-bow lakes and swamps. There are luxuriant tea gardens (Fig. 35.1c) in the area. Tamabil is also located at the border with India, 2 km from Jaflong, a spectacular glimpse on the hill slope of Shillong Plateau characterized by beautiful waterfalls (Fig. 35.1d). Jaintia Rajbari (palace of king), adjacent to Jaintia Bazar, about 7 km from Jaflong, is a very significant archeological site in this region, because it was the capital of Jaintia Kingdom from 1680 to 1835. The most visible features of the palace are a partly destroyed entrance with

fabulous Mughal influenced architecture and a small temple. A huge number of tourists visit this place due to the historical background of Jaintia Kingdom. The Sylhet city is also described as a City of Saints.

### 35.4 Discussion and Conclusions

The present endangered entity and area have carefully been evaluated based on the methodology of Reis and Henriques (2009), whereas, quantitative and qualitative assessment of the geoheritage are followed from Lima et al. (2010), Mansur and Carvalho (2011) and Bruschi et al. (2011). Endangered outcrops of the Eocene Sylhet Limestone with associated stratigraphic units and adjoining areas have enormous geo-scientific and educational contents. Geochemical characteristics suggest that limestone is a high quality calcite-rich and general observation indicates that limestone was deposited in a shallow marine environment. This limestone (48–50 Ma) contains abundant microfossil faunas including larger foraminifer assemblage (*Nummulites*, *Discocyclina*, *Alveolina*, *Operculina*, *Assilina*) and a sparse diverse ostracode assemblage. This limestone also contains a very rich and diversified dasycladalean algal assemblage, including eleven species of the dasycladalean algae. The foraminifer assemblage has zoogeographic affinities with Eocene Indopacific assemblages. The algal assemblage suggests their luxuriant growth in the open lagoonal to shelf environment in the warm waters.

Spectacular geomorphological features including endangered outcrops of Jaflong area typically covers geoscientific and aesthetic with scenic contents for executing a geoheritage and a geopark. The area extends some anthropogenic cultural heritage events from different tribes (e.g., Khasia, Monipuri, Tippera and Garo) and their primitive lifestyle, practicing age-old rites, rituals, customs and traditions, and a prominent Mughal archaeological event of Jaintia King Palace. The present geosite abide adequate scientific, economic, research, educational, cultural, aesthetic and functional values with intrinsic and extrinsic features, having indicial and symbolic contents with highly socialized place largely due to recreational reasons and having landscape value. The Sylhet Limestone also contains highly scientific influence bias documental contents, which is remarkably regional scale content. Moreover, the areas have intrinsic and aesthetic values, mainly scenic beauty with anthropogenic and archeological events. The area corresponds certainly to the scenic content indicating regional scale content, providing high recreational function. Results and level of rank from different quantitative and qualitative assessment provide excellent geoheritage category (Rank III; Fig. 35.1e) (e.g., Reis and Henriques 2009; Mansur and Carvalho 2011; Bruschi et al. 2011). Jaflong area with endangered outcrops

has significant scenic and documental contents and its rarity or aesthetic appeal, which accomplish the most of the criteria or values for geopark. So, it is very imperative to protect this geoheritage, spreading collected knowledge and promoting sustainable social and economic development through geotourism. However, the main entity (Sylhet Limestone) of the area is in extremely vulnerable conditions, which advise strong rationalization to grant protection at the level of geoheritage as well as geopark and it is so much important to make legal base for geoconservation. Therefore, overall observations provide excellent (Rank III) geoheritage category that needs to be preserved for future generation.

---

## References

- Brouwers EM, Khan MR, Akhter A (1992) Microfossil assemblages from the Eocene Sylhet limestone and Kopili formation, Sylhet district, Northern Bangladesh. U.S. Geological Survey, pp 1–46
- Bruschi VM, Cendrero A, Albertos JAC (2011) A statistical approach to the validation and optimisation of geoheritage assessment procedures. *Geoheritage* 3:131–149. doi:[10.1007/s12371-011-0038-9](https://doi.org/10.1007/s12371-011-0038-9)
- Evans P (1932) Explanatory notes to accompany a table showing the tertiary successions in Assam. *Trans Min Geol Inst India* 27:155–260
- Humane SK, Chaurpagar SN, Humane SS, Kundal P (2010) Dasycladalean algae and their depositional environments in the Sylhet limestone formation (lower-middle Eocene), Bengal Basin. *J Geol Soc India* 76(1):75–85
- Khan FH (1963) Preliminary report on limestone, coal, and glass sand Lamakala-Bhangarghat area, Sylhet district, East Pakistan. Pakistan Geological Survey Minerals Information Circular, vol 11
- Lima FF, Brilha JB, Salamuni E (2010) Inventorying geological heritage in large territories: a methodological proposal applied to Brazil. *Geoheritage* 2:91–99. doi:[10.1007/s12371-010-0014-9](https://doi.org/10.1007/s12371-010-0014-9)
- Mansur KL, Carvalho IS (2011) Characterization and valuation of the geological heritage identified in the Peró dune field, state of Rio de Janeiro Brazil. *Geoheritage* 3:97–115. doi:[10.1007/s12371-011-0036-y](https://doi.org/10.1007/s12371-011-0036-y)
- Reis RP, Henriques MH (2009) Approaching an integrated qualification and evaluation system for geological heritage. *Geoheritage* 1:1–10. doi:[10.1007/s12371-009-0002-0](https://doi.org/10.1007/s12371-009-0002-0)

# Estimation of Recreation Attractiveness and Geomorphic Risks for Recreational Purposes: Case of Nalychevo Nature Park (Kamchatka, Russia)

Iuliia Blinova and Andrey Bredikhin

## Abstract

During the past decades recreational activity has become one of the major socio-economic factors of sustainable development in many countries. Its organization is complex and appears a significant constituent of anthropogenic impact on landscape. Creation of a new tourism cluster or expansion of natural recreation resource, along with other scientific and applied problems of recreation, requires precise assessment of the territory. Geomorphology often determines technological peculiarities of land use, such as location and territory zoning, means of transport, safety for recreational system and people involved in recreational activity. To identify interrelationships between geomorphological features and recreational activities the notions of “fields of risk and attractiveness” are considered. Comprehensive study and assessment of each qualitative field gives a value of relief influence on a person. In this sense the territory of Russian Kamchatka is considered as a model. The recreational and geomorphic system in Nalychevo was first investigated by the authors during the field season 2010. The results of this research expedition underlie the assessment procedure of the Nature Park. Taking into account the structure of recreational and geomorphic space is the information basis for effective functioning of existing system and for creation new clusters.

## Keywords

Geomorphological risks • Attractiveness • Recreation and geomorphic potential • Nalychevo • Kamchatka

## 36.1 Introduction

Interrelationship between geomorphology as a principal component of landscape and recreation has become a topical issue over past decades. Studies in this field open new perspectives not only for scientific activities but also for

solution of various applied tasks. The solution of various problems of recreational activities, such as tourist product selection, optimal route search, creation of a new tourism cluster or expansion of natural recreation resources requires precise assessment of the territory. In this context society faces necessity of respective resource assessment.

Geomorphology, as a basic component of landscape, often determines technological peculiarities of land use. Mutual influence of relief and recreation can be divided into two general domains: recreational and geomorphic (RG) risks and RG attractiveness (Bredikhin 2010; Blinova and Bredikhin 2011). One of the principal attributes for efficient recreational usage of territory, landscape or relief is uniqueness. It is related to particular relief forms and associations which differ from the others in structure, or have

I. Blinova (✉) · A. Bredikhin  
Faculty of Geography Geomorphology and Paleogeography,  
Moscow State Lomonosov University, GSP-1, Leninskie gory, 1,  
Moscow 119991, Russia  
e-mail: ljuljawa@gmail.com

A. Bredikhin  
e-mail: avbredikhin@yandex.ru

some geomorphological and morphometric characters, which are not common in other forms of the earth's surface. Unique landforms are often considered as part of geoheritage and therefore defined as geosites and geomorphosites (Reynard et al. 2009). Such monuments form the main natural functional kernel for a recreation system which is created and exists around them. They also increase local recreational attractiveness of the area.

Natural monuments are particularly vulnerable to dangerous occurrence of endogenous and exogenous processes as guarantee of environmental stability is an essential condition for a proper system functioning. This requires a comprehensive study of relief dynamics, monitoring and forecasting its evolution in protected areas.

## 36.2 Study Area

The region of Kamchatka has unique tectonic location that generally promoted maturation of diverse landscapes. However recreational development of the area is very slow due to its bad accessibility and remoteness. In spite of general fame of Far East recreational resources there are still

areas which are not affected by human activities (including recreation and tourism) in immediate proximity to the regional center. One of them is Nalychevo Nature Park which is included in the "Volcanoes of Kamchatka" UNESCO's World Heritage List.

Natural Park Nalychevo, located in the south-east of Kamchatka Peninsula 50 km NE from Petropavlovsk-Kamchatsky (Fig. 36.1), represents an example of wild area not involved in human activities. The Park has an area of 2870 km<sup>2</sup> within an intermountain depression with clear geomorphological boundaries. All the currently known mineral water sites of Nalycheva basin are concentrated in this depression.

At present the territory of Nalychevo Park is a complex recreational system that mainly focuses on eco-tourism. The diversity of environmental conditions and relief forms on this area (Fig. 36.1c) creates necessary prerequisites for assignment a wide range of recreation specialization: balneal, hillwalking, sports (skiing, hiking etc.), environmental education. However, hierarchical polycentric structure of Natural Park and disengaged database impedes its management and sustainable development.

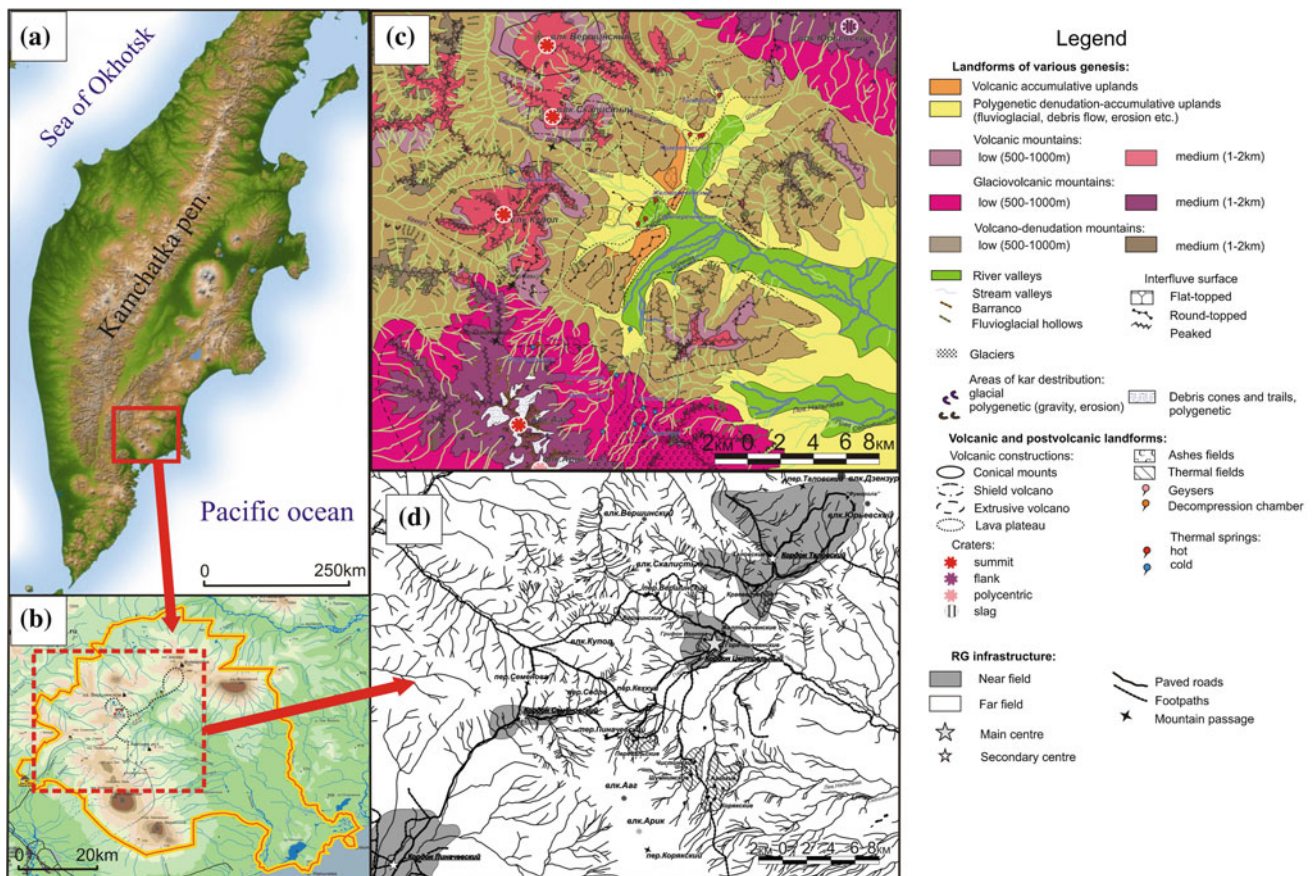


**Fig. 36.1** Recreation and geomorphic system Nalychevo: **a** Position of natural park on Kamchatka peninsula, **b** Position of studied area, **c** Geomorphic scheme of central part of Nalychevo, **d** Scheme of recreational structure of Nalychevo

### 36.3 Methodology

Currently, there are methods for assessing the recreational potential of the territory, including its location, climatic conditions, attractiveness and other factors which are valuable for recreational purposes (Blinova and Bredikhin 2011; Eringis and Budriūnas 1975).

There are two general domains of geomorphology and recreation mutual influence: recreational and geomorphic (RG) risk (threat) and RG attractiveness. Estimation of attractiveness and danger value must be carried out by means of composite indexes which include particular rates of relief features (rareness, diversity, aesthetical attractiveness etc.). The value of relief capacity for having positive influence on a person (physical, psychological etc.) can be placed in it. This quantity which indicates a complex functional suitability of an area for recreational purposes should be called “recreational and geomorphic potential” (RGP).

The impact of the various relief characteristics is determined by the objectives of holidaymakers. For example, in organization of recreational sports morphometric parameters are the most significant (absolute height, steepness, dismemberment). However, various types of recreation require different values of these parameters. For the attractiveness and risk assessment it is important to give a numerical score in each of the claimed relief properties taking into account the selected recreational activities. Therefore we assign several criteria and evaluate each of them on a scale of 1–4 points. Numerical approach allows us to conduct the assessment procedure impartially and to establish the ranking based on final scores. For all types of recreational use,

the criteria are similar: for instance, quality of exposure, diversity or accessibility. In order to evaluate the potential more precisely, for the final assessment, these criteria have been given different weights (Tables 36.1 and 36.2). Taking into account the obtained averages of RGP components the whole potential for organizing a particular type of recreational activity can be attributed to one of four types: insufficient, medium, optimum or extreme. Therefore a single geomorphosite or an association acquires some kind of “coordinates” in relation to its recreational and geomorphic potential.

### 36.4 Assessment of Nalychevo

After estimating recreational and geomorphic potential of a studied area we can analyze its structure, i.e. the set of presented or potentially possible recreational activities. Visually this classification could be represented as a pie chart (Fig. 36.2).

The diagram consists of two parts: the inner circle, divided into 4 parts and the outer cells. The inner part of the diagram reflects different functional groups of recreational activities. Then, for each group there is a set of specific recreational activities, realized or potential within the touristic system. The latter are represented in the form of cells. Depending on the value of RGP for each of them, the cell is painted in different colours.

According to our assessment the studied area is particularly prospective for balneal recreation, environmental education and some sport activities (skiing,

**Table 36.1** Criteria used to evaluate potential recreational uses of a geomorphosite and corresponding weights (modified from Lima et al. 2010)

Criteria	Criteria weight for different functional types of recreational use			
	Educational	Sport	Medical	Health-improving
Representativeness	5	5	5	0
Quality of the exposure	10	5	5	0
Diversity at the state level	5	5	5	0
Educational potential	30	0	0	0
Logistics	15	10	15	15
Inhabitants around 25 km	10	0	5	0
Accessibility	10	10	10	10
Vulnerability caused by human activities	5	15	5	10
Association with other values	5	5	10	10
Monumentality	5	0	0	0
Recreational potential	0	0	0	20
Social setting	0	5	10	5
Proximity to recreational facilities	0	10	10	10
Morphological prerequisites	0	30	20	20
Total	100	100	100	100

**Table 36.2** Criteria used to evaluate the risk of degradation of a geomorphosite and corresponding weights (modified from Lima et al. 2010)

Criteria	Weight
Vulnerability caused by natural or human factors	35
Proximity to potential damaging areas	20
Present protection status	20
Accessibility	15
Inhabitants within 25 km	10
Total	100

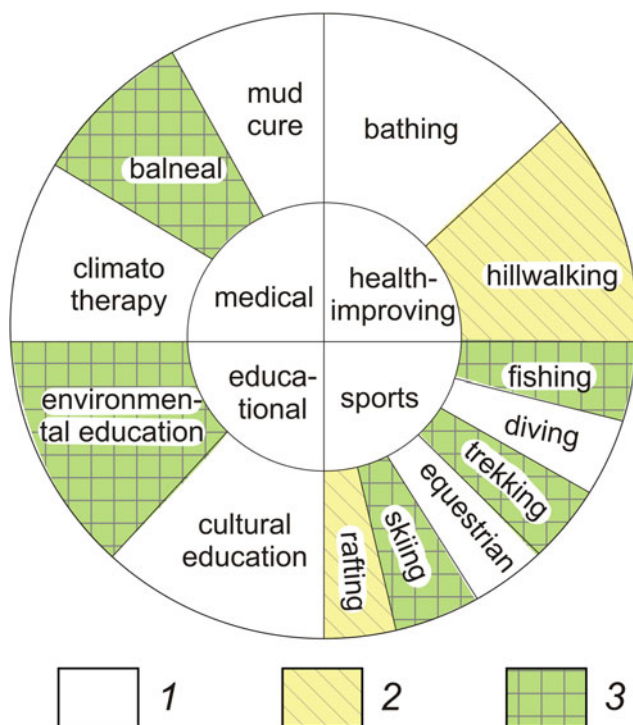


**Fig. 36.2** Scheme of recreational and geomorphic potential structure of Nalychevo nature park. Types of recreational and geomorphic potential: 1 Insufficient, 2 Medium, 3 Optimum

trekking and fishing). Geomorphological settings of this territory also make it suitable for hillwalking and rafting.

## 36.5 Conclusions and Perspectives

Such assessment allows us to compare specializations and recreational and geomorphic potential of different territories. Thereby it is possible to optimize decisions on the proper tourist product choice, or on organization of recreational activity. The last confirms the necessity to assess the RGP for different parties of recreational system—the organizers and tourists. Estimation of recreation attractiveness and geomorphic risks is particularly important for prospective recreational regions. The decision-making concerning to creation a new tourist cluster depends basically on resource assessment. Various functional types of activity within a recreational and geomorphic system could have different potential. Taking into account the structure of recreational and geomorphic space is the information basis for effective functioning of existing systems and for creating new ones.

The approach to assessment of recreational and geomorphic potential introduced in this paper allows elaborating concrete recommendations in organizing recreational activities (for well-known touristic areas and also for areas of new recreational development).

Next phase in the development of prospective recreational system is to compare the results of recreation and geomorphological assessment with the economic potential of the area and use value.

## References

- Bredikhin AV (2010) *Rekreatsionno-geomorfologicheskie sistemy* (Recreational and geomorphic systems). Oikumena, Moscow-Smolensk
- Blinova I, Bredikhin A (2011) *Rekreatsionno-geomorfologicheskii potentsial: Otsenka geodinamicheskii aktivnikh regionov* (Recreational and geomorphic potential: Assessment of regions with high geodynamics). LAP Lambert Academic Publishing, Saarbrücken, Germany
- Erings K, Budriūnas AR (1975) *Essence and method of detailed aesthetical and ecological investigations of sceneries*. Landscape Ecology and Aesthetics, Vilnius, pp 160–162
- Lima FF, Brilha JB, Salamuni E (2010) *Inventorying geological heritage in large territories: a methodological proposal applied to Brazil*. Geoh Heritage 2:91–99. doi:10.1007/s12371-010-0014-9
- Reynard E, Coratza P, Regolini-Bissig G (2009) *Geomorphosites*. Verlag Friedrich Pfeil, München, Germany

---

# Recovery of Ancient Groundwater Supply Systems and Old Abandoned Mines: Coupling Engineering Geosciences and Geoheritage Management

# 37

Maria Eugénia Lopes, Maria José Afonso, José Teixeira, João P. Meixedo, J. Filinto Trigo, Maria João Dias Costa, Luís C. Gama Pereira, and Helder I. Chaminé

---

## Abstract

This work aims to highlight the coupling of engineering geosciences and geoheritage studies on an integrative multidisciplinary approach to the recovery processes of abandoned mining heritage. In order to fulfil these goals an experimental site was selected in S. Martinho de Tibães Monastery enclosure. Some abandoned water mines were part of an impressive water supply system of the monastery between 17th and 19th centuries. The Aveleiras Mine site was also exploited in the first half of the 20th century as a wolfram mine for over 23 years. Specific actions were developed to rehabilitate some sites, in order to facilitate their inclusion in selected hydrogeo-itineraries to the wide public. This will demonstrate their early purpose, i.e., to provide water to the gardens and orchards of the monastery. In addition, the recovery of abandoned mining sites is a worthy example of an organization transformative process towards a second life-cycle in geotourism, natural heritage and cultural assets. Such interventions represent important measures for sustainability and the surrounding environment.

---

## Keywords

Groundwater systems • Abandoned mines • Engineering geosciences • Mining geoheritage • NW Portugal

---

## 37.1 Introduction

The main goal of geoconservation is the development and protection of geological heritage (Gray 2004). A geosite can be regarded as a geological setting with particular scientific,

educational or tourist value (e.g., Wimbledon 1996; Lima and Leal Gomes 1999; Brilha 2002; Brilha et al. 2005; Carcavilla et al. 2009; Burek and Prosser 2008; Meixedo et al. 2011; Lopes 2012). Therefore, geological heritage is an expression of geodiversity. In addition, geodiversity has

---

M.E. Lopes · M.J. Afonso (✉) · J. Teixeira · J.P. Meixedo · J.F. Trigo · H.I. Chaminé (✉)  
Laboratory of Cartography and Applied Geology (LABCARGA), DEG, DEC, School of Engineering (ISEP), Polytechnic of Porto, Porto, Portugal  
e-mail: mja@isep.ipp.pt

H.I. Chaminé  
e-mail: hic@isep.ipp.pt

M.E. Lopes  
e-mail: mel@isep.ipp.pt

J. Teixeira  
e-mail: joaat@isep.ipp.pt

---

J.P. Meixedo  
e-mail: jme@isep.ipp.pt

J.F. Trigo  
e-mail: jct@isep.ipp.pt

M.J. Dias Costa  
Mosteiro de Tibães, Direcção Regional de Cultura do Norte, Mire de Tibães, Braga, Portugal  
e-mail: diascosta@culturanoorte.pt

L.C. Gama Pereira  
Department of Earth Sciences, Faculty of Sciences and Technology, University of Coimbra, Coimbra, Portugal  
e-mail: lcgpereira@gmail.com

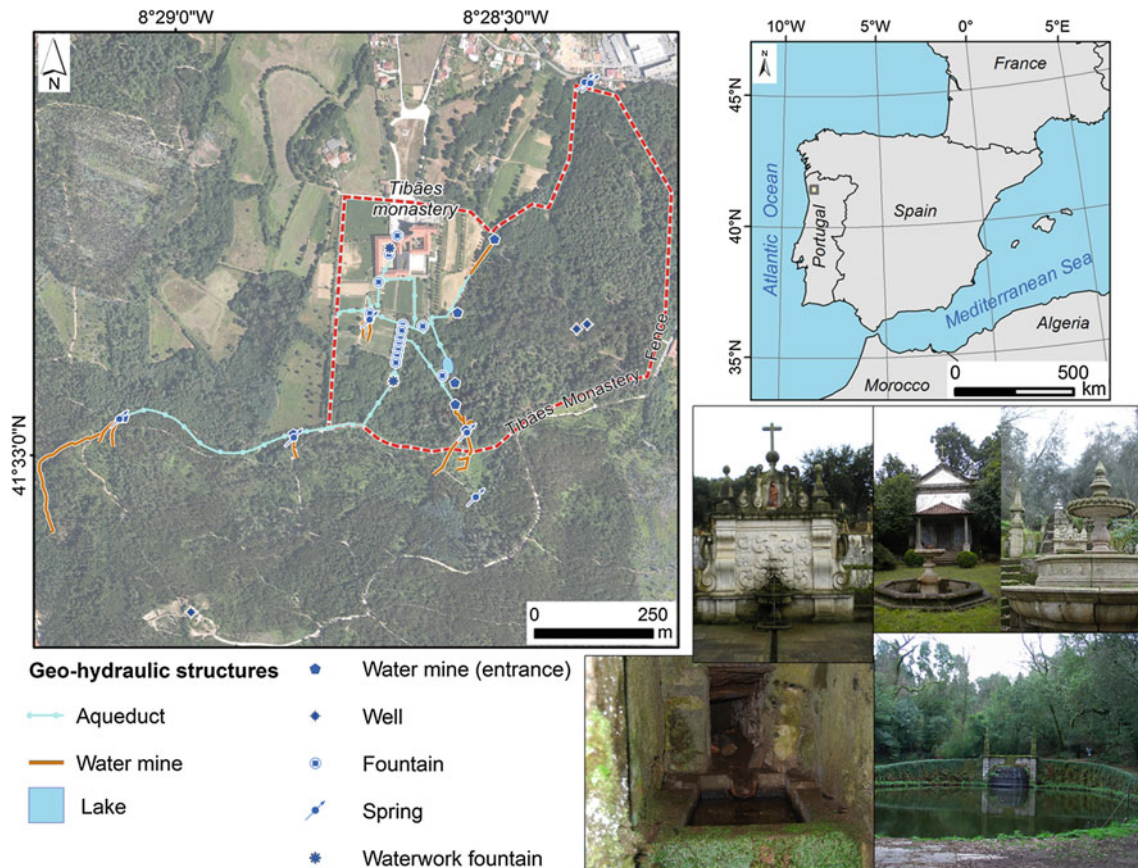


**Fig. 37.1** Geographical framework of S. Martinho de Tibães Monastery enclosure (Braga, NW Portugal). Main geo-hydraulic structures mapped and some images (top left on counter clockwise direction:

S. Bento fountain / spring, S. Bento Chapel fountain, waterworks' set fountains along a stairway, Aveleiras water mine, Lake)

a set of values such as intrinsic, cultural, aesthetic, economic, functional, scientific and educational (Gray 2004). The so-called geomining parks are old abandoned mining exploitation sites, where a geoheritage framework protection order is applied. These parks are designed to permit public visits with entertainment, educational or scientific investigation purposes. In summary, there is a triple goal to achieve (e.g., Orche 2003, Lima and Leal Gomes 1999; Meixedo et al. 2011; Lopes 2012): (i) to recover a degraded area with an important heritage value; (ii) to rehabilitate, both socially and economically, a specific community, and (iii) to offer the public the possibility to contact with geomining activity.

This work intends to emphasize the importance of combining engineering geosciences and geoheritage studies on an integrative multidisciplinary approach to the recovery processes of abandoned water supply systems related to old mines, as well as geomining sites of cultural relevance. In addition, an inventory and assessment for mining geoconservation purposes was applied following the main recommendations from several authors (e.g., Muñoz 1988; Orche 2003; Wolkersdorfer and Bowell 2005; García-Cortés 2008;

García-Cortés and Urquí 2009; López-García et al. 2011, and references therein).

This study involved a geomorphologic and geotectonic characterisation of the study area and, in a subsequent stage, an engineering geology assessment. A high-precision GPS was used for the fieldwork surveys. The scanline sampling technique was applied to the study of basic geotechnical description of free rock mass surfaces (ISRM 2007). In addition, engineering geoscience mapping was performed, both at surface and underground framework (Trigo et al. 2012). All the information was integrated on a Geographic Information System mapping platform, and combining geoenvironmental methodologies and techniques (Manoliu and Radulescu 2008), namely mining geology, engineering geoscience and hydrogeomechanics.

The opportunity to restore activity and interest in these abandoned sites provides a second cycle of life. Such interventions offer the potential for sustainable development, both of the geomining organization and of the surrounding environment. At a socio-economic level, the main advantage is the promotion of regions where the economy depended heavily on exploitation of natural resources.

## 37.2 The Study Area

The study area is located in the S. Martinho de Tibães Monastery and its surroundings, near Braga city, NW Portugal. This monastery was founded in the late 11th century, and was the mother house of the Order of Saint Benedict for Portugal. Most of the magnificent construction dates back to the 17th and 18th centuries. S. Martinho de Tibães Monastery was closed in 1834 because of liberal policies and sold in 1864, and 30 years later a fire destroyed part of the refectory cloister. In 1986, despite the degradation of the monastery over the last few decades, the Portuguese Government acquired it and began its heritage protection; the extensive recovery project was started and still continues to the current day (Dias Costa 2002), Fig. 37.1.

S. Martinho de Tibães region is located in the vicinity of regional shear zones. The regional tectonic framework comprises a Palaeozoic metasedimentary highly fractured and folded basement rock. It defines some main tectonic lineaments orientation, trending NW-SE and NE-SW (Ferreira et al. 2000). The geological units that outcrop in the study area are, mainly, micaceous clayish phyllites,

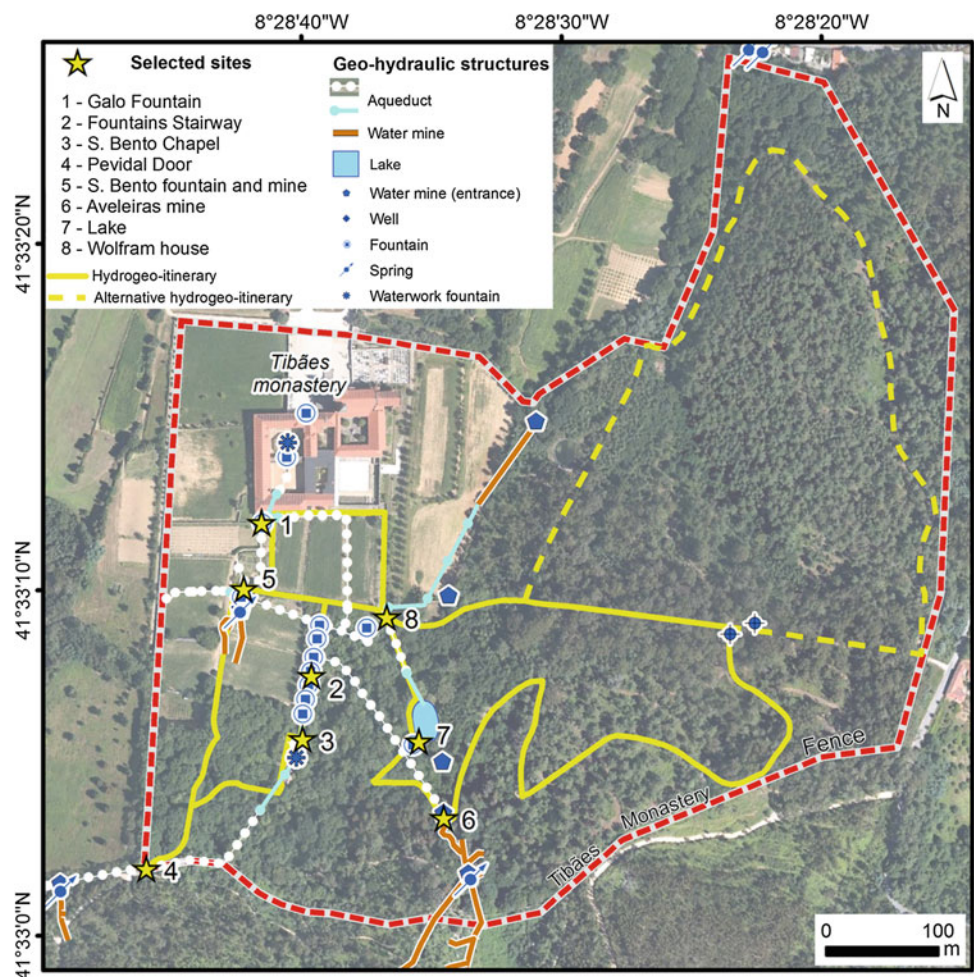
metagraywackes interbedded with metasiltites, metapelites and quartz hornfels, and granitic rocks (Lopes 2012). The presence of wolfram-bearing quartz shear veins in the study area led, in the 1930s, to the exploration and exploitation of these hydrothermal deposits (Meixedo et al. 2011; Lopes 2012; Trigo et al. 2012).

The monastery was supplied for many centuries by a complex water mine system and nowadays most of these mines are abandoned sites (Coelho Dias 2010; Lopes 2012). In this area several natural springs were reported, such as S. Bento spring (TERMARED 2011).

Conversion into selected hydrogeo-itineraries can be an important path to organizational sustainability, both internally and in interaction with the environmental issues. This approach offers hope for a sustainable new life for these abandoned water supply systems (Fig. 37.2).

These studies already led to preliminary cultural activities, namely an itinerary inside the S. Martinho de Tibães Monastery enclosure, where some aspects of the hydrogeodiversity and geoconservation were highlighted, particularly, a visit to the abandoned Aveleiras Mine site (Chaminé et al. 2008/2013). This activity was included in

**Fig. 37.2** Selected hydrogeo-itinerary proposals for the Monastery of S. Martinho de Tibães site: water sites related with groundwater supply systems and geo-hydraulic structures



the “Geology in the Summer” by “Ciência Viva” program (<http://www.cienciaviva.pt/>), promoted by a Portuguese agency for scientific dissemination by a wide public (Vargas and Noronha 2002).

### 37.3 Concluding Remarks

The cultural tourism around old abandoned groundwater supply and mining related areas has a great potential for geoscientific tourism. It must be highlighted that sites could play a forum for an educational key-role. The value of the geoheritage legacy can be transformed into museums, parks or protected natural areas for recreation, educational and scientific purposes. This kind of approach lead on conducting of educational activities related to a better public understanding of groundwater supply systems. Among the tourist activities primarily recommended there are guided tours, exhibits of geological features and groundwater supply methods. The converted outdoor spaces can accommodate children theme parks, picnic and selected camping areas, as well as guided tours on trekking, biking, hiking or horseback, to access the specific geological and mining features of the sites.

**Acknowledgements** This study was performed within the scope of the HYDROURBAN (“Hydrogeology, geomechanics and geoconservation of ancient water mines”) supported by the re-equipment programme IPP-ISEP|PADInv’2007/08 and the LABCARGA|ISEP /IPPAR–Mosteiro de Tibães consultancy R&D Project. This work was also under the framework of R&D projects (Aveiro: PESt-C/CTE/UI4035, Porto: PESt-OE/CTE/UI0668, Coimbra: PESt-OE/CTE/UI0611). We acknowledge the anonymous reviewers for the constructive comments.

### References

- Brilha J (2002) Geoconservation and protected areas. *Environ Conserv* 29(3):273–276
- Brilha J, Andrade C, Azevedo A, Barriga FJAS, Cachão M, Couto H, Cunha PP, Crispim JA, Dantas P, Duarte LV, Freitas MC, Granja HM, Henriques MH, Henriques P, Lopes L, Madeira J, Matos JMX, Noronha F, Pais J, Piçarra J, Ramalho MM, Relvas JMRS, Ribeiro A, Santos A, Santos VF, Terrinha P (2005) Definition of the Portuguese frameworks with international relevance as an input for the European geological heritage characterisation. *Episodes* 28(3):177–186
- Burek CV, Prosser CD (2008) The history of geoconservation. *Geological Society special publication*, vol 300. Geological Society, London, pp 1–312
- Carcavilla L, Durán J, García-Cortés A, López-Martínez J (2009) Geological heritage and geoconservation in Spain: past, present, and future. *Geoheritage* 1(2–4):75–91
- Chaminé HI, Lopes ME, Afonso MJ, Gomes A, Trigo JF (2008/2013) As antigas minas de água do Mosteiro de São Martinho de Tibães (Braga): um percurso pela geoconservação e geodiversidade. *Geologia no Verão*, ISEP, Porto. (Cd-Rom edition)
- Coelho Dias GJA (2010) Tibães: o encanto da Cerca, o silêncio dos monges e os últimos abades gerais dos beneditinos. *Museu de S. Martinho de Tibães / Mosteiro de S. Bento da Vitória*, p 116
- Dias Costa MJ (2002) A cerca do mosteiro de São Martinho de Tibães. *Património e Estudos*. IPPAR, Lisboa 2:86–95
- Ferreira N, Dias G, Meireles C, Braga MAS (2000) Carta Geológica de Portugal, na escala 1/50000. *Notícia Explicativa da Folha 5-D (Braga)*. 2ª edição. Instituto Geológico e Mineiro, Lisboa, p 68
- García-Cortés A (ed) (2008) Contextos geológicos españoles: una aproximación al patrimonio geológico español de relevancia internacional. *Instituto Geológico y Minero de España, Madrid*, p 235
- García-Cortés A, Urquí L (2009) Documento metodológico para la elaboración del inventario Español de lugares de interés geológico. *Instituto Geológico y Minero de España*, p 61
- Gray M (2004) *Geodiversity: valuing and conserving abiotic nature*. Wiley, West Sussex 434 p
- ISRM [International Society for Rock Mechanics] (2007) The complete ISRM suggested methods for characterization, testing and monitoring. In: Ulusay R, Hudson JA (eds) *Suggested methods prepared by the commission on testing methods*. ISRM, Ankara, Turkey, pp 1974–2006
- Lima F, Leal Gomes C (1999) Locais de interesse para a arqueologia mineira do Alto Minho (N de Portugal). *Estado actual: métodos de caracterização e estratégias de aproveitamento*. *Cadernos Laboratório Xeológico de Laxe* 23:89–99
- Lopes ME (2012) *Geoconservação e valorização do património geológico-mineiro de espaços subterrâneos antigos*. University of Coimbra, p 325 (unpublished PhD Thesis)
- López-García JA, Oyarzun R, Andrés SA, Martínez JIM (2011) Scientific, educational, and environmental considerations regarding mine sites and geoheritage: a perspective from SE Spain. *Geoheritage* 3(4):267–275
- Manoliu I, Radulescu N (eds) (2008) *Education and training in geoenvironmental sciences: soil mechanics, geotechnical engineering, engineering geology and rock mechanics*. CRC Press, Taylor & Francis Group, London, p 514
- Meixedo JP, Lopes ME, Dias Costa MJ, Trigo JF, Chaminé HI (2011) Geological and mining heritage in NW Portugal (Mire de Tibães): threats and opportunities for a sustainable second life-cycle. In: Cloughton P, Mills C (eds) *Mining perspectives: proceedings of the 8th international mining history congress 2009*. Cornwall and West Devon Mining Landscape World Heritage Site, Cornwall Council, Truro, pp 97–103
- Muñoz E (1988) *Georrecursos culturales*. *Geología Ambiental*. ITGE, Madrid, pp 85–100
- Orche E (2003) Puesta en valor del patrimonio geológico-minero: el proceso de adaptación de explotaciones mineras a parques temáticos. *Villas Bôas et al. (eds.) Patrimonio Geológico y Minero en el Contexto del Cierre de Minas*, p 51–68
- TERMARED (2011) *Catálogo de nascentes termais do espaço SUDOESTE*. Programa de Cooperação Territorial do Espaço Sudoeste Europeu (SUDOESTE), Xunta de Galicia, Santiago de Compostela, p 135
- Trigo JF, Chaminé HI, Afonso MJ, Almeida H, Lopes ME, Teixeira J, Pereira R, Pinheiro R, Meixedo JP, Gomes A, Teixeira JFA, Dias Costa MJ (2012) A antiga mina de volfrâmio das Avelas (Mosteiro de Tibães, NW Portugal): estudos interdisciplinares para a valorização do património geomineiro. *Boletim de Minas, DGEG*, Lisboa 47(2):139–156
- Vargas R, Noronha A (2002) Schools can be inspired by a summer of science. *Nature* 420:605
- Wimbledon WAP (1996) *Geosites: a new conservation initiative*. *Episodes* 19(3):87–88
- Wolkersdorfer C, Bowell R (2005) Contemporary reviews of mine water studies in Europe. *Mine Water Environ* 24:1–76

# Influence of Geological Structures and Weathering in Formation and Destruction of Cone-Shaped Rocky Houses of the Kandovan Village, Iran

Ebrahim Asghari Kaljahi, Farideh Amini Birami, and Masoud Hajjalilue

## Abstract

The Kandovan is a touristic and historical village which is located 65 km far from the Tabriz city, Northwest of Iran with views of cone-shaped rocky houses. These rocky houses created by erosion and weathering of pyroclastic rocks (ignimbrite) of Sahand volcano. Based on geological studies, it is recognized that the discontinuity systems of rocks and erosion have an important role in the formation of these cone-shaped rocks. Destructive factors in the study area can be divided into natural processes (weathering and erosion) and human activities. The XRD analysis carried out on surface rocks samples, highlighted that there are no traces of clay minerals and chemical weathering. So, physical weathering of rocks is dominant. To assess their durability physical properties test has been used. In this study, emphasis is placed on hardness, density, porosity, water absorption and saturation coefficient of rock mass of Kandovan. The rock mass of Kandovan has hardness, porosity, water absorption and dry density equal to 20–25 MPa, 45–50 %, 8–12 % and 15 kN/m<sup>3</sup> respectively. Test results highlight that the high value of porosity and water absorption and low density of rocks are main effective factors to assess durability of rocks to environmental factors. These properties along with human activities have important roles in the destruction of the cone-shaped rocky houses of Kandovan village.

## Keywords

Kandovan village • Physical properties • Weathering

## 38.1 Introduction

The Kandovan village its cone-shaped rocky houses is one of the tourist attractions in East Azarbaijan province of Iran. Due to its spectacular and unique landforms with cone—

shaped formed rocks. Approximately, 700 years ago, local people have carved them and made suitable for living. A typical view of cone-shaped rocky houses in the Kandovan is presented in Fig. 38.1. The rock mass of Kandovan is affected by natural destructive elements such as wind, rain, snow, etc. Weathering and erosion, however, are still active and these natural processes threaten the stability the rocky houses. Therefore, for conservation studies, an understanding of the physical and engineering geological properties of the rock mass is essential. In this study, emphasis is placed on both material and mass properties of the rocky houses. The rock mass of Kandovan is non-welded ignimbrite with rhyolitic to dacitic composition that it is types of the pyroclastic deposits (Less than 10 million years) of the Sahand volcano (Gauri and Moeinvaziri 2002). The study area is located in altitude ranges between 2,220 and 2,250 m and it has semi-arid and cold climate. The annual mean value of

E. Asghari Kaljahi (✉) · F.A. Birami  
Department of Geology, University of Tabriz, Tabriz, Iran  
e-mail: e-asghari@tabrizu.ac.ir

F.A. Birami  
e-mail: amini\_birami@yahoo.com

M. Hajjalilue  
Department of Civil Engineering, University of Tabriz,  
Tabriz, Iran  
e-mail: hajjalilue@tabrizu.ac.ir

rainfall and temperature are 352 mm and 7.5 °C respectively. The dry season occurs between June and September. The minimum temperatures values sometimes reach up to  $-20$  °C and the annual average number of rock wetting—drying and freezing—thawing cycles are 28 and 14 cycles respectively.

### 38.2 Genesis of the Cone-Shaped Rocky Houses

Within the thickly bedded of non-welded ignimbrite, the joints constitute the discontinuities. The orientations of the joints (i.e. dip and dip direction) were determined using geological compass. In the field, 72 joint orientation measurements were taken. In order to determine the dominant sets, the joint orientation measurements were evaluated using a computer program called “Dips”. For the pole plots, a Schmidt diagram with lower hemisphere projection was adopted. The contour diagram was then obtained from the pole plots. The diagrams yield three dominant joint sets : 65/228, 60/350 and 75/132°. Weathering and erosion of rocks along these discontinuities created the cone-shaped forms in Kandovan village. Figure 38.2 show the schematic steps of the erosion and making of cone-shaped forms.

### 38.3 Destruction Factors of the Cone-Shaped Rocky Houses

Several factors are involved in the destruction of rocks. The most important ones are physical and chemical weathering. Physical weathering is the breakdown of rock into small fragments by physical processes without a change in chemical composition. No chemical elements are added to,

or subtracted from, the rock. One of the most important physical weathering processes is rock consecutive freezing-thawing. It is generally known that the 9 % volumetric expansion upon phase change of water is the major cause of rock breakdown. The freezing process causes stress up to 200 MPa. This pressure may exceed the tensile strength of rocks several times within a year. Crystallization processes such as freezing-thawing weathering can be particularly deleterious to rock materials even for short periods of time (Hamblin and Christiansen 2008). Due to physical weathering processes the rocks of Kandovan have been weathered and caused to exfoliate the surface cone (Fig. 38.3).

Chemical weathering is the breakdown of minerals by chemical reactions with the atmosphere or hydrosphere (Eklund 2008). Chemical weathering reactions are largely controlled by access to water, nature of gases and acid components dissolved in water. Minerals of rocks are altered by chemical weathering and converted to new minerals with lower-strength. As a result, physical weathering becomes more severe. The rock chemical weathering and the presence of clay minerals causes weakening of the stone because of the presence of low energy bonds in their structures; therefore, they are more easily affected by mechanical erosion and they are formed when a rock has weathered by the presence of high water and temperature (Garcia-Vallés et al. 2003). Thus, to assess chemical weathering of kandovan rocks X-ray diffraction analysis were performed of 1cm thick of the Kandovan rock surface sample (probably chemical weathered). The typical XRD pattern for a sample is depicted in Fig. 38.4. The results show that there are no traces of clay minerals and chemical weathering in Kandovan rocks.

As previously mentioned, local people have carved rocks and made suitable for living. The human presence in the Kandovan village through activities that do besides natural

**Fig. 38.1** A typical view of *cone shaped* rocky houses in the Kandovan village



**Fig. 38.2** Schematic steps of formation of *cone shaped* rocks in the Kandovan

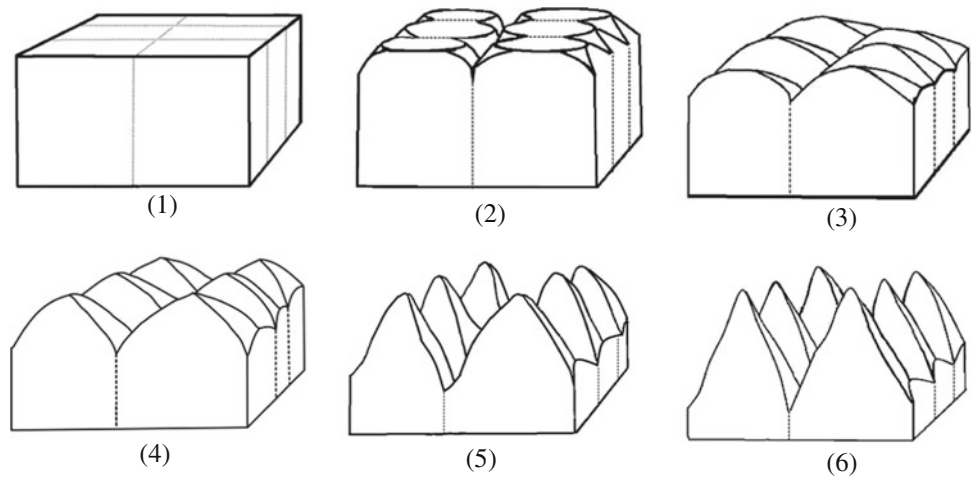
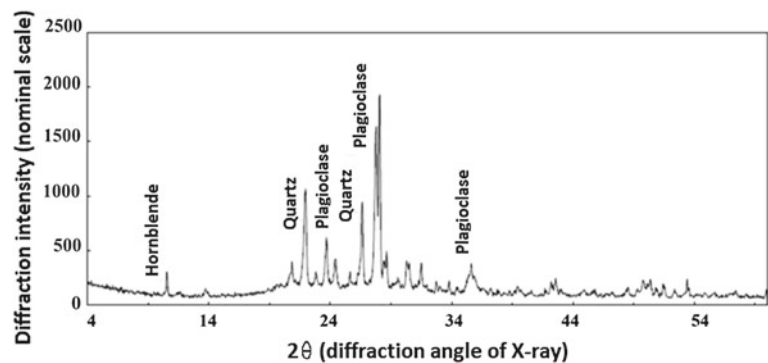


**Fig. 38.3** Flaking on Kandovan rocks surface due to weathering



**Fig. 38.4** Typical results of XRD analyses on samples obtained from surface of Kandovan rocks



factors (weathering and erosion) cause damage to the cone-shaped rocky houses. The most important human destructive factors are too much excavation inside of old houses for enlarging, resulting in walls getting fine and the increase in their vulnerability, unsanitary disposal of sewage, resulting in its penetration into rocks, use of modern materials for improving living space and repairing damaged units, construction not based on rules and regulations in the area of cone-shaped rocks, etc.

### 38.4 Physical Properties of the Cone-Shaped Rocky Houses

The internal factors such as physical properties of rocks control the mechanical behavior of theirs (Selby 1993). One way to assess the impact of these characteristics on durability of rock is physical properties tests. To determining of physical properties of Kandovan rocks, some samples were

obtained from fresh parts of rock mass and they were tested based on ASTM D4543 and ASTM D2216. Hardness is the characteristic of a solid material expressing its resistance to permanent deformation. Hardness values obtained using the Schmidt hammer on rock mass is often measured between 20 and 25 MPa, so the rocks are classified weak and weathered rocks (Brand and Philipsonm 1984).

Rock density depends from the pores, joints, cracks and other open spaces in the rock. Weathering process decreases density of rocks (Fahimifar and Soroush 2001). Low density in rock is due to high porosity and intense weathering. Dry density of fresh rock mass is equal to  $15 \text{ kN/m}^3$ . Porosity increases greatly by weathering processes and this causes a decrease of the rocks mechanical strength. The porosity of the rock mass is between 45 and 50 %. Kandovan rocks have high porosity and low density based on Anon classification (Anon 1979). Water absorption is an important feature affecting the rock resistance against weathering and other processes. Water absorption test on a relatively fresh samples returned values between 8 and 12 %. Saturation coefficient (S) of a rock is the ratio of natural capacity of a rock to absorb water after complete immersion under atmospheric pressure for a definite time, and the total pore volume that is accessible to water. A rock with a very high saturation coefficient may be deteriorated by freeze-thaw activity (Schaffer 1972). Therefore, this test can be useful for giving information on the freeze-thaw durability of a rock. Saturation coefficient greater than 0.8 indicates low durability (susceptible to frost activity). The saturation coefficient of cone-shaped rocky houses in the Kandovan village is found up to 0.8 and they are susceptible to frost activity.

### 38.5 Conclusions

The geological structures, especially discontinuities, have an important role in the formation of cone-shaped rocky houses in the Kandovan village. Weathering and erosion along discontinuities have created these shapes. Of course, some

cones are being destroyed by continuous erosion along them. Based on the results of the physical properties of rock mass classification, Kandovan village rocks have high porosity and low density and are susceptible to frost activity. Therefore, the rock with these features can be considered as a rock with low durability to environmental factors. High porosity and water absorption increase water content in the rock. High water absorption along with consecutive thawing and freezing provides conditions for weathering especially physical weathering. Moreover, we cannot ignore the role of human activity in destroying rock mass of Kandovan. The cone-shaped rocky houses in the Kandovan touristic village is being in destroying rock mass by these factors and preservation of this village will be one of the most important principles to prevent it from destruction.

### References

- Anon (1979) Classification of rocks and soils for engineering geological mapping, part 1: rocks and soils material. *Bull Int Assoc Eng Geol* 19:355–371
- Brand WE, Philipsonm HB (1984) Site investigation and geotechnical engineering practice in Hong Kong. *Getech. Eng (J Southeast Asian Geotech Soc) Sci* 2:105
- Eklund S (2008) Stone weathering in the monastic building complex on mountain of St Aaron in Petra, Jordan. Master's Thesis, University of Helsinki, Institute for Cultural Studies, Department of Archaeology, pp 114
- Fahimifar A, Soroush H (2001) Rock mechanics tests, theoretical and standards. Soil Mechanics Laboratory, Technical Publications, (in Persian)
- Garcia-Vallés M, Topal T, Vendrell-Saz M (2003) Lithenic growth as a factor in the physical deterioration or protection of Cappadocia monuments. *Environ Geol* 43:776–781
- Gauri N, Moienvaziri H (2002) Stratigraphy, petrology and geochemistry of ignimbrite layers of Sahand. Master Science Thesis, University of Tarbiat Moalem, Tehran, pp 167 (in Persian)
- Hamblin WK, Christiansen EH (2008) Earth's dynamic systems, 10th edn. Prentice Hall, Brigham Young University, chapter 10
- Schaffer RJ (1972) The weathering of natural building stones. *Dept. Sci. Ind. Res. Building Research Spec. Rept. NO.18*, pp 149
- Selby MJ (1993) Hillslope material and processes. Oxford University Press, Oxford, pp 451

# The Ivrea Morainic Amphitheatre as a Well Preserved Record of the Quaternary Climate Variability (PROGEO-Piemonte Project, NW Italy)

Franco Gianotti, Maria Gabriella Forno, Roberto Ajassa, Fernando Cámara, Emanuele Costa, Simona Ferrando, Marco Giardino, Stefania Lucchesi, Luigi Motta, Michele Motta, Luigi Perotti, and Piergiorgio Rossetti

## Abstract

In the Piedmont plain of NW Italy the Ivrea Morainic Amphitheatre (IMA) is a remarkable evidence of the Quaternary glaciations. It consists of a wide (505 km<sup>2</sup>) complex of lateral moraines (i.e. the Serra d'Ivrea), end moraines and kame terraces, encircling a 200 km<sup>2</sup> wide flat internal depression above which a subglacially moulded rocky hills (the Colli d'Ivrea) elevates. The glacial successions range from the end of the Early Pleistocene (dated on palaeomagnetic basis) to the end of the Late Pleistocene (<sup>14</sup>C radiometric and <sup>10</sup>Be exposure ages) (about 900–20 ky BP). The IMA has recently been parted into ten stratigraphical units, potentially correlable to the whole sequence of the main Quaternary glaciations recorded by the marine oxygen isotope stratigraphy. Natural (glacial deposits and forms) and archaeological (i.e. the Roman gold mines) features make the IMA a very interesting topic for a multidisciplinary research with educational, cultural and tourist purposes. Some recent and present activities for the land promoting are presented. A candidature to the UNESCO global geopark network is considered as a suitable and ambitious goal.

## Keywords

Ivrea morainic amphitheatre • Glaciations • Geoheritage • Quaternary • Piedmont

## 39.1 Introduction

The morainic amphitheatres are the main field evidence of the extent of the mountain glaciers during the Pleistocene glaciations. Although the amphitheatres are preserved in all the middle latitude mountain chains, they form wide and long time existing end moraine systems almost exclusively

in the Andes and in the European Alps, where glaciers have spread out over the piedmont plains. Among the south-alpine end moraine systems, the Ivrea Morainic Amphitheatre (IMA) is well-known for its outstanding geomorphology, but also its stratigraphical, archaeological and cultural features are particularly remarkable.

### Present Address:

F. Gianotti (✉) · M.G. Forno · R. Ajassa · F. Cámara · E. Costa · S. Ferrando · M. Giardino · S. Lucchesi · L. Motta · M. Motta · L. Perotti · P. Rossetti  
Dipartimento di Scienze della Terra, Via Valperga Caluso, 35,  
Turin, Italy  
e-mail: franco.gianotti@unito.it

M.G. Forno  
e-mail: gabriella.forno@unito.it

## 39.2 Geomorphological and Stratigraphical Features

The IMA is the third of the Italian amphitheatres for size (505 km<sup>2</sup>). It extends in the Piedmont region, at the outlet of the Dora Baltea Valley, between the internal edge of the Western Alps and the Po Plain (Fig. 39.1). Its 3,400 km<sup>2</sup> wide mountain catchment area comprises some of the highest peaks in Europe (Monte Bianco, Monte Rosa, Monte Cervino, Gran Paradiso). The most external end moraines lie



**Fig. 39.1** Sketch map with the IMA location at the outlet of the Dora Baltea Valley. The Serra d'Ivrea lateral moraine **a**, the Colli d'Ivrea rocky hills **b** and the two parks of Bessa and Candia Lake (light dotted lines) are indicated

at great distance (130 km) from the present front of the Monte Bianco glaciers.

Morphologically, the IMA forms a wide complex of lateral and terminal moraines and kame terraces (300 km<sup>2</sup>) around a large internal depression (200 km<sup>2</sup>). Its most typical elements are: (i) an exceptionally regular and very long (16 km) lateral moraine, named the *Serra d'Ivrea*, regarded as the biggest of the Alps (Fig. 39.2); (ii) a very large fluvial plain occupying the internal depression; and (iii) a wide sector of rocky reliefs (21 km<sup>2</sup>) connected to subglacial shaping, named the *Colli d'Ivrea*, cropping out above the internal plain. The spectacular landscape of the IMA is

**Fig. 39.2** View of the SW flank of the Serra d'Ivrea moraine from the internal proglacial plain



precisely based on the contrast between the flat internal plain and the surrounding high morainic reliefs, with a sharp difference of level reaching 700 m. Because of its morphological evidence, it has already been defined in the past as the most significant amphitheatre of the alpine glaciation (Penck et al. 1894).

From a cultural point of view, the IMA and the Rivoli-Avigliana Amphitheatre have been the first morainic amphitheatres studied in Italy (Martins and Gastaldi 1850), after the identification of the glacial genesis of the *Serra d'Ivrea* by Studer (1844).

About the IMA stratigraphy, the most distal moraine has been attributed to the Lower Pleistocene on paleomagnetic basis (Carraro et al. 1991), while the most proximal end moraine was referred to the Last Glacial Maximum (LGM) based on <sup>14</sup>C radiometric dating (Arobba et al. 1997) and <sup>10</sup>Be exposure ages (Gianotti et al. 2008). Three groups of moraines were initially distinguished on pedostratigraphical ground (Sacco 1927; Carraro et al. 1975). Some interglacial/interstadial markers (paleosols and lacustrine-palustrine layers interposed within the glacial deposits) allowed at last to recognize 10 stratigraphical units referred to as many glaciations (Gianotti et al. 2008) (Fig. 39.3). Consequently an exceptionally nearly complete glacialigenic succession outcrops and could be possibly correlated to the whole sequence of the main Quaternary glaciations recorded by the marine oxygen isotope stratigraphy from MIS 22 to MIS 2.

Moreover, the IMA hosts very important archaeological sites. An impressive example of ancient landscape modifications is represented by various alluvial gold placers distributed along the outer edge of the IMA (Gianotti 2011) (Fig. 39.3). Gold placers were exploited in pre-Roman period and mainly under the Roman Republic rule, as Strabo (Geography, V, 1.12) and Pliny the Elder (Nat. Hist., 33) reported. The Bessa “*aurifodinae*” mines, dated to 2nd–1st century B.C., are the widest mine dumps (10 km<sup>2</sup>) of the IMA, forming a man-made accumulation of rounded cobbles and boulders and several anthropic bedded sandy-gravel fans. Only the Bessa mines are protected by a regional park since 1985 (Baio and Gianotti 1996; Gianotti 1996).

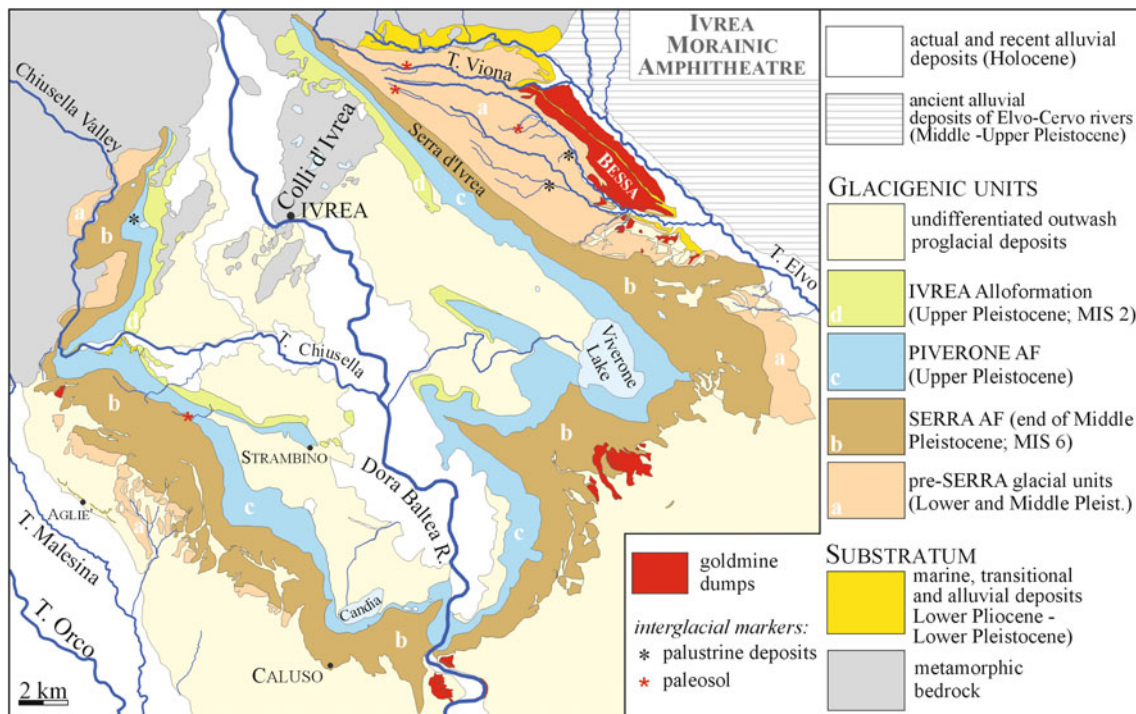


**Fig. 39.3** Geological sketch of the IMA. The pre-Serra group comprises seven glacial units, separated by palaeosols or palustrine layers. The main ancient gold mines, located at the outer edge of the IMA, are also shown

In the IMA internal depression, the pile-dwelling villages of the Viverone lake are also remarkable. These Middle Bronze Age settlements were included in 2011 in the list of UNESCO World Heritage Sites.

### 39.3 Actions

The IMA natural and anthropic features make it an excellent topic for scientific education and divulgation, mainly geologic and geomorphologic, palaeoclimatic and hydrogeological, with major implication for historical and archaeological aspects and tourist outlets. Above all the *Serra d'Ivrea* and the *Colli d'Ivrea* represent very didactic examples of the glacial sedimentation and erosion respectively. The value of the two potential geosites is increased by their closeness to the Ivrea town and their accessibility due to a dense network of roads and paths.

Furthermore, in spite of its remarkable human occupation (150,000 inhabitants into 80 communes between the provinces of Turin, Biella and Vercelli), wide breadth of country (in the internal plain) and woody land (on the moraines) are still preserved in the IMA. Yet, a more committed soil protection policy is still necessary for the agricultural and natural landscape preservation.

The IMA candidature to the UNESCO global geopark network could be a good opportunity to convey all of the actions promoting this region. The IMA certainly has the physical requirements to be a geopark, also taking into account that none of the present 100 geoparks corresponds to a big morainic amphitheatre. Unfortunately only 2 % of the IMA is actually under protection (Bessa and Baragge Regional Park and Candia Lake Provincial Park, Fig. 39.1), while an already operative park authority is necessary to become a geopark. This ambitious goal can be achieved only if all the society members, from the local population to the public authority, are aware of the high value of their land. Primarily, the scientific community has to support this action making much effort to reveal to people the essential scientific knowledge.

Various steps were recently carried out by the Earth Sciences Department of the Turin University in order to disseminate an understanding of the IMA geological features. Supported by the IMA Ecomuseum, a travelling exhibition about the IMA geology is going round the local municipalities and schools, where a series of lectures have been made and a popular book has been published (Gianotti and Marra 2012). Other actions are undertaken in the PROGEO-Piemonte Project "Proactive management of geological heritage in the Piedmont Region: innovative

methods and functional guidelines for promoting knowledge and supporting geoconservation activities”. In detail, specific researches are carried out with the aim to clarifying some geological questions about the IMA. The palynological analysis of two lacustrine successions drilled in a 55 m long sediment core should improve our knowledge about the NW Italy palaeoclimate. A detailed study of the different glacial deposits forming the *Serra d’Ivrea* moraine is conducting to best characterize the relation between clast features (composition, morphology and roundness) and transport/deposition processes. A morphological and geochemical analysis of the gold nuggets from the IMA placers is carrying out to recognize their primary source. We made a erratic blocks register (Motta and Motta 2013) according to the Piedmont regional law about the protection of erratics. A significant aim of this project is the dissemination of the results by coordinated brochures, posters and geologic itineraries books, as well as lectures, workshops and short courses for teachers and naturalistic guides.

## References

- Arobba D, Calderoni G, Caramiello R, Carraro F, Giardino M, Quagliolo P (1997) Palynological and radiometric evidence of a last glacial-interstadial from peat sediments in the Ivrea morainic amphitheatre (NW-Italy). *Geologia Insubrica* 2(2):143–148
- Baio M, Gianotti F (1996) Studio geologico e giacimentologico dell’area della “Bessa” (Biella, Italia). *Geologia Insubrica* 1(1–2):29–48
- Carraro F, Medioli F, Petrucci F (1975) Geomorphological study of the Morainic Amphitheatre of Ivrea, Northwest Italy. *Bull R Soc New Zealand* 13:89–93
- Carraro F, Lanza R, Perotto A, Zanella E (1991) L’evoluzione morfologica del Biellese occidentale durante il Pleistocene inferiore e medio, in relazione all’inizio della costruzione dell’Anfiteatro Morenico d’Ivrea. *Boll Museo Reg Sc Nat Torino* 9(1):99–117
- Gianotti F (1996) Bessa, paesaggio ed evoluzione geologica delle grandi aurifodine biellesi. *Eventi e Progetti*, Biella, p 83
- Gianotti F (2011) Geological setting of the Pleistocene placers and roman gold mines of the Ivrea Morainic Amphitheatre (Piedmont, NW Italy). Abstracts Convegno AIQUA “Il Quaternario italiano. Conoscenze e prospettive”, Roma, 24–25 febbraio 2011. *Il Quaternario, Ital J Quater Sci* 24(2), 183–185
- Gianotti F, Forno MG, Ivy-Ochs S, Kubik PW (2008) New chronological and stratigraphical data on the Ivrea Amphitheatre (Piedmont, NW Italy). *Quater Int* 190:123–135
- Gianotti F, Marra D (2012) L’impronta del Ghiacciaio. Anfiteatro Morenico di Ivrea: un unicum geologico. *Ecomuseo AMI*, Bolognino, Ivrea, p 63
- Martins C, Gastaldi B (1850) Essai sur les terrains superficiels de la vallée du Pô, aux environs de Turin, comparés a ceux de la plaine suisse. *Bull Soc Géol France* 7:554–605
- Motta L, Motta M (2013) The protection Law and the Register of erratic Blocks in Piedmont (Italy), as Example of Protection of a widespread Geosite in a densely populated Region. In: Mokriš M, Lieskovský A (eds) *Advanced research in scientific areas, Section 10 Natural Sciences*. EDIS, Zilina, Slovak Republic, pp 1534–1539
- Penck A, Bruckner E, du Pasquier L (1894) *Le Système glaciaire des Alpes*. *Guide Congr Géol Int Zurich Bull Soc Neuch Sc Nat* 22:86
- Sacco F (1927) *Il glacialismo nella Valle d’Aosta*. *Min LL PP Uff Idrog Po*, p 66
- Studer B (1844) *Lehrbuch der physikalischen Geographie und Geologie*, vol 1. Dalp, Bern, Chur und Leipzig

# The Monviso Ophiolite Geopark, a Symbol of the Alpine Chain and Geological Heritage in Piemonte, Italy

Franco Rolfo, Gianni Balestro, Alessandro Borghi, Daniele Castelli, Simona Ferrando, Chiara Groppo, Pietro Mosca, and Piergiorgio Rossetti

## Abstract

The Monviso Ophiolite Geopark (MOG) is one of the strategic geothematic areas chosen to represent the geodiversity of Piemonte within the research project “PROactive management of GEOlogical heritage in the PIEMONTE region”. The MOG is an extraordinary well preserved ophiolite body in the Italian Western Alps. It is one of the best known relics of oceanic crust in the Alps and formed during opening of the Mesozoic western Alpine Tethys and underwent high pressure metamorphism during Alpine subduction. The MOG encompasses the whole lithological spectrum of the Piemonte-Ligurian ophiolites, i.e. metamorphosed peridotite, gabbro, dolerite, basalt, and cover sediments. The MOG gives the almost unique chance for everybody to see and appreciate different portions of the ancient ocean along a mountain trail; from the Po river springs at Pian del Re, to Lago Fiorenza, Lago Lausetto and Lago Superiore, a path rises from 2,000 up to about 2,350 m a.s.l. and shows all different ophiolitic lithologies within few kilometers. The inventory of a number of different geosites at the MOG, whose conservation and development require different expertises, is considered as the first and essential starting point for the geoconservation of geological heritage and geosites.

## Keywords

Monviso massif • Cottian alps • Piemonte • Geological heritage

## 40.1 Introduction and Aim of the Study

Following the methodological approach of the ProGEO association (<http://www.progeo.se>), a multidisciplinary research group was created to carry out a research project (“PROactive management of GEOlogical heritage in the

PIEMONTE region”) aiming to conceive new conceptual and operational protocols in the management of geoheritage in the Piemonte Region of NW Italy.

Within the project, the Monviso Ophiolite Geopark (MOG) is a strategic geothematic area chosen to represent the geodiversity of Piemonte and its high potential for scientific studies, enhancement of public understanding of science, recreation activities and economic support to local communities (Rolfo et al. 2014).

The MOG is a composite ophiolite body in the Italian Alps, and a prominent rocky pyramid, 3841 m high a.s.l. It gives a great chance to see and appreciate different portions of the ancient Tethys ocean along a mountain trail; from the Po river springs at Pian del Re, to Lago (lake) Fiorenza, Lago Lausetto and Lago Superiore, a path rises from

F. Rolfo (✉) · G. Balestro · A. Borghi · D. Castelli · S. Ferrando · C. Groppo · P. Rossetti  
Department of Earth Sciences, University of Torino, 10125 Turin, Italy  
e-mail: franco.rolfo@unito.it

F. Rolfo · D. Castelli · P. Mosca  
IGG—CNR, 10125 Turin, Italy

2,000 m up to about 2,350 m a.s.l. and shows all different ophiolitic lithologies—modified after the Alpine evolution—within few kilometers.

## 40.2 The Monviso Ophiolite Geopark

### 40.2.1 Geological Setting

Ophiolites are portions of oceanic crust and underlying upper mantle, uplifted and emplaced onto continental crust in collisional orogens (e.g. Coleman 1977).

Among ophiolite bodies in the Alps, the MOG is one of the most representatives. It is a N-S trending body, 35 km long and up to 8 km wide, tectonically emplaced between

the underlying continental-derived Dora-Maira thrust units and the ocean-derived Piemonte Zone metasedimentary units. The MOG, one of the best preserved relics of oceanic crust in the western Alps, formed during the Mesozoic opening of the western Alpine Tethys and underwent high pressure (eclogitic) metamorphism during Alpine subduction (e.g. Lombardo et al. 1978). The MOG encompasses the whole lithological spectrum of the Piemonte-Ligurian ophiolites: metamorphic rocks after former peridotite, gabbro, dolerite, basalt, as well as cover sediments, will thus be found (Fig. 40.1). Interestingly, the metagabbros derive from two types of protolith (Mg-Al-rich gabbro and Fe-Ti-rich gabbro) probably produced by fractional crystallization from tholeiitic melts at different fractionation stages (Lombardo et al. 1978).

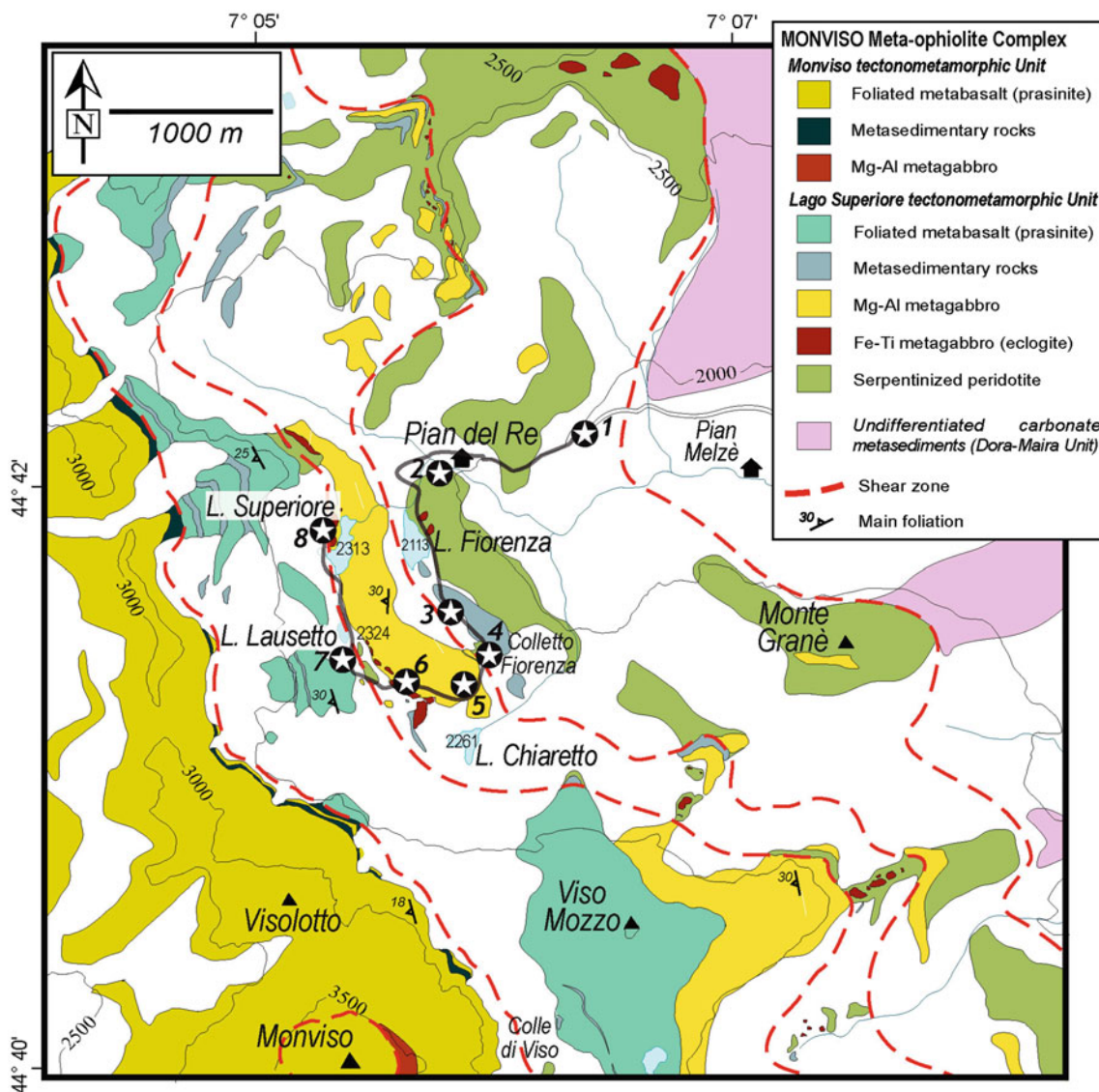


**Fig. 40.1** Geological map of the Monviso Ophiolite Geopark in the Monviso–Pian Melzè area, with the excursion route and location of Stops 1–8 (in italics) described in the text (modified from Castelli et al. 2014)

As a whole, the MOG comprises two major tectono-metamorphic units, trending north-south and dipping to the west, separated by a major shear zone: the “Monviso Upper Unit” to the west (overturned according to its original geometry) and the “Lago Superiore Lower Unit” to the east (Castelli et al. 2014).

As concerning its geologic evolution, recent advances in petrology, geochemistry and geochronology all suggest a short duration of igneous activity in the MOG and a short time span (from ca 170 to ca 150 Ma) for the entire Piemonte-Ligurian Tethys, portraying a scenario with an embryonic ocean (max 380 km wide; Piccardo et al. 2001) rather than a mature, slow spreading, Atlantic-type ocean model (Lagabrielle and Cannat 1990). The oceanic crust preserved in the MOG experienced first an oceanic hydrothermal alteration (Nadeau et al. 1993) and then, during the Alpine subduction, an high pressure eclogite-facies metamorphism (e.g. Lombardo et al. 1978). Later exhumation produced re-equilibration under progressively lower pressure conditions at blueschist- and greenschist-facies.

#### 40.2.2 A Geologic Trail Across the Tethys Ocean

A general view of the MOG internal structure is evident from a small hut along the road (7.5 km) from Pian Melzè to Pian del Re (Fig. 40.1, stop 1), by looking southward to the ridge from Monte Grané (2314 m) to Viso Mozzo (3019 m) and Monviso (3841 m). Along this section are exposed, from left to right and from bottom to top: the serpentinite at Monte Grané and in the lower ridge above Pian Melzè; the metagabbro at the foot of Viso Mozzo and the low ridge above Pian del Re; the Viso Mozzo metabasite and the Colle di Viso serpentinite, which crops out in the low ridge between Viso Mozzo and Monviso. This latter serpentinite sliver separates the two main tectonometamorphic units composing the MOG.

Along the path from Pian del Re to Lago Fiorenza, the first outcrop of serpentinite can be reached with a few minutes walk (Fig. 40.1, stop 2). The serpentinite, deriving from primary spinel-lherzolite of the upper mantle underlying the oceanic crust, is either massive or sheared (Fig. 40.2a). It mainly consists of antigorite, with variable amounts of clinopyroxene, brucite, Mg-rich chlorite, Ti-clinohumite, metamorphic olivine and chrysotile; the ore minerals are magnetite, FeNi-alloys and sulphides. Different generations of metamorphic veins crosscut the serpentinite.

About 500 m SSE of Lago Fiorenza (Fig. 40.1, stop 3), the path crosses a folded elongated body of metasediments—originally covering the former oceanic crust—tectonically embedded within serpentinite. This sliver, about 50 m-thick, belongs to an eclogite-facies shear zone which passes through Colletto Fiorenza. The metasediments consist of

impure marbles, calcschists and micaschists grading to quartzite (Fig. 40.2b). Rare cm-thick layers of metabasite are interbedded with metasediments.

At Colletto Fiorenza (Fig. 40.1, stop 4), a tectonic contact between calcschists and the overlying metagabbro (Fig. 40.2c) is marked by a zone from a few m to a few tens of m thick of strongly sheared serpentinite and talc-carbonate-amphibole-schist, with tectonic inclusions of banded eclogitic rocks.

Between Colletto Fiorenza and Lago Chiaretto (Fig. 40.1, stop 5), beautiful smaragdite metagabbro—former Mg-Al-rich plutons in the lower oceanic crust—locally includes transposed cm- to dm-thick dykes of metabasalts. The metagabbro shows a well developed foliation and consists of a whitish matrix, in which emerald-green porphyroclasts of “smaragdite” (the local name for Cr-omphacite) are preserved (Fig. 40.2d). Locally, a layering in the smaragdite metagabbro suggests a cumulus structure. The greenish-gray to pinkish metabasaltic dykes, now eclogite, are very fine-grained and locally preserve remnants of a porphyritic structure. Few boulders preserve igneous layering textures, with emerald-green bands (enriched in Cr-omphacite) corresponding to layers with high modal clinopyroxene.

West of the smaragdite metagabbro, along the path leading to Lago Lausetto and Rifugio Giacoletti, layered eclogitic rocks polished by the glacier are exposed (Fig. 40.1, stop 6). They consist of alternating layers of eclogite and metagabbro from a few cm- to several dm-thick. Eclogite largely prevails over metagabbro. The melanocratic layers (now eclogite) derive from primary FeTi-oxide gabbro, whereas leucocratic layers derive from Mg-Al gabbro protoliths. The eclogitic foliation is cut by different generations of metamorphic veins.

South of Lago Lausetto, along the path leading to Rifugio Giacoletti (Fig. 40.1, stop 7), a narrow alluvial plane hides a shear zone separating Fe-Ti metagabbro mylonites (to the E) from foliated prasinite (to the W). No primary features of the upper effusive portion of the oceanic crust, such as pillow structure or porphyritic texture, are preserved within the prasinite (nice pillows can be observed not far from here, for instance in the Vallone dei Duc, at the foot of Cima delle Lobbie). However, the prasinite may be considered as the metamorphic product of original basaltic flows. Homogeneous prasinite is fine-grained and mainly composed of albite, clinozoisite/epidote, chlorite, amphibole, and accessory rutile, titanite, apatite and opaque ores.

Finally, at the western side of Lago Superiore (Fig. 40.1, stop 8), a layered eclogitic sequence preserves small (10 × 10 cm) lenses of low-strain domains still preserving the igneous microstructure and surrounded by large volumes of eclogite-facies mylonites. Cigar-shaped boudins of eclogite within the metagabbro outline a complex interference pattern of folds. Eclogite-facies veins are spectacular—and indeed

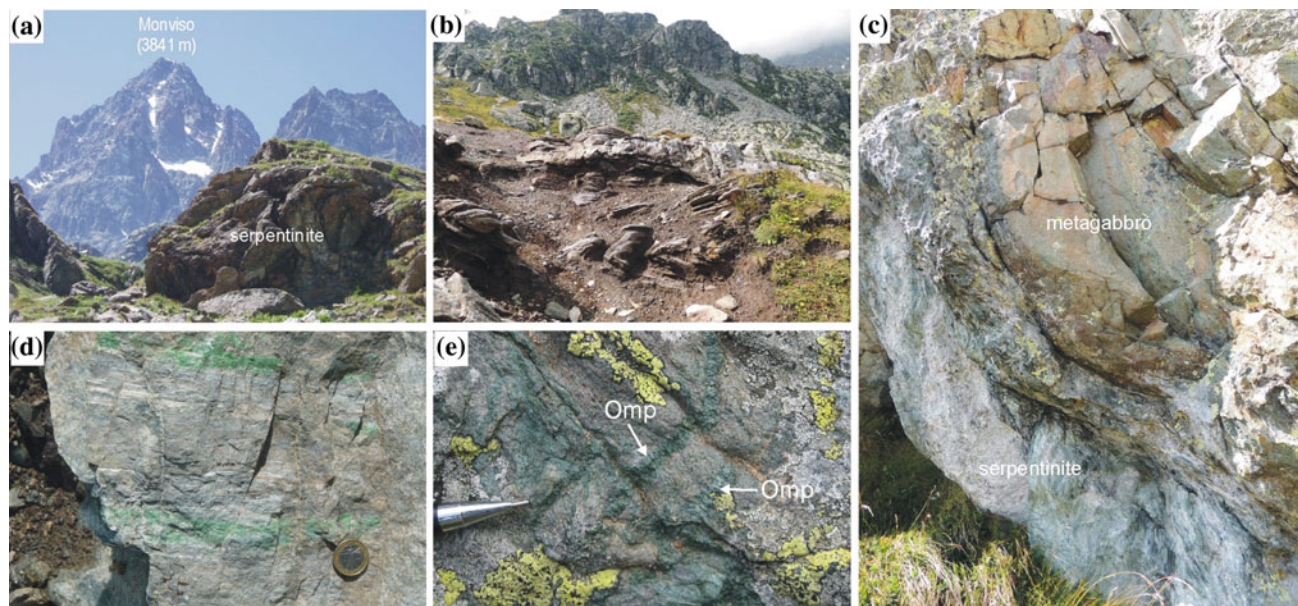


**Fig. 40.2** **a** Stop 2: outcrop of serpentinite of the Basal Serpentinite Unit above Pian del Re; **b** Stop 3: folded calcschists and impure marbles of the Basal Serpentinite Unit; **c** Stop 4: contact between serpentinite and metagabbro at Colletto Fiorenza; **d** Stop 5: smaragdite

metagabbro at Lago Chiaretto; **e** Stop 8: eclogite-facies omphacite-bearing veins cross-cutting the eclogitic FeTi-oxide metagabbro foliation

very rare worldwide—and witness the fluid migration during subduction (Fig. 40.2e). They contain mostly Na-pyroxene and minor garnet, rutile and apatite. In tension gashes, most pyroxene is fibrous.

### 40.3 Perspectives

A number of authors developed different methodologies and techniques for identifying, characterizing and managing geoheritage at the national, international and global scale (e. g. Wimbledon 1996). There is general agreement that the first and essential starting point for the geoconservation of geological heritage and geosites has to be an inventory of suitable resources and their detailed characterization and evaluation. Inventory and evaluation procedures play a decisive role on the implementation of subsequent conservation, valuing and monitoring of the geological heritage and may correspond to a sort of “Basic Geoconservation” (Henriques et al. 2011).

The inventory of a number of different geosites at the MOG, is provided here and further discussed by Rolfo et al. (2014). As concerning the geological concepts and geodiffusion interests we aim: (i) to show, describe and explain the preserved evidence of the fossil ocean; (ii) to explain the birth and development of an orogenic chain. Planned geodiffusion actions include concepts and design of geologic paths along the most interesting and representative cross

sections, mostly devoted to show features of the palaeo-ocean floor.

After these first steps, further actions described in detail by Giardino et al. (2012) will include coupling of scientific concepts and techniques, together with products focused either on geosites and also on museum collections, science exhibits and nature trails.

Moreover, within the research project “PROactive management of GEOlogical heritage in the PIEMONTE region”, multimedia and virtual reality approaches are planned, for imaging and communicating this unique natural heritage to an audience as broad as possible. Last but not least, further activity steps are the development of geodiversity action plans, including educational impacts and promotion of a “geodiversity economics”.

### References

- Castelli D, Compagnoni R, Lombardo B, Angiboust S, Balestro G, Ferrando S, Groppo C, Hirajima T, Rolfo F (2014) Crust-mantle interactions during subduction of oceanic & continental crust. *Geol Field Trips* 6(1.3):1–73. ISSN: 2038–4947 doi:10.3301/gft.2014.03
- Coleman RG (1977) Ophiolites: ancient oceanic lithosphere?. Springer Verlag, Berlin, p 229
- Giardino M, The PROGEO-Piemonte Research Team (2012) A multidisciplinary research project for developing a PROactive management of GEOlogical heritage in the PIEMONTE Region. *Geologia dell’Ambiente Suppl* 3:196–197

- Henriques MH, Pena dos Reis R, Brilha J, Mota T (2011) Geoconservation as an emerging geoscience. *Geoheritage* 3:117–128
- Lagabrielle Y, Cannat M (1990) Alpine Jurassic ophiolites resemble the modern central Atlantic basement. *Geology* 18:319–322
- Lombardo B, Nervo R, Compagnoni R et al (1978) Osservazioni preliminari sulle ofioliti metamorfiche del Monviso (Alpi Occidentali). *Rend Soc It Mineral Petrol* 34:253–305
- Nadeau S, Philippot P, Pineau F (1993) Fluid inclusion and mineral isotopic compositions (H-O-C) in eclogitic rocks as tracers of local fluid migration during high-pressure metamorphism. *Earth Planet Sci Lett* 114:431–448
- Piccardo GB, Rampone E, Romairone A, Scambelluri M, Tribuzio R, Beretta C (2001) Evolution of the ligurian Tethys: inference from petrology and geochemistry of the ligurian ophiolites. *Per Mineral* 70:147–192
- Rolfo F, Benna P, Cadoppi P et al (2014) The Monviso massif and the Cottian Alps as symbols of the alpine chain and geological heritage in Piemonte, Italy. *Geoheritage*, in press. doi:[10.1007/s12371-014-0097-9](https://doi.org/10.1007/s12371-014-0097-9)
- Wimbledon WAP (1996) GEOSITES, a new IUGS initiative to compile a global comparative site inventory, an aid to international and national conservation activity. *Episodes* 19:87–88

# The Morainic Amphitheatre Environment: A Geosite to Rediscover the Geological and Cultural Heritage in the Examples of the Ivrea and Rivoli- Avigliana Morainic Amphitheatres (NW Italy)

Stefania Lucchesi, Franco Gianotti, and Marco Giardino

## Abstract

The Ivrea Morainic Amphitheatre (IMA), at the Aosta Valley outlet, and the Rivoli-Avigliana Morainic Amphitheatre (RAMA), at the Susa Valley outlet, are the two main and well preserved Pleistocene end moraine systems of the North-Western Italian Alps. These two morainic amphitheatres are geosites containing high environmental, naturalistic, landscape and cultural values. The comparison between the geological and geomorphological features of the two amphitheatres evidenced that they can be considered a *unicum* and a “not renewable resource”. Analyses of the relationships between man and the morainic environment put in evidence synergies and conflicts, exploitation and conservation in relation to geodiversity. A deeper knowledge of the territory within a holistic approach allows to increase a sense of responsibility towards it, to favour better perception of the environmental problems and to develop proper engineering solutions for territorial planning.

## Keywords

Ivrea morainic amphitheatre • Rivoli-Avigliana amphitheatre • Geoheritage • Geosites • Cultural landscape

## 41.1 Introduction

Morainic amphitheatres are geosites containing high environmental, naturalistic, landscape and cultural values. We considered two morainic amphitheatres in the Piemonte Region (NW Italy, Fig. 41.1), two of the most significant examples of Pleistocene end moraine systems in the Alpine

area for their well-preserved morphology and size. The Ivrea Morainic Amphitheatre (IMA) and the Rivoli-Avigliana one (RAMA) are similar for genesis, stratigraphical and geomorphological setting, and for geological, ecological and cultural significance: indeed each shows particular and sometimes unique features.

A deep and holistic interaction between man and nature has been developed in these places since ancient times. A good knowledge on their resources and vulnerable assets is essential for safeguarding and valorizing these significant alpine Quaternary geosites, especially nowadays that the growing urbanization and the exploitation of natural resources are often responsible for vulnerability rise and landscape/ecosystem defacing. We analyzed synergies and conflicts between exploitation and conservation of geodiversity in the area. Particularly, we considered the geological and geomorphological elements of the morainic amphitheatres not only having naturalistic and scientific meaning, but also representing social, economic and cultural values.

S. Lucchesi (✉) · F. Gianotti · M. Giardino  
Dipartimento Di Scienze Della Terra, Università Di Torino,  
Via Valperga Caluso 35, 10125 Turin, Italy  
e-mail: srstefanialucchesi@libero.it

F. Gianotti  
e-mail: franco.gianotti@libero.it

M. Giardino  
e-mail: marco.giardino@libero.it

S. Lucchesi  
National Research Council—IRPI, Strada Delle Cacce,  
10135 Turin, Italy

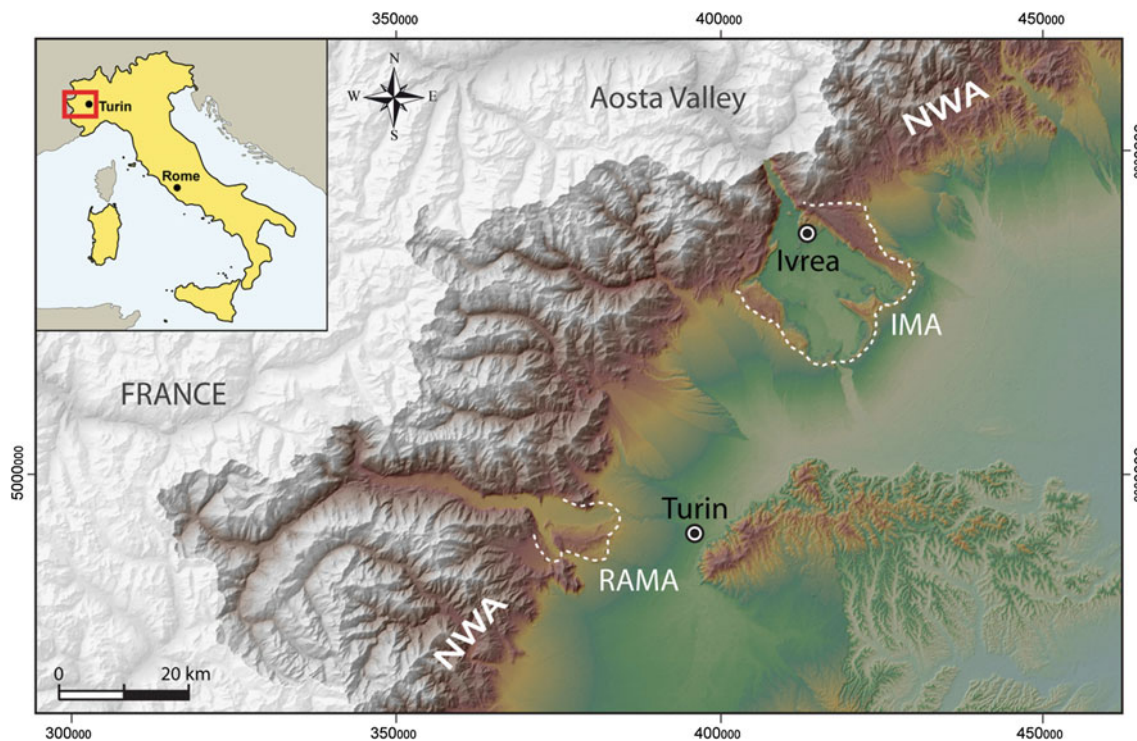


**Fig. 41.1** Location of the Ivrea morainic amphitheatre (IMA) and of the Rivoli-Avigliana morainic amphitheatre (RAMA) in the North-Western Italian Alps (NWA)

## 41.2 The Geological and Geomorphological Contexts

The IMA extends for over 500 km<sup>2</sup> in the Piedmont plain at the NNW-SSE trending Aosta Valley outlet. The Ivrea town lies into its internal depression, where 20 km<sup>2</sup> wide sub-glacially-molded rocky reliefs outcrop. The RAMA is located some tens of km southward, at the W-E trending Susa Valley outlet. It is smaller than the IMA (nearly 100 km<sup>2</sup>), but it is particularly significant because of its closeness to the Turin town. The building of the two morainic amphitheatres covers a long time from the end of the Lower Pleistocene (about 900 ky BP) to the end of Upper Pleistocene (around 20 ky BP), but their post-glacial modelling proceeded till present (Gianotti et al. 2008).

## 41.3 The Interaction Between Man and Morainic Amphitheatre

Bedrock geology and hills morphology conditioned local human settlements, activities, usages and traditions. Historical data indicate inhabitants during some periods pursued a substantial agreement with their territory, learning to well-managing its natural resources. On the contrary other periods

showed a break in the balanced man-nature relationships, with consequences also for life quality.

In Table 41.1 are described some of these different relationships between the glacial environment and man, the cultural meaning of different landforms and deposits and how they have changed in time.

### 41.3.1 Cultural Meaning of Glacial Landforms

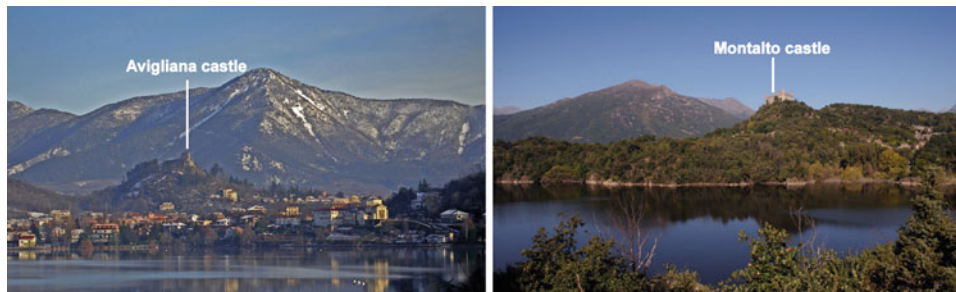
Moraines are lengthened reliefs constituted by glacial deposits. They can represent effective geographical boundaries between different peoples and cultures (e.g. the Serra moraine in the IMA, separating Canavese and Biellese territories), strategic locations for castle or guard towers (e.g. the Rivoli castle in the RAMA) and healthy rises for the human settlements over the marshy plains below.

Striated roches moutonnées mark the expansion of past glaciers and indicate their flow direction. Because of their peculiar forms, they became foundation sites of significant historical (e.g. the Avigliana castle in the RAMA, Montalto castle in the IMA, Fig. 41.2) or religious (e.g. the Sacra di San Michele in the RAMA) buildings.

Erratic blocks (more than 100 inventoried and protected in the RAMA), now useful for scientific purposes (datings

**Table 41.1** Classification of glacial landforms and deposits according to their scientific and past and present-day cultural meanings

	Scientific meaning	Cultural meaning -Past	Cultural meaning -Present day
Moraines	Trace of glacial phases	Geographical boundaries Strategic military locations Healthy rises for human settlements	Boundaries between peoples and local cultural heritages
Roches moutonnées	Trace of glacial flow	Foundation of strategic sites for military and religious purposes	Historical and religious sites
Erratic blocks	Datings of glacial phases	Stone quarries Sites for magic rites	Touristic and sporting (bouldering) sites
Lakes	Palaeo-environment and palaeoclimate indicators	Prehistoric settlements Fishing sites Sites for hemp cultivation	Naturalistic parks, touristic and sporting sites
Inter-morainic valleys	Traces of ancient spill way channels	Fertile cultivated land Drinking water exploitation Easy passes and local roads	Local roads or industrial areas Preservation of historical trails
Fluvioglacial gravels	Indicator of cataglacial environment	Building inert material Placers exploited for gold	Building inert material
Silty sediments	Indicator of cataglacial environment	Exploited for the pottery production	Quarries Artificial lakes
Peat bogs	Indicator of palaeo-lakes infilling	Industrial exploitation of material	Settlement of industrial areas Naturalistic areas and parks

**Fig. 41.2** On the *left* the Avigliana castle on the morainic ridge bordering the Avigliana lake in the RAMA; on the *right* the Montalto castle on the morainic ridge bounding the Sirio Lake in the IMA

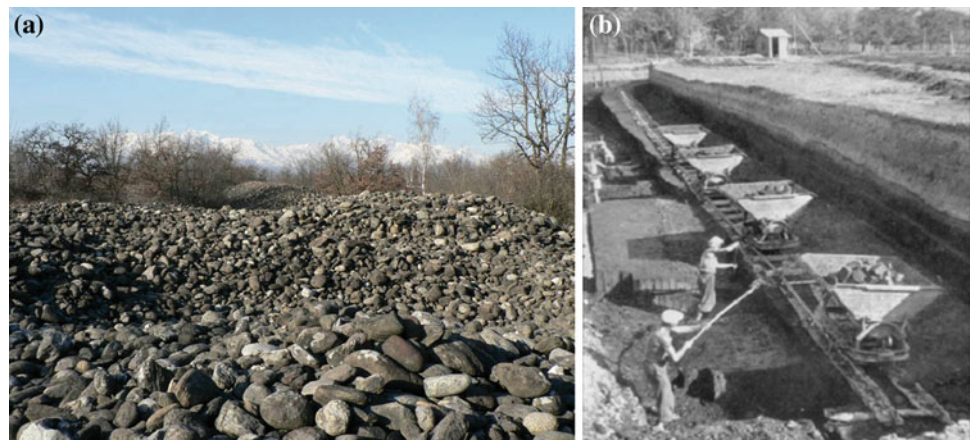
and reconstruction of past glacial advances), had always been considered important for man: in the past they have been easily exploited as stone quarries, so that most boulders got lost, or they have been regarded as mysterious objects suitable for religious or magic rites (e.g. the cupelled surfaces of Truc Monsagnasco in RAMA, Lorzán and Zubiena in IMA). Now the largest blocks are frequented for touristic and sporting purpose (bouldering).

The numerous intermorainic lakes (Avigliana in the RAMA; Viverone, Sirio, Candia, Bertignano, Alice, Meugliano in the IMA) or the lakes hosted into subglacial rocky hollows, are not only significant features concerning geomorphology and hydrology but also important as naturalistic and touristic-sporting sites. In the past, their

shores hosted prehistoric settlements (villages built on piles at Viverone and Avigliana), were frequented for fishing and also became suitable places for the hemp cultivation.

The intermorainic valleys, where fluviglacial streams flowed (“spill way”), corresponding to long plains between two moraines, became cultivated land, sites of water exploitation for drinking use (e.g. the Sangano aqueduct), favorable places for local roads or industrial areas (Avigliana ironwork industries). The passes across a moraine derived from the floodway of the ancient melt-out waters then have been crossed by important roads (as the Roman route for Gallia and the actual highway through the IMA) or by historical trail (Franks trail) or country paths.

**Fig. 41.3** Two examples of environment exploitation: the accumulations of rounded cobbles and boulders are the wastes of the Bessa Roman gold mine dump in the IMA (a); the Condove industry exploiting the peat bog of the RAMA, active till the middle of the XX century



### 41.3.2 Cultural Meaning of Glacial Deposits

Concerning the amphitheatre-forming deposits, materials of different genesis and lithofacies are exploited for their economic and social value.

Fluvioglacial gravels are commonly used as building inert material, but during the Roman occupations many alluvial placers around the IMA were intensively exploited for gold (where the Bessa aurifodinae are the main placer, with mine dumps 10 km<sup>2</sup> wide; Fig. 41.3a) (Baio and Gianotti 1996).

Ancient aeolian silts (loess) and silty alluvial sediments, partially weathered into clay by pedogenesis, were extensively exploited for the pottery production (“terracotta”, bricks, tiles and crockery), as many kiln ruins testify. Today a few big quarries are active on the highest terraced outwash plains (Fogliizzo and Carisio in the IMA and Alpnigano in the RAMA).

The peat bogs represent the final filling up of palaeo-lakes; they were almost all intensively exploited especially during the second half of the nineteenth-century, in a few cases by a real industrial activity (e.g. at San Giovanni dei Boschi in the IMA and at Condove in the RAMA and at Alice, Fig. 41.3b).

## 41.4 Conclusions

The comparison between the geological and geomorphological knowledge of the IMA and RAMA amphitheatres and the analysis of human activities within their territory evidenced some peculiar characteristics for the relationships between man and the morainic environment. Unique geological and geomorphological contexts are tied up with peculiar climatic and environmental conditions: they made each site as a *unicum* and a “not renewable resource”.

Some of the georesources exploited in the morainic amphitheatre in the past (e.g. the Bessa aurifodinae), later on have been neglected, becoming real enigmas to be interpreted. Their recent rediscovery enacted their definition as

cultural resources. Both in the past aurifodinae and in the present-day geomorphological landscape there exist some ethical implications to their exploitation: for the massive gold extraction, the Romans forced local people to pay their taxes by means of their labor. Today we exploit to the limit of the sustainability the landscape and natural resources, with the risk of exhausting those not renewable, to jeopardize those renewable for future generations.

In a context of engineering planning and environmental impact is therefore important to consider also the social and cultural value, even if hardly quantifiable, of the geological and geomorphological heritage that can be involved in the realization of such works.

To mature in a holistic approach of the territorial engineering it is necessary to find again the sense of relationship, affiliation and reciprocity that binds man to his own territory: this awareness increases a sense of responsibility towards the man “house-Earth”, favors the perception of the environment as a space where man is not only living, but a vital place to be inhabited, of which taking care and with which establish a synergic relationship (Lucchesi and Giardino 2012). Man is not the last of the exploiters of the resources, but he himself is a resource able to operate changes for the best (Simon 1981), also through new technologies and strategies of mitigation and reduction of the damages.

## References

- Baio M, Gianotti F (1996) Studio geologico e giacimentologico dell’area della “Bessa” (Biella, Italia). *Geol Insubrica* 1(1–2):29–48
- Gianotti F, Forno MG, Ivy-Ochs S, Kubik PW (2008) New chronological and stratigraphical data on the Ivrea Amphitheatre (Piedmont, NW Italy). *Quatern Int* 190:123–135
- Lucchesi S, Giardino M (2012) The role of geologists in cultural and human progress. In: *Geoethics and geological culture. Reflections from the Geoitalia conference 2011*. *Ann Geophys* 55(3) (Special issue). doi:10.4401/ag-5535
- Simon JL (1981) *The ultimate resource*. Princeton University Press, Princeton

Ludovic Ravanel, Philip Deline, and Xavier Bodin

---

## Abstract

Geomorphosites in high alpine areas show limited development of their geoheritage because of the heavy constraints to their use. Moreover, they are extremely vulnerable to global warming: glaciers and permafrost areas are currently affected by major changes due to the increasing temperatures. Research on alpine geomorphosites needs the use of methods of high-resolution topography. Among them, the Light Detection And Ranging (LiDAR) and particularly the Terrestrial Laser Scanning (TLS) plays a particular important role. Carried out on nearly 40 high altitude sites across the Alps since the beginning of the 2000s, this method is particularly interesting for the recognition and development of high-alpine geomorphosites. Indeed, it can be implemented for both identifying and characterizing the geomorphic objects (survey, monitoring, mapping), helping planning policies and protection (patterns of development/adaptation), and serving the geotouristic development.

---

## Keywords

High alpine geomorphosites • Terrestrial laser scanning • Rock glacier • Rockwall • Geotourism

---

## 42.1 Introduction

A geomorphological geotope—a geomorphosite—refers to a landform with a particular value (scientific, cultural, economic, etc.) due to human perception and/or exploitation (Panizza 2001). In high-alpine areas (>2000 m a.s.l.), where glacier and permafrost are evidences of a specific range of glacial, periglacial, and even supra-glacial processes, very few landforms are recognized as geomorphosites because of

access, recognition and valorisation difficulties (see Martin et al. 2010). The rapidly evolving geomorphological conditions of those areas (Kaab et al. 2007), especially because of the global warming, can severely impact any geomorphosites.

Capturing the glacio-geomorphological changes that affect the high mountain cryosphere is a challenging task. An accurate, robust, repeatable and flexible methodology has to be designed that must also support harsh environmental conditions without perturbing the studied object. Laser scanning, which directly collects dense point clouds, appears as particularly advantageous in mountain regions, especially in high mountain where rough surfaces make topographic surveys often difficult.

Here we raise the question of the interest in the Terrestrial Laser Scanning (TLS) techniques to recognize, characterise and valorise the high-alpine geomorphosites (Ravanel et al. 2014).

---

L. Ravanel (✉) · P. Deline · X. Bodin  
EDYTEM Lab, University of Savoie–CNRS, Le Bourget Du Lac,  
Chambéry, France  
e-mail: Ludovic.Ravanel@univ-savoie.fr

L. Ravanel  
Institute of Geography and Durability, University of Lausanne,  
Lausanne, Switzerland

## 42.2 Method and Use

TLS is an innovative method in the field of topography but is still poorly used to monitor the dynamics of high mountain rock slopes (Rabatel et al. 2008) or rock glaciers (Avian et al. 2009; Bodin et al. 2008). The time of flight of the laser beam allows measuring distances of several hundred meters with centimeter accuracy. It allows quickly surveying large areas with very high resolution and accuracy and provides high quality 3D models, which diachronic comparison authorizes the measurement of morphological changes (Abellan et al. 2006; Oppikofer et al. 2008). TLS appears as a promising technology despite its limitations (weight of equipment, cost of scanners and processing softwares, and high processing time).

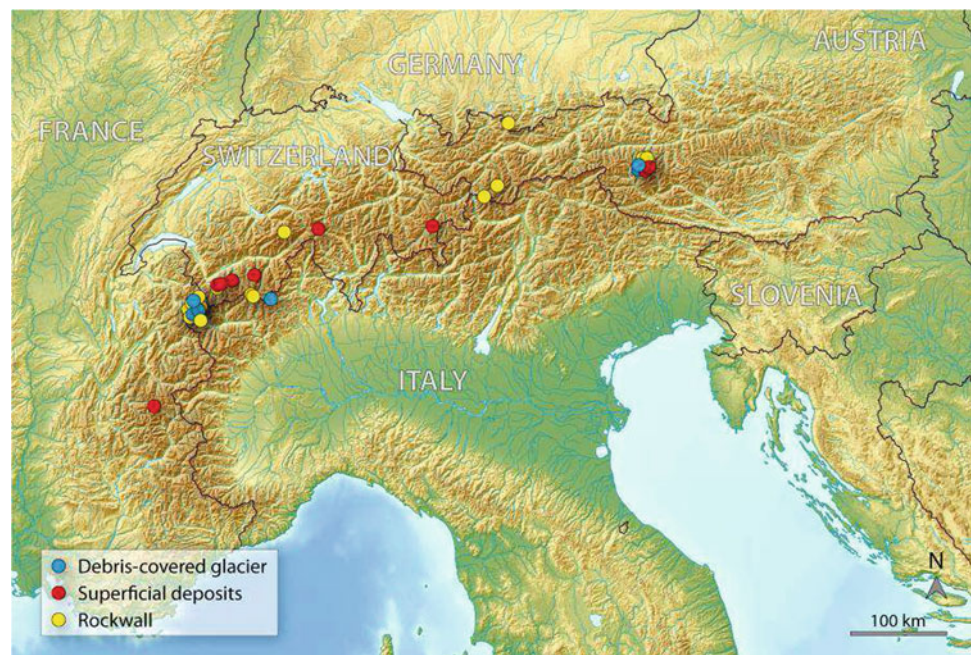
According to our inventory of studies and work in progress using TLS, the method was/is used on around forty sites (not necessarily geomorphosites) through the Alps, mainly in Austria, France and Switzerland (Fig. 42.1).

These sites correspond to some of the major landforms of the periglacial, glacial and supra-glacial belts in the Alps. These are mainly debris-covered glaciers (Avian and Bauer 2006; Bauer et al. 2006; Conforti et al. 2005), superficial deposits i.e. rock glaciers, screes and moraines (Bauer et al. 2003; Avian et al. 2009; Otto et al. 2012; Ravelin et al. in rev.) and rockwalls (Rabatel et al. 2008; Martelli et al. 2008; Oppikofer et al. 2008; Deline et al. 2009; Kenner et al. 2011; Ravelin et al. 2011, 2013; Viero et al. 2012; Fey et al. 2012, Hartmeyer et al. 2012). Such landforms, beside their aesthetic value for most people that come into high mountain, are evidences of specific processes and indicate the present (or past) state of climate and/or glacio-geomorphic systems.

## 42.3 What the Method Can Bring to High-Alpine Geomorphosites?

A geomorphosite has tangible and intangible components (Regolini 2012). It is therefore necessary, for a possible geomorphosite, to assess these two components and TLS can help. Generally, landforms that are TLS surveyed are thought to be active. Scientific issues prevailing in determining sites which have to be topographically modeled are oriented on processes in action, glacial processes and peri- or supra-glacial processes in high mountain. When TLS is not carried out in a monitoring purpose, scientific issues focused on processes are however present. In the realm of geoheritage recognition and valorization, TLS constitutes a very precious complement of the observation, which is one of the bases of the scientific reasoning in geomorphology, often followed by mapping. In the characterization of the tangible component of a landform, TLS indeed provides the finest possible information on its spatial settings and gives access to various embedded scales of interpretation. The possibility of 3D visualization of geomorphic objects greatly improves the inspection capabilities of scientists. What is qualified as intangible refers to scientific and additional values of a geomorphosite. Since a scientific issue predates to any TLS measurements, all sites where TLS is carried out could therefore be considered as geomorphosites. Nevertheless, all sites are not necessarily geomorphosites, especially in high mountain where access and development conditions differs from the valley floors. About scientific values, we follow Reynard (2009) who mentions for example the importance of the scarcity.

**Fig. 42.1** High alpine (>2000 m a.s.l.) study sites where TLS is used (Ravelin et al. 2014)



The morphodynamics of the active sites can pose difficulties for the management of geomorphosites. Processes that affect them can indeed destroy the sites and/or pose a threat to human activity and infrastructures. Geomorphosites vulnerability affects both their tangible and intangible components (Regolini 2012). In its tangible form, the vulnerability is expressed by the modification of a site. The origin of this change can be natural or anthropogenic. High mountain geomorphosites are particularly vulnerable because of the presence of ice. The detailed study of the processes and factors influencing the spatial and temporal evolution of a site allowed by TLS is therefore often relevant to better manage a dynamic site. Consequences of the melting of mountain glaciers and the permafrost degradation on the natural and cultural heritages have not yet been studied in detail, and only preliminary studies have been conducted to date (e.g. Haeberli 2008). The TLS method helps to identify and quantify the evolution of the glaciated areas and possibly leads to the production of landscape evolution models. These models can afterwards be used by local authorities and tourism infrastructure managers to determine patterns of development/adaptation. Among geomorphosites which are monitored by TLS, rapid change of some of them—possibly seen as destruction—can enhance their scientific value.

Whether it is related to geoconservation or geotourism, the development of a geomorphosite involves many initiatives. Any development activity implies communication between specialists and non-specialists through personal or impersonal (exhibitions, brochures, maps, etc.) media (Regolini 2012). Even if TLS seems to have never been carried out in the only purpose of developing a geomorphosite, it can be of great service. On the one hand, the TLS—and in particular the TLS monitoring—allows to better characterize and understand the site to develop. On the other hand, 3D models themselves can easily be used to help the development of a geomorphosite. They can be the basis for scientific, educational and popularization documents. 3D models can appear on brochures, exhibition panels or panels installed outdoor to help reading landscape (aids to interpretation). These 3D models can also be used in geomatic and multimedia tools. Such tools are becoming more and more frequent (Ghiraldi et al. 2010; Giardino et al. 2010). The use of new technologies is indeed growing rapidly.

## 42.4 Conclusions

TLS is undergoing fast progresses in geosciences. The opportunity of acquiring 3D information of natural objects with such high accuracy and high spatial resolution is opening up new ways of investigations about geomorphosites in high alpine areas where such sites are still misunderstood or low developed.

Until today, this method has been carried out on around 40 high altitude sites across the Alps since the beginning of the 2000s, mainly on debris-covered glaciers, superficial deposits and rockwalls. Usually responding to questions on physical processes, this method may also get involved for questions on geomorphosites at different levels: identification/characterization, planning policies and protection, and geotouristic development.

With global warming and associated accelerating processes, we presume that TLS will be a recognized method in the near future for evaluating and developing geomorphosites.

## References

- Abellan A, Vilaplana JM, Martinez J (2006) Application of a long-range terrestrial laser scanner to a detailed rockfall study at Vall de Nuria (Eastern Pyrenees, Spain). *Eng Geol* 88:136–148
- Avian M, Bauer A (2006) First results on monitoring glacier dynamics with the aid of terrestrial laser scanning on Pasterze Glacier (Hohe Tauern, Austria). *Grazer Schriften der Geographie und Raumforschung* 41:27–36
- Avian M, Kellerer-Pirklbauer A, Bauer A (2009) LiDAR for monitoring mass movements in permafrost environments at the cirque Hinteres Langtal, Austria, between 2000 and 2008. *Nat Haz Earth Syst Sci* 9:1087–1094
- Bauer A, Paar G, Kaufmann V (2003) Terrestrial laser scanning for rock glacier monitoring. In: *Proceedings of the 8th international conference on permafrost, Zurich*, p 55–60
- Bauer A, Kaufmann V, Kellerer-Pirklbauer A, Avian M, Paar G (2006) Terrestrial laser scanning for glacier monitoring: a comparison to standard geodetic and photogrammetric methods, and documentation of the glacier retreat of Goessnitzkees (Schober group, Austria) between 2000 and 2005. In: *Abstract of the 9th international symposium on high mountain remote sensing cartography, Graz, Austria*, p 1
- Bodin X, Schoeneich P, Jailliet S (2008) High-resolution DEM extraction from terrestrial LiDAR topometry and surface kinematics of the creeping alpine permafrost: the Laurichard rock glacier case study (southern French Alps). In: *Proceedings of the 9th ICOP, vol 1. Fairbanks, Alaska*, p 137–142
- Conforti D, Deline P, Mortara G, Tamburini A (2005) Terrestrial scanning LiDAR technology applied to study the evolution of the ice-contact Miage lake (Mont Blanc, Italy). *Report on the Joint ISPRS Com. VI, WG IV/4*, p 5
- Deline P, Bolhert R, Coviello V, Cremonese E, Gruber S, Krautblatter M, Jailliet S, Malet E, Morra di Cella U, Noetzli J, Pogliotti P, Rabatel A, Ravel L, Sadier B, Verleysdonk S (2009) L'Aiguille du Midi (massif du Mont Blanc) : un site remarquable pour l'étude du permafrost des parois d'altitude. *Collection EDYTEM* 8:135–146
- Fey C, Zangerl C, Haas F, Rutzinger M, Sailer R, Bremer M (2012) Rock slide deformation measurements with Terrestrial Laser Scanning in inaccessible high mountain areas. *Geophys Res Abs* 14:11944–1
- Ghiraldi L, Coaratta P, Marchetti M, Giardino M (2010) GIS and geomatics application for the evaluation and exploitation of Piemonte geomorphosites. In: *Regolini-Bissig G, Reynard E (eds) Mapping geoheritage. Geovisions* 35:97–113
- Giardino M, Perotti L, Carletti R, Russo S (2010) Creation and test of a mobile GIS application to support field data collection and mapping

- activities on geomorphosites. In: Regolini-Bissig G, Reynard E (eds) Mapping geoheritage. *Geovisions* 35:115–127
- Haerberli W (2008) Changing view of changing glaciers. In: Orlove B, Wiegandt E, Luckman BH (eds) Darkening peaks: glacier retreat, science and society. University of California Press, Los Angeles, pp 23–32
- Hartmeyer I, Keuschnig M, Delleske R, Schrott L (2012) Reconstruction of the Magnetkoeפל rockfall event—Detecting rock fall release zones using TLS, Hohe Tauern Austria. *Geophys Res Abs* 14:12488
- Kaab A, Chiarle M, Raup B, Schneider C (2007) Climate change impacts on mountain glaciers and permafrost. *Glob Plan Change* 56:7–9
- Kenner R, Phillips M, Danioth C, Denier C, Thee P, Zraggen A (2011) Investigation of rock and ice loss in a recently deglaciated mountain rock wall using TLS: Gemsstock. *Swiss Alps Cold Reg Sc Tech* 67:157–164
- Martelli D, Alberto W, Tamburini A (2008) Rilievi laser scanner nell'ambito del Progetto Interreg IIIA Alcotra n. 196 PERMAdatROC. IMAGEO S.r.l., unpublished report.
- Martin S, Regolini G, Perret A, Kozlik L (2010) Elaboration et evaluation de produits geotouristiques. *Propositions methodologiques Teoros* 29:55–66
- Oppikofer T, Jaboyedoff M, Keusen HR (2008) Collapse at the eastern Eiger flank in the Swiss Alps. *Nat Geosc* 1:531–535
- Otto JC, Keuschnig M, Gotz J, Marbach M, Schrott L (2012) Detection of mountain permafrost by combining high resolution surface and subsurface information. *Geogr Ann A* 94:43–57
- Panizza M (2001) Geomorphosites: concepts, methods and example of geomorphological survey. *Chi Sc Bull* 46:4–6
- Rabatel A, Deline P, Jaillat S, Ravanel L (2008) Rock falls in high-alpine rock walls quantified by terrestrial LiDAR measurements: a case study in the Mont-Blanc area. *Geophys Res Let* 35:L10502
- Ravanel L, Deline P, Jaillat S (2011) Quatre annees de suivi de la morphodynamique des parois rocheuses du massif du Mont Blanc par laserscanning terrestre. *Collection EDYTEM* 12:69–76
- Ravanel L, Deline P, Lambiel C, Vincent C (2013) Instability of a highly vulnerable high alpine rock ridge: the lower Arete des Cosmiques (Mont Blanc massif, France). *Geogr Ann A*. doi:10.1111/geoa.12000
- Ravanel L, Bodin X, Deline P. (2014) Using terrestrial laser scanning for the recognition and valorisation of high-alpine geomorphosites. *Geoheritage*. 6(2):129–140
- Ravanel L, Lambiel C, Jaboyedoff M, Oppikofer T. (in review) Terrestrial laser scanning monitoring of a highly vulnerable moraine at the Gentianes Pass (2894 m a.s.l., Valais Alps, Switzerland). *Arc., Antarc., Alpine Res.*
- Regolini G (2012) Cartographier les geomorphosites. *Geovisions* 38:294
- Reynard E (2009) Geomorphosites: definitions and characteristics. In: Reynard E, Coratza P, Regolini G (eds) *Geomorphosites*. Munchen, p 63–71
- Viero A, Furlanis S, Squarzoni C, Teza G, Galgaro A, Gianolla P (2012) Dynamics and mass balance of the 2007 Cima Una rockfall (Eastern Alps, Italy). *Landslides* doi:10.1007/s10346-012-0338-4

Heldal Tom and Meyer Gurli

---

## Abstract

In addition to displaying geological features, stone quarries may provide important ‘pools of knowledge’ of ancient technology, social organisation, trade and communications. Since many quarry landscapes were exploited over thousands of years, quarries can also be ‘indicators’ of important events or changes in society: there are many stories to quarries that deserve to be told. As with many mining sites, quarries tend to fall between two chairs regarding conservation and management. The exercise of viewing quarries and quarry landscapes from different angles do lead to a path along which the value of such sites can be analysed. This may lead to a better appreciation of such sites and initiate better conservation strategies and management practises.

---

## Keywords

Geoheritage • Stone • Quarries

---

## 43.1 Introduction

It is no coincidence that active or abandoned stone quarries frequently are mentioned in geological field guides. Quarries are often important sites for displaying geology, in having more or less fresh cuts into the bedrock that elsewhere may be difficult to find. But stone quarries may also display other values that may be relevant in a geoheritage context, and in particular when taking a more holistic view of such sites as heritage objects. The richness and significance of quarry sites can only be fully acknowledged if an assessment take into account other perspectives, such as the why’s and how’s that made people go to large efforts in extracting stone.

In the present paper, we explore different perspectives that can be used in the assessment of quarry sites. In addition to various geoheritage assessment systems (i.e., dos Reis and

Henriques 2009) we have used a characterisation method for quarry sites as described by Heldal (2009) and archaeological and historical methods for statement of significance given by Bloxam (2009; see also Bloxam and Heldal 2007).

---

## 43.2 Geology and Resource

In addition to being good showcases of for instance stratigraphic sections, stone quarries also describe the interaction between humans and a geological resource within a short or long period of time. An outstanding example is found at the Aswan West bank, Egypt. Silicified sandstone has been subject to quarrying from the Middle Palaeolithic until the present day (Heldal 2009). The numerous layers of quarries display the importance of this resource throughout the whole human history; from Achulian flake industries, 16000 years of saddle quern production, ornamental stone production in Dynastic Egypt and the Roman Period, to building-stone in modern times. Hence, this quarry site display a complete record of human evolution mirrored in one particular stone resource (Fig. 43.1a).

---

H. Tom (✉) · M. Gurli  
Geological Survey of Norway, 6315 Sluppen, 7491 Trondheim,  
Norway  
e-mail: tom.heldal@ngu.no

**Fig. 43.1** Quarries and quarry landscapes. **a** Saddle quern quarries at the Aswan West bank, Egypt, **b** high-mountain millstone quarries in Central Norway, **c** depiction of the Aix en Provence sandstone quarries by Cezanne, **d** the ‘unfinished obelisk quarry’, Aswan, Egypt, **e** sunken marble quarry at Aliki, Thassos, **f** sandstone gallery quarry, Egypt



Millstone quarrying in Norway did, for 1300 years, engage resources of porphyroblastic mica schist (Grenne et al. 2008), due to the bimodal distribution of hard and softer minerals, causing sufficient relief on grinding surfaces for grinding cereals efficiently. This particular geological resource made Norwegian millstone production unique compared with the rest of Europe. Adding ancient quarries for the production of baking slabs (greenschist; Baug 2013) and cooking pots (soapstone), a complex of resources (and quarries) emerges, all dedicated to the processing and making of food.

### 43.3 The Human Impact: Technology, Use and Historical Significance

Stone quarries contain marks from tools and other traces of the people working in them. These tell us about the production process and the available technology at the time of

extraction. The introduction of iron tools in Egyptian granite quarrying in the Roman Period can be read in the quarries (Klemm and Klemm 2008).

The purpose of stone quarrying is to produce tools and utensils, buildings and monuments. The significance of a quarry site is thus strongly linked to the application of the stone. The quarries employed for constructing the medieval cathedral in Trondheim, Norway, do not only draw importance from this national monument, but also add value to the monument itself, through visualizing the organisation behind the stone procurement system for the cathedral (Storemyr et al. 2010). Similarly, the quarries used for constructing the pyramids in Egypt may deserve outstanding global heritage values for that reason alone (Bloxam and Heldal 2007).

A wide distribution of stones from a quarry site may add more value to it than simply local use, as is the case for many Greco-Roman quarry sites in the Mediterranean (Lazzarini 2004). The link between the giant columns of the Pantheon in

Rome and tonalite gneiss quarries far out in the Egyptian desert are among the most impressive links (Peacock and Maxfield 1997). Quarries may be a primary source for constructing a city, such as Portland stone for London and brownstone for New York. Bloxam (2009) defines such connections between quarries and cities, monuments or distribution areas as ‘contact landscapes’, underlining the importance of such perspectives in the assessment of quarry sites.

The introduction of rotary querns to Norway probably represent a turning point in food production—bread baking became common practice. This introduced a 1300 years quarrying of rotary querns and millstones (Fig. 43.1b). In the 10th Century AD (Baug 2013) water mills were probably introduced in Norway, making another turn on the technology wheel, and the most likely sites to find solid evidence are the quarries. Thus, the quarries associate to important societal changes.

The association of quarries to a specific period or culture may add significant value to such sites. The Hyllestad Millstone quarry, western Norway, has a strong component of Viking Age quarries (Baug 2013). For this reason, the quarry has been selected as a part of a transnational, serial nomination of Viking world heritage sites. Similarly, quarries all over the world are reflections of a dynamic and changing society, of lost civilizations and technologies, of wars, architectural evolution, progress and regress.

---

### 43.4 Symbols and Monuments

Saddle quern quarries in Australia did not only have a practical function, but the procurement of such items were carried out within a powerful symbolic framework: the quarries were important steps along the dream path (McBryde 1997). In Ancient Egypt, solar symbolism reached great heights in the New Kingdom, resulting in exploitation of red and yellow rocks for statues and obelisks; the colours of the sun (Bloxam et al. 2007). The floors in the mortuary temples in front of Old Kingdom pyramids were made from black basalt, symbolising the life-giving mud of the Nile. The Roman stone quarrying in the Eastern Desert in Egypt during the 2nd and 3rd centuries AD can be viewed as a manifestation of imperial power; the display of Egyptian stones in Rome became a symbol of that power (Peacock 1992).

The monumental sandstone quarries in the hillside above Aix en Provence had probably gone into oblivion if wasn't for the artist Cezanne, who immortalised them with his paintings (Fig. 43.1c). Because of his fascination, one can now walk through the quarries that made the city grow from the Roman Period onwards.

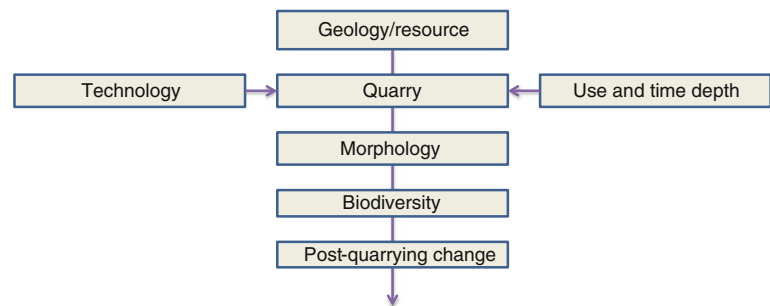
Also for us, stone quarries are often impressive, human made features, either due to the evidence of extreme human efforts or extreme reshaping of the landscape. The ‘Unfinished Obelisk’ quarry in Aswan, Egypt, is a monument of itself. The unfinished granite obelisk is 42 m tall and would have weighed 1,100 tons if finished (Fig. 43.1d). At Aliko, Thassos, a white marble peninsula has been completely removed by quarrying from the Archaic Greek to the Byzantine Period, leaving an impressive monument (Fig. 43.1e). So do numerous underground gallery quarries (Fig. 43.1f). However, not only the ornamental quarries from the ancient world appear impressing. In a Norwegian high-mountain area, 1,500 millstone quarries over a distance of 30 km construct a unique landscape of stone procurement (Grenne et al. 2008).

---

### 43.5 The Post-Quarrying Quarries

Quarrying operations transform landscapes by making deep cuts in the bedrock, turning or removing the soil and leaving huge heaps of debitage from quarrying. Quarries tend to create anomalies in the surrounding nature, that can give birth to new and deviating ecosystems. A nature reserve in western Norway (deciduous forest) proved later to be a result of long forgotten millstone quarrying, were the fine debitage from stone dressing created conditions for these trees to grow. Bats populates underground quarries, and water filled deep quarries may represent a completely new type of habitat in an area. Bétard (2013) gives a case study of biodiversity in hard rock quarries in Northern France. In many cases, the geological processes after quarrying can be as interesting as the ones that created the stone resource. The sole of the above mentioned marble quarry at Thassos is now below sea level, displaying evidence of earthquake movement. In the same quarry, debitage from working has been cemented to an anthropogenic conglomerate. The sole of a Mesolithic to Neolithic stone axe quarry in western Norway is found 4 m above sea level, illustrating the post-glacial rebound of the land. Quarries are particularly well suited for weathering studies, since they often provide good dating of one or several stages when the rock was fresh. The Widan el-Faras basalt quarry in Faiyum, Egypt, makes a stunning example. Old Kingdom (c. 4700 years BP) and Roman Period quarrying mark two starting points for weathering in a desert environment. The results are surprising; The Old Kingdom basalt pieces has suffered a complete loss of surface and deterioration of large blocks to piles of cobbles. The Roman stones do still keep their original shape, but have a centimetre thick, discoloured rim.

**Fig. 43.2** Possible path for assessing values of ancient stone quarries



### 43.6 Conclusion

The exercise of viewing quarries and quarry landscapes from different angles do lead to a path along which the value of such sites can be analysed. This may lead to a better appreciation of such sites and initiate better conservation strategies and management practises. As proposed by dos Reis and Henriques (2009), the assessment of geoheritage sites should include cultural and aesthetic aspects in addition to the educational and research values. Quarries may provide good examples of such challenges, how a combined and holistic assessment may add new pieces to a framework of values. Figure 43.2 gives a simplified assessment path: the geology and resource as the target for quarrying, the re-shaping of the landscape by quarrying aided by specific technologies and driven by a particular use of the stone. The quarry may define a unique biological habitat, and post-quarrying geological processes may have changed the site later. Hopefully, quarry sites will be more acknowledged, as natural or cultural monuments—or geocultural heritage.

### References

- Baug I (2013) Quarrying in Western Norway—an archaeological study of production and distribution in the Viking period and the middle ages. Ph.D. thesis, University of Bergen (ISBN 978-82-308-2363-7)
- Bétard F (2013) Patch-scale relationships between geodiversity and biodiversity in hard rock quarries: case study from a disused quartzite quarry in NW France. *Geoheritage* 5(2):59–71
- Bloxam EG, Haldal T (2007) The industrial landscape of the Northern Fayum desert as a World heritage site: modelling ‘outstanding universal value’ of 3rd millennium BC stone quarrying in Egypt. *World Archaeol* 39(3):305–323
- Bloxam E, Haldal T, Storemyr P, Kelany A, Degryse P, Bøe R, Müller A (2007) Characterisation of complex quarry landscapes; an example from the West Bank Quarries, Aswan. Report QuarryScapes, EU FP6 INCO-MED, 015416/Deliverable 4, p 275
- Bloxam EG (2009) New directions in identifying the significance of ancient quarry landscapes: four concepts of landscape. In: Abu-Jaber N, Bloxam EG, Degryse P, Haldal T (eds) *QuarryScapes: ancient stone quarry landscapes in the Eastern Mediterranean*. Geological Survey of Norway Special Publication 12:165–183
- dos Reis RP, Henriques MH (2009) Approaching an integrated qualification and evaluation system for geological heritage. *Geoheritage* 1(1):1–10
- Grenne T, Haldal T, Meyer GB, Bloxam, E (2008) From Hyllestad to Selbu: Norwegian millstone quarrying through 1500 years. In: Slagstad T (ed) *Geology for society*. NGU Special publication 11, Norway, pp 47–66
- Haldal T (2009) Constructing a quarry landscape from empirical data. General perspectives and a case study at the Aswan West Bank, Egypt. In: Abu-Jaber N, Bloxam EG, Degryse P, Haldal T (eds) *QuarryScapes: ancient stone quarry landscapes in the Eastern Mediterranean*. Geological Survey of Norway Special Publication 12, Norway, pp 125–155
- Klemm R, Klemm DD (2008) *Stones and quarries in Ancient Egypt*. British Museum Press, London
- Lazzarini L (2004) *Pietre e Marmi Antichi: Natura, Caratterizzazione, Origine, Storia D’uso, Diffusione, Collezionismo*. CEDAM
- McBryde I (1997) The landscape is a series of stories. Grindstones, quarries and exchange in Aboriginal Australia: a Lake Eyre case study. In: Ramos-Millán A, Bustillo MA (eds) *Siliceous rocks and culture*. Editorial Universidad de Granada, Granada, pp 587–607
- Peacock DPS (1992) *Rome in the desert: a symbol of power*. Inaugural Lecture, University of Southampton
- Peacock D, Maxfield V (1997) *Mons Claudianus Survey and Excavation 1987–1993*. Vol. I. Topography and Quarries, Cairo, Institut Français d’Archéologie Orientale. Fouilles de l’IFAO, 37
- Storemyr P, Lundberg N, Østerås B, Haldal T (2010) Arkeologien til Nidarosdomens middelaldersteinbrudd. In: Bjørlykke K, Ekroll Ø, Syrstad Gran B (eds) *Nidarosdomen – ny forskning på gammel kirke*. Trondheim: Nidaros Domkirkes Restaureringsarbeiders forlag

# Multimedia and Virtual Reality for Imaging the Climate and Environment Changes Through Earth History: Examples from the Piemonte (NW Italy) Geoheritage (PROGEO-Piemonte Project)

E. Giordano, A. Magagna, L. Ghiraldi, C. Bertok, F. Lozar, A. d'Atri, F. Dela Pierre, M. Giardino, M. Natalicchio, L. Martire, P. Clari, and D. Violanti

## Abstract

The dissemination of the knowledge of critical geological issues, such as past environmental and climate change and their correct placement in the geological time scale, is essential to rise the awareness of the huge potential impact of the Earth Sciences on the current and future generations. We selected two examples (the Marguareis and the Langhe and Monferrato areas) to disseminate these topics to a broad audience. Virtual tours, hosted on the PROGEO-Piemonte project website ([www.progeopiemonte.it](http://www.progeopiemonte.it)), have been developed with special care to educational purposes and made suitable for mobile devices. These allow us to overcome theoretical problems related to the complexity of geological items (spatial and evolutionary complexity, deep time dimension), with plain language explanations, detailed pictures and dynamic 3D models. The virtual visit overcomes practical difficulties, such as restricted access to high mountain or dangerous areas, and improves the access to detailed geological information at different scales, not readily available in the outcropping rocks. Dynamic or static information, stored on the website, are available on Google Earth or Google Maps in the field (mobile navigation) or at home (PC-based navigation). The virtual tours thus become an alternative to the visit on site, or a tool for deepening knowledge before or after the visit. This is especially helpful for schools, because virtual tours could be used in classroom with many different goals. The virtual tours, once accessed on-line by many visitors, will in turn push public administrators to realize geotouristic facilities on site and fund educational projects on these important issues.

## Keywords

Geoheritage • Geological time • Virtual tour • Education • Geotourism

## 44.1 Introduction

The multidisciplinary research project “PROGEO-Piemonte” (PROactive management of GEOlogical heritage in the Piemonte region; Ferrero et al. 2012) is funded by the University of Torino and the Compagnia di San Paolo and aims to achieve a new conceptual and operational discipline in the management of the geological heritage of Piemonte by means of the development of techniques for recognizing and managing its rich geodiversity at the local and regional scale. Among the main goals of the project is the dissemination of geological knowledge and concepts to the general public, teachers and pupils, and public administrators. In fact,

E. Giordano (✉) · A. Magagna · C. Bertok · F. Lozar · A. d'Atri · F. Dela Pierre · M. Giardino · M. Natalicchio · L. Martire · P. Clari · D. Violanti

Dipartimento di Scienze della Terra, Università degli Studi di Torino, via Valperga Caluso 35, 10125 Turin, Italy  
e-mail: [enrico.giordano@unito.it](mailto:enrico.giordano@unito.it)

M. Giardino  
e-mail: [marco.garden61@gmail.com](mailto:marco.garden61@gmail.com)

L. Ghiraldi  
Museo Regionale di Scienze Naturali di Torino, Via Giolitti 36, 10123 Turin, Italy

knowledge of geological heritage could improve awareness of “the huge potential within the Earth Sciences to create a healthier, safer and wealthier society” (de Mulder et al. 2006) among local communities as well as among occasional visitors.

In order to disseminate the knowledge on past environmental and climate change issues, we selected two examples within the geological heritage of Piemonte, i.e. the stratigraphic successions exposed in the Marguareis area (Maritime Alps, SW Piemonte), and in the Langhe and Monferrato areas (SW Piemonte). In both areas, geological tours have been developed to disseminate their geological content to a broad audience. These have been developed as virtual tours and are hosted on the PROGEO-Piemonte project website ([www.progeopiemonte.it](http://www.progeopiemonte.it)); they have been developed with special care to educational purposes and made suitable for mobile devices. Moreover, the digital virtual tours allow to overcome the different theoretical and practical problems related to the development of geological fieldtrips.

#### 44.2 Geological Tours: Theoretical and Practical Problems

Theoretical difficulties related to the development of geological fieldtrips involve complexity of geological items; to be fully understood (King 2008), the latter need:

- high level spatial ability (3D visualization)
- ability to visualize the geological objects at different scale (micro- to macro-scale)
- awareness of the deep time dimension involved.

The field only approach (mesoscale) does not favour the visualization at larger or smaller scales of the outcropping objects and of their peculiar features, nor their integration in the regional picture or in the correct time frame, usually very far from human time perception.

Main practical problems related to the development of geological fieldtrips are:

- accessibility of the selected sites
- their spatial and evolutionary complexity.

In fact, several sites, among those proposed, are not easily accessible or should be restricted to the general public for two main reasons: dangerous or rough terrains, or sites needing conservation (e.g. fossiliferous sites). Nevertheless, these sites have significant cultural contents, highly valuable for the community, and deserve dissemination. Thus the development of virtual geological tours is suitable to overcome the possibly limited physical and cultural skills of the users and the restricted access of several sites.

← Back

**Codice: IT - PP3**  
**Nome: Pollenzo**



**Ubicazione: Pollenzo**  
**Tipologia: Escursione a piedi**  
**Lunghezza: 700 m**  
**Dislivello: 0 m**  
**Partenza: 44°41'9.16"N 7°55'35.66"E**  
**Arrivo: 44°41'12.83"N 7°54'57.32"E**  
**Numero Tappe: 1**

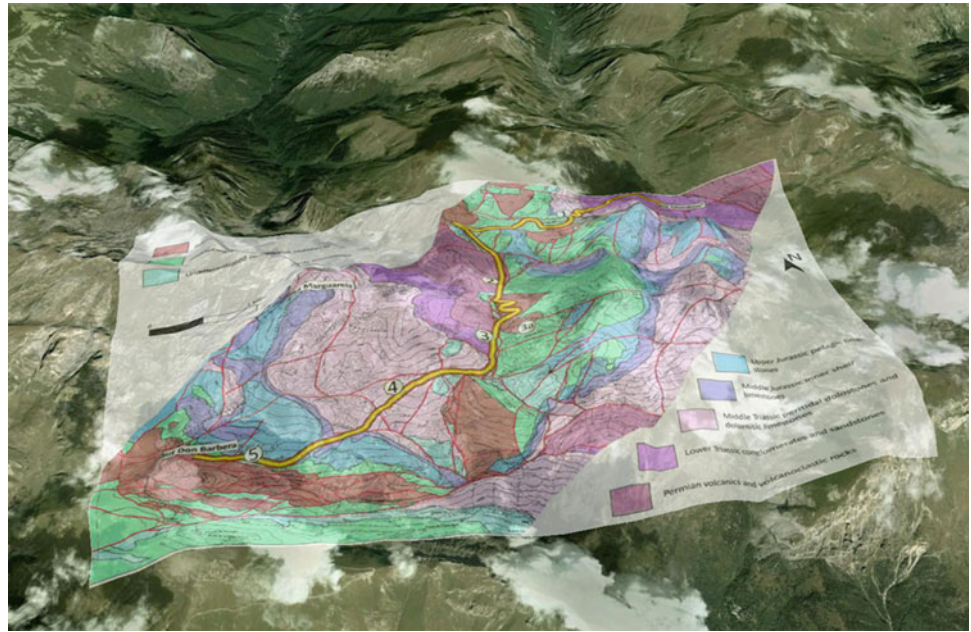
**Descrizione:** This tour illustrates the events occurred from 5.971 to 5.332 Million years ago. We take the visitors through the discovery of the rock record that testifies this dramatic regional scale environmental change, which involved the whole Mediterranean Sea, with the progressive isolation of the latter from the Atlantic Ocean, causing profound changes in the geosphere, the biosphere and the microclimate. The dramatic environmental and climatic changes occurred during a relatively short time interval during the Messinian (from 7.2 to 5.332 Million years ago), are known to the specialists as the Messinian salinity crisis; these changes are recorded in the rock record of the Tertiary Piedmont Basin and in several other localities around the Mediterranean region. These rocks show that a deep marine basin full of life (as testified by marine fishes and microplankton fossils) in

**Fig. 44.1** The Marguareis geo-tour displayed on Google Earth

#### 44.3 Foreseen Solutions

Development of dynamic virtual tours has been selected, among other more traditional solutions such as static geological maps, as the best tool to overcome the above mentioned problems. The geological tours in the Langhe and Monferrato and Marguareis areas include some easy to visit sites, characterized by a high grade of accessibility and enjoyable both to the general public and to the geological expert, and some other sites, highly valuable for the scientific community, but not easy to approach for the general public. The virtual visit enables a gradual knowledge deepening to both kind of sites: plain language explanations,

**Fig. 44.2** Example of a caption on Google Maps



detailed pictures and dynamic 3D models are available to both the general public and the expert visitors; moreover, both the expert visitors and those wishing to improve their geological knowledge have the option to access more detailed information on the subject, such as scientific publications. In general, the availability of digital material allows people to virtually visit these interesting sites and, at the same time, to gather more information about their cultural content. This different communication would eventually increase the awareness of people about the value of the geological heritage and of its importance for the society and will provide the opportunity to acquire information about the territory, both on site and at home.

Several different IT tools have been analysed in order to select those more suitable to develop geological virtual tours, keeping in mind that:

Each tour is composed of many stops, indicated with tracks and points on a map;

Each stop is provided with photographic material, including field pictures, panoramic photographs, as well as microscopic images and, eventually, drawings, schemes and 3D models;

Interactive photographs have been realized, where main geological features are underlined; these queried objects contain detailed information not directly readable from the landscape.

Materials are available both online and offline, so that they could be used in many different situations and with different tools. Besides, a downloadable and printable PDF version of the tours is offered.

Nowadays there are many tools that can meet these needs, but we think that the best ones are Google Earth or Google Maps for three fundamental reasons:

- easy to program;
- easy to use;
- mass-diffusion.

The Google Maps API lets to embed Google Maps in the project web pages. The API also provides a number of utilities for manipulating maps and adding content to the map through a variety of services (Butler 2006; Martin and Ghiraldi 2011).

The production of virtual tours follows the process specified below:

- Collecting data—it includes data collection on the ground, bibliographic research and remote sensing;
- Analysis—the analysis is performed through a GIS in order to get vector files (a point for each stop, a line for each track and a polygon for the geological map);
- Visualization—the files produced are converted into KML format so that they can be used on the web mapping software;
- Dissemination—all the material produced is published on the website through the creation of a relational database and /or Google © Fusion table.

Google maps API (Advanced Programming Interface) joined with programming language as javascript and HTML allows the customization of the default interface adding specific tools for performing query and visualizing personalized thematic maps (e.g. geologic and geomorphologic maps). The option of connecting to external data sources, downloading pictures and descriptions, etc., will allow experts to access a large amount of information, whereas the general public will take advantage of a free tool for deepening its geological knowledge. The geological features are described with plain, but scientifically rigorous, language. Different levels of visitor expertise are expected, so the

information is provided with free access from the basic to the top scientific level. Virtual tours and their related information are thus enjoyable on-site, from home or in classroom. The use of smart devices allows direct access to information stored in the PROGEO-Piemonte website, or via QR-codes readable on panels in each geosite or on tour-guides that will be provided by the local tourist boards (Figs. 44.1 and 44.2).

#### 44.4 Conclusions

Geological time and climate and environmental change themes are perfectly addressed by the two proposed virtual tours (Bertok et al. 2014; Lozar et al. 2014): the stratigraphic successions exposed in the Marguareis area document the deep time evolution of a sector of the European margin of the Mesozoic Tethys ocean; the outcrops selected in the Langhe and Monferrato regions record the Messinian time, a crucial interval of dramatic environmental and climatic changes, not only in the Piemonte region but also in the whole Mediterranean area.

In the Marguareis area the virtual tour runs through rocks of different nature (volcanic and sedimentary), and depositional environment (continental alluvial plains, carbonate tidal flats, deep sea basins); they provide the solid record of a very long time span (from Permian to Eocene: over 200 million years). On the whole, these rocks record the main stages of the geological evolution of the European margin related to the opening and closure of the Alpine Tethys ocean and consequent genesis of the Alpine chain. The proposed tour, moreover, enables to show how the stratigraphic successions may be discontinuous with prolonged gaps, and how the occurrence of ancient faults may be documented by the geometrical relationships between rock bodies. The tour is located within the protected area of the Marguareis Park and can be easily integrated in the park touristic activities.

The Messinian Salinity crisis (MSC) is a major palaeoceanographic event which occurred some 6 Ma ago during the late Miocene; it was characterized by dramatic palaeobiological, palaeoenvironmental, and palaeoclimatic changes that affected the whole Mediterranean area. Messinian rocks outcropping in the Piedmont Basin record the three MSC stages and the correlative environmental and climate changes. Focusing on the rock record of these changes, we aim to improve people knowledge and awareness of environmental modification and past climate variability and to address the crucial question whether it could happen again in the future.

In conclusion, the PROGEO-Piemonte project is developing virtual tours on two crucial geological issues (geological time and climate and environmental changes), with the aim to disseminate geological knowledge and enhance people awareness, thus improving the effective integration among general public and members of the geological, educational and ICT (Information and Communications Technology) communities.

The information stored on the website, both dynamic or static ones, are available from home via PC-based navigation and on site on mobile devices, and could be an alternative to the real visit on site, or a tool to deepen the knowledge before or after the visit. This fruition is especially interesting for schools, because virtual tours could be used in classroom with many different goals (e.g. preparing a field trip, deepening a topic, studying the Piemonte landscape, using maps etc.).

Moreover, the realization of virtual tours is much less expensive than traditional on-site equipment of geo-itineraries, thus overcoming present fund shortening for educational and touristic activities.

We hope that the virtual tours, once accessed on-line by many visitors, will push public administrators to realize geotouristic facilities on site (panels, panoramic view points, etc.) and informative materials (leaflets, tour-guides), and fund educational projects dealing with such important issues.

#### References

- Bertok C, d'Atri A, Martire L, Barale L, Piana F, Vigna B (2014) A trip through deep time in the rock succession of the Marguareis area (Ligurian Alps, South Western Piemonte). *Geoheritage* doi:10.1007/s12371-013-0096-2
- Butler D (2006) Virtual globes: the web-wide World. *Nature* 439:776–778
- de Mulder EFJ, Nield T, Derbyshire E (2006) The international year of planet Earth (2007–2009): Earth sciences for society. *Episodes* 29 (2):82–86
- Ferrero E, Giardino M, Lozar F, Giordano E, Belluso E, Perotti L (2012) Geodiversity action plans for the enhancement of geoheritage in the Piemonte region (North-Western Italy). *Ann Geophys* 55(3):487–495
- King C (2008) Geoscience education: an overview. *Study Sci Educ* 44 (2):187–222
- Lozar F, Clari P, Dela Pierre F, Natalicchio M, Bernardi E, Violanti D, Costa E, Giardino M (2014) Virtual tour on past environmental and climate changes: the Messinian succession of the Tertiary Piedmont Basin (Italy). *Geoheritage* doi:10.1007/s12371-014-0098-8
- Martin S, Ghiraldi L (2011) Internet au service du patrimoine. Cartographie dynamique de l'inventaire des géotopes d'importance nationale. Les géosciences au service de la société, Actes du colloque en l'honneur du Professeur Michel Marthaler, 24–26 juin 2010. *Géovisions* 37:106–117

# Relationships Between Geoheritage, and Environmental Dynamics in the Tanaro Valley (NW Italy): Geological Mapping and Geotourist Activities for a Proper Management of Natural and Cultural Landscapes

E. Giordano, M. Natalicchio, L. Ghiraldi, M. Giardino, F. Lozar, and F. Dela Pierre

## Abstract

This paper analyzes a cultural landscape in the SW sector of the Piemonte region, along the Tanaro riverside, where the relationships between geo-resource and human activities are evident and give rise to landscapes of great cultural value but also to some environmental issues. A geo-tour allows us to deal with different topics based on geological and geomorphologic aspects, and gives special emphasis to the relationships between 'Earth's resources' and human activities. The illustration of the stratigraphic, sedimentologic and micropalaeontologic characteristics of the sediments exposed along the trail allows us to illustrate the complex palaeoenvironmental and palaeoclimatic changes that affected the study area during the Messinian Salinity Crisis. Moreover from the geomorphologic analysis of the present landscape it is possible to decipher its recent evolution and to evaluate the risks connected with the touristic fruition, thus improving the potential use of anthropogenic landforms for geo-environmental education.

## Keywords

Landscape • Geo-resources • Messinian salinity crisis • Tanaro river

## 45.1 Introduction

The UNESCO Convention for the Protection of the World Cultural and Natural Heritage defines 'cultural landscapes' as the product of the combined action between nature, man and their changing relationship over time, under the influence of internal and external forces. The enhancement of these cultural landscapes, as well as the recognition of the risks they are exposed to, both for the natural degradation

and the social changes, led to the development of several actions at different scales of survey, management and protection.

Italy contains a remarkable diversity of cultural landscapes (1) designed and created intentionally by man, (2) composed of only natural elements or (3), as usual, combining the interaction between the previous ones. Some landscapes are included in and protected by the World Heritage list, but many others should be further analyzed, protected and valued to avoid the risk of loss of the local landscape as fundamental cultural value of the memory of the relationship between human beings and nature.

The aim of this paper is to analyze a cultural landscape in the SW sector of the Piemonte region, along the Tanaro riverside. Here the relationships between nature (as geo-resource) and human activities are evident and give rise to landscapes of great cultural value but also to some environmental issues.

E. Giordano (✉) · M. Natalicchio · M. Giardino · F. Lozar · F. Dela Pierre  
Earth Sciences Department, University of Turin, Turin, Italy  
e-mail: enrico.giordano@unito.it

M. Giardino  
e-mail: marco.garden61@gmail.com

L. Ghiraldi  
Natural Sciences Museum of Turin, Turin, Italy

**Fig. 45.1** The Pollenzo geosite is threatened by the fluvial erosion; for this reason only the right bank is easily accessible and with safety



The multidisciplinary research project ‘PROGEO-Piemonte’ (PROactive management of GEOlogical heritage in the Piemonte region) is funded by the University of Torino and the Compagnia di San Paolo and aims to achieve a new conceptual and operational discipline in the management of the geological heritage of Piemonte through the development of techniques suitable for recognizing and managing its rich geodiversity at the local and regional scale and is now addressing the subject of this paper (Ferrero et al. 2012).

## 45.2 Study Area Overview

The examined area includes part of the SW Piemonte region between Narzole and Monticello d’Alba. It is drained by the middle-lower part of the Tanaro river (tributary of the Po river) locally flowing from south-west to north-east; the area is bounded by the Roero hills to the north, by the Langhe hills to the east and by a series of alluvial terraces to the west.

From the geological point of view the study area is located in the Langhe basin which is part of the Tertiary Piedmont Basin, filled with a thick succession of marine sediments spanning the Middle Eocene-Messinian time interval. In particular, the area is composed of fossiliferous marine sands, clays, marls and gypsum formations and of fluvial deposits. Here geological studies have mainly addressed the sedimentological characteristics of the Miocene and Pliocene formations and their palaeontological content. These sediments record the Messinian Salinity Crisis, a major palaeoceanographic event that affected the whole Mediterranean basin around 6 Ma ago, leading to dramatic palaeoenvironmental, palaeobiological and palaeoclimatic changes (Clari et al. 2008) and currently the subject of a major scientific debate. In this area the rock record shows that in less than one million years deep marine environments were replaced by shallow marine and fluvial

environments (Colombero et al. 2013); the end of the Crisis is testified by the return to deep marine conditions.

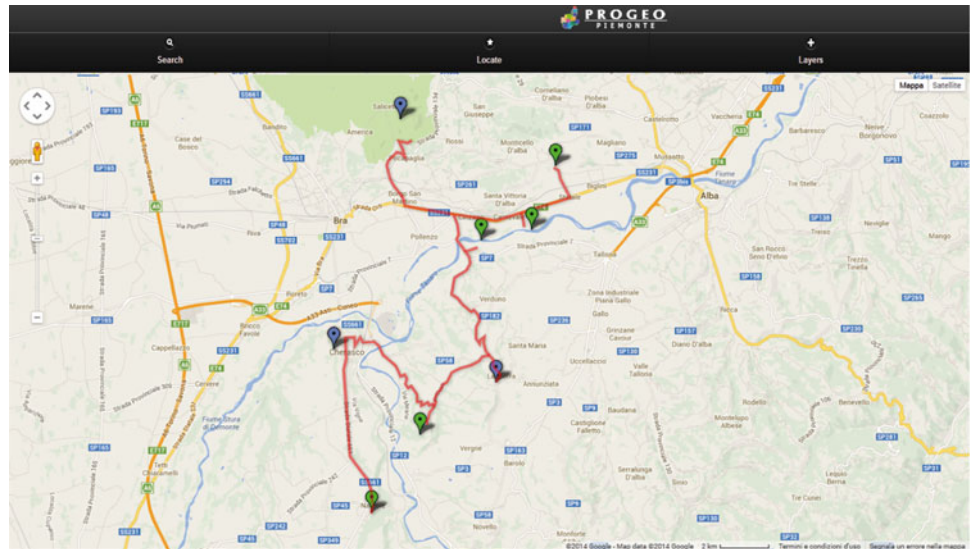
Moreover, the study of the effects of these changes in the rock record and the dissemination of the results can help to improve people knowledge and awareness of environmental modification and past climate variability and to address the crucial question whether it could happen again in the future (Bernardi et al. 2010; Dela Pierre et al. 2011).

From the geomorphologic point of view, the area is located in the south-eastern part of the Cuneo plain, at the foot of the Langhe hills, where heterogeneous forms mainly related to fluvial dynamic processes, both active and relict, are observed; until the Late Pleistocene—Holocene, the river Tanaro flowed to the north into the palaeo-Po near Caramagna (Ghiraldi 2010). The following river piracy, probably happened during the last interglacial period, combined with tectonic activity and climate changes, has modified and rejuvenated the landscape. The actual morphodynamics of the area is characterized by landforms and processes influenced by slope stabilization and fluvial activity. Some geosites have been identified to simplify the reconstruction of the evolution of the area and to highlight the use of the georesources, but tourist activity could be affected by geomorphologic risks due to the instability of river slopes and abandoned quarries and to flooding events. Moreover the artificial decrease of Tanaro river-bed and the construction of roads and infrastructures, in areas previously occupied by the river, amplified dangerous flooding (Fig. 45.1).

## 45.3 Mapping Geoheritage

Knowledge of a territory necessarily implies its cartographic representation that consequently is an essential part of every geotourist activity. A geotourist map should merge tourist with simplified geoscientific information (geological and geomorphologic), suitable to facilitate the understanding of

**Fig. 45.2** A PROGEO Piemonte webpage showing the itinerary and the geosites (blue = geomorphosites, green = geosite about the MSC)



the landscape evolution. In order to disseminate information to a wider audience, virtual globe systems such as Google Maps, are recognized as important tools in geosciences research and applications. Within the PROGEO-Piemonte project website, we created a dynamic map where users can display all the geosite/geoitineraries inventoried for the project or only the levels they need (Ghiraldi et al. 2012; Lozar et al. 2014). Moreover, users can display more detailed maps (e.g. geological or geomorphologic), made specifically for some selected areas. This system also enable researchers to conveniently collaborate and share their research projects and results.

#### 45.4 The Geo-Tour

Starting in Narzole and ending in Monticello d'Alba, the geo-tour allows us to deal with different topics based on geological and geomorphologic aspects, and gives special emphasis to the relationships between 'Earth's resources' and human activities.

The observation and analysis of the geological heritage allows us to reconstruct the geological evolution of the area since the Miocene to date. Besides geology and geomorphology, the tour also allows us to understand the use of the available physical and cultural resources by the human being.

The historical analysis clarifies the human influence on the landscape management: there is an artificial decrease in the whole area of the Tanaro riverbed, a reduction and fragmentation of natural areas and an increase of infrastructures. Today, as in the past, a large number of different quarries in the valley testifies the close link between human activities and natural resources. On the other hand, the illustration of the stratigraphic, sedimentologic and

micropalaeontologic characteristics of the sediments exposed along the trail explains the complex palaeoenvironmental and palaeoclimatic changes that affected the study area during the Messinian Salinity Crisis. Moreover from the geomorphologic analysis of the present landscape it is possible to decipher its recent evolution and to evaluate the risks connected with the tourist fruition (Fig. 45.2).

#### 45.5 Conclusion

The analyses of the relationships between geoheritage, environmental dynamics and risks in the Middle Tanaro valley have been conducted by means of detailed geological mapping and interpretations. These allowed targeted planning of geotourist activities. The possibility of working in a small basin that can be used as a model for the Messinian Salinity Crisis in the Mediterranean area allowed us to develop a comprehensive model of the desiccated deep basin, contributing to the present-day strong scientific debate. Knowledge on geomorphologic evolutionary stages of the river network and present-day morphodynamic processes allowed a safe plan for the geo-trails and a proper management of natural and cultural landscapes. Making the processes that shape the morphologies at the Earth's surface understandable to a wider public and helping people to read the signs of recent or remote environmental changes might help to retain society's memory of these phenomena and therefore enhance future management and resilient behaviour. The landforms and geologic materials in the present landscape that remind, if adequately interpreted, past natural and/or human-induced changes are ideal spots for geo-environmental education and should therefore be the subject of a scientific program able to protect them and to exploit their didactic value.

**Acknowledgement** This research was conducted within the project “PROactive Management of GEOlogical Heritage in the PIEMONTE Region” ([www.progeopiemonte.it/en](http://www.progeopiemonte.it/en)) co-founded by the University of Turin—Compagnia di San Paolo Bank Foundation “JCAPC - Progetti di Ateneo 2011” grant on line B1 “Experimental Sciences and Technology” (Project Id: ORTO11Y7HR, P.I. Prof. Marco Giardino).

---

## References

- Bernardi E, Dela Pierre F, Irace A, Lozar F, Natalicchio M, Clari P, Martire L, Violanti D (2010) The Messinian sediments of the Tertiary Piedmont Basin: new data from outcrop sections. Torino 19–25 Sept. GEOSSED 2010. Post congress Field trip, p 38
- Clari P, Bernardi E, Cavagna S, Dela Pierre F, Violanti D (2008) Alba e tramonto della crisi messiniana. Alba, 10-11 ottobre 2008 Guida all’escursione, p 43
- Colombero S, Bonelli E, Kotsakis T, Pavia G, Pavia M, Carnevale G (2013) Late Messinian rodents from Verduno (Piedmont, NW Italy): Biochronological, paleoecological and paleobiogeographic implications. *Geobios* 46(1–2):111–125
- Dela Pierre F, Bernardi E, Cavagna S, Clari P, Gennari R, Irace A, Lozar F, Lugli S, Manzi V, Natalicchio M, Roveri M, Violanti D (2011) The record of the Messinian salinity crisis in the Tertiary Piedmont Basin (NW Italy): the Alba section revisited. *Paleogeogr Paleoclimatol Paleoecon* 310:238–255
- Ferrero E, Giardino M, Lozar F, Giordano E, Belluso E, Perotti L (2012) Geodiversity action plans for the enhancement of geoheritage in the Piemonte region (North-Western Italy). *Ann Geophys* 55(3):487–495
- Ghiraldi L (2010) Geomatics application for evaluation and exploitation of geomorphosites in piemonte region (NW Italy). Ph.D. thesis, school in Earth sciences system for environment, resources and cultural heritage Università di Modena e Reggio Emilia, p 204
- Ghiraldi L, Giordano E, Perotti L, Giardino M (2012) Metodologie di catalogazione, valutazione, raccolta e visualizzazione dei dati geoscientifici. Caso studio della Media Valle Tanaro (Piemonte, NW Italy). *Geologia dell’ambiente* 1:27–32
- Lozar F, Clari P, Dela Pierre F, Natalicchio M, Bernardi E, Violanti D, Costa E, Giardino M (2014) Virtual tour on past environmental and climate changes: the Messinian succession of the Tertiary Piedmont Basin (Italy). *Geoheritage* doi:10.1007/s12371-014-0098-8

Emmanuel Reynard, Christian Kaiser, Simon Martin,  
and Géraldine Regolini

---

## Abstract

Urban areas are interesting places for developing geotourism because of a large audience and connections with other forms of cultural tourism. The presence of very good communication infrastructures allows the development of geotourism products using smartphone and tablet technologies. This paper presents the objectives, the procedure for choosing and organizing the content, and the technical aspects of the GeoGuide, an application developed in the city of Lausanne (Switzerland).

---

## Keywords

Geotourism • Geoheritage • Education • Smartphone

---

## 46.1 Introduction: Urban Geotourism

Geotourism is a form of tourism—at the interface between cultural tourism and ecotourism—which proposes the tourists a set of activities, products, services and infrastructures that aim to promote Earth sciences (Hose 1996; Dowling and Newsome 2006). Geotourism is linked with geoheritage—that is geosites and geomorphosites—which constitute a large part of the sites visited by geotourists.

Even if, at the origins, geotourism was mainly focused at the discovery of natural landscapes, urban areas may also be considered as interesting places for developing geotourism for several reasons: (1) large cities and historical towns

generally propose a large offer in cultural tourism, a sector attracting quite the same public as geotourism (interest for culture in a broad sense); (2) because of their location, a large number of cities have a specific natural framework (riverside cities, coastal cities, etc.) where storytelling about the interactions between human activities and natural features is quite easy to develop (Larwood and Prosser 1996); (3) they benefit from modern infrastructures, in particular communication networks.

This paper presents an experience carried out in Lausanne (Switzerland) to promote urban geotourism through the use of smartphones and tablets. Within the framework of the 10 year celebration of the Faculty of Geosciences and Environment of Lausanne University (UNIL), it was decided to develop a set of thematic itineraries aiming to diffuse to a large public the results of research carried out in the Faculty. One of these itineraries is developed in the urban context of Lausanne. The project had two main objectives: thematic and technical. The thematic concern was to focus on the relationships existing between the geoenvironment (rocks, water and atmosphere) and urban development: objective of environmental education). The technical aspects dealt with the development of an easy-to-use application for smartphones and tablets.

---

E. Reynard (✉) · C. Kaiser  
Institute of Geography and Sustainability, University of Lausanne,  
Géopolis, 1015 Lausanne, Switzerland  
e-mail: emmanuel.reynard@unil.ch

C. Kaiser  
e-mail: christian.kaiser@unil.ch

S. Martin · G. Regolini  
Relief (Private Company), Oisillons 9, 1860 Aigle, Switzerland

## 46.2 Lausanne: Geological, Geomorphological and Urban Contexts

Lausanne's topography is quite complicated, with the presence of numerous hills, deep river valleys, and alternations of very steep and flat areas. This context has greatly impacted on the development of the town, in particular on the street networks. The geological bedrock is mainly made of sandstones and marls of the Molassic Basin dating back to the Oligocene, and in the past sandstones were intensively exploited for building stones. The geomorphology is mostly depending on glacial and fluvial processes. Former glaciers have modeled the molassic bedrock and deposited moraines, whereas rivers have incised very deep valleys.

The city of Lausanne exists since the Roman times with a former town and harbor near the shoreline of Lake of Geneva; it developed then during the Middle Ages around a defense site (a geological promontory isolated by two deep valleys). Due to intense population growth the town increased rapidly in the 19th century, and the agglomeration reaches now a population of 345,000 inhabitants (2012). Lausanne is a city particularly interesting for communicating on the close relationships existing between the geological and geomorphological frameworks and the urban activities and on the impacts of urban development on geomorphological features. For years, the University of Lausanne has, therefore, organized field trips with students in the town, and a booklet on the theme of "Urban waters" was published some years ago. This project is part of this effort to communicate on geofoms in the agglomeration.

## 46.3 The GeoGuide Project

The GeoGuide project (<http://igd.unil.ch/geoguide/>) was initiated in 2013 by the Faculty of Geosciences and Environment (FGSE) to celebrate its 10th anniversary. An original method for the selection of the content was applied, and a specific application—called GeoGuide—was developed.

### 46.3.1 Content

The global approach to non-personal interpretation that was developed for the elaboration and assessment of geotourism products (Martin et al. 2010) guided the thematic part of the application. This approach is based on recommendations for good practices in the fields of natural sciences education (Giordan 1991) and heritage interpretation (Tilden 1957; Beck and Cable 2002).

It considers four fundamental aspects and their interplay: the site and objects, the message and content of the product,

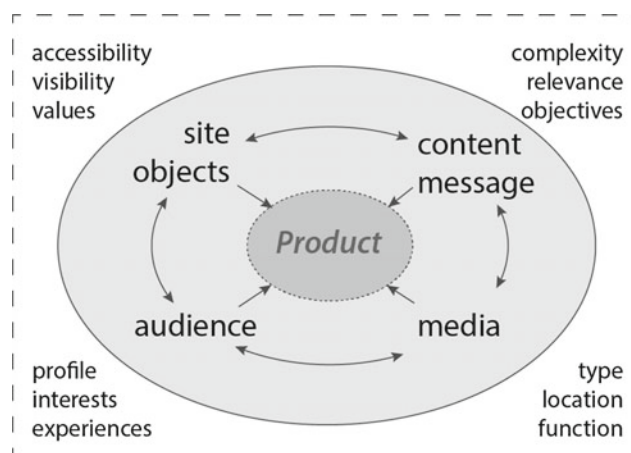


**Fig. 46.1** Four fundamental aspects interacting in the creation of a geotourist product

the media, and the audience (Fig. 46.1). The four variables are considered to be equivalent and interdependent. Therefore, each aspect has to be carefully analyzed in order to obtain a coherent product that is in line with the interests of the public and has a clearly stated communication goal.

In practice, the developers of a geotourist product are often restricted in their decision-making. The choices are limited by the financial resources or by the requirements of the customer. In the case of the GeoGuide there were two initial constraints: the general media (mobile phones and tablets) and some of the general contents (communication on the research carried out by members of the FGSE).

The general theme chosen for the application is the relationships existing between three spheres: (A) the climate, water and atmosphere; (B) the town and human activities; (C) the substratum, rocks and landscape. This highly geographical theme was intended to link the stops despite their very individual and diverse content. Each of the 30 stops focuses, therefore, on one specific relationship, e.g. alteration of the molassic rocks (relationship A C); urban development of a fluvial valley (B C); derivation of a watercourse for reducing rainwater volumes reaching wastewater treatment plants (A B), etc. In a specific menu of the application, stops can be sorted and accessed by choosing one relationship (Fig. 46.2).

As the GeoGuide is aimed at a wide, generally non-specialized, audience, some fundamental adaptations were made to allow for communication and education on rather complex and poorly known subjects. Firstly, in the main page of each stop, the information is organized in different levels of complexity: the title (attractive, not always explicit); an explanatory picture with extended legend; and the text, made as short as possible. For people with more interest, another page shows additional information, like simplified abstract of scientific papers, diagrams or references. Secondly, interpretive writing methods (Moscardo et al. 2007) were



**Fig. 46.2** The three themes of the Lausanne GeoGuide

applied for writing titles and texts: surprising statements, personal questions, invitation to observe the environment, etc. Finally, all pictures—except historical photographs—were created specifically for the GeoGuide. They are therefore always adapted to the location of the stop and strongly connected to the textual content.

The sites proposed along the itinerary are located where a particular feature can be observed, linked with the content: panorama, landform, urban object (road, bridge, park). The place is usually used as a concrete anchor for the theoretical content. This aspect relies to the objective of making non-specialist people curious about what geosciences can teach or reveal about their environment and preoccupations.

### 46.3.2 An Application for Smartphones and Tablets

Many electronic mobile guides especially in the field of tourism have already been created, and a rich literature exists on the topic (see Kenteris et al. 2011 for a review); they differentiate between application-led research and technology-led research where the former is generally done by

usability designers while the latter is typically done by software engineers. From a technical perspective, the GeoGuide project was realized through a flexible multi-platform mobile application, which can also be used as a Web application on desktop computers. It is clearly an application-led research project with focus on facilitating the communication of complex themes. During the design process, the technical requirements of the application were defined as follows:

- The application should be usable on any kind of Web-enabled device, such as smartphones with varying screen sizes (from 3-inch mini smartphone displays to 30-inch desktop screens), various tablet computers, and traditional desktop computers.
- On mobile devices, the guide can be accessed through Internet, or a native application can be installed and the complete content accessed without need for an Internet connection.
- Detailed multi-scale cartographic material for an interactive map is available, with the recommended guide route and information points displayed on the map. On mobile devices featuring some location service, such as a GPS sensor, the current position of the user is displayed directly on the map.
- The application was designed in a way to be easy to adapt to other locations, other languages, and other types of environments, for example a mountain area or a natural park.
- The thematic content was organized in several layers, and the user should be able to access the information from both the interactive map and a simple list.
- The whole application should be easy and straightforward to use. The base maps and the databases are uploaded on the mobile device when uploading the application.
- The application should be easy to extend, by adding additional features such as animations or an interactive quiz.

### 46.3.3 Strengths/Limitations and Future Perspectives

The application main strengths are the following:

- The GeoGuide is a digital medium that allows putting a lot of organized information of different types on a single device. Users can access only the needed information (for instance: localization (interactive map and GPS), text of a selected stop) and the content adapted to their interests (different levels of complexity).
- The GeoGuide is not only a mobile application, but is also accessible online, as website. The user can therefore also access the information at home, for preparing the visit, and after the trip, for accessing advanced content.

The opportunity to use the application on different platforms and different times is highly appreciated by geotourists (Martin 2013).

- The GeoGuide project is highly innovative and several novelties were developed: flexible use over the Web or by downloading a self-contained native mobile application; application usable on an extremely wide variety of devices; integrated detailed multi-scale cartographic material with use of device-specific location services for navigation purpose along with an easy access to the thematic content through both the map and list views; easy adaptation to another developing context; development as an open-source framework freely available for use in other locations or environments (available under GPL licence at <http://github.com/christiankaiser/geoguide>).
- For urban geotourism (and also for geotourism in protected areas), there is no impact in the field (panels, signs, etc.), a fact that is particularly important in towns where authorizations for adding street signs are long to obtain. The application has also some limitations:
- Room is reduced for the content (screen size, especially on smartphones), but this is also the case for educational panels (this limit is smoothed by the presence of two levels of knowledge and possibilities to download some specific material).
- At the moment, the GeoGuide uses little interactivity and augmented reality, except GPS localization, despite their potential opportunities for geotourism (Martin 2013). Adding interactive quiz and gamification might increase the attractiveness of the application and lead to better motivation and education (Prensky 2007).
- Finally, user studies need to be conducted to better understand the usability of such a system, the interest of the content for the users, and find new ways of presentation and interaction.

## References

- Beck L, Cable T (2002) *Interpretation for the 21st century. Fifteen guiding principles for interpreting nature and culture*, 2nd edn. Sagamore, Champaign
- Dowling R, Newsome D (2006) (eds) *Geotourism*. Elsevier, Amsterdam
- Giordan A (1991) La modélisation dans l'enseignement et la vulgarisation des sciences. *Impact: science et société* 41(4):337–355
- Hose TA (1996) Geotourism, or can tourists become casual rock hounds? In: Bennett MR et al (eds) *Geology at your doorstep: the role of urban geology in Earth Heritage Conservation*. Geological Society, London, pp 207–228
- Kenteris M, Gavalas D, Economou D (2011) Electronic mobile guides: a survey. *Pers Ubiquit Comput* 15(1):97–111
- Larwood JG, Prosser CF (1996) The nature of the urban geological resource: an overview. In: Bennett MR et al (eds) *Geology at your doorstep: the role of urban geology in Earth Heritage Conservation*. Geological Society, London, pp 18–30
- Martin S (2013) Valoriser le géopatrimoine par la médiation indirecte et la visualisation des objets géomorphologiques. Université de Lausanne, Institut de géographie et durabilité (Géovisions 41)
- Martin S, Regolini-Bissig G, Perret A, Kozlik L (2010) Elaboration et évaluation de produits géotouristiques. *Propositions méthodologiques*. *Téoros* 29(2):55–66
- Moscardo G, Ballantyne R, Hughes K (2007) *Designing interpretive signs. Principles in practice*. Fulcrum, Golden
- Prensky M (2007) *Digital game-based learning*. Paragon House, St. Paul
- Tilden F (1957). *Interpreting our heritage. Principles and practices for visitor services in parks, museums, and historic places*. University of North Carolina Press, Chapel Hill

---

# Methodologies and Activities to Promote Geotourism. The Case Study of the Cannobina Valley (NW Italy)

47

Luca Ghiraldi, Marco Bacenetti, Luigi Perotti, Marco Giardino,  
and Paolo Millemaci

---

## Abstract

During the last decade there has been a growing attention by citizens and public Administration towards the protection and preservation of the landscape. This has contributed to develop alternative offers including those whose main focus is related with the geological and geomorphological components of the territory. Over the last 10 years in Piemonte region several projects aimed at the definition of methodologies for collecting data, evaluating and promoting sites with geological and geomorphological interests have been carried out. This work produces a further contribution using an integrated approach combining the fundamental elements of geology and geomorphology with cultural, historical and artistic aspects of the Cannobina Valley (Piemonte, Verbania province, Italy). The main difficulties encountered during the promotional phase were, beyond the complexity of geological phenomena, also the spatial and temporal scale. For these reasons strategies and specific tools have been implemented in order to facilitate the comprehension by general public.

---

## Keywords

Geoheritage • Geotourism • Geosites • Web-Mapping

---

## 47.1 Introduction

The social, economic and cultural context that is affecting these last years, constrain the small organizations and institutions, not included in the main network of touristic offers, to plan and develop promotion and exploitation projects of their territory, integrating different resources in

order to set-up new experiences able to attract a vast and heterogeneous public. During the last decade there has been a growing attention by citizens and public administration towards the protection and preservation of the landscape and its components. This has contributed to changing the touristic offers, including within the classic historical, cultural and eno-gastronomic itineraries also those with a naturalistic and environmental focus. Among the latter a distinct sub-sector is the so called geotourism. Following the definition provided by Newsome and Dowling (2010), geotourism is a form of natural area tourism that specifically focuses on geology and landscape. It promotes tourism to geosites and the conservation of geo-diversity, contributing to increase the awareness of the importance of the Earth Sciences through appreciation and learning. Piemonte region (NW Italy) offers an extraordinary wealth of history, culture, art, legend and traditions that combined with the great heterogeneity of the landscapes makes it an ideal laboratory for testing alternative touristic offers, where the added value is the provision of interpretive and service facilities to enable

---

L. Ghiraldi (✉)  
Museo Regionale di Scienze Naturali di Torino, Via Giolitti 36,  
10123 Turin, Italy  
e-mail: luca.ghiraldi@gmail.com

P. Millemaci  
Geologist Freelance, Studio Ambiente, 103017 Cannobio,  
VB, Italy

M. Bacenetti (✉) · L. Perotti · M. Giardino  
Dipartimento di Scienze della Terra, Università di Torino,  
via Valperga Caluso 35, 10125 Turin, Italy  
e-mail: marco.garden61@gmail.com

tourists to acquire knowledge and understanding of the geological and geomorphological evolution of an area beyond the level of mere aesthetic appreciation.

## 47.2 Motivation and Goals

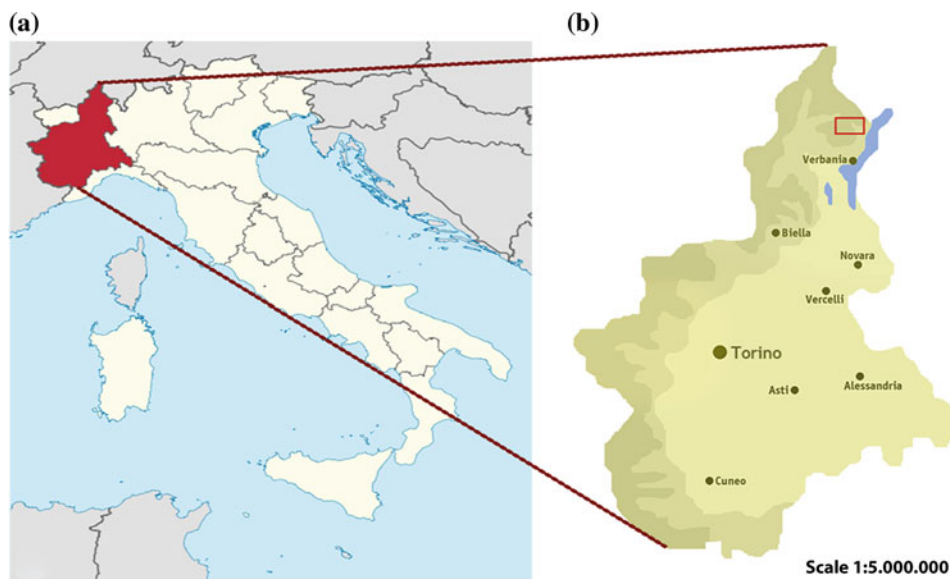
Over the last 10 years in Piemonte region several projects aimed at the definition of methodologies for collecting data, evaluating and promoting sites with geological and geomorphological interests, has been carried out by public or private organizations and institutions (Ferrero et al. 2012; Ghiraldi et al. 2012). However, in many sectors of the region such kind of activities has not yet been tested. With this work we want to produce a further contribution using an integrated approach combining the fundamental elements of geology and geomorphology with cultural, historical and artistic aspects of a territory very well known at international level for his high scientific value, but almost unknown by general public. The main goal was to make approachable, for people different for age and culture, the geology and the geomorphology of the valley and highlight how they have conditioned the life and the habit of its inhabitants.

## 47.3 Study Area

The Cannobina Valley (Verbania Province) is located in the northern sector of the Piemonte region at the border with Switzerland (Fig. 47.1), covers about 110 km<sup>2</sup> completely mountainous and did not suffer the processes of urbanization typical of other alpine valleys and for this reason has maintained a very high naturalistic value, which is added

with an equally high values of cultural and historical heritage. Furthermore the Cannobina Valley has remarkable tourist potentiality due to its position, located in the middle of an important tourist district that for the most part of the year attracts a remarkable number of visitors and because of its territory has been recently included within the boundary of the new-born Valsesia and Valgrande Geopark. The main valley has an East-West direction and opens onto Maggiore Lake. Geographically it belongs to the Lepontine Alps and it is drained by the Cannobino River and its tributaries. The valley has a length of almost 17 km and the maximum wide is 10 km. The maximum elevation is the Mount Limidario (2189 m) located on the right divide, while the Mount Zeda (2,156 m) and Mount Cimone di Cortechiuso (2,183 m) are on the left divide. Analyzing the present morphology different features derived both from glacial and river erosion can be recognized. The first are located at elevation between 600 and 1,300 m especially in the sector next to the head and to the mouth of the valley, while the latter characterize the central part of the basin where the fluvial incision shaped the valley with very steep sides and very narrow floors. From the geological point of view the Cannobina Valley belongs to the western sector of the Southern Alpine complex. It has characteristics of uniqueness since it is possible to observe with relative ease very well exposed section of intermediate and deep Earth's crust up to the border with uppermost mantle. Going along the road from Cannobio to Finero (Fig. 3.2), the main units characterizing the Hercynian basement: the "Serie dei Laghi" (SDL) and the "Ivrea-Verbano Zone" (IVZ) can be observed. Following the legend of the geological map of the Cannobina Valley (Borioni and Burlini 1995) the SDL consists of two subunits:

**Fig. 47.1** The red square shows the location of the Cannobina Valley (b) located in northern sector of Piemonte region (a)



- Strona-Ceneri: characterized by the presence of gneiss of different types;
- Scisti dei laghi: consisting mainly in micaschist and paragneiss rocks.

These units form a large fold with the gneiss of Strona Ceneri at the core and the micaschists of Scisti dei Laghi at the flanks. The IVZ outcrops at the northern and western part of the basin. The IVZ is considered a fragment of crust-mantel transition. Its outer part consists of mafic and ultramafic rocks, while the inner part is the so called Kinzigitic zone, which consists mostly of metapelites with frequent intercalation of amphibolites and pegmatite veins (Boriani et al. 1977). SDL and IVZ are separated by two tectonic lines: the Cossato-Mergozzo-Brissago and the Pogallo-Lake Orta. The first represents the oldest contact between the two units, and it is characterized by lithological contrast and the presence, both in Scisti dei Laghi and kinzigitic zone, by the intrusion of gabbro-dioritic magma: commonly known as appinitic dykes (Boriani et al. 1977). The second is located in the eastern part of the basin and seems to coincide with the boundary between the kinzigite and granulite rocks of the IVZ.

#### 47.4 Methodology

On the basis of the considerations mentioned above, a well-defined methodology (Ferrero et al. 2012; Ghiraldi et al. 2012) extensively tested in other projects has been adopted

in order to identify and select a list of sites. In addition several thematic tours whose focus is always represented by the geological and geomorphological features of the landscape have been designed. The itineraries passing through the Valley make use of existing trails (Fig. 47.2) and aims at analyzing the relationships between:

- lithology and landscape;
- lithology and the local architecture;
- Settlement and geomorphological conditioning;
- Morphology, climate and neo-tectonics activities.

Each tour proposes several stops; each stop is provided with description, images and schemas of selected features as well as multimedia products. For promoting an attractive tourists offers was necessary to consider the geological sites, not as individual elements disconnected from the local context, but as part of a network able to explain the origin, the story and the change of the landscape over millions years of evolution. The main difficulties in the promotion of itineraries focused on geology and geomorphology concerns, beyond the complexity of geological phenomena, also the spatial and temporal scale. For these reasons strategies will be implemented for facilitating the comprehension and for increasing the awareness by general public. Besides the preparation of specific panels along the paths, a pocket field guide with geo-tourist map will be published and thanks to the contribution of local authorities of the villages of Gurro and Cannobio a small geological and mineralogical museum and a visitor center will be purposely set-up. Special training

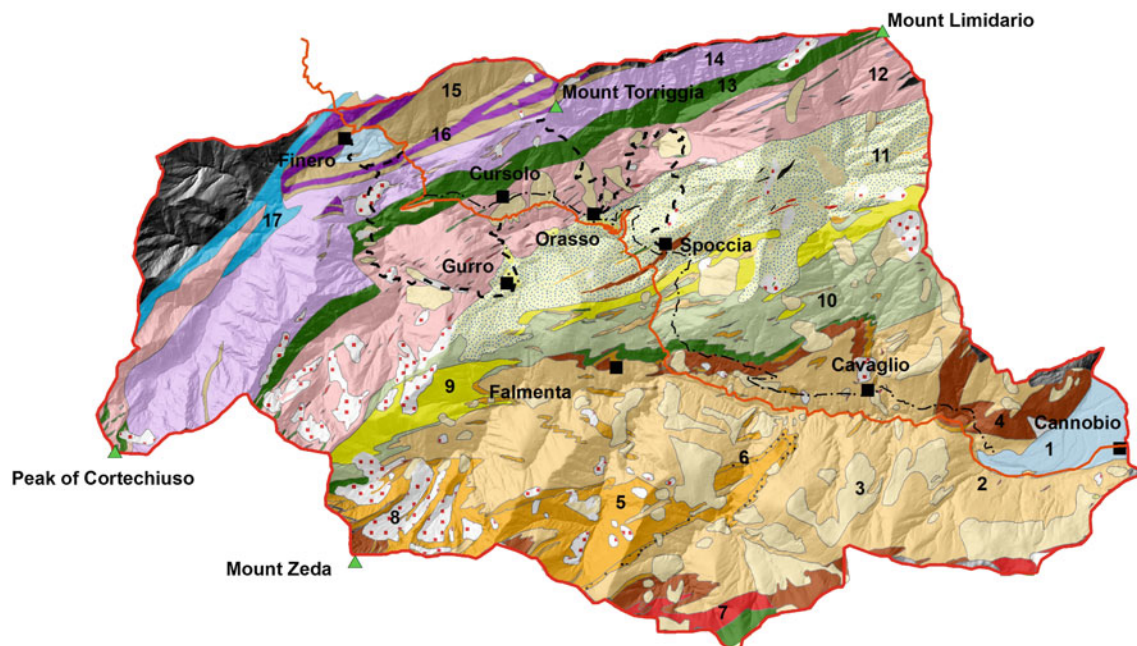


**Fig. 47.2** Geological map of the Cannobina Valley and the indication of the geo-touristic itineraries. Legend: Quaternary: 1 Floodplain. 3 Glacial and fluvioglacial deposits. 8 Slope debris. Serie dei Laghi Uni: 2 Fine-grained paragneiss of the Strona Ceneri. 4 Medium to coarse grained paragneiss of the Strona Ceneri. 5 Granitic orthogneiss with augen texture (Ordovician metagranites). 6 Granitic orthogneiss

with flaser texture. 7 Grano-dioritic orthogneiss. 9 Fine-grained paragneiss of the Strona Ceneri border zone. 10 Fine to coarse grained paragneiss of the Strona Ceneri border zone. 11 Scisti dei Laghi (micaschists). Ivrea-Verbano Unit: 12 Kinzigite. 13 Amphibolite. 14 Mafic granulite. 15 Peridotite. 16 Pyroxenite and layered gabbro. 17 Phyllonite. Dotted lines geo-itineraries. Orange line main road

activities for teachers and guides will be planned, as well as the development of Web and mobile application (Martin and Ghiraldi 2010).

## 47.5 Discussion and Conclusion

The analysis of the existing relationship between geological, cultural and historical heritage in the Cannobina Valley has been carried out following a well-known methodology developed by Department of Earth Sciences of Turin University and the Natural Sciences Museum of Torino. In order to plan geo-tourist activities combining different topics was necessary to create a multidisciplinary working group and inform the local administrators on the potential impact of the project. An aspect of fundamental importance was the methodology for preparing the itineraries. Planning different trails able to satisfy the different needs of the public is a question of primary importance for the success of the initiative, furthermore is important to use languages and illustrations simple and intuitive. With the technological advances that have characterized the last years and the increasing accessibility to the Web and mobile devices, setting up solutions capable of reaching a large number of potential users could be useful not only as advertising poster, but also for informing and sharing the knowledge of a ter-

ritory in an integrated manner; taking into account the cultural, historical and artistic aspects with those related to the Earth Sciences.

## References

- Boriani A, Bigioggero B, Orioni Bobbi E (1977) Metamorphism, tectonic evolution and tentative stratigraphy of the “Serie dei Laghi”. Geological map of the Vebania area (Northern Italy). *Mem Soc Geol It* 32:26p
- Boriani A, Burlini L (1995) Carta Geologica della Valle Cannobina. Scala 1:25.000. Comunità Montana Valle Cannobina, Dip. Sc. della Terra dell’Università degli Studi di Milano, Centro di studio per la geodinamica alpina e quaternaria. Consiglio Nazionale delle Ricerche
- Ferrero E, Giardino M, Lozar F, Giordano E, Belluso E, Perotti L (2012) Geodiversity action plans for the enhancement of geoheritage in the Piemonte region (North-Western Italy). *Ann Geophys* 55(3):487–495
- Ghiraldi L, Giordano E, Perotti L, Giardino M (2012) Metodologie di catalogazione, valutazione, raccolta e visualizzazione dei dati geoscientifici. Caso studio: i geositi nel paesaggio della Media Valle Tanaro (Piemonte, NW Italy). *Geologia dell’ambiente* 1:27–31
- Martin S, Ghiraldi L (2010) Internet au service du patrimoine. Cartographie dynamique de l’inventaire des géotopes d’importance nationale. Les géosciences au service de la société, Actes du colloque en l’honneur du Professeur Michel Marthaler, 24-26 juin 2010. *Géovisions* 37:106–117. Lausanne: Université, Institut de Géographie
- Newsome D, Dowling RK (2010) *Geotourism: the tourism of geology and landscape*. Goodfellow Publishers, Oxford

---

# Geomorphological Hazard in Hypogeum Karst Touristic Landscape: An Example from Frasassi Cave (Central Italy)

48

P. Farabollini, D. Aringoli, M. Materazzi, and G. Pambianchi

---

## Abstract

The study of geomorphological hazards in tourist areas has been addressed only recently, mostly because in areas of high touristic value any risk for excursionists or for simple nature lovers represents a strong conditioning factor to the fruition and therefore to the economy of an entire area. The geomorphological hazard can turn into a considerable risk, if one takes into account the increasing human pressure even in remote areas. The development of tourism, in fact, brings an increasing number of people to discover and attend both areas prone to hazards for some time, both in areas where these hazards are being increased. The complexity and multiplicity of these changes require necessarily a greater attention not only for a correct comprehension of natural phenomena but mostly for their possible interactions with tourism attendance and fruition. Based on previous experiences, also as a result of research projects funded by the Italian Ministry for the University and the Research (MIUR). A study on the natural hazards related to the touristic fruition in the area of Frasassi Cave in the Marche region (central Italy) is following presented.

---

## Keywords

Geomorphological hazard • Geotourism • Frasassi cave • Italy

---

## 48.1 Geomorphological Hazard and Geotourism

Many researches and the latest international and national projects funded, show how it is increasingly crucial the knowledge of the natural and induced hazards and their monitoring in the enjoyment of the natural environment in terms of geo-tourism (Mathieson and Wall 1987; Cipriani 2001; Diolaiuti et al. 2001; Brandolini et al. 2004; Terranova et al. 2005; Farabollini and Spurio 2007).

The hazard may increase due to the intensification of some natural phenomena but at the same time, it can lead to different reactions from the user in relation to its physical-technical-cultural characteristics (knowledge of the phenomenon, skill, training, etc.). The tourist will therefore be exposed to a greater or lesser vulnerability in occasion of a natural event. A very frequented, steep and overhanging track, when affected by precipitation, is characterized by an increased probability of slippery conditions; the risk associated will be therefore inversely proportional to the degree of preparation and to the proper equipment of the visitor.

In order to adopt a common operating model for the assessment of geo-environmental risk in tourist areas also to support the management and the territorial planning, a methodology based on qualitative and semi-quantitative evaluation of geomorphological risk and touristic vulnerability (Aringoli et al. 2007) has been tested. This model provides for the compilation of “inventory cards”, arranged

---

P. Farabollini (✉) · D. Aringoli · M. Materazzi · G. Pambianchi  
School of Science and Technology, University of Camerino, via  
Gentile III da Varano, 62032 Camerino, MC, Italy  
e-mail: piero.farabollini@unicam.it

so as to be usable even in the field, and prepared for entering data into a georeferenced database.

In particular, both the so-called “objective” geomorphological hazards (process, landforms and deposits involved) and the “subjective” ones (the set of features that can increase the risk, Brandolini et al. 2004) are described, classified and quantified. In the meanwhile, data on territorial vulnerability, such as the degree of fruition and facilities and infrastructures present, are collected. The division in classes of risk, arising from the interaction of the different degrees of hazard and vulnerability previously recognized, is the goal of the analysis.

## 48.2 The Frasassi Gorge and the Complex of the Frasassi Caves

The karst complex of Frasassi, discovered in September 1971 and accessible from 1974 for a length of approximately 1.5 km, is one of Europe’s most important speleological areas. The karst area includes more than one hundred cavities among which the complex Mezzogiorno-Frasassi constitutes one of the most extensive karst systems of the central Apennine. These caves are present on the right side of Frasassi Gorge, deeply incised by the Sentino river into the Calcare massiccio formation. In particular, the large cave “Grotta del Vento”, which is one of the largest in Europe (200 m high, 180 m long and 120 m wide), is visited every year by 300,000 tourists.

The whole karst complex known as “Grotta del Fiume-Grotta del Vento” (Fig. 48.1a), a system extended for more than 19 km, develops within the northern portion of the Mount Valmontagnana anticline, mainly constituted by the Calcare massiccio formation. The base level of the karst system is represented by the Sentino river that cuts the anticline with approximately WNW-ESE direction; all the caves are present at different elevation on the hydrographic right.

The karst process is set both on fractures related to Jurassic faults with NW-SE direction and on neotectonic faults with NE-SW direction along which the initial portion of the Frasassi Gorge is aligned (Coltorti et al. 1996). The dissolution of carbonate rocks, begun after the erosion of the formations overlying the Calcare massiccio and the reactivation of jurassic faults, seems to be mainly connected to H<sub>2</sub>S oxidation and to the excess of CO<sub>2</sub> present in the groundwater (Galdenzi and Menichetti 1990).

The superficial karst phenomena are represented by rare dolines and sinkholes, as well as some hanging valleys. Karren morphologies and dissolution holes are also present (Galdenzi and Menichetti 1990; Farabollini and Materazzi 2004). The hypogeous karst, on the contrary, is well developed and exceeds tens of kilometers. The karst

complex consists of at least seven sub-horizontal levels, located at different height with respect the base level and interconnected by sinkholes, dissolution pipes and pits, ravines: different typologies of concretions (stalactites, stalagmites, columns, veils, etc.) are visible inside of the cavities. Among these, frequent gypsum deposits related to the presence of sulphurous water and microforms such as “vortex niches”, “mud cones” and “mud pyramids”; inside the “Grotta del Fiume” in particular, remains of ibex and brown bear have been reported (Coltorti and Sala 1978).

At the base of the lowest karst system, the presence of groundwaters creates tunnels and lakes also of considerable size. Sub-horizontal cavities in fact represent, as a whole, stages of groundwaters stationing during time (Cattuto 1977; Galdenzi and Menichetti 1990).

The setting of the karst network at different levels of the water table has been conditioned by the interaction between tectonic uplift and river deepening: traces of past base levels are represented by pebbly deposits (visible along the gorge), referring to the four orders of alluvial terraces found throughout the river basin (Cattuto 1977; Coltorti et al. 1996).

The air temperature inside the Frasassi caves is around 13 °C and remains almost constant, but in the period of maximum attendance (especially in summer) the temperature can reach 15–16 °C. However, thermometric data relating to the hypogeous atmosphere indicate that especially in summer, when visitors are numerous, the cave fails to restore, during the night closure, the original environmental conditions. For the same reason the values of relative humidity, usually close to 100 %, can drop down to values of 97 % in summer. The CO<sub>2</sub> concentrations, measured in summer at various points of the touristic route, indicate values between 500 and 1,000 ppm, while minimum values of about 350 ppm are recorded in winter (Menichetti et al. 1996).

## 48.3 Geomorphological Hazard in the Karst Environment

The most visited touristic caves in the world convey, as a total attendance, about 170 million visitors each year; similarly in Italy, karst cave tourism involves about 2.5 million people/year (Chiesi 2000; Burri 2002). Based on these data it is possible to realize that, given the sensitivity of the karst environment, the chance of occurrence of environmental degradation episodes from excessive tourist fruition of the caves, is real and contingent, allowing to recognize a tolerance threshold of the caves, also concerning the number of visitors, both simple tourists and expert speleologists.

Associating speleologists to simple tourists is not a strangeness: for the ecosystem of the cave, there is no substantial difference, both in terms of problem (single cavity or

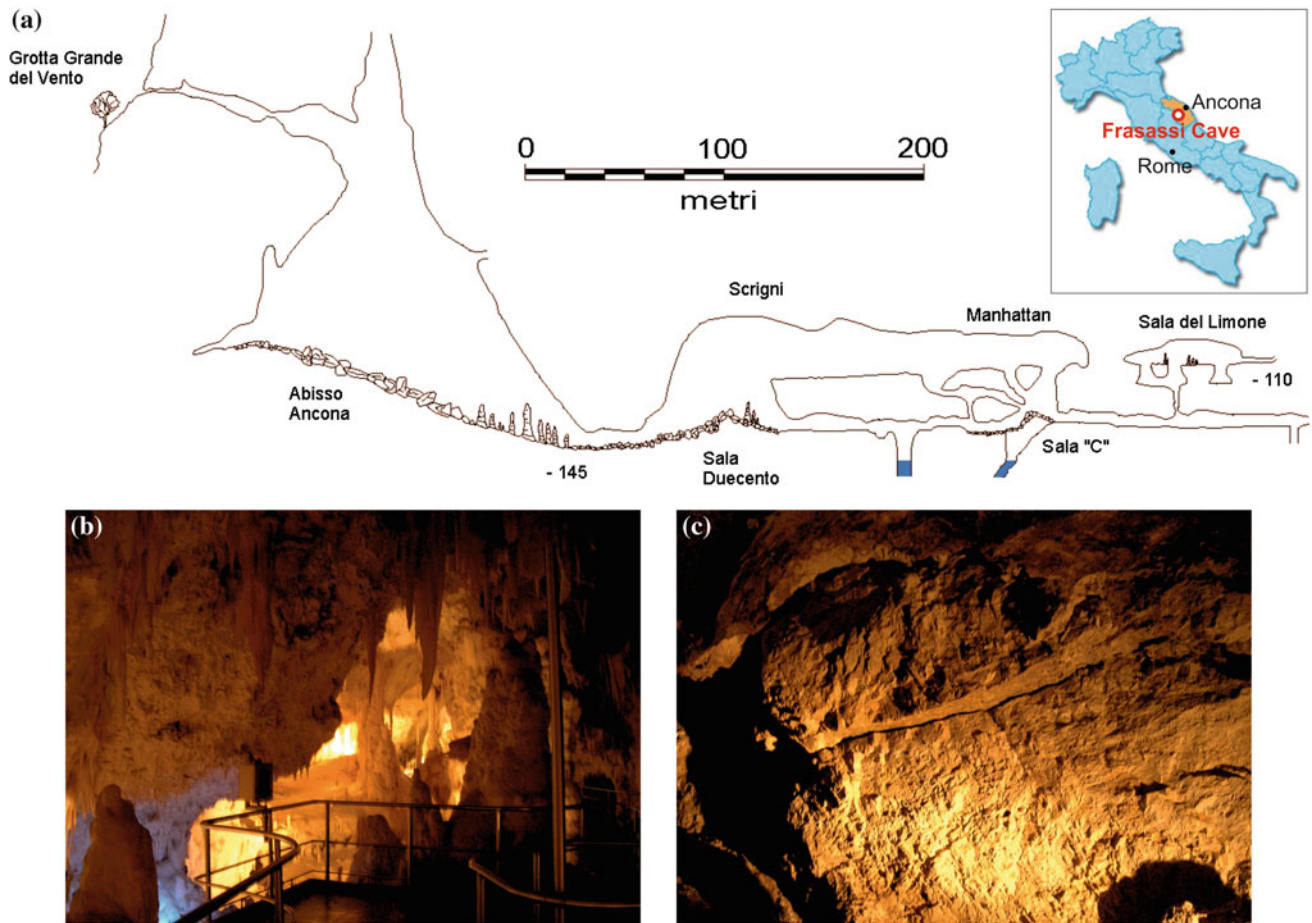


**Fig. 48.1** a Partial cross-section of the “Grotta del Fiume-Grotta del Vento” karst system; b detail of the route with protruding stalactites; c detail of the fault step on the Calcare massiccio formation

cave system) both in terms of possible degradation factors (Chiesi 2000; Burri 2002). Also the speleologists, careful to safeguard the cave environment, are sometimes themselves a serious and irreversible danger of deterioration: in many cases, concretions are irreversibly damaged to allow the passage and the exploration of new cavities. In addition to this, there is the awareness, more and more increasing, that many caves have to be adapted to a mass tourism in their shallower portions for socio-economic returns; new concrete paths, handrails, panels and other fixed structures, lights, etc. result from this recurrent need.

Alternative to mass tourism is starting to be more and more practiced the “speleologic tourism”. The aim is to “adapt” the tourist to visit in safety the cave, rather than adapt the cave to the needs of the tourist. Speleo-tourists, however, must always be guided and educated with great care, since they could cause great damages to the cave. This problem has been already experienced in the caves of Frasassi, where parts of the non-touristic route is today in disastrous conditions right because of an unchecked.

Even though numerous studies are available about human-induced hazard (Heathon 1986; Chiesi 2000; Cigna et al. 2000), the geomorphological hazard connected to caves has been not exhaustively studied. The risk for the human safety connected to the fruition of karst environments is, actually, rather limited and certainly typologically less diversified than those that can be found outside the cave. However, even in this context, they represent a significant percentage and of sure scientific and socio-economic interest.

The environmental conditions are generally inhospitable to man: the general rule is that the air of the caves is saturated of water, with almost constant temperature, generally corresponding to that of the average of the water entering the system and therefore roughly corresponding with the rain-falls temperature of that location. The risks facing occasional or expert visitors are of different types. The former are mainly related to the fact that occasional tourists have no specific adaptations to visit a cave (risk to be lost, to remain without light etc.). Speleologists, on the contrary, are usually

protected from some of these incidents, but they are exposed to others through excess of confidence (very prolonged descents, floods and collapses in areas not yet explored, rockfalls etc.). Most of the accidents, however, happen in very remote areas and this always involves a large effort to a high number of rescuers, from which a remarkable specific preparation is required.

The most significant geomorphological hazards are connected to the presence of internal phenomena (i.e. collapses, fractured areas etc.) and to those induced by external causes (i.e. earthquakes).

Inside the “Grande Grotta del vento” at Frasassi, materials from the collapse of the roof of the main cave (Ancona Abyss) are still present and visible along the left side of the cave entrance. These materials, sometimes larger than few tens of cubic meters, show signs of recent mobilization (Holocene) and may be subject to subsequent downward movements related to the circulation of aggressive waters or waters with a load of silty-sandy materials that could fill the voids and bring up the level of the water with consequent increases of the hydraulic pressures. Moreover, rockfall deposits, present at the foot of the cave, overlap and create a natural arch of limited height, under which passes the tourist route, with clear problems for the passage of visitors.

Inside the cave is also possible to recognize the presence of faults, which in some cases are visible through steps projecting on the route. Seismic studies have shown that the area in question is subject to considerable microseismicity with a main extensive character (Barchi et al. 1991); at the same time geomorphological studies carried out in the cave, evidenced bands of calcite related to levels of stationing of underground lakes with high horizontal development: these bands showed phenomena of tilting at least since 9000 years B.P. (Mariani 2002). Because the ongoing tectonic deformations, the seismicity of the area and the processes of weathering and degradation the above mentioned landforms (rockfall deposits, stalactites, stalagmites, fault steps), could be destabilized and there fore should be adequately monitored, these should be adequately monitored (Fig. 48.1c).

In the case of caves equipped for tourism, such as at Frasassi, there are other reasons for degradation and consequent hazard. The waters used for cleaning the caves, especially along the routes, and the use of hypochlorite for the concretions, are a source of concern both for the underground life and groundwaters, and for the tourist, who will benefit the same routes: due to the natural conditions of moisture, the possibility of slip will increase significantly. Moreover, the equipped routes for tourists, usually develop taking into account the morphology of the environment and the possibility to closely observe spectacular landforms and concretions: this means that tourists have to pass under groups or isolated stalactites (Fig. 48.1b) and these, especially the most light and thin, as a consequence of a

fortuitous event (seismic shocks, strong current of air, etc.) may break and fall on some unfortunate visitor.

Additional hazards arise from the particular and articulated development of the equipped route. The high moisture and the considerable seepage from the roof of the cave, make it particularly slippery. Moreover, the presence of numerous steps to overcome the differences in height between different rooms for their visit, make this route very difficult, especially for old people or visitors with walking difficulties. However, it should be pointed out that in many cases, is the curiosity of tourists, attracted by the natural beauty of the caves, responsible to create accidents to themselves or others.

## References

- Aringoli D, Farabollini P, Pambianchi G (2007) Valutazione della pericolosità geomorfologica lungo i sentieri escursionistici del Parco Nazionale dei Monti Sibillini (Appennino centrale). In: Piccazzo M. (ed) “Clima e rischio geomorfologico in aree turistiche”, Patron Editore, Bologna, 147–180
- Barchi M, Lavecchia G, Menichetti M, Minelli G, Piali G (1991) Analisi della fratturazione del Calcere massiccio in una struttura anticlinale dell’Appennino Umbro-Marchigiano. *Le grotte d’Italia*, serie V, 1:3–18
- Brancucci G, Burlando M (2001) La salvaguardia del patrimonio geologico. Franco Angeli Ed., pp 96
- Burri E (2002) Fruizione turistica dei geositi di natura carsica. *Geologia dell’Ambiente* 2:45–48
- Butler RW (1980) The concept of a tourist area cyclic evolution. Implications for management of resource. *Canadian Geogr Montreal* XXIV:5–12
- Brandolini P, Farabollini P, Motta L, Motta M, Pambianchi G, Pelfini M, Piccazzo M (2004) Geomorphologic hazards along tourist itineraries: some examples from Italy’s territory. In: The 32nd international geological congress (32IGC), Florence, Italy, 20–28 Aug 2004
- Cattuto C (1977) Correlazione tra i piani carsici ipogei e i terrazzi fluviali nella valle del fiume Esino (Marche). *Boll Soc Geol It* 95(1–2)
- Chiesi M (2000) Problemi di protezione ambientale nella fruizione e nell’adattamento turistico delle grotte. *Geologia dell’Ambiente* 3:28–33
- Cigna A, Cucchi F, Forti P (2000) Engineering problems in developing and managing show caves. *J Nepal Geol Soc* 22:85–94
- Cipriani E (2001) L’arrampicata sulle falesie: quando anche il turismo “verde” si rivela una minaccia per l’ambiente. *Atti del XXVII Congr. Geografico Italiano: “La geografia delle sfide e dei cambiamenti”*. Patron, Bologna, pp 747–752
- Coltorti M, Farabollini P, Gentili B, Pambianchi G (1996) Geomorphological evidences for anti-Appennines faults in the Umbro-Marchean Apennines and in the peri-Adriatic basin, Italy. *Geomorphology* 15:33–45
- Coltorti M, Sala B (1978) Resti fossili nella Gola di Frasassi. *Natura e Montagna* 1:27–31
- Diolaiuti G, D’Agata C, Pavan M, Vassena G, Lanzi C, Pinoli M, Pelfini M, Pecci M, Smiraglia C (2001) The physical evolution of and the anthropic impact on a glacier subjected to a high influx of tourists: Vedretta Piana Glacier (Italian Alps). *Geogr Fis Dinam Quat* 24:199–201
- Farabollini P, Materazzi M (2004) Pericolosità geomorfologica e pianificazione territoriale in un’area a tutela ambientale: l’esempio

- del Parco Naturale Regionale della Gola della Rossa e di Frasassi (Regione Marche). Studi Geol. Camerti, seconda serie, I, 57–69
- Farabollini P, Spurio E (2007) Geositi e Geoescursionismo. Quaderni del Parco n.8. Comunità Montana Alta Valle dell'Esino, pp 144
- Galdenzi M, Menichetti M (a cura di) (1990) Il carsismo della gola di Frasassi. Memorie dell'Ist. Ital. Di Speleologia, 4, serie III, pp 242
- Mariani S (2002) Indagini idrologiche e idrochimiche in un nuovo ramo della Grotta del Fiume (Frasassi—AN): contributi della speleologia alla ricostruzione dell'evoluzione carsica e tettonica dell'area. Tesi di laurea inedita, Università di Camerino, pp 77
- Mathieson A, Wall E (1987) Tourism: economic, physical and social impacts. Longman Scientific and Technical, New York
- Menichetti M, Galdenzi S, Marinelli G, Pierini A, Tosti S (1996) Monitoraggio ambientale e flusso turistico nella Grotta Grande del Vento a Frasassi (Ancona, Italia). Bossea MCMXCV, Proc. Int. Symp. "Show Caves and Environmental Monitorino", Cuneo, 193–199
- Terranova R, Firpo M, Brandolini P (ed) (2005) La valorizzazione turistica dello spazio fisico come via alla salvaguardia ambientale. Pàtron Editore, Collana "Geografia e organizzazione dello sviluppo territoriale", Studi regionali e monografici, 36, Bologna, pp 408

**Monitoring and Modelling Applications for the  
Diagnosis of the Actual Conditions, Preservation  
and Management of Cultural Heritage**

---

# Instrumental Geophysical Diagnose: Help to Historical Monuments Reconstruction Works

49

Mihai Mafteiu, Cristian Marunteanu, Victor Niculescu, and Sanda Bugiu

---

## Abstract

The necessity of knowing the underground state of historical monuments subject to damage demanded the use of some rapid geophysical methods (electrometric, magnetometric and GPR) in archaeological fields and geotechnical studies. An image of the ground structure can be presented and thus the rehabilitation study can be led by applying the geoelectric method of the non-destructive research to the foundation ground of the historical monuments. Therefore, an optimal choice of the electro-sounding array is required, the measures being connected to the structural parameter of the building (columns, long curtains, changes of the foundation depth). The resistivity pseudosections by electro-soundings, correlated both with the land survey, the monument sections and the lithological column from geotechnical drillings, emphasize a series of geoelectric effects of the natural or anthropic damaging causes on the geophysical image. Three case studies of historical monuments illustrate the results of geoelectric investigations and the conclusive rehabilitation measures.

---

## Keywords

Historical monument • Earthwork • Seepage • Apparent resistivity • Reconstruction

---

## 49.1 Introduction

A tomographic image of the geological structure can be obtained by applying optimal, simple, economical and operative devices and investigation networks with an appropriate processing and an integrated interpretation of all

the information and by applying the geoelectric method. This is possible by separating the abnormal effects of some problematic, natural or anthropic elements from the general natural structure through resistivity parameter in view of the stabilization of some historic or cultural monuments. Simultaneously, deciphering the causes of the anomalies creates the premises of proposals for preserving or rehabilitating these monuments. (Heimmer 1992; Cammarano et al. 2000). This paper describes the geophysical effects of the interactions between the buildings and the foundation ground which resulted from the geoelectric researches through vertical electric sounding method on some historic monuments. The geoelectric research linked with contiguous information outlined the effect of the surface, pluvial and drain waters and causes suffusion followed by differentiated settlements which lead to cracks in foundations and walls.

---

M. Mafteiu · V. Niculescu  
SC MM Georesearch SRL, Bucharest, Romania

C. Marunteanu (✉)  
University of Bucharest, Bucharest, Romania  
e-mail: crimarunteanu@yahoo.com

S. Bugiu  
SC Sami Consult SRL, Rm.Valcea, Romania

## 49.2 Methods and Premises of Resistivity Research

### 49.2.1 Resistivity Method

The resistivity method investigates the influence of the inferior semi-infinite space structure in the surface current distribution through apparent resistivity. The geoelectric parameter represents a complex average of the resistivity of the investigated environment (Barker 1989).

The ground technique VES (vertical electrical sounding) with Schlumberger device implies the determination of the apparent resistivity of a sequence of geological layers or rocks by applying a quadrupole device with two AB plug sockets through which a known current and two MN sockets are introduced in the ground for measuring the potential difference associated to this current. This AMBN quadrupole device has different configurations according to the prospecting necessities. Basically, they are varied in order to remove different factors which influence the current distribution (ground inhomogeneities, humidity, relief, etc.) which are reflected in the size and variation mode of the measured resistivity (Morris et al. 1997).

The depth of investigation in the geotechnical field depends on the buildings foundation depth and on the thickness of the bearing layer. The ground equipment for data acquisition is a high resolution resistivity-meter with self-compensated natural potential type SUPERSTING R1 (AGIE USA) or SAS 4000 (ABEM-SWEDEN).

### 49.2.2 Research Premises

The geoelectric research in civil, industrial and cultural fields, which this paper is about, is determined by a series of specific factors:

- The geoelectric contrast foundations/ adjacent environment;
- The constructive parameters and the degree of anthropic activity;
- The characteristics of the bearing layer and the ground.

From the perspective of the research technique, choosing an optimal network of observation and some adequate parameters of the field working devices are required by processing the information according to the geological and geotechnical data. The result of the integrated interpretation of the collected data in geotechnical terms is, geologically speaking, a complex image of the underground, that is similar to a tomographic image, in which the electric resistivity parameter “shapes” the geologic environment state. A series of effects connected to the relations between the researched object and the environment appear depending on

the nature of the phenomena reflected in the geoelectric images (case studies below):

- Warping of the buildings on the flooded filling materials (Sulina);
- Earthflows due to pipe infiltrations (Hurezi);
- Settlement due to local increase of ground wetness (Bucharest). Appropriate rehabilitation measures have been proposed and applied.

## 49.3 Case Studies

### 49.3.1 Sulina Orthodox Cathedral (Tulcea County)

An image of apparent resistivity on a cross section under the southern front part of the Orthodox Cathedral from Sulina, Tulcea County (Romania) located 30–35 m away from the touristic port of the Danube Canal is presented (Fig. 49.1).

The body of the church is made out of bricks in 1894 on a base bulged by stone blocks. The underground water Table (1.00–1.50 m depth) is tributary to the Danube River and climate excesses. The mechanical effort caused by the mooring of big ships but also by the infiltrations in the base of the wrongly drained rain water towards the outer surface of the building produced damage of the foundation on the central surface (church nave). The compressions between the pro narthex—narthex and nave—altar led to a horizontal crack at the jointing of the spandrels with the columns of the front wall (Chilton et al. 1997). As a result of these findings and after the uncovering of the basement, a rehabilitation solution through technical examination was suggested, that is implanting some micro piles at 1–2 m in between and approx. 4.00 m depth. The rehabilitation method applied to areas of phreatic level under the depth of the foundation brought good results. In case of a high and varying level, a mortar injection in the foundation ground could be important.

### 49.3.2 Hurezi Monastery (Valcea County)

The monastery of Hurezi, founded by the enlightened prince Constantin Brancoveanu in 1693, endured a lot of weathering and human damage along its history. In 2011 a restoration program proposed a geotechnical study accompanied by geoelectrical tomography. A detailed VES survey grid was attained around the church and the external wall facades founding out a lot of anomalies effect of wall damages due to seepage generating shallow landslides and mortar dampness. The domestic and rainwater leak off into fillings and beneath overburden create some minor and local earth flows near the walls.

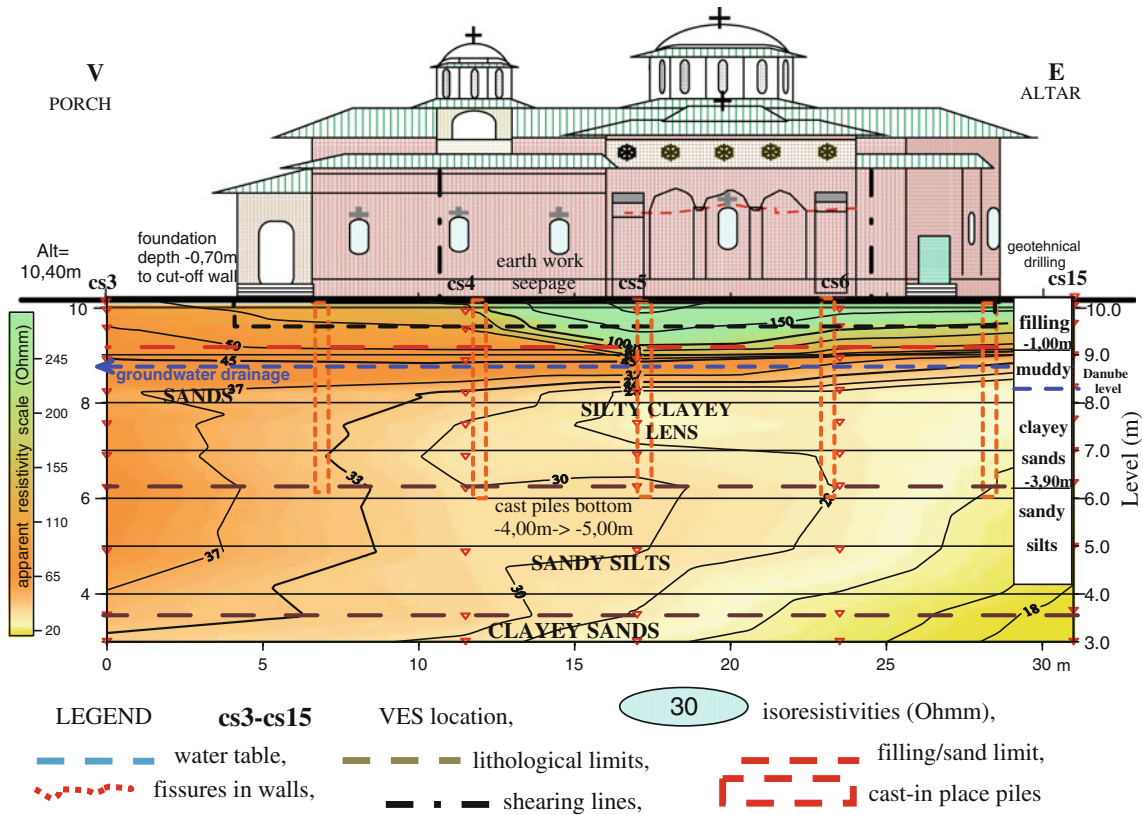


Fig. 49.1 Interpretative geoelectrical cross section—southern front part of the Orthodox Cathedral, Sulina, Tulcea County, Romania

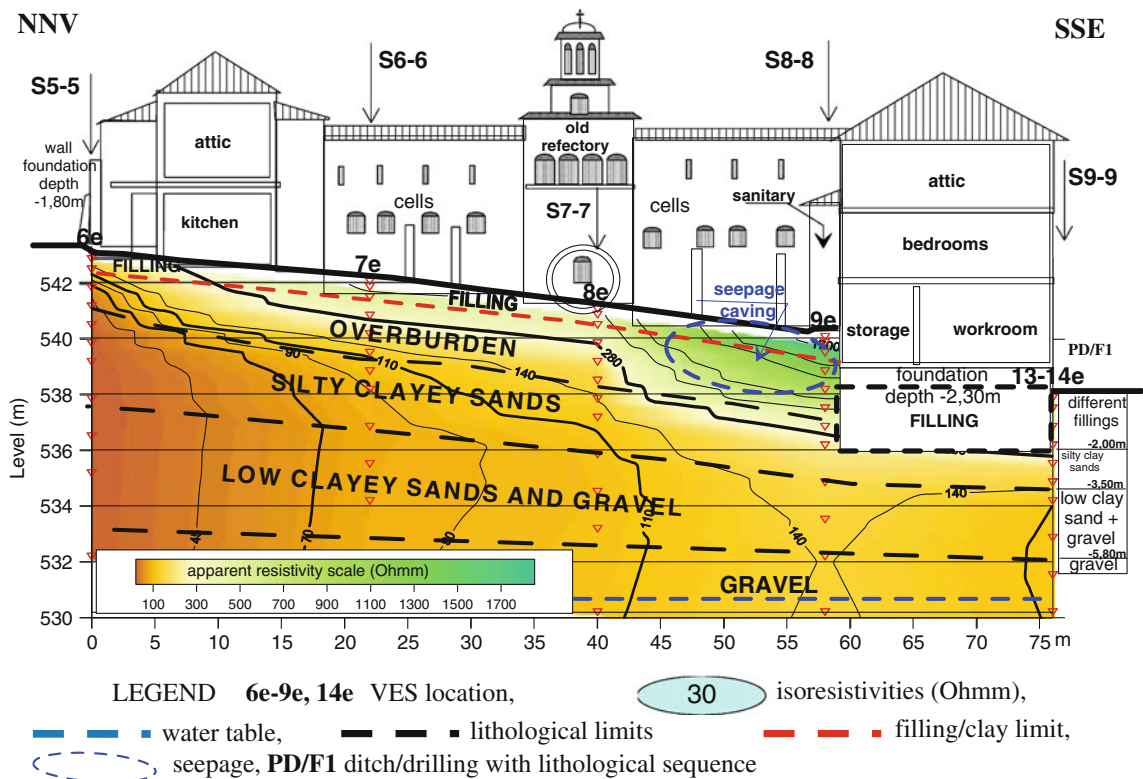
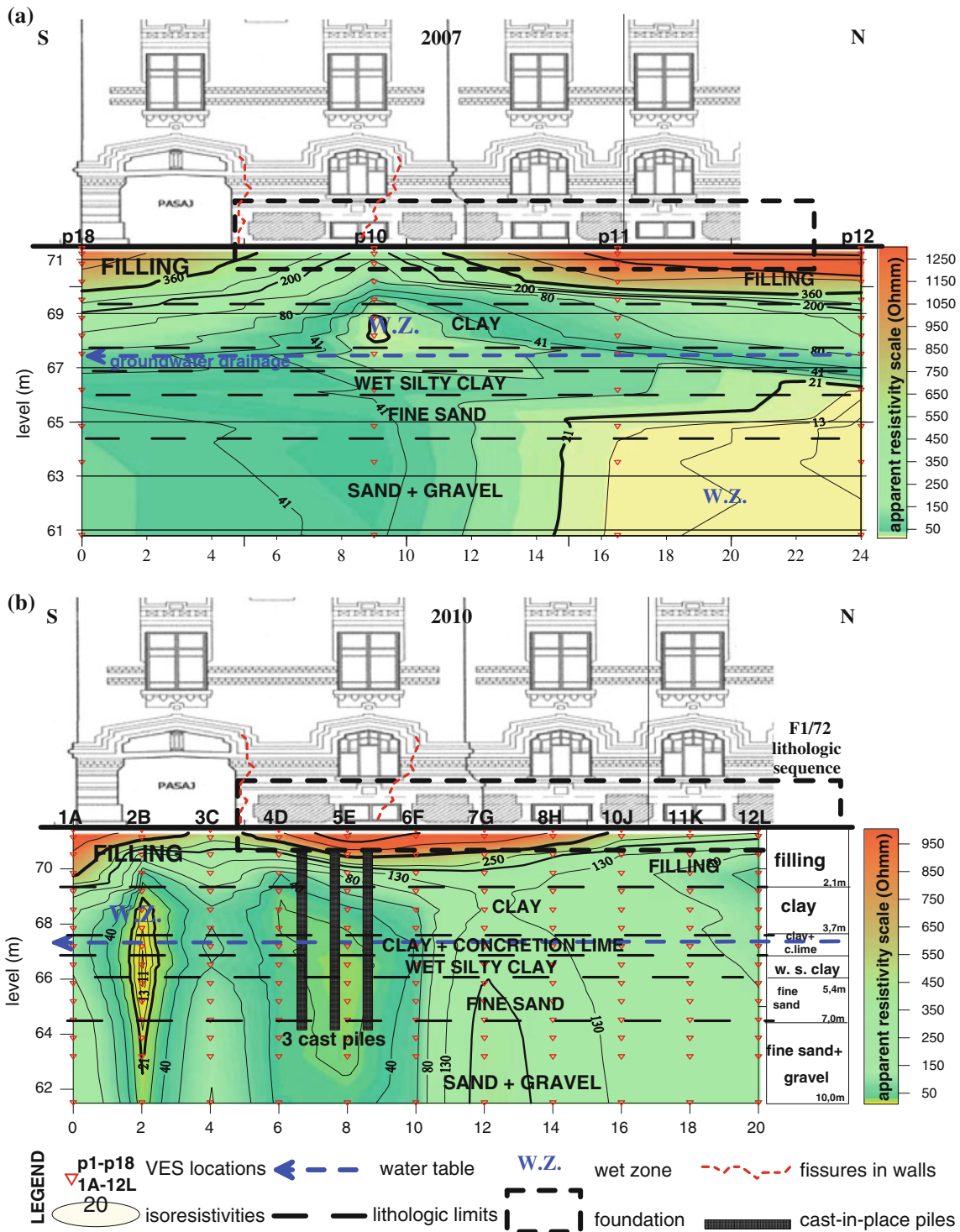


Fig. 49.2 Interpretative geoelectrical cross section—inner facade of the northern wall of the Orthodox Hurezi Monastery, Valcea County, Romania

The geoelectric image (Fig. 49.2) shows higher resistivities where water flow bleaches the silt part of soil and minor values where the liquid concentration grows. The rehabilitation solution is hydrogeotechnical:

- To build a deep drainage channel inside and outside the walls under the basement sill draining the rain water far from the fences;
- To build a shallow channel as a coarse filter near the wall base filled with fine gravel in order to aerate the basement.



**Fig. 49.3** Comparative geoelectrical cross section—Eastern façade of General City Hall of Bucharest before (a) and after (b) cast-in-place piles positioning

### 49.3.3 General City Hall (Bucharest)

In the rehabilitation program, under the walls of the City Hall in Bucharest, a historic monument built in 1910 in neo-Romanian style, the method of drilling piles of 6.50 m deep was tested in order to pass over the levels which are subject to pluvial and drain infiltrations.

The measurements of the initial geoelectric sounding (2007) have marked up an anomaly at VES p10—an infiltration in clay layer, under the fillings (Fig. 49.3a). After casting three piles every 3 m (2010) the geoelectric cross section was restored. The rehabilitation effect on the section casted with piles is a leveling of the resistivity under the fillings from 69.9 to 64.0 m at the clay level being sensitive to wetting and having an infiltration level. Statistically speaking, if the average of the values before casting the piles was 33.5  $\Omega$  m with a standard deviation of 11.1, the effect of piles led to an average of 35.8  $\Omega$  m with a standard deviation of 3.7. However, the geoelectric image shows that the cementation over pushed the humidity areas towards the NS drainage of the phreatic. The chosen retrieval solution seems to be efficient (Fig. 49.3b).

## 49.4 Conclusions

In the process of preserving the cultural heritage this method offers the architects and civil engineers a tomographic image of the foundation ground of the historical monuments which were subject to damage in time. The non-destructive technique on surface means portable equipment with research

devices in contact with built areas or with erected or buried walls. Above the geological and geotechnical mapping we attach the information about the subsurface obtained by geoelectrical sounding.

Through processing the VES cross sections, tomographic images can be obtained in real time regarding the petrophysical aspect of the foundation ground. Monitoring by restoring the electrometric measurements in different climate periods (after drought or heavy rainfall) can separate the geoelectric effects of the rainwater seepage from those of the pipe networks seepage in the ground. The different chemistry of the two water seepage fluids (visible through apparent resistivity anomalies) is another aspect which is outlined well on the tomographic images.

## References

- Barker RD (1989) Depth of investigation of collinear symmetrical four-electrode arrays. *Geophysics* 54/8:1031–1037
- Cammarano F, Di Fiore B, Mauriello P, Pattella D (2000) Examples of application of electrical tomographies and radar profiling to cultural heritage. *Annali di Geofisica*. 43(2):309–324
- Chilton J et al (eds.) (1997) Groundwater in the urban environment, vol. 1, problems, processes and management. In: Proceedings of the XXVII congress on groundwater in urban environment, Nottingham, UK
- Heimmer HD (1992) Near-Surface, high resolution geophysical methods for cultural resource management and archaeological investigation. GeoRecovery Systems, Inc, USA
- Morris M, Ronning JS, Lile OB (1997) Detecting lateral resistivity inhomogeneities with the schlumberger array. *Geophys Prospect* 45:435–448 (EAGE Netherlands)

---

# Rockfalls Monitoring Along Eastern Coastal Cliffs of the Favignana Island (Egadi, Sicily): Preliminary Remarks

50

Luca Falconi, Alessandro Peloso, Claudio Puglisi, Augusto Screpanti, Angelo Tati, and Vladimiro Verrubbi

---

## Abstract

Favignana island (Sicily, Italy) is a historical and environmental attraction site frequented by tourists during the long warm season of the year. For several centuries the calcareous sandstone outcropping in the east side of the island has been extracted and used as building stone. Actually the quarries and the caves are undergoing to erosional and gravitational processes that are influencing the touristic use. As well as putting at risk the safety of people attending the area, the diffused rock falls are likely to jeopardize sites of great anthropological value that, once destroyed, can no longer be reconstructed. An integrated monitoring project of the cliffs is aimed to identify the most active areas and to provide support to the local government's policies in the implementation of mitigation measures. If adequate measures will be taken in the future, operators and users of the tourist circuit will have the opportunity to enjoy these amazing areas with lower level of landslide risk.

---

## Keywords

Rock falls • Monitoring • Favignana Island • Sicily • Italy

---

## 50.1 Introduction

In the Favignana island outcrops a quaternary calcareous sandstone, improperly called as tuff. Its good resistance brought this rock to be extracted and used as building stone. The exploitation of the Favignana sandstone is ancient, but it was mainly in the period between 1700 and 1950 that reached its maximum development. Many buildings were constructed in Tunis with the “tuff” of Favignana and Messina was rebuilt with it after the earthquake of year 1908. After the II world war the “tuff” has gone out of the market and the mining areas have been abandoned to a

degradation process which increased the risk of walls collapse. Among the quarry areas there are also the high cliffs overlooking the sea situated along many parts of the eastern coast.

The landslides along these rock slopes, often highly fractured and exposed to the intense activity of aggressive exogenous agents, occur mainly with the detachment and fall of blocks extremely variable in sizes (Fig. 50.1). The ongoing climate change and particularly the variation in temperature regimes and fluctuations in sea level in the Mediterranean and Sicily seem to intensify the falls activity (Puglisi et al. 2007). These climatic dynamic indeed increase thermoclastic processes and erosion at the foot of the cliffs. The low human activity in these areas reduces the real risk conditions that remain concentrated in some bays frequented by tourists during the long warm season of the year. Local government of Favignana pays special attention to the evolution of the coastal system, consisting in the high coast and the emerged and submerged beach below. Rock falls, in fact, can heavily influence the availability of the beaches below,

---

L. Falconi (✉) · A. Peloso · C. Puglisi · A. Screpanti · A. Tati · V. Verrubbi  
ENEA, National Agency for New Technologies, Energy and Sustainable Economic Development, Via Anguillarese, 301, 00123 Rome, Italy  
e-mail: luca.falconi@enea.it

**Fig. 50.1** Rock blocks fallen at Cala del Bue Marino



resulting in a partial and/or total access and bathing ban in places that for their beauty are often a popular tourist attraction. In addition, the quarries and the caves are a natural and cultural heritage of great anthropological value that, once destroyed, can no longer be reconstructed.

## 50.2 Objective of the Study

The aim of the study is to contribute to the mitigation of geomorphological risk in the Favignana island. The cliffs monitoring and the movements characterization are aimed to identify the most active areas and to provide support to the local government's policies in the implementation of mitigation measures. Given the characteristics of the sites, inserted into the largest European marine protected area, the intervention measures will must also be characterized by a high degree of environmental sustainability. If valid, effective and pleasant measures will be taken in the future, operators and users of the tourist circuit will have the opportunity to enjoy these amazing areas with lower level of landslide risk.

## 50.3 Study Area

The study is focused on Cala Rossa, Cala del Bue Marino and Cala Azzurra, located in the eastern portion of the island, in areas classified with high and very high landslide hazard (Regione Siciliana 2006). A calcareous sandstone rich in marine fossils (bivalves, corals,...), with nearly horizontal layers of about half a meter thickness, are outcropping all over the area (Fig. 50.2). In the west side of Cala Rossa and Cala Azzurra, underlying the rock slab, whose thickness varies from few meters up to 30 and more meters, plastic clays are outcropping. The overlapping of hard rock masses on a plastic substratum leads to mechanical instability due to the diverse response of the materials to the applied perturbations, such as man-made excavations,

weathering or erosion (Gigli et al. 2012). The mass movements can be classified into two different but strictly interconnected typologies: lateral spread and rock blocks fall (Cruden and Varnes 1996)

## 50.4 Methodology

The monitoring activity, launched in October of 2012, will end in November 2014 and is led through the use of direct and indirect instruments. The direct measurements are made through mechanical joints gauges of different kind (tell-tale, removable joint-meters, 3D joint-meters) in relationship with the different characteristics of the walls, discontinuities and types of movement (one-dimensional or three-dimensional). Overall were installed 70 mechanical joint-meters, distributed along the cliffs of the three bays and also within the numerous cavities that open inside of the cliffs. The indirect measurements are carried out through laser scanner and GPS instruments with two substantially different purposes. The laser scanner is used for the acquisition of areal data in all the three areas object of the study and will permit to identify any movements of each of the points highlighted by the laser beam along the entire cliffs. For the identification of possible displacements along the cliffs, several scanning spaced in time will be acquired (Abellán et al. 2010; Stock et al. 2012). Various Digital Terrain Models will be processed and their comparison will permit to derive displacement maps of the observed cliffs. The GPS, instead, is used only in Cala Rossa and is directed at the control of 4 points identified in specific portions behind the cliff edge. The GPS technique will permit to identify movements with sub-centimetric detail level. For this purpose a local GPS network has been designed, consisting in four presumably stable vertices (Fig. 50.3). Accurate geological and geomechanical surveys of the selected sites were carried out with the aim of identifying predisposing parameters to be subsequently used in the rock fall susceptibility GIS analysis (Frattini et al. 2008).

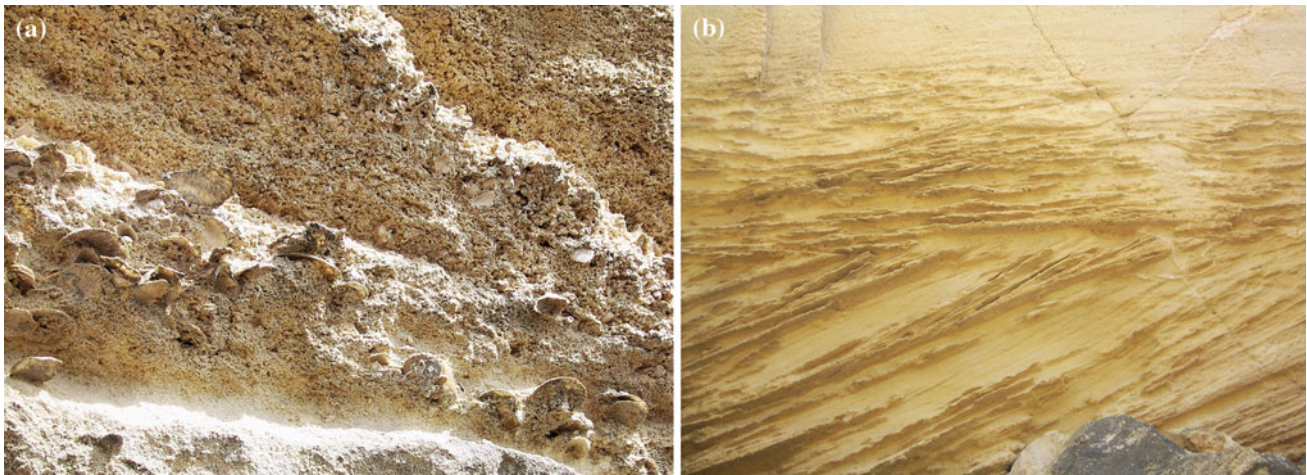


**Fig. 50.2** Bivalves (*left*) and layers (*right*) in the calcareous sandstones

**Fig. 50.3** The GPS network at Cala Rossa (A, B, C and D) and the four measuring points (O1, O2, E1 and E2)



## 50.5 Results

The rock mass shows a high degree of fracturing and evidence of previous blocks falls is also visible all over the study area. Several blocks of different sizes appear to be in conditions of high instability and in proximity of falling.

An example is given by the block of approximately  $0.3 \text{ m}^3$  collapsed on the morning of October 26, 2012 from the west cliff of Cala Rossa and recorded by the Laser

Scanner monitoring (Fig. 50.4). In the inner part of the same cliff, approximately 25 m from the edge, have been recognized two important discontinuities, longer than 100 m, 50 cm open and 40 cm offset (Fig. 50.5). Nevertheless the integrated monitoring system did not return evidences of significant movements in the first months of the project. This can be explained with the discontinuous nature of the processes of rock collapse and does not exclude the possibility of future movements.

**Fig. 50.4** Comparison between the laser scanner images registered before (*fuchsia dots*) and after (*blue dots*) the block fall from the west side of Cala Rossa (*blue circle*) occurred in October 26, 2012. Where the rock has moved the points lie on the same surface

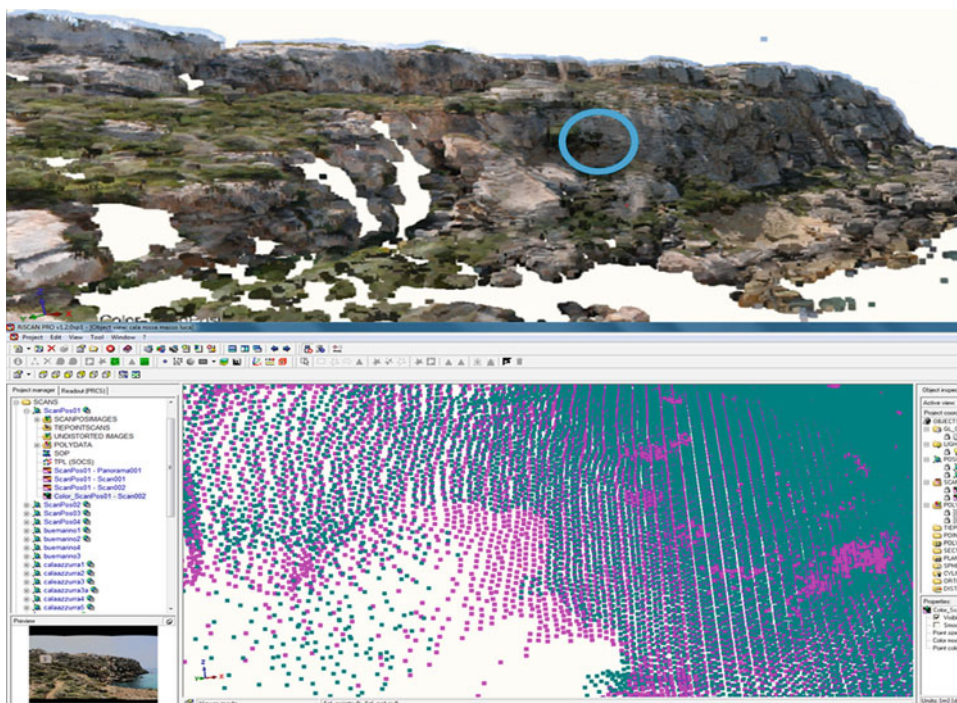


**Fig. 50.5** Giant joint of Cala Rossa



## 50.6 Conclusions

The results of the project will give to the local authorities information about the movements in the monitored areas, useful to the implementation of effective mitigation measures. The monitoring of the ancient mining areas of Favignana is a necessary and appropriate action to prevent that the cliffs and the most significant quarries at least become abandoned to an inexorable degradation process of the historical and environmental features. The enhancement of the safety level of these areas is an essential step for a sustainable and secure tourism in the island. This is the way to ensure that what was left of the quarries, back to being an economic resource, while respecting the historical and the environmental context.

## References

- Abellán A, Calvet J, Vilaplana JM, Blanchard J (2010) Detection and spatial prediction of rockfalls by means of terrestrial laser scanner monitoring. *Geomorphology* 119(3–4):162–171
- Cruden DM, Varnes DJ (1996) Landslide types and processes. In: Turner AK, Schuster RL (eds) *Landslides: investigation and mitigation*. Sp. - Rep. 247, Transportation Research Board, National Research Council, National Academy Press, Washington D.C, pp 36–75
- Frattoni P, Crosta G, Carrara A, Agliardi F (2008) Assessment of rockfall susceptibility by integrating statistical and physically-based approaches. *Geomorphology* 94(3–4):419–437
- Gigli G, Frodella W, Mugnai F, Tapete D, Cigna F, Intriери E, Lombardi L (2012) Instability mechanisms affecting cultural heritage sites in the Maltese Archipelago. *Nat Hazards Earth Syst Sci* 12(1883–1903):2012

- Puglisi C, Falconi L, Leoni L, Pino P, Rasà R, Tripodo A (2007) Analisi della Suscettibilità da frana in Sicilia (1:250.000): Relazioni con scenari climatici futuri. Workshop “Cambiamenti Climatici e Dissesto Idrogeologico: Scenari Futuri per un Programma Nazionale di Adattamento; Napoli, 9–10 Luglio 2007
- Regione Siciliana (2006) Piano Stralcio di Bacino per l’Assetto Idrogeologico (P.A.I.) Isole Egadi (105)
- Stock GM, Martel SJ, Collins BD, Harp EL (2012) Progressive failure of sheeted rock slopes: the 2009–2010 Rhombus Wall rock falls in Yosemite Valley, California, USA. *Earth Surf Proc Land* 37:546–561

---

# Landslide Hazard Assessment, Monitoring and Conservation of Vardzia Monastery Complex

51

Claudio Margottini, Jordie Corominas, Giovanni Battista Crosta, Paolo Frattini, Giovanni Gigli, Ioshinori Iwasaky, Giorgio Lollino, Paul Marinos, Claudio Scavia, Alberico Sonnessa, Daniele Spizzichino, and Daniele Giordan

---

## Abstract

The rock-cut city of Vardzia is a cave monastery site in south-western Georgia, excavated from the slopes of the Erusheti mountain on the left bank of the Mtkvari River. The main period of construction was the second half of the twelfth century. The caves stretch along the cliff for some eight hundred meters and up to fifty meters within the rocky wall. The monastery consists of more than six hundred hidden rooms spread over thirteen floors, which made possible to protect the monastery from the Mongol domination. The site was largely abandoned after the Ottoman takeover in the sixteenth century. The site is by the time affected by frequent slope instability processes along the entire volcanic tuff façade of the slope. Due to this phenomena the National Agency for Cultural Heritage Preservation of Georgia (NACHPG) has promoted, with the support of ISPRA, a landslide hazard assessment for the entire area through rock mechanics characterization, geotechnical engineering survey, geostructural and kinematic analysis, slope stability model, 3D laser scanner acquisitions and elaborations, and a real time monitoring system (GB\_Radar interferometry) for the identification of deformation path of the most hazardous areas. A field analysis was conducted to reconstruct geometry of the rocky cliff, characteristics of discontinuities, main failure modes and volume of potential unstable blocks and geomechanical parameters.

---

## Keywords

Landslide • Monitoring • Georgia • GB-Radar • Laser scanning

---

C. Margottini · D. Spizzichino (✉)  
ISPRA—Geological Survey of Italy, Via Vitaliano Brancati 60,  
00144 Rome, Italy  
e-mail: daniele.spizzichino@isprambiente.it

J. Corominas  
Department of Geotechnical Engineering and Geosciences,  
Technical University of Catalonia, Barcelona, Spain

G.B. Crosta · P. Frattini  
Department of Geological Sciences and Geotechnologies,  
University of Milano-Bicocca, Milan, Italy

G. Gigli  
Earth Sciences Department, University of Firenze, Florence, Italy

I. Iwasaky  
IGS, Osaka, Japan

---

G. Lollino · D. Giordan  
Consiglio Nazionale delle Ricerche - Istituto di Ricerca per la  
Protezione Idrogeologica, 10135 Turin, Italy

P. Marinos  
NTU Athens, Athens, Greece

C. Scavia  
Department of Structural, Geotechnical and Building Engineering,  
Technical University of Turin, Turin, Italy

A. Sonnessa  
Department of Civil, Constructional and Environmental  
Engineering, Sapienza University of Rome/SurveyLab, Sapienza  
Spinoff, Rome, Italy

## 51.1 Vardzia Monastery

The town-monastery of Vardzia is an absolutely unique example of rock-cut architecture not only at national level, but world-wide as well and it is an outstanding and incomparable example of Georgian medieval art. The majestic complex was founded by order of King George III and enlarged by his daughter Queen Tamara (1184–1213 AD). Organized along the rock wall on thirteen levels for a height of 50 m and a length of about 800 m, it consists of several hundred rooms with aqueducts, subterranean tunnels and vertical connections between the various storey. The History of Georgia also relates how Vardzia escaped the Mongol invaders in the 1290s (Stephen 2003). After the arrival of (Gaprindashvili 1975) the Ottomans in 1578, the monks departed and the site was largely abandoned. Infrastructure includes access tunnels, water facilities, and provision for defence (UNESCO 2012; ICOMOS 2001). In 1999 Vardzia Khertvisi was submitted for inscription on the UNESCO World Heritage List as a Cultural Site. In 2007 Vardzia Khertvisi was resubmitted as a mixed Cultural and Natural Site.

## 51.2 Geodetic Survey and Topographical Setting

In order to carry out a site-scale specific analysis and to support the monitoring system activities, a detailed geodetic 3D Laser Scanning survey has been performed and implemented. The geodetic surveying was aimed at the three-dimensional (3D) reconstruction of the cave monastery, and collection of data for future potential slope stability analysis. All 3D data were collected in a Local Reference Frame by means of a terrestrial high-resolution laser scanner (TLS), and then georeferenced by using high-precision dual frequency geodetic GNSS receivers (Baldo et al. 2009). Laser scanning is an automatic contact-free surveying technique (scanning laser range-finder) able to collect 3D surface coordinates at a very high spatial and geometric accuracy.

The intensity of the reflected laser pulse can be recorded, providing an indication of the reflection characteristics of the surface and enabling the creation of quasi images, but high resolution digital RGB images can be acquired with a built-in calibrated camera. All these characteristics make of TLS an extremely useful tool in the field of conservation and protection of Cultural Heritage. Surveying activities at the Vardzia site were performed using a topographical Riegl Z210i laser scanner both for measuring the 3D coordinates of the models and acquiring the RGB information linked to the point clouds. Ten TLS scans were acquired, in order to exactly reconstruct the topography of the site (Fig. 51.1), from two different scan positions by applying the multi-

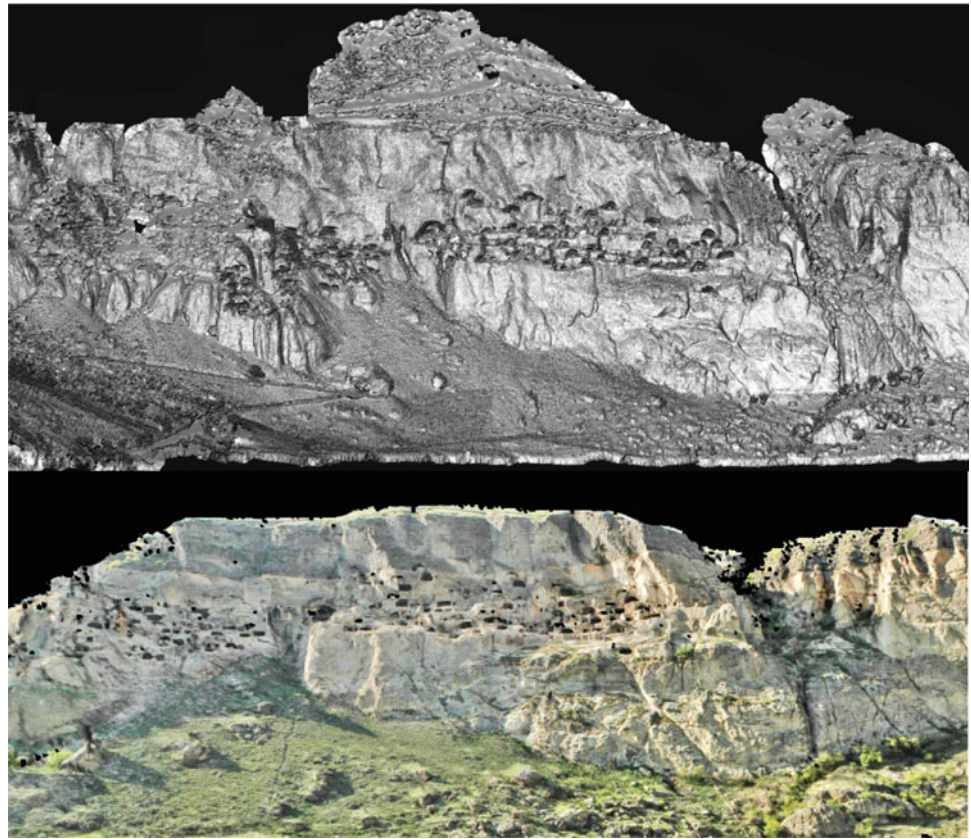
scanning technique. Average spatial resolution ranges from  $10 \times 10$  cm up to some meters, depending on the distance between the laser and the object. In our study area such distance vary from 400 m (along the Line Of Signal) up to 550 m (average distance between the laser and the monastery). Purpose-built targets were used to link the scans together and to build up a high-resolution 3D model of the cave monastery. The final model consists of a point cloud made of about 8,000,000 points from which a DTM with a  $1 \text{ m} \times 1 \text{ m}$  cell size has been derived.

## 51.3 Geological Structural and Geomorphological Setting

The Vardzia monastery is entirely cut and carved in volcanic and pyroclastic rocks (Gillespie and Styles 1999) formations (upper Moitsen–lower Moitsen) (Gudjabidze and Gankrelidze 2003). A representative lithologic cross section of the slope has been accomplished during the last field mission. The entire geologic sequence is the final result of several volcanoclastic and pyroclastic falls, characterized by different explosion dynamics and chemical lava compositions. Concerning the structural setting, at the slope scale, it is possible to define two main discontinuity systems, the first (sub vertical) due to cooling of the volcanoclastic sequence and a second one (locally parallel to the slope face) mainly due to stress release caused by the valley erosion. The spacing decreases at depth moving within the rock mass as visible through some minor tunnels. The boundary between the different volcanoclastic levels are not always clearly marked but they are all sub-parallel according to the style of deposition.

Vardzia is an excellent example of the so called Cultural Landscape (Margottini and Spizzichino 2009). in which human activities (e.g. excavation, construction and implementation of the cave monastery, painting) and natural, geological and geomorphological processes are strictly connected and interdependent. Vardzia slopes are the final result of local seismicity, different volcanoclastic and pyroclastic falls, erosion and deposition cycles of the Mtkhvari river. The entire rock wall has a length of about 800 m for a height of 130 m with a general E-W orientation. The slopes, as a general rule, present a rupestrian aspect, mainly stratified and alternatively massive. Nevertheless, discontinuities of various types are present, potentially related to: cooling phase after volcanic activity (vertical); tectonic activity (faults, minor joints, mainly sub-vertical) geomorphological activity (stress release caused by valley incision). Sub-vertical and high-angle dipping joints intersecting horizontal bedding (layers of different pyroclastics falls) are quite frequent in the area and have been observed during field investigation (Ershov et al. 1999). This situation causes

**Fig. 51.1** DSM of the rock-cut city Monastery of Vardzia (textured)



potential falls, sliding and toppling of blocks, whose type, dimension and kinematics depend on local orientation, mechanical properties of pyroclastic layers, spacing and persistence of joints.

#### 51.4 Monitoring System

Considering the morphological settings (slope extent ca.  $10^5 \text{ m}^2$ ) and slope instability processes (different typologies in size, magnitude and probability of occurrence), a new advanced simple and flexible monitoring system has been implemented in order to obtain: measurements, processing and remote control in real time, and to transform in the future, the monitoring system into a warning system. The system adopted for the monitoring of the entire cliff is based on a ground based interferometric radar. This equipment allows the monitoring of displacement in the line of sight with a resolution of mm.

The radar system is a Stepped-Frequency Continuous Wave (SF-CW) coherent radar with SAR and interferometric capabilities. The acquisition station has been realized with the valuable support of the NACHPG and the pre-acquisition and start up activities have been finalised and calibrated during the last field mission. The above mentioned technique (SF-CW) allows the resolution of the scenario along range

direction independently from the distance (range resolution up to 0.75 m).

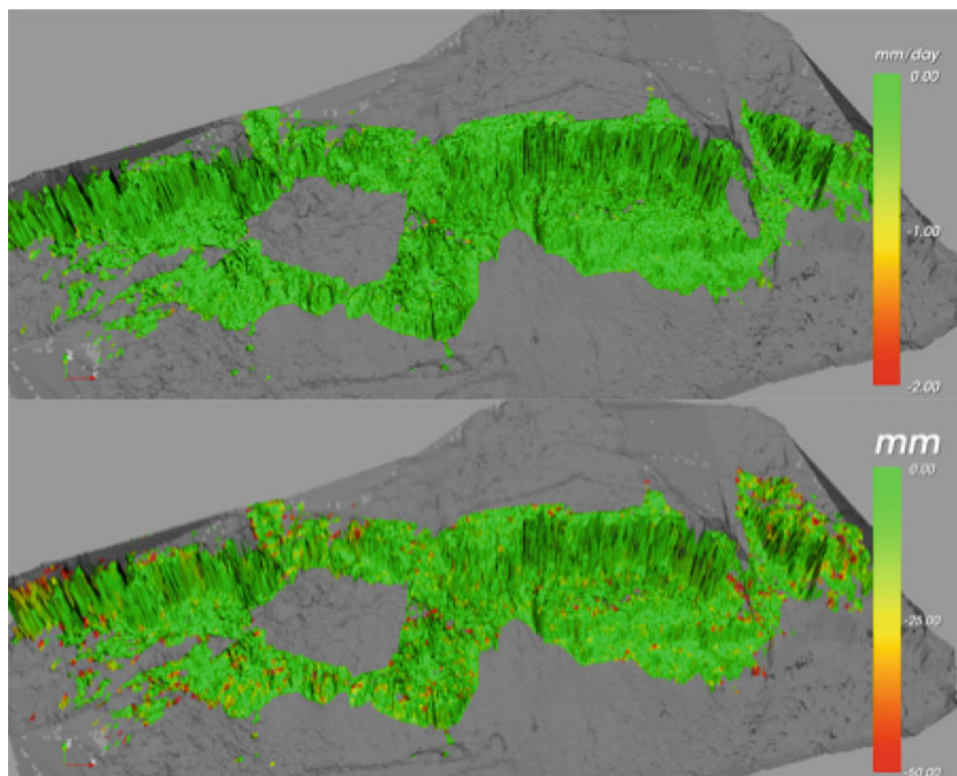
The SAR technique also allows the resolution of the scenario along cross-range direction independently (in the angular value) from the distance (cross-range resolution up to 4.3 mrad). The differential interferometry technique enables the measure of the displacement of the objects resolved through coupling SF-CW analysis. The system has been installed during the May 2012 field mission. During the period May–October 2012 the system has been initialized and tested. The radar configuration adopted is reported in the following table, the “selection mask” contains about 50,000 points (Table 51.1).

The TLS derived DTM has been used as 3D model for the visualization of the main monitored quantities (displacement and velocity) as collected and stored in real time by the

**Table 51.1** Main parameters of radar configuration

Distance from the slope	(m)	350–500
Antenna beam width	(deg)	>70
Number of points	–	50,000
Range resolution	(m)	0.5
Cross range resolution	(mrad)	4.3
Scanning time	(min)	5

**Fig. 51.2** Average velocity and displacement maps for the whole 5-month monitoring period



monitoring system. The monitoring system is actually close to the end of the first 6 months of acquisition and the preliminary results are quite stable and comfortable.

With the exception of some individual control points (mainly due to noise factors related to vegetation) the investigated area is stable and under control (Fig. 55.2). In the next 6 months on site verification of the main critical outcomes of the monitoring systems will be carried out along the cliff in order to calibrate and correct the results and define the most active zones in which downscaling of the landslide hazard and risk assessment is recommended.

## 51.5 Conclusion

The main geomorphological, geo-structural and geomechanical evidences obtained after two field missions (October 2011 and May 2012) suggest the following observations and recommendations:

1. the potential instability processes and mechanisms observed for the entire rock cliff can be referred to different failure modes (or their combination): rock fall; planar rock slide; roto translational rock slide; wedge and toppling failure;
2. such instability processes differ along the whole cliff in terms of activity, their state (temporal evolution),

distribution (spatial evolution), style (combination and repetition of different failure mechanism) and magnitude (landslide intensity and potential volumes);

3. actual and/or potential instability processes at the Vardzia monastery are the result of a combination of different predisposing factors such as: lithology, presence, frequency and orientation of discontinuities versus slope orientation, physical and mechanical characteristics of materials, morphological and hydrological boundary conditions;
4. the coupling of different survey techniques (e.g. 3D laser scanner, engineering geological and geomechanical field surveys, Ground based radar Interferometry) is the best strategy to be adopted in the interdisciplinary field of Cultural Heritage protection and conservation policies.

## References

- Baldo M, Bicchocchi C, Chiochini U, Giordan D, Lollino G (2009) LIDAR monitoring of mass wasting processes: the Radicofani landslide, Province of Siena, Central Italy. *Geomorphology* 105: 193–201
- Ershov AV, Brunet MF, Korotaev MV, Nikishin AM, Bolotov SN (1999) Late Cenozoic burial history and dynamics of the Northern Caucasusmolasse basin: implication for foreland basin modeling. *Tectonophysics* 313:219–241

- Gaprindashvili G (1975) (in English, Russian, Georgian). Ancient monuments of Georgia: Vardzia. Aurora art publishers, Lenin-grad, pp 7–25. ISBN 978-1-135-68320-7
- Gillespie MR, Styles MT (1999) BGS ROCK classification scheme volume 1 classification of igneous rocks. British geological survey research reports, (2nd edn) RR 99-06
- Gudjabidze GE, Gamkrelidze IP (2003) Geological map of Georgia, 1:500,000. Georgian State Department of Geology and National Oil Company “Saqnavtobi”
- ICOMOS (2001) Evaluations of cultural properties. UNESCO report, pp 18–21. Retrieved 1 May 2012
- Margottini C, Spizzichino D (2009) The management of cultural and environmental heritage sites: a pivot for conservation and enhancement. In: Proceedings of the first international symposium on Danxia landform. The 2nd collection. Danxiashan, Guadong (China), 26–28 May 2009
- Stephen H (2003) Rapp. Studies in medieval Georgian historiography: early texts and Eurasian contexts, passim. Peeters Publishers. ISBN 90-429-1318-5. Retrieved 26 April 2009
- UNESCO (2012) Internal report “Vardzia-Khertvisi”. Retrieved 1 May 2012

Giuseppe Delmonaco, Gabriele Leoni, Claudio Margottini, and Daniele Spizzichino

---

## Abstract

The paper summarizes field survey results and analysis in the framework of a UNESCO project (Siq Stability Project) for the implementation of remote and field integrated monitoring systems aimed at the detection and control of active deformation of the Siq slopes (Petra, Jordan). Petra is located on the eastern side of the Dead Sea-Wadi Araba tectonic depression, in SW Jordan. The Siq is a 1.2 km long natural deep gorge in the sandstone mountains that connects the urban area of Wadi Musa with the monumental area of Petra. Since Nabataean times, the Siq is the main narrow entrance for some thousands tourists that access the archaeological area every day. Discontinuities of various type (bedding, joints, faults), mainly related to stratigraphic setting, tectonic activity and geomorphological evolution of the slope can be recognized. Rock-fall potential activity can be catastrophic according to evolution of the movement (extremely rapid) and involved rock mass volumes. Slope instability, acceleration of crack deformation and consequent increasing of rock-fall hazard conditions could threaten the safety of people walking through the Siq.

---

## Keywords

Rock fall • Landslide • Cultural Heritage • Monitoring • Petra

---

## 52.1 Geological and Geomorphological Features of Siq

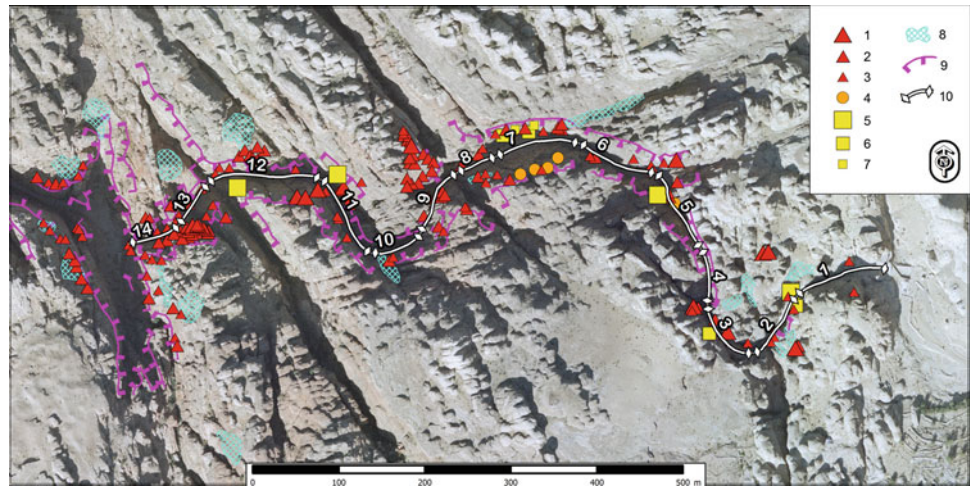
The Siq is a 1.2 km long natural structure formed by very steep slopes with variable heights by the ground level, from few meters, at the entrance, to several tens of meters at the end of the path. Outcropping rocks belong to the Cambrian-Ordovician sandstone of Disi and Umm Ishrin formations. The hand-carved rock monuments of Petra are almost entirely cut in the Umm Ishrin sandstone that can be subdivided into three main units, according to their texture,

mineralogical composition and geotechnical characteristics. The geomorphology of the Siq is the result of long and short-term factors affecting this part of the Petra territory such as tectonic uplift, erosion due to runoff, differential erosion and weathering of sandstone materials. The Siq has a main E-W orientation and a meandering course, governed by intersection of faults and master/secondary joints. The slopes generally presents a rupestral aspect, mainly massive. Nevertheless, discontinuities of various types are present, mainly related to bedding (generally horizontal), tectonic activity (faults, master joints, mainly sub-vertical), geomorphological activity (from vertical to medium-inclined joints). Sub-vertical and medium-angle dipping joints intersecting horizontal bedding are quite frequent and observed during field investigation. This situation may cause potential sliding of blocks, whose dimensions are depending on local orientation, density and persistence of discontinuities. Potential and actual rock slope failures are strictly depending on type and degree of structural control. They can be classified as: (i)

---

G. Delmonaco (✉) · G. Leoni · C. Margottini · D. Spizzichino  
ISPRA—Geological Survey of Italy, Via Vitaliano Brancati 48,  
00144 Rome, Italy  
e-mail: giuseppe.delmonaco@isprambiente.it

**Fig. 52.1** Landslide inventory map of Petra area: 1 rockfall large; 2 rockfall medium; 3 rockfall small; 4 toppling large; 5 slide large; 6 slide medium; 7 slide small; 8 unstable debris; 9 scarp; 10 Siq sector. Landslide volume: large  $>15 \text{ m}^3$ ; medium  $5\text{--}15 \text{ m}^3$ ; small  $<5 \text{ m}^3$



planar failures, (ii) wedge failures, (iii) toppling failures, (iv) unstable isolated blocks (toppling/sliding) (Delmonaco et al. 2013). All the above geomorphological processes have been collected and elaborated in a geo-database. An inventory map of potential unstable blocks has been implemented reporting types and magnitude of the inventoried phenomena (Fig. 52.1). Geostructural and landslide kinematic analysis have detected the probability of the main failure modes of the Siq slope-forming rocks.

- automated crack-gauge network, with wireless connection, to monitor main cracks and isolated potentially unstable blocks, with a low environmental impact technology;
- high resolution total station network measuring a prisms network, individual reflectorless points network and reflectorless grid network in the Siq slopes, for monitoring slope/blocks deformation;
- manual crack gauge network on 25 main discontinuities.

## 52.2 Monitoring System Proposal

According to the above results, and considering the morphological setting and slope instability processes, the following monitoring techniques have been proposed, designed, implemented and installed for the monitoring of the Siq slopes in Petra (Fig. 52.2):

- Satellite SqueeSAR<sup>TM</sup> analysis with permanent scatters techniques, to evaluate potential regional deformation pattern of the site and possible Siq border effects;

### 52.2.1 Satellite SqueeSAR<sup>TM</sup>

A large area of Petra Park, involving the Siq and major monuments, was analyzed with SqueeSAR<sup>TM</sup> technique, provided by TRE®. The SqueeSAR<sup>TM</sup> algorithm, recently developed, provide further improvement of PSInSAR<sup>TM</sup> technology, providing distinct properties of the signal from radar satellites to detect millimeter-scale changes of the ground. The analysis has provided 62.000 PS measurement points from 2003 to 2010 and related time histories of the

**Fig. 52.2** Monitoring system map: 1 gateway; 2 repeater; 3 air temperature/humidity sensor; 4 crackmeter, 5 wire deformometer; 6 meteorological station; 7 tiltmeter; 8 TM30 robotized station; 9 TM30 monitoring prism; 10 TM30 reference prism; 11 Manual crack gauge, 12 Siq sector

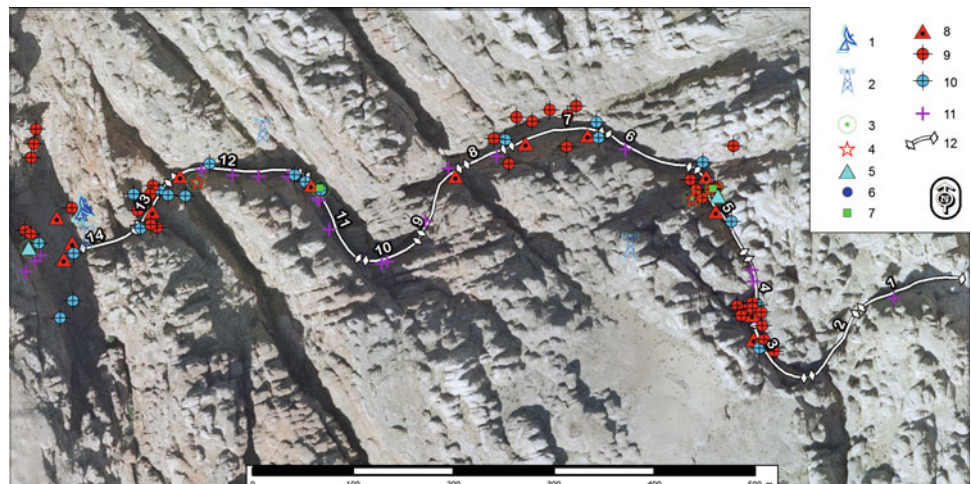
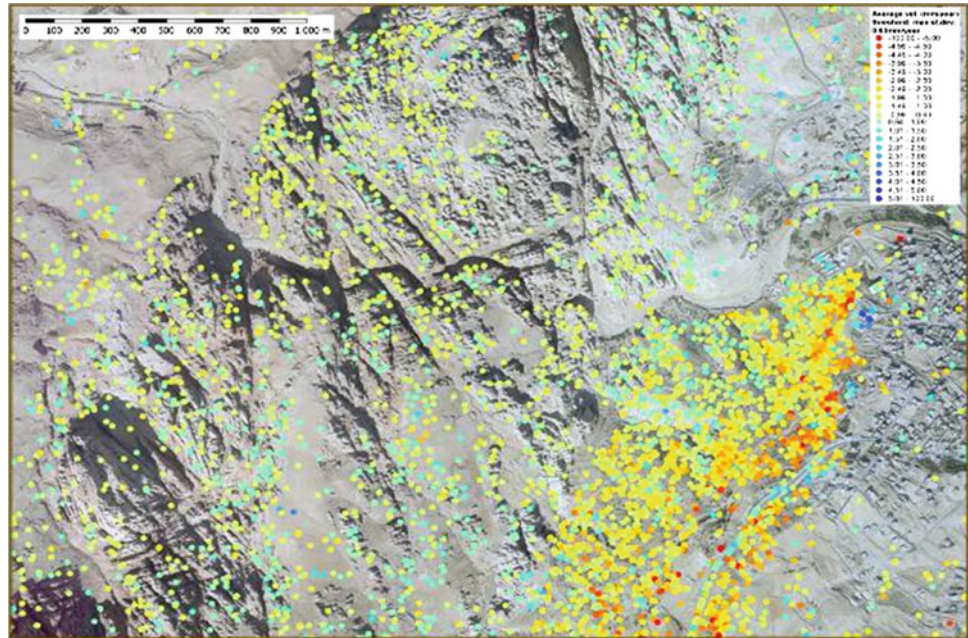


**Fig. 52.3** Annual average velocity with 0.63 mm/year threshold (maximum standard deviation)



yearly average displacement velocity (Fig. 52.3). In the analysis, 38 images with only a descending orbit have been used; this means that any potential displacement along the main E-W and vertical components cannot be distinguished. This is related to the available dataset of ENVISAT images, used in this project. The theoretical time difference of an ENVISAT satellite image acquisition is 35 days, but the time series of the image used for the analysis exhibit a much higher temporal gap with a maximum of 280 days. This type of problem has a low influence on area affected by slow or very slow deformation. The minimum pixel resolution is  $20 \text{ m} \times 5 \text{ m}$  for the acquisition of a reliable PS so that actual deformation processes involving surfaces  $<100 \text{ m}^2$  cannot be evidenced with the PS technique. The C-band utilized in the analysis corresponds to a wave-length ( $\lambda$ ) of 5.66 cm that allows the detection and measurement between two consecutive images (on a single isolated target) equal to 1.4 cm. All PS dataset actually displayed consist of coherent measurement point with a ground deformation  $<1.4 \text{ cm}$  during the all temporal distance covered by two consecutive images; any deformation exceeding such a threshold during the acquisition of two consecutive images has not been recorded due to loss of coherence and no longer displayed in the final dataset. All measurement points have a geographic accuracy variable from 7 (along E direction) and 2 m (along N direction so that the respective deformation data can be actually attributed to a different position in that field of accuracy, whereas the precision of the average velocity is equal to  $\pm 1 \text{ mm/year}$  with differential displacement measures of  $\pm 5 \text{ mm}$ .

Taking into account the above considerations, that derive from the quality of the available dataset of ENVISAT images, the following results have been obtained:

- there is no evidence of main ground deformation in the Petra valley affecting the Siq and the monuments during the time interval analyzed (2003–2010);
- the type of deformation and instability evolution (i.e. small rock falls) are hardly detectable with interferometric data due to decorrelation phenomena that might occur considering volumes/magnitude or involved surfaces of potentially unstable rocks with respect to the minimum detectable area of the technique (with ENVISAT about  $20 \text{ m} \times 5 \text{ m}$ ) and the geotechnical behavior of the Petra sandstone, characterized by a brittle rupture mode;
- for rock fall phenomena occurred during the time of observation (i.e. Tomb 609, High Place of Sacrifice) the analysis can be theoretically performed by concentrating the analysis of deformation in a smaller time window (pre and post-collapse) with the limits previously mentioned (i.e. availability of as many images as possible with high quality, use of a X-band images);
- the analysis performed to the Siq and Petra areas confirms limits and applicability for the specific landslide types (mostly rock falls) that affect the study area.

### 52.2.2 Direct Rock Block Monitoring with Wireless Network

An integrated network composed by 2 wire deformometers, 2 crack deformometers and 2 tiltmeters, 6 air-temperature sensors, a meteorological station, provided by Minteos® s.r.l., with wireless technology sensors for on-time registration and transmission of data, has been installed in the Siq in June 2013 (Fig. 52.4). Displacement of the main fractures,

**Fig. 52.4** Installation of wireless instrumentation network



inclination of the blocks and meteorological parameters are the main data collected by the system.

The general structure of the platform for the storage and management of the collected data from the sensors is based on the following components: field devices, constituted by wireless sentries that measure and send via radio the values of displacement (resolution 0.01 mm) and inclination (resolution 0.01°) to a Short-Range Repeater (SSR); the SSR routes the sentries radio message in the Siq adding temperature and humidity data forwarding these to the Long-range Repeater (LRR); the LLR add rainfall, shielded temperature, humidity and wind direction forwarding all data to the main gateway, located in front of the Treasury (end of the Siq); the gateway collects and send the data to the Minteos server via GPRS and, in turn, to the main Siq Project servers for storage and analysis of results. The sensors will be provided with long-life batteries capable to manage 24 h measures per day per 5 years and further provided with solar cells in order to assure measurements in the event of a breakdown.

The system, at this stage of the research, is not purposely aimed to work as a near-time alarm or early warning system device (Giordan et al. 2013), but to provide displacement

data and trends to be analyzed with those of meteo-climatic parameters.

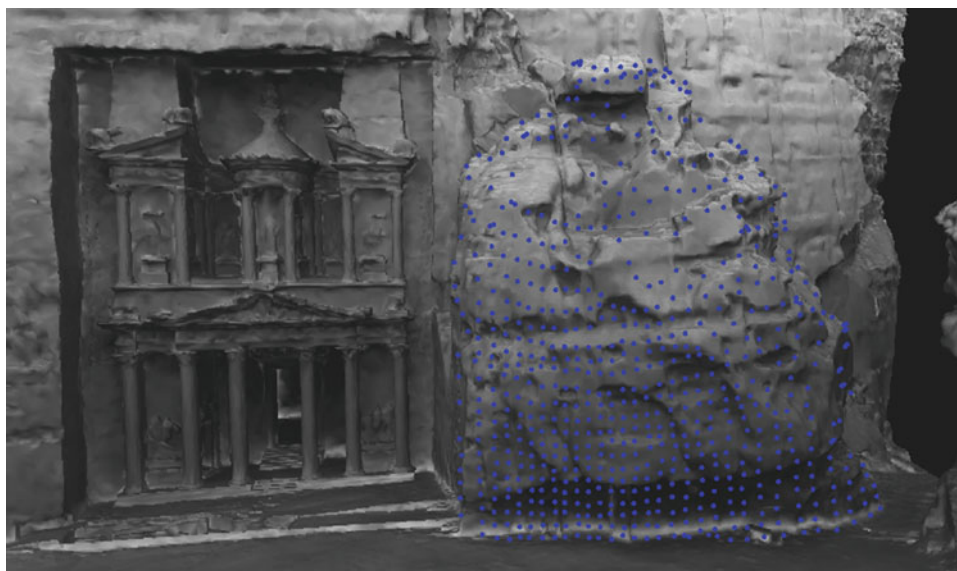
### 52.2.3 Reflectorless Total Station Monitoring Network

A Leica® TM30 reflectorless total station has been used to extend deformation control and analysis of the 6 potentially unstable blocks as well as provide information on movements of 15 slope faces located inside the Siq and in the Outer Siq (Treasury area).

A total of 81 micro prisms, (22 prisms in stable areas as reference points and 59 as monitoring targets) properly designed to reduce visual impacts, have been installed by local climbers. The technique (acquisition and elaboration of different 3D model compared during time) will provide 3D movement of unstable blocks/slope sectors and further movement (2D analysis) of the deformation slopes through the acquisition of some thousands reflectorless monitoring points (Fig. 52.5).

In detail, the TM30 monitoring system is based on a polygonal constituted by prisms located in the lower

**Fig. 52.5** TM30 reflectorless monitoring points in the area of the Treasury



portions of the Siq, working as reference points. Bimonthly lectures with the total station along the base polygonal will provide a regular time-space acquisition of control point clouds in the slope sectors to be monitored. Point clouds are constituted by prisms, working as base monitoring points, and reflectorless points that the total station is capable to detect and measure in the field between consecutive acquisitions. The precision with such a topographic monitoring system is sub-millimetric. The monitoring output is given by differences between distinct lectures and 3D topographic models derived by point clouds analysis in any monitored sector of the Siq. Such differences will provide deformation of points in the slopes for further analysis of actual/potential unstable areas of the Siq.

---

### 52.3 Preliminary Results and Conclusions

An integrated set of direct and remote distinct monitoring systems and techniques has been implemented for the analysis of rock slope deformations in the Siq of Petra. The overall system has been designed and installed according to potential capability of the different techniques as well as cost/benefit and long-term sustainability, considering the specific geological and cultural environment of the Siq of Petra.

A regional scale analysis of the measurement points derived by SqueeSAR™ technique has provided evidence of a general stability of the Petra area in the time span considered (2003–2010). The areas where some movement (>2 mm/year) occurred, are characterized by presence of incoherent material (e.g. debris, sands) removed by human activities and/or natural erosion and mostly located out of the Siq.

The crack and wire-gauge system, based on 6 months-observation data set, has provided a generally constant trend of movements, with negligible displacements (<1 mm), mostly related with daily temperature and humidity fluctuations.

The analysis with reflectorless total station is actually in the stage of set up finalization (i.e. reference and monitoring prisms georeference, implementation of reflectorless monitoring plan, zero cycle measurement) so that no data are

available. For this technique, a correct design of the network is fundamental to determine and assess relative movements of points, so that a particular attention and intense field work is being devoted to provide the highest accuracy in the system configuration.

Measurements of the manual crack gauge network, since June 2011, has provided records that exhibit a general enlargement of the monitored discontinuities (average of ca. 1 mm) during the 2011–2012 winter seasons and a slight shrinking of the fractures apertures in the summer seasons. Nevertheless, considering the limited number of measurements taken, it is still insufficient to define a clear displacement trend versus climate-related parameters and local geomorphic conditions of the blocks/slope portions examined.

In conclusion, in the Siq of Petra, conventional geotechnical and topographic instrumentation, with innovative and powerful components, has been installed to provide a wide set of techniques to produce evidence of displacement in the Siq slopes. These site-scale field techniques have been integrated with a satellite interferometric analysis in order to provide also a large-scale analysis of ground displacement in the Petra Park. It is expected that the adopted approach will provide in the development of the project, a discrimination of the most critical blocks/areas where to focus a geotechnical modeling for the analysis of actual slope stability conditions and suggestion of mitigation strategies for the benefit of the site managers.

---

### References

- Delmonaco G, Margottini C, Spizzichino D (2013) Rock fall assessment in the Siq of Petra, Jordan. In: Canuti P, Margottini C, Sassa K (eds) *Landslide science and practice. volume 6: risk assessment, management and mitigation*. Springer, Heidelberg, pp 441–449. ISBN 978-3-642-31312-6
- Giordan D, Allasia P, Manconi A, Baldo M, Santangelo M, Cardinali M, Corazza A, Albanese V, Lollino G, Guzzetti F (2013) Morphological and kinematic evolution of a large earthflow: the Montaguto landslide, southern Italy. *Geomorphology* 187:61–79

John Cripps, Nurul Liyana B. Awang Rosli, Barney Harris,  
and Roger Lewis

---

## Abstract

Durrington Walls is one of Britain's largest prehistoric henge monuments. Approximately 3 km northeast of Stonehenge, it is situated nearby the River Avon on the chalk of Salisbury Plain. The construction of Durrington Walls entailed the extraction and transport of approximately 110,000 tonnes of Lower Cretaceous Chalk, a monumental task that current evidence suggests took place no later than 2500BC. Residual tool marks on chalk spoil recovered from Durrington Walls suggest sophisticated digging practices and antler tools were employed during its construction. This study investigates how the saturation degree of chalk may impact on its strength and the formation of tool marks created by replicative experimentation. Tests were carried out in which grooves were formed by human manipulation of antler tines on tests pieces of chalk from Durrington at different levels of saturation. Forces imposed on specimens during the tests were measured and compressive strength and porosity tests were also carried out. Parallel tests were performed on chalk from South Ferriby, Lincolnshire, which is stronger and denser than the Durrington Chalk, to investigate the effects of chalk density, texture and structure on these properties. The results show that an increase in saturation of less than 1 % above dry resulted in a large decrease in strength of about 30–50 %, where the change is less for the stronger rock. The size of the grooves is influenced by rock strength, load applied and level of saturation.

---

## Keywords

Chalk • Saturation • Strength • Rock wear • Durrington walls

---

J. Cripps (✉) · N.L.B. Awang Rosli  
Department of Civil and Structural Engineering,  
University of Sheffield, Sheffield S1 3JD, UK  
e-mail: j.c.cripps@sheffield.ac.uk

N.L.B. Awang Rosli  
e-mail: liyana2306@gmail.com

B. Harris  
Department of Archaeology, University of Sheffield,  
Sheffield S1 3JD, UK

R. Lewis  
Department of Mechanical Engineering, University of Sheffield,  
Sheffield S1 3JD, UK

---

## 53.1 Introduction

Durrington Walls is a subcircular ditch and bank henge monument situated near to the River Avon, approximately 3 km northeast of Stonehenge. Like many of Britain and Ireland's henge monuments, it was constructed within the 3rd millennium BC. The structure and its location in southern England are illustrated in Figs. 53.1, 53.2 and 53.3. As Fig. 53.1 shows several houses belonging to a late Neolithic settlement have recently been excavated at the site. The settlement dates to the middle of the 3rd millennium BC (Marshall, In press) and is thought to be one of the largest in North West Europe of this time (Parker Pearson et al. 2007, 2011). Shortly after the settlement was abandoned the henge was constructed which still survives in parts today. When

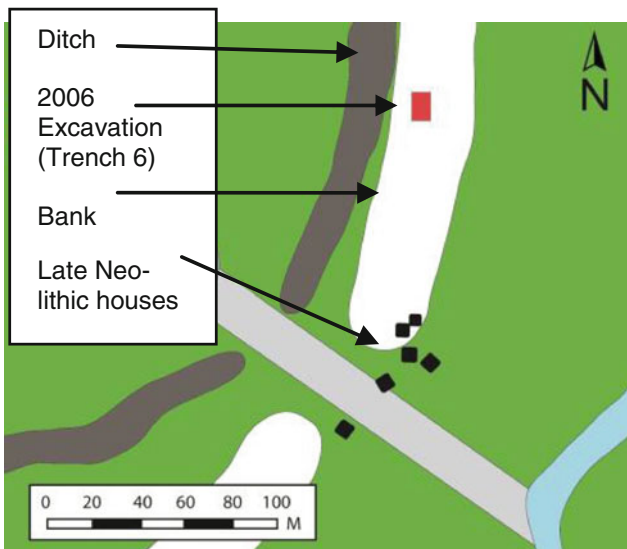


**Fig. 53.1** Plan view of SE part of Durrington Walls site

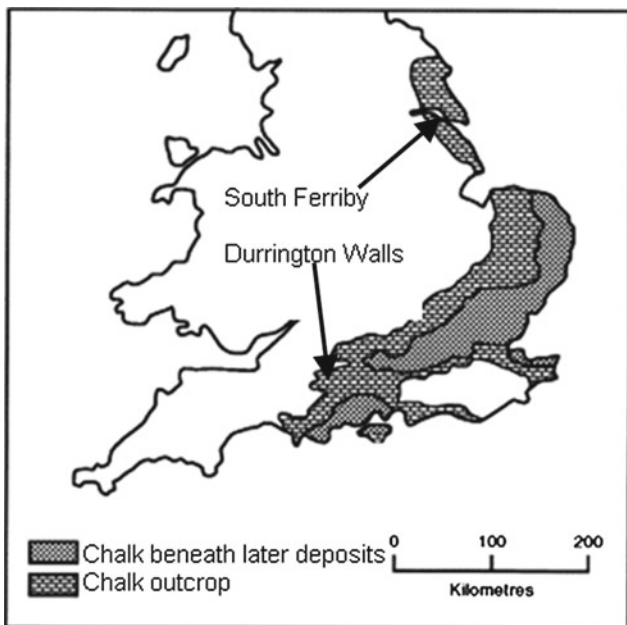


**Fig. 53.2** Approximate locations of sample sites (After Bell et al. 1999)

originally constructed the ditch was approximately 5 m deep by 5 m wide and encircled by a chalk bank around 5 m high. The henge has a circumference of approximately 1.6 km and it is estimated that the construction of this giant earthwork required the extraction and transport of approximately 110,000 tonnes of Lower Cretaceous Chalk.

As part of the Stonehenge Riverside Project, carried out by The University of Sheffield from 2004–2009, samples of fragmentary chalk were removed from the bank of Durrington Walls in order to investigate the technology used originally to extract it. Some of the chalk fragments show

tool marks (see Fig. 53.4) which can be attributed to the use of antler tools during the extraction process (Harris, In press).

The objectives of the present study were to (a) obtain values for the strength and wear resistance of the chalk encountered by prehistoric henge builders and (b) investigate the effects of rock moisture content on the above properties and the morphology of experimental grooves created with antler tines. Accordingly, strength and tribological sliding wear tests at different states of saturation were carried out on chalk from Durrington Walls. Similar tests were carried out on chalk from South Ferriby, Lincolnshire, UK (see Fig. 53.2) in order to investigate the effects of chalk density, texture and structure on these properties.

## 53.2 Laboratory Tests

### 53.2.1 Uniaxial Compressive Strength

It is well-known that dry rocks are stronger than wet ones which is attributed by Colback and Wiid (1965) to the effects of moisture on the surface-free energy of the rock grains. This they argue directly influences the molecular cohesive strength of the material. These authors reported a strength reduction of about 50 %, in shale and sandstone they tested, with most of this reduction occurring within an increase in moisture content of less than 1 or 2 %.

Chalk from archaeological excavations at Durrington and from the quarry at South Ferriby were prepared as 54 mm diameter cores with axes perpendicular to the bedding apparently present in the rock. The ends of the cores were trimmed perpendicularly to the axis, and they were ground flat. ISRM (1981) recommendations were followed with respect to the tests, where length to diameter ratios of 2.5–3 and a loading rate of 0.5–1.0 MPa/s were used.

Because of the size and low number of large blocks from Durrington available for testing, some of the cores were shorter than required by the standard, which necessitated the application of a correction recommended by Hawkins (1998). A further correction, (Hoek and Brown 1980), was applied to account for the core not being 50 mm diameter specified by ISRM (1981). Although it is recommended that at least 5 specimens are tested for each determination of strength, unfortunately there was insufficient Durrington material for more than 3 specimens to be tested at each moisture content, whereas between 3 and 6 specimens of the South Ferriby samples were used. In cases in which the direction of bedding in blocks was not discernible, the direction to give the best yield of samples was used and the failed specimen fragments were carefully examined to assess whether the failure had been affected by any non-horizontal bedding structures, or any inclusions or voids in the samples.

**Fig. 53.3** Durrington Walls viewed from the South during 2005 excavations. The remains of the partly eroded henge bank are highlighted in red (with thanks to Julian Thomas)



**Fig. 53.4** Chalk block from the Durrington site, with antler tool marking in box



### 53.2.2 Porosity, Moisture Content and Saturation

The moisture content of the samples was determined in the standard manner (British Standards BS 1377-2 1990) by drying at 105 °C until there was no further weight loss. Measurements were repeated on 1 or 2 specimens. The porosity tests were carried out according to the method specified by ISRM (1981), so after drying 105 °C the specimens were vacuum saturated for at least 1 h.

Strength and wear tests were performed on dry chalk, completely saturated chalk and chalk in various states of partial saturation. Full saturation was achieved by vacuum immersion in deionised water for up to 7 days, or until the mass was constant. Before a specimen was weighed the surfaces were carefully wiped dry. To attain a particular state of partial saturation (1, 2, 5, 10 or 15 %), the mass the sample needed to be for that moisture content was calculated by adding the necessary mass of water to the dry weight of

the sample and then either oven drying or immersing the sample until this was achieved. Once at the required state of saturation, the samples were wrapped in plastic cling film to prevent further change in moisture content and the sample was stored until required for testing. This was to assisted the creation of a uniform distribution of water in the through the sample.

### 53.2.3 Wear Tests

Manual unidirectional one-stroke sliding wear tests were carried out on 100 by 60 by 20 mm thick oblong slabs using a wet diamond saw. So far as possible the slabs were cut parallel to the bedding where this structure was identifiable. Initially the sliding test specimens were clamped to the instrumented force plate (see Fig. 53.5) and the test was performed by holding the antler tine firmly against the rock



**Fig. 53.5** Forming a groove on a sample of chalk clamped to a force plate



**Fig. 53.6** Measuring depth of surface markings

and drawing it over the surface in a single action. So that the moisture content of the specimen would remain at the required value, the cling film was removed from only the upper surfaces of the specimens immediately before the test was carried out. The average force and the widths and depths of resulting grooves were determined, where the dimensions were measured along 3 transepts, using respectively a vernier caliper and, as shown in Fig. 53.6, a digital depth gauge.

## 53.3 Experimental Results

### 53.3.1 Compressive Strength

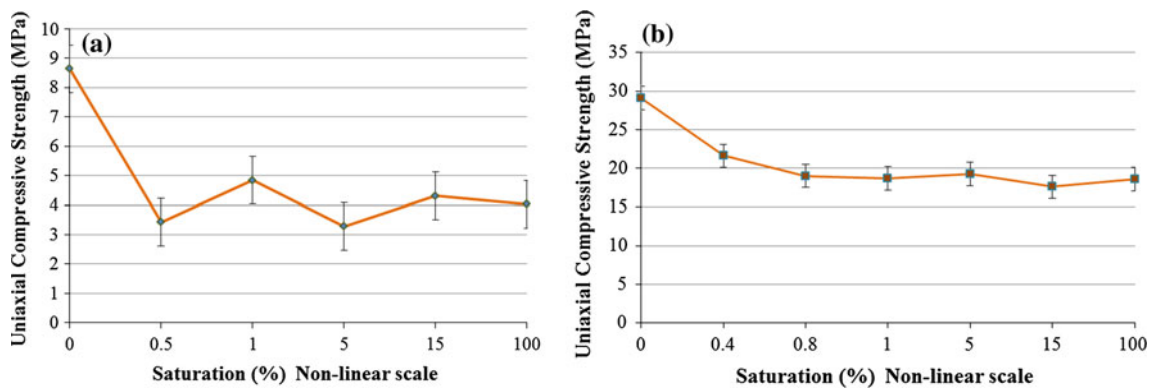
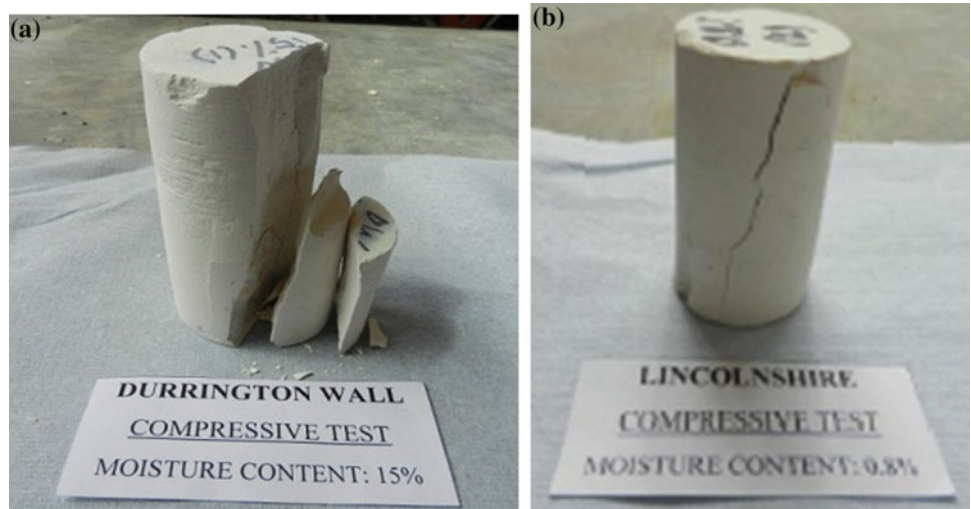
Examples of failed specimens are shown in Fig. 53.7. In most cases failure was along systems of vertical or sub-vertical, and occasionally inclined fractures. The results did not appear to have been influenced by any internal structures in the rock, although the test platens appear to have had an influence. Figure 53.8 shows the relationships between the average Uniaxial Compressive Strength (UCS) and the degree of saturation for the two types of chalk. The effect of only a slight increase in saturation is very clear, with a dramatic decrease in strength from 9 MPa for the dry rock to about 4 MPa; a drop of about 50 %, with an increase in saturation of 0.5 %. This is the equivalent of a moisture content of only 0.2 % in this rock. The drop in strength of the South Ferriby Chalk is about 30 %, where the dry value of 29 MPa reduces to about 18 MPa with an increase in saturation of 0.8 %; equivalent to a moisture content increase of 1.6 %.

The values of porosity in relation to strength for all states of saturation are shown in Fig. 53.9. Hence the porosity of Durrington Chalk is near to 40 %, whereas that of South Ferriby Chalk is around 20 % and as a consequence the former chalk is the weaker by a factor of about one third.

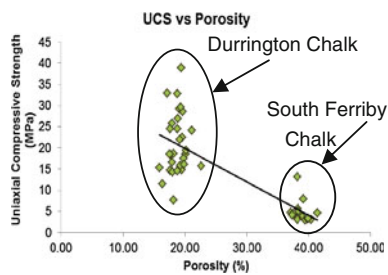
### 53.3.2 Wear

Figure 53.10 shows the amount of chalk removed in the series of groove tests for different saturations for both chalks at all loads. As would be expected, for the Durrington Chalk the amount removed increases as the saturation increases, however although the values increase rapidly to a saturation of 15–20 %, the rise appears to be more gentle as the saturation increases to 100 %. Clearly this is caused by the reduction of strength produced by the increase in saturation, but it appears that the groove size does vary over a wider range of saturations than the strength does. One implication of this finding is that it may be possible to estimate the saturation of tool-marked chalk over a wide range of saturations. Although the trend is not seen in the data for South Ferriby in Fig. 53.10b, this graph does demonstrate the control exerted by strength over groove size in the stronger chalk. The variations in groove size with the load applied to the antler tool are shown in Fig. 53.11 for both chalks at zero and 100 % saturations. The data demonstrate that volumes of chalk removed are generally lower for the dry chalk, and for the softer Durrington Chalk, there is a clearer relationship between the load applied to the tool and the amount of rock removed.

**Fig. 53.7** Compression tests on samples of chalk from **a** Durrington Walls and **b** South Ferriby



**Fig. 53.8** Strength of **a** Durrington Chalk and **b** South Ferriby Chalk at different degrees of saturation



**Fig. 53.9** Relationship between porosity and uniaxial compressive strength (all saturations)

### 53.4 Conclusions

The main findings of this research are as follows:

- Whereas the dry uniaxial compressive strength of dry Durrington Chalk is about 9 MPa which decreases to

about 5 MPa due to a small increase in moisture content of the order of 1 %. The strength changes little for further increases in saturation to 100 %.

- The results for South Ferriby Chalk follow a similar pattern, but the corresponding values are 29 and 18 MPa; thus this stronger chalk is less sensitive to the presence of water.
- Porosity is a key factor that influences the properties and whereas the weaker Durrington Chalk averages about 40 %, the value for the South Ferriby Chalk approximates to 20 %.
- The difference of about three-fold in the strengths of the Durrington and South Ferriby chinks accounts for a decrease of the order of ten-fold in the size of the grooves produced in the latter chalk.
- The size of the groove formed by holding an antler tool firmly against a rock surface and manually dragging is across the surface is a function of rock strength and degree of saturation of the rock.

**Fig. 53.10** Effect of saturation on size of grooves in **a** Durrington Chalk and **b** South Ferriby Chalk

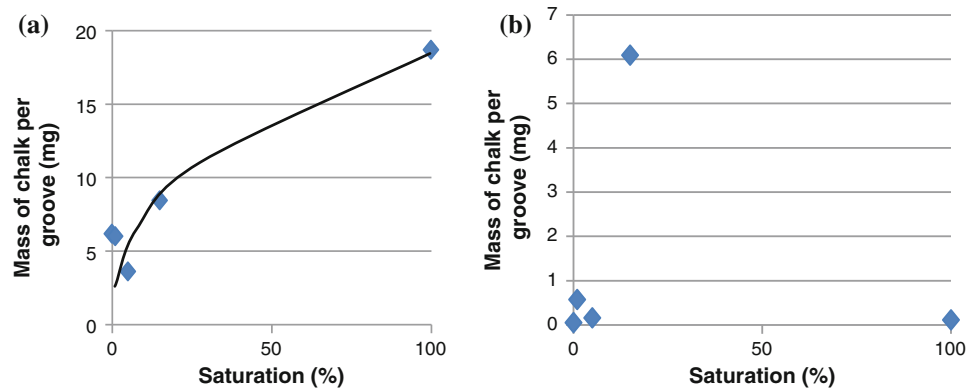
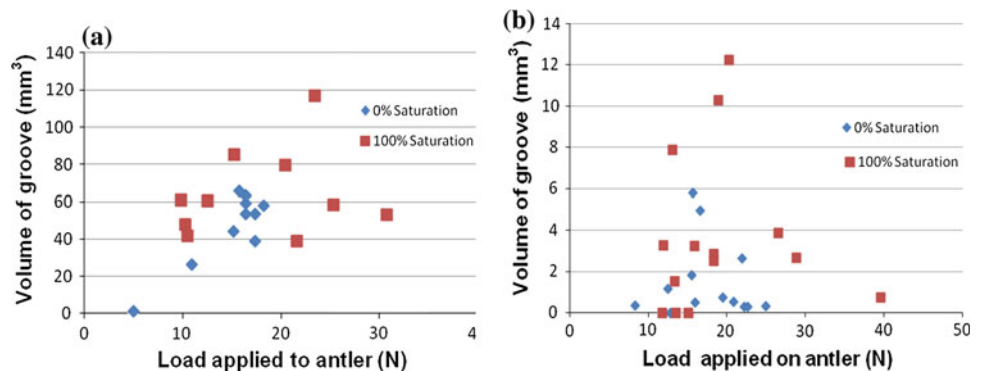


**Fig. 53.11** Effect of load on tool on size of grooves in **a** Durrington Chalk and **b** South Ferriby Chalk



- There is an approximate correlation between the load on the tool and the size of the grooves formed in the Durrington Chalk and the degree of saturation is also influential.
- If further research into prehistoric chalk extraction technology can establish an approximate upper limit for human applied loads with antler tools, the dimensions of archaeological tool marks may be used to determine the approximate saturation of the chalk at the time of working. In turn, this may assist in establishing whether the builders of Durrington Walls harnessed the strength reducing properties of water when excavating or dressing the chalk.

**Acknowledgements** N.L.B. Awang Rosli expresses thanks to the Ministry of Education, Brunei for financial support that enabled this work to be carried out. Thanks are also expressed to the Stonehenge Riverside Project and Cemex Cement, South Ferriby for samples of chalk.

## References

- Bell FG, Culshaw MG, Cripps JC (1999) A review of selected engineering geological characteristics of English chalk. *Eng Geol* 54:237–269
- British Standards BS 1377-2 (1990) Methods of test for soils for civil engineering purposes: classification tests. British Standards Institute, London
- Colback PSB, Wiid BL (1965) The influence of moisture content on the compressive strength of rocks. In: *Proceedings of the rock mechanics symposium: 3rd Canadian symposium*, pp 65–83
- Harris, BG (In press) Artefacts. In: Pearson MP, Bronk Ramsey C, Cook G, Pollard J, Thomas J, Richards C, Welham K (eds) *Durrington walls and woodhenge: a place for the living. The Stonehenge Riverside Project, vol 2. The Prehistoric Society, London*
- Hawkins AB (1998) Aspects of rock strength. *Bull Eng Geol Environ* 57:17–30
- Hoek E, Brown ET (1980) *Underground excavations in rock*. Inst Min Metall, London
- International Society for Rock Mechanics (ISRM) (1981) *Rock characterization testing and monitoring: suggested methods*. Pergamon Press, Oxford
- Marshall, PD (In press) Radiocarbon dating. In: Pearson MP, Bronk Ramsey C, Cook G, Pollard J, Thomas J, Richards C, Welham K (eds) *Durrington walls and woodhenge: a place for the living, vol 2. The Stonehenge Riverside Project, The Prehistoric Society, London*
- Parker Pearson M, Allen M, French C, Pollard J, Richards C, Robinson D, Thomas J, Tilley C, Welham K (2007) *The Stonehenge riverside project full interim report*, University of Sheffield
- Parker Pearson M, Pollard J, Richards C, Thomas J, Welham K, Albarella U, Chan B, Marshall P, Viner S (2011) *Feeding Stonehenge: feasting in late Neolithic Britain*. In: Aranda Jiménez G, Montón-Subías S, Sánchez Romero M (eds). *Guess Who's coming to dinner. Feasting rituals in the prehistoric societies of Europe and the Near East*. Oxbow Books, Oxford, pp 73–90

Elsa Pedro, Isabel Duarte, Humberto Varum, and António Pinho

---

## Abstract

In Angola, the earth construction constitutes part of the built and cultural heritage. Numerous buildings made of raw earth, built with ancient techniques and methods, are distributed throughout the country. There are a considerable number of structures in wattle and daub, mud and more recently on CEB (Compressed Earth Block). But, adobe constitutes itself as the most widely used technique based on raw earth. Given the current development of the country, and the possibility of integrating systems and alternative construction materials that respects the environment, adobe construction is one of the most suitable options. Associating the scientific work to the ancestral knowledge, it can be improved and optimized these solutions, responding to the current social, economic and environmental requirements. This paper presents the results of a survey on the characterization of construction with raw earth in Central Plateau of Angola, involving the identification of collecting sites of the raw material, building methods, and the determination of the properties of representative materials used in the adobe buildings. The methodology followed in this research was based on the compilation of the information available in the literature, on interviews to the local populations and on laboratory tests to characterize the physical properties (texture, consistency, density, etc.). The results of the research will identify and characterize the materials and methods used in the constructions with raw earth in Central Plateau of Angola, contributing to the development of knowledge of these sustainable solutions with a strong presence in this region.

---

## Keywords

Earth construction • Adobe • Characterization of built heritage • Central plateau • Angola

---

## 54.1 Introduction

A large part of the buildings of the Central Plateau of Angola is built with adobe. Adobe units are sensitive to degradation by water. Due to the climate, subtropical, hot and humid, in

most of the Angolan territory (60 % are plains with about 1,000–2,000 m high and an extensive river system), these constructions are vulnerable and may present early

---

E. Pedro  
Methodist University of Angola, Rua Nossa Sr<sup>a</sup> da Muxima, 10,  
6739 Luanda, Angola  
e-mail: elsapedr@gmail.com

I. Duarte (✉) · A. Pinho  
Geosciences Department, University of Évora, Rua Romão  
Ramalho, 59, 7000-671 Évora, Portugal  
e-mail: iduarte@uevora.pt

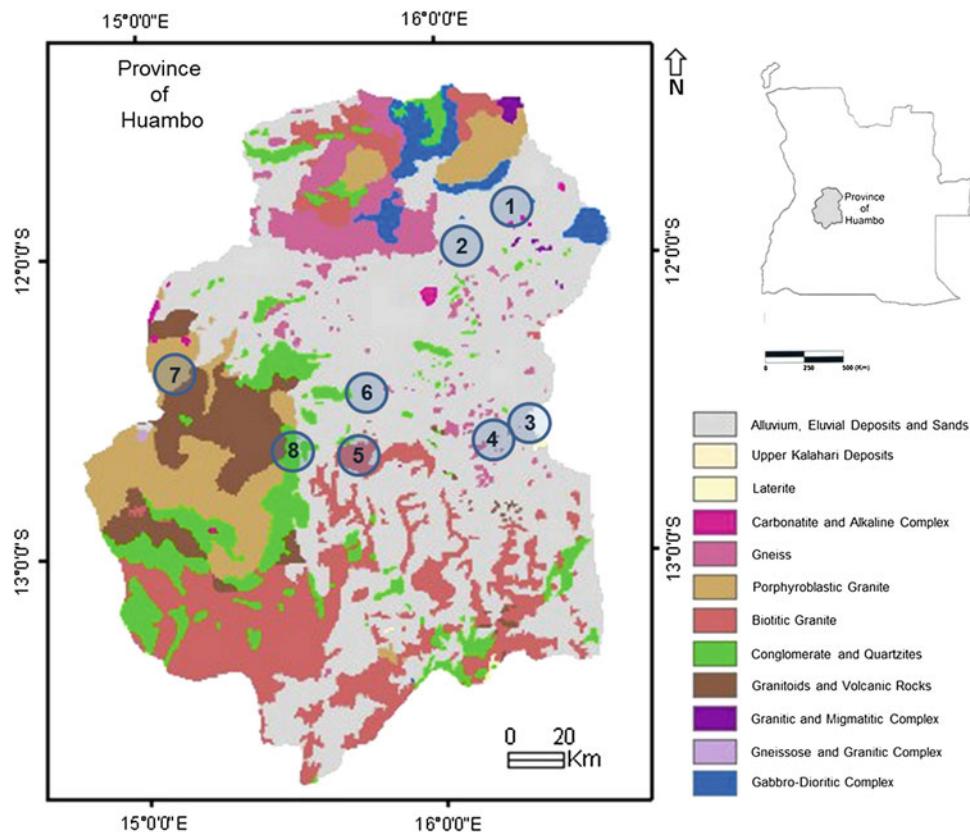
---

A. Pinho  
e-mail: apinho@uevora.pt

I. Duarte · A. Pinho  
GeoBioTec Research Centre, FCT, University of Aveiro, Aveiro,  
Portugal

H. Varum  
Civil Engineering Department, University of Aveiro, Campus  
Universitário de Santiago, 3810-193 Aveiro, Portugal  
e-mail: hvarum@ua.pt

**Fig. 54.1** Area under study (Province of Huambo, Angola) with sample locations: 1 Mungo; 2 Catolo; 3 Chinguar; 4 Chianga; 5 NDondo; 6 Lomanda; 7 Quinjenje; 8 Calenga. (Modified from Araújo and Guimarães 1992)



degradation, enforced by the loose of knowledge about the characteristics of the materials used and techniques for their conservation.

It is desirable, therefore, to find solutions to improve the durability and performance of adobe in the area under study. For this purpose, the geomaterials used in the construction of adobes should be characterised and should be identified the most common construction typologies and maintenance strategies adopted in those buildings.

For the development of this study, a historical record on building typologies and traditional construction methods using the raw earth, within Angolan communities of Central Plateau, was developed. The present paper presents the results of the survey done relatively to construction with raw earth on the studied area, namely intending to identify the collecting sites of the raw materials, e.g. the origin of the soils, the determination of the properties of different materials used in the production of adobes, and the characterization of the building methods in different regions of the Central Plateau of Angola.

## 54.2 Geography, Geomorphology and Lithology

Located on the west coast of Africa, Angola is a country with a total area of 1,246,700 km<sup>2</sup> and about 12,531,357 inhabitants (Fig. 54.1). Considering the specific features of the relief, the territory of the country is divided into two parts: East and West. The most important morphological unity of the West is the Central Plateau and the zone of Relief in Steps (Araújo and Guimarães 1992). The area under study, about 22,500 km<sup>2</sup> in the Province of Huambo, is located in the Central Plateau, with absolute values of altitudes that can reach 2,600 m. The main feature of the area is the escarpment relief from the Central Plateau to the north, with the gaps ranging from 1,500 m to 400–800 m. To the west, the plateau is limited by Chain Marginal Mountains, corresponding to the highest altitudes of Angola (Marques 1977). The lateritic soils are formed on the interflues and the foothills of the mountains. These soils are used in most of the existing earth buildings in the Central Plateau.

In the Central Region of Angola abound granitoids rocks, whose alteration “in situ” originated the “residual soils”. The geochemical, mineralogical and textural properties of these soils depend not only on the chemical composition of the parent rock, but mostly on local climatic and geomorphological characteristics (Duarte et al. 2013). Approaching the coast, the construction materials will vary accordingly to local lithology. The climate will also modify and, consequently, also varies the strength and durability of this type of construction in relation to the meteorological agents.

### 54.3 Methodology

The methodology adopted in this research is based on the compilation of the information available in the literature, and on surveys and interviews with local people in order to record the testimonies and experiences in relation to traditional materials and techniques used in earth construction, the lifespan of the construction and the need for periodic maintenance. On the other hand, 25 representative soil samples were collected with shovels and hoes, and were conditioned in appropriate bags and boxes. Based on laboratory tests, it were determined the physical properties of the materials used in the production of adobes by traditional methods.

The compilation of information was performed at two levels: (1) the information obtained from the master responsible for the construction of the building; (2) reports from the elders about the history of the buildings in the surveyed area (Fig. 54.2). The interviews were recorded, because the majority of the country’s rural population cannot read or write

and “know-how” was, and still is, based on experience transferred orally from generation to generation. Thus, films were recorded in the form of a questionnaire, combined with visits to construction sites to better understand the techniques used and the construction details and methods.

The questionnaire was structured in two parts: the first dedicated to the raw material used in the construction, and the second part reports the aspects related to production processes (mixtures, curing time of the adobe, moulds, transport and storage, utensils used in production, mortar joints and connections, amount of water used, plaster, foundations, materials and dimensions of the spans, roof covering, geometry, etc.). Some interviews (films) were made in the native language, *Umbundu*, due to limitations in communication, whose contents have been translated faithfully. In the Province of Huambo were selected the localities of Calenga, Quinjenje, NDondo, Lomanda, Catolo, Mungo, Chianga and Chinguar for this study.

### 54.4 Results

The results of the work are presented in Tables 54.1 and 54.2. The physical characteristics of the soils used in the production of adobes are listed in Table 54.1, namely: particle size analysis, specific gravity of grains ( $G_s$ ), sand equivalent (SE), Unified System Classification of Soil (USCS) and the lithological description. Regarding consistency, all soil samples analysed have no plastic behaviour, and the values of water content in the natural state are very different (2.3–21.4 %), depending on the location, sun exposure and sampling depth.

**Fig. 54.2** Example of existing adobe constructions



**Table 54.1** Physical characteristics and classification of soil samples used in the production of adobes in Province of Huambo

Place	Samples	USCS	Lithology	Particle size analysis (%)			Physical characteristics	
				<4.75 (mm)	<2.00 (mm)	<0.075 (mm)	G <sub>s</sub>	SE (%)
Calenga	1	ML	Brownish sandy silt	91.1	88.4	49.1	2.46	11
Quinjenje	2	SM	Grey silty sand	95.7	81.2	22.3	2.64	33
Chianga	7	SM	Brown silty sand	94.1	74.5	31.7	2.36	18
Chinguar	13	SM	Brown silty sand with gravel	82.2	61.6	16.8	2.68	47
Ndondo	14	SM	Brownish silty sand	97.8	86.4	30.8	2.64	24
Lomanda	17	SM	Dark brown silty sand with gravel	83.5	66.1	16.5	2.68	36
Catolo	18	SM	Dark brown silty sand	93.6	81.2	15.7	2.69	29
Mungo	19	SM	Dark brown silty sand	91.1	88.4	49.1	2.77	47
	20	SM	Dark red silty sand	92.2	74.4	33.5	2.71	31

Table 54.2 presents the methods of manufacture of adobes in selected localities in the province of Huambo. As can be seen, adobes are always produced in the transition from the wet season and dry season. The mortar is made of the same soil and water (but without straw). The methods applied in the buildings construction within the studied area are: (a) Construction team – 1 master and 1, 2 or 3 helpers; (b) Average time of house construction—5 days to 3 weeks; (c) Foundations—Inexistent, stones or stabilized adobes; (d) Types of walls—Internal (single) and external (single or double); (e) Plaster—Inexistent, sandy earth mortar or sand and cement mortar; (f) Roof covering—Laths for Eucalyptus wood covered with straw, tiles or zinc sheets.

It is interesting to note that the adobes are usually produced by the women, while children carry the water and men build the walls, being therefore the construction a family activity.

#### 54.5 Final Remarks

From the results obtained in this research, it can be seen that the physical characteristics of the soils used in adobe constructions are similar, being almost all samples classified as SM—silty sand.

**Table 54.2** Methods of manufacture of the adobes in the Province of Huambo

Place	Adobe				
	Manufacture	Size (cm × cm)	Construction season	Curing time (days)	Mould
Calenga	Mix with a hoe/shovel: soil, water, fresh straw	40 × 20	April–July	3–4 sundried	Simple wooden
Quinjenje	Mix with a hoe/shovel: soil, water, straw	47 × 22	May–July	6–8 sundried	Simple wooden
Chianga	Mix with a hoe/shovel: soil, water, straw	40 × 20	May	8 max. sundried	Double wooden
Chinguar	Mix with a hoe/shovel: soil, water, straw	40 × 20	May–July	8 max.	Simple and double wooden
Ndondo	Mix with a hoe: soil, water, straw	30 × 20	June–July	15 max. sundried	Double wooden
Lomanda	Mix with a hoe and with feet: soil, water and straw	40 × 20	June	6–8 sundried	Simple wooden
Catolo	Mix with a hoe: soil, water and straw	40 × 20	June	8 sundried	Double wooden
Mungo	Mix with a hoe: soil, water and straw	40 × 20	May	6–8	Simple wooden

The construction methods adopted in adobe buildings, materials (soils, water, and straw), eucalyptus wood moulding, mixing utensils, construction season and building methods, do not differ greatly from location to location.

However, it was found that the lifespan of the buildings can vary greatly. It were found adobe houses with more than 100 years in a good conservation state, but, on the other hand, some adobe houses with less than 10 years present serious pathologies with loss of material in adobe, compromising in some cases the structure stability. It is thought, by the testimony referred by the elders, that this discrepancy may be related to the mixing procedure: formerly adobes were made with the feet and currently with hoes and shovels, which influences the voids ratio. Thus, durability and

erodibility tests on adobes produced by these two methods are recommended to prove this hypothesis.

---

## References

- Araújo AG, Guimarães F (1992) Geologia de Angola. Notícia Explicativa da Carta Geológica à escala 1:1,000,000. Serv. Geol. de Angola. Luanda. 137p
- Duarte IMR, Mirão JAP, Rocha FTF, Bonito F, Queta F, Falcão W (2013) Pathway weathering in granitoid rocks from central region of angola: geochemical and mineralogical data. Angolan J Sci. EDUAN. Luanda, 28p (in press)
- Marques MM (1977) Esboço das grandes unidades geomorfológicas de Angola. Instituto de Investigação Científica Tropical, Garcia de Orta, Serviços Geológicos, Lisboa 2(1):41–43

# Remote Sensing Techniques in a Multidisciplinary Approach for the Preservation of Cultural Heritage Sites from Natural Hazard: The Case of Valmarecchia Rock Slabs (RN, Italy)

Margherita Cecilia Spreafico, Francesca Franci, Gabriele Bitelli,  
Valentina Alena Girelli, Alberto Landuzzi, Claudio Corrado Lucente,  
Emanuele Mandanici, Maria Alessandra Tini, and Lisa Borgatti

## Abstract

The Valmarecchia area (RN, Italy), located between the Emilia-Romagna and Marche regions, displays peculiar geological features, being characterized by rocky slabs lying on gentle slopes. The main fortified villages of the area, remarkable for historical and artistic assets, were built in the medieval period on these slabs for defense purposes. The area is affected by widespread landslide phenomena, involving both the rocky slabs and the underlying clayey shales. The main phenomena acting on the slabs are lateral spreading, with associated rock falls and topples. In this area, a multidisciplinary project, involving different expertise, like geology, geodesy, geomorphology, hydrogeology, soil and rocks mechanics is ongoing. In this particular context, in order to achieve a clear recognition of the instability phenomena, it is necessary to understand the movement patterns and the eventual differential displacement occurring in the slabs. Monitoring activities, joined with geological and geomorphological interpretation, are one of the fundamental step for a deep understanding of the movements and for the risk management purposes. In many cases, the monitoring system is missing or only poor data are available, therefore an approach for the Permanent Scatterers (PS) data analysis has been used, combining analysis on the PS velocity, on the direction of the movement and statistical consideration on the time series trend. Some preliminary results regarding the rock slab on which the town of Verucchio (RN, Italy) is located are here presented.

## Keywords

Satellite interferometry • Monitoring • Cultural heritage • Valmarecchia • Italy

## 55.1 Introduction

In Italy slope instability phenomena affecting natural and cultural heritage sites are very common: some of these affect historical towns built on the top of rock slabs, like Pitigliano in Tuscany (Fanti et al. 2012), Orvieto in Umbria (Tommasi et al. 2004), and many others.

The area between the Emilia-Romagna and Marche regions, called Valmarecchia, is characterized by a typical landscape, spotted with high grounds carved in Epiligurian rock slabs. These slabs developed during the Pleistocene and Holocene, especially in the latest glacial phase; their limits are usually marked by steep cliffs or rock walls, thus offering ideal locations to build fortresses or military settlements; for this reason, in the Medieval period, villages were usually built on the top of them. Widespread instability phenomena

M.C. Spreafico (✉) · F. Franci · G. Bitelli · V.A. Girelli ·  
A. Landuzzi · E. Mandanici · M.A. Tini · L. Borgatti  
Department of Civil, Chemical, Environmental and Materials  
Engineering - DICAM, ALMA MATER STUDIORUM,  
University of Bologna, Viale Risorgimento 2, 40136  
Bologna, Italy  
e-mail: margherita.spreafic2@unibo.it

F. Franci  
e-mail: francesca.franci2@unibo.it

C.C. Lucente  
Servizio Tecnico di Bacino, Sede di Rimini, Ferrara, Regione  
Emilia Romagna, Italy

affect these slabs and the clayey substratum on which they rest. The evolution of these instability phenomena can pose a severe risk to the fortified villages.

In these cases a deep knowledge of slope instability processes, taking into account the different factors that influence the evolution of the movements, is fundamental. In the context of endangered historical and environmental assets, different approaches and multidisciplinary works are needed to lead to the definition of adequate low-visual impact countermeasures and eventual monitoring systems. For example, regarding the San Leo rock slab, located in the middle part of Valmarecchia, a Terrestrial Laser Scanner survey was performed all around the cliffs, with the aim to describe the 3D geometry and the structural features of the slab. Moreover, studies about the material properties, the hydrologic system and the ongoing displacements are in progress. In this framework, geomatic and monitoring techniques can result very useful for an in-depth understanding of the rate, type and evolution of instability phenomena, but sometimes available data are not enough for the selected area or period. The PSInSAR technique has proved to be applicable in different contexts to analyze ground displacements, from land subsidence to landslides. The Permanent Scatterers (PS) analysis, due to its characteristics of precision, to the availability of quite long historical data set and wide area coverage can support the conventional in situ monitoring methods.

## 55.2 Methodology

In this work different interferometric analysis techniques were integrated to enhance the knowledge of the instability phenomena acting on the slabs. The contribution of the radar interferometric analysis for the Valmarecchia area permits to provide information on the state of activity, on the direction and on the movement pattern of different types of slope instability phenomena. These information will be integrated with geological, structural and geomorphological data to achieve a better comprehension of the acting phenomena.

The Permanent Scatterers analysis was performed using different dataset acquired in the frame of the PST-A (Piano Straordinario di Telerilevamento Ambientale/Extraordinary Plan of Environmental Remote Sensing) project: San Marino, Marecchia and Urbino datasets were collected between 1992 and 2000 and they are originated from the ERS images processing; Arezzo and Rimini datasets were collected between 2003 and 2008 and they are the results of the interferometric analysis of ENVISAT images. The images were processed by the companies T.R.E. S.r.l. and e-GEOS with the PS InSAR technique. The PS time series were analyzed with a tool developed by T.R.E.

(TRECcustomerToolbar, T.R.E. s.r.l.) and using a method for automated classification (Berti et al. 2013).

Moreover, the data of average velocity provided by the 2 geometries, ascending and descending, were combined to obtain the orientation of the velocity vector on the horizontal plane (EW) and vertical axis. Analyzing the time series, it is possible to identify and map homogeneous areas with respect to the deformation processes. Differences in average velocity of deformation may be useful for the identification of areas with distinct evolution and for the discrimination of different deformation behavior within the same landslide area, i.e., of rock blocks affected by differential subsidence due to deep-seated lateral spreading phenomena.

### 55.2.1 Time Series Analysis

In order to provide a general overview of the time series and to investigate the spatial distribution of different time series trends with respect to topographic and geologic features, the PS data were processed with PS Time software (Berti et al. 2013), which allowed the automated classification of the PS movement based on their time series trends. In particular, the datasets were subjected to a conditional sequence of statistical tests to classify each time series into one of the six predefined target trends: uncorrelated, linear, quadratic, bilinear, discontinuous with constant velocity and discontinuous with variable velocity. These trends describe different modes of ground deformation (Berti et al. 2013); uncorrelated time series represent random fluctuations of displacements around zero, and therefore PS with no significant movements during the observation period; linear trends indicate ground displacements with constant velocity and deformation phenomena acting over long time scales like creep, natural subsidence and slow and steady motion of so-called “dormant” landslides. Non-linear trends, quadratic, bilinear and discontinuous, denote the displacement rate variation during the analyzed period: velocity varies continuously in time for the PS with quadratic trends; for the PS characterized by a bilinear trend, the time series is segmented in two linear tracts of different velocity separated by a breakpoint in which the function is continuous; for the PS with a discontinuous trend, the time series is segmented in two linear tracts of similar or different velocity separated by a breakpoint in which the function is discontinuous.

### 55.2.2 Displacements Direction Analysis

The possibility to combine the velocity of PS data processed in ascending and descending orbit improves the amount and quality of information obtainable on the analyzed phenomena. The analysis procedures described in PST-A Guidelines

(MATTM 2009) were followed. In areas where both acquisition geometries for the same satellite are available, velocity measurements along the two different Line Of Sight (LOS) can be combined. It is almost never verified that a PS is considered as a target in both acquisition geometries, it is therefore necessary to proceed with a re-sampling of the ascending and descending datasets on a square grid mesh in order to make them comparable. The average velocity value of the Permanent Scatterers (PS) located inside each grid cell can be assigned to the cell center. The velocity values recorded along the ascending and descending orbits are then geometrically combined to obtain the velocities along the vertical and E-W horizontal direction. Estimation of the N-S horizontal velocity of deformation is not feasible, as one of the main limitations of the PS technique is the difficulty in recording horizontal movements along the North-South direction since the sensors operating orbits are oriented approximately along the meridians.

### 55.3 Valmarecchia Geology and Geomorphology

From a geological point of view, the study area is marked by a unique geodynamical phenomenon, known as Valmarecchia thrust sheet. In the sheet, the most ancient Ligurian Units and the younger Epiligurian Units, which are related to different depositional cycles, overthrust autochthonous Units of the Umbro-marchean-romagnan domain sedimented on the Adria continental microplate. The Epiligurian Units (hard rocks) rest unconformably on the Ligurian Units (varicoloured clays, marly and limestones) creating high grounds named Epiligurian plates or slabs. The slabs are often tectonized and crossed by several joint sets and faults, often interested by lateral spreading phenomena and associated rock falls, topples and tilting. Moreover, the underlying clayey substratum is involved in plastic movements, like earth flows and slides (Casagli 1994). The main cause of instability, which brings about these widespread movements, is the high deformability contrast between the plates and the underlying clays (D'Ambra et al. 2004). Other factors that predispose the instability are the structural setting of these slabs, the groundwater flow inside the plates and the consequent destabilization of the basal clays, which, together with creep and flows in the underlying clay, undermines the foot of the rock plates and causes the opening and widening of vertical fractures in the limestone rock masses. Therefore, the understanding of the movement patterns and of the differential displacement occurring in the slab is fundamental in order to achieve a clear description of the phenomena.

### 55.4 Discussion

Some preliminary results regarding Verucchio site are here described. The town of Verucchio is located on a rock slab, in Valmarecchia area, about 20 km SW of Rimini, at an average altitude of about 300 m a.s.l. The slab, formed by the so-called San Marino and Monte Morello geological units (limestones and sandstones) and crossed by several small faults or joints, lies on a clay substratum. Finally it is worth to emphasize the presence of a vast overthrust on the east side of the slab having a roughly North-South direction, that testifies the movement of the plate on the older Ligurian units occurred in the past. ERS dataset, acquired between 1992 and 2000, was analyzed to infer the behavior of the rock slab. Three areas with different trends of movements were identified from the study of the PS data, even if an higher density dataset would be certainly useful for a better characterization of the phenomenon. The presence of an area located in the central part of the slab, showing higher velocities can be observed from the PS velocity map (Fig. 55.1); in the eastern sector of this area the landslide inventory map reports an active landslide, classified as rock fall or toppling. In this area damages to buildings were reported but the definition of the landslide type and evolution is not clear, since no in situ geotechnical instruments are available at present. Interferometric results can confirm the existence of an unstable area and suggest some features, i.e. the rate, the direction and the pattern of the movement; this can be the starting point on which further specific investigation and monitoring activities can be proposed.

Moreover, in the western sector of the central area, where no landslides were previously mapped, some clusters of point with a mean velocity reaching values of  $-12$  mm/year along the LOS in the descending geometry, are detectable; these points are located on the San Marino geological unit. The PS velocities suggest the presence of unstable areas, requiring specific investigations. The northern area appears to be more stable, while in the south one velocity between 2 and 3 mm/year, along descending LOS, were registered.

The synthetic PS obtained from Ascending and Descending geometries combination are fewer than the original points, because they can be obtained only in cells in which targets from the two geometries are present. By analyzing PS trends, part of the slab is roughly characterized by E to W displacements. PS showed velocities reaching  $-4.0$  mm/year; further investigations are required to better understand the main cause of the movement. The Vertical displacements range between  $-1.5$  and  $0.7$  mm/year, for the analyzed period. Almost the same results were obtained with a slightly different procedure. Each descending geometry PS was joined with the closest ascending geometry PS using a 50 m maximum radius distance. Different types of

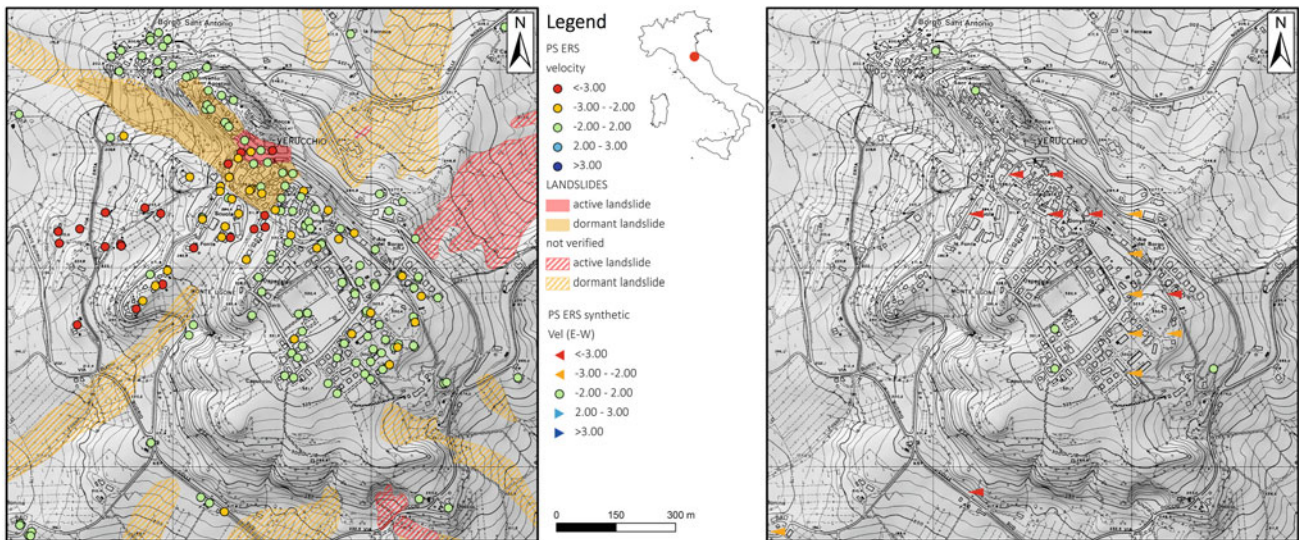


**Fig. 55.1** Velocity class along LOS of ERS PS (ascending and descending geometries) and direction of the movement on E-W axis

movement patterns are identifiable analyzing the LOS velocity. Uncorrelated and linear trends, probably indicating no movements and/or dormant landslides, are predominant in the north area, where, in fact, a dormant landslide is located. Quadratic and bilinear trends are prevalent in the central part, in correspondence of the above mentioned mapped and newly detected landslides; a mix of quadratic, uncorrelated and bilinear trends characterize the south area (Fig. 55.2).

Obviously, these preliminary results need to be interpreted, validated and integrated with others techniques, but they show how the applied methodology can give an overview of the movements occurring in this particular context; these data are useful for the interpretation and the understanding of the phenomena, mostly in the cases in which others monitoring data are not available or cover only limited periods. These indications, deriving from interferometric analysis, can give a first idea of the type and of the movement rate, useful to choose

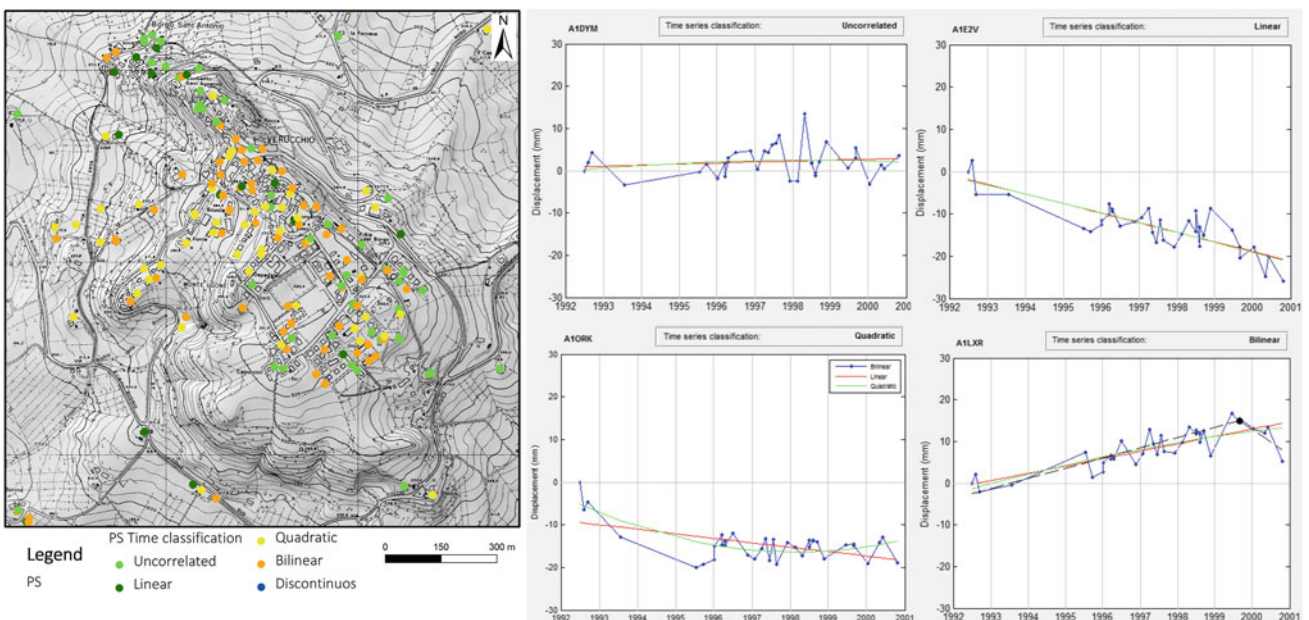


**Fig. 55.2** PS-Time classification and examples of the different movement patterns

where and how to continue or focus the monitoring activity. Another interesting issue can be the correlation between these results and the rainfall or the seismic records in a selected area, especially for points showing displacement rate variations during the analyzed period. Interferometric techniques permit also to update landslide boundaries or to highlight unstable areas where no mapped landslides were previously detected, as in the Verucchio case. This information have to be integrated with other data, like geological and geomorphological maps and on site investigations.

---

## References

- Berti M, Corsini A, Franceschini S, Iannacone JP (2013) Automated classification of persistent scatterers interferometry time series. *Nat Hazards Earth Syst Sci* 13:1945–1958
- Casagli N (1994) Fenomeni di instabilità in ammassi rocciosi sovrastanti un substrato deformabile: analisi di alcuni esempi nell'Appennino settentrionale. *Geol Romana* 30:607–618
- D'Ambra S, Giglio G, Lembo-Fazio A (2004) Interventi di sistemazione e stabilizzazione della Rupe di San Leo. In: *Proceedings of the 10th Congress Interpraevent*, Riva del Garda
- Fanti R, Gigli G, Lombardi L, Tapete D, Canuti P (2012) Terrestrial laser scanning for rockfall stability analysis in the cultural heritage site of Pitigliano (Italy). *Landslides* 10:409–420
- Ministero dell'Ambiente e della Tutela del Territorio e del Mare (MATTM) (2009) Linee guida per l'analisi di dati interferometrici satellitari in aree soggette a dissesti idrogeologici, Direzione Generale per la Difesa del Suolo
- Tommasi P, Pellegrini P, Boldini D, Ribacchi R (2004) Influence of rainfall regime on hydraulic conditions and movement rates in the overconsolidated clayey slope of the Orvieto hill (central Italy). *Can Geotech J* 43:1
- PSInSAR: Manuale d'uso. Tele-Rilevamento Europa T.R.E. s.r.l.
- Treuropa: ArcMap. Customer Toolbar Setup. Installazione e Manuale d'Uso. Tele-Rilevamento Europa T.R.E. s.r.l.

Maurizio Ripepe, Massimo Coli, Giorgio Lacanna, Emanuele Marchetti, Maria Teresa Cristofaro, Mario De Stefano, Valentina Mariani, Marco Tanganelli, and Paolo Bianchini

---

## Abstract

An ambient vibration survey of a structure represents an efficient and accurate technique for the characterization of its dynamic response to wind and seismic excitation. The dynamic response of the Giotto's bell-tower has been monitored with four velocimetric stations placed along the tower. The frequencies values and modal shapes have been evaluated by analyzing the data in the frequency domain and time domain respectively. Two translational modes for each direction and a torsional mode have been detected. An iterative back-analysis procedure has been set up to define a realistic elastic modulus of the stone masonry. The soil-structure interaction has been included in the identification process. The elastic modulus of the stone masonry represents an important mechanical parameter for the definition of reliable finite element models of the structure, that could be an useful tool for further investigations on the tower seismic behavior.

---

## Keywords

Historical tower • Ambient vibration • Dynamic identification • Model updating • Giotto's bell-tower

---

## 56.1 Overview of the Monument and Geological Setting

Firenze is one of the most well-known worldwide city and since 1982 its historical centre is under the UNESCO protection as Human Cultural Heritage. Among the many outstanding monuments of Firenze, Giotto's bell-tower, close to Brunelleschi's Dome, is one of the most emblematic

ones and represents a pole of attraction for thousands of tourists per year (Fig. 56.1a).

The Firenze area has been historically subjected to earthquakes, with maximum local magnitude  $M_L < 5$  and intensity  $I_{max} = VIII$  MCS (Mercalli-Cancani Sieberg scale). The strongest earthquakes occurred in 1454, 1895 and 1919. Therefore the definition of the dynamic response of the Giotto's bell-tower results of primary importance, in order to plan appropriate actions for its seismic protection.

Giotto's bell-tower is squared in plan, perfectly NS and WE oriented, with a side of 14.45 m, and a height of 84.7 m (Fig. 56.1b). It has four polygonal buttresses at the corners and is crossed by four floors. The substructure is constituted by a massive body of mortared stone, 6 m in depth, embedded into gravels. The substructures were dug in 1298 when Arnolfo di Cambio, maybe its designer, was director of the nearby Cathedral building yard. The construction works begun in 1334 and went on till 1359. At the 5th floor there is a high bell's cell with seven bells, with a total mass of more than 10 tons. The bells swing in the E-W direction and are blocked in the N-S direction. The tower is made of stone masonry

---

M. Ripepe · M. Coli · G. Lacanna · E. Marchetti  
Dipartimento di Scienze della Terra, University of Florence,  
Florence, Italy

M.T. Cristofaro · M. De Stefano · V. Mariani (✉) · M. Tanganelli  
Dipartimento di Architettura, University of Florence,  
Florence, Italy  
e-mail: valentina.mariani@unifi.it

P. Bianchini  
Opera Santa Maria del Fiore, Florence, Italy

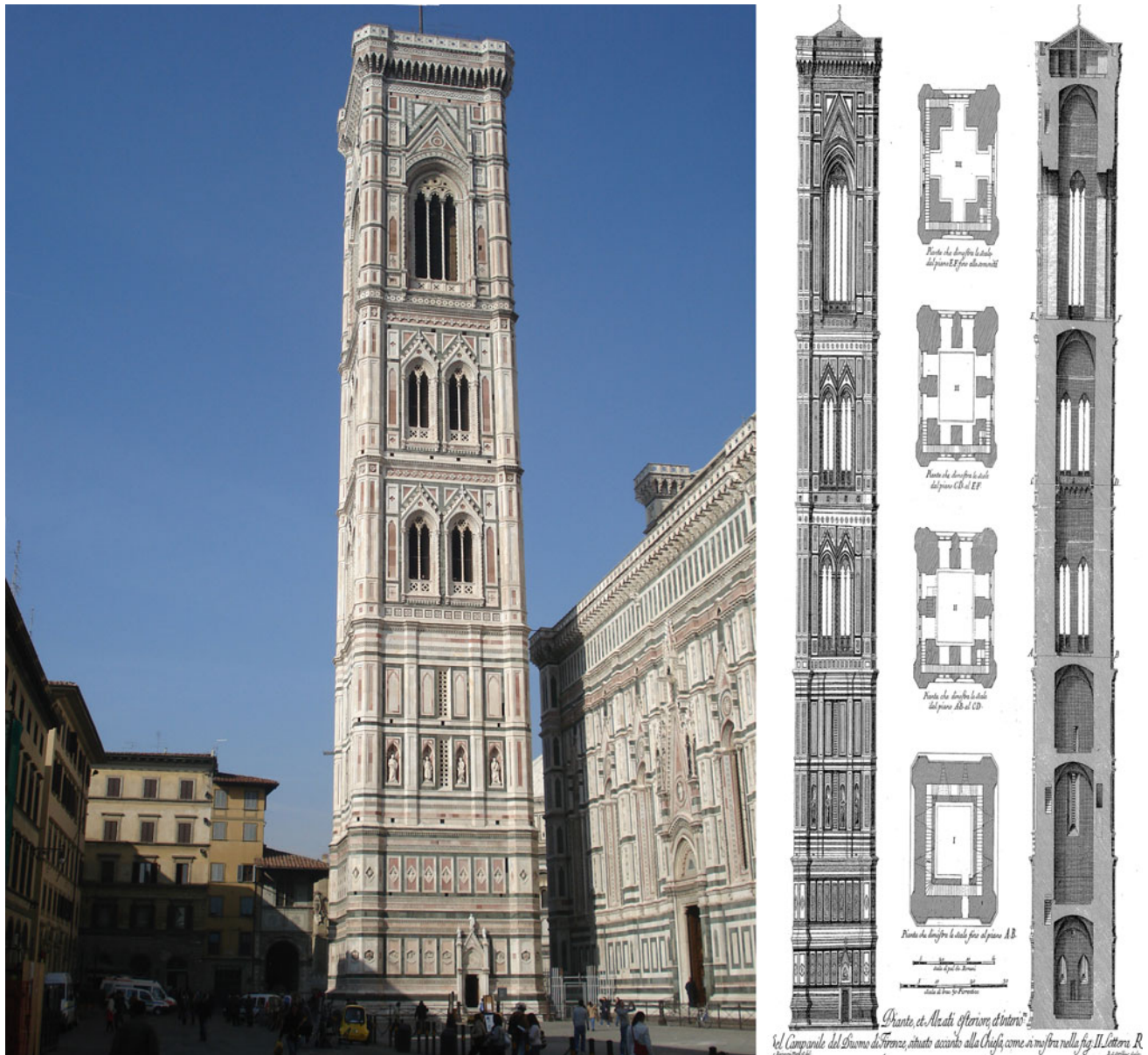


**Fig. 56.1** a Giotto's bell-tower East view. b Frontal view, vertical and horizontal sections above the street datum (© Opera del Duomo di Firenze)

(Pietraforte: a quartz-calcareous sandstone turbidite which was quarried in the near hill south of Firenze) with mortar joints. The bell-tower has an external revetment of white Carrara Marble and other colored marble tiles.

Firenze was settled by the Romans close to a ford along the Arno river in the middle Valdarno plain. This plain is a sedimentary basin developed in the last million years because of the role played by the NW–SE Fiesole master-fault (Briganti et al. 2003). The Medieval city lies on a layer of recent deposits, that are river bed-deposits mainly made of pebbles and gravel, from clean to silty, with layers and lenses of graded sands. A 3–5 m layer, irregularly composed by silty-sands, can be found on top, according to the fluvial

course (Coli and Rubellini 2007). The gravels display geotechnical parameters as follow: USCS = GP;  $c' \approx 10$  kPa;  $\phi' \approx 40^\circ$ ;  $V_p \approx 1.400$  m/s;  $V_s \approx 380$  m/s; the calculated areal seismic amplification factor due to the soil is  $1.4 \div 1.5$ . The water table is stable at about 7 m below the ground level and has a seasonal excursion up to  $\pm 1.5$  m.

## 56.2 Dynamic Monitoring

The oscillation modes of a structure can be analyzed by recording its frequency response to ambient noise, e.g. wind, microtremors, microseisms, at selected locations in the

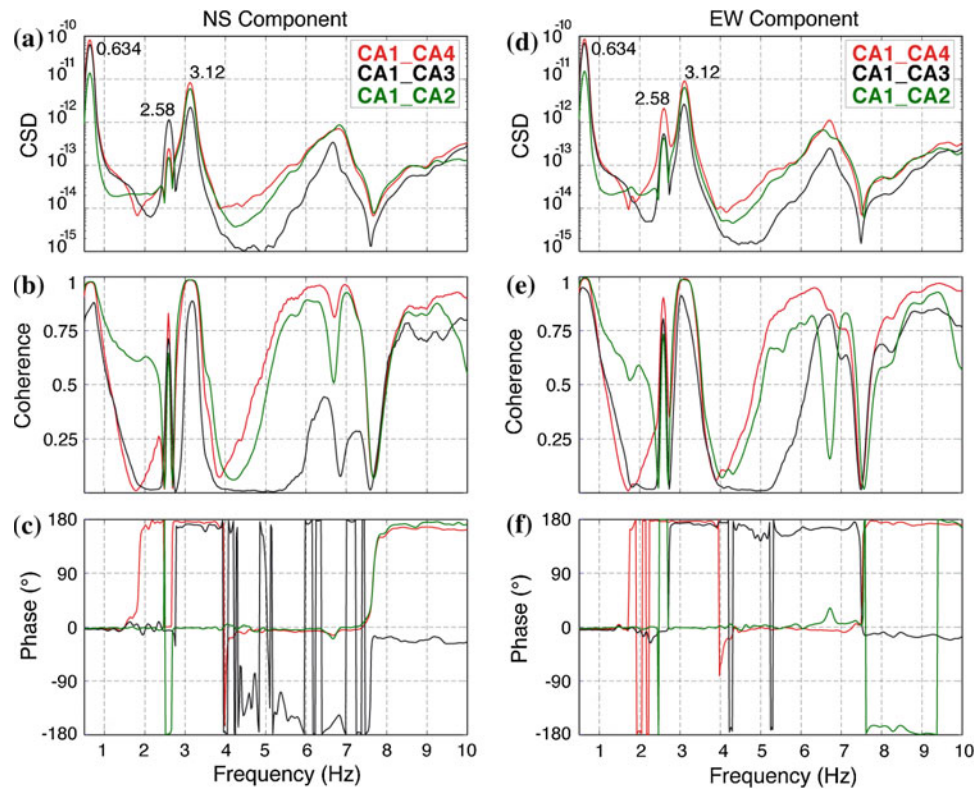


**Fig. 56.2** Cross-spectrum amplitude for **a** NS direction and **d** EW direction. Coherence for **b** NS direction and **e** EW direction. Phase angle for **c** NS direction and for **f** EW direction; for each couple analyzed CA1–CA2 (green line), CA1–CA3 (black line) and CA1–CA4 (red line)

structure itself (Ivanovic et al. 2000). The instrumentation is chosen to cover the amplitude and frequency range of interest. The 4 stations were installed along the vertical direction at four different levels from the ground level (CA1) up to the roof (CA4). The long time recording interval has allowed to check stability of the vibration and to get robust average values of the frequency response. Data processing was performed in the frequency domain by calculating, for each selected couple of records (Rinaldis et al. 2004), the cross spectral density (CSD) function (Fig. 56.2a, d) and the corresponding coherence (Fig. 56.2b, e) and phase functions (Fig. 56.2c, f).

The CSDs between the reference station CA1 and the other stations (CA2–CA3–CA4) in NS and EW directions identify 3 vibration modes of the structure for the same frequencies in both directions. The Cross-spectral amplitude at 0.634 Hz (Fig. 56.2a, d) increases with increasing height, showing high coherence values and phase angles of zero degree which confirm that this frequency is associated to the 1st translational movement of the bell-tower in the NS and EW directions. Frequency-domain analysis evidences amplitude peaks at 2.58 and 3.12 Hz with high coherence for significant phase shift, indicating a torsional mode and a 2nd translational mode of the structure in the NS and EW directions.

By performing a time domain analysis (Ditommaso et al. 2010), filtering the signal around these peaks, it was possible to calculate the modal-shape at the corresponding frequencies. The procedure has been done for all the detected modal shapes in both directions (Fig. 56.3).

### 56.3 Soil-Structure Interaction, Numerical Modeling and Dynamic Identification

The study of the soil-structure interaction has been carried out according to the theory of impedances by Gazetas (1991). Such method can be applied for the calculation of the dynamic stiffness  $K$  of shallow or embedded foundations harmonically oscillating in an homogeneous half-space. In the present study, the rotational stiffness of the soil-foundation system has been evaluated to be consequently used in the dynamic identification process. The main aspects involved into the method are: the geometry of the soil-foundation interface (shape, dimensions and level of embedment), the features of the soil profile and the geotechnical characteristics, the frequency of the exciting action.

The calculation has been done according to formulas and charts reported in Gazetas (1991) that lead to a value of  $K_\phi$  equal to  $3.14 \times 10^{12}$  Nm. The obtained value of rotational

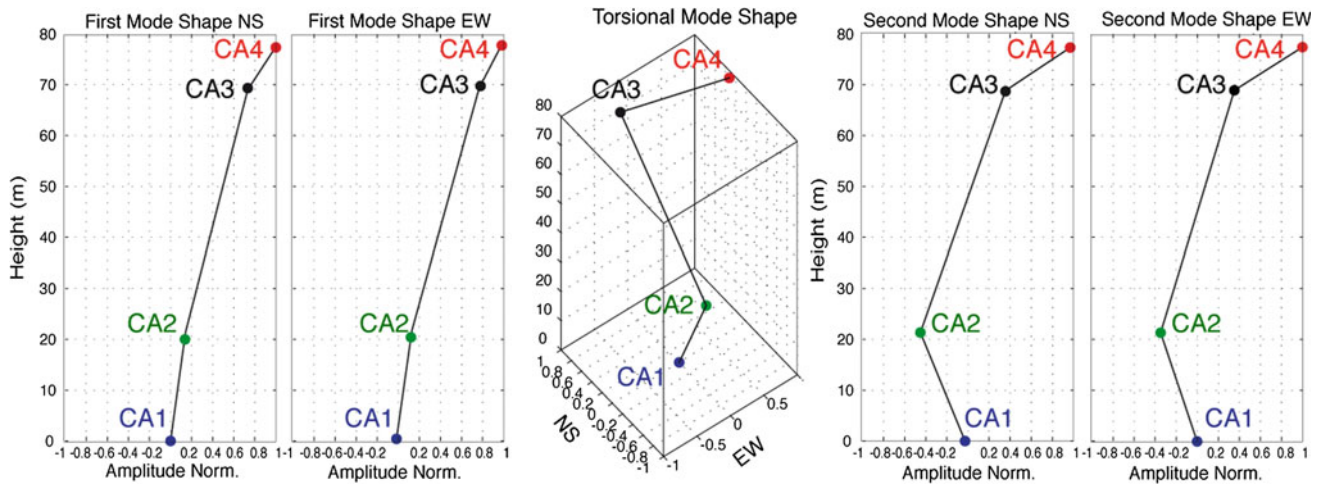


**Fig. 56.3** Modal shapes with respect to level

**Table 56.1** Comparison of experimental and analytical frequencies and modal shapes

	NS				EW			
	Freq1 [Hz]	Freq2 [Hz]	Normalized modal displacement		Freq1 [Hz]	Freq2 [Hz]	Normalized modal displacement	
			CA2	CA3			CA2	CA3
Experimental	0.634	3.120	0.1424	0.7330	0.634	3.120	0.1476	0.7863
Analytical	0.607	3.246	0.1242	0.8493	0.607	3.251	0.1243	0.8496
Error %	-4.2	4.0	-12.8	15.9	-4.2	4.2	-15.8	8.1

stiffness has been considered for both NS and EW directions, due to the substantial symmetry of the tower-foundation-soil system.

The aim of the performed structural identification was the evaluation of the Young modulus  $E$  of the stone masonry. Considering the symmetry of the structure and the independence of the two fundamental frequencies highlighted by the experimental survey, two 2D finite element models of the tower have been implemented to identify the parameters  $E$  (D'Ambrisi et al. 2012), one for each direction. The identification process is based on an iterative procedure that performs the modal analysis until the objective function:

$$F = \frac{(\Omega_{exp} - \Omega_{an})^2}{\Omega_{exp}^2} + (1 - MAC)^2 \quad (56.1)$$

is minimized (Friswell and Mottershead 1995). In the Eq. (56.1)  $\Omega_{exp}$  and  $\Omega_{an}$  are the experimental and the analytical frequencies respectively, while MAC is the modal assurance criterion defined by Allemang and Brown (1982) as:

$$MAC = \frac{\left( \left\{ \Phi_{exp}^T \right\} \cdot \left\{ \Phi_{an} \right\} \right)^2}{\left( \left\{ \Phi_{exp}^T \right\} \cdot \left\{ \Phi_{exp} \right\} \right) \cdot \left( \left\{ \Phi_{an}^T \right\} \cdot \left\{ \Phi_{an} \right\} \right)} \quad (56.2)$$

The MAC index measures the level of correlation between the experimental modal shape  $\{\Phi_{exp}\}$  and the analytical modal shape  $\{\Phi_{an}\}$ . The first two translational frequencies has been included in the Eq. (56.1), while only the 1st modal shape has been considered in the Eq. (56.2).

The identification process leads to values of  $E$  equal to 4,880 and 4,855 MPa in the EW and NS directions respectively. These values are quite high compared to values reported in literature and in the current Italian code (NTC 2008), that suggests a range equal to 2,400–3,200 MPa for regularly cut stone masonry. Nevertheless, the identified elastic modulus results from ambient vibrations measurements, therefore it is a dynamic modulus. A ratio of 1.2–1.3 can be assumed between the dynamic and the static moduli (D'Ambrisi et al. 2012), leading to values closer to those reported in literature and codes.

The comparison of experimental frequencies and modal shapes with the analytical ones associated to the identified modulus, is reported in Table 56.1. Percentage errors around 4 % have been found for the frequencies, while higher values, ranging between 12.8 and 15.9 % have been detected for normalized modal displacements (Table 56.1). An increased number of control points would be desirable to improve the accuracy of the identified modal shapes.

## 56.4 Conclusions

An experimental survey with ambient vibrations has been carried out on the Giotto's bell-tower. Four velocimetric stations were placed along the height of the tower for 4 days, recording the vibrations due to anthropic action, wind and bell's tolling. The signals have been processed in frequency and time domain and five main frequencies have been identified with the associated modal shapes (two translational modes for each main direction and one torsional mode). Subsequently, two 2D finite element models of the tower have been set up to identify the elastic modulus of the stone masonry, by an iterative procedure that minimizes the difference between experimental and analytical modal results. The soil-structure interaction has also been included in the identification process, assigning a rotational stiffness equal  $3.14 \times 10^{12}$  Nm at the tower base, calculated through the theory of impedances by Gazetas. Values of dynamic elastic modulus in the range 4855–4880 MPa have been found. A ratio of 1.2–1.3 between the dynamic and static moduli could be assumed to evaluate the static elastic modulus of the masonry, that is a fundamental mechanical parameter, necessary to perform further seismic vulnerability numerical analyses.

## References

- Allemang RJ, Brown DL (1982) A correlation coefficient for modal vector analysis. In: Proceedings of 1st international modal analysis conference. Orlando, USA
- Briganti R, Ciufegni S, Coli M, Polimeni S, Pranzini G (2003) Underground Florence: plio-quaternary evolution of the Florence area. *Boll Soc Geol It* 122:435–445
- Coli M, Rubellini P (2007) Note di geologia fiorentina. SELCA, 37 p
- D'Ambrisi A, Mariani V, Mezzi M (2012) Seismic assessment of a historical masonry tower with nonlinear static and dynamic analyses tuned on ambient vibration tests. *Eng Struct* 36:210–219
- Ditommaso R, Parolai S, Mucciarelli M, Eggert S, Sobiesiak M, Zschau J (2010) Monitoring the response and the back-radiated energy of a building subjected to ambient vibration and impulsive action: the Falkenhof Tower (Postdam, Germany). *Bull Earthq Eng* 8:705–722
- Friswell MI, Mottershead JE (1995) Finite element model updating in structural dynamics. Kluwer Academic Publishers, Dordrecht
- Gazetas G (1991) Formulas and charts for impedances of surface and embedded foundations. *J Geotech Eng ASCE* 117(9):1363–1381
- Ivanovic S, Trifunac MD, Todorovska MI (2000) Ambient vibration tests of structures. A review. *ISET J Earthq Technol* 37(4):165–197
- NTC (2008) Norme tecniche per le costruzioni. D.M. Ministero Infrastrutture e Trasporti 14 gennaio 2008, G.U.R.I. February 4th 2008, Rome, Italy
- Rinaldis D, Celebi M, Buffarini G, Clemente P (2004) Dynamic response and seismic vulnerability of a historical building in Italy. In: 13th world conference on earthquake engineering, Vancouver, B.C. Canada, paper no 3211

Su-Gon Lee, Steve Hencher, Ji-Won Kim, Sung-Bu Cho, Ho-Dam Lee, Sun-Hyun Park, Gun-Su Kim, and Young-Suk Lee

## Abstract

The Bangudae petroglyph is one of the most important examples of Korean prehistoric art. The petroglyph however has been subjected to annual submergence and drying since the impounding of a reservoir in 1965, which has led to some deterioration. The deterioration and need to preserve the petroglyphs has become an important matter of public concern. This paper presents some of the options for conservation of the Bangudae petroglyph and reviews their various advantages and disadvantages.

## 57.1 Introduction

The Bangudae petroglyph is located beside a river near Ulsan metropolitan city in the southeastern part of the Korean peninsula (Fig. 57.1). The petroglyph consists of a 10 m wide and 3 m high near-vertical cliff with about 300 land and sea animal features carved in the rock. The carvings were made in a period between the end of the Neolithic Age and the Bronze Age, about 7,000 years BP (Jeon et al. 2013) (Fig. 57.2). The cliff comprises mainly sedimentary rocks

such as sandstone, siltstone and shale and partially hornfels on the surface of cliff. The Bangudae petroglyph was discovered in 1971 by a Korean archaeologist and was designated as Korean National Treasure (No. 285) in 1995.

In the period between 1962 and 1965, a dam was built to provide water for Ulsan metropolitan city. Since the construction of the dam and impounding of the reservoir, the Bangudae petroglyph is now submerged for 8 months of the year (from early spring to autumn) and is exposed above water for 4 months (during winter) (Fig. 57.3). The periodic wetting and drying is causing deterioration to the rock and it is estimated that 25 % of the surface has already suffered some damage since 1965 (Fig. 57.4).

Since 2003 the Korean Cultural Heritage Administration has argued that the water level of dam should be lowered, but the Ulsan metropolitan government is reluctant due to the shortage of water resources. The newly elected president of Korea wishes to register the Bangudae petroglyph as a UNESCO cultural heritage site before 2017 in accordance with her presidential election campaign pledge. Therefore the conservation scheme of the Bangudae petroglyph has become an important matter of public interest.

This paper describes the deterioration the rock material over the past 48 years and presents the advantages and disadvantages of various possible conservation schemes of the Bangudae petroglyph.

S.-G. Lee (✉) · J.-W. Kim · S.-B. Cho · H.-D. Lee · S.-H. Park  
Department of Civil Engineering, University of Seoul, Seoul,  
Korea  
e-mail: sglee@uos.ac.kr

S. Hencher  
Department of Earth Science, University of Leeds, Leeds, UK  
e-mail: s.hencher@see.leeds.ac.uk

S. Hencher  
Halcrow China Limited, A CH2M HILL Company, Hong Kong,  
China

G.-S. Kim  
Department of Civil and Environmental Engineering, University  
of Ulsan, Ulsan, Korea

Y.-S. Lee  
Department of Electronic Engineering, Hanyang University,  
Seoul, Korea

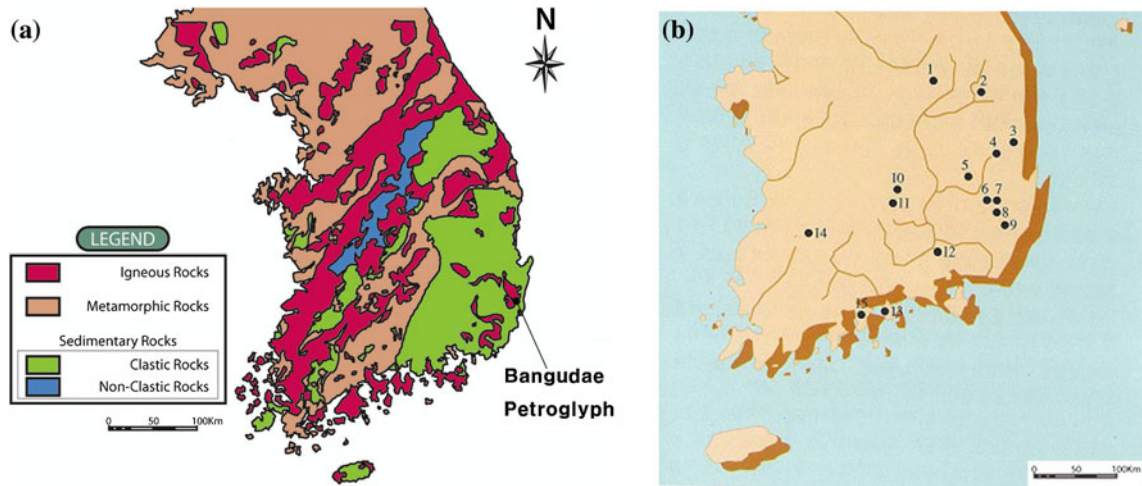


**Fig. 57.1** a Geology of South Korea and b distribution of petroglyphs in Korea (Yim 1999); note No.9 (Bangudae petroglyph)

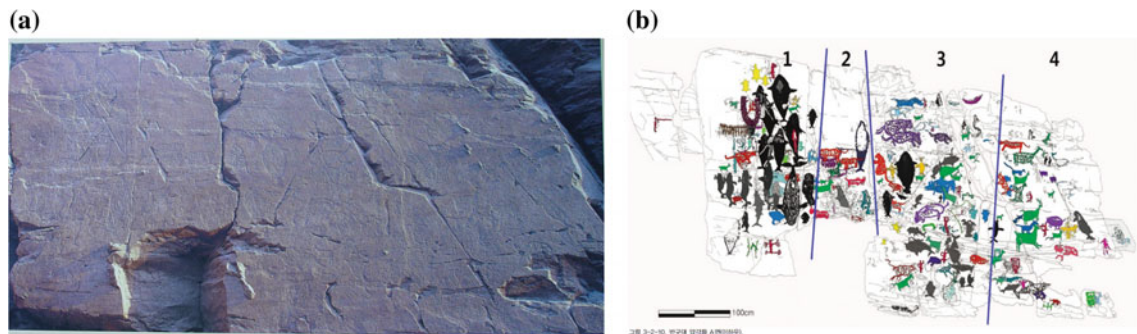


**Fig. 57.2** a Front view of Bangudae petroglyph and b an animation of Bangudae petroglyph



**Fig. 57.3** Submerged 8 months (*wet seasons*) and dry out for 4 month (*dry seasons*) since 1965

**Fig. 57.4** Evidence of deterioration of rock surface with time: the Bangudae petroglyph becomes obscured with time from the left (1972) to the right (2008) (Modified from Jeon 2012)

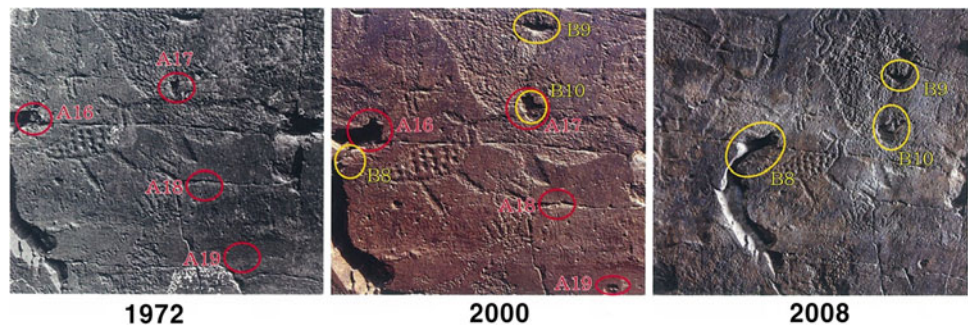
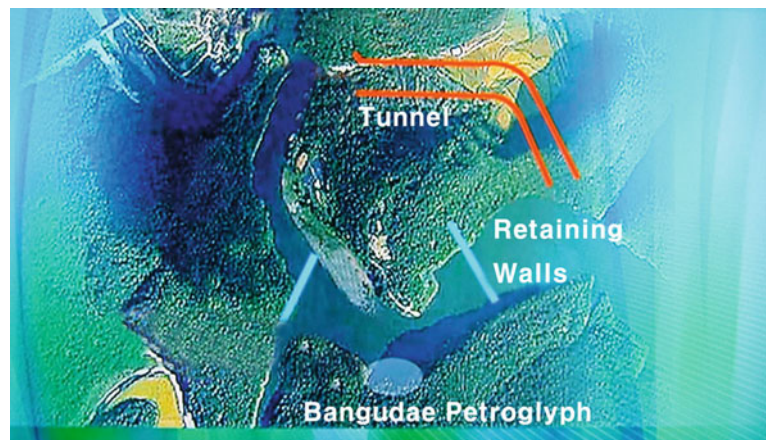


**Fig. 57.5** Convert of water course using by construction of small retaining wall in both upper and lower parts of river or by construction of a tunnel (Kim 2003)



## 57.2 Preservation Schemes

Due to increasing public concerns on culture preservation, various preservation schemes have been considered since 2003. There were 4 preservation schemes as follows: In response to increasing public concern over the deteriorating state of the Bangudae petroglyphs, various preservation schemes have been proposed since 2003 as follows:

### 57.2.1 Training of Water Course Away from Petroglyph

Kim (2003) suggested diverting the river. This would involve construction of small retaining walls along the river or construction of a tunnel (Fig. 57.5). This method was not accepted because of the expense and potential damage to the environment. Ironically during investigations for the study, Schmidt hammer tests were carried out on the surface of the Bangudae petroglyph and rock samples were collected and these actions have contributed to the deteriorating condition of the monument (Fig. 57.6).

### 57.2.2 Protection of Rock Surface

Seo (2010) examined the cliff and concluded that about 25 % of the rock surface was damaged. They recommended strengthening the surface of Bangudae petroglyph using silicon. This method was not accepted by the cultural properties protection committee because they feared some unexpected long-term behavior such as frost and ice wedging after silicon treatment. As for the earlier study conducted by Kim (2013), some damage was done during the field studies by Seo (2010) due to invasive investigation causing broken rock.

A large excavation to carry the river. (a) Plan view (b) cross-sectional view (c) before embankment (d) after embankment (Song et al. 2013).

### 57.2.3 Construction of Transportable Kinematic Dam

Ham (2013) recommended constructing a removable dam in front of the Bangudae petroglyph and this proposal is currently under review (Oct 2013) (Fig. 57.7a). It is understood

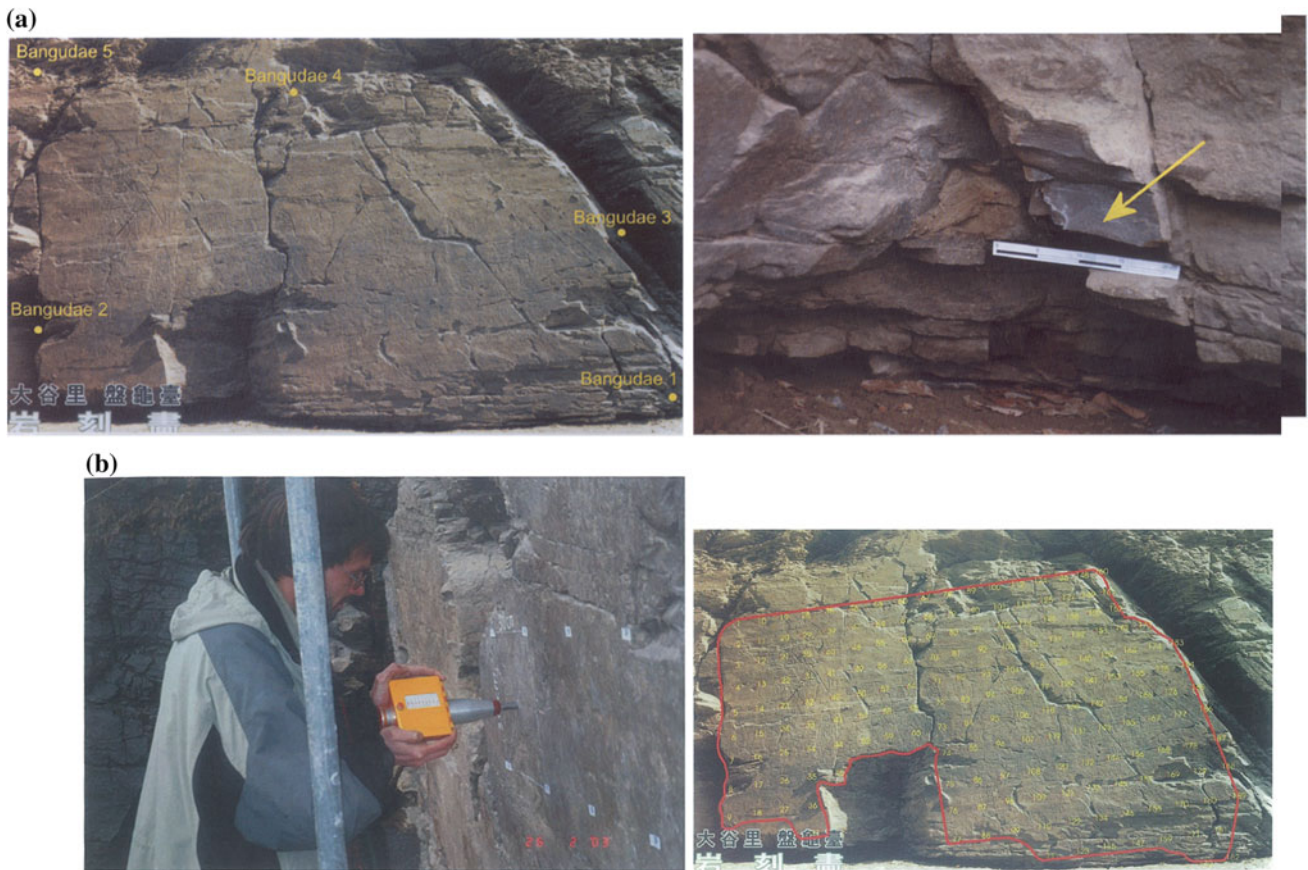


**Fig. 57.6** Damage to rock surface due to **a** rock sampling near the Bangudae petroglyph and **b** Schmidt hammer tests at 189 locations on the rock surface of Bangudae petroglyph (Kim 2003)

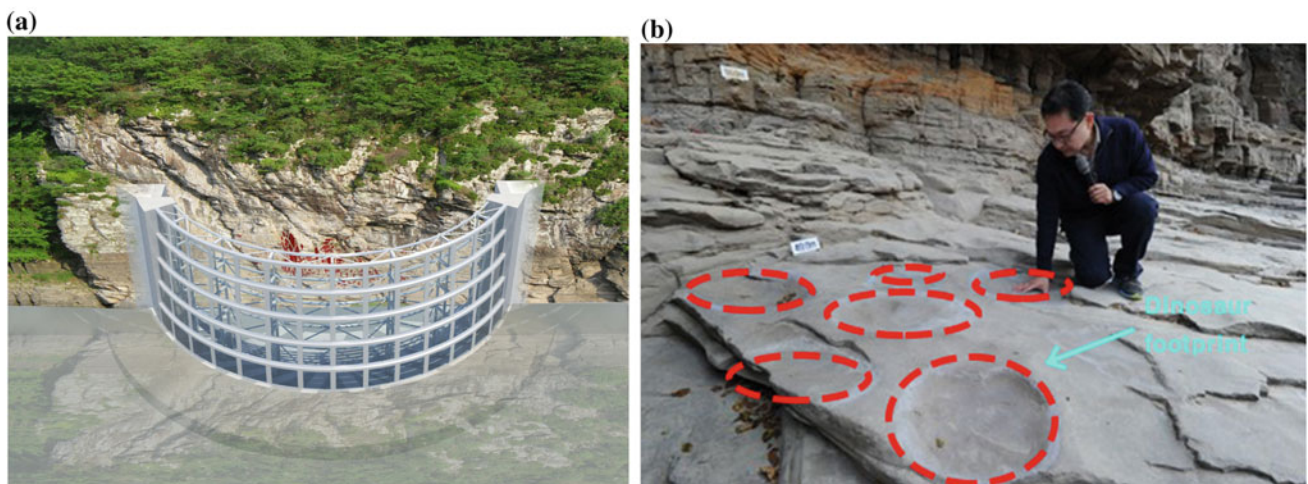


**Fig. 57.7** **a** A proposal to construct a removable dam to protect the Bangudae petroglyph is under review at present (Oct 2013): Bird-eye view (Ham 2013). **b** Numerous dinosaur footprints (see red-circle)

found on the rock surface below water level during site investigation in October 2013. These footprints might be hidden or damaged by construction of a dam

that the Korean central government lends support to this solution partly to facilitate reaching an agreement with local government (Ulsan metropolitan city). However recently (Oct 2013) during site investigation dinosaur footprints were

found on the rock surface below water level in front of the petroglyph (Fig. 57.7b). The need to preserve these important footprints may hinder or prevent the construction of the foundations for the removable dam.

### 57.3 Conclusion

Four solutions have been proposed to limit future deterioration of the Bangudae petroglyph. To date however it has proved very difficult to find a solution that meets all the requirements for preserving the monument without causing unacceptable damage to the setting and general environment. Ironically careless research activity in preparation of various schemes has caused accelerated deterioration of the Bangudae petroglyph.

---

### References

- Fitzner B, Heinrichs K, La Bouchardiere D (2004) The Bangudae petroglyph in Ulsan, Korea: studies on weathering damage and risk prognosis. *Environ Geol* 46:504–526
- Ham SM (2013) A suggestion of transportable kinematic dam for Bangudae petroglyph preservation scheme. Korean Central Government (in Korean)
- Jeon HT (2012) A report on deterioration of Bangudae: petroglyph in Ulsan, Korea. Bangudae Petroglyphs Institute, University of Ulsan, 38 p
- Jeon HT, Bahn PG, Tepfer EJ, Francfort HP, Solomon A, Yim SG, Han JH (2013) Bangudae: petroglyph panels in Ulsan, Korea, in the contest of world rock art. *World Petroglyphs Research I*, Bangudae Petroglyphs Institute, University of Ulsan, Hollym Publishing Co., Ltd, 231 pp
- Kim SJ (2003) Damage diagnosis on the Bangudae petroglyph and its conservation scheme. Seoul National University (in Korean)
- Seo JC (2010) Research on preservation of the surface of Bangudae petroglyph. University of Kongju (in Korean)
- Song JH (2003) A suggestion of embankment for Bangudae petroglyph preservation scheme. University of Hongik (in Korean)
- Yim S (1999) Petroglyph of Korea. Series of favorite books 102–44, Daewonsa Publishing Co., Ltd

---

# Consolidation and Restoration of the Moletta's Tower (Circus Maximus: Roma): Site Investigation and Monitoring

# 58

Roberto Brancaleoni, Federico Celletti, Fabio Garbin, Giuliano Padula, Luigi Serio, and Daniele Spizzichino

---

## Abstract

This paper describes the investigations carried out for the Moletta's Tower. The investigations were finalized at the consolidation and restoration of the building, in the work of environmental restoration and enhancement of archaeological sites of the Circus Maximus in Rome, with particular attention to the verification of the interaction soil-foundations of this tower. The surveys were focused mainly to provide information and data for the following aspects: (i) the project of the works necessary to prevent or reduce any differential subsidence resulting from the reduction of the water; (ii), a general static and seismic check of the tower; (iii) design the most appropriate consolidation work needed to building safety and make it accessible to the public for turistic exploitation. The geological, stratigraphic, geotechnical and seismic characteristics of the substrate have been defined by field of surveys carried out in the following stages: realization of 3 geognostic drillings (boreholes); sampling of 12 undisturbed soil samples, analyzed and tested in a specific and standard geotechnical laboratory; execution of 6 Standard Penetration Test S.P.T; execution of 2 multichannel analysis of surface waves (MASW) seismic stretched; realization of 1 well drilling inclined to identify the foundations of the tower's walls.

---

## Keywords

Circus Maximus • Consolidation and restoration • Geological and geotechnical investigation

---

R. Brancaleoni (✉) · F. Garbin · G. Padula  
Geoplanning Servizi per il Territorio s.r.l., Rome, Italy  
e-mail: roberto.brancaleoni@geoplanning.it

F. Garbin  
e-mail: fabio.garbin@geoplanning.it

G. Padula  
e-mail: giuliano.padula@geoplanning.it

F. Celletti  
Studio 3 + 1 di Federico Celletti s.a.s., Rome, Italy  
e-mail: federico.celletti@gmail.com

L. Serio  
Fabrica Studio Associato, Rome, Italy  
e-mail: luigiserio@fabricaassociati.it

D. Spizzichino  
Ispra, Italy

---

## 58.1 Introduction

The Moletta's Tower is located in the center of the semi-circular part of the track of Circus Maximus, (side Piazza di Porta Capena); stands out from the ruins of the Circus Maximus, as it seems almost a foreign object in a space that contains the remains of what was one of the major monuments of antiquity, the Tower is in fact the only architectural dating back to medieval times of this site.

Its origin is dated back the eleventh century, when the whole area between the slopes of the Palatine and the remains of the triumphal arch of the Circus Maximus was transformed into a fortified complex by the monks of S. Gregorio. Since 1145 the whole fortified complex passed to the Frangipane family.

With the exception of the period the end of the thirteenth century, when the tower results to have been shortened, its appearance remains essentially unchanged up to the present day.

In the age between the XIV and XVIII century, zone configuration will remain unchanged: that complex which crossed from the ditch of Velabro, with a mill backing onto the SE facade of Tower; the Tower is always incorporated into other buildings until 1934, when it was subjected to restoration and freed from the substructions.

In the early twentieth century the aspect assumed by the area of the Circus Maximus appeared far away from the current configuration: the area seems to be a vast space covered with industrial buildings arranged in accordance with random logic in which it was difficult to distinguish the archaeological remains from the buildings that rises in recent times.

A deep transformation occurs in the years between 1926 and 1934, when the restoration work and demolition of the substructures not coherent, brings the Circus Maximus to the aspect we know today.

In 2009 work began, currently underway, which finally turn to the roman citizens, the original configuration of the Circus Maximus: the isolated location of Moletta tower and the indication of the area where stood the triumphal arch of access to the Circus. These works will allow the exploitation of the archaeological area of the Circus Maximus and the Moletta's tower will be consolidated and restored.

For a correct approach to this work the geological, geotechnical and seismic parameters of ground belonging to the Tower were been defined (Fig. 58.1).



**Fig. 58.1** Tower of Moletta

## 58.2 Geological and Geomorphological Setting of the Area

From the geomorphological point of view the area is part of the Circus Maximus More in details it belongs to the valley between the Palatine Hill and the Aventine Hill (NNE to SSW) where once stood the ditch of the Velabrum, a tributary of the left bank of the Tiber.

In particular the study area is almost flat and is characterized by a share of approximately topographical 14–16 m to sea level.

The area, under a significant layer of backfill, is characterized by the presence of alluvial deposits (a2—Funciello and Giordano 2008) consist mainly of fine silty-clay deposits alternating with sandy levels and levels of peats at different depths (Fig. 58.2).

### 58.2.1 Detailed Geological Model

The investigations carried out have allowed to recognize the following successions subdivided as follows due to their characteristics stratigraphic, granulometric and geotechnical of the various encountered soils.

#### 58.2.1.1 Level 1: Greyish-Brown Backfill

It appears from loose to medium density, heterogeneous and heterometric, a predominantly grain size of a sand-gravel weakly clayish. Inside are found fragments of brick, mortar and pozzolanic pieces of marble. The measured thickness is between about 7 and 10 m.



**Fig. 58.2** Geology of area, from Funciello and Giordano (2008)

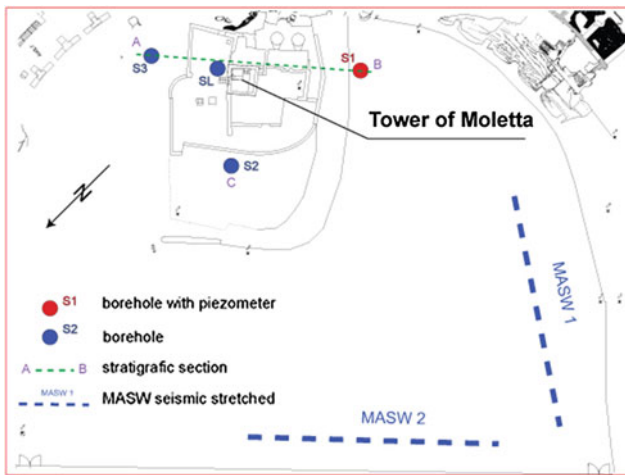


Fig. 58.3 Location of the investigation

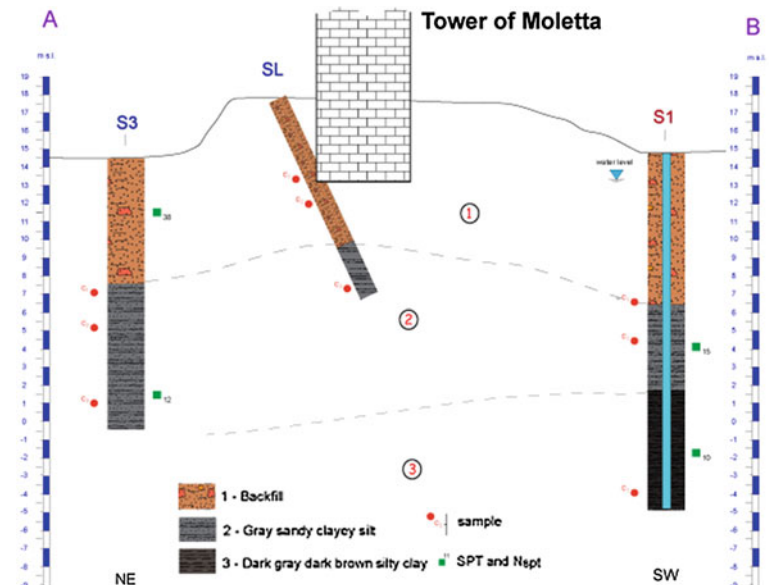
### 58.2.1.2 Level 2: Gray Sandy Clayey Silt

This level looks like stiff, at times occurs dark gray silty clay with the presence of organic matter. The thickness is approximately 7 m.

### 58.2.1.3 Level 3: Dark Gray Dark Brown Silty Clay

Abundant frustules and partially decomposed vegetation are present; fragments of wood and remains of shells. In places the clay fraction prevails. The thickness remains open and unconfined downwards because the investigations carried out have not intercepted the lower limit (Figs. 58.3 and 58.4).

Fig. 58.4 Stratigraphic correlation



## 58.3 Geotechnical Characterization of the Foundation Soils

Starting from the geological model, implemented by the stratigraphy of the geological surveys, a geotechnical characterization of soils was carried out by analyzing the laboratory tests performed on 12 samples taken during the surveys jointly with the 6 SPT performed during the same field investigation.

The main physical-mechanical characteristics detected for each level by granulometric analysis and physic-mechanical tests (direct shear tests with Casagrande box of 36 cm<sup>2</sup> diameter; triaxial tests and oedometric tests UU and CID), are summarized as follows :

physical properties

- $\gamma$  = natural unit weight of the soil;

mechanical properties

- $c'$  = drained cohesion (in terms of effective stress);
- $\phi'$  = friction angle (in terms of effective stress);
- $c_u$  = undrained cohesion;
- $E'$  = oedometric modulus (Table 58.1).

## 58.4 Structural Works: The Seismic Improvement of the Tower

The structural project consists in the seismic improvement of the tower. It has been necessary because of its refurbishment—in view of its opening to the public—and also because of the works to reduce the aquifer in the surrounding archeological area.

**Table 58.1**

	$\gamma$ (kN/m <sup>3</sup> )	$c'$ (kPa)	$c_u$ (kPa)	$\phi'$ (kPa)	$E'$ (kPa)
Level 1 <i>Greyish-brown backfill</i>	16.00–19.00	0–3		26–30	
Level 2 <i>Gray sandy clayey silt</i>	16.69–17.59	3–28	51–81	24–32	5,106–5,543
Level 3 <i>Dark gray dark brown silty clay</i>	15.01		64		2,355

$E'$  = load range between 98 and 196 kPa

These works allow to decrease the height of the entrance further down to about 1.5 m where the digs of Circus Maximus are actually. With this purpose an existing door has been reopened and strengthened.

In addition to widespread injections of hydraulic lime mortar in masonry, the seismic improvement consists in both the reinforce of the foundations inserting a steel ribbed slab and the emptying of the tower destroying all the floors and also with the insertion of steel rings on the inner side of the walls. On the steel a rings system of tie rods with outer end-plates is placed.

In the inner space a lightweight staircase made of a steel structure and wooden steps is designed and will allow to enter (placed at about 9.5 m above the height of the entrance). Through the glass windows placed between the crenellations of the perimeter walls it will be possible to enjoy a large view of the Circus Maximus.

The consolidation won't increase the mass of the tower, on the contrary, it will slightly reduce it.

Together with the consolidation of the structure also the strength of foundations and masonry will be improved with the steel structures designed and the injections of hydraulic lime mortar.

So a general enhancement of the structural behavior and the seismic capability of the tower will be obtained in addition to a substantial increase of the resistance to vertical loads.

Choosing steel structures, even in foundation, allows a total removability of the intervention and offers the possibility to recognize vertical parts and roofs and ensures a minimum visual impact respecting the original structures.

Also a long-time monitoring campaign should be implemented with aiming at estimate seismic response characteristics of the tower both on structures and at ground surface. An integrated monitoring system (wi-fi sensor) should be implemented in order to prevent future damages and to control the effectiveness of the proposed restoration work. More in detail in the second stage of the restoration project a

simple monitoring instruments composed by tilt meters will be installed.

## References

- Bozzano F, Funicello R, Marra F, Rovelli A, Valentini G (1995) Il sottosuolo dell'area dell'Anfiteatro Flavio in Roma. *Geologia applicata e idrogeologia* 30:405–422
- Capelli G, Mazza R, Taviani S (2008) La cartografia idrogeologica alla scala 1:50.000 dell'area di Roma. *Mem Descr Carta Geol d'Italia*, vol LXXX
- Corazza A, Lanzini M, Rosa C, Salucci R (1999) Caratteri stratigrafici, idrogeologici e geotecnici delle alluvioni tiberine nel settore del centro storico di Roma. *Il Quaternario* 12(2):215–235
- Corazza A, Lombardi L, Leone F, Brancaleoni R, Lanzini M (2004) Le acque sotterranee nei terreni di riporto della città di Roma. *Convegno Ecosistema Roma, Accademia dei Lincei*. Roma 14–16 aprile 2004
- Faccenna C, Funicello R, Marra F (1995) Inquadramento geologico strutturale dell'area romana. *Mem Descr della Carta Geol d'Italia*, vol I—“La Geologia di Roma: il Centro Storico”
- Funicello R, Giordano G (2008) Carta geologica del Comune di Roma (nuova edizione 2008)—Volume 1. *Mem Descr della Carta Geol d'Italia*, vol LXXX
- Funicello R, Praturlon A, Giordano G (2008) La geologia di Roma, dal centro storico alla periferia. *Mem Descr della Carta Geol d'Italia*, vol LXXX
- Gasparini C, Leone F, Brancaleoni R, Garbin F (2005) I rischi geologici nell'area urbana di Roma. *Convegno di Geologia Urbana nella Capitale, viaggio nella IV dimensione*. Roma 28 novembre 2005
- Mancini M, Moscatelli M, Stigliano F, Cavinato GP, Milli S, Pagliaroli A, Simionato M, Brancaleoni R, Cipolloni I, Coen G, Di Salvo C, Garbin F, Lanzo G, Napoleoni Q, Scarapazzi M, Storoni Ridolfi S, Vallone R (2013) The Upper Pleistocene-Holocene fluvial deposits of the Tiber River in Rome (Italy): lithofacies, geometries, stacking pattern and chronology. *J Mediterr Earth Sci* 95–101 (Special Issue)
- Marra F, Rosa C (1995) Stratigrafia e assetto geologico dell'area romana. In: “La geologia di Roma. Il centro Storico”. *Memorie descrittive della Carta Geologica d'Italia*, 50, 49–118
- Moscatelli M, Milli S, Patera A, Stigliano F, Storoni Ridolfi S, Brancaleoni R, Garbin F (2004) Caratteristiche geologiche e geotecniche dei terreni della Città di Roma. *Il Convegno Geosed*. Roma 20–21 settembre 2004

---

# Multi-scale Detection of Changing Cultural Landscapes in Nasca (Peru) Through ENVISAT ASAR and TerraSAR-X

59

Deodato Tapete, Francesca Cigna, Rosa Lasaponara, and Nicola Masini

---

## Abstract

Usefulness of archive C-band Synthetic Aperture Radar (SAR) imagery and recently acquired X-band SAR data was explored in Nasca (Peru) for condition monitoring of cultural features threatened by various natural and anthropogenic hazards. Amplitude information from medium resolution ENVISAT ASAR IS2 time series (2003–2007) acquired along ascending and descending orbits was exploited to depict recent landscape changes. Beneficial impacts on temporal analysis of surface processes are discussed, also in light of the promising perspectives of high resolution SpotLight TerraSAR-X images for feature detection. The approach demonstrates its suitability for regional/local-scale applications.

---

## Keywords

Landscape change • Condition monitoring • Synthetic aperture radar • Cultural heritage • Nasca

---

## 59.1 Synthetic Aperture Radar on Nasca Heritage

This research investigates the region of the Nasca Civilization, Southern Peru, dominated by the Rio Grande catchment basin, and its archaeological heritage (Fig. 59.1a). UNESCO WHL Lines and Geoglyphs of Nasca and Pampas de Jumana are certainly the most famous cultural sites, along with the World's largest adobe Ceremonial Centre of Cahuachi and the ancient aqueduct systems (the so-called 'puquios'). The latter were designed by the ancient inhabitants of the region for water supply, and testify their adaptation capabilities to the local environment.

As highlighted by several authors (Ruescas et al. 2009; Baade and Schmullius 2010), this heritage is currently exposed to surface erosion and deposition from flash floods events and run-off from the surrounding Andean foothills. Indeed, historical records confirm this issue is chronic, if it is true that a series of mudslides and severe earthquake accelerated the decline of Cahuachi in the fourth phase of its history (AD 350–400; Masini et al. 2012, and references

---

D. Tapete (✉)  
Department of Geography, Institute of Hazard, Risk and Resilience (IHRR), Durham University, South Road, Durham DH1 3LE, UK  
e-mail: deodato.tapete@gmail.com

F. Cigna  
British Geological Survey (BGS), Natural Environment Research Council (NERC), Nicker Hill, Keyworth, NG12 5GG, UK  
e-mail: fcigna@bgs.ac.uk

R. Lasaponara  
Institute of Methodologies for Environmental Analysis (IMAA), National Research Council (CNR), Contrada S. Loja, Tito Scalo, Potenza, Italy

N. Masini  
Institute for Archaeological and Monumental Heritage (IBAM), National Research Council (CNR), Contrada S. Loja, Tito Scalo, Potenza, Italy

R. Lasaponara · N. Masini  
Italian Mission of Heritage Conservation and Archaeogeophysics (ITACA) in Peru, Lima, Peru

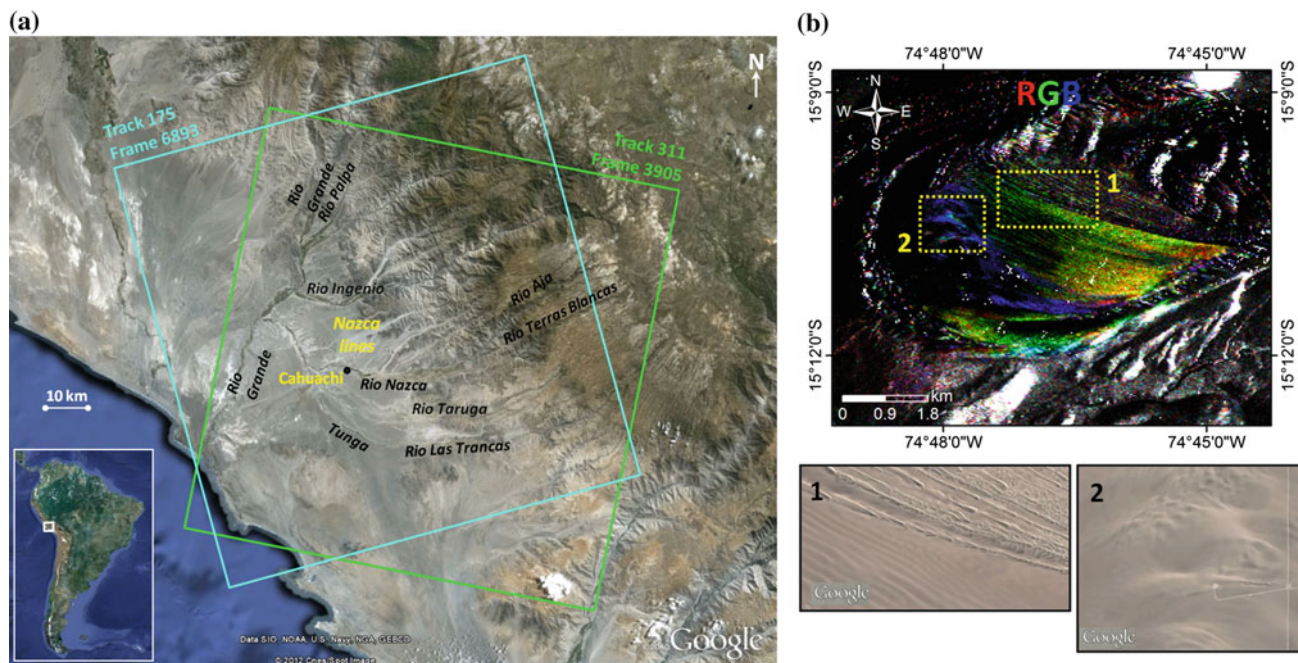


**Fig. 59.1** **a** Study area with ascending/descending ENVISAT ASAR IS2 footprints over the Nasca region, Peru (Google earth © 2012 Cnes/Spot Image). **b** RGB colour composite of a sand dune shows surface changes south of Cahuachi as recorded along ASAR descending

geometry on 04/02/2003, 15/04/2003 and 24/06/2003 (RGB channels respectively; modified from Cigna et al. 2013). Google Earth zoomed views come from Google earth (© 2013 DigitalGlobe)

therein). The same authors also applied methods of environmental change detection by using the interferometric coherence of Synthetic Aperture Radar (SAR) imagery. By contrast, this study demonstrates how surface changes revealed by exploiting SAR amplitude information can be referred to natural or human-induced processes of alteration, thereby supporting a sustainable satellite-based approach of condition monitoring of the heritage and its environmental context.

## 59.2 SAR Data and Methodology

Time series of the radar signatures and associated back-scattering coefficient ( $\sigma^0$ ) were reconstructed over the period 2003–2007, especially for the targets on the grounds related to the local cultural heritage and landscape. Although the whole catchment basin of the Rio Grande was analyzed, particular attention was given to the riverbeds of Rio Nazca and Rio Taruga (Fig. 59.1a).

The following SAR stacks from the archive of the European Space Agency (ESA) were accessed and exploited in the framework of Cat-1 project Id.11073:

- 8 ENVISAT ASAR IS2 scenes acquired in descending mode between 04/02/2003 and 15/11/2005;

- 5 ENVISAT ASAR IS2 scenes acquired in ascending mode between 24/07/2005 and 11/11/2007.

The stepped methodological approach used in this research included: raw data focusing into Single Look Complex (SLC); absolute radiometric calibration and co-registration; and, geocoding of the co-registered Multi Look Intensity (MLIs) images and derived products. The reader should refer to Cigna et al. (2013) for a full description of the methodology, as well as for the integration with Advanced Spaceborne Thermal Emission and Reflection Radiometer (ASTER) and VHR-optical imagery.

Among the products retrieved, it is worth mentioning here:

- the image ratios ( $R\sigma^0$ ) of different pairs of spatially filtered MLIs which enhance  $\sigma^0$  changes occurred during the time interval between two MLIs;
- RGB (Red-Green-Blue) or RC (Red-Cyan) colour composites of three or two MLIs respectively, where the colours of tint within the observed scene give information on the date when surface changes occurred.

The second part of this paper also introduces the advantages and potential offered by high to very high resolution data acquired between 2008 and 2012 by the TerraSAR-X mission to perform local-scale analysis. These data are made available by the German Space Agency (DLR) via the TSX-Archive-2012 LAN1881 project.

### 59.3 Hazards Depicted by ENVISAT ASAR Imagery

The amplitude-based change detection carried out by using ENVISAT ASAR imagery allowed us to demonstrate the usefulness of this approach to:

- Detect and map land surface processes, thereby following their spatial and temporal evolution, and overcoming some limitations intrinsic to phase-based approaches (such as Persistent Scatterer Interferometry—PSI);
- Monitor condition of an archaeological site and identify the causes of surface alteration (e.g., illegal digging activities, natural erosion) based also on integration with conservation history and ground truth;
- Characterize variations of soil moisture and vegetation in agricultural areas where archaeological features, such as the *puquios*, are commonly found and whose changes in terms of surface properties can be used to assess impacts of human activities and climate-change pressure.

Figures 59.1b and 59.2 summarize some of the main outcomes of these tests.

By combining the MLIs from different descending ASAR acquisitions on 04/02/2003, 15/04/2003 and 24/06/2003 into RGB colour composites, the evolution of a sand dune south of Cahuachi was reconstructed, proving that the major movements occurred between April and June 2003 (Fig. 59.1b). The advantage of working with SAR amplitude instead of phase is that the surface changes can be followed and mapped, whatever is the magnitude of the event affecting the area investigated. Land motion certainly modifies the local backscattering properties, but the surface still reflects the incident radiation. Hence,  $\sigma^0$  changes can be still estimated over time. Conversely, a scene modification such that former radar targets disappear does normally prevent further PSI analysis to be performed (cf. for instance the results obtained over a vegetated archaeological site severely

damaged by a collapse which are described in Tapete et al. 2012, 2013a).

With regard to site condition monitoring, ratioing between different pairs of scenes highlights how and where the radar backscattering changed. Figure 59.2 relates to  $\sigma^0$  variations detected in 2003–2005 within Cahuachi (cf. also Tapete et al. 2014). Looking at the whole period covered by the descending data (04 February 2003–15 November 2005), two blue-coloured patterns were discovered over the Pirámide Naranja and the southeastern corner of Sector B (Fig. 59.2b), with the latter not being attributable to legal excavations as the former (cf. Tapete et al. 2013b for more details on these results). Integration with ground truth and records of the archaeological excavations also allowed us to exclude effects of surface erosion or other type of disturbance.

### 59.4 Perspectives for Monitoring with X-Band SAR Imagery

A step towards an effective local scale analysis is undoubtedly represented by the exploitation of X-band TerraSAR-X and TanDEM-X archives, which can provide spatial resolution ranging from 1.1 to 3.5 m with High Resolution SpotLight (HS) Image Mode data. That leads to an unprecedented level of detail with which even shallow features raising few centimetres from the bare soil can be detected and distinguished based on the radar backscattering signal.

This is, for instance, the case of the Nasca Lines. These ‘negative geoglyphs’ are scratched on the ground surface by removing the dark gravels of the valley and exposing the underlying unpatinated and lighter coloured ground. Their detection within medium resolution SAR imagery (e.g., ENVISAT ASAR IS2) is strongly influenced by the size of the feature with regard to the pixel cell and ground resolution of the imagery itself (Tapete et al. 2013b). As shown in

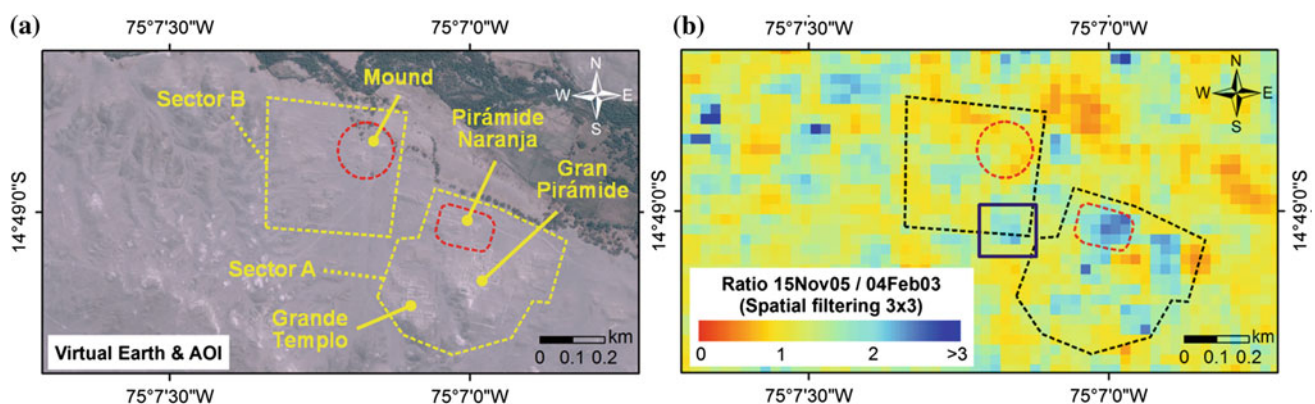


**Fig. 59.2** a Virtual Earth image of Cahuachi (Sector A) and Sector B enclosing archaeological mounds, and b the corresponding amplitude change detection map based on  $R\sigma^0$  in February 2003–November 2005.

The blue pattern within the black square over the southeast corner of Sector B is not due to authorized archaeological excavations (modified from Tapete et al. 2013b)

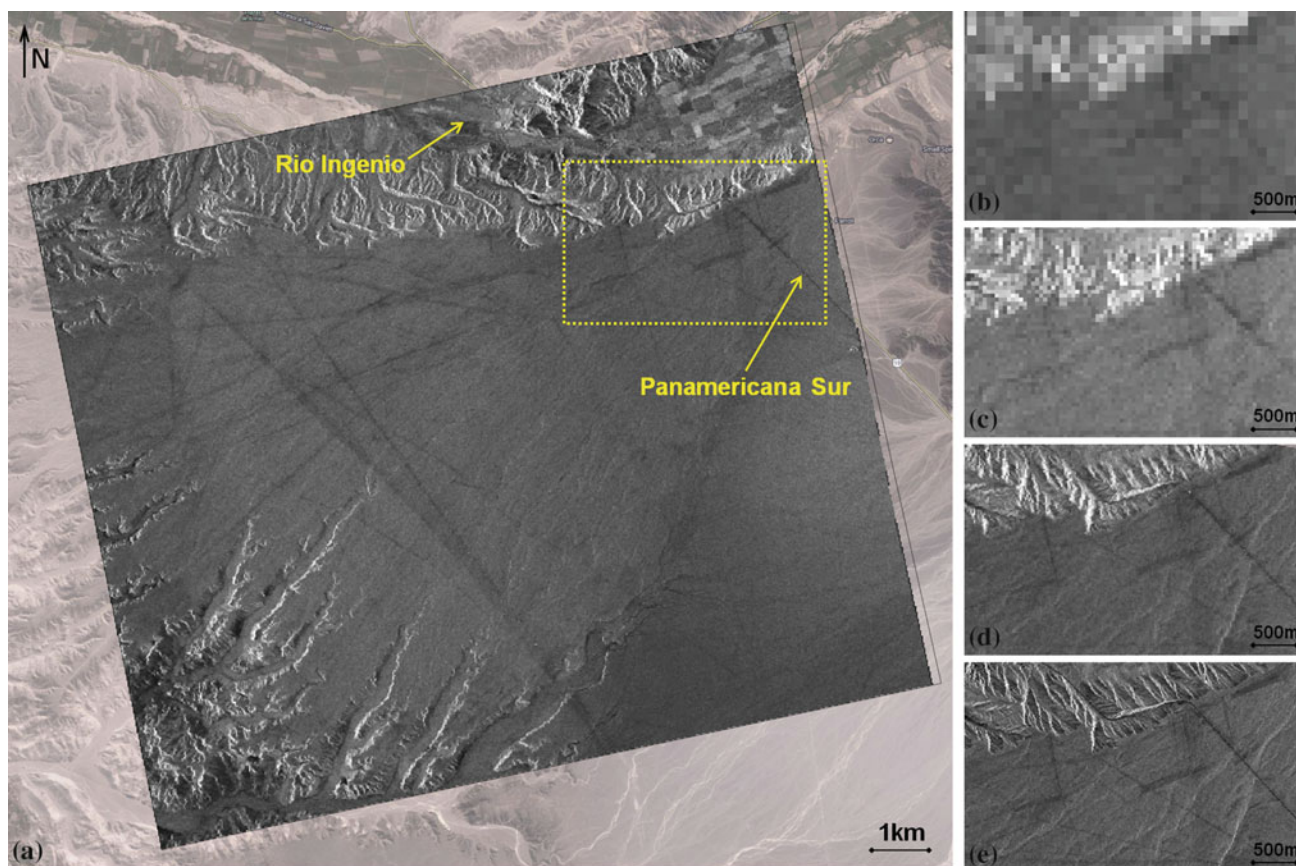


**Fig. 59.3** a TerraSAR-X (TSX) SpotLight scene acquired on 13/08/2008 in ascending mode with VV polarization and  $32.5^{\circ}$ – $33.6^{\circ}$  incidence angles over the Nasca Lines (© DLR 2014), overlapped onto optical imagery (©2013 Google Imagery ©Cnes/Spot Image, DigitalGlobe, Map data ©Google). Comparison of: b ScanSAR TSX,

HH, ascending, range res. 17.0–19.2 m; c StripMap TanDEM-X (TDX), HH, ascending, range res. 3.3–3.5 m; d SpotLight TSX, HH, descending, range res. 1.7–3.5 m; e High Resolution SpotLight TDX, HH, descending, range res. 1.1–3.5 m (© DLR 2014)

Fig. 59.3, the significant improvement of the spatial resolution is immediately appreciable directly comparing ScanSAR (SC), StripMap (SM), SpotLight (SL) and HS images acquired over the same area with same polarisation (in this case, horizontal-horizontal—HH). Evidently that has positive effects also on the change detection capabilities at the local scale, as the ongoing research is expected to prove.

margins of the main archaeological areas. Hence, the possibility to track through time the displacements of such landforms and surface changes can add important information for wide-context hazard assessment.

**Acknowledgments** ENVISAT ASAR data were made available through ESA Cat-1 project Id.11073. TerraSAR-X and TanDEM-X data are sourced from DLR archives via the TSX-Archive-2012 LAN1881 project.

## 59.5 Conclusive Remarks

The SAR-based approach used to investigate the Nasca region provides a suitable tool for a sustainable condition monitoring in time from remote. The multi-scale perspective offered by the multi-platform/band SAR data nowadays available is enhanced by the choice of exploiting the amplitude information. As demonstrated by the tests over sand-dunes, wind-driven and run-off water-controlled surface processes can be quite hazardous over such an arid region, especially for archaeological remains located at the

## References

- Baade J, Schullius CC (2010) Interferometric microrelief sensing with TerraSAR-X—first results. *IEEE Trans Geosci Remote Sens* 48(2):965–970
- Cigna et al (2013) Amplitude change detection with ENVISAT ASAR to image the cultural landscape of the Nasca region, Peru. *Peru Arch Prosp* 20(2):117–131. doi:[10.1002/arp.1451](https://doi.org/10.1002/arp.1451)
- Masini et al (2012) Integrated remote sensing approach in Cahuachi (Peru): studies and results of the ITACA mission (2007–2010). In: Lasaponara R, Masini N (eds) *Satellite remote sensing: a new tool for Archaeology*. Springer, Berlin, Heidelberg, pp 307–344. doi: [10.1007/978-90-481-8801-7\\_14](https://doi.org/10.1007/978-90-481-8801-7_14)

- Ruescas et al (2009) Change detection by interferometric coherence in Nasca Lines, Peru (1997–2004). In: Fringe 2009, 30 Nov–4 Dec, ESRIN, Frascati, ESA SP-677
- Tapete et al (2014) Investigating natural hazards in the Peruvian region of Nasca with space-borne radar sensors. In: Sassa K (ed) *Landslide science for a safer geo-environment*, vol 3. Springer International Publishing, Switzerland, 6 p. doi: [10.1007/978-3-319-04996-0\\_54](https://doi.org/10.1007/978-3-319-04996-0_54)
- Tapete et al (2013a) Radar interferometry for early stage warning of monuments at risk. In: Margottini C et al (eds) *Landslide science and practice. Early warning, instrumentation and monitoring*, vol 2. Springer, Berlin, pp 619–625. doi: [10.1007/978-3-642-31445-2\\_81](https://doi.org/10.1007/978-3-642-31445-2_81)
- Tapete et al (2013b) Prospection and monitoring of the archaeological heritage of Nasca, Peru, with ENVISAT ASAR. *Arch Prosp* 20 (2):133–147. doi:[10.1002/arp.1449](https://doi.org/10.1002/arp.1449)
- Tapete et al (2012) Satellite radar interferometry for monitoring and early-stage warning of structural instability in archaeological sites. *J Geophys Eng* 9(4):S10–S25. doi:[10.1088/1742-2132/9/4/S10](https://doi.org/10.1088/1742-2132/9/4/S10)

---

# Structural Assessment of Case Study Historical and Modern Buildings in the Florentine Area Based on a PSI-Driven Seismic and Hydrogeological Risk Analysis

60

Fabio Pratesi, Deodato Tapete, Gloria Terenzi, Chiara Del Ventisette, and Sandro Moretti

---

## Abstract

C-band medium-resolution Persistent Scatterer Interferometry (PSI) data from ERS-1/2, ENVISAT and RADARSAT-1 were used to establish a classification method preparatory to seismic and hydrogeological risk assessment of historical buildings in urban areas. Tests were conducted over the heritage city of Florence, Italy, using a multidisciplinary approach which takes into account geological and environmental factors of hazards, along with parameters related to conservation history of the monuments and the possible sources of damage commonly found within an urban context. The case study herein presented confirm the advantages of PSI against its well-known limitations, and demonstrate how PSI can be used to support subsequent structural analyses of buildings.

---

## Keywords

Structural deformation • Monitoring • Synthetic aperture radar • Persistent scatterer interferometry • Cultural heritage

---

## 60.1 Introduction

Recent works have showed how radar-based remote sensing techniques (e.g., Cigna et al. 2011, 2012; Spizzichino et al. 2013; Tapete and Cigna 2012; Tapete et al. 2012, 2013; Trigila et al. 2011), can be successfully exploited in the field of cultural heritage conservation threatened by natural and

anthropogenic alteration of landscape (e.g., subsidence, landslides, land-use changes). In particular, Persistent Scatterer Interferometry (PSI) data from multi-interferogram processing of satellite Synthetic Aperture Radar (SAR) imagery allow the investigation and monitoring of displacement trends of single man made objects spread on the ground. We propose here a PS data-based classification of monuments intended as an investigation method preparatory to seismic and hydrogeological risk assessment of historical buildings in urban areas.

---

F. Pratesi (✉) · C.D. Ventisette · S. Moretti  
Earth Sciences Department, University of Florence, Florence, Italy  
e-mail: ing.pratesi@gmail.com

F. Pratesi · G. Terenzi  
Department of Civil and Environmental Engineering,  
University of Florence, Florence, Italy

D. Tapete  
Department of Geography, Institute of Hazard, Risk and  
Resilience (IHRR), Durham University, South Road,  
Durham DH1 3LE, UK  
e-mail: deodato.tapete@gmail.com

---

## 60.2 Methodology

Many authors indeed have demonstrated the connection between displacements revealed by InSAR and the observed building damages, but it is not so immediate and easy to identify the real causes to which the detected deformation are to be referred. On the author's opinion, such goal can be achieved only after a 'categorization' of the monitored monuments based on the relationships between their intrinsic

structural properties and the geological susceptibility of their foundation ground.

To simplify the identification process, a matrix of possible damage scenarios is defined using mainly the following input parameters: (i) structural typology of the monument; (ii) geological bedrock; (iii) history of recent displacement as imaged by means of monitoring data; and (iv) past and recent conservation history of the building.

The importance of developing a standard procedure comes from the need to classify a large number of buildings in short time and even to give an effective and shared tool which guarantees uniformity and reproducibility in the evaluation of the vulnerability. The quick recognition of the expected criticalities is eased by multi-layering multi-source data within a GIS environment and analyzing structural and ground deformation, passing from a global to micro-scale. This allows us to check which target on the ground the displacements observed are referred to, thereby decreasing

the percentage of unrelated PS that might be misleading to assess the stability of the monument of interest.

Data sheets (Fig. 60.1) have been purposely designed to report all the information collected during this survey and screening activity, and summarize the criticality factors. These form aim to a rapid identification of the monitored monuments in terms of: (i) geographic position, (ii) geometric complexity, (iii) structural typology, (iv) detected displacements and (v) characteristics and criticalities of the foundation ground. Pre-defined criteria for compilation derived also from the existing approaches of building classification and survey, are thought to guide the operators to express a qualitative to quantitative judgment on the degree of PS coverage, and classify the degree of criticality following an increasing scale with six classes (from 1 to 6). Such organized database provides an inventory to correlate architectural typologies, structural weaknesses and ground stability within a same urban area.

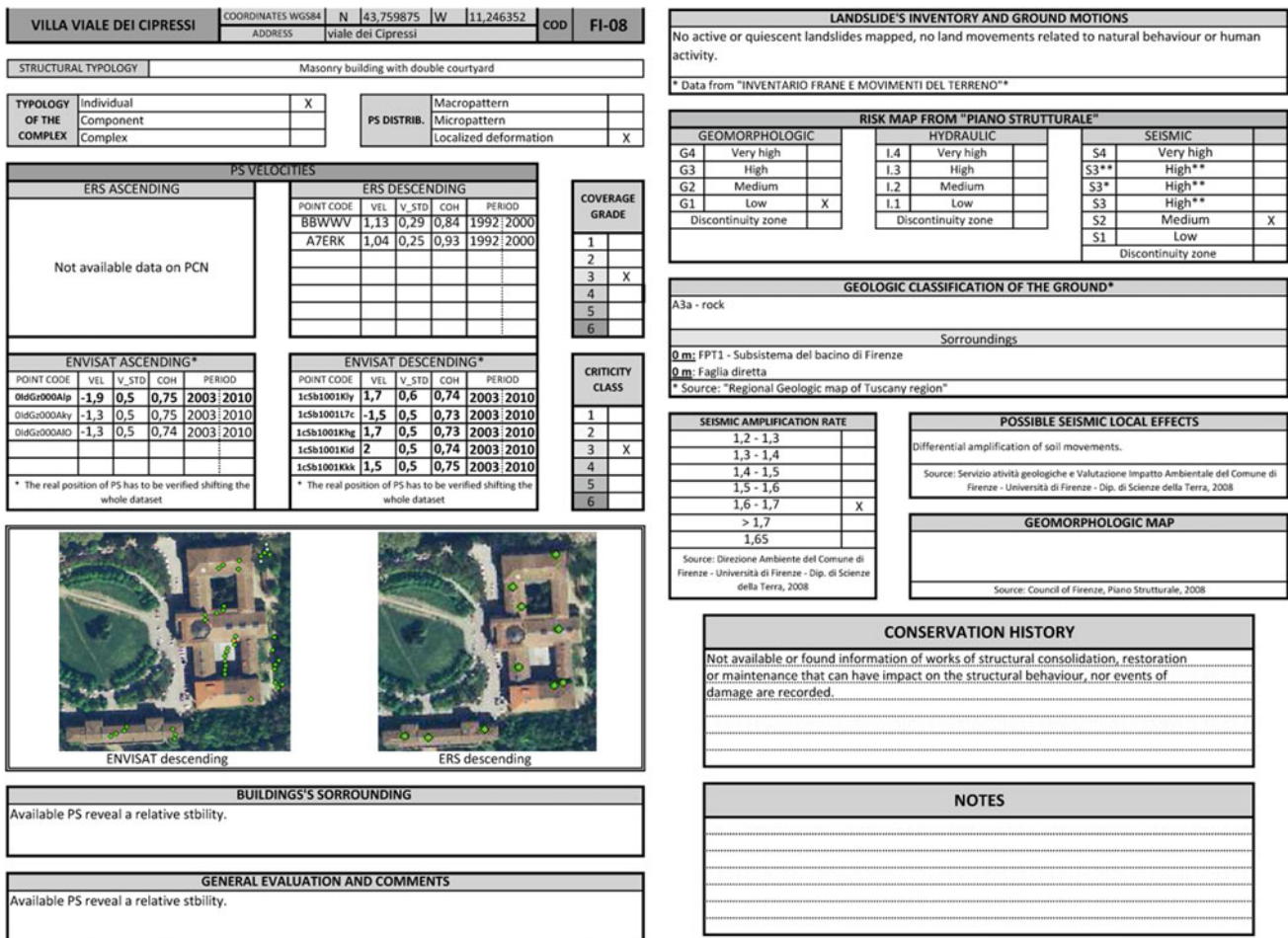


**Fig. 60.1** Example of the data sheets used for the PSI-based classification, including a section of “Conservation history” containing comments on (beneficial or detrimental) effects of human actions (e.g.

recorded restorations, engineering works carried out in the proximity of the monuments, etc.)

We applied the above method to the case study of Florence, to set parameters and procedures to be used for the PSI-driven classification we would like to propose for the assessment of the structural behavior of historical buildings, and their vulnerability and risk under expected hazard scenarios. This urban area is emblematic because it contains a high density of monuments, within a complex environment characterized by alluvial plain surrounded by slope areas, with different susceptibility to seismic amplification and/or ground motions.

### 60.3 First Results and Discussion

We show here a selection of the outcomes from this preliminary screening over the Florentine built heritage by means of PSI ERS-1/2 (1992–2000) and ENVISAT (2002–2010) data from the Extraordinary Plan of Environmental Remote Sensing (EPRS-E), made available in the framework of DIANA project with Tuscany Region. PSI RADARSAT-1(2003–2007) data were also included.

Table 60.1 shows the sample of monuments we selected to have a statistically sufficient representation of the main categories of the Florentine historical buildings. It is quite obvious that the categories and their population are based on simplified criteria of selection and classification and they give a figure of the majority of the historic environment in Florence, not including ‘minor’ historical buildings or places (e.g. tabernacles, small churches, etc.). The sampling was also influenced by the actual PS density provided by the datasets available.

Throughout the different datasets, most of the PS data indicate a relative stability as detected displacements are lower than the selected stability threshold of  $\pm 1.5$  mm/year. In several cases localized deformation are highlighted by single and isolated PS, however velocities are mostly lower than  $\pm 3$  mm/year of motion rate along the Line-Of-Sight (LOS) of the satellite. These results are consistent with the following evidences and records:

- (1) general stability of the Florentine ground as inferable by the bedrock geology underneath most of the monuments;
- (2) good condition of the structures, in some cases periodically maintained and checked;
- (3) absence of relevant seismic events occurred in the last 20 years.

Figure 60.2 shows a couple of examples of relatively stable PS over the Uffizi Gallery and Vasarian Corridor in the town centre along the Arno River side, and San Miniato Church complex on the top of the namesake hill over the period 2003–2010. ENVISAT ascending data LOS estimates do not show any critical movements which can warn about the stability of the museum due to possible collapses along

**Table 60.1** Categories of the Florentine monuments and related samples analyzed in this study

Category	Total number	Analyzed	%
Gates and arches	11	3	27.3
Stadiums	3	1	33.3
Churches (before 1900)	74	5	6.8
Churches (after 1900)	38	1	2.6
Villas	147	9	6.1
20th century architecture	74	7	9.5
Fortifications	4	2	50.0
Palaces (before 1900)	311	3	1.0
Convents	15	3	20.0
Archaeological sites	3	1	33.3
Bridges	12	1	8.3

the riverbank, nor structural displacements of the church potentially due to the ground motions historically threatening the hill (cf. Fanti 2006).

Among the newly built-up areas located in the suburbs of Florence which are currently experiencing urban sprawl and its consequences, we here briefly illustrate the case study of the research center of CNR (National Research Council of Italy). This building complex located in the Council of Sesto Fiorentino, 7 km far from the city center of Florence, was completed in early 2000s and all the research institutes and laboratories completed their move-in in 2005. It consists of three main RC courtyard buildings with two levels facing other linear and low rise blocks. In this case the satellite radar monitoring system has recorded the progressive subsidence affecting the structures, as expected from the dynamics of compression and consolidation during the settling-in of the soil. As shown in Fig. 60.3, the average LOS displacements rates retrieved from ENVISAT ascending data (and the corresponding descending dataset) grow gradually from the south part of the complex to the north. This differential condition seems to be related to the different period of construction of the buildings and to the typical dynamics of the consolidation process. The latter is characterized by high deformation velocities in the first loading period and by a non-linear decrease after. The north buildings were built first and the construction works advanced gradually from north to south. From the interpretation of the velocity field we can infer that the north building have just experienced the great part of the consolidation deformation while the consolidation process of the south ones is in the peak phase. A further contribution to this subsidence that cannot be excluded a priori can be the local groundwater exploitation for the daily usage of the entire complex. Such assessment needs to be taken into account in future stages of this research aimed to understand the structural behaviour in response to possible stresses, such as those from local seismic activity.

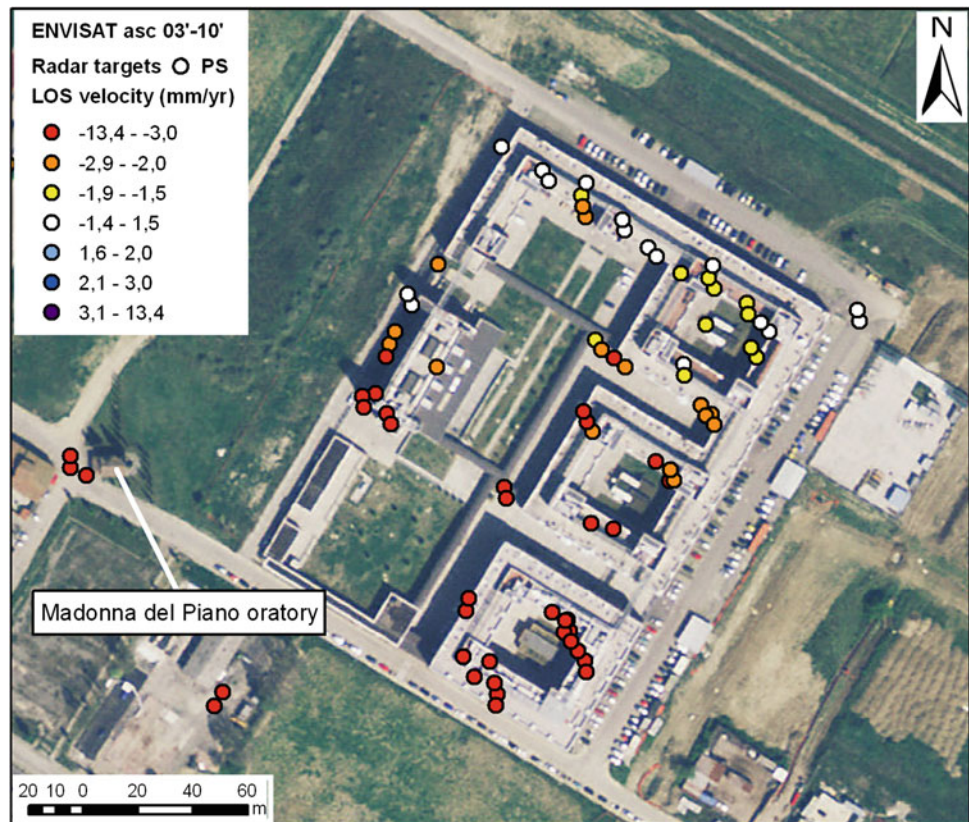


**Fig. 60.2** ENVISAT ascending average LOS displacement rates estimated over the Uffizi Gallery and Vasarian Corridor (*left*) and San Miniato Church complex (*right*) in Florence

A further proof of the instability processes currently active locally are the subsidence movements detected also in the surroundings of the CNR complex, with impacts that need to be verified. For instance, some downward moving

PS are detected within both ascending and descending ENVISAT imagery in the area of the small church of Madonna del Piano, a 17th-century building erected to protect a more ancient tabernacle (Fig. 60.3).

**Fig. 60.3** ENVISAT ascending average LOS displacement rates estimated over the CNR buildings in Sesto Fiorentino, Florence



## 60.4 Conclusions and Upcoming Research

The results of this PSI-based screening led us to cream off among the most important architectural and historical features of Florence, as well as the main new buildings and complexes in the Florentine suburban areas. These case studies will be subsequently reported to proper simplified structural categories (the so-called ‘structural categorization’), prior to proceeding with computational modeling, characterization of dynamic and deformation properties of the monitored buildings, and assessment of the structural interaction with the foundation ground under certain external factors imposed (e.g. seismic waves and rate and direction of ground displacement to simulate earthquake and landslide events, respectively). At this preparatory stage, the method of PSI-driven classification here illustrated makes the best out of the PSI technique and deals suitably with the typical limitations of PS datasets thereby demonstrating their exportability to other urban contexts and usability by conservators, building managers and local planning authorities.

## References

- Cigna F et al (2011) Advanced radar-interpretation of InSAR time series for mapping and characterization of geological processes. *Nat Hazards Earth Syst Sci* 11:865–881
- Cigna F et al (2012) Ground instability in the old town of Agrigento (Italy) depicted by on-site investigations and Persistent Scatterers data. *Nat Hazards Earth Syst Sci* 12:3589–3603
- Fanti R (2006) Slope instability of San Miniato hill (Florence, Italy): possible deformation patterns. *Landslides* 3:323–330
- Spizzichino D et al (2013) Cultural Heritage exposed to landslide and flood risk in Italy. *Geophysical research abstracts*, Vol 15, EGU2013-11081, EGU General Assembly 2013
- Tapete D, Cigna F (2012) Rapid mapping and deformation analysis over cultural heritage and rural sites based on Persistent Scatterer Interferometry, vol 2012, Article ID 618609, 19 p, 2012
- Tapete D et al (2012) Satellite radar interferometry for monitoring and early-stage warning of structural instability in archaeological sites. *J Geophys Eng* 9:S10–S25
- Tapete D et al (2013) Integrating radar and laser-based remote sensing techniques for monitoring structural deformation of archaeological monuments. *J Archaeol Sci* 40(1):176–189
- Trigila A et al (2011) Cultural heritage, landslide risk and remote sensing in Italy. In: Catani F, Margottini C, Trigila A, Iadanza C (eds) 2011. *The second world landslide forum—abstract book*, 3–9 Oct 2011, FAO, Rome, Italy, ISPRA, WLF2-2011-0397, p 603

---

# Documentation, Digital Survey and Protection for a Multidisciplinary Knowledge of Some Urban Historic Landscape in Italy

# 61

Alessandro De Masi

---

## Abstract

The introduction of digital 3D modeling in the field of Cultural Heritage enables the use of models as an interface to share and visualize information collected in databases with web-based tools. CyberCity generates 3D city models semi-automatically from stereo aerial images or laser scanner data with specialized software CyberCity-Modeler that provides easy use of texturing of facades with both terrestrial and aerial images. Moreover, the laser scanner with the software Gexcel JRC 3D Reconstructor, and the photo-scanning systems (ZScan and the Z-Map Laser Mencilsoftware) have provided a detailed picture of the cityscape; associated then the scanner with photo-scanning techniques, extremely precised orthophotos are implemented in a timely manner considered unimaginable with classical photogrammetric processes. With the integration of all the techniques used, a 3D model with a relevant rich database of information was obtained. It ensures today a proper preservation of the monuments, and an understanding of their evolution within the urban environment for the future, because of the various economic incentives.

---

## Keywords

Districts • Digital 3D modeling • 3D survey • Gexcel JRC 3D reconstructor • Photo-scanning systems

---

## 61.1 Introduction and Objectives

The Urban Landscape of the Historical Italian cities has a very complex structure because of its cultural, technological and representative values, and therefore the techniques of laser detection and software, as well as the integrated use of these systems, provide a complex and a challenging vision of the environment. Also, these systems serve to define the processes of maintaining the historic urban landscape. The scope of the research consists in a net of territory cultural and information technology districts, identified by “characterizing

aggregation systems” (urban, rural-manufacturing, rural-cultural and landscape-environmental-cultural), a competences network and a Knowledge-network in tune with a strategic vision of the new planning of the urban anthropic. This research focuses on Milan urban landscape and its most significant neoclassical architectural buildings. In Milan, the areas populated by the neoclassical buildings represent a territorial dimension of great importance due to the special architectural values of the sites. The nineteenth-century city of the enlightened Milanese bourgeoisie, at the time, was conceived as a place for experimenting with the social culture, with the evolution of the spirit and of the science according to the Enlightenment principles and the extraordinary vision of the French culture embodied in Diderot’s Encyclopedia. These motivations above all have led the author of this study to choose laser detection and software with innovative technological systems as modelling technologies—CyberCity 3D—use as his tools of investigation, being both compatible with

---

A. De Masi (✉)  
Department of Architecture, Built Environment and Construction  
Engineering (ABC), Milan Polytechnic - II School of Architecture,  
Via Durando 10, 20158 Milan, Italy  
e-mail: alessandro.demasi@unina.it

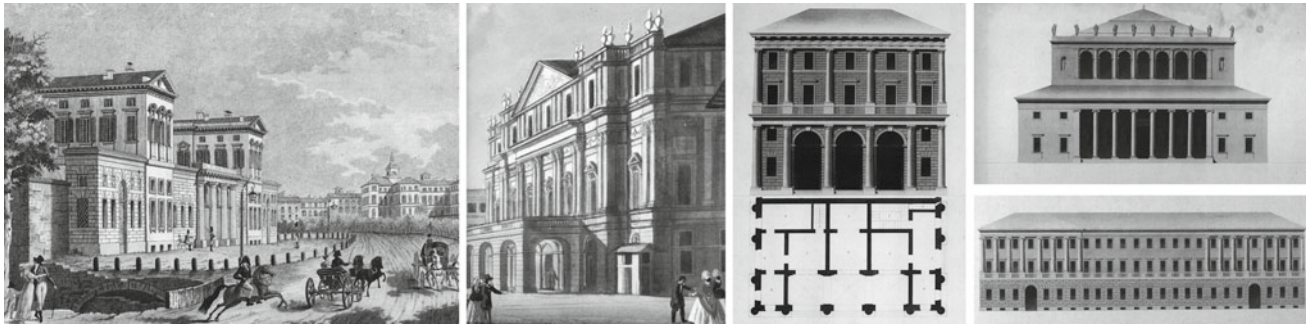


**Fig. 61.1** From *left*, Villa Belgiojoso Bonaparte today Villa Reale—Milan, Teatro alla Scala incision, Milan, L. Cagnola project for the bridge of Porta Ticinese 1801, L. C. Palazzo dei giardini pubblici,

1810, L. C. project for Palazzo Arese 1810—Civica Raccolta delle Stampe Bertarelli, Milan (Italy)

the neoclassicism's top priority of creating architectural models sans optical deformations. In fact, with laser technology we can obtain a precise image of the historical buildings and of their surrounding areas, and a punctual report on the preservation state of the nineteenth-century architectural heritage. Moreover, the digital 3D modelling enables the use of models as an interface to share and visualizes information collected in databases with web-based tools. This is order to disseminate and share the collected data with other research institutions and scholars using remote access. At the same time, the combined use of softwares reduces time-consuming operations for the detection and eliminates unnecessary components in the cloud of points of the following data processing stage. The most relevant engineer-architects for this study are undoubtedly Simone Cantoni, Giacomo Quarenghi, Leopold Pollak, the Abbot Joseph Zanoja and especially Luigi Canonica and Luigi Cagnola. Their most significant works (whose drawings of the Passaggio Centrale in Armorari Street and Politecnico di Milano in Leonardo Place are reported in this research) cannot be studied apart from the schools in which they served as professors, specifically named polytechnics (Fig. 61.1).

## 61.2 Line of Research Methodology

From the methodological point of view, the research was articulated according to: (1) Program of Digital Representation of the architecture and the urban landscape consisting of a set of cultural, geometric, morphological and dimensional knowledge for the formation of a digital 3D model all implementable with multidisciplinary themes; (2) human semiology, natural and absolute views of the territory to identify new forms of visibility and accessibility of the sites; (3) definition of territorial macro-areas and micro-areas having a landscape value resulting from territorial dynamics, to establish a cultural and managerial presence interfacing with technical Institutions, cultural Institutions, Universities;

(4) levels of sensitivity (trend threshold) of anthropogenic territories to encourage the process of interchange between urban systems on the territory (e.g. cultural-tourist-archaeological, urban system, manufacturing system and landscaping) that occur in fixed points known as “critical” within the neoclassical urban environments, and which are or may become characterizing places of attraction (De Masi 2012).

### 61.2.1 3D Survey and the Program of Digital Representation for District Areas

The Program of Digital Representation promotes the representation of district areas understood as homogeneous areas from the standpoint of historical and cultural awareness and to identify new ways of visibility and usability of sites with innovative technological systems as modelling technologies, CyberCity 3D. The use of these programs also allows the analysis of the buildings through techniques of 3D Surveying, Photo-Scanning Systems. My goal is to obtain models “complex” of the territory and urban architecture relevant to international culture. Aspects of the evolution of the cultural landscape can be documented and represented by the combined use of laser scanner (ground and airborne) and techniques of photo-scanning (ZScan and Z-Map Menci software) through the use of specialized software the latest generation of which the CyberCity-Modeler generates 3D models of the landscape, both natural and urban. For visualization uses software for the geometry and the texture of the objects photographed. These data are then managed by a final software which disposes of all the enormity of the data collected to properly display the pattern that is developing. It was preferred the combined use of FARO Scene 4.8 and Gexcel JRC 3D Reconstructor softwares. The FARO Scene software allows to compare two scans of the same structure in which the magnitude of the displacements of the structure, the filtering and the interpolation from point clouds to polynomial curves are reported. This leads to a

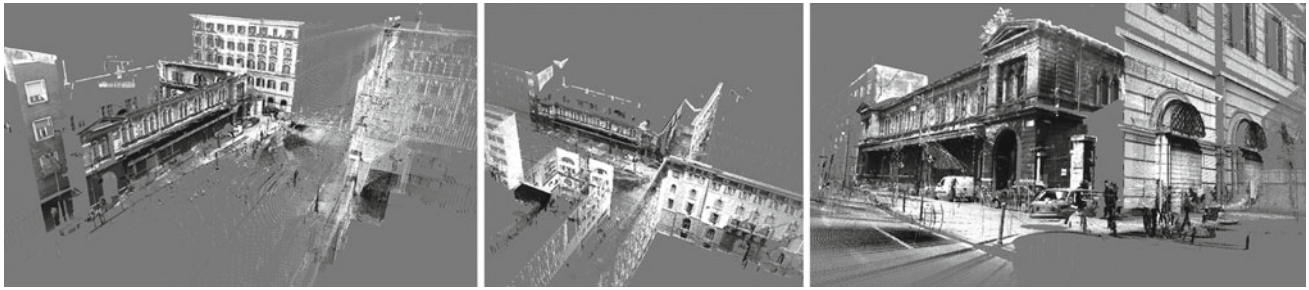


**Fig. 61.2** Instrumental survey of the building with the laser scanner FARO Photon 120 and 3D IMAGER 5006

simplification of point clouds with a considerable reduction in computation times as millions of 3D points are processed in systems of equations controlled by a few variables that represent curves in 3D space. In the phase of data processing the numerical methods give different options both in the equations assembly and in the phase of post-processing through a huge amount of collected metric data. It was necessary to consider the issues relating to the alignment of each scan and to contain the error in a tolerance limit proportionated to that of the measuring instrument. The alignment of the scans occurred with the use of iterative algorithms which carry out an automatic search of all the homologous points by performing a spatial roto-translation, without change of scale, compared to the reference system of the adjacent scanning. The reconstruction of the surface of the studied object was carried out in order to generate an IMMerge triangulated model to be inspected with IMinspect

application. The survey returned a complete discrete model (point of clouds) and then a DSM model (triangular mesh) mapped with ortho-photos and digital photos from which you can obtain the geometries of the complex. The point of clouds are intended as a flexible tool and data base from which it is possible to extract different information at different times and in which each point has the same degree of precision (Fig. 61.2).

### 61.2.2 3D Modelling and Photo-Scanning Systems for Cultural Heritage

The construction of a 3D-RGB digital model, obtained by some digital images of a real model, makes possible to acquire not only geometric data but also chromatic and thematic data. Among the photogrammetric surveying techniques the

**Fig. 61.3** Digital photogrammetric straightening and drawings and models of Passaggio Centrale, Armorari Street 8—Milan

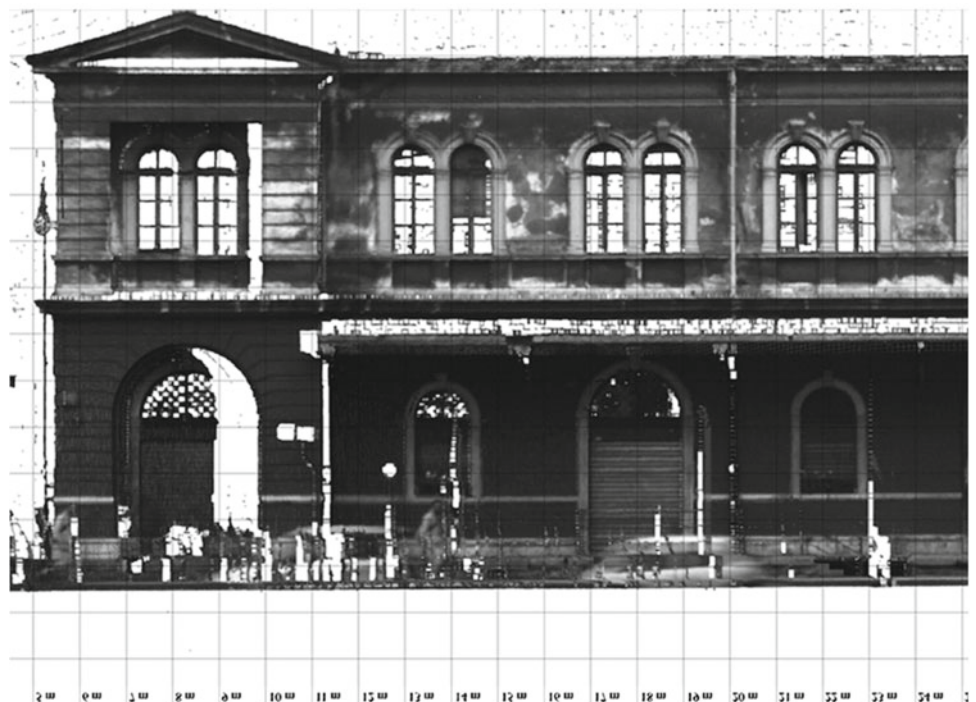




**Fig. 61.4** Drawings and models of Politecnico di Milano, Leonardo Place (Italy)

applications of three-dimensional acquisition systems, which allow the return of 3D models at high density of information, have become increasingly frequent and widespread (Ceccaroni 2008). The acquisition and importation of images allowed us to discretize the detected object in a finite number of pixels with specific algorithms, representative of a similar type of perspective transformation. The data acquisition phase with ZScan was obtained by simultaneous acquisition of point of clouds and “photo-scanning” textures based on an algorithm of tri-multifocal analysis of the image. The latter, using coloured point of clouds, sees the images as input of information being metrically and chromatically valid in 3D coordinates of the points. The resulting models were exported for the subsequent phases of editing and generation of plans, sections, profiles, contour lines, up to Digital Elevation Model (DEM). The ability to process and filter the clouds of points with the images shows a further step towards the analysis of the degradation of the materials on monuments. The colorimetric information is a very valuable representation in both the stages of diagnosis and monitoring. The mapping of

several images of the scanned architecture, even at different times of the day, allows the assessment of conditions that are completely hidden from the mere visual inspection (Carbognara 2008). The use of multi-level images, obtained with overlapped colored filters, can return as a photometric light curve resulted from the amount of absorbed light. This is a procedure to represent the reflectance values derived from the scans with altered colors. Furthermore, the use of the Z-Map Laser has allowed the alignment of the various clouds, the correction of errors, the generation of the orthophotos and the subsequent and possible vectorization (Figs. 61.3 and 61.4).

### 61.2.3 Reality-Based 3D CyberCity-Modeler

CyberCity 3D models generate urban landscape semi-automatic aerial images or using data taken from laser scanners and photogrammetry that are developed through a specific software CyberCity-Modeler (CC-Modeler™). With CC-Modeler the points which define the shape of the roof of the

building (x, y, z), from a scan area, are measured on workstation of photogrammetry. The points are labeled as points of perimeter or interior points concerning the conformation of the roof. Therefore, the CC-Modeler software will automatically convert the point cloud that has implemented and is assigned as the external points (perimeter) or as internal points with exceptional accuracy 0.1–0.2 m. The geometric shapes of the buildings as well as the structure of roofs and roofing are automatically generated using LIDAR data. The data collected by the software CyberCity-Modeler are displayed with the CAD model and the software CC-Edit is possible to display correctly the geometry of the models. The displaying oblique images of facades for large 3D City Models, obtained from scanning the air, can be through a composition of synthesis between images taken from the ground. These will be included adapting the polygon facade oblique through the 3D model in CC-Mapping and attention being given to the digitization of corner points in the image of the facade. Moreover, CC-Star is a visual digital photogrammetric station, which was developed specifically for the 3D modeling of cities. CC-visual Stella also offers standard features such as orientation photogrammetric stereo-model, the measure automatic and semi-automatic aerial triangulation, DTM and DSM, orthophoto mosaic of calculation. For the update of 3D models, the current City of the 3D model is imported from a GIS database or file system and is displayed along with the model stereo antenna. This means that the historical pattern of the city overlaps with the new information and image differences and changes are immediately visible. The management of all the recovered data in the database of information retrieved are generally handled by the ESRI which contains the two systems based on ArcSDE and Arc GIS. Therefore, the real-time visualization of urban landscape, can be done by exporting the data as Open Format Flight (FLT), respecting the level of detail (LOD) for the geometry and textures. Indeed, the visualization system called TerrainView™ (ViewTec AG), which includes sophisticated features for real-time visualization of 3D of information and provides many features for a vision purified by foreign elements, allows Web-streaming models of cities to high speed.

### 61.3 Results and Conclusion

In this paper different approaches to the acquisition and visualisation of 3D information from images have been examined. The Milanese neoclassical environment has a very complex structure because of its cultural, technological and representative values, and therefore the research methodology with the Program of Digital Representation of the architecture and the urban landscape show the potential of modern technologies of detection for digitally document and preserve our Cultural Heritage, as well as share and manage

them. Moreover, provide a complex and a challenging vision of the landscape of this historical period. The need to investigate the territory by identifying “characterizing aggregation systems” and their exchanges with nature and the anthropic reality allows to stress the physiographic systems of the “Territorial Areas”, opposite to the smaller “territorial districts”. The construction of “sensitivity levels” (De Masi 2009) of the macro (historic areas) or micro-areas (district) is the final process of articulation of urban and peri-urban landscapes, and depends on the items listed in the methodological lines of the research. The knowledge of the “sensitivity levels” with which the production, cultural and infrastructure systems—existing within Districts or Multi-district Areas—interact both among themselves and with the neighbouring territory to verify or to promote a steady relationship with the modern town planning (infrastructure and housing planning) and compare it with the historical, landscape and archaeological culture of the sites. The level of sensitivity depends on the specificity of the exchange on which the territorial dominant features related to biodiversity and landscape are also shown according to quality and quantity of items being present in the process of exchange between social environment and territory. This process determines a development of the district and its connections with the emergencies on the territory. Moreover, the Program of Digital Representation promotes the representation of district areas understood as homogeneous areas from the standpoint of historical and cultural awareness and to identify new ways of visibility and usability of sites with innovative technological systems as modelling technologies, CyberCity 3D. With the integration of all the techniques used a 3D model with a relevant rich database of information was obtained. The scanning technique and its application appears extremely appealing not only in terms of acquisition of metric data, but also in respect to the representation, the display of architectural objects and their contextualization in the territory. The 3D scanners ensures today a proper preservation of the monuments, and an understanding of their evolution within the urban environment for the future, because of the various economic incentives. In addition, the 3D laser scanner returns three-dimensional models “inspected” with a *continuous*, acquisition, which highlights a cloud of points evenly distributed over the geometric model. The digital 3D modelling enables the use of models as an interface to share and visualizes information collected in databases with web-based tools. This is order to disseminate and share the collected data with other research institutions and scholars using remote access. At the same time, the combined use of softwares reduces time-consuming operations for the detection and eliminates unnecessary components in the cloud of points of the following data processing stage. The image-based modeling approach is still the most complete, flexible and widely used for large sites with

integration of range sensors. It can produce accurate and realistic-looking models, even in some cases comparable to models resulting from laser scanning. Many of the problems of converting a measured point cloud into a realistic 3D polygonal model that can satisfy high modelling and visualisation demands have not been completely solved.

---

## References

- Baltsavias E (1999) Airbone lase scanning: existing systems and firm and other resources. *ISPRS J Photogram Remote Sens* 54:2–3
- Bartolucci D (2009) Principi di laser scanning 3D: hardware, metodologie applicative, esempi. Dario Flaccovio, Palermo
- Biagini C (2002) Information technology ed automazione del progetto. Firenze University Press, Firenze
- Birn J (2006) Digital lighting and rendering. New Riders, Berkley
- Brovelli MA, Cannata M (2002) DTM recostruction in urban areas from airborne laser scanner data: the method and the example of the town of Pavia (Italy). *Int Arch Photogram Remote Sens* 24:43–48
- Ceccaroni F (2008) Zscan: generazione di modelli 3D per la ricognizione metrica e radiometrica dei beni culturali tramite immagini. In AA.VV. Atti della III Conferenza ASITA, Napoli
- Celona T, Mariani Travi EeL (1983) Scrittori e architetti nella Milano napoleonica. Provincia di Milano, Amilcare Pizzi S.p.A. – arti grafiche
- Crosilla F, Galetto R (2003) La tecnica del laser scanning. Teoria ed applicazioni, CISM, Udine
- De Masi A (2009) Governance of new landscape (vol. 2). In: Abstract, Forum UNESCO, University and Heritage, 12th International Seminar “Historic urban landscapes: a new concept? A new category of world heritage sites?”. Hanoi, The Socialist Republic of Viet Nam (Vietnam)
- De Masi A (2012) Visibility, recognition and integrated digital survey for interpretation and promotion of the architectural heritage (vol. 2). In: Heritage 2012 Proceedings of 3 international conference world heritage and sustainable development, Porto, Portugal
- Guidi G, Russo M, Beraldin JA (2010) Acquisizione 3D e modellazione poligonale. Mc Graw-Hill, Milano
- Muller F, Zeng G, Wonka P, Van Gool L (2007) Image-based procedural modelling of facades. In: Proceedings SIGGRAPH, ACM Transaction on graphic
- Sacerdote F, Tucci G (2007) Sistemi a scansione per l’architettura e il territorio, Alinea Firenze
- Salvadori F (2002) Three dimensional scanning techniques applied to 3D modelling of pottery find Wien. In: Proceedings in workshop 7 archaologie and computer
- Vassena G, Sgrenzaroli M (2007) Tecniche di rilevamento tridimensionale tramite laser scanner

# Analysis of Rockfall Individual Risk at the Feifeng Underground Caves (Zhejiang Province, China) by Using 2D and 3D Runout Models

X.L. Wang, L.Q. Zhang, P. Frattini, S. Lari, G.B. Crosta, and F. Agliardi

## Abstract

The Feifeng Mountain tourist resort is famous for the ancient caves and drifting activities along the Yongan River. Because of steep slope, lithology (tuff overlying a thick soft layer), tectonic structure, and the underground excavation in ancient times, the area is seriously affected by rockfalls. A quantitative rockfall individual risk assessment has been performed, by using either a 2D and a 3D modelling approach. The 2D approach results in an overestimation of risk along the a priori defined paths, due to the impossibility to consider lateral spread of rockfall trajectories. The 3D approach allows for simulating the lateral dispersion and the trajectories along convergent topography, locally increasing the Individual Risk level.

## Keywords

Rockfall • Tuff • Individual risk • China • 2D and 3D simulation • Hy-Stone

## 62.1 Study Area

The large underground quarry of Feifeng Mountain (Fig. 62.1), in Zhejiang Province, eastern of China, were formed by excavating (areal extent 30,000 m<sup>2</sup>), the tuffaceous rocks to be used as building stone in the ancient China. The southern slope of the Feifeng Mountain is composed of Upper Jurassic cineretic tuff, intercalated by a soft 15 m muddy-siltstone layer. Three main faults control the structural setting of Feifeng Mountain: a thrust-compressional

fault (75°/300° of dip and dip direction respectively); a NW fault, 80°/210°; and a EW subvertical fault nearest to Feifeng Mountain.

Engineering geological properties of the tuff were analysed by in situ rock mass characterization and laboratory tests (according to ISRM 2007) (Table 62.1). A reduction of uniaxial compressive strength due to saturation has been observed, up to 15 %.

Rock mass is intensely jointed, and discontinuity persistence ranges between 2 and 15 m, and the aperture is tight to open (from 1 mm to 10 cm), sometimes with clay infilling. Discontinuity spacing shows an exponential distribution with a mean value of 1.34 m (Fig. 62.2). The joint surfaces can be classified as planar-rough and undulated-rough, according to ISRM recommendations. Groundwater seepage was observed through some of the discontinuities.

The discontinuity among the rock mass has significant influence on the stability of blocks. The rock mass was characterized by identifying 57 daylighting discontinuity planes using Terrestrial Laser Scanner point cloud and the software COLTOP 3D (Jaboyedoff et al. 2004). Discontinuities cluster in five main sets (Fig. 62.2) statistically characterized in terms of their mean vector orientations and dispersion (2 and 3 standard deviations, according to Priest).

X.L. Wang (✉) · L.Q. Zhang  
Key Laboratory of Engineering Geomechanics, Institute of  
Geology and Geophysics, Chinese Academy of Sciences,  
Beijing 100029, China  
e-mail: wxljl@163.com

P. Frattini · S. Lari · G.B. Crosta · F. Agliardi  
Department of Geological and Environmental Sciences,  
University of Milano-Bicocca, Piazza della Scienza 4,  
20126 Milan, Italy

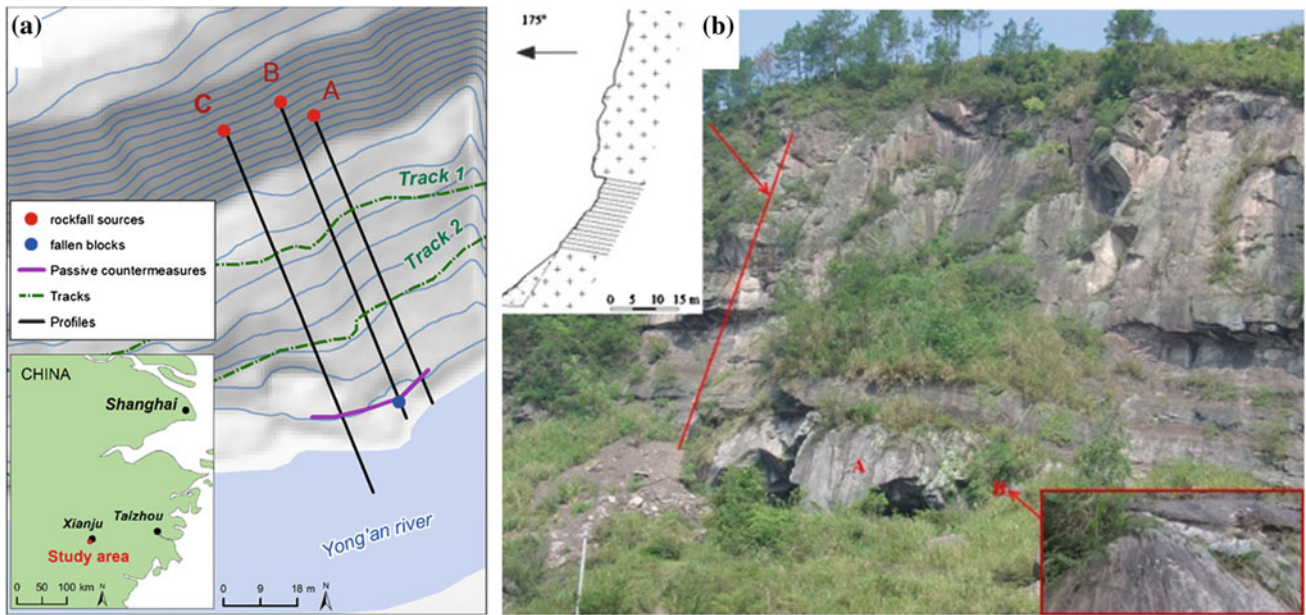


**Fig. 62.1** a The Feifeng Mountain study area, with identified unstable blocks A, B, and C; b picture of the southern slope with a sketch and geological profile and an inset with the main fault (A and B)

**Table 62.1** Laboratory test results for tuff

Property	Value
Saturated unit weight (kg/m <sup>3</sup> )	2,187
Dry unit weight (kg/m <sup>3</sup> )	2,001
Cohesion (MPa)	14.2
Friction angle (°)	42
Water absorption in atmospheric pressure (weight %)	0.56
Dry uniaxial compressive strength (MPa)	74.5–104.5
Saturated uniaxial compressive strength (MPa)	73.2–89.2
Tensile strength (MPa)	8.2–11.8

It could be easily observed that the orientations of the three main joint sets (84°/314°, 67°/209° and 74°/358°) correspond with the orientations of the three faults.

### 62.1.1 Definition of the Initiation of Potential Rockfall

Rockfalls in Feifeng mountain are controlled by the combined action of many factors, including slope morphology, lithology, and the excavation of caves in ancient time. The EW trending fault contributed to shape a rocky cliff with

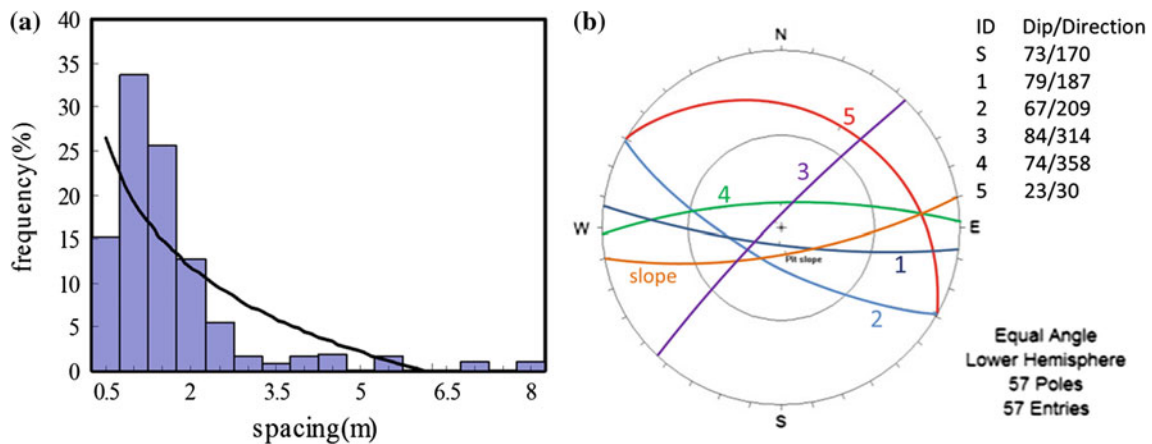


**Fig. 62.2** a Discontinuity spacing histogram and best fitting exponential distribution; b contour plot and great circles of the main discontinuities surveyed

slope gradients between  $73^\circ$  and  $85^\circ$ . The intense weathering of the muddy-siltstone layer produced vertical extensional discontinuities and under-excavation of the toe of the cliff, with the detachment of single blocks. The average height of each cave, excavated more than 700 years ago, exceeds 6 m, and generally the distances between pillars are among 30–40 m, leaving significant unsupported spans. Based on field investigations and on the stereographic technique, the stability of the rock mass on the slope was determined, and three main potential unstable blocks were found (the volume of block A, B, and C is 6.4, 2.7 and 22.7 m<sup>3</sup> respectively, more details could be found in the paper wrote by Wang et al. 2013) (Fig. 62.1).

## 62.2 Rockfall Individual Risk Assessment

Individual risk (IR) is defined, after Bottelberghs (2000), as the probability that an average unprotected person, permanently present at a certain location, is killed due to a rockfall:

$$IR = P_{(L)} \cdot P_{(T|L)} \cdot V \quad (61.1)$$

where  $P_{(L)}$  is the annual probability of occurrence of a rockfall (or, more generally, landslide, L) event in a given magnitude (i.e. volume) class;  $P_{(T|L)}$  is the probability for blocks related to a rockfall event to reach the exposed target, T (i.e. reach probability); V is the vulnerability (i.e. expected degree of loss) of a given exposed element.

The annual exceedance probability,  $P_{(L)}$ , was calculated, on the basis of the MCF curve starting from block volume data collected in the field (Wang et al. 2013). Values of 0.043, 0.072, and 0.019 were obtained for blocks A, B and C, respectively. For the assessment of vulnerability we assumed that the velocity of rockfall is too high for people to escape. Hence, vulnerability for walking people was defined as equal to 1 (e.g. all rockfall impacts on people result in death), and vulnerability for people sailing on the boats as 0.5, assuming that, in case of impact, only part of the boat would be destroyed. The reach probability for a location,  $P_{(T|L)}$ , is here evaluated as the ratio of the total number of blocks passing a specified location to the total number of blocks launched in the model (Agliardi et al. 2009). Runout distance, bounce height, kinetic velocity and reach probability of the three blocks A, B and C were simulated by means of

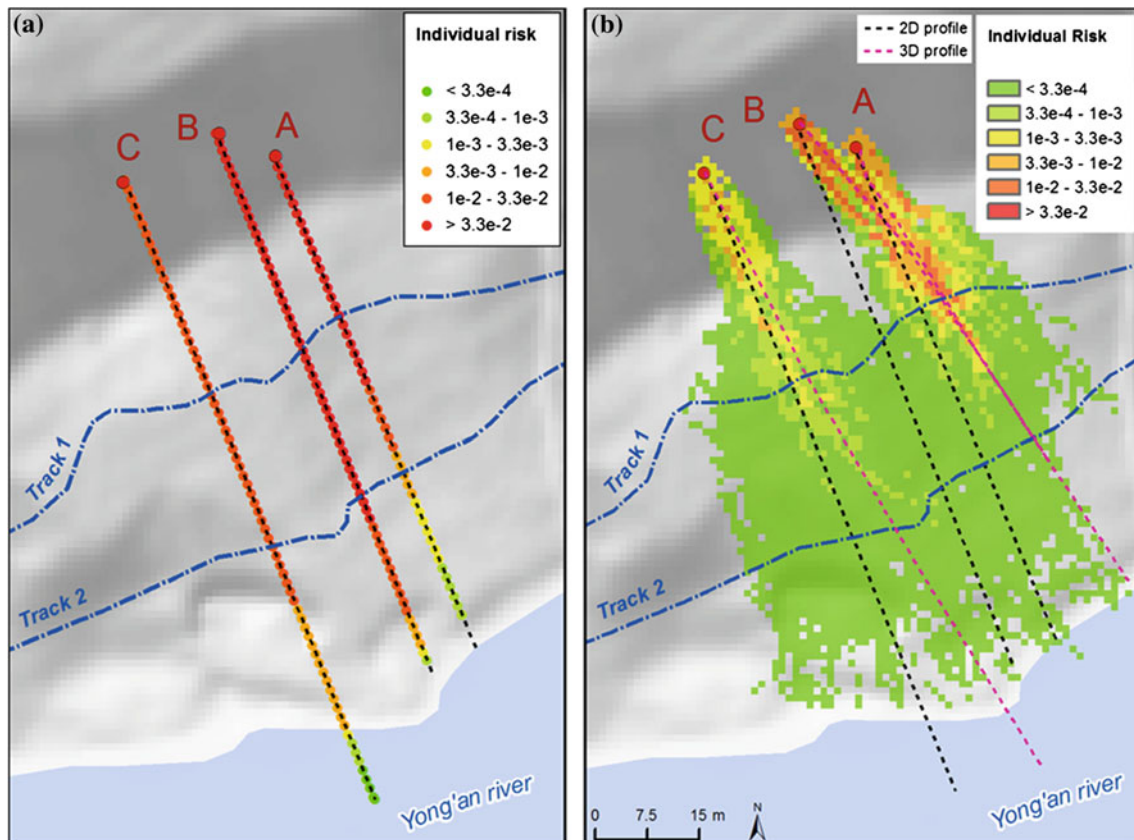
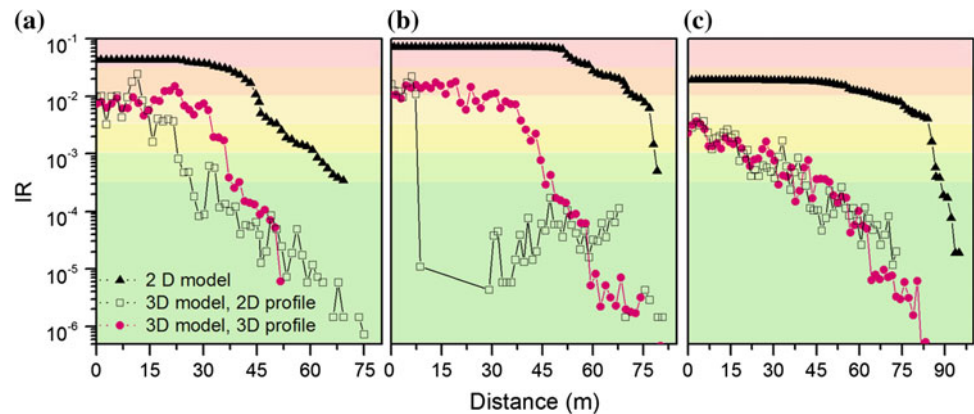


**Fig. 62.3** Individual risk for **a** 2D modelling and **b** 3D modelling

**Fig. 62.4** Individual risk values calculated by means of 2D and 3D models, sampled along 2D and 3D profiles (see Fig. 62.3)



2D and 3D codes. The 2D simulation, performed through Rockfall (Stevens 1998), provides values of block velocity and bounce height for any point along a predictive slope profile, and the locations of arrested blocks. Since the slope is steep and almost planar (i.e. its topography is neither significantly channelled nor convex), the use of 2D rockfall runout modelling is usually considered appropriate for local-scale analysis (Volkwein et al. 2011). However, 3D effects such as lateral dispersion are observed on planar slopes due to the effect of slope roughness and/or block shape (Crosta and Agliardi 2004). The 3D simulation was performed through HY-Stone (Crosta and Agliardi 2004; Frattini et al. 2012), which allows to simulate the motion of non-interacting rocky blocks in a three-dimensional framework, using a DEM to describe slope topography. It is based on a hybrid (mixed kinematic-dynamic) algorithm with different damping relationships available to simulate energy loss at impact or by rolling. Among the parameters used in both models, the morphology, the coefficients of restitution and friction are the most significant. The former was acquired on the field by using a Terrestrial Laser Scanner (TLS). The others by back-calibrating 2 historical rockfall events, and have been assigned to slope profiles of rockfall scenarios A, B and C (Figs. 62.3 and 62.4).

In the 2D modelling approach, the IR values are higher because the onset probability is entirely concentrated and propagated along the a priori defined profile. The 2D model approach does not account for the possibility that rockfall may follow different paths, showing lateral dispersion. In other words, the 2D modelling assumes that the a priori defined path is certain. This assumption leads to strong consequences on the risk calculation and makes the choice of the simulation paths extremely important.

The 3D modelling shows lower IR values because the lateral dispersion of trajectories reduces the probability to transit in a single cell. On the other side, this dispersion allows for superimposition of the trajectories in areas of slope convergence, locally increasing the Individual risk, as

observed for blocks A and B. Regarding dispersion, it has been shown that it depends on the surface roughness (Frattini et al. 2012) but also on the resolution and quality of the DEM (Crosta and Agliardi 2004). Hence, the quality of the DEM is fundamental for the IR calculation. This example also demonstrates that interpolation of IR values from 2D profiles can produce strong errors in the assessment and slope risk zonation.

**Acknowledgments** The authors would like to thank the support of China Postdoctoral Science Foundation (No. 2013M530722).

## References

- Agliardi F, Crosta GB, Frattini P (2009) Integrating rockfall risk assessment and countermeasure design by 3D modelling techniques. *Nat Hazards Earth Syst Sci* 9(4):1059–1073
- Bottelberghs PH (2000) Risk analysis and safety policy developments in the Netherlands. *J Hazard Mater* 71(1):59–84
- Crosta GB, Agliardi F (2004) Parametric evaluation of 3D dispersion of rockfall trajectories. *Nat Hazards Earth Syst Sci* 4(4):583–598
- Frattini P, Crosta GB, Agliardi F (2012) 22 Rockfall characterization and modeling. In: Clague JJ, Stead D (eds) *Landslides: types, mechanisms and modeling*, p 267
- ISRM (2007) Ulusay R, Hudson JA (eds) *The complete ISRM suggested methods for rock characterization, testing and monitoring: 1974–2006*. Kozan, Ankara
- Jaboyedoff M, Baillifard F, Couture R, Locat J, Locat P (2004) Toward preliminary hazard assessment using DEM topographic analysis and simple mechanic modeling. In: Lacerda WA, Ehrlich M, Fontoura AB, Sayo A (eds) *Landslides evaluation and stabilization*. Balkema, Rotterdam, pp 191–197
- Stevens W (1998). *Rockfall: a tool for probabilistic analysis, design of remedial measures and prediction of rockfalls*. M.A.Sc. Thesis, Department of Civil Engineering, University of Toronto, Ontario, Canada
- Volkwein A, Schellenberg K, Labiouse V, Agliardi F, Berger F, Bourrier F, Jaboyedoff M (2011) Rockfall characterisation and structural protection—a review. *Nat Hazards Earth Syst Sci* 11:2617–2651
- Wang XL, Frattini P, Crosta GB, Zhang LQ, Agliardi F, Lari S, Yang ZF (2013) Uncertainty assessment in quantitative rockfall risk assessment. *Landslides*. doi:10.1007/s10346-013-0447-8

# Rock Mass Instabilities in Tatlarin Underground City (Cappadocia-Turkey)

63

İsmail Dinçer, Ahmet Orhan, Paolo Frattini, and Giovanni B. Crosta

## Abstract

Cappadocia is one of the most important touristic sites in Turkey due to its spectacular and unique landforms, fairy chimneys, underground cities and historical heritages. Tatlarin underground city is one of the many rock-cut structures of Cappadocia. The Cappadocia Region mainly consists of Pre-Miocene basement rocks, Lower Miocene sedimentary rocks, Miocene volcano-sedimentary unit and Quaternary volcanic rocks. The underground city was built in slope consist of Miocene Tuff and it was generally threatened by rock mass instabilities. The most commonly observed stability problem at Tatlarin Underground City and its vicinity is the fall of rock blocks from the basalt outcrops. Potential rockfalls have been simulated by using the 3D model HY-STONE to recognize the most critical sectors and to provide a support for long-term urban planning and cultural heritage protection.

## Keywords

Rockfall • Tuff • Basalt • Cappadocia • 3D simulation

## 63.1 Introduction

The natural, historical and cultural heritages are seriously threatened by rock mass instabilities in Cappadocia (Turkey). Tatlarin underground city is one of the many rock-cut structures of Cappadocia. It is located approximately 35 km west of “Göreme National Park and the Rock Sites of Cappadocia” which has been included to the Word Heritage List by UNESCO in 1985. In the region, this city is not popular like others, and it was opened to visitors in 1991. It was caved during the Roman and Byzantine times, and is

separated from the other underground cities with designed toilets in the structure. The historical heritage and its vicinity are seriously threatened by rock mass instabilities as well as many historical heritages in Cappadocia. Most of the underground structures and fairly chimneys are found near or on rock slopes consisting of tuffs and/or ignimbrites.

Engineering geological problems related to rock mass instabilities of historical heritages in Cappadocia have been investigated by many researchers (Doyuran 1976; Topal and Doyuran 1997; Aydan and Ulusay 2003; Ulusay et al. 2006; Tunusluoğlu and Zorlu 2009; Zorlu et al. 2011). The Cappadocia Region mainly consists of Pre-Miocene basement rocks, Lower Miocene sedimentary rocks (red mudstone, sandstone, and conglomerates), Miocene volcano-sedimentary unit (Ürgüp Formation) and volcanic rocks (ignimbrite, andesite and basalt) of Neogene-Quaternary period (Temel et al. 1998) (Fig. 63.1). The Ürgüp Formation has widespread in the region and unconformably overlies the Yeşilhisar formation.

İ. Dinçer · A. Orhan  
Engineering Architecture Faculty, Geological Engineering  
Department, Nevşehir University, 50300 Nevşehir, Turkey

P. Frattini (✉) · G.B. Crosta  
Department of Earth and Environmental Sciences, University  
of Milano-Bicocca, Piazza della Scienza 4, 20126 Milan, Italy  
e-mail: paolo.frattini@unimib.it

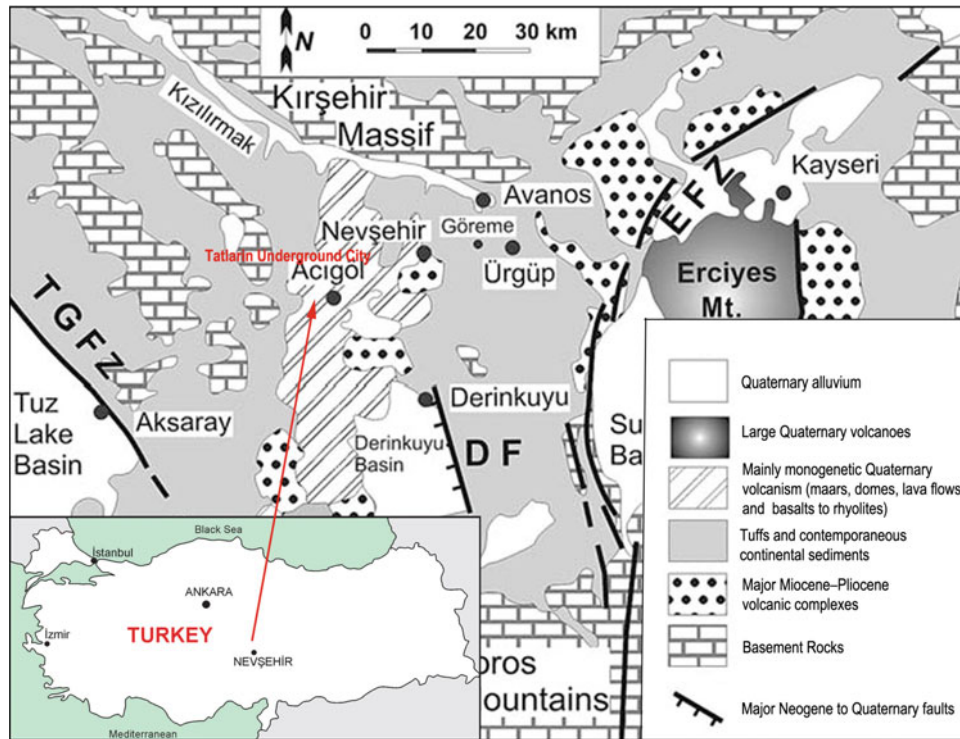


**Fig. 63.1** Cappadocia geological map (Ulusay et al. 2006; Temel et al. 1998; Le Pennec et al. 1994)

A big part of the underground structures and fairly chimneys are located in this unit (Aydan and Ulusay 2003). Ürgüp formation is intensively observed in the Tatlarin Underground City and its vicinity. In the study area four different tuff levels, which are belonging to Ürgüp formation, are observed.

These are, from bottom to top, reddish poor welded tuff, yellowish–grey tuff, sandstone–claystone alternations and welded beige tuff. Big parts of Tatlarin underground city are mostly caved within the welded beige colored tuff (Fig. 63.2). These units, are overlain by Quaternary reddish–black basalts. The massive basalts comprise intense cooling cracks and the upper parts represent a porous structure. The thickness of the high strength basalts varies between 10 and 15 m.

## 63.2 Engineering Geological Conditions

In order to evaluate the hazard against to rock mass instabilities, a detailed engineering geological mapping of Tatlarin Underground City and its vicinity was carried out. The underground city was caved in slope consist of Miocene–Pliocene tuff and it was generally threatened by rock mass instabilities such as rock fall. Recently a big rock fall, which is approximately 45 m<sup>3</sup>, occurred at the October 28, 2011, damaging the access roads and menacing residential

buildings (Fig. 63.2a). In the past, a number of rockfalls have damaged the underground city (Fig. 63.2a, d), as witnessed by numerous blocks (different volume).

The rock mass characterization has a primer importance on the stability of the underground structures and rock slopes. Therefore, detailed scan line surveying including all rock units (basalts and tuffs), was carried out at the study area for the evaluation of discontinuities properties. Joints were the main discontinuity type observed in basalts and tuffs. Both basalts and tuff are intersected by five main sub-vertical joint sets (Fig. 63.3).

In some places, joints are parallel to slope direction and they can be observed as the rock slope in tuff. The spacing of the joints in the tuffs and basalts varies from 0.20 to 2.30 m. Joints surface are classified as planar-rough and undulated-rough. The JRC was estimated from the roughness profiles by comparing them with the joint surfaces in the tuffs, and ranges from 8 to 12. Schmidt Hardness of basalts and tuffs are 42 and 19 in average, respectively. The values of JCS were obtained from the Schmidt hammer tests (mean JCS is 20 for Tuff and 80 for basalts). While the mean unit weight of the tuff varies from 11.20 to 15.40 kN/m<sup>3</sup>, mean unit weight of the basalts is 25.40 kN/m<sup>3</sup>. The basic friction angle of tuffs observed in the Cappadocia Region is determined as 30° by Ulusay et al. (2006) for saw-cut smooth rock surfaces.



**Fig. 63.2** General views of the slope with unstable basalt layer (a) and Tatlarin Underground City (b)

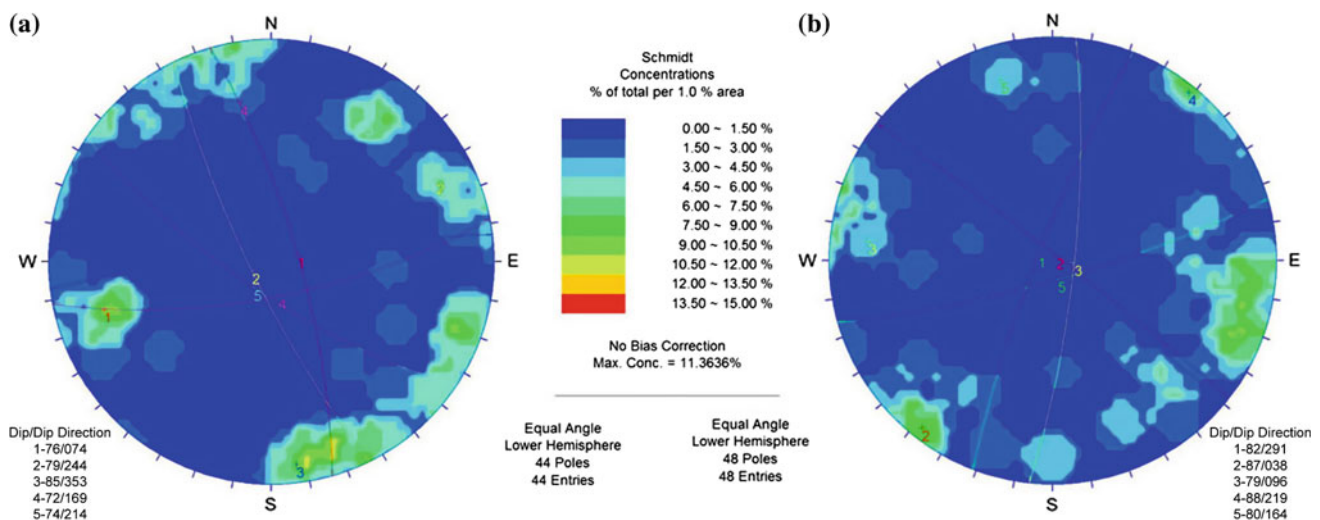


**Fig. 63.3** Contour diagrams of the main discontinuities in the basalts (a) and tuffs (b)

### 63.3 3D Rockfall Simulation

Rockfall behavior along the slope was simulated with the 3D simulation model HY-STONE (Crosta et al. 2004; Frattini et al. 2012) that allows simulating the motion of blocks in a three-dimensional framework, using a DEM to describe slope topography. The code is based on a hybrid algorithm with different damping relationships to simulate energy loss at impact or by rolling. The stochastic nature of rockfall processes and the variability of parameters are introduced by randomly sampling most parameters from different probability density distributions. Rockfall model calibration was performed by back-simulating the 2011 rockfall event. By using the available 1:2000 photogrammetric topographic data, a 2 m gridded DEM was created. Due to the

smoothness of the topography, an unrealistically straight propagation of blocks was obtained, mainly due to rolling (Fig. 63.4a). For this reason, in areas characterized by coarse debris deposits, the DEM was improved by adding randomly generated blocks.

The simulation with this topography shows a more complex and realistic behavior, with significant lateral spreading (Fig. 63.4b). The improved topography has been used to simulate the future potential scenarios (Fig. 63.5). In the first scenario, 100 blocks were simulated from each unstable point recognized on field (Fig. 63.5a). This scenario represents the most likely scenario, and can be expected in the next years. It is only limited to a central portion of the area, without impact on the underground city. Considering as unstable all rocky cliffs steeper than  $50^\circ$ , a second

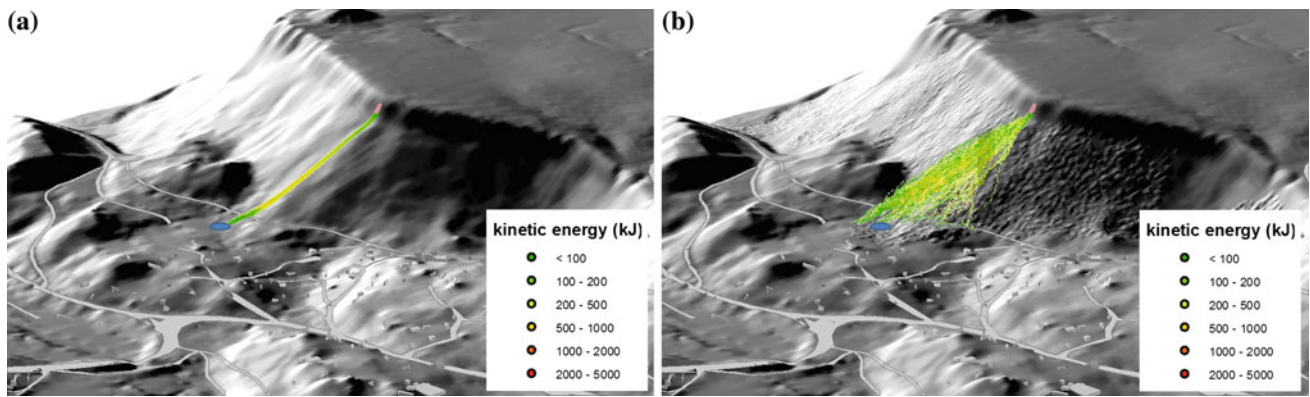


**Fig. 63.4** Back-calibration of October 28, 2011 rockfall event (see Fig. 63.2) showing the kinetic energy of blocks: **a** simulation with 1:2000 photogrammetric DEM; **b** simulation with DEM improved with random generated blocks in correspondence to coarse debris deposits

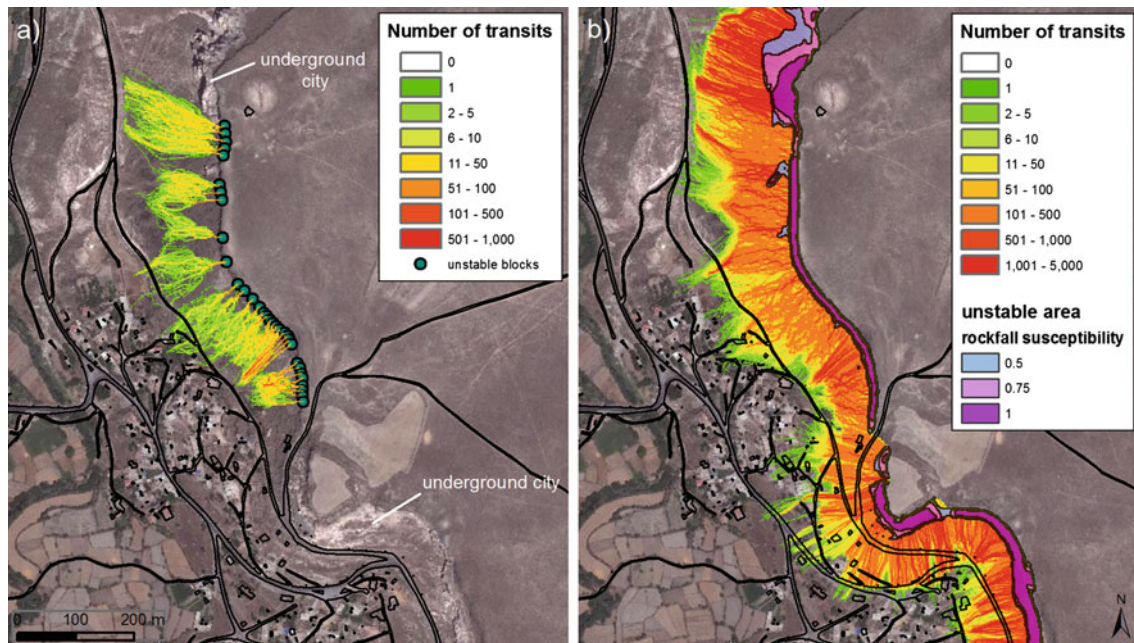


**Fig. 63.5** Results of potential future scenarios showing the number of blocks passing through each grid cell: **a** rockfalls from unstable blocks recognized on field. **b** rockfalls from rocky cliffs with slope gradient steeper than  $50^\circ$

scenario was simulated, launching 50 blocks from each unstable cell (Fig. 63.5b). In this scenario, an onset susceptibility as a function of slope gradient ( $0.5$  for cells between  $50^\circ$  and  $55^\circ$ ;  $0.75$  for cells between  $55^\circ$  and  $60^\circ$ ;  $1.0$  for cells steeper than  $65^\circ$ ) was considered and incorporated into the model. This scenario represents the worst-case low-probability scenario, which needs to be taken into account for long-term urban development and the risk management of the underground city tourist development.

## 63.4 Conclusion

Tatlarin underground city is one of the many rock-cut structures of Cappadocia. Although the archeological site is not frequently visited by tourist, a future development of tourism in this site could be important for both the conservation of cultural heritage and the economic development of the local community. As frequently happens in Cappadocia, the site is menaced by rockfalls that threaten the underground city

integrity and the safety of roads and track driving to the site. On site, geological and engineering geological survey, coupled with 3D rockfall simulation, allowed to recognize the potentially critical sectors of the area: the northern part of the village (Fig. 63.5a), being threaten by critically stable blocks that will likely fail in the next years; the entire eastern sector of the village; and the underground city, with a lower probability (Fig. 63.5b). For the future, a protection of the main access roads with barriers and embankments is fundamental, together with a careful review of the urban development plan of Tatlarin in order to avoid a further increase of risk. Regarding the underground city, it should be necessary to plan active mitigation structures on the cliff in order to avoid the onset of rockfalls.

## References

- Aydan Ö, Ulusay R (2003) Geotechnical and geo-environmental characteristics of man-made underground structures in Cappadocia, Turkey. *Eng Geol* 6:245–272
- Crosta GB, Agliardi F, Frattini P, Imposimato S (2004) A three-dimensional hybrid numerical model for rockfall simulation. *Geophys Res Abs* 6:04502
- Doyuran V (1976) Ortahisar'ın Çevresel Jeolojik Koşulları. *Türkiye Jeoloji Kurumu Bülteni* 19:83–88 (in Turkish)
- Frattini P, Crosta GB, Agliardi F (2012) Rockfall characterization and modeling. In: Clague JJ, Stead D (eds) *Landslides types, mechanisms and modeling*. Cambridge University Press, Cambridge, pp 267–281
- Le Pennec JL, Bourdier JL, Temel A, Camus G, Gourgaud A (1994) Neogene tuffs of Nevşehir plateau (Central Turkey): stratigraphy, distribution and source constrains. *J Volcanol Geotherm Res* 63: 59–87
- Temel A, Gündoğdu MN, Gourgaud A, Le Pennec JL (1998) Ignimbrites of Cappadocia (Central Anatolia, Turkey): petrology and geochemistry. *J Volcanol Geotherm Res* 88:447–471
- Topal T, Doyuran V (1997) Analysis of deterioration of the Cappadocian tuff. *Environ Geol* 34(1):5–20
- Tunusluoglu MC, Zorlu K (2009) Rockfall hazard assessment in a cultural and natural heritage (Ortahisar Castle, Cappadocia Turkey). *Environ Geol* 56:963–972
- Ulusay R, Gökçeoğlu C, Topal T, Sönmez H, Tuncay E, Ergüler ZA, Kasmer Ö (2006) Assessment of environmental and engineering geological problems for the possible re-use of an abandoned rock-hewn settlement in Ürgüp (Cappadocia), Turkey. *Environ Geol* 50:473–494
- Zorlu K, Tunusluoglu MC, Gorum T, Nefeslioglu HA, Yalcin A, Turer D, Gokceoglu C (2011) Landform effect on rockfall and hazard mapping in Cappadocia (Turkey). *Environ Earth Sci* 62: 1685–1693

---

**Part VII**

**Preservation of Cultural Heritage  
from Natural Hazards**

Zbigniew Bednarczyk

---

## Abstract

St. John of Dukla Chapel located in SE Poland in Beskidy Mountains is visited by tens of thousands of pilgrims from Poland and the world every year. Pope John Paul II also visited the Chapel several times. Unfortunately this unique place located on a flysch slope was seriously threatened by landslide hazard several times in 1998, 2000 and 2002. A very dangerous landslide, 400 m length 100 m wide was formed few meters under the chapel in 2004. Landslide was stabilized within the National Landslide Counteraction Framework (SOPO) Project in 2005. Remediation financed by the loan from the EIB Bank and state budget included slope stabilization by retaining wall built on micropiles foundation and surface and internal drainage systems. The main objective of the presented work was to control the stabilization works. Inclinometer measurements performed during 7 year time allowed observation of slope behavior. The remediation was effective, however small incremental deflections up to 2.5 mm were observed. These measurements due to the difficult soil conditions should be performed also in the next years.

---

## Keywords

Preservation • Cultural heritage • Landslide hazard • Monitoring

---

### 64.1 History of the Chapel

St. John of Dukla Chapel is located in SE Poland on a hill of Zaspit approximately 1.5 km from the village of Trzciana (Fig. 64.1). St. John of Dukla was a famous preacher and confessor, who, according to historical sources, was born in 1414 and led the life of a hermit in the surrounding forest. Around 1435, he joined the Franciscan Order and in 1463 the Bernardine Order. He became famous as a prominent preacher in Lviv, where he died in 1484. In 1769, he was officially beatified. In 1773, after the beatification of Saint John, Maria Amalia Mniszchow founded a chapel in the place where, according to tradition, St. John Hermitage was placed. The chapel was burned down twice, last time in

1883. The current chapel, preserved to the present day as a neo-Gothic brick building, was built in the years 1906–1908. Chapel was designed by Saint Bernard Father Camille Zarnowski. Historical paintings depicting the life of Blessed John painted by artist Wladyslaw Lisowski from Sanok are located on the walls inside the chapel. Next to the church a wooden house, called hermit's house, terrace, pilgrims house and artificial cave with spring water were located.

Pope John Paul II canonized St. John of Dukla in 1997 and now popular Pope's route passes through here. The water from a source at the Hermitage was considered miraculous.

---

### 64.2 Geological Conditions

Beskid Niski Mountains where the chapel was placed are built of flysch sedimentary rocks—mainly sandstones, shales and conglomerates in the Upper Cretaceous and Paleocene

---

Z. Bednarczyk (✉)  
Poltegor-Institute, Parkowa 25, 51-616 Wrocław, Poland  
e-mail: zbigniew.bednarczyk@igo.wroc.pl



**Fig. 64.1** Saint John of Dukla Chapel, interior and painting

Era. The Southern and western part of the so-called Magura Nappe pushed the Dukla Unit, which in turn raises the Silesian Unit. The most important formation of the Magura Nappe is Magura sandstones. Within the Dukla Unit high and sharp mountain ridges are formed by Cergowskie sandstones, whose highest peak, called Beskid Dukielski, is at an elevation of 759 m above sea level. Beskid Niski Mountains are characterized by one of highest landslide density in Poland (Starkel 1996). In this area there is one landslide for every one square kilometer of area (Raczkowski and Mrozek 2002). Dangerous mass movements are favoured by its steep slopes. Landslides often occurred in the frontal area of the Dukla Unit built of claystones, on the northern slopes of Cergowa Mountain and on the eastern slopes of the Mszana Mountain. Claystones in such a condition after being saturated with water become preferential slip surfaces for upper layers of sandstones. This type of processes was also observed in some parts of a hill of Zaspit where the Chapel is located. The first large

displacements near the Chapel were registered in Spring 1998 as a result of high precipitations. In Spring 2000 the edge of the landslide approached within a few meters to chapel entrance. Large mass movement activation occurred also in the Spring of 2002, but after then the movements were limited. In 2004 the earth significantly moved again, next to the existing landslides. After the Spring thaw, a landslide, 400 m long and 100 m wide, moved on a relatively steep slope ( $>20^\circ$ ) (Fig. 64.2). It moved dangerously close to the house of pilgrims (Figs. 64.3 and 64.4). Deep scratches were observed on this time on the walls and floor of the chapel of St. John. Cracks were also highlighted in the courtyard before entrance to the chapel. Right flank of the landslide edge approached within a few meters to the chapel entrance. In right part of the landslide crown, at the length of 4 m, the ground moved down by almost half a meter next to the existing landslides. Temporary remediation including retaining wall on pile foundation near the chapel and drainage works was realized in 2002.



**Fig. 64.2** Landslide crown near the Chapel



**Fig. 64.3** The Chapel and house of pilgrims, 2005



**Fig. 64.4** Initial phase of stabilization, 2006

### 64.3 Landslide Remediation

In 2005 the landslide was selected for stabilization realized inside the National Landslide Counteraction Framework Project (SOPO) Component A. Remediation works were financed by a loan from the European Investment Bank and from the Polish state budget. The investment on behalf of the Bernardine monastery, to which the chapel belongs, oversees the Community of Dukla. Design project was prepared by the Building Research Institute ITB Warsaw. It included drainage of the landslide area and construction of retaining wall on the micropiles foundation (Figs. 64.4 and 64.5). Micropiles were drilled to the depth of 10–12 m. Grouted-in-place micropiles were constructed from steel pipe diameter of 305 mm and cement grout. This technology had beneficial impact on slope stability conditions. The construction of retaining wall was founded on this type of foundation in stiffer geotechnical layers. Drainage system was built as a system of trenches filled by drainage stones and geo-textile collecting rainwater downhill. Renovation of the chapel included also building of retaining wall and the cave with two water intakes below the chapel. It contained repair of existing joints on the walls and building of temporary road to the chapel. All the stabilization works improved the stability conditions. The Bernardine order reported no additional movements near the chapel after the remediation works in 2006. However, this conclusion was based only on site inspection and it was unknown if remediation were sufficient enough, because the monitoring system was not implemented the stabilization.



**Fig. 64.5** Landslide after remediation works, 2009

### 64.4 Landslide Monitoring

The Carpathian Branch of the Polish Geological Survey in Krakow advised to check the stabilization works near the chapel by monitoring measurements. The author of this paper had an opportunity to install inclinometer and piezometer instrumentation near the chapel (Fig. 64.6). Instrumentation included typical monitoring devices as installed by the author at surrounding locations for 23 engineering geology site investigations inside SOPO Project (Bednarczyk 2008, 2012). Seventy millimeters ABS, grooved, quick joint casings were installed in the borehole near the chapel to a depth of 20 m to be sure to reach the bedrock formation. During this installation the adequate quality of cement-bentonite grout was paced into the borehole. The main groove direction A was oriented in the direction of slope inclination (Fig. 64.7). Measurements were performed using UK produced biaxial inclinometer probe. The inclinations of various points inside the casings was measured every 0.5 m in the direction of slope inclination and repeated after turning the probe at angle of 180°. In the first 4 years after stabilization 10 monitoring series were measured every year. In the last 2 years measurements were performed 2–4 times a year due to high travel costs. Totally 50 sets of monitoring measurements without official financing were realized. It was possible due to the others landslide projects conducted by the author in surrounding areas. The last measurement realized in June 2013 showed that incremental deflections in direction A (+) with the slope inclination varied from (–) 2.5 to (+) 1.7 mm.

**Fig. 64.6** Control measurements 2007–2013

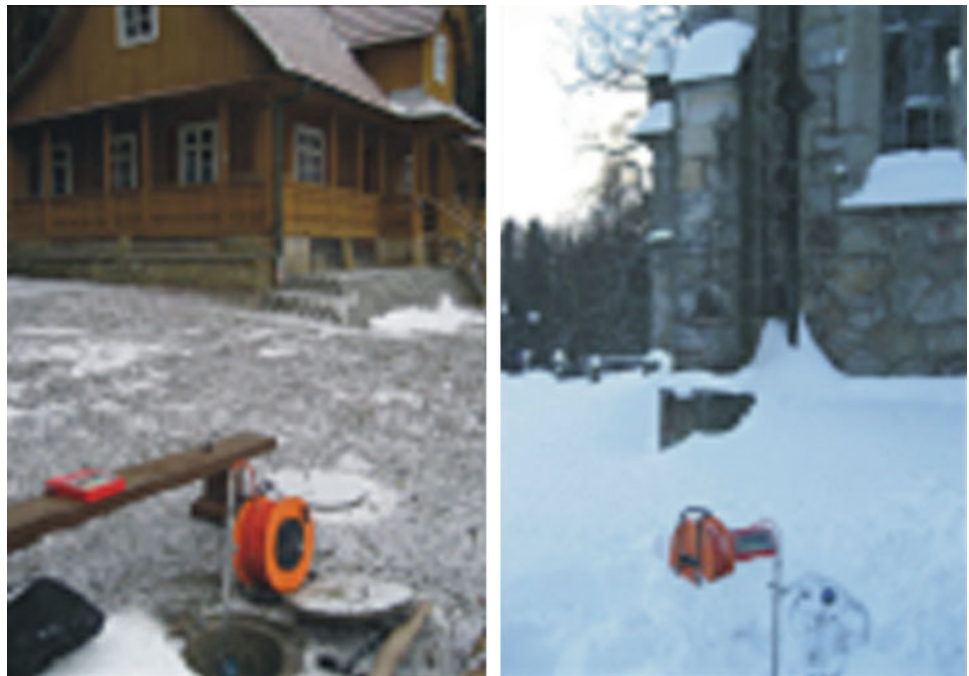
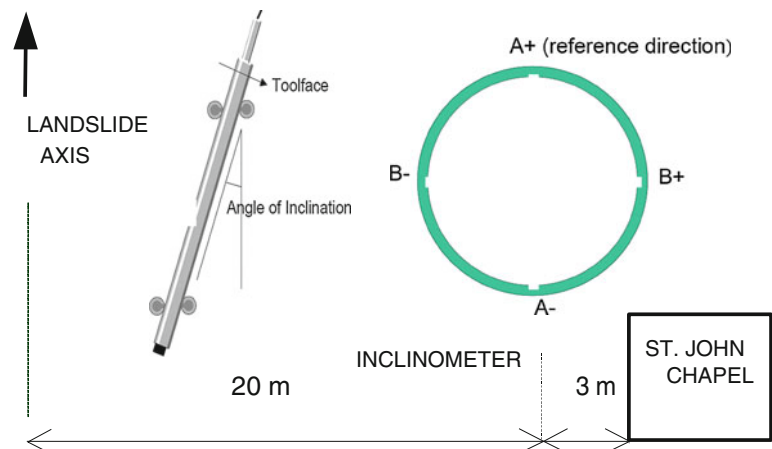


**Fig. 64.7** Directions of inclinometer measurements



In direction B (+) perpendicular to the slope inclination these varied from (–) 1 mm to (+) 0.1 mm (Fig. 64.8). The values of cumulated deflection were the highest at the relatively shallow depth of 1.3 m, where in direction of slope inclination, varied from (+) 10 to (–) 10 mm (Fig. 64.9). In the direction B—towards the landslide axis deflections reached 17 mm in 7 years time. The cumulated deflections indicated that movements of up to 6 mm occurred at depths of 14–16 m. However, the values of cumulated deflections are not fully representative because these could be used only as indicators of sliding body depth. Better characterization of mass movements at different depths was possible using

incremental displacements. The observed shear strains in direction of slope inclination A (+) were the highest below depth of 12 m (Fig. 64.10). In direction perpendicular to the slope inclination and landslide axis B (–) the cumulated displacements reached 4 mm to the depth of 5.8 m, 6 mm to the depth of 11.8 m and 7 mm below this depth (Fig. 64.11). The highest cumulative displacements were registered in years 2006–2007. In years 2007–2013 they ranged within 2–3 mm. It is planned that the measurements will be conducted at least two times a year in the future but it will depend on other projects in surrounding areas and possible financing possibilities.

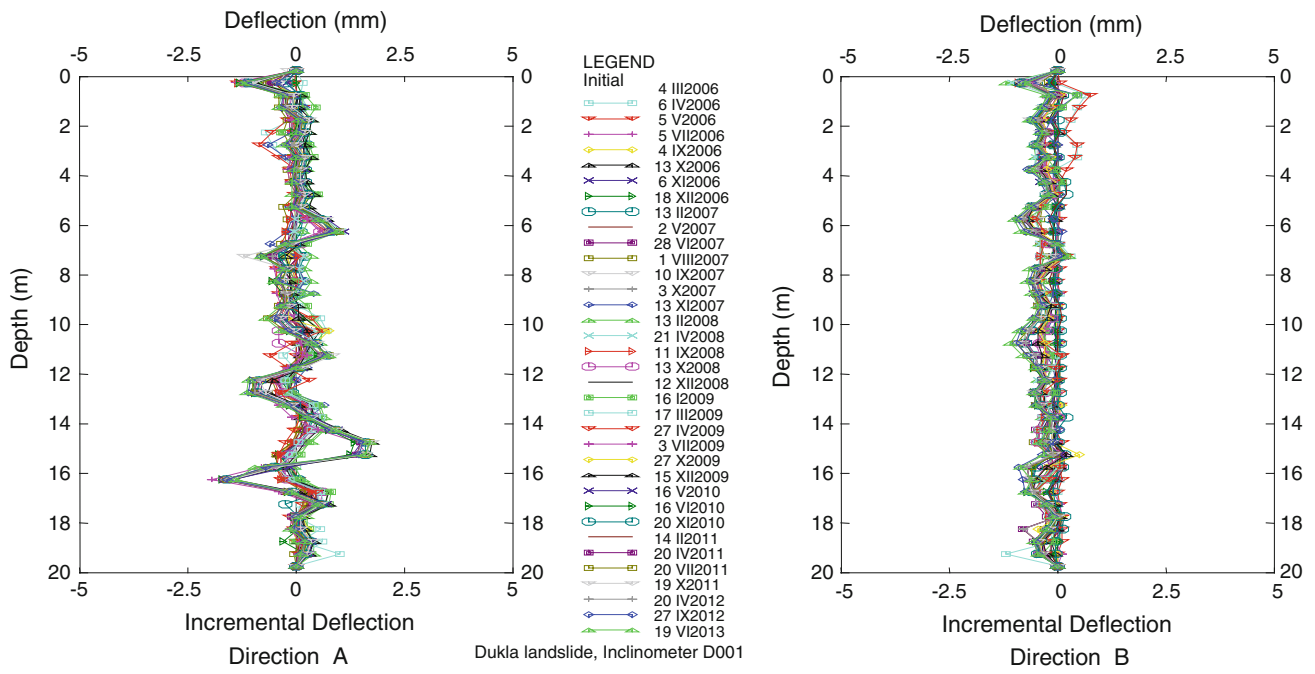


**Fig. 64.8** Incremental displacements 2006–2013

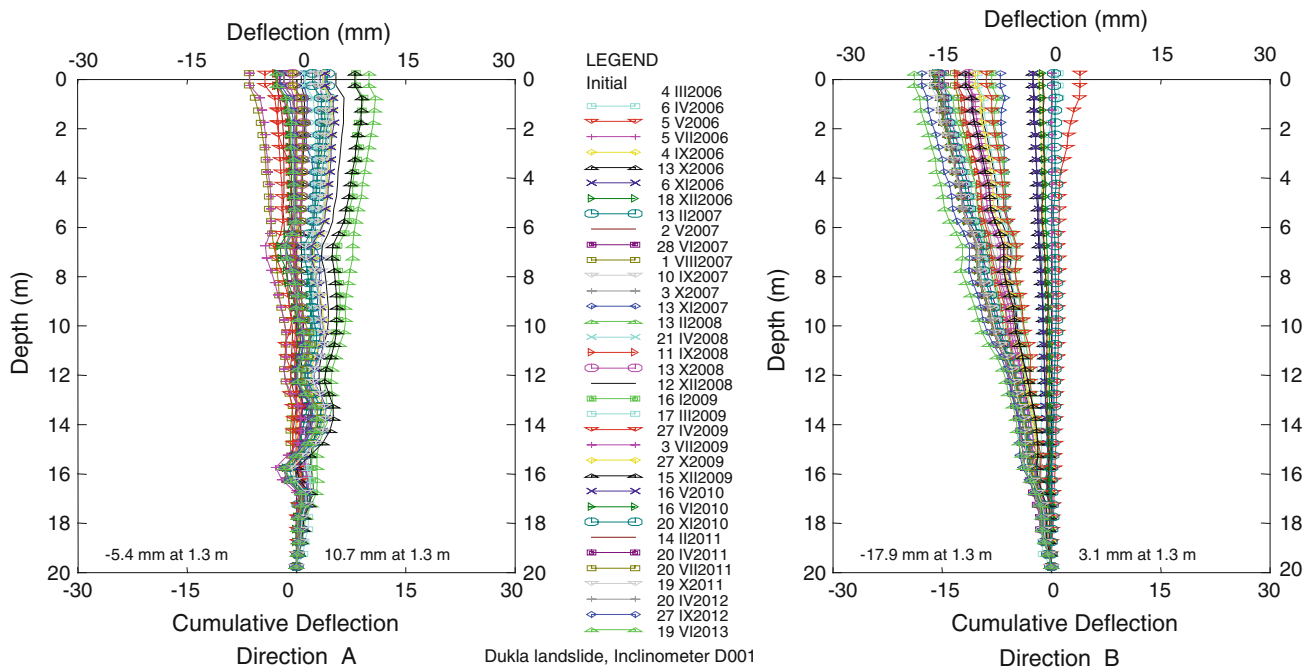


**Fig. 64.9** Cumulative displacements 2006–2013

**Fig. 64.10** Shear strains, direction A, 2006–2013

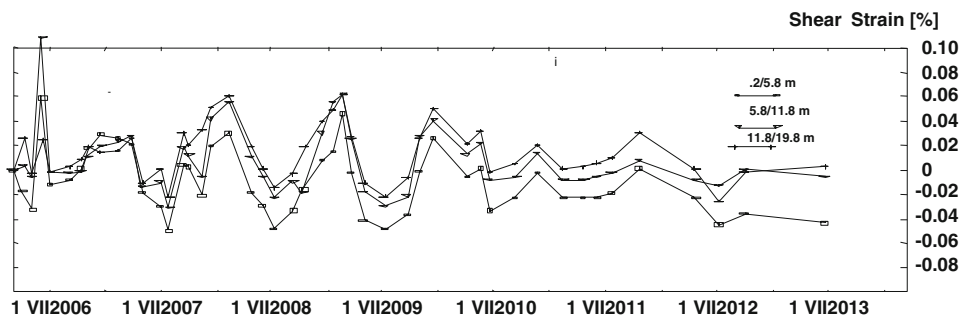
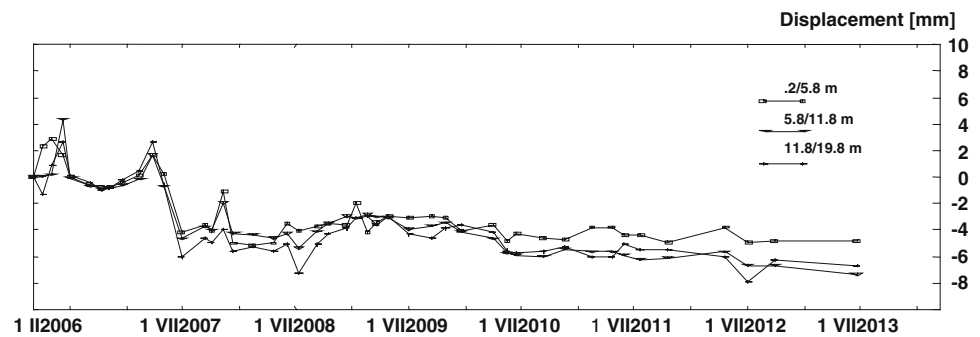


**Fig. 64.11** Cumulative displacements, direction B, 2006–2013



## 64.5 Summary and Conclusions

In the paper results of landslide remediation and monitoring, near the historical Saint John Chapel in Dukla, were shortly described. So far, in 7 years after remediation, the incremental deflections showed the maximum value of  $-2.5/+1.7$  mm to the depth of 19.5 m. However in the direction towards the landslide axis cumulative displacements of 4–7 mm to the depth of 5.8 m, 6 mm to the depth of 11.8 m and 7 mm below this depth were observed. These were the highest in years 2006–2007 and then ranged within 2–3 mm. The measurements confirmed the fact that remediation works limited the risk. For preservation of this unique Chapel the measurements need to be performed in the next years.

## References

- Bednarczyk Z (2008) Landslide geotechnical monitoring network for mitigation measures in chosen locations inside the SOPO Landslide Counteraction Project, Carpathian Mountains, Poland, The First World Landslide Forum, Tokyo, ICL, UN, UNU, pp 71–75
- Bednarczyk Z (2012) Geotechnical modeling and monitoring as a basis for stabilization works at two landslide areas in Polish Carpathians. In: Proceedings of 11th International & 2nd North American symposium on landslides. Canadian Geotechnical Society, Banff, Canada, Balkema, pp 1419–14259
- Raczkowski W, Mrozek T (2002) Activating of landsliding in the Polish Flysch Carpathians by the end of 20th century. *Studia Geomorphol Carpatho-Balcanica* 36:91–111
- Starkel L (1996) Geomorphology role of extreme rainfalls in the Polish Carpathians. *Studia Geomorphol Carpatho-Balcanica* 30:21–38

Samir Bouhedja, Boualem El Kechebour, and Ahmed Boukhaled

---

## Abstract

The Goal of this study is an analysis of the behavior of buildings in reinforced concrete during the earthquake of Boumerdes, on May 21th 2003, in the region of Algiers. This earthquake characterized by a magnitude of 6.8 on Richter scale and duration of 40 s is considered as very strong for the Algerian seismic historicity. Until this event, the site is not declared as high seismic zone. So, this situation has been the cause of great destructions and damages. The level of the damages induced by this earthquake on the structures can be explained by the interaction between the soil and the building. These collapses are caused by the real behavior between the soil and the foundations and in others cases, they are caused by the lack of ductility of the reinforced concrete frame elements. The work begins by the presentation of the site and the analysis of the damages sustained by the buildings, then by the study of the seismic risk factors in the region of Algiers. The study finishes by the recommendations about the conception of the structural elements to reduce the seismic risk and a conclusion on the necessity to consider the behavior of structures as result of interaction of elements composing a system. In conclusion, this study attests that the behavior of structures is linked to the interaction of system elements and that the multi-risk approach to improve the safety of urban and cultural heritage is required.

---

## Keywords

Building • Behavior • System • Earthquake • Heritage

---

## 65.1 Introduction

Natural and environmental hazards as the floods, landslides, and earthquakes, threaten all Euro-Mediterranean countries. The manifestations of these natural phenomena are the main causes of the degradation of urban environment and of the destruction of architectural structures. The preservation of

urban heritage represented by the different structures like the religious, educational and cultural buildings is actions that have as goal the sustainable development. Monumental buildings and historical masonry buildings are existing constructions having important cultural values. Indeed, every human community wants to conserve and transmit it heritage to the future generation. Actually, in Algeria, Codes for the cultural buildings doesn't exist.

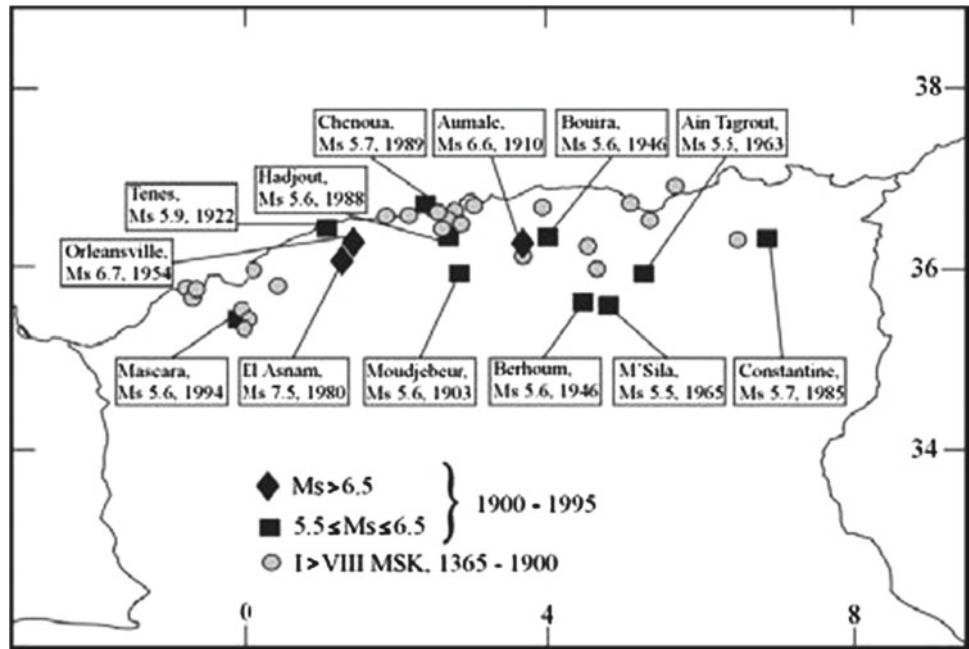
---

S. Bouhedja · B.E. Kechebour (✉) · A. Boukhaled  
Faculty of Civil Engineering, Laboratoire Eau, Environnement,  
Geomécanique et Ouvrages (LEEGO), University of Science and  
Technologie Houari Boumedién (USTHB), Bab Ezzouar, Algiers,  
Algeria  
e-mail: belkechebour@yahoo.fr

### 65.1.1 Historical Earthquakes in Algeria

The 21st May 2003 earthquake in North Algeria (Mw ~ 6.8) was a very destructive event which killed 2,273 people, injured more than 8,000 and left over 200,000 homeless, while total economic impact is estimated to US\$65 billion

**Fig. 65.1** Great earthquakes in Algeria during the last century (Benouar 1994)

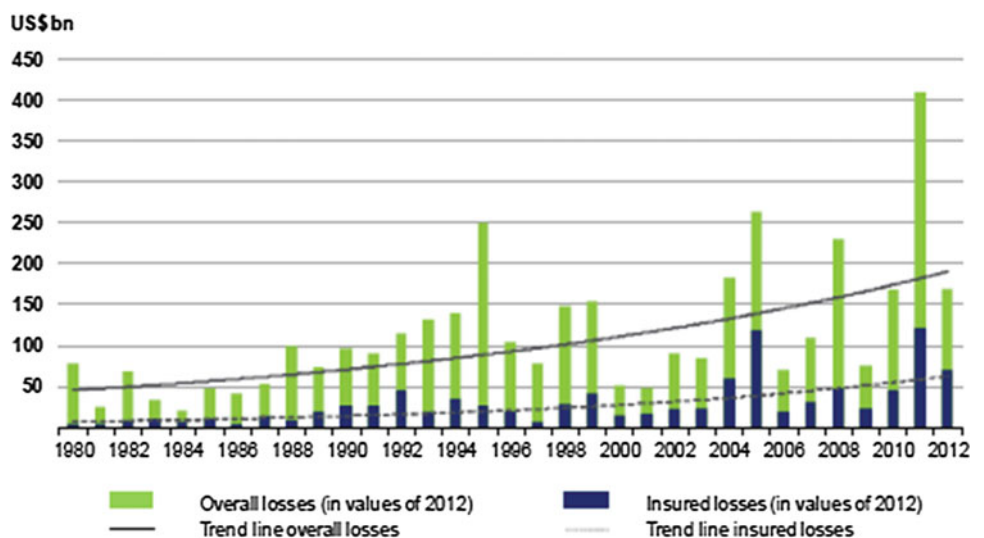


(EERI 2003). The causative fault is presumed to be an offshore structure, trending approximately NE–SW. Seismological data suggest that the length of the fault is around 40 km (Delouis and Vallée 2003), while focal mechanism solutions showed reverse faulting, coherent with the compression regime, which is present along this collision zone (Meghraoui 1988). In the old time, Algeria country has known many seismic disasters (Benouar 1994). The Fig. 65.1 gives the seismic zone in Algeria. The seismic fault of Boumerdes is discovered in 2003.

**65.1.2 The Relationship Between Disasters and Development**

Developments whether technological, economical and /or physical bring with them threats and risks. The disasters siphon the national resources by their effects, and must not become a necessary and inevitable consequence of development. The Fig. 65.2 illustrates the estimation of the loss cost generated by the natural catastrophes during the last years.

**Fig. 65.2** Estimation of the disaster cost in the world (Natural catastrophes worldwide 1980–2012: Source Munich Re NatCatSERVICE)



## 65.2 Presentation of the Site of Boumerdes Zone

The area hit by the earthquake corresponds to the easternmost part of the Mitidja basin, an ENE–WSW elongated structure, bounded from the south by the Mts Dahra and Blida, members of the Tellian Atlas mountain range.

### 65.2.1 Geology and Tectonics of Boumerdes Zone

The basin was formed in the Miocene, as a result of the N–S extensional stress field that was present there (Philip 1983); however, in the last 5 million years (since the Pliocene), the Africa–Eurasia convergence has led to the establishment of a compression al stress regime, oriented approximately N–S to NNW–SSE (Philip 1987). The deposits in the alluvial plain consist mostly of sand and silt, which cover the Pliocene–Miocene sediments of the basin (mostly sandstones and silt of considerable thickness). The geological basement of the basin comprises rocks deformed in the Tertiary and Precambrian metamorphic. The fault that was activated in the May 21 earthquake was found to be an offshore structure, trending approximately N45E (“Zemmouri Fault”). The analysis of the earthquake parameters showed that it is a dip-slip, reverse fault that was previously unknown (Delouis and Vallée 2003). It is oblique to the well-known Thenia Fault, an active dextral strike-slip structure, which also displays some amount of reverse displacement (Boudiaf et al. 1998). The line of the Thenia fault is WNW–ESE and is linked to the arcuate thrust front of the Tellian Atlas (Kabylie), which, in turn, is also considered to be an active fault (Boudiaf et al. 1999), running from Bouira at the SW of Kabylie, to Bejaia in the east, on the Mediterranean coast.

### 65.2.2 Geotechnical Conditions and Site Effects

The Algerian earthquake was aggravated by various factors, such as the shallow focal depth (15 km) and the presence of

phreatic water layer which is superficial (between 3 and 6 m). The water level is 3 m deep, so just the first 3 m of the sand layer is dry and the liquefaction may happen. In the cities Boumerdes, Zemmouri, Djinet and Dellys, the liquefaction was quite widespread. The effect was quite serious close to the Zemmouri and Djinet, but occurred mainly in rural, uninhabited areas. Sand was liquefied and ejected through linear ground fissures of considerable length. There were also manifestations of lateral spreading on the banks of Isser River. Rockfalls and other slope failure occurrences were limited in number and magnitude. The former affected well consolidated but densely fractured sandstones exposed on steep road cuts; the latter were noticed on loose sand dunes. Coastline retreat and uplift of the sea was also observed: the magnitude of uplift ranged between 0.4–0.8 m, between Boumerdes and Zemmouri (Yelles et al. 2003). The Fig. 65.3a, b show the cracking of the ground that can amplify the seismic effect.

## 65.3 Structural Damages

The early studies have determined some basic characteristics of this seism like: the duration of earthquake and the lack of ductility of the concrete.

### 65.3.1 Damages Caused by the Effect of Lack of Building Resistance

Earthquake duration is one of the causes of the damaging effects of strong ground motions on structures. The quantification of the effect of the earthquake duration on the structural reliability is a procedure that combines the non linear static and the non-linear dynamics. Ultimate strength and low-cycle structural damage limit states were applied within a framework in order to estimate the probability of failure for a suite of idealized structures. Linearly elastic structures as well as inelastic structures subjected to applied dynamic force or earthquake-induced ground motion are considered (Chopra 1995). The phenomenon fatigue of

**Fig. 65.3** **a** Craking of banks of CORSO River (suburb of Boumerdes). **b** Cracking of the ground in clayey zones (suburb of Boumerdes)



**Fig. 65.4** **a** Total destruction of a building of three floor situated on alluvial site (liquefaction of soil) in the suburb of Boumerdes. **b** Weakness of the stiffness of columns causing collapse (city of Boumerdes)



structures depends of seismic duration. In this vision, the seismic replica can destroy the structures because the original resistance of buildings is very reduced by the strong motion. This case has been reported about the Boumerdes earthquake. One day after the disaster, a replica causes the collapse of many buildings. Many studies are engaged in the United States in this field. This problematic concerns the probability to exceed the duration of a normative seismic peak (Van de Lindt and Gin-Huat 2004). The Fig. 65.4a, b illustrate the lack of building resistance.

### 65.3.2 Damages Caused by the Lack of Ductility of the Concrete

The disproportion of geometric sections between the columns and the beams induces plastic deformations on the columns earlier, then in the beams and causes the building collapse. The problem has been recognized during Boumerdes earthquake, as reported in Fig. 65.5a, b.

## 65.4 Discussion About Algerian Code

The Algerian code has been release during the last year of 1999 (RPA99 1999) and revised in 2003. After this disaster, the code (RPA 2003) have been reviewed and updated at sever rules in August 2003 (RPA99 2003) and in 2008. The

important innovation is the factor of building behavior ( $R > 1$ ) and the factor of reduction of force ( $V$ ) according this relation:  $R = V_{\text{elastic}}/V_{\text{calcul}}$ . The  $V_{\text{elastic}}$  corresponds to the structure's elastic response strength and  $V_{\text{calcul}}$  corresponds to allowable design strength. Many phenomena cannot be explained with rational method as the random collapses of neighbor structures and the site effect. But, the seismic engineering can reduce the damages of the structures and mitigate the loss of human live. Globally, the collapse of columns and the plasticization of nodes are the main cause of the ruin of buildings.

In order to reduce the effect of earthquake duration on structures, and to enhance the behavior of the structures, it is necessary:

- To use a procedure that combines order static and non-linear dynamics loads during the design.
- To implement into the new Algerian concrete standards, some rules to provide sufficient ductility at reinforced concrete members.
- To increase ductility for concrete structures subjected to bending in order to limit the depth of the compression zone ( $x/d$ ).
- To put a sufficient transversal reinforced pins at the node beam-column.
- To have the inertia of columns more greater than the inertia of beams.
- To drain the foundations of the site.
- To use seismic joint between the neighbor walls.

**Fig. 65.5** **a** Lack of ductility and discontinuity of the rebars in the node column-beam. **b** Lack of rebars in the column at the node



As the United States, Japan, and Europe move towards the implementation of Performance Based on engineering philosophies in seismic design of civil structures. The new seismic design requires performing a nonlinear analysis of the structures. These analyses can take the form of a full, nonlinear dynamic analysis, or a static nonlinear Pushover Analysis. The Pushover Analysis is a very attractive method for use in a design office, because the computational time required to perform a full, nonlinear dynamic analysis is acceptable.

---

## 65.5 Conclusion

The behavior of structures is linked to the interaction of system elements and the multirisk approach to improve the safety of cultural heritage, with particular regard to historical centers, is very suitable. The City of Algiers, Capital City, which is near to the Boumerdes City (40 km at west from Boumerdes), is very vulnerable. Indeed, more than half of national heritage is concentrated in this site and the elaboration of Codes for the cultural buildings is very required.

**Acknowledgments** The authors thank the Director of urbanism of Boumerdes District and the colleagues of seismic engineering Center of Algiers (CTC) for their collaboration.

---

## References

Benouar D (1994) Materials of investigations of the seismicity of Algeria and adjacent regions. *Ann Geofis* 37(4):860

- Boudiaf A, Ritz JF, Philip H (1998) Drainage diversion as evidence of propagating active faults: example of the El Asnam and Thénia faults, Algeria. *Terra Nova* 10:236–244
- Boudiaf A, Philip H, Coutelle A, Ritz JF (1999) Découverte d'un chevauchement d'âge quaternaire au sud de la Grande Kabylie (Algérie). Editions Lavoisier, France 1999
- Chopra AK (1995) *Dynamics of Structures*. Prentice Hall, New Jersey
- Delouis B, Vallée M (2003) The 2003 Boumerdes (Algeria) earthquake: source process from teleseismic data. *Newslett EMSC* 20:8–10
- EERI (2003) The Boumerdes, Algeria Earthquake, May 21, 2003. Earthquake Engineering Research Institute, Oakland, California
- Meghraoui M (1988) Géologie sismique du Nord de l'Algérie: paléosismologie, tectoniques active et synthèse sismotectonique, Thèse de doctorat des sciences, Université de Paris 11, France
- Philip H (1983) La tectonique actuelle et récente dans le domaine Méditerranéen et ses bordures, ses relations avec la sismicité, Thèse de Doctorat, Université des Sciences et Techniques du Languedoc, France
- Philip H (1987) Plio-Quaternary evolution of the stress field in Mediterranean zones of subduction and collision. *Ann Geophys* 5 (B):301–320
- RPA2003 (2003) Règles Parasismiques Algériennes, Alger, DTR (CGS), Janv
- RPA99 (1999) Règles Parasismiques Algériennes, Alger, DTR (CGS)
- RPA99 Addenda (2003) Règles Parasismiques Algériennes, DTR (CGS), Alger, Août
- Van de Lindt JW, Gin-Huat G (2004) Effect of earthquake duration on structural reliability. *J Struct Eng* 130(5):821–826
- Yelles C, Djelil H, Harndache M (2003) The Boumerdes-Algiers (Algeria) earthquake of May 21st, 2003 (Mw = 6.3). *Newslett EMSC* 3(5):20

# Stabilization of the Landslide in the Brda River Scarp at the Abutment of the Historical Bridge of the Narrow-Gauge Railway (Koronowo, Poland)

Marek Kulczykowski, Lesław Zabuski, Teresa Mrozek, Izabela Laskowicz, and Waldemar Świdziński

## Abstract

The paper presents the analysis of the catastrophic landsliding that affected the embankment at the western bank of the Brda river and the bridge abutment of the abandoned narrow-gauge railway from Bydgoszcz to Koronowo (central Poland). The bridge (18 m max. height, 120 m long) was set in use in 1895. It is the highest truss bridge in Europe and it is assigned a technical monument status according to Polish legislation. The railway trail was closed in 1992, so after the bridge served as a pathway. The catastrophic landsliding occurred as effect of unfavourable lithology (loose soils underlain by clay), river valley-side geometry and cumulative triggering action of rain and melt-water. The initial slide exceeding a 10 m displacement developed almost perpendicularly to the embankment axis. Following slips, developed under the bridge, resulted in removal of buttressing and the abutment exposure. The sliding process was simulated using Universal Distinct Element Code and applying a back analysis procedure. Based on the above, a remedial treatment was worked out which comprises stabilizing by retaining, slope profiling around the abutment as well as artificial drainage of the landslide area.

## Keywords

Narrow-gauge railway • Historical bridge • UDEC simulation • Landslide stabilization

M. Kulczykowski · L. Zabuski · W. Świdziński  
Institute of Hydro-Engineering, Polish Academy of Sciences,  
7 Kościarska Str., 80-328 Gdansk, Poland  
e-mail: marek@ibwpan.gda.pl

L. Zabuski  
e-mail: lechu@ibwpan.gda.pl

W. Świdziński  
e-mail: waldek@ibwpan.gda.pl

T. Mrozek (✉) · I. Laskowicz  
Polish Geological Institute—National Research Institute,  
Carpathian Branch, 1 Skraźtów Str., 31-560 Cracow, Poland  
e-mail: teresa.mrozek@pgi.gov.pl

I. Laskowicz  
e-mail: izabela.lakowicz@pgi.gov.pl

## 66.1 Introduction

The paper presents the results of the study on causes and effects of the catastrophic landsliding that affected the embankment at the western bank of the Brda river close to the bridge abutment of the abandoned narrow-gauge railway from Bydgoszcz to Koronowo, central Poland (Fig. 66.1). This is the highest truss bridge in Europe (max. height 18 m) and a technical culture monument. Since the bridge setting in use in 1895, the rail serviced passengers until 1969 while freight transport till 1992. Then, the bridge was used as a passageway by pedestrians.

The surroundings of Koronowo are susceptible to landsliding due to geologic setting (glacial deposits resting over Miocene clays) and geomorphologic situation, e.g. steep valley-sides of the river. Particularly instable are the settings where loose soils (sands, gravels) rest on less permeable cohesive grounds (clays, loams). Such arrangement of layers

**Fig. 66.1** Location of the study area and the historical narrow-gauge railway bridge

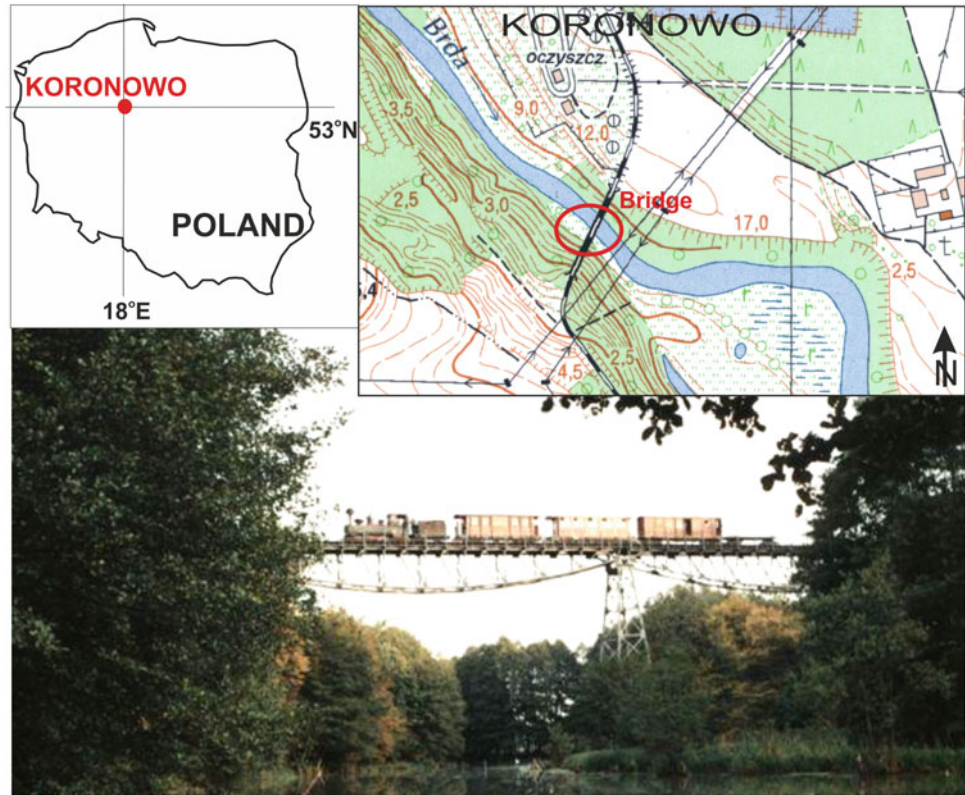


**Fig. 66.2** Landslide developed at the historical bridge. **a** Scarp of the landslide and broken sewage pipe, **b** bridge abutment exposed by the landslide



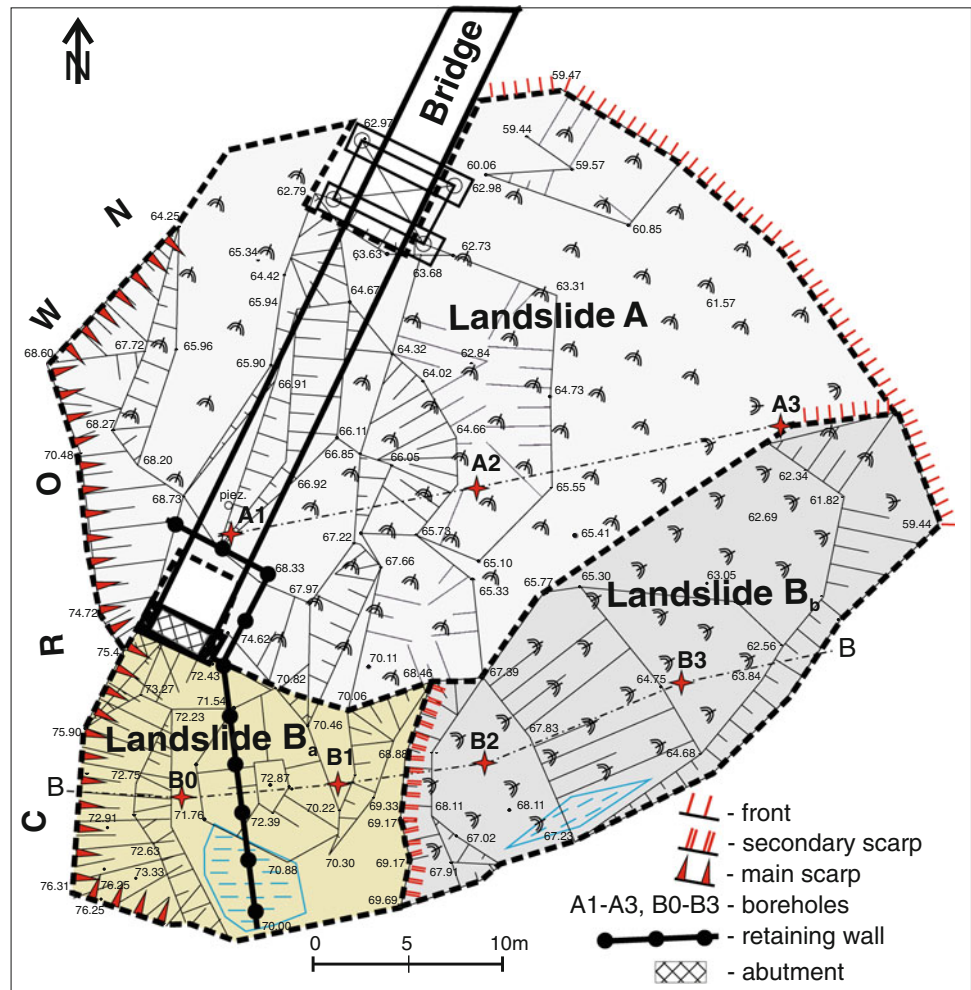
is observed in the examined site. Additional modifications are related to human impact (artificial embankment).

The landslide that occurred at the contact of the embankment and bridge abutment caused threat to the bridge stability due to removal of buttressing and resultant abutment exposure (Fig. 66.2). Due to historical-cultural importance of the bridge and its practical meaning, stabilization of the landslide, reconstruction of the damaged embankment and safety treatment of the abutment have been attempted.

## 66.2 Development of the Landslide

First signs of landsliding were cracks and a slight subsidence that appeared at the crown of the embankment in February 2011. Then, an initially slow movement accelerated suddenly, and severe deformations took place on 13 March, making the landslide almost fully developed by the end of month. At that time the landslide was 45 m long, and its front (toe) was at the level of the Brda river flood terrace. Although the rate of displacement decreased with time from ca. 1 m/day in March

**Fig. 66.3** Plan of the developed landslides A and B



to few cm/day in the next months (precise measurements were not conducted), the embankment material was sliding down continuously for a couple months. In parallel, the landslide scarp was enlarging while other morphologic features became buried by displaced soil. At the same time and later on in 2011, deformations occurred under the bridge as well, where the slip was generally NE oriented.

Figure 66.3 shows a plan of landslides A and B. Both were initiated in the same time, although the failure signs of landslide A were not so significant as B. In case of landslide B two parts were distinguished: the toe (front) of the upper part ( $B_a$ ) was worn out by a secondary scarp delimiting the lower part ( $B_b$ ). Observations carried out later on revealed that it was a complex movement.

### 66.3 Causes of Landslide Formation

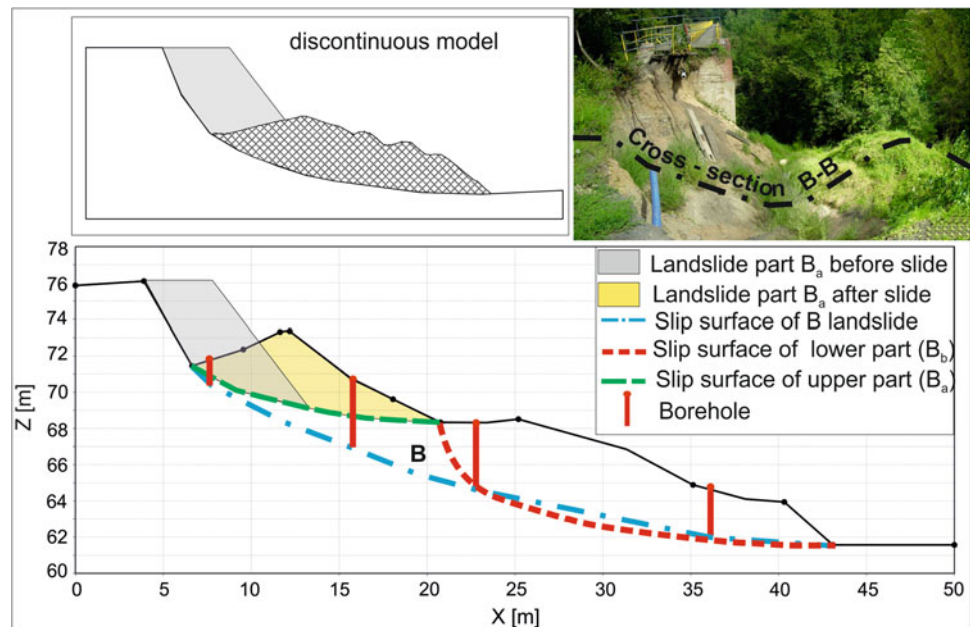
Landsliding was related to predisposing (causative) and triggering factors. In case of the former, a steep slope gradient of the embankment and bedding attitude sustained a propensity to sliding. Lithologically, 1.2–2.5 m thick loose

soils, forming the embankment upper layer, were underlain by clay and loam, that is by generally water-impermeable cohesive soils. Because of that, water percolating through loose soils when reaching the interface acted as a “lubricant” and promoted the slip. Slickenlines were very visible in natural outcrops in the landslide scarp.

Identification of active (triggering) factors was more complicated. To assess the influence of rainfall and melt waters on the embankment stability, precipitation pattern versus air temperature in the period preceding the failure was examined. The year of 2010 was characterised by extreme precipitation totals significantly exceeding multi-year means (e.g. 976 mm in 2010 versus 727 mm being the average annual precipitation total in Koronowo in 2004–2011). Indeed, for the landslide generation the period since November 2010 was important, that is a 3–4 month long period antecedent to the failure onset.

In November air temperature was positive and precipitation was high. As evapotranspiration was close to none, practically all available water infiltrated into the slope massif. Water infiltration was facilitated owing the fact that in 2005 the embankment was excavated to accommodate a

**Fig. 66.4** Landslide B simulation using discontinuous model. Location of cross-section B-B as shown in Fig. 2.1



sewage collector (Fig. 66.2). Although a trench for collector was filled-up, the soil was not consolidated, and this way a sort of a “drain” had formed. Negative temperatures in December 2010 and January 2011 led to freezing in sub-surface layer, so the outflow of “November water” from the slope was impossible. Winter snowfall, especially intensive in December, resulted in thick snow cover. With temperature increase in February, the ice-bound water from November rainfalls was released and additionally recharged with snow meltwater. In effect the soils were highly saturated, and because of that slope deformations were easily initiated. First cracks in the embankment crown gave a way for a free water inflow into deeper parts of the slope.

## 66.4 Geotechnical Investigations and Stability Analysis

Inspection of the borehole cores, standard penetration tests and vane shear tests allowed for identifying soil lithology as well as a slip surface. The shear parameters obtained in tri-axial compression tests were equal: cohesion  $c = 11.08$  kPa, angle of friction  $\varphi = 25.5^\circ$ ; specific weight  $\gamma = 20$  kN/m<sup>3</sup>.

Stability calculations based on above geomechanical parameters yielded the stability coefficient  $F$  significantly higher than 1.0. Thus, it was necessary to find shear strength parameters, for which limit equilibrium would be satisfied.

Therefore, sliding process of landslide  $B_a$  was simulated using Universal Distinct Element Code UDEC (2004) and applying a back analysis procedure. It aimed at finding

values of shear strength parameters for which displacement would be identical, as well as the position and the shape of slipped mass would be close to real (Fig. 66.4). Shear parameters along slip surface found this way were as follows:  $c = 10$  kPa,  $\varphi_r = 6^\circ$  for  $\gamma = 20$  kN/m<sup>3</sup>. These parameters differ from the laboratory ones quite significantly which might have been attributed to differences in moisture, scale effects and possible disturbance of soil structure.

For the above parameters, the stability coefficient both in case of landslide A and B, calculated by Morgenstern-Price method (Geo-Slope 2007), was approximately equal to 1.0, i.e. practically equivalent to the limit equilibrium state.

## 66.5 Stabilisation of Landslides A and B

In view of remedial treatment to landslides A and B, reconstruction of the embankment adjacent to the bridge abutment as well as buttressing of the abutment was proposed (Zabuski et al. 2011). As the major trigger of landsliding was rain- and melt-water, diverting water out from the landslides and the endangered area by artificial drainage would be compulsory. An additional measure was reprofiling of the terrain down-slope of the bridge-pier (around the abutment). The remedial engineering structures included a retaining wall anchored below the slip surface of the landslides (Fig. 66.1) gabions and a fill-ground for reconstructing the embankment (Wysokiński and Kotlicki 2007). According to the literature retaining walls and appropriate artificial drainage were applied in similar cases of bridge abutment

stabilization and can be treated almost as standard protective measures (e.g. Berry et al. 2004; Chirica and Galer 1998; Deniaud and Saunders 2007).

The proposed remedial measures revealed the stability factor higher than 1.5 for both landslides A and B, that has been accepted as satisfactory.

---

## 66.6 Closing Remarks

Visual, field observation of the landslide development from the moment of its formation to the state of serious deformations, geotechnical and stability analyses allowed for reconstructing a landslide process and for identifying its causes. The primary cause (predisposing factor) resulted from geology of the massif—loose soils underlain by cohesive soils. The fundamental triggering cause of sliding was water. Melt-water and water stored earlier under the frozen subsurface resulted in saturation of clay and sliding along that layer. The results of the study facilitated the choice of the countermeasures, such as remediation of the embankment and supporting of the bridge abutment. Stabilization works started in June 2013 and will be continued in 2014.

## References

- Berry K, Lauer R, Miller A, Olson S (2004) Landslide at a Bridge Abutment in St. Louis, Missouri. In: Yegian MK, Kavazanjian E (eds) *Geotechnical engineering for transportation project GeoTrans 2004*, Los Angeles, California, United States, vol 1. 27–31 July 2004, pp 479–487. doi:10.1061/40744(154)33
- Chirica A, Galer M (1998) Stability analysis corresponding to a New Bridge abutments. In: *Proceedings of the 4th international conference on case histories in geotechnical engineering*, St. Louis, March 1998, pp 1031–1036
- Deniaud C, Saunders T (2007) Emergency bridge stabilization at Mile 189.70 Vatrov Subdivision. In: *Proceedings of the AREMA 2007 annual conference*, Chicago, 9–12 Sept 2007
- Geo-Slope (2007) *GeoSlope Slope User's Manual*. Calgary, Canada
- UDEC (2004) *Itasca C.G:UDEC Manual*. Minneapolis
- Wysokiński L, Kotlicki W (2007) *Projektowanie konstrukcji oporowych stromych skarp i nasypów z gruntu zbrojonego*. Instrukcja nr 429/2007. ITB, Warszawa
- Zabuski L, Świdziński W, Kulczykowski M (2011) *Ekspertyza geotechniczna dotycząca przyczyn powstania osuwiska nasypu kolejowego wpływu osuwiska na stateczność prawobrzeżnego przyczółka mostu kolejki wąskotorowej w Koronowie oraz koncepcji jego zabezpieczeń*. IBW PAN, Gdańsk

---

# Importance of Mortars Characterization in the Structural Behavior of the Monumental and Civil Buildings: Case Histories in L'Aquila (Italy)

# 67

Elena Pecchioni, Raimondo Quaresima, Fabio Fratini, and Emma Cantisani

---

## Abstract

Aim of the present work is the characterization of mortars coming from religious, monumental and civil buildings significantly damaged by the 2009 earthquake in L'Aquila (Italy). The mortar characterization is performed in order to understand their characteristics (quality) in terms of raw materials, production and mix proportion. Moreover, in order to understand the role of the mortars in the mechanical behaviour of the masonries, non destructive mechanical tests have been performed in situ by Pin Penetration Resistance Test. The non destructive tests were correlated to the mineralogical and petrographical data. A whole characterization of the mortars is in fact fundamental, according to the last national technical standards, to reach adequate levels of knowledge as well as factors of confidence in order to design a proper structural project.

---

## Keywords

Historical mortars • L'Aquila • NTC 2008

---

## 67.1 Introduction

Due to their diffusion and function, mortars play a fundamental role in Cultural Heritage in terms of mural paintings, mosaics, plasters or component of the masonries (Pecchioni et al. 2008). Recently the study of masonries mortars have become particularly significant to design and plan a

structural project of recovery of buildings damaged by earthquakes, according to the last Italian national standard *Norme tecniche per le costruzioni* (NTC 2008). This standard, when designing a structural project, foresees the possibility to reach several “levels of knowledge” and to operate with different “factors of confidence” depending on the characterization of the structures and of the constitutive materials (Pecchioni et al. 2011). In case of repairing based on injection grouts, the mortars, which are responsible of the elastic modulus and compressive strengths of the masonries, play a fundamental role. In this paper the characteristics of mortars, belonging to civil and monumental buildings, significantly damaged in the 2009 L'Aquila earthquake, are reported. In particular, in situ mechanical non-destructive test were performed through a Windsor Pin System and the results were correlated with the mineralogical and petrographical data. The results of the analyses show the low quality of the mortars, dependent on the characteristics of the raw materials, the mix proportions and the manufacture, which, besides the natural decay, determined their low

---

E. Pecchioni (✉)  
University of Florence, Via G. La Pira, 4, 50121 Florence, Italy  
e-mail: elena.pecchioni@unifi.it

R. Quaresima  
University of L'Aquila, Via Campo Di Pile, Zona Industriale Di Pile, 67100 L'Aquila, Italy  
e-mail: raimondo.quaresima@univaq.it

F. Fratini · E. Cantisani  
C.N.R.- I.C.V.B.C., 50019, Sesto Fiorentino, Florence, Italy  
e-mail: f.fratini@icvb.cnr.it  
e-mail: e.cantisani@icvb.cnr.it

mechanical features and the consequent weakness of the masonries stricken by the earthquake (Corpora et al. 2007).

## 67.2 Materials and Analytical Methods

Mortar samples were chosen according to their characteristics in terms of diffusion and typology of the masonry. Two samples (SR2, SR3) come from the inner core of the masonry of a civil residence in Santa Ruffina, three samples come from a civil residence in Roio Piano (R1-arch, R2-indoor plaster, R3-outdoor plaster), three samples come from Santa Giusta Church in L'Aquila (SC1-inner core of the apse, SG2- inner core of the masonry along Santa Giusta square, SG3- mortar on bricks from the left vault of the Baroque phase of the church), four samples from Camponeschi Palace in L'Aquila (CAMP1- inner core of the masonry along Rome Street, CAMP1A- brown impurities of sample CAMP1, CAMP1B- lump of sample CAMP1, CAMP2- inner core of the masonry along Camponeschi street). All the procedure and analyses carried out, were performed according to the Italian and European standards (UNI, CEN Standards and Nor.Ma.L Recommendations). The different mortars were subjected to a mineralogical, petrographical and mechanical characterization by means of:

- *Stereomicroscopy*: morphological and surface features of all the samples, were observed under a stereomicroscope (Leica S8 APO) equipped with a 10x eyepiece lens and objective magnifications from 0.65x up to 4.5x and videocamera (EC3);
- *X-ray Diffraction (XRD)*: principal mineralogical composition of the powdered samples was determined through powder X-ray Diffraction (XRD) Philips PW 1050/37 diffractometer, with a Philips X'Pert data acquiring system, operating at 40 kV–20 mA, Cu anode, graphite monochromator, 2°/min goniometry speed, scanning range 2 $\theta$  between 5°–70°; the percentage of the single minerals were determined with the PANalytical Highscore software;
- *Polarised Light Microscopy (PLM)*: minero-petrographic and fabric features were assessed observing the thin sections under a ZEISS Axio Scope.A1 polarised light microscope equipped with 5 Megapixel resolution digital camera and dedicated software Axio Vision, both in plane and cross-polarised light.
- *Pin Penetration Resistance Test*: the measures were performed in situ, on the surface of each mortar, by a Windsor Pin System (WPS, W-P-2000), previously calibrated. After smoothing of the mortar surface, each measure was performed seven times rejecting the highest

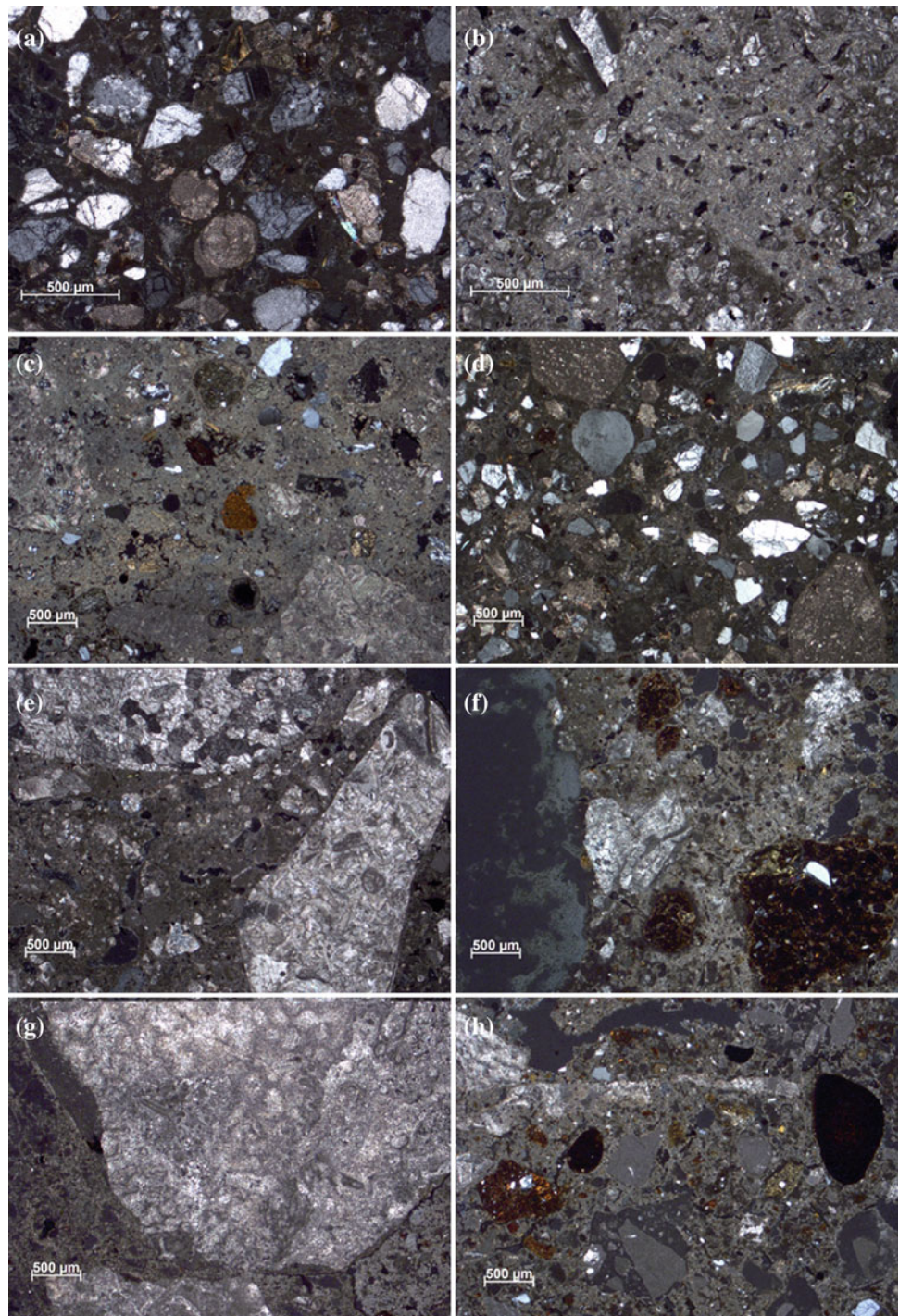
and lower value of the series. Average of the five remaining point readings (with the respective standards deviations), made it possible to calculate the compressive strength.

## 67.3 Results and Discussion

The mineralogical composition and the compressive strength of the different mortars are reported in Table 67.1. The composition of the mortars of the monumental buildings is different from those of the civil residences and the petrographical study (PLM) shows better their different characteristics (Fig. 67.1). The relatively compact yellowish mortars of the civil residence SR2 shows a well sorted aggregate made of quartz, feldspars and carbonatic rock fragments; the binder is a calcic lime, and the binder/aggregate (b/a) ratio is 1/3. The mortar of the civil residence SR3 has a poorly sorted aggregate constituted by a great amount of carbonatic rock fragments; the binder is a calcic lime with presence of shrinkage fractures, the b/a ratio of 1/2; the compactness is lower than in the sample SR2. The Roio mortars look like friable earth of ocher color. Sample R1 shows a calcic lime with an aggregate constituted mainly by carbonatic rock fragments and unmixed lime fragments besides rare quartz and pyroxenes; the b/a ratio is 1/2. Sample R2 has a poorly sorted aggregate made of quartz, feldspars and carbonatic rock fragments in a calcic lime, the b/a ratio is 1/3.

The R3 has a textural appearance similar to R2 but the aggregate has an higher content of carbonatic rock fragments also of millimetric size and a higher b/a ratio (1/2). Also the Onna sample (ON1) which looks like a friable earth, ocher in colour, shows a calcic-magnesian binder with an aggregate constituted by a great amount of carbonatic rock fragments and rare silicatic grains, besides to pyroxenes and underburnt magnesian limestone fragments; the b/a ratio is 1/3. The characteristics of the relatively compact whitish mortars of *St. Giusta Church* are slightly different among them; the samples SG1 and SG2 show a low amount of sub-rounded “clusters of fired clay” (reddish in colour), the aggregate is poorly sorted with centimetric fragments of carbonate rocks, underburnt magnesian limestone fragments and rare ceramic fragments, in a calcic-magnesian binder, the b/a ratio is 1/3; the sample SG3 (Baroque phase) shows a calcic lime with a high amount of sub-rounded “clusters” possibly to be referred to fired clay and rare ceramic fragments; the b/a ratio is always 1/3. The friable light brown mortars of CAMP1 show sub-rounded “clusters of fired clay” of millimetric grain size, dispersed in the calcic- magnesian lime

**Fig. 67.1** Optical images on PLM of: **a** SR2 (xlp) lean mortar with a well sorted aggregate in a calcic binder; **b** SR3 (xlp) mortar with abundant calcic binder and bad sorted aggregate; **c** R1 (xlp) pyroxenes and on the right an unmixed lime fragment, in a calcic lime; **d** R2 (xlp) bad sorted and heterogeneous silicatic aggregate in a calcic binder; **e** ON1 (xlp) great carbonatic rock fragments in a calcic-magnesian binder; **f** CAMP1 (xlp) on the right a sub-rounded “clusters of fired clay” and on the left an unmixed lime inclusion; **g** SG2 (xlp) centimetric fragments of carbonate rocks; **h** SG3(xlp) sub-rounded “clusters of fired clay”, dispersed in the binder. (xlp = cross polarized light)



and an aggregate constituted mainly of carbonatic rocks fragments and rare quartz; unmixed lime inclusions (of magnesian limestone) are present, the b/a ratio is 1/3. The mortar CAMP2 is similar to the previous one, it shows also underburnt magnesian limestone fragments in addition to rare pyroxenes. The binder of *Onna*, *St. Giusta* and *Camponeschi Palace*, is probably realized by burning a partially dolomitized limestone (lithotype present in the area of l'Aquila – Carta Geologica d'Italia 1955) as confirmed by

the presence of dolomite, brucite and magnesite (XRD data) besides by the presence of underburnt magnesium limestone fragments (PLM). The mortars of the civil residences show a relevant content of clay (XRD), probably earth residues in the aggregate, giving rise to a lower durability. The mortars of the monumental buildings do not show the presence of clay/earth residues (XRD), nevertheless they are characterized by the presence of sub-rounded “clusters” possibly to be referred to fired clay (PLM). The recorded presence of fired

**Table 67.1** Mineralogical composition (%) and compressive strength (MPa)

Samples	Qz	Ca	Fds	Phy	Gy	Dol	Other	Compressive strength (MPa)
SR2	42	30	20	8	–	–	–	4.5 ± 0.15
SR3	10	80	–	10	–	–	–	2.8 ± 0.27
R1	15	60	10	10	–	–	Py 5	1.1 ± 0.09
R2	40	32	18	10	tr	–	–	1.9 ± 0.11
R3	25	55	12	8	–	–	–	2.4 ± 0.12
ON1	10	75	–	5	–	10	Py/tr	1.9 ± 0.09
SG1	8	92	–	tr	–	tr	–	2.4 ± 0.13
SG2	15	85	–	tr	–	–	–	2.5 ± 0.11
SG3	18	82	–	tr	–	–	–	3.7 ± 0.09
CAMP1	8	87	–	tr	–	tr	Ar 5	2.2 ± 0.13
CAMP1A	18	62	20	tr	–	–	–	nd
CAMP1B	–	90	–	tr	–	–	Br 5, Mg 5	nd
CAMP2	–	95	–	–	tr	tr	Py 5	1.9 ± 0.11

Qz (quartz), Ca (calcite), Fds (feldspars), Phy (phyllosilicates), Gy (gypsum), Dol (dolomite), tr (traces), Ar (aragonite), Br (brucite), Mg (magnesite), Py (pyroxenes), nd (not determined). Percentage determined with the PANalytical Highscore software

clay can be explained as impurities of red soils stuck to the limestone and fired together with the stone blocks in the kiln. As a matter of fact in Abruzzo the most diffused practice to produce the lime was by digging a hole (pit furnaces) which was filled with limestone blocks and covered with mud and wood (Petrella 2009). In this way, during burning, the mud, became amorphous and reddish, sticking to the quick lime blocks. As regards to the presence of the rare pyroxenes (samples R1, ON1, CAMP2), this may be due to a pyroclastic component coming from the volcanic activity of the Latium-Abruzzi Apennines (D'Orefice et al. 2006), or from the activity of the Monti Sabatini - Colli Albani area, present in the rivers sand and utilized as aggregate in the mortars and/or as product of the reaction between the calcium/magnesium oxide and the baked clay. Concerning the mechanical features, all the mortars, except sample SR2, show similar range of low values. Generally the low value could be attribute mainly to a bad state of conservation and sometimes to bad grain size distribution. This is particular evident in sample R2, R3 and ON1 in which the loss of mechanical resistance is strictly correlated to the state of decay (Quaresima et al. 2006). This is further evidenced in samples R2 and R3, coming respectively from an indoor and an outdoor location. Such higher resistance of sample SR2 could be put in relation to the presence of an abundant well sorted aggregate on which the tip of the WPS device may have exerted the force, with consequent higher data. The mortars from monuments show values relatively a little bit higher than those of the civil buildings and this can be put in relation to a different quality both of the raw materials and of the manufacturing, anyway some higher values (WPS) could

be associated to mortars generally realized in L'Aquila in most recent period (after the 1703 earthquake). In the case of *Camponeschi Palace* the different values of the two samples CAMP1 and CAMP2, even having similar characteristics, correspond to diverse wings of the building, therefore to different constructive phases and maybe to a different state of conservation of the latter mortar. The WPS as method to mechanically characterize mortars, although has many limits, (heterogeneous composition of the mortars, planarity of the surface, precision and accuracy, limitation of the area of measure) but seems to be the tool able to correlate the traditional characterization to those information needed by the designers, according to the NTC (2008).

## 67.4 Conclusions

The characterization of mortars of some monumental and civil buildings stricken by the 2009 earthquake of L'Aquila, shows that these materials are different in terms of composition and mechanical features. The mortars from monumental buildings, characterized by a calcic magnesian binder show a slightly good state of conservation while the mortars from the civil buildings, characterised by a high content of clay/earth residues, according to a rural and poor manufacture tradition, show a lower durability. The compressive strength, measured by WPS, is generally low and around 2–3 MPa. In the monumental buildings these values are a little bit higher. The low values of resistance have been mainly correlated with the strong decay conditions and with characteristics of the mortars.

## References

- Carta Geologica d'Italia 1:100.000 (1955) Foglio 139 – L'Aquila. IGM, Servizio Geologico d'Italia
- Corpora H, Fiocchetti C, Meloni P, Quaresima R (2007) Lo Stato dell'Arte 5, vol 1. Nardini Firenze 2007, pp 435–441
- D'Orefice M, Graciotti R, Capitano F, Stoppa F, Rosatelli G, Barbieri M (2006) Mem. Descr. Carta Geol. d'It. LXXII, Selca Firenze 2006, pp 7–67
- NTC (2008) Norme Tecniche per le costruzioni. D.M.14 Gennaio. Gazzetta Ufficiale, Roma
- Pecchioni E, Fratini F, Cantisani E (2008) Le malte antiche e moderne tra tradizione ed innovazione. Pàtron (ed). Bologna
- Pecchioni E, Cantisani E, Fratini F, Quaresima R (2011) Florence cost strategic workshop. In: Grafica C (ed) Sesto Fiorentino Firenze, 2011, pp 170–172
- Petrella G (2009) Produzione e tecniche artigianali all'Aquila tra medioevo e Età Moderna. Dati Archeologici e archivistici. In: Paper presented at the V Congresso Nazionale di Archeologia Medievale, Foggia 30 Settembre–3 Ottobre 2009
- Quaresima R, Corpora H, Volpe R (2006) Heritage, weathering and conservation HWC-2006 Madrid, Taylor & Francis Group, Balkema, London, pp 91–96

Claudio Margottini, Daniele Spizzichino, Alberico Sonnessa,  
and Luca Maria Puzzilli

## Abstract

The present work reports the main results of a preliminary assessment of the stability condition affecting the Katskhi Pillar Monastery in western Georgian. The research activities have been carried out with the support of National Agency for Cultural Heritage of Georgia in Tbilisi, following field survey activities conducted during May and December 2012. The field mission was aimed at the implementation of the following activities: (i) collection of preliminary geological, geomorphological and geomechanical data in order to define the main strength and deformation parameters; (ii) geodetic surveying with TLS techniques for the 3D model reconstruction of the site and collection of geometric data for future slope stability analyses; (iii) seismic survey with passive technique to achieve information about resonant frequency of the site; (iv) preliminary analysis of rock pillar stability; (v) monitoring project design for a full analysis on long-term risk assessment for the Katskhi pillar.

## Keywords

Landslide • Katskhi • Cultural heritage • Natural hazard • Georgia

## 68.1 Historical Setting of the Katskhi Pillar Monastery

The Katskhi pillar is a natural limestone monolith located close to Katskhi village in the western Georgian Region of Imereti, near the town of Chiatura. It is approximately 40 meters high, and overlooks the small river valley of Katskhura, a right affluent of the Q'virila river (Fig. 68.1). The rock, with

visible church ruins on its top surface (areal extent: around 150 m<sup>2</sup>), has been venerated by locals as the Pillar of Life, symbolizing the True Cross, and has surrounded by several legends concerning its origin. It remained unclimbed by researchers and unsurveyed until 1944 and has been more systematically studied from 1999 onward. These studies revealed the early medieval hermitage, dating from the 9th or 10th century. A Georgian inscription dated to the 13th century suggests that the hermitage was still extant at that time. Religious activity associated with the pillar started to revive in the 1990s. Between 2005 and 2009, the monastery building on the top of the pillar was restored within the framework of a state-funded program with the support of the National Agency for Cultural Heritage Preservation of Georgia. The Katskhi pillar complex, in its current state, consists of a church, a crypt (burial vault), three hermit cells, a wine cellar, and a curtain wall on the uneven top surface of the column. At the base of the pillar there are the newly built church of Simeon Stylites and ruins of an old wall and belfry. A small church constituted by a single hall (with the dimensions of 4.5 × 3.5 m), is the final

C. Margottini · D. Spizzichino (✉) · L.M. Puzzilli  
ISPRA - Geological Survey of Italy, Via Vitaliano Brancati 60,  
00144 Rome, Italy  
e-mail: daniele.spizzichino@isprambiente.it

C. Margottini  
e-mail: c.margottini@gmail.com

A. Sonnessa  
Department of Civil, Constructional and Environmental  
Engineering, Sapienza University of Rome – SurveyLab, Spinoff,  
Rome, Italy

**Fig. 68.1** Panoramic view of Katskhi Pillar in the Katskhura valley. At the top of the calcareous column the small church of the Monastery is located



result of restoration of the ruined medieval church. Beneath and south of the church is an elongated rectangular crypt with the dimensions of  $2.0 \times 1.0$  m, which had served as a burial vault. At the very base of the pillar there is a cross in relief, exhibiting parallels with similar early medieval depictions found elsewhere in Georgia. The rock is now accessible through an iron ladder running from its base to the top.

### 68.2 Geo-Mechanical Characteristics of the Pillar

From a geological point of view the rocks cropping out in the area belong to the Upper Cretaceous formations (Adamia 2004) and more in detail to “shallow marine carbonate rocks” (Fig. 68.2).

**Fig. 68.2** Geological settings of Katskhi pillar monastery (red circle)

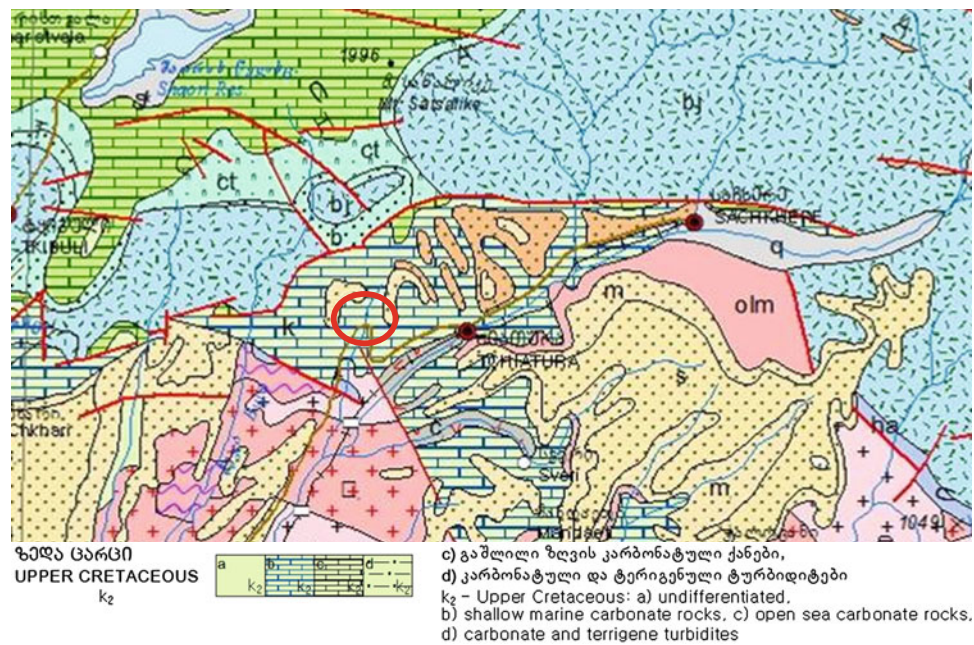


**Table 68.1** Preliminary geo-mechanical parameters

Lithology	Natural unit weight (KN/m <sup>3</sup> )	JRC	UCS from Schmidt—Hammer test (MPa)	$\phi$ Tilt test (°)	UCS from point load test (MPa)
Limestone	22,6	6–8	50–70	46	153

Geo-mechanical characteristics of rock mass forming the pillar have been reconstructed through field techniques and in situ laboratory tests, performed on rock blocks. Several rock mass classification methods and failure criteria have been implemented (Hoek 2007). More in detail, the following activities have been carried out during 2012 field survey (Table 68.1): geostructural and geomechanical survey through scan lines in order to define the main geomechanical parameters and indexes (e.g. RMR, GSI, Q system); collection of strength and deformation parameters from scientific and technical literature; Schmidt-hammer tests on joint surfaces and intact rock blocks for in situ analysis of Uniaxial Compressive Strength (UCS); sampling of blocks in the field for the laboratory tests; Point Load tests to provide UCS data from sampled blocks and compare them with in situ data (ISRM 1981).

More in detail the column is not exhibiting geomechanical homogeneity along its entire height. The lowest part is, in fact, characterized by a higher density of discontinuities with an estimated GSI around 60; the middle part of the column shows a GSI equal to 65 and the upper part (the more massive), shows a GSI index equal to 70. The decreasing of interlocking in rock pieces in the lowest part is responsible for the reduction of rock strength in this sector, which is also demonstrated by the lowest GSI value here detected with respect to the entire column. Accordingly, there is a higher rate of erosion in the lowest part of the column and generation of an overhanging structure in the upper part (Fig. 68.1).

Finally, the above described inhomogeneity is producing a similar instability mechanism on the entire pillar but with smaller size in the lowest part.

### 68.3 Types of Rock Slope Failures

Due to its morphological and geo-structural trend, the Katskhi pillar has been divided into different portions in order to provide zoning on potential landslide types affecting each single portion. Rock slope failures occurring at Katskhi can be classified into one of the following categories listed below depending on the type and degree of structural control and mechanical properties of rock masses. The whole pillar is affected (mainly in the lower/middle portion) by diffused small size rockfalls and wedge failures (size < 1 m<sup>3</sup>). These phenomena, although not directly correlated to the overall

stability of the pillar, can be very dangerous for pilgrims and visitors. In the middle portion of the column small block sliding phenomena have been identified and mapped (block size from 1 to 2 m<sup>3</sup>). Also in this situation there is not a real hazard for the stability of the entire column but there is a high risk for tourists, pilgrim and the community of monks and hermits of the site. In the upper part of the pillar big portions of unstable rock masses (toppling/sliding) have been detected and mapped. Due to the dimensions of the unstable rock masses also the edge and the boundary of the monastery could be involved. This situation is the most dangerous, since it involves both the safety of persons and the same Monastery edge.

### 68.4 Terrestrial Laser Scanning Survey

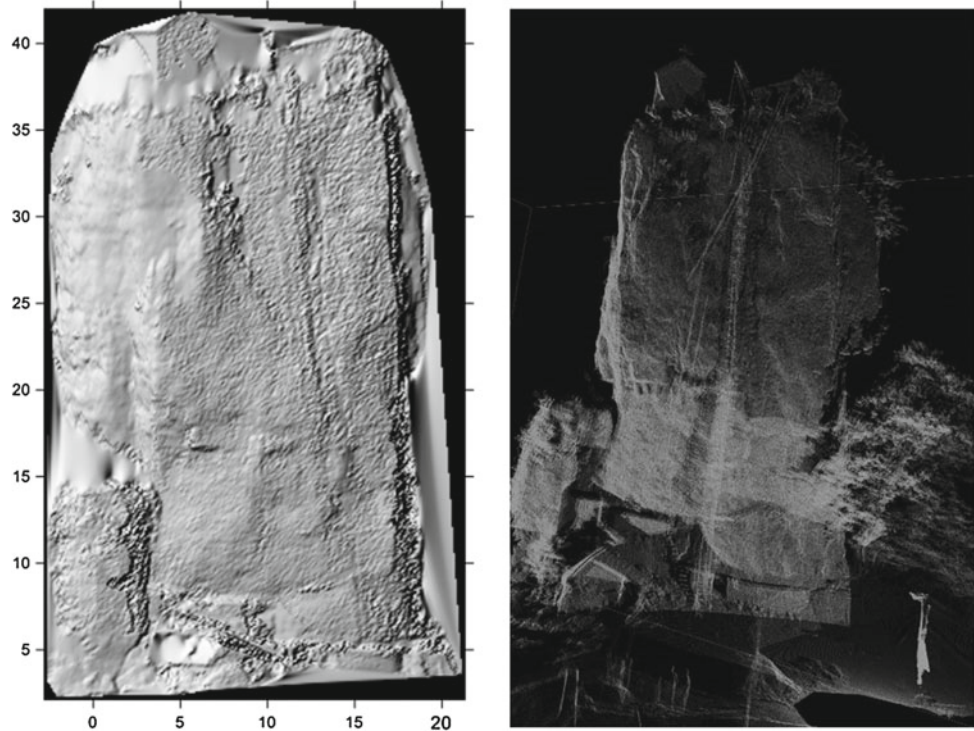
In order to carry out a site-scale specific analysis, a detailed geodetic 3D Laser Scanning survey has been performed and implemented during the May 2012 field mission. The geodetic surveying was aimed at the three-dimensional (3D) reconstruction of the pillar, and the collection of data for future slope stability analysis of the site (Fig. 68.3).

All these characteristics make TLS an extremely useful tool in the field of conservation and protection of Cultural Heritage. The detailed 3D geometry reconstruction is fundamental to reconstruct unstable mass and to extract 2D section for stability model. Surveying activities at Katskhi site were performed using a topographical Riegl Z210i laser scanner both for measuring the 3D coordinates of the models and acquiring the RGB information linked to the point clouds. This allows obtaining very accurate 3D surface models for archiving uses or for further quantitative analyses.

### 68.5 Passive Seismic Survey

During the field survey some ambient vibrations measurements were collected to achieve relevant information about possible site-resonance effects, associated with local geological conditions. Registrations were implemented with the digital three-component acquisition system Tromino<sup>®</sup> (Micromed S.p.A.), specifically designed for the application of the spectral ratio technique introduced by Nakamura (Nakamura 1989). Over the last decade many researchers

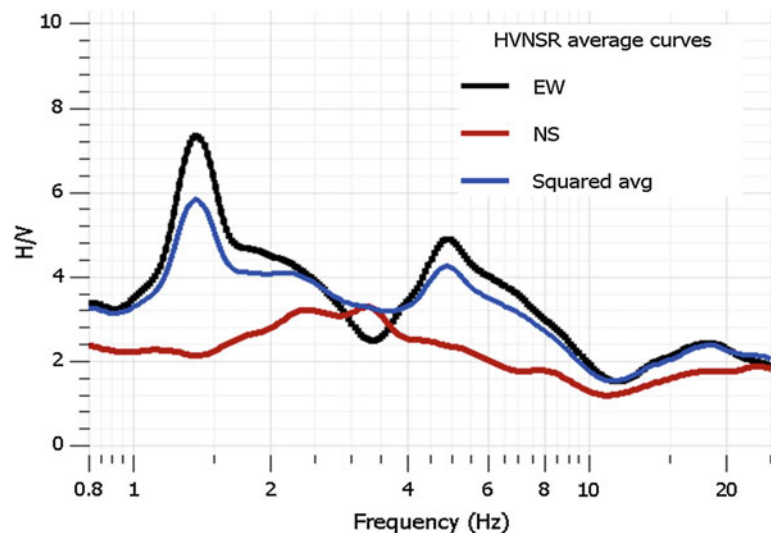
**Fig. 68.3** TLS 3D implemented model



have shown that the peak frequencies correlate closely to those computed from shear-wave transfer function for a high number of soil-rock structures, also providing useful indications about seismic behavior of soils in the same frequency range as earthquake energy. Five measurements were carried out around the pillar and two measurements on top of the pillar, the former to check the geological conditions and the presence of resonance effects, the latter in order to retrieve meaningful information about possible double-resonance effects of the pillar. Each test was performed using a sampling frequency of 128 Hz and an acquisition time of 16 min, following the SESAME guidelines to process data and for

the implementation of the H/V spectral ratio technique by using Geopsy software ver. 2.5.0 (SESAME 2004). From application of the spectral ratio technique, an average H/V curve with its corresponding peak frequency  $f_0$  and peak amplitude  $a_0$  were retrieved for each site (Fig. 68.4). Registrations made at the base with the ones collected at the top of Katskhi pillar were also processed together, aiming at estimating the Transfer function of the system by computing the spectral ratio between the input (ambient vibration at base) and the output signals (ambient vibration on top). We retrieved a narrow band of resonant frequencies  $f_0$  regardless of the position of measurements (at base or on top of pillar),

**Fig. 68.4** HVNSR average curves from all measurements, considering different directions on a horizontal plane



also that the horizontal signals for each site are almost entirely focused on EW direction. Further, we found that the double-resonance effects could be possible both in case of long and short-period earthquakes.

## 68.6 Conclusions

The present work allowed, through a multidisciplinary approach, the identification of different instability processes affecting the Katskhi pillar Monastery. Although it seems that there actually is not a high risk of rapid collapse for the entire Katskhi pillar, further analysis should be carried out in order to control and reduce the instability processes.

TLS techniques may allow a high resolution detailed 3-D model of the investigated sites as well as the semi-automatic detection of rock discontinuities and potential instability mechanisms (Gigli and Casagli 2011).

From the preliminary passive seismic investigation by using HVNSR technique it was possible to retrieve that the structure seems to be influenced by a relative motion almost entirely focalized in the EW direction, also susceptible to both short and long-period earthquakes. Therefore specifically designed seismic investigation are highly recommended, in order to retrieve a reliable shear wave profile for the subsoil, to compute fundamental site-period ( $1/f_0$ ) and comparing it with the preliminary estimates made by using H/V technique from ambient vibrations. Also a long-time seismic monitoring campaign should be implemented aiming at estimate seismic response characteristics of the pillar by spectral ratios of ambient vibrations and earthquakes, measured simultaneously on structures and at ground surface. An

integrated monitoring system should be implemented in order to prevent future small rock collapse of the column especially under dynamic condition. More in detail the following measures could be sufficient: scaling of small blocks along the façade of the pillar; nails and bolts for the medium size phenomena (reducing the dismantling of the column section and avoiding excessive eccentricity of the pillar loads); installation of Wi-Fi sensors (tiltmeters, crack-meters and accelerometers) in order to monitor future instability processes.

## References

- Adamia S (2004) Geological map of Georgia. 1:500.000 scale. Georgian Department of Geology. ISTC Project Union GEO-ECO (GIS and RS Consulting Center Geographic)
- Gigli G, Casagli N (2011) Semi-automatic extraction of rock mass structural data from high resolution LIDAR point clouds. *Int J Rock Mech Min* 48:187–198
- Hoek E (2007) *Practical Rock Engineering*, 2007 edn. <http://www.roscience.com>
- ISRM (1981) Commission on classification of rocks and rock masses—Basic geotechnical description of rock masses. *Int J Rock Mech Min Sci Geomech Abstracts* 18:85–110
- Nakamura Y (1989) A method for dynamic characteristics estimation of subsurface using micro-tremor on the ground surface. *Q Rep Railway Tech Res Inst* 30–1:25–33
- SESAME (2004) SESAME Project- Site EffectS assessment using Ambient Excitations (2004). European Commission—Research General Directorate Project No. EVG1-CT-2000-00026. Deliverable 23.12 Guidelines for the implementation of the H/V spectral ratio technique on ambient vibrations: measurements, processing and interpretation. [http://sesame-fp5.obs.ujfGrenoble.fr/Papers/HV\\_UserGuideline.pdf](http://sesame-fp5.obs.ujfGrenoble.fr/Papers/HV_UserGuideline.pdf)

# Ambient Noise Recordings in the Circo Massimo and *Vallis Murciae* Areas: Main Results Compared with the Dynamic Response of the XII Cen. A.D. Torre Della Moletta

Emiliano Di Luzio, Francesco Fazio, Sebastiano Imposa, and Giuseppe Rannisi

## Abstract

In this work we present the results of ambient noise recordings carried out in the Circo Massimo area, within the central archaeological district of Rome. The study area was part of a Quaternary alluvial valley, the *Vallis Murciae*, a secondary feeder of the Tiber River. Ninety-two recordings of ambient noise were performed in 2013 on a 20 meters regularly-spaced grid. By applying the Horizontal-to-Vertical Spectral Ratio (HVSr) technique, the first-mode resonance frequency ( $f_0$ ) of the Holocene-Upper Pleistocene alluvial infilling was determined, ranging between 1.2 and 1.8 Hz. The  $f_0$  local spatial variation was analyzed and a trend of  $f_0$  increase moving south-eastwards was confirmed by a noise recording taken at the eastern termination of the *Vallis Murciae* (Terme di Caracalla site). To characterize also the dynamic response of local monumental buildings, vibration recordings were done at the Torre della Moletta, a stony-tower built at the south-eastern limit of the Circo Massimo area during the Middle Age (XII cen. A.D.). The vibration pattern features a Hi/Ho peak at a frequency of about 3 Hz, that is close to the ground resonant frequency. This evidence reveals potentially destructive site effects for the Torre della Moletta building during seismic events and set the basis for further studies on seismic hazard assessment in the Rome downtown area.

## Keywords

Ambient noise • Building vibration • Seismic hazard • Rome • Italy

E. Di Luzio (✉)  
Institute for Technologies Applied to Cultural Heritage. Research Area RM1, CNR-ITABC, Via Salaria Km. 29.300, 00171 Monterotondo, Rome, Italy  
e-mail: ediluzio@libero.it

F. Fazio · G. Rannisi  
Geodixi s.r.l, Via Alfonsetti, 46, 95100 Catania, Italy

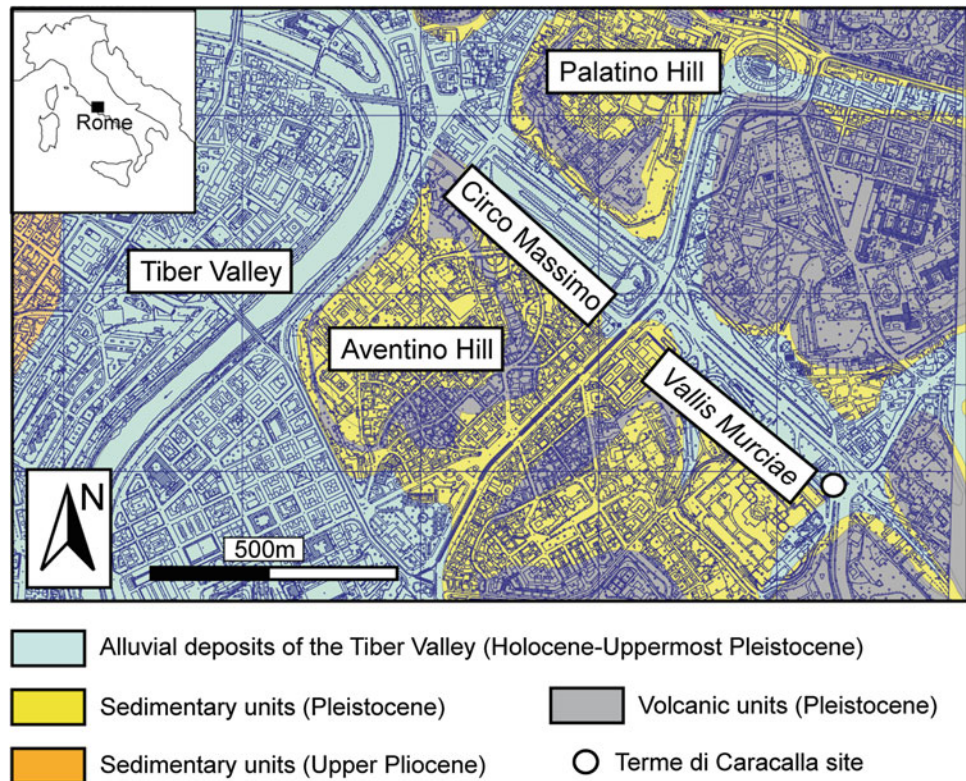
S. Imposa  
Department of Biological, Geological and Environmental Science Section—Earth Science Section, University of Catania, Corso Italia, 57, 95129 Catania, Italy

## 69.1 Introduction

Macroseismic studies (e.g. Sbarra et al. 2012) and numerical modelling of ground motion (e.g. Rovelli et al. 1995) evidenced that severe damages and site effects in the Rome historical centre have to be expected within the Tiber Valley and its tributaries (Fig. 69.1). However, despite the incomparable cultural heritage potentially threatened by seismic hazard, a relative lack of data persists on the dynamic characterization of the subsoil (e.g. Bozzano et al. 2008; Moscatelli et al. 2012).

In this study we present the results of several (92) recordings of ambient noise carried out in 2013 within the Circo Massimo area, that belongs to the ancient course of the *Vallis Murciae*, a former tributary of the Tiber River on its eastern bank (Fig. 69.1). Main aims of this work are: (i) a further contribute to the dynamic characterization of the

**Fig. 69.1** The Circo Massimo area and the *Vallis Murciae* in the central archaeological area of Rome. Location of the Terme di Caracalla site is indicated



geological substratum in Rome in terms of first mode resonant frequency ( $f_0$ ) of the Quaternary alluvial terrains; (ii) the analysis of the  $f_0$  spatial variation over short distances within an alluvial valley in the downtown area.

Moreover, the dynamic response of the XII cen. A.D. Torre della Moletta—located at the south-eastern limit of the Circo Massimo area—was analyzed and compared to the ground resonant frequencies revealing potential destructive site effects for the medieval building and, perhaps, for other monumental structures.

## 69.2 Ambient Noise Recordings

### 69.2.1 Field Survey, Parameters Setting and Results

Recordings of ambient noise (Fig. 69.2) were taken at different dates by using a Tromino Engy<sup>®</sup> tromograph placed on a rectangular grid (490 × 40 m) with a regular 20 m step (see Fig. 69.2). Each of the 92 recording was carried out with a sampling frequency of 128 Hz and lasted 14 min. Traces were elaborated by applying the HVSR (Horizontal to Vertical Spectral Ratio) technique and removing transients incoherent noise. Figure 69.2 shows the 18 H/V

average curves preserving more than 50 % of the processed signal after removal and fully respecting the Sesame criteria (Sesame 2004). A clear, stable H/V peak lies between 1.2 and 1.8 Hz and should be related to the bottom of the alluvial infilling (plus backfill deposits) found at 40 meters of depth in the CM1 well (Fig. 69.3); a greater variability exists at higher frequencies (15–40 Hz), while in the low frequencies field a less pronounced, wider peak can be observed within 0.3 and 0.4 Hz.

### 69.2.2 H/V Spatial Variation

Values of  $f_0$  for the main peak between 1.2 and 1.8 Hz were countered over the whole study area (Fig. 69.3). Higher values (1.5–1.8 Hz) were observed in the central part of the Circo Massimo at its south-eastern termination. Over a distance of about 500 m along the NW–SE longitudinal axis of the Circo Massimo valley, a  $\Delta f_0$  of about 0.6 Hz is realised. A trend of  $f_0$  increase moving south-eastwards is confirmed by a measurement taken at the eastern termination of the *Vallis Murciae*, at the Terme di Caracalla site. (Figure 69.2, see Fig. 69.1 for location), where the main H/V peak related to the bottom of the alluvial cover is both less pronounced and shifted towards  $f_0$  between 3 and 4 Hz.

**Fig. 69.2** Results of ambient noise recordings in the Circo Massimo area (selected 18 traces) and at the Terme di Caracalla site

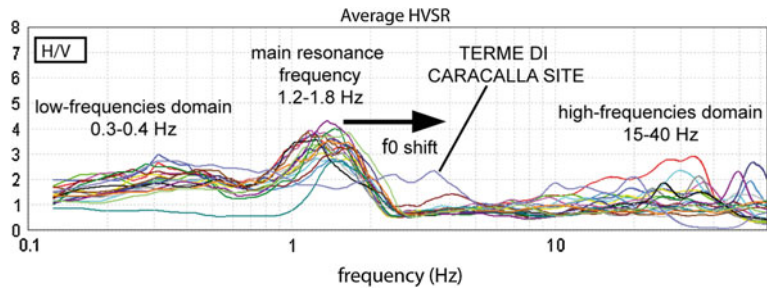
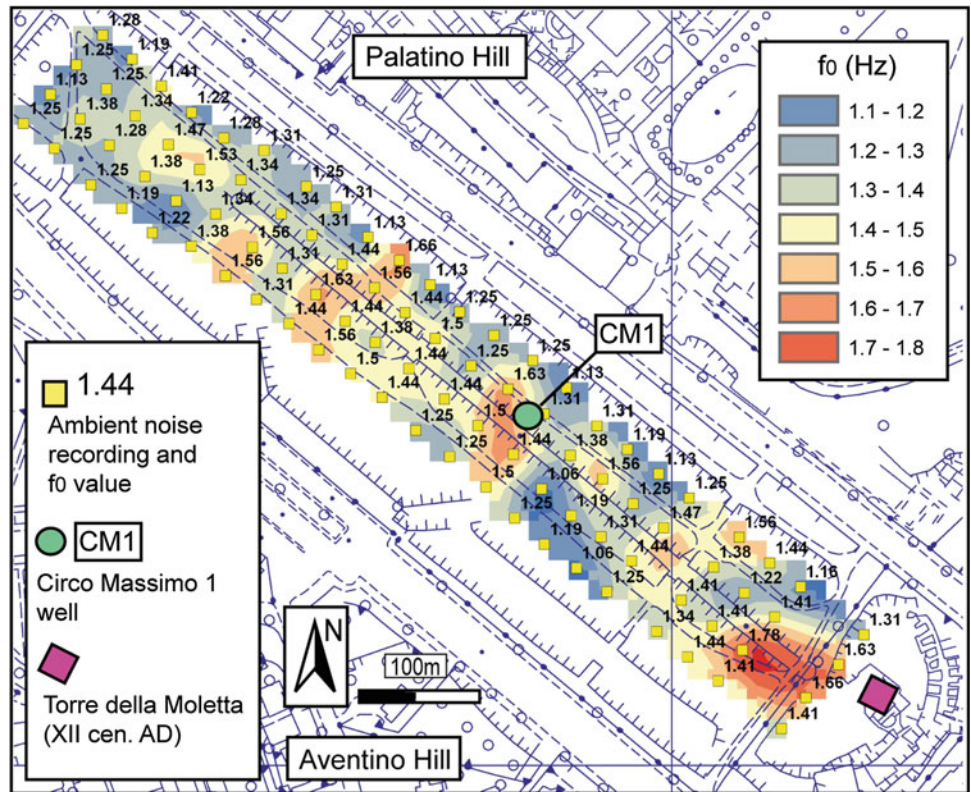


**Fig. 69.3** H/V spatial variation over the Circo Massimo area and location of the Torre della Moletta building



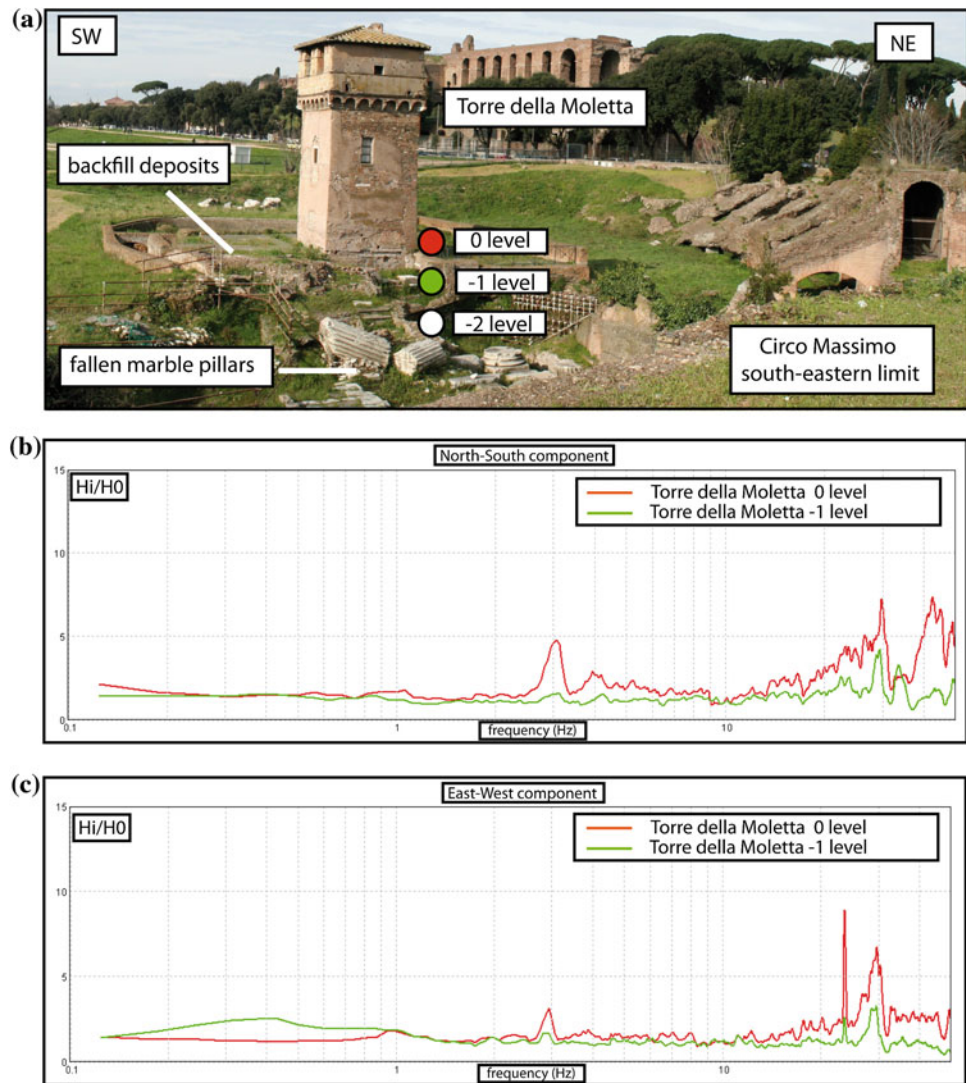
**69.3 Vibration Recordings at the Torre Della Moletta Building (XII Cen. A.D.)**

Vibration recordings were taken into the Torre della Moletta medieval building (Fig. 69.4a), at the south-eastern limit of the Circo Massimo area. The tower was built in the XII cen. A.D. using stony materials and is about 10 meters high from the present basal ground level (0 level). Backfill deposits around the tower mask the lowermost two levels (-1 and -2 levels). Hi/H0 values were determined by setting the

Tromino Engy<sup>®</sup> on a vertical alignment into the tower and assuming the -2 level as the reference (H0). A Hi/H0 peak can be observed at a vibration frequency of 3 Hz, clearly visible on the North-South component, and partially on the East-West component (Fig. 69.4b, c, respectively).

This values is coherent with the vibration frequencies of small-to-medium sized monuments in Rome such as free-standing columns, walls, arches (e.g. Marzi et al. 1990) and is close to f0 values for the alluvial cover in the south-eastern zone of the Circo Massimo area (1.5–1.8 Hz). Therefore, a

**Fig. 69.4** **a** The Torre della Moletta medieval building (XII cen. A.D.) at the south-eastern limit of the Circo Massimo area; **b** North-South component of the Hi/Ho curve; **c** East-West component



potential destructive double resonance effect during seismic events can be inferred for the medieval building; possible site effects on monumental buildings in the area are also suggested by ruins of two Imperial Age marble pillars which lie close to the Torre della Moletta, both fallen along the North-South direction (Fig. 69.4a).

## 69.4 Concluding Remarks

Processing and elaboration of 92 ambient noise recordings performed in the Circo Massimo area revealed a stable H/V peak in a  $f_0$  range between 1.2 and 1.8 Hz for the anthropic backfill and the alluvial cover filling the former alluvial valley. Spatial variation of  $f_0$  values over the area account for a trend of  $f_0$  increase moving south-eastwards along the longitudinal valley axis, whereas shorter wavelength

variations are likely due to an irregular morphology of the valley bottom.

The analysis of the dynamic response of the Torre della Moletta building (XII cen. A.D.), once compared to the local  $f_0$  values, suggests potential double resonance effects for the medieval tower; site effects in the Circo Massimo area can also be inferred by other archaeo-seismological evidence.

## References

- Bozzano F, Caserta A, Govoni A, Marra F, Martino S (2008) Static and dynamic characterization of alluvial deposits in the Tiber River Valley: new data for assessing potential ground motion in the City of Rome. *J Geophys Res* 113:B01303. doi:10.1029/2006JB004873
- Marzi C, Bongiovanni G, Clemente P (1990) Seismic preservation of historical monuments in Roma, preliminary results from ambient vibration tests. In: Marinos P, Koukis G (eds). *Engineering*

- geology of ancient works, monuments and historical sites, pp 2133–2134
- Moscatelli M, Pagliaroli A, Mancini M et al (2012) Integrated subsoil model for seismic microzonation in the Central Archaeological Area of Rome (Italy). *Disaster Adv* 5(3):109–124
- Rovelli A, Malagnini L, Caserta A, Marra F (1995) Using 1-D and 2-D modelling of ground motion for seismic zonation criteria: results for the city of Rome, *Annali di Geofisica* 38:591–605
- Sbarra P, De Rubeis V, Di Luzio E, Mancini M, Moscatelli M, Stigliano F (2012) Macro seismic effects highlight site response in Rome and its geological signature. *Nat Hazards* 62(2):425–443. doi:[10.1007/s11069-012-0085-9](https://doi.org/10.1007/s11069-012-0085-9)
- SESAME (2004) Guidelines for the implementation of the H/V spectral ratio technique on ambient vibrations. Measurements, processing and interpretation. WP1 2 European commission—Research general directorate project no. EVG1-CT-2000-0026 SESAME, report D23.12, 62 pp

---

# Susceptibility Assessment of Subaerial (and/or) Subaqueous Debris-Flows in Archaeological Sites, Using a Cellular Model

# 70

Valeria Lupiano, Maria Vittoria Avolio, Marco Anzidei, Gino Mirocle Crisci,  
and Salvatore Di Gregorio

---

## Abstract

This study analyzes landslide susceptibility for archaeological sites in the Albano lake and Nemi lake areas, both in subaerial and in submerged zones by simulations of SCIDDICA-SS2, a Cellular Automata (CA) model for subaerial, subaqueous, both subaerial-subaqueous debris/mud/granular flows. Successful applications of SCIDDICA-SS2 permitted to simulate past events for the Albano lake area. New numerical simulations allowed susceptibility evaluations for gravitational instability related to the above-mentioned archaeological sites.

---

## Keywords

Archaeological sites • Debris-flow • Landslides susceptibility • Cellular automata

---

## 70.1 Introduction

Many archaeological sites are frequently interested by slope instability phenomena, sometimes with significant consequences such as partial or total destruction (Canuti et al. 2000). Often these sites are located in areas prone to flow-like landslides. The hazard in the archaeological sites, related to the evolution of these phenomena, has increased in recent decades because of changes in land use and negligence in controlling runoff practices. Forecasting techniques for debris-flows range from simple empirical correlations to dynamical models. Each method can “satisfactorily” cover

only some typologies of cases according to data quality, geological features and so on. These considerations suggested us to approach the problem by making use of alternative methodologies in order to obtain effective tools for forecasting the path and extension of debris flows. We selected the SCIDDICA CA model (Avolio et al. 2008, 2009) for a preliminary susceptibility assessment in the study areas, affected by flow-type landslides. The research goal is the creation of an integrated computational system, based on the computational paradigm of CA, coupled to a GIS, in order to simulate debris-flows in subaerial, subaqueous and mixed cases. Such a system is structured so that it can be effectively used for the susceptibility evaluation of debris-flows in archaeological areas. The sites of high archaeological importance, which were chosen as test cases, are located in Albano Lake and in Nemi Lake (Italy, Fig. 70.1). Both sites are, in fact, particularly exposed to debris-flows (Mazzanti et al. 2009).

---

V. Lupiano (✉) · G.M. Crisci  
Department of Biology, Ecology and Earth Sciences, University of  
Calabria, 87036 Rende, Italy  
e-mail: valeria.lupiano@unical.it

M.V. Avolio · S. Di Gregorio  
Department of Mathematics and Computer Science, University of  
Calabria, 87036 Rende, Italy

M. Anzidei  
National Institute of Geophysics and Volcanology, 00143 Rome,  
Italy

### 70.1.1 Study Area

Albano and Nemi lakes, respectively 293 and 316 m a.s.l., are located in the central part of volcanic apparatuses of the Alban Hills. The two volcanic cones are characterized by

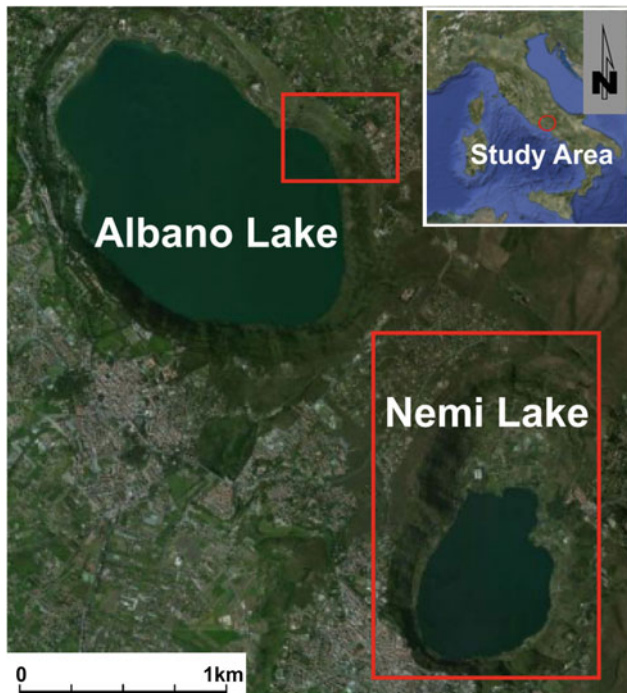


**Fig. 70.1** Study area (Bing Aerial Photo)

steep internal walls subject to intense erosion, due to gravitational processes. These landslides are developed in outcrops of pyroclastic deposits and/or poorly cemented detrital. Such pyroclastic covers give rise to falls, debris-flows and roto-translational landslides (that can evolve in very rapid debris-flows).

Nemi and Albano Lakes were formed in the last stage of the evolution of Lati-um Volcano. The rock types, which are found in this territory, are related to the products of the Colli Albani volcanic district, whose activity lasted from about 600,000 to 30,000 years ago with the emplacement of pyroclastic flows, lava flows and pyroclastic deposits. The area is still active today with repeated seismic swarms and crustal deformations (Anzidei et al. 1998, 2010; Riguzzi et al. 2009). Additionally, the lake level is continuously decreasing after the last seismic swarm that struck this area in 1987–1989 (Anzidei and Esposito 2010).

Along coasts and slopes near the lakes of Albano and Nemi lakes, very important archeological remains of pre-historic and Roman age are preserved. Moreover, on the NW shore of Lake of Nemi, the “Museum of the ships” is located, which houses many artifacts. Even in underwater environment the lakes are rich in archaeological finds. In fact, during Roman the Naumachiae, performances of naval battles took place on the lakes. Moreover, ruins of numerous roman villas collapsed on the bottom of the lakes can nowadays be found.

## 70.2 SCIDDICA-SS2, a CA Model for Flow-Type Landslides

CA represents a computational paradigm, for modelling complex systems, evolving on the basis of local interactions. SCIDDICA-SS2 =  $\langle T, X, Q, P, \tau \rangle$  is a deterministic CA for simulating subaerial, subaqueous flow-type landslides (Avolio et al. 2008, 2009), where:  $T$  is the finite hexagonal tessellation, corresponding to the region where the phenomenon evolves;  $X$ , the cell neighbourhood, identifies the geometrical pattern of cells, which influence any state change of the generic cell (the cell itself and six adjacent ones); cell relevant physical features as altitude, depth of erodible soil, landslide matter and outflows, their kinetic head and barycentre specify the set of states  $Q$ ; the set of the global physical and empirical parameters  $P$  accounts for the CA general frame related to the phenomenon, e.g. the cell apothem; eventually,  $\tau: Q^7 \rightarrow Q$  is the cell transition function. Debris in a cell is modelled as a block that can split into many parts, representing outflows, whose size minimizes locally differences of “height” (altitude plus debris thickness plus kinetic head) (Avolio et al. 2008, 2013a, b). Flow displacement is estimated by simple motion equations: slope movement with friction in the subaerial part and a modified Stokes equations with a form factor proportional to mass and gravity acceleration alteration by buoyancy rules motion in the subaqueous part. Computation of detrital cover erosion and kinetic head dissipation by turbulence completes the transition function (Avolio et al. 2008, 2013a, b).

Two main phases are needed for verifying the reliability of CA simulation models: the calibration phase identifies an optimal set of parameters capable of adequately reproducing the considered case; the validation phase tests the model on a sufficient (and different) number of cases similar in terms of physical and geomorphological properties. Once we have determined the optimal set of parameters, the model can be considered applicable in the same homogeneous geological context in which the parameters are derived. The likelihood between the area involved by the real landslide and the area involved in the simulation can be measured by the fitness function  $f: \sqrt{(R \cap S)/(R \cup S)}$  where  $R$  is the set of cells interested by the real landslide and  $S$  is the set of cells interested by the simulated landslide. These function returns values from  $0$  (completely wrong simulation) to  $1$  (perfect match); values greater than  $0.7$  are considered acceptable.

The adopted version SCIDDICA-SS2 was calibrated on the basis of simulations regarding debris-flows occurred on the eastern side of Albano Lake in 1997 (Avolio et al. 2009). It is a peculiar example because the path of the debris-flow was initially subaerial and afterward subaqueous. The intersection between real and simulated event (Fig. 70.2)

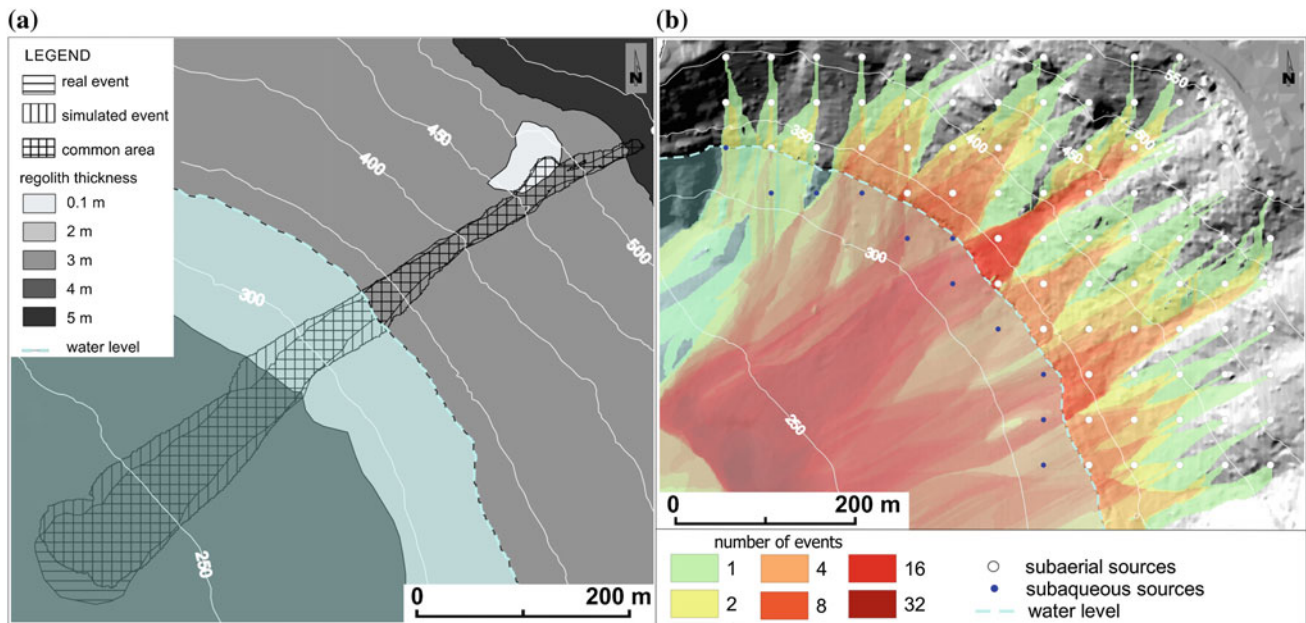


**Fig. 70.2** a Intersection between real and simulated event; b Albano Lake susceptibility zonation

returns a fitness value  $f = 0.85$  (Avolio et al. 2009). Other seven events, occurred on the shores of Albano Lake, were used for the SCIDDICA-SS2 validation. All of these events give results with  $f > 0.72$ .

### 70.3 Susceptibility Assessment

The SCIDDICA-SS2 CA model was used for a preliminary evaluation of the spatial hazard in the study area. Basics information required for such analysis are: (1) detailed

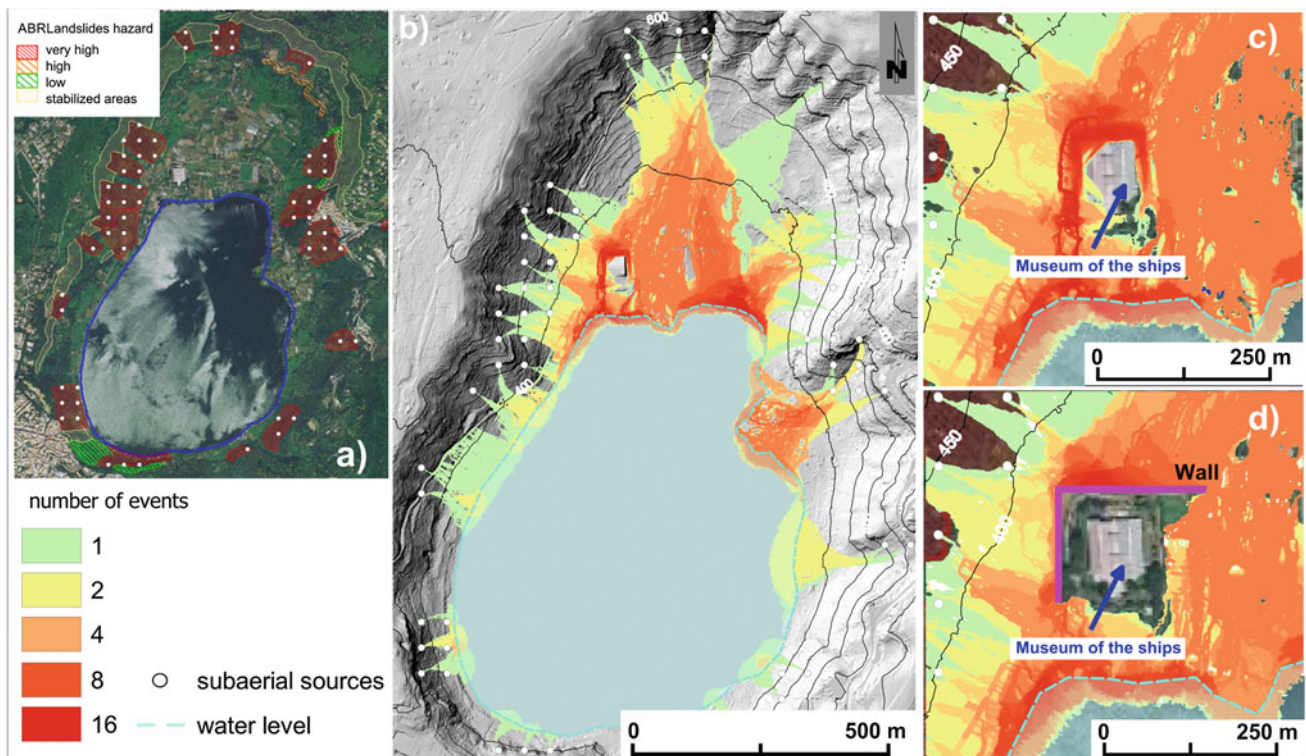


**Fig. 70.3** Nemi Lake a ABR landslides hazard; b susceptibility zonation; c "Museum of the ships" area first and d after placing of wall

DTM; (2) map of soil thickness overlying the bedrock, in this case consists of pyroclastic deposits poorly cemented; (3) location of landslide sources; (4) areal and volumetric size of landslide sources. Hexagonal cells with apothem equal to 0.5 m were adopted.

A very high resolution DTM (1:1000), based on LIDAR and Multibeam bathymetric data for the terrestrial and the lacustrine surfaces (Anzidei et al. 2006; Baiocchi et al. 2007; Anzidei et al. 2008), was available for analyzing the landslide occurrences, except the subaqueous part of the Nemi area, whose surveys were performed only by sounding apparatuses. Therefore, the susceptibility analysis excludes this zone. Figure 70.2a shows pyroclastic soil cover thickness detected for Albano Lake on geological observations. Regarding the detrital cover of Lake Nemi, literature data reported values of thicknesses between 3 m and 5 m. For this reason, not having available detailed surveys, a uniform thickness of 5 m was imposed.

89 hypothetical debris-flows, including 11 subaqueous ones, were simulated in the Lake of Albano area and their sources located at the vertices of a square grid with side length 50 m. A simple susceptibility scenario (Fig. 70.2b) was generated in a GIS by overlapping both subaerial and subaqueous flow paths.

Accurate analyses and studies of the *Autorità di Bacino* (ABR) of the Italian Lazio region (Regione Lazio 2012) were examined in order to select the most dangerous areas for debris-flows in Lake of Nemi. ABR records very high hazard areas (Fig. 70.3a), affected by landslides from extremely rapid to very rapid (such as rockfalls, debris flows, etc.), and/or landslides that are characterized by high volumes. A grid of hypothetical sources with side length 100 m was considered about these areas and 61 simulations were carried out. A susceptibility scenario (Fig. 70.3b) was obtained by simulation and overlapping of these hypothetical debris-flows.

The proposed methodology may be applied for assessing the effectiveness of protective measures, e.g. ground barriers for flows deviation. An application example was carried out placing a wall (height = 4 m), as morphological alteration in DEM, upstream of the “Museum of the ships”. New simulations of debris-flows were performed with such a modified morphology and compared with previous simulations without alterations. A new susceptibility scenario was created

(Fig. 70.3c, d) in order to verify the validity of the barrier and to analyse the effects in the areas affected by diverted flows.

## References

- Anzidei M, Esposito A (2010) The lake Albano: bathymetry and level changes. The Colli Albani Volcano. Special Publication of IAVCEI, 3. The Geological Society, London, pp 229–244
- Anzidei M, Carapezza ML, Esposito A, Giordano G, Lelli M, Tarchini L (2008) The Albano Maar Lake high resolution bathymetry and dissolved CO<sub>2</sub> budget (Colli Albani volcano, Italy): constraints to hazard evaluation. *J Volcanol Geoth Res* 171:258–268
- Anzidei M, Riguzzi F, Stramondo S (2010) Current geodetic deformation of the Colli Albani volcano: a review. The Colli Albani Volcano. Special Publication of IAVCEI, 3. The Geological Society, London, pp 299–310
- Anzidei M, Esposito A, De Giosa F (2006) The dark side of the Albano crater lake. *Ann Geophys* 49(6)
- Anzidei M, Baldi P, Casula G, Galvani A, Riguzzi F, Zanutta A (1998) Evidence of active crustal deformation of the Colli Albani volcanic area (central Italy) by GPS surveys. *J Volcanol Geoth Res* 80:55–65
- Avolio MV, Lupiano V, Mazzanti P, Di Gregorio S (2008) Modelling combined subaerial-subaqueous flow-like landslides by cellular automata. ACRI 2008, LNCS 5191. Springer, Berlin, pp 329–336
- Avolio MV, Lupiano V, Mazzanti P, Di Gregorio S (2009) A cellular automata model for flow-type landslide with simulations of subaerial and subaqueous cases. *EnviroInfo*, Berlino, Germania 1:131–140
- Avolio MV, Bozzano F, Di Gregorio S, Lupiano V, Mazzanti P (2013a) Simulation of submarine landslides by Cellular Automata methodology. In: Margottini C et al (eds) *Landslide science and practise*, vol 5. Springer, pp 65–72
- Avolio MV, Di Gregorio S, Lupiano V, Mazzanti P (2013b) SCIDDICA-SS3: a new version of Cellular Automata model for simulating fast moving landslides. *J Supercomput* 65:682–696
- Baiocchi V, Anzidei M, Esposito A, Fabiani U, Pietrantonio G, Riguzzi F (2007) *Intégrer Bathymétrie et lidar*. *Géomatique* 55
- Canuti P, Casagli N, Catani F, Fanti R (2000) Hydrogeological hazard and risk in archaeological sites: some case studies in Italy. *J Cult Heritage* 1:117–125
- AdBR Lazio (2012). [http://www.regione.lazio.it/binary/rl\\_ambiente/tbl\\_contenuti/piano\\_assetto\\_idrogeologico/Tav2\\_aree\\_tutela\\_sud/TAV\\_2.02\\_Sud.pdf](http://www.regione.lazio.it/binary/rl_ambiente/tbl_contenuti/piano_assetto_idrogeologico/Tav2_aree_tutela_sud/TAV_2.02_Sud.pdf). PAI, Tav. 02 Feb 2012
- Mazzanti P, Bozzano F, Avolio MV, Lupiano V, Di Gregorio S (2009) 3D numerical modeling of submerged and coastal landslides propagation. *Adv Nat Technol Hazards Res Springer* 28:127–138
- Riguzzi F, Pietrantonio G, Devoti R, Atzori S, Anzidei M (2009) Volcanic unrest of the Colli Albani (central Italy) detected by GPS monitoring Current Geodetic Deformation 309 test. *Phys Earth Planet Inter* 177:79–87

Mastelloni Maria Amalia, Ercoli Laura, Nocilla Alessandra, Nocilla Nicola, Sciortino Rosanna, and Zimbardo Margherita

## Abstract

The archeological site of the *Latomia del Paradiso* (Syracuse) is endangered by severe instability phenomena due to the shape of walls, underground excavation and poor rock mechanical characteristics. The failure of large blocks from the vault of the underground areas and the detaching of rock “flakes” from the walls surfaces make the geotechnical zoning of the walls particularly complex. The zoning is based on the characteristics of the rock wall surfaces that, in first approximation, can be distinguished in regularized surfaces because of mining, and in irregular surfaces characterized by fracture propagation. The elaboration of reflectivity values obtained from a laser scanner survey provides a quick and reliable method, which can be very useful to assess the localization of alteration processes and their intensity. Alteration processes affect the mechanical characteristics and a decay of a rock mass shear strength is associated to them. Therefore, it has been possible to obtain a differentiated assessment of the safety conditions of the rock mass walls in areas where a direct assessment was too expensive or difficult because of the wall extension, or impossible. The measurements of reflectivity have been correlated to the Hammer Schmidt rebound values  $r$  both in soft rocks, such as those under consideration, and in stone formations of different rock types.

## Keywords

Latomiae • Soft rock • Rock weathering • Reflectivity • Geotechnical mapping

## 71.1 Introduction

The current arrangement of the east side of the *Latomiae del Paradiso*, ancient quarries that are partly open pit and partly underground, depends substantially from failure phenomena

M.M. Amalia

Parco Archeologico of Syracuse, Syracuse, Italy

E. Laura · N. Nicola · S. Rosanna · Z. Margherita (✉)

University of Palermo, Viale Delle Scienze, 90128 Palermo, Italy

e-mail: margherita.zimbardo@unipa.it

N. Nicola

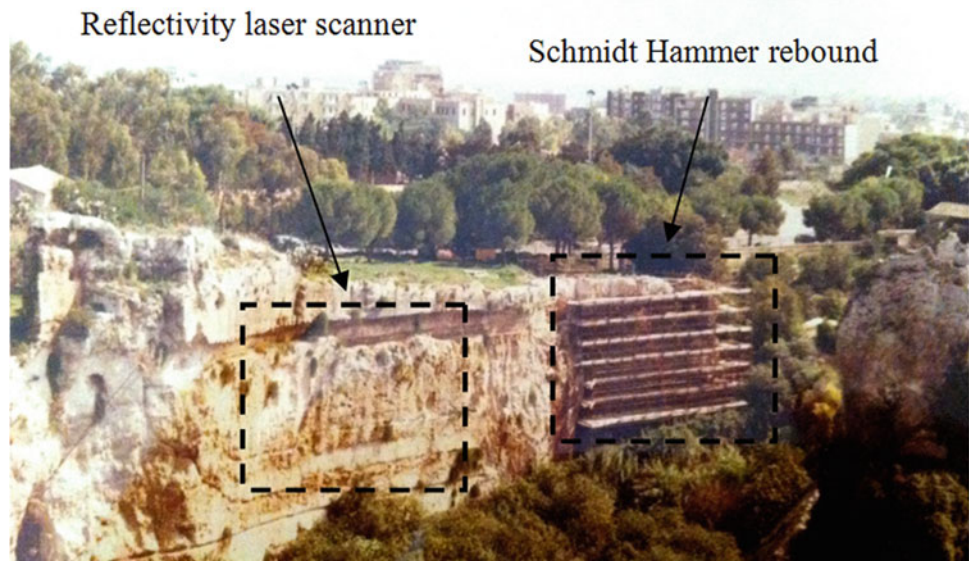
e-mail: nicola.nocilla@unipa.it

N. Alessandra

University of Brescia, Via Branze 43, 25121 Brescia, Italy

occurred over centuries. Previous studies have helped to provide a mechanical characterization of the rock and rock mass, in order to identify the factors that influence the stability of the walls (Ercoli and Speciale 1988). These studies have highlighted the difficulty to perform direct geotechnical measures because of the large size of the underground cavities and the vertical or overhanging configuration of walls. The *Servizio Parco* of Syracuse, which collaborates to a larger project on the study of Latomiae, has offered a considerable number of data which had been acquired with a laser scanner. This acquisition is part of a pilot project which is called “Polo museale di Syracuse” defined with INVITALIA in the Programma Operativo Interregionale Nazionale (POiN). The POiN is promoted by BB CC and IS, by MiBAC and MICT—Dipartimento Sviluppo e Coesione (2007–2013).

**Fig. 71.1** Investigated area:  
Latomia of Paradiso, eastern wall



As early as 1988 in an area of 300 m<sup>2</sup>, with the aid of a scaffolding, an investigation for geotechnical zoning of a wall sample area had been carried out by using direct methods (geological and meso-structural surveys, sampling for the physical and mechanical characterization of the rock, Schmidt hammer measurements) (Fig. 71.1). In this sector of the wall, surfaces regularized by mining, uneven surfaces caused by collapse, altered surfaces by water seepage and weathering agents coexisted.

The strength of the rock surface is strongly influenced by weathering processes (Zhao 1997), depending on the porosity of the material and on the presence of microcracks. The tendency of the material to absorb, reflect or transmit the electromagnetic radiation, varies with wavelength. This important property of matter allows the identification of the lithotypes by their spectral curve (spectral signature), (Johannsen and Sanders 1982). A correlation between the spectral signatures and the stone materials strength as a function of the alteration degree has therefore been considered as possible. Recent studies (Ercoli et al. 2013; Zimbaro et al. 2012) showed that the reflectivity measurements, carried out by means of laser scanner on rock surfaces, are correlated to strength characteristics. The opportunity to validate the laser scanner survey method for the geotechnical mapping was then taken into consideration for the present research. For the purposes of a more reliable zoning of the wall, in the investigated area particular attention was due to the recognition of the marks left on the wall by ancient hand excavation tool.

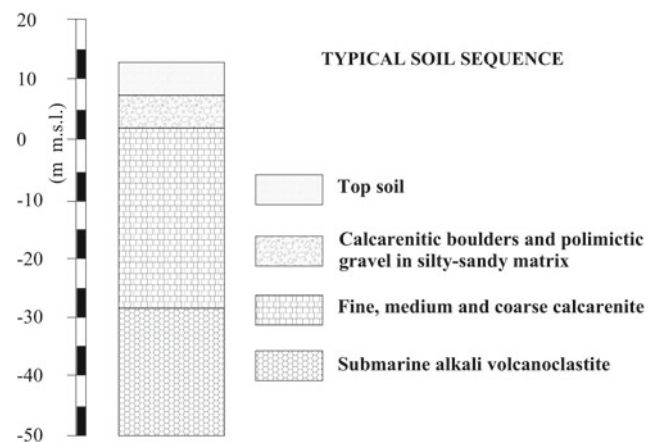


**Fig. 71.2** Typical soil sequence (Ercoli et al. 2014)

## 71.2 Geotechnical Characterization of the Rock Mass

A white or light-brown biocalcarenitic and calcirudite of Early-Middle Miocene with fine, medium and coarse-grained variations, outcrops on the Latomia wall; it is poorly or strongly cemented, belonging to the formation of the Climiti Mountains, Syracuse Member, overlaying submarine alkalin volcanoclastite (Fig. 71.2).

The physical and mechanical characteristics of intact rock, obtained by means of isotropic, triaxial and tensile tests, and of the rock mass both in dry or in the wet conditions are shown in Tables 71.1 and 71.2.

**Table 71.1** Physical and mechanical characteristics of intact rock

	Dry sample	Wet sample
Porosity n %	12–32	12–32
Unconfined compressive strength (MPa)	18–45	3.4–6.3
Tensile strength (MPa)	2.2	0.73

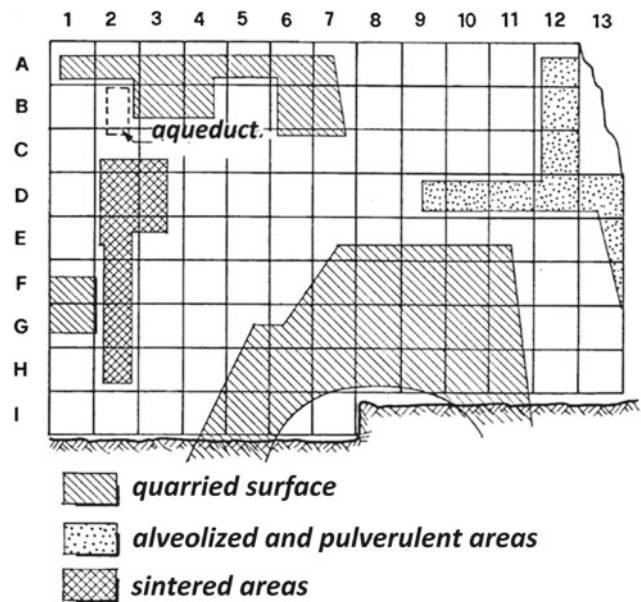
**Table 71.2** Mechanical characteristics of rock mass

	Dry rock mass	Wet rock mass
GSI (Hoek 1994)	55	30
Cohesion $c'$ (MPa)	0.93	0.25
Friction angle $\Phi'$	33°	21°

Saturation processes in the rock material are a direct result of the increased water leakages in the aqueducts carved in the rock and, as a consequence, a localized decay of the rock mass mechanical characteristics occurs.

### 71.3 Wall Zoning

The measurements of reflectivity (I) were carried out by means of the laser scanner Leica Scan Station, which has a field of scanning of  $360^\circ \times 270^\circ$ . The speed of acquisition can reach up to 4,000 points/s. The wavelength of the emitted ray  $\lambda$  is between 510 and 540 nm. The scan was performed with a density of 2 cm. The reflectivity measurements elaboration and their comparison with non-destructive investigation, (e.g. Schmidt hammer) was performed to validate the use of laser scanner not only for morphological and topographical reconstruction, but also for zoning the rock geomechanical conditions. The sector chosen for this study includes three types of surfaces: the upper level is constituted by an area of open pit (Classical and Early Hellenistic Age), below which a path was placed, whose residual wall is characterized by two *pinakes* (votive squared engravings in the rock) carved into the rock, according to a traditional use in Syracuse in the late Classical and Hellenistic periods (Mastelloni 2012). Below, a second level seems to retain traces of notches called “*pedarole*”, which had to allow the descent into a shaft. It is also thought that the “*pedarole*” could have perhaps given access to an underground quarry or be devoted to the inspections of underground water channels. The transformation of the same channel in a of open-air corridor path can be ascribed to a later stage, with the purpose of being an inspection path of the large underground channel now visible on the cliff. The western parts were canceled by a collapse so nowadays the remaining parts of the aqueduct are its upper vault, the eastern wall and its bottom. This water channel, whose height is between 1.70 and 2.30 m, is connected and functional to

**Fig. 71.3** Zoning obtained by the Schmidt hammer (Ercoli and Speciale 1988)

the water supply network of the area. Such a network can be attributed to the Hellenistic period. In the third level the traces of the collapse of an underground chamber’s vault are recognizable. The measures of rebound are useful to limit the areas with equal intensity of alteration or to identify poor quality rock areas. The zones of greater alteration are located below the aqueduct, orthogonal to the wall, where the dissolution process were more intense and the phenomena of collapse and detachment of rock “flakes” had already occurred. In the extreme southern sector, from a height of about 7 m from the top of the wall towards the basement, alveolization phenomena are diffused, with consequent localized decay of the mechanical characteristics. Rebound values, obtained from the Schmidt hammer, are between 10 and 40 and, in correspondence to these values, uniaxial compression strength values between 10 and 50 MPa have been measured. The zoning obtained by the Schmidt hammer is shown in Fig. 71.3. The laser scanner detection was performed on a contiguous visible portion of the same wall while the remaining part has been resulted hidden behind vegetation. The processing of the values of reflectivity index  $I$ , between 37 and 58 %, highlights the different levels of absorption of the rock (Fig. 71.4). The lowest values that correspond to the most intense weathering of the material have been recorded in areas next to the topographic surface. The highest values correspond to areas regularized by mining. For this almost flat areas, the regularity of the walls has reduced the vulnerability of the material because of the lower specific surface which is exposed to the weathering agents.

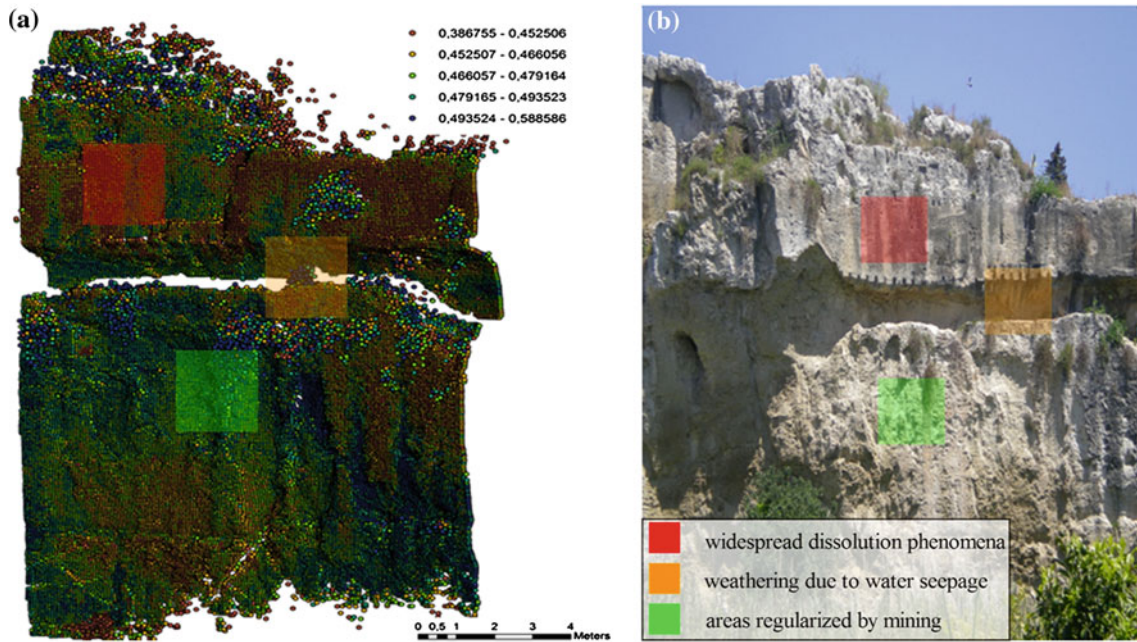


**Fig. 71.4** a Reflectivity values by laser scan. b Photo of the investigated area

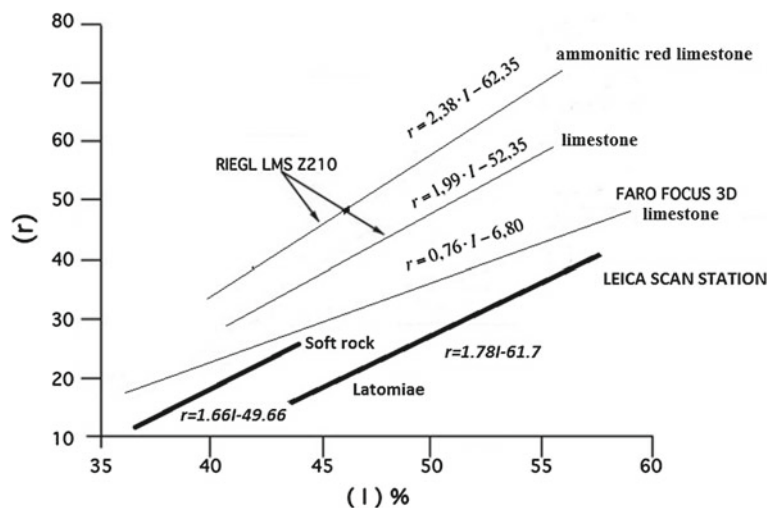
Below the aqueduct a reduction of the reflectivity values is present, the porosity of the rock has been modified by water seepage. Similar variability has been observed in the dry weight values variable between 14.4 and 23.5 kN/m<sup>3</sup>. Lowest values are associated to widespread dissolution phenomena, while the highest values are linked to a considerable degree of cementation. These three areas can be associated to three different decay classes for the rock mechanical characteristics, similar to those measured by means of the Schmidt hammer.

Given the relationship between dry unit weight and the rebound *r*, the data obtained by the Schmidt hammer were correlated to the reflectivity even if detected in neighboring

areas (Fig. 71.5). The slope of the fitted straight line is similar to that relating to another type of soft rocks (Calcarenite of Palermo and Marsala) which has been measured in the laboratory with the same technique on blocks with a length of 15 cm and a width of 20 cm (Zimbaro 2011). In the same figure the data obtained by different survey performed on other lithotypes are showed. In these cases, for each sampling area (approximately 20 × 20 cm) the rebound value *r* was obtained as the average value of about 20 measurements.

The study validated the possibility of a geomechanical zoning and highlighted the different responses of excavation anthropogenic surfaces through the elaboration of the reflectivity data recorded by means of the laser scanner.

**Fig. 71.5** Graph of correlations for reflectivity against rebound data



## References

- Ercoli L, Speciale G (1988) Rock weathering and failure processes in the Latomia del Paradiso (Syracuse, Italy). In: I.A.E.G. INT. SYMP, pp 771–778
- Ercoli L, Megna B, Nocilla A, Zimbardo M (2013) Measure of a limestone weathering degree using laser scanner. *Int J Archit Herit: Conserv Anal Restor* 7(5):591–607
- Ercoli L, Zimbardo M, Nocilla A (2014) Rock decay phenomena and collapse processes in the “Latomiae del Paradiso” in Syracuse. *Eng Geol* 178:155–165
- Johannsen CJ, Sanders JL (1982) Remote sensing for resource management. Soil Conservation Society of America, Ankeny
- Mastelloni MA (2012) Cave e materiali utilizzati in alcuni monumenti di Siracusa, in *Arqueología de la Construcción IV, Le cave nel mondo antico: sistemi di sfruttamento e processi produttivi*, Conv Int., Padova 22-24/11/2012
- Zhao J (1997) Joint surface matching and shear strength. *Int J Rock Mech Min Sci* 36:179–185
- Zimbardo M (2011) Valutazione dell’alterazione con laser scanner negli ammassi a struttura orientata e nella diagnostica dei beni monumentali. *Meccanica dei Materiali e delle Strutture* 2(1):41–51 (DICA)
- Zimbardo M, Nocilla N, Ercoli L, Sciortino R (2012) Valutazione dei parametri della resistenza al taglio delle discontinuità con l’ausilio del laser scanner. In: *Nuovi Metodi di indagine, monitoraggio e modellazione degli ammassi rocciosi*. CELID, Torino, pp 49–66

Izabela Laskowicz and Teresa Mrozek

---

## Abstract

Owing to intensification of extreme rainfall events since 1990s, widespread landsliding was observed in Central Europe. In Poland, devastating mass movements concentrated in the Flysch Carpathians (PFC) and at their foreland. This area is also known for many sacred cultural heritage objects, including those of spectacular Woodcraft Architecture Trail (WAT). Here, the natural (e.g. geologic) propensity to slope failure was often overlooked, so was a potential hazard. With selected examples of masonry and wooden structures, sacred historical heritage assets are discussed in the context of landsliding threats and related preventive measures. The landslide monitoring under the Landslide Counteracting System i.e. SOPO project is targeted on warning and performance purposes with reference to public buildings or infrastructure. If addressed to landslides affecting sacred historical objects, it contributes to better recognition and mitigation of hazard. The paper also shows that the structural stabilization implemented for the complex of the religious worship site in the eastern PFC was successful and withstood impact of extreme precipitation trigger of spring/summer 2010.

---

## Keywords

Landslide hazard • Sacred historical heritage • Wooden/masonry monuments • SOPO-project monitoring

---

## 72.1 Introduction

Poland is only moderately prone to natural hazards, however, disasters such as floods and landslides are the threats resulting in the major economic losses. They are also rapid-onset risk factors to cultural heritage (e.g. Canuti et al. 2009). Since the late 1990s extreme rainfalls have affected Central Europe. In relation to precipitation triggers, intensified widespread floods and landslides were observed in effect (e.g. Bissolli et al. 2011, Pánek et al. 2011). In Poland,

resultant damage was particularly severe in the Flysch Carpathians and did not save sacred cultural heritage. To outline the problems, in this paper selected sacred historical assets are discussed in the context of landslide hazard and related preventive measures or monitoring.

---

## 72.2 Geological Setting and Landslides Inventoried Under the SOPO Project

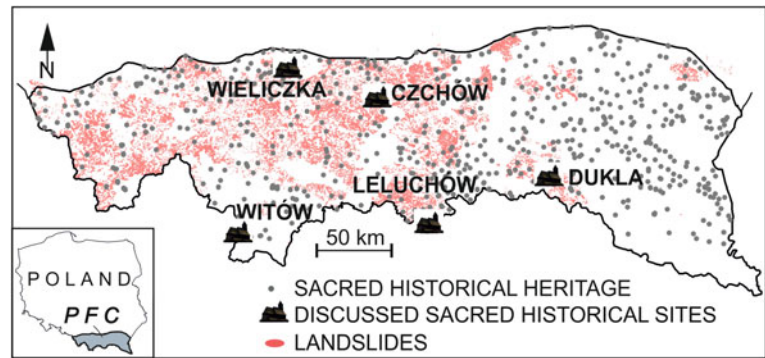
In Poland landslides concentrate in the Flysch Carpathians (PFC) and at their foreland. The PFC are built of flysch series (alternated sandstones, conglomerates, mudstones, shales) deposited by turbidity currents. The folded and detached flysch sediments formed uprooted nappes which all were thrust over northward onto the Miocene deposits of the Carpathian Foredeep. Structural anisotropy of the region is additionally enhanced by numerous transverse faults

---

I. Laskowicz · T. Mrozek (✉)  
Carpathian Branch, Polish Geological Institute – National  
Research Institute, 1 Skrzatów St., 31-560 Cracow, Poland  
e-mail: teresa.mrozek@pgi.gov.pl

I. Laskowicz  
e-mail: izabela.lakowicz@pgi.gov.pl

**Fig. 72.1** Location of sacred historical heritage assets on the background of landslides inventoried under SOPO project



(Margielewski 2006). The hillsides are often mantled with weathering covers, skeletal or loamy soils resting on loess-like deposits. Slope gradients are often steep (up to 50°). Indeed, particularly devastating multiple landsliding occurred just in 1997. Then, detrimental events of 2000–2006 were spatially more confined, but in 2010 almost all the PFC, from the boundary with the Czech Republic to that with Ukraine, were affected by landsliding. After slope failures experienced in 1997–2001 (estimated material losses in two Carpathian provinces amounted to ca.  $53.3 \times 10^9$  € in 2000–2001), the need for updated inventory of landslides became apparent. The national Landslide Counteracting System project (SOPO in Polish) for mapping landslides and terrains prone to mass movements in 1:10000 scale was effectively launched in 2008 (Mrozek et al. 2013). Until April 2014, up to 39,464 landslides affecting the PFC (ca. 20,000 km<sup>2</sup>) have been uploaded into the SOPO database. Apart from identifying landslides, the SOPO project is targeted on monitoring of ca. 100 landslides threatening goods of public interest.

### 72.3 Cultural Heritage in the Carpathians: General Setting

The National Cultural Heritage Register lists historical assets (i.e. estates) including here the sacred heritage, which (by definition) comprises churches of different faith, chapels, sites of religious worship, monuments, wayside shrines etc. ([http://www.nid.pl/pl/...](http://www.nid.pl/pl/)). Up to 19 % of all Polish sacred historical assets are found in the Carpathians and at their foreland. Therefore, this group of sacred assets is *par excellence* exposed to risk associated with natural disasters.

In the PFC, owing to a dense population and long-lasting expansion on slopes, man-made structures are wide-spread. With time, many gained the status of valuable historical monuments. Among them sacred objects form an outstanding class. In the remote past, their landscape setting had a traditional background. Roman Catholic churches were located closer to water courses, thus even on flood terraces or in mid-slopes. Orthodox churches (*tserkevs*), mainly

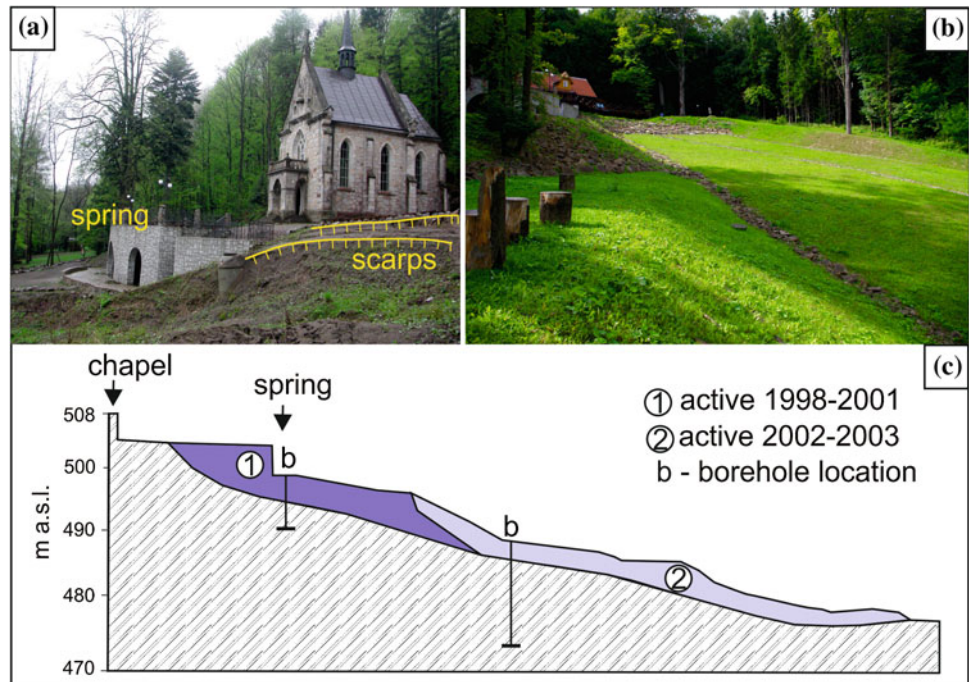
preserved in the eastern Polish Carpathians, were mainly located in summit parts of the hills. With progressing development and urbanization, the traditional setting of the churches was gradually ceasing, unfortunately hazardous locations were not avoided.

The marvellous feature of the region is the Woodcraft Architecture Trail (WAT), which also comprises precious churches. The latter are assigned to the National Cultural Heritage Register, while some (13) of them are also put into the UNESCO World Cultural Heritage List. Overlapping location of sacred cultural heritage objects with the landslide inventory map of the SOPO project evidences that many the sites are exposed to mass movement hazard (Fig. 72.1).

### 72.4 Sacred Cultural Heritage Objects at Risk: Exemplary Sites

An interesting example of the threat posed by landsliding to the sacred heritage is the worship site in the village of Trzciana near Dukla (Fig. 72.1). The hermitage of the 19th century with the later-built St. John of Dukla stony chapel and the cased spring (Fig. 72.2) were located on a slope which in itself was prone to failure (shale-sandstone flysch). Spectacular reactivation of the landslide was observed already in 1998 but the extreme displacements and damages occurred in 2000, and again later in 2002–2003. One of the landslide scarps had formed nearby the chapel wall and close to the miraculous (healing) spring (Fig. 72.2a). Examination of borehole cores indicated recurring sliding (multiple slickensides) and evidenced the slip surface in shales at maximum depth of 4.8 m. As the geo-engineering examination revealed the factor of safety (FS) less than 1, remedial actions were urgently undertaken to prevent damage of the object precious to pilgrims. Modelling of geophysical parameters showed that with a lowering of ground water level below the slip surface depth, FS would increase to 1.54 (Łukasik and Wysokiński 2001). Thus the crucial component of the remedial treatment was a system of subsurface drainage and open trenches (Fig. 72.2b, c). In the zone of the landslide scarp, stabilization comprised a retaining wall and

**Fig. 72.2** St John of Dukla sacred site affected by landsliding: **a** fissures of landslide scarp below the historical chapel and reconstructed spring chamber, **b** installed drainage system, **c** simplified landslide profile



a set of micropiles pinned in undisturbed substratum. The performance monitoring put into service showed that the undertaken measures are effective, as even extreme rainfall of May–June 2010, which triggered numerous landslides elsewhere, did not cause new failures here.

In relation to landsliding events of 2010 other precious sacred heritage objects were subjected to hazard. Although none of the sacred buildings were completely destroyed, many of them were seriously damaged. This was the case of the gothic church of 1364 in Czchów on the Dunajec river (Fig. 72.1). Obviously founders of the church were not aware of hazard. The masonry structure was set on a hillside so unfortunately as within a vast Holocene landslide (8 ha). The latter, being re-activated by the rainfall trigger in summer of 2010, made the church walls to crack. This landslide had been registered just under the SOPO project. Remedial measures are in a designing phase, as their implementing has to be taken with care in order to preserve historic and aesthetic values of the object.

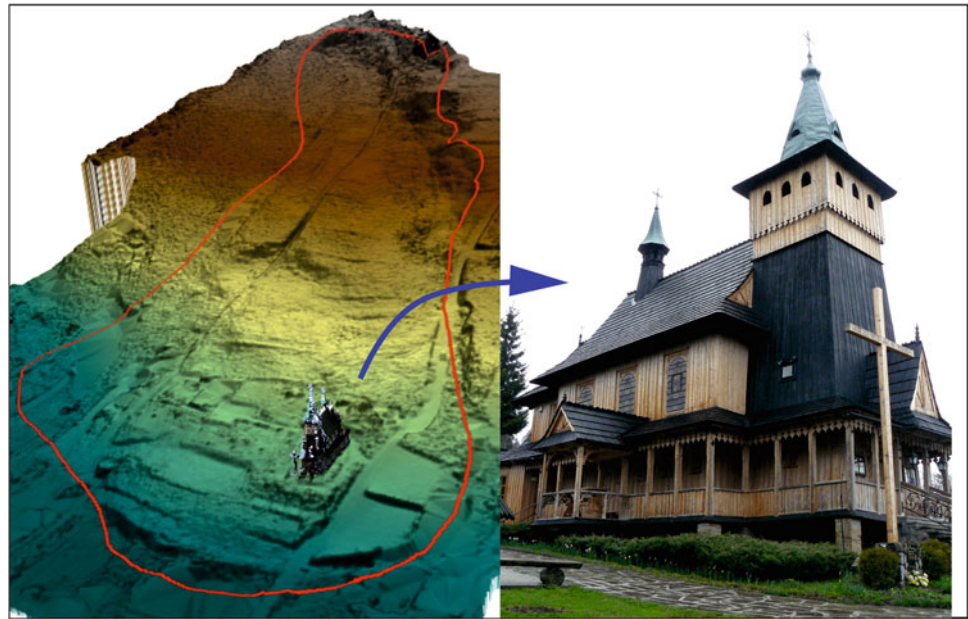
The St. Sebastian church of 1581 located in Wieliczka near Cracow and the 18th century Orthodox church in Leluchów (close to the Polish–Slovak border) demonstrate threatened wooden structures (Fig. 72.1). In the former case, the slope deformations of summer 2010 were serious, but remained the church structure intact, so the site is subjected only to systematic surface observations. In the second case, landslide activity in Leluchów was reported already in 1876. With no other reliable historic evidences, subsequent movements were observed in 1997 and 2001. At that time, the landslide seriously damaged the international road to

Slovakia, and because of that the landslide has been included in the SOPO project monitoring scheme. Since the measurements were initiated, the inclinometer records revealed three sliding surfaces and continual deformations. The total displacement of 70 mm (in 4-month period from 2009 to 2010) was recorded above the historic Orthodox church and, then, the inclinometer borehole was sheared. The monitoring continued in the remaining two boreholes located there, both for warning and protection purposes.

The wooden Roman catholic church of 1910–1920 in Witów (Fig. 72.1) is another object found in the WAT. At the time of the church erecting neither constructors nor a local society were aware of potential slope failures in the surroundings. Indeed, the church is located within an extent of the tongue of the Holocene landslide (Fig. 72.3), which is developed in sandstone-shale sediments.

The landslide used to be active in historic times, but it was not reactivated in 2010. Nonetheless, due to potential danger to the precious church, the landslide monitoring by terrestrial laser scanning (TLS) was set off for warning and preventive purposes. The laser point data, obtained using Riegl VZ-1000 scanner, were acquired with resolution 0.04 degree with laser Pulse Repetition Rate (PRR) of 300 kHz. The received final point cloud of the landslide contains 4,700 thousand of points measured with accuracy of about 8 mm. The TLS campaigns (scheduled twice per year) were performed already four times in low vegetation seasons (from September 2011). The data, after vegetation filtering, were used to generate precise DEMs of the landslide surface. The TLS data are verified by GNSS measurements of nine

**Fig. 72.3** Wooden Church in Witów (object of the woodcraft architecture trail) located on landslide monitored by TLS under SOPO project



geodetic points mounted within the landslide area. Both the methods have shown no deformations occurring on the landslide surface within the campaign period.

## 72.5 Closing Remarks

In the European context, the Carpathians are landslide susceptible (Holec et al. 2013), thus objects of historical cultural heritage located there can easily face a peril (e.g. Vlčko and Greif 2009). The PFC are not an exception in this respect as results from juxtaposition of environmental factors and human impact. First, owing to geologic and geomorphic setting, a number of recorded slope failures in the region as well as an area occupied by landslide deposits significantly exceed those in other parts of the country. Second, sacred cultural monuments, apart from having high historical and cultural values, are also important as lively sites of religious worship. To satisfy needs of numerous inhabitants sacred objects were set in many locations, often on flattened mid-slope segments. Unfortunately, these morphologically appealing sites turned out to be usually hazardous locations as their genesis was related to landslide processes. Third, as exemplified by extreme precipitation experienced in the Carpathian region since the turn of the 20th century, precipitation seems to be a major trigger of landslides which damaged or generated peril to sacred objects. At present the counteracting comprises two streamlines: (i) implementation of stabilization measures and remedial treatment of the historical structures that have been damaged by suddenly triggered slope failures (case-tailored countermeasures as it was the case of Dukla worship site), (ii) warning/preventive monitoring of landslides threatening the sacred objects (like

in Leluchów and Witów) to assess a rate of displacement and to mitigate detriments by devising a set of protective structural and non-structural measures. Finally, it is expected that the completion of landslide inventory under SOPO will contribute to improved evaluation of sacred objects at risk.

**Acknowledgments** Authors are grateful to their team colleagues, especially Z. Perski, W. Rączkowski and B. Bąk, for their support to the study and valuable discussions. SOPO project is financially supported by the National Fund for Environmental Protection and Water Management.

## References

- Bissolli P, Friederich K, Rapp J, Ziese M (2011) Flooding in eastern central Europe in May 2010 – reasons, evolution and climatological assessment. *Weather* 66(6):147–153
- Canuti P, Margottini C, Fanti R, Bromhead EN (2009) Cultural heritage and landslides: research for risk prevention and conservation. In: Sassa K, Canuti P (eds) *Landslides—disaster risk reduction*. Springer, Heidelberg, pp 401–405
- Holec J, Bednarik M, Sabo M, Minar J, Yilmaz I, Marschalko M (2013) A small-scale landslide susceptibility assessment for the territory of Western Carpathians. *Nat Hazard* 69(1):1081–1107. doi:10.1007/s11069-013-0751-6
- Łukasik S, Wysokiński L (2001) Osuwisko przy kościele św. Jana z Dukli. In: Kaszyńska M (ed) *Awarie budowlane: XX Konferencja Naukowo-Techniczna, Szczecin-Międzyzdroje, vol. 2, 22–26 maja, 2001*, pp 511–518
- Margielewski W (2006) Structural control and types of movements of rock mass in anisotropic rocks: case studies in the Polish Flysch Carpathians. *Geomorphology* 77:47–68
- Mrozek T, Wójcik A, Zimnal Z, Grabowski D (2013) Landslide inventory in 1:10000 scale in Poland—benefits and dilemmas of a national project. In: Margottini C, Canuti P, Sassa K (eds) *Landslide Science and Practice, vol 1., Landslide inventory and susceptibility and hazard zoning* Springer, Heidelberg, pp 51–55

- Pánek T, Brázdil R, Klimeš J, Smolková V, Hradecký J, Zahradníček P (2011) Rainfall-induced landslide event of May 2010 in the eastern part of the Czech Republic. *Landslides* 8:507–516
- Vlčko J, Greif V (2009) Environmental hazards: the results of engineering geological failures on cultural heritage. In: Sassa K, Canuti P (eds) *Landslides—disaster risk reduction*. Springer, Heidelberg, pp 407–411
- [http://www.nid.pl/pl/Informacje\\_ogolne/Zabytki\\_w\\_Polsce/rejestr-zabytkow/zestawienia-zabytkow-nieruchomych/](http://www.nid.pl/pl/Informacje_ogolne/Zabytki_w_Polsce/rejestr-zabytkow/zestawienia-zabytkow-nieruchomych/). Accessed 13 Sept 2013

---

# Preservation of Cultural Heritage of Sant'Agata de' Goti (Italy) from Natural Hazards

# 73

Anna Scotto di Santolo, Filomena de Silva, Domenico Calcaterra,  
and Francesco Silvestri

---

## Abstract

Sant'Agata de' Goti, Italy, is a small town resting on a tuff relief between two creeks, where many anthropic cavities, due to the tuff quarrying activity, are present. The tuff roof is few meters deep, so the adopted open-pit technique gave out superstructures strictly connected to the underlying cavities. This study is focused on the investigation of the possible failure mechanisms of a typical cavity, located along the edge of the cliff. After the collection and the interpretation of the geological and geotechnical data, a back analysis of the strength parameters of the fractured rock mass was carried out through the 2D FLAC code. Starting from the fissuring pattern observed in the field, a 'ubiquitous joint' constitutive model implemented into the code was utilized. The analyses confirmed that orientation, spacing and friction strength of the discontinuities affect the instability mechanisms of the cavity and play a very important role on the safety conditions of the building heritage of this attractive town.

---

## Keywords

Cavity • Numerical analyses • FLAC code • Pyroclastic rocks • Joints

---

## 73.1 Introduction

The historical center of Sant'Agata de' Goti, located in Campania region (Italy), rests on the flat top of a N–S oriented elliptical ridge (Fig. 73.1), about 50 m high, about 170 m wide and 600 m long, and delimited by the Riello and Martorano creeks. Both seismic and landslide hazards are due to the typical morphology consisting of a soft rock slab lying on a thick deformable soil layer, which is frequently detected for

other similar small historical towns in Central-Southern Italy (Fenelli et al. 1998). The damage suffered by some cavities, in static and dynamic conditions, testify that the interplay between seismic and landslide hazards might become particularly critical where the interaction between buildings and cavities is significantly intense. In this multi-risk scenario, the aim of the paper is the evaluation of the stability of a typical cavity, located along the edge of Martorano ridge. The stress state induced by the excavation in the tuff ridge has been reproduced through a numerical simulation with the 2D FLAC code (Itasca 2011), in order to compare the results to the joint pattern observed. Then a discontinuous equivalent model, consistent with the detected family of joints, has been adopted in order to evaluate the safety conditions.

---

A. Scotto di Santolo (✉)  
Università Telematica Pegaso, Centro Direzionale,  
Piazza Cenni, 2, 80143 Naples, Italy  
e-mail: anna.scottodisantolo@unipegaso.it

F. de Silva · F. Silvestri  
DICEA Università degli Studi di Napoli Federico II,  
Via Claudio 21, 80125 Naples, Italy

D. Calcaterra  
DISTAR Università degli Studi di Napoli Federico II,  
Largo San Marcellino, 10-80138 Naples, Italy

---

## 73.2 Subsoil Characterization

The rock formation constituting the ridge is the Campanian Ignimbrite in its yellow and grey lithofacies, lying on a thin loose layer of pyroclastic soil and a Miocene flysch

**Fig. 73.1** Western cliff of Sant'Agata de' Goti, along the Martorano creek. The red circle shows the location of the hypogean cavity analyzed in the paper



formation, cropping out in the Riello creek (Fig. 2a, b). In 1994 a comprehensive subsoil investigation was carried out through the whole historical centre, consisting of 40 boreholes, georadar measurements, down-hole tests and the installation of some inclinometers. The boreholes, drilled down to 40 m, intercepted about 4 m of made ground, sometimes mixed to pyroclastic soil (MG-PS), about 10 m of Lithified Yellow Tuff (LYT) and the Welded Grey Ignimbrite (WGI), without reaching the Miocene flysch formation. Both the grey and the yellow tuff lithofacies are crossed by joints belonging to various sets, which are evident along the slopes of the cliff (Fig. 73.2c) and inside the cavities. The discontinuities are partly syngenetic (i.e. the result of the sudden cooling of the volcanoclastic formation), partly related to mechanical processes, such as stress relief due to the proximity to the slopes, excavation and overburden load. A number of 64 discontinuities was detected in the cavities and interpolated in the equal angle or stereographic projection. Figure 73.2d shows the stereoplot of the structural joint system obtained; all the three dominant families are sub-vertical, being K1 aligned with the slopes direction, while K2 and K3 can be associated to the generation of unstable wedges, prone to toppling mechanisms along the tuff slopes. The presence of systematic geostructural features induces severe limitations to the applicability of classical material models based on the continuum mechanics; in previous investigations on cavity stability, the use of empirical classification and analysis methods was therefore preferred (de Silva et al. 2013).

### 73.3 The System of Cavities

The 160 hypogean cavities detected in the historical centre of Sant'Agata (Fig. 73.2a) were excavated for the extraction of the yellow tuff (LYT) and mainly utilized as storage. Due to the proximity of the rock mass to the ground level, the open-pit quarrying technique was mainly adopted. In other cases, the cavity was dug out through the preliminary excavation of a coated well. The hypogean ambiances are

constituted by one or more rooms, linked together by tunnels and often connected by stairwells to the building foundations. The interaction between cavity, foundation and building is more hazardous along the Martorano creek, where most of the cavities directly overlook the valley (Fig. 73.1). Their precarious stability is testified by the damages, consisting of block detachment from the roof and the walls, occurred during the 1980 Irpinia-Basilicata earthquake.

A typical cavity is shown in Fig. 73.3. It extends for 130 m<sup>2</sup> and is composed by three main rooms (A, B, C), one tunnel and two stairwells, accessed from inside the building and reaching the main rooms from different elevations. The roof of room A is a lowered vault presenting a cylindrical well covered with tuff bricks. The tunnel connecting the two main rooms A and B is about 3 m wide and 3.5 m high. The cavity presents systematic discontinuities, mainly N–S oriented, running on the ceiling and along the vertical walls (Fig. 73.3, pictures 2, 4, 5). The presence of some abutment walls testifies the damage occurred in the past.

### 73.4 Investigation on Failure Mechanisms

The results of preliminary numerical modeling were useful in providing a picture of the mechanism that may occur in the field and in estimating the parameters of interest on the stability conditions of the rock mass. Plane strain analyses were performed with the finite difference code FLAC 2D (Itasca 2011), with reference to the section A–A of the tunnel (Fig. 73.3b). The soil cover and the building were considered as overburden loads. The initial stress state was evaluated by assuming a value of the pressure coefficient at rest,  $k_0$ , equal to  $(1 - \sin\phi)$ .

The rock mass was assumed initially as a continuous, in order to reproduce the failure mechanisms observed and associated to the recent load history. The constitutive law of the tuff was assumed as elastic—perfectly plastic, with the Mohr Coulomb failure criterion. The parameters used for the intact rock are shown in Table 73.1. The volumetric bulk

**Fig. 73.2** Geological map showing the location of the cavities (a); A–A stratigraphic section (b); picture showing the typical aspect of the cliff (c); families of discontinuities (d)

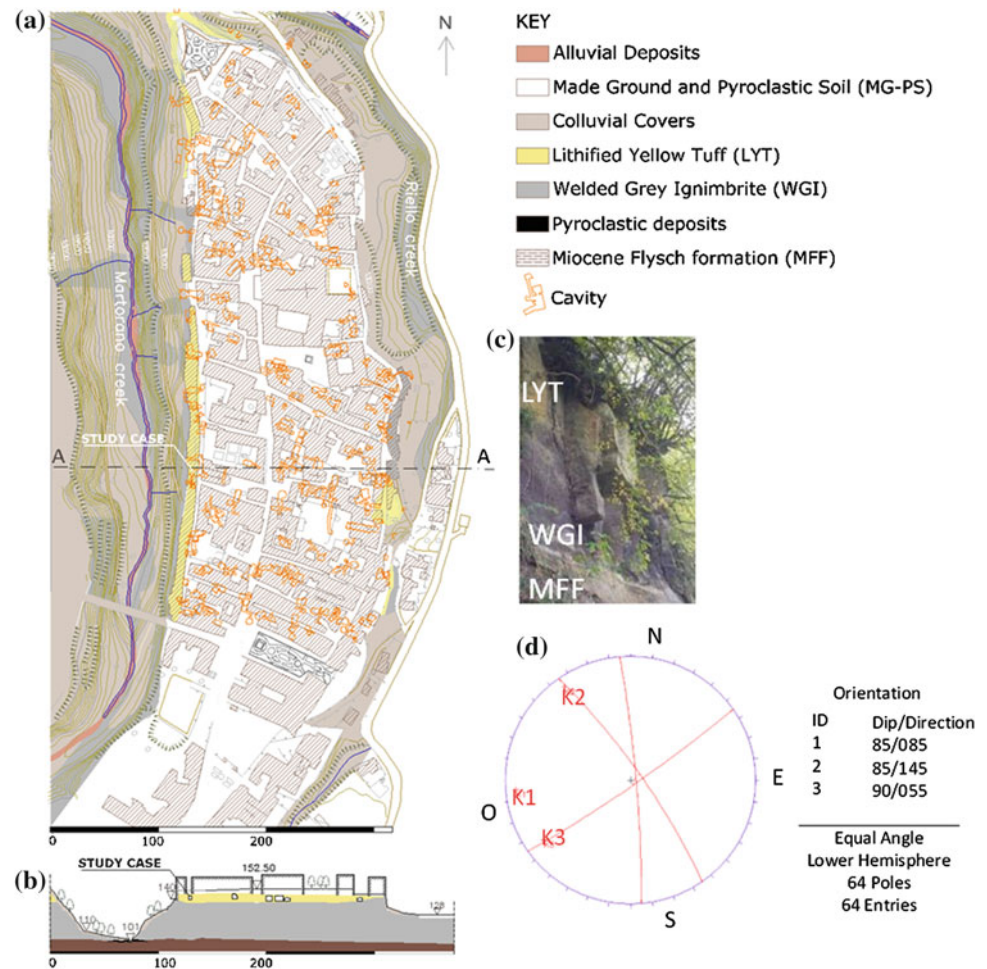


**Table 73.1** Mechanical parameters adopted in the numerical model

Analysis	Laboratory tests (intact rock)					Field tests (rock mass)			
	$\gamma$ (kN/m <sup>3</sup> )	$\sigma_c$ (MPa)	$\sigma_T$ (MPa)	$\phi$ (°)	$c$ (MPa)	$V_P$ (m/s)	$V_S$ (m/s)	$G_0$ (MPa)	$B$ (MPa)
Continuum	15.23	4	0.1	29	0.9	886	556	480	579
Ubiquitous joints			0.01 <sup>a</sup>	9 <sup>a</sup>	0.1 <sup>a</sup>				

<sup>a</sup> assumed from Q-system

modulus,  $B$ , and the shear modulus,  $G_0$ , were derived from the P and S wave velocities resulting from the down-hole tests. The unit weight,  $\gamma$ , and the uniaxial compression strength,  $\sigma_c$ , were taken equal to the mean values measured on 21 samples; instead, the tensile and shear strength parameters  $\sigma_T$ ,  $c$  and  $\phi$ , were derived from typical values reported in literature for pyroclastic weak rocks (Aversa and Evangelista 1998). The mechanical parameters assumed for the discontinuities are also reported in Table 73.1; these values were obtained from the Q-system index (Barton et al. 1974), being aware of the limitations of such empirical method.

The rock mass parameters have been obtained by means of the ‘strength reduction method’ built into the FLAC code. The safety factor, SF, is defined as the ratio between the

cohesion of the rock,  $c$ , to the critical value,  $c_{crit}$ , in correspondence of which the failure condition is triggered. For a Mohr–Coulomb material, the same factor is equal to the ratio between the compressive strength,  $\sigma_c$ , to that in correspondence of failure condition,  $\sigma_{crit}$ , if the friction angle is kept constant.

Figure 73.4a shows the plastic points obtained: the first evidences of instability are associated with the appearance of vertical cracks in the areas where the stress state reaches the tensile strength. The propagation of these fractures into the roof can trigger, as a first failure mechanism, a block fall (or local collapse for traction) consistent with the crack detected. The full development of fractures and yielding areas would eventually lead to the general collapse of the vault. The

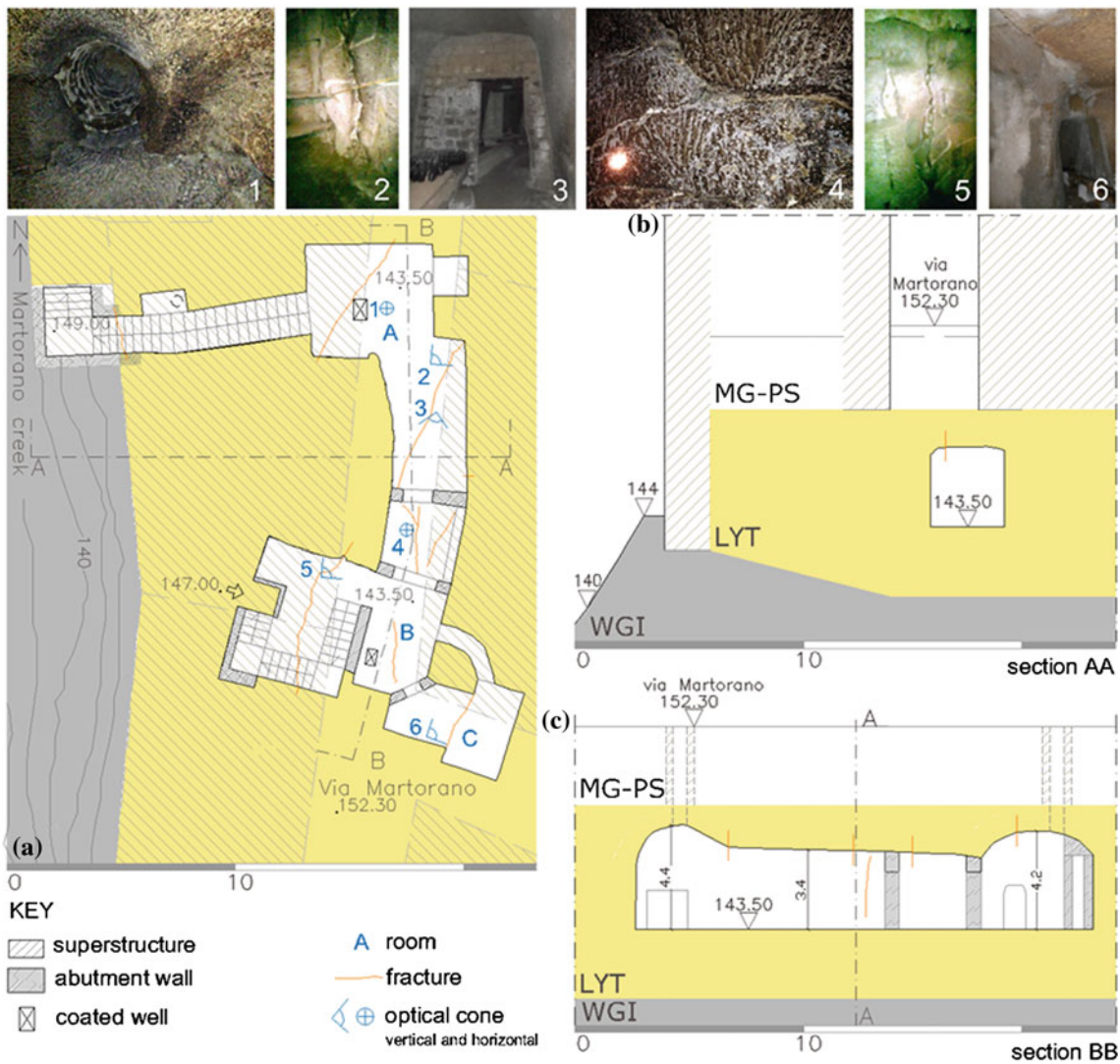


**Fig. 73.3** Plan (a) and sections (b and c) of the studied cavity with the joints observed

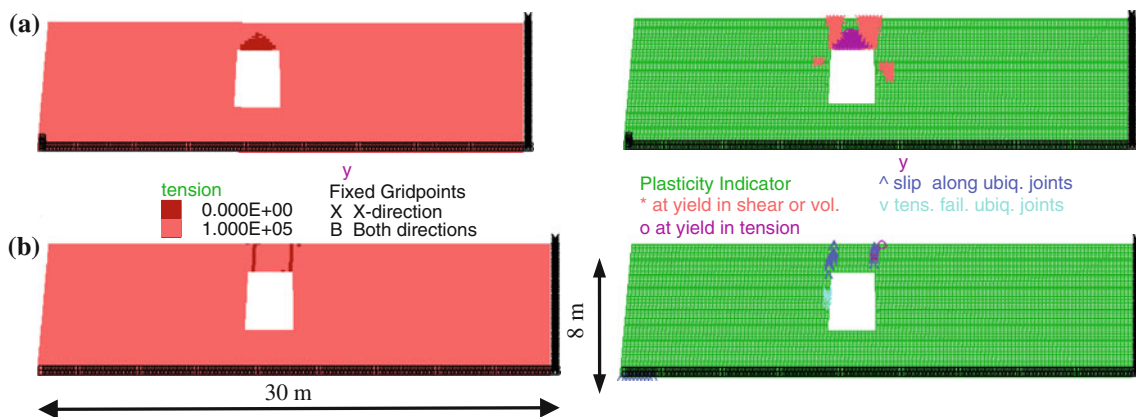


**Fig. 73.4** Tension and plasticity indicator for continuous (a) and ubiquitous joints models (b)

analyses were subsequently repeated with the ‘ubiquitous joint’ model, in order to investigate the potential failure mechanisms associated with the response of an equivalent

jointed rock mass. The presence of the first family of discontinuity observed in situ was used with the parameters reported in Table 73.1. The results are reported in Fig. 73.4b

in terms of plastic points obtained from the strength reduction method. In this case, the failure mechanism is associated mainly to the slip and tension failure along the imposed joints.

---

### 73.5 Conclusions

The paper reports the results of stability analyses on a typical anthropogenic cavity, located along the edge of the cliff at San'Agata de' Goti, Italy. The analyses were carried out by plane strain finite difference model with two different approaches. The results confirmed that orientation, spacing and friction strength of the discontinuities affect the instability mechanisms of the cavity. The approach, once extended to the whole territory, can be very useful to assess the degree of multi-hazard and to address the mitigation countermeasures, in order to increase the safety conditions of the building heritage of this attractive town.

### References

- Aversa S, Evangelista A (1998) Mechanical behaviour of a volcanic tuff: yield, strength and "destruction" effects. *Rock Mech Rock Eng* 31(1):25–42
- Barton N, Lien R, Lunde J (1974) Engineering classification of rock masses for the design of tunnel support. NGI Publication, Norwegian Geotechnical Institute, No. 106, Oslo
- de Silva F, Melillo M, Calcaterra D, Fascia F, Scotto di Santolo A, Silvestri F, Stendardo L (2013) A study for the requalification and safety against natural hazards of the environmental and building heritage of Sant'Agata de' Goti (Italy). In: Viggiani C et al (eds) *Proceedings of international symposium on geotechnical engineering for the preservation of monuments and historic sites*, Napoli. Taylor & Francis Group, London, pp 307–316
- Fenelli GB, Pellegrino A, Picarelli L (1998) Stability problems of old towns built on relict plateaux resting on clay deposits. In: Viggiani C (ed) *Proceedings of international symposium on geotechnical engineering for the preservation of monuments and historical sites*, Napoli. Rotterdam, Balkema, pp 163–173
- Itasca (2011) *FLAC (Fast Lagrangian Analysis of Continua) Version 7.0*. Itasca Consulting Group, Inc FLAC, Minneapolis

---

# A Study for Preserving the Freisa Terroir (Central Piedmont—Northwestern Italy) from Soil Erosion

74

Roberto Ajassa, Caterina Caviglia, Enrico Destefanis, Giuseppe Mandrone,  
and Luciano Masciocco

---

## Abstract

The potential soil loss has been evaluated at one of the hilly sites candidate as “Typical Piedmont Vineyard Landscapes: Langhe, Monferrato, Roero” to the World Heritage List of UNESCO. The geology of the study area is characterized by the Tertiary Piedmont Basin, sedimentary marine formations of Oligo-Miocene age. The soils belong to the medium and fine classes of *entisols* and, subordinately, *inceptisols*. In order to evaluate the annual soil loss caused by superficial runoff, the parametric empirical model USLE was applied. This method of simple structure has been integrated with the use of geographic information systems (GIS), which permitted to carry out the spatial analysis of the factors involved in the evaluation of the erosive process and the resulting erosion rate. Without grass cover, the areas most affected by the erosion are precisely those where the grapes grow. In this case, the average annual erosion rate has been estimated at 16.1 ton/ha with a 10 years return time rainfall. When the grass cover is present, instead, erosive phenomena are limited predominantly in the zones of outflow of the superficial water. The average annual erosion rate in areas planted with vines decreases in these conditions to 0.3 ton/ha, which shows how this method of management of the vineyards is appropriate against the danger of accelerated erosion.

---

## Keywords

Soil loss • Piedmont hills • USLE method • Freisa *terroir*

---

R. Ajassa · C. Caviglia · E. Destefanis · G. Mandrone ·  
L. Masciocco (✉)  
Dipartimento di Scienze della Terra, Università degli Studi di  
Torino, via Valperga Caluso 35, 10125 Turin, Italy  
e-mail: luciano.masciocco@unito.it

R. Ajassa  
e-mail: roberto.ajassa@unito.it

C. Caviglia  
e-mail: caterina.caviglia@unito.it

E. Destefanis  
e-mail: enrico.destefanis@unito.it

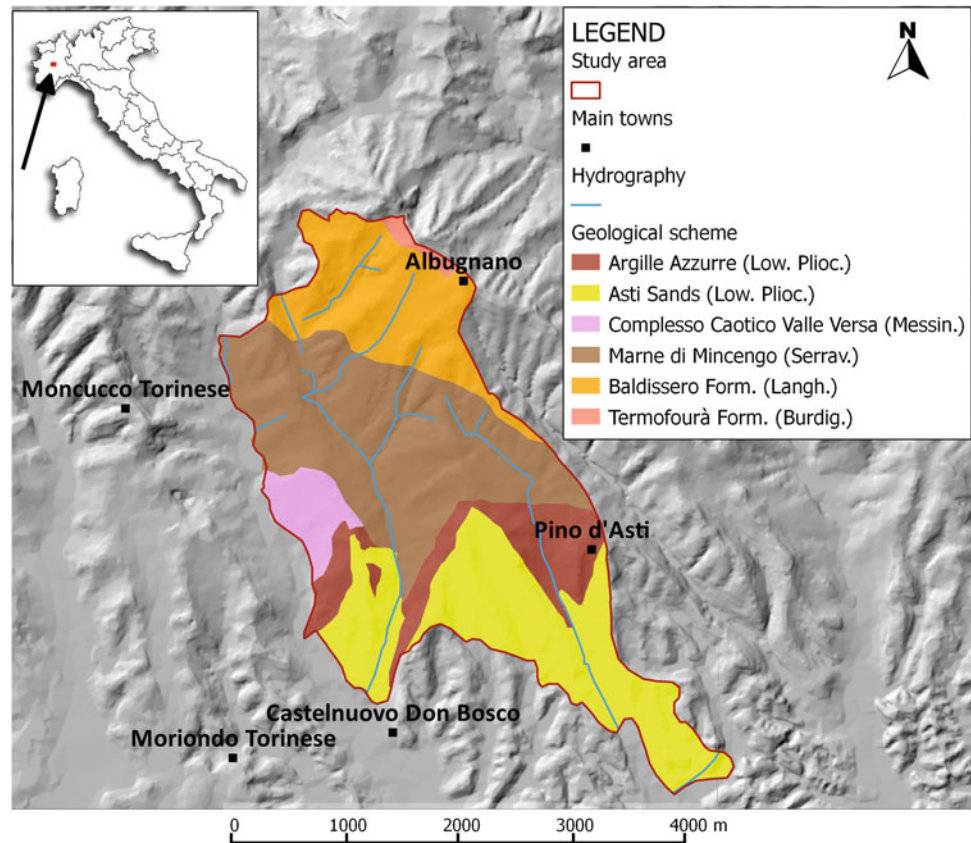
G. Mandrone  
e-mail: giuseppe.mandrone@unito.it

---

## 74.1 Introduction

The Freisa *terroir* is located in the central range of the Piedmont hills, in the municipalities of Albugnano, Castelnuovo Don Bosco, Pino D’Asti and Moncucco Torinese. This area is characterized by the cultivation of native grapes of Freisa and Malvasia wines: it is part of the landscape of the Langhe and Monferrato, candidates to UNESCO as World Heritage Site. The presence of Freisa crops at Piedmont Hills has been known since at least 500 years. Today it is cultivated in 116 municipalities but the production is concentrated around the town of Castelnuovo Don Bosco. “Freisa d’Asti” and “Freisa di Chieri” are the two wines DOC (*Denominazione di Origine Controllata*: controlled place of origin) related to the historic region of Freisa. Currently, the Freisa vine is experiencing a period of enhancement. Recent genetic studies,

**Fig. 74.1** Geological setting of the study area. Argille Azzurre: blue clays; Complesso Caotico Valle Versa: chaotic complex of the versa valley; Marne di Mincengo: Mincengo Marls



carried out by the IVV-CNR of Turin (Schneider et al. 2003), showed the first-degree family relationship between the Nebbiolo and Freisa vines.

## 74.2 Geological Setting and Pedological Features of the Area

The geology of the study area is characterized by the Tertiary Piedmont Basin (Piana and Polino 1995), generated by tectonic uplift of marine deposits of Oligo-Miocene age (Fig. 74.1).

In this sector, these sedimentary marine formations represent the northern flank of the Asti Syncline (whose axis is directed east–west) and so they are arranged from north to south in descending order of age (Festa et al. 2009).

The main geologic formations of the study area are represented by: the *Termofourà Formation* of Burdigalian age (divided in a silty conglomeratic member at the bottom and a marly-siliceous member at the top); the *Baldissero Formation* of Langhian—middle Miocene age (fossiliferous marls and arenites); the *Marne di Mincengo* of Serravallian age (whitish calcareous marls, sometimes with thin sandy intercalations); the *Complesso Caotico di Valle Versa* of Messinian age (blocks of varying size and composition—gypsum, vacuolar carbonates, fossiliferous micritic

limestones, marly limestones, carbonate breccias—embedded in a pelitic matrix); the *Argille Azzurre Formation* of lower Pliocene age, (clayey silts); the *Sabbie di Asti Formation* of Lower Pliocene age (medium-fine, homogeneous yellow sands, with a considerable degree of densification and a localized carbonate cementation). Holocenic silty and sandy-silty *fluvial deposits*, slightly weathered, with gravel interbedded, crop out in the creeks incisions.

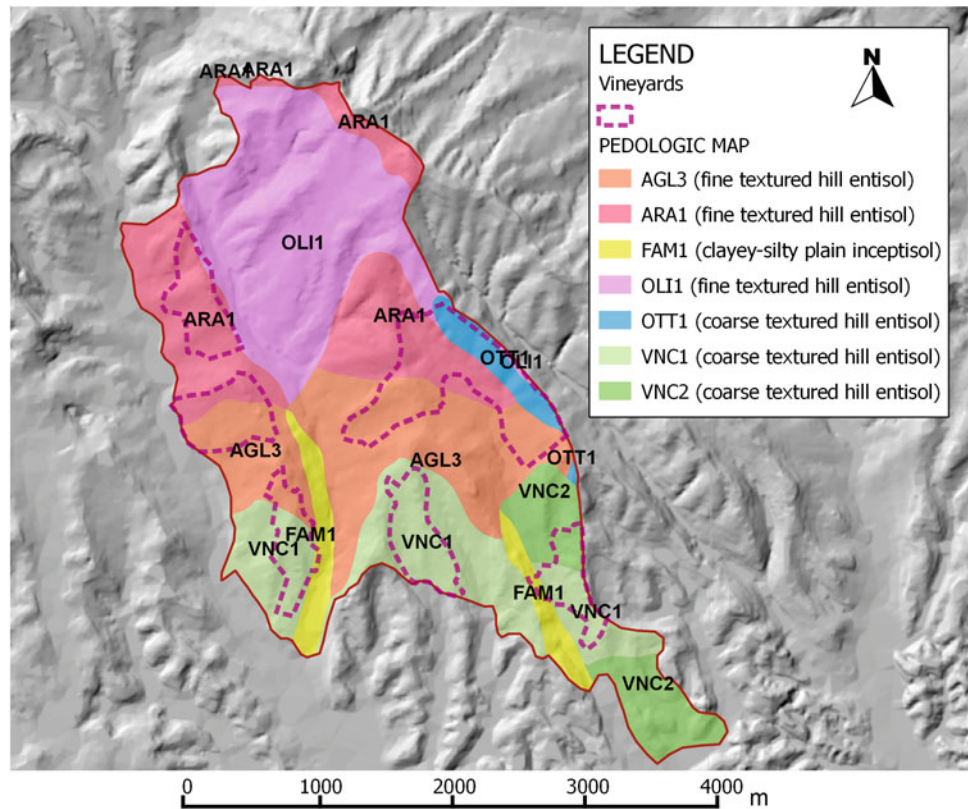
The soil features of the study area (Fig. 74.2) are described in the regional catalogue of the principal typological units of soils (Regione Piemonte 2010).

They are mainly represented by *fine textured hill entisols*, with fine-silty clay composition (AGL3, ARA1, OLI1), *coarse textured hill entisols* (OCT1, VNC1, VNC2), and *plain not idiomorphic and not gravelly clayey silty inceptisols* (FAM1).

## 74.3 Study Methodology

The USLE (Universal Soil Loss Equation) method for predicting soil erosion has been applied to the Freisa territory. It is a parametric empirical model that provides an evaluation of the annual soil loss caused by the superficial runoff erosion, using parcels homogeneous for dimension, type and use of the soil, topographic factors, cropping management

**Fig. 74.2** Pedologic map of the study area



factors and the rainfall energy (Wischmeier and Smith 1978). This method of simple structure has been integrated with the use of geographic information systems (GIS), which has permitted to carry out the spatial analysis of the factors involved in the evaluation of the erosive process and the resulting erosion rate. The annual soil loss  $A$ , expressed in ton/ha year, can be calculated with the following equation:

$$A = R \cdot K \cdot L \cdot S \cdot C \cdot P$$

where:

- $R$  = rainfall erosivity;
- $K$  = soil erodibility;
- $L$  = length of the slope;
- $S$  = degree of the slope;
- $C$  = cropping management;
- $P$  = conservation practice.

The rainfall erosivity factor  $R$  has been evaluated by means of the equation:

$$R = (E \cdot I_{30})/2540$$

where  $E$  is the specific energy of the rainfall event:

$$E = 916 + 313 \cdot \log(I_{30}/25.4)$$

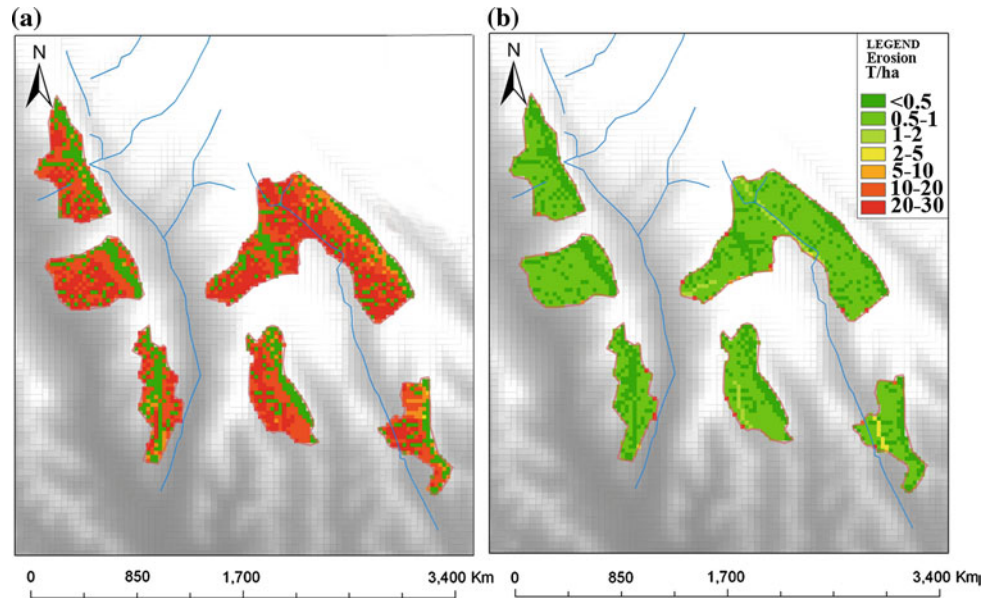
$I_{30}$ [mm/h] is the highest rainfall intensity, calculated considering the highest rainfall intensity of 30 min duration, obtained by the pluviometric data of the ARPA Piemonte monitoring network, taking into account the nearest station to the study area (Marentino). The pluviometric probability curve with a 10 years return time was calculated with the Gumbel equation (Gumbel 1941), to evaluate the hourly intensity of rainfall  $I_{30}$ .

The erodibility factor  $K$  of the soil coverage [ton/(ha · year · R)] was determined by means of a pedologic map with five classes defined on the basis of the percentage of fine material (<0.1 mm), coarse material (0.1–2.0 mm), organic matter, structure and soil permeability. A numerical value was attributed to each class using appropriate tables (Wischmeier and Smith 1978).

The length and the slope factors  $L$  and  $S$  and their information layers were calculated using specific tools of the ArcGis software. Slope and flow accumulation layers were derived from the digital elevation model (DEM) of the study area, (corrected for the presence of possible imperfections (sink). The evaluation of the  $L$  and  $S$  parameters was performed using the equation of Mitasova et al. (1996):

$$LS = (Flow\ acc \cdot cell\ size/22.13)^{0.4} \cdot [(\sin(slope) \cdot 0.01745)/0.09]^{1/4}$$

**Fig. 74.3** Annual potential soil erosion of the study area vineyards: **a** soil without grass cover; **b** soil with grass cover



where Flow Accumulation and Slope are raster layers of ArcGis that indicate respectively the water flux accumulation and the topographic surface slope. Cell size is the DEM resolution (grid mesh).

The cropping management factor  $C$  is a dimensionless coefficient that gives information about the use of the soil of the study area. It was obtained by the soil use map Corine Land Cover 2006 (Ispra 2010), assigning a value to each type of soil use, in agreement with literature data (Franzese et al. 2005). The difference between vineyards with or without grass cover was distinguished in the erosion evaluation using different coefficients.

The conservation practice factor  $P$  is a dimensionless coefficient ranging between 0 and 1. For the present study a unitary value was chosen as precautionary.

## 74.4 Results and Discussion

The USLE method was applied considering a project rainfall with a 10 years return time, at first on a bare soil. Without grass cover, in the vineyard areas, the average annual erosion rate has been estimated in 16.1 ton/ha (Fig. 74.3a), above the soil loss tolerance that, for a specific soil, ranges from 5 to 12 tons/ha/year (web ref. 4.1—[http://www.nrcs.usda.gov/Internet/FSE\\_DOCUMENTS/nrcs143\\_012269.pdf](http://www.nrcs.usda.gov/Internet/FSE_DOCUMENTS/nrcs143_012269.pdf)). When the grass cover is present, instead, erosive phenomena are limited predominantly in the zones of outflow of the superficial water (Fig. 74.3b). The areas affected by the higher values of erosion are rather limited. The average annual erosion rate in areas planted with vines is in this case estimated to 0.3 ton/ha, well below the soil loss tolerance.

The experience revealed the importance of the GIS system for a spatial evaluation of the soil erosion. Nevertheless, more precise information about topography (DEM) and litho-pedologic features of the soil would be necessary to obtain better results. Moreover, the importance of soil conservation practices like the grass coverage maintenance for such valuable territories has been emphasized.

## References

- Festa A, Dela Pierre F, Irace A, Piana F, Fioraso G, Lucchesi S, Boano P, Forno MG, Polino R (2009) Note illustrative della Carta Geologica d'Italia alla scala 1:50.000. Foglio 156 Torino Est. APAT, Dipartimento Difesa del Suolo, pp 143
- Franzese PP, Melchiorre R, Scopca A (2005) Erosione del suolo: l'applicazione del modello USLE al territorio della Regione Basilicata. Ecodinamica-Biologi Italiani
- Gumbel EJ (1941) The return period of flood flows. *Ann Math Stat* 12 (2):163–190
- Ispra-Istituto Superiore per la Protezione e la Ricerca Ambientale (2010) La realizzazione in Italia del Progetto Corine Land Cover 2006. Rapporti Ispra 131/2010
- Mitasova H, Hofierka J, Zlocha M, Iverson RL (1996) Modeling topographic potential for erosion and deposition using GIS. *Int J Geogr Inf Sci* 10(5):629–641
- Piana F, Polino R (1995) Tertiary structural relationships between Alps and Apennines: the critical Torino Hill and Monferrato area, Northwestern Italy. *Terra Nova* 7:138–143
- Regione Piemonte (2010) Catalogo regionale dei suoli capisaldo. [http://www.regione.piemonte.it/agri/suoli\\_terreni/suoli1\\_50/capisaldo.htm](http://www.regione.piemonte.it/agri/suoli_terreni/suoli1_50/capisaldo.htm)
- Schneider A, Boccacci P, Botta R (2003) Genetic relationships among grapevine cultivars from North-Western Italy. *Acta Hort* 603:229–235
- Wischmeier WH, Smith DD (1978) Predicting rainfall erosion losses: a guide to conservation planning. In: *Agriculture handbook no. 537*. USDA/Science and Education Administration, Govt. Printing Office, Washington, DC, pp 58

# Rockfall at the Arvanitia Pathway, Nafplio, Greece: Protection of the Site with Respect to Its Unique Natural Beauty and Archaeological Interest

Garyfalia Konstantopoulou, Natalia Spanou, and Vaia Kontogianni

## Abstract

The Akronafplia peninsula, located in the southern end of the historical town of Nafplio, the capital of Greece during the First Hellenic Republic (1821–1834), is an archaeological site which shows a special natural beauty and welcomes lots of visitors during the year. It consists mainly of Mesozoic blocky limestone, exposing 15–55 m high cliffs along the south and west slopes. Occasional rockfall events affect the popular 1 km long Arvanitia pathway, which extends along the foot of the slope. Stability analyses concerning various critical slopes along the pathway were carried out by IGME within a research project after a serious rockfall incident in January 2010. The aim of the project was to estimate the potential hazard and risk of the pathway by evaluating the slope stability in the study area and eventually to propose the appropriate mitigation measures. The high rockfall susceptibility of the rock mass combined to the height and steepness of the slopes, make the examined pathway extremely unsafe. The risk varies along the way, depending on the distance of the path from the cliffs, as well as on the thickness of vegetation in the inner zone, virtually acting as a natural trap of the falling rocks. However, where the trapping zone along the pathway is missing, protection measures are required, which may significantly alter the archeological and aesthetic character of Akronafplias' landscape. Thus, an additional requirement of the study involved minimization of the visual effect imposed by the mitigation measures.

## Keywords

Rockfall • Pathway • Archeological site • Mitigation measures

## 75.1 Introduction

Rockfall is an extremely rapid process, involving very high risk for human life and infrastructure. The rockfall hazard is a combination of a rock detachment source, a triggering

event and the at risk area, as defined by potential rockfall trajectories.

The falling blocks are generally created by sets of fractures. Natural fracturing patterns and incipient failure planes determine block sizes. The principal failure mechanism in this type of failure is loss of tensile strength on very steep slopes which is commonly triggered by infiltration of water, weather changes or earthquake events. Plant roots can also contribute to the rock mass instability widening rock cracks. Travel distance of rockfalls depends on factors such as the size of the block, the dip of the slope, the composition and the roughness of the slope surface.

The rockfall hazard and risk assessment is a complex procedure, requiring good knowledge of all hazard elements involved, as well as the vulnerability of the objects at risk.

G. Konstantopoulou (✉) · N. Spanou · V. Kontogianni  
IGME - Institute of Geology and Mineral Exploration, Athens,  
Greece  
e-mail: kongar@igme.gr

N. Spanou  
e-mail: spanou@igme.gr

V. Kontogianni  
e-mail: villy@igme.gr

Several authors have proposed different methods for rockfall hazard and risk rating (Pierson et al. 1990; Budetta 2004). Most of these methods were developed for evaluating rockfall risk to vehicles along highway roads, but appropriate rockfall hazard rating systems for pedestrian or bicycle trails are poorly defined.

A rockfall episode occurred on January 24, 2010 at a popular pathway located at the Arvanitia site, close to the historical city of Nafplio, Greece. The event occurred late at night, fortunately with no casualties. A heavy rainfall was evidently the triggering factor responsible for this rockfall. To mitigate the rock fall risk, the Nafplio municipality decided to investigate the in situ conditions in order to arrange the necessary remedial works. As part of this project a study of the rock fall stability and assessment of the associated risk was carried out by the Institute of Geology and Mineral Exploration of Greece (IGME).

Meanwhile the pathway was closed while not yet protected. However, several visitors overstep the warning signs and walk along the pathway. So, till today the Arvanitia site poses a constant threat to the public safety.

The primary objectives of this project were to identify long-term hazard and risk recognition and permanent mitigation. Although the geological factors contributing to rockfall hazards along the examined pathway are easily defined, the environmental and cultural limitations imposed on the site makes remediation quite challenging. The proposed mitigation measures must be cost-effective, while combining safety requirements with minimal aesthetic impact to the existing landscape.

## 75.2 Project Settings

### 75.2.1 Site Description

The Akronafplia peninsula is located in the southern end of the historical town of Nafplio (Fig. 75.1). It consists mainly of Mesozoic blocky limestone exposing 15–55 m high cliffs along the south and west slopes. The Arvanitia site is located at the southern coast of the peninsula, an area of significant archaeological interest and natural beauty that hosts numerous visitors. The popular pathway, used for both walking and cycling, is a paved up to 3 m wide path, running by-the-sea for a distance of about 1 km. It was constructed along the toe of steep high cliff with local use of controlled blasting.

The January 24, 2010 rockfall at Arvanitia pathway is the most serious event over the last years, being part of a long series of falls witnessed on the site. Two blocks of about 2 m<sup>3</sup> each detached and fell down the pathway lying at the slope toe, followed by multiple rock fragments (Fig. 75.2). A second minor rockfall event occurred the following July in a

nearby location, whereas scars of detached and falling down blocks are evident in many places along the cliffs.

### 75.2.2 Field Investigation

The field investigations were based on direct field-mapping techniques on the slopes along the pathway with the following objectives: (1) to describe the most relevant factors contributing to the slope instability hazards at the site; (2) to collect discontinuity data to obtain sufficient information regarding the geological structures and discontinuity patterns and the effect of their orientation on modes of failure (planar, wedge or topple failure analysis). Representative sampling was also conducted for rock mass strength testing. The quality of the rock mass was estimated with the RMR method (Bieniawski 1989); (3) to estimate the slope geometry in different slope sections in order to apply the rock fall simulation analysis of falling rocks and its impact on the pathway; (4) to input a rating zoning of rockfall hazard and risk in order to design a mitigation strategy for each zone section along the pathway.

### 75.2.3 Engineering Geological Conditions

The Akronafplia peninsula consists of Cretaceous limestone intersected by E-W faults, which are responsible for the geomorphology of the coastline and the trench of the Argolikos Gulf. Conglomerates are also found at the base of the cliff, yet not prone to failures due to its gentle inclination. The limestone rock mass is blocky to thickly bedded, moderately fractured in the lower part of the slope, whereas in the upper part it appears generally more disturbed. Randomly intersecting discontinuities include bedding, joint systems, fractures and open cracks caused by blasting practices during the construction of the pathway.

Karstified voids of various dimensions are also present, located mainly close to the base of the limestone slopes. The spacing between discontinuities defines the size and shape of the rock block, and discontinuity orientation defines the type of initial instability mechanism. The joint net is locally closely spaced, with planes of considerable length, generally dipping towards the slope. Kinematic analysis (DIPS, Rocscience Inc. 2010b, v.5.1) of discontinuities indicates a high rockfall susceptibility both at natural and artificial slope sections (Fig. 75.3), suggesting significant potential of toppling and wedge sliding (Fig. 75.3a and b). The rockfall events along the limestone slopes were caused by unfavorable rock mass characteristics, in combination with heavy rainfalls and the influence of improper slope interventions during path construction.

**Fig. 75.1** Aerial view of the Acronafplia peninsula landscape and the archaeological site on top of the cliff. The pathway at the toe of the cliff can also be seen. *Inset* location map of Nafplio, Greece



**Fig. 75.2** Two blocks falling on the Arvanitia pathway after the 24 January 2010 rockfall event



### 75.3 Rockfall Hazard and Risk Assessments

Based on the identified characteristics of potentially unstable rock mass along the pathway, analyses of the motion and resulting trajectories of potential rockfalls were conducted. Rockfall trajectories, impact energy and height of bouncing depend on the slope geometry, slope surface roughness and rockfall block characteristics (Guzzetti et al.

2003; Harris et al. 2001; Jaboyedoff et al. 2005). To determine the rock travel distance, different computer-modeling software has been developed using parameters that can influence the type of movement and the rock travelling distance.

The rockfall simulations were carried out on the most critical profiles. Thus, nine (9) profiles used for modeling were selected during field work at the most critical locations,

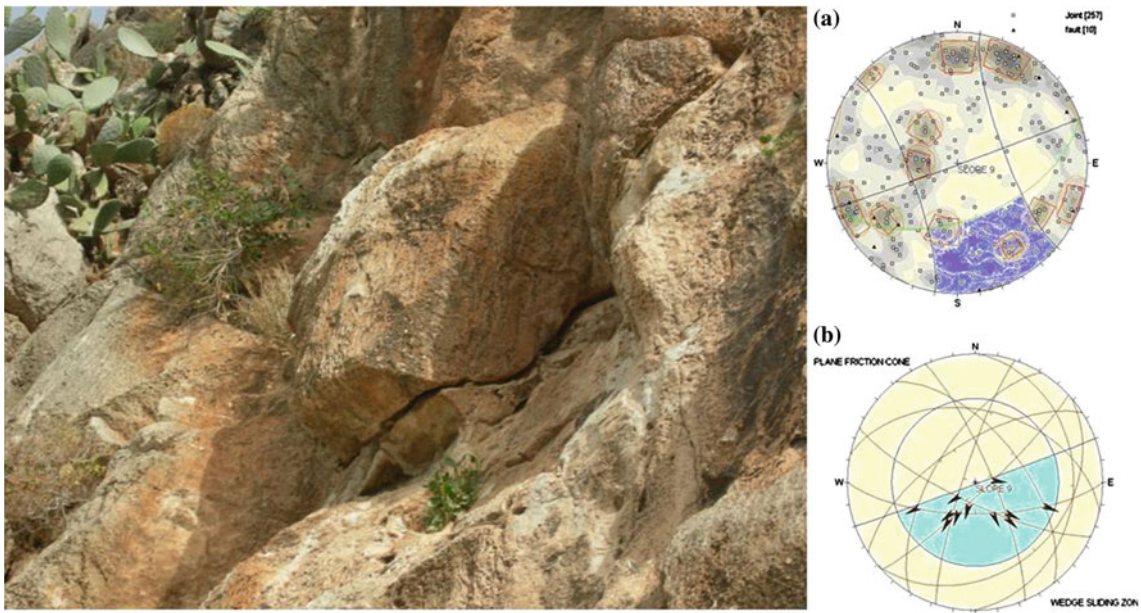
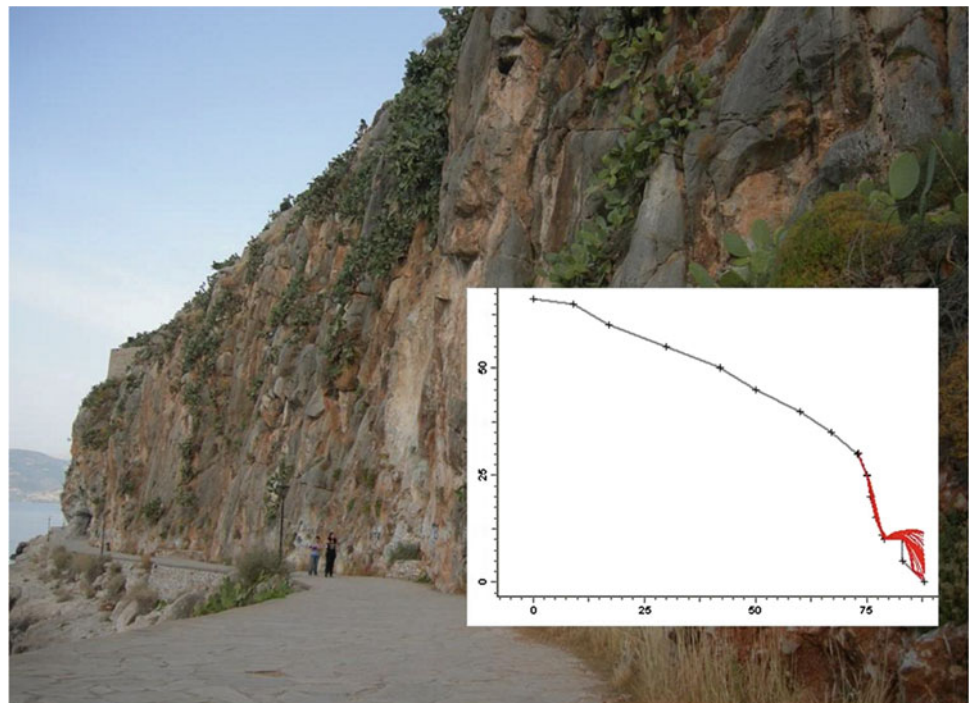


**Fig. 75.3** Typical limestone formation along the cliff. Stereographic projection made against **a** toppling and **b** wedge sliding at the section of the January 2010 event (with DIPS software). *Colored areas* suggest zones of potential instability

**Fig. 75.4** Rockfall analysis for slope sections along the Arvanitia pathway



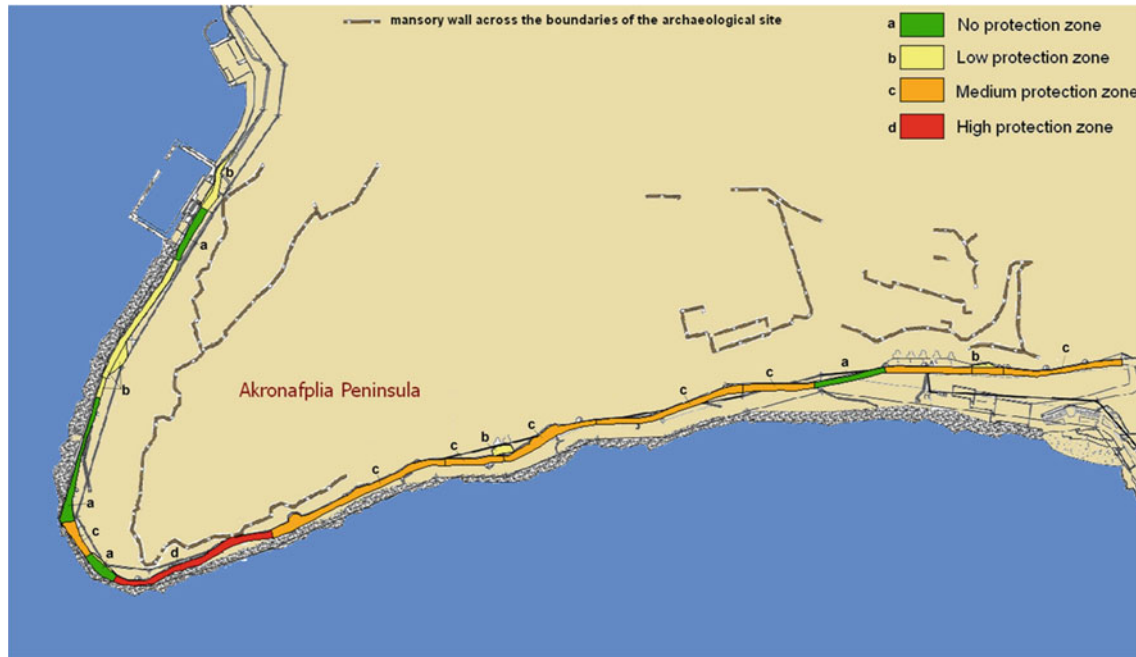
often corresponding to the highest point in the slope, where the slope angle or existing catchment geometry changed significantly, or locations where active rockfall was observed. Cross section geometry was developed using a 1:1,000 scale topographic map of the slope. Other input parameters, including source zones, block size, shape,

surface roughness, and friction coefficients, were based on field observations.

Rockfall modeling was completed for all analyzed slope sections using the computer simulation program RocFall (RocScience 2010a, v.4.0). RocFall is a statistical analysis program designed to assist with a risk assessment of rock

**Table 75.1** Level of protection and support measures selected for the Arvanitia pathway and impact to the natural environment

Level of protection	No protection	Low protection	Medium protection	High protection
Length (948 m total length of the pathway)	188 m	112 m	538 m	110 m
Support measures required with considerable visual impacts	–	Rock bolts and shotcrete	Barriers and/or wire mesh	Construction of shelter
Magnitude of the disturbance to the natural environment	No disturbance	Minor disturbance	Medium to high disturbance	Minor disturbance

**Fig. 75.5** Schematic zones of protection demand along the Arvanitia pathway

slopes and evaluation of mitigation measures. Modelling was conducted to analyze rockfall behavior rolling and falling down the slope. The models predict rockfall velocity, energy, bounce height, bounce location, and roll out distance (Fig. 75.4). This information was used during the rock slope evaluation to better understand falling rock behavior at each slope section and to help determine the appropriate mitigation measures. Field observations on detached rock blocks from different sites of the source were used to test the modelling results.

From the above considerations it is evident that long parts of the examined pathway are at rockfall risk. The degree of risk depends mainly on the local topography, the distance of the pathway from the slope as well as the density and species of the existing plants in the inner zone of the path. The existence of vegetation has an energy dissipative effect, acting as natural barrier. Whether this barrier effect is

effective or not, is determined by the size and kinetic energy of the rock block.

Based on the data, relatively crude rockfall simulation models are capable of producing reasonably accurate predictions of the rockfall trajectories, allowing a risk zoning of the examined pathway. For each one of the examined slope sections additional models, with mitigation options added, were evaluated to determine the most effective protection measure for each specific site. This was an iterative process, testing both the type and geometry of mitigation measures.

### 75.3.1 Limitations

The reliability of rockfall modeling and prediction of rockfall behavior is dependent upon the accuracy of the modeled slope geometry. This study relied on a limited number of

field developed cross sections, derived using a detail topographic map. This method to develop site specific models was appropriate for this preliminary evaluation, but more thorough cross-sections will be necessary for the final design development.

## 75.4 Support Measures

The in situ survey and the engineering geological mapping of the Arvanitia cliffs suggest a combination of remedial measures for the slope protection. The presence of trapping zones is the critical factor for deciding about necessity of measures since it can catch any fallen rocks before they reach the walkway. In cases of absence of a trapping zone the level of protection required is variable, depending on the extent of the fragmentation of the rock and the height of the cliff. In particular, four levels of protection were assumed to be necessary (see also Table 75. 1):

*No protection zone:* Areas with sufficient trapping zone.

*Low protection zone:* Removal of hanging blocks, rock bolts and shotcrete are advisable for clearance of specific locations of local rock fragmentation. Also prevision for existing walls, vegetation of catchment zone and elimination of visitors sightseeing stopovers (terraces with benches).

*Medium protection zone:* At sections of more extended fracturing and presence of unstable wedges, barriers or wire mesh are required.

*High protection zone:* At sections of up to 50 m height of the cliff, zero or negative inclination and minor catchment zone, construction of shelter should be considered.

In conclusion, along more than the half length of the pathway the cliff requires barriers and/or wire mesh, measures detracting the natural aesthetical value. To minimize the effect of these measures, determination of their capacity and position of installation was based on various possible scenarios of falling rocks and different heights of barrier installation, following stability analyses with the Rockfall software.

Preferable positions for support installation were places with vegetation extending sufficiently above the ground or positions not visible from the toe of the cliff with sufficient space for barrier installation. The results of this study are shown in Fig. 75.5.

## 75.5 Conclusions

The stability analysis of the Arvanitia cliff suggests that the site is very dangerous: The requirement to preserve pedestrian transit along the pathway is immediate protection of the slope. Therefore, proper measures are proposed for cost-effective solutions with minimum aesthetic impact on the unique natural beauty of the area.

## References

- Bieniawski ZT (1989) Engineering rock mass classifications: a complete manual for engineers and geologists in mining, civil, and petroleum engineering. Wiley-Interscience, Hoboken, pp 40–47
- Budetta P (2004) Assessment of rockfall risk along roads. *Nat Hazard Earth Syst Sci* 4:71–81
- Guzzetti F, Reichenbach P, Wieczorek GF (2003) Rockfall hazard and risk assessment in the Yosemite Valley, California, USA. *Nat Hazard Earth Syst Sci* 3(6):491–503
- Harris C, Davies M, Etzelmüller M (2001) The assessment of potential geotechnical hazards associated with mountain permafrost in a warming global climate. *Permafrost Periglac Process Special Issue: Permafrost Clim Eur* 12(1):145–156
- Jaboyedoff M, Dudt JP, Labiouse V (2005) An attempt to refine rockfall hazard zoning based on the kinetic energy, frequency and fragmentation degree. *Nat Hazard Earth Syst Sci* 5:621–632
- Marzorati S, Luzi I, De Amicis M (2002) Rockfalls induced by earthquakes: a statistical approach. *Soil Dyn Earthq Eng* 22 (7):565–577
- Pierson AL, Davis AS, Van Vickle R (1990) Rockfall hazard rating system—implementation manual. Federal Highway Administration (FHWA), Report FHWA-OR-EG-90-01. FHWA, U.S. Department of Transportation
- Rocscience Inc. (2010a) RockFall v.4.0: Statistical analysis of rockfalls Rocscience Inc. (2010b) DIPS v.5.1

Jesús Garrido and M<sup>a</sup> Lourdes Gutiérrez

---

## Abstract

Most of the Spanish cultural heritage is exposed to natural hazards. This fact is opposed to a sustainable development, which is the cultural heritage base, because its goal is to be passed down to future generations (Andalusian Cultural Heritage Law 2007). The impact of natural hazards on the Spanish cultural heritage has been checked over the Lorca earthquake (May 11th, 2011). The impact is higher for rapid onset phenomena, but prevention measures are not projected for avoiding them. Natural hazards prevention implies hazard identification, analysis and also risk assessment and management. The cultural heritage in urban areas of Andalusia (Spain) is very rich, but it is not completely considered in town planning, regardless of the fact that they might be placed in hazard-prone areas. Town planning cannot reduce the exposition of this cultural heritage but hazards and vulnerability can be reduced. Hazards and vulnerability of elements at risk must be known to design suitable prevention measures.

---

## Keywords

Natural hazards • Cultural heritage • Prevention • Town planning • Legislation

---

## 76.1 Introduction

Spain has the second largest number of Cultural World Heritage sites in the world. According to the Spanish Ministry of Education, Culture and Sports, the number of Properties of Cultural Interest in Spain is around 16,000. Most of them are castles, usually placed on promontories where they are exposed to landslides and rock falls, palaces or churches, usually constructed near rivers where they are

exposed to floods. Despite most of the cultural heritage is supposedly placed in safer places than modern buildings because those places were chosen some centuries ago, it could be affected by natural hazards. This fact is opposed to a sustainable development, because its goal is to be passed down to future generations (Andalusian Cultural Heritage Law 2007).

When this cultural heritage was built, the historical record of natural hazards was generally short, but long enough for destructive floods or earthquakes. Because of that, Rodríguez-Pascua et al. (2012) suggest that deterministic methods should be used when designing cultural heritage hazard maps.

The impact of natural hazards on the Spanish cultural heritage has been checked over the Lorca earthquake (May 11th, 2011). Some of Lorca's heritage damaged by the 2011 earthquake was also affected by the 1674 Lorca seismic crisis (Feriche et al. 2012). In the last centuries some Andalusian cultural heritage has been partially destroyed, for

---

J. Garrido (✉)  
Departamento de Ingeniería Civil, Universidad de Granada,  
Campus de Fuentenueva s/n, 18071 Granada, Spain  
e-mail: jega@ugr.es

M.L. Gutiérrez  
Departamento de Construcciones Arquitectónicas, Universidad de  
Granada, Campus de Fuentenueva s/n, 18071 Granada, Spain  
e-mail: mlgutier@ugr.es

example the historical center of Málaga by the 1680 earthquake (Goded et al. 2012).

The natural hazards impact is higher for rapid onset phenomena, but prevention measures have not been planned yet to avoid them. The Spanish cultural heritage exposed to natural hazards is studied just to project local corrective measures when it is affected by them. Town planning cannot reduce the exposition of this cultural heritage but hazards and vulnerability can be reduced. Prevention through non-structural measures, such as land use planning, is difficult to apply to cultural heritage. Moreover, preventive structural measures prior to natural hazards occurrence are better than corrective measures applied afterwards, because they are cheaper and safer.

---

## 76.2 Cultural Heritage and Natural Hazards

UNESCO adopted a Convention concerning the Protection of the World Cultural and Natural Heritage in 1972; meanwhile the Committee of Ministers of the Council of Europe adopted a Recommendation on the Protection of the Architectural Heritage against Disasters (93/9).

Italy is one of the pioneer nations establishing mechanisms, management operational protocols, and producing documents such as the Risk Map of Cultural Heritage (*Carta del Rischio*) in 1987 (Baldi 1992), which takes into account various natural hazards.

Initial approaches adopted by the international community in relation to risks and heritage have been focused on steps towards protection measures on the intentional destruction of this heritage (UNESCO 1954) but also on taking post-intervention measures, searching for the collaboration of competent services, avoiding any cultural heritage damage, and allocating funds for damage repair (UNESCO 1976). The Charter of Toledo (ICOMOS 1986) recognized the importance of the heritage protection and an expressed willingness to prevent and minimise the risks of its destruction according to criteria consistent with the protection of the cultural heritage.

Furthermore, the Charter of Noto (Noto Consultory 1986), on the Italian side, proposed a protection of historical centres towards seismic risks in the region of Eastern Sicily through seismic hazard maps; priority for intervention schemes; appropriateness of criteria definition; and intervention techniques for possible seismic risks. The Charter of Washington (ICOMOS 1987) highlighted the preventive measures against natural hazards, being these prevention or repair measures specific to the type of building or asset. The objectives of the Kobe Conference on Cultural Heritage Risk Management (2005) highlighted the integration of the cultural heritage into the disaster reduction policies, involving local communities in developing action plans on risk

management. In addition, the Xi'an Declaration (ICOMOS 2005) pointed out the need to respond to the changing process of heritage areas caused by natural disasters, establishing planning tools and practices to preserve and manage the environment. Moreover, the Lima Declaration (ICOMOS 2010) focused on prevention through urgent measures to possible damages caused in seismic prone areas. However, La Valletta Principles (ICOMOS 2011) focused on risks and the nature of the prevention and damage repair tools.

Multidisciplinary studies have primarily focused on the issues resulting from seismic natural hazards and, to a lesser extent, in floods and mass movements. Subsequent to the analysis of the effects and the consequences of disasters, planning and protocols on natural hazard management have necessarily followed, especially aimed at improving protection and future prevention measures, being effective in the educational training fields, and the preparation of management planning.

---

## 76.3 Natural Hazards in the Spanish Cultural Heritage

In the last decades, the Spanish Historical Heritage Law (Act 16/85) defined, at state level, the conceptual update of Historical Heritage, selecting the intervention criteria, providing a suitable use of them for the community and setting up a vigilant policy in order to create the necessary educative, technical and financial incentives. Some provisions established references to conservation matters and the setting up of preliminary studies on the analysis of the conservation status. However, Spanish Historical Heritage Law did not include direct and comprehensive measures referred to natural risks that may affect them. The update of the new cultural heritage catalogues and the inclusion of archaeological maps should be accompanied by the need of including a risk map into the cultural heritage conservation plans.

The National Plans are management tools for Cultural Heritage promoted by the Spanish Cultural Heritage Institute. Some of them are related to natural hazards prevention. Thus the Preventive Conservation National Plan (2011) establishes natural hazards prevention (specifically for earthquakes and floods) through the risk identification, analysis and assessment. The ideas of *Carta del Rischio* (Baldi 1992) are considered by the National Plan of Cathedrals and the National Plan of Abbeys, Monasteries and Convents, allowing to plan the conservation and restoration interventions in order to prevent stability and leak tightness problems related to earthquakes, rock falls or hydrology. They will be considered as urgent interventions. The National Plan for Cultural Landscape considers seismic hazard and rock falls.

In Spain, Culture affairs competence was transferred to the 17 Autonomous Communities (Spanish regions), which actually have a cultural or historical heritage legislation with no direct references to natural hazards. The Historical Heritage Andalusian Law was first enacted in 1991 and was amended during 2007 due to the integration into it of the Andalusian Urban Ordainment Law (Law 7/2002). They establish the competence of the Regional Government over Historical Heritage when "...there is a risk of destruction or deterioration of it". However, it is not compulsory to design a Conservation Project to conduct emergency works to prevent people or goods from that risk (Historical Heritage Andalusian Law).

## 76.4 National and Regional Spatial Planning and Urban Legislation

The recast text of the national Land Act, enacted by Royal Legislative Decree 2/2008, and most of the regional spatial planning and urban legislation, enforces to classify hazard-prone areas as unsuitable to development. The transposition of the Directive 2007/60/EC on the assessment and flood risk management into the national Royal Decree 910/2010 establishes that flood hazard maps and flood risk maps are compulsory at river basin district level. The land use planning will take into account both maps. Flood prone areas should also be considered as unsuitable to development. In accordance with the provisions of the Spanish Strategic Environmental Assessment (Law 6/2006), an Environmental Sustainability Report (ESR) is compulsory to be carried out, and must include a natural hazards map, as it is established by the Land Act. The ESR will be included in the General Urban Planning. The map is important in order to know the cultural heritage exposition to natural hazards and to plan structural countermeasures.

Most of the enacted regional laws about spatial and urban planning agree on carrying out natural hazards maps. According to the Civil Protection Basic Standards for floods a municipal civil protection plan is mandatory, and should also include a hazard map. Regarding earthquakes this plan is compulsory in towns with intensity higher than 7 (EMS) in the national seismic hazard map. However after analysing some Spanish urban plannings it is observed that most of them do not include natural hazards maps and when they are included, the map scale is too big.

One of the most visited monuments in Spain, the Alhambra of Granada, is placed in a highly seismic area. At least for the last five centuries, the fault of the San Pedro cliff and associated faults located at the bottom/on the foothills of the Alhambra hill, has been active (Justo et al. 2008). The

Alhambra walls were partially destroyed by different earthquakes several times. Nowadays the top of the cliff is closer to the Alhambra because the slope toe erosion by the river Darro during floods triggered some mass movements in the cliff. However, the Urban Planning of Granada city only includes a partial flood map and a mass movements map at scale 1:50,000.

Towns with a high seismic hazard, almost half of them in Andalusia, do not have a seismic civil plan (or a seismic hazard map).

Hazards maps are not enough. It is not possible to get a risk map without having vulnerability and exposition maps. Hazards and vulnerability of elements at risk must be known to design the preventive measures in the case that this cultural heritage is exposed to natural hazards. Due to the fact that some damage are related to restoration techniques, structural measures must be carefully studied. In addition, those measures cannot affect greatly the cultural heritage.

Town planning cannot reduce the exposition of cultural heritage but hazards and vulnerability can be reduced.

A detailed risk map of cultural heritage included in the General Urban Plannings would mean to operate researching on the identification and risk analysis of natural hazards; on conservation and techniques methods; on criteria selection and working methods; and on the coordination of activities and the optimization of resources (Preventive Conservation National Plan). All this would help to develop a multidisciplinary relationship and to integrate a technical-scientific methodology approach in the cultural heritage field. As a result of that, damage would be minimised and that, together with a good knowledge of the materials and construction technology, would allow proposing intervention models to agree with a suitable conservation (Baldi 1992) based on sustainability patterns.

## 76.5 Conclusions

In Spain, cultural heritage legislation have never considered town plannings and vice versa. The preventive conservation of cultural heritage to natural hazards is not present in town plannings. Hazard maps to be included in town plannings, according to the national Land Act, should be enforced at a detailed scale. The *Carta del Rischio* proposed by the Spanish Cultural Heritage Institute should focus on the study of the degree of conservation and the vulnerability of the cultural heritage. The coordination of all administrations which are competent in cultural heritage affairs and town plannings is recommended in order to save money and to spend it in preventive measures instead.

## References

- Baldi P (1992) La carta de riesgo del patrimonio cultural. In: La Carta de Riesgo. Una experiencia italiana para la valoración global de los factores del Patrimonio Monumental. Instituto Andaluz de Patrimonio Histórico, p. 9–14
- Ferliche M, Vidal F, Alguacil G, Aranda C, Pérez-Muelas J, Navarro M, Lemme A (2012) Performance of cultural heritage of Lorca (Spain) during the two small earthquakes of May 11th, 2011. In: Proceeding of the 15th world conference on earthquake engineering, Lisbon, Portugal, 2012. Paper No. 3163
- Goded T, Irizarry J, Buforn E (2012) Vulnerability and risk analysis of monuments in Málaga city's historical centre (Southern Spain). *Bull Earthq Eng* 10(3):839–861
- Noto Consultory (1986) Perspectives for the conservation and restoration of the historic city centre (The Noto Charter)
- ICOMOS (1986) The charter for the conservation of historic towns (The Toledo Charter)
- ICOMOS (1987) Charter for the conservation of historic towns and urban areas (The Washington Charter)
- ICOMOS (2005) Xi'an declaration on the conservation of the setting of heritage structures, sites and areas
- ICOMOS (2010) Lima declaration for disaster risk management of cultural heritage
- ICOMOS (2011) The Valletta principles for the safeguarding and management of historic cities, towns and urban areas
- Justo JL, Azañón JM, Azor A, Saura J, Durand P, Villalobos M, Morales A, y Justo E (2008) Neotectonics and slope stabilization at the Alhambra, Granada, Spain. *Eng Geol* 100:101–119
- Rodríguez Pascua MA, Pérez-López R, Silva PG, Giner-Robles JL, Martín-González F (2012) Descubriendo los terremotos “perdidos” en España: arqueosismología y paleosismología. *Aplicaciones al caso de Lorca. Patrimonio Cultural de España* 6:81–95
- UNESCO (1954) The Hague convention for the protection of cultural property in the event of armed conflict
- UNESCO (1976) Nairobi recommendation concerning the safeguarding and contemporary role of historic areas

---

**Part VIII**

**The Role of Historical Archives  
in the Assessment, Management  
and Valorization of Cultural Landscapes**

---

# Using Documentary Data to Reconstruct Social Responses and Local-Based Adaptation Strategies to Landslide and Flood Hazards in N Czechia

# 77

Pavel Raška, Vilém Zábranský, and Jakub Dubiřar

---

## Abstract

The role of social resilience and local-based adaptation strategies as efficient tools for natural risk reduction has been increasingly emphasised over the last decades. Many authors have noted that learning from historical disasters is a background process contributing to social resilience. In this study, three case studies examining multiple natural hazards, catastrophic landslides and flash floods in the study area of Northern Czechia are presented. The study of documentary data enabled us to reconstruct the social impacts of these hazards and the historical responses of communities to these impacts. Our results indicate that communities were frequently affected by various natural hazards and developed specific mitigation and recovery measures that might inspire present-day risk reduction strategies.

---

## Keywords

Natural hazards • Documentary data • Resilience • Risk reduction

---

## 77.1 Social Response and Resilience to Natural Hazards

During the last three decades, the social notion of natural risks and disasters has gained increasing attention in the literature (Bankoff et al. 2004; Wisner et al. 2004). Research within the social sciences has considered natural risks and their impacts as a social process, and significant effort has been expended to study the social production of natural risks and their impacts. According to this perspective, natural risk reduction must be based on social action at different institutional levels (Folke 2006; Hutter et al. 2013) with a crucial

role for local-based (community-based) strategies to mitigate the impacts of natural disasters. Local-based adaptation (mitigation) strategies are framed by the experiences of local communities with past natural hazards within the realm of specific environmental conditions and sociocultural traditions (Delica-Willison and Willison 2004).

Because the frequency and magnitude of natural hazards as well as the vulnerability of the affected communities change, local-based strategies need to be constantly reconsidered in the context of the environmental conditions of the investigated area and its sociocultural traditions. The “learning through the past” paradigm has been widely adopted to theoretically frame the developmental context of local-based strategies (Voss and Wagner 2010). Consequently, the research on learning from disasters has focused on the creation of local-based adaptation strategies in a certain area, the effectiveness of the strategies as well as at the ways in which these strategies have been passed on to future generations (Junea and Mauelshagen 2007; Schenk 2007).

---

P. Raška (✉) · J. Dubiřar  
Department of Geography, Faculty of Science, J. E. Purkyně  
University, Ústí Nad Labem, Czech Republic  
e-mail: pavel.raska@ujep.cz

V. Zábranský  
Department of History, Philosophical Faculty, J. E. Purkyně  
University, Ústí Nad Labem, Czech Republic

## 77.2 Documentary Data in Natural Hazard Studies

Documentary data play the fundamental role in reconstructing the historical occurrence of natural hazards, their social impacts and the resulting local adaptation strategies. Documentary sources are human-made written or iconographic data sources, which directly or indirectly reflect the past events of men (Glade et al. 2001). These data have been widely exploited in geology, geomorphology, climatology and hydrology to reconstruct the past spatiotemporal distribution of earthquakes, landslides, weather extremes and flood hazards and their impacts (e.g., Guzzetti et al. 1994; Raška et al. 2014). However, relatively less attention has been paid to the use of these data for the reconstruction of social responses to these natural hazards.

## 77.3 Revealing Social Responses to Natural Hazards Using Documentary Data: Case Studies

In 2013, we launched the 3-year research project, *Documentary data sources for research of social perception and adaptation strategies to selected historic natural hazards in the Czech Republic*. The project aims to analyse documentary data for information related to the social responses to historical natural hazards before 1950 and to index local-

based adaptation strategies, which would be relevant to present-day natural risk reduction. One of the major rationale for the research project was that the local-based adaptation strategies are currently not common in Czechia as they are not sufficiently supported by legal frameworks. This is a result of slow reestablishment and reinforcement of former social patterns after the fall of communism in late 1980s (Howard 2003).

As part of the project, we created a critical typology of available documentary sources (Raška et al. 2014), which were searched for information about individual natural hazard events. The documentary data have been analysed utilizing an interdisciplinary approach of geomorphologic, historical, and medial methods, including content analysis to build the database of events and their impacts and critical discursive analysis to study the specifics of social construction of these data.

In this study, we present three case studies from N Czechia (Fig. 77.1) that illustrate the usefulness of different types of documentary sources for reconstructing the social response to and mitigation strategies for natural hazards. Particular emphasis was placed on the social construction of reports on natural hazards, the social perception of natural hazard impacts and the specific community tools for natural hazard mitigation. The secondary aim of this research is to highlight the need to protect documentary data in local archives and find effective ways to make them available for present-day natural risk reduction.

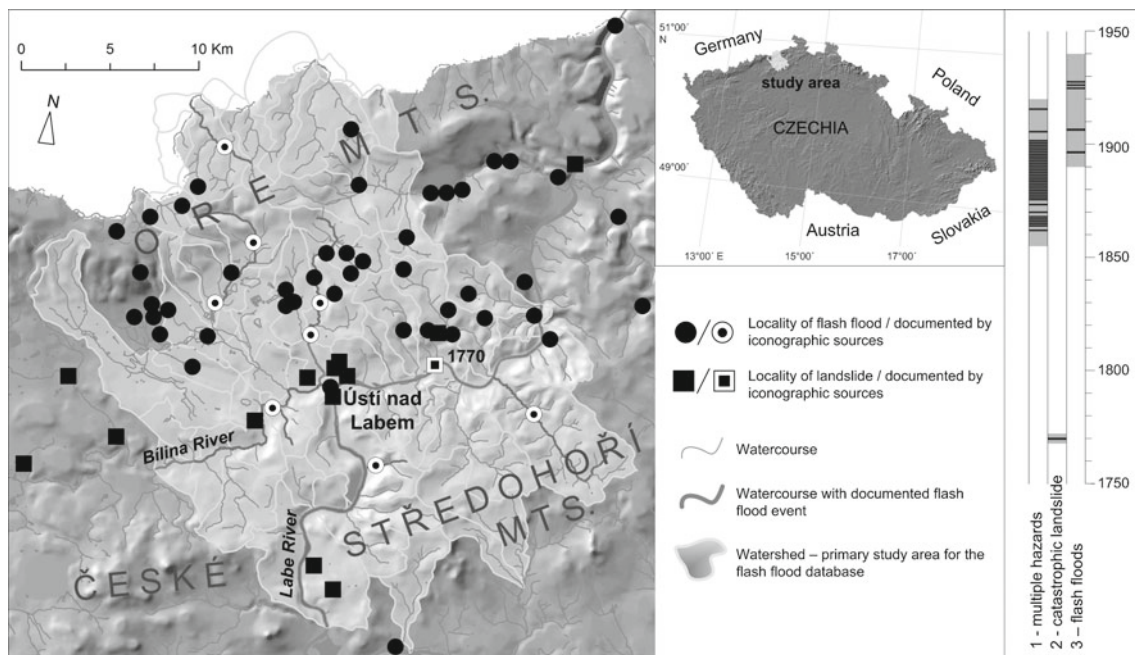


**Fig. 77.1** The study area with documented flash floods, landslides and rock fall events. Other hazards (e.g., hailstorms, heavy rains, etc.) are not shown as they occurred in most locations. Note the light grey

rectangle in a timeline indicates the monitored period within the case study; dark grey indicates events found

### 77.3.1 Social Responses to Multiple Natural Hazards Over Time

The first case study exploits local newspapers (Aussiger Anzeiger 1856–1902) to create a time series line of natural hazards in the city of Ústí nad Labem in N Czechia for the latter part of the 19th century. We found 599 reports on 275 different natural hazards (Fig. 77.2a, b), primarily floods and other hydrometeorological extremes, that caused 1 casualty per year and had significant impacts on buildings and infrastructure. The detailed discursive analysis focused on landslides and rock fall events (see locations in Fig. 77.1) indicates that there were three main modes of coping with the impacts of landslides, including (a) small-scale events without mitigation measures, (b) events affecting routes and land outside of the built-up areas with mitigation and recovery by locals, and (c) events affecting houses and regional transportation routes with mitigation and recovery planned and performed by committees consisting of city council members, geotechnicians and representatives of local organizations and communities.

### 77.3.2 Social Impacts of and Response to Catastrophic Landslide

The second case study was focused on the earliest catastrophic landslide documented near the city of Ústí nad Labem. The landslide at Koží vrch Hill occurred in January 1770 affecting the village of Veselí and one third of the Labe/Elbe River, the largest river in Czechia. Until now, the precise location and extent of the landslide was uncertain and were only indirectly inferred from protoscientific reports and comments on the social impacts of the event. A thorough exploration of the local archives produced several data. The most significant was a coloured manuscript (Fig. 77.2c) created only 2 weeks after the landslide, which depicted both the extent of the landslide and its impacts. Historical descriptions of the region by local authors revealed the social responses to the landslide, including interpretations of the causes of the landslide, the recovery measures and the emergence of a traditional notion of the event (e.g., a local poem describing the landslide events and the construction of a chapel with a painting of the landslide as a reminder of the event and as thanks to God for saving the houses).

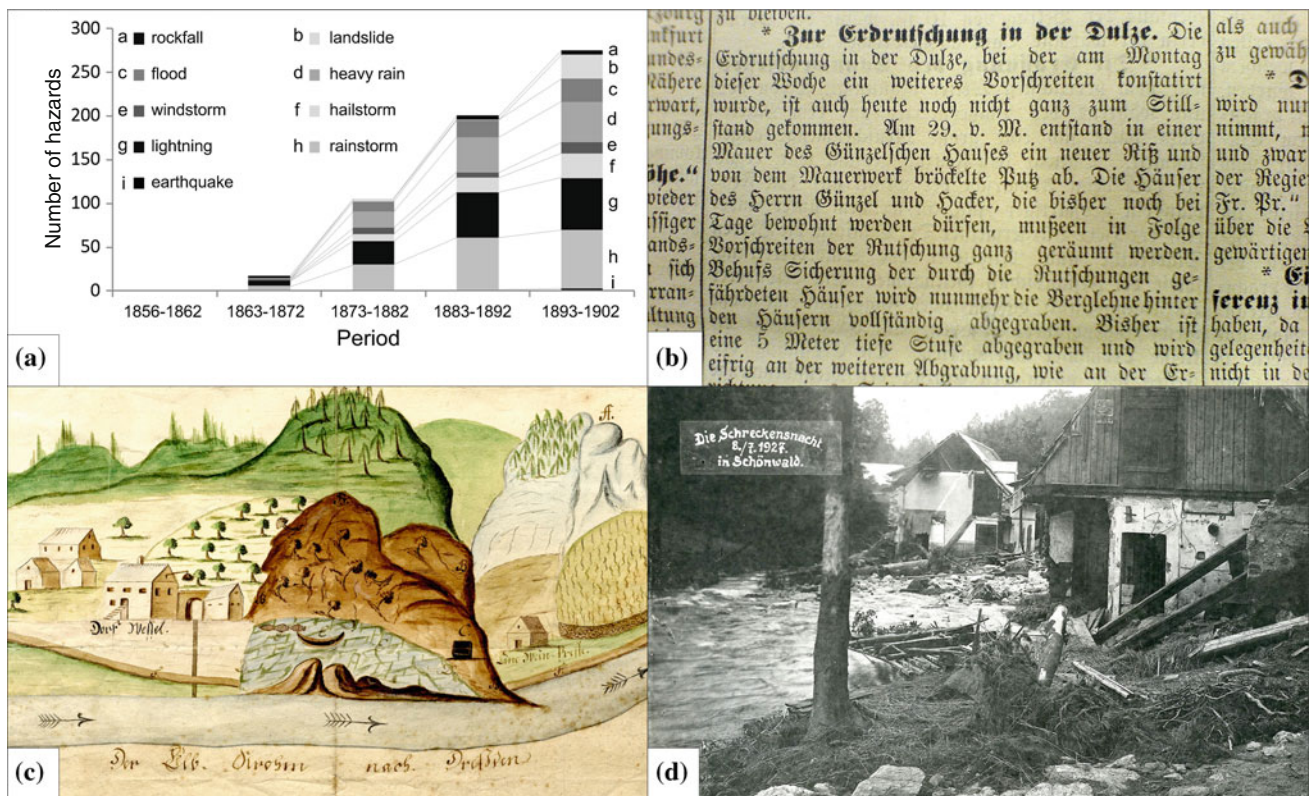


**Fig. 77.2** a Case study 1: the number of hazards in newspaper articles about natural hazards (1856–1902), b Case study 1: an example newspaper article about the landslide (Erdrutschung in the Ústí nad

Labem city), c Case study 2—depiction of the catastrophic landslide at the Koží vrch hill (1770), d Case study 3—photo of the flash flood impacts in Krásný Les village, Ore Mts. (1927)

### 77.3.3 Social Responses to Historical Flash Floods at Different Institutional Levels

The third case study analyses iconographic material (old photographs; see Fig. 77.2d) using visual sociology approaches and examines written documentary data (chronicles and stenographs from political meetings) to reveal the social responses to flash floods in the Ústí nad Labem region from the end of the 19th century until World War II. Inspection of the photographic archive of the local museum identified flash flood events at seven watercourses in the years 1897, 1907, 1925, 1926 and 1927 recorded in tens of photographs. All of the recorded events (see Fig. 77.1 for locations) affected technical infrastructure and buildings, and the catastrophic event in 1927 caused 2 casualties. The photographs indicate that the impacts of small-scale events, even in urban areas, were primarily mitigated by the locals themselves, and there was significant community help for those who were affected. The recovery efforts following a large-scale event, those resulting in the destruction of tens of houses (e.g., the event in Ore Mts. in 1927), were coordinated centrally. As indicated in the digital archives of the parliament of the Czechoslovak Republic, mitigation and recovery measures were repeatedly requested by representatives of the region. The political response to these events resulted in the implementation of a new legal act providing support during and after natural disasters.

### 77.4 Discussion and Conclusion: The Role of Documentary Data in Natural Risk Reduction

Each case study demonstrates that historical communities were frequently affected by natural hazards of different magnitudes. Some of these hazards fundamentally affected the local social system and its everyday function. Our results also indicate that these historical communities gradually developed a multilevel approach to natural risk reduction and recovery, which—originally not always codified—helped recovery from extreme geomorphologic and hydrometeorological events. In particular, the documentary proofs suggest the strong position of local communities in mitigation and recovery measures after these events and denote the presence of an implicit participatory approach in landscape planning and management (cf. Delica-Willison and Willison 2004; Voss and Wagner 2010). Present-day N Czechia lacks a participatory approach (an observation that is partly valid for the whole territory of Czechia), but the documentary data have revealed possible ways and specific tools to improve present-day natural risk reduction strategies.

In this respect, documentary data are a unique source of information and require the implementation of modern approaches with respect to how they are sought, conserved and disseminated. While the conservation and analyses of the data are subject to research and archiving institution (development of digital repositories, critical typologies of data sources), the collection and dissemination of the data may be well performed by creation of crowdsourced web-based databases (cf. Horita et al. 2013) that would be accessible to decision makers for the use in territorial planning as well.

**Acknowledgments** This research was supported by project No. 13-02080P “Documentary data sources for research of social perception and adaptation strategies to selected historic natural hazards in the Czech Republic” (Grant Agency of the Czech Republic) and the project IGA UJEP. The Language Editing Services is appreciated for English style corrections.

### References

- Bankoff G, Frerks G, Hilhorst D (eds) (2004) Mapping vulnerability: disasters, development & people. Earthscan, London
- Delica-Willison Z, Willison R (2004) Vulnerability reduction: a task for the vulnerable people themselves. In: Bankoff G, Frerks G, Hilhorst D (eds) Mapping vulnerability: disasters, development & people. Earthscan, London, pp 145–158
- Folke C (2006) Resilience: the emergence of a perspective for social-ecological system analysis. *Glob Environ Change* 16:253–267
- Glade T, Albini P, Frances F (eds) (2001) The use of historical data in natural hazard assessments. Kluwer, Dordrecht
- Guzzetti F, Cardinali M, Reichenbach P (1994) The AVI Project: a bibliographical and archive inventory of landslides and floods in Italy. *Environ Manage* 18:623–633
- Horita FEA, Degrossi LC, Assis LFFG, Zipf A, de Albuquerque JP (2013) The use of volunteered geographic information and crowdsourcing in disaster management: a systematic literature review. In: Proceedings of the nineteenth Americas conference on information systems, Chicago, pp. 1–10
- Howard MM (2003) The weakness of civil society in post-communist Europe. Cambridge University Press, Cambridge
- Hutter G, Kuhlicke Ch, Glade T, Felgentreff C (2013) Natural hazards and resilience: exploring institutional and organizational dimensions of social resilience. *Nat Hazards* 67:1–6
- Juneja M, Mauelschagen F (2007) Disasters and pre-industrial societies: historiographic trends and comparative perspectives. *Mediev Hist J* 10:1–31
- Raška P, Zábanský V, Dubišar J, Kadlec A, Hrbáčová A, Strnad T (2014) Documentary proxies and interdisciplinary research on historic geomorphologic hazards: a discussion of the current state from a central European perspective. *Nat Hazards* 70:705–732. doi:10.1007/s11069-013-0839-z
- Schenk GJ (2007) Historical disaster research. State of research, concepts, methods and case studies. *Hist Soc Res* 32:9–31
- Voss M, Wagner K (2010) Learning from (small) disasters. *Nat Hazards* 55:657–669
- Wisner B, Blaikie P, Cannon T, Davis I (2004) At risk: natural hazards, people's vulnerability, and disasters. Routledge, London

---

# Historical Archives Data for the Reconstruction of Geomorphological Modifications in the Urban Area of Turin (NW-Italy)

# 78

Stefania Lucchesi and Marco Giardino

---

## Abstract

The use of historical archives data is a fundamental tool for better reconstruction of evolutionary stages in the geomorphological history of urban areas. Often historical data constitute the unique testimony of past geomorphological phenomena: in fact, as in the case study of Turin (NW-Italy), many landforms have been partially or completely destroyed during historical times by increasing urbanization. In the investigated area, evidences of ancient landforms (river channels, aeolian dunes, morainic ridges) have been derived from various historical sources (papers, maps and images). They proved to be particularly meaningful for the reconstruction of palaeo-environmental and palaeo-climatic conditions and for the enhancement of preservation measures of the local geodiversity. Moreover, historical data about ancient trends of main rivers crossing the urban area allowed exploration of fluvial morphodynamic scenarios, useful for hazards assessment, risk management and town planning.

---

## Keywords

Geomorphology • Geodiversity • Urban geology • Holocene • Northern Italy

---

## 78.1 Introduction

The first settlement of the future city of Turin, named *Augusta Taurinorum* by the Romans, dates back to about 2000 years ago in the central Piedmont plain (NW-Italy). It was located on the fluvio-glacial apron developed at the

mouth of the Dora Riparia valley (Western Alps), near the confluence with the Po River (Fig. 78.1).

Landforms in the larger urban area of Turin and its suburbs progressively and deeply modified through times, due both to natural causes (particularly the oldest ones) and to anthropic causes (particularly those formed in the last two centuries).

The most evident and meaningful landforms used as tracers of the geo-morphological modifications of the Turin area are those related to hydrographic network and to micro-relief of ancient aeolian and glacial environments (scarps, dunes, incisions).

The analysis of various historical sources (papers, maps and images) from different archives aims to the reconstruction of different geomorphological settings of the urban area in recent and historical times. Then, evaluation of their modifications through the time is addressed to support activities of public interests, such as: spreading of Earth Science knowledge, valorization of geodiversity,

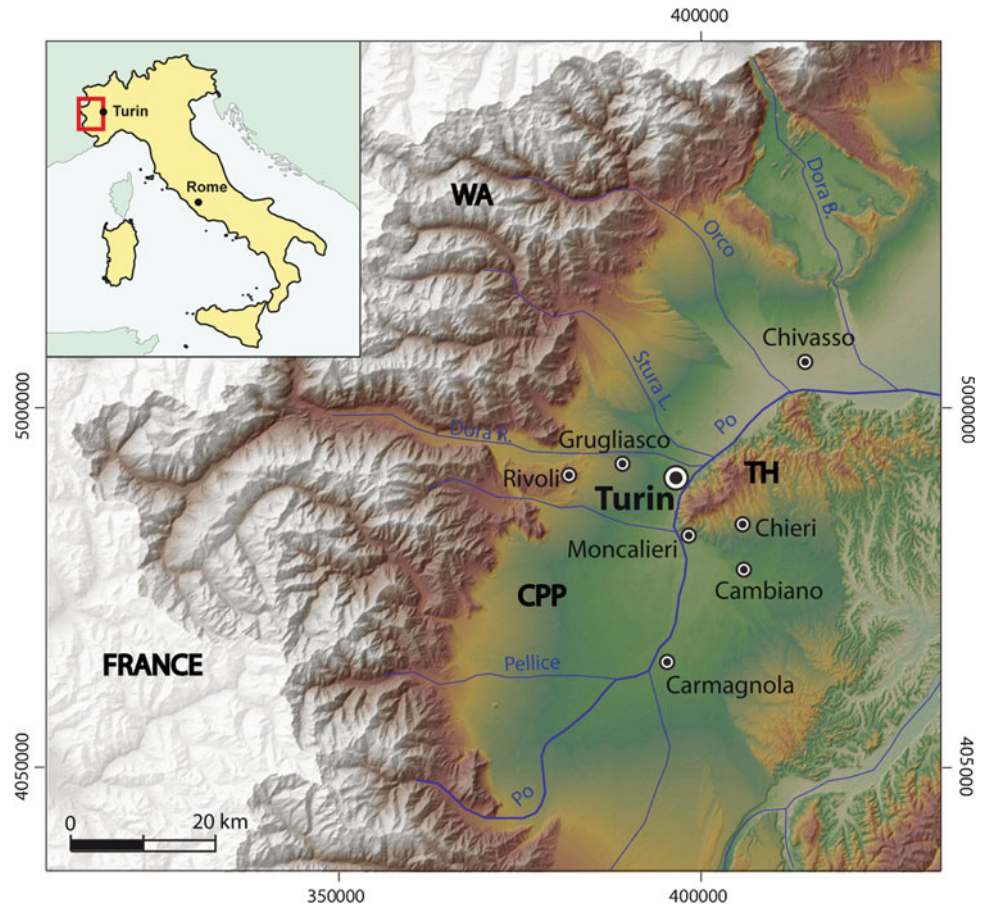
---

S. Lucchesi (✉) · M. Giardino  
Dipartimento di Scienze della Terra, Università di Torino,  
Via Valperga Caluso, 10125 Turin, Italy  
e-mail: srstefanialucchesi@libero.it

S. Lucchesi  
National Research Council, CNR-IRPI, Strada Delle Cacce, 10135  
Turin, Italy

M. Giardino  
NATRISK Research Centre, Università degli studi di Torino, Via  
Valperga Caluso 35, 10125 Turin, Italy  
e-mail: marco.giardino@unito.it

**Fig. 78.1** Location of the larger urban area of Turin (North-Western Italy) in the central Piemonte plain (CPP), between the Western Alps (WA) and the Turin Hill (TH)



enhancement of natural hazards assessment, risk management and town planning (Carraro and Lucchesi 2004).

## 78.2 The Historical Archives: Advantages and Limitations

During our research we used three types of data: (1) papers and textual documents, (2) pictorial representations, (3) ancient topographic maps. They were obtained from local, regional and national historical archives or sources (Archivio di Stato, Istituto Geografico Militare, CNR-IRPI, Archivio Storico della Città di Torino).

We took advantages of retrieving geomorphological data from historical archives: most papers, maps and pictures contain geographical constrains and are marked with a date, thus showing the geomorphological landscape of the area in a specific time interval, from present to past, whose length depends on the duration of the historical record. Therefore, geomorphological phenomena sometimes can be easily and precisely located in space and time, or at least contents and age of the documents point out the possible occurrence of a specific landform or process. On the contrary, by using classical geomorphological methods such as field survey or

aerial photointerpretation, only landforms preserved in the present-day landscape can be mapped and dated; sometimes, remnant of the oldest ones can be recognized and mapped, but other dating techniques are required for their chronological reference.

On the other side historical papers and pictures generally give punctual and/or qualitative indications that are hard to map with high detail. Historical maps give instead areal indications that can be easily overlapped and compared each other, even if a possible deformation of the topographical representation, depending on map detail and representation techniques, must be considered.

From the analysis of historical topographic maps we also draw some more general information on the environmental context of ancient landscapes. By considering some particular ancient toponyms no more recorded in modern maps (such as: *Gora*, or *Gorra*, *Porto*, *Le Basse*, *Molino* or *Molinello*, *la Marcia*, whose translations from local idioms are: “channel”, “fluvial harbour”, “lowland”, “mill”, “the march”) we pointed out the presence of lowland areas near river channels. *Fornace* (“kiln”) testifies the presence of exploited clays. The *Sabbioni* region is indicative of an area rich in sandy sediments due to relict aeolian dunes (Fig. 78.2), while the village of *Rivalta* is located, for

**Fig. 2** The area of “Sabbioni” (SW to Cambiano village), characterized by the presence of aeolian dune is now covered by a parking as can be seen comparing **a** the excerpt of the “Mappa del territorio di Torino a metà dell’Ottocento”—Stato Maggiore Sardo, 1854 and **b** the excerpt of the orthophoto Terraitaly it2000 (updating 2007)



example, near a high scarp (*ripa alta*) of the Sangone Stream.

A limitation to the use of historical documentation comes from different representation techniques of topographical and geomorphological elements with respect to the modern ones. In most ancient maps, drawn from land surveying without sophisticated positioning techniques, proportions among different topographical elements do not always correspond to the real ones. In addition, different historical maps usually have different symbols for representing the same elements, due to the lack of standards and to the subjectivity of the drawer. In any case, it is not possible to go back in time to the endless for the reconstruction of the ancient morphology: in our case study, maps with a good spatial reliability and with an acceptable detail (around 1:10.000, 1:20.000 scale) started off the eighteenth century. As a matter of fact, just by analyzing and comparing historical maps without any other additional information (texts, paintings, photos) it is very difficult to reconstruct geomorphological modifications of urban areas and to separate natural from artificial causes (e.g., discriminating between natural cut-off phenomena and artificial rectification of meanders; see next paragraph).

### 78.3 Reconstruction of the Hydrographic Setting in the Urban Area

In the Turin urban area, main hydrographic modifications of the local watercourses (Po, Stura di Lanzo, Dora Riparia Rivers and Sangone Stream) during the last 250 years have been drawn by three historical maps reproduced by the Istituto di Architettura Tecnica del Politecnico di Torino in 1968: “Carta topografica della caccia” dated to the last quarter of the 1700; “Plan Geométrique de la Commune de Turin” of the beginning of the 1800; “Carta dei contorni di Torino” of around 1850 and from four different updatings of the “Carta d’Italia” of the Istituto Geografico Militare (from 1875 to 1969).

Through the analysis of such historical maps it was possible to identify not only the main hydrographic modifications, but also their more or less detailed chronological references. Among the main natural modifications we identified lateral migration of watercourses, migration of the confluence point, meanders cut-off and formation of new small tributary channels.

Comparison of historical and present-day maps showed several modifications of the Po River course, either natural or artificial, during a time span of about 230 years. Till the end of the 1700, there was an active meander on the right side of the Po River at the foot of the Torino Hill where was built the ancient village of Moncalieri. Nowadays the only evidence of this meander is the arc-shaped depression articulating the hillside across the urban area of Moncalieri (Fig. 78.3).

Similarly, the relict meanders and the ox-bow lakes mapped in the “Carta topografica della caccia” (around 1785; A in Fig. 78.3) on the left side of the Po River near La Barauda (South of Moncalieri), are now no more recognizable neither in the field nor in modern maps.

### 78.4 Reconstruction of the Micromorphology of the Urban Area

Other important elements of the geomorphological landscape of Turin are represented by small reliefs and depressions (up to 100 m wide, and a few meters high) characterizing the local micromorphology of study area. They have been recognized in the “Carta dei contorni di Torino” (around 1850), an historical map 1:25.000 in scale; three examples are described below. Nowadays, many of these features are no more recognizable, because they have been progressively enclosed in a rapidly expanding and dense urban fabric.

At the Western boundary of the Torino hill, among the towns of Cambiano, and Chieri, depositional landforms have been indicated in maps and described in literature as “dunes” or “sabbioni” (Fig. 78.2). Field geomorphological surveys

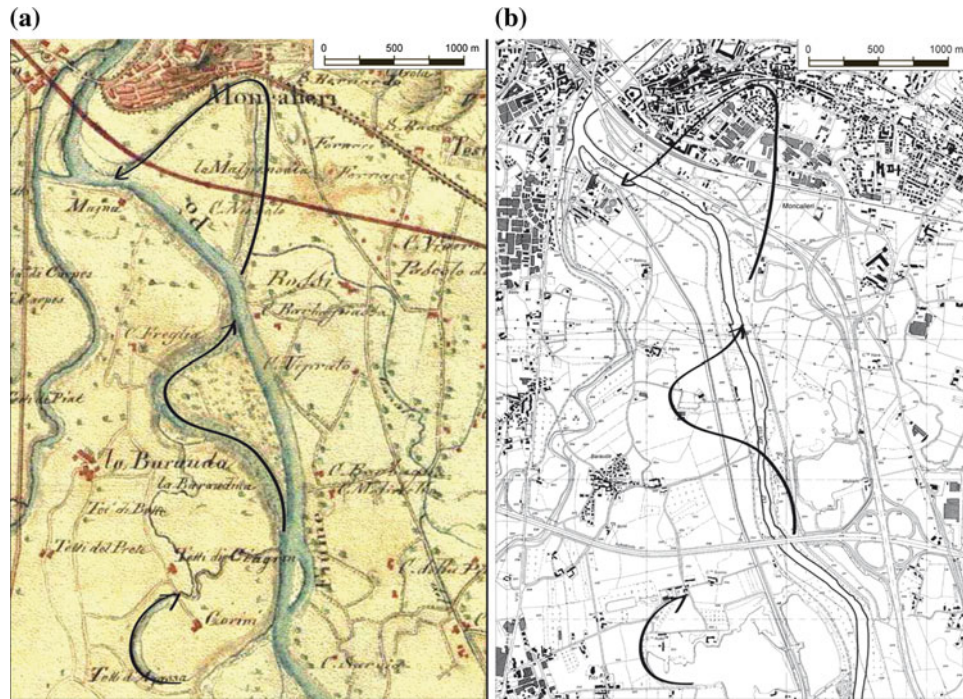


**Fig. 78.3** Comparison between the excerpt of: **a** “Carta topografica della caccia” dated around 1785 and **b** present-day Carta Tecnica Regione Piemonte—1:10,000 scale, sezione 174010. The arrows show previous meanders of the Po River that were artificially cut in the

nineteenth century for the construction of the national road and the urban expansion of the town of Moncalieri, at the boundary with Turin municipality

and granulometric analysis of sediment samples from these reliefs allowed to discriminate between aeolian and riverine dunes dated back to Upper Pleistocene-lower Holocene, for their palaeoenvironmental contexts.

At the western suburbs of Turin, near the town of Rivoli, similar microreliefs have been mapped and described. Field survey and laboratory analysis allow to interpret most of them as riverine dunes related to

Holocene fluvial modeling, only a few being relics of morainic ridges related to the Rivoli-Avigliana Morainic Amphitheater (i.e., Truc Garghera, Fig. 78.4), and one can be considered an aeolian dune. This latter is now quite destroyed by the urban expansion of the town of Grugliasco. In some local archeological sites we also found remains of necropolis partially settled in these sandy sediments (Lucchesi 2004).

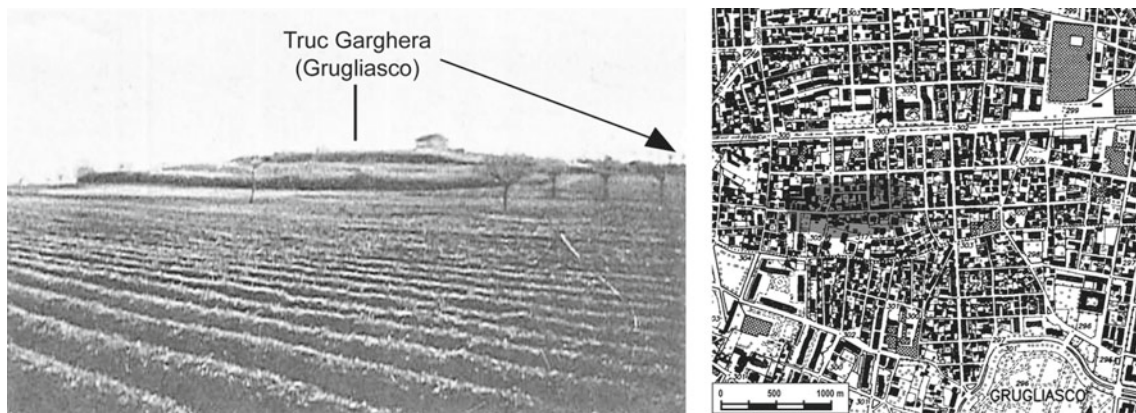


**Fig. 4** Truc Garghera (Grugliasco): the relief visible in a photo from Prever, dated 1907 (on the left) is now quite completely covered by buildings and no more recognizable, as shows the topographic map of

the Regione Piemonte, scale 1:10,000 (on the right). The relief is mapped in grey color

Similar but more isolated, reliefs have been also locally mapped in different parts of the urban area. Also some ancient authors like Promis (1869) pointed out that near the eastern city fortifications of the city there was an “isolated mound”, 6–7 m high, subsequently flattened by human activity. The genetic interpretation of these reliefs is difficult to define in absence of other data.

## 78.5 Conclusions

Data coming from the analysis of historical archives integrated with those from field surveys, remote sensing and laboratory analysis, allowed the acquisition of a better knowledge on geomorphological modifications of the urban area of Turin (NW-Italy) in recent and historical times. Ancient landforms, such as riverine dunes, aeolian dunes or morainic ridges, became important elements for their geological, scientific and cultural value: they offer information about ancient landscape, environment and climate changes; some of them are also archeological sites (e.g., the Grugliasco dune). All these data are relevant for identifying geodiversity and for enhancing earth science knowledge and preservation measures (e.g., Museo Torino Project: <http://www.museotorino.it>; Giardino et al. 2012).

Historical data regarding more recent landforms, such as those related to the hydrographic network, are very important for hazard assessment and risk management. The geodatabase

produced within this study have been useful for base geological mapping (Balestro et al. 2010; Festa et al. 2010), geomorphological analysis related to the General Town Plan of the city of Turin and for planning local watercourses regulation.

## References

- Balestro G, Cadoppi P, Piccardo GB, Polino R, Spagnolo G, Tallone S, Fioraso G, Lucchesi S, Forno MG (2010) In: Polino R (ed) Foglio 155, *Torino Ovest*, Carta Geologica d'Italia alla scala 1:50.000. A.R.P.A., Tip. Geda, Torino
- Carraro F, Lucchesi S (2004) Application of integrated allostratigraphy in the geological survey of the central Piedmont plain. In: Pasquare G, Venturini C (eds) Mapping geology in Italy. C.N.R.–A.P.A.T., Roma, pp 70–76
- Festa A, de la Pierre F, Irace A, Piana F, Fioraso G, Lucchesi S, Boano P, Forno MG (2010) In: Polino R (ed) Foglio 156, *Torino Est*, Carta Geologica d'Italia alla scala 1:50.000, A.R.P.A., Tip. Geda, Torino
- Giardino M, Pavia G, Lombardo V, Lucchesi S, Russo S (2012) *MuseoTorino: science and images tell the story of Turin (Italy) before the city*. In: Proceedings of the 7th European Congress on Regional Geoscientific Cartography and Information Systems (EUREGEO), Bologna, 12–15 June 2012, vol. 1, pp 282–283
- Lucchesi S (2004) Inquadramento geologico e geomorfologico del sito. In: Pejrani Baricco L (ed) Presenze longobarde. Collegno nell'Alto Medioevo. Min. Beni Attività culturali, Soprintendenza per i Beni Archeologica del Piemonte, Città di Collegno. Stamp. Art. Naz., Torino, pp. 13–15
- Promis C (1869) Storia dell'antica Torino Julia Augusta Taurinorum scritta sulla fede de' vetusti autori e delle sue iscrizioni e mura. Stamp. Reale, Torino, pp 34–37

# Reconstructions, Transfers and Forced Abandonments Brought About by Earthquakes and Landslides in the Historical Centres of Southern Italy: The Role of Primary Sources

Fabrizio Terenzio Gizzi , Maria Rosaria Potenza, Maria Sileo, and Cinzia Zotta

## Abstract

Italy is among the most prone Mediterranean countries to extreme natural menaces, such as earthquakes and landslides. These can cause serious damage to the properties and consequent changes in urban areas and historical centres especially, due to their high vulnerability. Starting from these preliminary remarks the paper deals with an ongoing research activity aimed at analyzing in depth and in a systematic way the damage and the consequent abandonments, transfers, and forced reconstructions caused by significant earthquakes and/or landslides in the historical centres of Southern Italy during the twentieth century. To make clear the methodology followed, the paper analyses three case studies related to the same number of historical centres menaced by mass movements and/or earthquake phenomena. The final aim of the research is to setup a reference Web Gis Atlas that will be a further tool that the stakeholders will find useful to improve mitigation risk actions against the two main geological menaces acting in Italy.

## Keywords

Natural disasters • Historical centres • Archive sources • Southern Italy

## 79.1 Introduction

Geological threatens are among the main factors conditioning the conservation of historical centres. Indeed, earthquakes, landslides, and floods caused changes in the urban frameworks worldwide and over the centuries.

These considerations are suitable especially for the historical centres located in Italy whose territory is prone to seismic and/or hydro-geological hazards, in the southern area especially (Boschi et al. 2000; Apat 2008).

As a matter of fact, the twentieth century saw the impact of significant seismic events or landslides (e.g.: 1908 Calabria, 1915 Marsica, and 1980 Irpina earthquakes; 1966

Agrigento slide, the persistent soil instability of Orvieto and Civita di Bagnoregio towns) on numerous towns and historical centres with the subsequent loss of tangible heritage.

In spite of the importance of bringing the “memory” of past events to light in order to mitigate the risks, a methodical work aimed to thoroughly analyse the losses and changes brought about by the geological events in old towns planning layout is still lacking.

Bearing these preliminary remarks in mind, we started a research aimed at filling this gap partially. The research consists of the archive documentary analysis and the drafting of thematic maps about the mid-to-long-term effects and consequences of earthquakes and landslides occurred in the last century (twentieth) in the historical centres located in Southern Italy and Southern Apennines particularly, areas characterized by a high seismic and hydro-geological hazard. In detail, the towns that will be considered are those of Basilicata, Molise, Calabria, Campania, Apulia, and Sicily (Fig. 79.1). As regards the amount of the sites being considered, it will depend mainly on the completeness and quality of historical data retrieved.

F.T. Gizzi (✉) · M.R. Potenza · M. Sileo · C. Zotta  
Institute of Archaeological and Monumental Heritage (IBAM),  
Potenza, Italy  
e-mail: f.gizzi@ibam.cnr.it

**Fig. 79.1** Overview of the Italian regions to be considered in the ongoing research activity on the historical urban changes. The figure also shows the location of the three case studies illustrated in the paper



However, a quick estimate can suggest a number of towns that exceeds one hundred at great length.

To make clear the work and methodologies that will be followed up, this paper shows three case studies relating to the same number of historical centres of Southern Italy involved in natural disasters. These sites were analysed in detail as regards two main aspects: the damage caused by the extreme natural events and the institutional actions taken to restore the disaster effects in the built-up area.

The methodology showed in this paper will be useful to maintain the research whose final aim is to edit a Web Gis Atlas whose thematic maps will resume the overall impact (e.g.: abandonments, transfers, and forced reconstructions) caused by twentieth century natural extreme events on the historical centres of Southern Italy. This will help the stakeholders to put into the field proper actions aimed to the built heritage safeguard.

### 79.1.1 Methodology

To reach the goals of the research, the extensive primary sources investigation is ongoing in the archives of local and central institutions. This will allow collecting and analysing

a very large amount of unpublished historical-technical and administrative sources such as: (1) multi-temporal basic and thematic maps of historical centres, (2) multi-temporal aerial and terrestrial photos of the old towns, (3) reports filled in by the technicians entrusted by the institutions with the survey of the damage caused by the landslides or earthquake on the built areas.

Through the analysis of the basic or thematic historical maps or photos, such as those drawn up by the Cadastral Office, Office staff of Civil Engineering, Italian Geological Survey, the Italian Military Geographic Institute, Superintendence of Monuments, we will be able to identify with high spatial detail:

- the urban layout of the site *before* the occurrence of the natural event;
- the areas of the historical centres affected by the landslide or earthquake damage. Depending on the quality of the sources we will be able to get information about effects at a quarter/street or at a building/housing scale;
- the areas where consolidation works, hydro-geological maintenance, reconstructions and transfer actions were put into the field by the institutions over the time.

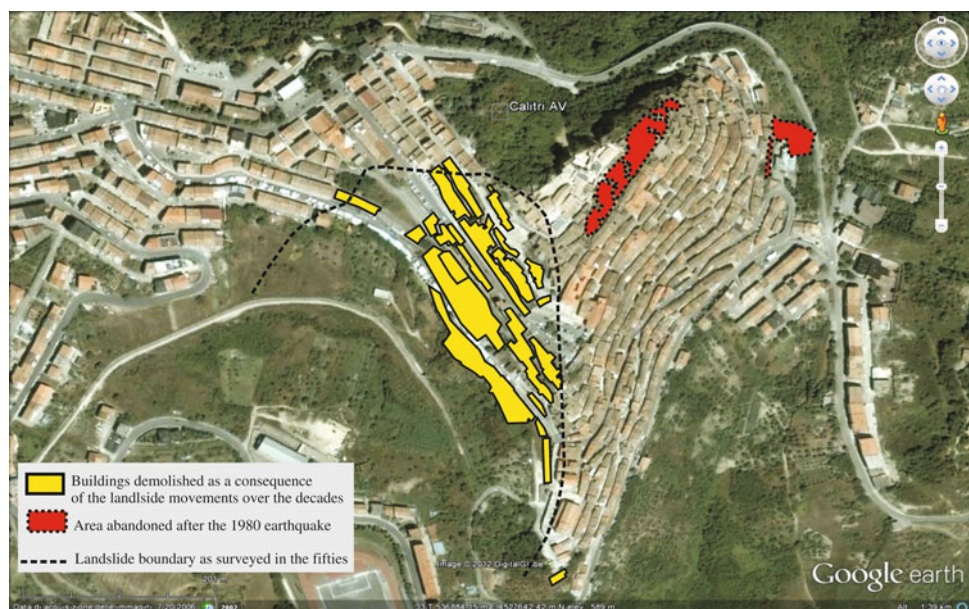
As mentioned, the cartographic data, ranging from late XIX century to late XX century, will be integrated with the technical reports filled in by the technicians entrusted with the survey of the areas involved in the disasters so as to better delineate the effects of the natural events and the actions planned by the institutions for the historical centres affected by the disasters. For example, getting new macroseismic information concerning the damage caused by the 23 November 1980 earthquake ( $M_e = 6.9$ ) was possible thanks to two main typologies of technical sources preserved in local archives: the “*Scheda A*” and “*Scheda B*” (the “*Survey Cards*”) drawn up in the aftermath of the earthquake, and the reports and maps elaborated within the framework of the “*Piani di Recupero*” (“*Plans of Recover*”) of the historical centres, scheduled by a law governing the rebuilding phase (Law n. 219/81). Therefore, thanks to the in-depth study of the Survey Cards it was possible to delineate the damage maps at an urban scale for about 90 towns located in the Basilicata Region (Southern Italy) (Gizzi et al. 2012).

All the information deriving from documentary investigations will be compared with the current setup of the historical towns to argue the real overall impact of the natural events on the built-up areas.

## 79.2 Case Studies

This section will put into evidence the methodological approach followed considering the analysis of three case studies of downtowns localised in three different regions of Southern Italy (Fig. 79.1). Each site is located in a geological background different from the other so as to deal with the methodology in the way as thoroughly as possible.

**Fig. 79.2** Changes imposed by the historical landslides reactivations and the 1980 seismic event in the town of Calitri (Avellino, Campania Region, Southern Italy)



### 79.2.1 Calitri

Calitri is a typical village of the Southern Apennines (Campania Region), a Neogene fold-and-thrust belt made up of Mesozoic-Paleogene sediments, that stands on a ridge localised on the left orographic side of the Ofanto River whose erosion causes a deep soil instability.

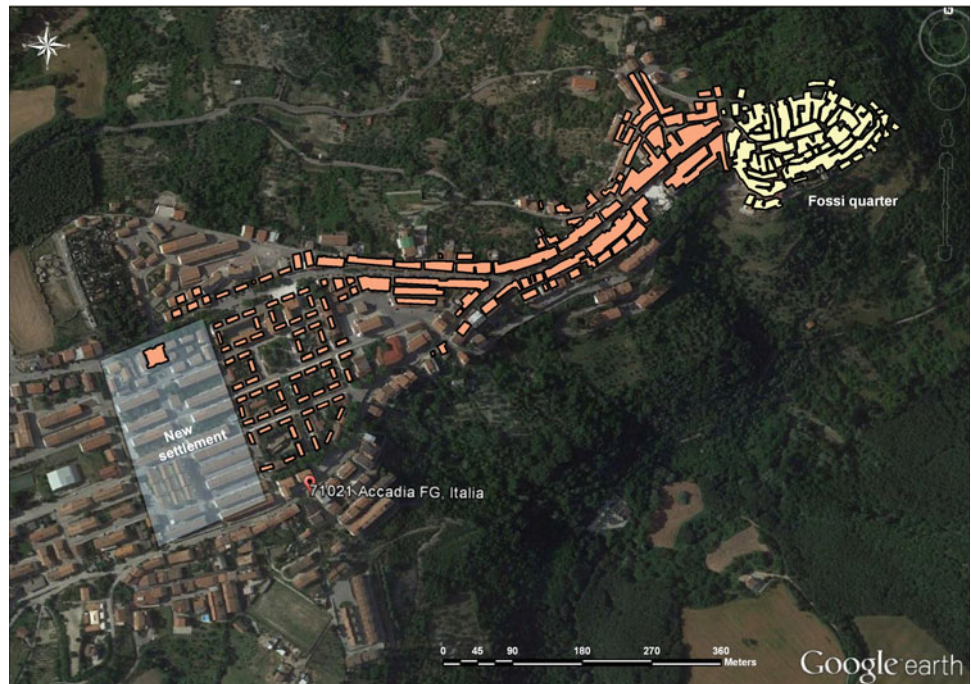
From a geological point of view, the inhabited area lies on sandy-arenaceous deposits (early-middle Pliocene) superimposed on grey-light blue clayey-marly deposits (early Pliocene).

The changes occurred in the urban town planning during the second part of the twentieth century are due to the joint actions of landslides and earthquakes.

In detail, according to the Italian Geological Survey the western area of the town was still subject to the soil instability in the early fifties. As a consequence, some buildings located on the landslide area were so seriously damaged that the authorities suggested shifting the town partially and putting into the field wide consolidations works of the entire historical centre. Nevertheless, the end of fifties saw new reactivations of the mass movement.

As for the 1694 and 1910 seismic events, also the 1980 earthquake caused the re-activation of the main landslide with heavy damage to many buildings that were demolished and the inhabitants transferred to other areas. Moreover, the 1980 earthquake brought about direct building damage in a wide area close to the landslide sector: this quarter was also abandoned and the inhabitant shifted to other areas (Fig. 79.2). The high vulnerability of the edifices, made up of poor materials and rough building techniques, worsened the effects of interacting natural disasters, thus “amplifying” their actions.

**Fig. 79.3** Accadia (Foggia, Apulia Region, Southern Italy). Satellite view with superimposed the transfer plan of *Fossi* quarter compiled in the 1950s. The quarter was abandoned after the damage caused by the 1930 and 1962 seismic events



## 79.2.2 Accadia

Accadia is a town located in the *Subappennino Dauno* (Apulia Region), a mountain range which is the eastern continuation of the Samnite Apennine, made up of calcarenite and arenaceous-marly-clayey sediments Miocene in age and sandy-arenaceous and clayey deposits Pliocene in age.

The town is located on a hill top placed at the confluence of two streams. The eastern quarter of the centre, known as *Rione Fossi*, lies on sandy-arenaceous deposits where many grottoes were dug by men over the centuries.

The strong natural event of the twentieth that marks the turning point of the town history is the 23 July 1930 earthquake ( $M_e = 6.7$ ) that caused significant damage to the entire town and *Rione Fossi* particularly (site intensity  $I_s = VIII$  MCS). The serious effects caused by the 1930 earthquake and the building collapses occurred in the early thirties obliged the authority to declare the *Fossi* quarter to be transferred. Such a decision was made considering the hydro-geological instability of the soil caused by the wide and interconnected network of unconsolidated and unstable grottoes. The conditions were made even worse by the fact that the buildings showed a bad state of conservation and a high structural vulnerability imputable to the poor building techniques and materials used that were typically formed by stream pebbles. However, the transfer of the quarter to the western historical centre was not carried out at least until the occurrence of the 21 August 1962 earthquake ( $M_e = 6.2$ ) whose effects on the built-up area ( $I_s = VII$  MCS) were conditioned by the high soil instability (Fig. 79.3).

## 79.2.3 Pisticci

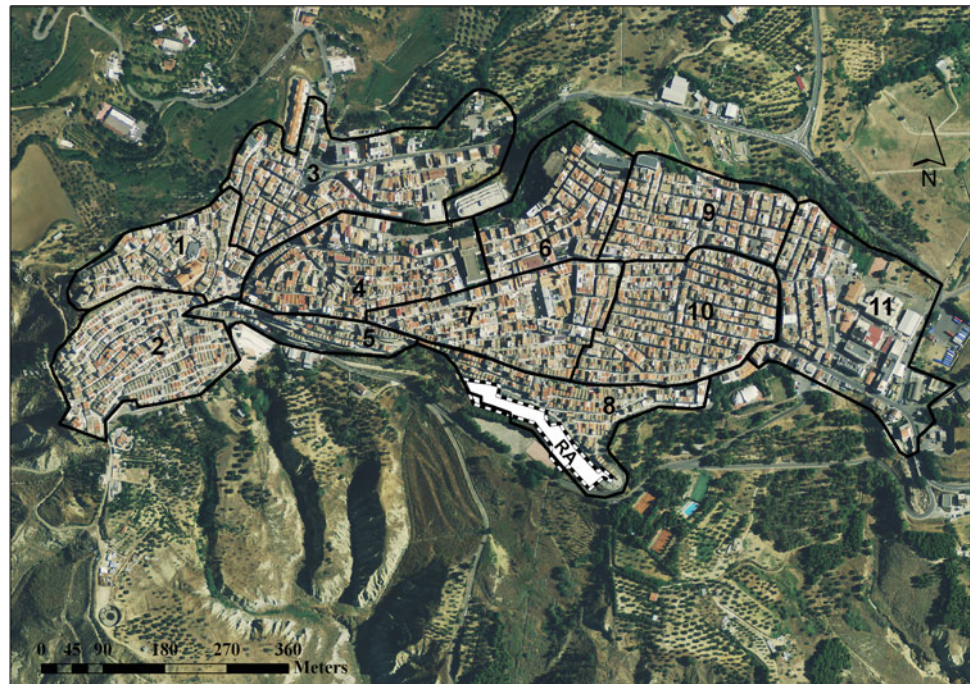
This is a town of the Basilicata region located in the Bradanic Trough, a Pliocene-Pleistocene sedimentary basin filled with clayey and sandy-conglomeratic deposits and placed between the Southern Apennines and the Apulia foreland.

Pisticci lies on a wide terraced surface bounded by steep slopes shaped by intense superficial erosive phenomena. The relief is made up of clayey deposits, Pliocene and Pleistocene in age and sandy-conglomeratic sediments, Pleistocene in age.

Since the past centuries the town has been involved in wide and disastrous landslides. To analyze these in depth, the systematic analysis of the bibliographic sources and unpublished primary technical documents is ongoing. The preliminary version of the data set, updated with several new events unknown in literature (not discussed here), indicates that the downtown area was hit by about forty landslides from the sixteenth century to the early 1970s.

The first event dates back to 1505, but the main landslide affecting the town happened in 1688, when two quarters (*Casalnuovo* and *Croci*) were almost completely destroyed. In consequence of the occurrence of the mass movements in 1850 the town was involved, for the first time, in the consolidation works (1864–1876). Nevertheless, about twenty events or reactivations were recorded in a time span of 70 years (1890–1959). The damage caused by these slides induced the competent authority to plan transfer actions in the early 1960s. The transfers were planned considering two priority levels: the “urgent transfer” of two quarters (*Rione*

**Fig. 79.4** Pisticci (Matera, Basilicata Region, Southern Italy). Superimposed on the aerial photo is the subdivision in quarters of the town. The ongoing historical investigations suggest that the most affected areas are those numbered 1, 5, 3 and 8. Due to such events almost all the town was considered to be transferred in the 1960s. However, only a small portion (RA) was really relocated in another area



*Croci* and *Rione Dirupo*) and the “normal transfer” of the other areas of the village. However, the other slide reactivations happened in the later sixties and early seventies persuaded the authorities to put into the field further consolidation works, putting away *de facto* the relocating plans. As a matter of fact, comparing the old and current layouts of the whole town it emerges that only a small portion of the original transfer hypothesis was carried out, whilst most neighborhoods currently show an urban layout comparable with that of the sixties. In addition, a limited urban growth is currently identifiable in some areas that the technical surveys performed in the fifties and sixties pointed out as involved in mass movements (Fig. 79.4).

### 79.3 Conclusion

The seismic history of Italy informs us that the country experienced numerous strong events that caused deep changes to the urban, socio-economic, and natural contexts. Similar consideration can be made if one considers the hydro-geological hazard and its relationship with human settlements. However, detailed analysis on the medium-to-long-term damage and consequences caused in the Italian towns is still not available and not accessible in a systematic way.

With this in mind, the paper has dealt with an ongoing research aiming to perform a methodical analysis of the damage and consequences, such as transfers, reconstructions,

and abandonments caused by the earthquakes and landslides in the urban areas, and historical centres in particular, of Southern Italy in the twentieth century. The requirement of such a study is an intensive and crossed use of historical sources, primary documents especially, to get as reliable and suitable information as possible.

Through three case studies, which are symbolic of the different site conditions that will be encountered, the paper has shown the entire methodology that will be followed during the research activity.

The long-term aim of this work is to supply a Web Gis Atlas, a tool of technical-historical knowledge useful to mitigate the risks in the Italian historical centres, especially.

### References

- APAT (2008) Report on landslides in Italy. IFFI Project. Methods, results and regional reports. Special Report. <http://www.isprambiente.gov.it/it/pubblicazioni/rapporti/landslides-in-italy-special-report-2008>. Accessed 8 Oct 2013
- Boschi E, Guidoboni E, Ferrari G, Mariotti D, Valensise G, Gasperini P (2000) Catalogue of strong Italian earthquakes from 461 B.C. to 1997. Introductory texts and CD-ROM, Version 3 of the Catalogo dei forti terremoti in Italia. *Annali di Geofisica* 43(4):55
- Gizzi FT, Potenza MR, Zotta C (2012) 23 November 1980 Irpinia-Basilicata earthquake (Southern Italy): towards a full knowledge of the seismic effects. *Bull Earthq Eng* 10(4):1109–1131. doi:10.1007/s10518-012-9353-Z

---

# Relevance of Database for the Management of Historical Information on Climatic and Geomorphological Processes Interacting with High Mountain Landscapes

80

Guido Nigrelli and Marta Chiarle

---

## Abstract

In the framework of the activities of the GeoClimAlp research group (Geomorphological impacts of Climate change in the Alps), a system of databases has been developed for the storage and management of glacial, periglacial and mountain digital resources, related to the Greater Alpine Region in general, and to the North-Western Italian Alps in particular. These resources are historical documents, publications, photos, aerial photographs, antique and recent maps, instrumental and survey data, related to: (i) alpine glaciers; (ii) natural instability processes and landforms in glacial/periglacial areas; (iii) hydro-climatic conditions of the alpine areas. This wealth of knowledge is mainly referred to the last 150 years. The GeoClimAlp digital resources stored in these databases are mainly used to: (i) study the spatial-temporal evolution of alpine glaciers; (ii) study the geomorphological processes, and in particular natural instability, that occur at high altitude (over 2000 m a.s.l.), in particular as a consequence of climate change; (iii) assess the hydro-climatic conditions of the glacial/periglacial and mountain areas; (iv) conduct research on climate change in the alpine environment.

---

## Keywords

Database • Geomorphology • Climatology • Alps • Italy

---

## 80.1 Introduction

The Alpine environment, and in particular the high-altitude one, is responding quickly and with great intensity to ongoing climate change, through evidences of geomorphological, hydrological and ecological type (Fig. 80.1). Mountain glacier shrinkage and related outcropping of rock walls and debris, changes of the precipitation and temperature patterns and of the hydrological regimes, the shift of

flora and fauna species to higher altitudes than the habitat they belong to, are some of the main terrestrial indicators of climatic change. The impact of these changes on slope stability, water resources and human activities is remarkable: however, the understanding of the ongoing phenomena and the forecasting of future scenarios still show large uncertainty.

GeoClimAlp (Geomorphological impacts of Climate change in the Alps) is a research group of CNR-IRPI (Consiglio Nazionale delle Ricerche, Istituto di Ricerca per la Protezione Idrogeologica), established with the intent to improve the knowledge on the role of climate change in the morphogenesis of the alpine environment in general and of high-altitude environments in particular. The geological-morphological and climatic-hydrologic research fields are the main ones to be integrated in the scientific activities of the research group.

---

G. Nigrelli (✉) · M. Chiarle  
Consiglio Nazionale delle Ricerche, Istituto di Ricerca per la  
Protezione Idrogeologica, GeoClimAlp Research Group, Strada  
delle Cacce 73, 10135 Turin, Italy  
e-mail: guido.nigrelli@irpi.cnr.it

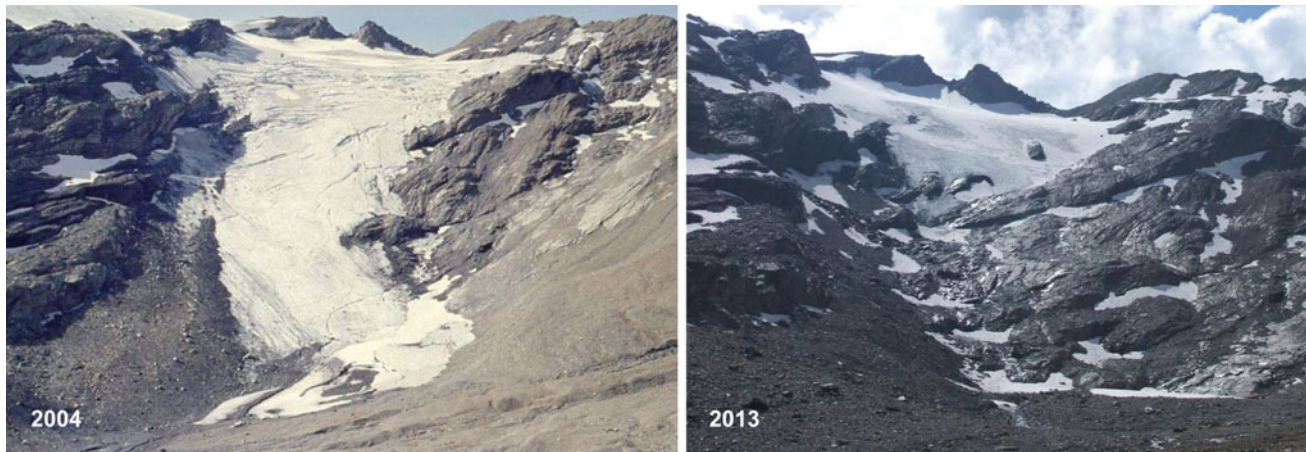


**Fig. 80.1** Recession of the Breuil Meridionale Glacier in the Aosta Valley (NW Italy) from 2004 to 2013. The compared pictures show a

strong retreat of the glacier snout in less than 10 years. (Sources 2004 photo by A. Viotti; 2013 photo by M. Chiarle)

The activities currently carried out by GeoClimAlp are mainly oriented to the study of natural instabilities occurring in mountain environments, with emphasis on morphodynamic processes in the glacial and periglacial environment, on environmental changes taking place due to the climate change, and on related geohazards. For these purposes, a systematic activity of documentation is carried out, which focuses on instability events that occur in mountain areas, with particular attention to paroxysmal events in high-altitude alpine environments, and on the recent evolution of glaciers, and of glacierized and recently deglaciated areas.

In order to achieve the above mentioned objectives, the geological-geomorphological research field is integrated with the climatic-hydrologic one. In accordance to this approach, investigations include: the study of climate variability and trends in the alpine environment through time series analysis, the analysis of precipitation and thermal conditions associated to morphodynamic processes in glacial and periglacial environments, the monitoring of key climate variables measured at ground level in glacial basins, and the study of the relations between these variables and large-scale circulation patterns.

In order to better store and manage different types of collected data, in consideration also of the continuously growing amount of available documentation, of the different formats of data, and of the perishability of historical documents, the GeoClimAlp research group, developed a system of databases for the management of the information related to the Greater Alpine Region (HISTALP 2010) in general, and to the North-Western Italian Alps in particular, with a preferential use of open source technological solutions. The stored information includes historical documents, images (terrestrial and aerial photos, satellite images), cartographic data, and thematic maps, in addition to new data generated during the development of several research projects.

## 80.2 Description of Databases

In order to meet the needs of the different research project, several databases have been realized in the last few years. According to modern approaches to the information management, allowed by the continuous development of new informatic tools, also open source, a system of databases was considered as the most suitable tool to manage all the information already stored. This system presently rely on seven databases developed in the framework of the activities of the GeoClimAlp research group, which are briefly described here below.

1. Alpine Glacier Inventory (AGI). In the framework of the Alcotra 2007–2013 project “GlaRiskAlp – Glacial Risks in the Western Alps” (GlaRiskAlp 2013), the need arose to compile a complete digital inventory of glaciers of Western and South-Western Piedmont (NW Italian Alps), in order to locate and quantify the glacial resource and its evolution over time. In this framework, the GeoClimAlp research group, in cooperation with the University of Turin (Departments of Computer Science and Earth Sciences), created a database to meet the project’s specific needs and to provide a modern tool for storing, processing and sharing glaciological data (Nigrelli et al. 2013). The main goals that have shaped the design and implementation of the database are the following: (i) to archive and store the huge amount of glaciological data collected and to plan for new types of data and data formats in current use; (ii) to develop a tool that could catalogue the data sources for each glacier according to the standards of the World Glacier Inventory and of the Italian Glaciological Committee; (iii) to share the collected data, making them accessible and useful for various purposes; (iv) to meet the above-mentioned demands with low-cost solutions.

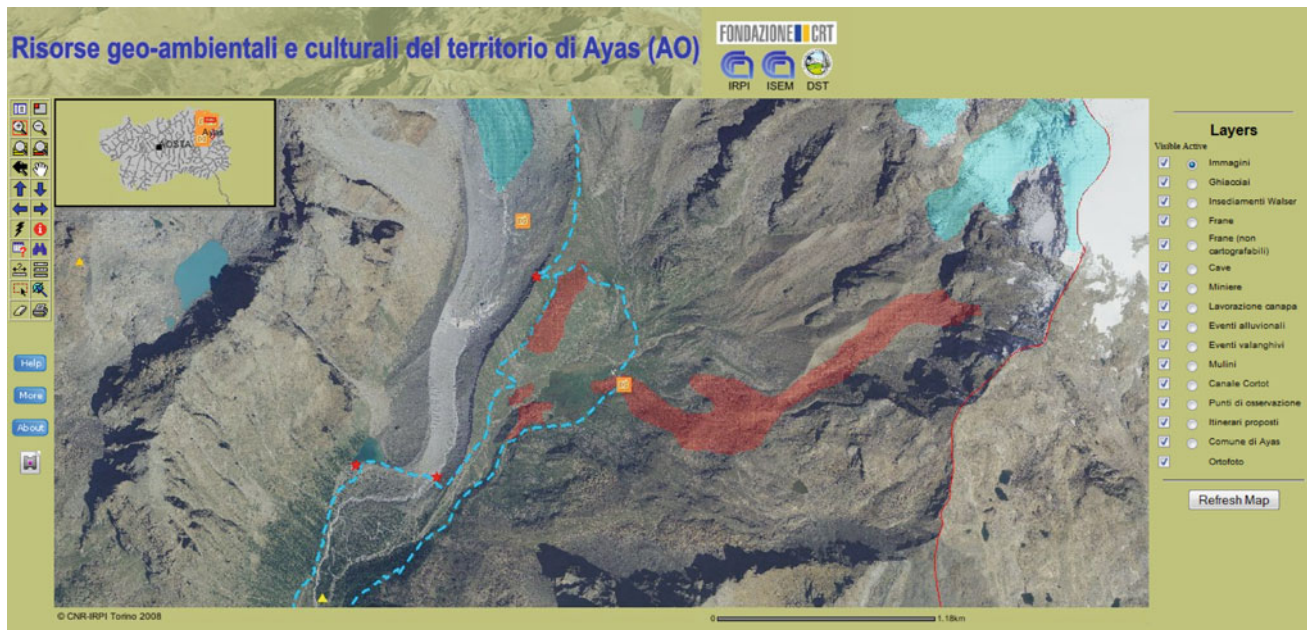
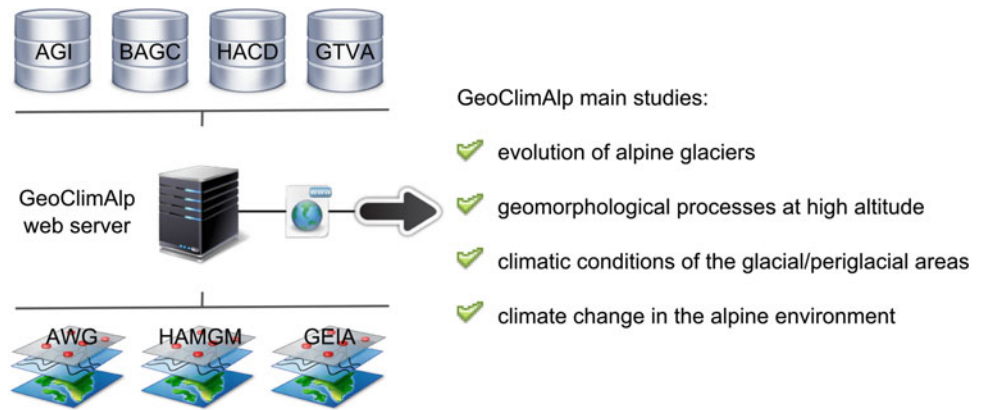


**Fig. 80.2** Screen shot from the AWG database illustrating the available information level (website: <http://s2irpito.to.cnr.it/Website/ayas/viewer.htm>)

2. Bibliographic database on Alpine environment, Glaciers and mountain Climate (BAGC). This database was designed to archive and manage a large amount of bibliographic resources in both paper and digital format. It serves two basic purposes: (i) to collect and store publications and unpublished reports (articles in international, national and local journals, monographs, conference proceedings, technical reports) and maps (historical, topographic and thematic maps); (ii) to provide access to information and products for use by researchers, decision makers, and students (Nigrelli and Vergnano 2012).
3. Historical Alpine Climate Data (HACD). This database was designed to manage an archive heterogeneous types of climatic data. Its basic purposes are to collect and store weather data, as well as to provide access to climatic data and products for use by researchers, climatologists, decision makers, and students. The database was designed and developed following the World Meteorological Organization standards and requirements for climate data management. The database can manage several climatic parameters: temperature, precipitation, rainfall, snow depth, atmospheric pressure, relative humidity, wind; solar radiation, water level and water flow (Nigrelli and Marino 2012).
4. GeoTourism Val d'Ayas (GTVA). This database is designed to be able to manage heterogeneous types of resources. The resources in this database have been used to design and plan some activities of geotourism in the Aosta Valley, with particular attention to the municipality of Ayas. For these purposes, the database can manage (i) aerial and terrestrial photos; (ii) historical documentation and recent publications; (iii) maps and images; (iv) videos.
5. Ayas WebGIS for geological, environmental and cultural resources (AWG). This is a geographic information system on the web designed to store, analyze, manage, and present geological, environmental and cultural data concerning the municipality of Ayas (North-Western Italian Alps). The database uses also the information contained in the database previously described. Through this web service, the viewer can display the different themes that make up the resources in terms of geotourism; these themes are: glaciers, geosites, landslides, mountain landscape, quarries, mines, mills, trails, historic Walser settlements, scenic spots of observation and related photos (Fig. 80.2).
6. High Alpine Mountain and Glacier Monitoring (HAM-GM). This data set consists of a collection of digital data acquired: (i) during field survey campaign related to glacier monitoring activities and to investigations in high-elevation alpine areas, collected with a gps receiver; (ii) by means of tools GIS. For this reason, the database has to manage data in different digital formats (in gpx, kml, kmz and shapefile format). The main files collected are: glacier terminus position, snout elevation, snow lines, lines of the moraine ridges, measures and photographs from fixed points, fixed points position, meteorological stations position, geodetic IGM benchmarks position, traces of the approach routes to the glaciers.

**Fig. 80.3** Schematic structure of the database system. For the meaning of the acronyms see the text



7. Glaciers Evolution in the Italian Alps (GEIA). This is a set of spatial data relating to the areas of the glaciers located in Western and South-Western Piedmont (NW Italian Alps), developed in the framework of the already mentioned Glariskalp project: data can also be viewed on the web page of the project (GlaRiskAlp 2013). These data refer to two different time-steps: (i) at the end of the Little Ice Age (approximately around the year 1850); (ii) in 2006.

### 80.3 Architecture and Technology of the System of Databases

The architecture of this system of databases is very simple (Fig. 80.3). The four databases and the other data set collections are stored in the GeoClimAlp web server that uses the Microsoft Windows Server 2003 operating system. The four server side databases are managed and used through a simple web interface. These databases and web applications associated with them have been developed using free open source software (Apache, MySQL, PHP, Java, phpMyAdmin). One data set collection is managed on local PC using QGIS and is used on line by a WebGIS system, a distributed GIS services over the web (ESRI ArcIMS). The other two data sets are stored in specific folders of the GeoClimAlp website and are used on line with the services of Google Maps and Google Earth, both in the field and in the office.

By means of this simple interconnection between databases and data collections, the GeoClimAlp research group has the possibility to manage a substantial amount of historical and recent glacial, periglacial and mountain digital resources, related to the alpine region.

### 80.4 Future Work and Conclusions

The use of databases for the management of historical and recent information on climatic and geomorphological processes interacting with high mountain landscapes becomes strategic in all those cases in which there is the need to analyze in detail a high number of natural variables, distributed in time and space. For these cases, the speed and accuracy in the research of information are the main strategic success factors. In order to improve these aspects, the GeoClimAlp research group is developing a system of metadatabase, able to simultaneously interrogate various databases located on different web servers.

### References

- HISTALP (2010) Historical Instrumental Climatological Surface Time Series of the Greater Alpine Region. Central Institute for Meteorology and Geodynamics, Wien, Osterreich. <http://www.zamg.ac.at/histalp> (accessed September 25, 2013)
- GlaRiskAlp (2013) Glacial Risks in Western Alps. ALCoTra, Italian Transborder Alpine Cooperation program 2007-2013. Fondazione Montagna Sicura, Courmayeur, Italia. <http://www.glariskalp.eu> (accessed September 27, 2013)
- Nigrelli G, Chiarle M, Nuzzi A, Perotti L, Torta G, Giardino M (2013) A web-based, relational database for studying glaciers in the Italian Alps. *Comput Geosci* 51:101–107
- Nigrelli G, Marino ALL (2012) Dbclim: a web-based, open-source relational database for rainfall event studies. *Comput Geosci* 48:337–339
- Nigrelli G, Vergnano M (2012) A web-based, relational database for landslide, mud-debris flow and flood studies in northern Italy. *GEAM Anno XLIX*: 67–70

---

# Dynamic Geomorphology and Historical Iconography. Contributions to the Knowledge of Environmental Changes and Slope Instabilities in the Apennines and the Alps

81

Giardino Marco, Mortara Giovanni, Borgatti Lisa, Nesci Olivia, Guerra Cristiano, and Lucente Corrado Claudio

---

## Abstract

In the unique Italian cultural context, the use of historical documents, among which iconography, may represent a powerful tool to describe past natural events and thus add pieces of information to the hazard and risk puzzles. Besides written documents, drawings, paintings, sketches and views allow geologists to acquire a special multitemporal data set on some important landslide features: geometry (volumes, areas, thickness, runout), kinematics (type, state of activity, distribution of activity), impacts etc. Here, some examples of the representation of dynamic geomorphological processes in historical archives are presented and commented with reference to the Apennines and the Alps.

---

## Keywords

Landslides • Historical archives • Paintings • Apennines • Alps

---

## 81.1 Introduction

Italy is a very young and dynamic terrain from a geological and geomorphological point of view, and the deposits of large landslides are widespread in the Apennines and in the Alps. Even if our country has been inhabited since ancient times, the knowledge and in particular the memory of past catastrophic landslide events are often very limited. This implies a poor documentation of the magnitude and frequency characteristics of large landslides. Anyhow, in our unique cultural context, the use of historical documents, among which iconography, may represent a powerful tool to describe past events and thus add pieces of information to the hazard and risk puzzles. Besides written documents, drawings, paintings, sketches and views allow geologists to acquire a special multitemporal data set on some important landslide features: geometry (volumes, areas, thickness, runout), kinematics (type, state of activity, distribution of activity), impacts etc. Of course, this dataset has a number of biases, mainly due to the representation techniques, the viewpoint, the artistic attitude of the author, and to some specific purposes of the artwork. However, with the expert look and knowledge of a landslide specialist, the value of this information in the frame of landslide hazard and risk

---

G. Marco (✉)  
Department of Earth Sciences and NatRisk Research Centre,  
University of Torino, Via Valperga Caluso 35,  
10125 Torino, Italy  
e-mail: marco.giardino@unito.it

M. Giovanni  
CNR-IRPI, Strada delle Cacce 73, 10135 Torino, Italy

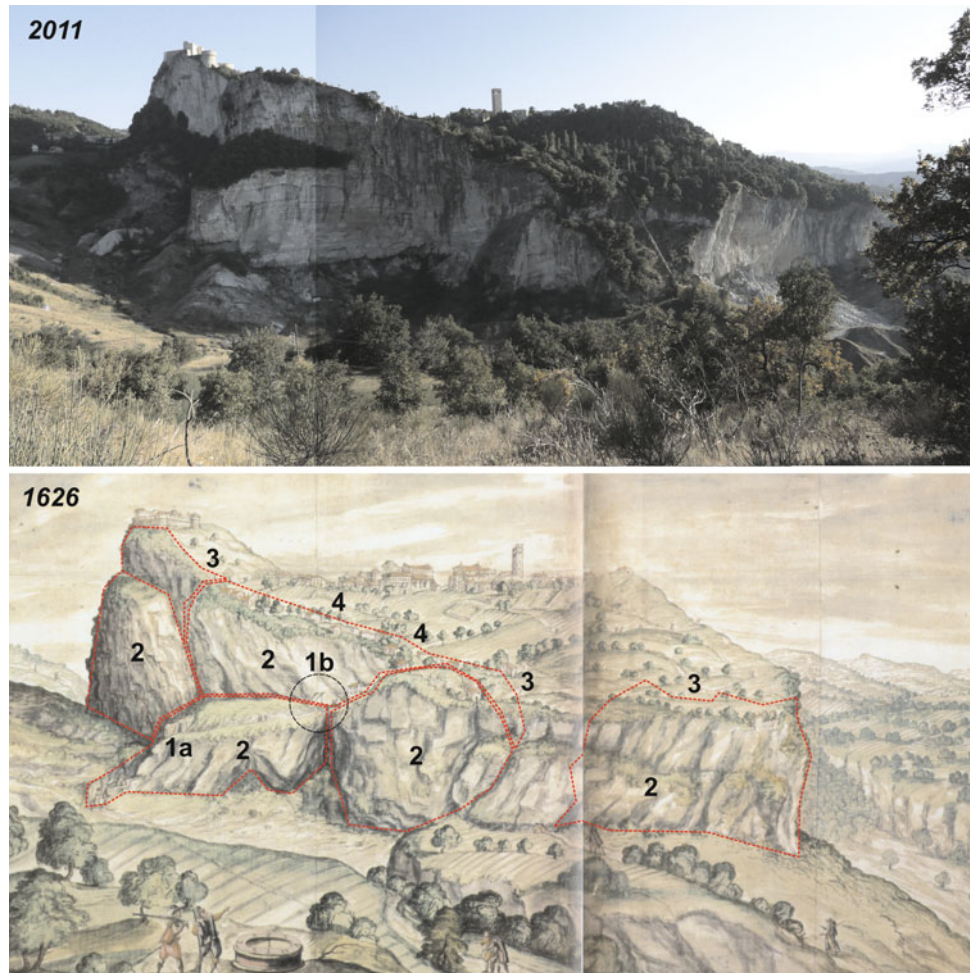
B. Lisa  
Department of Civil, Chemical, Environmental and Materials  
Engineering, University of Bologna, Bologna, Italy

N. Olivia  
Department of Earth, Life and Environment Sciences,  
University of Urbino, Urbino, Italy

G. Cristiano  
University of Bologna, Bologna, Italy

L.C. Claudio  
Romagna Basin Technical Service, Bologna, Italy

**Fig. 81.1** San Leo Cliff: comparison of an updated photo (2011) and a Mingucci watercolor (1626, Biblioteca Apostolica Vaticana). *1a* “Porta di Sotto” gate; *1b* drawbridge; 2 large fallen rock portions (compared to today); 3 current cliff edge; 4 disappeared town district



mitigation can be markedly enhanced. Here, some examples of the representation of dynamic geomorphological processes in historical iconography are presented and commented.

## 81.2 The Apennines

The Umbria-Marche Apennines are bounded to the North by the Val Marecchia Nappe, which in turn is embedded in lower Pliocene clays. The Nappe is formed by Ligurian Units overlain by Epi-Ligurian ones. The Epi-Ligurian Units consist of a wide variety of lithotypes ranging from conglomerates, sandstones, and biocalcarenes, to gypsum, marls, and clays. The Ligurian Units are represented by chaotic varicoloured shales associated with more competent lithotypes such as limestones, marly mudstones, and sandstones to form a melange. The Nappe structure is so complex that the overall geologic assemblage can be regarded as “chaotic”. The marked mechanical contrast between the Ligurian clay-rich rock masses and Epiligurian stiff rock slabs, together with climatic factors contributed to carve a

unique and fascinating landscape which, at the same time, is fragile and unstable. The Little Ice Age climate deterioration (cold winters and abundant precipitation) was recorded in the Valmarecchia by large landslides; a significant geomorphological changes with strong impacts over villages and man-made structures, up to influence the socio-economic framework.

### 81.2.1 Val Marecchia Landslides

Through the analysis of historical documents and antique maps, along with the contribution of new findings and field tests, it was possible to reconstruct the morphology and evolution of some major landslides during the 17<sup>th</sup>–19<sup>th</sup> century.

The ancient fortified city of San Leo (Fig. 81.1) rises at the top of a calcarenite and sandstone slab, bordered by subvertical and overhanging cliffs up to 100 m high, overlying clayey gentle slopes and badlands. The rock slab and the surroundings, due to these particular geological and morphological features, was affected by several and great

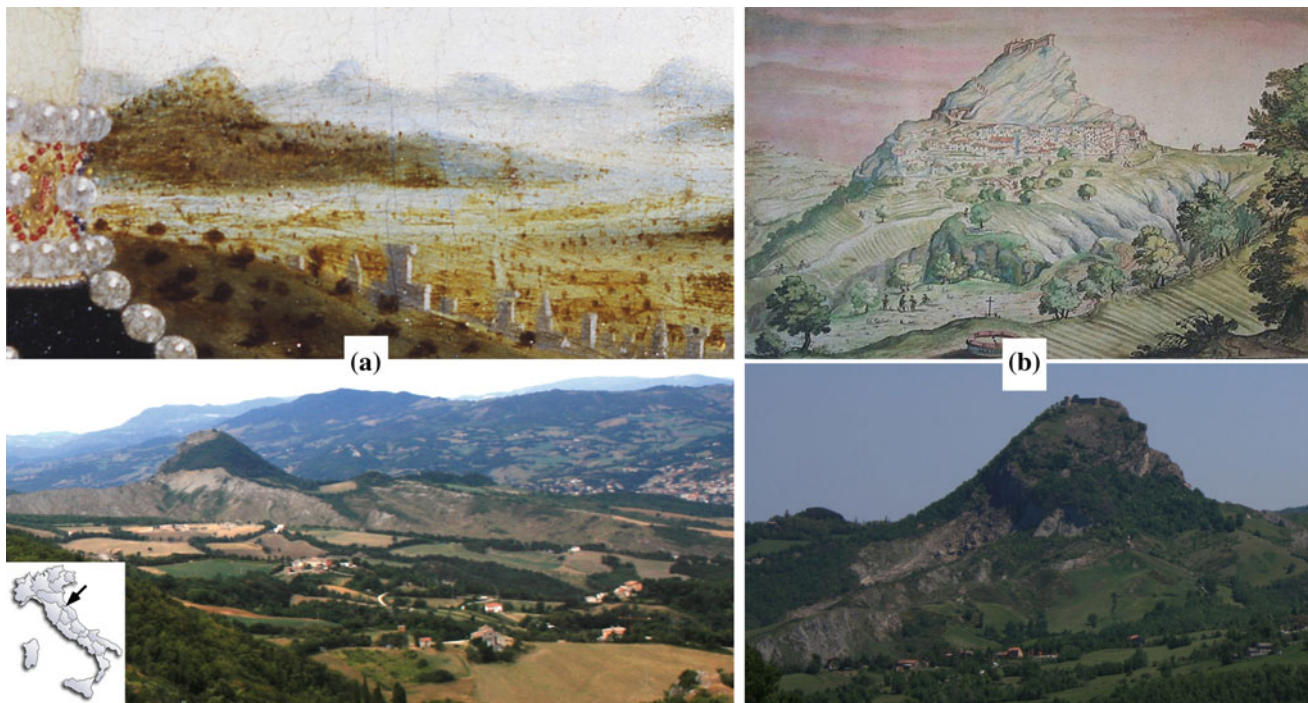


**Fig. 81.2** Maioretto Cliff: **a** Comparison between the Maioretto cliff today and in the portrait of Battista Sforza (diptych of the Dukes, Piero della Francesca, Galleria degli Uffizi, Florence). Note the truncated

profile, **b** Mingucci watercolor before the landslide (1626, Biblioteca Apostolica Vaticana) and at present

landslides (rock falls, mud flow and complex landslides) during the last four centuries (Bernardi et al. 2011).

The Rocca di Maioretto landslide affected an isolated hill 2 km west of the famous San Leo rock-plate (Fig. 81.2). The hilltop consists of sandstones and conglomerates overlying pelitic units, an outlier bordered on two sides by remarkable badlands and large landslides. The northern side of the outlier, whose top preserves ancient fortress ruins, was affected on 29 May 1700 by a devastating rock slide, which destroyed a village. The landslide rock materials fed, or perhaps caused, an earth-flow which is still active today: large blocks have been transported downslope the cliff for more than  $\sim 1$  km. Drawings and paintings depict the cliff before the large landslide, one was painted by Piero della Francesca in the famous diptych of the Dukes of Urbino, in 1465. The cliff behind the portrait of the Duchess Battista Sforza is still perfectly intact (Borchia and Nesci 2012). In a second painting by Mingucci (1626), the cliff and the village are still intact.

## 81.3 The Alps

The whole Alpine Chain is characterized by frequent and widespread slope instability phenomena of various types, distributed regardless of its general setting of a complex

double-verging structure. The large geodiversity of the Alps in term of lithological setting and the complex kinematic history cause different “static” condition to slope stability (Soldati et al. 2006). Litho-technical and geomechanical/structural properties of rock masses and superficial deposits couple with topographical/geomorphological contexts and meteo/climatic factors in posing local dynamic conditions to the types of instability processes, magnitude and frequency of instability events (Eisbacher and Clague 1984; Mortara et al. 1984). Three case studies have been selected for illustrating processes and related conditioning factors.

### 81.3.1 Elm Rock Avalanche

The catastrophic rock avalanche of Elm (Swiss Alps), occurred on September 11, 1881; it was masterfully portrayed by F. Weber two days later than its occurrence (Hardmeyer-Jenni 1884). The watercolored lithography allows appreciation of local geological structure of the slope, the characteristics of the whole landslide (impressive detachment scarp, long run-out, large blocks in the accumulation zone), geomorphological effects and related damages to infrastructures (valley dam, partial run up on the opposite valley side, destruction of buildings). Based on witnesses reports, the same artist reconstructed even the

**Fig. 81.3** Impressive and realistic reconstruction of the Elm rock avalanche collapse, portrayed by F. Weber, two days after its occurrence (in Hardmeyer-Jenni 1884)



dramatic moment of collapse: almost a snapshot that, with plausible realism, depicts the breath of the giant debris cloud that fills the valley, the impact of the blocks on buildings, the escape of the survivors (Fig. 81.3).

### 81.3.2 Noceno Landslide

In April 1810 a complex landslide involved part of the village of Noceno (on the eastern shore of Lake Como, Lombard Prealps). A contemporary map in full color describes with great accuracy

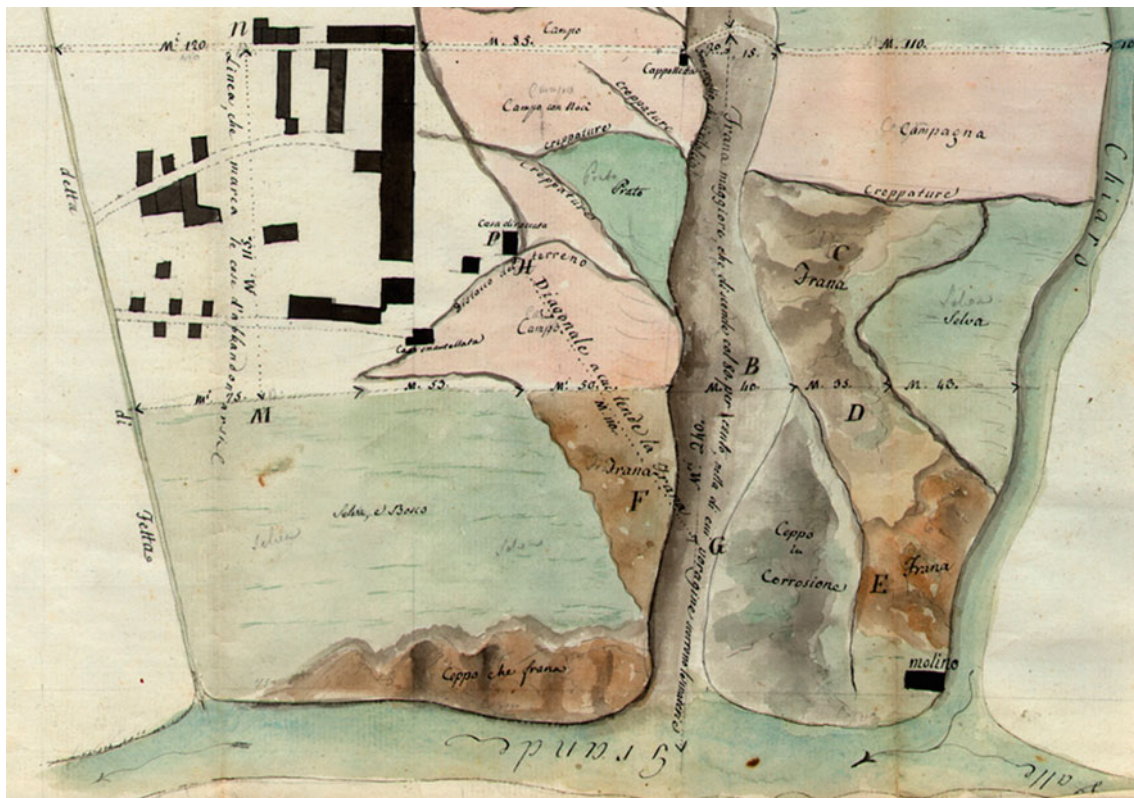


**Fig. 81.4** Detail of the map (June 1810), describing with great accuracy geomorphological elements and damages related to the Noceno landslide: *distacco del terreno* = landslide scarp; *diagonale a*

*cui tende la frana* = direction of the movement; *creppature* = tension cracks; *casa smantellata* = destroyed house). Courtesy of CNR-IRPI Archive, Turin

**Fig. 81.5** This water-colour of G.P. Bagetti (1822, Palazzo Reale, Turin) underlines with effectiveness the impressive geological and geomorphological context of the Gondo Gorges



the area involved, the size, the newly-formed system of fractures, the most unstable sectors and the prevailing direction of the movement, the incision in which the fluid fraction of the landslide flows, the dwellings most at risk. The map identifies also a sector, external to landslide area, where the village of Noceno could possibly be reconstructed. The slope instability of the area is still ongoing, even if dense vegetation totally cover the landslide of 1810: for this reason the historical document assumes a special importance (Fig. 81.4).

### 81.3.3 The Gondo Gorges

The Napoleonic road that links Italy and Switzerland, through the famous Simplon Pass is a remarkable alpine engineering work along the rough and deep Diveria Valley (NW Alps). Adventurous tales of travel and accurate vintage designs effectively illustrate the severe geological-geomorphological context (Garimoldi and Jalla 2006; Paolucci 2011). The descriptions of the wild gorges of Gondo emphasize the rushing streams, the extreme steepness of the slopes and the state of fracturing of rock masses. They hint at the difficulties faced by construction engineers and the natural risks to which travelers were exposed (debris flows, rock falls, snow avalanches) (Fig. 81.5).

## 81.4 Conclusions

Depicting landscape was a strong cultural need since XV century. The artists of the time began to draw less stylized natural scenes gradually and to make more and more realistic

and identifiable profiles of hills and mountains. Over four centuries, before the birth of photography, a documentary heritage of great scientific importance was established describing transformations of the physical landscape. Indeed, careful interpretations are needed, because a linear progression towards realism doesn't exist in the development of landscape painting. Infact the representation of Nature often maintained idealizing aspects through centuries, depending on the tendencies of different painting schools and authors.

Iconography presented in this article contributes to integrate the cognitive framework of some sites exposed to a risk of collapse and/or debris flows in the Alps and the Apennines. Their value is consistent but some cautions has been taken into account, for using them as sources for the study of past environments; contrasts between realism and romanticism are evident even in the landscape paintings of Bagetti, that generally were based on careful topographic surveying (Godlewska 2003).

The search for historical iconographies is not easy, given the dispersion in the territory of historical archives, museums, libraries, as well as is not simple, but essential, the validation of their significance. Moreover, an interdisciplinary work is needed, taking advantage of the abundant literature on the treatment of historic sources for the study of past geomorphologic and ecologic processes produced in the fields of Historical Geography and Historical Ecology (Cevasco 2007). A coordinated effort in this direction would make available to the scientific community and public administrations a temporally extensive database, highly relevant and useful for the geomorphologic reconstruction of an area.

## References

- Borchia B, Nesci O (2012) *The Invisible Landscape. A fascinating hunt for the real landscapes of Piero della Francesca among Montefeltro hills*. Il Lavoro Editoriale, pp. 1–86. ISBN: 9788876636646
- Bernardi M, Borgatti L, Ghirotti M, Guerra C, Landuzzi A, Lucente C, Marchi GF (2011) San Leo: ten centuries of coexistence with landslides, II World Landslide Forum, Session L24, Roma 3-7 ottobre 2011
- Cevasco R (2007) *Memoria verde. Nuovi spazi per la geografia*. Edizioni Diabasis, 318 pp
- Eisbacher GH, Clague JJ (1984) Destructive mass movements in high mountains: hazard and management. *Geol. Survey Canada, Paper 84-16*, 230 pp
- Garimoldi G, Jalla D (2006) *Alpi di sogno. La rappresentazione delle Alpi occidentali dal XIX al XXI secolo*. Silvana Editoriale, 239 pp
- Godlewska A (2003) Resisting the cartographic imperative: Giuseppe Bagetti's landscapes of war. *J Hist Geogr* 29:22–50
- Mortara G, Govi M, Sorzana PF (1984) Mouvements de versants avec des conséquences humaines graves ou catastrophiques dans les Alpes Italiennes. *Comptes Rendus 25e Congres Int. de Géographie "Les Alpes"* (Paris, août 1984)
- Hardmeyer-Jenni F (1884) *Der Bergsturz von Elm im Glarnerlande. Mit einem Anhang enthaltend die Trauerrede bei der Todtenfeier, gehalten von Fridolin Leuzinger, Pfarrer von Matt, und mit vier Ansichten in Farbdruck, nebst einem Situationsplan*. Fussli & Co, Zürich 1881, 30 pp
- Paolucci A (2011) *La bella Italia. Arte e identità delle città capitali*. Silvana Editoriale, 379 pp
- Soldati M, Borgatti L, Cavallin A, De Amicis M, Frigerio S, Giardino M, Mortara G, Pellegrini GB, Ravazzi C, Surian N, Zanchi A (2006) Geo-morphological evolution of slopes and climate changes in northern Italy during the late quaternary: spatial and temporal distribution of landslides and landscape sensitivity implications. *Geogr Fis Dinam Quat* 29:165–183

---

Part IX

**Weathering and Preservation of Building Stones  
and Other Materials**

---

# Stone Masonry Material of a Medieval Monastic Glass Production Centre, Pomáz (Hungary)

82

Á. Török, B. Szabó, and J. Laszlovszky

---

## Abstract

A ruined medieval monastic glass production centre (church, workshop buildings) is located in Central North Hungary a few kilometres North of Budapest. The recent archaeological excavations exposed the walls of the church of the monastic estate and also found a large complex providing evidence for the workshop buildings. This site has a primary importance since it is one of the best preserved glass making facilities in Central Europe, in Hungary. The present paper provides a brief overview of the history and development of the building, the construction activities by using computer aided reconstruction of the walls and masonry structures. It also outlines the most important stone types and binders of the walls. The masonry is composed of various lithologies. Cut blocks of andesite tuffs and rounded cobbles of andesite from a significant part of the masonry walls. Sedimentary rocks such as sandstone and a few blocks of travertine were also identified. The historic binder, a lime-based mortar was also identified in the structure. This site represents a unique religious and industrial heritage structure in Europe that was constructed by medieval methods by using local stones.

---

## Keywords

Andesite • Andesite tuff • Medieval • Church

---

## 82.1 Introduction

The site is located in Hungary 20 km north of Budapest. The medieval stone building complex is situated between two settlements, Pomáz and Pilisszentkereszt, on the right side of the road, on the top of an approximately 20 m high hill (Fig. 82.1). The most prominent structure of the area is the ruin of a medieval church (Fig. 82.2).

---

Á. Török (✉)

Budapest University of Technology and Economics, Műegyetem  
rkp. 3, Budapest 1111, Hungary  
e-mail: torokakos@mail.bme.hu

B. Szabó · J. Laszlovszky  
Department of Medieval Studies, Central European University,  
Budapest, Hungary

---

## 82.2 History and Excavations

The ruins detected on the hilltop raised the interest of local historians first in the 19th century, and based on its layout it was recognized as a monastic complex. The first archaeological surveys were carried out in the 1920s by László Krompecher, a professor at the Technical University in Budapest. In the 1990s, in the framework of a survey of the archaeological heritage of Pomáz settlement, József Laszlovszky initiated further field studies at the site. The works included the documentation of the surface features, and a systematic analysis of the previously unearthed finds and the already existing documentation. The surface features indicated the small church excavated by Krompecher oriented northeast-southwest, surrounded by three wings, the northwestern divided into two by a longitudinal ridge. It was well visible that the axis of the church diverged from that of the surrounding wings.

**Fig. 82.1** Location of the medieval monastic glass production centre in Hungary



**Fig. 82.2** Ruin of the medieval church



Based on a revision of the previous results and the new surveys József Laszlovszky offered a new interpretation of the site. As a church and an industrial center coexisted there, he identified the ruins as a monastic estate, that of the Pilis (today Pilisszentkereszt) monastery of the Cistercian order (Laszlovszky 2009, 192). He explained the difference between the orientation and the wall structure of the church

and the wings with a chronological difference and a shift in the function: the church had been built originally as the parish church of the Árpád Period village Kovácsi, and later, in the later Middle Ages it was incorporated into an industrial grange of the Cistercian Abbey. A charter issued by King Béla IV proved that by 1254 the village was possessed by the Abbey.

### 82.3 Methods

A topographical survey was carried out in the narrower area of the building complex, including the earthwork features and the visible walls. Additionally laser scanner was also used to describe the wall geometry. The obtained data set was further processed by using computer codes resulting to an architectural reconstruction. The stone masonry material was identified by using macroscopic and microscopic analyses. The lithotypes were described and characterized by using the terminology of EN 12407. The weathering features of the stone walls were classified according to the ICOMOS ISCS 2008.

### 82.4 Results

The results of the topographic survey and the landscape features situated in the broader territory showed further traces characteristic for the Cistercian granges: that of a complex water supply system and land management. On the eastern side of the hill, a recess can be observed the bottom of which is swampy even in dry summers due to a natural spring. This is an element of the water management system that consisted of three ponds equipped with dam and a ditch system connecting the ponds. Besides the water regulation system, the agricultural activity carried out on the territory in the Middle Ages is testified by a recognizable terrace system as well.

The archaeological excavations carried out at the site have revealed a number of new elements and architectural structures since 2011. The single nave church with a semicircular apse forms the center of the complex (Fig. 82.2). Based on the structural analysis of this building, the construction of the

church can be dated to the second half of the Arpadian period, most probably to the 12th century. The surviving remains of the church suggest that it has been constructed in one single phase, but it has suffered a number of alterations later, mainly related to a later, non-ecclesiastic use (workshop building) of the church. Graves excavated around the church are also dated to the Arpadian period, their presence correspond with the function of a parish church.

The workshop complexes around the church are clearly later additions, most probably in the 14–15th centuries. At least two of the wings were used as glass production buildings with kilns inside and also outside of the buildings. Several building phases can be identified in the case of the workshop wings. Some of the destruction layers excavated in front of the church are also connected to the workshop, dismantled kilns were placed and leveled in the courtyard with building elements of the kilns, products, by-products and waste materials of glass production. Building materials excavated in this layers as well as construction materials of the church and the workshop complex represent a wide range different stones, bricks, fire-resistant bricks and traces of wooden constructions attached to the workshop or erected in the church during the functional changes of it. The peak of the glass production period can be dated to the turn of the 15–16th century, while later changes occurring in the church can be dated to the 16th century. The site has been abandoned in the Ottoman period (16–17th century) and was used as a quarry for building material in the Early Modern and Modern Period.

The crushed stone walls of the church covered with finely cut ashlar on both the inner and the outer side appeared to be clearly different from that of the more irregular stone walling of the surrounding wings (Fig. 82.3). The laser aided

**Fig. 82.3** Ground plan of the monastic church ruin





**Fig. 82.4** Laser scan image of the church ruins

reconstruction also revealed that the structures of the internal and external walls are different (Fig. 82.4).

The external parts of the church wall were made of finely cut andesite tuff (Fig. 82.5a). It is light grey with high amount of lithic clasts such as pumice and andesite. In

between the ashlar lime-based mortar are found (Fig. 82.5b). The internal part of the walls was made of well rounded andesite cobbles, and crushed stone rubble of andesite tuff (Fig. 82.5c). The binder is also lime-based mortar (Fig. 82.5d).

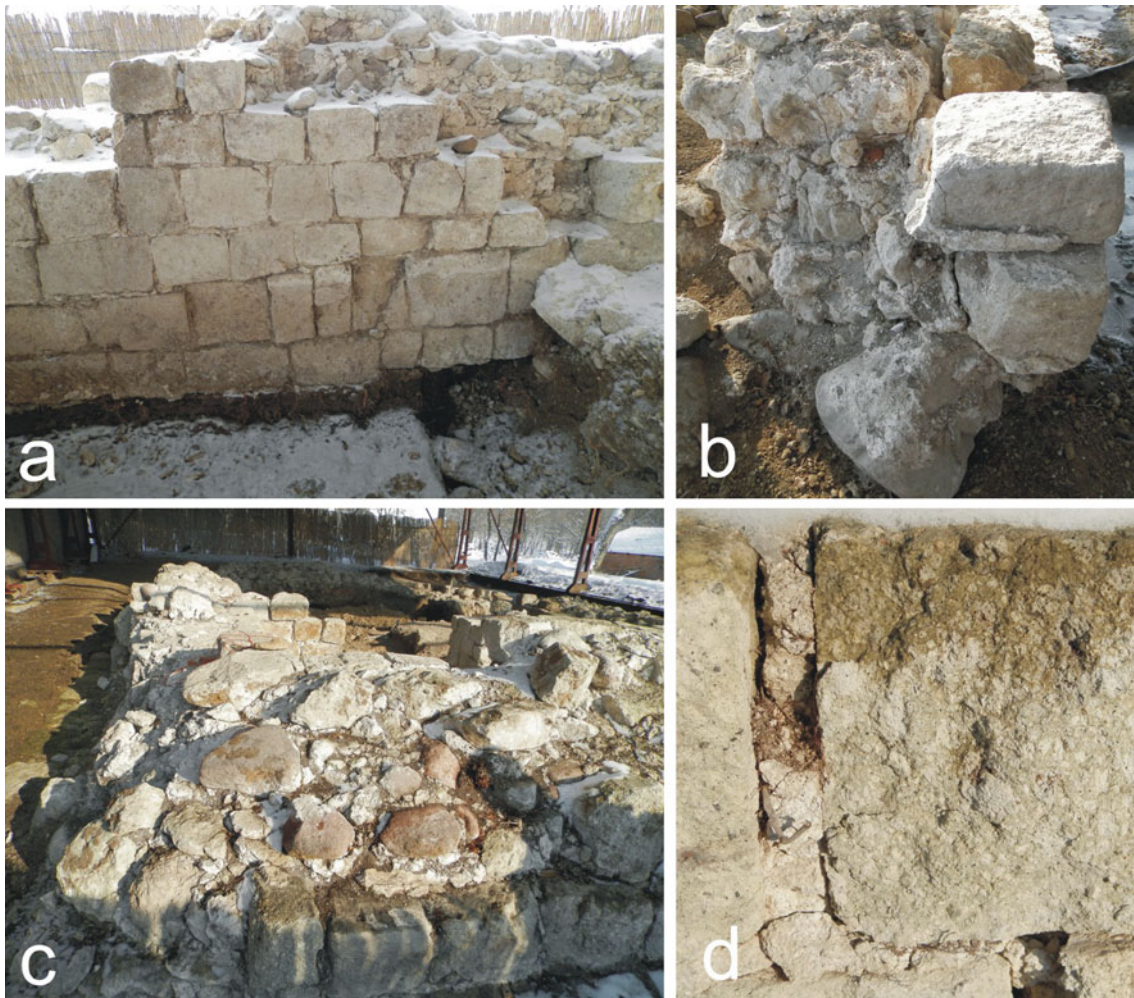


**Fig. 82.5** Stone masonry: **a** finely cut andesite tuff ashlar; **b** cross section of a wall; **c** rounded andesite cobbles at the central part of the wall; **d** lime-based mortar in the joints



**Fig. 82.6** Travertine in the wall of glass production centre

The lithology of the medieval glass production centre that is located west to the church is slightly different from the church itself. Beside andesite tuff and various types of andesite, sedimentary rocks such as sandstone and travertine were also identified within the ruined walls (Fig. 82.6). The most common weathering features of andesite tuffs are the micro-cracking and multiple flaking. Sandstone blocks display crumbling and scaling. Travertine blocks of Roman period were also found as re-cycled material from the nearby antique site.

## 82.5 Conclusions

The masonry is composed of various lithologies including different forms of andesite tuff and andesite. The provenance analysis of igneous stones revealed that most materials are originated from the vicinity of the buildings, from the nearby volcanic area of Visegrád Hills. Sedimentary rocks such as sandstone and a few blocks of travertine were also identified. Several forms of stones are used as masonry materials. Besides cut blocks of andesite tuffs rounded cobbles of andesite from the nearby stream deposits form also a significant part of the masonry walls. The analysis and identification of stone materials and their sources are also important, as the heat resistant special brick elements of the glass production kilns were probably produced locally, using specially tempered clay material.

---

## Reference

- Laszlovszky J (2009) Ciszterci vagy pálos? A Pomáz-Nagykovácsi-Pusztán található középkori épületmaradványok azonosítása. (Cistercian or Pauline? Identification of the medieval building complex in Pomáz-Nagykovácsi.) In: Guitman, B (ed) A ciszterci rend Magyarországon és Közép-Európában, (The Cistercian order in Hungary and in Central Europe.) Piliscsaba, pp. 191–208

# Statistical Models for Predicting the Mechanical Properties of Travertine Building Stones After Freeze-Thaw Cycles

Amin Jamshidi, Mohammad Reza Nikudel, Mashalah Khamehchiyan, and Ahmad Zalooli

## Abstract

Freeze-thaw is one of the most powerful weathering agents that may cause a rapid change in the mechanical properties of stones, and thus limit their durability. Consequently, determining the mechanical properties of stones after freeze-thaw is important to select the natural building stones for outdoor applications, which are exposed excessive freeze-thaw cycles. The purpose of this study is propose statistical models for predicting the mechanical properties of travertine building stones after freeze-thaw test. For this, 12 travertine samples were selected and their physical and mechanical properties including density ( $\rho$ ), water absorption ( $W_a$ ), uniaxial compressive strength (UCS), and P-wave velocity ( $V_p$ ) were determined. Then, freeze-thaw test up to 60 cycles was carried out and mechanical properties including the UCS and  $V_p$  of the samples were measured. Using data analysis, statistical models for predicting the mechanical properties of deteriorated samples after freeze-thaw test were proposed. In these models, the mechanical property of samples after freeze-thaw was considered to be the dependent variable—dependent on the independent variables of the initial mechanical property of the samples and their water absorption. The results show that statistical models are in good accuracy for predicting the mechanical properties of samples, and thus a rapid durability assessment.

## Keywords

Freeze-thaw • Statistical models • UCS •  $V_p$

## 83.1 Introduction

Travertine is a chemical sedimentary rock formed mostly in tectonic areas (Pentecost 2005). Nowadays travertine with different color, texture and pattern are widely used as building materials for construction and decoration purposes especially for outdoor applications such as flooring, paving and wall cladding.

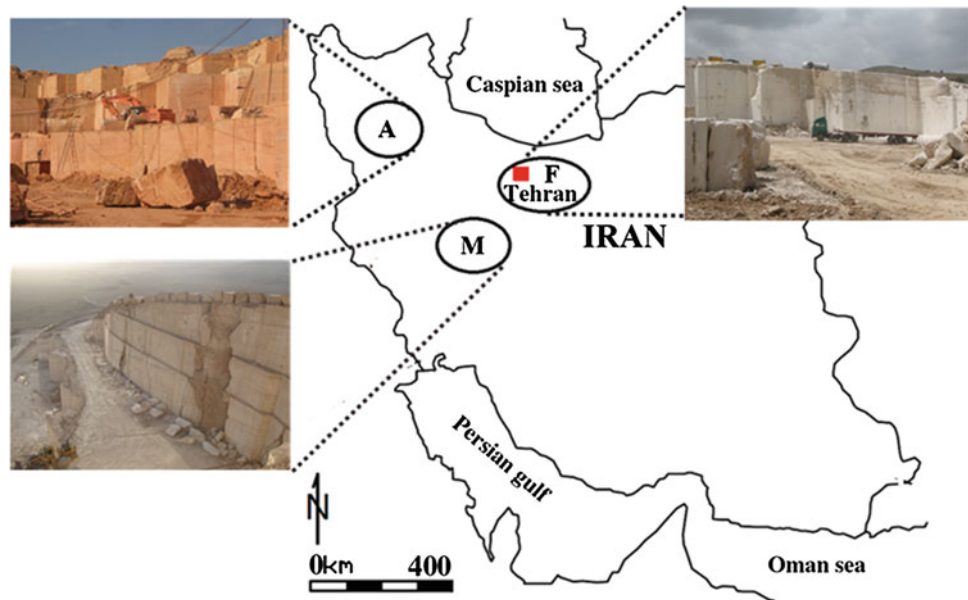
Freeze-thaw action is one of the most powerful physical weathering agents, which may cause a rapid change in the mechanical properties of travertines, and limit their durability. Therefore, the resistance to deterioration (durability) should be evaluated before the selection of an appropriate building stone (Zappia et al. 1998).

Uniaxial compressive strength (UCS), and P-wave velocity ( $V_p$ ), are one of the most important mechanical properties to assess stones durability against weathering agents (Zezza 1990; Valdeon et al. 1996; Goudie 1999; Nicholson 2001; Benavente et al. 2004). However, change in the mechanical properties of stones due to weathering agents can affect their durability in the course of time (Jamshidi et al. 2013). Thus it is necessary to understand the change of mechanical properties of stones when freeze-thaw is considered as one of the weathering agents.

A. Jamshidi (✉)  
Lorestan University, Khorramabad-Borujerd road,  
Khorramabad, Iran  
e-mail: jamshidi.geo85@yahoo.com

M.R. Nikudel · M. Khamehchiyan · A. Zalooli  
Tarbiat Modares University, Jalal Ale Ahmad Highway,  
Tehran, Iran

**Fig. 83.1** The location of sampling and some of the quarries



The aim of this study is propose the statistical models for predicting the mechanical properties (UCS and  $V_p$ ), of 12 travertine building stones after freeze-thaw test. In these models, the mechanical property of stones after freeze-thaw was considered to be the dependent variable—dependent on the independent variables of the initial mechanical property of the stones and their water absorption.

### 83.2 Materials and Methods

To carry out the research, 12 travertine building stones were selected from various quarries in Iran (Fig. 83.1). For each travertine, some of block that varied from  $0.2 \times 0.35 \times 0.35$  to  $0.30 \times 0.40 \times 0.40$  m in size were collected. The physical and mechanical properties including density, water absorption, uniaxial compressive strength and P-wave velocity of each sample were determined. Freeze-thaw test up to 60 cycles was carried out and mechanical properties of samples after treatment were measured. Using data analysis, statistical models for predicting the mechanical properties of samples after freeze-thaw test were proposed.

### 83.3 Physical Properties

To fulfill the aim of the study, some of physical properties of the samples including density ( $\rho$ ) and water absorption ( $W_a$ ) were determined in accordance with ISRM (1981). The results of these tests are given in Table 83.1. According to the rocks classification based on  $\rho$  suggested by Anon (1979), most of the samples were classified as to have moderate  $\rho$  ( $2.2\text{--}2.55 \text{ g/cm}^3$ ).

### 83.4 Freeze-Thaw Test

For freeze-thaw test, initially, the samples were saturated by submerging in tap water and then placing in a freezer conditioned at  $-12 \text{ }^\circ\text{C}$  for 12 h. After removing the samples, they were thawed by placing in a water bath at  $12 \text{ }^\circ\text{C}$  for 12 h. Each complete cycle of freeze–thaw lasted for 24 h, comprising 12 h for freezing and 12 h for thawing and the test procedure was repeated for 60 cycles.

Two series of samples were prepared for each stone type to identify their UCS and  $V_p$  before and after the treatment. The first series were utilized for determination of fresh stone properties (initial properties) and the second series were subjected to freeze-thaw cycles. After 60 cycles of freeze-thaw, for UCS and  $V_p$ , the measurements were made on five specimens under saturated conditions. The experimental procedure was performed according to the methods suggested by the ISRM (1981). The results of freeze-thaw test on the samples are given in Table 83.2.

### 83.5 Statistical Analysis of Results

In this study, the multivariate regression equations were used for predicting the mechanical properties of the deteriorated samples. In these equations, the mechanical properties of samples after 60 cycles of freeze-thaw test were considered to be the dependent variable, which dependent on the independent variables of the initial mechanical properties of the samples and their  $W_a$ . Multivariate regression equations were undertaken with 95 % confidence level and the best-fit curves were obtained using the least squares method.

**Table 83.1** The statistical distribution of physical properties of the samples under study

Commercial name	$\rho$ (g/cm <sup>3</sup> )			Wa (%)		
	Min.	Max.	Ave.	Min.	Max.	Ave.
Azarshahr silver	2.40	2.49	2.46	1.16	1.81	1.43
Dastjerd red	2.57	2.71	2.66	0.39	0.93	0.67
Dastjerd green	2.65	2.72	2.69	0.17	0.23	0.20
Dastjerd white	2.70	2.75	2.72	0.23	0.64	0.50
Atashkooch white	2.44	2.59	2.47	1.62	1.81	1.70
Abasabad light cream	2.40	2.48	2.43	1.82	2.10	2.00
Abasabad white	2.40	2.43	2.42	1.67	1.96	1.87
Abyar white	2.33	2.47	2.41	1.33	1.62	1.47
Dareh bokhari cream	2.31	2.43	2.38	2.52	2.77	2.69
Atashkooch cream	2.39	2.50	2.46	1.38	1.89	1.72
Firuzkuh chocolate	2.32	2.46	2.38	1.09	1.53	1.27
Firuzkuh cream	2.31	2.38	2.34	1.23	2.35	1.70

**Table 83.2** The mechanical properties of fresh and deteriorated samples

Commercial name	UCS (MPa)		V <sub>p</sub> (m/s)	
	<sup>a</sup> Fresh value	<sup>b</sup> Deteriorated value	Fresh value	Deteriorated value
Azarshahr silver	55.5	46.0	4930	4338
Dastjerd red	65.7	59.7	5260	4892
Dastjerd green	64.5	60.0	5310	4938
Dastjerd white	62.4	58.2	5450	5010
Atashkooch white	49.3	40.4	4600	3910
Abasabad light cream	41.3	32.7	4150	3445
Abasabad white	43.7	38.8	4410	3709
Abyar white	51.4	46.4	4690	4174
Dareh bokhari cream	37.4	30.1	4135	3300
Atashkooch cream	45.7	41.3	4510	3879
Firuzkuh chocolate	59.9	50.4	5010	4500
Firuzkuh cream	50.7	43.6	4470	3956

<sup>a</sup> Initial condition

<sup>b</sup> After 60 cycles of freeze-thaw test

Coefficient of multiple determinations ( $R^2$ ) and standard error of estimate (SEE) were used as the numerical measures of the goodness of fit for regression equations.

The general model for predicting the mechanical property after freeze-thaw test is expressed in the following form:

$$M_{60} = \alpha_0 + \alpha_1 M_0 + \alpha_2 W_a \quad (83.1)$$

where  $M_{60}$  is the predicted value of the mechanical property (UCS or  $V_p$ ) for the samples after 60 cycles of freeze-thaw test,  $M_0$  is the fresh mechanical property or, in other words, the initial mechanical property (initial UCS<sub>0</sub> or  $V_{p0}$ ),  $W_a$  is

the  $W_a$  of the fresh sample,  $\alpha_0$  is a constant,  $\alpha_1$  and  $\alpha_2$  are the regression coefficient of  $M_0$  and  $W_a$ , respectively.

The data given in Tables 83.1 and 83.2 were analyzed using Spss<sup>®</sup> v.16 code statistical software. The results of these analyses are given in Table 83.3.

The  $R^2$  of equations of E1 and E2 given in Table 83.3 is higher than 0.978 that is at acceptable level. The SEE values for equations of E1 and E2 is 1.63 and 59.25, respectively. These measures show that equations can be accepted as a highly reliable for predicting the mechanical properties after freeze-thaw with the coefficients given in Table 83.3.

**Table 83.3** Regression equations coefficients for predicting the mechanical properties of samples after freeze-thaw test from Eq. (83.1) and results of statistical tests

Equation code no.	Estimates mechanical property	Estimator	Coefficient	Coefficient of multiple determination ( $R^2$ )	Standard error of estimate (SEE)	F-ratio	Tabulated F-ratio
E1	UCS (MPa)	Constant	22.88	0.978	1.63	200.57	4.26
		UCS <sub>0</sub> (MPa)	0.605	–	–	–	–
		Wa (%)	–6.19	–	–	–	–
E2	V <sub>P</sub> (m/s)	Constant	–173.68	0.991	59.25	514.85	4.26
		V <sub>P0</sub> (m/s)	0.978	–	–	–	–
		Wa (%)	–206.55	–	–	–	–

**Fig. 83.2** Measured UCS versus estimated UCS from Eq. (E1) given in Table 83.3

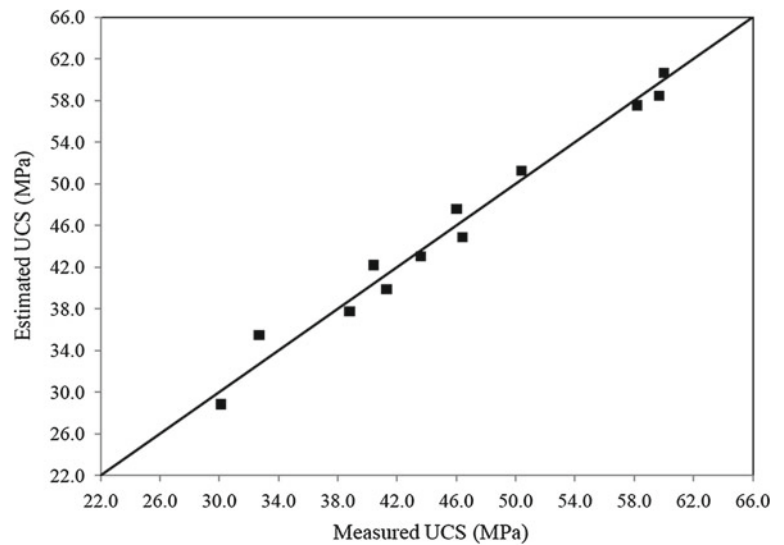
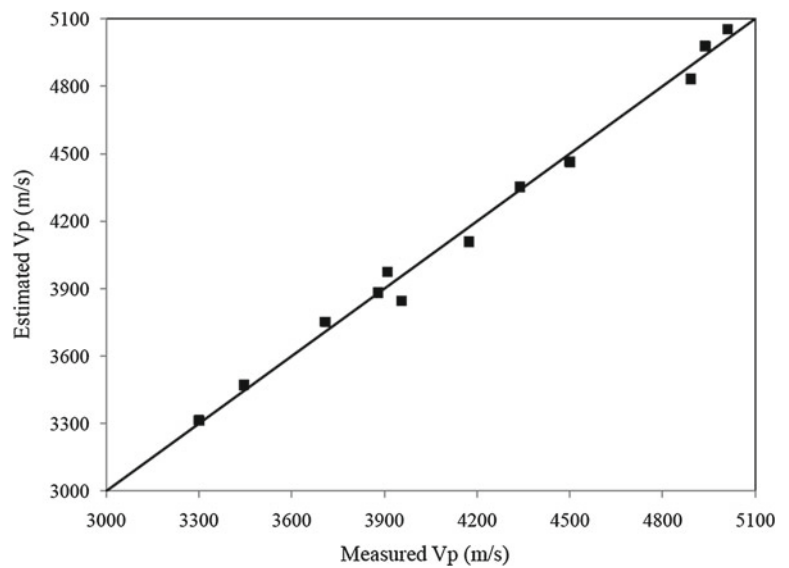


**Fig. 3** Measured V<sub>P</sub> versus estimated V<sub>P</sub> from Eq. (E2) given in Table 83.3



To test the global usefulness and the significance of equations, analysis of variance for the regressions were also performed. F statistics test is widely used in regression and

analysis of variance. The null hypothesis for this test is  $H_0: \alpha_1 = \alpha_2 = 0$ , against alternative hypothesis  $H_1$ : at least one of  $\alpha_1, \alpha_2$  is not equal to zero. Analysis of variance for the

regressions is given Table 83.3. For a significance level of 5 %, the tabulated F-ratio with degree of freedom  $\nu_1 = 2$  and  $\nu_2 = 9$  is 4.26. Since all the computed F-ratios for the equations are quite larger than tabulated F-ratio, the null hypothesis is rejected. So, it can be concluded that the equations given in Table 83.3 are appropriate for predicting the mechanical properties of samples after freeze-thaw test.

The relationship between the measured the mechanical properties and estimated values from equations given in Table 83.3 using 1:1 slope line is shown in Figs. 83.2 and 83.3. A point lying on the line indicates an exact estimation. The Figs. 83.2 and 83.3 indicate that the data points fall close to the 1:1 slope line and are scattered uniformly around it, suggesting that equations with the suggested coefficients are appropriate for predicting the mechanical properties after freeze-thaw test.

### 83.6 Conclusions

The freeze-thaw test is a well-known test for mechanical properties and durability assessment of building stones and construction materials. However, performing freeze-thaw test is a very laborious and time-consuming. In this paper, statistical models for predicting the UCS and  $V_P$  of 12 travertine samples after freeze-thaw were proposed.

The results show that statistical models are in good accuracy for predicting the UCS and  $V_P$ , and thus a rapid durability assessment. As a result, these models avoiding from performing freeze-thaw test, which is laborious and time-consuming.

However, it must be pointed out that travertine are notoriously variable and heterogeneous in their properties such as mechanical properties and porosity due to the nature of its porous media. As a result, these models can be used with care for rocks with the range of initial properties (fresh properties) of samples studied here.

### References

- Anon OH (1979) Classification of rocks and soils for engineering geological mapping. Part 1: rock and soil materials. *Bull Assoc Eng Geol* 19:355–371
- Benavente D, Garcia del Cura MA, Fort R, Ordonez S (2004) Durability estimation of porous building stones from pore structure and strength. *Eng Geol* 74:113–127
- Goudie AS (1999) Experimental salt weathering of limestone in relation to rock properties. *Earth Surf Process Land* 24:715–724
- ISRM (1981) Rock characterization testing and monitoring. In: Brown ET (ed) *ISRM suggested methods*. Pergamon Press, Oxford, pp 211
- Jamshidi A, Nikudel MR, Khamehchiyan M (2013) Predicting the long-term durability of building stones against freeze-thaw using a decay function model. *Cold Reg Sci Technol* 92:29–36
- Nicholson D (2001) Pore properties as indicators of breakdown mechanisms in experimentally weathered limestone. *Earth Surf Process Land* 26:819–838
- Pentecost A (2005) *Travertine*. Springer, Berlin
- Valdeon L, de Freitas MH, King MS (1996) Assessment of the quality of building stones using signal processing procedures. *Q J Eng Geol* 29:299–308
- Zappia G, Sabbioni C, Riontino C, Gobbi G, Favoni O (1998) Exposure tests of building materials in urban atmosphere. *Sci Total Environ* 224:235–244
- Zeza U (1990) Physical–mechanical properties of quarry and building stones. In: Veniale F and Zeza U (eds) *Advanced workshop; analytical methodologies for investigation of damage stones*. Pavia, pp 1–20

Bezhan Tutberidze and Tamara Tsutsunava

---

## Abstract

The Vardzia monastery complex hewn in the rock is dated to the XII–XIII centuries. The complex is hewn in a volcanogenic-sedimentary suite built up of facies of lower pyroclastic subsuite of the Late Miocene “Goderdzi suite”. One of the layers of the suite—alternating tuffs, known as the “Vardzia type tuffs” belongs to ignimbrite type tuffs. They are massive rocks characterized by different extent of cementation and intricate grain-size composition. The monastery complex is hewn right in these tuffs. A thick packet of volcanic breccias, which makes steep rocky slopes with a system of joints overlies the tuffs. In the suite of tuff-breccias due to weakening of the resistance along the vertical joints, an active process of disturbance of the stability takes place. Destructive processes taking place around the monastery complex is initiated by composition peculiarities of volcanic breccias and by intricate endogenetic and exogenetic geological processes that affect the monastery complex of Vardzia and the adjacent regions. Besides the collapse of separate small fragments provoked by inhomogeneous composition and different extent of cementation of rocks, increases a hazard of large block failure that will substantially change the structure of the monument and will endanger the visitors’ safety. To protect the monastery complex of Vardzia from the destruction processes it is necessary to evaluate the dynamics of endogenetic and exogenetic geological processes and to establish priorities in essential rehabilitation works. One of the most urgent preventive measures is to preserve stability of volcanic breccias on a steep slope.

---

## Keywords

Georgia • Cave monastery • Volcanic tuff • Destructive processes • Preventive measures

---

## 84.1 Location

The Vardzia monastery complex is situated on the territory of Georgia and belongs to the Aspindza municipal district. The cave monastery is located in the southeastern part of Erusheti volcanic plateau—1300 m above sea level. The monastery complex is hewn in a volcanogenic-sedimentary suite exposed on a left steep rocky slope of the Mtkvari river gorge.

---

## 84.2 Geology

The relief on the territory of the Vardzia monastery complex gained its recent form in late Late Miocene and Early Pliocene against the background of strong ascending tectonic

---

B. Tutberidze (✉)  
Faculty of Exact and Natural Sciences, Department of Geology,  
Ivane Javakhishvili Tbilisi State University, Tbilisi, Georgia  
e-mail: bejan.tutberidze@tsu.ge

T. Tsutsunava  
Alexandre Janelidze Institute of Geology, I. Javakhishvili Tbilisi  
State University, Tbilisi, Georgia  
e-mail: tsutsunava@yahoo.com

movement (Attic orogeny). At that time a thick volcanogenic and volcanogenic-sedimentary suite was formed on the Erusheti-Arsiani plateau that is known as “Goderdzi suite”. Lithologically it is divided into pyroclastic and effusive subsuites. In the geological structure of the area of the Vardzia Monastery complex participates the formations of pyroclastic subsuite represented by intercalation of tuffs, rudaceous volcanic breccias and conglomerates (Skhirtladze 1958; Tutberidze 2004).

Within the area of the monastery complex, the ascending geological section is given below (Fig. 84.1). Strait in the foot of the complex on the right side of the river Mtkvari exposures of bedrocks are not visible due to great thickness of hillside waste of different size tuff breccias and tuffs. In the eastern part of the complex at the level of riverbed, natural exposures of 7–8 m thick white and yellow-layered tuffs continued by a 12 m thick packet of rudaceous breccias and tuffs are observed. A 40–60 m thick massive, sometimes cross-bedded tuff packet concordantly covers the latter. The Vardzia monastery complex is hewn right in this tuff packet. The tuffs are of ignimbrite origin—deposited in subcontinental, rarely lacustrine basin conditions and are known as “Vardzia type tuffs”. Visually they are rocks of light grey, white or whitish color; they are loose, rather well treatable, characterized by different extent of cementation and excellent building features. The tuffs represent a mixture of volcanic ash and coarse clastic material. They contain great amount of white pumice inclusions and have intricate grain-size composition. The ash mass is of aleurolite-psammitic composition though contains great amount of coarse clastic psephitic material as well. There are distinguished pelite-aleurolitic, vitro- and crystalloclastic varieties (Skhirtladze 1958). Content of the tuffs correspond to andesites ( $\text{SiO}_2 = 58.79\text{--}62.00\%$ ). The K-Ar age of tuffs is  $8 \pm 1.5$  Ma.

A packet (15–20 m) of volcanic breccias, which makes a steep rocky slope with a system of joints (mainly vertical) and erosion gorges overlies the tuffs (Fig. 84.2). Size of breccia fragments vary in wide range (max. 50 cm in diameter). Grayish-red, black and light grey breccias are observed here. According to microscopic study and analytical data the breccias correspond to andesites and dacites ( $\text{SiO}_2$  59–65 %). The section is terminated by andesite and dacite lava flows of the effusive subsuite of the Goderdzi suite.

Like the Cave Monastery Complex of Vardzia, a world-known Cappadocia underground construction (fairy chimneys) is hewn in Late Tertiary-Early Quaternary (about 10 Ma) welded (ignimbrite type) tuffs (Ulusay et al. 2006; Yilmazer 1995; Topal and Doyuran 1997).

A large group of monastery complexes of worldwide or municipal importance is dug out in rocks of different age and different lithological composition. For example: in North

Ethiopia, particularly on the territory of Central and Eastern Tigray about 100 carved in rock churches of different history, size and age are known, which are hewn in Permian-Carboniferous, Triassic, Lower and Middle Jurassic sandstones (Asrat 2002); In North-East Bulgaria, the monuments of worldwide and municipal importance are hewn in Upper Cretaceous sandy limestones (Matova 2008).

In the hill built up of Oligocene-Miocene basalt volcanic scoriae of the Northwestern plateau of Ethiopia world-known Lalibela (North Ethiopia) churches are hewn (Asrat and Ayallew 2011; Sani et al. 2012). We can provide many other examples of such monuments.

---

### 84.3 Hazards Induced with Geological Processes and the Expected Results

The problems concerned with the damage of the Vardzia monastery complex are initiated mainly by intricate endogenous (earthquakes, tectonic movements) and exogenous (water, Aeolian and glacial impact and different types of weathering) geological processes that intensively affect the monastery complex of Vardzia and the adjacent region. The suite of volcanic breccias makes favorable conditions for large-scale damage of the monument. In this suite the probability of landslide and snow slide activity is rather high that will be most hazardous for the safety of the monastery complex. The above assumption is based on the fact that at present the rock stability—equilibrium in the tuff-breccia suite is disturbed under the intensive impact of geological processes. It manifested in the weakening of rock resistance along the fissures and cracks in tuff-breccias.

The safety of the monastery complex is endangered by the unpredictable and uncontrolled endogenous geological processes as well as by the exogenous ones involving abrupt variations of air temperature and especially waters in a form of snow, rain, ice and ground waters that are rather abundant in the region.

In the fissured-solid rocks of tuff-breccias due to the erosion processes induced with seasonal flows running in the fissures and temperature variations the extent of rock cementation considerably decreases provoking the widening of fissures and formation of new ones. They also intensify processes of differentiated weathering of the constituent inhomogeneous rocks causing disturbance of slope stability—real conditions for slope failures, landslides and avalanches. Under the impact of the above factors a real threat of detachment and failure (or gliding) of large blocks or boulders of volcanic breccias increase day by day substantially changing the structure and the integrity of the monument and will endanger the visitors' safety.

**Fig. 84.1** Schematic geological section of the Vardzia Cave Monastery Complex. 1 Founder (slump) of volcanic breccia and tuff; 2 psephte volcanic tuff and breccia; 3 pelite-alevrite, crystal, cristal vitrical and crystal lithic tuffs of Vardzia; 4 andezitic volcanic breccia; 5 andesite lava flow

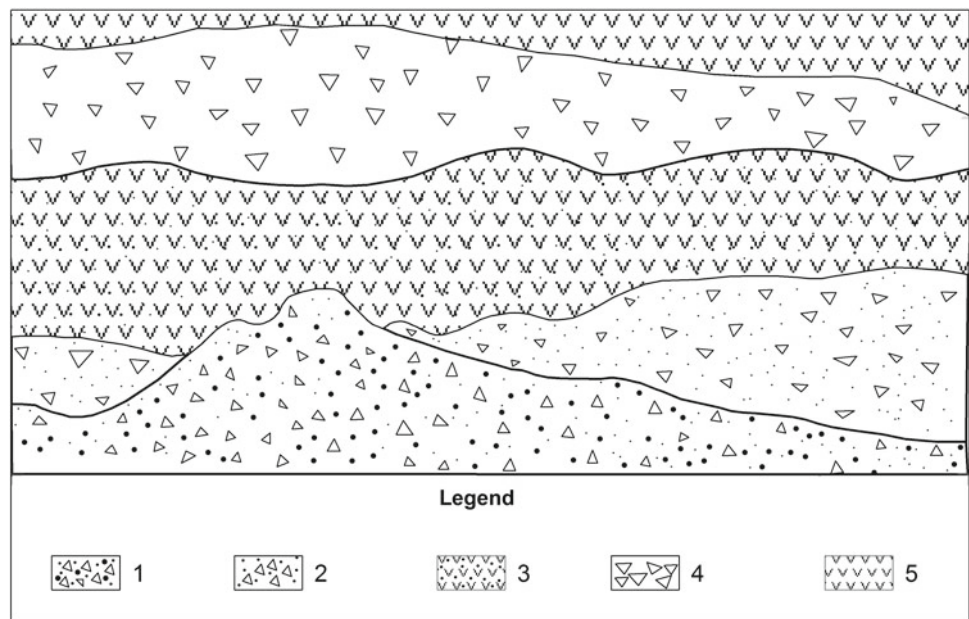


**Fig. 84.2** Cave monastery complex of Vardzia



#### 84.4 Preventive Activities

To maintain cultural heritage carrying out of conservation works is essential and urgent for all the countries. The main factors of disturbance of monument stability are: seismic events, groundwater- and wind-induced, weathering and erosion processes. These processes considerably deteriorate physical-mechanical properties of rocks and a real threat of destruction of the monument evolves. Special attention

should be focused on argillization (montmorillonitization) process that is the main reason of rocks physical-mechanical features deterioration and its progressive degradation (Delmonaco et al. 2010).

As the protecting activities of the rock-hewn Vardzia monastery complex—cleaning and restoration works are carried out annually, though this is insufficient. To stop further advance of exogenetic processes and to avert their destructive impact within the monastery complex area large-scale preventive works must be undertaken.

Urgent tasks to consider:

1. Evaluation of the dynamics of geological processes;
2. Evaluation of physical-mechanical properties of the building rocks (especially the breccias suite) from viewpoint of engineering geology and assessment of degree and rate of their alteration;
3. Reduction of inclination angle of active part of vertical slope of tuff breccias exposed to landslide and snow slide risk or to cut off an upper loaded part of tuff breccias (to reduce pressure) to preserve slope stability of the monastery complex area;
4. Arrangement of water regulating (flow diverting) walls and reinforcement of water course (concrete walls) to avoid the lateral and stream bed erosion provoked by surface waters running in fissures and cracks of the tuff breccias suite.

---

## References

- Asrat A, Ayallew Y (2011) Geological and geotechnical properties of the medieval rock hewn churches of Lalibela, Northern Ethiopia. *J Afr Earth Sci* 59(1):61–73
- Asrat A (2002) The rock-hewn churches of Tigray, Northern Ethiopia: a geological perspective. *Ge archaeology* 17(7):649–663
- Delmonaco G, Margottini C, Spizzichino D (2010) Weathering processes, structural degradation and slope-structure stability of rock-hewn churches of Lalibela (Ethiopia). *Geol Soc Lond Eng Geol Spec Publ* 23:131–147
- Matova M (2008) Geoenvironmental problems for the world cultural heritage in North-East Bulgaria. In: Kostov RI, Gaydarska B, Gurova M (eds) *Geoarchaeology and archaeomineralogy. Proceedings of the international conference*, Sofia, Publishing House “St. Ivan Rilski”, Sofia, pp 362–366
- Sani F, Moratti G, Coli M, Laureano P, Rovero L, Tonietti U, Coli N (2012) Integrated geological-architectural pilot study of the Biet Gabriel-Rufael rock hewn church in Lalibela Northern Ethiopia. *Ital J Geosci* 131(2):171–186
- Skhirtladze N (1958) Post-paleogenic effusive volcanism of Georgia. Publishing House, Academy of Sciences of GSSR, Tbilisi, 333p
- Topal T, Doyuran V (1997) Engineering geological properties and durability assessment of the Cappadocian tuff. *Eng Geol* 47(1):175–187
- Tutberidze B (2004) Geology and petrology of the late orogenic magmatism of the central part of the caucasian segment. TSU, Tbilisi 339 p
- Ulusay R, Gokceoglu C, Topal T, Sonmez H, Tuncay E, Erguler ZA, Kasmer O (2006) Assessment of environmental and engineering geological problems for the possible re-use of an abandoned rock-hewn settlement in Urgüp (Cappadocia) Turkey. *Environ Geol* 50(4):473–495
- Yilmazer I (1995) Engineering geologic factors in the design of a large underground structure in a tuff sequence in Cappadocia. *Eng Geol* 40(3):235–241

---

# Conserving Scotland's Built Heritage: A Petrographic Investigation on the Effects of De-icing Salts on Scottish Sandstones

85

Callum Graham, Martin Lee, Vernon Phoenix, and Maureen Young

---

## Abstract

In an attempt to understand the effects of high levels of de-icing salt deposition on sandstone masonry structures, samples of six blonde and two red sandstones were subject to salt crystallisation tests using three different de-icing salts. The impact of these salts on stone mass and integrity was initially evaluated by quantifying the mass gain/loss of samples via weighing and photography; subsequently Scanning Electron Microscopy (SEM), laser scanning and X-ray computed tomography scanning (CT scanning) were used to assess internal salt distributions and salt decay mechanisms across each stone type. Preliminary results indicate that both the salt type and microscopic texture of the stones play a significant role in salt accumulation within the pore structure and on observed decay characteristics. Samples immersed in  $\text{CaCl}_2$  show the greatest percentage of weight increase but with little observable decay. The red Locharbriggs samples on the other hand demonstrate the greatest percentage of weight change and decay across each salt type. This decay is related to the microscopic texture of the stone, specifically in relation to microscopic anisotropy at the pore scale.

---

## Keywords

Sandstone decay • Salt crystallisation • De-icing salts • Built heritage

---

## 85.1 Introduction

Scotland has a rich and complex geological history, and its traditional buildings showcase the varied and unique rock types used in their construction, so giving the towns and cities of Scotland their distinct character. During the mid-late 19th Century, Scotland had in excess of 700 working quarries (McMillan and Hyslop 2008) satisfying local, national and international demands for stone. Through increased trade links with North America, Scottish building

stone was frequently exported as ballast on returning trade ships. This ultimately led to Scottish stone being used as high quality building material internationally. Today however, Scotland has roughly 20 operating quarries, 12 of which supply sandstone (McMillan and Hyslop 2008). This puts increased stress on the age-old problem of sourcing suitable stone for replacement masonry. Many of these remaining quarries cannot provide building materials of sufficient quality and this has led to Scotland, formally a great stone nation, importing many of its building stones.

Through extensive investigation we have a good understanding of how the traditional stones decay (Smith et al. 2002), but long-term weathering responses of newly emplaced stones within historic building facades is often unknown, thus further exacerbating the problems faced by the heritage industry.

The present study seeks to better understand the process of salt crystallisation within sandstone. Salts are introduced into masonry via a number of pathways, including: (i) the alteration of materials that contain salt, such as the

---

C. Graham (✉) · M. Lee · V. Phoenix  
School of Geographical and Earth Sciences, University of  
Glasgow, Lilybank Gardens, Glasgow, G12 8QQ, UK  
e-mail: c.graham.1@research.gla.ac.uk

M. Young  
Conservation Directorate, Historic Scotland,  
7 South Gyle Crescent, Edinburgh, EH12 9EB, UK

mobilization of salt ions within stone mortars (Ruedrich and Siegesmund 2007); (ii) capillary rise from de-icing salts saturated into groundwater; (iii) vapour diffusion from air pollution or sea spray (Silva and Simão 2009); and (iv) from soils and fertilizers via absorption and capillary rise. Once in the stone salts cause damage by: (i) thermal expansion (Al-Naddaf 2009); (ii) hydration pressures; (iii) interaction with the hydric expansion of clays; and (iv) crystallisation pressures (Rodriguez-Navarro and Doehne 1999).

On average over six hundred thousand tonnes of de-icing salts are deposited on roads and pavements each year in Scotland (Transport Scotland 2014) and over two million tonnes throughout the UK (Salt Union 2014). With such widespread employment of de-icing practices, environmental mobilization of these salts has undoubtedly increased. The deleterious effect of certain de-icing salts on concrete and steel has been well documented (Valenza and Scherer 2007) but the effect and damage mechanisms of de-icing salts on masonry structures, and especially those constructed from the types of sandstones used throughout Scotland, is less well known. This study will ultimately help Historic Scotland to decide which are the most suitable de-icing salts to use around vulnerable buildings, and to make recommendations on the best types of replacement stone for future salt resilience.

Here we present results from an initial salt crystallisation test.

## 85.2 Materials and Methods

Eight sandstone samples were used in this study; six are representative of common replacement stones throughout Central Scotland and Northern England and the other two are stones used in the construction of the University of Glasgow at its current site at Gilmorehill in 1870 (Lawson

1981). These samples are tentatively identified as a Giffnock blonde sandstone and a Bonhill red sandstone. Three de-icing salts were used throughout the study: NaCl, CaCl<sub>2</sub> and a blended chloride salt containing NaCl (≥90 %) and bischofite (a common magnesium chloride additive).

### 85.2.1 Methods

The hydric behavior of each stone was measured using a range of British Standard tests including: (i) water absorption at atmospheric pressure; (ii) capillary coefficient; (iii) saturation coefficient; (iv) sorptivity; and (v) effective open porosity by buoyancy measurements. Pore size distributions were quantified by mercury intrusion porosimetry (MIP), allowing the classification of pore diameters as a percentage of the measured porosity to be made for each sample.

In order to assess the impacts of salt decay mechanisms on the internal structure and integrity of the various sandstone samples, salt crystallisation tests in accordance with the British standard BS EN12370.1999 were performed. The crystallisation behavior of each salt was studied by Environmental Scanning Electron Microscopy (ESEM) using a FEI field-emission instrument.

### 85.2.2 Stone Characterization

The petrographic characteristics of each stone sample were determined by characterisation of thin sections using transmitted light microscopy, a suite of hydric and permeability tests, MIP, computed tomography (CT) scanning and X-ray diffraction (XRD). Results were compared with data from the same stones obtained from the Building Research Establishment (BRE 2012). The mineralogy and porosity of each stone is listed in Table 85.1.

**Table 85.1** Mineralogy and average porosity

Name	Colour	Quartz (%)	K-Feldspar + mica (%)	Fe-oxide + other (%)	Clay + Cement (%)	Average porosity (%)
Cullalo	Pale white	76.0	2.0	nd	2.0	20.0
Scotch Buff	Buff	72.7	1.2	2.3	5.0	18.8
Stanton Moor	Blonde	73.0	4.7	2.0	5.5	14.8
Blaxter	Buff	72.0	5.0	1.5	6.0	15.5
Giffnock	Blonde	76.7	1.5	1.0	5.5	15.3
Clashach	Pale white	82.0	1.5	1.5	5.0	10.0
Locharbriggs	Red	71.0	2.0	4.5	3.0	19.5
Bonhill	Red	71.6	0.5	2.0	1.6	24.3

Average porosity calculated by helium porosimetry, water absorption and MIP  
*nd* denotes not detected

### 85.3 Results and Discussion

Resistance to salt crystallisation is expressed by the magnitude of changes to the petrographic properties and the petrophysical parameters of the stone and by salt crystallisation mechanisms and properties of the used salts. Thirty six cycles were carried out in this initial test, utilising thirty two samples. Each sample that was immersed in salt solution showed an initial weight increase, as expected (Ruedrich and Siegesmund 2007). This was followed, in samples exposed to NaCl and the chloride blend, by a secondary stage of weight decrease. CaCl<sub>2</sub> samples experienced a similar initial stage of enrichment, with a secondary stage of little fluctuation and a normalisation of values.

CaCl<sub>2</sub> accumulated in each stone type to a greater degree than NaCl and the chloride blend, and was the dominant factor in weight changes to these samples. The Clashach samples show the lowest amount of salt enrichment across each salt type, while Locharbriggs samples show the greatest amount of weight change with each salt.

A greater percentage of each salt is absorbed in the Locharbriggs, Stanton Moor and Scotch Buff samples, while significant weight losses are recorded for NaCl and the chloride blend in the Locharbriggs samples. The trend in these samples is therefore controlled significantly by the petrographic properties of the stone, as opposed to salt being the primary factor. The total connected porosity and the porosity of pores less than 5 µm in radius (P5) significantly influence water absorption and salt uptake, while the microporosity of pores less than 0.1 µm in radius (P0.1) is responsible for the generation of high crystallisation pressures (Yu and Oguchi 2010). Stanton Moor, Scotch Buff and Locharbriggs samples contain (P5) values of 13, 11.6 and 9.1 % and (P0.1) values of 5.7, 6 and 4.1 % respectively. With further salt enrichment, high crystallisation pressures would develop in Stanton Moor and Scotch Buff samples and deterioration would occur.

CaCl<sub>2</sub> did not damage any of the stone types, although was absorbed to a greater degree than NaCl and the chloride blend. Absorption of CaCl<sub>2</sub> controlled the final weight figures across each stone type while there is a strong relationship between final NaCl and chloride blend weight values and maximum weight loss in each stone type. This pattern indicates that both NaCl and the chloride blend caused more damage than CaCl<sub>2</sub>. Furthermore, correlation coefficients of 0.80 and 0.78 are found between: (i) final chloride blend and NaCl weight values and (ii) the difference between capillary uptake values measured at different orientations respectively. These results highlight the importance of microscopic anisotropy on fluid movement and susceptibility to salt induced decay.

ESEM work has demonstrated significant differences between the crystallisation behavior of CaCl<sub>2</sub> in comparison to NaCl and the chloride blend. CaCl<sub>2</sub> crystal growth

initiates at very low relative humidity (RH) (5 % RH), forming large, thin crystalline sheets that coat grains. At these low RH conditions, dynamic crystallisation and dissolution reactions are evident, forming small, hollow, bubbly and unstable globules of salt solution coating quartz grains. During the hydration of CaCl<sub>2</sub> dendritic crystals were evident, growing from an initial nucleation site at ~30 % RH. This is in contrast to the well documented crystallisation behaviour of NaCl, where NaCl forms small isometric hopper crystals (Rodriguez-Navarro and Doehne 1999).

Throughout these experiments, two main decay patterns can be distinguished. Various stones are characterized by a progressive rounding and smoothing of the corners and edges of the cubes, regarded as homogeneous decay, occurring across every sample susceptible to alteration. This is caused by evaporation, drying and a loss of sand grains taking place on all faces of the stone, a process unlikely to take place within a building facade. The other pattern is differential decay within layers in certain samples, caused by the heterogeneities in the rock. The Locharbriggs NaCl, chloride blend and Cullalo chloride blend samples show this progressive decay pattern concerning the loss of sand grains, focused in dark layers of grain alignment and variants of pore size distributions within the stone.

Colour measurements made using a chroma-meter also show a clear connection between stone and salt type. CaCl<sub>2</sub> caused a consistent darkening in all but the Stanton Moor sample, with the chloride blend causing significant "greening" across every stone type; a likely artifact of the green colourant mixed with the chloride blend salt forming efflorescence on the surface. Observations suggest that this discolouration penetrates less than a millimeter beneath the surface and within layers in the Cullalo and Locharbriggs samples.

---

### 85.4 Conclusions

With regards to those samples immersed in CaCl<sub>2</sub>, salt type was the dominant factor controlling solution uptake and stone alteration. CaCl<sub>2</sub> samples absorbed and retained a greater percentage of salt across each stone type, but showed little macroscopic alteration of the stone samples. The most significant factors influencing this pattern include specific properties to salt within the stone such as the hygroscopic behavior and hydrous phase changes. Crystals coating grains surfaces and possible pore clogging lead to a decrease in available and effective porosity caused by salt crystallisation throughout the stone or near the surface. Decay patterns on the studied stones are related to drying characteristics and the microscopic internal structure of the samples. This is specifically in relation to Locharbriggs samples where decay seems to concentrate in darkened layers of significant

heterogeneities such as pore size distributions, while clean, well sorted and mineralogically mature sandstones such as the Cullalo and Clashach samples show little alteration and a smaller proportion of dry weight change across each salt type. Salt uptake and eventual decay is influenced by the total connected porosity and the microporosities of pores less than 5 and 0.1  $\mu\text{m}$  in radius.

Results from these initial tests highlight the need for further analysis and a greater understanding of the pore network of each stone type. Through the results of other tests not presented in this paper, it is evident that many of the stones used are heterogeneous between samples and a larger sample set is required. Although in many cases the measurements of porosity, pore fractions and capillary uptake are sufficient for understanding the pore network, results suggest that gaining an understanding of the spatial relationship between these parameters within the pore network is crucial to our understanding of how they behave. This will help in the understanding of not only fluid flow through the stone but with the interaction between salt solution movement and the crystallisation mechanisms of different salts. It is with these considerations in mind that significant modifications and improvements have been made to the experimental design of repeat crystallisation and hydric tests but also with a more comprehensive set of larger samples, a greater sample set, the addition of more sandstone types and the inclusion of several novel investigative techniques.

The results presented here indicate that a suite of processes are taking place within the immersion and drying cycles of the stones that are dependent on both the

petrophysical and mineralogical properties of each sandstone type and the de-icing salt used.

---

## References

- Al-Naddaf M (2009) The effect of salts on thermal and hydric dilation of porous building stone. *Archaeometry* 51:495–505
- BRE (2012) Building Research Establishment website. <http://projects.bre.co.uk/ConDiv/stonelist/stonelist.html>
- Lawson J (1981) *Building stones of Glasgow*. Geological Society of Glasgow, Glasgow
- McMillan A, Hyslop E (2008) The city of Edinburgh—landscape and stone. In: ICOMOS 2008 scientific symposium
- Rodriguez-Navarro C, Doehne E (1999) Salt weathering: influence of evaporation rate, supersaturation and crystallisation pattern. *Earth Surf Process Land* 24:191–209
- Ruedrich J, Siegesmund S (2007) Salt and ice crystallisation in porous sandstones. *Environ Geol* 52(2):225–249
- Salt Union website (2014) [www.saltunion.com/news/quick-facts/](http://www.saltunion.com/news/quick-facts/)
- Silva ZSG, Simão JAR (2009) The role of salt fog on alteration of dimension stone. *Constr Build Mater* 23:3321–3327
- Smith BJ, Turkington AV, Warke PA, Basheer PAM, McAlister JJ, Meneely J, Curran JM (2002) Modelling the rapid retreat of building sandstones: a case study from a polluted maritime environment. *Natural stone, weathering phenomena, conservation strategies and case studies*. *Geol Soc Lond Spec Publ* 205: 347–362
- Transport Scotland website (2014) [www.transportscotland.gov.uk/road/maintenance/winter-maintenance/salt](http://www.transportscotland.gov.uk/road/maintenance/winter-maintenance/salt)
- Valenza II, John J, Scherer GW (2007) Mechanism for salt scaling of a cementitious surface. *Mater Struct* 40:259–268
- Yu S, Oguchi CT (2010) Role of pore size distribution in salt uptake, damage, and predicting salt susceptibility of eight Japanese building stones. *Eng Geol* 115:226–236

David Martín Freire-Lista, Vladimir Greif, Mónica Álvarez de Buergo, and Rafael Fort

## Abstract

Since troglodyte population has excavated their dwellings in the gypsum escarpment of the Risco de las Cuevas of Perales de Tajuña (Spain), atmospheric processes have preferentially sculptured the rockwall. This weathering has a negative effect on the future of the monument, and to preserve it, it is important to investigate how the different content of clay in the gypsum that constitute the escarpment, respond to the weathering. Three types of gypsum, with different amounts of clay, material that constitute El Risco de las Cuevas, were subjected to accelerated ageing tests in laboratory (freezing/thawing and wetting/drying). In addition to laboratory observations, results from field observations and digital photogrammetry were obtained, serving to draw the geometry of the escarpment, comparing with old photographs, taken by neighbors of the village of Perales de Tajuña, in which images of the detached tape block of gypsum can be seen, their dimensions and volume. All artificial accelerated ageing tests have led to gypsum caused decay, being the most aggressive the resistance to freezing in the gypsum specimens with the highest clay content.

## Keywords

Gypsum • Grottoes • Ageing test • Weathering • Photogrammetry

## 86.1 Introduction

El Risco de las Cuevas is a gypsum escarpment, (Fig. 86.1) in which grottoes have been excavated from late Neolithic to recent times (Reyes Téllez 2009). This rockwall is located in the province of Madrid, in Perales de Tajuña, 40 km Southeast of Madrid city, 40°14'0.3''N 3°19'55''O. The

environmental conditions and microclimate (Freire-Lista et al. 2014) produce several weathering processes (Hall et al. 2012) that might endanger this piece of cultural heritage.

This area was declared Historical-Artistic Monument in 1931. In 1998 it was listed as BIC (cultural asset of interest) by the regional government of Madrid with Monument category under the “historical, architectonic, archaeological, artistic, ethnographic and scientific (Spanish law 1998), for being a product of human activity of outstanding cultural interest.

The action of atmospheric agents (Ponziani et al. 2012), with a Mediterranean continental climate, since the Neolithic caused weathering of the whole escarpment, endangering the integrity of the caves, jeopardizing the whole monument (Ergüler 2009).

This research is focused on the evaluation of decay processes of the gypsum beds that constitute the natural and cultural heritage property of El Risco de las Cuevas. The aim is to establish the causes of its decay and to propose preservation measures for this area, studying the evident interactions

---

D.M. Freire-Lista (✉) · M. Álvarez de Buergo · R. Fort  
Instituto de Geociencias (CSIC, UCM), Spanish Research Council-Complutense, University of Madrid, Madrid, Spain  
e-mail: dafreire@geo.ucm.es

D.M. Freire-Lista · R. Fort  
CEI Campus Moncloa, UCM-UPM and CSIC, Madrid, Spain

V. Greif  
Faculty of Natural Sciences, Department of Engineering Geology,  
Comenius University in Bratislava, Mlynska Dolina G, Bratislava,  
Slovakia

**Fig. 86.1** View of the Risco de las Cuevas of Perales de Tajuña (Madrid)



between Man, natural slope evolution and heritage. Aiming at preventive conservation rather than an intervention.

## 86.2 Geological Setting

The escarpment where the caves were excavated belongs to the Lower Miocene unit of the Madrid Basin (Calvo et al. 1989). It is overlaid by the Lower-Mid Miocene Intermediate Unit, which is formed by carbonates (limestones and dolostones) along with other materials like clays, gypsum and flint. This forms the top of the sequence outcropping in this area. There are debris cones formed at the bottom of the rockwall made up of mixture of debris from the Lower, Medium and Upper Units. The escarpment, 70 m high and 500 m wide, was created by reactivation of Variscan faults during the Alpine orogeny (Garrote et al. 2008), which have determined the direction of the rockwall (SW-NE) as well as the Tajuña river valley (that gives name to the nearest village), located in its center.

## 86.3 Materials and Methods

In order to obtain the escarpment geometry, a series of photos were taken using a Canon 5D Mark II digital camera at focal lengths of 16 and 35 mm. The series of photos were processed using digital photogrammetry software Photomodeler Scanner to obtain 3D point cloud of the studied slope. By further processing and meshing the 3D pointcloud it was possible to calculate the slope height, volumes of selected fallen blocks, and areas of shear surfaces of sliding blocks. The point cloud will be used as the benchmark for

monitoring the erosion and material loss from the face of the rockwall in the future. To study the evolution of rockwall, old photographs have been used, which have been searched through the village and archaeological associations.

In order to analyze the effect of humidity and temperature on the rock, tree accelerated artificial ageing tests were reproduced in the laboratory: The freezing/thawing tests consisted of 24 h cycles: 17 h of total immersion in room temperature water ( $20^{\circ} \pm 5^{\circ}\text{C}$ ), and 7 h of freezing at  $-16^{\circ}\text{C}$ . The wetting/drying test was performed in 24 h cycles: 17 h in room temperature water immersion followed by 6 h in a laboratory oven at  $50^{\circ}\text{C}$  and 1 h in a dryer. Another accelerated ageing test by wetting/drying (modified) was performed, consisted of cycles of 17 h in a laboratory oven at  $50^{\circ}\text{C}$  and 1 h in a dryer for cooling to room temperature, and complete immersion during 6 h in room temperature water. Each accelerated ageing test was concluded at 105 cycles. The material decay evaluation has been carried out by means of the control of its weight loss in each one of the cycles.

Each one of these artificial ageing tests has been performed with 9 samples, divided in 3 groups (Fig. 86.2), based on the amount of clay minerals (Illite, Smectite and Kaolinite). Type 1 gypsum with less of 5 % in clay content, type 2, gypsum with clay content between 5 and 15 % and type 3 with a higher clay content, more than 15 %.

## 86.4 Results

A high number of old photographs was collected, taken since 1890, which have been processing. From them, it is know that the last great rock fall happened at the beginning

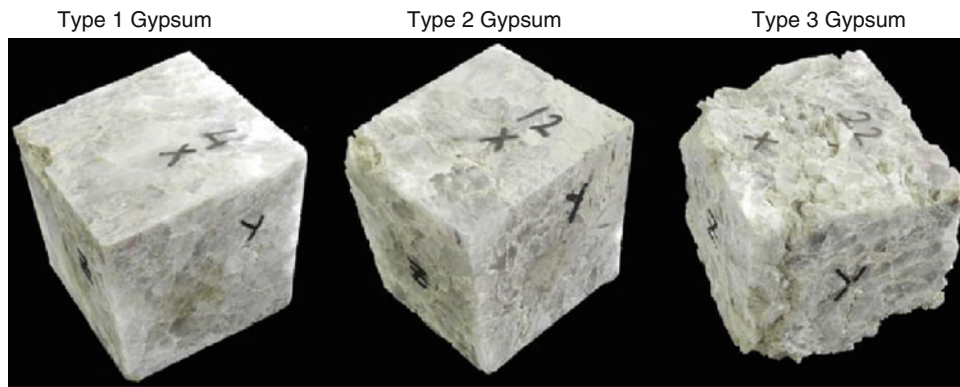


**Fig. 86.2** Different types of gypsum studied, divided by the amount of clay

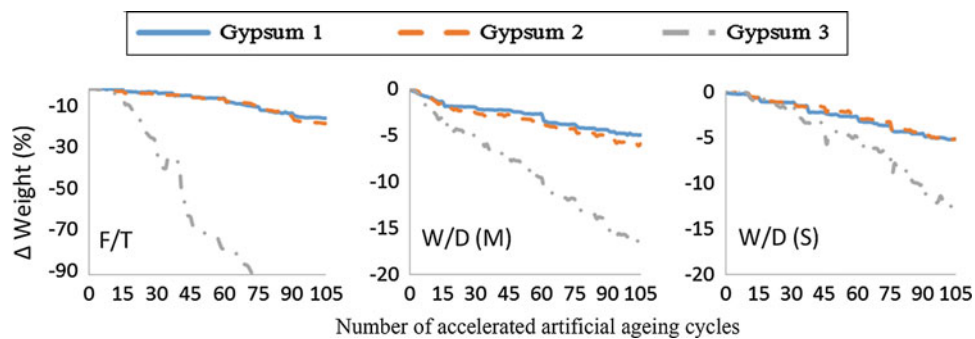


**Fig. 86.3** Number of accelerated artificial ageing cycles. Weight variation of three groups of gypsum in each testing artificial ageing-accelerated test. F/T (freezing/thawing), W/D (M) (modified wetting/drying test), W/D (S) (standard wetting/drying)

of the twentieth century, a gypsum block of about 736 m<sup>3</sup> and 1,600 tons weigh. It fell with a shear surface of about 354 m<sup>2</sup> area, measured by the photogrammetry analysis.

The gypsum durability has been evaluated measuring the weight loss of the specimens. The type 3 gypsum has experienced the most severe decay (Fig. 86.3) in all the test. These samples have undergone disintegration in its entire perimeter and in cycle number 75 of freezing/thawing test, these specimens have lost almost 90 % of its weight. For the modified wetting/drying test, 16.2 % and for the standard wetting/drying test, 12.9 %.

This weight loss was continuous throughout the cycles and, possibly, greater number of cycles performed, the specimens would lead to the complete disintegration if increasing the number of cycles. Mass loss occurred primarily during the melting step, with the test pieces of gypsum immersed in water at 20 °C.

The decay of the type 1 and 2 gypsum has been very similar, with less decay of type 1 gypsum, which its weight loss is due to the dissolution by artificial accelerated ageing tests. The samples belonging to the gypsum without clay (type 1) experienced less weight loss: 14.2 % for freezing/

thawing, 4.9 % for modified wetting/drying test and 5.2 % for the standard wetting/drying test.

## 86.5 Conclusions

The Risco de las Cuevas decay is favored by the mineral composition of the gypsum rocks, with different clay content of subhorizontal layers, the geomorphology (with an almost vertical slope) and by the climate, with a noticeable cyclical nature of temperature and humidity.

The artificial ageing tests allowed to determine how the clay mineral content is the key factor that controls the decay, being the most aggressive ageing test the freezing/thawing one, with a faster material loss of the samples with a higher content in these minerals. Although the deterioration process takes place in different ways, the water participates actively form in each one of them: ice water frost, dissolution, water retention with an increase of weight, and clays lixiviation. These factors generate specific damages and all of them contribute to the rock decay. It is important to minimize the water inflow.

The severity of wetting/drying cycles influences the gypsum durability. Modified wetting/drying test was more aggressive (a higher weight loss) than the standard wetting/drying test, which kept more uniform moisture conditions of gypsum samples (a shorter drying).

Another experience in terms of valuing cultural heritage that would contribute to its preservation is the so-called geomonumental routes (<http://www.madrimasd.org/English/Science-Society/scientific-heritage/Geomonumental-Routes/default.asp>), through which the geological features and the cultural value of the El Risco de las Cuevas are shown to the society. These activities have been carried out in the site during the last 2 years in the frame of the Science Week, with successful results.

**Acknowledgements** This paper is part of the program Geomateriales (S2009 /MAT-1629), funded by the Community of Madrid. Thanks to the Petrophysics Laboratory of the Institute of Geosciences, (CSIC, UCM), belonging to the Laboratories Network on Heritage Science and Technology (RedLabPat), CEI-Moncloa (UCM- UPM, CSIC), and to the laboratories Network of the Community of Madrid (RedLab) where the laboratory testing was performed. Funding from the UCM research group “Applied Petrology for Heritage Conservation Research Group” is also acknowledged.

## References

- Calvo JP, Ordóñez S, García del Cura MA, Hoyos M, Alonso-Zarza AM, Sanz E, Rodríguez Aranda JP (1989) Sedimentología de los complejos lacustres miocenos de la Cuenca de Madrid. *Acta Geológica hispánica* 24:281–298
- Ergüler ZA (2009) Field-based experimental determination of the weathering rates of the Cappadocian tuffs. *Eng Geol* 105:186–199
- Freire-Lista DM, Martínez-Garrido MI, Fort R (2014) Monitoring techniques for microclimatic analysis in cultural and natural heritage for decay evaluation. In: Art´14, 11th international conference on non-destructive investigations and microanalysis for the diagnostics and conservation of cultural and environmental heritage. Madrid 11–14 June (in press)
- Garrote J, Garzón G, Tom R (2008) Multi-stream order analyses in basin asymmetry: A tool to discriminate the influence of neotectonics in fluvial landscape development (Madrid Basin, Central Spain). *Geomorphology* 102:130–144
- Hall K, Thorn C, Sumner P (2012) On the persistence of weathering. *Geomorphology* 1–10:149–150
- Ponziani D, Ferrero E, Appolonia L, Migliorini S (2012) Effects of temperature and humidity excursions and wind exposure on the arco of Augustus in Aosta. *J Cult Heritage* 13:462–468
- Reyes Téllez F (2009) El Risco de las Cuevas, en Perales de Tajuña. *Anales de Arqueología Cordobesa* 20:203–230
- Spanish law 10/1998, July 9th, of historical heritage, Community of Madrid (Spain)

---

# Deterioration of Stone and Mineral Materials from the Roman Imperial “Villa of the Antonines” at Ancient Lanuvium

# 87

Gregory A. Pope, Deborah Chatr Aryamontri, Laying Wu,  
and Timothy Renner

---

## Abstract

The “Villa of the Antonines”, located at the 18th mile of the ancient Via Appia, is so far the least explored of the ancient Roman imperial residences in the area of the Alban Hills. Excavations at “Villa of the Antonines” permit an investigation of subsurface deterioration of cultural stone, addressing two primary questions: (1) What are the deterioration processes in the soil and sediment environment, and how do these compare to subaerial deterioration processes? (2) How might the deterioration impact other methodologies reliant on the analysis of the material, such as use and wear analysis, dating techniques, and provenience by chemical tracers? The deterioration characteristics of materials recovered thus far can be visually described. Marbles are discolored and exhibit a loss of polish and partial to extensive granular disintegration and powdering. Brick varies in color and composition due to manufacturing and material differences, but may also exhibit within-soil alteration. Glass tesserae exhibit frosting and pitting from chemical solution. Scanning electron microscopy (SEM) reveals surface microdeterioration such as pitting, etching, and glazing. Qualitative backscatter electron microscopy (BSEM) and energy dispersive spectroscopy (EDS) indicate the distribution of elements, including byproducts of chemical deterioration, likely within the soil environment.

---

## 87.1 Introduction

In 2010, Montclair State University began investigation of archaeological remains at the 2nd Century Roman imperial “Villa of the Antonines”, at the 18th mile of the ancient Via Appia near Genzano di Roma, Italy (Fig. 87.1). This imperial residence spread over a considerable extent, but remained largely unknown apart from the massive concrete remains of the bath complex and the partially excavated adjacent amphitheater (Chatr Aryamontri et al. in press; Chatr Aryamontri and Renner 2010, 2011, 2012; Cassieri and Ghini 1990). The villa has been neglected and poorly explored, as well as subject to looting, vandalism, and decay. Nevertheless, the lavish decoration of the complex is apparent in the large quantity of fragments of decorative white and colored marble and the thousands of multi-colored glass tiles (tesserae) used for flooring or wall decoration. Many of the construction and decorative materials that once were an integral part of the buildings of the villa lie loose

---

G.A. Pope (✉)  
Department of Earth and Environmental Studies, Montclair State  
University, Montclair, NJ 07043, USA  
e-mail: popeg@mail.montclair.edu

D.C. Aryamontri · T. Renner  
Department of Classics and General Humanities, Montclair State  
University, Montclair, USA

G.A. Pope · D.C. Aryamontri · T. Renner  
Center for Heritage and Archaeological Studies, Montclair State  
University, 10 Normal Avenue, Montclair, NJ 07043, USA

L. Wu  
Microscopy and Microanalysis Research Laboratory, Montclair  
State University, Montclair, USA  
e-mail: wul@mail.montclair.edu

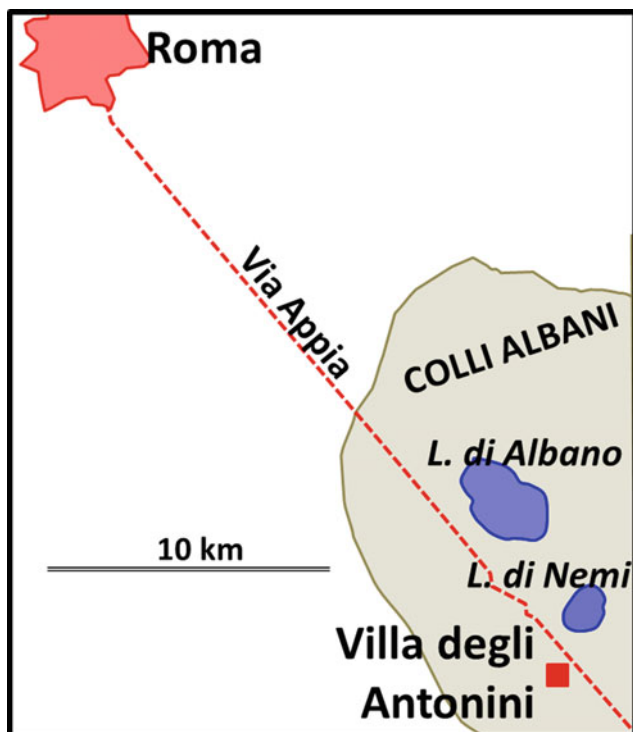


**Fig. 87.1** Location of the “Villa of the Antonines”

and scattered everywhere on the site, some in a sub-aerial setting, but the majority of them buried underground. The artifacts excavated from soil and sediment, especially fragments of brick, white marble, and the mosaic glass tesserae, have undergone differing levels of deterioration or corrosion.

The purpose of this paper is to provide an initial assessment of the deterioration of stone and mineral materials recovered from “Villa of the Antonines.” Deterioration in the soil matrix presents different weathering environments than the more-commonly understood subaerial deterioration. With a better understanding of stone deterioration in the soil matrix, researchers will be in a better position to assess sources of the materials, their working and production, and their eventual conservation. This goal is heightened at the “Villa of the Antonines” given the poor state of site preservation. With special permission from Italian authorities, the authors were able to obtain a number of stone, brick, and glass fragments, on loan, for this preliminary study.

## 87.2 Methods

Specimens were selected among existing recovered artifacts of the “Villa of the Antonines” site, by purposely choosing samples that demonstrated observable deterioration as well as less-deteriorated samples for comparison. Details of the

ongoing excavation can be read in Chatr Aryamontri et al. (in press, 2013), Chatr Aryamontri and Renner (2010, 2011, 2012), and Cassieri and Ghini (1990).

Analysis presented for this paper relies on the capabilities of scanning electron microscopy (SEM) and energy dispersive spectroscopy (EDS) at the Microscopy and Microanalysis Research Laboratory at Montclair State University. Glass samples were mounted on aluminum stubs, fixed with carbon tape, and coated with a thin layer of gold film in a Denton Desk IV Sputter Coater. In the case of marble and brick, samples were mounted in the same manner but coated with a thin film of carbon. The samples were imaged by a Hitachi S-3400 N SEM, under a high vacuum system, 15 kV,  $\sim 10$  mm working distance, spot size 30, and objective aperture size 2. Qualitative EDS spectrum analysis on the specimen surface was conducted at 15 kV accelerating voltage, beam spot size 70, and objective aperture size 2, working distance equal/close to 10 mm.

## 87.3 Results

### 87.3.1 Brick

Brick fragments at the study site varied in the degree of deterioration, some in good condition, others intact but soft and capable of being scratched with a fingernail. Samples recovered from the study site, all from the soil matrix, were deteriorated samples. The surface was dark brown in color, while the interior was yellow-tan. Samples analyzed were damp.

At the macroscopic scale, a cross-sectioned brick fragment exhibited a distinct discolored rim along the perimeter of the fragment surface, approximately 1 mm in width. This rind was a post-burial formation, developing parallel to the fragmented surface, not related to the original surface of the fired brick. Oxidation was probably involved; elucidation of other chemical alteration processes to the clay minerals will await further microanalysis.

One brick fragment was imaged with SEM, BSEM, and qualitative element mapping (EDS) (Fig. 87.2). At magnifications  $\sim 200$ – $2000\times$ , the surface appeared granular, with aggregate particles  $\sim 5$ – $20$   $\mu\text{m}$  in diameter. Fissures  $\sim 20$   $\mu\text{m}$  wide and up to several 100  $\mu\text{m}$  in length crossed the soft material, probably the result of wetting and drying cycles (Lopez-Arce and Garcia-Guinea 2005). EDS indicated elements expected for clay minerals: Si, Al, Ca, K, Mg, in homogeneous distribution. Iron was also present (visible in element mapping and likely visible as brighter areas in BSE images), contributing to the oxidized surface over  $\sim 20$  % of the fragment surface.

**Fig. 87.2** Weathered brick. **B1** showing fracture. **B2** showing granular texture

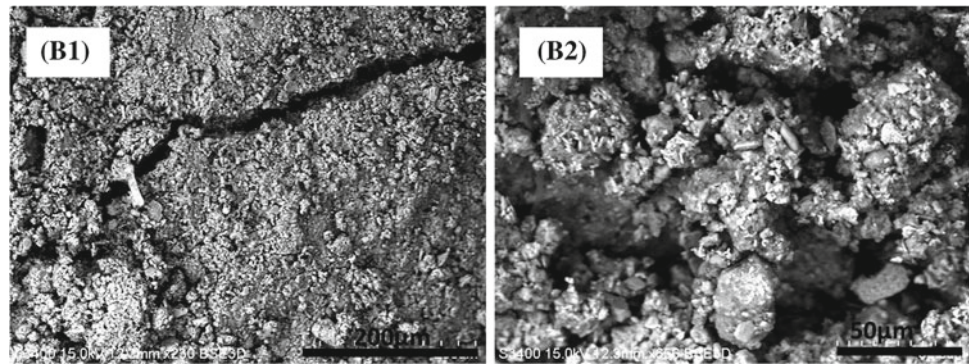


**Table 87.1** Marble samples

Sample	Name	Description
M1	Modern marble	White, granoblastic, unweathered
M2	“Marmo bianco”	White, granoblastic, weathered
M3	Striped white	White, granular, gray stripe inclusion (mica?), weathered
M4	Striped green	Green exterior, granular, stripe inclusions, weathered

### 87.3.2 Marble

Four marble fragments have been analyzed thus far, three from the “Villa of the Antonines” (from the soil matrix) and one a fresh-cut modern marble (Table 87.1).

Like the brick, marble fragments at the study site varied in the degree of deterioration, including some that retained polish. None of the “Villa of the Antonines” marble samples recovered from the soil retained any glassy polished surface, though they are presumed to have been polished at one time. The marbles did retain flat faces, often with granular disintegration. For comparison, the modern marble (M1) did have a polished surface evident at the macroscopic scale, while SEM revealed a polished surface covered with shallow roughness interspersed with striated smooth glazing (Fig. 87.3 upper). No cracking or deep intergranular pitting was seen in M1.

The granoblastic M2 sample was composed of elements consistent with calcitic and dolomitic marble, with prominent amounts of both Ca and Mg. M2 exhibited extensive surface weathering features. A relatively smooth area (Fig. 87.3 middle) showed an etched surface of shallow, oriented crystal points (<10 µm in relief) split by several parallel fissures 5–10 µm wide and ~100 µm long. The etching was a product of chemical solution, while the cracking may have been the result of one or more agents: calcite crystal thermal expansion, salt crystal growth, fire, or

physical stress on the stone (Rapp 2002). Elsewhere on the same sample, the surface was deeply pitted, resembling “grikes and clints” karst topography (Fig. 87.3 lower).

Under SEM analysis, marble sample M3 appeared the least-weathered of the analyzed samples. While not retaining polish, original surfaces had minimal relief, resembling the modern marble. Calcite crystals were in good condition, with little intergranular weathering. The weakest locations of the sample were associated with the gray stripe. SEM/EDS revealed this to be a type of mica mineral (probably biotite, given the Mg and Fe present), with fractures parallel to the phyllosilicate plates.

Sample M4 had a green-colored exterior that was lighter in color in the interior. Its composition was more heterogeneous than the other marbles, with inclusions of aluminosilicate minerals, some of these also containing Fe and Mg or K. There was minimal surface deterioration: some flaking and granular loss, but no deep pitting and no cracking.

### 87.3.3 Glass Tesserae

Four of the glass tesserae were analyzed thus far (Table 87.2), two each of green or red color, specifically selecting examples of both more and less deterioration. A general state of deterioration was visible at the macroscopic level. These macroscopic observations translated to later microscopic analysis (Fig. 87.4).

The chemical composition of the tesserae was variable. The major components of silica, calcium, and soda (Na) were apparent. Minor peaks of iron and chlorine were detected in some locations, due to impurities, colorants (Croveri et al. 2010; Fleming 1997), or possible use of evaporite salts for flux. Most components were homogenous throughout with the exception of T2, which gave indications of element segregation (Fig. 87.5).

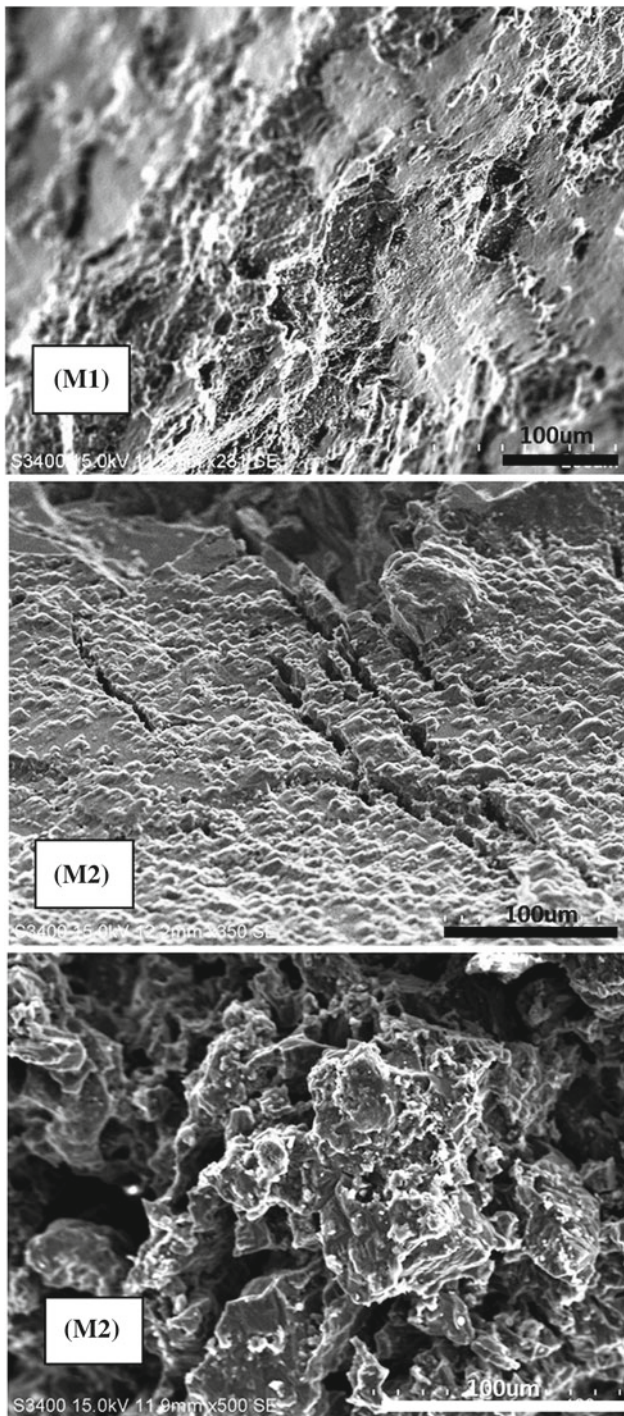


**Fig. 87.3** Marble samples. *Upper*, modern marble (M1), minimal deterioration. *Middle*, parallel cracking in M2. *Lower*, dissolution pitting in M2. 100 µm scale bar in each image

**Table 87.2** Tesserae samples

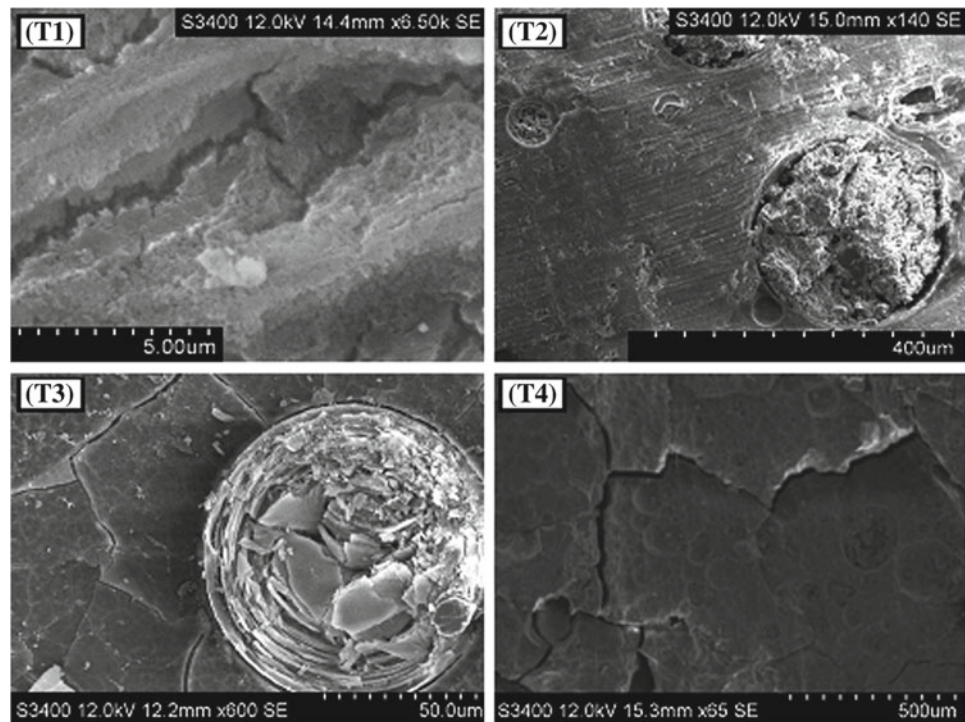
Sample	Description and macroscopic condition
T1	Green colored, good condition
T2	Red colored, good condition
T3	Red colored, poor condition
T4	Green colored, poor condition

The glass tesserae exhibited a variety of deterioration features including surface overgrowths, shallow pitting or cratering, linear and polygonal cracking, and surface flaking. The environment in which this deterioration occurred is uncertain, though burial in the soil is potentially responsible for much of the deterioration. Manufacturing features are also apparent, such as bubbles and striations, both contributing to later deterioration. Since the specimens of the same kind clearly presented different stages of deterioration, it is clear that the degree of deterioration is not reliant on the manufacturing process. We hypothesize the resulting order of deterioration of the tesserae as follows, in first to last order: (1) manufacturing faults (bubbles, striations); (2) pitting and cratering; (3) fine polygonal cracking and overgrowths; (4) large cracking; (5) flaking, biotic growth.

The most common features of the tesserae were shallow circular pits or craters, occasional on some surfaces such as T1 but ubiquitous and extensive on other surfaces, such as T3 and T4 (Fig. 87.4 lower right). The craters ranged in size from 20–80 µm in diameter and in depth <5 µm. We interpret these to be weathering features as they were limited to exposed surfaces and appeared to overlay manufacturing features, such as the striae. Cratering is probably related to chemical dissolution, described by Branda et al. (1999). Craters are not to be confused with often larger and deeper circular vesicles, interpreted as being bubbles in the glass, a product of manufacturing (Croveri et al. 2010). Bubbles do play a role in the surface deterioration, however. In the T1 sample, organic material filled several of these bubbles, which act as a protective location but also serve to retain biological weathering agents. (Fig. 87.4 upper right). In T3, an 80 µm bubble was completely filled with a flaked material, probably now clay (Fig. 87.4 lower left). This may have been an unmelted inclusion in the glass, perhaps of the sodic flux added to the raw material. It weathered into plates concentric to the circumference of the bubble.

Three types of cracking or fissuring were noted on the tesserae: small polygonal cracking; larger angular area cracking; and fine linear cracks. All represent mechanical

**Fig. 87.4** Surface weathering on tesserae: parallel cracking in grooves (**T1**); vesicle filled with organic material (**T2**); vesicle filled with clay, surrounded by mosaic fractures (**T3**); mosaic fracture patterns and shallow craters (**T4**)



surface stress, but from various causes. The smallest cracks define small ( $<20\ \mu\text{m}$ ) polygonal flakes, best seen on T3 (Fig. 87.4 lower left) and T4, but not observed on T1 and T2 (concordant with the visibly better condition of T1 and T2). The cracks and polygonal flakes are shallow surface features. Likely, polygonal cracking is a result of glass corrosion in either a subsoil or subaerial environment, described by Römich (1999). Atmospheric or soil acids are capable of leaching the alkaline elements of the sodic components. While SEM-EDS identified the presence of alkaline elements on the glass surface (Fig. 87.5), specific element loss (compared to the interior of the specimen) awaits cross-sectional microanalysis.

Fine polygonal cracks were in some instances contained within angular surface blocks, defined by larger cracks up to  $20\ \mu\text{m}$  wide. On the T4 specimen, these larger cracks cut through shallow craters or pits (Fig. 87.4 lower left and lower right). The crack-defined areas,  $\sim 100\text{--}500\ \mu\text{m}$  in diameter, resemble macroscopic exfoliation seen on rock surfaces, and may be caused by temperature stress, salt crystal growth, hydration or dehydration of glass (which may originally contain up to 20 % water, Römich 1999), or

clay hydration from the soda component (Ganio et al. 2012). The larger cracks would also allow deeper penetration of further weathering agents.

The third type of cracking, linear cracks (Fig. 87.4 upper left), appeared parallel to striations. We believe the striations, hundreds of  $\mu\text{m}$  long and  $5\text{--}10\ \mu\text{m}$  wide, to be manufacturing artifacts, possibly from irregular cooling or mixing of raw material, from cutting the glass into tesserae, or from polishing the glass. Striations were not apparent on all surfaces, and linear cracking not apparent on all striations. The linear cracks,  $\sim 0.5\ \mu\text{m}$  wide, formed in the “troughs” of the striations. Linear cracks may be the result of cooling and shrinking during manufacture, from post-manufacture exposure to temperature extremes, glass hydration/dehydration, clay expansion, or salt crystal growth below the plates (given the presence of Cl, Na, and K identified within the glass matrix, Fig. 87.5). The linear cracks are likewise large enough to allow entry for weathering agents, extending the deterioration feedback. Thin overgrowths or coatings were identified on flat surfaces, particularly on striated surfaces. These overgrowths are probably secondary deposits of silica.

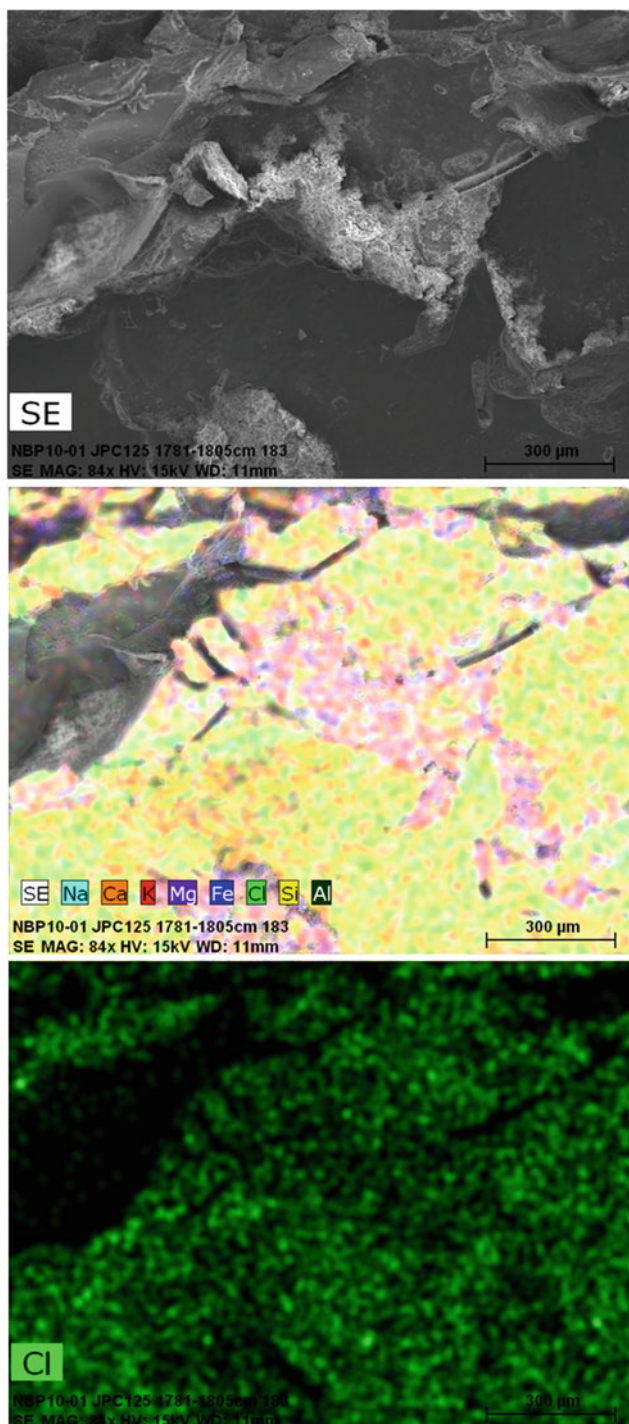


**Fig. 87.5** Qualitative element analysis of T2 with EDS. Identical areas imaged: secondary emission (*top*), mixed element mapping (*center*), chlorine content (*bottom*). Scale bar 300 µm in each

## 87.4 Conclusions

All samples analyzed thus far exhibited a degree of deterioration consistent with burial in a cyclically wet-dry soil environment. Soil moisture suitable for chemical weathering

likely contributed to the oxidation and softening of brick, solution and disintegration of marble, and pitting and micromosaic cracking of glass tesserae. Mechanical weathering processes were also important, exerting physical stress to produce cracks in the materials, attributed to anisotropic mineral stress, wetting and drying of clays, and possibly thermal stress.

Our study of the recovered artifacts is ongoing, and better detail of the deterioration process as well as the nature of the materials is forthcoming. Cross-sectional backscatter SEM and EDS will be able to discern the extent of physical stress into the interiors of the samples, as well as determine the loss (or addition) of elements from surface to interior during the chemical weathering process. Continued study of additional specimens will expand the data set, including different varieties of marble and tesserae. With scrap and leftover material, we will also attempt to assess bulk chemistry of the major and trace elements in the brick, marble, and glass. The composition analysis may assist in the establishing the provenance of the materials used, while also establishing the degree of loss of key elements (by weathering) that would render provenance comparisons uncertain. The assessment of the decorative and architectural materials from the “Villa of the Antonines” provides an unexpected, albeit fragmentary window into technological aspects of the Roman Imperial period.

## References

- Branda F, Laudisio G, Costantini A (1999) Weathering of a Roman glass: a new hypothesis for pit formation on glass surfaces. *Glass Technol* 40(3):89–91
- Cassieri N, Ghini G (1990) La cosiddetta villa degli Antonini al XVIII miglio della Via Appia. *Quaderni del Centro di studio per l'archeologia etrusco-italica*. 10(1):168–178
- Chatr Aryamontri D, Renner T, Cecchini C Indagini Archeologiche presso la ‘Villa degli Antonini’ (Genzano Di Roma) (2012–2013) in Lazio e Sabina. In: Ghini G (ed) *Atti del Convegno. Decimo Incontro di Studi sul Lazio e la Sabina (Roma 4–6 giugno 2013)* (in press)
- Chatr Aryamontri D, Renner T, Cecchini C (2013) Nuove esplorazioni della Montclair State University (New Jersey) presso la Villa degli Antonini a Genzano di Roma: i risultati degli scavi 2010–2011, in Lazio e Sabina. In: Ghini G (ed) *Atti del Convegno. Nono Incontro di Studi sul Lazio e la Sabina (Roma 27–29 marzo 2012)*, pp 291–298
- Chatr Aryamontri D, Renner T (2010) Villa degli Antonini: Season 2010 (“Villa of the Antonines”). *Fasti Online*. [http://www.fastionline.org/micro\\_view.php?fst\\_cd=AIAC\\_2694&curcol=sea\\_cd-AIAC\\_3783](http://www.fastionline.org/micro_view.php?fst_cd=AIAC_2694&curcol=sea_cd-AIAC_3783)
- Chatr Aryamontri D, Renner T (2011) Villa degli Antonini: Season 2011 (“Villa of the Antonines”). *Fasti Online*. [http://www.fastionline.org/micro\\_view.php?fst\\_cd=AIAC\\_2694&curcol=sea\\_cd-AIAC\\_4158](http://www.fastionline.org/micro_view.php?fst_cd=AIAC_2694&curcol=sea_cd-AIAC_4158)
- Chatr Aryamontri D, Renner T (2012) Villa degli Antonini: Season 2012 (“Villa of the Antonines”). *Fasti Online*. [http://www.fastionline.org/micro\\_view.php?fst\\_cd=AIAC\\_2694&curcol=sea\\_cd-AIAC\\_4548](http://www.fastionline.org/micro_view.php?fst_cd=AIAC_2694&curcol=sea_cd-AIAC_4548)
- Croveri P, Fragalà I, Ciliberto E (2010) Analysis of glass tesserae from the mosaic of the ‘Villa del Casale’ near Piazza Armerina (Enna,

- Italy). Chemical composition, state of preservation and production technology. *Appl Phys A* 100:927–935
- Fleming SJ (1997) Roman glass: reflections of everyday life. University of Pennsylvania Press, Philadelphia, p 80
- Ganio M, Boyen S, Fenn T, Vanhoutte S, Gimeno D, Degryse P (2012) Roman glass across the empire: an elemental and isotopic characterization. *J Anal Atom Spectrom* 27:743–753
- Lopez-Arce P, Garcia-Guinea J (2005) Weathering traces in ancient bricks from historic buildings. *Build Environ* 40:929–941
- Rapp GR (2002) *Archaeomineralogy*. Springer-Verlag, Berlin, p 326
- Römich H (1999) Historic glass and its interaction with the environment. In: Tennent NH (ed) *The conservation of glass and ceramics: research, practice, and training*. James and James, London, pp 5–14

---

# Stone Masonry Arch Bridges: In situ Testing and Stability Analyses by Using Numerical Methods; Examples from Hungary

88

Bögöly Gyula, Görög Péter, and Török Ákos

---

## Abstract

Maintenance and restoration is a common problem of historical stone structures. To control the stability and to verify the load-bearing capacity of these structures there are several modelling methods from the simple approximate calculations to the difficult numerical methods. Several Hungarian stone masonry arch bridges were investigated in the past few years. It was experienced that it is difficult to determine adequate input parameters for the numerical modelling from the in situ tests even for the simplest methods for instance trust line analysis and rigid block method. The modelling methods are able to describe the behaviour of the stone masonry arches but the results are depending on the quality of the input parameters, which are determined by the diagnostic tools. The analysis of these structures becomes more difficult since they are under protection for their historical value. The paper focuses on the most important in situ diagnostic methods of the stone masonry arch bridges according to different examples from Hungary. The investigated bridges have different stone materials (sandstone, andesite tuff) and different structures (single-span, multi-span). The applications and limitations of these diagnostic methods are also described. The paper also includes parametric analysis of the different input parameters of modelling such as the quality of the stone material (weathering, water content), strength of the blocks, shear strength between the blocks, quality of the joints. The aim of this research is to bring closer the numerical methods to the practice and develop the diagnostic methods to provide adequate information for the effective modelling.

---

## Keywords

Diagnostics • In situ tests • Stone masonry • Numerical methods

---

## 88.1 Introduction

Nowadays there are no new stone masonry arch bridge constructions, but the maintenance and restoration of the old ones represent a special challenge at the present time as well. There are more than 1,500 stone masonry arch bridges in Hungary which were built mostly in the 18th and 19th

century (Gálos and Vásárhelyi 2005). Since the condition of most of them increasingly deteriorates and the traffic with the related loads has increased significantly, thus their stability control and the verification of their load-bearing capacity became necessary in many cases. The main problem is to solve how their condition could be assessed simply and accurately enough in a way that it could be also applicable in practice. In order to find a solution several Hungarian stone masonry arch bridges with different types of structure and dimension stones were investigated in the past few years. The paper presents the experiences and results of these preliminary investigations.

---

B. Gyula (✉) · G. Péter · T. Ákos  
Budapest University of Technology and Economics, Műegyetem  
rkp. 3, Budapest 1111, Hungary  
e-mail: bogoly@gmail.com

## 88.2 Modelling

With the advancement of numerical modelling and due to the increased requirements in present time the conventional approximate calculations are not up to date anymore; therefore more specific methods were developed such as thrust line analysis, rigid-block method, finite element and discrete element method. These methods are capable of taking into account many different influential effects, thus the failure load can be calculated with great accuracy in theory. On the other hand in practice these modern methods are not applicable so easily. In these models several effects and attributes are taken into consideration by mechanical model parameters. These parameters can be measured often only with difficulty on existing structures, or it is difficult to characterize them with one factual value. Since the results are depending on the quality of the input parameters it is very important to know how precisely these parameters can be measured and how large is the effect of their deviations on the outcome.

### 88.2.1 Methods and Required Model Parameters

The Hungarian standard of masonry arch bridges defines three different levels of the investigations. It begins with approximate calculations like MEXE method. On the 2nd level it suggests a simple 2D modelling (thrust line analysis, rigid block method), and the top level of structural analysis advises more difficult 2D and 3D modelling (rigid block method, FEM, DEM) (Magyar Útügyi Társaság 2006). The expected accuracy of the analysis determines which method is suggested to be used. During the preliminary investigations the thrust line analysis was used with Archie-M, and the rigid block method was used with the program developed by the University of Sheffield, named Ring.

The Archie-M program can take into account multi-span bridges, masonry strength, masonry unit weight, mortar loss, and the angle of friction of the fill unit.

The Ring 3.0 program can identify the critical failure load factor and associated failure mechanism and distribution of internal forces. This allows the safety of the bridge to be assessed. The software can take into account multi-span bridges, compressive strength of the blocks, masonry unit weight, mortar loss, the angle of friction and cohesion of the fill unit, the favourable effect of passive pressure, angle of dispersion and a few damages. The bond between the blocks is taken into consideration by friction coefficients.

The more difficult 2D and 3D modelling (FEM, DEM) would require more specific and detailed parameters.

The traditional MEXE method is still widely used for assessing the carrying capacity of masonry arch bridges. For

this reason approximate calculations were carried out by the MEXE method to compare the results.

---

## 88.3 Determination of Input Parameters

### 88.3.1 In situ Tests

The parameters, which are necessary for the models, can be derived from site investigations and from laboratory tests. The site investigations include the inspections and recording of geometrical parameters, photo documentation. The most important parameters of the bridge or any arch and vault are the shape and the other geometrical details because these parameters are the ones that mainly determine how the loads will be dispersed by the influence of the backfill, and how the vault will bear the transmissive loads.

Lithotypes of the dimension stones also have to be observed on site and the differences between the strength of the blocks could be measured in situ by using Schmidt hammer (Fig. 88.1 left). It is a particularly suitable technique for the diagnostics of national monument structures to estimate the UCS of the rock materials when sampling is not an option. Many literature and research are concerned with this in situ technique (for example: Aydin and Basu 2005; Yasar and Erdogan 2004; Yilmaz and Sendir 2002; Kahraman 2001) because the correlation between the rebound value and the uniaxial compressive strength (UCS) is changing with the rock types (Zhang 2005). The rebound value is depending on more properties, for instance: weathering grade, dry density, porosity, grain size, moisture content and naturally the parameters of the Schmidt hammer (impact energy, plunger tip) (Aydin and Basu 2005). There are several contradictory suggestions about which type of the Schmidt hammer is recommended to be used. According to the International Society for Rock Mechanics (ISRM 1978) the L-type hammer, which has the lower impact energy, should be used for the hardness characterization of rocks between 20–150 MPa UCS. On the other hand some literatures say that the N-type hammer outperforms the L-type, because of the higher impact energy. The American Society for Testing and Materials (ASTM 2001) does not prefer a specific hammer type at all (Buyuksagis and Goktan 2007). Although both types of Schmidt hammers are capable for testing the surface hardness of the blocks, there is no widely used applicable formula or method to estimate the uniaxial compressive strength of stone materials from the rebound value of the Schmidt hammer test.

The moisture has a great influence on the UCS value (Vásárhelyi 2005) therefore moisture content also should be recorded on site (Fig. 88.1 right).

**Fig. 88.1** Schmidt hammer test (left), Moisture content measuring (right)



The condition of the mortar, the potential damages (missing blocks, cracks) have to be observed on site as well. If sampling is possible then core samples from the backfill and from the blocks should be taken for laboratory analysis.

Since in most cases these structures are under protection in situ non-destructive tests are the only way to get information for the modelling. Therefore it is very important to develop the diagnostic methods to provide adequate information for the effective modelling.

### 88.3.2 Laboratory Tests

Some petrophysical properties such as compressive strength, unit weight, angle of friction and cohesion of the backfill have to be identified under laboratory conditions. Usually stone masonry arches were built with different types of dimension stones, which make the structures inhomogeneous. If different levels of weathering are added this inhomogeneity is more significant. Therefore many times it is difficult to characterize the compressive strength of the blocks or the masonry strength with one factual value.

In the rigid block method the bond between the blocks is taken into account by friction coefficients. This value can not be measured in case of existing structure, but there are some literary suggestions from 1:1 scale laboratory model experiments whereby the friction coefficient could be derived (Melbourne and Gilbert 1995).

### 88.4 Sensitivity of Input Parameters

With the derived model parameters four bridges were analyzed and the failure loads were calculated by all the three methods. In order to see clearly the effects of each parameter

on the stability of the bridges, sensitivity analyses were made in case of the rigid-block method. In the sensitivity analyses the different input parameters were changed in the margin of error of their measurability. The results of the 70 runs show that the most significant parameters beyond the geometry are the compressive strength and the friction coefficient. The size of their effect depends on the failure mechanism. There are several different failure mechanisms: 4 hinges, 3 hinges with sliding, sliding only, and in case of multi-span bridges 7 hinges, 8 hinges mechanism. The span/rise rate of masonry arch bridges influences significantly the emergent failure mechanism. In case of lower rise arches (span/rise >4.0) generally 3 hinges mechanism emerges with sliding. In case of higher rise arches (span/rise <4.0) 4 hinges mechanism is expected. In case of lower rise arches with low fill depth (mostly below 1 meter) sliding mechanism could occur. In either of the mechanisms, where hinges occur, the friction coefficient *ceteris paribus* could bring down the failure load with ~15 %, the compressive strength could change ~5 % in either direction and the uncertainty of all parameters (friction coefficient, UCS, masonry and fill unit weight, the angle of friction and cohesion of the fill unit) could affect the outcome with ~20 %. In case of sliding, only the deviation of the friction coefficient between the blocks could change the failure load with even ~40 % and the effect of all the other parameters separately are neglectable.

### 88.5 Conclusions

The performed sensitivity analyses on stone masonry arches show that the calculated failure load is highly influenced by the accuracy of some input parameters. The difference of the outcome (~20 or 40 %) seems quite large but in most cases

these bridges have more than enough backup thus the acceptance of their stability are not queried. But these results clarify that the estimation of the friction coefficient would require further examinations. In case of lower rise arches with low fill depth, when sliding only failure mechanism emerges, the effect of the friction coefficient is especially important. Without more accurate values the modelling could be replaceable with simpler and faster approximate calculations, for instance the MEXE method. It is noticeable that the MEXE method assesses the results quite well in case of multi-span bridges with short pier as well. In fact it overestimates the carrying capacity of short span bridges.

The results show that the emergent failure mechanism could affect significantly the rate of the influence of the parameters. Therefore it is suggested to pay attention to the accuracy of these parameters depending on the failure mechanism.

Since in most cases stone masonry arches are under protection in situ non-destructive test are the only way to get information for the modelling. Still there is no widely used applicable formula or method which could estimate the uniaxial compressive strength of stone materials from the rebound value of the Schmidt hammer test. Therefore it is very important to develop the diagnostic methods and standards to provide adequate information for the effective modelling.

## References

- ASTM (2001) Standard test method for determination of rock hardness by rebound hammer method. ASTM Stand. 04.09 (D 5873-00)
- Aydin A, Basu A (2005) The Schmidt hammer in rock material characterization. *Eng Geol* 81:1–14
- Buyuksagis IS, Goktan RM (2007) The effect of Schmidt hammer type on uniaxial compressive strength prediction of rock. *Int J Rock Mech Min Sci* 44:299–307
- Gálos M, Vásárhelyi B (2005) Közúti boltozott kőhidaink, *Kő*, VII., pp 21–25
- ISRM (1978) Suggested methods for determining hardness and abrasiveness of rocks. *Int J Rock Mech Min Sci Geomech Abstr* 15:89–97
- Kahraman S (2001) Evaluation of simple methods for assessing the uniaxial compressive strength of rock. *Int J Rock Mech Min Sci* 38:981–994
- Magyar Útügyi Társaság (2006) Útügyi Műszaki Előírás 813/2005, pp 61–108
- Melbourne C, Gilbert M (1995) The behaviour of multiring brickwork arch bridges. *Struct Eng* 73:39–47
- Vásárhelyi B (2005) Statistical analysis of the influence of water content on the strength of Miocene limestone. *Rock Mech Rock Eng* 38(1):69–76
- Yasar E, Erdogan Y (2004) Estimation of rock physiomechanical properties using hardness methods. *Eng Geol* 71:281–288
- Yilmaz I, Sendir H (2002) Correlation of Schmidt hardness with unconfined compressive strength and young's modulus in gypsum from Sivas (Turkey). *Eng Geol* 66:211–219
- Zhang L (2005) Engineering properties of rocks. In: Elsevier geo-engineering book series, vol 4. Elsevier, Berlin, pp 180

---

# Quantitative Analysis of Salt Crystallization–Dissolution Processes on Rock-Cut Monuments in Petra/Jordan

89

Kurt Heinrichs and Rafiq Azzam

---

## Abstract

Salt weathering represents a major cause of damage on stone monuments worldwide. However, processes of salt weathering still cannot be explained satisfactorily. Further systematic investigation of stone monuments is required for the improvement of knowledge on active salt weathering processes and controlling factors. Assessment of the dynamics of salt crystallization–dissolution processes is a focus of modern salt weathering research. The overall aim of the ‘petraSalt’ research project are real-time/real-scale weathering models that depict characteristic interdependencies between stone properties, monument exposure regimes, environmental influences, salt loading, salt crystallization–dissolution behaviour and salt weathering damage. The rock-cut monuments of ancient Petra in Jordan were selected for studies. A main part of the project is the joint evaluation of salt load and environmental conditions acting on it, allowing a differentiated, depth-dependent quantification of the complex salt crystallization–dissolution processes, considering diurnal and seasonal variation. The approach is exemplified.

---

## Keywords

Stone monuments • Salt weathering • Wireless sensor network • Environmental monitoring • Salt crystallization models

---

## 89.1 The City of Petra and Salt Weathering Damage

The ancient city of Petra is located in a mountainous region of Southwest Jordan. In Petra many hundred monuments like tombs, sanctuaries and places of worship were carved by the Nabataeans from sedimentary bedrocks (mainly sandstones of Cambrian to Ordovician age) about 2,000 years ago. In 1985 UNESCO inscribed Petra on the list of World Heritage. All rock-cut monuments have suffered damage

from weathering, partly of alarming extent. Results of a previous research project (1996–1999) had revealed salt weathering as major cause of damage (e.g., Heinrichs 2008). This was the reason for focusing the ‘petraSalt’ project on this significant weathering process. Considering the huge masses of rock removed for monument creation, unweathered condition of the monuments can be assumed for their initial phase of exposure. Thus, active salt weathering processes can be limited to a period of about 2,000 years (Heinrichs and Nguyen 2011).

---

K. Heinrichs (✉) · R. Azzam  
Department of Engineering Geology and Hydrogeology,  
RWTH Aachen University, Aachen, Germany  
e-mail: heinrichs@lih.rwth-aachen.de

R. Azzam  
e-mail: azzam@lih.rwth-aachen.de

---

## 89.2 Environmental Monitoring

An autonomously operating wireless sensor network was applied in Petra as an innovative technology for high-resolution monitoring of environmental conditions affecting the monuments and acting as driving forces for salt weathering

processes (Heinrichs et al. 2012). The system was developed in cooperation with TTI GmbH—TGU Smartmote (Stuttgart, Germany). The system consists of sensor nodes and gateways. The sensor nodes comprise processor board, radio module, long-life batteries, sensors for the measurement of temperature, relative humidity and electrical impedance in various depths (1, 3, 6, 9, 13 and 18 cm) inside the stone and sensors for the measurement of temperature, relative humidity, stone surface temperature, wind, rain and light at the stone surface. The sensor nodes were programmed to collect data every 5 min. They sent the collected data to gateways in Petra, equipped with solar energy supply units. The gateways relayed the measurement data to a long-distance network (GSM) for remote access per internet. The sensor network collected data from September 2012 to June 2013. In this way, the sensor system provided an extraordinary information output regarding environmental conditions at the Petra monuments considering diurnal, seasonal and depth-dependent variation. The data were exported from the database on daily basis for further evaluation.

### 89.3 Case Study

The presented case study was chosen for reasons of rather high salt load and salt load to great depth. The investigation area was located at the right side of the ‘Silk Tomb’ (Monument No. 770). The case study refers to sensor node 770-10. It was installed in a height of 3.36 m above ground level. The stone surface steeply inclines to the north (direction of inclination: 10°, angle of inclination: 88°). The stone surface is mainly shadowed (effect of insolation rather low). The sensor node was positioned at the margin of a water run-off path, showing granular disintegration as weathering form. The case study concerns a grey-red variety of the multicoloured, matrix-rich, fine-grained sandstone of the Cambrian Umm Ishrin Sandstone Formation (middle part). Considering certain gaps in the series of climate data, mainly due to disturbances of the GSM network in Petra, complete sets of climate data were available for 208 days comprising 306,000 temperature and humidity data in total.

### 89.4 Salt Analysis and Salt Crystallization Models

Drill cores obtained from dry drilling in the course of the sensor network installation were taken for ionic analysis of soluble salts. The quantitative analysis of salt crystallization–dissolution processes requires knowledge about the salt crystallization behaviour under changing temperature and humidity conditions. The crystallization behaviour of mixed salt systems is rather complex and, thus, prediction not easy.

However, there has been considerable progress in the use of salt crystallization models such as ECOS-RUNSALT—used here—which allows prediction of the crystallization pathways and phase transitions even for complex salt mixtures (Steiger and Heritage 2012). RUNSALT serves as user interface to the ECOS program “Environmental Control of Salt Damage—thermodynamic model for the prediction of the crystallization behaviour of salt mixtures under changing climate conditions” (Bionda 2002–2005; Price 2000). Following ions are included in the ECOS-RUNSALT model parameterization:  $\text{Na}^+$ ,  $\text{K}^+$ ,  $\text{Mg}^{2+}$ ,  $\text{Ca}^{2+}$ ,  $\text{Cl}^-$ ,  $\text{NO}_3^-$  and  $\text{SO}_4^{2-}$ . These ions represent the typical constituents of salt mixtures found at the Petra monuments. The drill cores were analyzed segment-wise (0–0.5 cm, 0.5–1.5 cm, 1.5–2.5 cm, ... 17.5–18.5 cm). Application of the ECOS-RUNSALT program requires that the sum of the cation and anion charges is equal (Steiger and Heritage 2012). Thus, a charge balance has to be made first. In the samples of the case study a systematic cation excess was found. Besides salt minerals, calcite characteristically occurs in the Petra rocks as further secondary mineral. From experience it is known, that a certain fraction of calcite is mobilized by the eluting procedure as dissolved  $\text{Ca}^{2+}$  and  $\text{HCO}_3^-$  ions despite the low solubility of calcite. Therefore, the charge balance can be equalized by corresponding reduction of the  $\text{Ca}^{2+}$  content. The real content of calcite was determined by testing with hydrochloric acid. The corrected weight fractions of the ions were related to one kilogram salt-free and calcite-free stone material. These weight fractions represented the input data for the ECOS-RUNSALT program. Soluble salt was found in the drill core segments from 0 to 15.5 cm. With respect to weight fractions of ions, highest concentration of soluble salt occurs in the outermost part of the drill core (0–3.5 cm).  $\text{Na}^+$  is the prevailing cation in the outermost 4.5 cm, followed by  $\text{Ca}^{2+}$ . Further to depth,  $\text{Ca}^{2+}$  and  $\text{Mg}^{2+}$  become prevalent.  $\text{Cl}^-$  is the predominant anion all over the profile, followed by  $\text{NO}_3^-$  and  $\text{SO}_4^{2-}$ . The ECOS-RUNSALT cannot predict the crystallization behaviour in case of very complex salt solutions containing  $\text{Ca}^{2+}$  and  $\text{SO}_4^{2-}$  at the same time, like found in all segments of drill core 770-10. In this case the program asks for removal/reduction of  $\text{SO}_4^{2-}$  and  $\text{Ca}^{2+}$  fractions that may form gypsum. Although gypsum is a major salt in many stone monuments, also in the Petra rock-cut monuments, its removal from the system does not mean a great problem, because gypsum is considered as very inactive with respect to climate fluctuations due to its very low solubility (Steiger and Heritage 2012). Nevertheless, the concentration of gypsum was calculated separately from those portions of  $\text{Ca}^{2+}$  and  $\text{SO}_4^{2-}$  removed from the input data.

The ECOS-RUNSALT program offers the calculation of the salt crystallization behavior for range of temperature between  $-30$  and  $50$  °C and relative humidity between 15 and 98 %. Volume of crystallized salt was selected as mode of evaluation. Regarding the case study, the program

predicted halite (NaCl), sylvite (KCl), calcium nitrate ( $\text{Ca}(\text{NO}_3)_2$ ), niter ( $\text{KNO}_3$ ), carnallite ( $\text{KClMgCl}_3 \cdot 6 \text{H}_2\text{O}$ ) and nitrocalcite ( $\text{Ca}(\text{NO}_3)_2 \cdot 4 \text{H}_2\text{O}$ ) as potential salt phases. Due to too low salt concentration, only halite was confirmed by X-ray diffraction analysis. However, previous X-ray diffraction analysis of surface samples had identified sylvite, calcium nitrate, carnallite, nitrocalcite, niter and gypsum as potential salt phases. Based on export and evaluation of data obtained from systematic query, salt crystallization models were derived individually for all drill core segments displaying salt phase formation for the overall ranges of temperature and relative humidity. It is well known that the deliquescence relative humidity of a single salt can be considerably reduced by the influence of other salt phases. This was also found here. In case of complete salt crystallization, halite, carnallite, calcium nitrate and gypsum occur in all segments of the drill core, sylvite up to a depth of 5.5 cm, niter only down to 1.5 cm. The salt profile is clearly dominated by chloride salts. Halite represents the prevalent salt phase in the outermost segments, carnallite dominates further to depth. Highest volumes of salt (6–8  $\text{cm}^3/\text{kg}$  stone) are found in the outermost 3.5 cm of the drill core. Here the volume of completely crystallized salt corresponds to a degree of pore filling between 7 and 11 % (comparably low).

### 89.5 Merging of Salt Crystallization Models and Climate Data

The approach aimed at quantification of salt crystallization–dissolution processes over depth analogue to the segmentation of the drill core. This necessitated interpolation of climate data for certain depths. A program for such interpolation was developed. Furthermore, the approach was tailored to identification of salt crystallization–dissolution processes by number and intensity, considering total salt as well as individual salt phases. With respect to intensity, a subdivision of six levels according to volume-% of crystallized salt was made for total salt (0 %/salt completely dissolved, 0–25, 25–50, 50–75, 75–100, 100 %/salt completely crystallized). For the individual salt phases a similar subdivision was made. Corresponding limit values were determined for all drill core segments from the ECOS-RUNSALT data. Trend curves of high approximation and related mathematical functions were ascertained for the resulting graphs of the limit values over total range of temperature and relative humidity. On daily basis, climate data were entered in these crystallization models. By use of “If, then...else” functions for each data pair temperature/relative humidity of 1 day the corresponding level of crystallization was determined by the evaluation program. In this way, the distribution of salt crystallization levels over depth was assessed by day for total salt and single salt phases. For more detailed assessment of salt

crystallization–dissolution processes, the evaluation scheme was programmed to determine the salt crystallization levels at the beginning and the end of the day as well as minimum and maximum crystallization level. Considering these four parameters, each with six possibilities in case of total salt (6 levels of crystallization), this would mean 1,296 possible constellations regarding salt crystallization–dissolution processes. After removal of non-realistic cases (e.g., “minimum” cannot be higher than “start” or “end”), 196 cases remained regarding total salt. Aiming at clear presentability of results, these were summarized into 36 cases, considering three criteria: particular crystallization levels and total number of crystallization levels passed through, relation between crystallization and dissolution. Corresponding classifications were elaborated for the single salt phases. The evaluation scheme was programmed to identify the corresponding crystallization–dissolution cases by use of “If, then...else” mathematical functions applying to the combination of the parameters “start”, “end”, “minimum” and “maximum”.

### 89.6 Results, Discussion and Outlook

Salt crystallization–dissolution processes in the measuring period were found to be limited to the outer 8.5 cm of the profile 770-10. Further to depth, salt (except gypsum) was always completely dissolved. In the whole measuring period gypsum was crystallized all over depth. Crystallization–dissolution processes concerned halite, sylvite, niter, carnallite and calcium nitrate. Nitrocalcite never crystallized. Maximum depth of salt crystallization–dissolution processes decreased from later summer (September–November 2012) to minimum in winter (December 2012–February 2013). It increased again in early summer (March–May 2013) and further in high summer (only data from June 2013 available). Maximum depth of salt crystallization–dissolution processes was reached in high summer. With respect to total salt (except gypsum), 26 of the 36 potential cases of salt crystallization–dissolution processes occurred. The outer 4.5 cm of the depth profile (zone of highest salt loading) were affected by crystallization–dissolution processes almost every day! Frequency of crystallization–dissolution processes significantly decreased further to depth. Highest intensity (here: range of crystallization–dissolution processes over five levels of crystallization) was found in the outermost segment of the depth profile, however, only on few days. Crystallization–dissolution over 3–4 crystallization levels occurred frequently in the front 2.5 cm of the depth profile. Further to depth, intensity of crystallization–dissolution processes decreased. Complete salt crystallization was reached only in the front 3.5 cm of the profile. In the front 1.5 cm complete salt crystallization was reached on more than 100 days, most frequently in early and high summer.

Complete salt dissolution was reached rarely in the front 4.5 cm of the profile. Further to depth, frequency of days reaching complete dissolution increased considerably. Further evaluation addressed the identification of active salt phases.

Halite was found as main active salt phase, followed by sylvite, niter, carnallite and calcium nitrate. This concerns likewise frequency and depth of crystallization–dissolution processes. Only in the front 1.5 cm of the profile, the five salt phases were found as jointly active to high extent. The results indicate maximum stress due to salt crystallization processes in the outermost part of the depth profile, being such high to find expression in granular disintegration at the stone surface. This weathering behaviour must be considered as the cumulative result of almost daily crystallization–dissolution processes all over the year, although the results indicate early and high summer as seasons of maximum stress.

An evaluation strategy was worked out, focused on well-directed merging of climate data with data on salt loading. Meaningful quantitative information on salt crystallization–dissolution processes was obtained. The new approach to quantitative analysis of salt crystallization–dissolution processes is transferred to the further case studies included in the “petraSalt” project, thus considering different stone types, monument exposure scenarios, climate regimes and salt load. These results in all are expected to allow reliable

rating and interpretation of aggressiveness and damage potential of salt weathering regimes considering their variability.

---

## References

- Bionda D (2002–2005) RUNSALT computer program. Online available at: <http://science.sdf-eu.org/runsalt/>
- Heinrichs K (2008) Diagnosis of weathering damage on rock-cut monuments in Petra/Jordan. *Environ Geol* 56(3): 643–675 (special issue: Monument future: climate change, air pollution, decay and conservation—the Wolf-Dieter-Grimm volume)
- Heinrichs K, Azzam R, Krüger M (2012) The use of a wireless sensor network for high-resolution environmental monitoring of stone monuments in context with investigation of salt weathering—exemplified for rock-cut monuments in Petra/Jordan. In: *Proceedings of the 12th International Congress on the Deterioration and Conservation of Stone*, October 22–26, 2012, New York, USA (in press)
- Heinrichs K, Nguyen HT (2011) 3D terrestrial laser scanning of rock-cut monuments in Petra/Jordan. *Mitt. Ing.-u. Hydrogeol Lehrstuhl für Ingenieurgeologie und Hydrogeologie, RWTH Aachen* 104:27–37
- Price C (2000) An expert chemical model for determining the environmental conditions needed to prevent salt damage in porous materials. *Protection and Conservation of the European Cultural Heritage*, Research report No. 11, Archetype, London
- Steiger M, Heritage A (2012) Modelling the crystallization behaviour of mixed salt systems: input data requirements. In: *Proceedings of the 12th International Congress on the Deterioration and Conservation of Stone*, October 22–26, 2012, New York, USA (in press)

Maria Heloisa Barros de Oliveira Frascá, Fabiano Cabañas Navarro,  
and Eduardo Brandau Quitete

---

**Abstract**

Although building stones used in historic and modern buildings and monuments may have unlimited durability if adequate conservation methods are applied, the great diversity of their nature often impairs the choice of the most suitable maintenance or cleaning procedures. Aiming at to contribute to the improvement of stone conservation, this paper presents a laboratory simulation for the anticipation of possible alterations in the stone surface when in contact to chemical reagents typically used in cleaning products, both domestic and professional, as ammonium chloride, sodium hypochlorite, hydrochloric acid and potassium hydroxide. Tests indicated that hydrochloric acid was the most aggressive among the selected substances, usually causing intensive discoloration or bleaching of the selected granitic rocks (granites, charnockites etc.). In white granite, specifically a garnet granitic gneiss, the effect was a red-orange staining, rust-like. Thus, the results also reinforced the great susceptibility of the Fe element to chemical attack. Finally, it is emphasized the recommendation to preceded by tests any application of cleaning products, to ensure physical and aesthetics stone preservation.

---

**Keywords**

Building stones • Alteration • Cleaning • Granite • Microscopic investigation

---

**90.1 Introduction**

The weathering of stones begins as soon as they get in contact with atmospheric conditions on the Earth's surface. This process continues once used as building or monumental stones, when they may be subject to additional weathering agents such as pollution, climate aggressiveness (coastal or desert environments) and, also, lack of or poor maintenance.

Furthermore, the large diversity of the stones used in historic and modern buildings and monuments become very difficult the anticipation of possible alterations due to the action of industrial cleaning products (acidic or alkaline). Regarding silicate rocks, more specifically granites, this difficult is increased by the wide range of mineralogical constituents as well grain size, microcracking degree and secondary alteration and weathering.

The harmfulness of inadequate cleaning procedures is largely reported in the literature. The frequent cleaning of black soiling, which is the darkening of exposed surfaces by the accumulation of particulate matter (Grossi et al. 2003), generally cause physical changes to the surface of the objects (Koller 2000).

In the 1970s and 1980s, the removing of soiling from sandstone and granite façades in Scotland by inappropriate cleaning methods, as strong acids and alkalis, caused bleaching, staining and roughening in granites (Young et al. 2003). And, in spite of the damage caused at the time of cleaning is

---

M.H.B.d.O. Frascá (✉)

MHB Geological Services, São Paulo, SP, Brazil  
e-mail: mheloisa2@yahoo.com.br

F.C. Navarro

UNIFAL—Federal University of Alfenas - Campus Poços  
de Caldas, Poços de Caldas, MG, Brazil

E.B. Quitete

IPT—Institute for Technological Research, São Paulo, SP, Brazil

**Table 90.1** Chemical reagents, concentrations and time of contact

Solutions	Time (h)
Ammonium chloride—100 g/L	24
Sodium hypochlorite—20 g/L <sup>a</sup>	24
Hydrochloric acid—3 % (v/v) (parts by volume)	96
Hydrochloric acid—18 % (v/v) (parts by volume)	96
Potassium hydroxide—100 g/L	96
Potassium hydroxide—30 g/L	96

<sup>a</sup> Prepared from technical grade sodium hypochlorite (13 % active chlorine)

likely to be only superficial, aesthetical, the authors considered that the absence of definitive evidence does not exclude the possibility that increased rates of decay are one of the potential side-effects of cleaning.

Thus, aiming to contribute to granite conservation, it was carried out the simulation of chemical attack by selected reagents in some granitic rock material focusing on the observation of possible visual and mineralogical changes.

## 90.2 Test Method

The proposed method is based on a Brazilian standard test (ABNT 1997) which intends to check the alterability of ceramic tiles by common chemical reagents used for cleaning. Some adjustments were made, particularly in the examination method and results evaluation.

As the most usual chemical reagents used in cleaning products potentially harmful to stone there were selected: ammonium hydroxide, sodium hypochlorite, hydrochloric acid and potassium hydroxide. Solution concentrations and time of contact with the stone surface are given in Table 90.1.

The test procedure is briefly described as follows:

- Test specimen, measuring about 15 cm × 15 cm, is prepared from polished slabs, preferably;
- A PVC ring or square (~10.0 cm internal diameter or edges and 2 cm height) is adhered in the stone surface by silicon based resin;

(c) About 0.5 cm height of solution (Table 90.1) is placed inside the PVC and left by predetermined time;

(d) At the end of the test, the PVC is removed and the stone surface is washed in tap water.

Visual changes are then evaluated according to four grades: G1—no visual modification; G2—slight colour modification; G3—moderate colour modification; G4—intense colour modification. The new visible colour or tone should be mentioned, e.g. intense discoloration, moderate yellowing etc., as well as the occurrence of mineral disaggregation.

It is important the inspection of test specimens being made by at least two trained technicians, in order to minimize the subjectivity of colour evaluation.

## 90.3 Materials and Experimental Results

Tests were carried out in Brazilian granitic rocks selected on basis of colour—and related mineralogical content—, textural and structural features (Figs. 90.1, 90.2 and 90.3).

The main responsible for the visually observed changes was the hydrochloric acid, which promoted variable staining patterns and intensities, ranging from discoloration (bleaching) to yellowing (Figs. 90.1, 90.2 and 90.3).

A petrographic examination, comprising optical and electronic microscopy and associated EDS, was carried out to investigate the modifications.

### 90.3.1 Bleaching

The petrographic observation indicated the partial discoloration of biotite crystals, now showing alternated brown and light beige layers (Fig. 90.4a). In a selected biotite crystal submitted to EDS determination (Fig. 90.4b), the brown layer exhibited higher Fe content when compared to the beige layer (Fig. 90.4c, d).

Such results suggest that the physicochemical conditions given by the acidic attack allowed the leaching of some iron present in biotite, and possible in other ferromagnesian minerals, resulting in the discoloration of the stone.

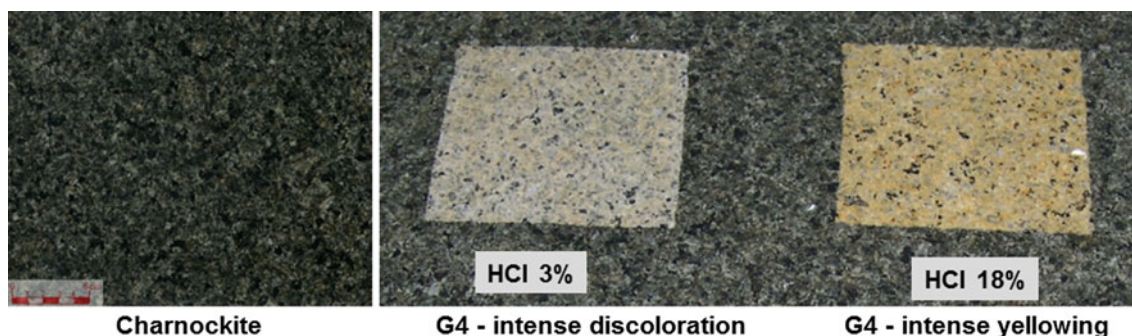


**Fig. 90.1** Charnockite before (*left*) and after (*centre and right*) chemical attack

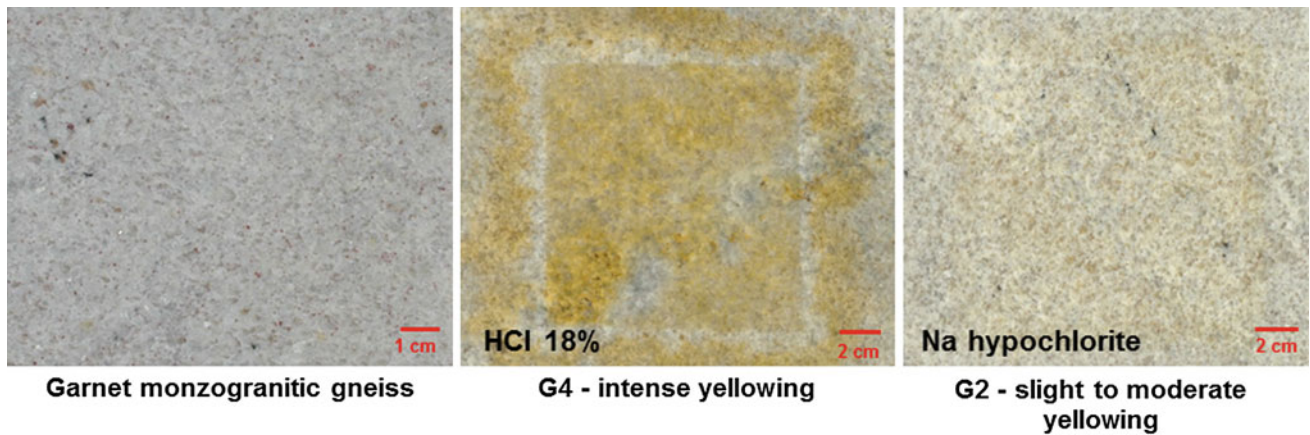


**Fig. 90.2** White-colour gneiss before (*left*) and after (*centre and right*) chemical attack

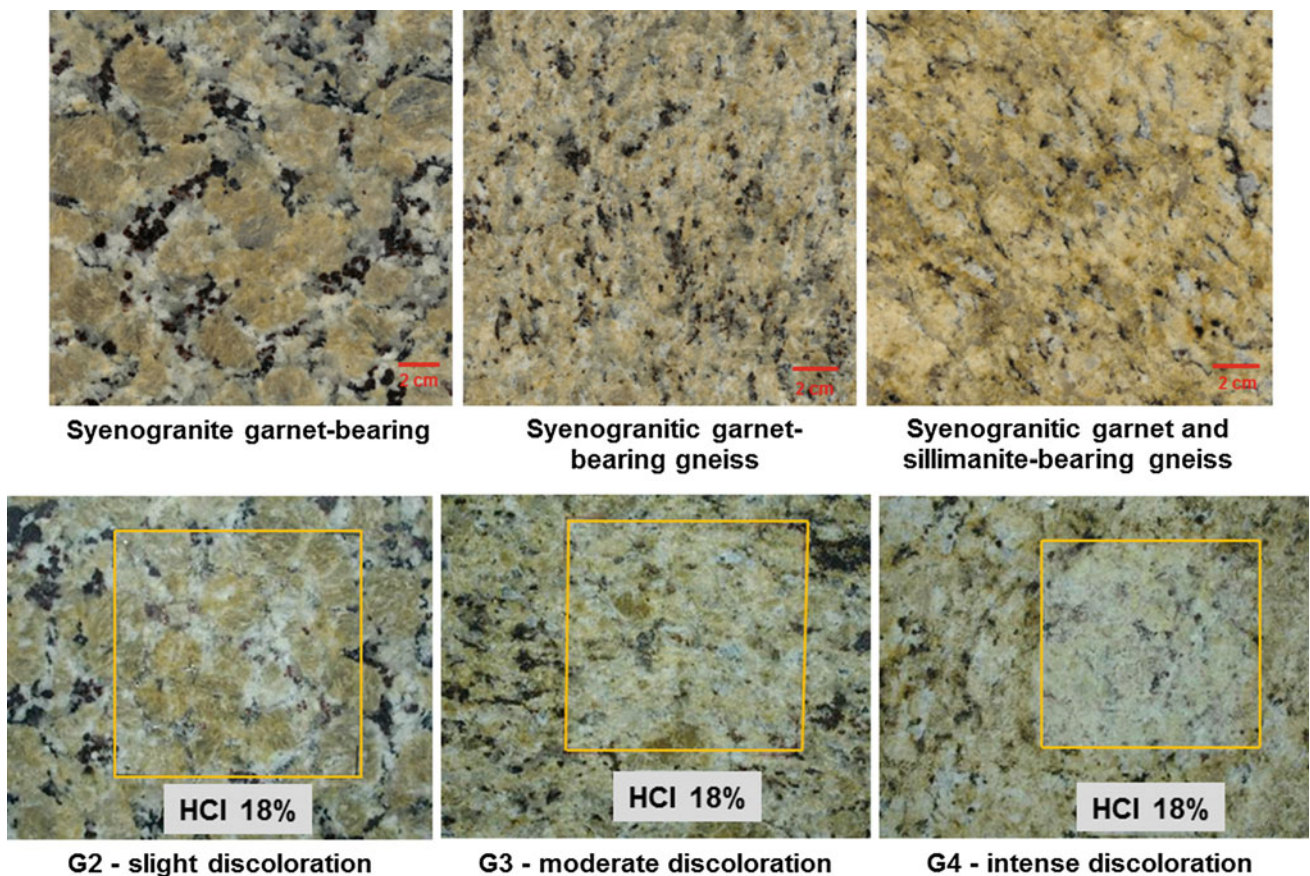


**Fig. 90.3** Yellow-colour gneisses before (*first row*) and after (*second row*) chemical attack

### 90.3.2 Yellowing

The microscopic investigation of white-colour granite, in which the acidic effect was an orange-red stain, like rust, showed an intense impregnation of fractures and cleavages by iron hydroxides, mainly in feldspars (Fig. 90.5), probably remobilized from pre-existing Fe-rich mineral oxidized after chemical attack.

### 90.4 Final Remarks

The proposed simulation demonstrated the significant susceptibility of silicate rocks to physicochemical variations that in this case was the pH conditions. The hydrochloric acid showed to be the most aggressive chemical reagent in the selected granitic rocks tested, causing discoloration or bleaching of green and yellow stones, and yellowing of white stone.

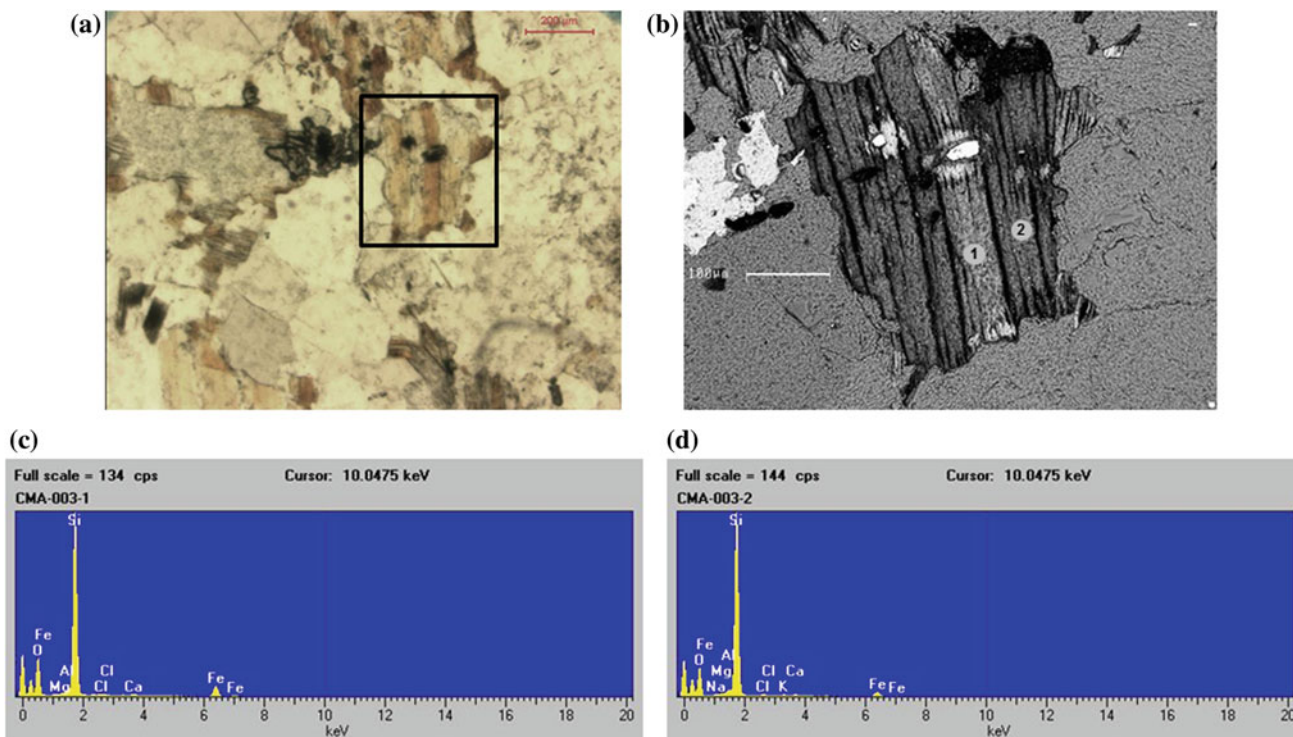


**Fig. 90.4** Biotite showing alternated brown and light beige layers under polarized (a) and electronic microscopes (b). EDS results for point 1 (brown layer), in (c), exhibiting higher Fe content than point 2 (beige layer), in (d)

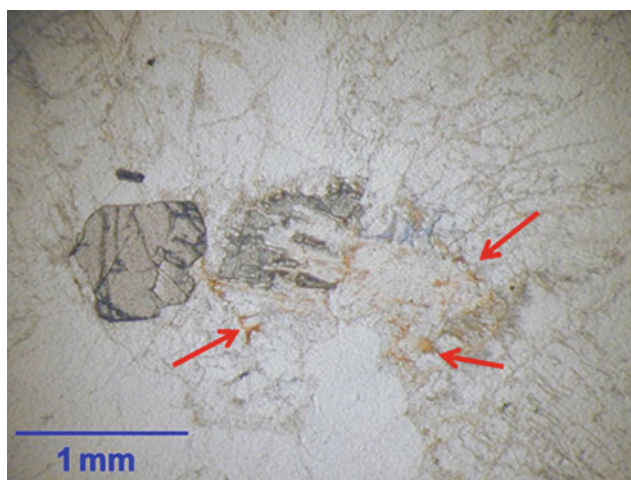


**Fig. 90.5** Iron hydroxides (pointed by arrows) in fractures and cleavages of feldspars

The results also reinforce the great susceptibility of the Fe element to acidic attack, in concordance to Winkler (1966), to whom the weathering rates of ferrous-ferric oxides and hydrates as well as of ferrous-ferric silicate minerals may approach the corrosion rates of iron.

Thus, the unpredictable answer of any rock type, due to the already mentioned large diversity of mineralogical content, strongly recommend to precede any cleaning by experimental investigations to ensure the proper physical and aesthetic conservation of the stone.

In addition, the proposed method is preliminary and restricted to the rock *in natura*. Further investigation should include the role of the several currently used stone treatments (water repellency, consolidation etc.) in the effective protection of the stone from chemical attack or even from the environmental aggressiveness.

## References

- ABNT (1997) Brazilian Association of Technical Standards. NBR 13° 818/97: ceramic tiles—specification and test methods. ABNT: Rio de Janeiro, p 78 (in Portuguese)
- Grossi CM, Esbert RM, Díaz-Pache F, Alonso FJ (2003) Soiling of building stones in urban environments. *Build Environ* 38:147–159
- Koller M (2000) Surface cleaning and conservation. *The Getty Conservation Institute Newsletter* 15(3):5–9
- Winkler EM (1966) Important agents of weathering for building and monumental stone. *Eng Geol* 1(5):381–400
- Young ME, Urquhart DCM, Lainga RA (2003) Maintenance and repair issues for stone cleaned sandstone and granite building façades. *Build Environ* 38:1125–1131

Harith E. Ali, Suhail A. Khattab, and Muzahim Al-Mukhtar

## Abstract

This study concerns the decay of a historical site Al-Namrud in the north of Iraq developed in the second millennium B.C. by the Assyrian Empire under the effect of bird droppings (BD) factor. The building stone (limestone) shows sever signs of damage. In order to analyse the bird droppings weathering effects, a number of complementary multi-scale characterization methods were carried out on the tested limestone. Results show great changes in the in situ altered stone compared with the fresh one: higher porosity and different pore size distribution, water transfer parameters (capillarity and water uptake) increase, bulk and skeletal densities decrease. Preliminary data confirm that applied accelerated weathering test induce changes approximately similar in the fresh to those observed in the in situ altered stones. The weathering by bird droppings seems to be an active factor of the structural, textural changes and deterioration in some of stones in the Al-Namrud monuments.

## Keywords

Historical monuments • Multi-scales characterization • Accelerated aging tests • Bird droppings weathering

## 91.1 Introduction

In situ observations concerning the state of the degradation of the building structure and stones of the city Calah—Al-Namrud shows sever signs of damaged in the Monuments. Al-Namrud, developed by Assyrian Empire in the second millennium B.C. located 37 km to the eastern south of Mosul city—in the north of Iraq. A number of stones samples are degraded due to time and weathering factors. This study is a part of a research work concerning weathering factors,

weathering processes and stone deterioration of the monuments in the city. In fact, some parts of the city are invaded by birds (or birds found refuge in some area of the monument) and stones are highly degraded. In this paper, weathering due to bird degradation is studied. In situ altered stones refer to samples highly affected by bird droppings factor collected from the monument site and analyzed. Fresh stones refer to samples collected from the quarry used in the construction of the monument from Eski-Mosul area.

The biological effect on the stone structure is representing by the bacteria activity through its initiating or augmenting of chemicals production that can attack stone directly. This activity is summarized as the oxidization of sulphur or one of its compounds in the stone components, forming sulphuric acid, which in turn attacks stone structure directly (Ashurst and Dimes 1998, Dahlin 2000 and Petushkova et al. 2007). However, damage is unquestionably done by the roosting and nesting of birds on stone. This decay is caused mainly by the accumulation of their droppings and nesting materials which breaks down as a result of bacterial

---

H.E. Ali  
Building and Construction Engineering Department,  
Technical College, Mosul, Iraq

S.A. Khattab  
College of Engineering - Mosul University, Mosul, Iraq

M. Al-Mukhtar (✉)  
CRMD, University of Orleans—CNRS, Orleans, France  
e-mail: Muzahim.al-mukhtar@univ-orleans.fr

action and releases acids, which in turn attack limestone stone (Ashurst and Dimes 1998).

Accelerated weathering tests were widely used in the laboratory to identify different mechanisms of decay of the stones. Immersion tests, wetting-drying cycles with distilled water or with solutions containing sodium sulphate or sodium chloride were mainly carried out to evaluate physicochemical and mechanical changes in the tested stones (Goudie 1999, Benavente et al. 2001, Van et al. 2007, Angeli et al. 2007, Beck and Al-Mukhtar 2010). In this paper accelerated immersion tests with bird dropping were carried out: the fresh limestone were immersed in a solution of air dry fine bird droppings (BD) powder and distilled water for a period of 48 days. Results of this biological weathering were analysed and compared with the characterization data of in situ altered and fresh limestone.

---

## 91.2 Experimental Program

### 91.2.1 Aging Test: Bird Droppings Weathering Test

A completely dry fresh limestone samples (105 °C for 24 h) of size ( $5 \times 5 \times 5 \text{ cm}^3$ ) have been immersed in a solutions of bird droppings. These solutions are prepared in distilled water with 10 and 20 % of bird dropping powder fully passing sieve N0.100 and about 0.5 % passing sieve N0.200. 100 samples were immersed for a period 48 days for each percentage of BD, and a daily measuring of wet and dry weights has been carried out.

Two samples for both wet and then dry weights were carried out for each measurement. Dry measurement process start with drying samples at 50 °C for 48 h., and then washed carefully to remove the bird droppings effect in order to follow the changing in the porosity and the water transfer properties in the altered stone. The process of washing was conducted by the immersion of the treated samples in distilled water and by changing of water every 1 h for about 24 h. Finally the samples dry at 50 °C for 48 h.

### 91.2.2 Characterization Methods

A multi-scale characterization is conducted on the tested samples in order to identify stone properties and deterioration effects and processes.

#### 91.2.2.1 Mineralogical Characterization: X-ray Diffraction (XRD) and Thermogravimetric Analysis (TGA)

X-ray diffraction patterns were obtained on powders of stone using Philips Apparatus with the  $K\alpha$  line of copper ( $\lambda_{Cu} = 1.5406 \text{ \AA}$ ) with  $2\theta$  from 1.5 to 60°. In order to

compare the obtained patterns, the main quartz reflection is used to scale the X-ray patterns intensities for all tested samples. In TGA test, the mass loss of a given sample is recorded under controlled temperature ramp. The apparatus used is a Setaram TG-DTG 92-16 electro-balance operating within the 20–1000 °C range, with a heating rate of 100 °C per hour and under argon atmosphere.

#### 91.2.2.2 Porosity and Pore Size Distribution Tests

Bulk density at dry state is determined by hydrostatic weighing method which is based on the Archimede's principle on a sample saturated and submerged in a wetting fluid as water (Beck et al. 2003). The mercury intrusion method was performed by applying pressure (up to 210 MPa) and monitoring continuously the intruded volume of mercury in the pores of the tested sample. The radii of pores were estimated using Young-Laplace equation. Theoretically, pores with a diameter between 350  $\mu\text{m}$  and 4 nm can be investigated with the apparatus used: a Poresizer 9320 porosimeter. Samples of about  $1 \text{ cm}^3$  were dried at 50 °C during 48 h and then tested.

#### 91.2.2.3 Water Transfer Properties

To determine capillary and water uptake coefficients, tests were performed on cylindrical samples (diameter: 50 mm/ height: 120 mm) placed in a sealed space on a fine plastic railing submerged in water. Samples were weighed after wiping the base with a wet rag and the height of the capillary front measured with a calliper at regular intervals. The average value of the capillary coefficient is calculated using three measurements of the height of the capillary front located on different zones on the sample to avoid the risk of local non-homogeneous pore structure (Beck et al. 2003).

---

## 91.3 Results and Analysis

### 91.3.1 Characterization of the Historical and Fresh Limestone Samples

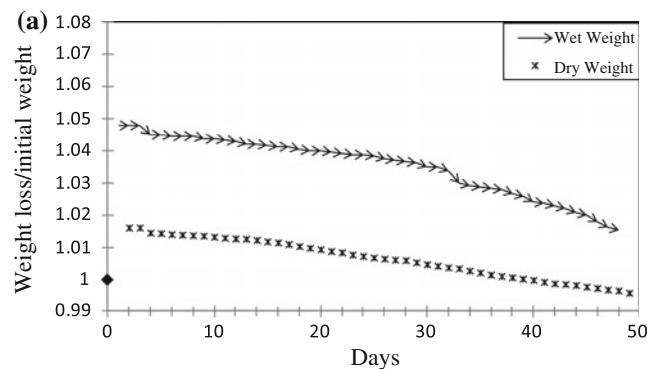
For the two stones in situ altered and fresh, XRD analyses show that the major mineralogical compositions are Calcite ( $\text{CaCO}_3$ ), silica ( $\text{SiO}_2$ ) in the form of quartz. From the thermo gravimetric (TGA) and ICP analyses, the calcium carbonate was about 90 % and 94 % in the in situ altered and fresh stones respectively. These two stones are practically pure limestone with some clay and siliceous impurities. Table 91.1 detail the main parameters obtained from mercury porosimetry and from hydrostatic density methods. The porosity determined by mercury porosimetry is 60 % higher in the in situ altered (34 %) to that in the fresh stone (21 %). Moreover, the average pore diameter is more than doubled; the bulk and the skeletal densities are decreased in the altered stone in comparison with the fresh stone.

**Table 91.1** Properties of the in situ altered and fresh limestones using mercury porosimetry and hydrostatic methods

	In situ altered limestone	Fresh limestone
Bulk density (gm/ml)	1.71	2.04
Skeletal density (gm/ml)	2.58	2.66
Water content at saturation (%)	23.8	13.5
Porosity by hydrostatic method (%)	38	26
Porosity by mercury intrusion (%)	34	21
Total volume of pores	0.191	0.115
% of pores having >6 $\mu\text{m}$	65	25
% of pores having <6 $\mu\text{m}$	35	75
Average pore diameter ( $\mu\text{m}$ )	0.73	0.28

### 91.3.2 Weathering Test: Immersion in Bird Droppings (BD) Solutions

The behavior of the stone samples during the immersion in bird droppings solutions is shown in Fig. 91.1. In the case of 10 % BD solution an increase in the wet and dry weights followed by a reduction in these weights with immersion time has been noticed. The increase in the wet weight could be explained by the absorption of the BD solution by the immersed stone. But the precipitation of the droppings particle on the stone surface leads probably to close the stone pores. Thus, a continuous reduction in the amount of the absorbed solution and in return a reduction in the wet weight occurs. The increase and decrease in the dry weight could be explained by the accumulation of the droppings particles inside the stone pores. However, the dissolution of the stone materials through the immersed process leads to a reduction in the dry weight in spite of the presence of BD particles. This behavior has been repeated with a higher amount in the case of 20 % BD solution (Fig. 91.1b).



The mineralogical study presented in Fig. 91.2 shows a formation of some amount of gypsum materials on the outer surface of the limestone immersed in 20 % BD solution for 48 days (Fig. 91.2b). However, this gypsum formation is extended to a depth of (5 mm) inside the stone structure (Fig. 91.2c), while this gypsum formation does not noticed in the case of limestone immersed in 10 % BD solution for 48 days. It can also be noted that the gypsum peaks decrease after the washing process of the immersed samples (Fig. 91.2d). This phenomenon could be attributed to the bacteria activities which oxidize sulphur or one of its components ( $\text{SO}_3$ ) in the stone components, forming sulphuric acid (acidity media) through the immersion process in the bird droppings solutions.

Figure 91.3 shows the mercury intrusion porosimetry results for fresh, altered with 10 and 20 % bird droppings solutions, and in situ altered stones. Important changes can be observed in the pore volume and pore size distribution of the altered stones due to biological (BD) effect process. All the curves of the altered stones are located between the two limit curves the fresh and in situ altered one with a matching in the zone (less than 6  $\mu\text{m}$ ), while no matching between immersed limestone and both fresh and in situ altered stone has been noticed in the zone (greater than 6  $\mu\text{m}$ ), with an increase in the values of total porosity and the nature of pore structure toward the historical (in situ) altered one.

### 91.4 Discussion

Table 91.2 summarizes the main results obtained on the tested stones. These results confirm as shown in Fig. 91.4 that the degradation due to bird dropping was considerable. Main properties of the tested stones during the applied weathering test were highly changes: porosity increases,

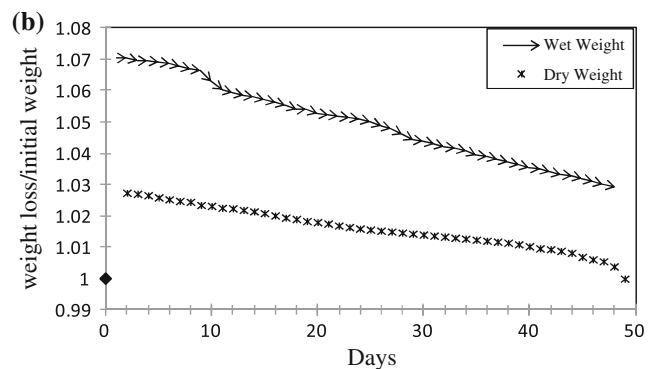


**Fig. 91.1** Weight changes of fresh limestone samples during immersion tests in bird droppings solutions. **a** 10 % bird droppings solution for 48 days. **b** 20 % bird droppings solution for 48 days

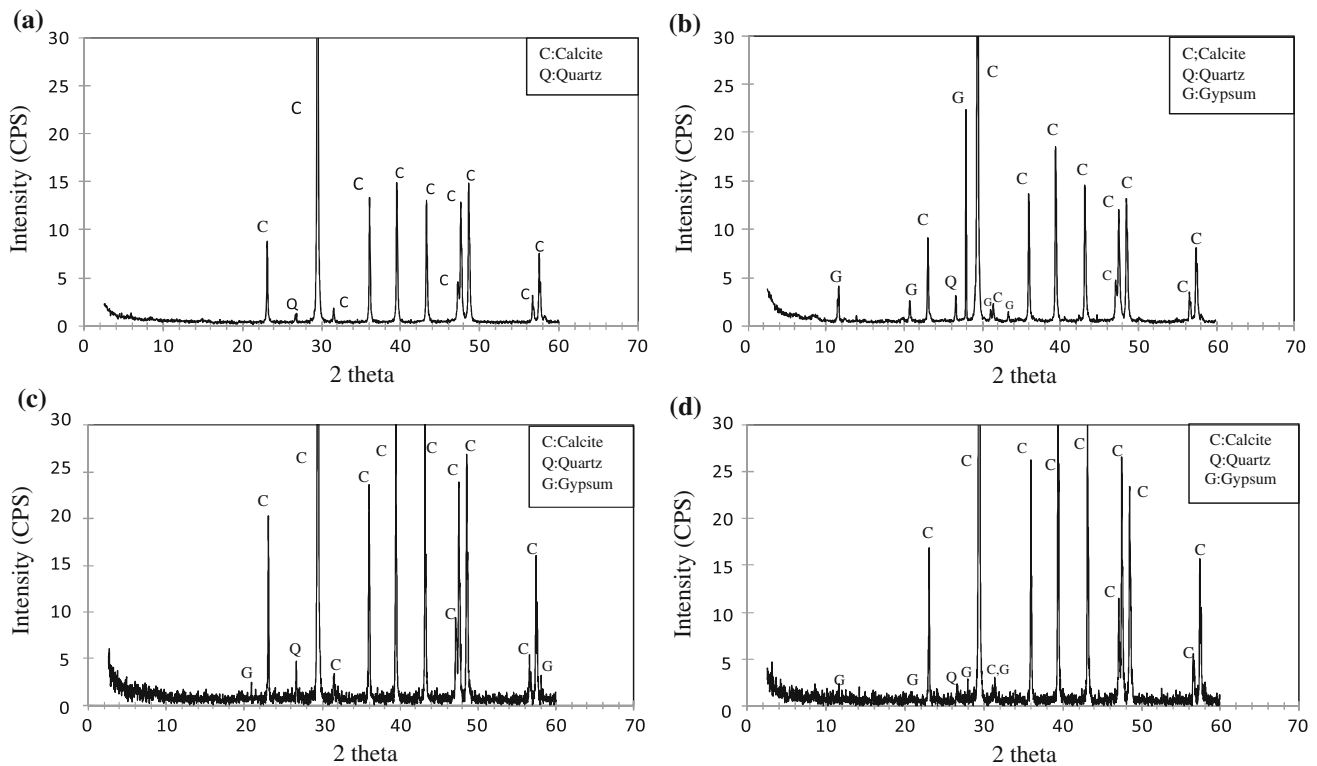


**Fig. 91.2** XRD analysis (a) fresh limestone. b and c treated limestone with 20 % BD for 48 days at depths (0 mm) and (5 mm) respectively. d the treated limestone with 20 % BD solution for 48 days after washing

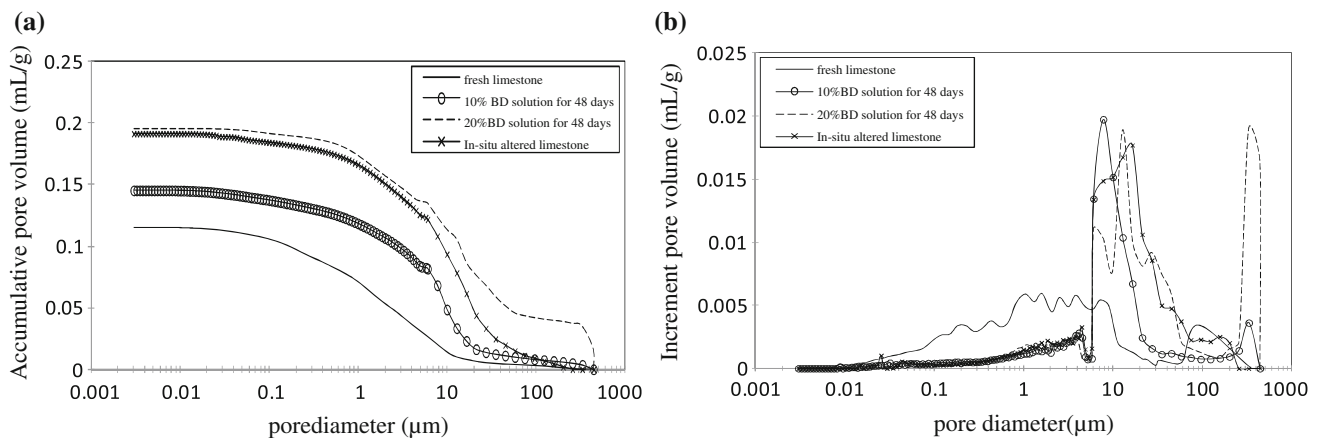


**Fig. 91.3** Mercury intrusion porosimetry curves showing cumulative pore volume (left) and incremental pore volume (right) for in situ altered, fresh and altered stone with 10 and 20 % bird droppings (BD) solutions

capillary-water uptake coefficients reduce and the anisotropy was varied in the range (31–36.5). Properties of the weathered stones change more with increase the percentage of bird droppings powder in the water used as a solution treatment. Moreover, these physical properties mainly porosity and pore size distribution of the samples decayed in the laboratory are

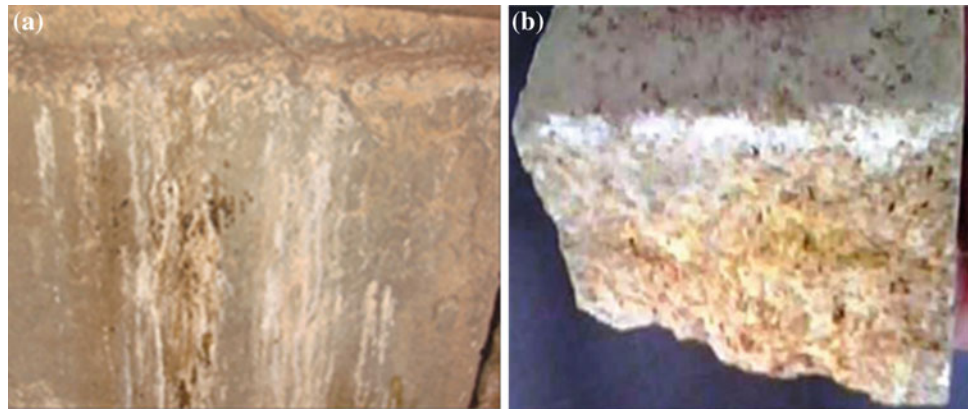
approximately similar to those of the in situ altered limestone sample. Change in the porosity parameters under the bird droppings effect mainly increase macropores of the altered stones which in turn induces a great modification in the water transfer properties approximately similar to that obtained concerning the in situ altered stones.

**Table 91.2** Main properties of fresh, in situ altered and altered stones in the laboratory

Properties	Fresh/In situ Altered limestone	Stone altered in the laboratory due to bird dropping tests during 48 days in	
		10 % BD solution	20 % BD solution
Average pore diameter, $\mu\text{m}$	0.28/0.73	0.45	0.63
Porosity by mercury intrusion, %	20.9/33.8	24.1	26.7
Porosity by hydrostatic method, %	26.4/38	30	34.1
Capillary Perpendicular (B1), $\text{cm}/\text{min}^5$	0.29/UD	0.252	0.212
Capillary Parallel (B2), $\text{cm}/\text{min}^{0.5}$	0.38/UD	0.344	0.284
Anisotropy B2/B1, %	31/UD	36.5	33.9

UD Undetermined, BD Bird droppings

**Fig. 91.4** Degradations due to bird dropping, in situ altered stone (a) and laboratory altered stone (b)



## 91.5 Conclusions

Results obtained from measured properties show weathering effects on the in situ altered stone of the monument Al-Namrud in the north of Iraq, constructed in the second millennium B.C. by the Assyrian Empire in comparison with the fresh stone. In the field, numerous mechanisms contribute in the degradation of the monument: dissolution of carbonate, damage which done by the roosting and nesting of birds on soft stone through the bacteria activity which oxidize sulphur or one of its compounds, forming sulphuric acid, which in turn attacks stone structure directly, formed gypsum material on the outer stone surface and extended to a depth of 5 mm. Since this gypsum material has been approximately removed by washing, lead to increase the porosity and reduce the capillary and water uptake coefficients. The biological effect represented by the immersion in the bird droppings solutions can be considered very important agent. This produces a pore size distribution approximately similar to that of in situ altered stones. This study shows that bird droppings weathering seem to be an active factor of the structural, textural changes and deterioration in some of stones in the Al-Namrud monuments. It's obvious that a lot of laboratory and field work must be done in order

to firstly evaluate the state of the degradation of different stones on the site and to study how remediate the main degradation to insure the stability of the different structures of the Al-Namrud monument.

## References

- Angeli M, Bigas J-P, Benavente D, Menendez B, Hebert R, David C (2007) Salt crystallization in pores: quantification and estimation of damage. *Environ Geol* 52:187–195
- Ashurst J, Dimes FG (eds) (1998) Conservation of building and decorative stone, vol 2. Routledge, London
- Beck K, AL-Mukhtar M, Rozenbaum O, Rautureau M (2003) Characterization, water transfer properties and deterioration in tuffeau: building material in the Loire Valley-France. *Build Environ* 38:1151–1162
- Beck K, AL-Mukhtar M (2010) Evaluation of the compatibility of building limestones from salt crystallisation experiments. *Geol Soc London SP* 333:111–118
- Benavente D, Garcia Del Cura MA, Bernabeua A, Ordenez S (2001) Quantification of salt weathering in porous stones using an experimental continuous partial immersion method. *Eng Geol* 59:313–325
- Dahlin E (2000) Preventive conservation strategies for organic objects in museums, historic buildings, and archives, damage assessment-causes-mechanisms and measurements. In: 5th EC conference report Cultural Heritage Research. pp. 57–60

- Goudie AS (1999) Experimental salt weathering of limestones in relation to rock properties. *Earth Surf Proc Land* 24:715–724
- Petushkova JuA, Petushkova JuP, Osipov GA (2007) Microbial diversity in biocides-treated stone of historical building. In: BioMicro World II International Conference on environmental, industrial and applied microbiology, Seville-Espagne
- Van TT, Beck K, AL-Mukhtar M (2007) Accelerated weathering tests on two highly porous limestones. *Environ Geol* 52(2):283–292

---

# Changes in Petrophysical Properties of the Stone Surface due to Past Conservation Treatments in Archaeological Sites of Merida (Spain)

92

Natalia Perez-Ema, Monica Alvarez de Buergo, Rosa Bustamante, and Miguel Gomez-Heras

---

## Abstract

Petrophysical properties, such as porosity, permeability, density or anisotropy determine the alterability of stone surfaces from archaeological sites, and therefore, the future preservation of the material. Others, like superficial roughness or color, may point out changes due to alteration processes, natural or man-induced, for example, by conservation treatments. The application of conservation treatments may vary some of these properties forcing the stone surface to a re-adaptation to the new conditions, which could generate new processes of deterioration. In this study changes resulting from the application of consolidating and hydrophobic treatments on stone materials from the Roman Theatre (marble and granite) and the Mitreo's House (mural painting and mosaics), both archaeological sites from Merida (Spain), are analyzed. The use of portable field devices allows us to perform analyses both on site and in laboratory, comparing treated and untreated samples. Treatments consisted of synthetic resins, consolidating (such as tetraethoxysilane TEOS) and hydrophobic products. Results confirm that undesirable changes may occur, with consequences ranging from purely aesthetic variations to physical, chemical and mechanical damages. This also permits us to check limitations in the use of these techniques for the evaluation of conservation treatments.

---

## Keywords

Archaeological sites • Stone • Marble • Granite • Conservation • Treatments • Petrophysical properties • Merida

---

N. Perez-Ema (✉) · M. Gomez-Heras  
CEI Campus Moncloa UCM-UPM, Edif. Real Jardín Botánico  
Alfonso XIII, Avda. Complutense s/n, 28040 Madrid, Spain  
e-mail: natalia.perez@upm.es

N. Perez-Ema · M. Alvarez de Buergo · M. Gomez-Heras  
Instituto de Geociencias IGEO (CSIC, UCM), C/ José Antonio  
Nováis 12, 28040 Madrid, Spain

N. Perez-Ema · R. Bustamante · M. Gomez-Heras  
Escuela Tecnica Superior de Arquitectura, Universidad Politécnica  
de Madrid, Avda, Juan de Herrera 4, 28040 Madrid, Spain

---

## 92.1 Introduction

The research project in which this study is included is focused on the analysis of the effects of conservation treatments applied on stone material from archaeological sites, in terms of effectiveness, durability and alteration processes derived from its application. Since alteration processes depends greatly on the interaction between the surface and the surrounding environment, either burial or aerial, the analysis of petro-physical properties is an essential task to characterize the material, as well as for the reasoned proposal of preservation treatments, but also in order to evaluate their effects.

The archaeological city of Merida was listed as World Heritage site by UNESCO in 1993 and includes several monumental remains from the Roman period. The sites in which this study is focused are the Roman Theater,

inaugurated in 15 B.C, and Mitreo's House, built in the late first or early second century.

Review of scientific literature regarding evaluation of conservation treatments for stone material allows us to state that: 1. Most of the studies are based on fresh/unaltered stone materials on which a specific treatment is tested (mainly consolidating and hydrophobic products), subjected, later on, to accelerated ageing tests; 2. It is mostly based on laboratory studies, being very different working on site, with original and specific materials and alterations; 3. These studies are focused on historic built heritage or outdoor sculpture, and very rarely on archaeological sites. Some negative effects of conservation treatments are already well known, such as, for example, the photo-oxidative degradation of synthetic resins (Favaro et al. 2006; Chiantore and Lazzari 2001) frequently used in the restoration of wall paintings. In the case of ethyl silicate there are studies analyzing its limited effectiveness caused by the presence of water (Rodrigues da Costa and Rodrigues 2011), or superficial alteration such as discoloration, darkening and brightness changes. Special attention has been paid on hydrophobic treatments in the last years, taking into account that in most of the alteration phenomena the water is present. These treatments can be extremely aggressive in the case of archaeological stone showing physical and mechanical damages, as well as color changes (Fort et al. 2000). The presence of salts inside the stone materials when applying superficial treatments, which act as impermeable barriers, can also lead to accelerated decay (Varas et al. 2007). Changes in the stone surface could lead to general degradation of the material; in this sense the superficial roughness and color are key parameters. The roughness affects the weatherability of the material against external agents; the rougher texture leads to a higher reactive surface area, moreover it promotes the deposition of particles from environment and the water retention, favoring surface soiling and eventually, the formation of crusts (Alvarez de Buergo et al. 2011). Color changes, besides aesthetic disturbance, may indicate also chemical and physical alterations (Fort et al. 2000).

## 92.2 Methodology and Techniques

The review of conservative interventions carried out in both selected archaeological sites permits the selection of treated and untreated areas where developing comparative analysis through the use of portable and non destructive equipments, listed below. On the other hand several samples of the original stone material were collected on site; marble (different types and colors) and granite from the Roman Theater, and wall painting fragments from the Mitreo's House. In addition to portable techniques, in the IGEO's Petrophysics

laboratory it is possible to complement on site measurement with some other techniques, always comparing pre- and post-treatment.

Portable field devices used are as follows:

- Measurements of the propagation velocity of ultrasound (Pundit equipment)
  - Optical surface roughnessmeter (TRACEiT, Innowep GMBH)
  - Hardness tester (Equotip 3)
  - Spectrophotometry color measurement (Minolta CM-700d/600D).
  - Infrared Termography (ThermaCAM™ B4)
- Laboratory tests and techniques:
- Scanning electron microscopy SEM and element microanalysis (EDS)
  - Mercury intrusion porosimetry (MIP)
  - Determination of hydric properties by Contact Angle test (static angle), or water saturation and capillarity tests.

## 92.3 Results

### 92.3.1 Measurements on Site

Regarding the Roman Theater, all measurements were focused on the evaluation of last general intervention, carried out on the Front Stage in 1996.

Treatments on marble were mainly based on chemical cleaning, punctual consolidation with ethyl silicate and a general protection with hydrophobic products.

Most of the outcomes in this case show differential values mainly due to the state of preservation. Thus, the treated areas were altered areas, and therefore show lower levels of, for instance, superficial hardness (Table 92.1), color ( $\Delta E^* = 3$ )<sup>1</sup> or water absorption (Table 92.2). In these cases laboratory tests and measurements on recently applied treated areas are imperative in order to evaluate such parameters in terms of effectiveness. The difference between roughness values, however, is very high, considering treated area, disaggregated, and the unaltered one (Table 92.3). Results obtained with infrared termography revealing, for example, different thermal behavior comparing treated and untreated parts of the same marble piece from the basement (Figs. 92.1 and 92.2).

In the case of the Mitreo's House, interventions are developed continuously since the 80's. Products used are mainly synthetic resins for the consolidation of the wall paintings and mosaics, but also, though less regularly, TEOS.

<sup>1</sup> Based on CIELab system, where  $\Delta E^* = \sqrt{(\Delta L^*)^2 + (\Delta a^*)^2 + (\Delta b^*)^2}$

**Table 1** Average values for superficial hardness (*Leeb hardness scale*)

	Treated areas	Untreated areas
Grey marble—columns	392 HLD ( $\pm 50$ )	522 HLD ( $\pm 31$ )
White marble—cornices	494 HLD ( $\pm 58$ )	544 HLD ( $\pm 36$ )

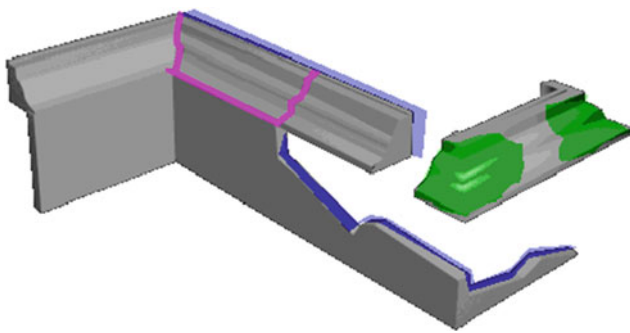
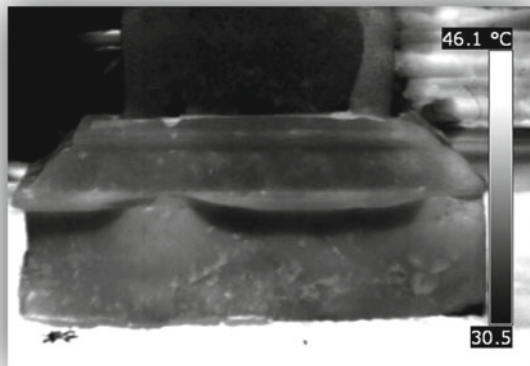
**Table 2**  $WA_{LP}$  values for water absorption

White marble—cornices	$WA_{LP} = 0.0004$	$WA_{LP} = 0.0000$
-----------------------	--------------------	--------------------

Based on CEN/TC 346 N. 244 protocol for the evaluation of water-repellents

**Table 3** Average values for superficial roughness measured on fragment A2cor31

White marble—cornices	$Rz = 8.7 (\pm 10)$	$Rz = 21.1 (\pm 19)$
-----------------------	---------------------	----------------------

**Fig. 1** Application of TEOS is in *green color* (Source Agora S.L)**Fig. 2** Image of the same cornice showed in Fig. 1 obtained with an IR Thermographic camera

Measurements carried out on wall painting show different degree of internal cohesion (Table 92.4), as well as changes in color parameters in the *Cosmologic Mosaic* with a  $\Delta E^*$  value of 7. Regarding hardness measurements the difficulty lays on the way the panel is attached to the mural support, not providing representative outcomes unless these conditions are identical for the whole panel extension. In most of

**Table 4** Values for ultrasound measurements, by indirect method, on Mitreo's House

Treated area	Untreated area
2,182 m/s	1,611 m/s

cases the edges of the panels were consolidated with plaster, leading to a differential level of adhesion to the support in the center of the panel, which has a poor adhesion, with respect to the wall, and the outer consolidated parts.

### 92.3.2 Laboratory Tests

Given limitations for comparative assessment on site, laboratory tests are essential. Treatments applied on laboratory reproduce those ones documented on each site, analyzing specimens before and after application and analyzing changes on the materials surface.

The results from the contact angle test show high efficiency for all cases when assessing hydrophobicity. Nevertheless, mercury intrusion porosity tests prove that, although an overall decrease of porosity, treatments change the pre-existing balance between macro and microporosity, increasing the first one and decreasing the second one in the case of marble.

Tests carried out on fragments of wall painting show an increase in superficial microroughness (Table 92.5) as well as remarkable changes in color parameters in the case of ethyl silicate treatment ( $\Delta E^* = 10$ ).

### 92.4 Conclusions

The analysis of the effects of conservation treatments should be based, as far as possible, on in situ measurements, in order to evaluate these effects in its original context. This involves some difficulties, first the access to accurate information about previous interventions, the use of portable and non-destructive techniques, then measurements must be numerous to be representative, but we must also know the limits of each technique, as the multitude of variables that act on outdoor environment are large and heterogeneous.

Regarding durability of treatments, SEM analyses show that there are still remnants and traces of treatment on marbles from the Theater, but its effectiveness has not been proved. Treated areas of marbles are currently disaggregated, affected by sugaring. In this case there are few differences between treated and untreated areas, and it cannot be deduced that, when existing, they are caused by the treatment.

Specimens studied on laboratory clearly show changes on the surface of all stone material treated. All of them will be placed in its original context in order to monitor changes

**Table 5** Changes in superficial roughness on wall painting fragments from Mitreo's house


MCM23-Estel 1,000©		MCM24-Acrl33©		MCM25-PB72©	
Rz-Pre-Treatment	20	Rz-Pre-T	23	Rz-Pre-T	22
Rz-Post-Treatment	40	Rz-Post-T	41	Rz-Post-T	26

periodically during at least one year and compare these results to those obtained from in situ measurements.

**Acknowledgements** This research was supported by the PICATA program from Campus of International Excellence of Moncloa. Our acknowledgements to GEOMATERIALES programme (S2009-MAT1629) within Instituto de Geociencias (CSIC, UCM), to AIPA Research Group (ETSAM, Polytechnic University of Madrid) and to the Research Group funded by the Complutense University of Madrid "Alteration and Conservation of heritage stone materials" (Ref. 921349). We thank Agora S.L, the "Consortio de la Ciudad Monumental de Merida", as well as the "Museo Nacional de Arte Romano de Merida", for its collaboration in this research.

## References

- Alvarez de Buergo M, Vázquez-Calvo MC, Fort R (2011) The measurement of surface roughness to determine the suitability of different methods for stone cleaning. *Geophysical research abstracts*, vol 13, EGU2011-6443
- Chiantore O, Lazzari M (2001) Photo-oxidative stability of paraloid acrylic protective polymers. *Polymer* 42:17–27
- Favaro M, Mendichi R, Ossola F, Russo U, Simon S, Tomasin P, Vigato PA (2006) Evaluation of polymers for conservation treatments of outdoor exposed stone monuments. Part I: photo-oxidative weathering. *Polym Degrad Stab* 91(12):3083–3096
- Fort R, Lopez de Azcona MC, Mingarro F, Alvarez de Buergo M, Ro Riguez J (2000) A comparative study of the efficiency of siloxanes, methacrylates and microwax-based treatments applied to the stone materials of the royal palace of Madrid, Spain. In: Fassina V (ed) 9th International Congress on Deterioration and Conservation of Stone. Amsterdam: Elsevier
- Rodrigues da Costa J, Rodrigues D (2011) The effect of water on the durability of granitic materials consolidated with Ethyl Silicates. In: Adhesives and Consolidants in Conservation: Research and Application. CCI Symposium-Ottawa, Canada
- Varas MJ, Alvarez de Buergo M, Fort R (2007) The influence of past protective treatments on the deterioration of historic stone façades: a case study. *Stud Conserv* 52:110–125

# Synthesis and Characterization of a Calcium Oxalate-Silica Nanocomposite for Stone Conservation

93

Noni Maravelaki, Anastasia Verganelaki, Vassilis Kilikoglou, and Ioannis Karatasios

## Abstract

A novel biomimetic nanocomposite, comprised of amorphous silica and calcium oxalate, has been efficiently synthesized by incorporating materials of low toxicity and cost, imitating a stable binary system occurring in well-preserved areas of monuments, plant biomineralization and the industrial processing of sugar. A simple two-step and cost-effective reaction route, involving calcium hydroxide and oxalic acid dihydrate in isopropanol as precursors, yielded a colloidal solution of nano-calcium oxalate; the latter, mixed with tetraethoxysilane produced a crack-free mesoporous xerogel with pore radius of approximately 15 nm. FTIR, XRD, DTA-TG and SEM studies demonstrated that the nano-calcium oxalate was embedded into the silica matrix resulting in a crack free nanocomposite, which was deeply penetrated and homogeneously distributed within the treated porous medium. The hygric properties and the tensile strength of treated samples were improved, without affecting the microstructural characteristics. The physico-chemical stability and compatibility of the nanocomposite with stone create a potential strengthening and protective agent for inorganic porous materials.

## Keywords

Biomimetic • Crack-free • Mesoporous • Consolidation • Construction materials

## 93.1 Introduction

Building materials of architectural structures and monuments are weathered through natural processes and anthropogenically induced environmental pollution. Over the last decades, a lot of research has been carried out towards the production of silicon-based polymeric resins to be used as strengthening and protective agents for the porous building

materials. This family of materials present many advantages but also several disadvantages like cracking and insufficient bonding to carbonaceous substrates.

In an attempt to improve the performance of this group of materials, a novel nanocomposite consolidant (SiO<sub>x</sub>) was designed and synthesized based on the modification of tetraethoxysilane (TEOS) after incorporating nano-particles of calcium oxalate monohydrate (COM) into the silica matrix. The COM was selected on the grounds of the remarkable weathering resistance of combined calcium oxalate and silica layers, often encountered on monuments as patina. In addition, the formation of calcium oxalate-silica component is a well-established process in plant biomineralization and sugar mill evaporators. Eventual non-reacted precursors, such as calcium hydroxide, can actually benefit the overall processing by acting as a catalyst or otherwise, can simply be transformed into harmless by-products.

N. Maravelaki (✉) · A. Verganelaki  
Technical University of Crete, Akrotiri 73100, Chania, Greece  
e-mail: pmaravelaki@isc.tuc.gr

V. Kilikoglou · I. Karatasios  
National Centre for Scientific Research “Demokritos”,  
Aghia Paraskevi 15310, Athens, Greece

## 93.2 Experimental Section

### 93.2.1 Materials and Synthesis of the Nanocomposite

TEOS, n-octylamine (Oct) and isopropanol (ISP) (puriss. p.a.) were supplied by Sigma-Aldrich, calcium hydroxide (CH) by Fluka and oxalic acid dihydrate (Oxac) by Panreac. The experimental part of this research included two stages; (a) two separate alcoholic solutions were prepared by dissolving CH 1.01 % w/v and Oxac 1.72 % w/v in ISP. The solutions were separately stirred for 10 min under ultrasonic agitation, and then they were mixed to give the CaOx-s. Afterwards, the CaOx-s was vigorously stirred with a magnetic agitator for other 24 h; this reaction time was computed according to analyses of powders from the drying CaOx-s, indicating that the maximum amount of COM nanocrystals was produced in 24 h (Maravelaki et al. 2011). The term CaOx-p refers to the dried powder obtained from the CaOx-s, in which the major part is COM with an amount of remaining CH; (b), TEOS was added into the entire CaOx-s, under ultrasonic agitation for 2 h. The water produced from the reaction between CH and Oxac, along with the amount of the remaining CH can facilitate the hydrolysis of TEOS. Afterwards, Oct acting as surfactant (Mosquera et al. 2010) was added under vigorous stirring in order to obtain the SiOx-s; the mole ratios of the materials TEOS/CaOx-p/H<sub>2</sub>O/ISP/Oct were 0.5/0.03/0.09/7.15/0.05. The SiOx-s was placed on a round bottom flask and stirred for approximately 3 h at room temperature. The SiOx-s was casted into transparent cylindrical molds 5.5 cm in diameter and 2 cm in height and was covered on top by a perforated parafilm in order to allow gentle evaporation of the solvent. Gelation and drying occurred by simple exposure of the cast sols to laboratory conditions (RH = 60 ± 5 %, T = 20 ± 2 °C) until a constant weight was achieved. A crack-free xerogel (SiOx-x) was produced within 35–40 days. For comparison purposes, another xerogel (TEOS-x) derived from a sol containing TEOS, ethanol (EtOH) and water in a molar ratio TEOS:EtOH:H<sub>2</sub>O equal to 1:4:16 was also synthesized and analyzed.

### 93.2.2 Characterization and Evaluation of the Consolidation of SiOx

Initially, the viscosity of the SiOx-s was measured. The qualitative and quantitative analysis of the CaOx-p was performed by FTIR and XRD, respectively. Textural characterization of both the xerogels SiOx-x and TEOS-x was performed by N<sub>2</sub> physisorption after curing of 12 months. The surface morphology of the CaOx-p and SiOx-x was examined under SEM. Aiming to evaluate the performance

of the SiOx in a laboratory scale case study, the SiOx-s was applied to bioclastic limestone specimens, mainly consisted of calcium carbonate (approximately 97 %). The test specimens were treated with the SiOx-s by capillarity for 24 h, in a closed chamber under laboratory conditions. Afterwards, the test specimens were dried in laboratory conditions. A constant weight was reached within 30–45 days. The evaluation was obtained by the comparative physical, morphological and mechanical characterization of untreated and treated stone specimens after a curing of 6 months.

## 93.3 Results and Discussion

### 93.3.1 Characterization of the Nano-materials

XRD analysis revealed that the CaOx-p corresponds to the minerals whewellite (COM) and portlandite (CH) (Fig. 93.1). By the Rietveld method indicated that the CaOx-p was composed of 75 % COM and 25 % CH; the latter, does not create any problems in the overall reaction process, since it can be transformed into calcite over time. The results of XRD analysis were verified with the FTIR analysis. SEM examination of the CaOx-p revealed that the above synthesis led to the formation of aggregates as shown in Fig. 93.2a. These aggregates are composed of rod-shaped crystals, where the majority of crystals exhibit a width of about 30–35 nm and a length of 70–170 nm (Fig. 93.2b and c). The choice of the CH and Oxac relies on the avoidance of harmful by-products, and can be considered an approach similar to that occurring in the well-preserved patinas; in the latter, COM was produced by the reaction of calcite and Oxac. Therefore, the approach followed for the COM synthesis can be considered biomimetic to natural ones occurring on monuments and in biomineralization. The designed hybrid SiOx-s was

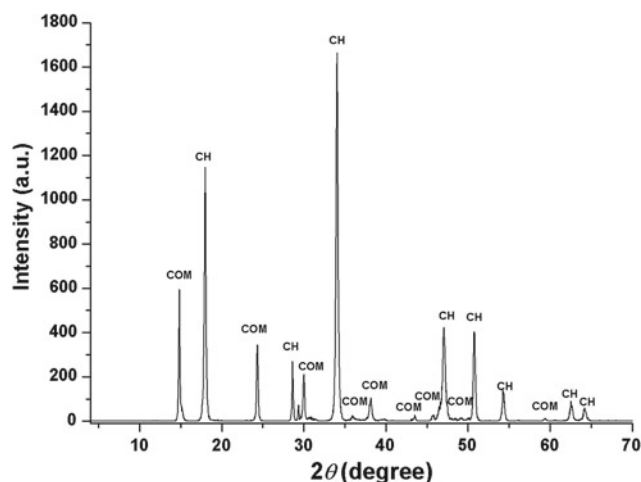


**Fig. 93.1** XRD pattern of the synthesized CaOx-p nanoparticles containing whewellite (COM) and portlandite (CH)

**Fig. 93.2** SEM micrographs of the synthesized CaOx-p: view of the aggregates (a); details of the crystals with a width of about 30–35 nm and a length of 50–170 nm (b, c)

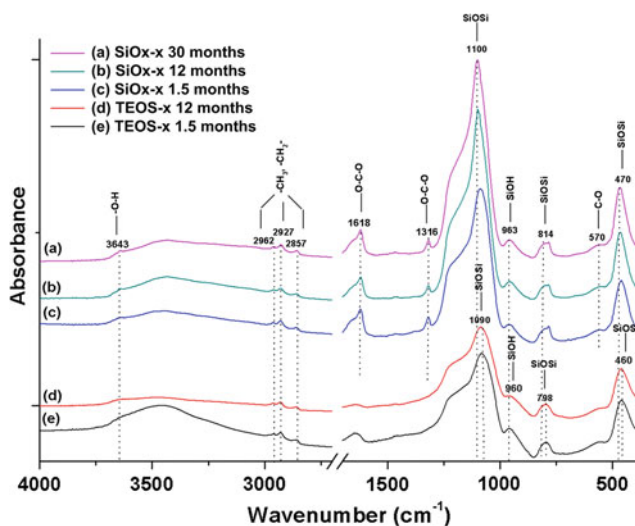
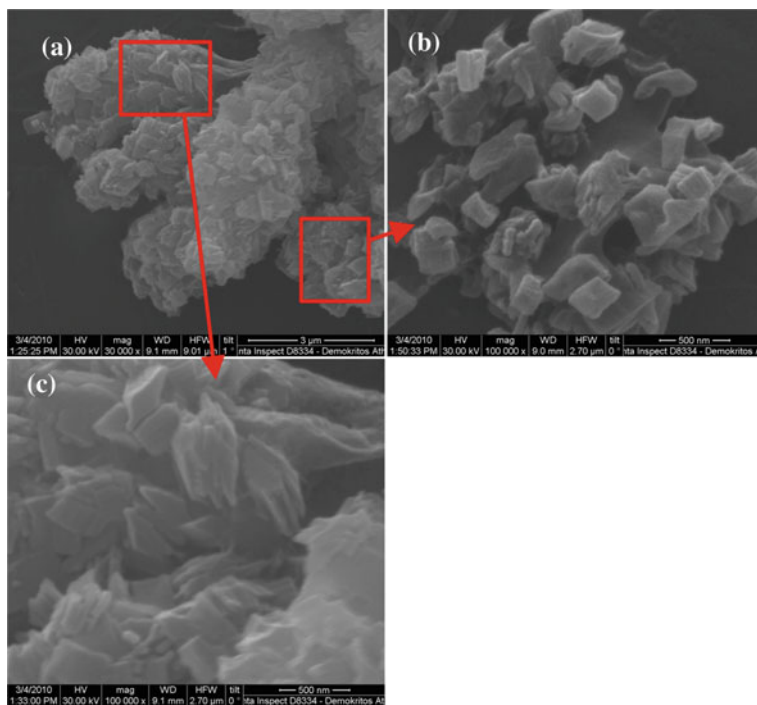


**Fig. 93.3** FTIR spectra of SiOx-x after a curing of 30 (a), 12 (b) and 1.5 (c) months, along with the TEOS-x after a curing of 12 (d) and 1.5 (e) months

characterized as a Newtonian liquid, with viscosity value 1.56 mPa s, close to that of the commercial products. In order to characterize chemically the product and more specifically the effect of the CaOx-s addition into the TEOS-Oct system, a comparative FTIR investigation was performed. Fig. 93.3 compares the infrared spectra obtained from TEOS-x and SiOx-x at different time intervals of curing. In all the spectra, the absence of the absorption at  $1,169\text{ cm}^{-1}$ , related to the rocking of the C-H bond in  $-\text{CH}_3$  of TEOS, suggests that the hydrolysis of TEOS was successfully completed (Rubio et al. 1998). Observing the infrared spectra of the TEOS-x cured for

12 and 1.5 months (d and e), it can be seen that the basic Si-O-Si bonds, formed upon hydrolysis and condensation of TEOS, showed characteristic absorptions at  $1,082$ ,  $798$  and  $460\text{ cm}^{-1}$  (Rubio et al. 1998). On the other hand, it is worth mentioning that in the spectra of the SiOx-x (a, b and c) cured for 30, 12 and 1.5 months, the main symmetric Si-O-Si stretching at  $1,082\text{ cm}^{-1}$  has been shifted to the higher wavenumber at  $1,100\text{ cm}^{-1}$ . This is an indication of the chemical differentiation induced by the CaOx-s addition, resulting in shifting the Si-O-Si symmetric stretching to higher wavenumbers (e.g.  $1,082 \rightarrow 1,100$ ,  $798 \rightarrow 814\text{ cm}^{-1}$ ). It is well-established that when an enhanced electronic density has to be accommodated in the same area of a chemical bond, this results in increasing the wavenumber. The presence of COM is denoted with the bands at  $1,618$  and  $1,316\text{ cm}^{-1}$  which are associated with the O-C-O anti symmetric and symmetric stretching, respectively (Petrov and Soptrajanov 1975).

Nitrogen adsorption isotherm of the SiOx-x exhibits type IV isotherms and a type H1 hysteresis loop, characterized by parallel and nearly vertical branches. These isotherms are typical of mesoporous materials, containing a portion of macropores. The average pore value of SiOx-x was approximately 15 nm; this large pore radius of SiOx-x can be attributed to the incorporation of nano-COM into its matrix, augmenting the pore size of the network. The micro-morphological characterization of the SiOx-x conducted through SEM provided supporting evidence to BET results. Fig. 93.4 indicated that SiOx-x comprises a compact assembly of uniform sphere-like nanoparticles ranging from 35 to 90 nm.

**Fig. 93.4** **a** Details of SiO<sub>x</sub>-x reveal that the nanoparticles range from 35 to 90 nm; **b** The SiO<sub>x</sub>-x particles resemble “distorted” spheres, while the interstices formed between the nanoparticles of SiO<sub>x</sub>-x measure around 30 nm

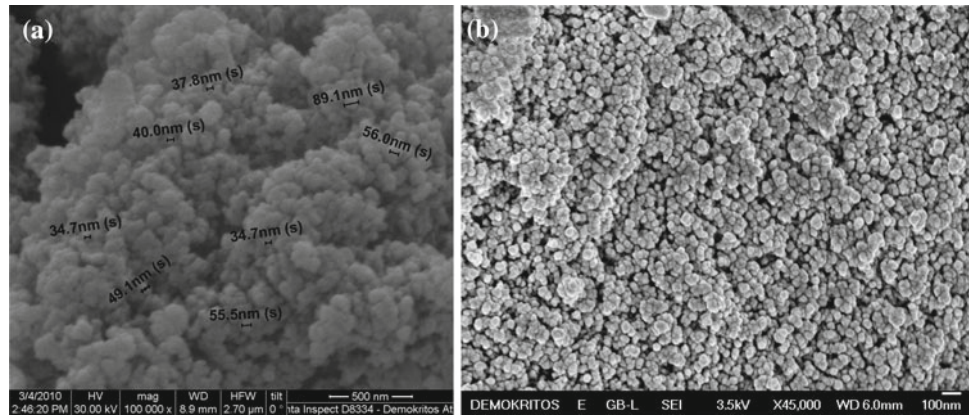


**Table 93.1** Coefficients of the WCA, WVP, TWAC, contact angle measurements, chromatic parameters and tensile strength measurements of untreated and treated limestone

	WCA ( $\text{g cm}^{-2} \text{s}^{-1/2}$ )	TWAC (%)	WVP ( $\text{g cm}^{-2} \text{d}^{-1}$ )	Chromatic parameters				Tensile strength (MPa)
				L*	a*	b*	$\Delta E^*$	
Untreated	0.0115 ( $\pm 0.0005$ )	13.78 ( $\pm 0.15$ )	0.140 ( $\pm 0.044$ )	81.32 ( $\pm 0.06$ )	2.10 ( $\pm 0.00$ )	12.42 ( $\pm 0.01$ )	–	2.81 ( $\pm 0.12$ )
SiO <sub>x</sub> - treated	0.0050 ( $\pm 0.0005$ )	12.5 ( $\pm 0.34$ )	0.093 ( $\pm 0.017$ )	80.80 ( $\pm 0.87$ )	2.23 ( $\pm 0.06$ )	14.18 ( $\pm 0.26$ )	2.01 ( $\pm 0.22$ )	3.46 ( $\pm 0.49$ )

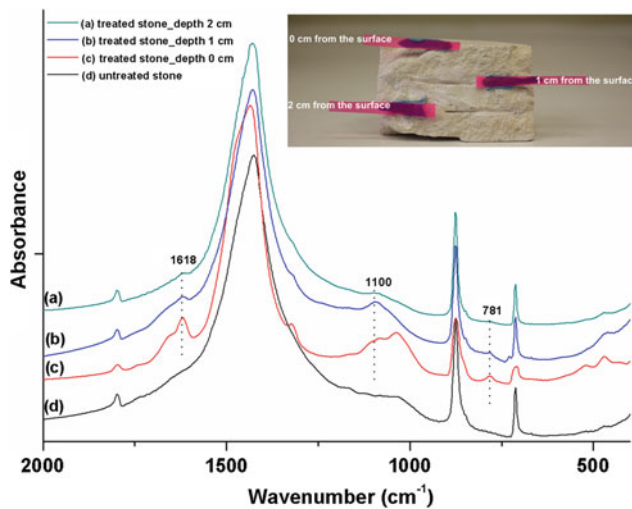


**Fig. 93.5** FTIR spectra of the SiO<sub>x</sub>-treated stone at various depths (*a*, *b*, *c*) from the surface and untreated stone (*d*)

### 93.3.2 Performance Evaluation of the SiO<sub>x</sub>

In the treated bioclastic limestone the chromatic changes and the coefficient of water vapor permeability decreased. More specific, after treatment the chromatic variation cannot be detected by the naked eye. The low viscosity value of SiO<sub>x</sub>-s facilitates its penetration in a depth more than 2 cm from the surface. In particular, the main oxalate absorption bands at 1,618 and 781  $\text{cm}^{-1}$  and the main Si-O-Si vibration at 1,100  $\text{cm}^{-1}$  (Rubio et al. 1998) were identified by the infrared spectroscopy at a depth of about 2 cm from the treated surface (Fig. 93.5). The microdrilling measurements directly used both for the mechanical

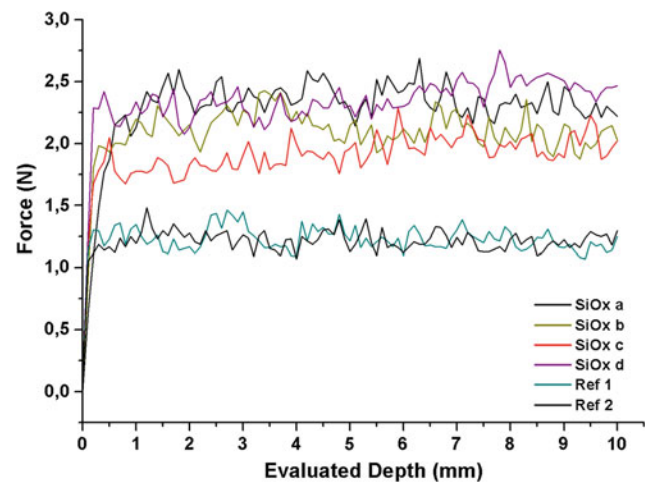


**Fig. 93.6** Drilling resistance of untreated and SiO<sub>x</sub>-treated stone

examination of the robustness of the stone and indirectly for the evaluation of the product penetration depth, supported the results obtained in the FTIR study (Fig. 93.6).

Table 93.1 compares the hygric behavior, as well as the microstructural and mechanical characteristics of the treated-untreated stone specimens. After treatment, the water capillary absorption (WCA) coefficient was decreased by 57 %, while the total amount of capillary absorbed water (TWAC) decreased by 8 %. Regarding the mechanical properties, the indirect tensile strength of the treated specimens increased up to 23 %, providing a considerable consolidation effect. In the treated samples, the water vapor permeability (WVP) coefficient was additionally reduced by approximately 34 %.

The SEM micrographs clearly indicated that the product was deposited on the walls of the pores without modifying the stone microstructure to such an extent that can further alter the stone hygric behavior.

---

### 93.4 Conclusions

The synthesized hybrid SiO<sub>x</sub> consolidates the porous limestone by improving the stone performance characteristics, without significantly altering the stone microstructure, thus allowing the liquid and vapor circulation within the porous matrix. The SiO<sub>x</sub>, which was derived from the incorporation of calcium oxalate into TEOS, has the advantage to be a crack-free material which is an important feature for the successful application of consolidants. The low viscosity value of the SiO<sub>x</sub> facilitates its penetration in a depth more than 2 cm from the treated surface. These beneficial prop-

erties were significantly ameliorated by the reduction of the water absorption mainly due to the presence of calcium oxalate, which is the main compound identified in well-preserved patina layer on monuments. Therefore, the designed SiO<sub>x</sub> provides a compatible structure to the deteriorated stone with the ability of strengthening and protecting it from the environmental loading.

---

### References

- Maravelaki P, Verganelaki A, Karatasios I, Kilikoglou V (2011) Industrial property organization, vol 1007392, p 54
- Mosquera MJ, de los Santos DM, Rivas T (2010) Surfactant-synthesized ormosils with application to stone restoration. *Langmuir* 26:6737–6745
- Petrov I, Soptrajanov B (1975) Infrared spectrum of whewellite. *Spectrochim. Acta Part A* 31:309–316
- Rubio F, Rubio J, Oteo JL (1998) A FT-IR study of the hydrolysis of tetraethylorthosilicate. *Spectrosc Lett* 31:199–219

---

# Freeze-Thaw and UV Resistance in Building Stone Coated with Two Permanent Anti-graffiti Treatments

94

Paula María Carmona-Quiroga, María Teresa Blanco-Varela,  
and Sagrario Martínez-Ramírez

---

## Abstract

Cultural heritage weathering by traditional agents (water, air pollutants, biological agents and so on) is aggravated by direct human action in the form of graffiti. New protective treatments have been developed to counter the visual impact and deterioration induced by such vandalism. While these coatings prevent paint from penetrating in the pore systems of construction materials or from adhering to their surface by lowering surface energy, their application to historic buildings and monuments is restricted. This study aims to contribute to the *acquis* on the performance and compatibility of these protective treatments in the context of the conservation of historic building materials. More specifically, it explores the durability of two stones (granite and limestone) protected with two permanent anti-graffiti coatings (a fluorosiloxane and a Zr-ormosil) when exposed to a total of 30 freeze-thaw cycles and 2,000 h of UVA radiation with water spray in a QUV weathering tester. The results of the two durability tests conducted revealed that both coatings accelerated limestone deterioration by obstructing the egress of water trapped in the pore systems during successive thawing episodes. By contrast, granite showed no external signs of damage. Colour analysis detected no visible decay in either of the coated limestone surfaces after UV radiation (no yellowing or darkening). The chromatic heterogeneity of granite rendered similar analysis impractical.

---

## Keywords

Anti-graffiti coating • Freeze-thaw • UV radiation • Ormosil • Stone

---

## 94.1 Introduction

Graffiti, a new form of damage to building façades, jeopardises the integrity of the architectural heritage (Chapman 2000). Such deliberate drawing or writing on building surfaces with paints or pigments is especially pernicious, since

removal with chemical or mechanical procedures often necessarily alters the surface of the building material, rendering it more vulnerable to penetration by pigment and dirt.

One possible solution may be the use of anti-graffiti coatings. These products prevent paint from penetrating into the pore systems of construction materials or adhering to their surface by lowering the surface energy of the substrate and facilitating the ready removal of spray paint and similar. They are classified as sacrificial, semi-permanent or permanent depending on the number of graffiti cleaning cycles they can withstand: one, several or more than ten, respectively (García and Malaga 2012).

Nonetheless, very few studies have been conducted on their performance/durability in historic buildings, whose façades are usually weathered.

---

P.M. Carmona-Quiroga (✉) · M.T. Blanco-Varela ·  
S. Martínez-Ramírez  
Eduardo Torroja Institute for Construction Science  
(IETCC-CSIC), 28033 Madrid, Spain  
e-mail: blancomt@ietcc.csic.es

S. Martínez-Ramírez  
Institute for the Structure of Matter (IEM-CSIC), 28006 Madrid,  
Spain

**Table 94.1** Water porosity and water vapour permeability of the substrates before and after anti-graffiti treatment

		Water accessible porosity	Water vapour permeability at 20 °C
Limestone	Untreated*	7 % vol	6.5 g cm/m <sup>2</sup>
	Decline with fluorinated product*	0 %	15 %
	Decline with Zr-ormosil	13 %	29 %
Granite	Untreated*	0.5 % vol	0.5 g cm/m <sup>2</sup>
	Decline with fluorinated product*	0 %	1 %
	Decline with Zr-ormosil	80 %	19 %

\*data from Carmona-Quiroga et al. (2008)

This study aims to expand on the existing knowledge of the interaction between two of these permanent protective treatments, a fluoroalkylsiloxane and a Zr-ormosil, and two stone materials, a granite (“Gris Quintana”) and a limestone (“Blanco Paloma”). Prior studies addressed the photochemical stability of the coatings alone and their effectiveness in protecting stone against sulfite and sulfate formation in simulated SO<sub>2</sub>-polluted environments (Carmona-Quiroga et al. 2010 and 2013, respectively).

Although the application of permanent coatings to heritage buildings and monuments has been banned in some European countries due to the irreversibility of the procedure, today reversibility appears to be less of a concern than compatibility and re-treatability (Price 1996).

Two durability tests were conducted on the coated stones to characterise treatment-stone interactions. Freeze-thaw cycles were conducted because water, the main decay-inducing agent in building materials, is normally used to clean protected surfaces. UV radiation trials, in turn, were performed to test the chemical stability of the coatings on the stone surfaces.

## 94.2 Experimental

Two stone surfaces with different compositions and porosities, “Blanco Paloma” limestone (Seville, Spain) and “Gris Quintana” granite (Badajoz, Spain) were treated with two anti-graffiti coatings. One was a commercial water-based fluoroalkylsiloxane and the other an organically modified silicate (ormosil) synthesised from polydimethylsiloxane (PDMS) and two network-forming alcoxides (Zr propoxide and MTES) dissolved in n-propanol (Oteo et al. 1999).

Two procedures were used to apply the coatings: (i) in one a single coat of product was brushed onto the surface of the materials (used for samples exposed to UVA radiation) and (ii) and in the other samples were submerged for 1 min in the anti-graffiti product (for the samples exposed to freeze-thaw

cycles) to ensure homogeneous distribution on all sample surfaces, and not only on one side.

The findings on stone petrography, mineralogical composition and hydric properties (porosity, permeability) and the cleaning efficiency of the (brush-on) coating were reported in a prior paper (Carmona-Quiroga et al. 2008). The results listed in Table 94.1 show that ormosil filled the pores, reducing material porosity and permeability, whereas the fluorinated treatment covered the pores only superficially.

Thirty freeze-thaw cycles were conducted on the treated and untreated stone specimens to determine their durability. The samples were immersed in a water tank at 15 ± 5 °C for 48 h prior to exposure. The samples were subsequently stored for 16 h at −18 °C and then allowed to thaw for 8 h. Treated and untreated stones were also exposed to 2,000 h of UVA radiation (0.71 W/m<sup>2</sup> at 340 nm) in a QUV/spray (Q-Lab Corporation) weathering chamber pursuant to the experimental conditions defined in ISO standard 4892-3 (water spray cycles during constant UV exposure). L\*a\*b\* colour coordinates were found for the stone before and after UV exposure with a Minolta CM 2500 D portable spectrophotometer.

## 94.3 Results and Discussion

### 94.3.1 Freeze-Thaw Cycles

The freeze-thaw cycles induced decay in the limestone specimens, which was hastened by the presence of the two anti-graffiti coatings, especially the fluorinated product. The granite specimens, by contrast, were unaltered (Fig. 94.1) by exposure to these cycles.

While the untreated limestone specimens began to exhibit minor pitting immediately after conclusion of the trial (Fig. 94.1a), the samples coated with the fluorinated product began to crack after the 15th cycle and had disintegrated entirely by the 30th (Fig. 94.1b). The earliest symptoms of

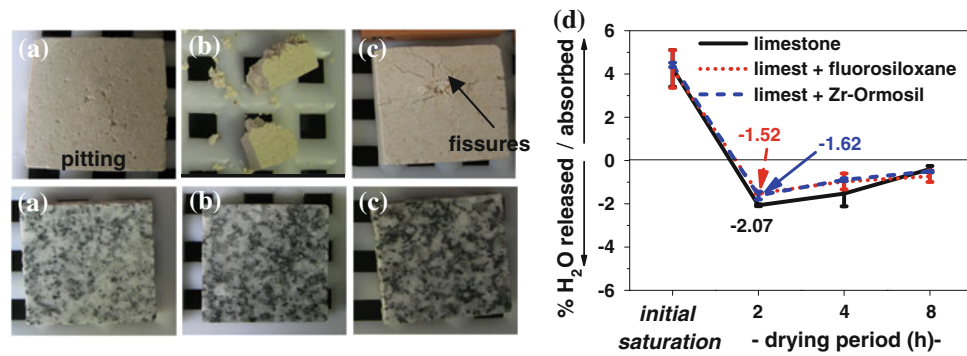


**Fig. 94.1** Limestone (*above*) and granite (*below*) after 30 freeze-thaw cycles: **a** uncoated; **b** coated with the fluorinated anti-graffiti product; **c** coated with Zr-ormosil; **d** water desorption at room temperature in treated and untreated limestone

**Table 94.2** Chromatic parameters for coated and uncoated stone after exposure to 2,000 h of UVA radiation and water spray

		$\Delta L^*$	$\Delta a^*$	$\Delta b^*$	$\Delta E^*$
Limestone	Untreated	$-1.15 \pm 0.79$	$-0.82 \pm 0.07$	$-0.33 \pm 0.70$	$1.61 \pm 0.39$
	Fluorinated	$1.05 \pm 0.52$	$-0.28 \pm 0.05$	$-2.92 \pm 0.54$	$3.15 \pm 0.32$
	Zr-ormosil	$0.19 \pm 1.52$	$-0.28 \pm 0.15$	$-0.61 \pm 0.53$	$1.29 \pm 0.50$
Granite	Untreated	$2.32 \pm 1.72$	$-0.11 \pm 0.01$	$0.04 \pm 0.35$	$2.35 \pm 1.69$
	Fluorinated	$2.42 \pm 1.58$	$0.22 \pm 0.08$	$-1.35 \pm 0.08$	$2.83 \pm 1.38$
	Zr-ormosil	$4.29 \pm 3.05$	$-0.02 \pm 0.07$	$-0.25 \pm 0.01$	$4.30 \pm 3.04$

$L^*$  = luminosity;  $a^*/-a^*$  = red/green axis,  $b^*/-b^*$  = yellow/blue axis.  $\Delta E^*$  (total colour variation) =  $(\Delta L^{*2} + \Delta a^{*2} + \Delta b^{*2})^{1/2}$

pitting in the ormosil-coated specimens appeared after 21 cycles and progressed rapidly (although more gradually than in the samples treated with the other coating), favouring material loss (Fig. 94.1c). The explanation for such accelerated decay is illustrated in Fig. 94.1d, which depicts water desorption at ambient temperature in the treated and untreated limestone specimens. Both treatments hindered the egress of the water absorbed by the specimens after submersion at atmospheric pressure for 48 h: after 2 h of drying at ambient temperature, 27 % less water was released by the fluorinated and 22 % less by the ormosil samples than by the untreated specimens. Consequently, during the freeze-thaw cycles, these coatings would favour a gradual increase in the initial saturated water content and ultimately generate higher pressure.

### 94.3.2 UV Radiation

The main agent of decay in surface treatments is ultraviolet radiation, which can alter the original colour of the impregnated materials (Fortes-Revilla and Blanco-Varela 2001). Hence the need for studies on the subject.

Prior to UV radiation, the chromatic variations generated in the substrates by the anti-graffiti coatings were recorded.

The limestone surface darkened and yellowed slightly under both, although the total colour variation,  $\Delta E^* < 3$ , was imperceptible to the naked eye (Prieto et al. 2010). In light of the chromatic heterogeneity of granite, changes in the colour of the stone ( $\Delta E^* \approx 6-12$ ) due primarily to a decrease in luminosity (from 73 to 67–61) could be not be analysed straightforwardly.

After 2,000 h of exposure to UV and water spray, the change in surface colour on the treated and untreated limestone was imperceptible (Table 94.2) to the naked eye, pursuant to the thresholds defined by Di Gennaro et al. (2002) and Prieto et al. (2010):  $\Delta E^* < 5$  and  $\Delta E^* < 3$ , respectively. The surfaces treated neither yellowed ( $b^*$  did not rise) nor darkened ( $L^*$  did not decline) after the ageing trials. Moreover, while the untreated limestone darkened after exposure to radiation and water spray, both the fluorinated and the ormosil coatings prevented such soiling-induced darkening.

In granite, the only variation in the colour coordinates recorded was for lightness ( $L^*$ ) on the ormosil-coated surfaces (Table 94.2), a finding that could not be regarded as significant, given the polymineral (polychromatic) nature of this substrate.

These results were consistent with the FTIR findings for the treatments themselves reported in a prior paper

(Carmona-Quiroga et al. 2013), according to which neither exhibited decay after exposure to 2,000 h of UV radiation.

#### 94.4 Conclusions

An understanding of the durability of new anti-graffiti coatings is imperative to ensure that their application to the architectural heritage will not induce decay in the long run. This study proved that the two permanent anti-graffiti coatings analysed hasten decay in limestone exposed to freeze-thaw cycles by hindering the egress of water from the pore system during the successive freezing episodes. Substrate permeability is nonetheless known to be affected by the manner in which the coatings are applied (here submersion instead standard brush application).

Both treatments are stable under photo-oxidising conditions, according to the minimal colour variations, imperceptible to the naked eye ( $\Delta E^* < 3$  or  $< 5$ ), detected on the limestone surface. The chromatic heterogeneity of granite ruled out similar analysis of this stone.

**Acknowledgments** This research was funded by the Spanish Ministry of Education and Science (MAT 2003-08343 and CONSOLIDER CSD2007-00058 Projects) and the Autonomous Community of Madrid (Geomaterials Programme S2009/MAT-1629). Author Carmona participated in this study on an integrated employability pathway pre-doctoral grant (I3P) awarded by the European Social Fund and the Spanish National Research Council (CSIC), under the aegis of the CSIC's Theme Network on Cultural Heritage.

#### References

- Carmona-Quiroga PM, Martínez-Ramírez S, Blanco-Varela MT (2008) Fluorinated anti-graffiti coating for natural stone. *Materiales de Construcción* 58(289–290):233–246
- Carmona-Quiroga PM, Panas I, Svensson J-E, Johansson L-G, Blanco-Varela MT, Martínez-Ramírez S (2010) Protective performances of two anti-graffiti treatments towards sulfite and sulfate formation in SO<sub>2</sub> polluted model environment. *Appl Surf Sci* 257(3):852–856
- Carmona-Quiroga PM, Blanco-Varela MT, Martínez-Ramírez S (2013) Permanent antigraffiti for artificial construction materials: lime mortar and brick. In: Rogerio-Candelera MA, Lazzari, M, Cano E (eds) *Science and technology for the conservation of cultural heritage*. CRC Press, The Netherlands, pp 311–314
- Chapman S (2000) Laser technology for graffiti removal. *J Cult Heritage* 1(1):S75–S78
- Fortes-Revilla C, Blanco-Varela MT (2001) Influence of water-repellent treatment on the properties lime and lime pozzolan mortars. *Materiales de Construcción* 51(262):39–52
- Di Gennaro F, Ferrari A, Pagella C, Cervellati G (2002) Petrographic study on effectiveness of antigraffiti protective treatment (Part 1-Stony materials of carbonatic composition). *Pitture e Vernici, European Coatings* 78:23–31
- García O, Malaga K (2012) Definition of the procedure to determine the suitability and durability of an anti-graffiti product for application on cultural heritage porous materials. *J Cult Heritage* 13(1):77–82
- Oteo, JL, Rubio, J and Rubio F (CSIC) 1999, *Materiales termohíbridos inorgánico-orgánicos de baja densidad y su procedimiento de obtención*, Spanish Patent 9901977
- Price CA (1996) *Stone conservation: an overview of current research*. The Getty Conservation Institute, California
- Prieto B, Sanmartín P, Silva B, Martínez-Verdú F (2010) Measuring the color of granite rocks: a proposed procedure. *Color Res Appl* 35(5):368–375

---

# Monitoring of Cultural Heritage Decay in Rome: Analysis of Soiling and Erosion Phenomena

95

Raffaella Gaddi, Mariacarmela Cusano, Patrizia Bonanni, Carlo Cacace, and Annamaria Giovagnoli

---

## Abstract

Particulate matter deposition on cultural heritage facades is a process that can produce optical and structural decay. Usually, the forms of superficial deterioration caused by atmospheric pollutants are related to erosion and soiling phenomena. During 2013 in Rome, a monitoring campaign was realized to collect data at local level to study, in time, the effects of soiling and erosion on the materials constituting cultural heritage. This experimental analysis was aimed to evaluate the damage caused by particulate matter deposition (PM<sub>10</sub> and PM<sub>2.5</sub>) and the material loss, due to the action of atmospheric pollutants and climatic factors, on marble, glass and copper. The monitoring campaign was managed exposing samples of the three materials close to seven air quality monitoring stations, located in Rome within the Great Ring Road, to have available also air pollutant concentration data. Concerning the soiling phenomena analysis, colour changing measurements have been realized periodically on marble and glass samples to verify the luminosity variation ( $\Delta L^*$ ) caused by particulate matter deposition. Regarding erosion assessment, weight change measurements were realized on marble and copper based samples. This approach, at local level, allows to follow the decay trend of those monuments potentially exposed to soiling and erosion risk and consequently, if necessary, to plan monitoring and maintenance activities of the works of art, reducing the dangerous effects of pollutant deposition.

---

## Keywords

Soiling • Corrosion • Marble • Glass • Copper

---

## 95.1 Introduction

The historical building decay, in polluted urban areas, can be caused by the synergic action of climatic factors (precipitation, relative humidity, temperature) and atmospheric

pollutants (gases and particulate matter). In this study, two deterioration typologies, which are commonly observed on the cultural heritage, have been examined: *soiling* and *material loss (erosion/corrosion)*.

The monitoring campaign was started in Rome, in March 2013, by the National Italian Institute for Environmental Protection and Research (ISPRA) and the Superior Institute for Conservation and Restoration (ISCR), in collaboration with Regional Environmental Protection Agency of Lazio (ARPA Lazio).

The experimental study aims to analyze the potential decay affecting some of the materials constituting the Italian Cultural Heritage such as marble, glass and metal.

---

R. Gaddi (✉) · M. Cusano · P. Bonanni  
ISPRA, National Italian Institute for Environmental Protection and Research, Via V. Brancati 48, 00144 Rome, Italy  
e-mail: raffaella.gaddi@isprambiente.it

C. Cacace · A. Giovagnoli  
ISCR, Superior Institute for Conservation and Restoration, Via di San Michele 23, 00153 Rome, Italy

In particular, the project is finalized to study in Rome, corrosion and soiling phenomena to identify specific algorithms (Brimblecombe and Grossi 2004; Watt et al. 2008) that can describe the correlation between the “dose” (the concentrations of air pollutants and climatic parameters) and the “response” (the damage suffered by exposed materials). Carrara marble and glass specimens (microscope slides) were exposed for the evaluation of soiling processes while marble and copper based samples were positioned for the analysis of corrosion/erosion mechanisms (Urosevic 2012; Lombardo et al. 2010).

The samples were placed vertically both rain-sheltered and unsheltered, in order to evaluate the pollutant effects on the exposed materials in these two different conditions. The experimental campaign, lasting 2 years, has been conducted at seven of the thirteen air quality monitoring public stations in Rome, where exposure racks, containing the samples to be analyzed, were set.

In this article, the preliminary results of the monitoring campaign, that will finish in March 2015, will be shown.

## 95.2 Monitoring Campaign and Samples

The monitoring campaign consists of exposure of different material samples, inside the fences surrounding the air quality monitoring stations in Rome, managed by ARPA Lazio. The study was carried out near four urban background stations (Arenula, Cinecittà, Cipro, Villa Ada) and near three urban traffic stations (Corso Francia, Fermi, Largo Magna Grecia) within the Great Ring Road.

In the considered monitoring stations, canopy exposure racks were placed. Each exposure rack contains: unpolished Carrara marble samples and microscope glass slides for soiling assessment; unpolished Carrara marble samples for measurements of deposited material composition by Scanning Electron Microscope (SEM) analysis.

In Corso Francia and Largo Magna Grecia stations, polished marble specimens and copper based samples were also exposed to assess the erosion/corrosion phenomena. In these two sites two uncovered exposure racks, containing marble, glass and copper based samples, were also positioned to compare the effects of air pollution and climate factors on rain- sheltered and unsheltered conditions.

## 95.3 Measures

The study of soiling is realized on the unpolished marble specimens and on microscope slides placed on each exposure rack.

The color measurements have been carried out by using a compact portable spectrophotometer Minolta CM-700d. This analysis allows to measure colorimetric parameters  $L^*$ ,  $a^*$  and  $b^*$ <sup>1</sup> in time, to check a possible variation caused by air pollutant deposition on exposed materials.

For the marble specimens, optical measurements have been made with the SCI method,<sup>2</sup> while for glass samples, the measure have been made using the SCI and SCE<sup>3</sup> methods. All optical measurements have been carried out by using the standard illuminant D65.

These measures have been periodically executed in situ and compared to the data collected before exposure. The obtained values will be correlated with annual concentrations of  $PM_{10}$  and  $PM_{2.5}$  (where the latter is measured) to identify the algorithm that best describes the relationship between the material decay and the air pollutant concentrations.

The erosion/corrosion phenomenon will be estimated on polished marble and copper specimens at the end of monitoring campaign (Tzanis et al. 2011). The evaluation of the possible corrosion is based on measures of weight for marble samples and on measures of weight and color variation (method SCI and SCE) for copper.

## 95.4 Preliminary Results

In this chapter the results, regarding soiling phenomena, obtained in the first year of the campaign are shown, although the dose-response functions for the soiling of the considered materials can be obtained only at the end of the monitoring campaign, after the collection of all data necessary for the definition of the algorithms. In the graphs below, the trend of luminosity ( $L^*$ ), measured in SCI method (Fig. 95.1) on marble specimens is reported from March 2013 (beginning of exposure) up to March 2014.

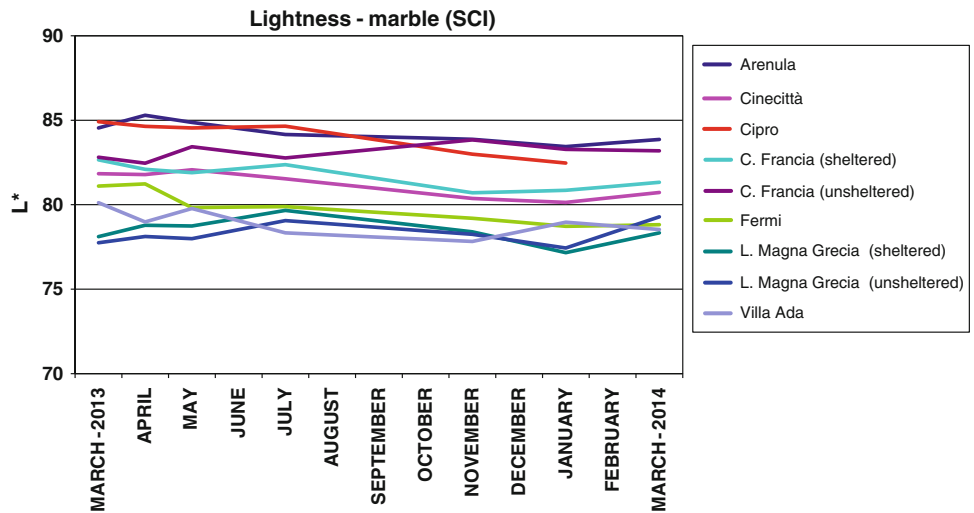
Figure 95.1, relating to marble specimens, shows a slight decrease of Luminosity except for unsheltered samples in Corso Francia and Largo Magna Grecia.

<sup>1</sup> The difference between two colors is defined by  $\Delta E = [(\Delta L^*)^2 + (\Delta a^*)^2 + (\Delta b^*)^2]^{1/2}$ .

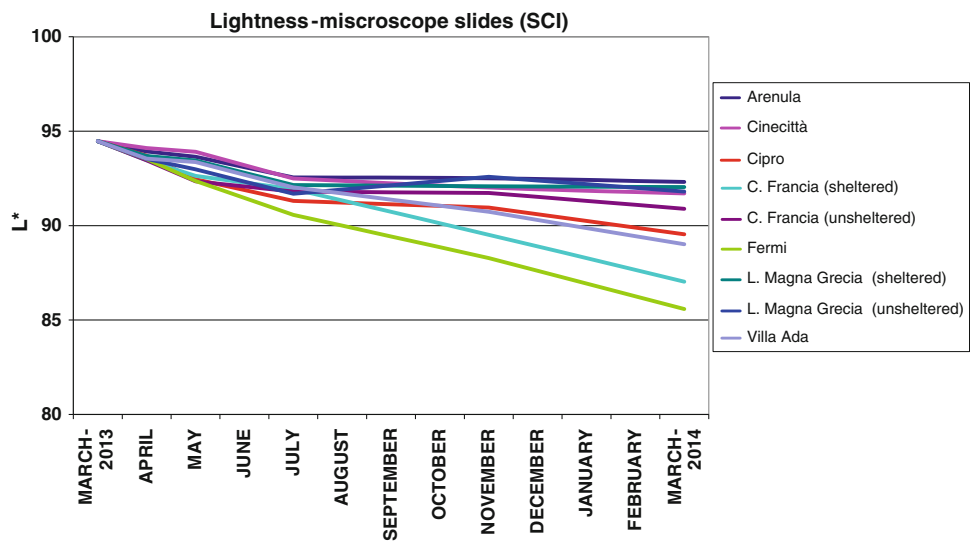
<sup>2</sup> SCI (Specular Component Included). SCI method measures the specular reflectance and the diffuse reflectance (total reflectance). This type of color evaluation measures total appearance regardless of surface conditions.

<sup>3</sup> SCE (Specular Component Excluded). In SCE mode, the specular reflectance is excluded from the measurement so this mode includes only the diffuse reflectance. For objects with shiny surfaces, the specularly reflected light is relatively intense and the diffused light is weaker. To measure the color of a sample in the same way that it is viewed, it is necessary to exclude the specular reflectance and measure only the diffuse reflectance.

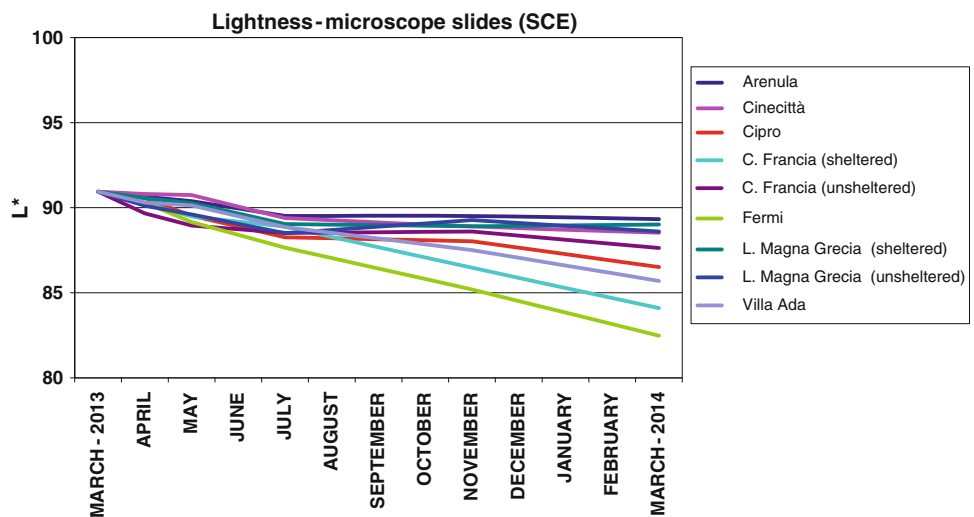
**Fig. 95.1** Luminosity L\*(SCI) trend for marble samples at the seven selected sites



**Fig. 95.2** Luminosity L\* (SCI) trend for glass samples at the seven selected sites

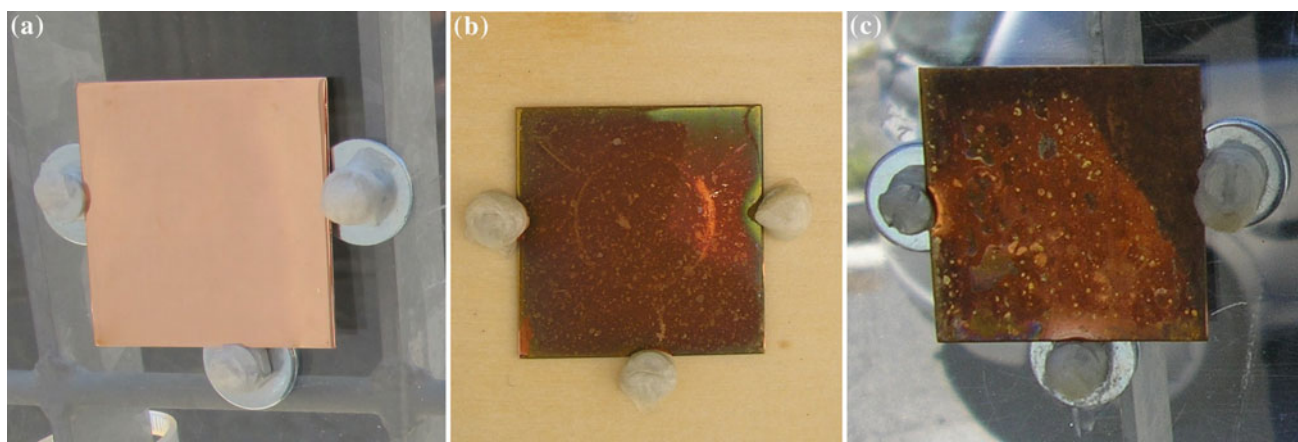


**Fig. 95.3** Luminosity L\*(SCE) trend for glass samples at the seven selected sites



**Table 95.1** L\*, a\*, b\* and  $\Delta E$  values for copper based samples in Corso Francia and Largo Magna Grecia monitoring sites after six month exposure

SCI	$\Delta L^*(t_6 - t_0)$	$\Delta a^*(t_6 - t_0)$	$\Delta b^*(t_6 - t_0)$	$\Delta E(t_6 - t_0)$
L.M. Grecia—S	-33.3	1.9	9.2	34.6
L.M. Grecia—U	-35.2	0.9	4.5	35.5
C. Francia—S	-33.0	1.2	10.6	34.7
C. Francia—U	-44.0	-6.8	-6.7	45.0
SCE	$\Delta L^*(t_6 - t_0)$	$\Delta a^*(t_6 - t_0)$	$\Delta b^*(t_6 - t_0)$	$\Delta E(t_6 - t_0)$
L.M. Grecia—S	32.0	11.9	33.6	47.8
L.M. Grecia—U	32.5	12.5	28.0	44.7
C. Francia—S	34.8	11.7	32.0	48.7
C. Francia - U	20.5	4.7	9.7	23.2

**Fig. 95.4** Copper samples: **a** sample before exposure; **b** sheltered sample after six-month exposure; **c** unsheltered sample after six-month exposure

In Figs. 95.2 and 95.3 measurements on glass specimens in SCI and in SCE methods are respectively shown from March 2013 (beginning of exposure) up to March 2014.

The exposed microscope slides (Figs. 95.2 and 95.3) appear to show a gradual decrease of L\* in time in all analyzed sites.

For copper based samples, currently, the color measures of L\*, a\* and b\* after six month exposure (from July 2013 up to January 2014), are reported in Table 95.1 for sheltered (S) and unsheltered (U) specimens in Largo Magna Grecia and in Corso Francia stations using SCI and SCE methods.

In both sites, after 6 months,  $\Delta E$  values are very high showing a significant change of surface characteristics; the coupon surface indeed appeared particularly opaque and grayish for the presence of copper corrosion products (Fig. 95.4).

## 95.5 Conclusion

The methodological approach appears to provide the expected results. During the reporting period, the copper based coupons seem to be a very react substrate for

calculating the corrosion rate, instead marble and glass materials are very appropriate for soiling evaluations. All results must be verified at the end of the experimentation.

## References

- Brimblecombe P, Grossi CM (2004) The rate of darkening of material surfaces. In: Saiz-Jimenez C (ed) Air pollution and cultural heritage, pp 193–198
- Lombardo T, Ionescu A, Chabas A, Lefevre RA, Ausset P, Candau Y (2010) Dose-response function for the soiling of silica-soda-lime glass due to dry deposition. *Sci Total Environ* 408:976–984
- Tzani C, Varatos C, Christodoulakis J, Tidblad J, Ferm M, Ionescu A, Lefevre R-A, Theodorakopoulou K, Kreislova K (2011) On the corrosion and soiling effects on materials by air pollution in Athens, Greece. *Atmos Chem Phys* 11:12039–12048
- Urosevic M, Yebra-Rodriguez A, Sebastian-Pardo E, Cardell C (2012) Black soiling of an architectural limestone during two-year exposure to urban air in the city of Granada (Spain). *Sci Total Environ* 414:564–575
- Watt J, Jarett D, Hamilton R (2008) Dose-response functions for the soiling of heritage materials due to air pollution exposure. *Sci Total Environ* 400:415–424

---

# Fluorescent Microscopy of Stained Thin Sections: A Direct Tool for the Evaluation of Pore Space Characteristics in Porous Rocks

96

Richard Přikryl

---

## Abstract

An enhanced microscopic analysis of pore spaces, as an important part of the entire rock fabric, is proposed. It is based on a special preparatory technique of thin sections. The technique consists of a two-step fixation of porous specimens: the staining of the pore space with a mixture of a low viscosity epoxy resin and a fluorescent dye. The technique is primarily designed to increase the contrast between the pores and rock-forming minerals, and to enhance their microscopic observability. This method can also be used for description of the crack/pore geometry, as well as for the interpretation of other porosimetric parameters.

---

## Keywords

Pore space • Staining technique • Ultraviolet microscopy

---

## 96.1 Introduction

Any types of voids (macro- or micropores and/or cracks) in a rock make up part of the pore space. The proportion of pore space to the unit bulk volume of a rock is usually expressed in petrophysics as the porosity ( $\phi$ ) (Schön 2004). However, the expression of porosity by one number is highly insufficient when the contribution of a complex pore space to that of the whole rock microfabric (or other rock properties) is to be studied. Although some indirect methods such as mercury porosimetry (Rübner and Hoffmann 2006) are conventionally used for the quantification of selected textural properties of pores, as well as the evaluation of pore types, size, geometry, and their relationships to other rock fabric elements, However, these can only be performed by direct (mostly microscopic) observation. From the numerous techniques proposed in the past for visualization of the pore space (Table 96.1), most present some limitations in terms of

their application to the broader range of rock types, the application of special observational techniques, and/or on the possibility to study the specimens by other methods.

This paper intends to summarize a modified procedure for pore space staining prior to the preparation of thin sections. The combination of favourable physical properties of the epoxy resin and the colourant allows for preparation of thin sections from specimens demonstrating various degrees of disintegration.

---

## 96.2 Procedure of Specimen Preparation

The specimen preparation procedure consists of the following steps:

- (1) penetration of the sample before cutting it with a diamond saw;
- (2) diamond-saw cutting of the plane that will later be glued to the glass plate;
- (3) fine grinding of the sawn surface by a diamond paste;
- (4) ultrasonic cleaning and removal of particles produced by the cutting and grinding;
- (5) drying of the sample to a constant weight at a temperature not exceeding 45 °C;

---

R. Přikryl (✉)  
Institute of Geochemistry, Mineralogy and Mineral Resources,  
Faculty of Science, Charles University in Prague, Albertov 6,  
128 43 Prague 2, Czech Republic  
e-mail: prikryl@natur.cuni.cz

**Table 96.1** Overview of methods used for the visualization of microcracks or micropores in rocks

Method of crack/pore pre-observational treatment	Study technique	Reference
Rock surface removal by ion-thinning	SEM, TEM	Barber (1970), Sprunt and Brace (1974), Dengler (1976)
Carbon decoration by precipitation from furfuryl alcohol	Naked eye or optical microscope	Simmons et al. (1975), Simmons and Richter (1976)
Electrochemical deposition of copper into the cracks	Optical microscope	Simmons and Richter (1976)
Suction of an index oil into the evacuated cracks	Optical microscope	Simmons and Richter (1976)
Pore casting technique with a suitable plastic under vacuum or elevated pressure and later leaching of rock material	Optical microscope	Nuss and Whiting (1947), Pittman and Duschatko (1970), Pittman (1971), Wardlaw (1976)
Replication of cracks by applying acetylcellulose replicating film on a polished surface	SEM or optical microscope	Kobayashi and Fourney (1978)
Spraying fluorescent dyes onto the polished surfaces	Naked eye	Ali and Weiss (1968), Gradner and Pincus (1968), D'Andrea and Condon (1971), Walsh (1974), Kelsall et al. (1986), Lindqvist et al. (1994)
Staining of a thin section after its preparation	Optical microscope	Ruzyla and Jezek (1987)
Staining of bulk samples in water soluble liquids (e.g., fluorescein, India ink, drawing ink)	Optical microscope, SEM	Rassineux et al. (1987), Alber and Hauptfleisch (1999)
Filling of voids and fractures by a molten metal with a low melting point (Wood's metal)	Optical microscope, SEM	Scrivener and Nemati (1996), Carpinteri et al. (1997), Nemati et al. (1998)
Polished sections deposited by a layer of gold-palladium	Ultraviolet light, naked eye	Friedman and Johnson (1978)
Chemical contact imagery by saturating cracks with sulphidic solution and imprinting of the surface on a photographic film wetted with sulphuric acid	Photographic film	Zinke et al. (1993), Zang et al. (1996)
Audioradiographic crack mapping	Photographic film	Wu et al. (1978)
Saturation of a sample with blue-dyed epoxy, with a methyl metacrylate—fluorescent dye mixture, or with an epoxy resin—fluorescent dye mixture under vacuum	Optical microscope equipped with UV light	Anselmetti et al. (1998), Caye et al. (1970), Nishiyama and Kusuda (1994, 1996), Chen et al. (1999, 2000), Montoto et al. (1980), Hakami (1995), Přikryl and Kou (1996), Persson (1998), Přikryl (1998)

- (6) a successive penetration on the cut plane in order to penetrate non-interconnected voids that had not been accessible during the first penetration; this step preferably conducted under vacuum, in which it was held until air bubbles stopped rising;
- (7) gentle grinding of excess hardened epoxy resin—fluorescent dye mixture from the surface of the sample;
- (8) preparation of an ordinary thin section (without a cover glass).

The rock slabs were diamond sawn from oriented blocks, and then carefully polished by diamond paste. The polished surfaces were washed with clean water. The additional cleaning with ultrasonic equipment ensured the removal of any particles loosened during polishing from the microcracks and/or pores. The slabs were then thoroughly dried.

Dry samples, stored in a mould, were placed in the vacuum chamber and kept under vacuum for about 20 min. An admixture of epoxy resin and fluorescent dye (EPODYE, Struers, Denmark) was introduced into the mould after vacuuming of the dry samples. Any commercial epoxy resin is applicable, but those with a low viscosity are highly advantageous. In this study, CHS EPOXY 513 (Spolchemie, Czech Republic) was applied because of its low viscosity (180 mPa.s at 25 °C), thus allowing its penetration into even minute microcracks. The vacuum was held until air bubbles stopped rising. The samples were removed from the mould when the resin started to polymerise.

After 24 h of hardening, the excess resin on the polished rock surface was carefully polished away. Uncovered thin sections were prepared by standard procedures.

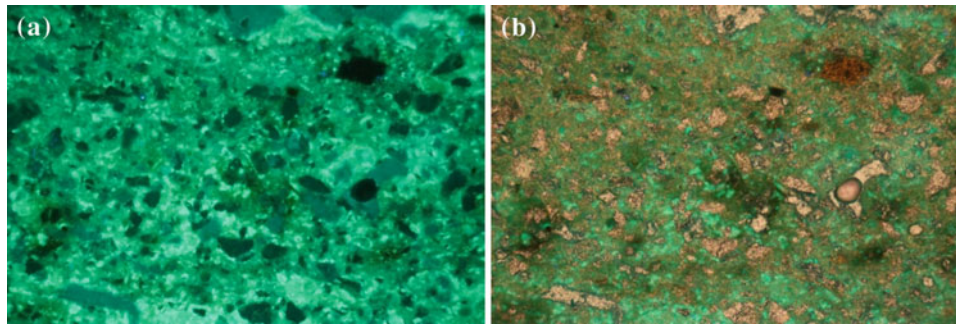


**Fig. 96.1** **a** Pore space of an extremely fine-grained, highly porous clayey-calcareous silicite, as seen under UV reflected light mode. The length of the observed field is about 4 mm, **b** Rock microfabric of the

same rock type, viewed by the combination of UV reflected light and transmitted non-polarized visible light

An uncovered thin section can be observed through a conventional optical polarizing microscope equipped with a source of ultraviolet light. The photomicrographs can either be captured on a sensitive film (KODAK GOLD 400 ASA) or recorded by means of digital photography (Fig. 96.1).

### 96.3 Discussion of the Various Preparatory Methods, and Summary

All of these techniques mentioned have their advantages and drawbacks. The proper method should be selected depending on the aim of the study. The technique of furfuryl alcohol (carbon decoration method) can be very dangerous for a sample from the point of view of introducing new microcracks due to the heating of the sample (compare Simmons et al. 1975). The high temperatures applied during carbon deposition can cause thermal stresses exceeding the strength of homogeneous minerals or intergrain bonds. Pore casting methods are advantageous when a realistic 3-D model of the pore/crack system is desirable, but are limited for readily soluble rocks such as limestones. The disadvantage arises from the fact that the original rock must be dissolved—and this can only be relatively easily applied for calcite-bearing carbonate rocks. Thus, it is not possible to simultaneously observe both the microcrack/pore fabric and the fabric of the crystalline framework.

The epoxy resin—fluorescent dye mixture is the only pore/crack casting method applicable for macro- as well as microfabric analysis of pores and cracks. The obvious advantage of using a low viscosity, slow hardening epoxy over quick hardening metacrylates (compare Nishiyama and Kusuda 1994; 1996; Chen et al. 1999) is evident due to the longer time available for the impregnation of even minute cracks. The impregnation of samples by an epoxy resin—fluorescent dye mixture facilitates the fluorescent dye's stability in the crack/pore space during thin section preparation compared to water soluble penetrants (Rassineux et al. 1987;

Alber and Hauptfleisch 1999). Epoxy can also increase the cohesion of some weak rocks such as highly porous sandstones or tuffs. On the other hand, the use of fluorescent dyes together with other liquids is restricted to the observation of larger cracks visible to the naked eye.

One controversial point involves the sample sawing prior to its impregnation. Nishiyama and Kusuda's approach (1994) of sample impregnation prior to sectioning presumes the connectivity of all microcracks/micropores in the sample. As this might not be valid for all rocks, it is helpful to carefully diamond saw the sample prior to impregnation; extensively weathered samples being the only exception.

The impossibility to distinguish among cracks of different origins presents a limitation of the current methods. For example, the laboratory stress-induced cracks cannot be fully separated from cracks originally present in the rocks. The only possibility is to study the crack density, geometry, and spatial distribution in the original intact rock, as well as in a stressed sample, and then to express the new (stress-induced) crack population as the difference between the two aforementioned crack fabrics. On the other hand, the advantages encompass clear crack detection due to the dye used, and increased cohesion of weak, non-cohesive (or weathered or stressed) materials.

**Acknowledgements** This study was kindly supported by the Czech Ministry of Education, Youth and Sports (Project MSM 0021620855 "Material flow mechanisms in the upper spheres of the Earth") and Czech Science Foundation (Project No. 13-13967S "Experimental study of crack initiation and crack damage stress thresholds as critical parameters influencing the durability of natural porous stone").

### References

- Alber M, Hauptfleisch U (1999) *Int J Rock Mech Min Sci Geomech Abstr* 36:1065  
 Ali SA, Weiss MP (1968) *J Sed Petrol* 38(2):681  
 Anselmetti FS, Luthi S, Eberli GP (1998) *AAPG Bull* 82(10):1815  
 Barber DJ (1970) *J Mater Sci* 5:1  
 Carpinteri A, Chiaia B, Nemati KM (1997) *Mech Mat* 26:93

- Caye R, Pierrot R, Ragot JP (1970) *Bull Soc Fr Min Crist* 93:571
- Chen Y, Nishiyama T, Kusuda H, Kita H, Sato T (1999) *Int J Rock Mech Min Sci Geomech Abstr* 36:535
- Chen Y, Nishiyama T, Terada M, Iwamoto Y (2000) *Eng Geol* 56:395
- D'Andrea DV, Condon JL (1971) In: 12th U.S. symposium on rock mechanics, AIME, New York, NY, 1971
- Dengler L (1976) In: Wenk H-R (ed) *Electron microscopy in mineralogy*. Springer, Berlin, p 550
- Friedman M, Johnson B (1978) In: Proceedings of the 19th U.S. symposium of rock mechanics, Reno, Nevada
- Gardner RD, Pincus HJ (1968) *Int J Rock Mech Min Sci* 5:155
- Hakami E (1995) Dissertation. Royal Institute of Technology, Stockholm
- Kelsall PC, Watters RJ, Franzone JG (1986) In: Proceedings of the 27th U.S. symposium on rock mechanics "Rock mechanics: key to energy production". Tuscaloosa (Alabama), June 23–25, 1986
- Kobayashi T, Fourney WL (1978) In: Proceedings of the 19th U.S. symposium of rock mechanics. Reno, Nevada
- Lindqvist P-A, Suarez LM, Montoto M, Tan XC, Kou SQ (1994) *Rock indentation database: testing procedures, results and main conclusions (SKB report: Pr 44-94-023, Sweden, 1994)*
- Montoto M, Montoto L, Röshoff K, Leijon B (1980) In: *Subsurface space, proceedings of the international symposium (Rockstore '80)*. Stockholm, Sweden, June 23–27, 1980
- Nemati KM, Monteiro PJM, Cook NGW (1998) *J Mat Civ Eng* 10 (3):128
- Nishiyama T, Kusuda H (1994) *Int J Rock Mech Min Sci Geomech Abstr* 31:369
- Nishiyama T, Kusuda H (1996) *Eng Geol* 43:247
- Nuss WF, Whiting RL (1947) *Bull AAPG* 31(11):2044
- Persson A-L (1998) *Eng Geol* 50:177
- Pittman ED, Duschatko RW (1970) *J Sed Petrol* 40(4):1153
- Pittman ED (1971) *AAPG Bull* 55(10):1873
- Příkryl R, Kou SQ (1996) Research Report 24. Luleå University of Technology, Luleå, Sweden
- Příkryl R (1998) Dissertation. Charles University in Prague, 1998
- Rassineux F, Beaufort D, Meunier A, Bouchet A (1987) *J Sed Petrol* 57 (4):782
- Rübner K, Hoffmann D (2006) *Part Part Syst Char* 23(1):20
- Ruzyla K, Jezek DI (1987) *J Sed Petrol* 57(4):777
- Schön JH (2004) *Physical properties of rocks: fundamentals and principles of petrophysics*. Elsevier, Amsterdam
- Scrivener KL, Nemati KM (1996) *Cem Concr Res* 26(1):35
- Simmons G, Todd T, Baldrige WS (1975) *Am J Sci* 275:318
- Simmons G, Richter D (1976) In: Strens RGJ (ed) *The physics and chemistry of minerals and rocks*. John Wiley & Sons, London, p 105
- Sprunt ES, Brace WF (1974) *Int J Rock Mech Min Sci Geomech Abstr* 11:139
- Walsh JD, CSIRO (1974) *Tech. Mem. 12, Commonwealth Scientific and Industrial Research Organization, Melbourne, Australia* (1974)
- Wardlaw NC (1976) *Bull Am Petr Geol* 60:245
- Wu CC, Freiman SW, Rice RW, Mecholsky JJ (1978) *J Mater Sci* 13:2659
- Zang A, Lienert M, Zinke J, Berckhemer H (1996) *Tectonophysics* 263:219
- Zinke J, Gehlen K, Lienert M, Berckhemer H (1993) In: Emmermann R, Lauterjung J, Umsonst T (eds) *Contribution to the 6th annual KTB-Colloquium, geoscientific results, Giesen, Germany, April 1–2, 1993*

# Influence of Fântânița Lake (Chalk Lake) Water on the Degradation of Basarabi–Murfatlar Churches

97

Rodica-Mariana Ion, Radu-Claudiu Fierascu, Irina Fierascu, Raluca-Madalina Senin, Mihaela-Lucia Ion, Mirela Leahu, and Daniela Turcanu-Carutiu

## Abstract

Discovered in 1957, the Ensemble Basarabi–Murfatlar is one of the most impressive archaeological sites from Europe. The monument is situated on a hill chalk cliff, and is built from amorphous calcium carbonate, very sensitive to moisture, frost, salts, as the most important and common causes of monuments degradation. The calcite dissolution is affected by the presence of foreign ions,  $Mg^{2+}$  (from  $MgSO_4 \cdot 7H_2O$  and  $MgSO_4 \cdot 6H_2O$ ) and  $Na^+$  (from  $Na_2SO_4 \cdot 10H_2O$  and  $Na_2SO_4$ ), being the major cations in seawater and groundwater. Also, the anions  $SO_4^{2-}$  and  $Cl^-$  are favouring the calcite conversion to gypsum and is responsible for stone wall dissolution. Some petrographic and physico-chemical (X-ray fluorescence energy dispersive (EDXRF), thermal analysis, ICP-AES of wall samples are presented in this paper. The influence of Fântânița Lake water (Chalk Lake) composition situated very close to the church is discussed, pointing out the salts migration from the lake to the church wall.

## Keywords

Basarabi–Murfatlar • Calcite • Degradation • Salts • Lake water

## 97.1 Introduction

The Basarabi–Murfatlar Ensemble has been discovered on 1957, and is one of the most impressive archaeological sites of Europe, consisting of four churches dated from 9th–11th century, recognized as the first religious monument from

medieval Dobrogea. Situated in the cliff of a chalk stone hill, this ensemble is built from amorphous calcium carbonate (calcite), very sensitive to humidity, frost, salts etc. Stone surfaces are continuously exposed to physical, chemical and biological degradation (Ion et al. 2013).

The high porosity allows penetration of water with corrosive ions, acids and salts inside the stone and cause it severe damages. The deterioration of stone is primarily due to the presence of different water-soluble salts. Salts crystallization is responsible for efflorescence (salt deposited on stone surfaces), sub-efflorescence (the salts beneath the surfaces) and crypto-efflorescence (the salts are deposited within the pore of the stone) (Gauri 1982). Sometimes, due to the increased salinity of the ground water, an increased stone degradation occurs, due to the reaction of calcite from limestone react with different oxides (El-Gohary 2011). Different anions (nitrates, sulphates, and chlorides) is facilitating the stone degradation. This situation has been identified for Basarabi–Murfatlar church.

R.-M. Ion (✉) · R.-C. Fierascu · I. Fierascu · R.-M. Senin  
Analytical Department, ICECHIM, 202 Splaiul Independentei,  
060021, Bucharest, Romania  
e-mail: rodica\_ion2000@yahoo.co.uk

R.-M. Ion · M.-L. Ion · M. Leahu  
Materials Engineering and Mechanics Department,  
Valahia University, 18-20 Unirii Blvd.,  
130082, Targoviste, Romania

D. Turcanu-Carutiu  
Art Faculty, Ovidius University, 124 Mamaia Blvd.,  
900527, Constanta, Romania

Calcite (the variety of calcium carbonate detected) dissolution is affected by the presence of foreign compounds,  $Mg^{2+}$  (from  $MgSO_4 \cdot 7H_2O$  and  $MgSO_4 \cdot 6H_2O$ ) and  $Na^+$  (from  $Na_2SO_4 \cdot 10H_2O$  and  $Na_2SO_4$ ), being the major cations in seawater and groundwater. Also, the anion  $SO_4^{2-}$  (from atmospheric pollution) is favouring the calcite conversion to gypsum and is responsible for stone wall dissolution. Petrographic and physico-chemical (X-ray fluorescence energy dispersive (EDXRF), thermal analysis, ICP-AES and X-ray diffraction (XRD)), are presented, too. Because in the close vicinity of the church is the Fântânița Lake or Chalk Lake, formed after construction of Danube-Black Sea Channel in 1975, the possible influence of the water composition on the weathering and deterioration of this church, is analysed in this paper. These analysis are original, nobody up to now discussed this water lake influence of these churches.

## 97.2 Materials and Methods

### 97.2.1 Sampling

Samples of stone were collected from Basarabi church (samples collected from the exterior of the monument, without any value for this church), Fig. 97.1.

### 97.2.2 Characterization Techniques

**The X-ray diffraction** analysis has been carried out with a DRON UM1 diffractometer using an iron filter for the  $CoK_{\alpha}$  radiation (1.79021 Å), and with a Philips Diffractometer PW 1840, 40 kV/20 mA, Cu  $K_{\alpha}$  radiation). **The energy-dispersive X-ray fluorescence analysis** was performed with an energy dispersive instrument, EDXRF PW4025, type Minipal- Panalytical, with a Si(Li)-detector of 150 eV resolution at 5.89 keV (Mn-K $\alpha$ -line) and a Rh-tube with an acceleration voltage of 50 kV. **Thermal analysis** has been performed on



Fig. 97.1 Picture of the prelevated sample

a Mettler Toledo Thermo-gravimetric Analyzer TGA/DSC/SDTA 823 $^{\circ}$ , in the range of temperature 25–1000  $^{\circ}$ C, in dynamic air, with 60 ml/min, at a heating rate of 10  $^{\circ}$ C/min, in alumina crucible. **ICP-AES elements analysis** has been recorded with ICP-AES spectrometer Varian, Liberty 110 System.

## 97.3 Results and Discussion

This ensemble is built from calcium carbonate (chalk) and is very sensitive to humidity, frost, salts etc. Usually, calcium carbonate is occurring as limestone, chalk and biomaterials. It can adopt three polymorphs forms: calcite, aragonite and vaterite (Goudie et al. 1970). From petrographical analysis, could be concluded that the wall is mainly composed of calcium carbonate ( $CaCO_3 = 91.4\%$ ), small amount of quartz and minerals clay as constituents, and an autigens chemical structure with iron oxides and hydroxides. It has a highly porous microstructure, with quite coarse pores (Fig. 97.2). The prelevated chalk sample is a clay bioclastic limestone (chalk), a variety of precipitation limestone, porous, finely granular and relatively friable (white powder). The identified vaterite, which coexist with calcite, is stable only under 10  $^{\circ}$ C, has the tendency to form framboidal structures, in the presence of  $CO_2$ , with an average size of these elementary spheres comprised between 36 and 150 nm (Nehrke 2007). Analyzing the metal content (by ICP and EDXRF) from samples prelevated from different church's locations, and lake water, too, besides the usual metals (Fig. 97.3 and Table 97.1) could be detected Sr, favouring the calcite stability, being able to interact primarily with the sterically open sites on the surface of calcite during dissolution (Lea et al. 2001). The growth of damaging salt crystals is usually attributable to crystallization, caused by the evaporation or

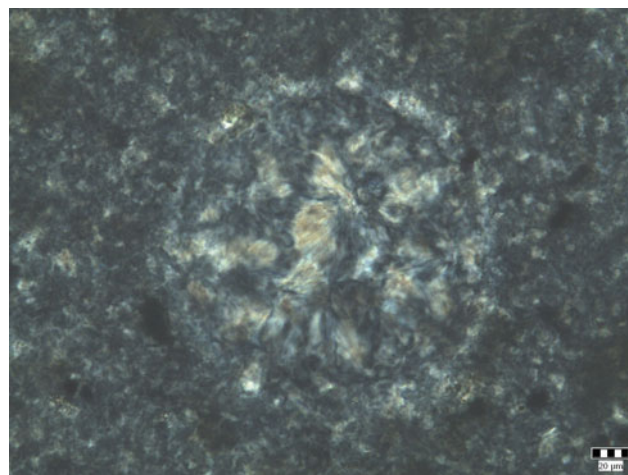
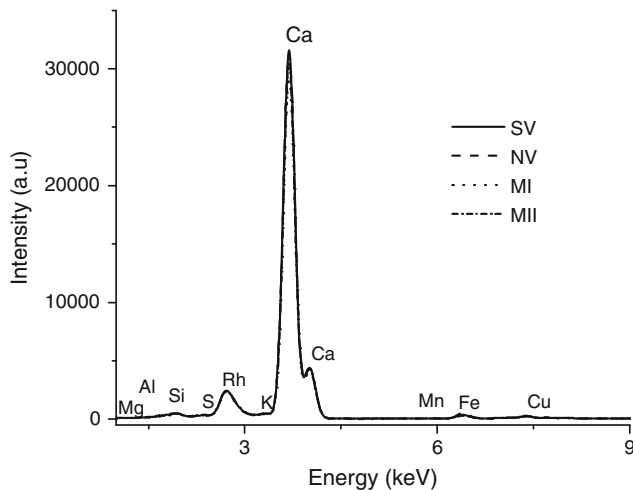


Fig. 97.2 Petrographic analysis of chalk stone sample



**Fig. 97.3** EDXRF semi-quantitative analysis of chalk samples

cooling of salt solutions within the stone. Most aggressive are:  $\text{Na}_2\text{SO}_4 \cdot 10\text{H}_2\text{O}$  (mirabilite), an extremely soluble salt which derives from hydration of  $\text{Na}_2\text{SO}_4$  (thenaride), which increases its volume for about 70–250 %, and kieserite ( $\text{MgSO}_4 \cdot 6\text{H}_2\text{O}$ ) which transforms in epsomite ( $\text{MgSO}_4 \cdot 7\text{H}_2\text{O}$ ) with a volume increase of 173 % (El-Gohary 2011).

For the lake water have been determined sulphates (1426.75 mg/L vs. 300 mg/L for Danube-Black Sea Channel)(STAS 8601-70), chlorides (645 mg/L vs. 200 mg/L in Danube-Black Sea) (SR ISO 9297/01) and hardness (53.93 °DH vs. 30 °DH) (SR ISO 6059/2008) all these being similar with literature data (Barac et al. 2011). The other water parameters have values not exceeding the standard values for Black Sea water. Their presence in the lake could be the main source for the salts responsible for wall degradation. Also, by analyzing the values obtained by ICP-EAS, could be observed identical or higher values for Na and Mg, for the lake water by comparison with the chalk samples prelevated from different locations of the church. From thermal analysis, in the chalk sample prelevated from the church, could be identified both hydrous and anhydrous Mg and Na sulphates (Table 97.2).

**Insoluble salts** (mostly carbonates) do not crystallize, mostly because of their poor solubility a stay either on or below surface. Because of their low solubility, **slightly soluble salts** often crystallize just below the surface and cause bulging, detachment and loss of fragments, calcium sulfate (*gypsum*) being the predominant salt ( $\text{CaSO}_4 \cdot 2\text{H}_2\text{O}$ ). **Highly soluble salts** are mostly chlorides and nitrates ( $\text{NaCl}$ ,  $\text{NaNO}_3$ ,  $\text{KNO}_3$ ). Their hygroscopic salts in humid environments remain in solution producing a dark patches. Because of high

**Table 97.1** The ICP-AES analysis for Basarabi churches sample (minor elements)

Element	Lake water (ppm)	Church stone from entrance Nord-West (ppm)	Church stone from entrance South-West (ppm)	Chalk sample (I) (ppm)	Chalk sample (II) (ppm)
Al	0.218	542.29	569.81	554.15	196.38
Sr	2.322	269.66	256.38	317.27	496.44
Ca	68.19	92,500	95,500	94,700	96,700
Ba	–	14.19	11.02	1.08	16.08
Mn	–	132.33	128.08	169.24	216.79
Fe	–	652.86	354.54	379.04	116.08
Mg	131.9	760.77	764.35	132.02	1304.20
Na	458.9	173.77	172.46	837.30	1745.81
Zn	1.566	78.57	36.90	2.46	82.16
Cu	–	–	4.77	0.27	3.44
K	6.845	481.43	387.80	528.83	127.44

**Table 97.2** Endothermic peaks of chalk sample with Na and Mg sulphates

Chalk sample	Endothermic peaks (°C)				
	100	150	198	275	–
$\text{Na}_2\text{SO}_4$	–	–	–	275.54	–
$\text{Na}_2\text{SO}_4 \cdot 10\text{H}_2\text{O}$	90.89	–	–	271.15	–
$\text{MgSO}_4 \cdot 6\text{H}_2\text{O}$	110	156	200	275	360
$\text{MgSO}_4 \cdot 7\text{H}_2\text{O}$	135	185	200	274	365

solubility, the crystallization occurs, efflorescence appears, but sometimes crystallization spreads below the surface layer, affecting cohesion—subefflorescence (Török 2010).

## 97.4 Conclusion

Some petrographic and physico-chemical (X-ray fluorescence energy dispersive (EDXRF), thermal analysis, ICP-AES of wall samples from Basarabi–Murfatlar church are presented in this paper. The calcite dissolution is affected by the presence of some cations,  $Mg^{2+}$  (from  $MgSO_4 \cdot 7H_2O$  and  $MgSO_4 \cdot 6H_2O$ ) and  $Na^+$  (from  $Na_2SO_4 \cdot 10H_2O$  and  $Na_2SO_4$ ) being detected in Fântânița Lake water, very close to the Basarabi–Murfatlar Churches and pointing out the salts migration from the lake to the church wall. Also, the anions  $SO_4^{2-}$  and  $Cl^-$  are favouring the calcite conversion to gypsum and is responsible for stone wall dissolution.

**Acknowledgments** This work was supported by a grant of the Romanian National Authority for Scientific Research, CNDI-UEFI-SCDI, project number 222/2012.

## References

- Barac M, Maria D, Arghirescu A, Antoniac C (2011) Acviferul Dobrobei de sud sub influenta canalului Dunare-Marea Neagra si a factorilor antropici, potential poluatori ai acestuia. *Ecoterra* 26:1–6
- Gauri L (1982) Stone conservation planning: analysis of intricate systems, science and technology in service of conservation. IIC, London, pp 46–50
- El-Gohary M (2011) Chemical deterioration of Egyptian limestone affected by saline water. *Int J Conserv Sci* 2(1):17–28
- Goudie A, Cooke R, Evans A (1970) Experimental investigation of rock weathering by salts. *Area* 2:42–48
- Ion RM, Bunghez IR, Pop SF, Fierascu RC, Ion ML, Leahu M (2013) Chemical weathering of chalk stone materials from Basarbi churches. *Met Int* 2:89–93
- Lea AS, Amonette JE, Baer DR, Liang Y, Colton NG (2001) Microscopic effects of carbonate, manganese and strontium ions on calcite dissolution. *Geochim Cosmochim Acta* 65:369–379
- Nehrke G (2007) Calcite precipitation from aqueous solution: transformation from vaterite and role of solution stoichiometry, Ph.D. thesis, pp. 67–96
- Török A (2010) In situ methods of testing stone monuments and the application of nondestructive physical properties testing. In: Dan Bostenaru M, Pšikryl R, Török Á (eds) *Materials, technologies and practice in historic heritage structures*. Springer, Netherlands, pp 177–193

---

# Condition Survey on XIV–XVIII Century Funerary Monuments in the Cloisters of St. Anthony Basilica in Padua

98

Vasco Fassina, Simone Benchiarin, and Gianmario Molin

---

## Abstract

Most of the funerary monuments in the cloisters of St. Anthony's Basilica, being located in the centre of Padua, have suffered of marked decay processes related to the recent industrialisation which has strongly increased sulphur based-compound in the atmosphere. Extensive sampling of the monuments were performed following the European guidelines of CEN TC 346. Surface samples were collected from those areas which showed severe symptoms of stone deterioration. Care was taken to ensure that the samples were representative of each monument. Petrographic analyses of all surface crusts showed gypsum, in both microcrystalline flakes and in acicular crystals. Gypsum is the predominant phase due to sulphation processes, according to the interactions of the atmosphere in contact with the stone surface. SEM analyses (BSE images) of cross sections showed extensive micro-cracks in the limestone, parallel to the stone/crust interface, completely filled with gypsum. The study of the decay products, their extent on the surface and in depth of the stone and the causes that have led to their formation have allowed an important evaluation of decay degree and consequently the most appropriate procedure of restoration to be carried out.

---

## Keywords

Monuments' condition • Stone decay • Black crust • Stone polychromy

---

## 98.1 Introduction

The present work aims to define the type and extent of deterioration processes in a series of Renaissance funerary monuments in the Cloisters of the Basilica of St. Anthony in Padua. As these funerary monuments are unique memorials

to the history of distinguished Paduan scholars, intervention is urgently required to halt the fading of precious inscriptions from their surfaces. A condition assessment of the monument surfaces was therefore the first step taken by the conservation process. The condition of more than a hundred objects found in the cloisters was qualitatively evaluated to prioritise restoration works according to the severity of the damage.

This paper presents and discusses the results obtained on two monuments that are subjected to severe decay processes.

The funerary monument to Giovanni Calurnio (1443–1503) was executed in the early 16th century by the sculptor Antonio Minello de' Bardi. Until 1871, the artwork was kept inside the church of San Giovanni da Verdara in Padua, and was successively moved to the Cloister of the Novitiates (Basilica of St. Anthony), in an area protected from direct water runoff. The monument is made of Nanto stone, a yellow-brown, marly-arenaceous limestone of the Middle

---

V. Fassina (✉)

Soprintendenza per i Beni Storici Artistici ed Etnoantropologici  
per le province di Venezia, Padua, Treviso, Belluno, Italy  
e-mail: vasco.fassina@gmail.com

S. Benchiarin · G. Molin  
Dipartimento dei Beni Culturali, Università degli Studi di Padova,  
Padua, Italy  
e-mail: benk@libero.it

G. Molin  
e-mail: gianmario.molin@unipd.it

Eocene, outcropping near Vicenza (Veneto, north-eastern Italy) and quarried along the slopes of the south-western sector of the Berici Hills. As restoration work is urgently required, stone characterisation and identification of decay products were carried out using classic mineralogic-petrographic and chemical methods. Photographic documentation collected in the past century enabled us to make a preliminary visual assessment. The surface showed extensive decayed areas which may be associated with the increased concentrations of sulphur pollutants measured in the atmosphere. This was thoroughly explained by many authors who carried out studies on Venetian monuments (Fassina 1978, 1988a, 1993, 1994; Fassina et al. 2001, 2002; Camuffo 1998).

The monument, located along the west wall of the cloister, is sheltered from direct rain and exposed to rain spray, fog deposition, air turbulence due to frequent condensation-evaporation cycles, and water rising from the ground by capillary migration. A north-north-easterly wind favours evaporation processes which are enhanced on the left side of the artwork, probably due to a stronger ventilation in that corner. The most severe damage is on the upper parts showing spalling and crumbling due to the combined action of salts and expansion of clay minerals. Black fly ash crusts are widespread on all stone surfaces, and crumbling, flaking, surface deposits and missing parts are visible on all surfaces. Large patches of dense efflorescence, caused by rising damp, affect the lower parts of the monuments up to a height of 70 cm above the ground (Fig. 98.1a).

The second monument examined is a St. George and dragon bas-relief, which was initially located on the external façade of St. George's oratory and was transferred inside the General Cloister in 1931. When the original bas-relief was removed, it was replaced by a copy made in the same Nanto stone. The original bas-relief, which has been preserved in a

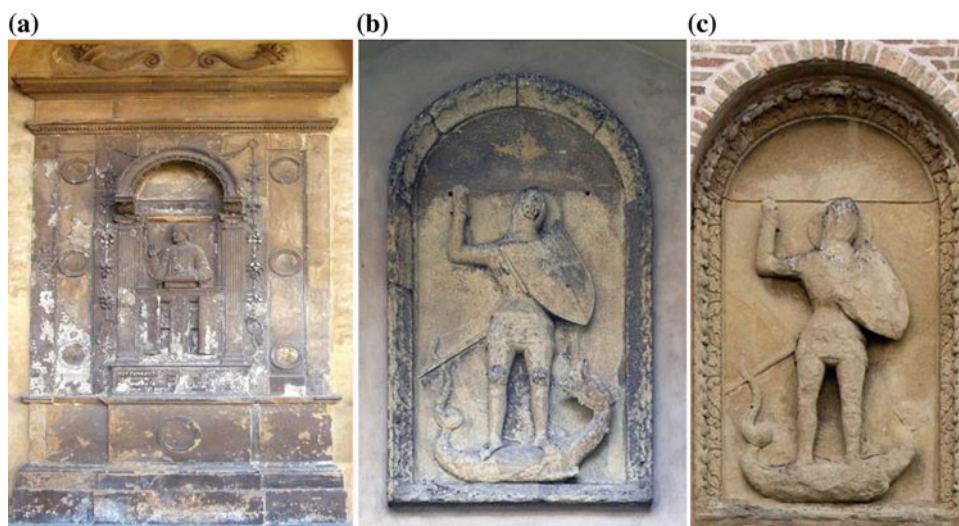
sheltered environment, exhibits widespread spalling in its most exposed sections. However, although its severe conditions of decay prompted conservation experts to shelter it inside the cloister, the extent of the damage is actually less than that observed on the copy now on the façade of St. George's oratory. In fact, several carved parts are missing from the outside work, especially on St. George's face, as clearly shown in photographs (Figs. 98.1b, c). Visual observation led us to conclude that the bas-relief copy exposed to weathering agents for 70 years has larger missing parts than the original one, which was exposed to the outside environment for four centuries (1552–1931). The more severe decay on the outside copy is closely associated with the sharp increase of atmospheric pollutant concentration that occurred after the 1960s during urbanisation and industrialisation periods (Fassina 1978, 1988b; Sabbioni 1995). The original bas-relief, which was exposed to the atmospheric agents for a much longer period (400 years) was only subjected to natural weathering, i.e., atmospheric agents of the pre-industrial period which deteriorated the artefact very slowly because only moderately aggressive.

From the visual observations we can conclude that preservation of the old bas-relief in a sheltered environment has contributed to its conservation.

## 98.2 Sampling and Analytical Methods

Surface samples were collected from areas showing severe signs of stone deterioration: damaged layers were scraped off, fragments of black crusts and stone were removed and salt efflorescence was sampled on the outer surface of the slabs of the ornamental stone. Special care was taken to ensure that the samples were representative of the whole monument.

**Fig. 98.1** a Calturnio monuments in 2004. b St. George carved in the 16th century. c The copy exposed to the outside environment since 1931



The stone and its decay products were qualitatively and quantitatively characterised by mineralogic-petrographic and chemico-physical analyses. Optical microscope (OM) and scanning electron microscope equipped with a dispersive energy micro-analyser (SEM-EDS) were used for thin section examination. Ion chromatography (IC) measured anion concentrations such as sulphates, nitrates, chlorides and oxalates. The morphological characteristics of the black crusts were observed by examining 3D samples using secondary electrons collected by scanning electron microscopy (SEM). Organic compounds were identified by infrared spectroscopy (FT-IR).

### 98.3 Results

Petrographic analyses of all surface crusts of Calturnio monument revealed the presence of gypsum, both in microcrystalline flakes and in acicular crystals. It is now well known that the gypsum formation is due to sulphation processes caused by the interactions between the atmosphere and the stone surface (Amoroso and Fassina 1983; Fassina 1983, 1988a, b). SEM analyses (back-scattered electrons—BSE images) of decayed scab cross-sections showed a dendritic crust between 30  $\mu\text{m}$  and 1 mm thick. These crusts have two main features:

- (i) Irregular aggregates of needle-shaped gypsum crystals (lenticular and minute crystals), sometimes arranged in a fan shape, the structure of which causes the high crust porosity. The stone/crust interface is transformed into microcrystalline calcite, which shows chemical transformation in progress.
- (ii) Embedded in the gypsum crust are iron, titanium and porous carbonaceous particles whose diameters range between 10 and 40  $\mu\text{m}$  and concentrations from a few percent to about 30 %-volume.

Three-dimensional images (SEM-BSE) of the black crusts show platy crystals of gypsum (Fig. 98.2a), spherical and porous carbonaceous particles emitted by heavy oil combustion (Fig. 98.2b) and smooth spherical particles mainly composed of iron and other metals due to fossil fuel combustion (Sabbioni 1995) (Fig. 98.2c).

Ion Chromatography analyses of stone materials taken by a micro-drilling technique at different depths from the stone surface (Amoroso and Fassina 1983) identified sulphates as the most abundant anions, with trends decreasing from the surface downwards. These sulphates, as previously noted, are clearly associated with the presence of gypsum. IC analyses show gypsum concentrations ranging from 27 to 36 % on the surface and falling to 1 % in depth (Table 98.1). Quantitative determination of sulphate salts may explain some of the decay phenomena affecting the monument.

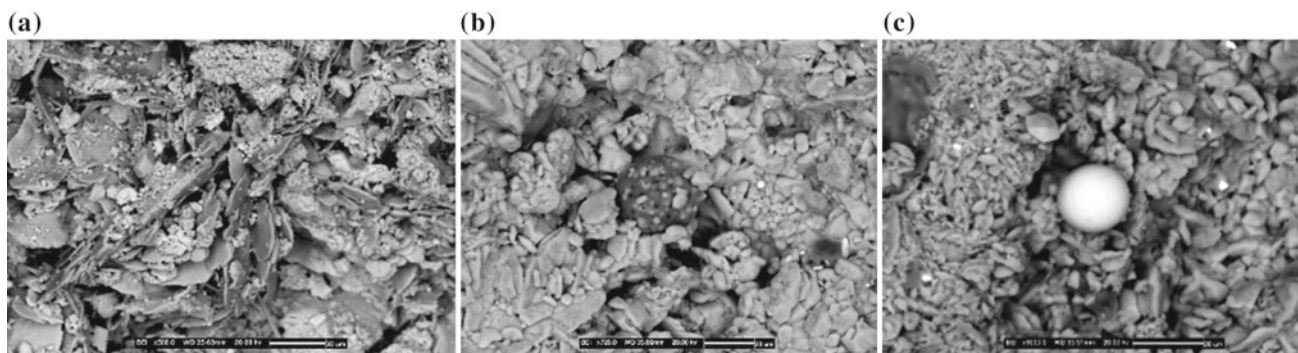
### 98.4 Discussion

Cross-section SEM analyses (BSE images) show extensive micro-cracks in the limestone, parallel to the stone/crust interface and completely filled with gypsum.

These cracks, between 5 and 30  $\mu\text{m}$  thick, may be up to a few millimetres long and up to 5 mm deep inside the stone, perhaps even deeper. These micro-fissures were observed in the samples classified as bindstone.

Although spalling is certainly enhanced by deterioration, this seems to have acted on originally discontinuous surfaces of probable cyanobacterial structure.

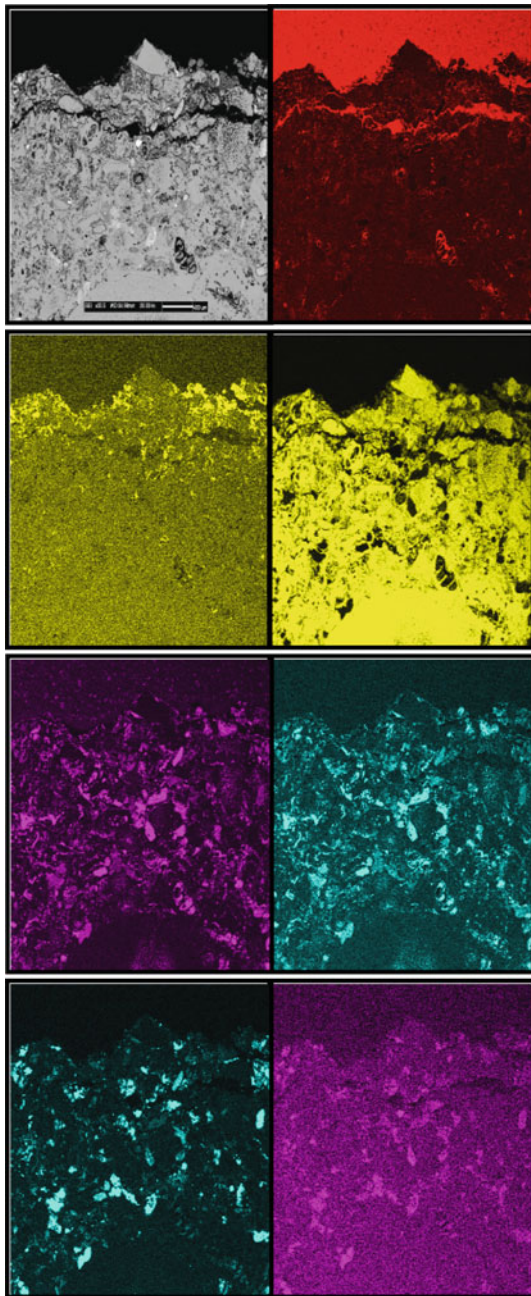
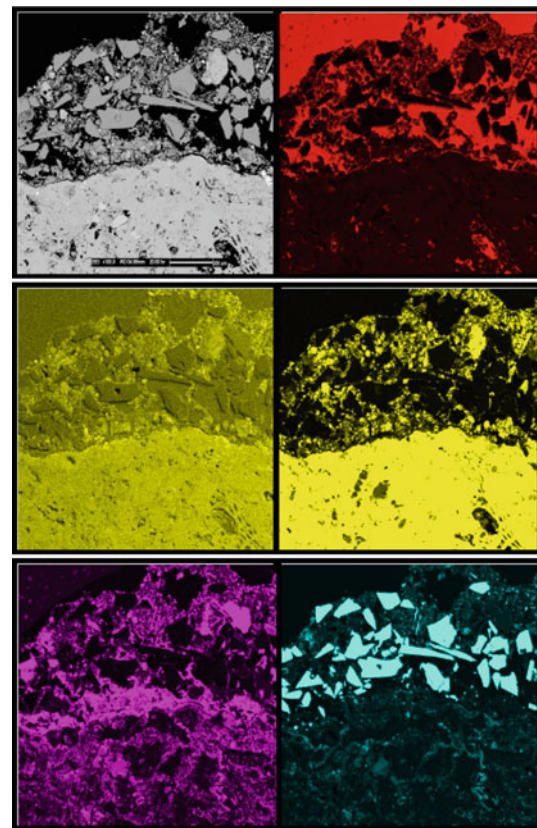
IC revealed different concentrations of nitrates all over the stone. Evidence of water migration through porous stone is given by efflorescence at the base of the monument, and is made up of niter, as identified by XRD analysis. Niter is probably closely related to capillary rising damp transporting salts from decomposing organic matter.



**Fig. 98.2** a Platy crystals of gypsum (*left*); b carbonaceous particle (*middle*). c smooth metal particles (*right*)

**Table 98.1** Ion chromatography (IC) was used to measure anion concentrations (%) of stone material sampled at different depths

Sample/depth	Height (cm)	SO <sub>4</sub> <sup>2-</sup>	Cl <sup>-</sup>	NO <sub>3</sub> <sup>-</sup>	Oxalate
19a (0–1 mm)	370	20.10	–	0.23	–
19b (1–2 mm)	370	3.36	–	0.35	–
19c (2–3 mm)	370	3.15	–	0.33	–
23a (0–1 mm)	120	15.44	0.39	1.70	–
23b (1–2 mm)	120	1.14	0.33	1.32	–
23c (2–3 mm)	120	0.68	0.34	1.70	–

**Fig. 98.3** Map distribution of elements in a sample cross-section taken from the original bas-relief preserved inside (*from left* BS electron, C, S, Ca, Si, Al, Fe, Ti)**Fig. 98.4** Map distribution of elements in a sample cross-section taken from the copy placed outside (*from left* BS electron, Fe, Ti, P, K, Mg, Na)

Samples were also taken from the original St. George bas-relief and from the outside copy to compare the amount of deterioration products. The sample taken from the original shows that the artefact was affected by greater surface sulphation, up to 50  $\mu\text{m}$  (Fig. 98.3). Instead, the outside copy showed greater sulphur penetration deep within the crust (Fig. 98.4). The presence of phosphates in this same specimen was attributed to an organic maintenance treatment.

Two samples were taken from the copy, one from an area protected from water runoff and one from an area exposed to it. Sulphate concentration was 39 % in the sheltered area sample and 22 % in the exposed area one. How can these

baffling results be explained? The lower gypsum concentration in the exposed area sample is probably due to the efficient cleansing action of the rain. Comparison of sulphate concentration data from these two samples show that in areas sheltered from water runoff, gypsum concentration is greater on the outside copy.

## 98.5 Conclusions

The study of decay products, their surface extent and depth, and the causes of their formation enable us to assess the degree of decay and to plan restoration work accordingly. SEM analyses (back-scattered electrons-BSE images) of cross-sections of decayed scabs showed a dendritic crust between 30  $\mu\text{m}$  and 1 mm thick. Porous carbonaceous particles were found in the irregular aggregates of needle-shaped gypsum crystals. Spherical and porous carbonaceous particles are emitted by heavy oil combustion, while smooth spherical particles, mainly composed of iron and other metals, are due to fossil fuel combustion. SEM analyses (BSE images) of cross-sections showed extensive micro-cracks in the limestone, parallel to the stone/crust interface and completely filled with gypsum. These cracks, between 5 and 30  $\mu\text{m}$  thick, may be up to a few millimetres long and up to 5 mm deep inside the stone, perhaps even deeper.

## References

- Amoroso GG, Fassina V (1983) Stone decay and conservation atmospheric pollution-cleaning-consolidation and protection. Elsevier, Amsterdam, pp 1–453
- Camuffo D (1998) Microclimate for cultural heritage. Elsevier, Amsterdam
- Fassina V (1978) A survey on air pollution and deterioration of stonework in Venice. *Atmos Environ* 12:2205–2211
- Fassina V (1988a) Stone decay of Venetian monuments in relation to air pollution. In: Marinos PG, Koukis G, Balkema AA (eds) Proceedings of international symposium on the engineering geology of ancient work, monuments and historical sites, Rotterdam, pp 787–796
- Fassina V (1988b) Environmental pollution in relation to stone decay. *Durab Build Mater* 5:317–368
- Fassina V (1993) The weathering mechanisms of marble and stone of Venetian monuments in relation to the environment. In: Proceedings of the 10th triennial meeting of ICOM, Committee for conservation, Washington, August 22–28, pp 345–351
- Fassina V (1994) The influence of atmospheric pollution and past treatments on stone weathering mechanisms of Venetian monuments. *Eur Cult Herit Newsl* 8(2):23–35
- Fassina V, Favaro M, Crivellari F, Naccari A (2001) The stone decay of monuments in relation to atmospheric environment. *Anal Chim* 91 (2001):767–774
- Fassina V, Favaro M, Naccari A (2002) Principal decay patterns on Venetian monuments, in natural stone, weathering phenomena, conservation strategies and case studies. In: Siegesmumg S, Weiss T, Volbrecht A (eds) Geological Society special publication, London, vol 205, pp 381–391
- Sabbioni C (1995) Contribution of atmospheric deposition to the formation of damage layers. *Sci Total Environ* 167:49–55

Zita Pápay and Ákos Török

---

## Abstract

Miocene porous limestone from Sós-kút (Hungary) is one of the most common building stone in Hungarian monuments. This porous limestone has wide variety in fabric, porosity and pore-size distribution. These properties also influence the behaviour of limestones and control their durability against environmental hazards. Our study shows that pore structure has a primary role in weathering susceptibility, and it also influences the compatibility with different consolidants and the efficiency of consolidation. Fine-, medium- and coarse-grained porous limestones were tested under laboratory conditions. Cylindrical samples were consolidated by immersion under atmospheric pressure until full saturation was reached. In the tests three consolidants were applied: one type of silicic acid ester, an aliphatic urethane resin and Paraloid B72. Physical parameters such as density, ultrasonic pulse velocity, total porosity, pore-size distribution by mercury intrusion porosimetry and water absorption were measured on natural and consolidated samples. Our analyses have shown that the tested consolidants have different penetration depth which depends on fabric and pore-structure of limestone types.

---

## Keywords

Limestone • Consolidation • Apparent porosity • Pore-size distribution

---

## 99.1 Introduction

Porous stone in historical buildings shows a lot of weathering forms caused by attacking physical, chemical and biological processes especially in polluted environment (Török 2002). A number of studies explained that fabric, porosity and pore-size distribution has primary role in behavior of porous stones against weathering processes (Fitzner and Basten 1992; Török et al. 2007; Molina Ballesteros et al. 2010). During restoration of buildings a key question is the selection of proper consolidants. The present paper provides information on the role of pore-size distribution that controls the

penetration depth of consolidants, and thus controls the efficacy of consolidation. Three commonly used consolidants were tested on three types of Hungarian porous limestone from Sós-kút under laboratory conditions. Porous limestone from Sós-kút is often used in historical and public buildings of Budapest because it is light, easy to work with and has a decorative value (Török 2003).

---

## 99.2 Materials

Stone blocks were extracted from Sós-kút quarry located 20 km from Budapest (capital of Hungary). Figure 99.1 shows the macroscopic appearance and pore-size distribution of the analyzed limestones. Three different limestone types were used for tests: fine-, medium, coarse-grained ones. The medium and coarse-grained varieties have yellowish white colour, the fine-grained type is white. The

---

Z. Pápay (✉) · Á. Török  
Budapest University of Technology and Economics, Műegyetem  
rkp. 3, Budapest, 1111, Hungary  
e-mail: zita.papay@gmail.com

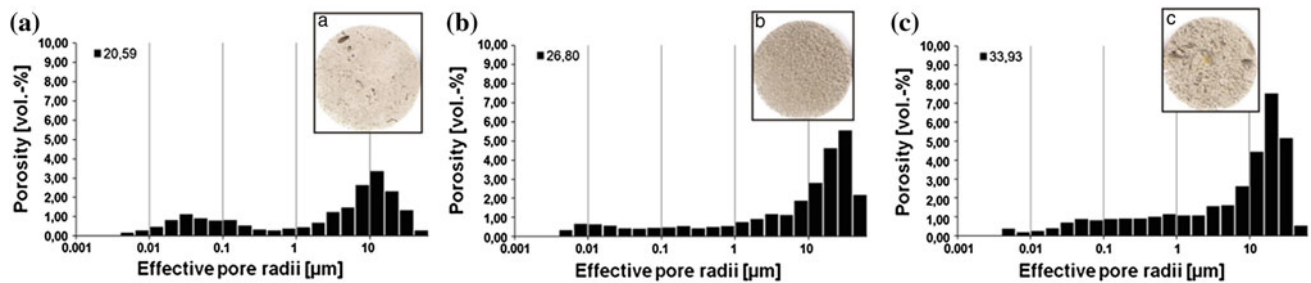


**Fig. 99.1** Macro image and pore-size distribution of fine-, medium and coarse porous limestone

fine-grained limestone has compact fabric with very small, micrometer-sized pores. Its bulk density is  $1,981 \text{ g/cm}^3$  and it has 20.59 V% total porosity (Fig. 99.1a). The medium-grained type is a typical oolitic grainstone with dominantly millimeters-sized pores (Fig. 99.1b). It has  $1,705 \text{ g/cm}^3$  and 26.8 V% total porosity. The coarse-grained variety contains shell fragments which can be observed by naked eyes (Fig. 99.1c). Its bulk density is  $1.599 \text{ g/cm}^3$  and its pore-size distribution shows larger millimeter-size pores with 33.93 V% total porosity (Pápay and Török 2007). As consolidants three agents were used for the experiments: silicic acid ester (SAE) with 20 m%, Paraloid B72 (PB72) with 4 m% and aliphatic urethane resin (AUR) with 50 m% effective substance, respectively.

### 99.3 Methods

Cylindrical specimens with a diameter of 5 cm and a height of 5 cm were drilled from the stone blocks. The tests were performed according to the recommendations of the previous Hungarian Standard and new EU norms. Specimens were classified into analytical groups on the basis non-destructive

testing methods (MSZ 18282/4) to minimize the standard deviation of the results. Specimens were treated under laboratory conditions at normal atmospheric pressure. Apparent porosity determined by water saturation under atmospheric pressure (MSZ 18284/1). Water absorption test was carried out according to EN 13755:2008. Capillary rise was observed on specimens with a diameter of 5 cm and a height of 10 cm. Specimens were immersed in water and agent in 5 mm. Pore diameter and total porosity were determined with mercury porosimetry. In course of porosimetry measurement mercury is intruded by porosimeter at high external pressure into porous material. The pore size distribution can be estimated on basis of the pressure values needed to penetrate mercury into a pore.

### 99.4 Results

The physical properties of treated and untreated samples such as ultrasonic pulse velocity and apparent porosity were compared (Table 99.1). Consolidant absorption and the amounts of the reacted agent are also presented in Table 99.1. The data are average values of 3, 4 or 5 samples, respectively.

**Table 99.1** Physical properties of treated and untreated porous limestones

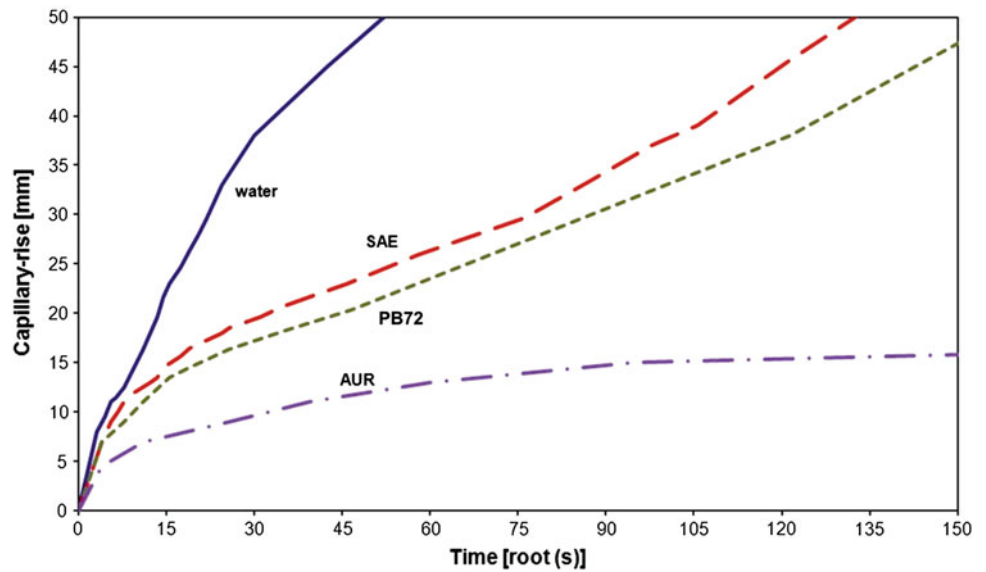
Type	Group	ultrasonic pulse v. (km/s)	Agent absorption (m%)	Reacted agent (m%)	Apparent porosity/total porosity (V%)
Fine-grained lime-stone	Untreated	2.47	–	–	18.72/20.59
	Silica acid ester	2.71	5.10	0.97	15.77
	Paraloid B72	2.58	7.96	0.44	19.73
	Aliphatic urethane resin	2.55	3.97	0.51	14.21
Medium-grained lime-stone	Untreated	2.32	–	–	26.18/26.80
	Silica acid ester	2.40	11.03	1.72	27.26
	Paraloid B72	2.19	13.39	0.43	31.57
	Aliphatic urethane resin	2.54	12.77	1.63	10.23
Coarse-grained lime-stone	Untreated	1.95	–	–	26.34/33.93
	Silica acid ester	2.15	12.5	2.09	30.07
	Paraloid B72	2.12	13.13	0.50	29.67
	Aliphatic urethane resin	2.24	14.49	1.80	12.07

Table 99.1 shows that the ultrasonic pulse velocity values increase due to consolidation for all the three limestones and three consolidants except with Paraloid B72 treated medium-grained limestone where  $-5.6\%$  was measured.

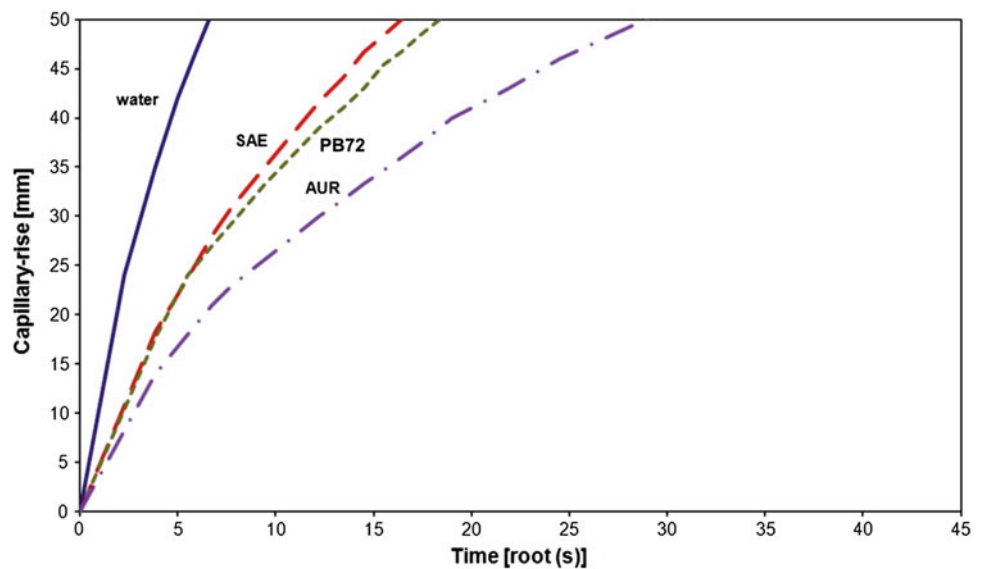
The agent absorption before drying and the mass of treated samples after agent reacting were also monitored and recorded. The largest absorption rate was observed by Paraloid B72 treatment: in fine-grained limestone  $7.96\%$ , in medium-grained  $13.39\%$  and in coarse-grained  $13.13\%$  with one exception in coarse-grained variety aliphatic uretan resin penetrated by  $14.49\%$ . Silicic acid ester showed the smallest rate of absorption: in medium-grained porous limestone ( $11.03\%$ ) and in coarse-grained porous limestone ( $12.5\%$ ) where aliphatic urethane resin represents larger absorptions  $12.77$  and  $14.49\%$ . The fine-grained porous limestone behaves different silicic acid ester

showed  $5.10\%$ , aliphatic urethane resin showed smaller  $3.97\%$  absorption. The mass of the treated specimens after drying shows another trend. The largest quantity of solid-phase consolidant was measured in silica acid ester treated stones: in fine-grained  $0.97\%$ , in medium-grained  $1.72\%$  and in coarse-grained  $2.09\%$  consolidant were found. The smallest quantity from consolidants was found from Paraloid B72 in the tested stones: in fine-grained  $0.44\%$ , in medium-grained  $0.43\%$  and in coarse-grained  $0.50\%$ . The values of aliphatic uretan resin were between the former ones; in fine-grained  $0.51\%$ , in medium-grained  $1.63\%$  and in coarse-grained  $1.80\%$  aliphatic urethane resin was found (Table 99.1). Apparent porosity values show that silicic acid ester and Paraloid B72 increase apparent porosity. In fine-grained porous limestone  $-2.95$  and  $+1.01\%$ , in medium-grained porous limestone  $+1.08$ ,  $+5.39\%$  and in

**Fig. 99.2** Capillary rise in fine-grained porous limestone



**Fig. 99.3** Capillary rise in medium-grained porous limestone



coarse-grained porous limestone +3.73 and 3.33 V% for silicic acid ester and Paraloid B72, respectively. Significant decrease in apparent porosity was observed in all of the three limestone varieties by treatment with aliphatic urethane resin (−4.51, −17.03 and −14.27 V% for fine-, medium and coarse-grained limestone).

Figures 99.2, 99.3 show the capillary rise for fine-, medium-grained limestone as a function of the square root of time in seconds. Figures represent the average of 2 samples for fine- and 3 samples for medium-grained limestone. The same trend is observable for all the limestone varieties. Silicic acid ester rises the quickest and aliphatic urethane resin the slowest. Paraloid B72 is between the former two ones. Capillary rise of aliphatic urethane resin in fine-grained limestone do not exceed 15 mm after 6 h (Fig. 99.2).

## 99.5 Conclusions

The studied three different types of porous limestones have different pore-size distributions and porosity. The penetration of the three consolidant was also different due to the differences in porosity and pore-size distribution. The experiments have shown that aliphatic urethane resin had the lowest penetration into the limestones. The measured high amount of consolidant partly evaporates and partly forms a crust on the limestone surface. The larger the pore diameters the deeper the penetration of the aliphatic urethane resin, as it is marked by the measured resins of 1.63 m% in the medium-grained, 1.8 m% in the coarse-grained and 0.51 m% in the fine-grained limestone after consolidation.

From the tested three consolidants the silica acid ester show the highest rate of capillary rise, and the largest amount of solid consolidant in the porous limestones. The penetration and gel formation of this consolidant seems to perform the best at porous limestones from all the tested ones.

## References

- Ballesteros Molina E, Martín Cantano M, Talegón García J (2010) Role of porosity in rock weathering processes: a theoretical approach. *Cadernos Lab. Xeolóxico de Laxe Coruna* 35:147–162
- Pápay Z, Török Á (2007) Evaluation of the efficiency of consolidants on Hungarian porous limestone by non-destructive test methods. *Cent Eur Geol* 50(4):299–312
- Török Á (2002) Oolitic limestone in polluted atmospheric environment in Budapest: weathering phenomena and alterations in physical properties. In: Siegesmund S, Weiss TS, Vollbrecht A (eds) *Natural stones, weathering phenomena, conservation strategies and case studies*. Geological Society, London, Special Publications 205, pp 363–379
- Török Á (2003) Surface strength and mineralogy of weathering crusts on limestone buildings in Budapest. *Build Environ* 38(9–10):1185–1192
- Török Á, Forgó LZ, Vogt T, Löbens S, Sieemund S, Weiss T (2007) The influence of lithology and pore-size distribution on the durability of acid volcanic tuffs, Hungary. In: Prikyl R, Smith BJ (eds) *Building stone decay from diagnoses to conservation*. Geological Society, London, Special Publications 271, pp 251–260
- Fitzner B, Basten D (1992) Gesteinporosität—Klassifizierung, meßtechnische Erfassung und Bewertung ihrer Verwitterungsrelevanz. In English: Stone porosity—classification, measurement methods and evaluation of its role in weathering processes. In: Sneath R (ed) *Jahresberichte Steinerfall—Steinkonzervierung 1992*. Ernst & Sohn GmbH. Verlag, pp 19–32, Berlin

---

# The Bentheim Sandstone: Geology, Petrophysics, Varieties and Its Use as Dimension Stone

# 100

C. Wim Dubelaar and Timo G. Nijland

---

## Abstract

The shallow-marine Bentheim Sandstone was deposited in one of the NW-SE trending basins north of the London-Brabant and Rhenish massifs during the Valanginian (Early Cretaceous). The Bentheim Sandstone forms an important reservoir rock for petroleum, but has also proven itself as a very durable natural stone quarried since about 1100 AD. This paper focuses on the geology and the petrophysics of the Bentheim Sandstone as a building stone. The Bentheim Sandstone is exposed in outcrops just east of the Dutch-German border, in the vicinity of Bad Bentheim and Gildehaus. Two varieties are distinguished, a pale yellow sandstone characteristic for the Gildehaus area and a darker, ochre and locally even reddish type. The red variety is found in an area around Bad Bentheim. In the red variety different generations of hematite coatings, from the early phase of burial history to later stages in the formation of the Bentheim Sandstone could be recognized in thin sections and on SEM images. Thick iron crusts along fault planes originated from the percolation of iron-rich groundwater in the joints crossing the sandstone beds. The historic use of the Bentheim Sandstone and the weathering aspects of the dimension stone are shortly dealt with.

---

## Keywords

Bentheim • Building stone • Lower cretaceous • Hematite coating

---

## 100.1 Introduction

Bentheim Sandstone is the reservoir rock of several oil and gas fields of northwest Germany and the northeastern Netherlands (Füchtbauer 1955, 1963; Knaap and Coenen 1987; De Jager and Geluk 2007). Most of the studies of the Bentheim Sandstone have concentrated on its sedimentary origin (e.g. Kemper 1976; Kortmann 1983; Wonham et al. 1997) and on its reservoir properties as a host rock for oil and gas

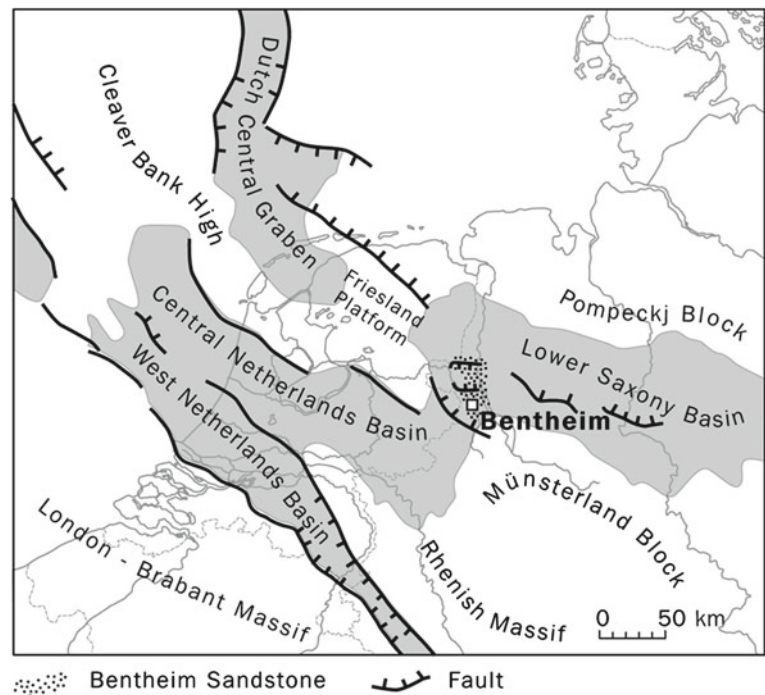
(e.g. Füchtbauer 1955, 1963; Vos 1990; Malmberg 2002; PGK 2009). Only a few papers are devoted to the varieties and the rock properties of the Bentheim Sandstone in light of its use as building stone (Becker 1987; Grimm 1990; Voort 2000; Ehling and Lepper, *submitted*). Quarrying of the Bentheim Sandstone started around 1100 AD in the area of Bad Bentheim and Gildehaus (Voort 2000), so its application as a construction stone spans almost a thousand years. Two varieties are distinguished, a pale yellow sandstone, characteristic of the Gildehaus area, and a darker, ochre and locally even reddish stone, found in the area east of Bad Bentheim. This paper focuses on the geology and the petrophysical aspects of the Bentheim Sandstone, with particular attention for thin-section and SEM- analyses of the red variety. The historic use of the Bentheim Sandstone and the weathering aspects of the dimension stone are shortly dealt with.

---

C. Wim Dubelaar (✉)  
Geological Survey of the Netherlands—TNO, PO Box 800153508  
TA, Utrecht, The Netherlands  
e-mail: wim.dubelaar@tno.nl

T.G. Nijland  
TNO, PO Box 492600 AA, Delft, The Netherlands

**Fig. 100.1** Early Cretaceous structural elements and basin configuration in the Netherlands and the adjacent part of Germany (adapted from De Jager and Geluk 2007; Kombrink et al. 2012)



## 100.2 Geology of the Bentheim Sandstone

### 100.2.1 Regional Setting and Structural Model

The Bentheim Sandstone is of Early Cretaceous (Valanginian) age. It was deposited in a shallow-marine environment in the western part of the Lower Saxony Basin, a basin extending from the east of the Netherlands to the Harz Mountains in Germany. The Bentheim Sandstone is composed of several sheet-like sand bodies up to 80 metres thick. In the Bentheim area, the unit consists of massive or cross-bedded quartz arenites, separated from the underlying marine claystones by an erosive contact (Kemper 1976; Wonham et al. 1997). The Bentheim Sandstone grades upwards and eastwards into marine claystones and sandstones. The Bentheim depositional area is part of a small pull-apart basin formed as a result of dextral strike-slip movements along a basement fault (PGK 2009; Geluk et al. 2009). The provenance of the sediments are the surrounding highs: the Münsterland Block and the Rhenish Massif to the south and the Friesland Platform to the northwest (Fig. 100.1). Sediments of the Bunter Sandstone Formation in those highs presumably provided most of the sands of the Bentheim Sandstone (Kemper 1976). Originally, the main source area of the Bentheim Sandstone was thought to be the area to the southwest of Bentheim, in the eastern Netherlands. This high was known as the Triassic High (e.g. Schott et al. 1967; Kemper 1976). New insights take into account that at that time, in the Early Cretaceous, the presumed high was in fact the eastern extension of the Central Netherlands

Basin, and therefore could not have been the provenance area of the Bentheim Sandstone (Geluk et al. 2009). More likely, the Friesland Platform, situated NW of the Bentheim area, provided most of the clastic sediments bordering the deeper parts of the Lower Saxony Basin (Fig. 100.1). The cross-bedded sands from different outcrops in the Bentheim area show that paleocurrents were mainly directed towards the SSE, which is in accordance with a northwesterly source area. The basin sediments were inverted in Late Cretaceous times resulting in the present-day East Netherlands High.

### 100.2.2 Bentheim Sandstone Outcrops

The main outcrops of Bentheim Sandstone occur in a circa 9-km-long east-west aligned ridge with an average width of some 400 m (Fig. 100.2). The ridge is part of a limb of an east-west trending anticline formed during Alpine folding of the basin sediments, dipping 10–20° to the south. The only outcrop exposing the northern limb of the anticline is the small and isolated Isterberg (Kemper 1976). The folded area of the inverted part of the Lower Saxony Basin, marked by the anticlinal remnant, is covered with a few scattered patches of Neogene and Paleogene (mainly Eocene) clayey sediments and by a thin sheet of Quaternary glacial and fluvial deposits (Hinze 1988). The present-day morphology of the landscape reflects the weathering profile and is highlighted by differences in land use; the resistant sandstones form wooded ridges and the softer claystones are used as farmland.

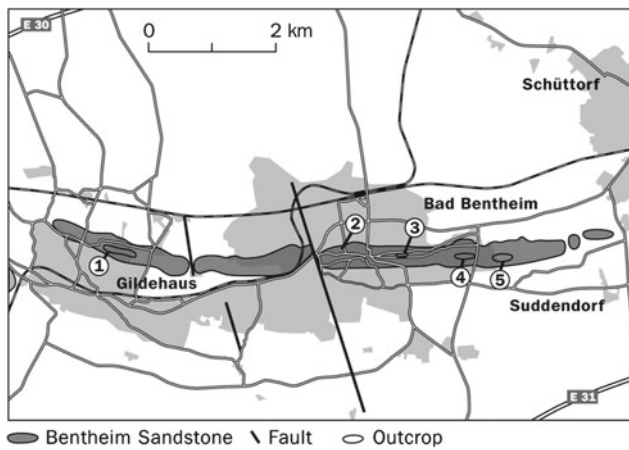


**Fig. 100.2** Outcrops of Bentheim sandstone between Gildehaus and Suddendorf (modified after Kemper 1976). 1 Romberg Quarry, 2 Bentheim Castle, 3 Am Kathagen, 4 Freilichtbühne, 5 Wood Quarry

The Bentheim Sandstone can be studied in great detail in the abandoned quarries of the intensively exploited sandstone beds near Gildehaus, Bad Bentheim and farther east to Suddendorf (Fig. 100.2). The type section of the Bentheim Sandstone was established in the Romberg Quarry, situated in Gildehaus, and is divided into three units: the Lower Bentheim Sandstone (c. 20 m thick), the Romberg Claystone (3 m thick) and the Upper Bentheim Sandstone (6–10 m thick), locally called the ‘Obere Flaserzone’ (Kemper 1976; Kortmann 1983). Most Bentheim Sandstone building blocks were quarried from the so-called ‘Hauptsandstein’, medium-grained, massive beds that dominate the Lower Bentheim Sandstone unit. Bed thickness in this unit varies from 1.5 to 4 m. East of Bad Bentheim, the Lower Bentheim Sandstone is divided into two sand units, separated by sandy claystone beds (‘Zwischenmittel’, Kemper 1976). In the Romberg

Quarry, the Bentheim Sandstone is still being excavated. The limited volume of quarried rock is mainly used for restoration purposes (Fig. 100.3).

### 100.2.3 Mineralogy, Petrophysics and Material Properties

The Bentheim Sandstone consists of well-sorted medium-grained sand with an average grain size between 180 and 300 micrometer (Vos 1990; Louis et al. 2005). Quartz is the main constituent (>90 %, usually up to 97 % in building-stone varieties) with accessory feldspars (microcline, in most cases strongly corroded), heavy minerals (tourmaline, zircon, rutile) and Fe-(hydr)oxides such as goethite and hematite. Stone quarried for building purposes is almost devoid of clay minerals (<1 %) and carbonates (Füchtbauer 1955; Kemper 1976; Becker 1987; Grimm 1990).

Samples from the sandstone beds in the Romberg Quarry as analyzed by Vos (1990) and new samples taken by the authors from abandoned quarries east of Bad Bentheim show booklets of the clay mineral kaolinite on the surfaces of the quartz grains (Figs. 100.4 and 100.5). Kaolinite also forms thin clay coatings marking the walls of the pore spaces. The quartz particles often show overgrowth of newly formed quartz at the edges of the crystals and in the sutured boundaries between the grains (Fig. 100.7). This secondary silica presumably became available as feldspar crystals decomposed during burial-related diagenesis, releasing SiO<sub>2</sub> and also forming kaolinite. A second mechanism was the solution of quartz along the grain contacts and its deposition elsewhere in the granular matrix.

Porosity of the Bentheim Sandstone is high, up to 26 volume % (Füchtbauer 1963). Measured water permeability ranges from 0.97 to 2.14 Darcy in samples from the Romberg

**Fig. 100.3** Romberg Quarry, Gildehaus, 2006. Extracted Bentheim sandstone layer in the center is 2 m in height



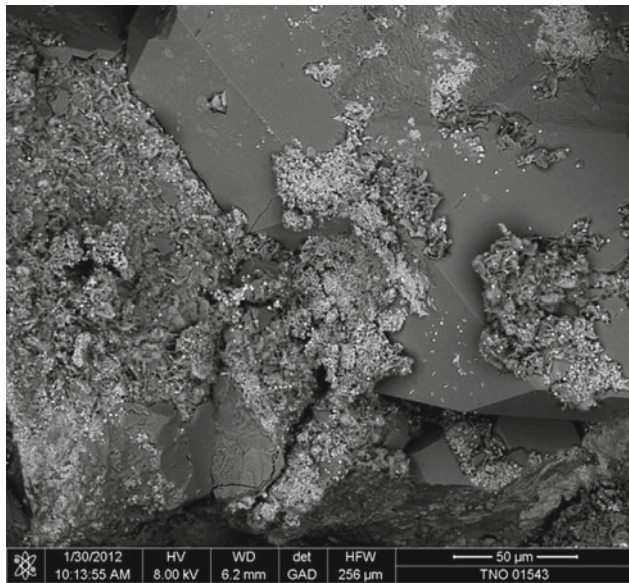


**Fig. 100.4** SEM image of Bentheim sandstone, *red* variety. White kaolinite and hematite on quartz crystals

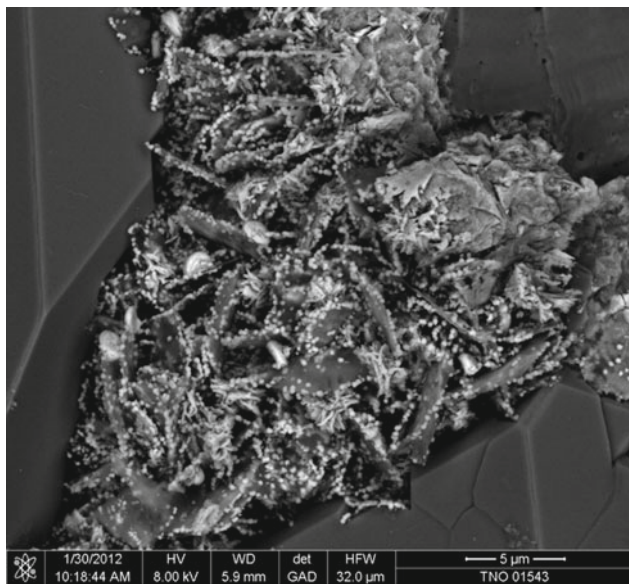


**Fig. 100.5** SEM image of Bentheim Sandstone, *red* variety. Hematite on top of booklets of white kaolinite

Quarry (Vos 1990). Most pores have a diameter between 0.025 and 0.1 mm (Grimm 1990). Oversized pores occur frequently and are mostly caused by dissolution of the feldspars. Malmberg (2002) stated that quartz cementation presumably helped to preserve primary porosity. Although precipitated in limited amounts, the silica cement helped the framework to withstand the effect of overburden pressure and thus limited mechanical compaction. In their microstructural analysis of the Bentheim Sandstone, Louis et al. (2005) observed an anisotropy of elastic and transport properties in samples taken from the Romberg Quarry. The anisotropic

**Table 100.1** Material properties of Bentheim sandstone. Data from Füchtbauer (1955), Müller (1993), Grimm (1990), Louis et al. (2003), (2005) and unpublished data from the authors

Density	$\text{g cm}^{-3}$	2.65
Apparent density	$\text{g cm}^{-3}$	2.04–2.12
Compressive strength	$\text{N mm}^{-2}$	48–77
Bending tensile strength	$\text{N mm}^{-2}$	4.2
Young's modulus	GPa	8.3–12
Porosity	vol.%	20–26
Water absorption (atm. pressure)	wt%	7.1
Water absorption (vacuum)	wt%	11–12
Frost resistant		yes
Specific surface area	$\text{m}^2 \text{g}^{-1}$	1.69

characteristics were attributed to the non-spherical shape of the pores having an elongation direction parallel to bedding. They observed that most of the grains have their long axis aligned with the bedding plane. The authors do not elaborate on the genesis of that property, but in our opinion, this anisotropy should be attributed to the primary process of a current-dominated sedimentary environment. No significant anisotropy was detected in the orientation of grain contacts with respect to the direction of the bedding plane. We assume that grain-contact orientation is a diagenetic feature that is unrelated to the original sedimentary bedding.

A summary of material properties relevant to the use of Bentheim Sandstone as dimension stone is given in Table 100.1. Some varieties may have considerably lower compressive strengths than usually reported in literature, and the difference between water-saturated (vacuum) and dry samples is significant (e.g. average 34 and 48  $\text{N mm}^{-2}$ , respectively, for a single sample). Strength depends in part on orientation with respect to the bedding plane (Louis et al. 2005).

### 100.3 Off-White and Red Stone Varieties

The most typical Bentheim Sandstone blocks used as a building stone are off-white ('cream'). This colour variety was mainly quarried near Gildehaus, and the presently exploited stone in the Romberg Quarry is also of this variety. Darker, ochre to red stones are typical of the Bad Bentheim area, especially east of the town where they crop out in the former quarries Am Kathagen and Freilichtbühne (Fig. 100.2). Its reddish appearance is caused by the presence of the iron oxide hematite ( $\text{Fe}_2\text{O}_3$ ) coating the quartz grains. These red sandstones are also characterized by higher concentrations of clay minerals than its pale counterpart, with clay minerals filling the larger pores in the stone (Figs. 100.6, 100.7 and 100.8). The local abundance of hematite is remarkable. The origin and nature of the clay minerals, filling some of the oversized pores (Fig. 100.8) is

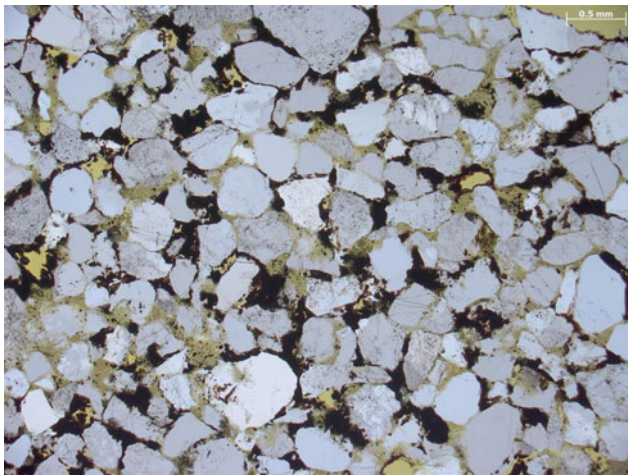


**Fig. 100.6** Microphotograph of Bentheim sandstone, *red* variety, showing the abundance of hematite between the quartz grains

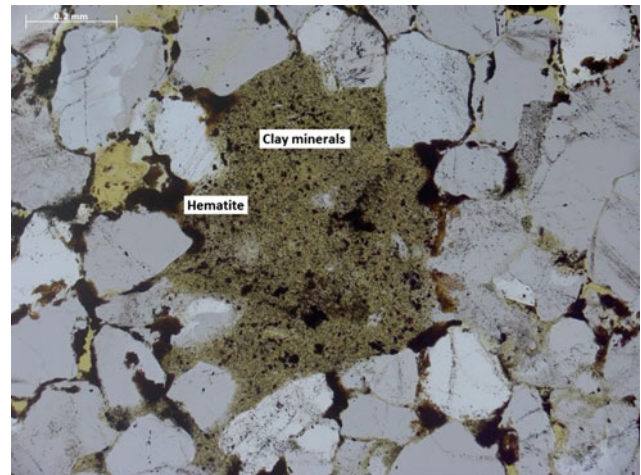


**Fig. 100.8** Microphotograph of Bentheim sandstone, *red* variety. Oversized pore filled with clay minerals and hematite

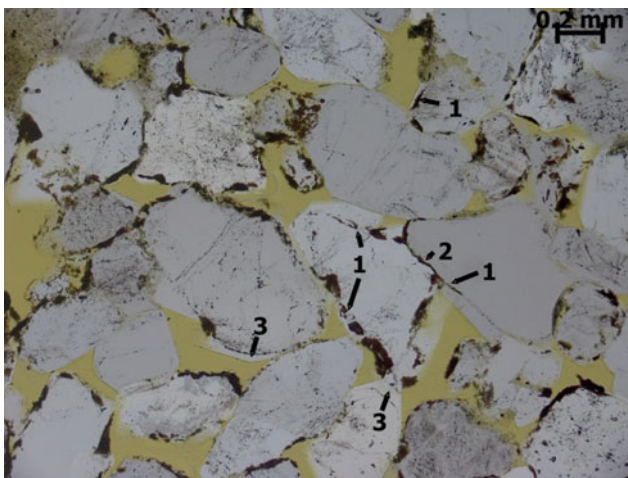


**Fig. 100.7** Microphotograph of Bentheim Sandstone, *red* variety. Thin coatings of hematite (1) formed prior to pressure solution of quartz grains during compaction (2). Coatings are overgrown by newly formed quartz, locally developing clear crystal faces (3)

not completely understood. An option is that those clay minerals originally were fecal pellets, which were concentrated in burrows. During the burial history of the Bentheim Sandstone those clay minerals (originally glauconite?) presumably were squeezed in the pores (personal comment Harmen Mijnlief). An indication to the fecal pellet origin is the occurrence of Ichnofossils, such as *Ophiomorpha* and *Rhizocorallium* which have been recognized on many bedding planes in the Bentheim Sandstone (Kemper 1976).

Thin sections show that a thin veneer of hematite was already present before the overgrowth with seams of newly formed quartz took place (Fig. 100.6). Therefore, the first iron coating probably formed soon after deposition of the sand grains, in an early stage of the burial history. During later stages in the geological history of the Bentheim

Sandstone, perhaps up to quite recently, new coatings with iron oxides were formed. The red discoloration is in many cases a local phenomenon and it usually ends abruptly within a sequence of sandstone layers. It should be noted that large joints in the sandstone beds below Bentheim Castle, in the centre of Bad Bentheim, show cm-thick iron crusts along the fault planes. These crusts originated from the percolation of iron-rich groundwater in the fracture system, from which it locally impregnated the intact sandstone beds (Becker 1987; Nijland and Dubelaar 2014). As most of the larger faults in the Bentheim Sandstone occur in the central and nearby eastern part of the sandstone ridge, it can be understood why the red variety of the Bentheim Sandstone is mainly restricted to that specific area.

## 100.4 Historic Use of Bentheim Sandstone

The Bentheim Sandstone has been quarried since about 1100 AD and was at first used in the area around Bentheim (Voort 2000). In the Middle Ages, most of the dimension stone was exported to Twenthe, the nearby eastern part of the Netherlands, with St. Plechelmus' basilica in Oldenzaal (c. 1150 onwards) as the most prominent example. Between 1200 and 1425, baptismal fonts, made out of a single block Bentheim Sandstone, were transported to churches in the northern Netherlands (De Leeuw 1977) and northern Germany (Petersen 1997). Application of the red type of Bentheim Sandstone has mostly been restricted to Bad Bentheim and a few villages in the neighborhood (Kaplan 2009).

Around 1400 AD, first buildings in Bentheim Sandstone appear in the west of Overijssel province, farther west from the German-Dutch border (De Vries 1994). From 1450 A.D. onwards, with its introduction at the Dom in Utrecht, the Bentheim Sandstone was widely used in many cities in the

Netherlands. Well-known examples of its application include St. John's Cathedral in 's-Hertogenbosch (c. 1500 onwards), the New Church in Delft (1494) and the Royal Palace in Amsterdam (1648–1654). To a lesser extent, Bentheim Sandstone was also used in Flanders (Mechelen, Antwerp), Denmark (Aarhus) and in northwestern Germany, where the town halls of Bremen (1595 onwards) and Münster (from the 14th century onwards) are prominent examples. In 1629 the VOC (United Dutch East India Company) sent a ship to Batavia (now Jakarta) in Indonesia. In its cargo were blocks of Bentheim Sandstone destined for a large portico, but the ship was wrecked off the coast of Western Australia (Weber and Lepper 2005). Bentheim Sandstone was also used for sculptures and as a decorative stone, especially in the 17th and 18th centuries (e.g. Slinger et al. 1980; Dubelaar 1990; Nijland et al. 2007). In the 19th and 20th century, its exploitation gradually decreased and nowadays there is only a limited exploitation in Romberg Quarry (Fig. 100.3).

### 100.5 Weathering and Durability

Bentheim Sandstone usually is quite a durable rock. The high quartz content, small amounts of clay and carbonate and the slightly consolidated framework by thin coatings of secondary silica on the quartz grains, give the Bentheim Sandstone its long-lasting properties. The lack of or only slightly developed lamination within generally massive beds prevents the sandstone from easily splitting apart. Flaking and blistering are rare. The high porosity and permeability promote a large uptake of water during rainy periods, but also helps it to dry up in a relatively short period of time.

Black weathering of Bentheim Sandstone is a widespread phenomenon. Microscopically, the thin black layers are composed of algae and fungi, gypsum, airborne particles such as fly ash, and Fe-(hydr)oxides, present on the surface and in directly adjacent pores. Relative to the original, unaltered stone, black layers show significant increases in loss on ignition, total and organic carbon, total sulfur and iron, as well as Pb, Cu, Zn and Sn (Nijland et al. 2004, Tables 3 and 4). Formation of thin black layers is evidently not due to a single process, but involves formation of gypsum, deposition of airborne material, microbial activity and solution and re-deposition of Fe-(hydr)oxides. The difference in the development of black weathering crusts in another, in some aspects, comparable building stone, the Obernkirchener Sandstone, is striking (Fig. 100.9). The Obernkirchener Sandstone is an Early Cretaceous sandstone excavated near Hannover (Germany) and was also regularly used in the Netherlands (Slinger et al. 1980; Nijland et al. 2007). It has



**Fig. 100.9** Allard Pierson Museum Amsterdam. Facade with contrasting appearance of Bentheim Sandstone (*above*) and Obernkirchener Sandstone (*below*) due to different porosity, permeability and grain-size. Photo Niek Dubelaar

lower porosity and permeability values than the Bentheim Sandstone.

### 100.6 Conclusions

The Bentheim Sandstone is a natural stone quarried since about 1100 AD in the vicinity of Gildehaus and Bad Bentheim. Its high quartz content, small amounts of clay and carbonate and the slightly consolidated framework strengthened by thin coatings of secondary silica on the quartz grains, make the Bentheim Sandstone a durable building stone. Two varieties are distinguished, a pale yellow sandstone, presently exploited in the Romberg Quarry near Gildehaus, and a ochre-to-reddish type found in the area east of Bad Bentheim. The reddish appearance of this latter variety is caused by the presence of the iron oxide hematite ( $\text{Fe}_2\text{O}_3$ ) coating the quartz grains. Different generations of hematite coatings, from the early phase of burial history to later stages in the formation of the Bentheim Sandstone could be recognized in thin sections and on SEM images. Thick iron crusts along fault planes originated from the percolation of iron-rich groundwater in the joints crossing the sandstone beds.

**Acknowledgments** Harmen Mijnlief and Sytze van Heteren, Geological Survey of the Netherlands—TNO read an early version of the manuscript. Han Bruinenberg, Geological Survey of the Netherlands—TNO designed Figs. 100.1 and 100.2.

## References

- Becker U (1987) Zur Geologie des Bentheimer Sattels (Nordteil; TK 3608, Niedersachsen); sowie petrologische, gesteinsphysikalische und bausteingeschichtliche Untersuchungen des Bentheimer Sandsteins (Valangin). Diplomarbeit, Phillips Universität Marburg/Lahn, pp 182
- De Jager J, Geluk MC (2007) Petroleum geology. In: Wong ThE, Batjes DAJ, De Jager J (eds) *Geology of the Netherlands*. Royal Netherlands Academy of Arts and Science, Amsterdam, pp 241–264
- De Leeuw G (1977) Drentse doopvonten van Bentheimer zandsteen. Drents Museum, Assen, p 64
- Dubelaar CW (1990) A geological view of the Royal Palace, Amsterdam, The Netherlands. In: Marinos PG, Koukis GC (eds) *Geology of ancient works, monuments and historical sites*. IAEG Athens, pp 2057–2066
- Ehling A, Lepper J (Coord.) (in press): Bausandsteine in Niedersachsen und Nordrhein-Westfalen sowie nordische Sandsteine
- Füchtbauer, H., 1955. Zur Petrographie des Bentheimer Sandsteins im Emsland. *Erdöl und Kohle*, Hamburg, 8, pp 616–617
- Füchtbauer H (1963) Paleogeography and reservoir properties of the lower cretaceous Bentheim sandstone. In: 6th World Petroleum Congress Excursion Guide Book I, Hannover, 42–43
- Geluk MC, Grötsch J, Van der Veen H, Van Ojik K (2009) Hydrocarbons in the NE Netherlands—past, present and future. In: 71st EAGE Conference and Exhibition—Workshops and Fieldtrips, Field trip 1
- Grimm WD (1990) Bildatlas wichtiger Denkmalgesteine der Bundesrepublik Deutschland. Bayerisches Landesamt für Denkmalpflege, Arbeitsheft 50, München, p 655
- Hinze C (1988) Geologische Karte von Niedersachsen 1: 25.000. Erläuterungen zum Blatt 3608 Bad Bentheim, Niedersächsisches Landesamt für Bodenforschung, Hannover, p 120
- Kaplan U (2009). Naturbausteine historische Bauwerke des Münsterlandes und seiner angrenzende Gebiete. In: *Geologie und Paläontologie in Westfalen*, LWL-Museum für Naturkunde, Heft 73, pp 176
- Kemper E (1976) Geologischer Führer durch die Grafschaft Bentheim und die angrenzenden Gebiete mit einem Abriss der emsländischen Unterkreide. Das Bentheimer Land. Verlag Heimatverein der Grafschaft Bentheim e.V., Nordhorn-Bentheim, 64, pp 206
- Knaap WA, Coenen MJ (1987) Exploration for oil and natural gas. In: Visser WA, Zonneveld JIS, Van Loon AJ (eds) *Seventy-five years of geology and mining in the Netherlands (1912–1987)*. Royal Geological and Mining Society of the Netherlands, Den Haag, pp 207–242
- Kombrink H, Doornenbal JC, Duin EJT, Den Dulk M, Van Gessel SF, Ten Veen JH, Witmans N (2012) New insights into the geological structure of the Netherlands; results of a detailed mapping project. *Neth J Geosci* 91:419–446
- Kortmann H (1983) Sedimentologische Untersuchungen über den Bentheimer Sandstein (Valangin) der Umgebung von Bad Bentheim. Diplomarbeit, Universität zu Köln, p 132
- Louis L, David C, Robion P (2003) Comparison of the anisotropic behaviour of undeformed sandstones under dry and saturated conditions. *Tectonophysics* 370:193–212
- Louis L, David C, Metz V, Robion P, Menéndez B, Kissel C (2005) Microstructural control on anisotropy of elastic and transport properties in undeformed sandstones. *Int J Rock Mech Min Sci* 42:911–923
- Malmborg P (2002) Correlation between diagenesis and sedimentary facies of the Bentheim Sandstone, the Schoobeek field, The Netherlands. Examenarbeite Geologiska Institutionem Lunds Universitet 150:1–20
- Müller F (1993) *Internationale Naturstein Kartei (INSK)*, 3rd edn. Ebner Verlag, Ulm
- Nijland TG, Dubelaar CW, Van Hees RPI, Van der Linden TJM (2004) Black weathering of Bentheim and Obernkirchener sandstone. In: Kwiatkowski D, Löfvendahl R (eds) *Proceedings 10th International congress on deterioration and conservation of stone*, Stockholm, pp 27–34
- Nijland TG, Dubelaar CW, Tolboom HJ (2007) De historische bouwstenen van Utrecht. In: Dubelaar W, Nijland TG, Tolboom HJ (eds) *Utrecht in steen. Historische bouwstenen in de binnenstad*. Matrijs, Utrecht, pp 31–109
- Nijland TG, Dubelaar CW (2014) Rode Bentheimer zandsteen. *Grondboor and Hamer* 68(3):64–69
- Petersen F (1997) *Romanische Taufsteine in Ostfriesland*. Sollermann, Leer, p 127
- PGK (Petroleum Geological Circle) (2009) Development of the Emlichheim/Schoonebeek oilfields and Reservoir characteristics of the Bentheim Sandstone. TNO unpublished report, p 39
- Schott W, Jaritz W, Kockel F, Sames C-W, Stackelberg U, Stets J, Stoppel D (1967) Zur Paleogeographie der Unterkreide im nördlichen Mitteleuropa mit Detailstudien aus Nordwestdeutschland. *NBemerkungen zu einem Atlas, Erdöl und Köhle* 20:149–158
- Slinger A, Janse H, Berends G (1980) *Natuursteen in monumenten*. Zeist, Rijksdienst voor de Monumentenzorg 120 pp
- Voort H (2000) *Abbau, Absatz und Verwendung von Bentheimer Sandstein in 800 Jahrhunderten*. Schriftenreihe des Sandsteinmuseums Bad Bentheim, 1: S. pp 3–18
- Vos M (1990) Selection of outcrop samples for acoustic measurements on reservoir rock. Internal report Delft University of Technology, p 63
- Weber J, Lepper J (2005) Tracing a 17–20th century Odyssey. The Provenance of the Batavia Sandstone Portico. – *Bulletin of the Australian Institute for Maritime Archaeology* 29:53–60
- Wonham JP, Johnson HD, Mutterlose, J, Stadler A, Ruffell A (1997) Characterization of a shallow marine sandstone reservoir in a syn-rift setting: the Bentheim Sandstone Formation (Valanginian) of the Rühlermoor field, Lower Saxony Basin, NW Germany. In: *GCSEPM foundation 18th annual research conference shallow marine and nonmarine reservoirs*, 7–10 December, pp 427–448

B. Vásárhelyi and Á. Török

---

## Abstract

Volcanic tuffs were tested under laboratory conditions to obtain data on the influence of water content on the strength. The studied lithologies included rhyolite tuff from NE Hungary, andesite tuff from Central Hungary and basalt tuff from central western Hungary. Tests included the determination of density, ultrasonic pulse wave velocity, the uniaxial compressive strength (UCS) and modulus of elasticity of both dry and water saturated specimens. The samples were fully immersed into water until full saturation was reached, following the descriptions given in EN 13755:2008 and densities were measured prior and after the saturation (EN 1936:2007). The ultrasonic pulse velocities were measured according to EN 14579:2005, while uniaxial strength was determined as described in EN 1926:2007 standard. Modulus of elasticity was calculated. The mechanical properties of dry and water saturated specimens were compared and the relationships between these parameters were analyzed by using statistical methods. A linear relationship was found between air dry and water saturated UCS of tuffs. Density and UCS were also correlated, with exponential equations for both air-dry and water saturated tests conditions.

---

## Keywords

Volcanic tuff • Water saturation • Uniaxial compressive test • Mechanical properties

---

## 101.1 Introduction

Volcanic tuffs are important stones that are widely used in monuments worldwide. Examples are known from Easter islands and from many European countries. The present work brings examples on how the water content influences the mechanical properties of volcanic tuffs. In the previous

works similar studies have been performed on sandstone (Vásárhelyi 2002a) on porous limestone (Vásárhelyi 2005) on travertine (Török and Vásárhelyi 2010) and on rhyolite tuff (Vásárhelyi 2002b, Kleb and Vásárhelyi 2003). It has been also demonstrated that the water content significantly changes the strength of various lithologies (Vásárhelyi and Ván 2006). The paper based on one mechanical test results of volcanic tuffs provides mathematical equations that can be used to calculate water saturated physical properties from measured dry parameters, such as density, ultrasonic pulse velocity. It also suggests a formulae how to calculate saturated Uniaxial Compressive Strength (UCS) and modulus of elasticity (E) from dry values.

---

B. Vásárhelyi (✉)  
Department of Structural Engineering, University of Pécs,  
Pécs, Hungary  
e-mail: vasarhelyib@gmail.com

Á. Török  
Department of Construction Materials and Engineering Geology,  
Budapest University of Technology and Economics,  
Budapest, Hungary

## 101.2 Test Methods

Specimen preparation and testing were performed in the Rock Mechanics Laboratory at the Technical University of Budapest. Each test was carried out in two petrophysical states: dry and water saturated and measured the bulk density ( $\rho$ ) and the ultrasonic wave velocity ( $v$ ) in which the impedance was calculated. Right circular cylinders were prepared, following the ISRM suggested methods (ISRM 1978), with a diameter of 54 mm and the height: diameter ratio is 2:1 or slightly above. In addition to the standard values of unconfined compressive strength (UCS) and modulus of elasticity (Young's modulus,  $E$ ), the complete stress-strain curve was measured.

### 101.3 Relationship Between Dry and Saturated Densities and Pulse Velocities

Before disturbed rock mechanical investigations, both the density and the ultrasonic wave velocity were measured. Firstly, the measured density of the different tuffs are analyzed, secondly the influence of the water content for the ultrasonic wave velocity is presented.

Knowing, that the density of the water ( $\rho_{\text{water}}$ ) is  $1 \text{ g/cm}^3$ , the theoretical connection between the dry and the saturated density should have to start at 0; 1 point (i.e. pure air; water condition). Plotting the measured points, the following regression was determined with this condition:

$$\rho_{\text{sat}} = 0.523\rho_{\text{dry}} + 1 \quad (R^2 = 0.854) \quad (101.1)$$

or:

$$\rho_{\text{sat}} = \exp(0.369\rho_{\text{dry}}) \quad (R^2 = 0.922) \quad (101.2)$$

The experimental results are always under the theoretical line, which indicates the saturation was not complete (note: in order to represent the field conditions, pressure was not applied in the saturation of samples). The relationship between the two constituent is:

$$\rho_{\text{sat}} = 0.742\rho_{\text{dry}} + 0.629 \quad (R^2 = 0.941) \quad (101.3)$$

or:

$$\rho_{\text{sat}} = 0.945 \exp(0.402\rho_{\text{dry}}) \quad (R^2 = 0.929) \quad (101.4)$$

These regressions are presented in Fig. 101.1.

Similar results were found analyzing the measured ultrasonic wave velocities both dry and saturated conditions. The results were plotting in Fig. 101.2. The linear regression in case of beginning the line from the origin is:

$$V_{\text{sat}} = 1.119 v_{\text{dry}} \quad (R^2 = 0.802) \quad (101.5)$$

According to the experimental results, the following linear relationships were determined:

$$V_{\text{sat}} = 1.314 v_{\text{dry}} - 0.426 \quad (R^2 = 0.822) \quad (101.6)$$

or using logarithmic regression:

$$V_{\text{sat}} = 2.763 \ln(v_{\text{dry}}) + 0.436 \quad (R^2 = 0.867) \quad (101.7)$$

### 101.4 Relationship Between Dry and Saturated Compressive Strength and Modulus of Elasticity

During the uniaxial compressive tests, the strength of the rock and the Young modulus were determined both dry and saturated petrophysical conditions. Using the best fit method, both parameters decrease linearly due to the water saturation.

$$\text{UCS}_{\text{sat}} = 0.729 \text{UCS}_{\text{dry}} \quad (R^2 = 0.892) \quad (101.8)$$

Using the squared fit method for determining the relationship between the dry and saturated Young's modulus were found that the squared regressions coefficients for linear and exponential laws were not significantly different. The linear equation is:

$$E_{\text{sat}} = 0.807 E_{\text{dry}} \quad (R^2 = 0.895) \quad (101.9)$$

The exponential equation is:

$$E_{\text{sat}} = 0.403 E_{\text{dry}}^{1.329} \quad (R^2 = 0.957) \quad (101.10)$$

The UCS was represented in function of the density in Fig. 101.3. In this case the following form of the relation was found:

$$\sigma = ae^{b\rho} \quad (101.11)$$

where  $a$  and  $b$  are material constants. The calculated values are summarized in Table 101.1.

**Fig. 101.1** Relationships between the dry and water saturated density of tuffs

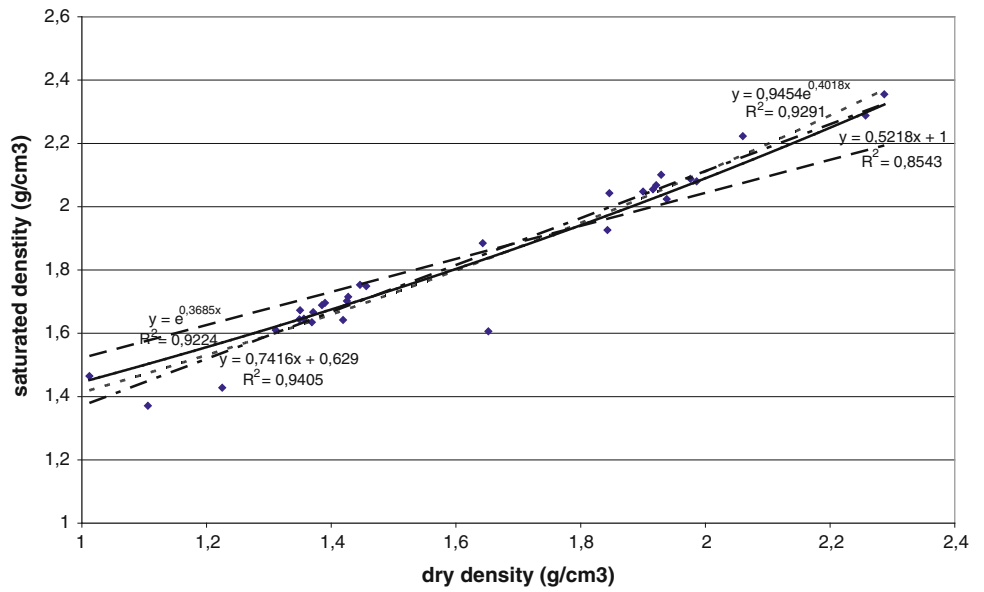


**Fig. 101.2** Regression lines between the dry and saturated ultrasonic wave velocities

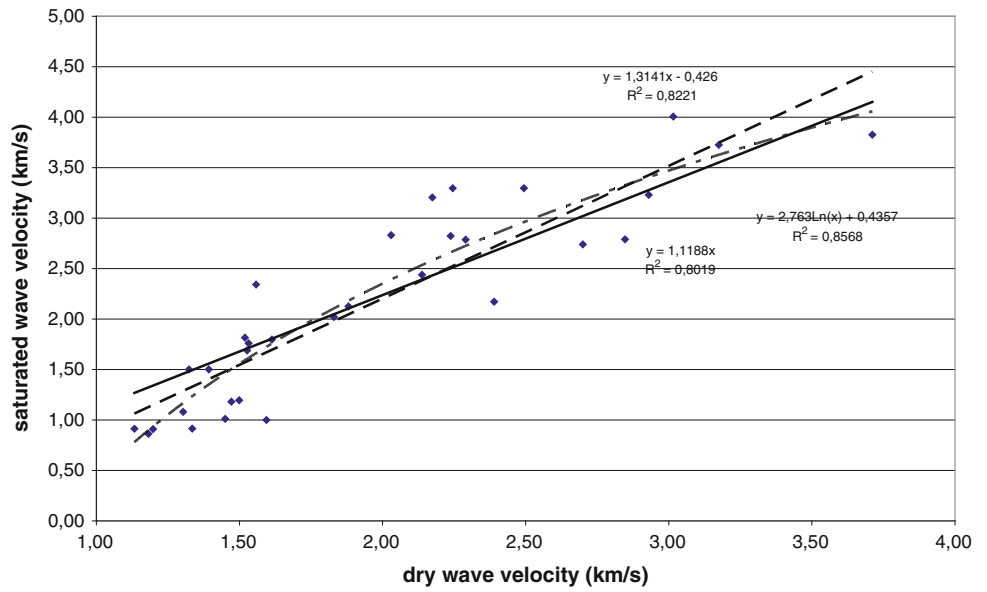


**Fig. 101.3** Effect of density on uniaxial compressive strength. UCS in log scale

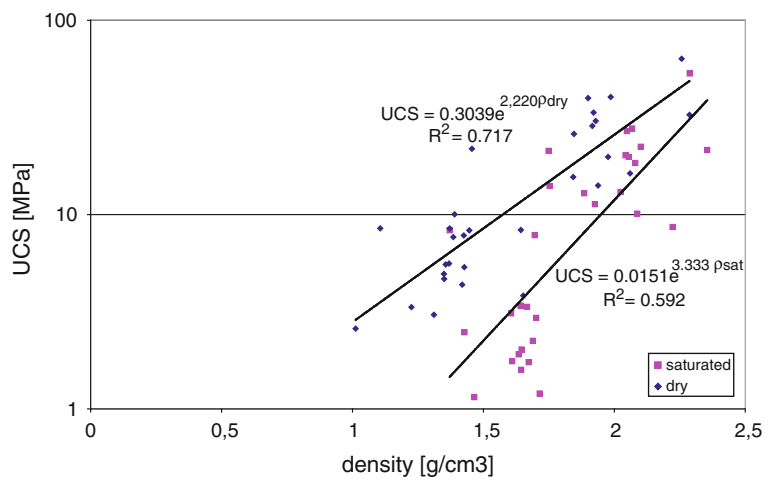


**Table 101.1** The measured material constants for Eq. (101.11). The R-square is 0.717 and 0.592 in case of dry and saturated condition, respectively

	dry	saturated
a	0.304	0.015
b	2.220	3.333

## 101.5 Conclusion

A correlation was found between the air dry and water saturated densities of the studied volcanic tuffs. Regression analyses have shown that the best fit is found with a logarithmic equation between the saturated and dry ultrasonic pulse velocities. An exponential equation was given to describe the relationship between density and uniaxial compressive strength. For this equation two material constants, the dry and the saturated ones were calculated.

## References

- ISRM (1978) Suggested methods for determining the uniaxial compressive strength and deformability of rock materials. *Int J Rock Mech Mining Sci Geomech Abst* 16:137–141
- Kleb B, Vásárhelyi B (2003) Test results and empirical formulas of rock mechanical parameters of rhyolitic tuff samples from Eger's cellars. *Acta Geol Hung* 46:301–312
- Török Á, Vásárhelyi B (2010) The influence of fabric and water content on selected rock mechanical parameters of travertine, examples from Hungary. *Engng Geol* 115:237–245
- Vásárhelyi B (2002a) Some observation regarding the strength and deformability of sandstones in case of dry and saturated conditions. *Bull Engng Geol Env* 62:245–249
- Vásárhelyi B (2002b) Influence of the water saturation on the strength of volcanic tuffs. In: Dinis da Gama C, Ribeiro e Sousa L (eds) *Eurock 2002, Madeira. Proceedings of Workshop on Volcanic Rocks*, pp 89–96
- Vásárhelyi B (2005) Statistical analysis of the influence of water content on the strength of the Miocene limestone. *Rock Mech Rock Eng* 38:69–76
- Vásárhelyi B, Ván P (2006) Influence of the water content for the strength of the rock. *Eng Geol* 84:70–74

# Influence of Salt and Moisture on Weathering of Historic Stonework in a Continental-Humid, Urban Region 102

I. Egartner, H. Schnepfleitner, and O. Sass

---

## Abstract

On the long term, the presented project deals with the processes involved in salt weathering at monuments and natural rock outcrops in climatically different areas. As a pilot study we investigated an example of a cultural heritage structure in the continental-humid, urban region of Graz, Austria using a range of methods for moisture and salt monitoring. The aim was to assess the influence and the interaction between moisture and salts in the formation of the observed weathering structures of the involved limestones. In the spirit of an integrative, multi-method approach we use a range of techniques: (1) Mapping of weathering phenomena; (2) ERT (Electrical Resistivity Tomography); (3) Handheld Moisture Meter; (4) Paper pulp poultices; (5) Laboratory investigation (IC—Ion Chromatography). The various methods were applied to investigate the causes of weathering phenomena at the columns of the city gate ‘Paulustor’ in Graz.

---

## 102.1 Introduction

The weathering of building stones results from a number of physical and chemical processes affecting the stone, interacting and leading to development of various stone decay phenomena. The processes are influenced by environmental conditions and rock properties. Moisture and salts play a particularly important role for weathering and decay (Franzen and Mirwald 2009; Doehne 2002; Leucci et al. 2007). On the long term, the presented project deals with the processes involved in salt weathering at monuments and natural rock outcrops in climatically different areas. As a pilot study we investigated an example of a cultural heritage structure in the continental-humid, urban region of Graz using a range of methods for moisture and salt monitoring. One of the studied structures is presented here. The aim was to assess the influence and the interaction between moisture

and salts in the formation of the observed weathering structures of the involved limestones. The investigations aim at the following topics: (1) Salt and moisture distribution at the stone surface and subsurface and their relationship to weathering phenomena; (2) Infiltration paths and transport of moisture into the masonry and (3) Characteristics of surface and near-surface salts and their sources.

### 102.1.1 Study Site and Material

Mapping and 2D-geoelectric profiling were applied to investigate the causes of weathering phenomena at the columns of the city gate ‘Paulustor’. The four inner columns are built of marine limestone, called ‘Aflenzer Kalksandstein’. It is a fossiliferous, porous limestone mainly built up of calcite and belonging to the rock complex of Leitha-limestone, which developed in shallow marine milieu in the Styrian Basin in the Miocene (Hiden 2001; Gross 2007). Every column measures 1.80 to 1.50 m in width and ~3.70 m in height. The columns show varying signs of weathering like flaking and blistering which was reason for several repairs (e.g. mortar facing) in the past. Through the city gate passes a moderately used road. The road is de-iced in winter by use

---

I. Egartner (✉) · H. Schnepfleitner · O. Sass  
Department of Geography and Regional Science, University  
of Graz, Graz, Austria  
e-mail: isabel.eg@gmx.at

of salt. Situated between the internal four columns is a great roof opening. Through this wide mouth, rain water can reach the street-orientated column fronts while the pavement sides of the columns are water-protected under the roof. The pavement walls are, except of the corners, covered with a thick render and are partially painted by graffiti.

---

## 102.2 Methods

### 102.2.1 Mapping and Sampling

The weathered parts of the Paulustor' extend from the base of the column up to a height of c. 1.30 m. The mapping focused on type, location and intensity of the weathering phenomena using mapping codes as proposed by Fitzner and Heinrichs (2002, 2005). Sampling was carried out mainly by removing already detached layers of deposits and crusts on the masonry surface. The sampling locations are provided as serial numbers on the mapping sheets. Drilling was not allowed for reasons of monument protection.

### 102.2.2 2D-Geoelectrics (ERT)

Electrical Resistivity Tomography (ERT) is a geophysical profiling technique which detects zones of different electrical conductivity and displays them in 2D- or 3D-sections. In stonework, different electrical properties are generally caused by heterogeneous water contents. Thus, ERT can be used to monitor water penetration into, and drying of, historic masonry walls and to get insights into water movement and water distribution inside the stonework. It makes possible to compare the patterns of deterioration of a building wall to the patterns of moisture content or moisture ingress. This non-destructive approach is also helpful for the investigation of salt weathering because water and water vapour are the transport media for soluble salts. However, it is currently not possible to differentiate if zones of high resistivity are caused by high water content, by soluble salts, or by a combination of both.

We used a GeoTom ERT device with 20 self-adhesive ECG electrodes connected by a multi-core cable to the control unit. The adhesive pads of the ECG electrodes (normally used for medical purposes) have a diameter of 5.5 cm and the conductive silicone gel spot measures 2 cm in diameter. The electrode to electrode distance reached from 8 to 10.1 cm. Wenner and Schlumberger configuration were applied for the 2D-survey. The Wenner configuration provides a particularly high resolution for surface-parallel structures while the Schlumberger configuration gives a good resolution of vertical structures within the stone wall. The applied current is automatically chosen by the GeoTom

device (0.05 or 0.5 mA). For the inversion routine (calculation of the final 2D-resistivity section from the array of measurements) we used the Res2DInv software (Loke and Barker 1995). Spatial patterns and resistivity changes were visualized in isoline plots using Surfer® software. At the 'Paulustor' two sets of horizontal ERT profile sections were located around one of the internal columns (column 1) at a height of 0.45 and 1.20 m above ground. Furthermore, four vertical ERT profiles were measured in the middle of each side of the column up to a height of ~1.40 or 1.80 m. The resistivity measurement reaches to a depth of 25–35 cm inside the wall.

---

## 102.3 Handheld Moisture Meter

We used the handheld moisture sensor 'Voltcraft MF-50 Moisture Meter' to measure the moisture content of the wall surface at different heights along the vertical ERT Profiles on each side of the column. The sensor is a non-destructive, handheld and relatively cheap approach to assess the moisture content of stone materials (Mol and Viles 2010; Eklund et al. 2013). As it is mainly used by engineers and practitioners for a quick assessment of wetting patterns, there is no readily available calibration function from instrument reading to absolute moisture content. Thus, we used the instrument only to detect spatial distribution of higher or lower moisture content.

### 102.3.1 Paper Pulp Poultices

Paper pulp poultices were used as salt sampling method for non-destructive application. Pulp poultices (20 cm diameter and 3–5 cm thick) soaked in de-ionized water with a pulp-to-water weight ratio of about 1/8 were applied to the sampling points for 3 h. The poultices were then removed, soaked in 100 ml deionized water and filtered to remove the paper poultice (Martinho et al. 2012; Dionisio et al. 2012; Backbier and Rousseau 1993). The saline solutions were analyzed using the ion chromatograph (Dionex ICS-3000 Reagent-Free) at the Institute of Applied Geoscience of the Technical University of Graz. Ion chromatography is a type of fluid chromatography and is used to separate inorganic anions and cations.

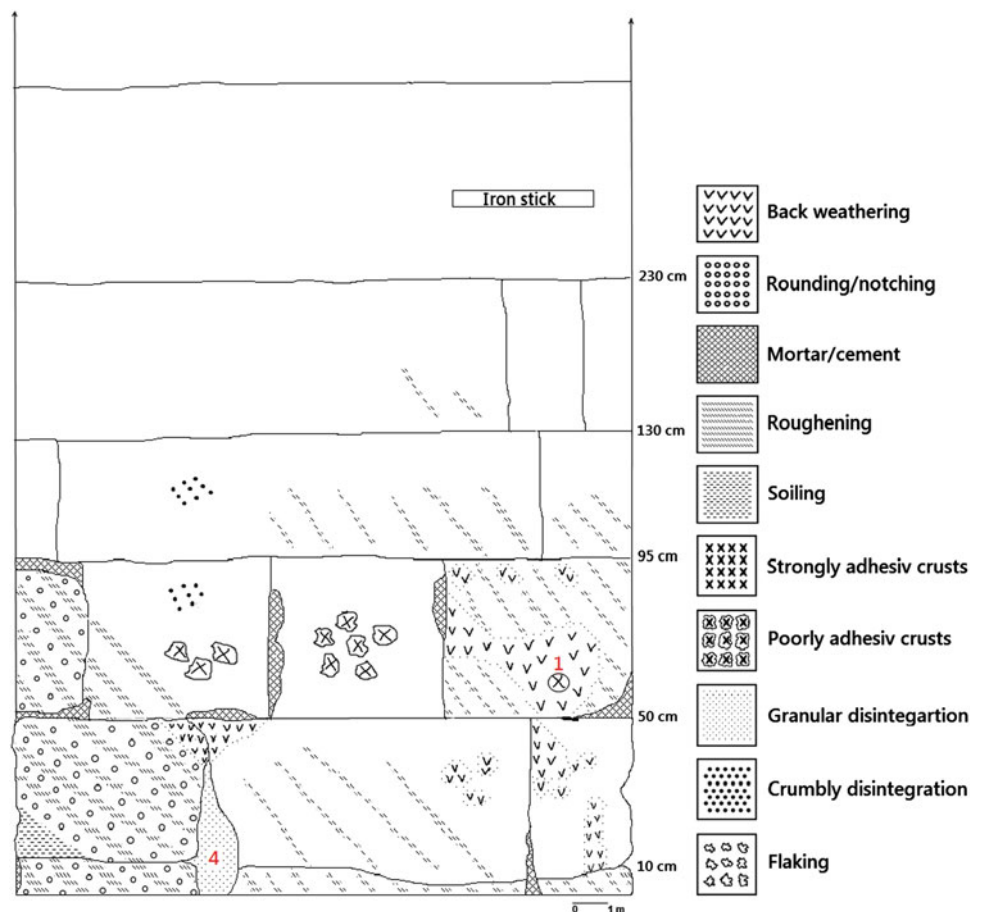
---

## 102.4 Results

### 102.4.1 Mapping

The weathering zone is situated in the lower half of the columns and reaches from the column base upward to an

**Fig. 102.1** Mapping of back weathering and detachment on the surface of the park-side wall of column 1



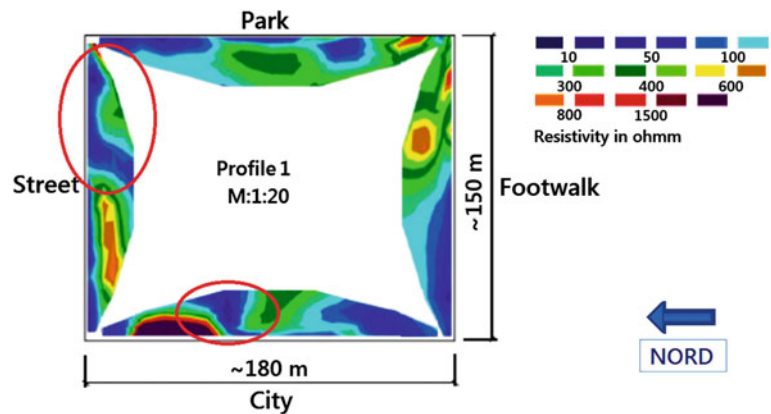
elevation of 0.80–1.30 m above ground, depending on the side of the wall. Above this threshold, the surface of the walls is covered by a thick render and on these parts, almost no weathering was observed. The pavement-side walls of the columns are rendered from the base upwards, except of the corners where weathering occurs. Considerable back-weathering and detachment of stone surface are visible at almost all sides, except of the pavement-side faces where these weathering phenomena are less common. The edges of the corners of the columns are often rounded due to partial weathering. Dark-colored spots, which may belong to soiling deposits and flake-like, poorly adhesive crusts, exist in several places of the weathering zone. The mapping of weathering features on the surface of the park-side wall of column 1 is shown in Fig. 102.1. A crystallized salt deposit was found in the middle of a back weathering hollow. The position of the efflorescence is marked as number 1 (written in red) in Fig. 102.1. According to the ERT (see next section), this efflorescence seems to extend into the subsurface of the masonry.

#### 102.4.2 2D-Geolectric (ERT)

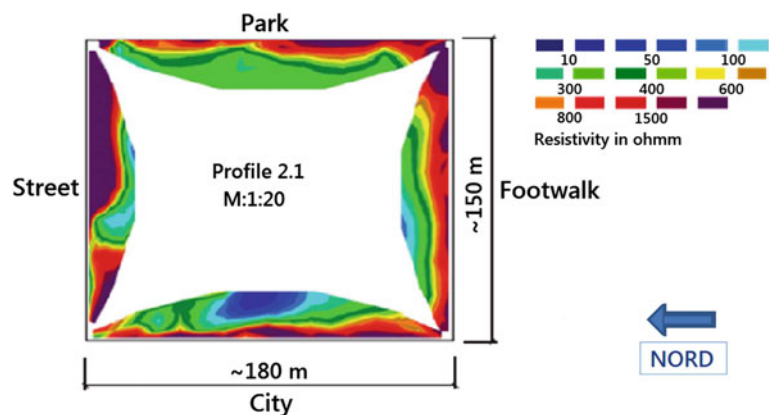
Figure 102.2 displays all profiles of the horizontal ERT section 1 and their position at the column. This section is located in the lower part of the column, in the middle of the weathering zone. The overview at the upper left side of the figure shows that most of the lower resistivity areas (wetness or salts, blue colours) are situated immediately at the surface and at a shallow depth (approx. 10 cm); however, at some sections of the column they extend to greater depth. At the corner of the park- and pavement-side walls much higher resistivity is visible (red colours) which points to drier conditions especially near the surface. The highest resistivity was measured in a zone of some decimeters width at the city-facing side.

Figure 102.3 illustrates all profiles of the horizontal ERT section 2 and their position at the column. The profiles of this ERT section are well above the weathering area, in the upper part of the column. Much higher resistivity values appear in the shallow subsurface of all profiles of this section

**Fig. 102.2** Horizontal ERT section 1 with their position at the column 1. *Red circles* Paths of moisture ingress (see discussion)



**Fig. 102.3** Horizontal ERT section 2 with their position at the column 1



which is in correlation with the render covered surface of the masonry. This pattern is in sharp contrast to the lower ERT section with low resistivities near the surface. In some areas in the deeper region of the column low resistivity areas are visible (green colours) which are broadly similar to the interior parts at the lower profile section. Very lower resistivities occur (for unknown reasons) in the subsurface on the city-facing side.

Figure 102.4 shows all vertical ERT profiles and their position at the column. All profiles show very high resistivities at the uppermost part, which correlate with the render covered zone of the stonework. The lower resistivity of the weathered zone (ground to c. 0.8–1.3 m) is well visible at all column faces. However, the street and city orientated walls show particularly low resistivity which also reaches much deeper into the masonry. At the park-side wall the driest conditions of all vertical profiles are found with the exception of one wet or salty patch near the surface at 0.5–0.88 m. At the wall orientated to the pavement, the base and the

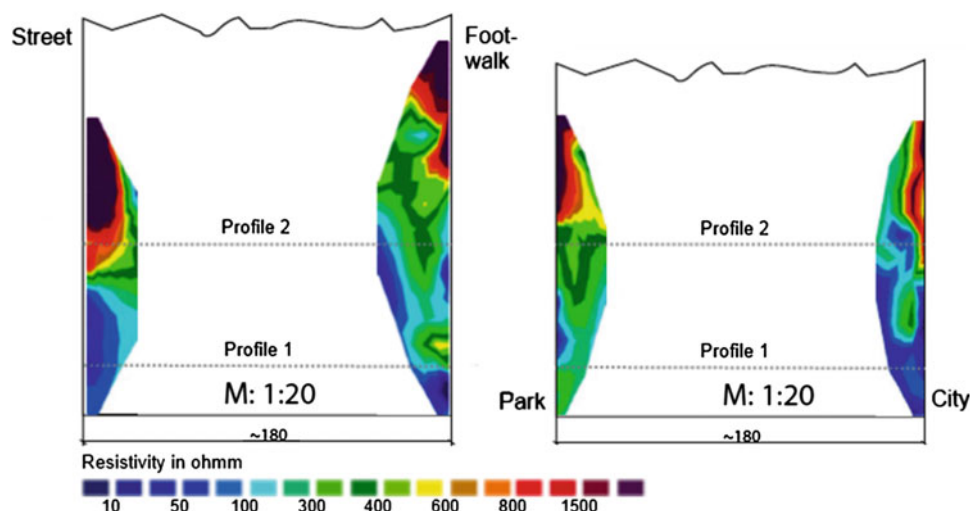
upper zone of the weathered area stand out for their lower resistivity.

## 102.5 Handheld Moisture Meter

The moisture was measured on the surface of each wall of column 1. About 35 measure points were detected on each side, up to a height of 2.20 m (Table 102.1). The moisture decreases with height of the column. The base (the upper 10 cm) at the street-side wall is drier than above. The results of the moisture meter measurements reveal a pronounced wetting zone at the base of the column.

### 102.5.1 Paper Pulp Poultices

Five samples were taken from the surface of column 1 to investigate the salt concentrations and their types. The points

**Fig. 102.4** Vertical ERT section with their position at the column 1**Table 102.1** Results of the handheld moisture meter measurements (Digit)

Height (cm)	Park-side wall			Pavement-side wall			City-side wall			Street-side wall		
	Right side	Middle	Left side	Right side	Middle	Left side	Right side	Middle	Left side	Right side	Middle	Left side
2.2	0	0	0	0	0	0	0	0	0	0	10.8	0
2	14.1	10.1	0.8	5	5.6	2.3	7.7	2.4	13.5	1.5	15.6	6.7
1.8	19.4	8.8	2.8	0.4	14.3	10.4	10.6	9.8	38.5	5.5	3	20.1
1.6	34.8	23.2	0	13.6	21.8	15.3	34.2	29.7	14	14	11	11.6
1.4	15.5	22.3	24.6	5.7	2.9	11.3	49.3	11.7	36	33.6	76.2	12.3
1.1	22.6	19.9	47.5	4.2	15.8	11.1	55.5	50.1	23.5	42	85.3	51.6
0.8	42.1	51	71.5	37.7	22.1	29.8	76.5	71	47.9	69.6	94	42.5
0.5	82.4	29.3	83.7	19.1	22.8	44.6	98	77.4	60.1	85	100	80.7
0.2	100	23.3	100	66.6	87.2	33.8	100	96	80	100	25	100
0	100	61	100	100	84.4	100	100	100	100	30	56.8	54.6

of sampling were places with visually strong decay. In Table 102.2 the results of the sampling points were compared to basic values, which belong to a non-weathered surface of the rock. Two sampling points (nr. 1 and 4) are marked as red numbers in Fig. 102.1. One sampling point (nr. 1) shows an efflorescence of 10–15 cm diameter. It is

one of the ‘hot spots’ of weathering decay at the column. Such formation was also described for halite (NaCl) deposits on limestone in the Namib (Goudie et al. 1997). Three samples (nr. 2, 3 and 5) were picked up at the base of the column, near the ground and two samples (nr. 1 and 4) are originated from a height of about 60–70 cm. The results of

**Table 102.2** Results of the Ion chromatography (mg/l) for paper pulp poultices sampling

Test	Orientation	Note	Na <sup>+</sup>	K <sup>+</sup>	Mg <sup>2+</sup>	Ca <sup>2+</sup>	Cl <sup>-</sup>	NO <sub>3</sub> <sup>-</sup>	SO <sub>4</sub> <sup>2-</sup>
0	Basic values		8.92	2.59	0.86	5.24	4.75	4.38	20.22
1	Park-side wall	Efflorescence	256.96	33.98	21.15	166.45	591.25	156.66	139.28
2	City-side wall	Back weathering	300.99	2.85	4.28	38.04	524.69	6.45	5.63
3	Street-side wall	Back weathering	357.85	13.92	20.27	142.87	699.14	145.45	110.97
4	Park-side wall	Flacking	295.95	4.42	4.86	35.70	515.87	4.29	13.33
5	Pavement-side wall	Soiling	570.35	161.40	47.01	278.43	1031.48	977.84	118.92

the ion chromatography show different anion concentrations (chlorides, sulfates and nitrates). At all walls of the column chlorides were found, although the highest amount at sample number 5. Near-ground sampling positions (nr. 3 and 5) and the point with the efflorescence (nr. 1) exhibit higher amounts of sulfates and nitrates. The samples number 2 and 4 show negligibly low amounts of sulfates and nitrates. The highest amount of chlorides, sulfates and nitrates shows the sampling point number 5, which is located at the pavement-side wall. Also an amount of 6.47 mg/l ammonium ( $\text{NH}_4$ ) was found at this place, which originates from organic acids (probably bird droppings).

## 102.6 Discussion

2D-resistivity turned out to be a valuable tool for visualising moisture distribution in the investigated masonry. As the stone type is very similar in all parts of the investigated columns (apart from the render facing in the higher parts), observed zones of low surface resistivity can in all probability be associated with higher moisture and/or salt content. At some spots, iron bars stick out of the stone surface at different height which might be influencing the 2D-geolectric survey the profiles. However, as we did not observe heightened conductivity around these features, we assume that they don't go deep into the masonry and do not obstruct the measurement. As pointed out earlier, it is hard to discriminate salt from water from resistivity measurements alone (Sass and Viles 2010b). The supplementary measurements help to clarify this point. The capacitive hand sensor (which is unaffected by salts) clearly shows that surficial water content is heightened in the lower parts of the column. However, considering the results derived from the paper pulp poultices, salts contribute to low resistivities as well. This is underlined by the fact that the sampled area with the highest ion content (column base at pavement side) stands out for the lowest resistivity of all geoelectrical profiles.

The most conspicuous pattern is the much lower resistivity around the base of the column and up to a height of 0.8–1.3 m which is particularly apparent in the vertical profiles. This elevation above ground roughly corresponds to the upper fringe of the observed weathering features. We assume that capillary rise of groundwater and surface water, together with spray from passing vehicles are the main reasons for dampness near the base of the columns. In turn, this is also the main explanation for the concentration of weathering features in this area. Similar patterns were observed at artificial walls in Oxford (UK) (Sass and Viles 2010a, b). The upper profile section is very different with a markedly drier surface zone. We assume that this area is well above the spray and capillary rise zone. However, the thick render also contributes to the high resistivity which makes it

difficult to compare the near surface resistivity between the lower and the upper profiles.

Apart from small-scale variations, the mean wetness of all sides of the column appears to be relatively similar. This is valid both for the lower (horizontal section 1) and for the upper section (horizontal section 2). However, the largest area of very low resistivity ( $<20 \Omega\text{m}$ ) at the surface is found on the street- and city-facing sides. Some areas seem to be noticeably drier, e.g. the pavement/park corner in the lower section, which is probably due to the distance to the street and shielding from rainfall, as well as to better drying conditions near the corners (Fig. 102.2). The resistivity deeper inside the column is quite similar between the lower and the upper section (c. 300–500  $\Omega\text{m}$ —greenish colours) which means that from a certain depth, the stonework of the column remains largely unaffected by surficial moisture fluctuations (Fig. 102.4). Some of the observed small-scale patterns in the lower section can be related to weathering features or stone properties observed at the surface. The highest resistivity of all profiles was found in the lower horizontal ERT section at the city-facing column front. It correlates to an air-filled cavity behind the visual surface of one of the square stones. Lower subsurface resistivity exists at the corner of the street- to park-side and at the corner of the city- to pavement-side. Probably it has to do with zones of enhanced moisture, which reach from each of the mentioned corners until the middle of the respective column side and reach from surface to visible 25.5 cm and possibly much deeper. At the street-side and city-side there seem to be lower resistivity paths from the surface to deeper regions (red-rimmed areas in Fig. 102.2). These zones probably reflect the ashlar margins between limestone blocks.

The vertical profiles of the ERT survey clearly mirror the weathered zone of the column by means of high conductivity values from the base up to ca. 1.30 m. This is a strong indication that the ongoing decay at the column is caused by heightened moisture at the surface and shallow subsurface caused by capillary rise of groundwater and surface water. The absence of visible weathering at greater elevation might be caused by the water-protective character of the thick render cover. However, it is more plausible that the render initially covered the entire column and has come down due to decay in the lower parts. Considerable salt weathering is presumed by the visible efflorescence and by the results of ion chromatography. The salts are probably introduced by road de-icing and spray water which only reaches the lower part of the columns (Doehne 2002). The results of the ion chromatography expect that salts are very present at the stone surface which makes it rather improbable that the salts derive from the capillary rise of ground water. Sulfates and nitrates are located at the stone surface near the ground. At areas of strong decay, sulfates and nitrates are also present. The latter might derive from organic acids like pidgeon

droppings. Surprisingly, the shielded position of the columns within the gate does not seem to be a valid protection against decay; the lack of direct rainfall might even promote salt weathering as the abundant salts are not washed down.

## 102.7 Conclusion

Intensive stone decay was observed at four rain-shielded columns of the Paulustor gate in Graz. The weathering features concentrate on the base of the columns up to c. 1.3 m; in this zone, the protective render has weathered off. Geoelectric profiles, supplemented by capacitive measurements and paper pulp poultices, show that both water and salt content are heightened in this area which is probably the reason for effective salt weathering. Water and salts mostly derive from surface spray and to some extent from capillary rise; the shielded position prevents the salts from being washed down. Furthermore, patterns of water ingress could be observed (which is, however, of little relevance for surficial weathering). 2D-resistivity, when combined with other methods like mapping and sampling, proved to be a very helpful approach for visualizing patterns of moisture and salt concentration.

**Acknowledgements** The author wish to thank the Institute of Applied Geoscience of the Technical University of Graz for analysing the paper pulp poultice samples by means of the ion chromatograph (Dionex ICS-3000 Reagent-Free).

## References

- Backbier L, Rousseau J (1993) Analytical study of salt migration and efflorescence in a mediaeval cathedral. *Anal Chim Acta* 283:855–867
- Dionisio A, Martinho E, Grangeia C, Almeida F (2012) Non-invasive techniques for the evaluation of stone conservation. In: *Global Stone Congress 2012*, Borba, Portugal, pp 170–177
- Doehne E (2002) Salt weathering: a selective review. *Natural stone, weathering phenomena, conservation strategies and case studies*. Geological Society. Special Publications, vol 205, pp 51–64
- Eklund JA, Zhang H, Viles HA, Curteis T (2013) Using hand-held moisture meters on limestone: some factors affecting their performance and guidelines for best practice. *Int J Architect Herit* 7 (2):207–224
- Fitzner B, Heinrichs K (2002) Damage diagnosis on stone monuments—weathering forms, damage categories and damage indices: understanding and managing stone decay. In: *Proceedings of the international conference ‘stone weathering and atmospheric pollution network (SWAPNET)’ 2001*, Prague, Czech Republic, pp 11–56
- Fitzner B, Heinrichs K (2005) Kartierung und Bewertung von Verwitterungsschäden an Natursteinbauwerken. *Zeitschrift der deutschen Gesellschaft für Geowissenschaften* 156(1):7–24
- Franzen Ch, Mirwald PW (2009) Moisture sorption behaviour of salt mixtures in porous stone. *Chem Erde* 69:91–98
- Goudie AS, Viles HA, Parker AG (1997) Monitoring of rapid salt weathering in the central Namib Desert using limestone blocks. *J Arid Environ* 37:581–598
- Gross M (2007) Das Neogen des steirischen Beckens. *Exkursionsführer. Joannea—Geol Paläontol* 9:117–193
- Hidden H (2001) Das “Leithakalk”-Areal von Retznei-Aflenz-Wagna südlich von Leibnitz. *Geologie, Fossilführung und Bergbaugeschichte. Der Steirische Mineralog* 11:14–19
- Leucci G, Cataldo R, De Nunizio G (2007) Assessment of fractures in some columns inside the crypt of the Cattedrale di Otranto using integrated geophysical methods. *J Archaeol Sci* 34:222–232
- Loke MH, Barker RD (1995) Least-squares deconvolution of apparent resistivity pseudosections. *Geophysics* 60(6):1682–1690
- Martinho E, Alegria F, Dionisio A, Grangeia C, Almeida F (2012) 3D-resistivity imaging and distribution of water soluble salts in Portuguese Renaissance stone bas-reliefs. *Eng Geol* 141–142:33–44
- Mol L, Viles HA (2010) Geoelectric investigations into sandstone moisture regimes: implications for rock weathering and the deterioration of San Rock Art in the Golden Gate Reserve, South Africa. *Geomorphology* 118:280–287
- Sass O, Viles HA (2010a) Wetting and drying of masonry walls: 2D-resistivity monitoring of driving rain experiments on historic stonework in Oxford, UK. *J Appl Geophys* 70:72–83
- Sass O, Viles HA (2010b) Two-dimensional resistivity surveys of the moisture content of historic limestone walls in Oxford, UK: implications for understanding catastrophic stone deterioration
- Turkington AV, Smith BJ (2000) Observation of three-dimensional salt distribution in building sandstone. *Earth Surf Process Landf* 25:1317–1332

---

# Monitoring of the Thermal-Moisture Regime at St. Jacob's Church in Levoča UNESCO Site, Eastern Slovakia

# 103

Jan Vlcko, Vladimír Greif, Ľudovít Kubičár, Danica Fidiriková, and Kralovičová Lenka

---

## Abstract

The paper deals with the monitoring of thermal-moisture regime, as one of the deterioration factors within the rock material at UNESCO historic site, particularly in the supporting pillars of St. Jacobs's church in Levoča, Eastern Slovakia. The moisture sensor consists of a small cylinder having the diameter and length of 20 mm in which a small ball of 2 mm diameter is placed that delivers the heat in step-wise regime and simultaneously measures temperature. Two sensors have been positioned in South-North orientation and embedded in the church supporting pillars. During monitoring we have identified diffusion of moisture associated with cycle day/night and cycle wetting/drying caused by meteorological precipitation.

---

## Keywords

Moisture sensor • Rock deterioration • Sandstone • Levoča

---

## 103.1 Introduction

Degradation of building stones is strongly influenced by moisture that in combination with temperature, salt and various biofactors, have high correlation with geographical location, microclimate and with the local hydrological and hydrogeological conditions. Historic structures frequently suffer from structural failures which might be triggered by both highly deteriorated subgrade and/or by deteriorated decorative and ornamental parts having structural function. In both cases, especially when the rock/stone is easily cut and porous the moisture in rock triggers the deterioration processes.

The absorption and transport of water in porous materials combined with the effects of moist air movement through these structures are complex processes. Understanding the moisture content in the historic structure, its distribution and temporal variation is crucial in the prediction of porous material decay. Moisture in the rock/stone (masonry) has a destructive impact caused by cycles of wetting/drying, freezing and thawing. Modern building and conservation techniques can significantly suppress the diffusion of moisture into foundations or rock/stone (masonry). The open question is the efficiency of taken measures as well as the variability in moisture distribution within the historic structure as the response to permanently changing environmental conditions, including human impact. The best tool to observe the complex process of moisture migration in the rock/stone is appropriate on-site monitoring (Fidiriková et al. 2013a). Therefore, moisture monitoring and the knowledge of moisture-thermal regime of rocks has assumed high priority in various branches of civil engineering, geotechnical engineering and engineering geology, especially in the field of appropriate remedial and preservation measures selection within the historic structure restoration process.

---

J. Vlcko (✉) · V. Greif · K. Lenka  
Department of Engineering Geology, Faculty of Natural Sciences,  
Comenius University Bratislava, Mlynska dolina G, 84215,  
Bratislava, Slovakia  
e-mail: vlcko@fns.uniba.sk

L. Kubičár · D. Fidiriková  
Institute of Physics, Slovak Academy of Sciences, Dúbravská  
cesta 9, 84511 Bratislava, Slovakia

This paper presents results of the monitoring of thermal moisture regime of St Jacob's Church in Levoča by thermal conductivity sensor. Data on temperature and moisture variation were recorded. Time series gained during the monitoring period were correlated with the meteorological data. The theory of the sensor, its construction and measuring regime is described briefly.

### 103.2 Site Description

City of Levoča is located in the historical region of Spiš, which was inhabited as early as the Stone Age. In the 11th century, this region was conquered and, subsequently, became part of the Kingdom of Hungary and remained such until 1918. After the Mongol invasions of 1241/1242, the area was also settled by Germans. The oldest written reference to the city of Levoča dates back to 1249. The 14th century Roman Catholic Church of St Jacob (Fig. 103.1) is the real pearl of the historic town. It houses a magnificently carved and painted wooden Gothic altar, the largest in Europe, (18.62 m in height), created by Master Paul around 1520.

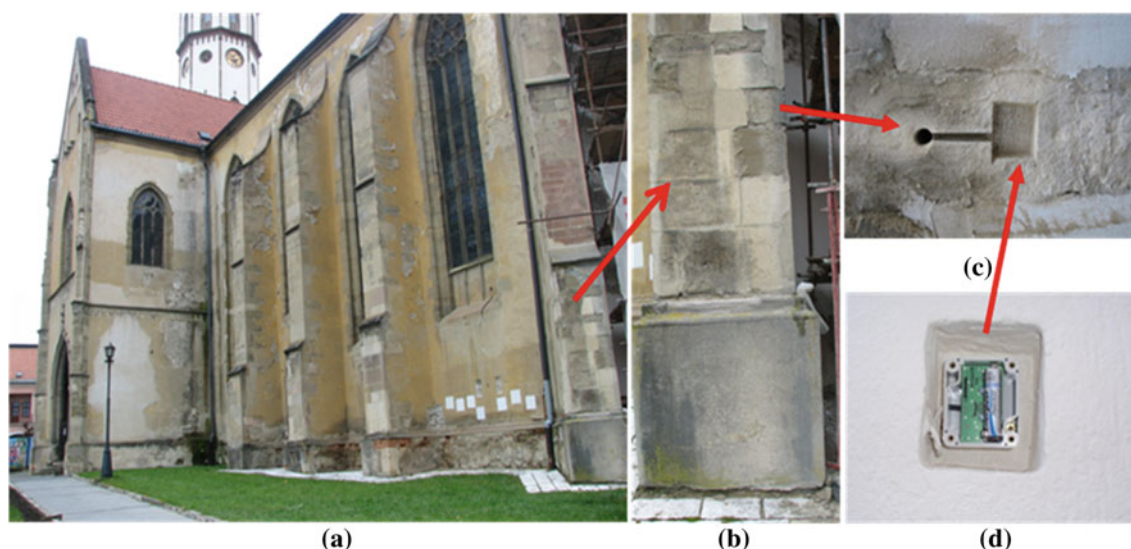
From the geological point of view Levoča historic centre is situated on a small hill, which is a part of Levoča Mts. composed of Paleocene flysh formation where sandstones prevail over claystones. Sandstones form not only the sub-grade of the St Jacob's church they also form construction material in the foundations (sandstone slabs reaching 60–80 cm in length and 10–15 cm in height) and substantial part of upper structure. In places where the sandstones were deteriorated, bricks were used as the replacement material

(Fig. 103.1). Detailed geotechnical investigation revealed that the foundations depth of spread footings varies between 1.2 and 2.25 m, the supporting pillars are of the same foundation depth. The groundwater depth is at the level of 2.5–4.0 m and does not reach the foundations. At the positions of exploration pits below foundations tubes of old sewage system were discovered which are of poor quality and leakages in rainy season may occur and thus in some period of year the foundations more or less are in direct contact with waste water.

Frequent precipitation in combination with frost during the winter is a deteriorating factor that causes the sandstone blocks decay in the upper structure, mainly in the supporting pillars (Fig. 103.1a, b). Two positions were chosen for moisture monitoring, namely the north and south pillars of the St Jacobs Church in a height of 2.5 m above the ground (Fig. 103.1b). Holes in diameter of 30 mm to depths of 150 mm were drilled into the sandstone blocks (Fig. 103.1). Body for moisture sensor was prepared from the cylindrical core sample drilled from sandstone block with a length of 30 mm. A hole in diameter of 2 mm was bored along the longitudinal axis and the sensing element in a form of a ball in diameter up to 2 mm was fixed inside the sample. Figure 103.1c, d shows overall arrangement of the monitoring location.

### 103.3 Sandstone Properties

Sandstone is fine-grained, brown to grey in color with uniform distributed mineral components (quartz, feldspar and lithic fragments of shale, limestone, phyllite, silicite). As far

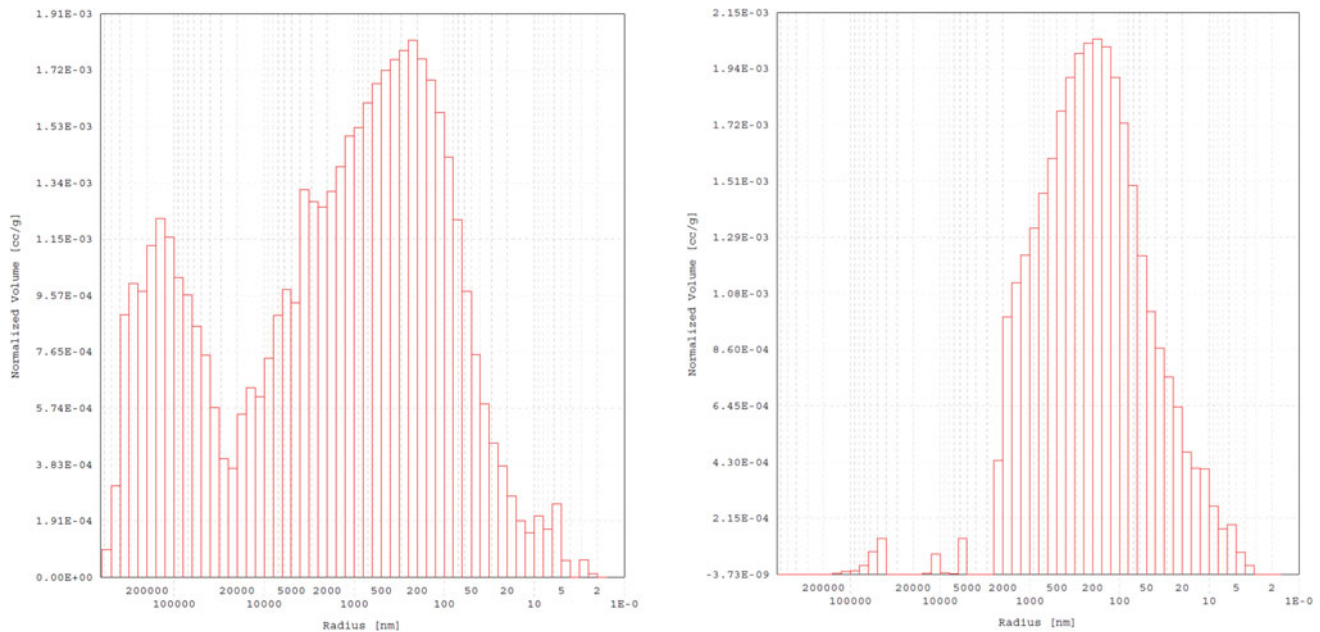


**Fig. 103.1** Church of St Jacob (a), pillar made of sandstone blocks (b) and overall arrangement of the monitoring position before installation and after finalizing of the instrument set-up (c, d)

**Table 103.1** Physico-mechanical properties of sandstone from St Jacob's church in Levoča

	Bulk density [kg/m <sup>3</sup> ]	Density [kg/m <sup>3</sup> ]	Porosity [%]	Saturation [%]	UCS [MPa]	Elasticity modulus [GPa]	Deform modulus [GPa]	Poisson's ratio [-]
W*	2.504	2.75	8.94	3.19	–	–	–	–
NW*	2.455	2.739	10.28	3.67	36.7	8.82	7.12	0.248

W\* weathered sample, NW\* not weathered sample

**Fig. 103.2** Distribution functions of the pore sizes in sandstone not weathered (*left*) and weathered (*right*)

as the physico-mechanical properties concerns there were taken samples from sandstone blocks located in a window sill of the church, from the interior, relatively fresh ones-not-weathered, and from the exterior weathered samples.

As shown in the Table 103.1 the rock properties of weathered samples are clearly recognized, especially as far as the porosity and saturation concerns. Some of thermo-physical parameters reach these vales: coefficient of linear thermal expansion  $1.0710 \times 10^{-5}$  (not weathered) and for weathered  $1.0910 \times 10^{-5}$  [m/mK], thermal diffusivity 0.84407 [mm<sup>2</sup>/s], specific heat 1006.84 [J/kg.C] and thermal conductivity 2.091996 [W/m.K].

The differences in both types of sandstones were also confirmed by the Hg porosimetry test when pore size distribution was determined. Pore size distribution function (Fig. 103.2) of not weathered sandstone has two maxima, the first one corresponds to 120 nm and the second one to 200 nm, while by the weathered sandstone the first peak corresponding to the pore size of 120 nm was not detected. Its absence can be probably attributed to deposits from acid rains. As the atmosphere before year 1800 was probably less polluted it can be assumed that a real time of weathering

corresponds to 200 years, though sandstone blocks were exposed to climatic factors over last 600 years.

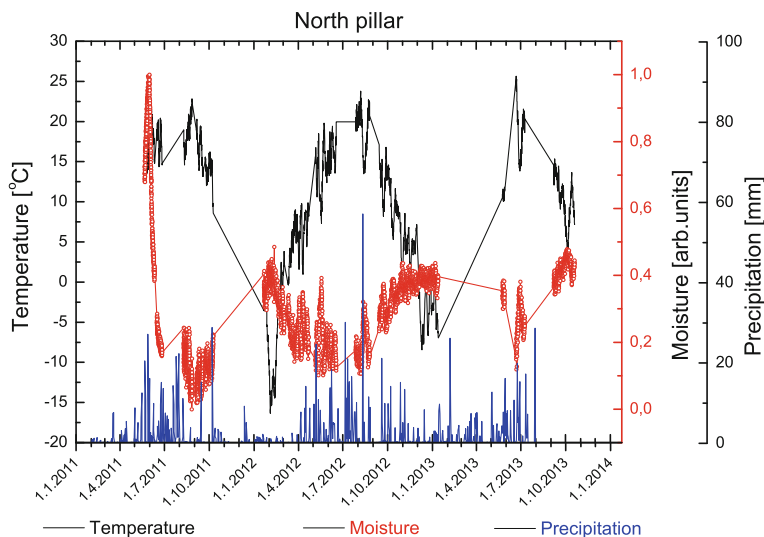
#### 103.4 Moisture Sensor

Body of the moisture sensor(s) is manufactured of the sandstone core drilled directly from the supporting pillars. Sensor body has shape of cylinder in diameter and length of 30 mm. A hole in diameter of 2 mm was drilled in the longitudinal axis of the cylinder in which a sensing element is fixed using epoxy resin (Fig. 103.3). The principle of sensing element is based on the transient hot-ball method for measuring thermal conductivity (Kubičár et al. 2010). The signal of the sensing element is not sensitive to ionic radicals of the pore medium. Sensing element (hot ball) is inserted back into the drilled hole to ensure that the porous structure of both the sensor body and the investigated material are identical and is capable to provide the contact for heat and water transport at the interface surrounding sandstone block and the sensor. Thermal conductivity of the porous material is a function of the pore content (Fidriková et al. 2013b).

**Fig. 103.3** Photo of moisture sensor with sensing element (*hot ball*) inside it



**Fig. 103.4** Temperature–moisture regime recorded from the North pillar at St Jacob’s church in Levoča



Therefore the moisture sensor can be used to determine the water content in the sandstone block when calibration is carried out prior to the inserting the sensor into rock block. The calibration is performed in dry and water saturated conditions using “classic” gravimetric method. Then linear relation between the water content in sensor body and the sensor signal is used.

A simple instrument RTM (Transient MS, s.r.o.) that is constructed for use in a harsh environment. The instrument can be pre-programmed over the USB channel by a PC.

Monitoring procedure starts when the bond stabilizes and thermodynamic equilibration between the sensor and the surrounding medium is attained. This can be recognized by acquired monitored data (Fig. 103.4).

### 103.5 Results and Discussion

As can be seen from the monitoring data series recorded during last 3 years the temperature–moisture curves in the North pillar correspond to diurnal and annual temperature cycles. After stabilization period (approx two months) real temperature–moisture data were recorded. Sudden fall of moisture curve during the stabilization period is depending

on material properties bonding the interface of sensor body and rock wall. In the case of North pillar milled sandstone served as the natural bond medium. This proved to be appropriate assembly acting as a single structural unit securing thermodynamic equilibration and recorded data are of high relevance. Despite the knowledge we gained, additional study needs to be performed in order to find out proper bond material to accelerate the stabilization period.

**Acknowledgments** This work was supported by the Slovak Research and Development Agency under the contracts No. APVV-0641-10, APVV-0330-10 as well by VEGA 2-0190-12.

### References

- Fidriková D, Vretenár V, Šimková I, Greif V, Vlčko J, Dieška P, Kubičár L (2013a) Sensor for monitoring the moisture in porous materials. *Int J Thermophys* (published online August, 2013a) doi:[10.1007/s10765-013-1493-0](https://doi.org/10.1007/s10765-013-1493-0)
- Fidriková D, Greif V, Dieška P, Štofanič V, Kubičár L, Vlčko J (2013b) Monitoring of the temperature–moisture regime in St. Martin’s Cathedral tower in Bratislava. *J Environ Earth Sci* 69:1481–1489
- Kubičár L, Vretenár V, Štofanič V, Boháč V (2010) Hot-ball method for measuring thermal conductivity. *Int J Thermophys* 31(10):1904–1918

---

## Author Index

### A

Accattino, Edoardo, 207  
Afonso, Maria José, 227  
Agliardi, F., 357  
Ahmad, Zalooli, 477  
Ajassa, Roberto, 235, 427  
Alberico, Sonnessa, 293  
Alberto, Landuzzi, 317  
Alena, Girelli Valentina, 317  
Alessandra, Nocilla, 409  
Alessandra, Tini Maria, 317  
Ali, Harith E., 515  
Al-Mukhtar, Muzahim, 515  
Álvarez de Buergo, Mónica, 491  
Amalia, Mastelloni Maria, 409  
Amin, Jamshidi, 477  
António, Pinho, 311  
Antoniou, Andreas, 95  
Anzidei, Marco, 405  
Aringoli, D., 273  
Aryamontri, Deborah Chatr, 495  
Avolio, Maria Vittoria, 405  
Awang Rosli, Nurul Liyana B., 305  
Azzam, Rafig, 507

### B

Bacchetti, Marco, 269  
Balestro, Gianni, 239  
Battista, Crosta Giovanni, 293  
Bednarczyk, Zbigniew, 369  
Belhocine, B., 169  
Benchiarin, Simone, 547  
Bernhard, Lempe, 107, 113  
Bertok, C., 257  
Bianchini, Paolo, 323  
Birami, Farideh Amini, 231  
Blanco-Varela, María Teresa, 531  
Blinova, Iuliia, 223  
Bodin, Xavier, 249  
Bollati, Irene, 213  
Bonanni, Patrizia, 535  
Borghi, Alessandro, 207, 239  
Borostyáni, Márta, 153  
Bouhedja, Samir, 375  
Boukhaleh, Ahmed, 275  
Boumezeur, A., 169  
Brancaleoni, Roberto, 335  
Bredikhin, Andrey, 223

### C

Cacace, Carlo, 535  
Caielli, Grazia, 59  
Calcaterra, Domenico, 421  
Cámara, Fernando, 235  
Cantisani, Emma, 387  
Carmona-Quiroga, Paul María, 531  
Castellanza, Riccardo, 59, 65  
Castelli, Daniele, 239  
Caviglia, Caterina, 427  
Cecilia, Spreafico Margherita, 317  
Celletti, Federico, 335  
Chaminé, Helder I., 227  
Chen, Wenwu, 193, 199  
Chen, Yi, 189  
Chiarle, Marta, 459  
Chiba, Tatsuuro, 99  
Chikaosa, Tanimoto, 71  
Chiotinis, Nikitas, 95  
Cho, Sung-Bu, 329  
Christaras, Basile, 139  
Christian, Kaiser, 265  
Chunze, Piao, 71  
Ciantia, Matteo Oryem, 65  
Cigna, Francesca, 339  
Cinzia, Zotta, 453  
Clari, P., 257  
Claudio, Lucente Corrado, 463  
Claudio, Margottini, I., 293, 299  
Claudio, Scavia, 293  
Coli, Massimo, 323  
Coratza, Paola, 213  
Corrado, Lucente Claudio, 317  
Costa, Emanuele, 235  
Cripps, John, 305  
Crisci, Gino Mirocle, 405  
Cristian, Marunteanu, 281  
Cristiano, Guerra, 463  
Cristofaro, Maria Teresa, 323  
Crosta, Giovanni B., 59, 357, 361  
Cuccuru, Francesco, 139  
Cusano, Mariacarmela, 535

### D

d'atri, Anna, 207, 257  
Danica, Fidriková, 577  
Daniele, Giordan, 293  
Daniele, Spizzichino, 293, 299

Dela Pierre, F., 257, 261  
 Deline, Philip, 249  
 Deng, Xiaolong, 123  
 Destefanis, Enrico, 427  
 Di Gregorio, Salvatore, 405  
 di Prisco, Claudio, 65  
 di Santolo, Anna Scotto, 47, 421  
 Dias Costa, Maria João, 227  
 Dinçer, İsmail, 361  
 Dino, Giovanna Antonella, 207  
 Dubiřar, Jakub, 443

**E**

Egartner, I., 569  
 Elsa, Pedro, 311  
 Emanuele, Mandanici, 317  
 Emmanuel, Reynard, 265  
 Evangelista, Aldo, 47  
 Evangelista, Lorenza, 47

**F**

Fais, Silvana, 139  
 Falconi, Luca, 287  
 Fan, Yuquan, 183  
 Farabollini, P., 273  
 Fassina, Vasco, 37, 547  
 Ferrando, Simona, 207, 235, 239  
 Fierascu, Irina, 543  
 Fierascu, Radu-Claudiu, 543  
 Forno, Maria Gabriella, 235  
 Fort, Rafael, 491  
 Francesca, Franci, 317  
 de Franco, Roberto, 59  
 Frascá, Maria Heloisa Barros de Oliveira, 511  
 Fratini, Fabio, 387  
 Frattini, Paolo, 357, 361  
 Freire-Lista, David Martin, 491  
 Frigerio, Gabriele, 59, 65  
 Fujii, Yukiyasu, 75

**G**

Gabriele, Bitelli, 317  
 Gabriele, Leoni, 299  
 Gaddi, Raffaella, 535  
 Gama Pereira, Luís C., 227  
 Garbin, Fabio, 335  
 Garrido, Jesús, 437  
 Gaspari, Giuseppe M., 129  
 Géraldine, Regolini, 265  
 Ghiraldi, Luca, 257, 261, 269  
 Gianotti, Franco, 235, 245  
 Giardino, Marco, 213, 235, 245, 257, 261, 269, 447  
 Giordano, E., 257, 261  
 Giorgio, Lollino, 293  
 Giovagnoli, Annamaria, 535  
 Giovanni, Gigli, 293  
 Giovanni, Mortara, 463  
 Giuseppe, Delmonaco, 299  
 Gopeenatha, Namita, 129  
 Graham, Callum, 487  
 Greif, Vladimir, 491  
 Groppo, Chiara, 207

Groppo, Chiara, 239  
 Guo, Qinglin, 31, 177, 183  
 Gurli, Meyer, 253  
 Gutiérrez, M<sup>a</sup> Lourdes, 437  
 Gyula, Bögöly, 503

**H**

Hajjalilu, Masoud, 231  
 Harris, Barnabas, 305  
 Hasegawa, Shuichi, 99  
 He, Faguo, 193, 199  
 Heinrichs, Kurt, 507  
 Hencher, Steve, 329  
 Hmaidia, H., 169  
 Hossain, Ismail, 219  
 Huisman, Hans, 103  
 Humberto, Varum, 311

**I**

Ion, Mihaela-Lucia, 543  
 Ion, Rodica-Mariana, 543  
 Ioshinori, Iwasaky, 293  
 Isabel, Duarte, 311  
 Isabella, Bianco, 159  
 Ishikawa, Yuzo, 31, 177  
 Iwasaki, Yoshinori, 31, 53, 177

**J**

Jan, Vlcko, 577  
 de Jayawardena, Upali Silva, 43  
 Jordie, Corominas, 293  
 Judith, Festl, 107

**K**

Kageura, Ryota, 99  
 Kaljahi, Ebrahim Asghari, 231  
 Karatasios, Ioannis, 525  
 Kathrin, Scherzer, 107  
 Kawato, Katsushi, 99  
 Kazuhiro, Oda, 71  
 Kechebour, Boualem El, 375  
 Keigo, Koizumi, 71  
 Khattab, Suhail A., 515  
 Kikuchi, Katsuhiko, 75  
 Kilikoglou, Vassilis, 525  
 Kim, Gun-Su, 329  
 Kim, Ji-Won, 329  
 Koizumi, Keigo, 31, 177  
 Konstantopoulou, Garyfalia, 431  
 Kontogianni, Vaia, 431  
 Kouki, Athanasia, 89  
 Koukis, George, 89  
 Koyama, Tomofumi, 53  
 Kralovičová, Lenka, 577  
 Kulczykowski, Marek, 381  
 Kuroschi, Thuro, 107, 113

**L**

Lacanna, Giorgio, 323  
 Lari, S., 357

Lasaponara, Rosa, 339  
 Laskowicz, Izabela, 381, 415  
 Laszlovszky, J., 471  
 Laura, Ercoli, 409  
 Laureti, Lamberto, 213  
 Leahu, Mirela, 543  
 Lee, Ho-Dam, 329  
 Lee, Martin, 487  
 Lee, Su-Gon, 329  
 Lee, Young-Suk, 329  
 Lekkas, Efthymis, 95  
 Leonelli, Giovanni, 213  
 Lewis, Roger, 305  
 Li, Lihui, 123  
 Liang, Qiao, 147  
 Lin, Weiren, 135  
 Lisa, Borgatti, 317, 463  
 Lollino, Piernicola, 65  
 Longo, Sergio Enrico Favero, 207  
 Lopes, Maria Eugénia, 227  
 Lozar, F., 257, 261  
 Lucchesi, Stefania, 235, 245, 447  
 Lucia, Mehnert, 107  
 Ludovít, Kubičár, 577  
 Lupiano, Valeria, 405

**M**

Magagna, A., 257  
 Mandrone, Giuseppe, 427  
 Maravelaki, Noni, 525  
 Marchetti, Emanuele, 323  
 Marco, Giardino, 463  
 Marco, Zerbinatti, 159  
 Margherita, Zimbardo, 409  
 Margottini, Claudio, 393  
 Maria, Sileo, 453  
 Mariani, Valentina, 323  
 Martínez-Ramírez, Sagrario, 531  
 Martire, Luca, 207, 257  
 Masciocco, Luciano, 427  
 de Masi, Alessandro, 351  
 Mashalah, Khamehchian, 477  
 Masini, Nicola, 339  
 Maslov, Yuriy, 83  
 Materazzi, M., 273  
 Mavlyanova, N. G., 165  
 Meixedo, João P., 227  
 Merodo, Jose Antonio Fernandez, 65  
 Mihai, Maftciu, 281  
 Millemaci, Paolo, 269  
 Misae, Ito, 71  
 Mitsugu, Yoshimura, 71  
 Mocsár-Vámos, Mariann, 153  
 Molin, Gianmario, 547  
 Moretti, Sandro, 345  
 Mosca, Pietro, 239  
 Motta, Luigi, 235  
 Motta, Michele, 235  
 Mrozek, Teresa, 381, 415  
 Mulder, Arno, 103  
 Muller, Axel, 103  
 Muniyappa, Prathap, 129

**N**

Nahar, Mowsumi, 219  
 Nakagawa, Koichi, 31, 177  
 Natalicchio, M., 257, 261  
 Navarro, Fabiano Cabañas, 511  
 Ngan-Tillard, Dominique, 103  
 Nicola, Nocilla, 409  
 Nigrelli, Guido, 459  
 Nijland, Timo G., 557  
 Nonomura, Atsuko, 99

**O**

Oike, Kazuo, 31, 177  
 Olivia, Nesci, 463  
 Onoda, Satoshi, 99  
 Orhan, Ahmet, 361

**P**

Padula, Giuliano, 335  
 Pambianchi, G., 273  
 Panizza, Mario, 213  
 Panizza, Valeria, 213  
 Paolo, Frattini, 293  
 Paolo, Piumatti, 159  
 Papanikolaou, Helen, 139  
 Pápay, Zita, 553  
 Park, Sun-Hyun, 329  
 Paul, Marinos, 293  
 Pecchioni, Elena, 387  
 Pei, Qiangqiang, 183  
 Pelfini, Manuela, 213  
 Peloso, Alessandro, 287  
 Pengcheng, Peng, 147  
 Perotti, Luigi, 235, 269  
 Peter, Ellecosta, 113  
 Péter, Görög, 153  
 Péter, Görög, 503  
 Phoenix, Vernon, 487  
 Piacente, Sandra, 213  
 Pica, Alessia, 213  
 Piervittori, Rosanna, 207  
 Pope, Gregory A., 495  
 Poretti, Giulia, 207  
 Pratesi, Fabio, 345  
 Prikryl, Richard, 539  
 Puglisi, Claudio, 287  
 Puzzilli, Luca Maria, 393  
 Pyrgiotis, Lambros, 89

**Q**

Qinglin, Guo, 71  
 Qiuping, Zhu, 147  
 Quresima, Raimondo, 387  
 Quitete, Eduardo Brandau, 511

**R**

Raška, Pavel, 443  
 Ravanel, Ludovic, 249  
 Renner, Timothy, 495

Reza, Nikudel Mohammad, [477](#)  
 Ripepe, Maurizio, [323](#)  
 Rolfo, Franco, [207](#), [239](#)  
 Rosanna, Sciortino, [409](#)  
 Rosaria, Potenza Maria, [453](#)  
 Rossetti, Piergiorgio, [235](#), [239](#)  
 Russo, Filippo, [213](#)

**S**

Sanda, Bugiu, [281](#)  
 Saroglou, Charalambos, [117](#)  
 Sass, O., [569](#)  
 Sato, Minoru, [135](#)  
 Schnepfleitner, H., [569](#)  
 Screpanti, Augusto, [287](#)  
 Senin, Raluca-Madalina, [543](#)  
 Serio, Luigi, [335](#)  
 Shanlong, Yang, [71](#)  
 Shaojun, Yan, [147](#)  
 Shimoda, Ichita, [53](#)  
 Shogaki, Takaharu, [75](#)  
 Silvestri, Francesco, [421](#)  
 Simon, Martin, [265](#)  
 de Silva, Filomena, [421](#)  
 Sonnessa, Alberico, [393](#)  
 Sotiriou, Andreas, [117](#)  
 Spanou, Natalia, [431](#)  
 Spizzichino, Daniele, [335](#)  
 Spizzichino, Daniele, [393](#)  
 de Stefano, Mario, [323](#)  
 Sun, Guanping, [199](#)  
 Świdziński, Waldemar, [381](#)  
 Szabó, B., [471](#)

**T**

Takada, Naoki, [135](#)  
 Takahashi, Manabu, [135](#)  
 Tanganelli, Marco, [323](#)  
 Tanimoto, Chikaosa, [31](#), [177](#)  
 Tapete, Deodato, [339](#), [345](#)  
 Tati, Angelo, [287](#)  
 Teixeira, José, [227](#)  
 Terenzi, Gloria, [345](#)  
 Terenzio, Gizzi Fabrizio, [453](#)  
 Tian, Lei, [193](#), [199](#)  
 Tom, Heldal, [253](#)  
 Török, Ákos, [153](#), [503](#), [553](#), [565](#), [471](#)  
 Trigo, J. Filinto, [227](#)  
 Tsutsunava, Tamara, [483](#)

Turcanu-Carutiu, Daniela, [543](#)  
 Tutberidze, Bezhan, [483](#)

**U**

Uchida, Jun'ichi, [99](#)

**V**

Vásárhelyi, Balázs, [153](#), [565](#)  
 Ventisette, Chiara Del, [345](#)  
 Verganelaki, Anastasia, [525](#)  
 Verubbì, Vladimiro, [287](#)  
 Verwaal, Wim, [103](#)  
 Victor, Niculescu, [281](#)  
 Villa, Alberto, [59](#)  
 Violanti, D., [257](#)  
 Vladimir, Greif, [577](#)

**W**

Wang, Jinfang, [189](#)  
 Wang, Lanming, [31](#), [177](#)  
 Wang, X. L., [357](#)  
 Wang, Xudong, [31](#), [177](#), [183](#)  
 Watanabe, Kunio, [75](#)  
 Wim Dubelaar, C., [557](#)  
 Wu, Laying, [495](#)

**X**

Xudong, Wang, [71](#)

**Y**

Yang, Bo, [189](#)  
 Yang, Shanlong, [183](#)  
 Yang, Zhifa, [123](#)  
 Yoshinori, Iwasaki, [71](#)  
 Young, Maureen, [487](#)  
 Yun, Fang, [147](#)

**Z**

Zábranský, Vilém, [443](#)  
 Zabuski, Lesław, [381](#)  
 Zerboni, Andrea, [213](#)  
 Zhang, Huyuan, [189](#)  
 Zhang, Jingke, [193](#), [199](#)  
 Zhang, L. Q., [357](#)